REPORT ON THE ENVIRONMENTAL IMPACT ASSESSMENT OF THE BALTICA-1 OFFSHORE WIND FARM

APPENDIX 1

THE INVENTORY REPORT



MEWO
SUBSEA SOLUTIONS

AUTHORS:

Marek Bogucki, Patryk Dombrowski, Sara Foit, Łukasz Gajewski, Karol Ginał, Olha Hruzdieva, Mateusz Kołakowski, Sandra Korczak, Emilia Leszczyńska, Elżbieta Maszloch, Marcelina Mazur-Petka, Jędrzej Patejko, Karolina Rogowska, Angelika Słomska, Kacper Sokół, Marcin Sontowski, Marta Szafrańska, Radosław Wróblewski, Szymon Zabrocki, Janusz Dworniczak, Tomasz Kusio, Maja Lange, Marta Grabowska, Marek Marciniak, Krzysztof Załęski, Ewelina Misiewicz, Jarosław Kapiński, Maciej Kałas, Katarzyna Galer-Tatarowicz, Grażyna Dembska, Grażyna Pazikowska-Sapota, Agnieszka Flasińska, Aleksandra Bojke, Aleksandra Dzendrowska, Ewelina Duljas, Małgorzata Littwin, Agata Szpiech, Katarzyna Szczepańska, Olga Jażdżewska, Dominika Ostrowska, Agnieszka Cichowska, Tomasz Dziarkowski, Paweł Jasiński, Jadwiga Kargol, Angelika Rybakowska, Martyna Dąbrowska, Izabela Wittstock, Jakub Obszarski, Aliaksandr Lisimenka, Anna Barańska, Diana Dziaduch, Tomasz Nermer, Aleksander Drgas, Lena Szymanek, Katarzyna Horbowa, Krzysztof Radtke, Zuzanny Mirny, Szymon Smoliński, Włodzimierz Grygiel, Małgorzata Dembek, Beata Schmidt, Irmina Balicka, Olga Brocławik, Magda Chreptowicz, Marta Nocoń, Urszula Sadowska-Maksym, Frank Thomsen, Włodzimierz Meissner, Thomas W. Johansen, Maans Karlson, Lucyna Pilacka, Liliana Schönberger, Henrik Skov, Aneta Zapart, Magdalena Wybraniec

CONTRACTORS:

Justyna Edut, Izabela Zelewska, Natalia Kaczmarek, Teresa Moroz-Kunicka, Mateusz Kunicki, Kamila Gałka, Marta Cieżyńska, Jacek Ksepko, Krzysztof Gajko, Dominika Górnowicz, Karolina Rogóż-Badzińska

TABLE OF CONTENTS

ABBREVIATIONS AND DEFINITIONS 44

1 GEOPHYSICAL SURVEYS – THE BASIC SCOPE 51

1.1 Non-specialist summary 51

1.1.1 Bathymetric surveys 51

1.1.2 Side-scan sonar survey 51

1.1.3 Magnetometric measurements 52

1.1.4 Surveys of man-made or unidentified objects on the seabed 52

1.1.5 Shallow seismo-acoustic profiling 52

1.1.6 Seismic surveys 52

1.1.6.1 Single-channel seismic surveys 52

1.1.6.2 Multi-channel seismic surveys (2D UHR) 53

1.1.7 Soil sampling 53

1.1.7.1 Surface sediment sampling 53

1.1.7.2 Core sampling 53

1.2 Spatial scope of the surveys 54

1.3 Methodology 57

1.3.1 Bathymetric surveys 57

1.3.1.1 Bathymetric survey methodology 57

1.3.1.2 Bathymetric data post-processing methodology 57

1.3.2 Side-scan sonar survey 59

1.3.2.1 Side-scan sonar survey methodology 59

1.3.2.2 Sonar data post-processing methodology 59

1.3.3 Magnetometric measurements 61

1.3.3.1 Magnetometric survey methodology 61

1.3.3.2 Magnetometric data post-processing methodology 62

1.3.4 Surveys of man-made or unidentified objects on the seabed 63

1.3.4.1 Methodology for the surveys of man-made or unidentified objects on the seabed 63

1.3.4.2 Methodology for processing the data from the surveys of man-made or unidentified objects on the seabed 63

1.3.5 Shallow seismo-acoustic profiling 64

1.3.5.1 Methodology for seismo-acoustic surveys using sediment profiler 64

1.3.5.2 Seismo-acoustic data post-processing methodology 65

1.3.6 Seismic surveys 67

1.3.6.1 Single-channel seismic surveys 67

1.3.6.1.1 Single-channel seismic survey methodology 67
1.3.6.1.2 Single-channel seismic data post-processing methodology 67
1.3.6.2 Multi-channel seismic profiling 69
1.3.6.2.1 Methodology of multi-channel seismic surveys (2D UHR) 69
1.3.6.2.2 Multi-channel seismic data post-processing methodology 70
1.3.7 Soil sampling 71
1.3.7.1 Surface sediment sampling 71
1.3.7.1.1 Surface sediment sampling methodology 71
1.3.7.1.2 Methodology for the laboratory testing of sediment samples 72
1.3.7.2 Core sampling 73
1.3.7.2.1 Core sampling methodology 73
1.3.7.2.2 Methodology for the laboratory tests of core samples 73
1.4 Activities performed 74
1.5 Results 75
1.5.1 Bathymetric surveys 75
1.5.2 Side-scan sonar survey 78
1.5.3 Magnetometric measurements 79
1.5.4 Surveys of man-made or unidentified objects on the seabed 82
1.5.5 Shallow seismo-acoustic profiling 85
1.5.6 Seismic surveys 86
1.5.6.1 Single-channel seismic surveys 86
1.5.6.2 Multi-channel seismic surveys (2D UHR) 86
1.5.7 Soil sampling 86
1.5.7.1 Surface sediment sampling 86
1.5.7.2 Core sampling 96
1.6 Summary of results and conclusions 96
1.6.1 Interpretation of the seabed surface character 96
1.6.2 Geological structure 109
1.7 Shortcomings and gaps in the state-of-the-art 125
2 ABIOTIC ELEMENTS IN MARINE SURVEYS – THE BASIC SCOPE OF SURVEYS CONTRACTED 126
2.1 Hydrological and meteorological monitoring including sea currents 126
2.1.1 Non-specialist summary 126
2.1.2 Spatial scope of the surveys 127
2.1.3 Methodology 129
2.1.4 Activities performed 132

2.1.5 Results 139
2.1.5.1 Meteorological measurements 139
2.1.5.2 Hydrological measurements 143
2.1.5.2.1 Wave motion 143
2.1.5.2.2 Water depth (thickness of the sea deep) 151
2.1.5.2.3 Water flow 154
2.1.5.3 Hydrophysical measurements 166
2.1.5.3.1 Continuous recordings 166
2.1.5.3.1.1 Water temperature 166
2.1.5.3.1.2 Electrical conductivity of water 168
2.1.5.3.1.3 Water salinity 170
2.1.5.3.1.4 Water turbidity 172
2.1.5.3.2 CTD measurements performed during the water and sediment sampling 174
2.1.5.3.2.1 Water temperature 174
2.1.5.3.2.2 Electrical conductivity of water 175
2.1.5.3.2.3 Water salinity 176
2.1.5.3.2.4 Water turbidity 177
2.1.5.3.2.5 Depth 178
2.1.5.4 Ice conditions 179
2.1.6 Summary of results and conclusions 179
2.1.6.1 Meteorological measurements 179
2.1.6.2 Hydrological measurements 180
2.1.6.2.1 Wave motion 180
2.1.6.2.2 Water depth (thickness of the sea deep) 180
2.1.6.2.3 Water flows 180
2.1.6.3 Hydrophysical measurements 181
2.1.6.3.1 Continuous recordings 181
2.1.6.3.1.1 Water temperature 181
2.1.6.3.1.2 Electrical conductivity of water 181
2.1.6.3.1.3 Water salinity 181
2.1.6.3.1.4 Water turbidity 181
2.1.6.3.2 CTD measurements performed during the water and sediment sampling 182
2.1.6.3.2.1 Water temperature 182
2.1.6.3.2.2 Electrical conductivity of water 182
2.1.6.3.2.3 Water salinity 182

2.1.6.3.2.4 Water turbidity 182
2.1.6.3.3 Water depth 182
2.1.6.4 Ice conditions 182
2.1.7 Shortcomings and gaps in the state-of-the-art 182
2.2 Surveys of physicochemical properties of water 183
2.2.1 Non-specialist summary 183
2.2.2 Spatial scope of the surveys 185
2.2.3 Methodology 187
2.2.3.1 Survey methodology 187
2.2.3.2 Methodology for data post-processing 190
2.2.4 Activities performed 191
2.2.5 Results 194
2.2.5.1 Physical state indicators (suspended solids) 194
2.2.5.2 Indicators of oxygen conditions 196
2.2.5.3 Acidification indicators 201
2.2.5.4 Indicators of nutrient conditions 204
2.2.5.5 Particularly harmful and priority substances 216
2.2.5.5.1 Metals and metalloids 216
2.2.5.5.2 Phenol index and cyanides (free and bound) 218
2.2.5.5.3 Mineral oil index 219
2.2.5.5.4 Polycyclic aromatic hydrocarbons (PAHs) 220
2.2.5.5.5 Polychlorinated biphenyls (PCBs) 225
2.2.5.6 Radionuclides 227
2.2.6 Summary of results and conclusions 228
2.2.6.1 Physical state indicators (suspended solids) 228
2.2.6.2 Indicators of oxygen conditions 230
2.2.6.2.1 Dissolved oxygen 230
2.2.6.2.2 Biochemical oxygen demand (BOD_5) 231
2.2.6.2.3 Total organic carbon content (TOC) 232
2.2.6.3 Acidification indicators 233
2.2.6.3.1 Reaction (pH) 233
2.2.6.3.2 Alkalinity 235
2.2.6.4 Indicators of nutrient conditions (nutrients) 237
2.2.6.4.1 Nitrites 237
2.2.6.4.2 Nitrates 237

2.2.6.4.3 Ammoniacal nitrogen (ammonia) ... 239
2.2.6.4.4 Mineral nitrogen (DIN) ... 240
2.2.6.4.5 Total nitrogen ... 241
2.2.6.4.6 Phosphates ... 243
2.2.6.4.7 Total phosphorus ... 245
2.2.6.5 Specific synthetic and non-synthetic contaminants and a group of chemical indicators characterising the presence of substances particularly harmful to the aquatic environment and the priority substances in the field of water policy ... 247
2.2.6.5.1 Metals and metalloids ... 247
2.2.6.5.2 Phenol index and cyanides (free and bound) ... 248
2.2.6.5.3 Mineral oil index ... 248
2.2.6.5.4 Polycyclic aromatic hydrocarbons (PAHs) ... 249
2.2.6.5.5 Polychlorinated biphenyls (PCBs) ... 250
2.2.6.6 Radionuclides ... 251
2.2.6.7 A summary of results obtained for the survey area ... 252
2.2.7 Shortcomings and gaps in the state-of-the-art ... 253
2.3 Seabed sediments ... 253
2.3.1 Non-specialist summary ... 253
2.3.2 Spatial scope of the surveys ... 254
2.3.3 Methodology ... 256
2.3.3.1 Survey methodology ... 256
2.3.3.2 Methodology of data post-processing ... 259
2.3.4 Activities performed ... 259
2.3.5 Results ... 262
2.3.5.1 Indicators characterising the physicochemical properties of sediments (LOI, moisture content, TOC) ... 262
2.3.5.2 Nutrient indicators (total nitrogen, total phosphorus) ... 262
2.3.5.3 Specific synthetic and non-synthetic contaminants, as well as metals from the group of substances particularly harmful to the aquatic environment ... 262
2.3.5.3.1 Metals and metalloids ... 262
2.3.5.3.2 A group of chemical indicators characterising the occurrence of substances harmful to the aquatic environment ... 263
2.3.5.3.2.1 Crude oil derivative hydrocarbons (mineral oils) ... 263
2.3.5.3.2.2 Polycyclic aromatic hydrocarbons (PAHs) ... 263
2.3.5.3.2.3 Polychlorinated biphenyls (PCBs) ... 264
2.3.5.3.2.4 Organotin compounds (TBT, DBT, MBT) ... 264

2.3.5.3.3 Radionuclides 265
2.3.5.4 Grain size analysis 265
2.3.6 Summary of results and conclusions 265
2.3.6.1 Indicators characterising the physicochemical properties of sediments (LOI, moisture content, TOC) 265
2.3.6.2 Nutrient indicators (total nitrogen, total phosphorus) 265
2.3.6.2.1 Total nitrogen 265
2.3.6.2.2 Total phosphorus 266
2.3.6.3 Specific synthetic and non-synthetic contaminants, as well as metals from the group of substances particularly harmful to the aquatic environment 267
2.3.6.3.1 Metals and metalloids 267
2.3.6.3.1.1 Metal and metalloid content 267
2.3.6.3.1.2 Content of labile metal form 267
2.3.6.3.2 Polycyclic aromatic hydrocarbons (PAHs) 269
2.3.6.3.3 Polychlorinated biphenyls (PCBs) 270
2.3.6.3.4 Crude oil derivative hydrocarbons 270
2.3.6.3.5 Organotin compounds (TBT, DBT, and MBT) 271
2.3.6.4 Radionuclides 272
2.3.6.5 Grain size analysis 272
2.3.6.6 Summary of the analysis results 273
2.3.7 Shortcomings and gaps in the state-of-the-art 273
2.4 Aggregates 273
2.4.1 Non-specialist summary 273
2.4.2 Spatial scope of the surveys 274
2.4.3 Methodology 274
2.4.4 Activities performed 275
2.4.5 Results 275
2.4.6 Summary of results and conclusions 285
2.4.7 Shortcomings and gaps in the state-of-the-art 285
2.5 Acoustic background 285
2.5.1 Non-specialist summary 285
2.5.2 Spatial scope of the surveys 287
2.5.3 Methodology 289
2.5.4 Activities performed 291
2.5.5 Results 294

2.5.6 Summary of results and conclusions 337
2.5.7 Shortcomings and gaps in the state-of-the-art 338
3 BIOTIC ELEMENTS IN MARINE SURVEYS – THE BASIC SCOPE OF SURVEYS CONTRACTED 340
3.1 Phytobenthos 340
3.1.1 Non-specialist summary 340
3.1.2 Spatial scope of the surveys 340
3.1.3 Methodology 340
3.1.4 Activities performed 342
3.1.5 Results 342
3.1.6 Summary of results and conclusions 344
3.1.7 Shortcomings and gaps in the state-of-the-art 344
3.2 Macrozoobenthos 344
3.2.1 Non-specialist summary 344
3.2.2 Spatial scope of the surveys 345
3.2.3 Methodology 345
3.2.4 Activities performed 349
3.2.5 Results 351
3.2.5.1 Soft bottom 351
3.2.5.1.1 Taxonomic composition 351
3.2.5.1.2 Macrozoobenthos abundance 353
3.2.5.1.3 Macrozoobenthos biomass 354
3.2.5.1.4 Bivalve size structure 355
3.2.5.1.5 B index 358
3.2.5.2 Hard bottom 358
3.2.5.2.1 Taxonomic composition 358
3.2.5.2.2 Macrozoobenthos abundance 359
3.2.5.2.3 Macrozoobenthos biomass 359
3.2.5.2.4 Bivalve size structure 360
3.2.5.2.5 TSP index 361
3.2.6 Summary of results and conclusions 361
3.2.7 Shortcomings and gaps in the state-of-the-art 369
3.3 Ichthyofauna 369
3.3.1 Non-specialist summary 369
3.3.2 Spatial scope of the surveys 371
3.3.3 Methodology 371

3.3.3.1 Ichthyoplankton 371
3.3.3.2 Hydroacoustic surveys and pelagic hauls 373
3.3.3.3 Demersal fish surveys 376
3.3.3.4 Herring concentration surveys 379
3.3.4 Activities performed 381
3.3.4.1 Ichthyoplankton 381
3.3.4.2 Hydroacoustic surveys and pelagic hauls 382
3.3.4.3 Demersal fish surveys 384
3.3.4.4 Herring concentration surveys 389
3.3.5 Results 394
3.3.5.1 Ichthyoplankton 394
3.3.5.1.1 Ichthyoplankton species composition and abundance in individual survey seasons 395
3.3.5.1.1.1 Winter 395
3.3.5.1.1.2 Spring 396
3.3.5.1.1.3 Summer 397
3.3.5.1.1.4 Autumn 398
3.3.5.1.2 Variability of ichthyoplankton species composition and abundance between seasons 399
3.3.5.1.3 Spatial distribution 403
3.3.5.2 Hydroacoustic surveys and pelagic hauls 413
3.3.5.3 Demersal fish surveys 423
3.3.5.4 Herring concentration surveys 425
3.3.5.5 Biological survey results 428
3.3.5.5.1 Sprat 428
3.3.5.5.2 Herring 432
3.3.5.5.3 Cod 435
3.3.5.5.4 Flounder 439
3.3.6 Summary of results and conclusions 442
3.3.6.1 Ichthyoplankton 442
3.3.6.2 Hydroacoustic surveys and pelagic hauls 444
3.3.6.3 Results of catches and biological analyses 445
3.3.6.4 Conclusions 449
3.3.7 Shortcomings and gaps in the state-of-the-art 452
3.4 Marine mammals 453
3.4.1 Non-specialist summary 453
3.4.2 Spatial scope of the surveys 455

3.4.2.1 Passive acoustic monitoring 455
3.4.2.2 Aerial visual monitoring 458
3.4.2.3 Visual observations (marine mammal counting) during seabird surveys 460
3.4.3 Methodology 460
3.4.3.1 Passive acoustic monitoring 460
3.4.3.2 Aerial visual monitoring 462
3.4.3.3 Visual observations (marine mammal counting) during seabird surveys 462
3.4.4 Activities performed 462
3.4.4.1 Passive acoustic monitoring 462
3.4.4.2 Aerial visual monitoring 464
3.4.4.3 Visual observations (marine mammal counting) during seabird surveys 464
3.4.5 Results 464
3.4.5.1 Passive acoustic monitoring 464
3.4.5.2 Aerial visual monitoring 493
3.4.5.3 Visual observations (marine mammal counting) during seabird surveys 496
3.4.5.4 Summary of the visual monitoring results 497
3.4.6 Summary of results and conclusions 499
3.4.6.1 Harbour porpoise 499
3.4.6.2 Seals 502
3.4.7 Shortcomings and gaps in the state-of-the-art 506
3.5 Avifauna 506
3.5.1 Bird counts from aboard vessels (seabirds) 506
3.5.1.1 Non-specialist summary 506
3.5.1.1.1 Subject matter and objective of the project 506
3.5.1.1.2 Survey methods 506
3.5.1.1.3 Survey results 507
3.5.1.2 Spatial scope of the surveys 508
3.5.1.3 Methodology 509
3.5.1.4 Activities performed 515
3.5.1.4.1 Survey area 515
3.5.1.4.1.1 Weather conditions 517
3.5.1.4.1.2 The presence of other vessels within the transect strip 518
3.5.1.4.2 Reference area 519
3.5.1.4.2.1 Weather conditions 521
3.5.1.4.2.2 The presence of other vessels within the transect strip 522

3.5.1.5 Results....523
3.5.1.5.1 Avifauna species composition 523
3.5.1.5.1.1 Survey area 523
3.5.1.5.1.1.1 Wintering period 523
3.5.1.5.1.1.2 Spring migration period 525
3.5.1.5.1.1.3 Summer period 529
3.5.1.5.1.1.4 Autumn migration period 531
3.5.1.5.1.2 Reference area 534
3.5.1.5.1.2.1 Wintering period 534
3.5.1.5.1.2.2 Spring migration period 537
3.5.1.5.1.2.3 Summer period 539
3.5.1.5.1.2.4 Autumn migration period 541
3.5.1.5.2 Changes in avifauna abundance 544
3.5.1.5.3 Altitude of bird flights 551
3.5.1.5.3.1 Survey area 551
3.5.1.5.3.2 Reference area 553
3.5.1.5.4 Bird distribution 556
3.5.1.5.4.1 Wintering period 560
3.5.1.5.4.2 Spring migration period 564
3.5.1.5.4.3 Summer period 568
3.5.1.5.4.4 Autumn migration period 570
3.5.1.5.5 Conservation status of the seabird species identified 574
3.5.1.5.6 Comparison of species composition of birds present in the survey area and in the reference area 577
3.5.1.5.6.1 Species composition and average abundance of seabirds in the wintering period 577
3.5.1.5.6.2 Species composition and average abundance of seabirds in the spring migration period 578
3.5.1.5.6.3 Species composition and average abundance of seabirds in the summer period .. 579
3.5.1.5.6.4 Species composition and average abundance of seabirds in the autumn migration period 579
3.5.1.5.6.5 Comparison of the abundance indices of the bird grouping 580
3.5.1.6 Summary of results and conclusions 581
3.5.1.7 Shortcomings and gaps in the state of the art....586
3.5.2 Surveys of bird movements (migratory birds) 587
3.5.2.1 Non-specialist summary 587
3.5.2.2 Spatial scope of the surveys 590

3.5.2.3 Methodology 593
3.5.2.3.1 Visual observations 593
3.5.2.3.2 Radar observations 599
3.5.2.3.2.1 Horizontal radar surveys 599
3.5.2.3.2.2 Vertical radar surveys 600
3.5.2.3.3 Acoustic monitoring 601
3.5.2.4 Activities performed 602
3.5.2.5 Results....614
3.5.2.5.1 Visual observations 614
3.5.2.5.1.1 Local bird movements in the wintering period 614
3.5.2.5.1.2 Spring migration 616
3.5.2.5.1.3 Autumn migration 621
3.5.2.5.2 Migration fluxes (flight intensity) 625
3.5.2.5.3 Flight altitude from visual observations 653
3.5.2.5.3.1 Local bird movements in the wintering period 653
3.5.2.5.3.2 Spring migration 656
3.5.2.5.3.3 Autumn migration 662
3.5.2.5.4 Horizontal radar bird tracking.... 668
3.5.2.5.4.1 Local bird movements in the wintering period 668
3.5.2.5.4.2 Spring migration 676
3.5.2.5.4.3 Autumn migration 688
3.5.2.5.5 Vertical radar results.... 704
3.5.2.5.5.1 Local bird movements in winter (wintering birds) 704
3.5.2.5.5.2 Spring migration 709
3.5.2.5.5.3 Autumn migration 715
3.5.2.5.6 Acoustic monitoring.... 725
3.5.2.5.6.1 Spring migration 725
3.5.2.5.6.2 Autumn migration 729
3.5.2.6 Summary of results and conclusions 733
3.5.2.7 Shortcomings and gaps in the state-of-the-art....742
3.6 Chiropterofauna (bats) 743
3.6.1 Non-specialist summary 743
3.6.2 Spatial scope of the surveys 743
3.6.3 Methodology 746
3.6.4 Activities performed 748

3.6.5 Results 750
3.6.5.1 Bat species composition 750
3.6.5.2 Seasonal activity dynamics 751
3.6.6 Summary of results and conclusions 753
3.6.7 Shortcomings and gaps in the state-of-the-art 754
4 REFERENCES 755

LIST OF TABLES

Table 1.1 Factors enabling the performance of activities as part of ROV inspections in a manner ensuring the acquisition of survey data of appropriate quality 63

Table 1.2. A standard set of sieves for sieve analysis 72

Table 1.3. The statistics of magnetic anomalies based on their shape 80

Table 1.4. The types of man-made objects or objects of unidentified origin on the seabed 82

Table 1.5. A macroscopic description and the result of grain size analysis of the sediment samples collected in the survey area 87

Table 1.6. The number of boulders in individual size classes 107

Table 1.7. The classification of the seismic units differentiated (the character of reflections in the seismo-acoustic recording) 110

Table 1.8. A correlation of seismic units with the sediments collected during drilling with a vibrocorer (core examples) 111

Table 2.1. The coordinates of the survey stations in the survey area 129

Table 2.2. Threshold values of devices for measured physical parameters at sea 130

Table 2.3. The recording parameters of the measured atmosphere and sea properties 131

Table 2.4. A specification of the activities performed as part of the hydrometeorological monitoring 133

Table 2.5. The percentage data yields for the survey area 137

Table 2.6. The dates of measuring individual parameters included in the Report on the survey area 138

Table 2.7. The statistical analysis of the meteorological parameters measured at survey station B_MFW_3 located within the survey area 140

Table 2.8. A summary of selected characteristics of wind-generated wave motion at the survey stations located in the survey area recorded throughout a measurement period of one full year 143

Table 2.9. A summary of the number of the maximum wave heights occurrences at the survey stations in the survey area according to the Douglas scale 144

Table 2.10. The characteristics of the water flow measured across the water depth profile at the survey stations located within the survey area throughout a measurement period of one full year .. 154

Table 2.11. A statistical analysis of the water temperature measured at survey stations B_MFW_1, B_MFW_3, and B_MFW_5 located within the survey area throughout the entire measurement period 166

Table 2.12. A statistical analysis of the electrical conductivity of water measured at survey stations B_MFW_1, B_MFW_3, and B_MFW_5 located within the survey area throughout the entire measurement period 168

Table 2.13. A statistical analysis of the water salinity calculated for the survey stations B_MFW_1, B_MFW_3 and B_MFW_5 located within the survey area for the entire measurement period 170

Table 2.14. A statistical analysis of the water turbidity measured at survey stations B_MFW_1, B_MFW_3, and B_MFW_5 located within the survey area for the entire measurement period 172

Table 2.15. A statistical analysis of water temperature measured during the water and sediment sampling throughout the entire measurement period 174

Table 2.16. A statistical analysis of the electrical conductivity of water measured during the water and seabed sediment sampling throughout the entire measurement period 175

Table 2.17. A statistical analysis of water salinity calculated during the water and seabed sediment sampling throughout the entire measurement period 176

Table 2.18. A statistical analysis of water turbidity measured during the water and seabed sediment sampling within the entire measurement period 177

Table 2.19. A statistical analysis of water depth measured during the water and seabed sediment sampling within the entire measurement period 178

Table 2.20. Methods and techniques applied in the in situ testing of water samples in the mobile and stationary laboratories 188

Table 2.21. A list of activities conducted in relation to water sampling in the survey area 192

Table 2.22. The scope of the tests conducted on the water samples collected as part of all six water sampling campaigns carried out in the survey area 193

Table 2.23. The mean, minimum, and maximum contents of total suspended solids in the water samples collected in the survey area 194

Table 2.24. The mean, minimum, and maximum content of total suspended solids in the profile water samples collected in the survey area 194

Table 2.25. The mean, minimum, and maximum values of the content of dissolved oxygen, BOD_5, and TOC in the water samples collected in the survey area 196

Table 2.26. The mean, minimum, and maximum content of dissolved oxygen, BOD_5, and TOC in the profile water samples collected in the survey area 197

Table 2.27. The mean, minimum, and maximum value of reaction (pH) and alkalinity in water samples collected in the survey area 201

Table 2.28. The mean, minimum, and maximum value of reaction (pH) and alkalinity in the profile water samples collected in the survey area 202

Table 2.29. The mean, minimum, and maximum values of nitrogen and phosphorus compounds in the water samples collected in the survey area 205

Table 2.30. The mean, minimum, and maximum values of nitrogen and phosphorus compounds in the water samples collected in the survey area 207

Table 2.31. The mean, minimum, and maximum concentration values of metals and metalloids in the water samples collected in summer 2023, in the survey area 216

Table 2.32. The mean, minimum, and maximum metal concentration values in the profile water samples collected in summer 2023 in the survey area 216

Table 2.33. The mean, minimum, and maximum concentrations of phenols and free and bound cyanides in the water samples collected in July 2023 in the survey area 218

Table 2.34. The mean, minimum, and maximum concentration values of phenols and free and bound cyanides in the profile water samples collected in summer 2023 in the survey area 219

Table 2.35. The mean, minimum, and maximum concentration values of petroleum hydrocarbons (mineral oil index) in the water samples collected in July 2023 in the survey area 219

Table 2.36. The mean, minimum, and maximum concentration values of petroleum hydrocarbons (mineral oil index) in the profile water samples collected in summer 2023 in the survey area 220

Table 2.37. The mean, minimum, and maximum concentration values of the sum of 16 PAHs in the water samples collected in July 2023 in the survey area 220

Table 2.38. The mean, minimum, and maximum concentration values of PAHs and the sum of 16 PAHs in the profile water samples collected in summer 2023 in the survey area 221

Table 2.39. The mean, minimum, and maximum concentration values of the sum of 7 PCBs in the water samples collected in July 2023 in the survey area 225

Table 2.40. The mean, minimum, and maximum concentration values of the sum of 7 PCBs in the profile water samples collected in summer 2023 in the survey area 226

Table 2.41. The mean, minimum, and maximum values of the caesium (^{137}Cs) and strontium (^{90}Sr) radioactivity in the water samples collected in summer 2023 in the survey area 227

Table 2.42. The methods and techniques used for analysing seabed sediment samples with the indication of the limit of quantification of a particular method 257

Table 2.43. A standard set of sieves for sieve analysis 258

Table 2.44. A list of activities conducted as part of sediment sampling in the survey area 260

Table 2.45. The scope of the analyses of seabed sediment samples collected within the survey area 261

Table 2.46. The mean, minimum, and maximum values of LOI, moisture content, and TOC in the sediment samples collected within the survey area 262

Table 2.47. The mean, minimum, and maximum values of total nitrogen and total phosphorus concentrations in the sediment samples from the survey area 262

Table 2.48. The mean, minimum, and maximum values of trace metal concentrations (total content and labile form) in the sediment samples from the survey area 262

Table 2.49. The mean, minimum, and maximum values of mineral oil concentration in the sediment samples from the survey area 263

Table 2.50. The mean, minimum, and maximum values of PAH concentrations in the sediment samples from the survey area 263

Table 2.51. The mean, minimum, and maximum values of PCB concentrations in the sediment samples from the survey area 264

Table 2.52. The mean, minimum, and maximum concentrations of organotin compounds in the sediment samples from the survey area 264

Table 2.53. The mean, minimum, and maximum values of caesium (^{137}Cs) radioactivity in the sediment samples from the survey area 265

Table 2.54. A summary of the obtained survey data 292

Table 2.55. Survey campaign no. 1. The statistical values of the sound pressure level values SPL [dB re 1 µPa] in two 1/3-octave frequency bands with central frequencies of 63 Hz and 125 Hz and in the 20–20 000 Hz broadband 308

Table 2.56. Survey campaign no. 2. The statistical values of the sound pressure level values SPL [dB re 1 µPa] in two 1/3-octave frequency bands with central frequencies of 63 Hz and 125 Hz and in the 20–20 000 Hz broadband 308

Table 2.57. Survey campaign no. 3. The statistical values of the sound pressure level values SPL [dB re 1 µPa] in two 1/3-octave frequency bands with central frequencies of 63 Hz and 125 Hz and in the 20–20 000 Hz broadband 309

Table 2.58. Survey campaign no. 4. The statistical values of the sound pressure level values SPL [dB re 1 µPa] in two 1/3-octave frequency bands with central frequencies of 63 Hz and 125 Hz and in the 20–20 000 Hz broadband 309

Table 2.59. Survey campaign no. 5. The statistical values of the sound pressure level values SPL [dB re 1 µPa] in two 1/3-octave frequency bands with central frequencies of 63 Hz and 125 Hz and in the 20–20,000 Hz broadband 309

Table 2.60. Survey station H_1. The statistical values of the sound pressure level values (SPL) [dB re 1 µPa] in two 1/3-octave bands with central frequencies of 63 Hz and 125 Hz and in the 20–20,000 Hz broadband in individual wind speed classes according to the Beaufort scale [°B] Survey session no. 1 (03.12.2022–07.02.2023) 320

Table 2.61. Survey station H_4. The statistical values of the sound pressure level values (SPL) [dB re 1 µPa] in two 1/3-octave bands with central frequencies of 63 Hz and 125 Hz and in the 20–20,000 Hz broadband in individual wind speed classes according to the Beaufort scale [°B] Survey session no. 1 (03.12.2022–07.02.2023) 320

Table 2.62. Survey station H_1. The statistical values of the sound pressure level values (SPL) [dB re 1 µPa] in two 1/3-octave bands with central frequencies of 63 Hz and 125 Hz and in the 20–20,000 Hz broadband in individual wind speed classes according to the Beaufort scale [°B] Survey campaign no. 2 (19.03.2023– –24.04.2023)* 321

Table 2.63. Survey station H_2. The statistical values of the sound pressure level values (SPL) [dB re 1 µPa] in two 1/3-octave bands with central frequencies of 63 Hz and 125 Hz and in the 20–20,000 Hz broadband in individual wind speed classes according to the Beaufort scale [°B] Survey session no. 2 (19.03.2023–24.04.2023)* 321

Table 2.64. Survey station H_3. The statistical values of the sound pressure level values (SPL) [dB re 1 µPa] in two 1/3-octave bands with central frequencies of 63 Hz and 125 Hz and in the 20–20,000 Hz broadband in individual wind speed classes according to the Beaufort scale [°B] Survey session no. 2 (19.03.2023–24.04.2023)* 322

Table 2.65. Survey station H_4. The statistical values of the sound pressure level values (SPL) [dB re 1 µPa] in two 1/3-octave bands with central frequencies of 63 Hz and 125 Hz and in the 20–20,000 Hz broadband in individual wind speed classes according to the Beaufort scale [°B] Survey session no. 2 (19.03.2023–24.04.2023)* 323

Table 2.66. Survey station H_1. The statistical values of the sound pressure level values (SPL) [dB re 1 µPa] in two 1/3-octave bands with central frequencies of 63 Hz and 125 Hz and in the 20–20,000 Hz broadband in individual wind speed classes according to the Beaufort scale [°B] Survey session no. 3 (24.04.2023–12.08.2023) 323

Table 2.67. Survey station H_3. The statistical values of the sound pressure level values (SPL) [dB re 1 µPa] in two 1/3-octave bands with central frequencies of 63 Hz and 125 Hz and in the 20–20,000 Hz broadband in individual wind speed classes according to the Beaufort scale [°B] Survey session no. 3 (30.04.2023–12.08.2023) 324

Table 2.68. Survey station H_4. The statistical values of the sound pressure level values (SPL) [dB re 1 µPa] in two 1/3-octave bands with central frequencies of 63 Hz and 125 Hz and in the 20–20,000 Hz broadband in individual wind speed classes according to the Beaufort scale [°B] Survey session no. 3 (24.04.2023–12.08.2023) 324

Table 2.69. Survey station H_1. The statistical values of the sound pressure level values (SPL) [dB re 1 µPa] in two 1/3-octave bands with central frequencies of 63 Hz and 125 Hz and in the 20–20,000 Hz broadband in individual wind speed classes according to the Beaufort scale [°B] Survey session no. 4 (13.08,2023–12.11.2023) 325

Table 2.70. Survey station H_3. The statistical values of the sound pressure level values (SPL) [dB re 1 µPa] in two 1/3-octave bands with central frequencies of 63 Hz and 125 Hz and in the 20–20,000 Hz broadband in individual wind speed classes according to the Beaufort scale [°B] Survey session no. 3 (12.08.2023–13.11.2023) 325

Table 2.71. Survey station H_4. The statistical values of the sound pressure level values (SPL) [dB re 1 µPa] in two 1/3-octave bands with central frequencies of 63 Hz and 125 Hz and in the 20–20,000 Hz broadband in individual wind speed classes according to the Beaufort scale [°B] Survey session no. 4 (13.08,2023–12.11.2023) 326

Table 2.72. Survey station H_1. The statistical values of the sound pressure level values (SPL) [dB re 1 µPa] in two 1/3-octave bands with central frequencies of 63 Hz and 125 Hz and in the 20–20,000 Hz broadband in individual wind speed classes according to the Beaufort scale [°B] Survey session no. 4 (12.11,2023–03.12.2023) 326

Table 2.73. Survey station H_2. The statistical values of the sound pressure level values (SPL) [dB re 1 µPa] in two 1/3-octave bands with central frequencies of 63 Hz and 125 Hz and in the 20–20,000 Hz broadband in individual wind speed classes according to the Beaufort scale [°B] Survey session no. 4 (12.11.2023–15.02.2024) 327

Table 2.74. Survey station H_3. The statistical values of the sound pressure level values (SPL) [dB re 1 µPa] in two 1/3-octave bands with central frequencies of 63 Hz and 125 Hz and in the 20–20,000 Hz

broadband in individual wind speed classes according to the Beaufort scale [°B] Survey session no. 4 (12.11.2023–15.02.2024)..... 327

Table 2.75. Survey station H_4. The statistical values of the sound pressure level values (SPL) [dB re 1 µPa] in two 1/3-octave bands with central frequencies of 63 Hz and 125 Hz and in the 20–20,000 Hz broadband in individual wind speed classes according to the Beaufort scale [°B] Survey session no. 4 (12.11,2023–03.12.2023)..... 328

Table 3.1. Coordinates of the transects along which the seabed inspection was conducted to establish the phytobenthos occurrence within the survey area..... 342

Table 3.2. List of activities conducted as part of phytobenthos surveys in the survey area..... 342

Table 3.3. Characteristics of the transects along which the seabed inspection was conducted to establish the phytobenthos occurrence in the survey area..... 343

Table 3.4. A compilation of examples of zoobenthos taxa sensitivity used to calculate index B*..... 347

Table 3.5. The limit values of index B used for the assessment of the ecological status of the soft-bottom zoobenthos..... 348

Table 3.6. The limit values of the TSP index used for the assessment of the quality status of the hard-bottom macrozoobenthos communities..... 348

Table 3.7. The list of fieldwork activities conducted as part of the macrozoobenthos surveys in the survey area in 2023 on soft bottom and hard bottom..... 349

Table 3.8. The list of activities conducted as part of the laboratory tests of macrozoobenthos sampled in the survey area in 2023..... 351

Table 3.9. The taxonomic composition in macrozoobenthos samples from the soft bottom in the survey area..... 351

Table 3.10. The constancy of macrozoobenthos taxa presence in the samples from the soft bottom in the survey area..... 353

Table 3.11. The taxonomic composition in two macrozoobenthos samples from the hard bottom in the survey area..... 358

Table 3.12. Compilation of the results of macrozoobenthos surveys in the survey area..... 362

Table 3.13. A compilation of the ichthyoplankton catches conducted in the survey area..... 381

Table 3.14. A compilation of pelagic trawl hauls conducted in the survey area..... 383

Table 3.15. A compilation of the catches with bottom-set gillnets conducted in the survey area..... 385

Table 3.16. A list of the catches with herring gillnets carried out as part of the herring concentration surveys within the survey area..... 390

Table 3.17. Frequency of larvae occurrence in the samples and the number of survey periods, in which they were found in the survey area..... 394

Table 3.18. Abundance of larvae [ind.·10 m^{-2}] of individual fish taxa at survey stations located in the survey area in winter..... 395

Table 3.19. Average larval length [mm SL] of individual fish taxa at survey stations located in the survey area in winter..... 396

Table 3.20. Abundance of larvae [ind.·10 m^{-2}] of individual fish taxa at survey stations located in the survey area in spring..... 396

Table 3.21. Average larval length [mm SL] of individual fish species at survey stations located in the survey area in spring..... 397

Table 3.22. Abundance of larvae [ind.·10 m^{-2}] of individual fish taxa at survey stations located in the survey area in summer..... 397

Table 3.23. Average larval length [mm SL] of individual fish species at survey stations located in the survey area in summer 398

Table 3.24. Abundance of larvae [ind.·10 m^{-2}] of individual fish taxa at survey stations located in the survey area in autumn 398

Table 3.25. Average larval length [mm SL] of individual fish species at survey stations located in the survey area in autumn 399

Table 3.26. The number of individuals caught [pcs], abundance [pcs/ind.·10 m^{-2}] (average for the entire survey area) and the average standard length [mm SL] of the larvae of individual taxa in the annual cycle for the survey area 403

Table 3.27. The acoustic parameters for the survey area 413

Table 3.28. The abundance proportions and average weights of the herring and the sprat determined based on the survey hauls carried out during four survey campaigns in the survey area 413

Table 3.29. The abundance, biomass and areal biomass density of pelagic fish determined using acoustic methods 414

Table 3.30. The weight of individual species of fish caught in bottom-set gillnet sets within the survey area during all survey campaigns 423

Table 3.31. The abundance of individual species of fish caught in bottom-set gillnet sets within the survey area during all survey campaigns 423

Table 3.32. The weight of individual species of fish caught in herring gillnets in the survey area during all survey campaigns 425

Table 3.33 Abundance of individual species of fish caught in herring gillnets in the survey area during all survey campaigns 426

Table 3.34. A comparison of daily herring catch rates and densities of piscivorous birds on seabird observation days in the survey area 427

Table 3.35. The areal biomass density of pelagic fish, determined using acoustic methods based on SPRAS and BIAS vessel passages conducted in the years 2017–2021 445

Table 3.36. All taxa recorded during the survey catches conducted within the survey area 445

Table 3.37. The coordinates of the survey stations for the passive acoustic monitoring of porpoises in the survey area 455

Table 3.38. The coordinates of observation transects during the monitoring of marine mammals from the plane in the survey area 458

Table 3.39. A summary of activities performed during the reporting period as part of acoustic monitoring of marine mammals in the survey area 463

Table 3.40. A summary of the observation flights performed within the reporting period 464

Table 3.41. A summary of acoustic data obtained from passive acoustic monitoring conducted in the survey area. Data have been divided into sets collected during five service vessel passages 466

Table 3.42. Data obtained during the passive acoustic monitoring conducted in the survey area 472

Table 3.43. A summary of harbour porpoise detections obtained during the acoustic monitoring in the OWF Baltica 1 survey area, between 3 December 2022 and 28 February 2024. Results are shown as days (DPD) and minutes (DPM) of porpoise positive detections, obtained with the use of the KERNO-F classifier and followed by a visual validation 485

Table 3.44. A summary of marine mammal observations recorded during the seabird survey vessel passages, in the survey area and the reference area 496

Table 3.45. The transect effective strip width (ESW) values for calculated for individual species and for the entire group of waterbirds staying in the survey area 513

Table 3.46. A list of dates of seabird observations in the survey area, including the names of people conducting the observations and the vessel used 516

Table 3.47. A list of dates of seabird observations in the reference area, including the names of people conducting the observations and the vessel used 520

Table 3.48. The abundance and proportion in the grouping of individual taxa of birds observed sitting on the water during successive survey campaigns within the survey area in the wintering period 523

Table 3.49. The abundance of seabirds found within the survey area during the wintering period, broken down by the method of their recording 524

Table 3.50. The abundance and proportion in the grouping of individual taxa of birds observed in flight during successive survey campaigns within the survey area in the wintering period 525

Table 3.51. The abundance and proportion in the grouping of individual bird taxa sitting on water observed during subsequent campaigns in the survey area during the spring migration period 526

Table 3.52. The abundance of seabirds found within the survey area during the spring migration period broken down by the method of their recording 527

Table 3.53. The abundance and proportion in the grouping of individual taxa of birds observed in flight during successive survey campaigns within the survey area in the spring migration period 527

Table 3.54 The abundance and proportion in the grouping of individual taxa of birds observed sitting on the water during successive survey campaigns within the survey area in the summer 529

Table 3.55. The abundance of seabirds recorded within the survey area during summer, broken down by the method of their recording 530

Table 3.56. The abundance and proportion in the grouping of individual taxa of birds observed in flight during successive survey campaigns within the survey area in the summer 530

Table 3.57. The abundance and proportion in the grouping of individual taxa of birds observed sitting on the water during successive survey campaigns within the survey area in the autumn migration period 532

Table 3.58. The abundance of seabirds found within the survey area during the autumn migration period, broken down by the method of their recording 532

Table 3.59. The abundance and proportion in the grouping of individual taxa of birds observed in flight during successive survey campaigns within the survey area in the autumn migration period 533

Table 3.60. The abundance and proportion in the grouping of individual taxa of birds observed sitting on the water during successive survey campaigns within the reference area in the wintering period 535

Table 3.61. The abundance of seabirds found within the reference area during the wintering period, broken down by the method of their recording 535

Table 3.62. The abundance and proportion in the grouping of individual taxa of birds observed in flight during successive survey campaigns within the reference area in the wintering period 536

Table 3.63. The abundance and proportion in the grouping of individual taxa of birds observed sitting on the water during successive survey campaigns within the reference area in the spring migration period..... 537

Table 3.64. The abundance of seabirds found within the reference area during the spring migration period broken down by the method of their recording 538

Table 3.65. The abundance and proportion in the grouping of individual taxa of birds observed in flight during successive survey campaigns within the reference area in the spring migration period 538

Table 3.66. The abundance and proportion in the grouping of individual taxa of birds observed sitting on the water during successive survey campaigns within the reference area in the summer 540

Table 3.67. The abundance of seabirds recorded within the reference area during summer, broken down by the method of their recording 540

Table 3.68. The abundance and proportion in the grouping of individual taxa of birds observed in flight during successive survey campaigns within the reference area in the summer 541

Table 3.69. The abundance and proportion in the grouping of individual taxa of birds observed sitting on the water during successive survey campaigns within the reference area in the autumn migration period..... 542

Table 3.70. The abundance of seabirds found within the reference area during the autumn migration period, broken down by the method of their recording 542

Table 3.71. The abundance and proportion in the grouping of individual taxa of birds observed in flight during successive survey campaigns within the reference area in the autumn migration period 543

Table 3.72. The abundance of individual bird species flying over the survey area at the heights specified and the proportion of flights in these zones 552

Table 3.73. The abundance of individual bird species flying over the reference area at the heights specified and the proportion of flights in these zones 555

Table 3.74. A list of seabird species present in the survey area, together with their conservation status and abundance indices [ind./10 km]. Species present in extremely low abundance were excluded 574

Table 3.75. A list of seabird species present in the reference area, together with their conservation status and abundance indices [ind./10 km]. Species present in extremely low abundance were excluded 575

Table 3.76. A list of seabird species with an elevated conservation status present in the areas surveyed, together with their conservation status and maximum abundance indices [ind./10 km]. Species present in extremely low abundance were excluded 576

Table 3.77. Average abundance of seabirds per survey campaign and their abundance indices [ind./10 km] within the survey area and in the reference area during the wintering period 578

Table 3.78. The average abundance of seabirds per survey campaign and their abundance indices [ind./10 km] within the survey area and in the reference area during the spring migration period 578

Table 3.79. The average abundance of seabirds per survey campaign and their abundance indices [10 ind./10 km] within the survey area and in the reference area during the summer 579

Table 3.80. The average abundance of seabirds per survey campaign and their abundance indices [ind./10 km] within the survey area and in the reference area during the autumn migration period 579

Table 3.81. Total survey effort at LP_01 station in December 2022, January and February 2023 603

Table 3.82. Total survey effort at LP_02 station in December 2022, January and February 2023 603

Table 3.83. Total survey effort at MB_01 station in March, April and May 2023 606

Table 3.84. Total survey effort at MB_02 station in March, April and May 2023 607

Table 3.85. Total survey effort at MB_01 station in July, August, September, October, November and December 2023 611

Table 3.86. Total survey effort at MB_02 station in July, August, September, October, November and December 2023 612

Table 3.87. The local (L) and migratory (M) taxa observed at survey station LP_01 in December 2022, and January and February 2023 615

Table 3.88. The local (L) and migratory (M) taxa observed at survey station LP_02 in December 2022, and January and February 2023 616

Table 3.89. The bird taxa observed at survey station MB_01 in the spring migration period 617

Table 3.90. The bird taxa observed at survey station MB_02 in the spring migration period 619

Table 3.91. The bird taxa observed at survey station MB_01 during the autumn migration surveys 621
Table 3.92. The total observations of bird taxa recorded at survey station MB_02 during the autumn migration surveys 623
Table 3.93. The effective sample width for long-tailed duck, common scoter, common chaffinch, white wagtail, and razorbill 629
Table 3.94. The migration fluxes of bird taxa in the survey area in subsequent months in the spring and autumn migration periods 629
Table 3.95. The migration fluxes of species groups in the survey area in subsequent months in the spring and autumn migration periods 650
Table 3.96. The flight altitude of birds observed at survey station LP_01 survey station in December 2022, and January and February 2023 654
Table 3.97. The flight altitude of birds observed at survey station LP_02 survey station in December 2022, and January and February 2023 655
Table 3.98. The flight altitude of birds observed at survey station MB_01 in the spring migration period 657
Table 3.99. The flight altitude of birds observed at survey station MB_02 in the spring migration period 660
Table 3.100. The flight altitude of birds observed at survey station MB_01 in the autumn migration period 663
Table 3.101. The flight altitude of birds observed at survey station MB_02 in the autumn migration period 665
Table 3.102. The total number of birdtracks recorded at two survey stations during the wintering period (December 2022, January, and February 2023) 668
Table 3.103. The number of tracks of species and bird categories recorded at survey station LP_01 during the wintering period (December 2022, January and February 2023) 668
Table 3.104. The flight directions of individual bird taxa recorded at survey station LP_02 in the entire survey period (December 2022, January and February 2023) 672
Table 3.105. The total number of all bird tracks recorded on the two survey stations during the spring migration period 676
Table 3.106. The number of tracks of individual bird taxa recorded at survey station MB_01 during the spring migration period 676
Table 3.107. The number of tracks of individual bird taxa recorded at survey station MB_02 during the spring migration period 682
Table 3.108. The total number of all bird tracks recorded at both survey stations during the autumn migration period 688
Table 3.109. The number of tracks of species and bird categories recorded at survey station MB_01 during the autumn migration period 688
Table 3.110. The number of tracks of species and bird categories recorded at survey station MB_02 during the autumn migration period 696
Table 3.111. The summary of bird calls recorded at daylight and night hours at survey station MB_01 during the spring migration period 726
Table 3.112. The summary of bird calls recorded at daylight and night hours at survey station MB_02 during the spring migration period 728
Table 3.113. The summary of bird calls recorded at daylight and night hours at survey station MB_01 during the autumn migration period 730
Table 3.114. The summary of bird calls recorded at daylight and night hours at survey station MB_02 during the autumn migration period 732

Table 3.115. The conservation status of migrating bird species observed and recorded during the local winter movement studies, and the spring and autumn surveys conducted from December 2022 to December 2023 739

Table 3.116. The coordinates of particular survey transect sections within the survey area 743

Table 3.117. The coordinates of the acoustic monitoring points in the survey area 743

Table 3.118. The boundaries of bat activity categories for individual taxa according to Kepel et al. (2013) 748

Table 3.119. A list of dates of bat survey vessel passages along the transects within the survey area including the names of people carrying out the observations and the vessel used 749

Table 3.120. A list of dates of bat survey vessel passages to the survey stations within the survey area including the names of people carrying out the observations and the vessel used 749

Table 3.121. A list of results of bat survey vessel passages at the acoustic monitoring point within the survey area including the bat species recorded and the level of the activity index for the survey night 752

Table 3.122. A list of activity indices obtained for the survey periods (01.04–31.05 – spring migration, 01.08–15.09 and 15.09–31.10 – autumn migration) during the bat survey vessel passages at the monitoring stations and along the survey transect*,** 753

LIST OF FIGURES

Figure 1.1. The locations of surface sediment sampling stations within the survey area 55

Figure 1.2. The locations of the survey stations for core sampling within the survey area 56

Figure 1.3. Bathymetric data processing flow chart 58

Figure 1.4. Sonar data processing flow chart 60

Figure 1.5. Magnetometer installation diagram, including distances between individual devices 61

Figure 1.6. Magnetometric data processing flow chart 62

Figure 1.7. Seismo-acoustic and single-channel seismic data processing flow chart 66

Figure 1.8. The distribution of offsets for the streamer and sparker 69

Figure 1.9. Multi-channel seismic data processing flow chart 71

Figure 1.10. The bathymetry of the survey area 76

Figure 1.11. The map of the seabed slopes in the survey area 77

Figure 1.12. The sonar mosaic of the survey area 78

Figure 1.13. The map of the residual field strength in the survey area together with the magnetic anomalies detected 79

Figure 1.14. The map of the residual geological signal in the survey area 81

Figure 1.15. The location of objects of man-made or unknown origin designated for ROV inspection within the survey area 83

Figure 1.16. An example of an object – ROV_149 (an air plane wreck); visible in the bathymetric data (MBES), in the sonar mosaic (SSS), and the data from an ROV inspection – an ROV inspection video still frame 84

Figure 1.17. An example of an object – ROV_155 (fishing nets); not visible in the bathymetric data (MBES), visible in the sonar mosaic (SSS) and the data from an ROV inspection – an ROV inspection video still frame 85

Figure 1.18. The seabed types in the survey area 97

Figure 1.19. A fragment of a bathymetric map; an undulating surface of the accumulation plain; visible signs of the seabed irregularities within the sand accumulations divided by depressions resulting from the periodical seabed surface washout, where mega-ripples can be seen in the MBES and SSS data 98

Figure 1.20. A fragment of a bathymetric map; an undulating surface of the accumulation plain; visible signs of sand extraction (depressions) 99

Figure 1.21. A fragment of a bathymetric map; an uneven surface of the abrasive-accumulative plain; visible single boulders and boulder clusters 99

Figure 1.22. The traces of icebergs in the survey area 101

Figure 1.23. An area with the seabed relief modified by the mining works conducted 102

Figure 1.24. The surface sediments in the survey area 103

Figure 1.25. A fragment of a sonar mosaic; an undulating surface of the accumulation plain; visible signs of the seabed irregularities within the sand accumulations divided by depressions resulting from the periodical seabed surface washout, within which mega-ripples can be seen in the MBES and SSS data 104

Figure 1.26. A fragment of a sonar mosaic; an undulating surface of the accumulation plain; visible signs of sand extraction (depressions) 104

Figure 1.27. A fragment of a sonar mosaic; an uneven surface of the abrasive-accumulative plain; visible single boulders and boulder clusters 105

Figure 1.28. The occurrence of ripple-marks and mega-ripples in the survey area 106

Figure 1.29. The distribution of boulders in the survey area 108

Figure 1.30. The top of unit IA [m BSB] – fine to medium sands, locally silty sands, with coarse sands and gravels (marine, fluvial, and fluvioglacial) in places 113

Figure 1.31. The top of unit IB [m BSB] – fine and medium sands, locally sands with gravel (lagoonal, fluvial, fluvioglacial) 114

Figure 1.32. The top of unit ID1 [m BSB] – clayey tills or silty tills, locally clays or silty clays with an admixture of sand and gravel fractions (subaquatic) 115

Figure 1.33. The top of unit ID2 [m BSB] – sands with gravel, gravels, tills (fluvioglacial and glacial) 116

Figure 1.34. The top of unit IF1 [m BSB] – sediments filling the valleys in the Silurian top 117

Figure 1.35. The top of unit IF2 [m BSB] – Silurian deposits 118

Figure 1.36. Geological cross-section along the survey line 21001_OWF_056_1 119

Figure 1.37. Geological cross-section along the survey line 21001_OWF_056_2 120

Figure 1.38. Geological cross-section along the survey line 21001_OWF_242_1 121

Figure 1.39. Geological cross-section along the survey line 21001_OWF_242_2 122

Figure 1.40. Geohazards in the survey area 124

Figure 2.1. The locations of survey stations for hydrological and meteorological monitoring including sea currents distributed within the survey area 128

Figure 2.2. The wind speed measured at survey station B_MFW_3 throughout a measurement period of one full year 140

Figure 2.3. A wind rose presenting the directional distribution of the wind velocities and directions measured at survey station B_MFW_3 throughout a measurement period of one full year 141

Figure 2.4. The air humidity measured at survey station B_MFW_3 throughout a measurement period of one full year 141

Figure 2.5. The air pressure measured at survey station B_MFW_3 throughout a measurement period of one full year 142

Figure 2.6. The air humidity measured at survey station B_MFW_3 throughout a measurement period of one full year 142

Figure 2.7. The maximum wave heights H_{max}, significant wave heights H_{m0}, and mean wave heights H_{mean} measured at survey station B_MFW_1 throughout a measurement period of one full year ... 144

Figure 2.8. The maximum wave heights Hmax, significant wave heights Hm0, and mean wave heights H_{mean} measured at survey station B_MFW_2 throughout a measurement period of one full year ... 145

Figure 2.9. The maximum wave heights H_{max}, significant wave heights H_{m0}, and mean wave heights H_{mean} measured at survey station B_MFW_3 throughout a measurement period of one full year ... 145

Figure 2.10. The maximum wave heights H_{max}, significant wave heights H_{m0}, and mean wave heights H_{mean} measured at survey station B_MFW_4 throughout a measurement period of one full year ... 146

Figure 2.11. The maximum wave heights H_{max}, significant wave heights H_{m0}, and mean wave heights H_{mean} measured at survey station B_MFW_4 throughout a measurement period of one full year ... 146

Figure 2.12. The peak wave periods T_p and mean wave periods T_{mean} measured at survey station B_MFW_1 throughout a measurement period of one full year 147

Figure 2.13. The peak wave periods Tp and mean wave periods T_{mean} measured at survey station B_MFW_2 throughout a measurement period of one full year 147

Figure 2.14. The peak wave periods Tp and mean wave periods T_{mean} measured at survey station B_MFW_3 throughout a measurement period of one full year 148

Figure 2.15. The peak wave periods Tp and mean wave periods T_{mean} measured at survey station B_MFW_4 throughout a measurement period of one full year 148

Figure 2.16. The peak wave periods Tp and mean wave periods T_{mean} measured at survey station B_MFW_5 throughout a measurement period of one full year 149

Figure 2.17. The wave rose diagram for the values measured at survey station B_MFW_1 throughout a measurement period of one full year 149

Figure 2.18. The wave rose diagram for the values measured at survey station B_MFW_2 throughout a measurement period of one full year 150

Figure 2.19. The wave rose diagram for the values measured at survey station B_MFW_3 throughout a measurement period of one full year 150

Figure 2.20. The wave rose diagram for the values measured at survey station B_MFW_4 throughout a measurement period of one full year 151

Figure 2.21. The wave rose diagram for the values measured at survey station B_MFW_5 throughout a measurement period of one full year 151

Figure 2.22. Changes in the sea depth (thickness of the water column) recorded at survey station B_MFW_1 throughout a measurement period of one full year 152

Figure 2.23. Changes in the sea depth (thickness of the water column) recorded at survey station B_MFW_2 throughout a measurement period of one full year 152

Figure 2.24. Changes in the sea depth (thickness of the water column) recorded at survey station B_MFW_3 throughout a measurement period of one full year 153

Figure 2.25. Changes in the sea depth (thickness of the water column) recorded at survey station B_MFW_4 throughout a measurement period of one full year 153

Figure 2.26. Changes in the sea depth (thickness of the water column) recorded at survey station B_MFW_5 throughout a measurement period of one full year 154

Figure 2.27. The water flow velocities measured at survey station B_MFW_1 throughout a measurement period of one full year 156

Figure 2.28. The water flow velocities measured at survey point B_MFW_2 throughout a measurement period of one full year 157

Figure 2.29. The water flow velocities measured at survey point B_MFW_3 throughout a measurement period of one full year 157

Figure 2.30. The water flow velocities measured at survey point B_MFW_4 throughout a measurement period of one full year 158

Figure 2.31. The water flow velocities measured at survey point B_MFW_5 throughout a measurement period of one full year 158

Figure 2.32. The directional distributions of the water flow velocities measured at survey station B_MFW_1 in the layer from the free sea surface to the depth of 4 m throughout a measurement period of one full year 159

Figure 2.33. The directional distributions of the water flow velocities measured at survey station B_MFW_1 in the layer from the depth of 16 m to the depth of 20 m below the sea surface throughout a measurement period of one full year 159

Figure 2.34. The directional distributions of the water flow velocities measured at survey station B_MFW_1 in the layer from the depth of 32 m to the seabed 160

Figure 2.35. The directional distributions of the water flow velocities measured at survey station B_MFW_2 in the layer from the free sea surface to the depth of 4 m throughout a measurement period of one full year 160

Figure 2.36. The directional distributions of the water flow velocities measured at survey station B_MFW_2 in the layer from the depth of 16 m to the depth of 20 m below the sea surface throughout a measurement period of one full year 161

Figure 2.37. The directional distributions of the water flow velocities measured at survey station B_MFW_2 in the layer from the depth of 44 m to the seabed 161

Figure 2.38. The directional distributions of the water flow velocities measured at survey station B_MFW_3 in the layer from the free sea surface to the depth of 4 m throughout a measurement period of one full year 162

Figure 2.39. The directional distributions of the water flow velocities measured at survey station B_MFW_3 in the layer from the depth of 16 m to the depth of 20 m below the sea surface throughout a measurement period of one full year 162

Figure 2.40. The directional distributions of the water flow velocities measured at survey station B_MFW_3 in the layer from the depth of 32 m to the seabed throughout a measurement period of one full year 163

Figure 2.41. The directional distributions of the water flow velocities measured at survey station B_MFW_4 in the layer from the free sea surface to the depth of 4 m throughout a measurement period of one full year 163

Figure 2.42. The directional distributions of the water flow velocities measured at survey station B_MFW_4 in the layer from the depth of 8 m to the depth of 12 m below the sea surface throughout a measurement period of one full year 164

Figure 2.43. The directional distributions of the water flow velocities measured at survey station B_MFW_4 in the layer from the depth of 16 m to the seabed throughout a measurement period of one full year 164

Figure 2.44. The directional distributions of the water flow velocities measured at survey station B_MFW_5 in the layer from the free sea surface to the depth of 4 m throughout a measurement period of one full year 165

Figure 2.45. The directional distributions of the water flow velocities measured at survey station B_MFW_5 in the layer from the depth of 16 m to the depth of 20 m below the sea surface throughout a measurement period of one full year 165

Figure 2.46. The directional distributions of the water flow velocities measured at survey station B_MFW_5 in the layer from the depth of 40 m to the seabed 166

Figure 2.47. The water turbidity measured at survey station B_MFW_1 throughout the entire measurement period..... 167

Figure 2.48. The water turbidity measured at survey station B_MFW_3 throughout the entire measurement period..... 167

Figure 2.49. The water turbidity measured at survey station B_MFW_5 throughout the entire measurement period..... 168

Figure 2.50. The electrical conductivity of water measured at survey station B_MFW_1 throughout the entire measurement period 169

Figure 2.51. The electrical conductivity of water measured at survey station B_MFW_3 throughout the entire measurement period 169

Figure 2.52. The electrical conductivity of water measured at survey station B_MFW_5 throughout the entire measurement period 170

Figure 2.53. The water salinity calculated for survey station B_MFW_1 for the entire measurement period 171

Figure 2.54. The water salinity calculated for survey station B_MFW_3 for the entire measurement period 171

Figure 2.55. The water salinity calculated for survey station B_MFW_5 for the entire measurement period 172

Figure 2.56. The water turbidity measured at survey point B_MFW_1 for the entire measurement period 173

Figure 2.57. The water turbidity measured at survey point B_MFW_3 for the entire measurement period 173

Figure 2.58. The water turbidity measured at survey point B_MFW_5 for the entire measurement period 174

Figure 2.59. The mean water temperature values measured in the survey area during individual water sampling campaigns conducted from January to November 2023 175

Figure 2.60. The mean values of electrical conductivity of water measured in the survey area during individual water sampling campaigns from January to November 2023 176

Figure 2.61. The mean values of water salinity calculated for the survey area during individual water sampling campaigns from January to November 2023..... 177

Figure 2.62. The mean values of water turbidity measured in the survey area during individual water sampling campaigns in the period from January to November 2023 178

Figure 2.63. The mean values of water depth measured in the survey area during individual water sampling campaigns in the period from January to November 2023 179

Figure 2.64. The location of the survey stations for water sampling within the survey area 186

Figure 2.65. The mean concentration of suspended solids in the near-surface and near-seabed layers tested under individual survey campaigns 229

Figure 2.66. The mean concentration of dissolved oxygen in the near-surface and near-seabed layers of water from the survey area under individual survey campaigns..... 230

Figure 2.67. The diversification of the average dissolved oxygen concentration with depth from the six profiles surveyed in the survey area under individual survey campaigns 231

Figure 2.68. The mean concentration of TOC in the near-surface and near-seabed water layers from the survey area under individual survey campaigns..... 232

Figure 2.69. The diversification of the TOC concentrations with depth in the six profiles surveyed in the survey area under individual survey campaigns 233

Figure 2.70. The mean pH value in the near-surface and near-seabed layer of water in the survey area in individual survey campaigns 234

Figure 2.71. The mean pH value changing alongside the depth in the six profiles surveyed in the survey area under individual survey campaigns 235

Figure 2.72. The mean alkalinity value in the near-surface and near-seabed layer of water in the survey area during the individual survey campaigns 236

Figure 2.73. The diversification of the mean alkalinity value with depth in the six profiles surveyed in the survey area under individual survey campaigns 236

Figure 2.74. The mean nitrate nitrogen concentration values in the near-surface and near-seabed layers from the survey area under individual survey campaigns 238

Figure 2.75. The diversification of the average nitrate nitrogen concentration value with depth in the six profiles surveyed in the survey area under individual survey campaigns 239

Figure 2.76. The mean values of the mineral nitrogen concentrations (DIN) in the near-surface and near-seabed water in the survey area in individual survey campaigns 240

Figure 2.77. The diversification of the mean mineral nitrogen concentration (DIN) value with depth in the six profiles surveyed in the survey area under individual survey campaigns 241

Figure 2.78. The mean total nitrogen concentration values in the near-surface and near-seabed layer of water in the survey area under individual survey campaigns 242

Figure 2.79. The diversification of the mean total nitrogen concentration value with depth in the six profiles surveyed in the survey area under individual survey campaigns 242

Figure 2.80. The mean total phosphorus concentration values in the surface and near-seabed layer of water in the survey area under individual survey campaigns 244

Figure 2.81. The diversification of the mean phosphate phosphorus concentration value with depth in the six profiles surveyed in the survey area under individual survey campaigns 245

Figure 2.82. The mean total phosphorus concentration values in the surface and near-seabed layer of water in the survey area under individual survey campaigns 246

Figure 2.83. The diversification of the mean total phosphorus concentration value with depth in the six profiles surveyed in the survey area under individual survey campaigns 246

Figure 2.84. The change of the mean concentration values of PAHs in the water sampled in the survey area in August 2023 250

Figure 2.85. The location of the survey stations for core sampling within the survey area 255

Figure 2.86. The proportion of metal labile forms (lab.) and forms permanently bound with the sediment (perm.) in the survey area 268

Figure 2.87. The survey area against the background of a fragment of the map of surface sediments [Source: internal materials based on Kramarska, 1995b] 276

Figure 2.88. The survey area against the background of a fragment of the map of “Deposits and prospective areas of aggregate resources” [Source: internal materials based on Kramarska et al., 2005] .. 277

Figure 2.89. The extent and thickness of the potential aggregate deposit (with a thickness > 2 m) located in the survey area 279

Figure 2.90. A geological cross-section along survey line 21001_OWF_083; the survey area 280

Figure 2.91. A geological cross-section along survey line 21001_OWF_202_1; the survey area 281

Figure 2.92. A geological cross-section along survey line 21001_OWF_202_2; the survey area 282

Figure 2.93. A geological cross-section along survey line 21001_OWF_X35; the survey area 283

Figure 2.94. A geological cross-section along survey line 21001_OWF_X18; the survey area 284

Figure 2.95. The deployment locations of the SM4M noise recorders in the survey area 288

Figure 2.96. Noise recorder SM4M Submersible (Wildlife Acoustics, USA) with a single HTI-96 hydrophone (on the left) and the measuring instrument deployment scheme (on the right) 289

Figure 2.97. The vertical profiles of temperature T [°C], salinity S [PSU], and sound velocity c [$m \cdot s^{-1}$] recorded at survey station H_1 on 3 December 2022 (dashed blue curves), 7 February 2023, 24 April 2023, 13 August 2023, 12 November 2023 (respectively, solid black, blue, red, and yellow curves) and 27 February 2024 (dashed black curves) 294

Figure 2.98. The vertical profiles of temperature T [°C], salinity S [PSU], and sound velocity c [$m \cdot s^{-1}$] recorded at survey station H_2 on 3 December 2022 (dashed blue curves), 15 February 2023, 29 April 2023, 12 August 2023, 12 November 2023 (respectively, solid black, blue, red, and yellow curves) and 2 March 2024 (dashed black curves) 295

Figure 2.99. The vertical profiles of temperature T [°C], salinity S [PSU], and sound velocity c [$m \cdot s^{-1}$] recorded at survey station H_3 on 15 February 2022 (dashed blue curves), 30 April 2023, 12 August 2023, 13 November 2023 (respectively, solid black, blue, red, and yellow curves) and 26 February 2024 (dashed black curves) 295

Figure 2.100. The vertical profiles of temperature T [°C], salinity S [PSU], and sound velocity c [$m \cdot s^{-1}$] recorded at survey station H_4 on 3 December 2022 (dashed blue curves), 7 February 2023, 24 April 2023, 12 August 2023, 12 November 2023 (respectively, solid black, blue, red, and yellow curves) and 27 February 2024 (dashed black curves) 296

Figure 2.101. A sample time series of ambient noise signals with a time duration of 1 min. (left) and its PSD levels [dB re 1 $\mu Pa^2 \cdot H^{-1}$] (right) 297

Figure 2.102. The low frequency "cutoff" phenomenon in shallow waters. The vertical axis Y – the "cutoff" frequency [Hz]; the horizontal axis X – sea depth [m] 297

Figure 2.103. Survey station H_1. The statistical distribution of the averaged power spectral density (PSD) [dB re 1 $\mu Pa2 \cdot Hz^{-1}$] values of the ambient noise in 1/3-octave bands. The central frequencies F_{centr} of individual bands are marked on the horizontal axis 299

Figure 2.104. Survey station H_2. The statistical distribution of the averaged power spectral density (PSD) [dB re 1 $\mu Pa2 \cdot Hz^{-1}$] values of the ambient noise in 1/3-octave bands. The central frequencies F_{centr} of individual bands are marked on the horizontal axis 300

Figure 2.105. Survey station H_3. The statistical distribution of the averaged power spectral density (PSD) [dB re 1 $\mu Pa2 \cdot Hz^{-1}$] values of the ambient noise in 1/3-octave bands. The central frequencies F_{centr} of individual bands are marked on the horizontal axis 301

Figure 2.106. Survey station H_4. The statistical distribution of the averaged power spectral density (PSD) [dB re 1 $\mu Pa2 \cdot Hz^{-1}$] values of the ambient noise in 1/3-octave bands. The central frequencies F_{centr} of individual bands are marked on the horizontal axis 302

Figure 2.107. Survey station H_1. The mean values of the power spectrum density levels of the ambient noise in 1/3-octave bands $PSD_{1/3\ oct}$ [dB re 1 $\mu Pa^2 \cdot Hz^{-1}$] calculated for individual percentiles 304

Figure 2.108. Survey station H_2. The mean values of the power spectrum density levels of the ambient noise in 1/3-octave bands $PSD_{1/3\ oct}$ [dB re 1 $\mu Pa^2 \cdot Hz^{-1}$] calculated for individual percentiles 305

Figure 2.109. Survey station H_3. The mean values of the power spectrum density levels of the ambient noise in 1/3-octave bands $PSD_{1/3\ oct}$ [dB re 1 $\mu Pa^2 \cdot Hz^{-1}$] calculated for individual percentiles 306

Figure 2.110. Survey station H_4. The mean values of the power spectrum density levels of the ambient noise in 1/3-octave bands $PSD_{1/3\ oct}$ [dB re 1 $\mu Pa^2 \cdot Hz^{-1}$] calculated for individual percentiles 307

Figure 2.111. Survey station H_1. The time series of the sound pressure level SPL [dB re 1 µPa] in 1/3-octave bands of 63 Hz and 125 Hz (black and blue curves, respectively) and the 20–20 000 Hz broadband (red curve) – upper panel. The histograms of the sound pressure levels $SPL_{63\ Hz}$, $SPL_{125\ Hz}$ and $SPL_{20–20\ 000\ Hz}$ – bottom panel. Red line – the mean SPL value, green line – the median SPL value, blue line – the mode SPL value. Survey session no. 1 (03.12.2022–07.02.2023) 310

Figure 2.112. Survey station H_4. The time series of the sound pressure level SPL [dB re 1 µPa] in 1/3-octave bands of 63 Hz and 125 Hz (black and blue curves, respectively) and the 20–20 000 Hz broadband (red curve) – upper panel. The histograms of the sound pressure levels $SPL_{63\ Hz}$, $SPL_{125\ Hz}$, and $SPL_{20–20\ 000\ Hz}$ – bottom panel. Red line – the mean SPL value, green line – the median SPL value, blue line – the mode SPL value. Survey session no. 1 (03.12.2022–07.02.2023) 311

Figure 2.113. Survey station H_1. The time series of the sound pressure level SPL [dB re 1 µPa] in 1/3-octave bands of 63 Hz and 125 Hz (black and blue curves, respectively) and the 20–20 000 Hz broadband (red curve) – upper panel. The histograms of the sound pressure levels $SPL_{63\ Hz}$, $SPL_{125\ Hz}$ and $SPL_{20–20\ 000\ Hz}$ – bottom panel. Red line – the mean SPL value, green line – the median SPL value, blue line – the mode SPL value. Survey session no. 2 (07.02.2023–24.04.2023) 311

Figure 2.114. Survey station H_2. The time series of the sound pressure level SPL [dB re 1 µPa] in 1/3-octave bands of 63 Hz and 125 Hz (black and blue curves, respectively) and the 20–20 000 Hz broadband (red curve) – upper panel. The histograms of the sound pressure levels $SPL_{63\ Hz}$, $SPL_{125\ Hz}$ and $SPL_{20–20\ 000\ Hz}$ – bottom panel. Red line – the mean SPL value, green line – the median SPL value, blue line – the mode SPL value. Survey session no. 2 (16.02.2023–29.04.2023) 312

Figure 2.115. Survey station H_3. The time series of the sound pressure level SPL [dB re 1 µPa] in 1/3-octave bands of 63 Hz and 125 Hz (black and blue curves, respectively) and the 20–20 000 Hz broadband (red curve) – upper panel. The histograms of the sound pressure levels $SPL_{63\ Hz}$, $SPL_{125\ Hz}$ and $SPL_{20–20\ 000\ Hz}$ – bottom panel. Red line – the mean SPL value, green line – the median SPL value, blue line – the mode SPL value. Survey session no. 2 (15.02.2023–30.04.2023) 312

Figure 2.116. Survey station H_4. The time series of the sound pressure level SPL [dB re 1 µPa] in 1/3-octave bands of 63 Hz and 125 Hz (black and blue curves, respectively) and the 20–20 000 Hz broadband (red curve) – upper panel. The histograms of the sound pressure levels $SPL_{63\ Hz}$, $SPL_{125\ Hz}$ and $SPL_{20–20\ 000\ Hz}$ – bottom panel. Red line – the mean SPL value, green line – the median SPL value, blue line – the mode SPL value. Survey session no. 2 (07.02.2023–24.04.2023) 313

Figure 2.117. Survey station H_1. The time series of the sound pressure level SPL [dB re 1 µPa] in 1/3-octave bands of 63 Hz and 125 Hz (black and blue curves, respectively) and the 20–20 000 Hz broadband (red curve) – upper panel. The histograms of the sound pressure levels $SPL_{63\ Hz}$, $SPL_{125\ Hz}$ and $SPL_{20–20\ 000\ Hz}$ – bottom panel. Red line – the mean SPL value, green line – the median SPL value, blue line – the mode SPL value. Survey session no. 3 (24.04.2023–13.08.2023) 313

Figure 2.118. Survey station H_3. The time series of the sound pressure level SPL [dB re 1 µPa] in 1/3-octave bands of 63 Hz and 125 Hz (black and blue curves, respectively) and the 20–20 000 Hz broadband (red curve) – upper panel. The histograms of the sound pressure levels $SPL_{63\ Hz}$, $SPL_{125\ Hz}$ and $SPL_{20–20\ 000\ Hz}$ – bottom panel. Red line – the mean SPL value, green line – the median SPL value, blue line – the mode SPL value. Survey session no. 3 (30.04.2023–12.08.2023) 314

Figure 2.119. Survey station H_4. The time series of the sound pressure level SPL [dB re 1 µPa] in 1/3-octave bands of 63 Hz and 125 Hz (black and blue curves, respectively) and the 20–20 000 Hz broadband (red curve) – upper panel. The histograms of the sound pressure levels $SPL_{63\ Hz}$, $SPL_{125\ Hz}$ and $SPL_{20–20\ 000\ Hz}$ – bottom panel. Red line – the mean SPL value, green line – the median SPL value, blue line – the mode SPL value. Survey session no. 3 (24.04.2-23–13.08.2023) 314

Figure 2.120. Survey station H_1. The time series of the sound pressure level SPL [dB re 1 µPa] in 1/3-octave bands of 63 Hz and 125 Hz (black and blue curves, respectively) and the 20–20 000 Hz broadband (red curve) – upper panel. The histograms of the sound pressure levels $SPL_{63\ Hz}$, $SPL_{125\ Hz}$ and $SPL_{20–20\ 000\ Hz}$ – bottom panel. Red line – the mean SPL value, green line – the median SPL value, blue line – the mode SPL value. Survey session no. 4 (13.08.2023–12.11.2023) 315

Figure 2.121. Survey station H_3. The time series of the sound pressure level SPL [dB re 1 µPa] in 1/3-octave bands of 63 Hz and 125 Hz (black and blue curves, respectively) and the 20–20 000 Hz broadband (red curve) – upper panel. The histograms of the sound pressure levels $SPL_{63\ Hz}$, $SPL_{125\ Hz}$ and $SPL_{20–20\ 000\ Hz}$ – bottom panel. Red line – the mean SPL value, green line – the median SPL value, blue line – the mode SPL value. Survey session no. 4 (12.08.2023–13.11.2023) 315

Figure 2.122. Survey station H_4. The time series of the sound pressure level SPL [dB re 1 µPa] in 1/3-octave bands of 63 Hz and 125 Hz (black and blue curves, respectively) and the 20–20 000 Hz broadband

(red curve) – upper panel. The histograms of the sound pressure levels $SPL_{63\ Hz}$, $SPL_{125\ Hz}$ and $SPL_{20–20\ 000\ Hz}$ – bottom panel. Red line – the mean SPL value, green line – the median SPL value, blue line – the mode SPL value. Survey session no. 4 (13.08.2023–12.11.2023) 316

Figure 2.123. Survey station H_1. The time series of the sound pressure level SPL [dB re 1 µPa] in 1/3-octave bands of 63 Hz and 125 Hz (black and blue curves, respectively) and the 20–20 000 Hz broadband (red curve) – upper panel. The histograms of the sound pressure levels $SPL_{63\ Hz}$, $SPL_{125\ Hz}$ and $SPL_{20–20\ 000\ Hz}$ – bottom panel. Red line – the mean SPL value, green line – the median SPL value, blue line – the mode SPL value. Survey session no. 5 (12.11.2023–03.12.2023) 316

Figure 2.124. Survey station H_2. The time series of the sound pressure level SPL [dB re 1 µPa] in 1/3-octave bands of 63 Hz and 125 Hz (black and blue curves, respectively) and the 20–20 000 Hz broadband (red curve) – upper panel. The histograms of the sound pressure levels $SPL_{63\ Hz}$, $SPL_{125\ Hz}$ and $SPL_{20–20\ 000\ Hz}$ – bottom panel. Red line – the mean SPL value, green line – the median SPL value, blue line – the mode SPL value. Survey session no. 5 (12.11.2023–15.02.2024) 317

Figure 2.125. Survey station H_3. The time series of the sound pressure level SPL [dB re 1 µPa] in 1/3-octave bands of 63 Hz and 125 Hz (black and blue curves, respectively) and the 20–20 000 Hz broadband (red curve) – upper panel. The histograms of the sound pressure levels $SPL_{63\ Hz}$, $SPL_{125\ Hz}$ and $SPL_{20–20\ 000\ Hz}$ – bottom panel. Red line – the mean SPL value, green line – the median SPL value, blue line – the mode SPL value. Survey session no. 5 (12.11.2023–15.02.2024) 317

Figure 2.126. Survey station H_4. The time series of the sound pressure level SPL [dB re 1 µPa] in 1/3-octave bands of 63 Hz and 125 Hz (black and blue curves, respectively) and the 20–20 000 Hz broadband (red curve) – upper panel. The histograms of the sound pressure levels $SPL_{63\ Hz}$, $SPL_{125\ Hz}$ and $SPL_{20–20\ 000\ Hz}$ – bottom panel. Red line – the mean SPL value, green line – the median SPL value, blue line – the mode SPL value. Survey session no. 5 (12.11.2023–03.12.2023) 318

Figure 2.127. Survey station H_1. The time series of the sound pressure levels (SPL) [dB re 1 µPa] in 1/3-octave bands of 63 Hz and 125 Hz (black and blue curves, respectively) and in the 20–20,000 Hz broadband (red curve) – upper panel. The time series of wind velocity V [$m \cdot s^{-1}$] – middle panel. The dependence of sound pressure levels $SPL_{63\ Hz}$, $SPL_{125\ Hz}$, and $SPL_{20–20\ 000\ Hz}$ on the wind velocity – bottom panel. Survey session no. 1 (03.12.2022–07.02.2023) 329

Figure 2.128. Survey station H_4. The time series of the sound pressure levels (SPL) [dB re 1 µPa] in 1/3-octave bands of 63 Hz and 125 Hz (black and blue curves, respectively) and in the 20–20,000 Hz broadband (red curve) – upper panel. The time series of wind velocity V [$m \cdot s^{-1}$] – middle panel. The dependence of sound pressure levels $SPL_{63\ Hz}$, $SPL_{125\ Hz}$, and $SPL_{20–20\ 000\ Hz}$ on the wind velocity – bottom panel. Survey session no. 1 (03.12.2022–07.02.2023) 329

Figure 2.129. Survey station H_1. The time series of the sound pressure levels (SPL) [dB re 1 µPa] in 1/3-octave bands of 63 Hz and 125 Hz (black and blue curves, respectively) and in the 20–20,000 Hz broadband (red curve) – upper panel. The time series of wind velocity V [$m \cdot s^{-1}$] – middle panel. The dependence of sound pressure levels $SPL_{63\ Hz}$, $SPL_{125\ Hz}$, and $SPL_{20–20\ 000\ Hz}$ on the wind velocity – bottom panel. Survey session no. 2 (19.03.2023–24.04.2023) 330

Figure 2.130. Survey station H_2. The time series of the sound pressure levels (SPL) [dB re 1 µPa] in 1/3-octave bands of 63 Hz and 125 Hz (black and blue curves, respectively) and in the 20–20,000 Hz broadband (red curve) – upper panel. The time series of wind velocity V [$m \cdot s^{-1}$] – middle panel. The dependence of sound pressure levels $SPL_{63\ Hz}$, $SPL_{125\ Hz}$, and $SPL_{20–20\ 000\ Hz}$ on the wind velocity – bottom panel. Survey session no. 2 (19.03.2023–29.04.2023) 330

Figure 2.131. Survey station H_3. The time series of the sound pressure levels (SPL) [dB re 1 µPa] in 1/3-octave bands of 63 Hz and 125 Hz (black and blue curves, respectively) and in the 20–20,000 Hz broadband (red curve) – upper panel. The time series of wind velocity V [$m \cdot s^{-1}$] – middle panel. The dependence of sound pressure levels $SPL_{63\ Hz}$, $SPL_{125\ Hz}$, and $SPL_{20–20\ 000\ Hz}$ on the wind velocity – bottom panel. Survey session no. 2 (19.03.2023–30.04.2023) 331

Figure 2.132. Survey station H_4. The time series of the sound pressure levels (SPL) [dB re 1 µPa] in 1/3-octave bands of 63 Hz and 125 Hz (black and blue curves, respectively) and in the 20–20,000 Hz broadband (red curve) – upper panel. The time series of wind velocity V [$m \cdot s^{-1}$] – middle panel.

The dependence of sound pressure levels $SPL_{63\ Hz}$, $SPL_{125\ Hz}$, and $SPL_{20–20\,000\ Hz}$ on the wind velocity – bottom panel. Survey session no. 2 (19.03.2023–24.04.2023) 331

Figure 2.133. Survey station H_1. The time series of the sound pressure levels (SPL) [dB re 1 µPa] in 1/3-octave bands of 63 Hz and 125 Hz (black and blue curves, respectively) and in the 20–20,000 Hz broadband (red curve) – upper panel. The time series of wind velocity V [$m \cdot s^{-1}$] – middle panel. The dependence of sound pressure levels $SPL_{63\ Hz}$, $SPL_{125\ Hz}$, and $SPL_{20–20\,000\ Hz}$ on the wind velocity – bottom panel. Survey session no. 3 (24.04.2023–12.08.2023) 332

Figure 2.134. Survey station H_3. The time series of the sound pressure levels (SPL) [dB re 1 µPa] in 1/3-octave bands of 63 Hz and 125 Hz (black and blue curves, respectively) and in the 20–20,000 Hz broadband (red curve) – upper panel. The time series of wind velocity V [$m \cdot s^{-1}$] – middle panel. The dependence of sound pressure levels $SPL_{63\ Hz}$, $SPL_{125\ Hz}$, and $SPL_{20–20\,000\ Hz}$ on the wind velocity – bottom panel. Survey session no. 3 (30.04.2023–12.08.2023) 332

Figure 2.135. Survey station H_4. The time series of the sound pressure levels (SPL) [dB re 1 µPa] in 1/3-octave bands of 63 Hz and 125 Hz (black and blue curves, respectively) and in the 20–20,000 Hz broadband (red curve) – upper panel. The time series of wind velocity V [$m \cdot s^{-1}$] – middle panel. The dependence of sound pressure levels $SPL_{63\ Hz}$, $SPL_{125\ Hz}$, and $SPL_{20–20\,000\ Hz}$ on the wind velocity – bottom panel. Survey session no. 3 (24.04.2023–12.08.2023) 333

Figure 2.136. Survey station H_1. The time series of the sound pressure levels (SPL) [dB re 1 µPa] in 1/3-octave bands of 63 Hz and 125 Hz (black and blue curves, respectively) and in the 20–20,000 Hz broadband (red curve) – upper panel. The time series of wind velocity V [$m \cdot s^{-1}$] – middle panel. The dependence of sound pressure levels $SPL_{63\ Hz}$, $SPL_{125\ Hz}$, and $SPL_{20–20\,000\ Hz}$ on the wind velocity – bottom panel. Survey session no. 4 (13.08.2023–12.11.2023) 333

Figure 2.137. Survey station H_3. The time series of the sound pressure levels (SPL) [dB re 1 µPa] in 1/3-octave bands of 63 Hz and 125 Hz (black and blue curves, respectively) and in the 20–20,000 Hz broadband (red curve) – upper panel. The time series of wind velocity V [$m \cdot s^{-1}$] – middle panel. The dependence of sound pressure levels $SPL_{63\ Hz}$, $SPL_{125\ Hz}$, and $SPL_{20–20\,000\ Hz}$ on the wind velocity – bottom panel. Survey session no. 4 (12.08.2023–13.11.2023) 334

Figure 2.138. Survey station H_4. The time series of the sound pressure levels (SPL) [dB re 1 µPa] in 1/3-octave bands of 63 Hz and 125 Hz (black and blue curves, respectively) and in the 20–20,000 Hz broadband (red curve) – upper panel. The time series of wind velocity V [$m \cdot s^{-1}$] – middle panel. The dependence of sound pressure levels $SPL_{63\ Hz}$, $SPL_{125\ Hz}$, and $SPL_{20–20\,000\ Hz}$ on the wind velocity – bottom panel. Survey session no. 4 (13.08.2023–12.11.2023) 334

Figure 2.139. Survey station H_1 The time series of the sound pressure levels (SPL) [dB re 1 µPa] in 1/3-octave bands of 63 Hz and 125 Hz (black and blue curves, respectively) and in the 20–20,000 Hz broadband (red curve) – upper panel. The time series of wind velocity V [$m \cdot s^{-1}$] – middle panel. The dependence of sound pressure levels $SPL_{63\ Hz}$, $SPL_{125\ Hz}$, and $SPL_{20–20\,000\ Hz}$ on the wind velocity – bottom panel. Survey session no. 5 (12.11.2023–03.12.2023) 335

Figure 2.140. Survey station H_2. The time series of the sound pressure levels (SPL) [dB re 1 µPa] in 1/3-octave bands of 63 Hz and 125 Hz (black and blue curves, respectively) and in the 20–20,000 Hz broadband (red curve) – upper panel. The time series of wind velocity V [$m \cdot s^{-1}$] – middle panel. The dependence of sound pressure levels $SPL_{63\ Hz}$, $SPL_{125\ Hz}$, and $SPL_{20–20\,000\ Hz}$ on the wind velocity – bottom panel. Survey session no. 5 (12.11.2023–15.02.2024) 335

Figure 2.141. Survey station H_3. The time series of the sound pressure levels (SPL) [dB re 1 µPa] in 1/3-octave bands of 63 Hz and 125 Hz (black and blue curves, respectively) and in the 20–20,000 Hz broadband (red curve) – upper panel. The time series of wind velocity V [$m \cdot s^{-1}$] – middle panel. The dependence of sound pressure levels $SPL_{63\ Hz}$, $SPL_{125\ Hx}$, and $SPL_{20–20\,000\ Hz}$ on the wind velocity – bottom panel. Survey session no. 5 (12.11.2023–15.02.2024) 336

Figure 2.142. Survey station H_4. The time series of the sound pressure levels (SPL) [dB re 1 µPa] in 1/3-octave bands of 63 Hz and 125 Hz (black and blue curves, respectively) and in the 20–20,000 Hz broadband (red curve) – upper panel. The time series of wind velocity V [$m \cdot s^{-1}$] – middle panel. The dependence of sound pressure levels $SPL_{63\ Hz}$, $SPL_{125\ Hz}$, and $SPL_{20–20\,000\ Hz}$ on the wind velocity – bottom panel. Survey session no. 5 (12.11.2023–03.12.2023) 336

Figure 2.143. The hearing thresholds of selected fish and mammal species occurring in the Baltic Sea [Source: herring (Enger, 1967); cod (Chapman and Hawkins, 1973); salmon (Hawkins and Johnstone, 1978); harbour porpoise (Kastelein et al., 2002); grey seal (Ridgway and Joyce, 1975); harbour seal (Kastak and Schusterman, 1998; Terhune, 1988; Møhl, 1968); ringed seal (Terhune and Ronald, 1975)] 338

Figure 3.1. The locations of the survey transects within the survey area on the surface sediment types basemap 341

Figure 3.2. Image of the stony seabed along transect FB_01 in the survey area 343

Figure 3.3. Image of the stony seabed along transect FB_02 in the survey area 344

Figure 3.4. The location of the survey stations at which macrozoobenthos samples were collected in 2023 on soft bottom and hard bottom in the survey area 350

Figure 3.5. The dominance structure in the total abundance of the macrozoobenthos from the soft-bottom stations in the survey area 354

Figure 3.6. The dominance structure in the total macrozoobenthos biomass from the soft-bottom stations in the survey area 355

Figure 3.7. The distribution of Macoma balthica shell lengths in 5 mm size classes on the soft bottom in the survey area (N = 8660) 356

Figure 3.8. The distribution of Macoma balthica biomass in 5 mm size classes on the soft bottom in the survey area (N = 8660) 356

Figure 3.9. The shell length distribution of Mytilus trossulus, Mya arenaria and Cerastoderma glaucum in 5-mm size classes on the soft bottom in the survey area (Mytilus trossulus N = 1103; Mya arenaria N = 68; Cerastoderma glaucum N = 57) 357

Figure 3.10. The biomass distribution of Mytilus trossulus, Mya arenaria and Cerastoderma glaucum in 5 mm size classes on the soft bottom in the survey area (Mytilus trossulus N = 1103; Mya arenaria N = 68; Cerastoderma glaucum N = 57) 358

Figure 3.11. The dominance structure in the total macrozoobenthos abundance from the hard-bottom stations in the survey area 359

Figure 3.12. The dominance structure in the total macrozoobenthos biomass from the hard-bottom stations in the survey area 360

Figure 3.13. The distribution of Mytilus trossulus shell lengths in 5 mm size classes on the hard bottom in the survey area (N = 464) 360

Figure 3.14. The distribution of Mytilus trossulus biomass in 5 mm size classes on the hard bottom in the survey area (N = 464) 361

Figure 3.15. The macrozoobenthos abundance distribution in the survey area 364

Figure 3.16. The macrozoobenthos biomass distribution in the survey area 365

Figure 3.17. The Macoma balthica biomass distribution in the survey area 366

Figure 3.18. The Mytilus trossulus biomass distribution in the survey area 367

Figure 3.19. The ecological status distribution in the survey area based on macrozoobenthos quality status assessment 368

Figure 3.20. The locations of the survey stations for ichthyoplankton sampling within the survey area 372

Figure 3.21. The routes of the hydroacoustic transect and pelagic hauls within the survey area 375

Figure 3.22. The locations of the survey stations for gillnet deployment within the survey area 378

Figure 3.23. The locations of survey stations for the deployment of nets used in commercial herring fishing, together with multi-mesh nets, within the survey area 380

Figure 3.24. Number of larvae caught during the entire survey period in the survey aread 395

Figure 3.25. Number of ichthyoplankton taxa during individual survey periods in the survey area 399
Figure 3.26. Average abundance of fish larvae [ind.·10 m^{-2}] during individual survey periods in the survey area 400
Figure 3.27. The proportion of individual taxa of fish larvae in the average total larval abundance in the survey area during individual survey periods 401
Figure 3.28. Abundance of larvae [ind.·10 m^{-2}] of individual fish species (average for the entire area) in the survey area during individual survey periods 402
Figure 3.29. Spatial distribution of sprat larvae in the annual cycle within the survey area 405
Figure 3.30. Spatial distribution of ammodytid larvae in the annual cycle within the survey area 406
Figure 3.31. Spatial distribution of flounder larvae in the annual cycle within the survey area 407
Figure 3.32. Spatial distribution of goby larvae in the annual cycle within the survey area 408
Figure 3.33. Spatial distribution of common seasnail larvae in the annual cycle within the survey area 409
Figure 3.34. Spatial distribution of fourbeard rockling larvae in the annual cycle in the survey area 410
Figure 3.35. The spatial distribution of herring larvae in the annual cycle within the survey area 411
Figure 3.36. The spatial distribution of rock gunnel larvae in the annual cycle in the survey area 412
Figure 3.37. Herring areal biomass density [t·NM^{-2}] based on hydroacoustic surveys conducted in the survey area during the winter campaign 415
Figure 3.38. Herring areal biomass density [t·NM^{-2}] based on hydroacoustic surveys conducted in the survey area during the spring campaign 416
Figure 3.39. Herring areal biomass density [t·NM^{-2}] based on hydroacoustic surveys conducted in the survey area during the summer campaign 417
Figure 3.40. Herring areal biomass density [t·NM^{-2}] based on hydroacoustic surveys conducted in the survey area during the autumn campaign 418
Figure 3.41. Sprat areal biomass density [t·NM^{-2}] based on hydroacoustic surveys conducted in the survey area during the winter campaign 419
Figure 3.42. Sprat areal biomass density [t·NM^{-2}] based on hydroacoustic surveys conducted in the survey area during the spring campaign 420
Figure 3.43. Sprat areal biomass density [t·NM^{-2}] based on hydroacoustic surveys conducted in the survey area during the summer campaign 421
Figure 3.44. Sprat areal biomass density [t·NM^{-2}] based on hydroacoustic surveys conducted in the survey area during the autumn campaign 422
Figure 3.45. The average daily catch rates reported for the catches conducted using bottom-set gillnet sets during successive survey campaigns in the survey area 425
Figure 3.46. The correlation between herring occurrence and the average density of piscivorous birds in the survey area 427
Figure 3.47. A correlation between the occurrence of all fish species and the average density of piscivorous birds in the survey area 428
Figure 3.48. The length distribution of sprat caught in pelagic trawl in the survey area, by the season of 2023 430
Figure 3.49. The age structure of sprat caught in pelagic trawl in the survey area, by the season of 2023 . 431
Figure 3.50. The distribution of gonad maturity stages of sprat caught in pelagic trawl in the survey area, by the season of 2023 431
Figure 3.51. The distribution of stomach fullness degrees of sprat caught in pelagic trawl in the survey area, by the season of 2023 432

Figure 3.52. The length distribution of herring caught in pelagic trawls in the survey area, by the season of 2023 434

Figure 3.53. The age structure of herring caught in pelagic trawls in the survey area, by the season of 2023 434

Figure 3.54. The distribution of gonad maturity stages of herring caught in pelagic trawls in the survey area, by the season of 2023 435

Figure 3.55. The distribution of stomach fullness degrees of herring caught in pelagic trawls in the survey area, by the season of 2023 435

Figure 3.56. The length distribution of cod caught in gillnets in the survey area, by the season of 2023 437

Figure 3.57. The age structure of cod caught in gillnets in the survey area, by the season of 2023 437

Figure 3.58. The distribution of gonad maturity stages of cod caught in gillnets in the survey area, by the season of 2023 438

Figure 3.59. The distribution of stomach fullness degrees of cod caught in gillnets in the survey area, by the season of 2023 438

Figure 3.60. The length distribution of flounder caught in gillnets in the survey area, by the season of 2023 440

Figure 3.61. The age structure of flounder caught in gillnets in the survey area, by the season of 2023 441

Figure 3.62. The distribution of gonad maturity stages of flounder caught in gillnets in the survey area, by the season of 2023 441

Figure 3.63. The distribution of stomach fullness degrees of flounder caught in gillnets in the survey area, by the season of 2023 442

Figure 3.64. The locations of survey stations for passive acoustic monitoring in the survey area 457

Figure 3.65. The location of the observation transects during the monitoring of marine mammals from the plane, in the survey area 459

Figure 3.66. The anchoring system used for the deployment of F-POD detectors at the seabed 461

Figure 3.67. The harbour porpoise occurrence recorded at different survey stations during the acoustic monitoring in the survey area between 3 December 2022 (stations in Poland)/14 February 2023 (stations in Sweden) and 28 February 2024. Data is shown as a percentage of DPD recorded over all the recording days per survey station..... 474

Figure 3.68. The harbour porpoise occurrence recorded at different survey stations during the acoustic monitoring in the survey area between 3 December 2022 (stations in Poland)/14 February 2023 (stations in Sweden) and 28 February 2024. Data is shown as a percentage of DPM recorded over all the recording minutes per survey station 475

Figure 3.69. The harbour porpoise occurrence recorded at different survey stations during the acoustic monitoring in the survey area between 3 December 2022 (stations in Poland)/14 February 2023 (stations in Sweden) and 28 February 2024. Data is shown as a percentage of DPD recorded over all the recording days per survey station..... 476

Figure 3.70. The harbour porpoise occurrence recorded at different survey stations during the acoustic monitoring in the survey area between 3 December 2022 (stations in Poland)/14 February 2023 (stations in Sweden) and 28 February 2024. Data is shown as a percentage of DPM recorded over all the recording days per survey station..... 477

Figure 3.71. The harbour porpoise occurrence recorded seasonally at the survey stations during the acoustic monitoring in the survey area between 3 December 2022 (stations in Poland)/ 14 February 2023 (stations in Sweden) – 28 February 2024. Data is shown as a percentage of DPD recorded over all the recording days within a season, obtained at a given station* 479

Figure 3.72. The harbour porpoise occurrence recorded seasonally at the survey stations during the acoustic monitoring in the survey area between 3 December 2022 (stations in Poland)/ 14 February 2023

(stations in Sweden) and 28 February 2024. Data is shown as a percentage of DPM recorded over all the recording minutes within a season, obtained at a given station* 479

Figure 3.73. The harbour porpoise occurrence recorded monthly at the survey stations during the acoustic monitoring in the survey area between 3 December 2022 (stations in Poland)/ 14 February 2023 (stations in Sweden) and 28 February 2024. Data is shown as a percentage of DPD recorded over all the recording days within a month, obtained at a given station* 480

Figure 3.74. The harbour porpoise occurrence recorded monthly at the survey stations during the acoustic monitoring in the survey area between 3 December 2022 (stations in Poland)/ 14 February 2023 (stations in Sweden) and February 2024. Data is shown as a percentage of DPM recorded over all the recording minutes within a month, obtained at a given station* 480

Figure 3.75. The harbour porpoise occurrence recorded seasonally during the acoustic monitoring in the survey area between 3 December 2022 (stations in Poland)/ 14 February 2023 (stations in Sweden) and 28 February 2024. Data is shown as a percentage of DPD recorded over all the recording days within a season, obtained at a given station* 482

Figure 3.76. The harbour porpoise occurrence recorded seasonally during the acoustic monitoring in the survey area between 3 December 2022 (stations in Poland)/ 14 February 2023 (stations in Sweden) and 28 February 2024. Data is shown as a percentage of DPM recorded over all the recording minutes within a season, obtained at a given station* 483

Figure 3.77. The harbour porpoise occurrence recorded seasonally during the acoustic monitoring in the survey area between 3 December 2022 (stations in Poland)/ 14 February 2023 (stations in Sweden) – 28 February 2024. Data is shown as a percentage of DPD recorded over all the recording days within a season, obtained at a given station* 484

Figure 3.78. The flight route and seal observations during the aerial visual monitoring conducted on 22 April 2023 in the survey area 494

Figure 3.79. The flight route and seal observations during the aerial visual monitoring conducted on 22 May 2023 in the survey area 495

Figure 3.80. The number of seal observations recorded in individual months of the visual monitoring between December 2022 and November 2023 in the OWF Baltica-1 survey area and the reference area 498

Figure 3.81. The number of seal observations recorded in individual seasons of the visual monitoring between December 2022 and November 2023 in the survey area 498

Figure 3.82. The probability of detecting porpoises in two seasons: May–October (left) and November–April, demonstrated during the SAMBAH project (2011–2013) (source: own study based on SAMBAH data] 500

Figure 3.83. The location of survey stations during the acoustic monitoring under the SNMP projects (2017–2020). Black denotes stations with the highest porpoise detection rates during the project. Dashed lines denote the boundaries of the Natura 2000 site Hoburgs bank och Midsjöbakarna. The locations of the monitoring stations under the SNMP program were the same as those under the SAMBAH project [Source: Owen et al., 2021] 500

Figure 3.84. The observations of live grey seals in 2020–2023 [Source: WWF, 2023a] 503

Figure 3.85. The observations of live harbour seals in 2020–2023 [Source: WWF, 2023a] 503

Figure 3.86. The observations of live ringed seals in 2020–2023 [Source: WWF, 2023a] 504

Figure 3.87. The observations of live unidentified seal species in 2020–2023 [Source: WWF, 2023a] 504

Figure 3.88. Migration routes of young grey seals for 2022 and 2023 [SMIOUG press materials available online] 505

Figure 3.89. The location of observation transects along which seabird counts were conducted in the survey area and the reference area 509

Figure 3.90. A diagram illustrating the method of determining the distance from the horizon; b – distance of the calliper from the eye of the observer (cm), c – opening of the calliper (cm), d – width of the transect on one side of the vessel (m), h – height of the observer's eye above the water surface (m), v – distance of the observer from the horizon, which is calculated using the formula: v = 3838 ($h^{0,5}$) 512

Figure 3.91. The scheme of an exemplary boundary of the transect effective strip width (ESW) in a 300-m wide strip of bird-counting 513

Figure 3.92. The proportion of the sea state categories recorded during all the campaigns in the survey area 518

Figure 3.93. The proportion of the specific precipitation intensity categories recorded during all the campaigns in the survey area 518

Figure 3.94. The proportion of the sea state categories recorded during all the campaigns in the reference area 522

Figure 3.95. The proportion of the specific precipitation intensity categories recorded during all the campaigns in the reference area 522

Figure 3.96. The changes in the abundance index of the entire bird grouping during successive survey campaigns within the survey area and the reference area 546

Figure 3.97. The changes in the abundance index of the long-tailed duck during successive survey campaigns within the survey area and in the reference area 547

Figure 3.98. The changes in the abundance index of the European herring gull during successive survey campaigns within the survey area and in the reference area 548

Figure 3.99. The changes in the abundance index of the razorbill during successive survey campaigns within the survey area and in the reference area 549

Figure 3.100. The changes in the abundance index of the common guillemot during successive survey campaigns within the survey area and in the reference area 550

Figure 3.101. The changes in the abundance of birds flying over the survey area at various heights during successive inspections 551

Figure 3.102. The changes in the abundance of birds flying over the reference area at various heights during successive inspections 554

Figure 3.103. The spatial distribution of the average densities of all birds within the survey area and the reference area between December 2022 and November 2023 557

Figure 3.104. The spatial distribution of the average densities of the long-tailed duck within the survey area and the reference area between December 2022 and November 2023 558

Figure 3.105. The spatial distribution of the average densities of the European herring gull within the survey area and the reference area between December 2022 and November 2023 559

Figure 3.106. The spatial distribution of the average densities of all birds within the survey area and the reference area during the wintering period 561

Figure 3.107. The spatial distribution of the average densities of the long-tailed duck within the survey area and the reference area during the wintering period 562

Figure 3.108. The spatial distribution of the average densities of the European herring gull within the survey area and the reference area during the wintering period 563

Figure 3.109. The spatial distribution of the average densities of all birds in the survey area and the reference area during the spring migration period 565

Figure 3.110. The spatial distribution of the average densities of the long-tailed duck within the survey area and the reference area during the spring migration period 566

Figure 3.111. The spatial distribution of the average densities of the European herring gull within the survey area and the reference area during the spring migration period 567

Figure 3.112. The spatial distribution of the average densities of all birds within the survey area and the reference area during summer 569

Figure 3.113. The spatial distribution of the average densities of all birds in the survey area and the reference area during the autumn migration period 571

Figure 3.114. The spatial distribution of the average densities of the long-tailed duck within the survey area and the reference area during the autumn migration period 572

Figure 3.115. The spatial distribution of the average densities of the European herring gull within the survey area and the reference area during the autumn migration period 573

Figure 3.116. A comparison of abundance indices of the entire grouping of seabirds in the survey area and the reference area in successive phenological periods. The difference in percentage is provided in relation to the index value for the reference area 580

Figure 3.117. The spatial distribution of the long-tailed duck density in the transect strip within the survey area and in the reference area on 22 April 2023 584

Figure 3.118. The location of survey stations as part of the surveys of bird movements during the wintering period against the background of the Natura 2000 sites and the Southern Middle Bank 591

Figure 3.119. The location of survey stations as part of the surveys of bird movements during the spring and autumn migration periods 592

Figure 3.120. Transect segments (marked with numbers) and buoys (marked with dots and letters) 593

Figure 3.121. An illustration of headwinds and tailwinds during spring and autumn migration (marked in blue) for the dominant migratory bird flight directions (marked in black) 596

Figure 3.122. A flow chart illustrating the main steps taken when estimating the total passage of migratory birds through the survey area based on visual daytime observations* 597

Figure 3.123. A screenshot of the Robin Visualiser display with radar screen as a background image on the left and editing console on the right. Continuous lines indicate flight trajectories automatically determined in real time by the horizontal radar 600

Figure 3.124. A screenshot of the Robin Visualiser display of a vertical radar presenting the passage routes of birds migrating at different altitudes 601

Figure 3.125. The probability of detection depending on the distance from the observer taking account of the observer effect (detection error) for the long-tailed duck 626

Figure 3.126. The probability of detection depending on the distance from the observer taking account of the observer effect (detection error) for the common scoter 627

Figure 3.127. The probability of detection depending on the distance from the observer taking account of the observer effect (detection error) for the common chaffinch 627

Figure 3.128. The probability of detection depending on the distance from the observer taking account of the observer effect (detection error) for the white wagtail 628

Figure 3.129. The probability of detection depending on the distance from the observer taking account of the observer effect (detection error) for the razorbill 628

Figure 3.130. The proportion of all birds observed at individual altitudes at survey station LP_01 in December 2022, and January and February 2023 655

Figure 3.131. The proportion of all birds observed at individual altitudes at survey station LP_01 in December 2022, January and February 2023 656

Figure 3.132. The proportion of all birds observed at individual altitudes at survey station MB_01 in the spring migration period 659

Figure 3.133. The proportion of all birds observed at individual altitudes at survey station MB_01 in the spring migration period 662

Figure 3.134. The proportion of all birds observed at individual altitudes at survey station MB_01 in the autumn migration period 665

Figure 3.135. The percentage share distribution of all observations at different flight altitudes recorded at survey station MB_02 in the autumn migration period 667

Figure 3.136. The flight directions of all tracked birds recorded at survey station LP_01 during the entire survey period (December 2022, January and February 2023) 669

Figure 3.137. The flight directions of all tracked auks recorded at survey station LP_01 in the entire survey period (December 2022, January and February 2023) 670

Figure 3.138. The flight directions of all tracked long-tailed ducks recorded at survey station LP_01 in the entire survey period (December 2022, January and February 2023) 670

Figure 3.139. The flight directions of all tracked divers recorded at survey station LP_01 in the entire survey period (December 2022, January and February 2023) 671

Figure 3.140. The flight directions of all tracked common scoters recorded at survey station LP_01 in the entire survey period (December 2022, January and February 2023) 671

Figure 3.141. The flight directions of all tracked velvet scoters recorded at survey station LP_01 in the entire survey period (December 2022, January and February 2023) 672

Figure 3.142. The flight directions of all tracked birds recorded at survey station LP_02 during the entire survey period (December 2022, January and February 2023) 673

Figure 3.143. The flight directions of all tracked long-tailed ducks recorded at survey station LP_02 in the entire survey period (December 2022, January and February 2023) 674

Figure 3.144. The flight directions of all tracked auks recorded at survey station LP_02 in the entire survey period (December 2022, January and February 2023) 674

Figure 3.145. The flight directions of all tracked divers recorded at survey station LP_02 in the entire survey period (December 2022, January and February 2023) 675

Figure 3.146. The flight directions of all tracked velvet scoters recorded at survey station LP_02 in the entire survey period (December 2022, January and February 2023) 675

Figure 3.147. The flight directions of all tracked birds at survey station MB_01 during the spring migration period 679

Figure 3.148. The flight directions of all tracked long-tailed ducks recorded at survey station MB_01 during the spring migration period 680

Figure 3.149. The flight directions of all tracked long-tailed ducks at survey station MB_01 during the spring migration period 680

Figure 3.150. The flight directions of all tracked velvet scoters at survey station MB_01 during the spring migration period 681

Figure 3.151. The flight directions of all tracked auks recorded at survey station MB_01 during the spring migration period 681

Figure 3.152. The flight directions of all tracked geese recorded at survey station MB_01 during the spring migration period 682

Figure 3.153. The flight directions of all tracked birds at survey station MB_02 during the spring migration period 685

Figure 3.154. The flight directions of all tracked long-tailed ducks at survey station MB_02 during the spring migration period 686

Figure 3.155. The flight directions of all tracked common scoters at survey station MB_02 during spring migration 686

Figure 3.156. The flight directions of all tracked velvet scoters at survey station MB_02 during the spring migration period 687

Figure 3.157. The flight directions of all tracked razorbills at survey station MB_02 during the spring migration period..... 687

Figure 3.158. The flight directions of all tracked birds recorded at survey station MB_01 during the autumn migration period 691

Figure 3.159. The flight directions of all tracked unidentified ducks recorded at survey station MB_01 during the autumn migration period 691

Figure 3.160. The flight directions of all tracked long-tailed ducks recorded at survey station MB_01 during the autumn migration period 692

Figure 3.161. The flight directions of all tracked common scoters at survey station MB_01 during the autumn migration period 692

Figure 3.162. The flight directions of all tracked auks recorded at survey station MB_01 during the autumn migration period 693

Figure 3.163. The flight directions of all tracked lesser black-backed gulls recorded at survey station MB_01 during the autumn migration period 694

Figure 3.164. The flight directions of all tracked little gulls recorded at survey station MB_01 during the autumn migration period 694

Figure 3.165. The flight directions of all tracked great cormorants recorded at survey station MB_01 during the autumn migration period 695

Figure 3.166. The flight directions of all tracked passerines recorded at survey station MB_01 during the autumn migration period 695

Figure 3.167. The flight directions of all tracked terns recorded at survey station MB_01 during the autumn migration period 696

Figure 3.168. The flight directions of all tracked birds recorded at survey station MB_02 during the autumn migration period 699

Figure 3.169. The flight directions of all tracked long-tailed ducks recorded at survey station MB_02 during the autumn migration period 699

Figure 3.170. The flight directions of all tracked unidentified ducks recorded at survey station MB_02 during the autumn migration period 700

Figure 3.171. The flight directions of all tracked auks recorded at survey station MB_02 during the autumn migration period 700

Figure 3.172. The flight directions of all tracked great cormorants recorded at survey station MB_02 during the autumn migration period 701

Figure 3.173. The flight directions of all tracked common scoters at survey station MB_02 during the autumn migration period 701

Figure 3.174. The flight directions of all tracked lesser black-backed gulls recorded at survey station MB_02 during the autumn migration period 702

Figure 3.175. The flight directions of all tracked little gulls recorded at survey station MB_02 during the autumn migration period 702

Figure 3.176. The flight directions of all tracked passerines recorded at survey station MB_02 during the autumn migration period 703

Figure 3.177. The flight directions of all tracked unidentified divers recorded at survey station MB_02 during the autumn migration period 703

Figure 3.178. The distribution of bird flight altitudes recorded using vertical radar in December 2022 at survey station LP_01. The number of tracks was averaged with the total monthly effort of the vertical radar data collection 704

Figure 3.179. The distribution of bird flight altitudes recorded using vertical radar January 2023 at survey station LP_01. The number of tracks was averaged with the total time devoted to the vertical radar data collection in that month 705

Figure 3.180. The distribution of bird flight altitudes recorded using vertical February 2023 at survey station LP_01. The number of tracks was averaged with the total time devoted to the vertical radar data collection in that month 706

Figure 3.181. The distribution of bird flight altitudes recorded using vertical radar in December 2022 at survey station LP_02. The number of tracks was averaged with the total time devoted to the vertical radar data collection in that month 707

Figure 3.182. The distribution of bird flight altitudes recorded using vertical radar January 2023 at survey station LP_02. The number of tracks was averaged with the total time devoted to the vertical radar data collection in that month 708

Figure 3.183. The distribution of bird flight altitudes recorded using vertical February 2023 at survey station LP_02. The number of tracks was averaged with the total time devoted to the vertical radar data collection in that month 709

Figure 3.184. The distribution of bird flight altitudes recorded using vertical radar in March 2023 at survey station MB_01. The number of tracks was averaged with the total time devoted to the vertical radar data collection in that month 710

Figure 3.185. The distribution of bird flight altitudes recorded using vertical radar in April 2023 at survey station MB_01. The number of tracks was averaged with the total time devoted to the vertical radar data collection in that month 711

Figure 3.186. The distribution of bird flight altitudes recorded using vertical radar in May 2023 at survey station MB_01. The number of tracks was averaged with the total time devoted to the vertical radar data collection in that month 712

Figure 3.187. The distribution of bird flight altitudes recorded using vertical radar in March 2023 at survey station MB_02. The number of tracks was averaged with the total time devoted to the vertical radar data collection in that month 713

Figure 3.188. The distribution of bird flight altitudes recorded using vertical radar in April 2023 at survey station MB_02. The number of tracks was averaged with the total time devoted to the vertical radar data collection in that month 714

Figure 3.189. The distribution of bird flight altitudes recorded using vertical radar in May 2023 at survey station MB_02. The number of tracks was averaged with the total time devoted to the vertical radar data collection in that month 715

Figure 3.190. The distribution of bird flight altitudes recorded using vertical radar in July 2023 at survey station MB_01. The number of tracks was averaged with the total time devoted to the vertical radar data collection in that month 716

Figure 3.191. The distribution of bird flight altitudes recorded using vertical radar in August 2023 at survey station MB_01. The number of tracks was averaged with the total time devoted to the vertical radar data collection in that month 717

Figure 3.192. The distribution of bird flight altitudes recorded using vertical radar in September 2023 at survey station MB_01. The number of tracks was averaged with the total time devoted to the vertical radar data collection in that month 718

Figure 3.193. The distribution of bird flight altitudes recorded using vertical radar in October 2023 at survey station MB_01. The number of tracks was averaged with the total time devoted to the vertical radar data collection in that month 719

Figure 3.194. The distribution of bird flight altitudes recorded using vertical radar in November 2023 at survey station MB_01. The number of tracks was averaged with the total time devoted to the vertical radar data collection in that month 720

Figure 3.195. The distribution of bird flight altitudes recorded using vertical radar in July 2023 at survey station MB_02. The number of tracks was averaged with the total time devoted to the vertical radar data collection in that month 721

Figure 3.196. The distribution of bird flight altitudes recorded using vertical radar in August 2023 at survey station MB_02. The number of tracks was averaged with the total time devoted to the vertical radar data collection in that month 722

Figure 3.197. The distribution of bird flight altitudes recorded using vertical radar in September 2023 at survey station MB_02. The number of tracks was averaged with the total time devoted to the vertical radar data collection in that month 723

Figure 3.198. The distribution of bird flight altitudes recorded using vertical radar in October 2023 at survey station MB_02. The number of tracks was averaged with the total time devoted to the vertical radar data collection in that month 724

Figure 3.199. The distribution of bird flight altitudes recorded using vertical radar in November 2023 at survey station MB_02. The number of tracks was averaged with the total time devoted to the vertical radar data collection in that month 725

Figure 3.200. The number of bird calls in daylight and night hours recorded at survey station MB_01 in the spring migration period 727

Figure 3.201. The number of bird calls in daylight and night hours recorded at survey station MB_02 in the spring migration period 729

Figure 3.202. The number of bird calls in daylight and night hours recorded at survey station MB_01 in the autumn migration period 731

Figure 3.203. The number of bird calls in daylight and night hours recorded at survey station MB_02 in the autumn migration period 733

Figure 3.204. The bat acoustic monitoring sites; NT_01–NT_04 – transects, NS_01–NS_04 – static monitoring points 745

Figure 3.205. The bat species composition and the total number of activity units recorded using ultrasound detection within the survey area between 1 April and 31 October 2023 750

Figurep 3.206. The bat species composition – the number of activity units recorded using ultrasound detection between 1 April and 31 October 2023 broken down by phenological seasons – spring migration and autumn migration 751

ABBREVIATIONS AND DEFINITIONS

2D UHR	multi-channel seismic surveys
Area A	the offshore WTG, substation, and cable line construction area
Area B	the cable line construction area
ASCII	American Standard Code for Information Interchange
AWAC	Acoustic Wave and Current (Profiler)
Baltica-1 OWF construction area	the area of the offshore WTG, substation, and cable line construction area (area A) and the cable line construction area (area B)
BIAS	Baltic International Acoustic Survey – a type of standardised survey passage conducted by all Baltic countries in the autumn to provide data for estimating stocks of pelagic species
Bird Life International	an international non-governmental organisation working to protect birds and their habitats. It is a federation of bird protection organisations from various countries
BOD_5	5-day Biochemical Oxygen Demand
BSB	below the seabed
BSL	below the sea level
CMP	common mid-point domain
CTD	sensors measuring conductivity, temperature, and depth
DBT	dibutyltin
DGPS	Differential Global Positioning System
DIN	Dissolved Inorganic Nitrogen
diving benthophages	a morphological-ecological group including bird species which feed on benthic organisms, in search of which they dive
diving ichthyophages	a morphological-ecological group including bird species which feed on fish, in search of which they dive
DPD	Detection Positive Days
DPM	Detection Positive Minutes

DW	dry weight
E	east
EBCDIC	Extended Binary-Coded Decimal Interchange Code
EDSU	Elementary Data Sampling Unit typically equal 1 NM, not counted directly in the calculations, but indicating that an area is covered by surveys
EEZ	Exclusive Economic Zone within the meaning of the Act of 21 March 1991 on the maritime areas of the Republic of Poland and maritime administration (Journal of Laws of 1991, No. 32, item 131 as amended)
EIA	Environmental Impact Assessment
EIA Report	Environmental Impact Assessment Report
EMODnet	European Marine Observation and Data Network
EPD MI GMU	Environmental Protection Department at the Maritime Institute of the Gdynia Maritime University
EQS	Environmental Quality Standard – a standard that specifies the degree of concentration of a pollutant that should not be exceeded to protect human life and the natural environment
ESW	effective strip width
EUROBATS	Agreement on the Conservation of Populations of European Bats
EVRF	European Vertical Reference Frame
FFT	Fast Fourier Transform
F-POD	a detector designed for passive acoustic monitoring of odontocetes (such as the harbour porpoise)
FTU	formazin turbidity unit
GC-FID	gas chromatography/flame ionisation detection
GC-MS	gas chromatography coupled with mass spectrometry
GDEP	General Directorate of Environmental Protection (Polish: *Generalna Dyrekcja Ochrony Środowiska,* GDOŚ)
GES	Good Environmental Status

GIS	Geographic Information System
GNSS	Global Navigation Satellite System
GPS	Global Positioning System
HELCOM	Baltic Marine Environment Protection Commission (Helsinki Commission)
H_{m0}	significant wave height based on the spectral analysis of the wave energy density
H_{max}	maximum wave height
H_{mean}	mean wave height
IBA	Important Bird Area
IBAS	International Baltic Acoustic Surveys
ICES	International Council for the Exploration of the Sea
ichthyofauna	the total number of fish species inhabiting water bodies
ichthyoplankton	eggs and larval forms of fish; ichthyoplankton is characterised by the lack of independent movement, it only drifts in the water depth; as part of the study, also juvenile stages of fish were analysed in the section on ichthyoplankton
ID	identifier
IHO	International Hydrographic Organisation
IMWM–NRI	Institute of Meteorology and Water Management – National Research Institute (Polish: *Instytut Meteorologii i Gospodarki Wodnej Państwowy Instytut Badawczy*, *IMGW–PIB*)
IOGP	International Association of Oil and Gas Producers
IQR	interquartile range
ISO	International Organisation for Standardisation
IUCN	International Union for Conservation of Nature
KERNO-F	an algorithm of the FPOD.exe software used in the analysis of data obtained by an F-POD

larva	an early stage in the development of fish starting after a fish hatches from the egg, from the stage of yolk-sac larva to a post-larva
LC	Least Concern species
LIM	Line Isolation Monitor
LOI	loss on ignition
LOQ	limit of quantification
LT	total length of a fish measured from the front of the fish body (its snout) to the end of the longest ray of the caudal (tail) fin (abbreviated from Latin *longitudo totalis*)
macrozoobenthos	synonym: benthic macrofauna; the fraction of organisms inhabiting the seabed surface (epifauna) or inside sediment (infauna), which remain washed out on a 1.0-mm sieve
MAG	magnetometer
MBES	multibeam echosounder
MBT	monobutyltin
MCS	multi-channel seismic profiling
MGD MI GMU	Maritime Geotechnics Department at the Maritime Institute of the Gdynia Maritime University
MI GMU	Maritime Institute of the Gdynia Maritime University (Polish: *Instytut Morski Uniwersytetu Morskiego w Gdyni*, *IM UM*G)
moulting area	an area where birds (usually Anseriformes) gather to shed old feathers including quills
MSFD	Marine Strategy Framework Directive
N	north
N/A	not applicable
NASC	Nautical Area Scattering Coefficient
NE	north-east
NMFRI	National Marine Fisheries Research Institute (Polish: *Morski Instytut Rybacki – Państwowy Instytut Badawczy*, *MIR-PIB*)

NMFS	National Marine Fisheries Service of the United States – the federal agency responsible for the management, conservation, and protection of living marine resources, which has published the criteria for the assessment of noise impact on marine mammals, including the frequency-weighted sound levels
NMO	normal moveout – a process of NMO correction that removes the moveout effect on travel times
NNW	north by north-west
NW	north-west
OSS	offshore substation
otolith	a calcium carbonate structure in the saccule or utricle of the inner ear of fish used as gravity, balance, movement, and directional indicator and in intercepting sound waves
OWF	Offshore Wind Farm
OWF B1	Offshore Wind Farm Baltica 1
PAHs	polycyclic aromatic hydrocarbons
PAM	passive acoustic monitoring
PCA	Polish Centre for Accreditation
PCB	polychlorinated biphenyls
pelagic fish	fish living in open water, the life of which is not connected to a solid substrate
pH	potential of hydrogen – the negative decimal logarithm of the hydrogen ion activity [H+]
Phytobenthos	aquatic plants which include vascular plants (e.g. sea-grass) rooted in the seabed and macroalgae, which attach themselves to hard surfaces
ppm	particles per million; 1 ppm means 1 mg of salt in 1 kg of seawater
PSD	power spectral density
QC	quality control
QPS Quinsy	QINSy (Quality Integrated Navigation System) hydrographic data acquisition, navigation, and processing software package

ROV	remotely operated vehicle
RTK	Real-Time Kinematic for the DGPS; the technology of the most accurate measurements of the position above sea level (with accuracy to centimetres) obtained in real-time (without calculations in the post-processing phase)
S	south
S/N	serial number
SAMBAH	the "Static Acoustic Monitoring of the Baltic Sea Harbour Porpoise" international research project
SBP	sub-bottom profiler
SCS	single channel seismic
SE	south-east
SEL	sound exposure level
SEM	State Environmental Monitoring (Polish: *Państwowy Monitoring Środowiska*, *PMŚ*)
SISP	Series of ICES Survey Protocols – the series of guidelines on survey vessel passages published by the International Council for the Exploration of the Sea
SL	standard length of a fish – the length of a fish measured from the tip of the snout to the posterior end of the last vertebra or the posterior end of the mid-lateral portion of the hypural plate
SM4M	Song Meter Acoustic Recorder – a weatherproof wildlife hydrophone
SMHI	Swedish Meteorological and Hydrological Institute
SPEC	Species of European Conservation Concern – the rank of special concern, considering the category of threat and the species occurrence in Europe and the world, given to bird species by BirdLife International
SPL	sound pressure level
SPRAS	Baltic Acoustic Spring Survey – a type of standardised survey vessel passage conducted by all Baltic countries in the spring to provide data for estimating the stocks of pelagic species

SSDM	Seabed Survey Data Model – a GIS database compliant with the guidance of the International Association of Oil & Gas Producers
SSE	south–south-east
SSS	side-scan sonar
survey station	a place designated for collecting samples, taking measurements, or conducting observations
SVP	sound velocity probe
SVS	sound velocity sensor
SW	south-west
TBT	tributyltin
TFDN	time-frequency denoising
Tm	mean wave period
TOC	total organic carbon
Tp	peak wave period – the period with waves presenting the highest amount of energy transported
TSP	the index of the presence of zoobenthos taxa on hard seabed
TVF (frame)	Transverse Gradiometer frame
TWT	two-way time
UTC	Coordinated Universal Time
WFD	Water Framework Directive
WGBIFS	Baltic International Fish Survey Working Group
WoRMS	World Register of Marine Species

1 GEOPHYSICAL SURVEYS – THE BASIC SCOPE

1.1 NON-SPECIALIST SUMMARY

To identify the character of seabed relief and structure in the survey area, geophysical surveys were conducted. The geophysical campaign comprised the following types of surveys: bathymetric (determination of the seabed depth and relief), sonar (identification of the seabed character), seismo-acoustic using a sediment profiler (determination of the deep-seabed structure), single- and multi-channel seismic surveys (identification of deeper geological structures), and magnetometric survey (identification of magnetic anomalies of the substratum and the potential objects deposited on the seabed or shallowly below its surface). The surveys were conducted along the survey lines delineated parallel to one another in such a way that the entire seabed within the area analysed was covered by bathymetric (MBES) and sonar (SSS) surveys. The measurement campaign, including bathymetric, sonar, and seismo-acoustic measurements using a sediment profiler, and single-channel seismic and magnetometric measurements, lasted from February to August 2023. In the period from 26 September 2023 to 1 February 2024, seismic surveys were performed in the survey area using multi-channel seismic imaging.

Additionally, to confirm the arrangement of shallow sediment layers and to identify the presence of potential aggregate deposits, surface sediment and core samples were collected. The locations of the survey stations for sediment core sampling using a vibrocorer were distributed evenly over a grid with a density of 1 station per 3 km^2 within the survey area. Surface sediment samples, however, were collected using a van Veen grab sampler at survey stations distributed in a parallel grid with a density of 1 station per 1 km^2 of the survey area.

To identify any potential objects deposited on the seabed at the pre-determined points, a visual inspection was carried out using a remotely operated vehicle (ROV). The visual inspection lasted from 28 November 2023 to 14 February 2024 and its purpose was to confirm and verify the objects that could not be unambiguously identified using the previously obtained data.

1.1.1 Bathymetric surveys

The bathymetric surveys were conducted using a multibeam echosounder (MBES) within the survey area. Based on the acquired bathymetric data and taking into account data from the European Marine Observation and Data Network (EMODnet), a bathymetric map was prepared and the characteristics of the seabed surface and the forms occurring on the seabed of the study area were identified.

The seabed surface in the survey area is located at a depth from 13.7 to 51.8 m BSL The depth increases towards the south and east. The shallowest parts of the seabed are located in the western section of the area. The seabed surface is diverse.

1.1.2 Side-scan sonar survey

Sonar surveys were carried out using a side-scan sonar (SSS) within the survey area. The results of sonar registrations from the survey area were collected and processed into a sonar image.

Based on the analyses of the sonar data collected, using bathymetric data as well as data from the sediment sample analyses obtained from the EMODnet, a map of surface sediments in the survey area was prepared. The prevailing part of the seabed surface consists of fine and medium-grained sands. In

the eastern and north-western parts of the area, the seabed consists of cohesive sediments with a thin, discontinuous sandy cover and an erosive pavement with single boulders on the surface.

1.1.3 Magnetometric measurements

Magnetometric measurements were carried out using a set of two magnetometers over the survey area.

Based on the surveys conducted, maps of the residual field and magnetic anomalies were developed for the survey area. In the survey area, 2 linear objects and 599 magnetic anomalies were identified.

1.1.4 Surveys of man-made or unidentified objects on the seabed

Based on the bathymetric, sonar and magnetometric data analysis, 152 man-made or unidentified objects were identified. All those objects were selected for visual inspection using a remotely operated vehicle (ROV). Additionally, after the MAG and SSS data analysis, three inspection points were selected (ROV_157, 158, and 159) as possible objects for verification due to the recorded signals of potential magnetic anomalies. The purpose of the ROV inspection was to confirm or verify the type of the object which cannot be unambiguously identified based solely on other data (SSS, MBES, MAG). Most objects that were identified during the ROV inspections were classified as man-made objects, with a small fraction being geomorphological formations. The video material acquired confirmed the presence of man-made objects such as fragments of shipwrecks, aeroplane components, fishing nets and ropes, logs, a tyre, tree branches, and wood debris.

1.1.5 Shallow seismo-acoustic profiling

Shallow seismo-acoustic profiling was conducted with the use of a sediment profiler over the survey area.

Based on the analysis of the data collected, the structure of the sediment layers forming the seabed of the survey area was identified. The seabed of the survey area is built mainly of sandy sediments. The form a layer with a thickness of up to several metres. Below the sandy sediments, glacial deposits were recognised, the top of which in the eastern part of the survey area is located shallow below the seabed surface or locally forms outcrops in the seabed.

1.1.6 Seismic surveys

1.1.6.1 Single-channel seismic surveys

As part of the seismic surveys, single-channel seismic surveys were carried out using a single-channel streamer and a sparker sound source over the survey area.

Based on the analysis of seismo-acoustic and seismic registration results, four main seismic units were differentiated. These units were interpreted geologically with the application of general knowledge of the method and the survey region. The units differentiated were described as:

- unit IA – fine- to medium-grained sands, locally silty sands, with coarse-grained sands and gravels (marine, fluvial and fluvioglacial) in places;
- unit IB – fine- and medium-grained sands, locally sands with gravel (lagoonal, fluvial, fluvioglacial);
- unit ID – sands with gravel, gravels, and tills (fluvioglacial and glacial). The following division into two sub-units within the fluvioglacial and glacial sediments was introduced:

  - unit ID1 – clayey tills or silty tills, locally clays or silty clays with an admixture of sand and gravel fractions (subaquatic);
  - unit ID2 – sands with gravel, gravels, and tills (fluvioglacial and glacial);
- unit IF – pre-Quaternary sediments:
  - unit IF1 – sediments filling the valleys in the Silurian top layer, the age of which is difficult to determine at the current stage of surveys;
  - unit IF2 – correlated as Silurian sediments.

1.1.6.2 Multi-channel seismic surveys (2D UHR)

As part of the research in the survey area, measurements were taken using a streamer, i.e. a towed hydrophone set, with 96 channels spaced every 1 m.

As a result of the conducted 2D MCS survey, there was prepared an interpretative model of the geological structure of the rock medium down to approx. 80–100 m below the seabed. The boundaries (ceilings) of the main stratigraphic units of the Quaternary level, and internal precipitates in tills (subunits) were marked, and the roof of the Silurian bedrock was mapped as well. In addition, the data were analysed for the occurrence of geological hazards, such as palaeo-channels, zones saturated with CH_4 marsh gas (methane), tectonic fault lines, and other amplitude anomalies that cannot be related to the local boundaries of geological units.

1.1.7 Soil sampling

1.1.7.1 Surface sediment sampling

Surface sediment samples were collected to determine the types of surface sediments and identify the areas with sediments which may constitute potential aggregate deposits. The sediment samples were collected at survey stations determined within the survey area. Surface sediment samples were collected using a van Veen grab sampler. As part of the surface sediment sampling campaign, 118 survey stations were established within the survey area (1 station per 1 km^2).

Thus collected surface sediment samples were transported to the Maritime Geotechnics Department at the Maritime Institute of the Gdynia Maritime University (MGD MI GMU). In the laboratory, the samples underwent a macroscopic analysis and the soil grain size was examined using a sieve and/or areometric analysis. After their collection, the samples were stored under thermally controlled conditions.

The entire seabed surface of the survey area consists of sandy and sand-gravel soils.

1.1.7.2 Core sampling

To confirm the arrangement of shallow sedimentary layers and determine the presence of areas with potential aggregate deposits, core samples were taken using a vibrocorer. The locations of the survey stations for core sampling were evenly distributed over the entire survey area, in a grid with a density of 1 station per 3 km^2. 39 core sampling stations were designated.

The collected core samples were transported to the laboratory of the MGD MI GMU. In the laboratory, they underwent a macroscopic analysis and the soil grain size was examined using a sieve and/or areometric analysis. After their collection, the samples were stored under thermally controlled conditions.

Core examinations confirm that most of the survey area is composed of sandy and sand-gravel soils (with fine sands as the dominant fraction). In a part of the survey area, Pleistocene soils occur under sandy cover, namely clays/silts with sand and gravel. In places, tills are found on the seabed surface.

1.2 SPATIAL SCOPE OF THE SURVEYS

Bathymetric, sonar, magnetometric, and seismoacoustic surveys were carried out in the survey area of 177.96 km^2 along longitudinal lines spaced at an interval of 50 m and transverse lines spaced at an interval of 500 m. Surveys using single-channel seismic and multi-channel seismic recording were carried out in the area of 108.19 km^2. For single-channel seismic measurements, the following distribution of measurement lines was used: longitudinal lines at 50-m intervals, and transverse lines at 500-m intervals, while for multi-channel seismic measurements, the measurement lines were distributed in the following manner: longitudinal lines at 200-m intervals, and transverse lines at 2000-m intervals.

The locations of survey stations for surface sediment sampling were planned in an evenly distributed grid with a density of 1 station per 1 km^2. 118 survey stations were designated for the survey [Figure 1.1].

The survey stations for core sampling were designated along seismo-acoustic survey lines using sediment and seismo-acoustic profilers as well as at the intersection of the lines along which the bathymetric, sonar, and magnetometric surveys were performed. The locations of the survey stations for core sampling were planned over the survey area in an evenly distributed grid with a density of 1 station per 3 km^2. 39 survey stations were designated for the survey [Figure 1.2].

Data from EMODnet were used for the bathymetric analysis and in the determination of surface sediment types and seabed types in the Swedish EEZ.

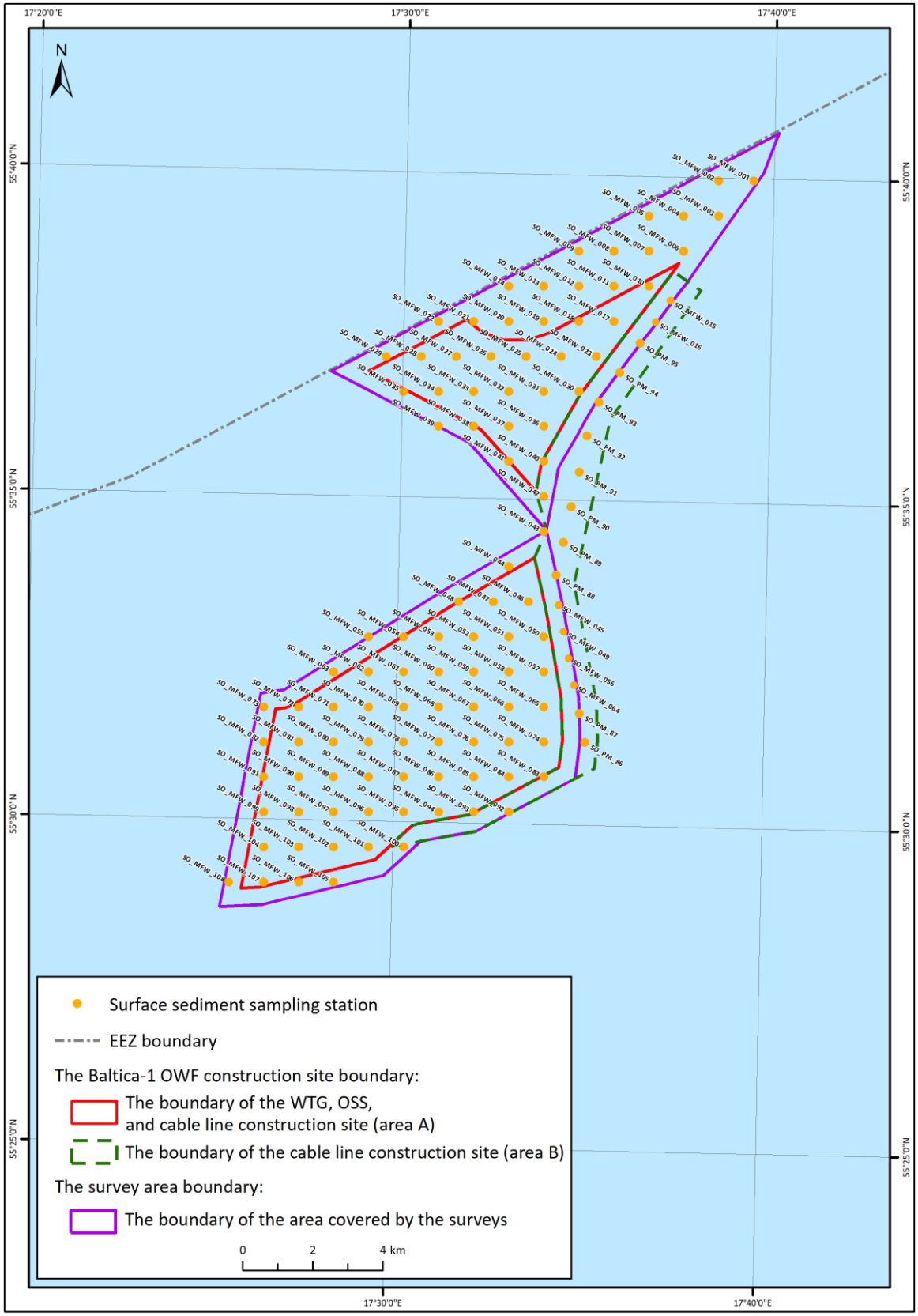


Figure 1.1. The locations of surface sediment sampling stations within the survey area

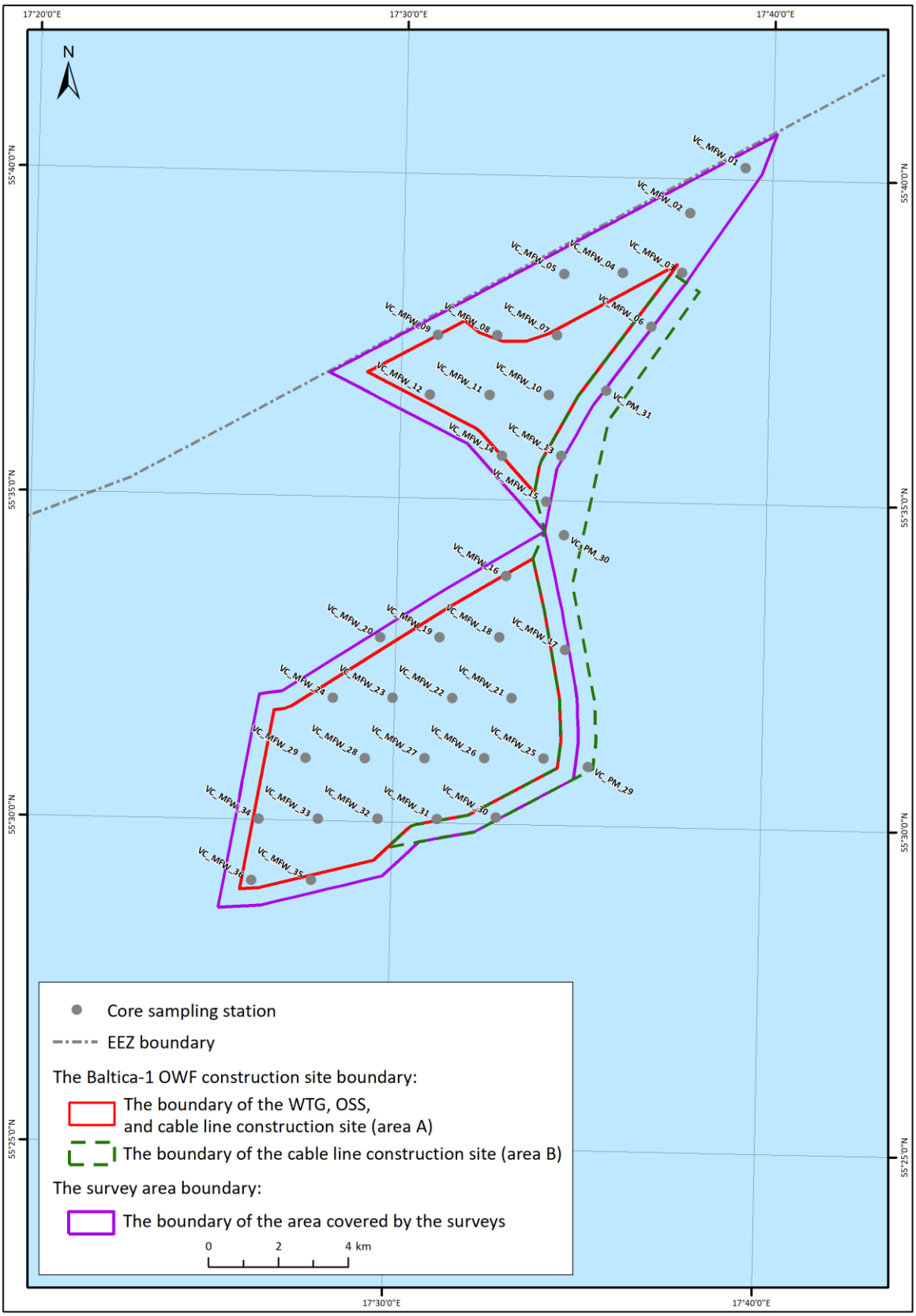


Figure 1.2. The locations of the survey stations for core sampling within the survey area

1.3 METHODOLOGY

1.3.1 Bathymetric surveys

1.3.1.1 Bathymetric survey methodology

Bathymetric surveys in the survey area were carried out using a multibeam echosounder along the designated survey lines running at 50-m intervals and along the transverse survey lines (cross-lines) at 500-m intervals.

The basic survey system used in the creation of the bathymetric image of the seabed in the area surveyed was the Reson SeaBat T50 multibeam echosounder manufactured by Teledyne Reson. The system that collected and saved data provided by the echosounder in real time was the QINSy software.

During recording, the data obtained from the multibeam echosounder were converted into bathymetric data in real-time. The QPS QINSy software automatically allowed for the corrections related to the sound velocity in the water column, readings from the motion reference unit and positioning. The depth data were correlated to the EVRF 2007 geoid model.

To ensure proper measurement accuracy, equipment for measuring the velocity of sound propagation in water was used. Both the equipment operating on-line at the multibeam echosounder head as well as the sound velocity profilers operating in the water column were used (SVPs/CTDs).

The SVPs/CTDs recorded sound velocity at intervals of at least 50 cm in the water column. The sound velocity measurement obtained with the SVPs/CTDs was compared with the measurement made with the SVS (Sound Velocity Sensor) head sensor. SVP/CTD measurements were carried out at least 4 times within 24 hours (or 2 times in the case of 12-hour work).

1.3.1.2 Bathymetric data post-processing methodology

The data obtained from bathymetric surveys were processed to eliminate acoustic noise, validate them for sea-level changes and next, subjected to quality control procedures. The processing of the bathymetric data was carried out in two steps. During the first stage, QPS Qinsy software was used for analysis and possible correction of the input data obtained from individual devices of the survey system. This stage ended with exporting the cleaned data to an adequate raster format or data in the ASCII (x, y, z) format.

At the first stage of the data processing, the positioning along with the reference level was verified and corrected if needed. The bathymetric data measured in the RTK system in the areas with access to differential corrections provided by the ASG EUPOS system were automatically referred to the GRS 80 ellipsoid.

Next, all survey profiles were checked in the QPS QINSy system to verify if the angle parameters resulting from the multibeam echosounder system calibration had been included.

Subsequently, each measurement profile was analysed to check whether the profile of sound dispersion in water had been entered correctly into the system.

In the second phase of the bathymetric data processing, the AutoClean software was used. At this step, it was possible to correct the local height deviations in the data in a given profile thanks to the varied visualisation methods. Also, the curvatures of the data strip caused by the occurrence of acoustic

refraction in the sea were corrected. Next, the data were cleaned of any interferences or the fish shoal echoes registered.

The bathymetric data processing flow chart is presented in Figure 1.3.

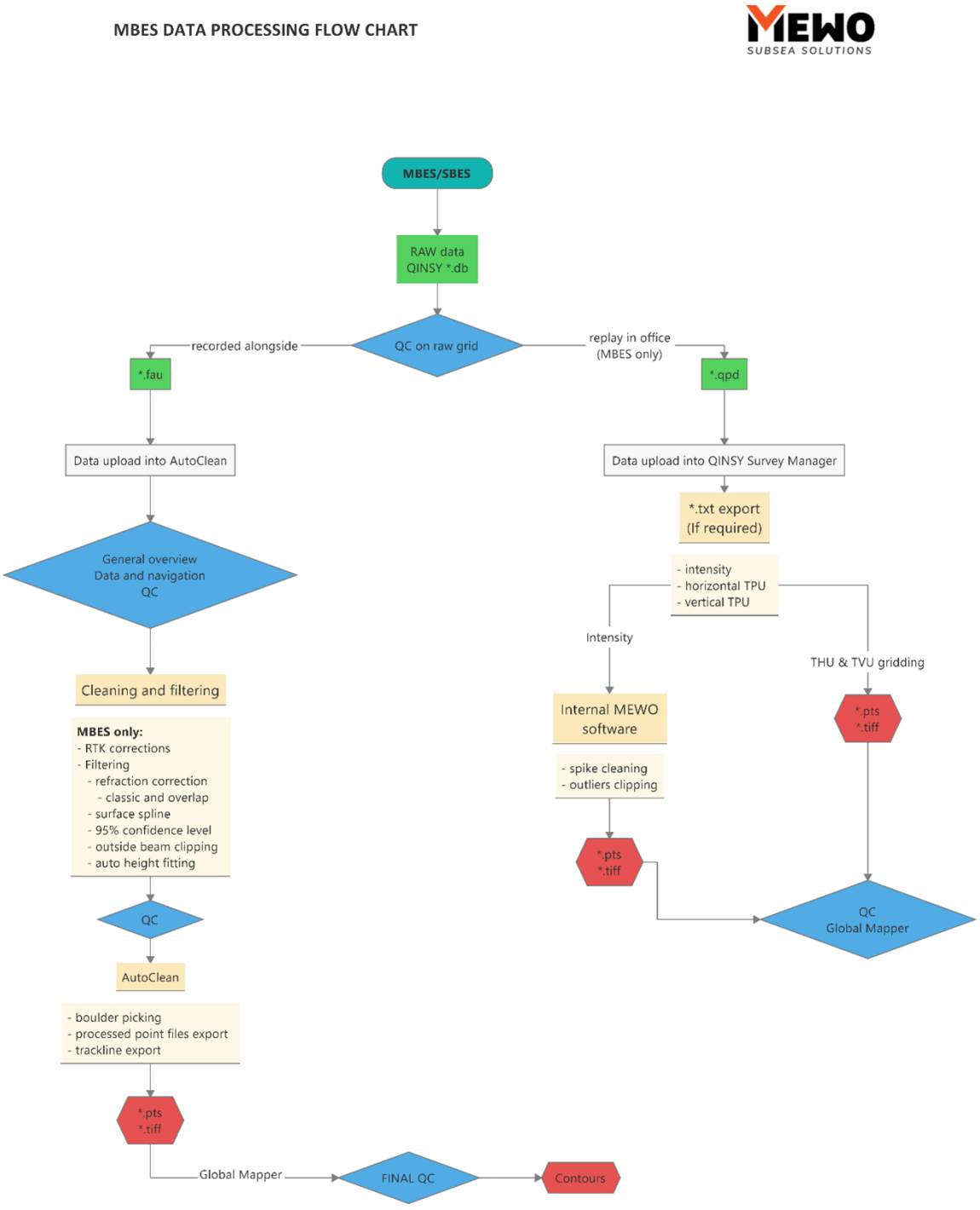


Figure 1.3. Bathymetric data processing flow chart

Data collected as part of the bathymetric surveys conducted meet the guidelines of IHO Standard Order 1a.

1.3.2 Side-scan sonar survey

1.3.2.1 Side-scan sonar survey methodology

Side-scan sonar surveys were carried out along the established survey lines running at 50-m intervals and along transverse survey lines (cross-lines) running at intervals of 500 m.

During the surveys, the side-scan sonar operated at the frequency of 230/850 kHz to enable better interpretation of the seabed images recorded. The spacing of the survey lines allowed the recognition of objects with minimum dimensions of 0.5 m.

The sonar surveys were carried out using an EdgeTech 4205 sonar. The sonar transducer array was towed in a manner that allowed its good stability in the water depth. The positions of the sonar towfish were determined in real-time using an acoustic positioning system. Digital data from the side-scan sonar were recorded using the EdgeTech Discover software, and next, processed in the SonarWiz software.

1.3.2.2 Sonar data post-processing methodology

The sonar mosaic was prepared using the SonarWiz software. Individual profiles obtained during side-scan sonar surveys were entered into the application according to their coordinates, resulting in a sonar image of the area analysed, which consisted of overlapping profiles. To visualise the character of the seabed surface, data collected using high frequencies (850 kHz) were used. Filters sharpening the edges of the forms occurring in the survey area (side-scan edge detection), and next, also the nav smoothing filters were applied for smoothing the image when making the mosaic. For areas located directly under the sonar, in the so-called dead zone, the slant range correction (i.e. approximation) of data from both channels was performed. To obtain a uniform sonar image, it was necessary to adjust the gain strength of the signal emitted by the sonar (using the time-varying gain).

The sonar image is used as a basis for distinguishing the seabed types and forms of seabed relief for the purposes of the environmental work planned. The sonar image was also used to determine the anthropogenic objects on the surface of the seabed in the surveyed area, which could pose a threat or difficulty for the planned investment.

The sonar data processing flow chart is presented in Figure 1.4.

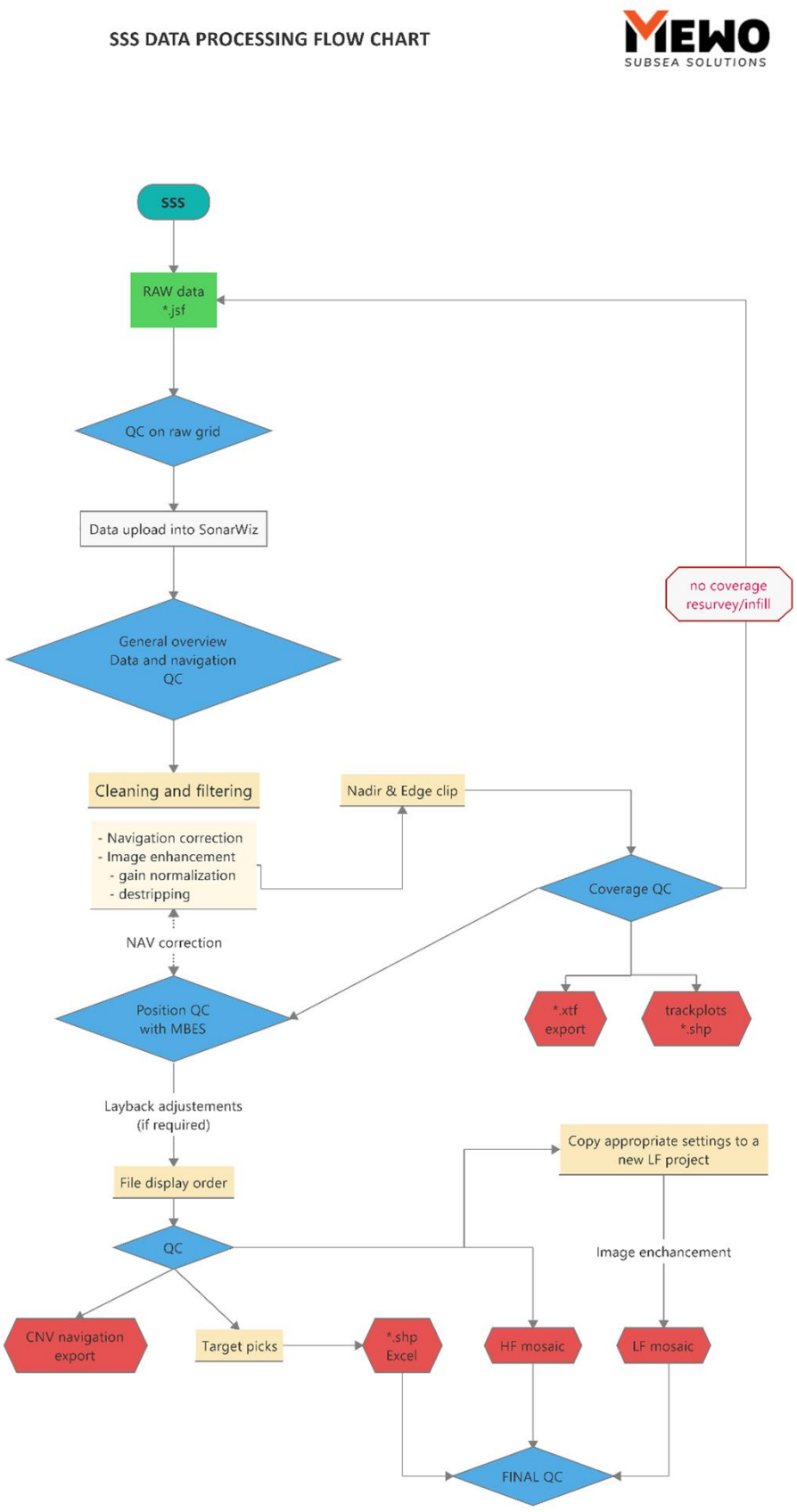


Figure 1.4. Sonar data processing flow chart

During the process of verifying the position of the objects found, the location of the objects on the seabed surface within the survey area was determined.

The correctness of the SSS positioning was confirmed based on MBES data.

1.3.3 Magnetometric measurements

1.3.3.1 Magnetometric survey methodology

Magnetometric surveys were carried out along the designated survey lines running at 50-m intervals and along cross-lines (transverse survey lines) running at 500-m intervals.

The magnetometric surveys were conducted using a set of two G882 caesium magnetometers (MAG1, MAG2) fitted on a TVG (Transverse Gradiometer) frame [Figure 1.5]. Data were collected using QPS QINSy software. The G882 magnetometer is characterised by a very high resolution (0.1 nT) and a sensitivity of 0.004 nT. Additionally, the device has built-in pressure sensors and an altimeter. The sampling rate was 10 Hz.

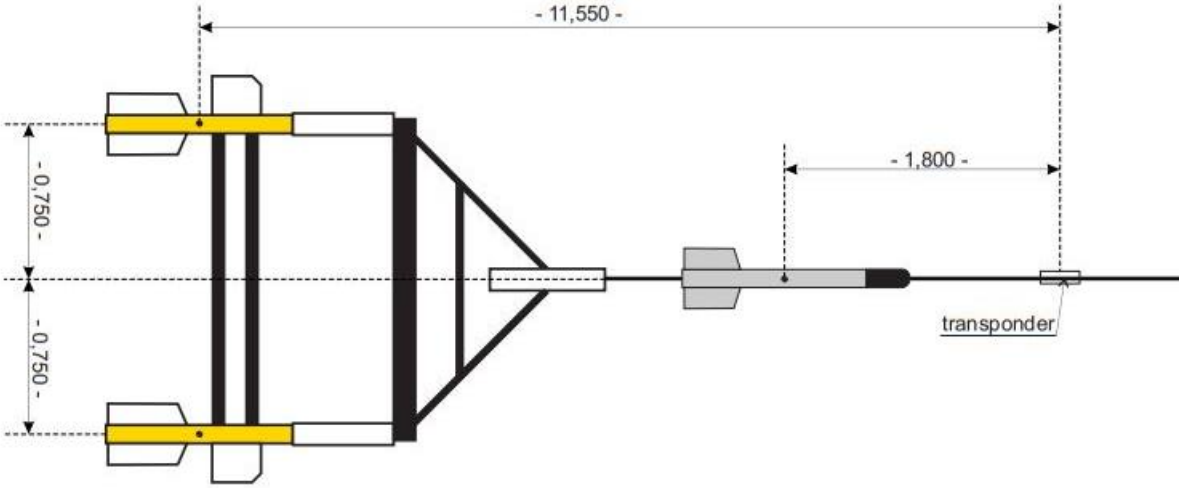


Figure 1.5. Magnetometer installation diagram, including distances between individual devices

During the surveys, the QPS QINSy system recorded the positions of the vessel, transponder installed on the umbilical cable, and magnetometer. The QPS QINSy system enabled the calculation of all the positions to obtain the actual position of the measuring sensor. Survey data were logged in the standard QPS QINSy format and ASCII format.

The character of the survey area and its natural conditions are the main factors determining the survey method. If the measuring instrument is towed too low above the seabed in conditions of variable bathymetry or varied seabed topography, it can hit the seabed or be dragged over it.

The size of the magnetic anomalies recorded depends primarily on the size (weight) of a given ferromagnetic object. Changes in the level at which the magnetometer is towed over an object can result in erroneous estimation of the anomaly value, whereas sudden changes in the altitude of the device above the seabed can lead to detecting false anomalies. It should also be taken into account that smaller objects can only be detected from a low altitude or at a short distance from the survey line. Only objects of considerable weight can be detected between survey lines.

The actual detection range depends on numerous factors, the most important of which are the distance from an object, the type of substance and its magnetic susceptibility as well as the burial depth. The detection range is calculated for the point sources of magnetic field anomalies. The detection range values lower than the actual altitude of the sensor above the seabed/the distance from an object mean that an object of a certain size will not be detected based on a magnetometric prospection.

1.3.3.2 Magnetometric data post-processing methodology

The magnetometric data collected were processed and analysed using the Oasis montaj software.

In the first stage of data processing, a non-linear filter and the nav smoothing filter for altimeter values were used to eliminate the resulting interference. Then, the X and Y coordinates were corrected. In the second stage, a preliminary low-pass filtering of the signal was performed, which eliminated all unwanted high-frequency components. After the filtering, altitude correction was applied, which removes the effects of differences in the altitude of the measuring device towing above the seabed between the survey lines. After satisfactory results were achieved, the field background values were calculated. The next stage aimed to obtain and analyse the residual field. For this purpose, the magnetic field background values were subtracted from the processed values obtained in the previous steps.

The remaining low-frequency components (magnetic field anomalies) indicated the presence of objects with ferromagnetic properties. Magnetic anomalies were marked using Blakely's method. Magnetic anomalies had been also identified along the measurement profiles before the initial data processing was started.

The diagram of magnetometric data processing is shown in Figure 1.6.

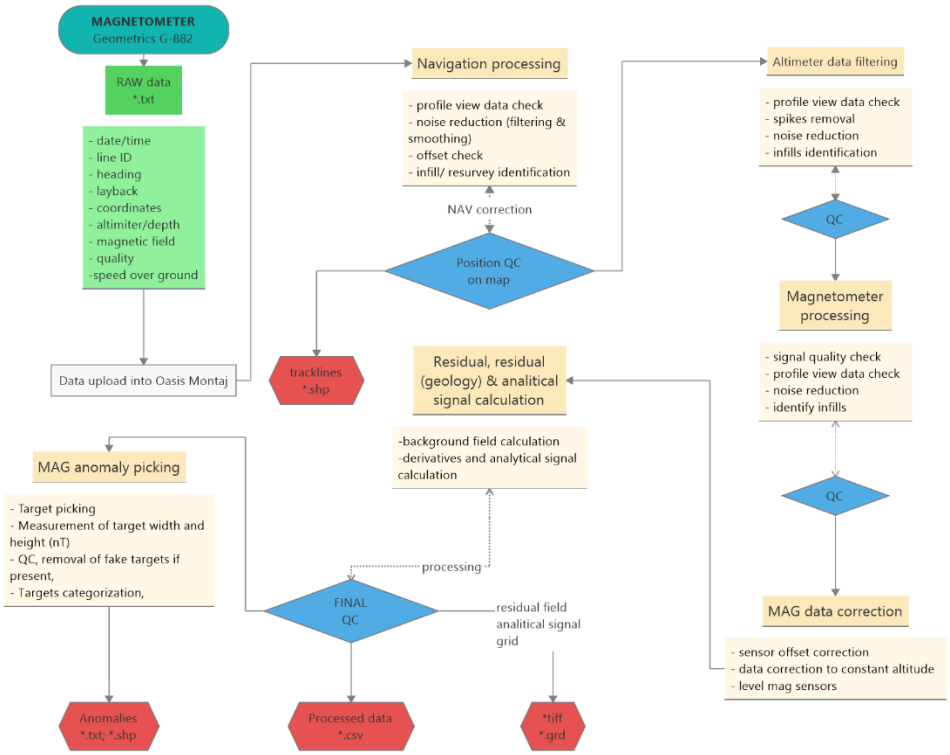


Figure 1.6. Magnetometric data processing flow chart

1.3.4 Surveys of man-made or unidentified objects on the seabed

1.3.4.1 Methodology for the surveys of man-made or unidentified objects on the seabed

The man-made or unidentified objects deployed on the seabed were identified based on previously gathered and processed bathymetric, sonar, and magnetometric data. The objects determined were marked for visual inspection using a remotely operated vehicle (ROV). The purpose of the ROV inspection was to confirm or verify the type of object, which cannot be unambiguously determined based on other data. Moreover, the nature of such objects, their role in the marine environment, and possible threats to the Investment resulting from the presence of these objects (especially wrecks and contaminants such as unexploded ordnance, duds, and chemical warfare agents) were verified together with their potential value in terms of cultural heritage and archaeology.

The inspections took place in previously designated inspection points. During the inspection process, observations of individual ROV parameters were carried out. Also, other possible messages displayed on the control panel which enable appropriate responses to non-compliance with the technical conditions were checked out.

1.3.4.2 Methodology for processing the data from the surveys of man-made or unidentified objects on the seabed

The Quality Control (QC) of the video data was carried out directly on the vessel during the ROV inspection conducted. If the video recording had an unsatisfactory image quality which prevented correct contact identification, a decision was made at that stage to repeat inspection whenever possible. If suspended solids agitated by mechanical factors associated with an ROV propeller operation were visible in the video image to an extent preventing object identification, the inspection was suspended until the conditions in the water stabilised and resumed only then. If a large content of suspended solids was due to natural and independent from ROV operation reasons (in which case it is difficult to predict the time needed for the conditions to improve), then a note describing these conditions was entered in the Survey Log.

A preliminary description of the ROV inspection results (analysis and interpretation) was made by the engineer carrying out the inspection. The final description of the results was made in the office. The video recordings were ultimately analysed and compared with the information from geophysical surveys.

Before each ROV inspection, weather conditions such as wind velocity and sea state, the accuracy of the vessel positioning, and the underwater positioning of the ROV were assessed and the correct operation of inspection devices was checked. During inspections, all changes in the survey conditions were recorded. The weather factors enabling the performance of surveys at sea as part of the ROV inspections in a manner ensuring the acquisition of survey data of appropriate quality are presented in Table 1.1.

Table 1.1 Factors enabling the performance of activities as part of ROV inspections in a manner ensuring the acquisition of survey data of appropriate quality

Weather factor	Activities affected by the weather factor	Permissible value
Wind	ROV inspection	<10 m s^{-1}
Sea state		Up to 4

GIS software was used to demonstrate object correlation. Due to the different methods of data acquisition, diverse buffers were used to correlate the different object types:

- MAG−SSS data correlation was performed by applying a buffer with a diameter equal to the distance between the survey lines designed and the magnetic anomalies. The magnetic anomalies inside the buffers were linked one by one using their unique IDs;
- the SBP–SSS data correlation was not applied because all SBP anomalies were marked as objects situated below the seabed surface;
- the SBP–MAG data correlation was applied in the same manner as SSS–MAG, but using a 15-m buffer;
- the ROV points did not require correlation as they were derived from the SSS data, which had been compared at an earlier stage.

1.3.5 Shallow seismo-acoustic profiling

1.3.5.1 Methodology for seismo-acoustic surveys using sediment profiler

Shallow seismo-acoustic profiling was carried out along the established survey lines running at 50-m intervals and along cross-lines (i.e. transverse survey lines) at 500-m intervals.

Shallow seismo-acoustic profiling was carried out using an Innomar SES-2000 Standard sediment profiler. The data obtained enabled the identification of the sub-surface sediment layers up to the required depth of approximately 6 m. The penetration depth depends on the type of sediments, therefore, penetration often reaches deeper than the indicated 6 m. This is particularly visible in the data collected within the seabed composed of fine-grained sediments, where no other horizon is distinguishable within the required scope of surveys. This provides information on the thickness of the fine-grained sediment. The sediment homogeneity in such a place is confirmed by, e.g., the top layer of the glacial sediments, visible much deeper (e.g. 15–20 m) in single-channel seismic data. In places, where another strong reflection appeared in the seabed structure, e.g. the top of glacial sediments, at a depth of approximately 7–9 m, this horizon was observed both in the sub-bottom profiler data and single-channel seismic data.

The Innomar SES-2000 Standard profiler set includes a console with a built-in computer for operating the measurement system and a transducer installed rigidly outboard. The device allowed operating in two frequency ranges: high, in which the primary frequencies (100 or 200 kHz) were used for precise determination of depth, and low (4–15 kHz), for the penetration of sediments forming the seabed. At the same time, the profiler was receiving the information on heave and pitch compensation thanks to which the data recorded are free from interferences caused by wave motion. SESWIN software was used for data acquisition.

To avoid accidental interferences between the Innomar SES-2000 Standard and the MBES system, both systems were synchronised during data acquisition. For this purpose, a multibeam echosounder was used as a trigger for the Innomar SES-2000 Standard system. Signal interferences were regularly checked and assessed during the data quality control.

The ping rate (signal emission frequency) was specified automatically by the recording software and was from 3 to 5 kHz, which results from the length of a single synchronisation cycle in external triggering, taking into consideration the recording length and the delay.

1.3.5.2 Seismo-acoustic data post-processing methodology

The processing of seismo-acoustic data obtained from a pinger sub-bottom profiler (SBP) was carried out in the DUG Insight software, whereas, their interpretation was performed in the Kingdom software manufactured by Markit Group Limited (S&P Global Limited).

Data were collected in *.raw format, which requires conversion into standardised *.sgy format. *.raw files were converted in the SES Convert software. In effect, low-frequency *.sgy files were obtained which underwent further processing. If navigation spikes occurred, they were levelled using the SGY TOOL software, which interpolates the correct equipment altitude based on the points surrounding the spike.

Processing of SBP data included, first of all, merging *.sgy files into a single file, if the size of the file saved for a given line exceeded the acquisition program defined. The SBP files which required merging into one file were uploaded into a data processing software in separate instances of the input process, with the application of the CMP renumbering, if needed, to maintain consecutive continuity. Successively, the products of each instance were merged into a single, coherent seismic image sorted to the CMP collection – given the good alignment, no need to apply further corrections to the statics between individual instances was observed.

After merging, an analytical moving average algorithm was applied, which compared the average square amplitudes between a wide (7 traces) and a narrow (1 trace) window and correlated the difference obtained with the pre-set scaling factor with a value of 3. If the amplitude of a given sample was smaller than or equal to that factor, it remained unchanged; however, if it exceeded the factor, it was replaced with the value of the amplitude computed using the alpha-median filter.

In the next step, the amplitude scaling was applied between adjacent tracks, due to their variable scaling by the acquisition programme.

The final step of the signal processing was a convolution with the pre-computed debubbling operator to minimise the intensity of mechanical wave reverberation below the seabed.

The flow chart for processing data acquired using a sub-bottom profiler is presented in Figure 1.7.

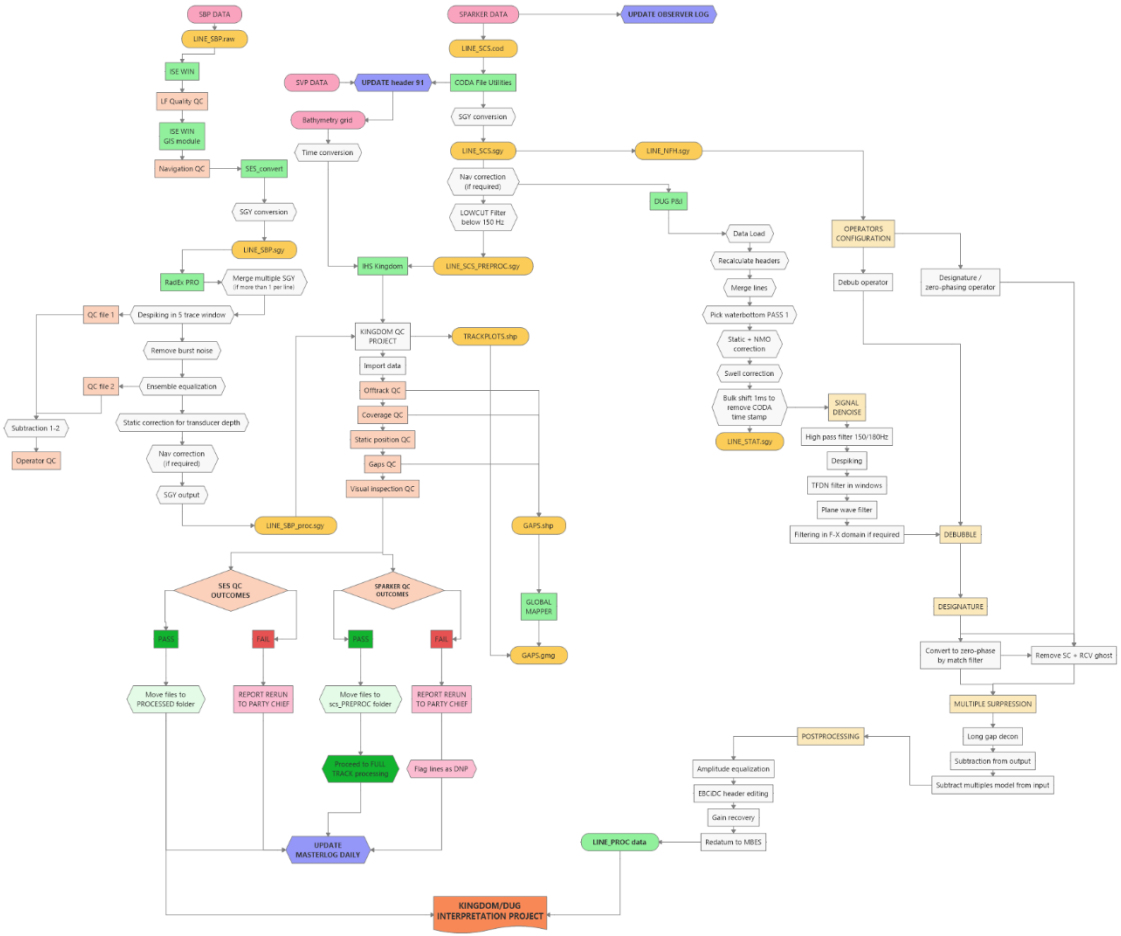


Figure 1.7. Seismo-acoustic and single-channel seismic data processing flow chart

1.3.6 Seismic surveys

1.3.6.1 Single-channel seismic surveys

1.3.6.1.1 Single-channel seismic survey methodology

To obtain a two-dimensional image used for determining the geological structure up to a depth of approximately 45 m, surveys were conducted using the seismic reflection method with a streamer, i.e. a single-channel set of receivers, and a sparker (an acoustic wave induction source) with a broad frequency band. A set of single-channel hydrophones (streamer) HYD-150/20 manufactured by Applied Acoustic and a Dura-Spark UHR Sparker induction source by the same company towed behind the vessel were used. Single-channel seismic surveys were carried out along the designated survey lines running at 50 m intervals and along cross-lines spaced at an interval of 500 m. The surveys were carried out with the participation of Marine Mammal Observers and a passive acoustic monitoring (PAM) operator on board a vessel, in accordance with the guidelines of the British Joint Nature Conservation Committee.

The sparker emits an acoustic signal in the form of a pulse, which is generated as a result of capacitors discharging along a system of electrodes installed on a frame. The electrical discharge created a vacuum bubble. When the burst, it generated a broadband, multi-directional acoustic pulse that penetrated individual geological layers.

The returning acoustic signal was received by a set of single-channel hydrophones distributed closely enough to treat them as a single element. The signal was transformed into electric energy and after that, converted by the transmitter into a digital signal for further processing.

CODA GeoSurvey DA 2000 software is used to acquire data collected using a streamer with a sparker source. Data are saved in *.cod format.

1.3.6.1.2 Single-channel seismic data post-processing methodology

Post-processing of single-channel seismo-acoustic data is done using the DUG Insight software. *.cod format requires conversion to the standardised *.sgy format. *.cod files were converted in the Coda File Utilities software. As a result of this operation, *.sgy files were obtained. The purpose of the data quality control is to eliminate navigational errors and indicate locations for re-runs (e.g. due to poor quality of data, gaps in data, etc.). During data processing, high-pass filters and swell filters were used. After offset calculation between the receiver and source, NMO correction was also added. Upon re-assessment and validation, the data were properly processed. At that stage, with the use of DUG Insight software, the data was processed via embedded filters, selected according to needs: low cut, TFDN, dip, signature de-ghosting, and multiple removal by decon.

The single-channel seismo-acoustic data processing flow chart is presented in Figure 1.7.

The number of SCS files for which re-runs were required was insignificant. Individual sections were subjected to CMP recalculation and then uploaded to the data processing software as a single raw seismic image sorted to the CMP collection. Applying a static correction as a standard processing procedure neutralised any potential vertical differences between the files, as it included corrections applicable to the SVP lines recording time and offsets.

SCS processing began with removing electrical interferences in the band of approximately 60–240 Hz using a low-pass filter. Each time, it was verified whether the coherent useful signal had not been removed.

The next step involved applying the Normal Move-Out (NMO) correction and static correction to data. The first stage of NMO correction was carried out using a theoretical offset of 11.25 m measured and computed during mobilisation together with the SVP data. In the data with the NMO filter applied, the direct acoustic wave arrival time was picked and the value was used to compute the actual offset for each shot, by estimating the difference between the theoretical and the observed DA time. After entering the new offset value, it was implemented into the input data set; next, NMO was applied again with that value, this time, with actual offset values for each shot. As a result, the data gained the actual vertical position, although still with a visible wave motion effect. To neutralise it, the first breaks of the signal reflected from the seabed were picked and a static correction was applied to each route, with a value equal to the difference between the pick and the bathymetry grid converted to the time domain.

After introducing a static correction, time-frequency denoise (TFDN) filtering was applied through separation and filtering of the data separately in two frequency bandwidths: 0–256 Hz and 256–512 Hz.

The next step was standard filtering. Concerning the data and lines, a filter was applied in 0–256 Hz and 256–512 Hz bands with threshold values of 2.5 and 1 for the data from 0–256 Hz range and 2.5–1.5 for the data from 256–512 Hz range.

In both cases, 21 adjacent traces were used in the filter estimation window and 8 traces were selected in each window to be converted to the T(f) domain using the Fourier transform. The data filtered were subtracted from the input data. Noise model muting was applied from approximately 1 ms below the seabed upwards to limit the modification of the seabed reflection that could result in an incorrect estimation of the far-field operator construction.

The last element of the noise reduction process was the plane wave dip filtering. To this purpose, the data were divided again into two components: first, 0–128 Hz and second, 128–512 Hz. Vibration propagation speed values were applied at a level of 1.11 ms/upper trace and 5 ms/upper trace in the case of both 0–128 Hz and 128–512 Hz windows. The same speed values were adopted for the upper and lower filters. The window adopted for the filter had a length of 25 ms with a 50% overlap.

Data filtered from the noise were then used to create debubble operators as well as de-ghosting and zero-phasing operators. A range of approximately 30–40 traces from the line was selected; next, the first input was moved to 0 TWT and cross-correlation was carried out to precisely position the first input – for the debubble operator, on the sample containing the local minimum phase extremum, whereas, for the zero-phase and de-ghosting operators, on the first sample opening the minimum oscillation. The traces aligned in that way were merged into one – operator input – and auto-correlated to determine the length of the deconvolution operator and its gap. Deconvolution parameters designed in that way were applied to the stacked track and a deconvolution operator was exported as the result of the operation, which was later on convoluted with the entire collection of tracks for a given line.

A very similar process was designed for converting traces in the minimum phase convention to zero phase. The difference was the application of a signature de-ghosting operation consisting of a predictive deconvolution of the complex operator trace to find the recurring component in inverted polarity, which is a back reflection from the water surface, by estimating its vertical position using data

on byte 41 and 45 of the trace headers, where the information about the approximate towing depth of the source and receivers is stored, and next, the adaptive subtraction from the input trace. Only then, the track prepared in that way underwent autocorrelation and subsequent construction of the Weiner filter, which was exported as a wavelet and imposed on each track in the input line after debubbling.

After zero-phasing, a deconvolution with a gap defined between horizon H1 – the seabed, and horizon H2, specified by the proportion H1 = H2*1.98, was applied to the data. In that way, multiple reflections from the seabed were removed from the seismogram.

Finally, spherical divergence correction was carried out by applying the gain in specified windows – with the following scalars: 0.001 on 0 TWT, 1 on the seabed position and 3 on the horizon H2 position, respectively.

1.3.6.2 Multi-channel seismic profiling

1.3.6.2.1 Methodology of multi-channel seismic surveys (2D UHR)

The surveys using the seismic reflection method were conducted to obtain a two-dimensional image used to identify the geological structure of the medium in the upper part of the subsurface zone, at least up to the depth of the WTG foundations. Multi-channel seismic surveys were performed using a set of Geoeel Silicone Gel multi-channel hydrophone array (streamer) made by Geometrix and an excitation source, which was the Double Deck Dura-Spark UHD 400+400 multi-electrode sparker, operating in the alternating mode, towed behind the vessel.

The multi-channel seismic surveys were carried out along the established survey profiles at 200-m intervals and along the cross-lines (transverse survey lines) at 2000-m intervals. The surveys were carried out with the participation of Marine Mammal Observers and a passive acoustic monitoring (PAM) operator on board a vessel, in line with the guidelines of the British Joint Nature Conservation Committee.

Figure 1.8 presents the distribution of offsets for the streamer and sparker.

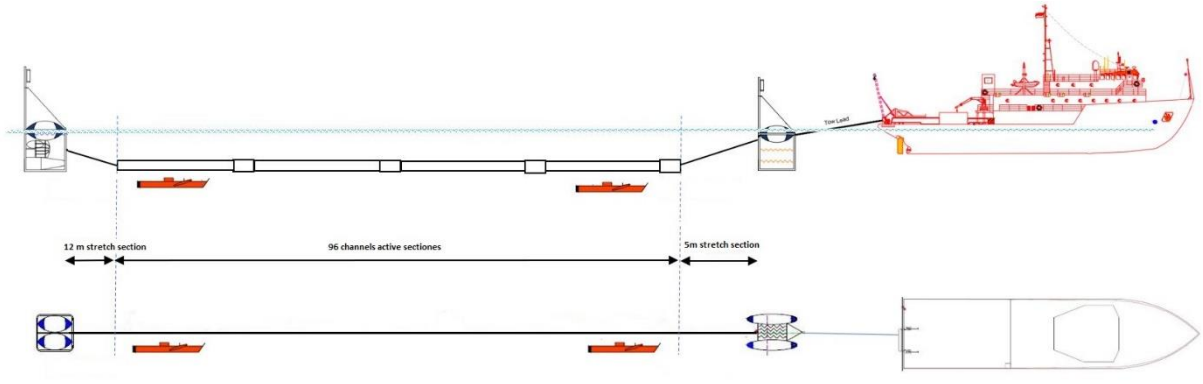


Figure 1.8. The distribution of offsets for the streamer and sparker

The streamer geometry applied assumes that the streamer is towed directly by the sparker, which makes the horizontal separation between the sparker and the streamer equal to zero. The geometry did not provide for the use of a front buoy as the main source of information on the close offset. To monitor the position and direction of the front part of the streamer during the acquisition, an AA 101G

MiniPod Submersible GNSS receiver antenna connected to the acquisition system, installed on the sparker, was used.

The sparker signature (stable and clear signal at the maximum power and frequency) was verified using a hydrophone installed on the sparker skid, while the characteristic features of the source signal were recorded on the recording oscilloscope.

All seismic data were recorded with the appropriate precision with the amplitude clipping unaccepted.

Source signature data in the Seg-D format were delivered together with the other data acquired.

To avoid the direct impact of the seismic source on marine mammals appearing within the seismic survey area, “soft-start” measures were used for the source, which involved a gradual increasing of its power over at least 30 minutes up to the level required.

1.3.6.2.2 Multi-channel seismic data post-processing methodology

The 2D multi-channel seismic data were recorded in SEG-D format, with each gather saved in a separate file. The position of each shotpoint was recorded in a navigation file based on the relationship between the vessel position and the assumed geometry or directly from the GPS antenna installed on the seismic wave source. In the first stage of processing, the data were loaded as SEG-D files into a program dedicated to seismic data processing and converted to the internal data format in this software.

Then, each shotpoint was assigned the appropriate coordinates, and imported from the navigation file. Next, data on the geometry of the system were entered. On this basis, the coordinates for each channel in each gather were calculated and, as a result, the exact coordinates of each Common-Mid-Point were obtained (which is known as CMP binning). After the positioning had been imported, its correctness was verified, e.g. by matching the theoretical direct wave hodograph to the recorded gathers.

In the next step, the data were pre-filtered, using the noise characteristics recorded on SoL and EoL and utilising mathematical tools available in the program, including the bandpass, Butterworth, and F-K filters, the removal of incoherent and random noise as well as the direct wave spectrum. After applying the filters, the first longitudinal wave inputs, which are the signal reflection from the seabed, were picked, and then muting of the paths above the picked TWTs, i.e. the water column, was introduced. After the initial cleaning of the data from noise, it was necessary to correct the amplitude losses associated with the spherical displacement of the seismic wave. The key process in the processing was the source designation and elimination of the ghost phenomenon in seismic data.

The data filtered in this way were stacked in a so-called super-gather, constituting a common-offset stack for a relatively large number of neighbouring gathers. For a better clustering of interval velocities, it was allowed to introduce the preliminary removal of multiple reflections (with demultiple techniques) at this stage. Next, an interactive analysis of NMO velocities was performed. Then, the velocities were picked and used for the NMO correction. It should be emphasised that the process of determining the NMO kinematic correction was iterative and repeated several times during the processing sequence with increasing resolution. The first result of the stacking was a control brute-stack, which was the starting point for further corrections of the velocity analysis.

After applying the NMO shift, the actual stacking took place with a fixed fold value; if necessary, additional filtering could be applied after stacking. In the next step, using algorithms specific to the program used, all events that were multiple reflections were eliminated.

The next procedure was data migration to obtain the correct dip angles of the reflection boundaries. For this purpose, the finite-difference (FD) migration was conducted in discretised space or the Kirchoff migration method with the assumption of Huygens hyperbolas was used.

After migration, the data were moved to MSL, based on the first reflection, which was a reflection from the seabed, compared with the bathymetry grid converted to the time domain (using SVP/CTD sounding data).

The data processed in this way were exported to the standard SEG-Y format with headers supplemented in accordance with the EBCDIC Standards.

The multi-channel seismic data processing flow chart is presented in Figure 1.9.

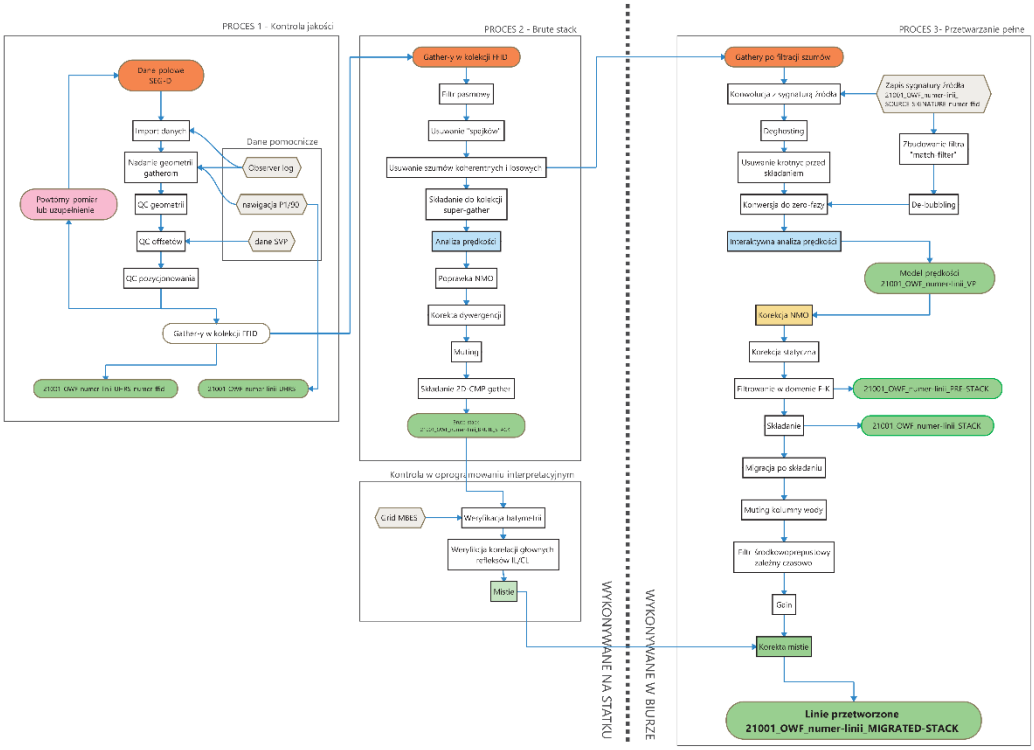


Figure 1.9. Multi-channel seismic data processing flow chart

1.3.7 Soil sampling

1.3.7.1 Surface sediment sampling

1.3.7.1.1 Surface sediment sampling methodology

Surface sediment sampling was carried out to identify the sediments forming the seabed surface and indicate the areas with potential aggregate deposits. Surface sediment samples (in a total of 118) were collected using a van Veen grab sampler.

The secured surface sediment samples were transported to the Geotechnical Laboratory of the Maritime Geotechnics Department at the Maritime Institute of the Gdynia Maritime University (MGD MI GMU). The samples were placed in a room with controlled and recorded temperature. The sample storing temperature is in the range of 5–25°C.

1.3.7.1.2 Methodology for the laboratory testing of sediment samples

The samples collected underwent analysis in compliance with the PN-EN ISO 14688-1:2018-05 and PN-EN ISO 14688-2:2018-05 standards.

Altogether, 118 surface sediment samples collected within the survey area using a van Veen grab sampler, were delivered to a stationary laboratory on land. In the Geotechnical Laboratory of the MGD MI GMU, the samples were stored in a room with a controlled temperature. The sample storing temperature was monitored and kept in the range of 5–25°C. The proper conditions were ensured thanks to the use of refrigerated containers with temperature regulation.

The surface sediment samples collected from the survey area were macroscopically examined in compliance with the PN-EN ISO 14688-1:2018-05 and PN-EN ISO 14688-2:2018-05 standards and a photographic documentation was prepared. The macroscopic description included the identification of the fractions (taking into account additional components such as shell and wood fragments, etc.), determination of the colour, carbonate content (on a 4-point scale) and consistency (for fine-grained soils). The information from the macroscopic description of the samples is presented in the form of a summary table. The photographs taken during the macroscopic description are provided in digital form.

The samples were subjected to sieve analysis in the case of coarse-grained sediments (sand ad gravel) and, if need be, areometric analysis in the case of fine-grained sediments (sands with silt, silts, and clays). The identification and classification of the sediments were conducted in line with the PN-EN ISO 14688-1:2018-05 standard.

As part of the sieve analysis, grain size analysis of coarse-grained sediments was determined by dry-sieving. A standard set of sieves used for the sieve analysis is presented in Table 1.2.

Table 1.2. A standard set of sieves for sieve analysis

Sieve number	Mesh aperture [mm]
1	63
2	32
3	16
4	6.3
5	4
6	2
7	1
8	0.5
9	0.2
10	0.125
11	0.063

The analyses were conducted with the use of a laboratory shaker. Before the analysis, the samples were dried for 24 hours at a temperature of 105°C.

The areometric analysis was carried out on the samples which contained more than 10% of particles with an equivalent diameter below 0.063 mm. The test procedure is based on Stokes's law. From each sediment sample, a suspension was prepared by mixing an appropriately sized sample with a water-

dispersant solution (in this case, sodium hexametaphosphate was used). The mixture was next strained through a sieve with a mesh aperture of 0.063 mm. The sediment that remained on the sieve was dried and sieved (in compliance with the procedure for coarse-grained soils), and the decanted suspension was poured into a cylinder. Density readings were taken using a suitably calibrated hydrometer at appropriate intervals over 24 hours. Changes in the suspension density occur as a result of the particles falling down. The equivalent particle diameters and the content of individual fractions were determined based on Stokes's law.

During the laboratory testing and sample storage, the material was not utilised.

1.3.7.2 Core sampling

1.3.7.2.1 Core sampling methodology

To confirm the arrangement of shallow sediment layers and to determine the presence of potential aggregate deposits, core samples were collected using a VKG 3-6-9 vibrocorer. The vibrocorer includes an approx. 250-kg vibrator mounted on a guide resting on a frame, which was placed on the seabed. A stainless-steel pipe with a protective PVC liner inside was driven into the ground using vibrations with a frequency of approx. 28 Hz. The liner was used to protect the core while driving the core barrel into the ground.

The core barrel had a one-way valve at one of its ends, which closed during the retraction of the device, thus generating a vacuum holding the core inside. At the other end, a special cutting head (cutting shoe) was screwed onto the barrel together with a basket-type core catcher (so-called “orange”), ensuring that the soil sample was cut off and kept inside the sampler during its retraction from the ground. A band was installed on the side surface of the core barrel, the location of which after sampling completion indicated the depth of penetration reached during the sampling attempt.

The vibrocorer was lowered from the vessel using a stern-mounted gantry. The vibrocorer and the electronic automation systems are powered and controlled using an umbilical connecting the device with the power supply and control system located on the vessel.

The sampled cores were up to 6 m in length. If the minimum yield length required for sampling acceptance, which is 4.5 m, was not obtained, a second attempt was made at a location offset by approximately 5 m. If the second attempt was also unsuccessful, no further attempts were made. The samples collected were divided into 1-m sections, and then the sediments located at the core cross-sections were described macroscopically in line with PN-EN_ISO 14688-1:2018-05 standard.

After the tests conducted aboard the vessel were completed, the samples were sealed in core barrel sections with caps and tape. Each core fragment was marked accurately. In the period between the sampling and the beginning of the tests, during the tests, as well as after their completion (during the storage period), the samples were kept in conditions which ensured a temperature range of 5–25°C maintained.

1.3.7.2.2 Methodology for the laboratory tests of core samples

Core samples, which had been collected using vibrocorer, were delivered to the laboratory on land. In the Geotechnical Laboratory of the MGD MI GMU, the samples were stored in a room with a controlled temperature. The sample storing temperature was monitored and kept in the range of 5–25°C. The proper conditions were ensured thanks to the use of refrigerated containers with temperature regulation.

The onshore laboratory tests were performed in an accredited facility – the Geotechnical Laboratory of the MGD MI GMU (PCA accreditation number: AB 1770).

After opening, single core parts were placed together on a table under special lights. The surface layer of the soil was slightly trimmed and cleaned to show its internal structure for the purpose of photographic documentation and further description. The macroscopic description was conducted in line with the PN-EN ISO 14688-1:2018 standard. The macroscopic examination included the determination of the main and secondary fractions, the contents of carbonates and organic substances (where possible). During the macroscopic description, geotechnical layers were determined (using lithological-genetic criteria) and soil colours were specified according to the PN-EN ISO 14688-1:2018 and Munsell Soil Colour Charts as a base scale. The results have been presented in the borehole logs.

The grain size analysis of granular soils was determined with the use of dry sieving. Sieve analyses were conducted in compliance with the PN-EN ISO 17892-4:2017-01 standard. The diameters of test sieves used during the tests are collated in Table 1.2.

To complete the tests, vibrating mechanical sieve shakers were used. The soil classification based on the PN-EN ISO 14688-2:2018-05 standard was used. Granular samples for which more than 10% of the total soil passed through the 0.063 mm sieve were selected for areometric analysis (including sieve analysis).

The grain size analysis of fine-grained soils (soils with more than 10% fine fractions) was determined by the combined sieve and sedimentation analysis with the use of the areometric method. The tests were conducted in accordance with the PN-EN ISO 17892-4:2017-01 standard. Demineralised water and a dispersing agent (sodium hexametaphosphate, approx. 40 $g \cdot l^{-1}$) were used for the tests. The soil classification based on the PN-EN ISO 14688-2:2018-05 standard was used.

1.4 ACTIVITIES PERFORMED

The sequence of activities conducted as part of the geophysical surveys was as follows:

- delineating the survey lines in the survey area;
- bathymetric, sonar, magnetometric, and seismoacoustic measurements using a sediment profiler and single-channel seismic profiling in the survey area from 18 February to 5 August 2023;
- collection of surface sediment samples using a van Veen grab sampler was carried out in the survey area on 22–23 and 27–28 February 2023. 118 samples were collected from 118 survey stations;
- surveys with the use of multi-channel seismic profiling in the period from 26 September 2023 to 1 February 2024;
- core sampling in the survey area from 1–12 December 2023. Altogether, 39 core samples were collected from 39 survey stations;
- ROV inspections of 155 man-made objects and objects of unknown origin in the period from 27 December 2023 to 14 February 2024;
- processing data obtained during the works conducted as part of geophysical measurements;
- preparing the result maps of the examined survey area.

1.5 RESULTS

1.5.1 Bathymetric surveys

For bathymetric surveys conducted with the use of a multibeam echosounder, full coverage of the seabed was ensured. Based on the data collected, a bathymetric map [Figure 1.10] and a map of seabed slopes [Figure 1.11] were developed.

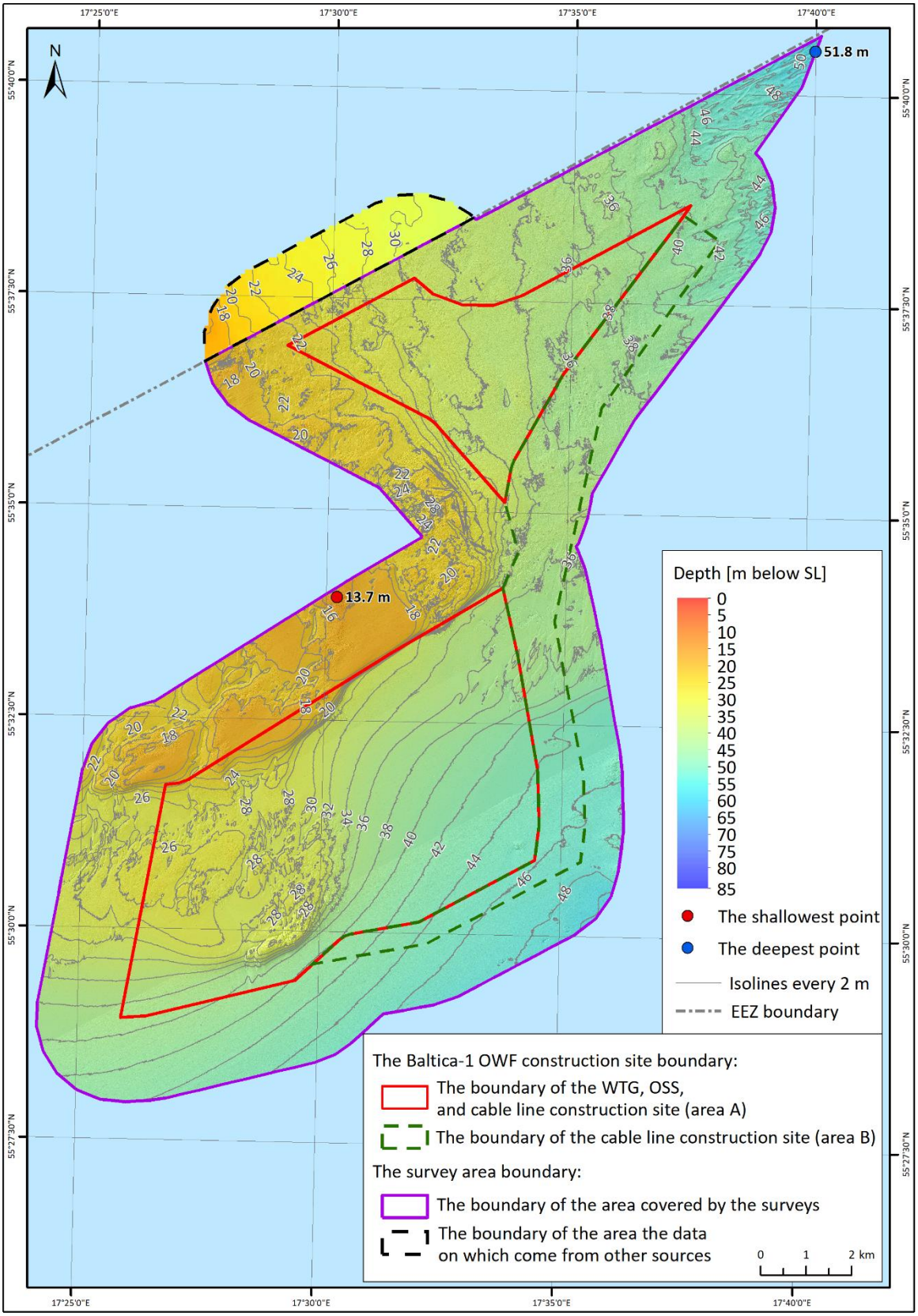


Figure 1.10. The bathymetry of the survey area

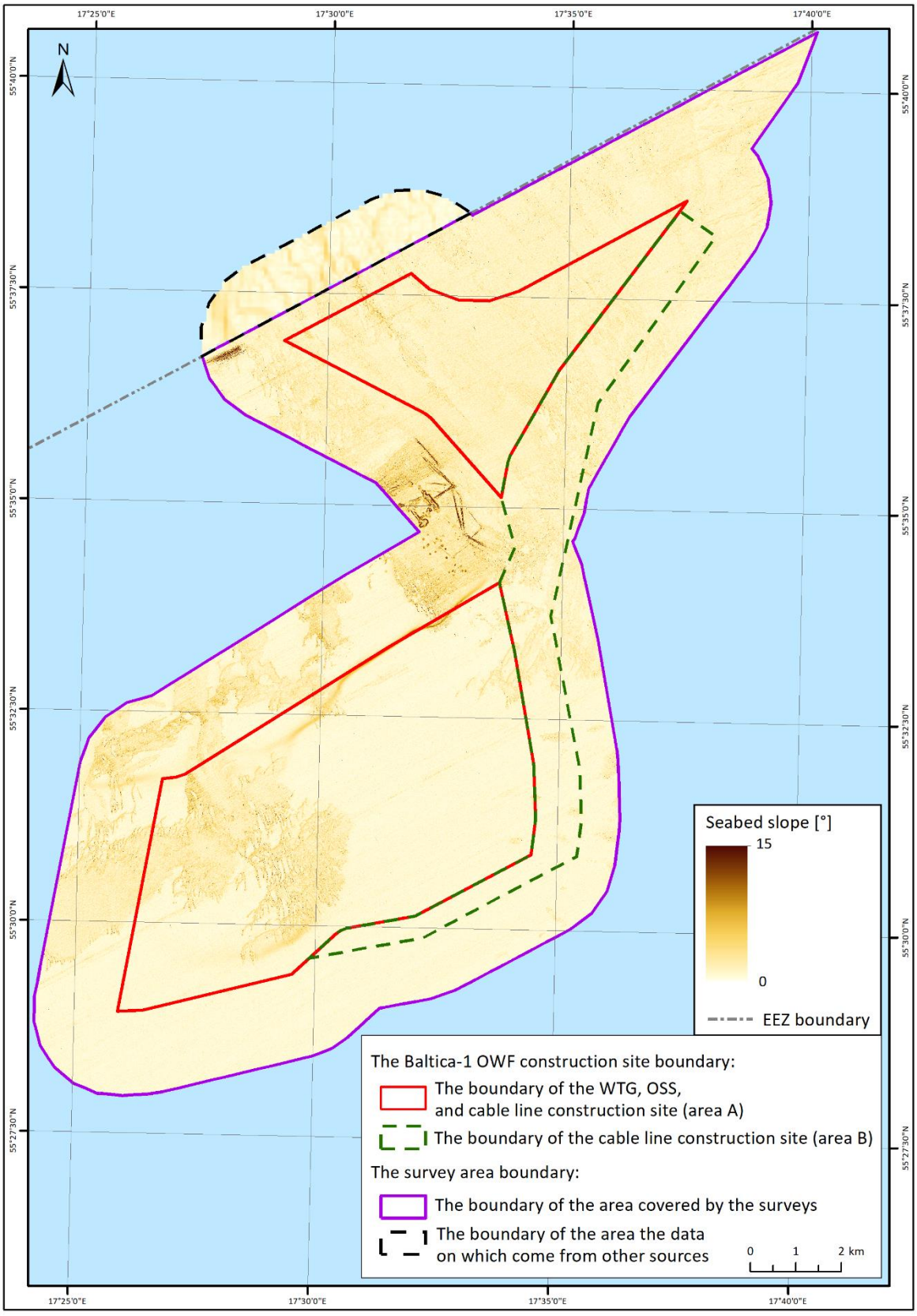


Figure 1.11. The map of the seabed slopes in the survey area

1.5.2 Side-scan sonar survey

Side-scan sonar surveys were performed in a way that ensured full coverage of the seabed. On their basis, a sonar mosaic was created for the survey area [Figure 1.12].

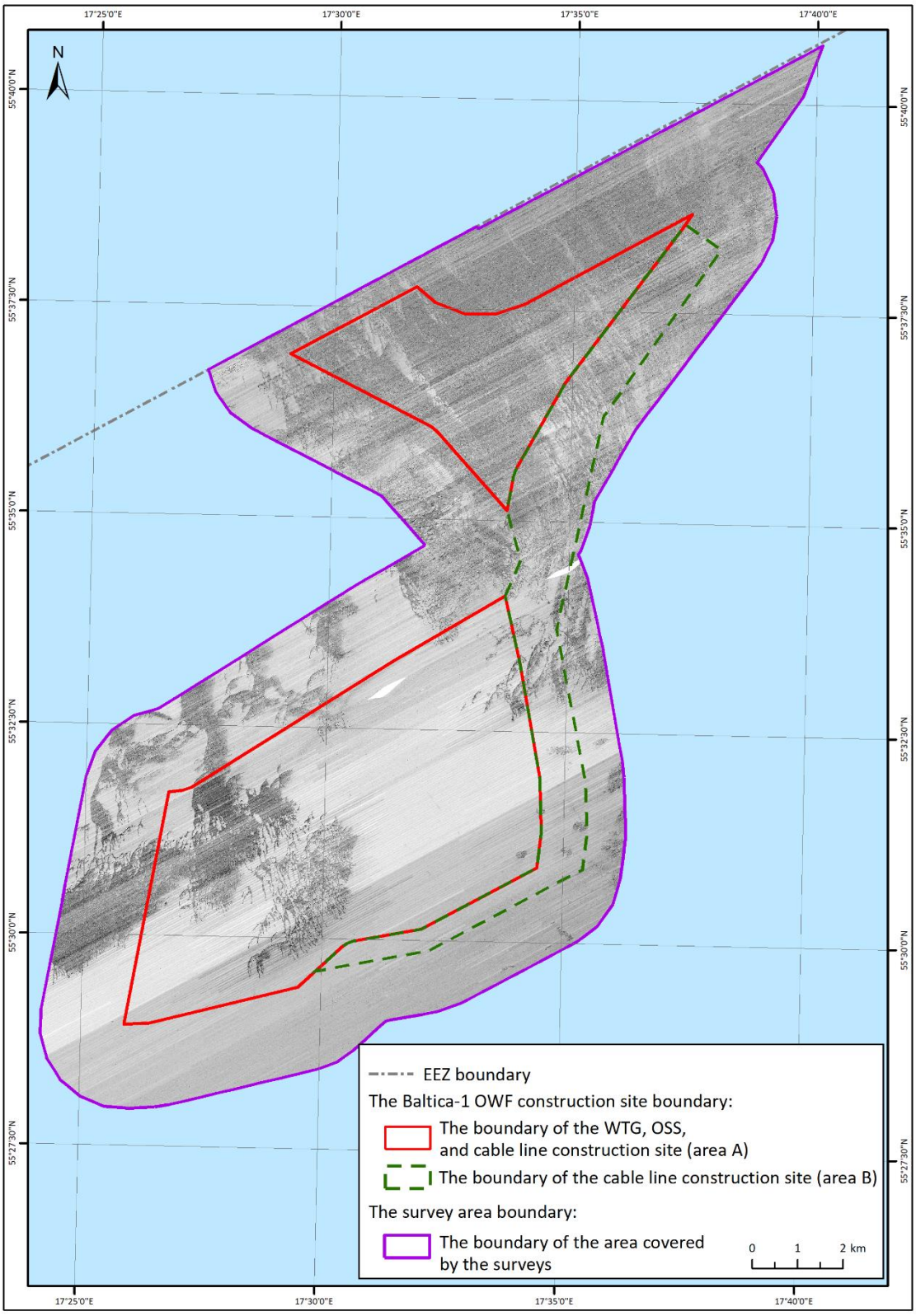


Figure 1.12. The sonar mosaic of the survey area

1.5.3 Magnetometric measurements

Magnetometric measurements were carried out along survey lines designated within the survey area. Based on the data collected, maps of the residual field and magnetic anomalies were developed [Figure 1.13].

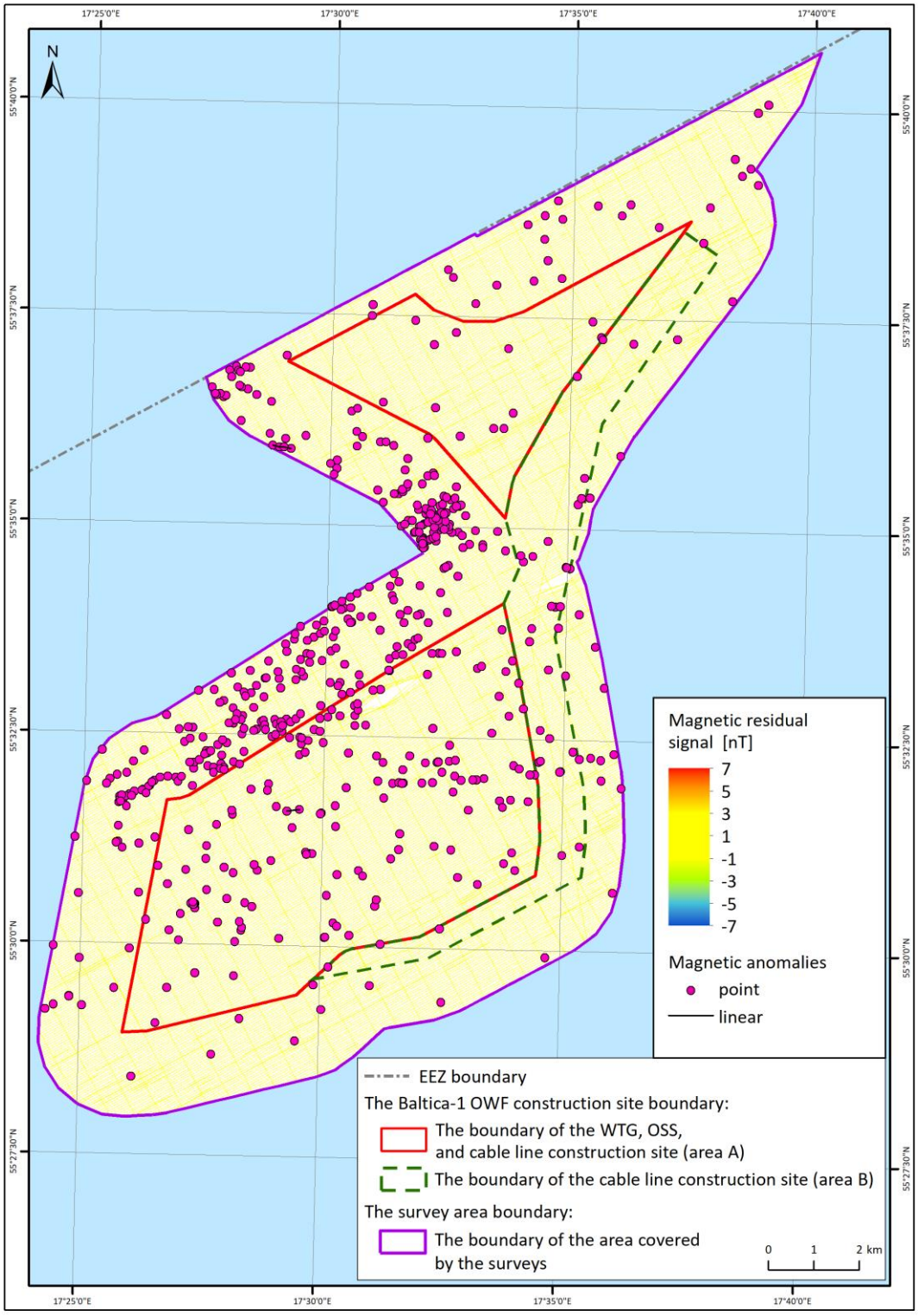


Figure 1.13. The map of the residual field strength in the survey area together with the magnetic anomalies detected

Based on the surveys conducted and the residual signal calculated, two linear objects and 599 point magnetic anomalies were identified in the survey area. One object was classified as linear due to the occurrence of magnetic anomalies on adjacent profiles. Most objects (63.77%) were recorded by the sensors as dipoles. All magnetic anomalies were compared with the bathymetric and sonar information to verify the possible presence of objects on the seabed. The area where the dredging works had been conducted within the framework of the extraction operations from the "Południowa Ławica Środkowa" (Southern Middle Bank) deposit in the Southern Baltic Sea, was clearly distinguishable in the magnetometer data due to the irregular shape of the seabed and the highly variable depths after sediment extraction.

Table 1.3 contains the number of magnetic anomalies detected in the form of points and lines. Most objects were recorded by the sensors as dipoles. Two objects were classified as linear due to the occurrence of magnetic anomalies on adjacent profiles.

Table 1.3. The statistics of magnetic anomalies based on their shape

Number of point anomalies	Number of linear anomalies	Monopoles [%]	Dipoles [%]
599	2	36.29	64.69

Additionally, based on the magnetometer surveys, the residual geological signal was determined [Figure 1.14]. The signal image obtained is homogeneous and uniform. Differences in field values are noticeable in areas with single boulder clusters on the seabed, usually around 3 nT relative to the 0 nT level. No areas which could point to a significant impact of the geological structure on the magnetometer surveys conducted were identified.

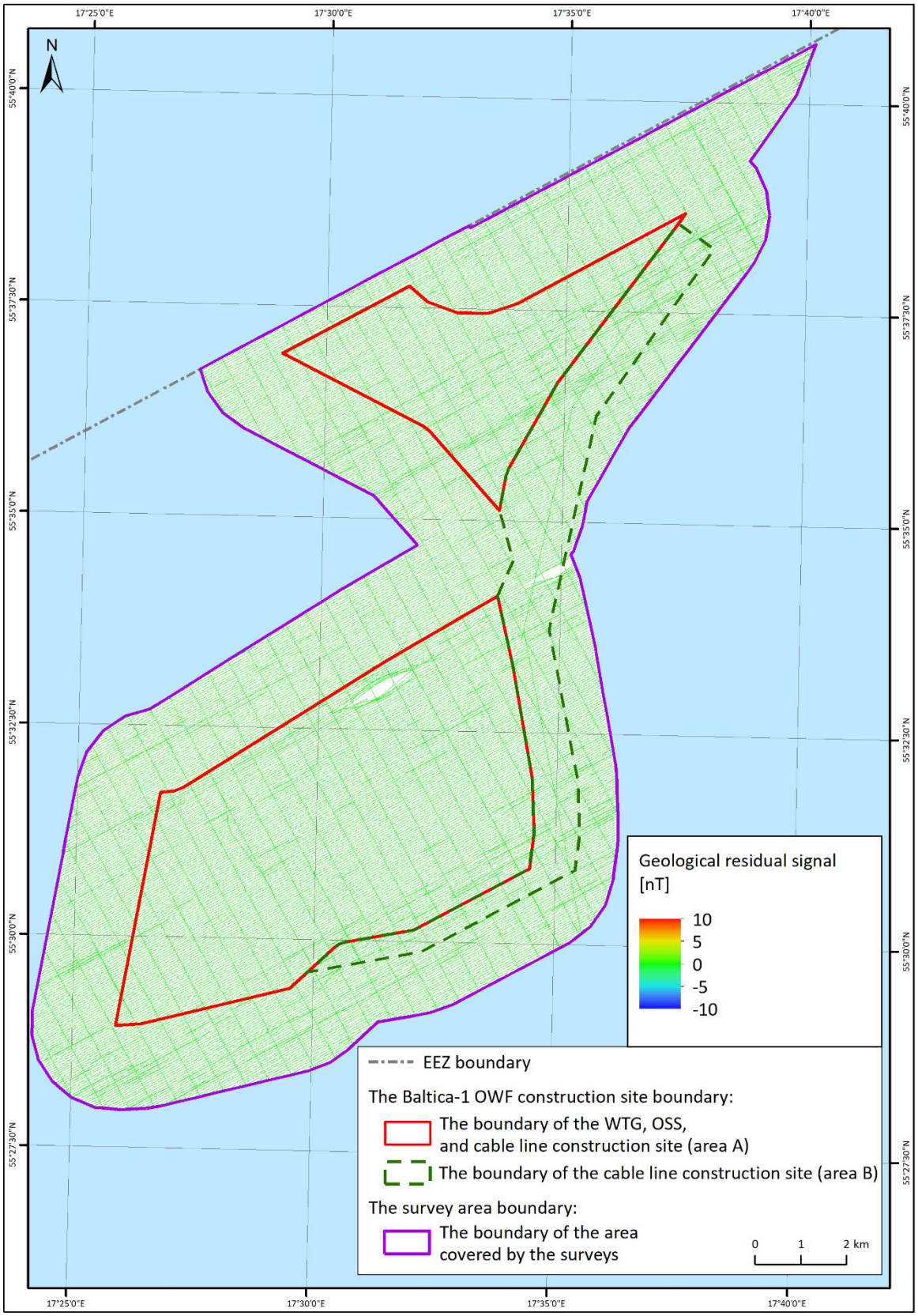


Figure 1.14. The map of the residual geological signal in the survey area

1.5.4 Surveys of man-made or unidentified objects on the seabed

A total of man-made or unidentified objects 1460 objects deployed on the seabed were marked based on the data collected. Based on the bathymetric, sonar and magnetometer data analysis, a total of 155 objects were selected for visual inspection using a remotely operated vehicle (ROV). The purpose of the ROV inspection was to verify potential unexploded ordnance and identify/confirm the presence of wrecks or other objects significant/dangerous for the implementation of the OWF. Most objects identified during the ROV inspections were classified as man-made objects or geomorphological formations. The video material acquired confirmed the presence of man-made objects such as fragments of shipwrecks, aeroplane components, fishing nets and ropes, logs, tyres, tree branches, and wood debris.

Table 1.4 below presents statistics on 1460 objects of anthropogenic or unidentified origin. The objects were classified based on all the surveys and observations conducted. The division of object classes was presented based on the guidelines of the International Association of Oil and Gas Producers (IOGP) for the SSDM database.

Table 1.4. The types of man-made objects or objects of unidentified origin on the seabed

Object type	Number of objects	Percentage of all objects [%]
Potential man-made objects	172	11.8
Wrecks	5	0.3
Linear objects (nets, ropes)	55	3.8
Cables	1	0.1
Unidentified object of uncertain origin	116	7.9
Accumulation of various types of debris of varied, uncertain origin	11	0.8
Other objects difficult to assign to other groups	42	2.9
Geological objects	23	1.6
Elongated objects	1035	70.9

The locations of the objects designated for the ROV inspection are presented in Figure 1.15. Example results of the inspections conducted are presented in Figure 1.16 and Figure 1.17, which include a fragment of the bathymetric map of the object area, a fragment of sonar mosaic, and an ROV inspection video still frame.

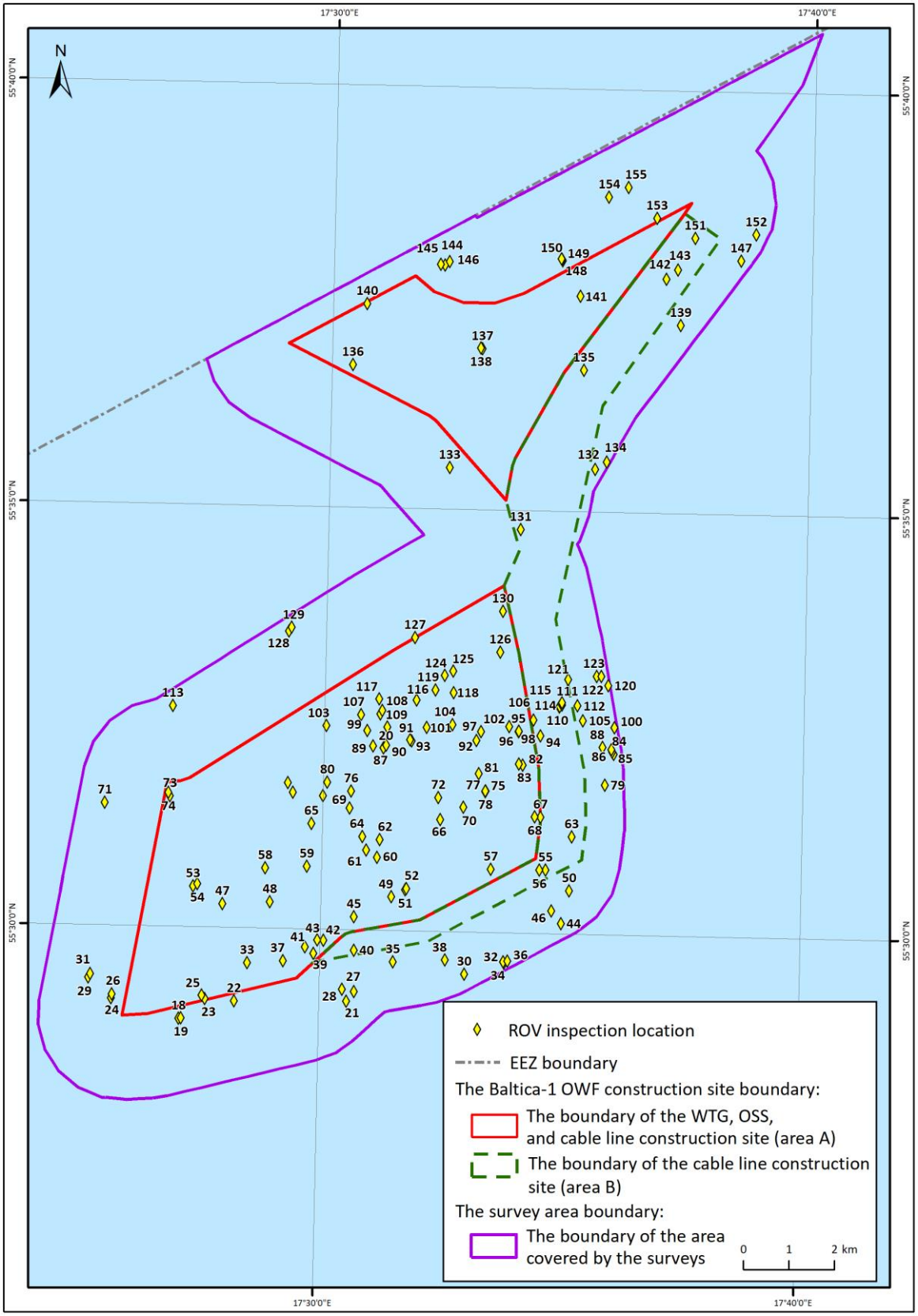


Figure 1.15. The location of objects of man-made or unknown origin designated for ROV inspection within the survey area

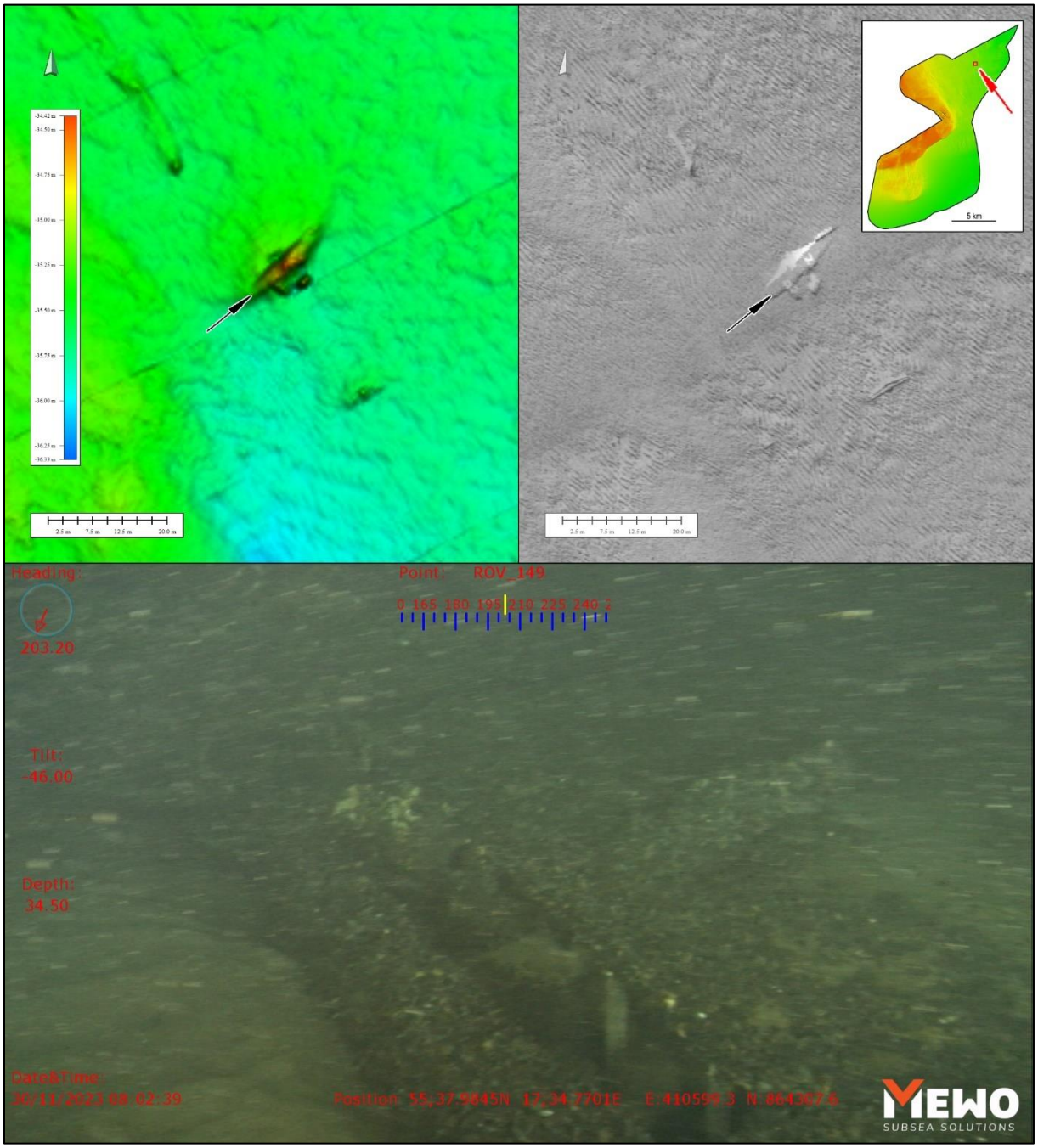


Figure 1.16. An example of an object – ROV_149 (an air plane wreck); visible in the bathymetric data (MBES), in the sonar mosaic (SSS), and the data from an ROV inspection – an ROV inspection video still frame

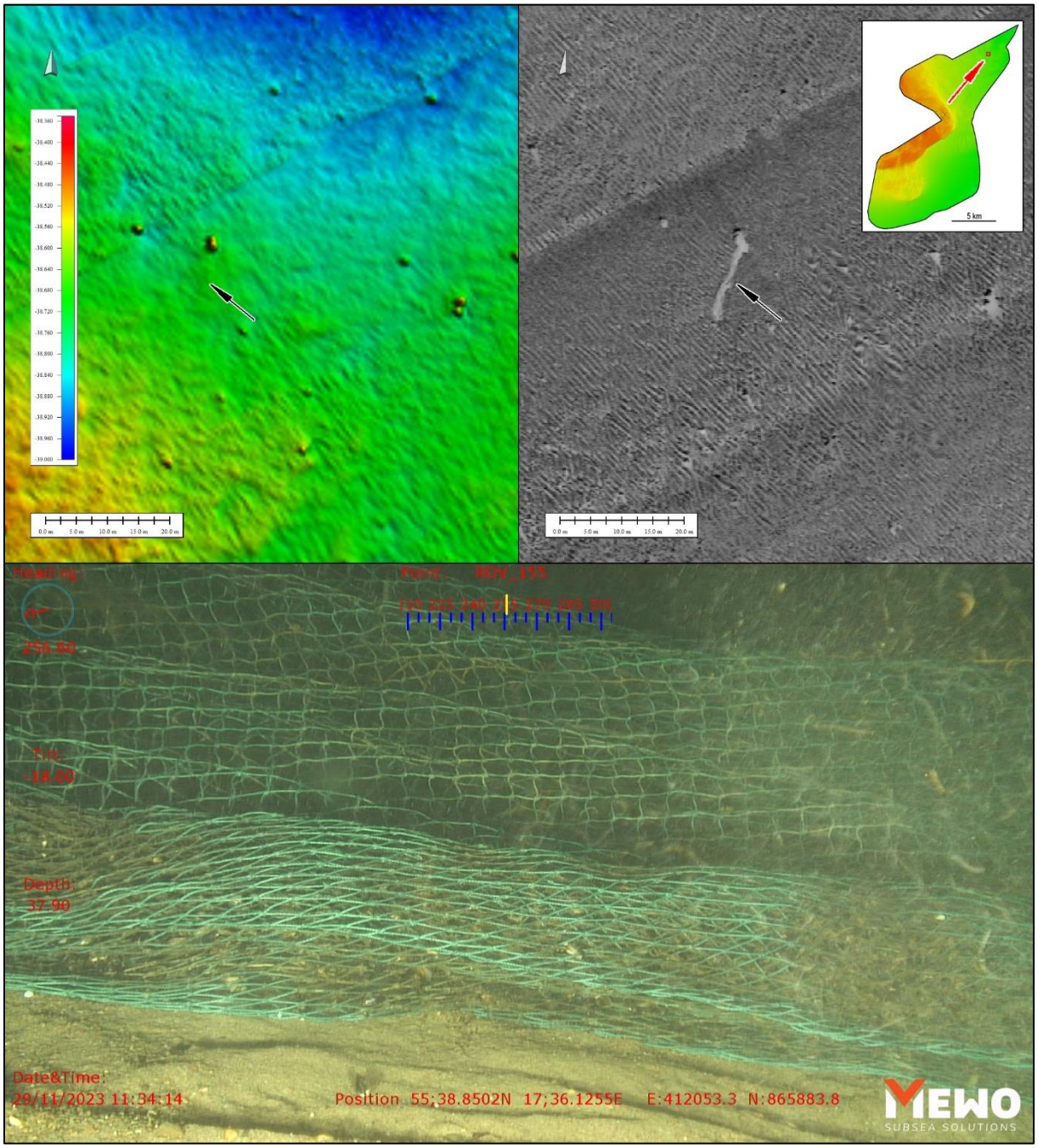


Figure 1.17. An example of an object – ROV_155 (fishing nets); not visible in the bathymetric data (MBES), visible in the sonar mosaic (SSS) and the data from an ROV inspection – an ROV inspection video still frame

1.5.5 Shallow seismo-acoustic profiling

Shallow seismoacoustic profiling was performed in the survey area. Based on the obtained measurement data from the profiling conducted along cross-lines at a distance of 500 m from each other, the geological structure of the analysed area was determined to a depth of 6.0 m.

1.5.6 Seismic surveys

1.5.6.1 Single-channel seismic surveys

Based on the analysis of data collected during seismic measurements using the reflection technique with a single-channel set of receivers, the structure of the seabed was determined to a depth of approximately 45 m.

1.5.6.2 Multi-channel seismic surveys (2D UHR)

The results of the seismic survey using the reflection technique, performed using a multi-channel set of hydrophones, allowed for the recognition of the geological structure of the analysed area to at least the depth of the WTG foundations.

1.5.7 Soil sampling

1.5.7.1 Surface sediment sampling

As part of the surveys, 118 sediment samples were collected from the survey area. Table 1.5 presents the results of the macroscopic analysis and grain size analysis of the sediment samples collected.

The grain size analysis of surface soil samples indicates the sandy and sand-gravel character of the sediments within the survey area. Locally, in the northern part of the survey area, higher contents of gravel fraction were observed (50% in sample SO_MFW_029). An increased content of fine fractions (silt and clay) was observed in the south-eastern part of the area. Only one surface soil sample from the survey area (SO_MFW_075) had a fine-particle content of more than 10% (15.3%) and was classified as sand with silt.

Table 1.5. A macroscopic description and the result of grain size analysis of the sediment samples collected in the survey area

Survey station	Macroscopic description	Soil symbol	Colour according to the Munsell colour chart	HCl	Description based on granulometric composition	Soil symbol based on granulometric composition
SO_MFW_001	Medium sand with gravel (from fine to coarse) and a large amount of clay	clgrmSa	multicoloured	0	Medium sand and coarse sand with gravel	grmSa/grcSa
SO_MFW_002	Fine sand with gravel (from fine to coarse) and a small amount of silt and clay, shells and fragments of *Macoma balthica* shells	grfSa	5Y 3/2 (dark olive-grey)	0	Fine sand with medium sand and gravel	grmsafSa
SO_MFW_003	Medium sand with fine sand and gravel (from fine to coarse) and a small amount of silt and clay, shells and fragments of *Macoma balthica* shells	grfsamSa	2.5Y 4/2 (dark grey-brown)	0	Medium sand with fine sand	fsamSa
SO_MFW_004	Coarse sand with medium sand and fine gravel	fgrmsacSa	multicoloured	0	Sand (from fine to coarse)	Sa
SO_MFW_005	Medium sand, fragments of shells	mSa	10YR 4/3 (brown)	0	Medium sand with fine sand	fsamSa
SO_MFW_006	Coarse sand with medium sand and a small amount of fine gravel, shell fragments	msacSa	multicoloured	0	Medium sand with coarse sand	csamSa
SO_MFW_007	Coarse sand with a small amount of medium sand and fine gravel, shells and fragments of *Macoma balthica* shells	cSa	multicoloured	0	Coarse sand and medium sand	cSa/mSa
SO_MFW_008	Medium sand and coarse sand with a small amount of gravel, shells and fragments of *Macoma balthica* shells	mSa/cSa	10YR 4/3 (brown)	0	Medium sand with coarse sand	csamSa
SO_MFW_009	Coarse sand with medium sand, shells and fragments of *Macoma balthica* shells	msacSa	10YR 4/3 (brown)	0	Medium sand with coarse sand	csamSa
SO_MFW_010	Medium sand and coarse sand with a small amount of gravel, shell fragments	mSa/cSa	multicoloured	0	Medium sand with coarse sand	csamSa
SO_MFW_011	Coarse sand with medium sand and a small amount of fine gravel	msacSa	multicoloured	0	Medium sand with coarse sand	csamSa
SO_MFW_012	Medium sand, visible muscovite lamellae, shell fragments	mSa	10YR 4/3 (brown)	0	Medium sand	mSa
SO_MFW_013	Medium sand	mSa	10YR 4/3 (brown)	0	Medium sand	mSa
SO_MFW_014	Medium sand, single gravel grains, fragments of shells	mSa	10YR 4/3 (brown)	0	Medium sand	mSa

Survey station	Macroscopic description	Soil symbol	Colour according to the Munsell colour chart	HCl	Description based on granulometric composition	Soil symbol based on granulometric composition
SO_MFW_015	Coarse sand with medium sand and a small amount of fine gravel, shells and fragments of *Macoma balthica* shells, soil discolouration resulting from oxidation	msacSa	multicoloured	0	Medium sand and coarse sand	cSa/mSa
SO_MFW_016	Medium sand with coarse sand, single gravel grains, shell fragments	csamSa	10YR 5/2 (grey-brown)	0	Medium sand with coarse sand	csamSa
SO_MFW_017	Coarse sand with medium sand and a small amount of fine gravel, shell fragments	msacSa	multicoloured	0	Medium sand with coarse sand and gravel	grcsamSa
SO_MFW_018	Medium sand with a small amount of coarse sand, single gravel grains, shell fragments	mSa	10YR 5/2 (grey-brown)	0	Medium sand	mSa
SO_MFW_019	Coarse sand and medium sand with a small amount of fine gravel	mSa/cSa	multicoloured	0	Medium sand with coarse sand	csamSa
SO_MFW_020	Coarse sand with medium sand, single gravel grains	msacSa	10YR 4/2 (dark grey-brown)	0	Medium sand with coarse sand	csamSa
SO_MFW_021	Coarse sand with gravel and a small amount of medium sand, shell fragments	grcSa	multicoloured	0	Medium sand with coarse sand and fine gravel	fgrcsamSa
SO_MFW_022	Medium sand with a small amount of coarse sand, shell fragments	mSa	10YR 4/3 (brown)	0	Medium sand with coarse sand	csamSa
SO_MFW_023	Gravel (from fine to coarse) with coarse and medium sand, shells and fragments of *Macoma balthica* shells, plant fragments	saGr	multicoloured	0	Gravel (from fine to coarse) with medium sand and coarse sand	csamsaGr
SO_MFW_024	Coarse sand with medium sand, single gravel grains	msacSa	10YR 4/2 (dark grey-brown)	0	Medium sand with coarse sand	csamSa
SO_MFW_025	Medium sand with a small amount of coarse sand, *Macoma balthica* shells and shell fragments	mSa	10YR 5/2 (grey-brown)	0	Medium sand with coarse sand	csamSa
SO_MFW_026	Coarse sand with a small amount of medium sand	cSa	10YR 5/2 (grey-brown)	0	Medium sand with coarse sand	csamSa
SO_MFW_027	Coarse sand with a large amount of fine and medium gravel, shell fragments	grcSa	multicoloured	0	Gravel with coarse sand and medium sand	msacsaGr

Survey station	Macroscopic description	Soil symbol	Colour according to the Munsell colour chart	HCl	Description based on granulometric composition	Soil symbol based on granulometric composition
SO_MFW_028	Medium sand with a small amount of coarse sand	mSa	10YR 5/3 (brown)	0	Medium sand	mSa
SO_MFW_029	Fine and medium sand with coarse sand and a small amount of medium sand, Macoma balthica shells and shell fragments	csafGr/csamGr	multicoloured	0	Medium gravel with medium sand and coarse sand	csamsamGr
SO_MFW_030	Medium sand, *Macoma balthica* shells and shell fragments	mSa	10YR 4/3 (brown)	0	Medium sand	mSa
SO_MFW_031	Medium sand with coarse sand, shell fragments	csamSa	10YR 4/2 (dark grey-brown)	0	Medium sand with coarse sand	csamSa
SO_MFW_032	Coarse sand with medium sand, single gravel grains, Macoma balthica shells and shell fragments	msacSa	10YR 4/3 (brown)	0	Medium sand with coarse sand	csamSa
SO_MFW_033	Medium sand, *Macoma balthica* shells and shell fragments	mSa	2.5Y 5/3 (light olive-brown)	0	Medium sand with fine sand	fsamSa
SO_MFW_034	Medium sand, *Macoma balthica* shells and shell fragments	mSa	10YR 5/2 (grey-brown)	0	Medium sand	mSa
SO_MFW_035	Medium sand and coarse sand with fine gravel	fgrmSa/fgrcSa	10YR 4/3 (brown)	0	Medium sand with medium gravel	mgrmSa
SO_MFW_036	Medium sand and coarse sand	mSa/cSa	10YR 4/3 (brown)	0	Medium sand with coarse sand	csamSa
SO_MFW_037	Medium sand and coarse sand	mSa/cSa	10YR 4/3 (brown)	0	Medium sand and coarse sand	mSa/cSa
SO_MFW_038	Medium sand with a small amount of coarse sand	mSa	10YR 4/3 (brown)	0	Medium sand	mSa
SO_MFW_039	Coarse sand with medium sand and fine gravel	fgrmsacSa	10YR 4/3 (brown)	0	Medium sand with coarse sand	csamSa
SO_MFW_040	Medium sand with coarse sand, shell fragments	csamSa	10YR 4/2 (dark grey-brown)	0	Medium sand with coarse sand	csamSa
SO_MFW_041	Medium sand with a small amount of coarse sand	mSa	10YR 5/2 (grey-brown)	0	Medium sand	mSa
SO_MFW_042	Medium sand with a small amount of fine sand	mSa	10YR 4/4 (dark yellow-brown)	0	Medium sand with fine sand	fsamSa
SO_MFW_043	Medium sand and coarse sand	mSa/cSa	10YR 4/2 (dark grey-brown)	0	Medium sand with coarse sand	csamSa

Survey station	Macroscopic description	Soil symbol	Colour according to the Munsell colour chart	HCl	Description based on granulometric composition	Soil symbol based on granulometric composition
SO_MFW_044	Medium sand, visible muscovite lamellae	mSa	10YR 5/2 (grey-brown)	0	Medium sand with fine sand	fsamSa
SO_MFW_045	Medium sand with a small amount of fine sand	mSa	10YR 5/2 (grey-brown)	0	Medium sand with fine sand	fsamSa
SO_MFW_046	Fine sand, *Macoma balthica* shells and shell fragments	fSa	10YR 5/1 (grey)	0	Fine sand	fSa
SO_MFW_047	Fine sand, fragments of *Macoma balthica* shells. Single fragments of shredded plants. Strong smell of rotting; after a reaction with HCl, there is a noticeable smell of H_2S	fSa	2.5Y 4/2 (dark grey-brown)	0	Fine sand	fSa
SO_MFW_048	Fine sand with medium sand, *Macoma balthica* shells and shell fragments, visible muscovite lamellae	msafSa	10YR 5/2 (grey-brown)	0	Fine sand with medium sand	msafSa
SO_MFW_049	Fine sand with a small amount of medium sand, fragments of *Macoma Balthica* shells	fSa	10YR 5/2 (grey-brown)	0	Fine sand with medium sand	msafSa
SO_MFW_050	Medium sand	mSa	10YR 5/2 (grey-brown)	0	Medium sand with fine sand	fsamSa
SO_MFW_051	Fine sand, *Macoma balthica* shells and shell fragments	fSa	2.5Y 5/2 (grey-brown)	0	Fine sand	fSa
SO_MFW_052	Fine sand, plant fragments, *Macoma balthica* shells and shell fragments	fSa	2.5Y 5/1 (grey)	0	Fine sand	fSa
SO_MFW_053	Fine sand, numerous plant fragments, *Mya arenaria* and *Macoma balthica* shells and shell fragments	fSa	10YR 5/1 (grey)	0	Fine sand	fSa
SO_MFW_054	Medium sand, fragments of shells	mSa	10YR 5/2 (grey-brown)	0	Medium sand with fine sand	fsamSa
SO_MFW_055	Medium sand with fine sand	fsamSa	10YR 5/2 (grey-brown)	0	Medium sand	mSa
SO_MFW_056	Fine sand, single fragments of plants, fragments of shells	fSa	10YR 5/2 (grey-brown)	0	Fine sand	fSa
SO_MFW_057	Fine sand, visible muscovite lamellae; *Macoma balthica* shells and shell fragments	fSa	2.5Y 4/2 (dark grey-brown)	0	Fine sand	fSa
SO_MFW_058	Fine sand, visible muscovite lamellae; *Macoma balthica* shells and shell fragments	fSa	2.5Y 4/2 (dark grey-brown)	0	Fine sand	fSa
SO_MFW_059	Fine sand, visible muscovite lamellae; *Macoma balthica* shells and shell fragments	fSa	2.5Y 5/2 (grey-brown)	0	Fine sand	fSa
SO_MFW_060	Fine sand, shell fragments	fSa	2.5Y 5/2 (grey-brown)	0	Fine sand	fSa

Survey station	Macroscopic description	Soil symbol	Colour according to the Munsell colour chart	HCl	Description based on granulometric composition	Soil symbol based on granulometric composition
SO_MFW_061	Fine sand, shells and fragments of *Macoma balthica* and *Cerastoderma edule* shells	fSa	2.5Y 5/2 (grey-brown)	0	Fine sand	fSa
SO_MFW_062	Fine sand with medium sand, shells and fragments of *Cerastoderma edule* and *Macoma balthica* shells	msafSa	2.5Y 5/1 (grey)	0	Fine sand with medium sand	msafSa
SO_MFW_063	Fine sand with medium sand, visible muscovite lamellae	msafSa	10YR 5/2 (grey-brown)	0	Fine sand with medium sand	msafSa
SO_MFW_064	Fine sand with a small amount of silt, *Macoma balthica* shells and shell fragments	fSa	2.5Y 5/2 (grey-brown)	0	Fine sand	fSa
SO_MFW_065	Fine sand with a small amount of silt, *Macoma balthica* shells and shell fragments	fSa	5Y 4/2 (olive-grey)	0	Fine sand	fSa
SO_MFW_066	Fine sand with a small amount of silt, single plant fragments, *Macoma balthica* shells and shell fragments	fSa	5Y 4/2 (olive-grey)	0	Fine sand	fSa
SO_MFW_067	Fine sand, *Macoma balthica* shells and shell fragments	fSa	2.5Y 5/2 (grey-brown)	0	Fine sand	fSa
SO_MFW_068	Fine sand, *Macoma balthica* shells and shell fragments	fSa	2.5Y 4/2 (dark grey-brown)	0	Fine sand	fSa
SO_MFW_069	Fine sand, fragments of plants, *Mya arenaria* and *Macoma balthica* shells	fSa	2.5Y 4/2 (dark grey-brown)	0	Fine sand	fSa
SO_MFW_070	Fine sand with medium sand, shells and fragments of *Mya arenaria* and *Cerastoderma edule* shells	msafSa	2.5Y 5/2 (grey-brown)	0	Fine sand with medium sand	msafSa
SO_MFW_071	Medium sand with a small amount of fine sand, *Macoma balthica* shells and shell fragments	mSa	10YR 5/2 (grey-brown)	0	Fine sand with medium sand	msafSa
SO_MFW_072	Fine gravel with coarse sand, *Cerastoderma edule* shells and fragments of shells	csafGr	multicoloured	0	Fine gravel with coarse sand	csafGr
SO_MFW_073	Fine sand with medium sand, visible muscovite lamellae; Cerastoderma edule shells and fragments of shells	msafSa	10YR 5/2 (grey-brown)	0	Fine sand with medium sand	msafSa
SO_MFW_074	fine sand with a small amount of silt, fragments of plants	fSa	2.5Y 4/2 (dark grey-brown)	0	Fine sand	fSa
SO_MFW_075	Fine sand with a small amount of silt, plant fragments, *Macoma balthica* shells and shell fragments	fSa	2.5Y 5/2 (grey-brown)	0	Sand with silt	siSa

Survey station	Macroscopic description	Soil symbol	Colour according to the Munsell colour chart	HCl	Description based on granulometric composition	Soil symbol based on granulometric composition
SO_MFW_076	Fine sand with a small amount of silt, *Macoma balthica* shells and shell fragments	fSa	2.5Y 5/2 (grey-brown)	0	Fine sand	fSa
SO_MFW_077	Fine sand with a small amount of silt, *Macoma balthica* shells and shell fragments	fSa	2.5Y 5/2 (grey-brown)	0	Fine sand	fSa
SO_MFW_078	Medium sand with fine sand, *Macoma balthica* shells and shell fragments	msafSa	10YR 4/2 (dark grey-brown)	0	Medium sand with fine sand	fsamSa
SO_MFW_079	Medium sand and fine sand, *Cerastoderma edule* shells and shell fragments, visible muscovite lamellae	mSa/fSa	10YR 5/2 (grey-brown)	0	Fine sand with medium sand	msafSa
SO_MFW_080	Coarse sand with medium sand and a small amount of gravel, *Macoma balthica* shells	msacSa	10YR 4/3 (brown)	0	Medium sand with coarse sand	csamSa
SO_MFW_081	Medium sand	mSa	10YR 5/2 (grey-brown)	0	Medium sand with fine sand	fsamSa
SO_MFW_082	Fine sand with a small amount of medium sand, shells and fragments of *Macoma balthica* and *Cerastoderma edule* shells	fSa	2.5Y 5/2 (grey-brown)	0	Fine sand	fSa
SO_MFW_083	Fine sand with a small amount of silt, plant fragments, *Macoma balthica* shells and shell fragments	fSa	2.5Y 5/2 (grey-brown)	0	Fine sand	fSa
SO_MFW_084	Fine sand with a small amount of silt, *Macoma balthica* shells	fSa	2.5Y 4/1 (dark grey)	0	Fine sand	fSa
SO_MFW_085	Fine sand with a small amount of silt, *Macoma balthica* shells and shell fragments	fSa	2.5Y 4/2 (dark grey-brown)	0	Fine sand	fSa
SO_MFW_086	Fine sand with a small amount of medium sand, shells and fragments of *Macoma balthica* and *Mya arenaria* shells.After a reaction with HCl, there is a noticeable smell of H_2S	fSa	2.5Y 4/2 (dark grey-brown)	0	Fine sand	fSa
SO_MFW_087	Medium sand, fragments of *Macoma balthica* shells	mSa	10YR 5/3 (brown)	0	Medium sand with fine sand	fsamSa
SO_MFW_088	Medium sand and coarse sand, shell fragments	mSa/cSa	multicoloured	0	Coarse sand and medium sand	cSa/mSa
SO_MFW_089	Fine sand with medium sand, shell fragments	msafSa	10YR 5/2 (grey-brown)	0	Fine sand with medium sand	msafSa

Survey station	Macroscopic description	Soil symbol	Colour according to the Munsell colour chart	HCl	Description based on granulometric composition	Soil symbol based on granulometric composition
SO_MFW_090	Coarse sand and medium sand, single gravel grains	cSa/mSa	multicoloured	0	Medium sand with coarse sand	csamSa
SO_MFW_091	Medium sand	mSa	10YR 4/3 (brown)	0	Medium sand	mSa
SO_MFW_092	Fine sand with a small amount of silt, *Macoma balthica* shells and shell fragments, single fragments of shredded plants (up to 1 mm)	fSa	2.5Y 4/2 (dark grey-brown)	0	Medium sand with fine sand	fsamSa
SO_MFW_093	Fine sand with a small amount of silt, plant fragments, *Macoma balthica* shells and shell fragments	fSa	2.5Y 4/2 (dark grey-brown)	0	Fine sand	fSa
SO_MFW_094	Fine sand with a small amount of silt, *Macoma balthica* shells and shell fragments, and single small plant fragments. After a reaction with HCl, there is a noticeable smell of H_2S	fSa	2.5Y 4/2 (dark grey-brown)	0	Fine sand	fSa
SO_MFW_095	Fine sand with medium sand, numerous plant fragments, shells and fragments of *Mya arenaria* and *Macoma balthica* shells. After a reaction with HCl, there is a noticeable smell of H_2S	msafSa	2.5Y 4/2 (dark grey-brown)	0	Fine sand	fSa
SO_MFW_096	Coarse sand with fine gravel and a small amount of medium sand	grcSa	multicoloured	0	Coarse sand with fine gravel	fgrcSa
SO_MFW_097	Fine sand; discernible muscovite lamellae	fSa	2.5Y 5/2 (grey-brown)	0	Fine sand	fSa
SO_MFW_098	Fine sand, shell fragments	fSa	2.5Y 5/3 (light olive-brown)	0	Fine sand	fSa
SO_MFW_099	Fine sand, *Macoma balthica* shells and shell fragments, visible muscovite lamellae	fSa	2.5Y 5/2 (grey-brown)	0	Fine sand	fSa
SO_MFW_100	Fine sand with a small amount of silt, plant fragments, shell fragments	fSa	2.5Y 4/2 (dark grey-brown)	0	Fine sand	fSa
SO_MFW_101	Fine sand with a small amount of silt; *Macoma balthica* shells and shell fragments; a few thin laminae of an organic matter. After a reaction with HCl, there is a noticeable smell of H_2S	fSa	2.5Y 5/2 (grey-brown)	0	Fine sand	fSa

Survey station	Macroscopic description	Soil symbol	Colour according to the Munsell colour chart	HCl	Description based on granulometric composition	Soil symbol based on granulometric composition
SO_MFW_102	Fine sand with a small amount of medium sand, thin laminae of organic matter, *Macoma balthica* shells and shell fragments. After a reaction with HCl, there is a noticeable smell of H_2S	fSa	2.5Y 5/2 (grey-brown)	0	Fine sand	fSa
SO_MFW_103	Fine sand with a small amount of medium sand	msafSa	2.5Y 4/2 (dark grey-brown)	0	Fine sand	fSa
SO_MFW_104	Fine sand, plant fragments, *Macoma balthica* shells and shell fragments	fSa	2.5Y 4/2 (dark grey-brown)	0	Fine sand	fSa
SO_MFW_105	Fine sand with silt, *Macoma balthica* shells and shell fragments, visible muscovite lamellae. After a reaction with HCl, there is a noticeable smell of H_2S	sifSa	2.5Y 4/2 (dark grey-brown)	0	Fine sand	fSa
SO_MFW_106	Fine sand, *Macoma balthica* shells and shell fragments	fSa	2.5Y 4/2 (dark grey-brown)	0	Fine sand	fSa
SO_MFW_107	Fine sand with a small amount of silt, *Macoma balthica* shells and shell fragments, plant fragments	fSa	2.5Y 5/2 (grey-brown)	0	Fine sand	fSa
SO_MFW_108	Fine sand, plant fragments, *Macoma balthica* shells and shell fragments. After a reaction with HCl, there is a noticeable smell of H_2S	fSa	2.5Y 5/2 (grey-brown)	0	Fine sand	fSa
SO_PM_86	Fine sand with a small amount of silt, single plant fragments, *Macoma balthica* shells and shell fragments	fSa	2.5Y 5/2 (grey-brown)	0	Fine sand	fSa
SO_PM_87	Fine sand, visible muscovite lamellae, shell fragments	fSa	2.5Y 5/2 (grey-brown)	0	Fine sand	fSa
SO_PM_88	Medium sand, plant fragments, *Macoma balthica* shells and shell fragments	mSa	10YR 4/2 (dark grey-brown)	0	Fine sand with medium sand	msafSa
SO_PM_89	Medium sand, fragments of *Macoma balthica* shells	mSa	10YR 4/2 (dark grey-brown)	0	Fine sand with medium sand	msafSa
SO_PM_90	Medium sand with coarse sand and a large amount of gravel; *Macoma balthica* shells and shell fragments	fgrSa	multicoloured	0	Medium sand and medium gravel	mGr/mSa
SO_PM_91	Coarse sand with a small amount of fine gravel	cSa	multicoloured	0	Coarse sand with medium sand	msacSa

Survey station	Macroscopic description	Soil symbol	Colour according to the Munsell colour chart	HCl	Description based on granulometric composition	Soil symbol based on granulometric composition
SO_PM_92	Fine sand with medium sand	msafSa	10YR 5/2 (grey-brown)	0	Fine sand	fSa
SO_PM_93	Coarse sand and medium sand with a small amount of fine gravel, shell fragments	cSa/mSa	2.5Y 5/3 (light olive-brown)	0	Medium sand with fine sand	fsamSa
SO_PM_94	Medium sand, *Macoma balthica* shells and shell fragments	mSa	10YR 5/2 (grey-brown)	0	Medium sand with fine sand	fsamSa
SO_PM_95	Coarse sand with medium sand, single gravel grains, Macoma balthica shells and shell fragments	msacSa	multicoloured	0	Medium sand with coarse sand	csamSa

1.5.7.2 Core sampling

As part of the surveys conducted, 39 core samples were collected in the survey area and analysed. In the cores, non-cohesive soils, cohesive soils and, in some places, organic soils were identified.

As a result of grain size analyses carried out on the samples taken with a vibrocorer, 26 types of soil were identified, from pure clay to sand with gravel. Some samples contained significant organic matter contents (up to almost 10%). The samples tested (recognised as carbonate during macroscopic description) showed carbonate content ranging from 0 to 19%, with the average for the entire test population being 10%.

1.6 SUMMARY OF RESULTS AND CONCLUSIONS

1.6.1 Interpretation of the seabed surface character

The seabed surface in the survey area is located at a depth from approximately 13.7 to approximately 51.8 m BSL. In the bathymetric image, the shallower central and western parts of the survey area can be distinguished. The seabed in that part of the area is located at a depth of approximately 13.7–23.0 m BSL, and it is separated from the rest of the survey area by a slope reaching, in places, up to 12 m in height and an inclination of several degrees. Below the slope, the seabed gently lowers in the eastern, north-eastern, south-eastern, and southern directions to a depth of approximately 51.8 m. The surface of that part of the seabed is even. The seabed slope in the survey area is from 0° to approximately 15°. In places, within the excavation walls, the seabed slope exceeds 15°.

The characteristics of the depth distribution and the character of the seabed relief in the survey area were prepared in the form of a map of seabed surface types [Figure 1.18] using a bathymetric map [Figure 1.10], a seabed slope map [Figure 1.11], and a sonar mosaic [Figure 1.12]. Within the survey area, two types of seabed surfaces were distinguished, comprising an accumulation plain and an abrasive-accumulative plain.

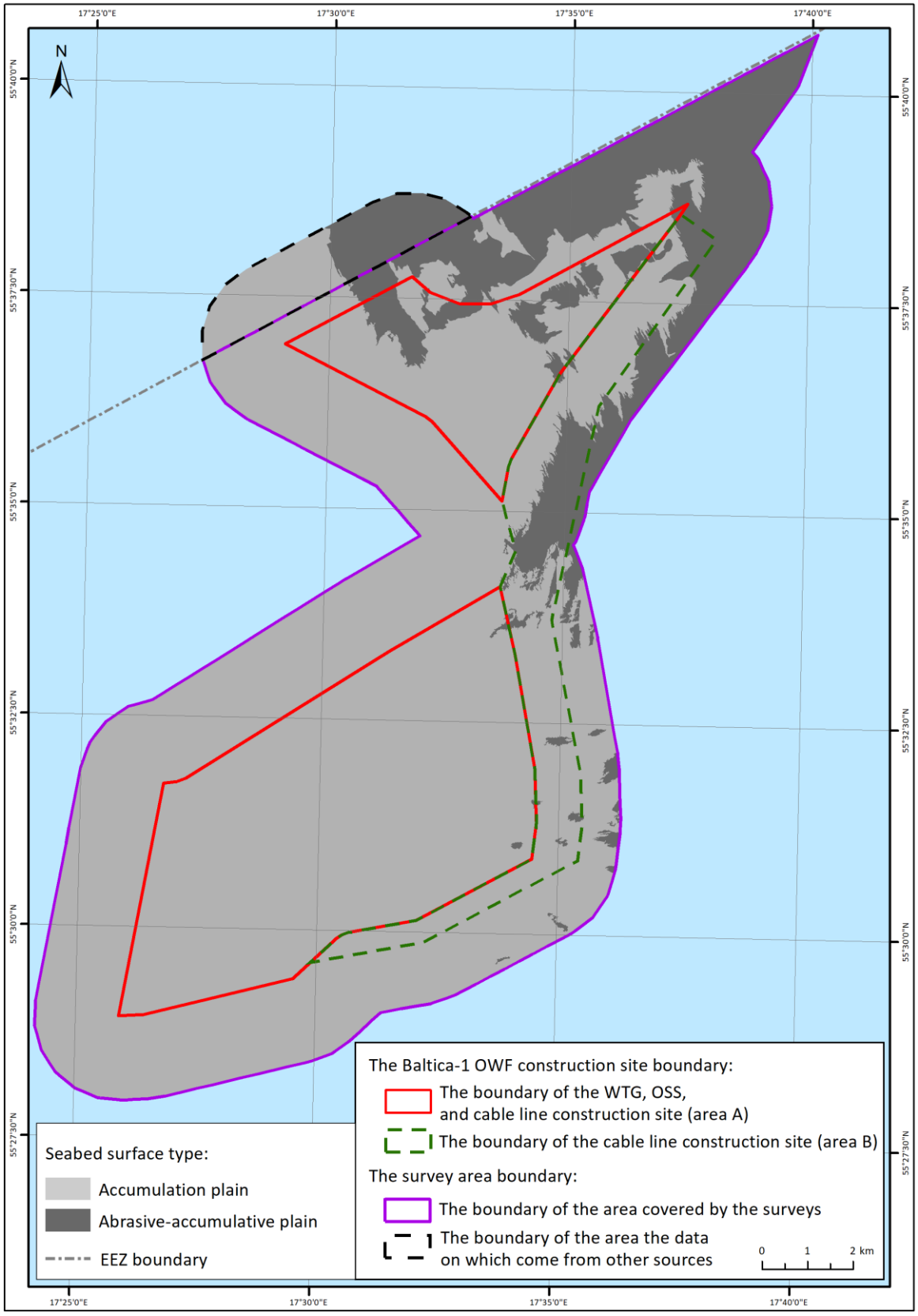


Figure 1.18. The seabed types in the survey area

The western and central parts of the survey area form an area with an accumulation plain character [Figure 1.19]. It covers the seabed with depths ranging from approximately 13.7 to approximately 35.0 m BSL. The seabed surface is slightly undulating, with minor changes in seabed altitudes related to the presence of sandy formations. The seabed relief bears signs of sand extraction [Figure 1.20]. The seabed slopes are 2–3°, up to a maximum of over a dozen degrees on the slope visible in the seabed relief in the central part of the survey area and within the sand extraction areas.

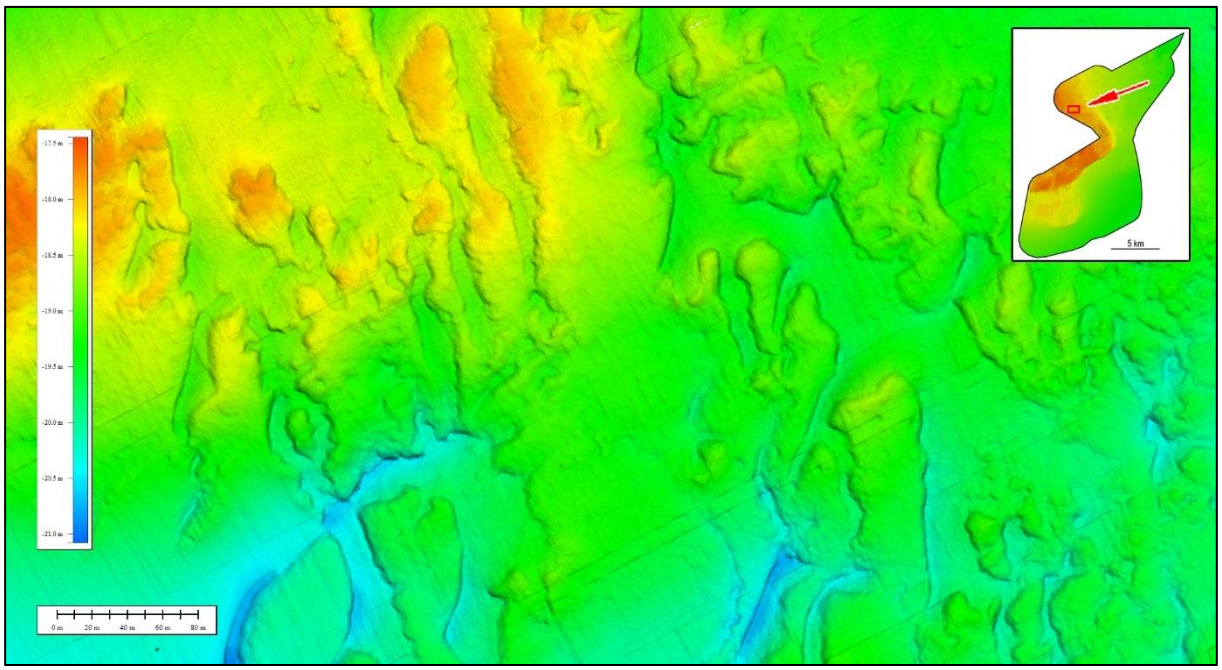


Figure 1.19. A fragment of a bathymetric map; an undulating surface of the accumulation plain; visible signs of the seabed irregularities within the sand accumulations divided by depressions resulting from the periodical seabed surface washout, where mega-ripples can be seen in the MBES and SSS data

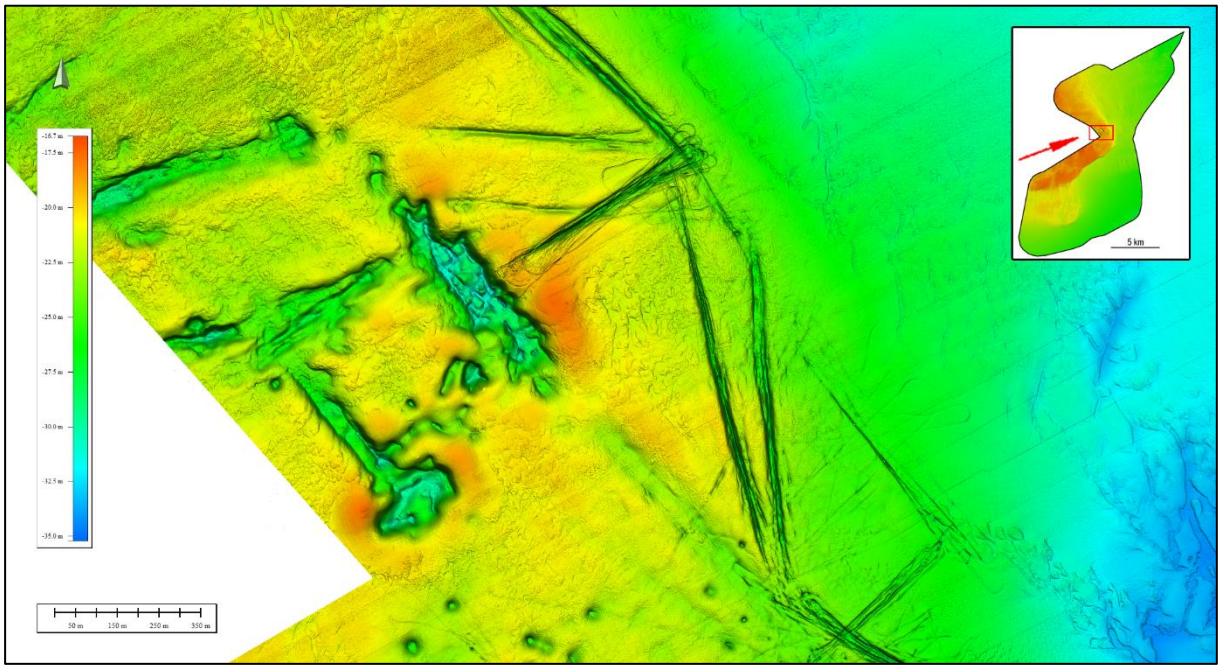


Figure 1.20. A fragment of a bathymetric map; an undulating surface of the accumulation plain; visible signs of sand extraction (depressions)

The eastern part of the seabed in the area analysed has the character of an abrasive-accumulative plain [Figure 1.21]. It covers the seabed at depths from approximately 35.0 to approximately 51.8 m BSL. The seabed is uneven, with 0.5–1.0 m changes in altitude due to the presence of sand accumulations and outcrops of older sediments (glacial and fluvioglacial sediments). The seabed slopes reach 2–3°, up to a maximum of over a dozen degrees within the slopes of the outcrops of older sediments.

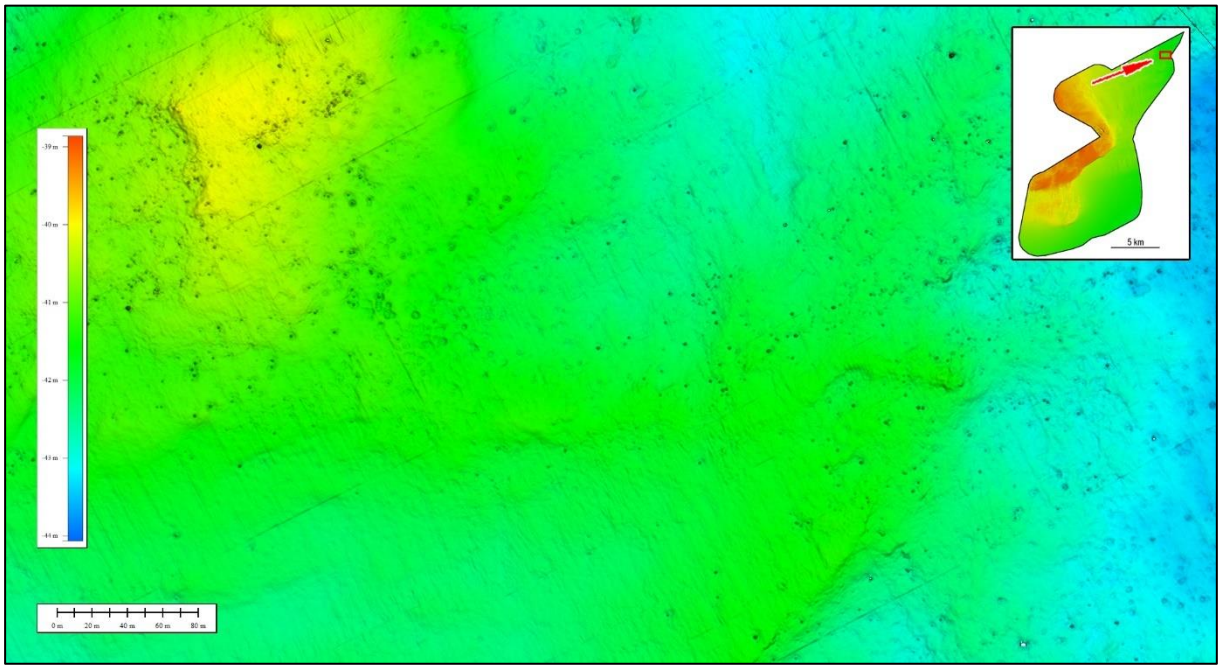


Figure 1.21. A fragment of a bathymetric map; an uneven surface of the abrasive-accumulative plain; visible single boulders and boulder clusters

In the north-eastern part of the survey area, numerous iceberg ploughmarks (scours or furrows) are visible in the seabed relief. They form a chaotic arrangement of elongated depressions of more than 2 km in length in places, up to 140 m in width, and up to 1.4 m in depth [Figure 1.22].

In the central part of the survey area, traces of sand extraction are visible in the seabed relief. A 1-NM wide strip of the survey area overlaps (from the west) with the mining areas “Południowa Ławica Środkowa B” and “Południowa Ławica Środkowa C” (covering the Southern Middle Bank) (igs.pgi.gov.pl; geolog.pgi.gov.pl). Those areas have been indicated as areas with seabed relief modified due to the mining and further works conducted and the natural processes taking place on the seabed as a result of such works [Figure 1.23].

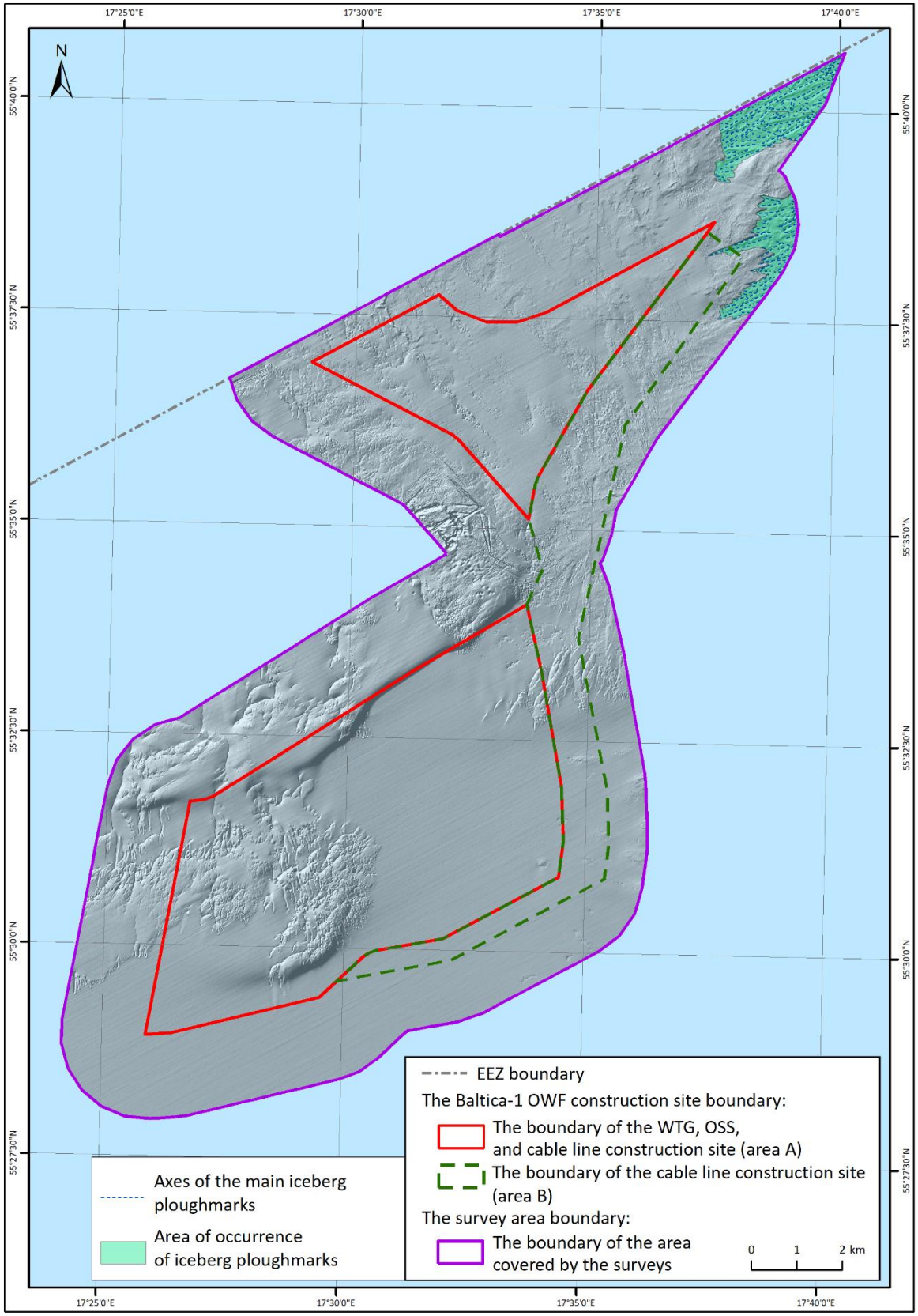


Figure 1.22. The traces of icebergs in the survey area

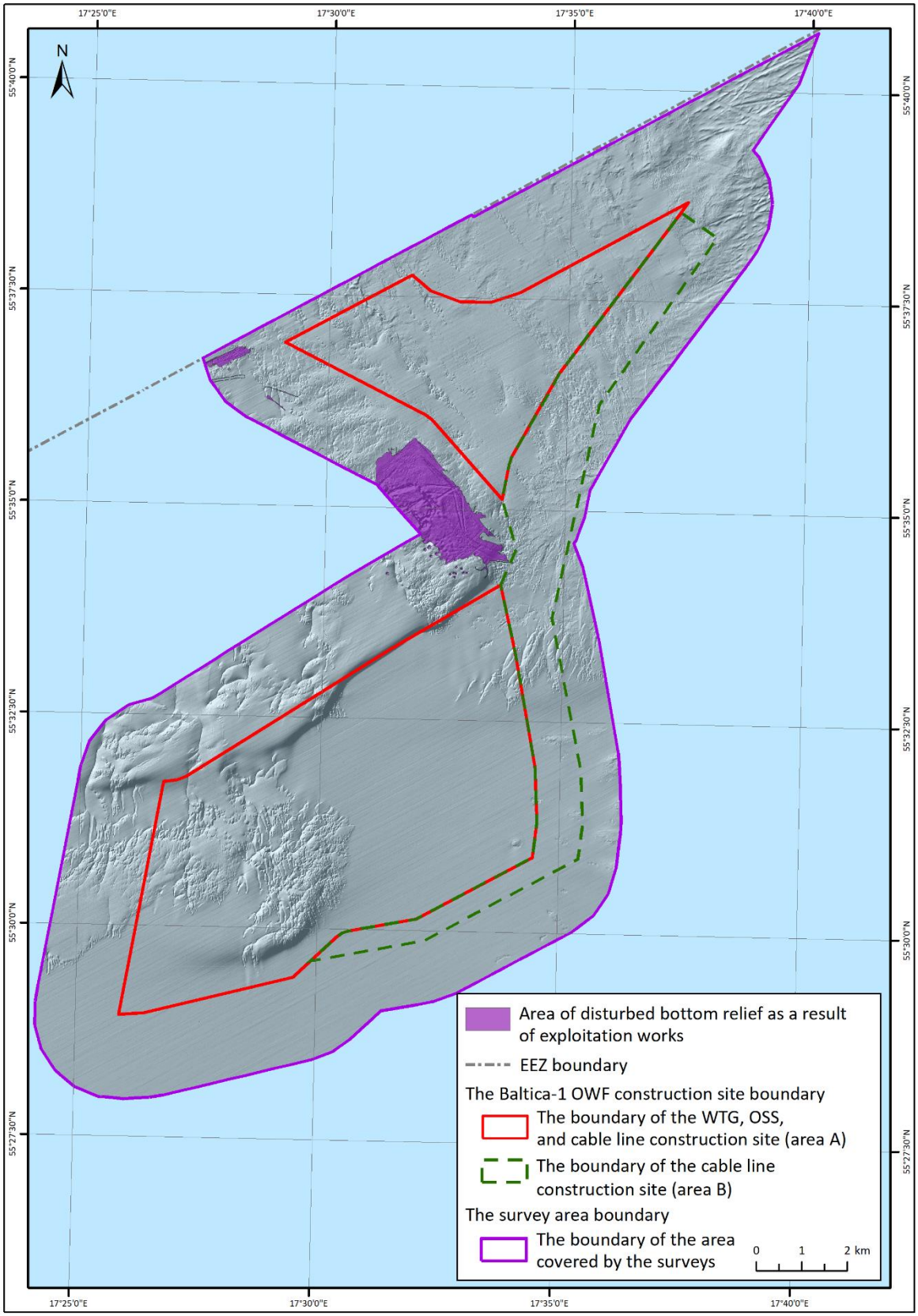


Figure 1.23. An area with the seabed relief modified by the mining works conducted

Based on the conducted analyses of bathymetric and sonar data, correlated with the data obtained from the analyses of sediment samples collected using a vibrocorer and a van Veen grab sampler, supplemented with EMODnet data, a map of surface sediments in the survey area was prepared [Figure 1.24].



Figure 1.24. The surface sediments in the survey area

The areas with uniform mosaic tones characterise level, locally undulating sandy seabed [Figure 1.25, Figure 1.26]. The parts of mosaic with uneven, rough texture featuring single points with long acoustic shadows are seabed areas most probably formed by cohesive sediments with a thin discontinuous sand cover and erosive pavement on the surface [Figure 1.27].

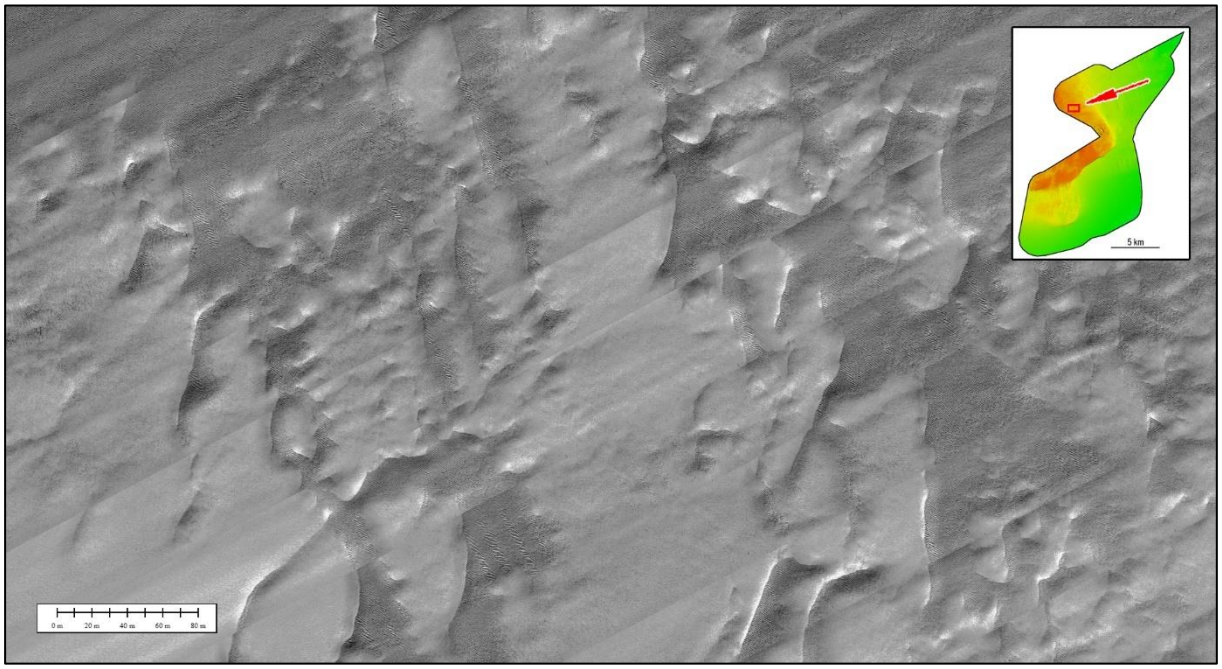


Figure 1.25. A fragment of a sonar mosaic; an undulating surface of the accumulation plain; visible signs of the seabed irregularities within the sand accumulations divided by depressions resulting from the periodical seabed surface washout, within which mega-ripples can be seen in the MBES and SSS data

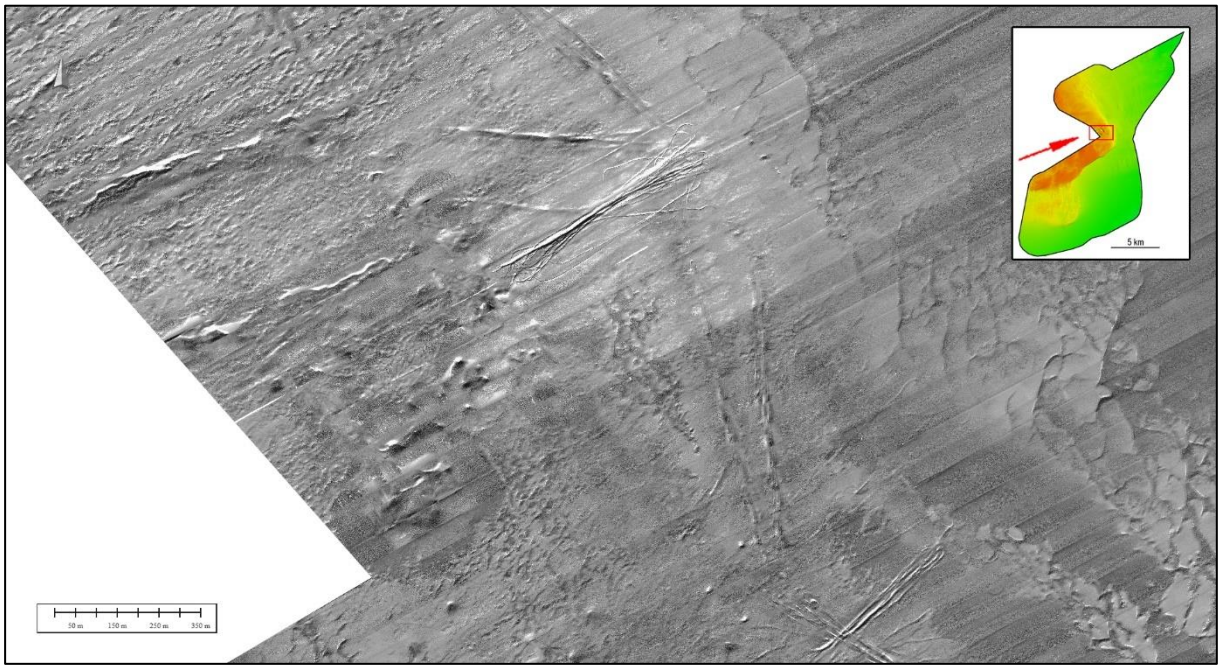


Figure 1.26. A fragment of a sonar mosaic; an undulating surface of the accumulation plain; visible signs of sand extraction (depressions)

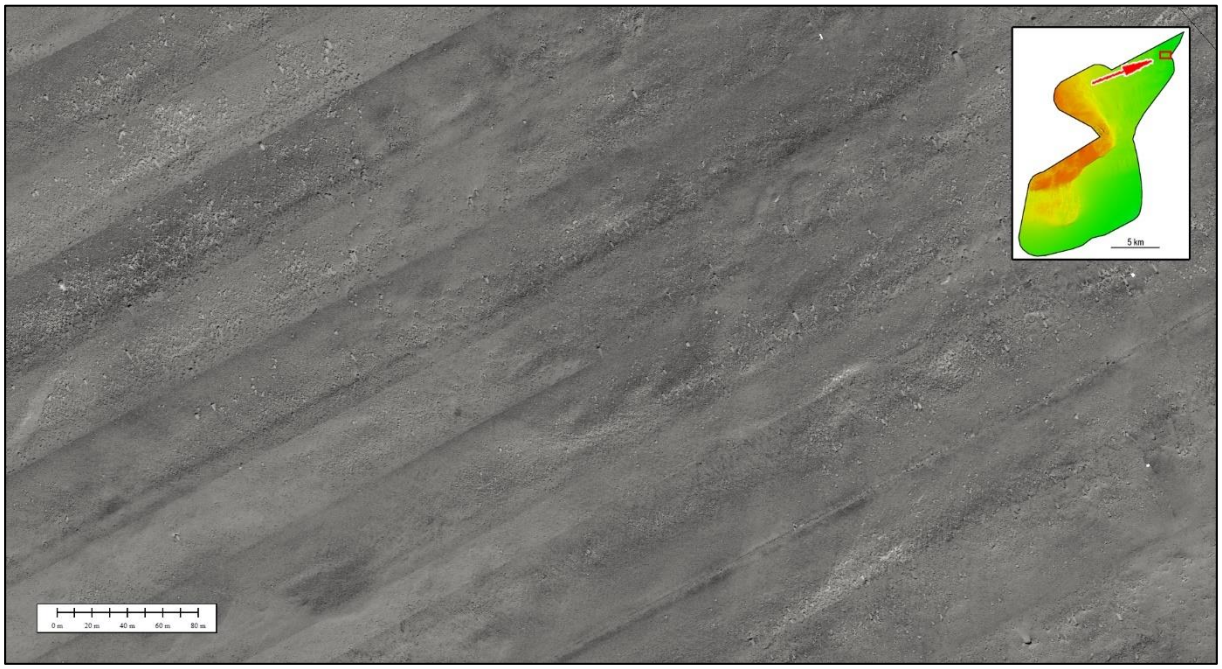


Figure 1.27. A fragment of a sonar mosaic; an uneven surface of the abrasive-accumulative plain; visible single boulders and boulder clusters

The western and central parts of the seabed of the survey area (accumulation plain) are formed by sandy sediments. The eastern and north-eastern parts of the survey area (abrasive-accumulative plain) are formed by cohesive sediments with a thin discontinuous sand cover and erosive pavement with single boulders on the surface.

Bathymetric and sonar data show areas of the seabed where series of mega-ripples are present on the seabed surface [Figure 1.28]. Ripple-marks are defined as sandy ridges with a height of 0.01–0.1 m and a cycle of 0.1–1 m between the crests, while mega-ripples have ridges with a height of 0.1–1 m and a cycle of 1–30 m between the crests (Secomandi et al., 2017). The features visible within the survey area reach a height of up to a dozen or so centimetres, while the cycle between the crests is approximately 1.8 m. They occur both within a sandy seabed and within a seabed formed by cohesive sediments with a thin, discontinuous sandy cover as well as erosive pavement with single boulders on the surface. It is within that thin sandy cover that the ripple-marks and mega-ripples are formed, which can be freely shifted across the hard seabed formed by cohesive sediments. On the surface of the seabed consisting of fine- to medium-grained sands, ripple-marks and mega-ripples are formed in areas where loose sandy sediments are shifted across the surface of more densely packed sands. Most ridges have a NW–SE or N–S orientation, however, in some places, the second generation of ridges with a NE–SW orientation can be found.

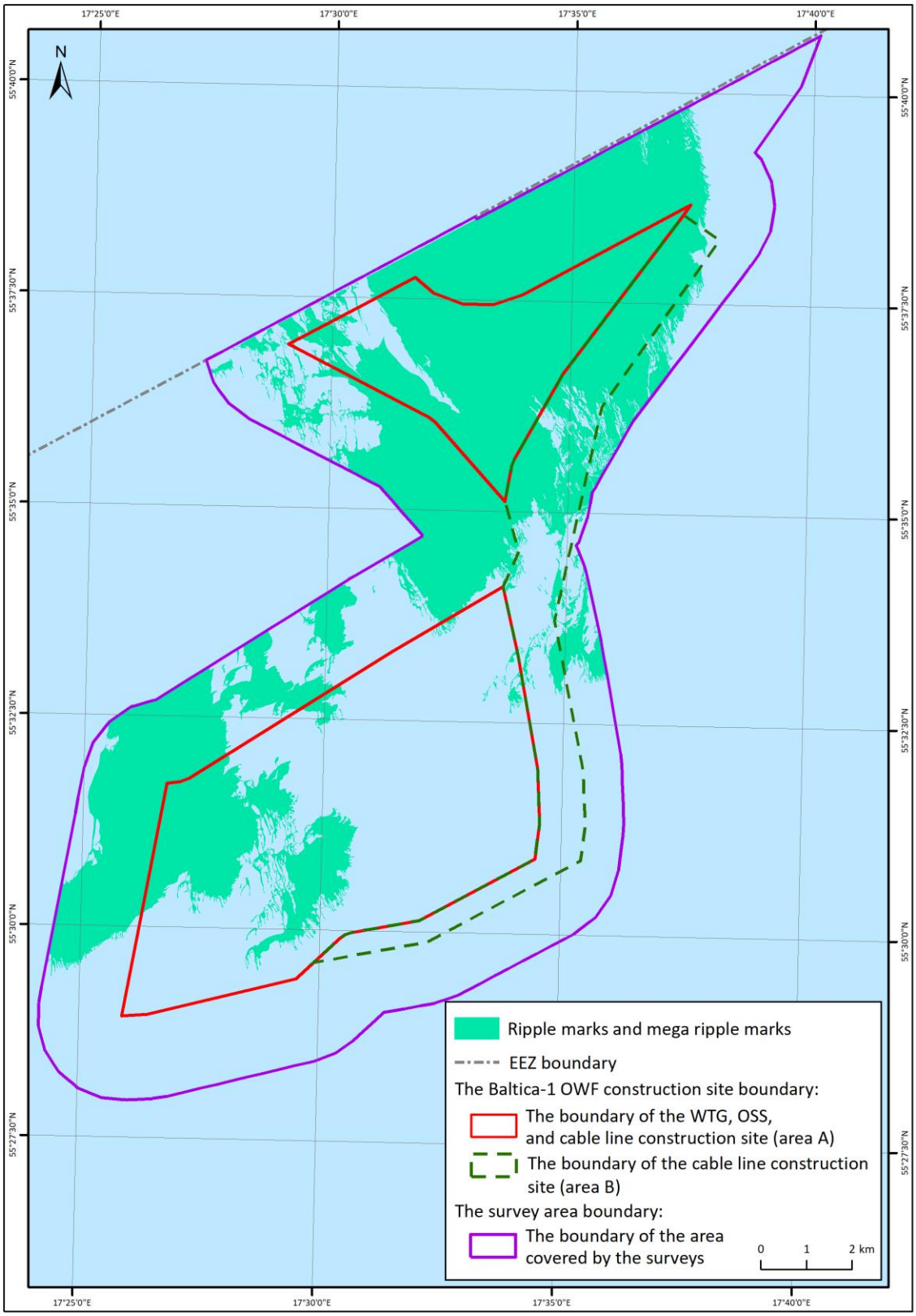


Figure 1.28. The occurrence of ripple-marks and mega-ripples in the survey area

Based on the SSS and MBES data, 16,717 boulders were identified in the survey area. Boulders were detected automatically by an algorithm available in the AutoClean package for MBES data processing,

developed by BeamworX. This algorithm is applied to cleaned, ungridded data which allows for the maximum number of soundings to be used. Boulders with at least one of the dimensions exceeding 0.25 m were identified. Out of the points generated automatically, the ones considered to be artefacts were removed manually. The number of boulders in individual size classes is presented in Table 1.6. In the survey area, a majority of the boulders occur individually or in small clusters in the northern, north-eastern and eastern parts of the area. The distribution of boulders in the survey area is presented in Figure 1.29.

Table 1.6. The number of boulders in individual size classes

Size class	**0.25–0.99 m**	**1.0–1.49 m**	**≥ 1.5 m**
The number of boulders	725	3396	12596

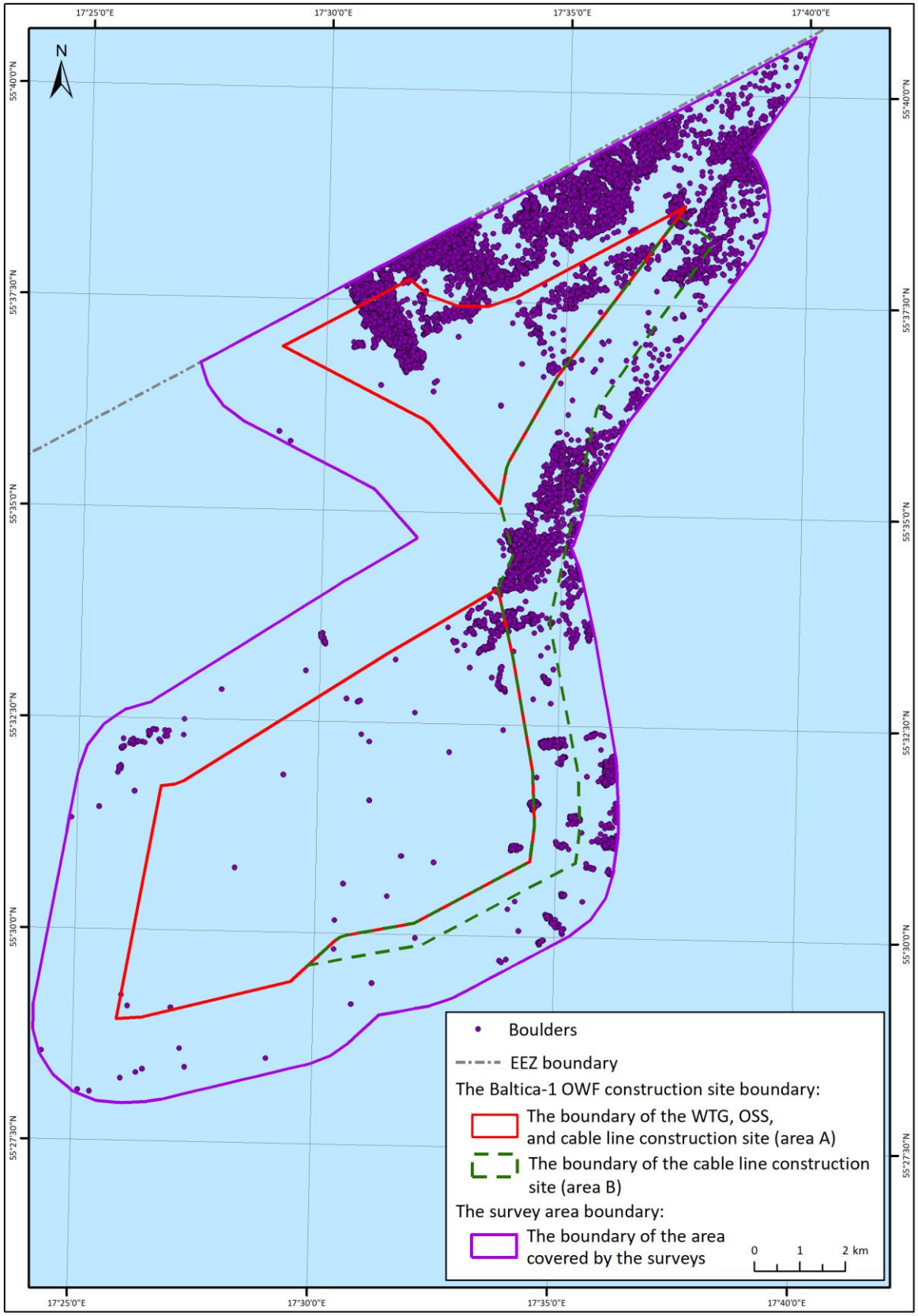


Figure 1.29. The distribution of boulders in the survey area

1.6.2 Geological structure

Based on the analysis of seismo-acoustic and seismic profiling results, six main seismic units were differentiated. These units were interpreted geologically with the application of general knowledge on the method and region of the survey conducted.

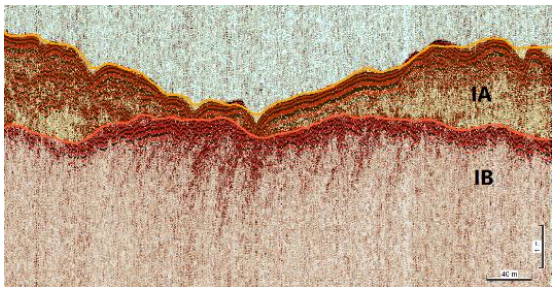
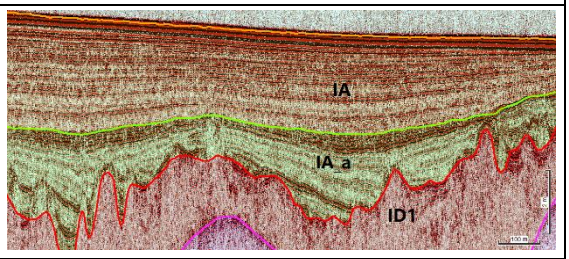
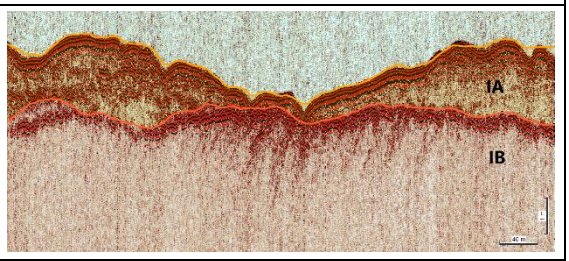
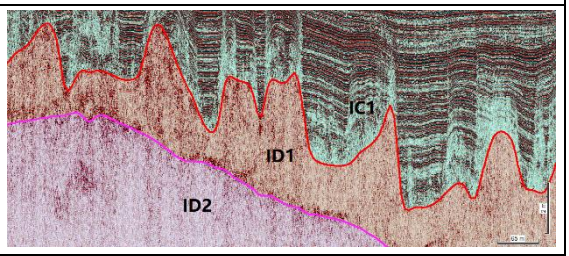
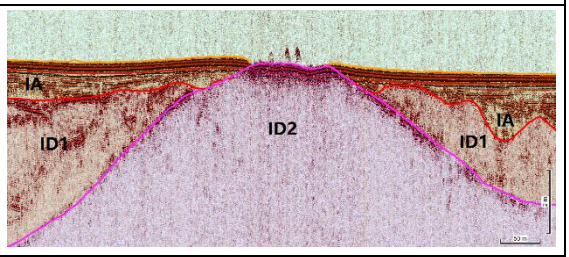
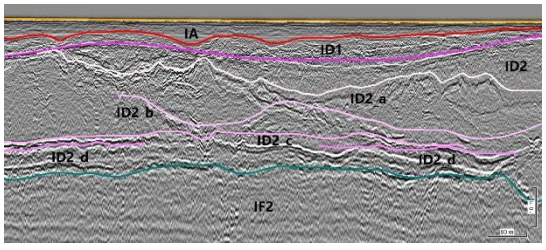
The basis for identification was the diversity of intensity and distribution of reflections, as well as the nature of the unit boundaries. The interpretation of the tops of individual seismic units was carried out manually by an interpreter and is the original result of the analysis of the data collected and the literature data (Dadlez, 1995; Kramarska, 1995a,b; Kramarska et al., 1999; Mojski, 1995; Uścinowicz, 1995; https://igs.pgi.gov.pl, https://geolog.pgi.gov.pl). This approach results from the specificity of the Pleistocene and Holocene sediments forming the seabed of the southern Baltic Sea. These are usually the sediments of great diversity (e.g. glacial sediments) with a significant number of internal horizons appearing in the sediments of similar genesis (glaciolacustrine deposits, fluvioglacial deposits, marine deposits).

The classification of the seismic units differentiated (the nature of reflections on the seismo-acoustic recording, including examples of fragments of seismic records) is shown in Table 1.7.

The units differentiated were described as:

- unit IA – fine- to medium-grained sands, locally silty sands, with coarse-grained sands and gravels (marine, fluvial and fluvioglacial) in places. These are sandy and sandy-silty marine deposits (Holocene) forming a layer together with the sandy deposits of fluvial and fluvioglacial origin (sands, gravels, locally silts; Pleistocene/Holocene). The top of unit IA forms the seabed surface of the sea area in which the deposits of this unit are present. The exceptions are the few places where outcrops of older sediments are visible on the seabed surface (glacial and fluvioglacial sediments, unit ID2). Because of a clear difference in the nature of reflections, an internal horizon IA_a was differentiated within unit IA. These are fine- to medium-grained sands, locally silty sand filling the depressions in the top of unit ID1;
- unit IB – fine and medium-grained sands, locally sands with gravel (lagoon, fluvial, fluvioglacial), form accumulations of varied character, heterogeneous, with alternating accumulations of sand and gravel. Possible presence of boulders. Boulders and gravels may form surfaces of an erosive pavement character, especially in the top part of the unit;
- unit ID – sands with gravel, gravels, tills (fluvioglacial and glacial); mainly glacial sediments with a large proportion of tills. This unit structure contains interbeddings and lenses of sand and sand and gravel sediments, with possible boulders present. In the top part, boulders may form surfaces of erosive pavement character. The following division into two sub-units within the fluvioglacial and glacial sediments was introduced:
    - unit ID1 – clayey tills or silty tills, locally clays or silty clays with an admixture of sand and gravel fractions (subaquatic);
    - unit ID2 – sands with gravel, gravels, tills (fluvioglacial and glacial); – within this unit, four internal horizons were differentiated, described as ID2_a, ID2_b, ID2_c and ID2_d (interpreted based on multi-channel seismic data only); these may be the tops of both glacial and fluvioglacial deposits;
- unit IF – pre-quaternary sediments:
    - unit IF1 – sediments filling the valleys in the Silurian top layer, the age of which is difficult to determine;
    - unit IF2 – correlated as Silurian sediments.

Table 1.7. The classification of the seismic units differentiated (the character of reflections in the seismo-acoustic recording)

Unit name	Reflection characteristics	Interpretation – lithology	An example of the seismic record
IA	Long, continuous reflections mostly parallel to the seabed surface; in areas of thicker accumulations, sometimes they form an arrangement of a diagonal horizon character within the bank	Fine- and medium-grained sands, locally silty sands, with coarse-grained sands and gravels in places	
IA_a	Long, continuous reflections mostly parallel and of similar shapes	Fine- to medium-grained sands, locally silty sand, filling the depressions in the top of subaquatic tills	
IB	Long, horizontal, continuous reflections of similar shapes, and/or short, slanting reflections; locally with small diffraction waves	Fine- to medium-grained sands, locally sands with gravel	
ID1	A chaotic arrangement of short reflections of various sizes and amplitudes; frequent diffraction waves, with the top surface undulated	Clayey tills or silty tills, locally clays or silty clays with an admixture of sand and gravel fractions	
ID2	A chaotic layout of short reflections of varied size and amplitude; frequent diffraction waves	Sands with gravel, gravels, tills	
ID2_a ID2_b ID2_c ID2_d	A chaotic layout of short reflections of varied size and amplitude; frequent diffraction waves	Glacial and fluvioglacial sediments	

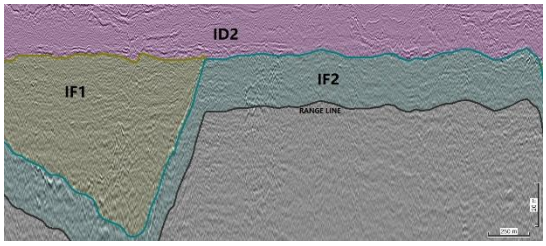
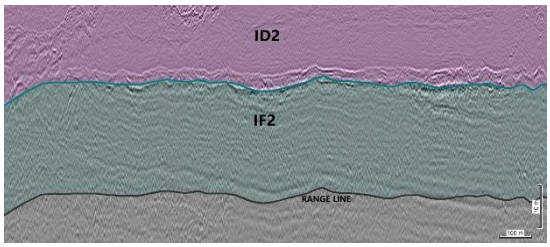
Unit name	Reflection characteristics	Interpretation – lithology	An example of the seismic record
IF1	A chaotic arrangement of short and medium reflections of various sizes and amplitudes; diffraction waves in places	Sediments filling the valleys in the Silurian top, the age of which is difficult to determine at the current stage of surveys	
IF2	Long, medium and strong reflections of similar shapes	Sediments correlated as Silurian deposits	

Table 1.8 presents a compilation of the macroscopic descriptions of the sediments collected as part of vibrocorer drilling together with the corresponding seismic units. Not all seismic units are represented in the samples of the sediments collected with the use of drilling. Sediments of older series are outside the reach of drilling at the points in which the drilling was planned or do not occur in the given area. All the data obtained during the analysis of the sediments collected with a vibrocorer were taken into account when interpreting the seismic data.

Table 1.8. A correlation of seismic units with the sediments collected during drilling with a vibrocorer (core examples)

Unit name	A group of sediment types assigned to a given seismic unit	Core number and macroscopic description of the collected sediment
IA	Fine- and medium-grained sands, locally silty sands, with coarse-grained sands and gravels in places	**VC_MFW_05** Core description: 0.0–6.0 m; fine and medium SAND, single grains of fine gravel, at a depth of 5.70–5.90 m an interbedding of medium sand with a small amount of fine and medium gravel, at the bottom (the last 5 cm) fine sand; soil symbol EN ISO 14688: fSa/mSa; soil colour: 2.5Y 5/2; carbonate content: calcareous
IB	Fine- to medium-grained sands, locally sands with gravel	**VC_MFW_16** Core description (only unit IB sediments): 1.5–2.0 m; medium SAND with fine to coarse gravel, at a depth of 1.75 m, a 6.5 cm diameter stone, at a depth of 1.75–1.85 m, an interbedding of compact clay with silt, medium sand, and fine and medium gravel; soil symbol EN ISO 14688: grmSa; soil colour: 2.5Y 5/2; carbonate content: calcareous
ID1	clayey tills or silty tills, locally clays or silty clays with an admixture of sand and gravel fractions	**VC_MFW_26** Core description (only unit ID1 sediments): 4.75–5.35 m; CLAY with silt, with thin and thick laminae of fine sand; soil symbol EN ISO 14688: siCl; soil colour: 2.5Y 4/2; carbonate content: calcareous
ID2	Sands with gravel, gravels, tills	**VC_MFW_03_A** Core description: 0.0–1.1 m; CLAY with silt, sand and fine to coarse gravel, at a depth of 0.15–0.20 m and 0.30–0.40 m interbeddings of firm clay; soil symbol EN ISO 14688: grsasiCl; soil colour: 2.5Y 4/2; carbonate content: calcareous;

Unit name	A group of sediment types assigned to a given seismic unit	Core number and macroscopic description of the collected sediment
		1.1–1.4 m; CLAY with silt, sand and fine to coarse gravel; soil symbol EN ISO 14688: grsasiCl; soil colour: 2.5Y 4/1; carbonate content: slightly calcareous

As a result of the interpretation conducted, the seabed structure was identified to a depth of approx. 45.0–40 metres, up to approximately 130 m in places.

In the south-western and central part of the survey area, the seabed is formed by fine- and medium-grained sands, locally silty sands, in some places coarse-grained sands and gravels (unit IA). They form a layer with a thickness of up to approximately 17 m consisting mainly of marine sands. In the northern and eastern part of the survey area, they form a discontinuous layer and occur on the seabed in the form of accumulations characterised by low thickness. Within this unit, an internal horizon IA_a was differentiated. It comprises fine- to medium-grained sands, locally silty sand filling the depressions in the top of unit ID1, in the south-eastern part of the area. Below the sandy sediments, in the western and southern parts of the survey area, fine- and medium-grained sands were identified, locally sands with gravel (unit IB) [Figure 1.31]. They form a layer with a thickness of up to approximately 20 m. The sediments of this unit are not homogeneous. They are sediments of lagoonal and fluvial origin, partially also fluvioglacial. Below the sediments of units IA and IB, in the southern part of the survey area, sediments of subaquatic origin were identified – clayey tills or silty tills, locally clays or silty clays with an admixture of sand and gravel fractions (unit ID1). They form a layer with a thickness of up to approximately 8 m; the exception is the fill of the buried valley identified in the central part of the survey area, which is mainly constituted by the sediments of unit ID1 with a thickness of up to approximately 16 m. Greater thicknesses (approx. 16 m) occurs also in the south-western part of the survey area. Another unit identified comprises the glacial and fluvioglacial sediments of unit ID2. These are mostly sands, gravels, and tills. The shallowest location in which they were identified is the eastern and north-eastern part of the area analysed, where they form outcrops on the seabed surface. Their top descends towards the west and south-west, to the depth of approximately 27 m BSB. Within Unit ID2, four internal horizons were differentiated: D2a, ID2b, ID2c,and ID2d, which may be the tops of both glacial and fluvioglacial deposits. Below the glacial sediments of unit ID2, sediments representing unit IF were identified, which were classified as pre-Quaternary sediments. Unit IF2 sediments were described as Silurian deposits. Their top is intersected with valleys of NW–SE to NE–SW orientation and lies at a depth from approximately 9 to approximately 129 m BSB. The valleys in the Silurian top are filled with Quaternary deposits, but two valleys in the western part of the southern fragment of the survey area may be filled with older deposits (unit IF1). This needs further, detailed reconnaissance.

Figure 1.30–Figure 1.35 illustrate the extent of occurrence and the location (m BSB) of the tops of individual seismic units in the survey area. Presented below are sample geological cross-sections illustrating the geological structure of the survey area [Figure 1.36–Figure 1.39].

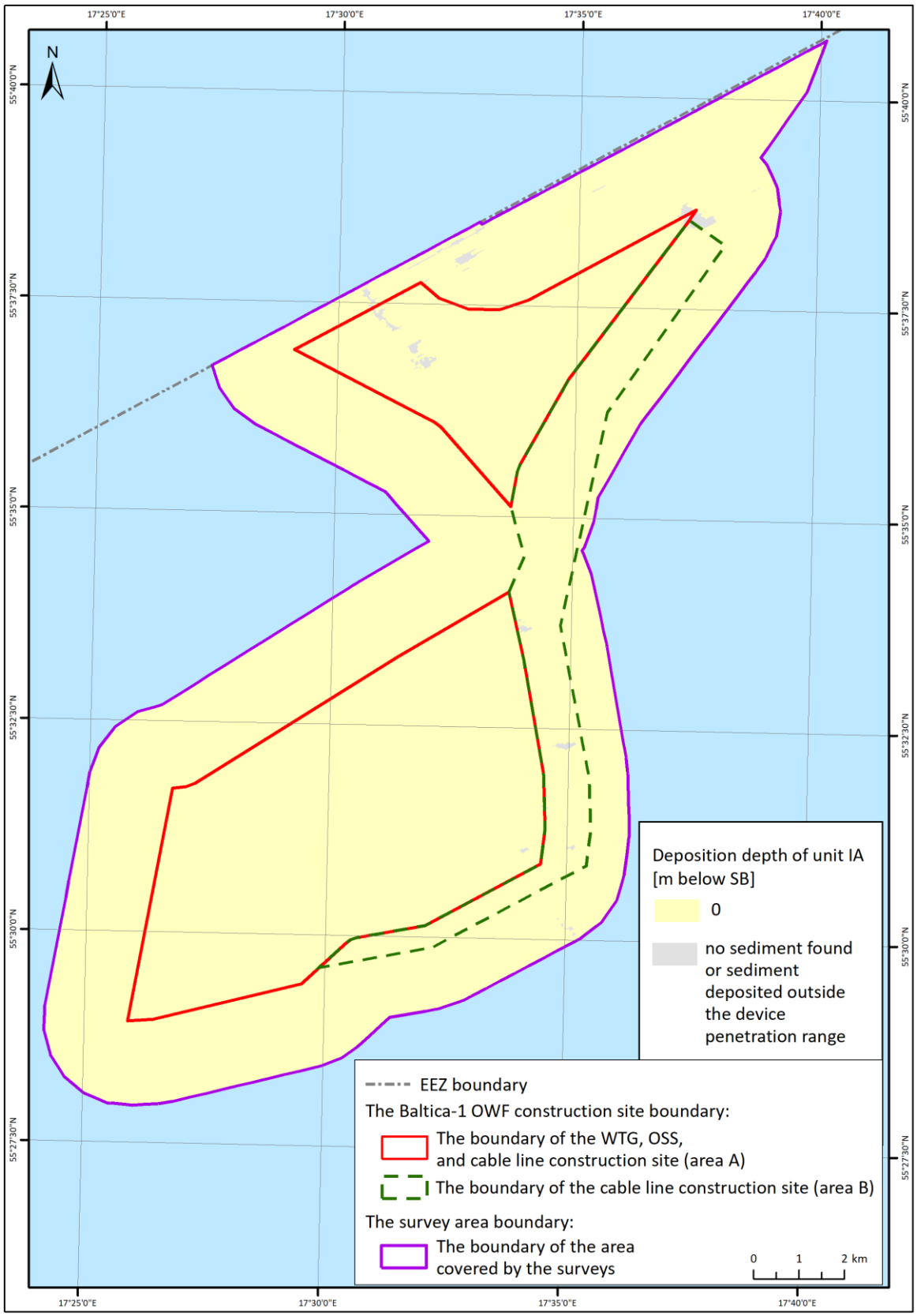


Figure 1.30. The top of unit IA [m BSB] – fine to medium sands, locally silty sands, with coarse sands and gravels (marine, fluvial, and fluvioglacial) in places

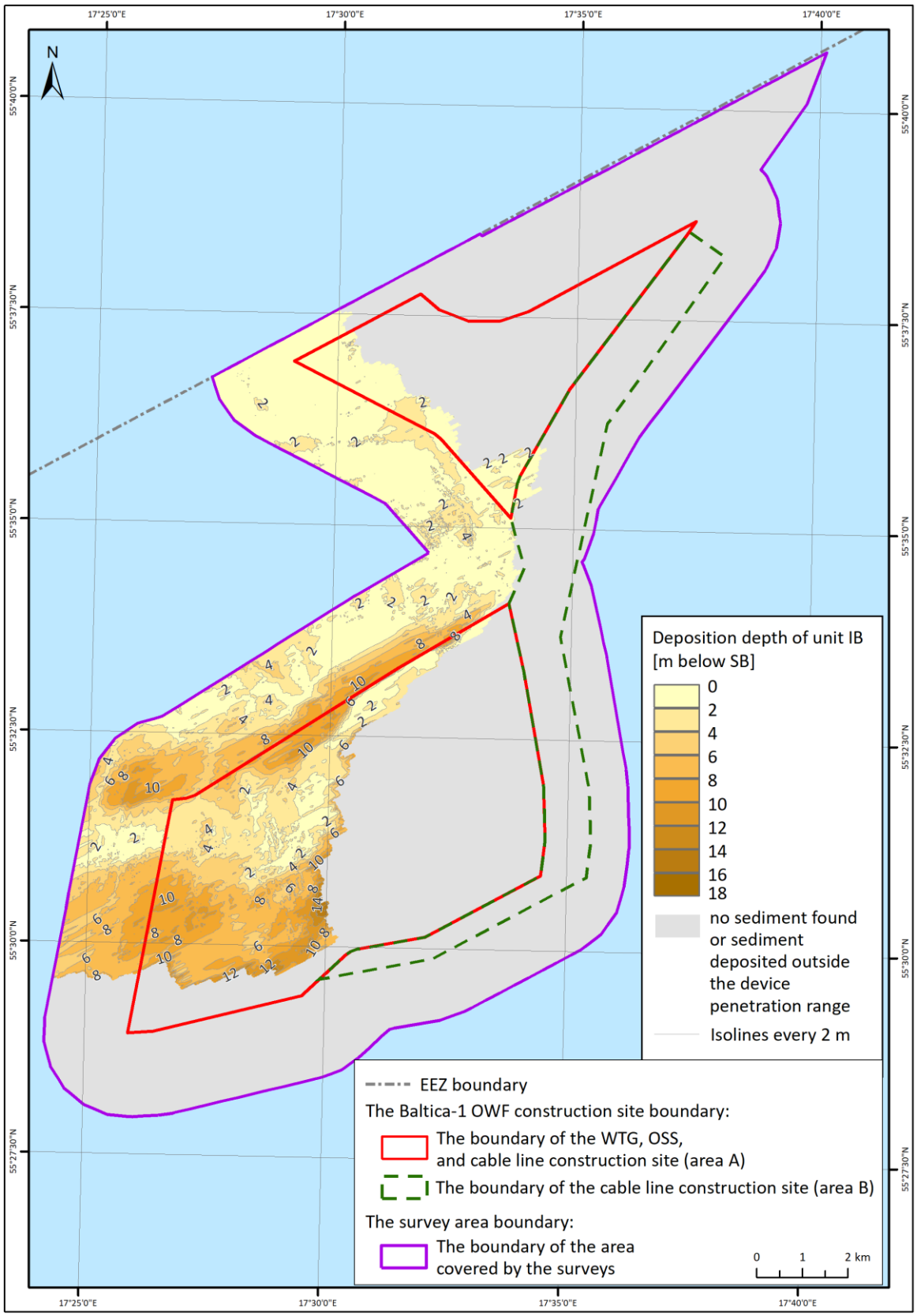


Figure 1.31. The top of unit IB [m BSB] – fine and medium sands, locally sands with gravel (lagoonal, fluvial, fluvioglacial)

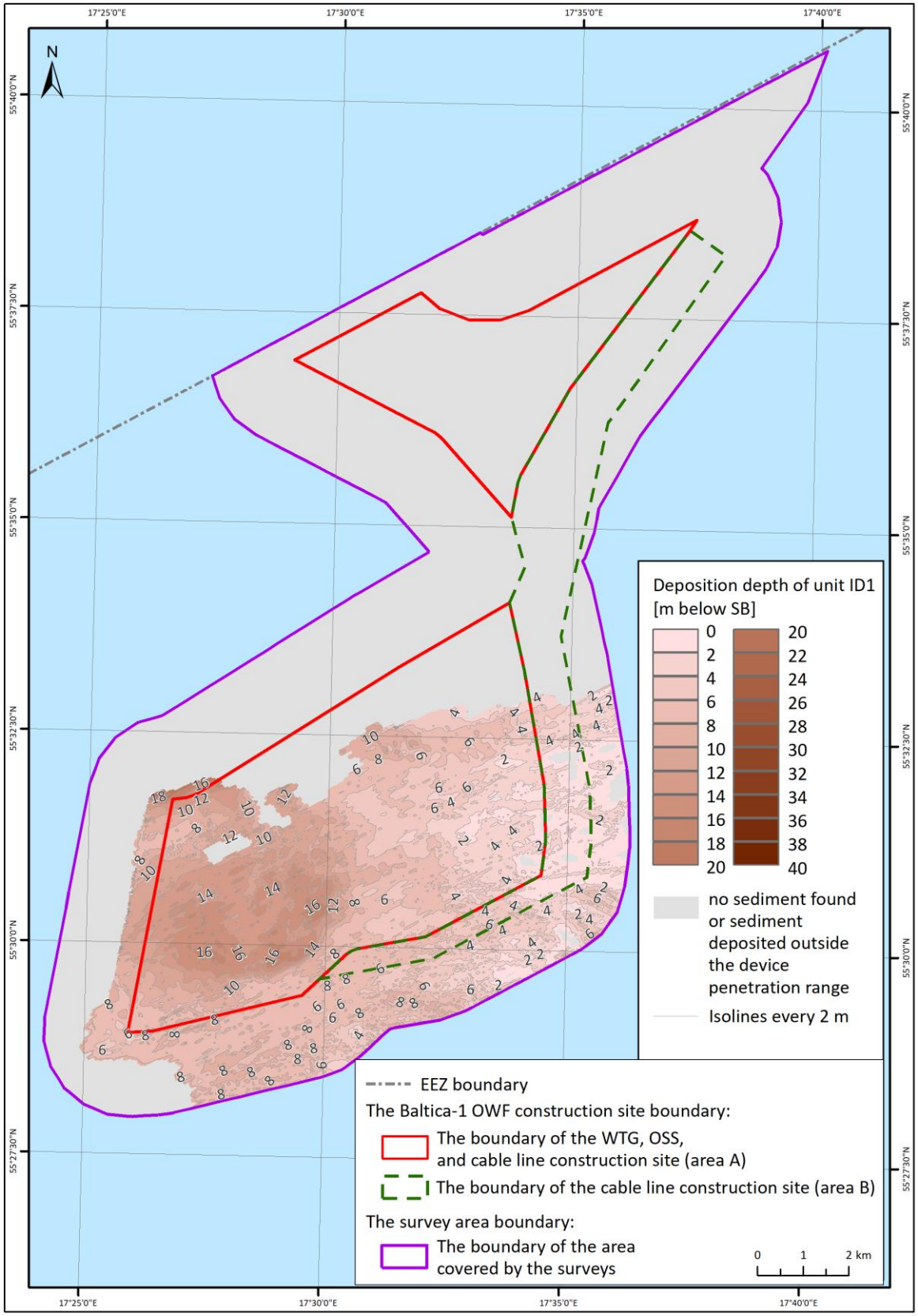


Figure 1.32. The top of unit ID1 [m BSB] – clayey tills or silty tills, locally clays or silty clays with an admixture of sand and gravel fractions (subaquatic)

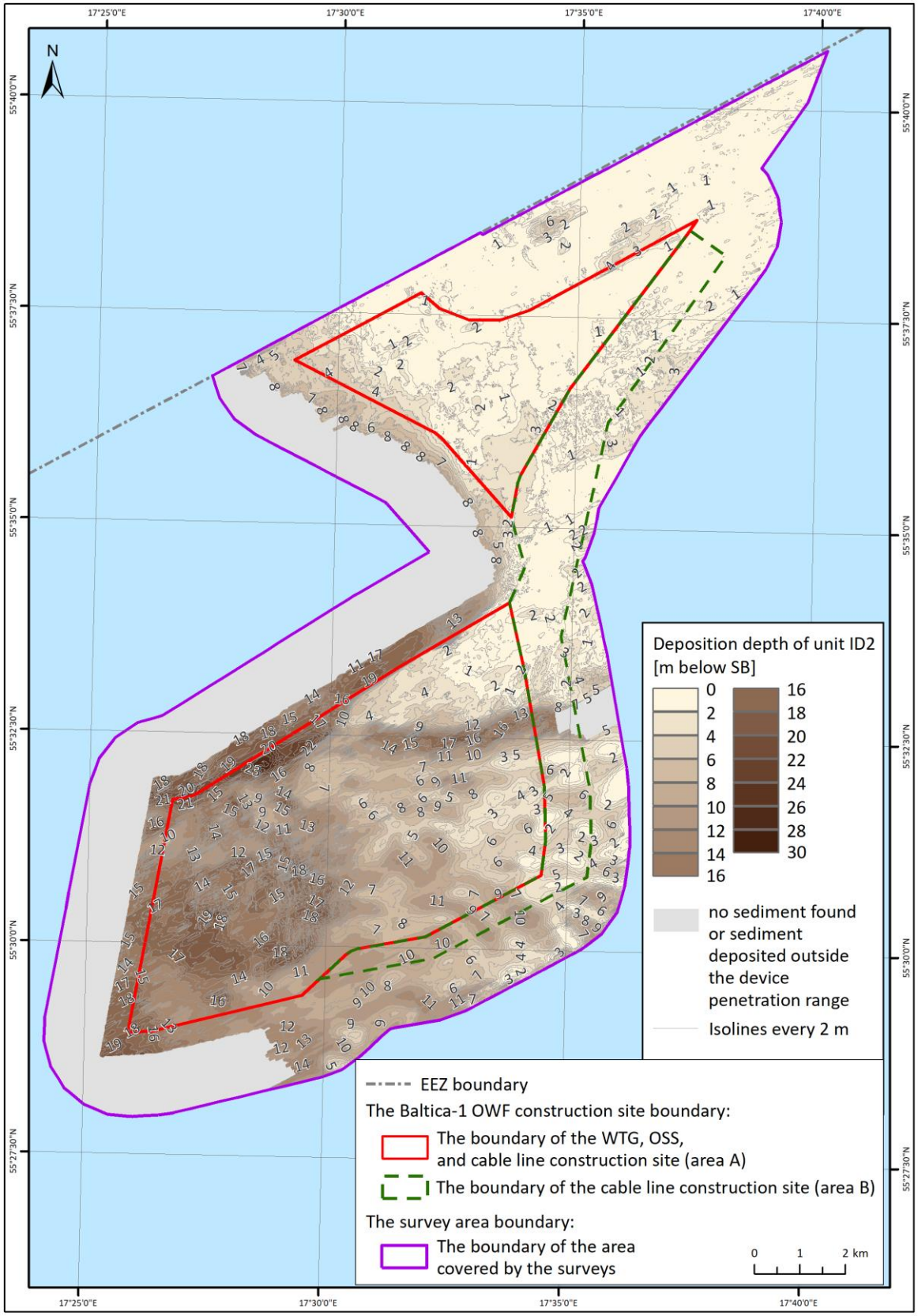


Figure 1.33. The top of unit ID2 [m BSB] – sands with gravel, gravels, tills (fluvioglacial and glacial)

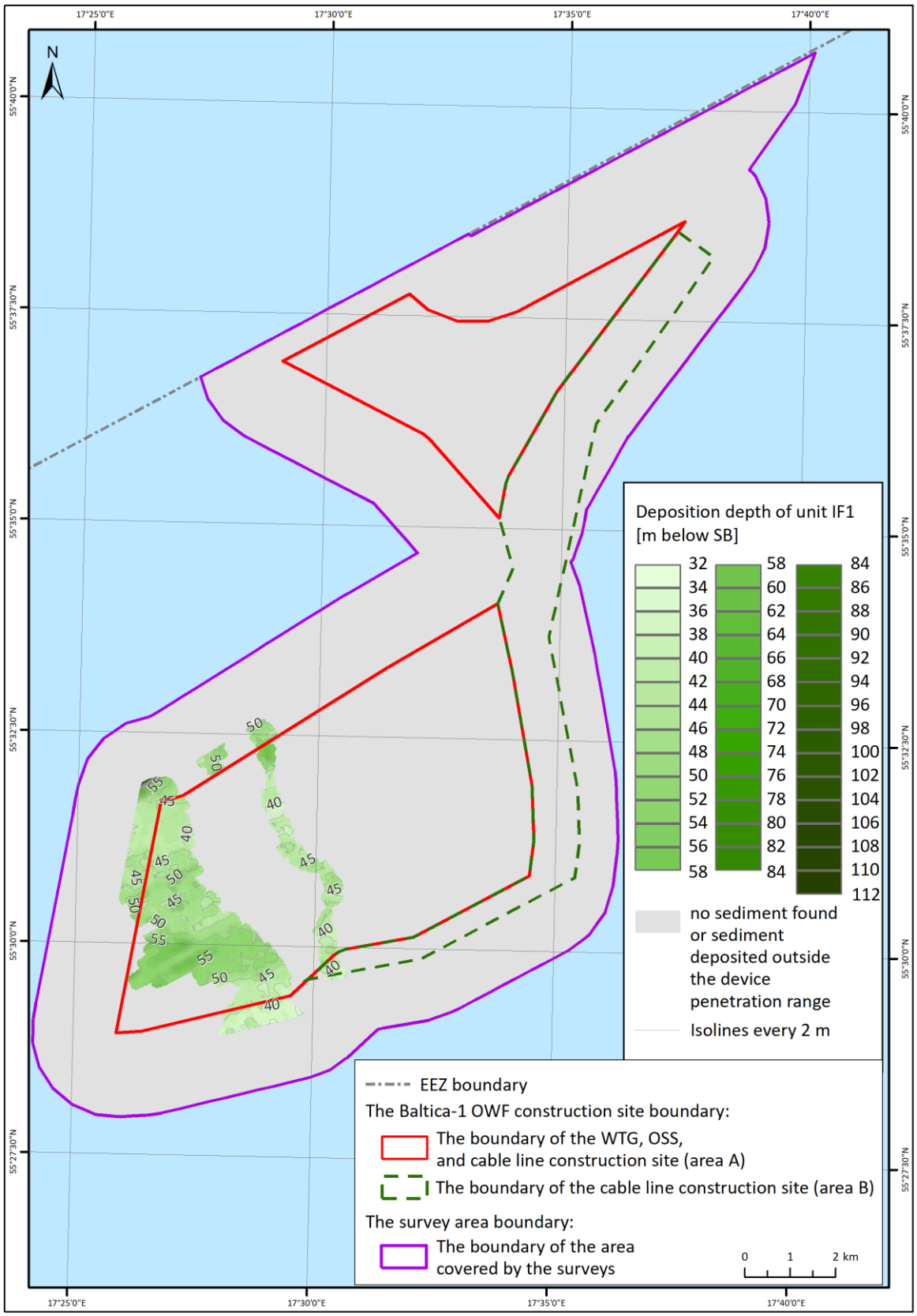


Figure 1.34. The top of unit IF1 [m BSB] – sediments filling the valleys in the Silurian top

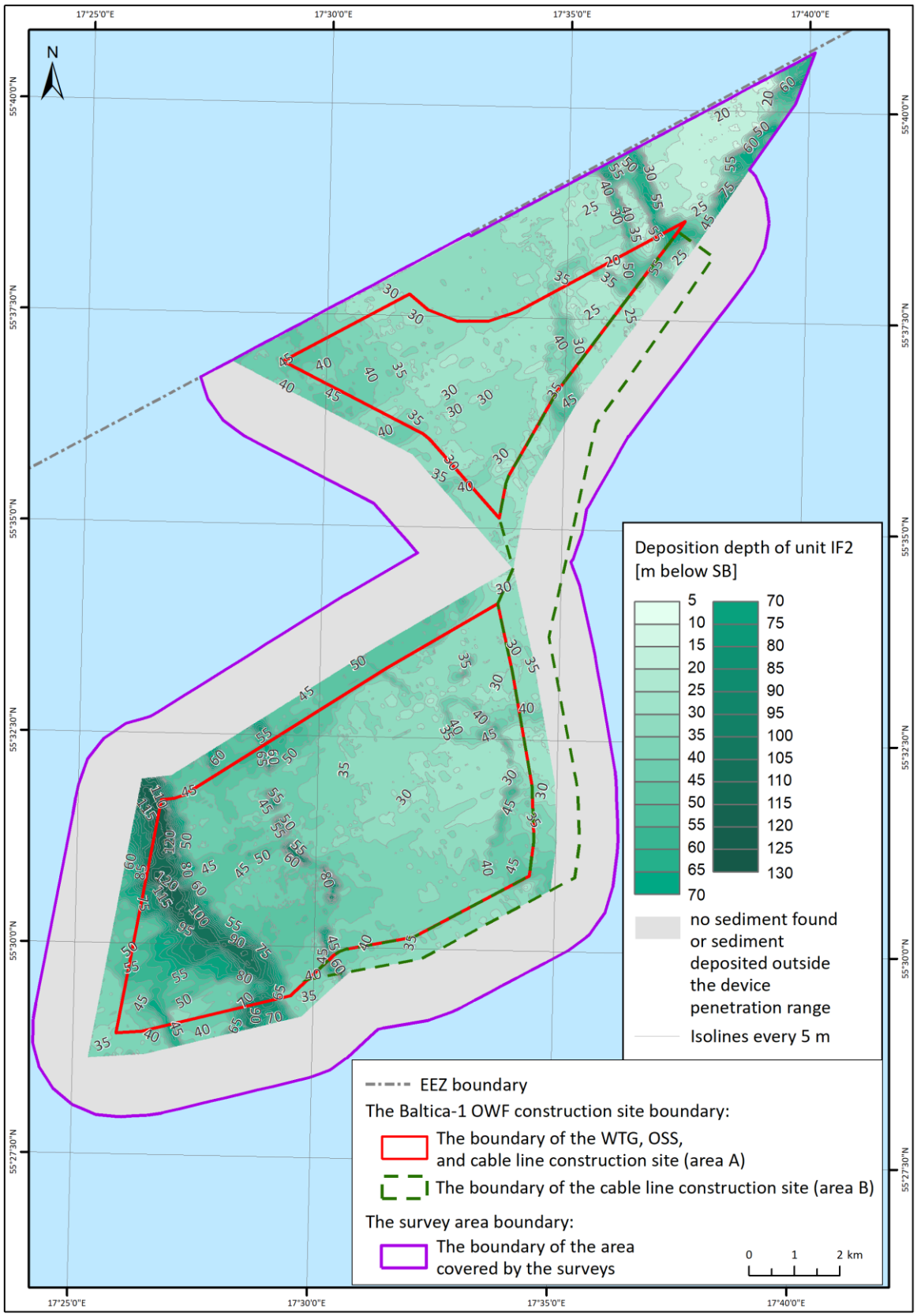


Figure 1.35. The top of unit IF2 [m BSB] – Silurian deposits

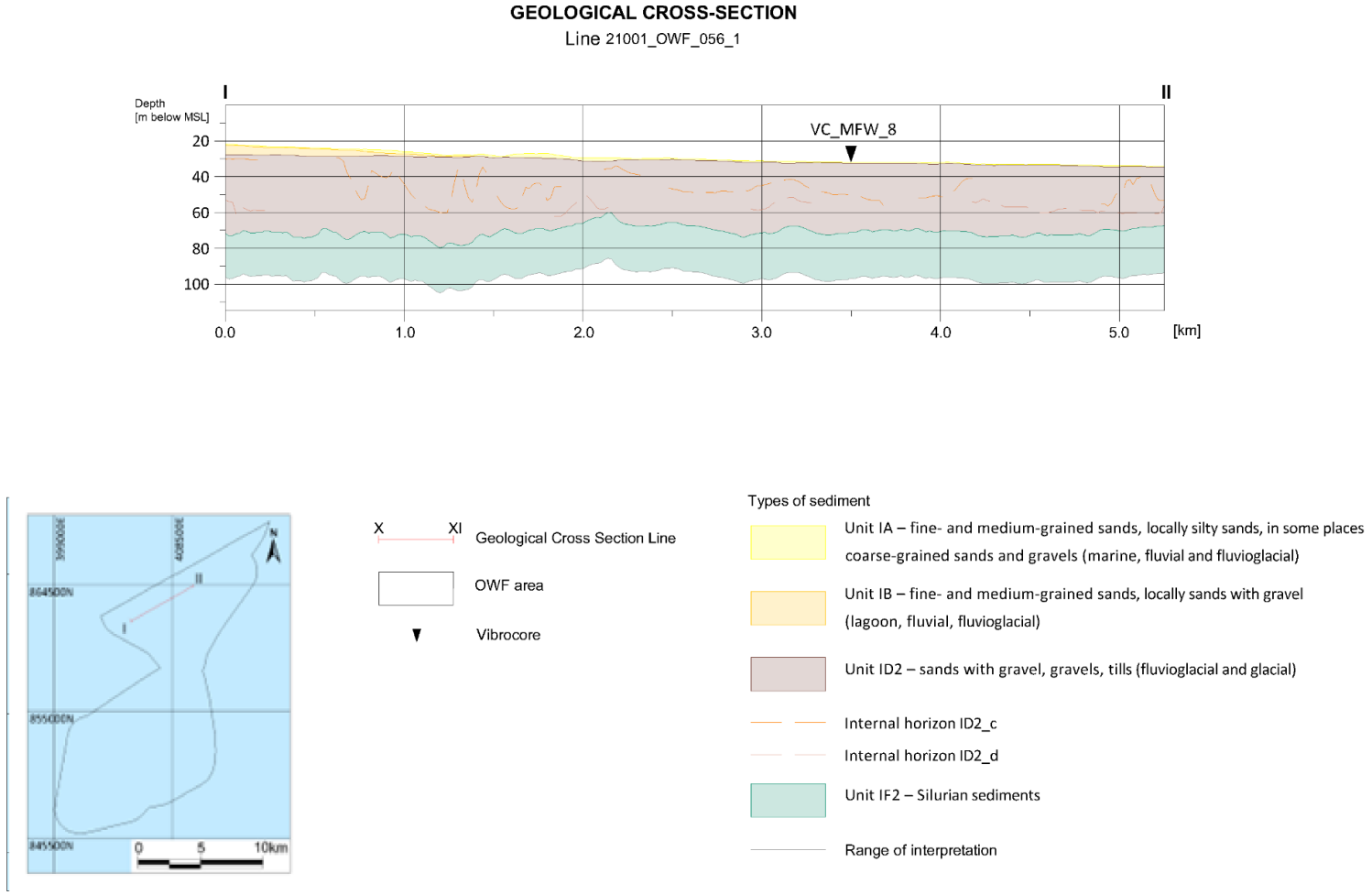


Figure 1.36. Geological cross-section along the survey line 21001_OWF_056_1

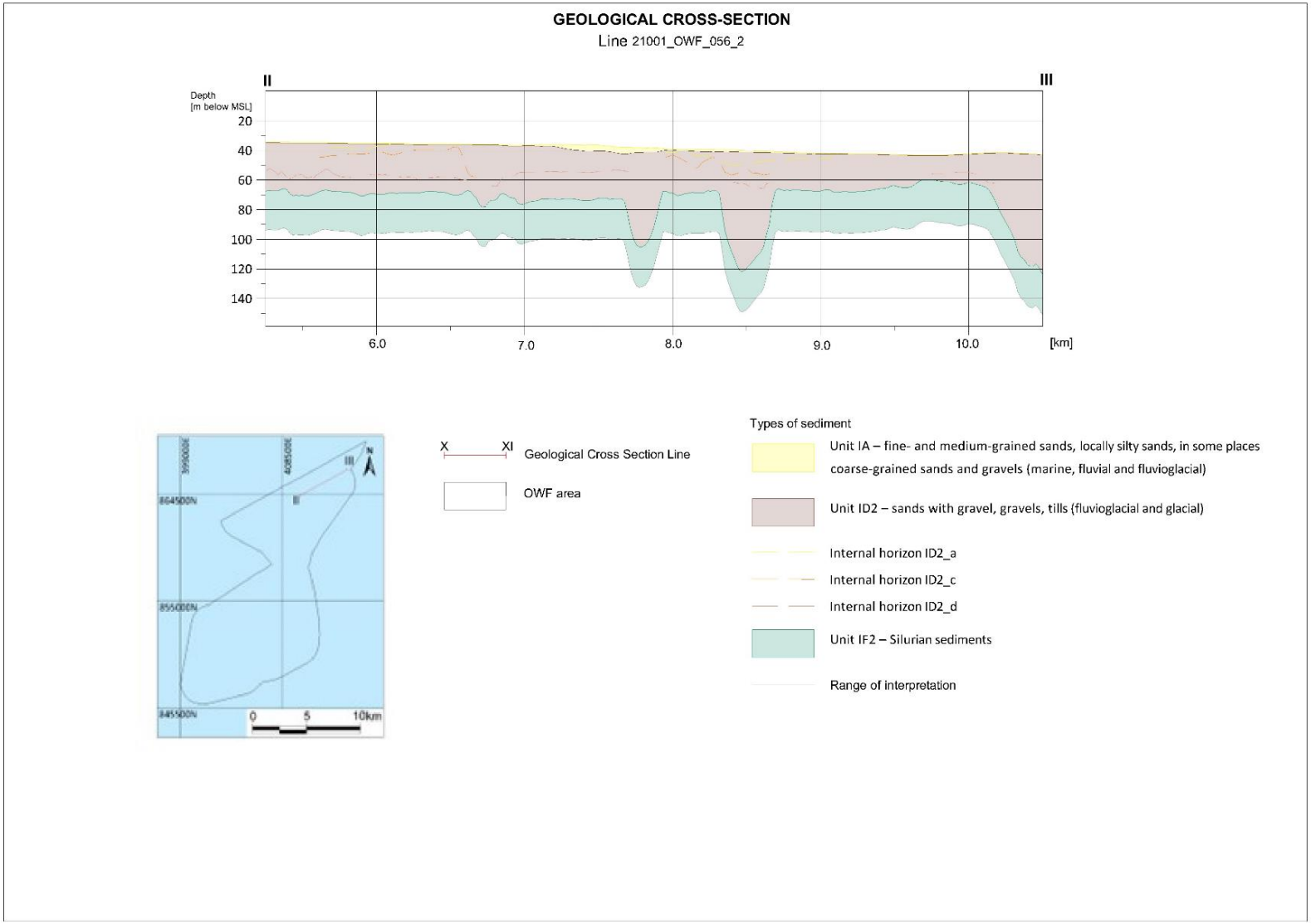


Figure 1.37. Geological cross-section along the survey line 21001_OWF_056_2

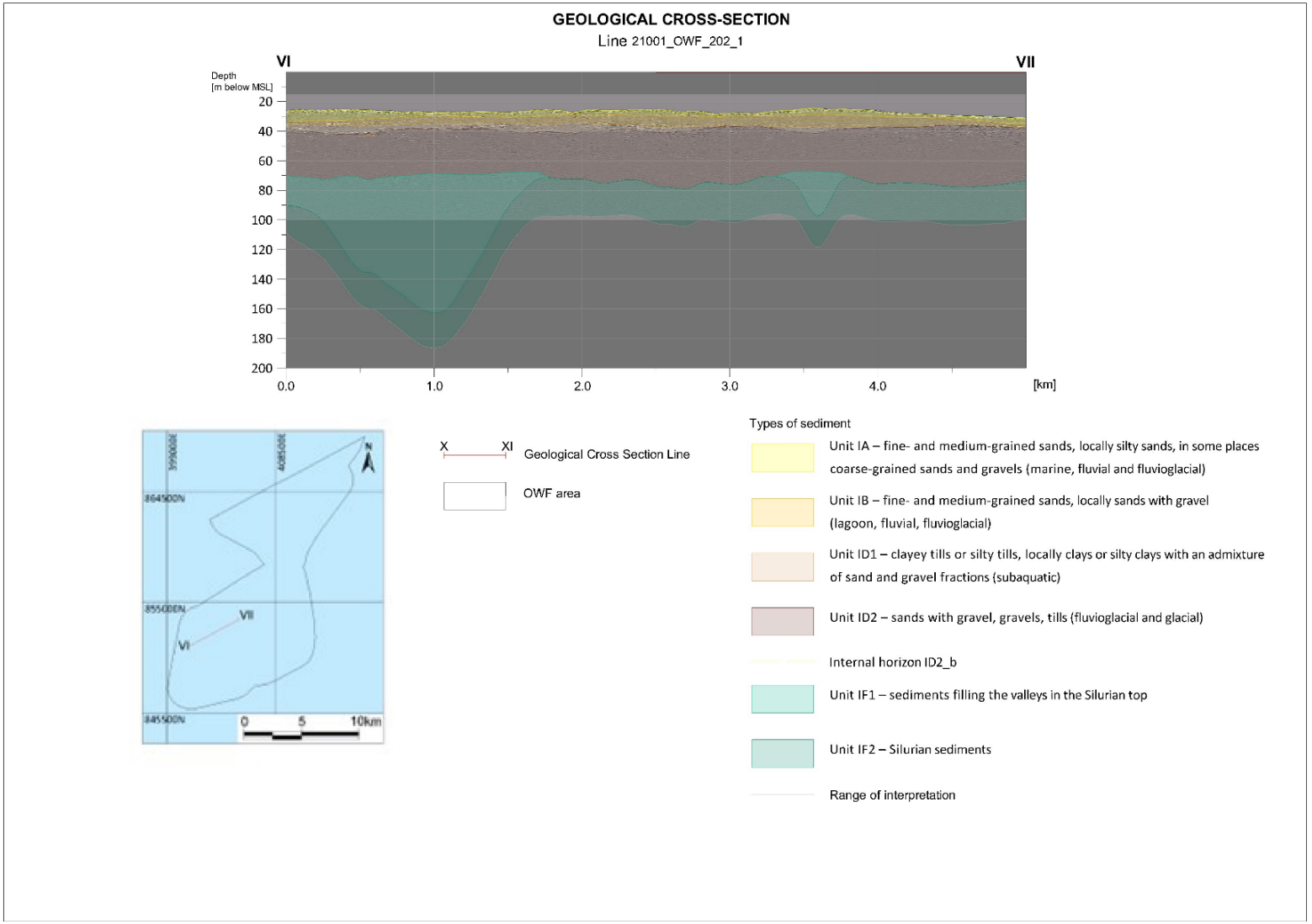


Figure 1.38. Geological cross-section along the survey line 21001_OWF_242_1

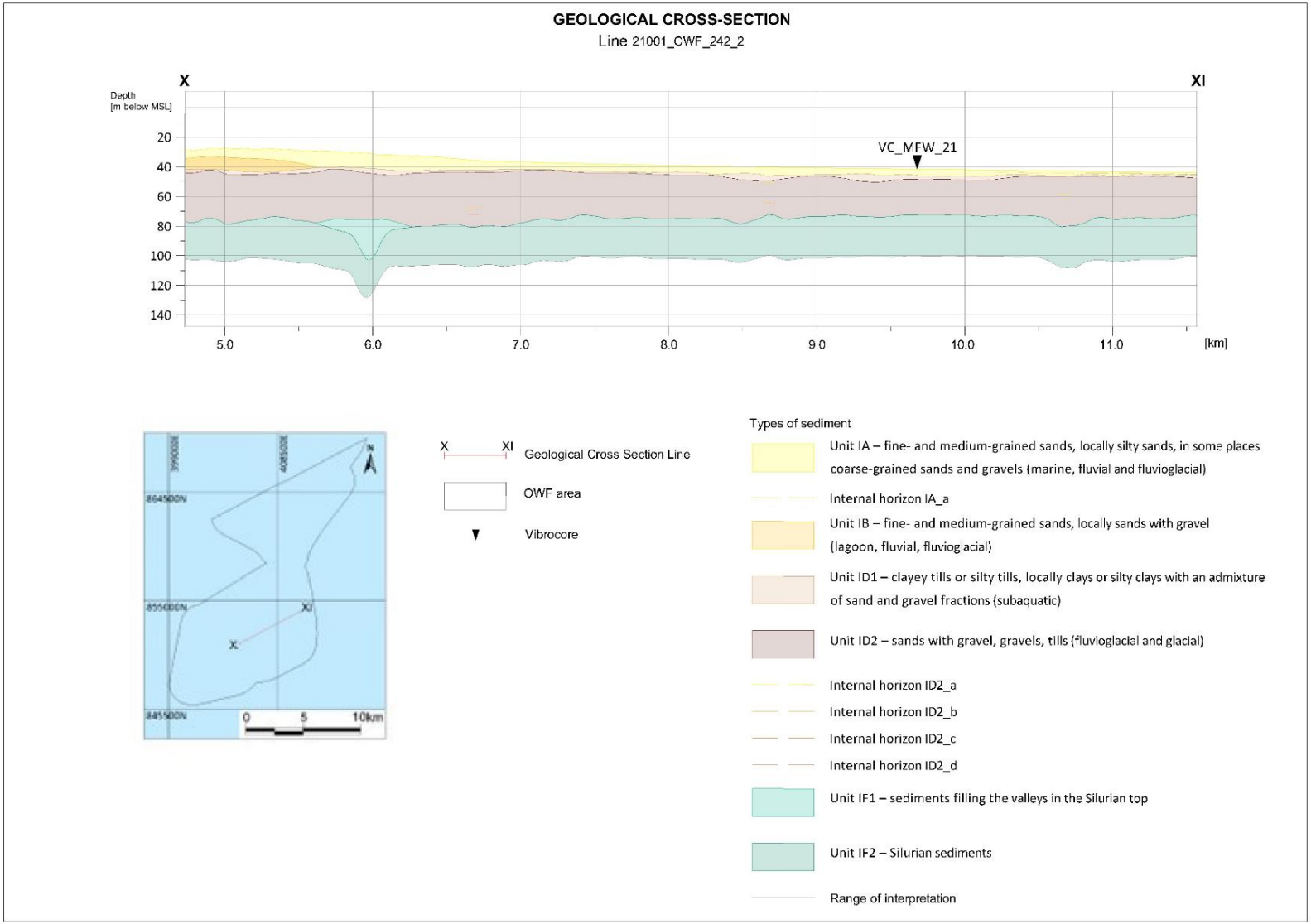


Figure 1.39. Geological cross-section along the survey line 21001_OWF_242_2

During the analysis of the seismic data collected in the survey area, 32 buried anomalies were detected. These anomalies are caused by oval-shaped objects, probably boulders or boulder clusters buried in the sediment or the presence of a sediment with a different fraction and packing from the sediment surrounding the anomaly indicated.

The buried anomalies identified were correlated with the anomalies visible on the magnetometer data. A maximum distance of 15 m between the locations of anomalies determined from these two types of data was assumed. In effect, in the survey area, 6 locations were obtained in which the buried anomalies correspond to magnetic anomalies.

In the survey area, a system of fossil valleys of NW–SE to NE–SW orientation cutting through the top of Silurian deposits was identified. The valleys are filled with Quaternary deposits, but two valleys in the western part of the southern fragment of the survey area may be filled with older deposits (unit IF1).

The valley bottoms are located at a depth of approximately 66–103 m BSB, their width is approximately 500–950 m, while the length is approximately 4300–9400 m. The largest of the valleys is located in the western part of the southern fragment of the survey area. Its bottom is at a depth of approximately 132 m BSB, the width is approximately 2100 m, and its length is approximately 6600 m.

In the central part of the survey area, a fossil valley cutting through unit ID2 sediments was identified. Its axis is more or less latitudinal, the width is approximately 500 m, while its length is approximately 3500 m. The valley bottom is located at a depth of approximately 33 m BSB and its filling constitutes mainly of unit ID1 sediments.

Probably, all valleys continue outside the survey area.

During the analysis of the seismic data, 8 normal faults and 3 reverse faults were detected. Their offsets range from approximately 2 to 5 m. All faults are located within the Silurian deposits and do not continue in younger deposits.

In the southern part of the survey area, potential locations of shallow gas occurrence in sediments were indicated. These locations were determined based on seismo-acoustic data analysis. Places of potential presence of shallow gas deposits were marked when distortions of reflections were observed in seismo-acoustic data records (bright spots, boosted reflections, seismic chimneys, acoustic blanking). In some of the places indicated, distortions of reflections were visible only on one profile, without extending the information about the potential presence of gas in the sediments onto the adjacent profiles. In most cases, reflection distortions were visible in a similar position also on subsequent, adjacent seismo-acoustic profiles. Potential shallow gas accumulations were identified within the sediments of units IA, ID1, and ID2.

The shallow gas indicated is associated with Quaternary deposits. Their occurrence results from the presence of organic matter in young (Pleistocene/Holocene) deposits rich in organic matter, currently covered with modern sediments of the Baltic Sea. The gas is a product of biogenic processes. The analyses conducted, did not provide the basis to indicate gas seeping from deeper geological structures (Jaśniewicz et al., 2019).

It should also be emphasised that no surface structures the genesis of which would be related to the gas escaping from the sediment (e.g. pockmarks), were identified in the seabed relief of the area analysed. High-resolution bathymetric data and sonar image were analysed.

The distribution of buried anomalies, fossil valleys, faults, and shallow gas occurrences is presented on the map of geohazards [Figure 1.40].

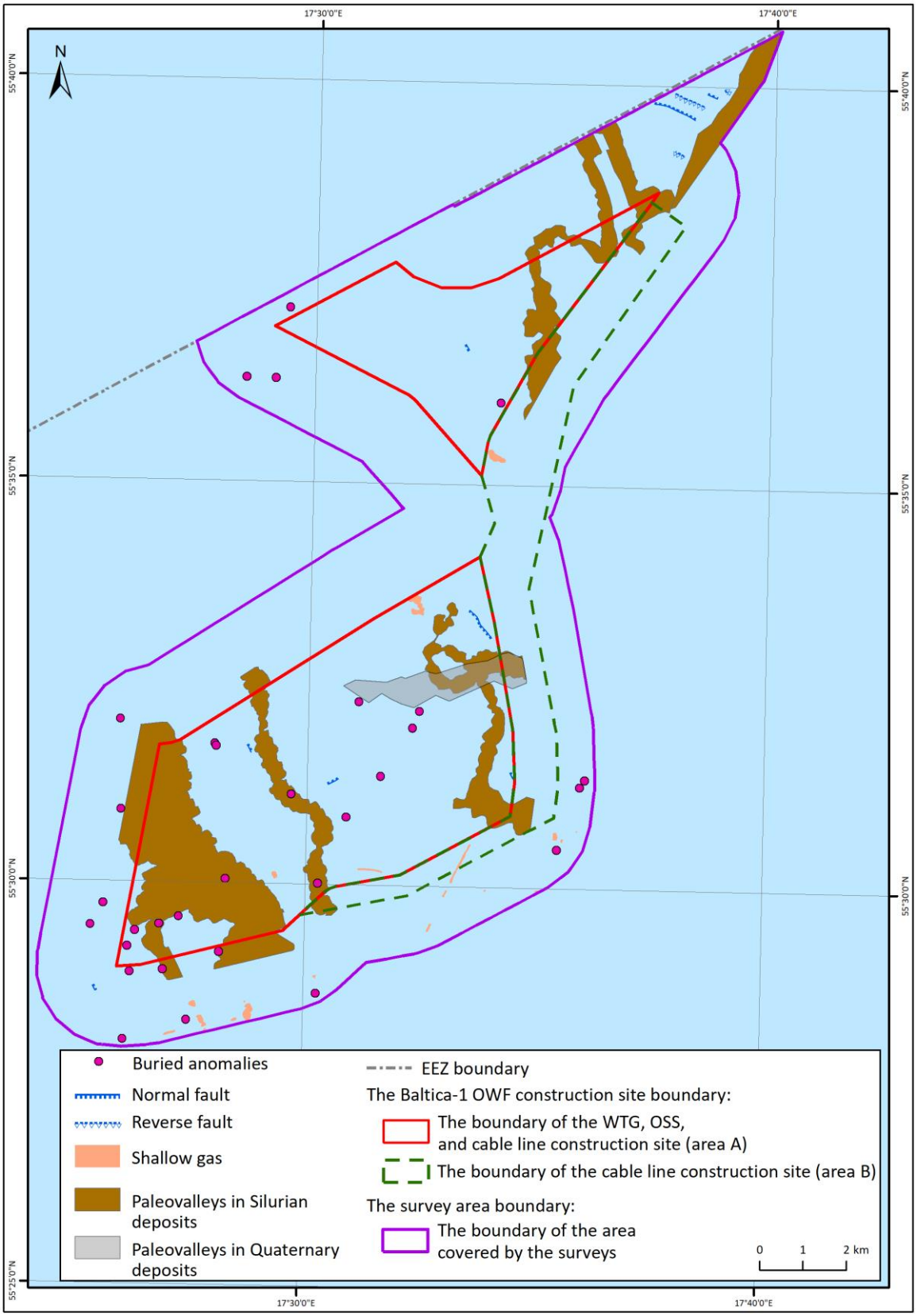


Figure 1.40. Geohazards in the survey area

1.7 SHORTCOMINGS AND GAPS IN THE STATE-OF-THE-ART

No research was carried out in the survey area within the Swedish EEZ due to the lack of the necessary permit. Therefore, the characteristics of this part of the area are based on data obtained from the European Marine Observation and Data Network (EMODnet).

Data collected did not allow profiling the part of the survey area located within the Swedish EEZ with the same resolution as the one used in the part of the survey area located within the Polish EEZ, where a complete set of the Contractors' own surveys was conducted. However, considering that the planned Investment will not be located within Swedish waters, the profiling of this part of the survey area based on data obtained from sources other than our own surveys is sufficient for the impact assessment.

2 ABIOTIC ELEMENTS IN MARINE SURVEYS – THE BASIC SCOPE OF SURVEYS CONTRACTED

2.1 HYDROLOGICAL AND METEOROLOGICAL MONITORING INCLUDING SEA CURRENTS

2.1.1 Non-specialist summary

In the period from 1 December 2022 to 30 November 2023, continuous measurements of electrical conductivity and temperature of water were performed at 101 vertical profiles in the area of the planned offshore wind farm. The measured parameters (atmosphere – wind speed and direction, air pressure, temperature, and humidity; water dynamics – the height, period, and direction of waves on the free sea surface, changes in depth of water, speed and direction of flows; and hydrophysical properties of water – temperature, electrolytic conductivity, salinity and turbidity) were presented in graphical form and as basic statistical information and briefly discussed.

The weather conditions at sea were recorded at a position in the southern part of the Southern Middle Bank, hence they represent the characteristics of the near-water layer of the atmosphere of the open sea area at a distance of approximately several dozen km from the Polish coast. The observations covered a full year, from December 2022 to November 2023. The recorded wind data show the full range of wind conditions variability over this part of the sea: from strong storms (with wind speeds exceeding 20 $m \cdot s^{-1}$, gusts of 28 $m \cdot s^{-1}$ (e.g. on 18.02.2023 and 22.11.2023) to periods of calm weather (e.g. on 08.09.2023). In this period, the mean wind velocity was 7.28 $m \cdot s^{-1}$. The winds from the south-western sector (from SSW to WSW) were clearly dominant, although there was also a visible share of directions from the north-eastern and eastern sectors (from NNE to ESE). Significant fluctuations in atmospheric pressure were recorded (in the range of approx. 980–1042 hPa; with the average for this period of 1012.87 hPa). The air temperature shows the full range of variability during the year from approx. -2.9°C (28.03.2023) to approx. 23.3°C (08.09.2023), with the average for the period of 10.16°C. Air humidity ranged from approx. 42% to 100%, with the average of 86%. No ice phenomena occurred in the surveyed sea area in the winter period.

The wave motion on the free sea surface was characterised by variable intensity depending on the season. The highest waves were recorded in winter, while the spring and summer were the calmest. The maximum wave height was 9.51 m, which was recorded at survey station B_MFW_3 (18.02.2023). Depending on the survey station, the mean wave motion height ranged from 0.64 m to 0.71 m. The dominant wave motion was from the west and south-west.

Registrations of flows in the entire cross-section of the water column, from the water surface to the seabed, were performed simultaneously at five survey stations located in places at sea with different depths and located at different distances from the shoreline. Such significant differences in sea depth combined with different distances from the coast influenced the visible differentiation of the characteristics of water flows in the water column, both in terms of the distribution of directions and mean velocities in the water column. However, all dominant flow directions, which were visible basically in the entire cross-section of the water column, specific to the individual measurement locations, were revealed in the area of the planned wind farm. A characteristic pattern of dominant flows in the southern and south-western sectors was revealed. The mean flow velocities recorded at the stations on the Southern Middle Bank are generally the highest in the near-surface layers (up to 12 m BSL) – from 0.10 to 0.12 $m \cdot s^{-1}$, and the lowest in the near-seabed layer – from 0.06 to 0.10 $m \cdot s^{-1}$,

with the maximum values ranging from 0.46 to 0.61 $m \cdot s^{-1}$. The recorded changes in the thickness of the water column (sea depth) for all survey stations were within the range of 0.7–1.2 m.

The hydro-physical parameters of water were typical of the shallow-water zone of the southern Baltic coast, e.g. water salinity oscillated around 7.45 PSU. The water temperature ranged from 2.97 to 21.16°C and was similar throughout the water column. The values of water turbidity at all measurement points were within the range between approx. 0.41 to approx. 139.89 FTU.

2.1.2 Spatial scope of the surveys

The spatial scope of hydrological and meteorological studies, taking into account sea currents, was the survey area covering the Baltica-1 OWF construction area, which is the site of construction of WTGs, OSSs, and cable lines (area A) and the site of construction of cable lines (area B) together with a zone of no less than 1 NM in width measured from the boundary of area A [Figure 2.1].

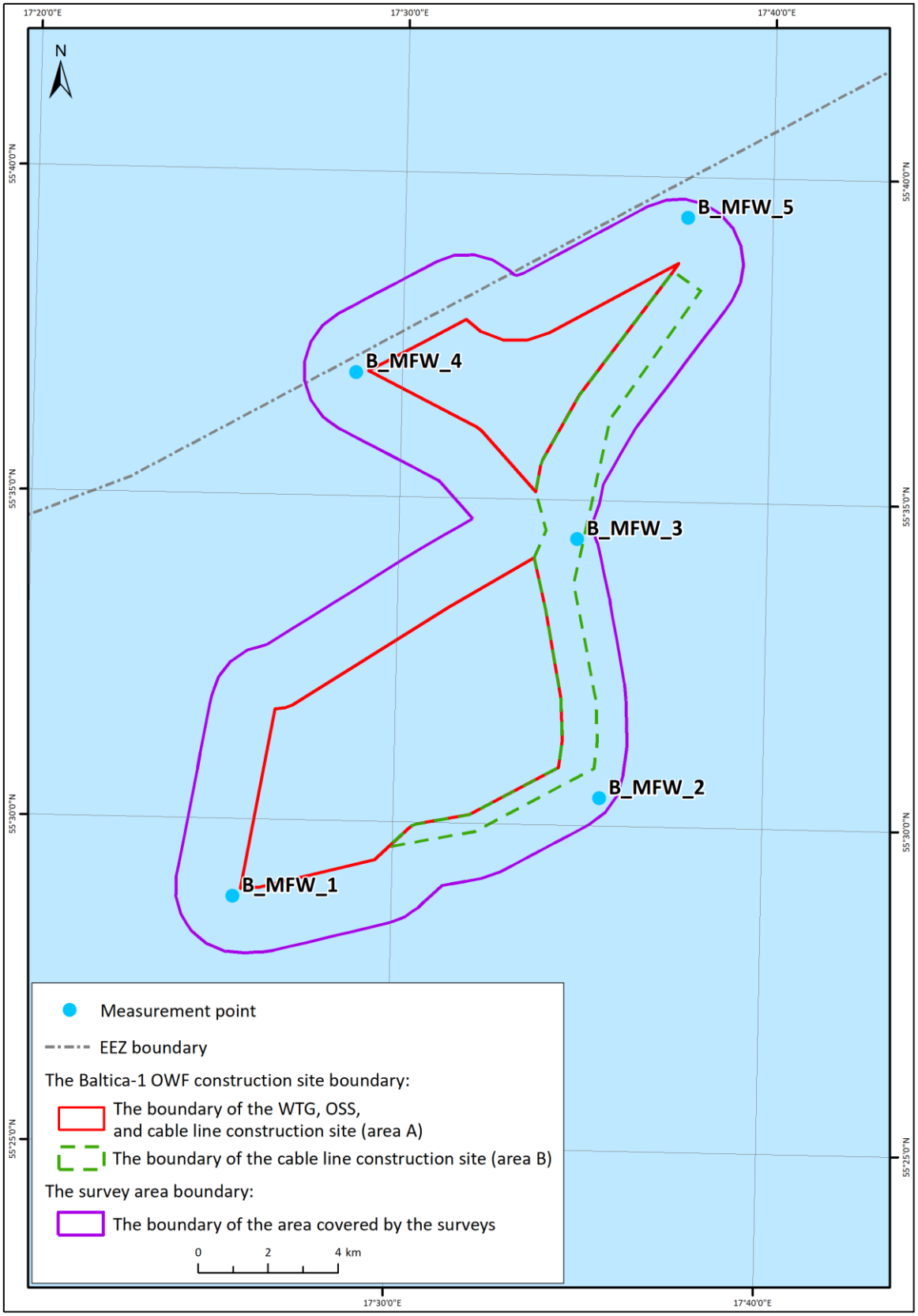


Figure 2.1. The locations of survey stations for hydrological and meteorological monitoring including sea currents distributed within the survey area

2.1.3 Methodology

The survey system in the survey area consisted of five survey stations. The survey buoy located at survey station B_MFW_3 was equipped with:

- a LUFFT WS500-UMB meteorological station, which was equipped with separate sensors for measuring individual meteorological parameters: relative humidity of the air, air temperature, wind velocity and direction;
- a Vaisala PTB210 barometer for measuring atmospheric pressure;
- a set of CTD probes for measuring hydrophysical parameters: temperature, electrolytic conductivity, and water pressure (depth) at five depths in the water depth: 1 m, 4 m, 8 m, 16 m, and above the seabed;
- a current profiler with a CTD probe and a turbidity sensor for measuring water flow (speed and direction) throughout the water depth, wave motion on the free sea surface (height, period, and direction of waves), water temperature above the seabed, and the current water depth (thickness) and turbidity.

Current profilers with CTD probes equipped with turbidity sensors were located at survey stations B_MFW_1 and B_MFW_5, while single current profilers were located at survey stations B_MFW_2 and B_MFW_4.

The locations of survey stations included in the system monitoring the survey area are presented in Figure 2.1 and described in Table 2.1.

Table 2.1. The coordinates of the survey stations in the survey area

Measurement point	Depth [m]	Two-dimensional Cartesian coordinate system PL-1992 [m]		Comments
		y	x	
B_MFW_1	36	400705.00	847510.00	Current profiler, CTD probe, turbidity sensor
B_MFW_2	47	411164.00	850290.00	Current profiler
B_MFW_3	34	410540.00	857679.00	A survey buoy (buoy), a meteo station, CTD probes, turbidity sensors, and a current profiler
B_MFW_4	19	404237.00	862451.00	Current profiler
B_MFW_5	44	413708.00	866848.00	Current profiler, CTD probe, turbidity sensor

The locations of measuring devices in the survey area had been selected so that the measured values of physical parameters were as representative as possible for the survey area. When selecting the indicated locations, the seabed relief was taken into account, which is characterised by significant inclinations towards the south and east in this region, and consequently – large changes in water depth.

The measuring devices in the survey area were located at survey stations with depths ranging from 19 to 47 m.

The locations of the measuring devices in the survey area had been selected so that the measured values of physical parameters were representative of the survey area. When selecting the indicated locations, the seabed relief was taken into account, which is characterised by a significant inclination towards the south and east in this region, and consequently – large changes in water depth. Therefore,

points with different depths were selected, located possibly on the outskirts of the survey area, so that their later extrapolation for the entire survey area would be possible. In addition, such a distribution of the measuring devices on the seabed did not interfere with the performance of other surveys at sea.

Additionally, as part of hydrological and meteorological monitoring, taking into account sea currents, hydrological monitoring was carried out at survey stations designated as part of water and seabed sediment sampling. Monitoring was carried out using CTD probes, and the measurement was performed over the entire vertical profile at intervals of no more than 0.5 m.

The following parameters were measured as part of the surveys of hydrological and meteorological conditions including sea currents in the survey area:

- air humidity;
- atmospheric pressure;
- wind speed;
- wind direction;
- air temperature;
- water flow velocity;
- water flow direction;
- wave height and period;
- the thickness of the sea deep;
- electrical conductivity of water;
- water turbidity;
- water temperature.

The specification of the parameters measured, which complied with the guidelines of the Word Meteorological Organisation (WMO No. 8. Guide to Meteorological Instruments and Methods of Observations) and other widely used and recommended standards, is presented in Table 2.2.

Table 2.2. Threshold values of devices for measured physical parameters at sea

Parameter	Minimum value	Maximum value	Unit	Accuracy	Resolution	Expected values	
						Minimum	Maximum
Relative humidity	< 5%	< 100%	-	2	< 1%	45	100
Atmospheric pressure	500	1100	hPa	0.15	0.01	960	1040
Wind velocity	0	75	$m \cdot s^{-1}$	0.3 $m \cdot s^{-1}$ or 3%	0.5	0	33
Wind direction	0	360	°	< 3	1	0	360
Air temperature	-30	45	°C	0.2	0.1	-10	30
Water flow velocity	0	10	$m \cdot s^{-1}$	< 1%	0.005	0	1.0
Water flow direction	0	360	°	2	0.1	0	360
Wave height	0	30	m	< 1%	0.1	0	9
Wave period	1	100	s	N/D	N/D	1	12
Wave direction	0	360	°	2	0.1	0	360
Water depth (thickness of the sea deep)	0	50	m	0.5% of the scale range	0.005% of the scale range	15	83

Parameter	Minimum value	Maximum value	Unit	Accuracy	Resolution	Expected values	
						Minimum	Maximum
Electrical conductivity of water	0	80	$mS \cdot cm^{-1}$	0.01	0.002	6	13
Water salinity	0	N/A	ppm	0.01	0.002	5	9
Water turbidity	0	4000	FTU	< 2%	< 0.002%	0.1	40
Water temperature	-5	35	°C	0.01	0.005	1	24
Sea level	350	650	cm	0.5% of the scale range	0.005% of the scale range	400	600

N/D – no data

The registrations of wind velocity and direction, and air temperature, humidity, and pressure, were carried out with the frequency of 1/10 Hz, for 10 minutes every hour. Next, the measurement results were averaged for every 10-minute period.

The pressure, conductivity, temperature, and turbidity sensors operated with the frequency of 1 Hz for a period of 1 minute within one hour. Next, the measurement results were averaged for each hour.

Physical parameters were measured every hour, and additionally, wave readings and current water depths were given as a mean value from every period of 1024 s (approx. 17 minutes). Water flow was averaged for every 5 minutes. Moreover, water flow in the sea was averaged for horizontal water layers of 1 m in thickness. The above-mentioned information is presented in Table 2.3.

Table 2.3. The recording parameters of the measured atmosphere and sea properties

Parameters	Sampling frequency	Survey period	The pause between the measurements
Meteorological parameters of the atmosphere	0.1 Hz	10 min.	1 hour
Hydrophysical parameters of the water deep	1 Hz	1 min.	1 hour
Dynamic parameters of the water; wave motion	400 or 600 kHz	Approx. 17 min.	1 hour
Dynamic parameters of the water; thickness	400 or 600 kHz	Approx. 17 min.	1 hour
Dynamic parameters of the water; flows	400 or 600 kHz	5 min.	1 hour

The meteorological data obtained (from the meteorological station) and hydrophysical data (from CTD probes and current profilers collecting meteorological data) are subject to a quantitative and qualitative assessment and verification of their accuracy, (including verification of possible values that do not fall within the expected range) [Table 2.2] and elimination of spikes. Information on the results of the qualitative analysis performed in this way is included in the processed data sets. Next, after the above-mentioned steps were completed, the readings underwent a statistical analysis and graphical rendering. The CTD values measured for the needs of hydrological monitoring were also determined by the number of measurements and the minimum, mean, and maximum values. The statistical and graphical data obtained this way were subjected to a comprehensive scientific analysis and expert evaluation. The results of these analyses have been included in this Report.

Water flow parameters, registered by a current profiler have been visualised using dedicated software. First of all, the working conditions of the instruments were assessed for the entire survey period, starting from their last deposition on the seabed. Most importantly, the assessment concerned features such as stability (tilt magnitude and vertical axis rotation, the strength of signal emitted and received by the acoustic sensors) and battery level state during the entire survey session. Subsequently, raw measurement data were analysed to eliminate values falling outside the range expected and accidental errors. The values expected were part of data control. The system checked and reported the exceedances of values expected. The scopes of the parameters measured in the surveys (the threshold values of measuring instruments) are presented in Table 2.2. After the completion of these actions, the proper analysis of the measured signals was conducted. The obtained correct series of data on the water flow elements measured in 1-m thick layers were used to calculate flows in three sea deep layers: near-surface, middle, and near-seabed, of 4 m in thickness each. The data string obtained this way have been presented here in the form of time charts and water flow roses. Raw data including data obtained from measurements for each current profiler are contained in a file in the *.wpr binary format.

The methodology for the correctness assessment of the recorded survey data on the surface wave motion and the average levels of the free sea surface were similar to the ones described for the water flows. Correct measurement data are presented in a form of temporary levels of the free water table. The heights, periods and directions of wave motion and wave spectra were determined using a dedicated program called Storm. The final results of the analysis are shown in a graphic form, as charts. The statistical and graphical data obtained this way were subjected to a comprehensive scientific analysis and expert evaluation. The results of these analyses have been included in this Report.

To visualise the measured data, the following software was used: Excel by Microsoft, Grapher by Golden Software and Storm – dedicated software for AWAC current profilers by Nortek.

The ice conditions that prevailed in the survey area during the period of recording meteorological and hydrological parameters in the winter season are determined based on available information from the Baltic Sea ice services:

- the Polish Ice Report, Baltic Sea Ice Chart, chart of ice in the Polish coastal zone, and the ice bulletin, all of which are published by the Hydrological Forecast Office of the IMWM-NRI;
- the ice reports and ice charts published by the SMHI (Swedish Meteorological and Hydrological Institute).

Information on the ice conditions is presented in a descriptive form.

2.1.4 Activities performed

Hydrological and meteorological monitoring in the survey area was carried out from 1 December 2022 to 30 November 2023. It included continuous recordings at designated survey stations at sea. In addition, periodic service work was carried out to: collect recorded data from individual measuring devices, maintain the devices, and replace power batteries.

The following list [Table 2.4] includes the service work performed during the reporting period.

Table 2.4. A specification of the activities performed as part of the hydrometeorological monitoring

Date	Activities performed	Measurement point	Measuring instrument	Comments
30.11.2022	Device deployment	B_MFW_3	At the station B_MFW_3: • Lufft WS-500-UMB weather station (S/N: 262.0922.0813.243); • Vaisala PTB210j barometer (S/N U3310465); • Monitor CTD+ DR probe installed on a buoy (S/N 58872): • Three Monitor CTD probes on a tether (S/N: 69478, 74680, 76760).	-
03.12.2022	Device deployment	B_MFW_2, B_MFW_3, B_MFW_5	At the station B_MFW_2: • current profiler (S/N: N-8241); At the station B_MFW_3: • current profiler (S/N: N-8255); • Monitor CTD+ probe with a turbidimeter (S/N 58871) installed above the seabed. At the station B_MFW_5: • current profiler (S/N: N-8243); • Monitor CTD+ probe with a turbidimeter (S/N 71681):	
04.12.2022	Device deployment	B_MFW_1, B_MFW_4	At the station B_MFW_1: • current profiler (S/N: N-8274); • Monitor CTD+ probe with a turbidimeter (S/N 69479): At the station B_MFW_4: • current profiler (S/N: N-8275).	-
24.01.2023	Service works and reading of data from the measuring instruments and deployment of backup measuring instruments	B_MFW_3	At the station B_MFW_3: • Lufft WS-500-UMB weather station (S/N: 262.0922.0813.243); • Vaisala PTB210j barometer (S/N U3310465); • Probes attached to the buoy at a depth of 1 m – Monitor CTD+ DR (S/N 58872, S/N 84189); • Three Monitor CTD probes on a tether (S/N: 69478, 84193, 76760, 84192, 84194, 84187);	-
15.02.2023	Service works and reading of data from the measuring instruments and deployment of backup measuring instruments	B_MFW_3, B_MFW_4, B_MFW_5	At the station B_MFW_3: • current profiler (S/N: N-8255); • Monitor CTD+ probe with turbidimeters (S/N 84190, S/N 58871) installed above the seabed; At the station B_MFW_4: • current profiler (S/N: N-8275); At the station B_MFW_5: • current profiler (S/N: N-8243); • Monitor CTD+ probe with turbidimeters (S/N 71681, S/N 84537):	-
16.02.2023	Service works and reading of data from the measuring instruments	B_MFW_1, B_MFW_2,	At the station B_MFW_1: • current profiler (S/N: N-8274); • Monitor CTD+ probe with turbidimeters (S/N 84188, S/N 69479) installed above the seabed; At the station B_MFW_2:	-

Date	Activities performed	Measurement point	Measuring instrument	Comments
			• current profiler (S/N: N-8241).	
19.03.2023	Service works and reading of data from the measuring instruments	B_MFW_3	At the station B_MFW_3: • current profiler (S/N: N-8255); • Monitor CTD+ probe with turbidimeters (S/N 84190):(S/N 84190, S/N 58871).	-
22–24.04.2023	Service works and reading of data from the measuring instruments	B_MFW_1, B_MFW_2, B_MFW_3, B_MFW_4, B_MFW_5.	At the station B_MFW_1: • current profiler (S/N: N-8274); • Monitor CTD+ probe with turbidimeters (S/N 84188, S/N 69479) installed above the seabed; At the station B_MFW_2: • current profiler (S/N: N-8241); At the station B_MFW_3: • current profiler (S/N: N-8255); • Monitor CTD+ probe with turbidimeters (S/N 84190, S/N 58871) installed above the seabed; At the station B_MFW_4: • current profiler (S/N: N-8275); At the station B_MFW_5: • current profiler (S/N: N-8243); • Monitor CTD+ probe with turbidimeters (S/N 71681, S/N 84537):	
04.06.2023	Service works and reading of data from the measuring instruments	B_MFW_3	At the station B_MFW_3: • Lufft WS-500-UMB weather station (S/N: 262.0922.0813.243); • Vaisala PTB210j barometer (S/N U3310465); • Monitor CTD+ DR probe (S/N 86078) mounted to a buoy at a depth of 1 m; • Three Monitor CTD probes on a tether (S/N: 84192, 84194, 84187).	-
25.06.2023	Service works and reading of data from the measuring instruments	B_MFW_3	At the station B_MFW_3: • Lufft WS-500-UMB weather station (S/N: 262.0922.0813.243); • Vaisala PTB210j barometer (S/N U3310465); • Monitor CTD+ DR probe (S/N 86078) mounted to a buoy at a depth of 1 m; • Three Monitor CTD probes on a tether (S/N: 84192, 84194, 84187).	-
29–30.07.2023	Service works and reading of data from the measuring instruments	B_MFW_1, B_MFW_2, B_MFW_3, B_MFW_4, B_MFW_5.	At the station B_MFW_1: • current profiler (S/N: N-8274); • Monitor CTD+ probe with turbidimeters (S/N 84188, S/N 69479) installed above the seabed; At the station B_MFW_2: • current profiler (S/N: N-8241); At the station B_MFW_3: • current profiler (S/N: N-8255);	

Date	Activities performed	Measurement point	Measuring instrument	Comments
			• Monitor CTD+ probe with turbidimeters (S/N 84190, S/N 58871) installed above the seabed; At the station B_MFW_4: • current profiler (S/N: N-8275); At the station B_MFW_5: • current profiler (S/N: N-8243); • Monitor CTD+ probe with turbidimeters (S/N 71681, S/N 84537):	
17.08.2023	Service works and reading of data from the measuring instruments	B_MFW_3	At the station B_MFW_3: • Lufft WS-500-UMB weather station (S/N: 262.0922.0813.243); • Vaisala PTB210j barometer (S/N U3310465); • Monitor CTD+ DR probe (S/N 86078) mounted to a buoy at a depth of 1 m; • Three Monitor CTD probes on a tether (S/N: 84192, 84194, 84187).	-
27–29.09.2023	Service works and reading of data from the measuring instruments	B_MFW_1, B_MFW_2, B_MFW_3, B_MFW_4, B_MFW_5.	At the station B_MFW_3: • Lufft WS-500-UMB weather station (S/N: 262.0922.0813.243); • Vaisala PTB210j barometer (S/N U3310465); • Monitor CTD+ DR probe (S/N 86078) mounted to a buoy at a depth of 1 m; • Three Monitor CTD probes on a tether (S/N: 84192, 84194, 84187); • Monitor CTD+ probes with turbidimeters above the seabed (S/N 84190, S/N 58871); • current profiler (S/N: N-8255); At the station B_MFW_1: • current profiler (S/N: N-8274); • Monitor CTD+ probes with turbidimeters above the seabed (S/N 84188, S/N 69479); At the station B_MFW_2: • current profiler (S/N: N-8241); At the station B_MFW_4: • current profiler (S/N: N-8275); At the station B_MFW_5: • current profiler (S/N: N-8243); • Monitor CTD+ probe with turbidimeters (S/N 71681, S/N 84537).	-
12.11.2023	Service works and reading of data from the measuring instruments	B_MFW_3	At the station B_MFW_3: • Monitor CTD+ DR (S/N 84194) mounted to a tether at a depth of 8 m.	-
15–19.02.2024	Service works and reading of data from	B_MFW_1, B_MFW_2, B_MFW_3,	At the station B_MFW_3: • Lufft WS-500-UMB weather station (S/N: 262.0922.0813.243);	-

Date	Activities performed	Measurement point	Measuring instrument	Comments
	the measuring instruments	B_MFW_4, B_MFW_5.	• Vaisala PTB210j barometer (S/N U3310465); • Monitor CTD+ DR probe (S/N 86078) mounted to a buoy at a depth of 1 m; • Three Monitor CTD probes on a tether (S/N: 84192, 84194, 84187); • Monitor CTD+ probes with turbidimeters above the seabed (S/N 84190, S/N 58871); • current profiler (S/N: N-8255); At the station B_MFW_1: • current profiler (S/N: N-8274); • Monitor CTD+ probes with turbidimeters above the seabed (S/N 84188, S/N 69479); At the station B_MFW_2: • current profiler (S/N: N-8241); At the station B_MFW_4: • current profiler (S/N: N-8275); At the station B_MFW_5: • current profiler (S/N: N-8243); • Monitor CTD+ probe with turbidimeters (S/N 71681, S/N 84537).	

In addition, as part of the measurements of the physicochemical properties of water and examination of seabed sediments at the planned survey stations, temperature, salinity, and turbidity were measured using a CTD probe.

Temperature, salinity, and turbidity measurements were taken at the survey stations for water sampling and seabed sediment testing. During the entire reporting period, CTD measurements were taken as part of:

- water sampling:
  - the first water sampling campaign conducted at survey stations SW_MFW_01 – SW_MFW_36 on 18–19 January 2023;
  - the second water sampling campaign conducted at survey stations SW_MFW_01 – SW_MFW_36 on 9–10 March 2023;
  - the third water sampling campaign conducted at survey stations SW_MFW_01 – SW_MFW_36 on 1–2 May 2023;
  - the fourth water sampling campaign conducted in the survey area at survey stations SW_MFW_01 – SW_MFW_36 on 11–13 July 2023;
  - the fifth water sampling campaign conducted in the survey area at survey stations SW_MFW_01 – SW_MFW_36 on 25 September 2023;
  - the sixth water sampling campaign conducted in the survey area at survey stations SW_MFW_01 – SW_MFW_36 on 29 November 2023;
- seabed sediment surveys:
  - the first campaign of seabed sediment sampling in the survey area at survey stations SO_MFW_001 – SO_MFW_108 and SO_PM_86 – SO_PM_95, on 22–23, 27–28 February 2023;

- the second campaign of testing seabed sediments in the survey area at survey stations SO_MFW_01 – SO_MFW_108 and SO_PM_86 – SO_PM_95 on 28–29 July 2023.

Table 2.5 summarises the percentage yields for data measured at survey stations designated in the survey area for the measurement period of 1 year (from 1 December 2022 to 30 November 2023). Table 2.6 summarises the dates on which measurements were performed at individual survey stations and on which the data analysed in this Report was obtained.

Table 2.5. The percentage data yields for the survey area

Parameters	Measurement point				
	B_MFW_1	B_MFW_2	B_MFW_3	B_MFW_4	B_MFW_5
Wind velocity and direction	N/A	N/A	< 92%	N/A	N/A
Atmospheric pressure	N/A	N/A	< 100%	N/A	N/A
Air temperature	N/A	N/A	< 92%	N/A	N/A
Relative air humidity	N/A	N/A	< 92%	N/A	N/A
Height, period, and direction of waves	< 99%	< 99%	< 79%	< 99%	< 99%
The thickness of the sea deep	< 99%	< 99%	< 79%	< 99%	< 99%
Water flow velocity and direction	< 99%	< 99%	< 79%	< 99%	< 99%
Water temperature	< 99%	N/A	< 93%	N/A	< 99%
Electrical conductivity of water	< 99%	N/A	< 86%	N/A	< 99%
Water turbidity	< 98%	N/A	< 93%	N/A	< 97%

The lower yield of some qualitative conductivity data from CTD probes on a tether resulted from sensor fouling, which resulted in the exclusion of some data in further analysis. The devices from which the data was read operated correctly in terms of electronics and were also properly connected to the recording and power supply systems.

This concerned water conductivity and salinity data from individual probes in the following periods:

- probe deployed at a depth of 1 m, period from 14 July 2023, 10:00 p.m. to 17 August 2023, 11:00 a.m. and from 11 September 2013, 8:00 p.m. to 27 September 2023, 10:00 a.m.;
- probe deployed at a depth of 4 m, 18 July 2023, 7:00 p.m.–17 August 2023, 3:00 p.m.;
- probe deployed at a depth of 8 m, 23 July 2023, 1:00 p.m.–17 August 2023, 3:00 p.m.;
- probe deployed at a depth of 16 m, 27 August 2023, 5:00 p.m.–27 September 2023, 10:00 a.m.

From 2 September, 4:00 p.m. to 27 September 2023, 10:00 a.m., the temperature, conductivity, and salinity data from the probe corresponding to a depth of 4 m indicated depth values outside the expected range, and therefore, were not included in further analyses. The probable cause of the erroneous depth data was the overgrowing of the depth sensor with living organisms. During the service, the probe was cleaned of the overgrowing organisms and measurements were resumed. The lack of some measurement data from a depth of 4 m from this period does not negatively affect the environmental impact assessment of the planned Baltica-1 OWF.

A similar situation occurred for the probe deployed at a depth of 8 m. The temperature, conductivity, and salinity data from the period 20 August, 12:00 p.m.–27 September 2023, 10:00 a.m. were not included in the further analysis due to erroneous depth measurement results for this probe. As for the probe located at a depth of 4 m, the probable cause was the fouling of the depth sensor in the probe.

During the service, the probe was cleaned of fouling organisms and measurements were resumed. The lack of some measurement data from a depth of 4 m from this period does not negatively affect the environmental impact assessment of the planned Baltica-1 OWF.

Table 2.6. The dates of measuring individual parameters included in the Report on the survey area

Parameters	Measurement point				
	B_MFW_1	B_MFW_2	B_MFW_3	B_MFW_4	B_MFW_5
Wind velocity and direction	N/A	N/A	30.11.2022–24.01.2023 24.01.2023–04.06.2023 04.06.2023–25.06.2023 25.06.2023–17.08.2023 17.08.2023 – 27.09.2023 27.09.2023–30.11.2023	N/A	N/A
Atmospheric pressure	N/A	N/A	30.11.2022–24.01.2023 24.01.2023–04.06.2023 04.06.2023–25.06.2023 25.06.2023–17.08.2023 17.08.2023 – 27.09.2023 27.09.2023–30.11.2023	N/A	N/A
Air temperature	N/A	N/A	30.11.2022–24.01.2023 24.01.2023–04.06.2023 04.06.2023–25.06.2023 25.06.2023–17.08.2023 17.08.2023 – 27.09.2023 27.09.2023–30.11.2023	N/A	N/A
Relative air humidity	N/A	N/A	30.11.2022–24.01.2023 24.01.2023–04.06.2023 04.06.2023–25.06.2023 25.06.2023–17.08.2023 17.08.2023 – 27.09.2023 27.09.2023–30.11.2023	N/A	N/A
Height, period, and direction of waves	04.12.2022–16.02.2023	03.12.2022–15.02.2023	04.12.2022–15.02.2023	04.12.2022–15.02.2023	03.12.2022–15.02.2023

Parameters	Measurement point				
	B_MFW_1	B_MFW_2	B_MFW_3	B_MFW_4	B_MFW_5
	16.02.2023–22.04.2023 23.04.2023–29.07.2023 29.07.2023–28.09.2023 28.09.2023–30.11.2023	16.02.2023–23.04.2023 23.04.2023–29.07.2023 30.07.2023–28.09.2023 28.09.2023–30.11.2023	15.02.2023–19.03.2023 19.03.2023–23.04.2023 23.04.2023–30.07.2023 30.07.2023–28.09.2023 28.09.2023–30.11.2023	15.02.2023–23.04.2023 23.04.2023–30.07.2023 30.07.2023–28.09.2023 28.09.2023–30.11.2023	15.02.2023–23.04.2023 24.04.2023–30.07.2023 30.07.2023–28.09.2023 28.09.2023–30.11.2023
The thickness of the sea-deep	04.12.2022–16.02.2023 16.02.2023–22.04.2023 23.04.2023–29.07.2023 29.07.2023–28.09.2023 28.09.2023–30.11.2023	03.12.2022–15.02.2023 16.02.2023–23.04.2023 23.04.2023–29.07.2023 30.07.2023–28.09.2023 28.09.2023–30.11.2023	04.12.2022–15.02.2023 15.02.2023–19.03.2023 19.03.2023–23.04.2023 23.04.2023–30.07.2023 30.07.2023–28.09.2023 28.09.2023–30.11.2023	04.12.2022–15.02.2023 15.02.2023–23.04.2023 23.04.2023–30.07.2023 30.07.2023–28.09.2023 28.09.2023–30.11.2023	03.12.2022–15.02.2023 15.02.2023–23.04.2023 24.04.2023–30.07.2023 30.07.2023–28.09.2023 28.09.2023–30.11.2023
Water flow velocity and direction	04.12.2022–16.02.2023 16.02.2023–22.04.2023 23.04.2023–29.07.2023 29.07.2023–28.09.2023 28.09.2023–30.11.2023	03.12.2022–15.02.2023 16.02.2023–23.04.2023 23.04.2023–29.07.2023 30.07.2023–28.09.2023 28.09.2023–30.11.2023	04.12.2022–15.02.2023 15.02.2023–19.03.2023 19.03.2023–23.04.2023 23.04.2023–30.07.2023 30.07.2023–28.09.2023 28.09.2023–30.11.2023	04.12.2022–15.02.2023 15.02.2023–23.04.2023 23.04.2023–30.07.2023 30.07.2023–28.09.2023 28.09.2023–30.11.2023	03.12.2022–15.02.2023 15.02.2023–23.04.2023 24.04.2023–30.07.2023 30.07.2023–28.09.2023 28.09.2023–30.11.2023
Water temperature	04.12.2022–30.11.2023	N/A	04.12.2022–30.11.2023	N/A	03.12.2022–30.11.2023
Electrical conductivity of water	04.12.2022–30.11.2023	N/A	04.12.2022–30.11.2023*	N/A	03.12.2022–30.11.2023
Water turbidity	04.12.2022–30.11.2023	N/A	04.12.2022–30.11.2023	N/A	03.12.2022–30.11.2023

2.1.5 Results

2.1.5.1 Meteorological measurements

A short statistical analysis of the meteorological values measured has been presented in Table 2.7. Measurements of meteorological parameters (wind velocity and direction, water temperature, air pressure and humidity) were carried out at the level of approx. 5 m above the free surface of the sea with a time step of 1 hour. For each time step, registrations were carried out with the frequency of 1/10 Hz for 10 minutes. Next, the measurement results were averaged for every 10 minutes. The analysis of meteorological data covers the period from 12:00 a.m. (midnight) on 1 December 2022 to 11:00 p.m. on 30 November 2023. In the period from 18 February to 19 March 2023, there was a break in the recording of data from the meteorological station located on a buoy due to its getting damaged

during a strong storm and waiting for weather conditions at sea that would allow for the necessary repairs to be made safely.

Table 2.7. The statistical analysis of the meteorological parameters measured at survey station B_MFW_3 located within the survey area

Measurement point	Value	Wind velocity [m·s^{-1}]	Dominant wind direction	Atmospheric pressure [hPa]	Air temperature [°C]	Relative humidity [%]
B_MFW_3	Mean	7.28	W, WSW, SW	1012.87	10.16	86.10
	Minimum	0.00		980.01	-2.90	42.41
	Maximum	20.84		1041.54	23.34	100.00

In the period discussed, according to the recordings made at the B_MFW_3 measuring point, the prevailing winds in the study area were winds from the following directions: W, WSW, SW, although a certain share of ESE, NNE, E, and ENE directions can be noted.

Figure 2.2 and Figure 2.3 present the results obtained from wind measurements at survey station B_MFW_3. The directions presented in the wind rose indicate the directions from which the wind blew.

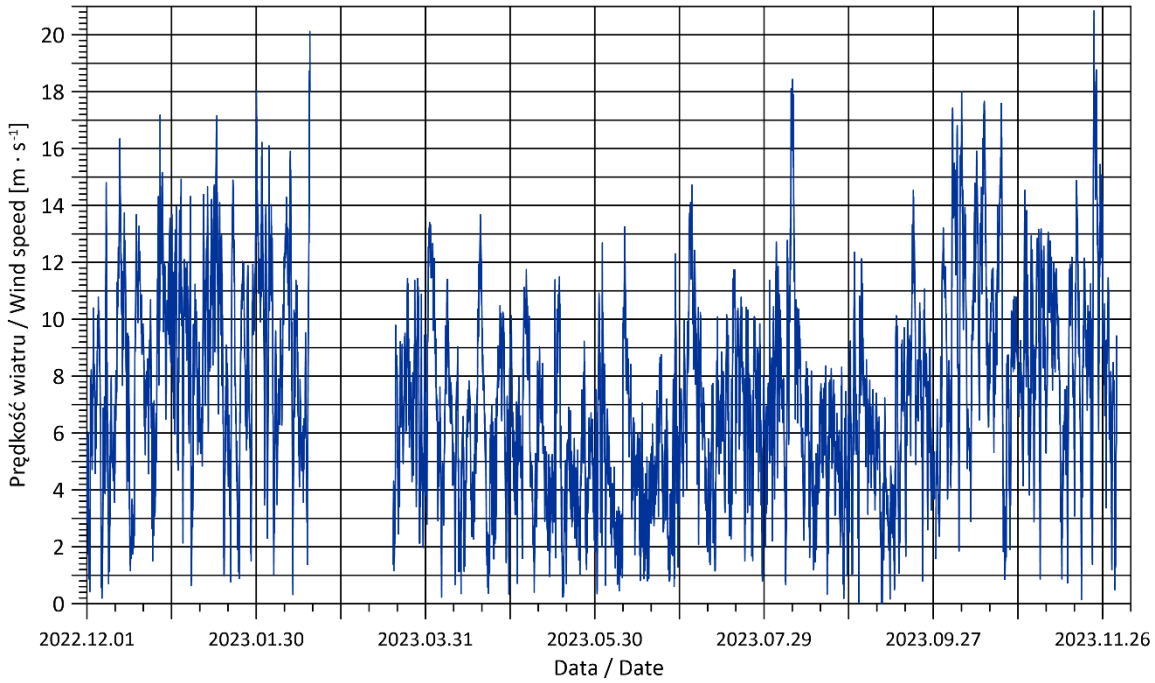


Figure 2.2. The wind speed measured at survey station B_MFW_3 throughout a measurement period of one full year

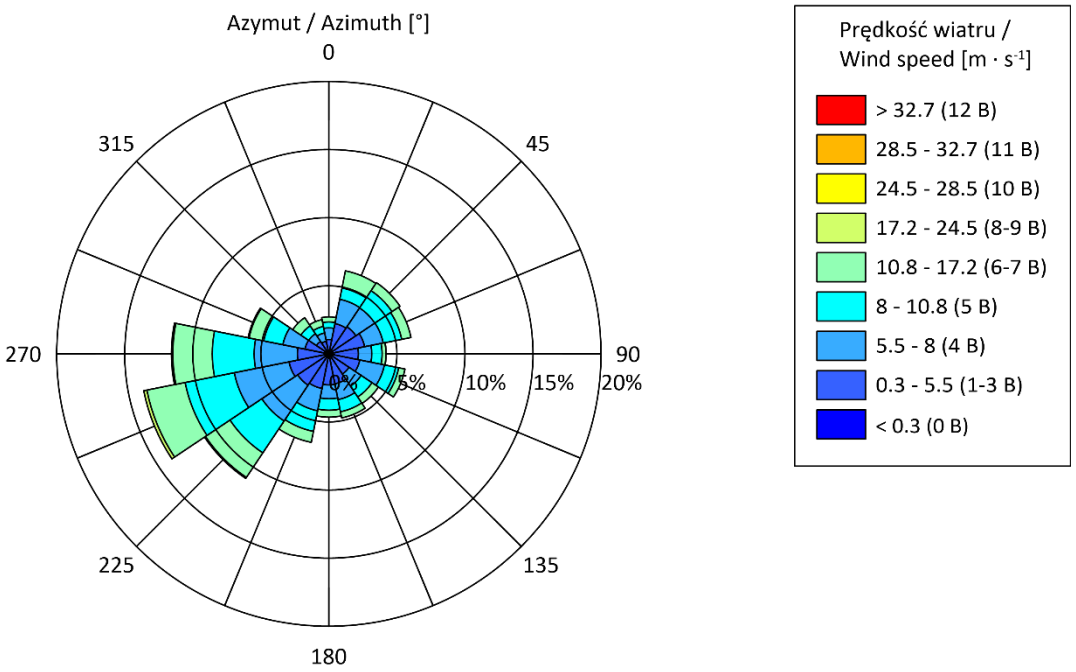


Figure 2.3. A wind rose presenting the directional distribution of the wind velocities and directions measured at survey station B_MFW_3 throughout a measurement period of one full year

The compiled results of the air humidity, pressure, and temperature measurements conducted at the survey station B_MFW_3 are presented in the subsequent plots [Figure 2.4, Figure 2.5, Figure 2.6].

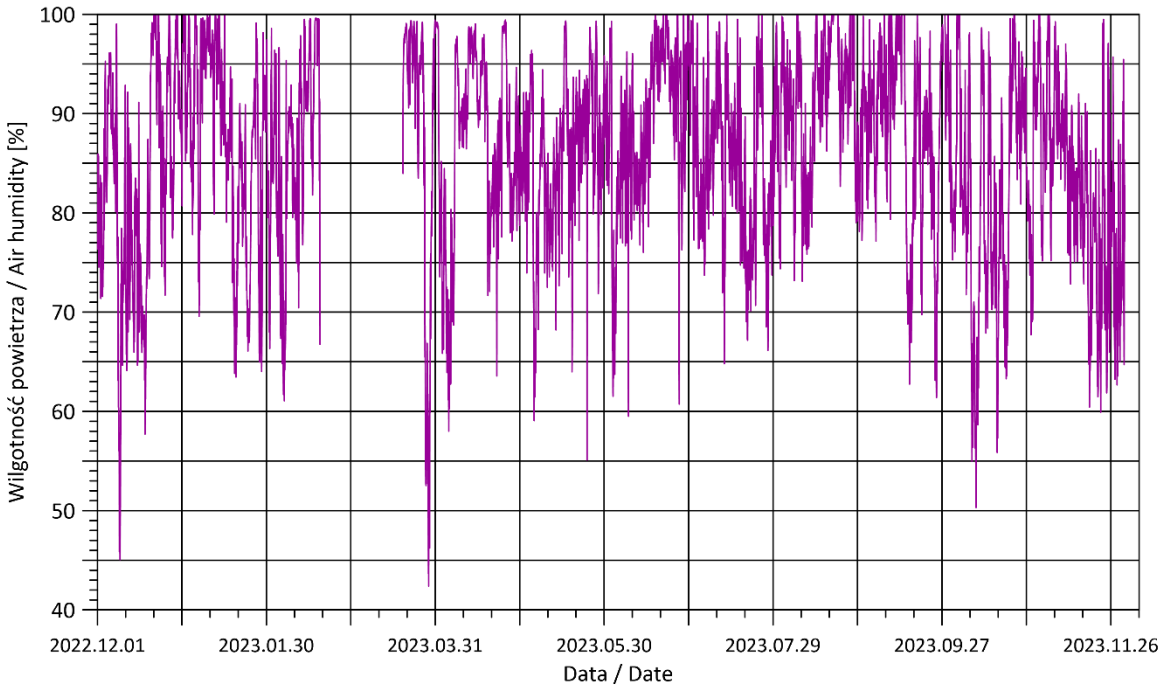


Figure 2.4. The air humidity measured at survey station B_MFW_3 throughout a measurement period of one full year

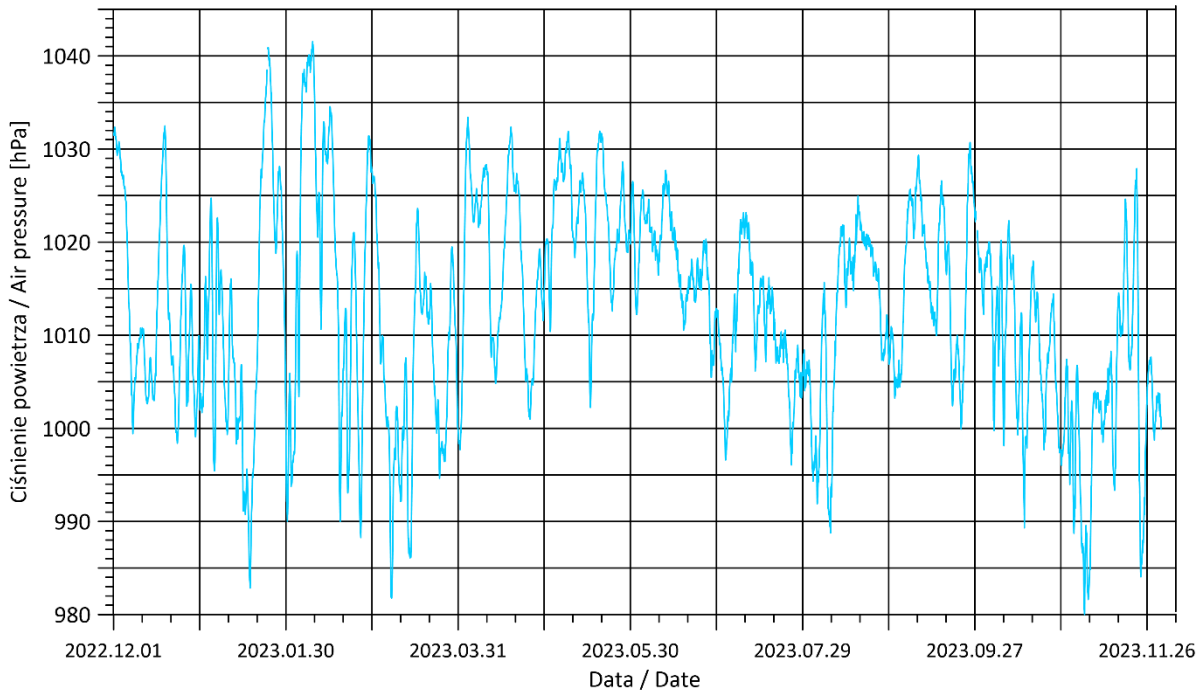


Figure 2.5. The air pressure measured at survey station B_MFW_3 throughout a measurement period of one full year

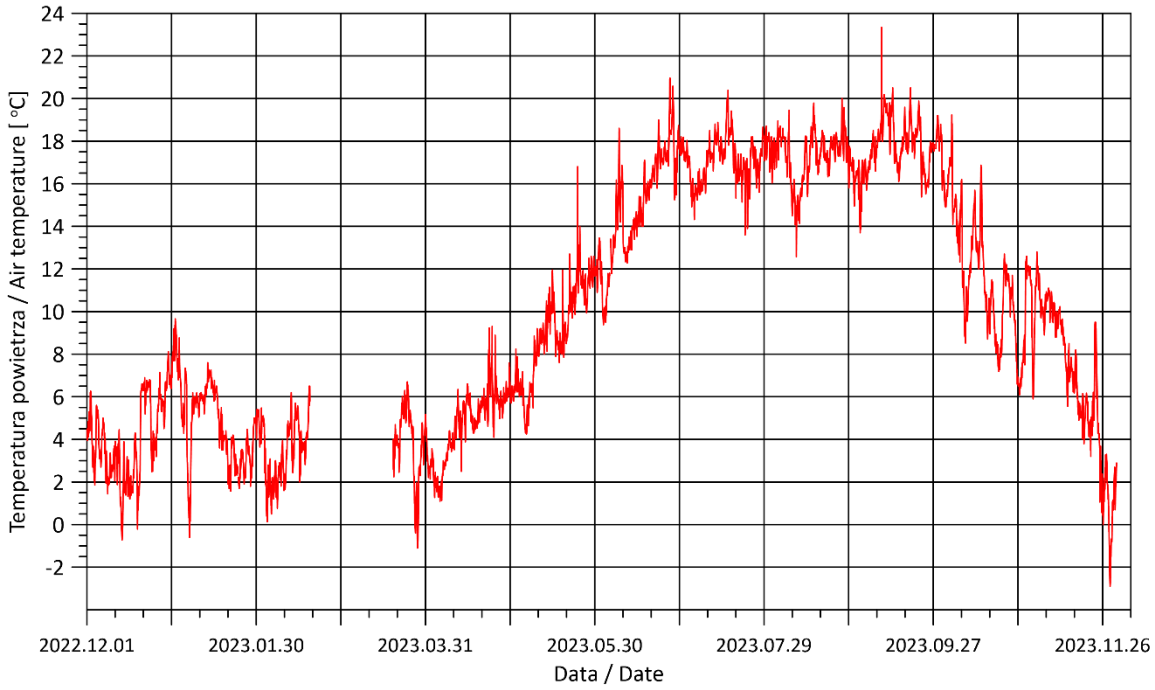


Figure 2.6. The air humidity measured at survey station B_MFW_3 throughout a measurement period of one full year

2.1.5.2 Hydrological measurements

2.1.5.2.1 Wave motion

The analysis below presents the results of continuous monitoring conducted from 1 December 2022 to 30 November 2023 from all survey stations located in the survey area.

Selected characteristics of wind-generated wave motion on the free sea surface are given in Table 2.8.

Table 2.8. A summary of selected characteristics of wind-generated wave motion at the survey stations located in the survey area recorded throughout a measurement period of one full year

Measurement point	Parameter	Mean	Minimum	Maximum	Standard deviation
B_MFW_1	Maximum wave height [m]	1.82	0.11	9.39	1.31
	Significant wave height [m]	1.18	0.08	5.73	0.85
	Mean wave height [m]	0.71	0.05	3.74	0.52
	Peak spectrum period [s]	5.20	1.70	9.90	1.40
	Mean wave motion period [s]	3.90	1.90	8.10	1.00
B_MFW_2	Maximum wave height [m]	1.85	0.14	8.96	1.30
	Significant wave height [m]	1.20	0.09	5.63	0.84
	Mean wave height [m]	0.70	0.05	3.40	0.51
	Peak spectrum period [s]	5.20	1.40	10.7	1.50
	Mean wave motion period [s]	4.00	2.10	7.80	1.00
B_MFW_3	Maximum wave height [m]	1.67	0.12	9.51	1.25
	Significant wave height [m]	1.08	0.08	5.90	0.81
	Mean wave height [m]	0.64	0.05	3.81	0.50
	Peak spectrum period [s]	5.00	1.60	10.30	1.40
	Mean wave motion period [s]	3.80	2.00	8.10	1.00
B_MFW_4	Maximum wave height [m]	1.77	0.13	7.26	1.17
	Significant wave height [m]	1.15	0.08	5.13	0.77
	Mean wave height [m]	0.69	0.05	3.19	0.47
	Peak spectrum period [s]	5.10	1.60	10.3	1.40
	Mean wave motion period [s]	3.90	1.90	7.50	0.90
B_MFW_5	Maximum wave height [m]	1.78	0.12	9.04	1.29
	Significant wave height [m]	1.15	0.09	5.68	0.84
	Mean wave height [m]	0.69	0.05	3.45	0.51
	Peak spectrum period [s]	5.10	1.80	10.3	1.40
	Mean wave motion period [s]	3.90	2.00	7.90	1.00

The significant wave height for each hourly measurement was obtained based on the spectral analysis of the wave energy density. The mean wave motion height and the mean wave motion period refer to the values averaged from mean heights and mean periods measured at one-hour intervals. The wave motion directions, under the generally adopted rule, refer to the directions from which waves approach.

Table 2.9 presents the number of the maximum wave occurrences at the survey stations within the survey area according to the Douglas sea scale.

Table 2.9. A summary of the number of the maximum wave heights occurrences at the survey stations in the survey area according to the Douglas scale

Douglas sea scale	Wave height	The number of occurrences at the survey station				
		B_MFW_1	B_MFW_2	B_MFW_3	B_MFW_4	B_MFW_5
0	0	0	0	0	0	0
1	0–0.1	0	0	0	0	0
2	0.1–0.5	896	676	851	875	1041
3	0.5–1.25	2827	2985	2468	2806	2863
4	1.25–2.5	2757	2803	2211	2893	2690
5	2.5–4	1554	1589	1003	1659	1485
6	4–6	543	532	289	417	520
7	6–9	93	97	82	30	84
8	9–14	1	0	2	0	1
9	>14	0	0	0	0	0

Figure 2.7–Figure 2.11 present the results compiled for the hourly wave motion measurements at the survey stations located within the survey area: B_MFW_1, B_MFW_2, B_MFW_3, B_MFW_4, and B_MFW_5.

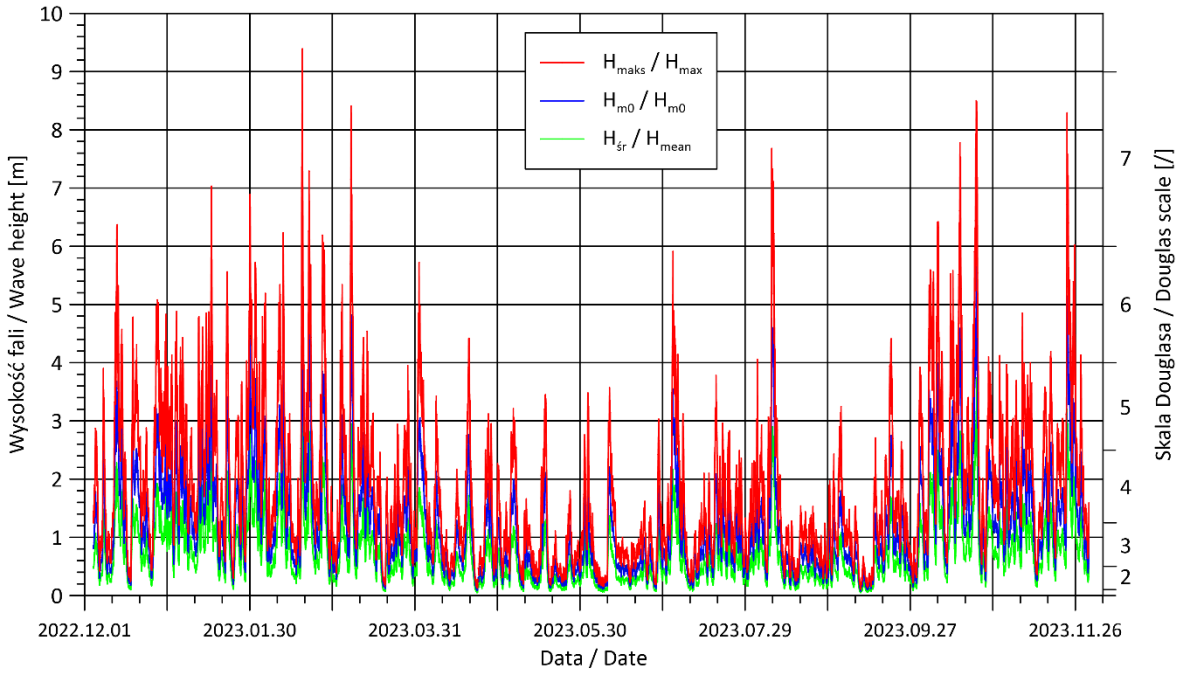


Figure 2.7. The maximum wave heights H_{max}, significant wave heights H_{m0}, and mean wave heights H_{mean} measured at survey station B_MFW_1 throughout a measurement period of one full year

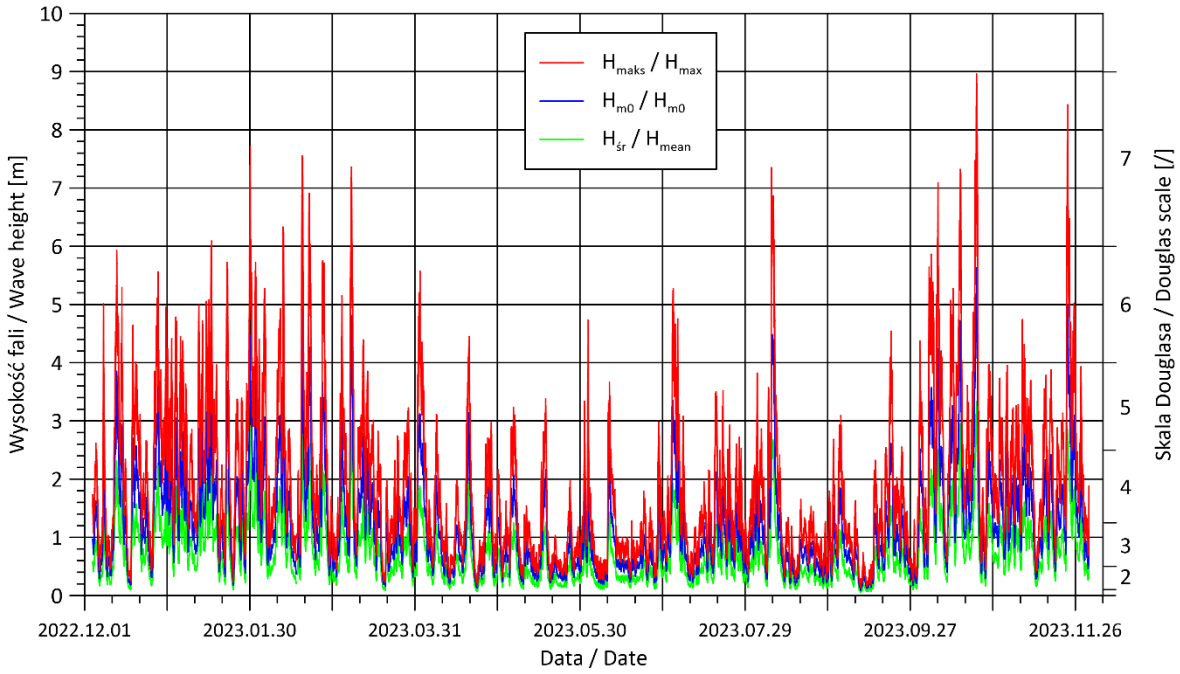


Figure 2.8. The maximum wave heights Hmax, significant wave heights Hm0, and mean wave heights H_{mean} measured at survey station B_MFW_2 throughout a measurement period of one full year

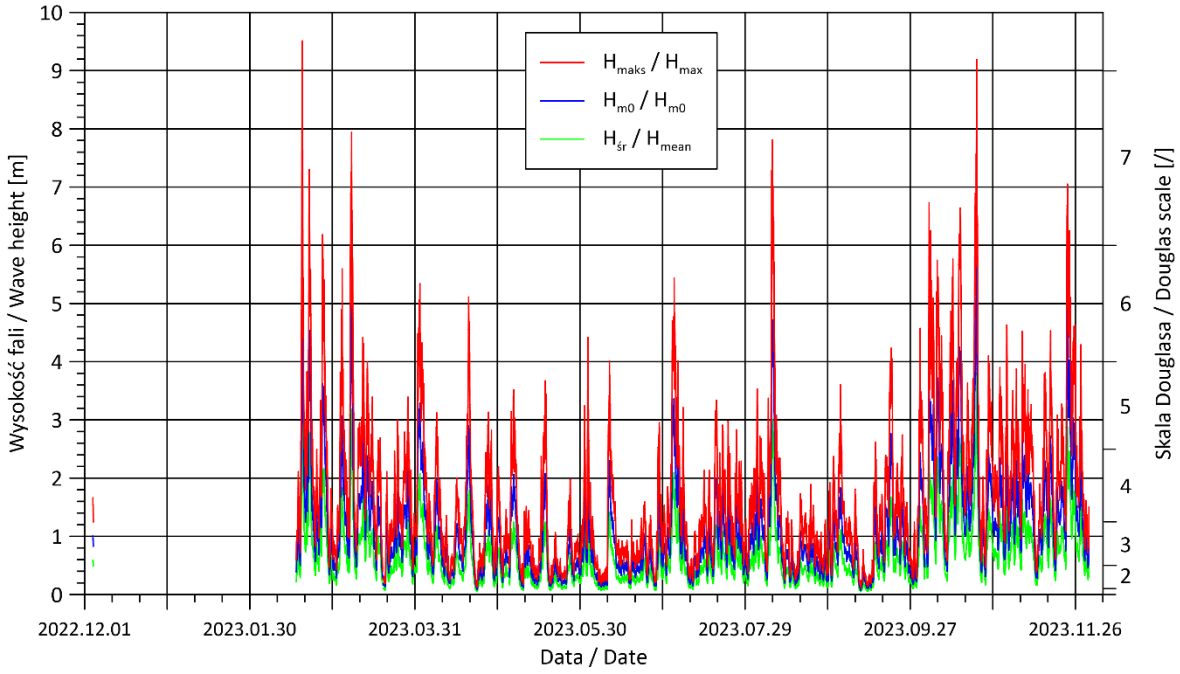


Figure 2.9. The maximum wave heights H_{max}, significant wave heights H_{m0}, and mean wave heights H_{mean} measured at survey station B_MFW_3 throughout a measurement period of one full year

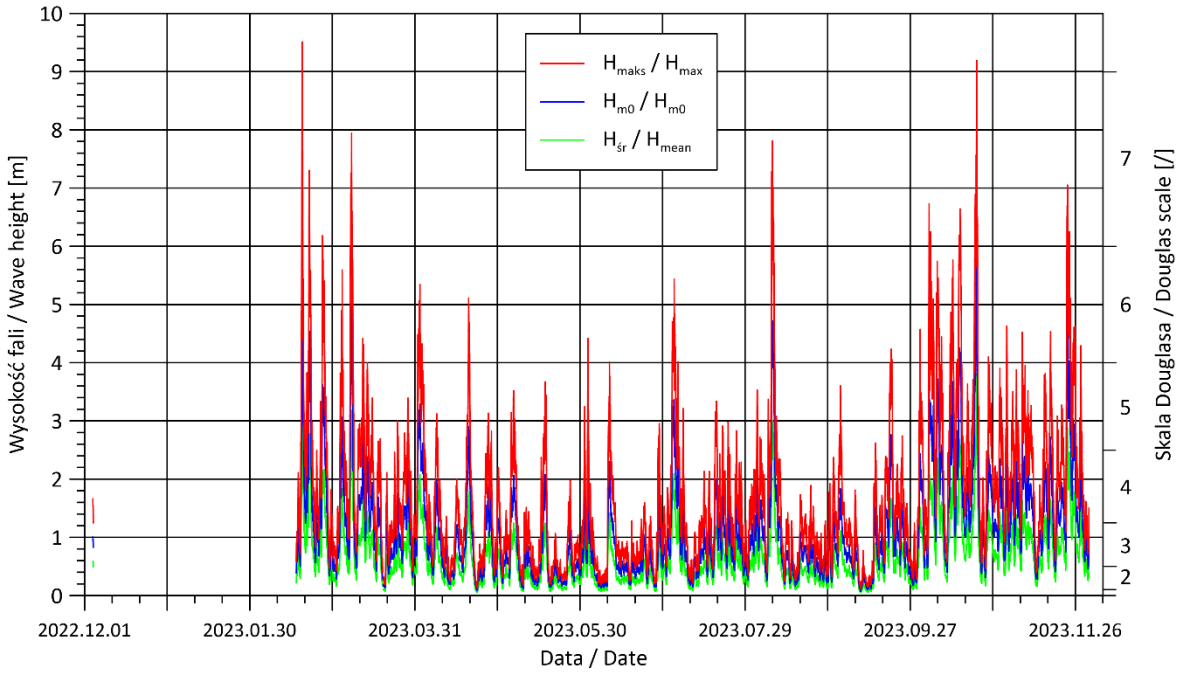


Figure 2.10. The maximum wave heights H_{max}, significant wave heights H_{m0}, and mean wave heights H_{mean} measured at survey station B_MFW_4 throughout a measurement period of one full year

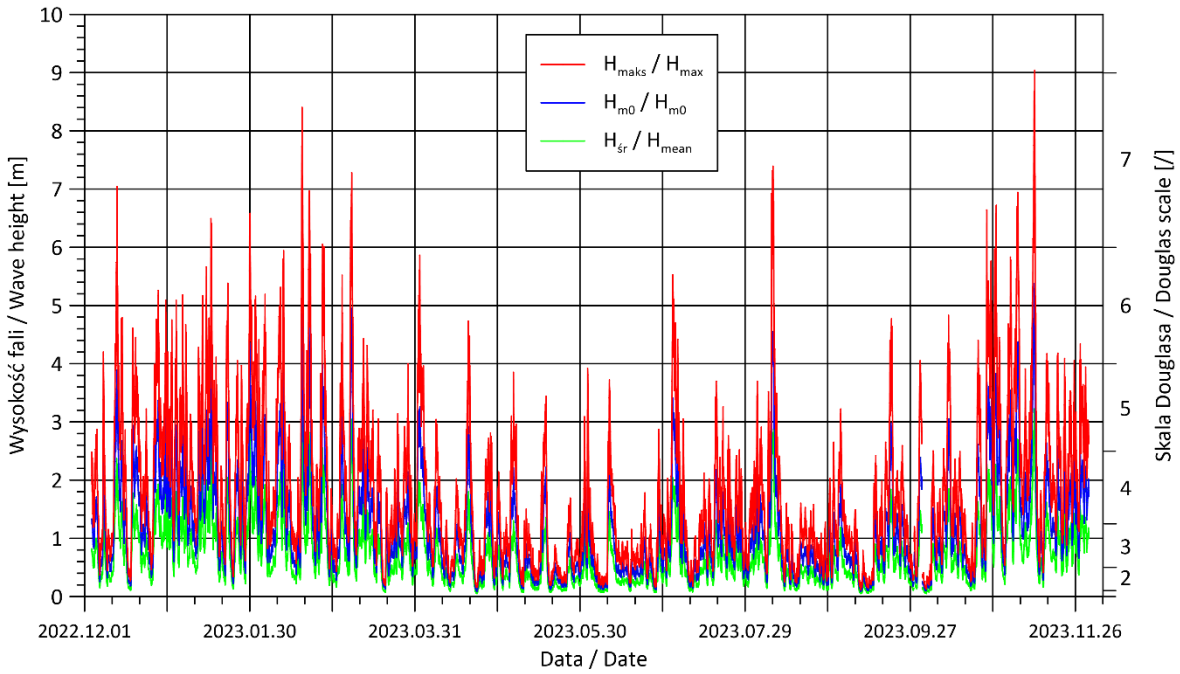


Figure 2.11. The maximum wave heights H_{max}, significant wave heights H_{m0}, and mean wave heights H_{mean} measured at survey station B_MFW_4 throughout a measurement period of one full year

Figure 2.12–Figure 2.16 present the results compiled for the hourly wave period measurements at the survey stations located within the survey area: B_MFW_1, B_MFW_2, B_MFW_3, B_MFW_4, and B_MFW_5.

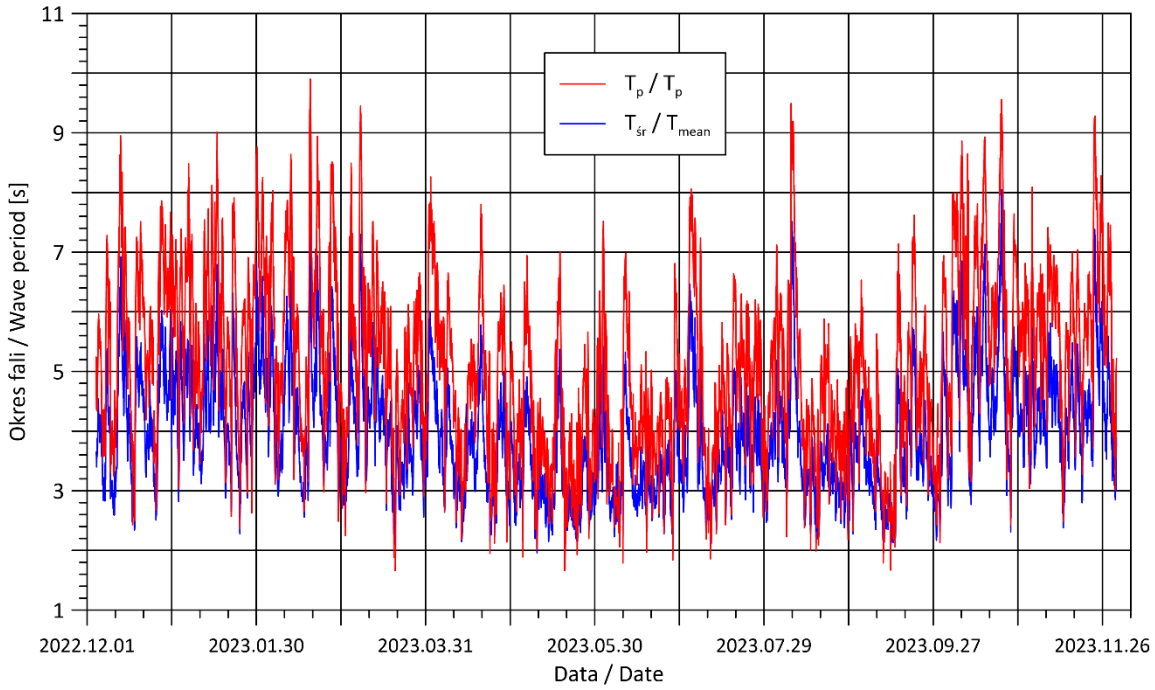


Figure 2.12. The peak wave periods T_p and mean wave periods T_{mean} measured at survey station B_MFW_1 throughout a measurement period of one full year

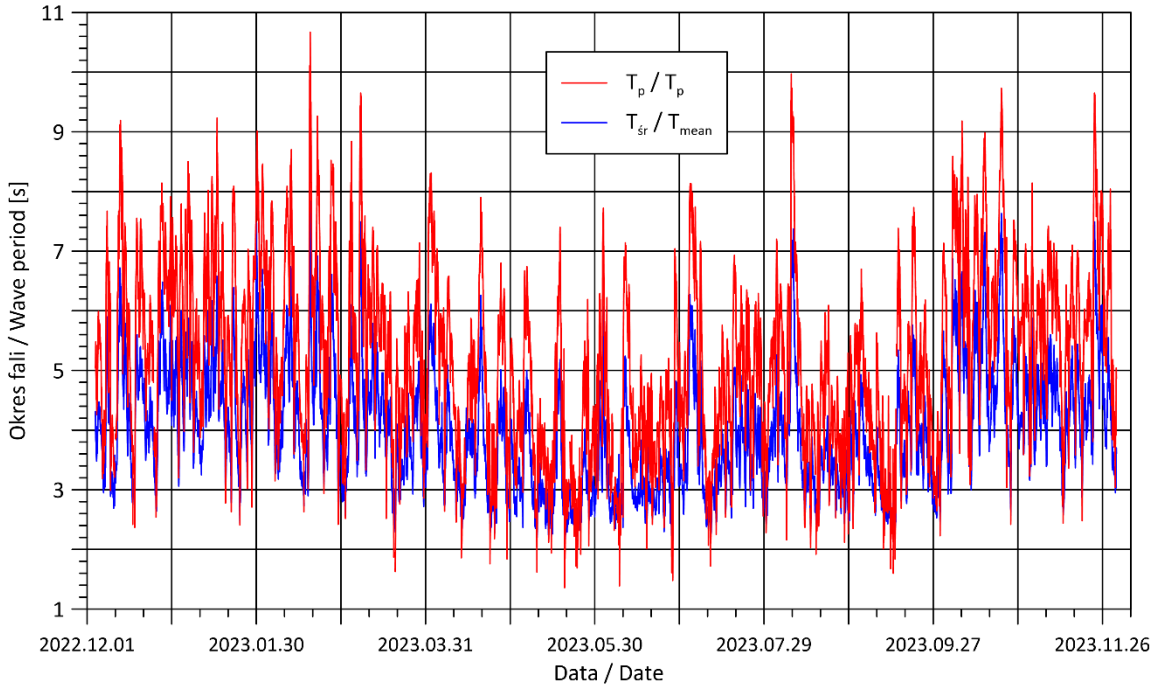


Figure 2.13. The peak wave periods Tp and mean wave periods T_{mean} measured at survey station B_MFW_2 throughout a measurement period of one full year

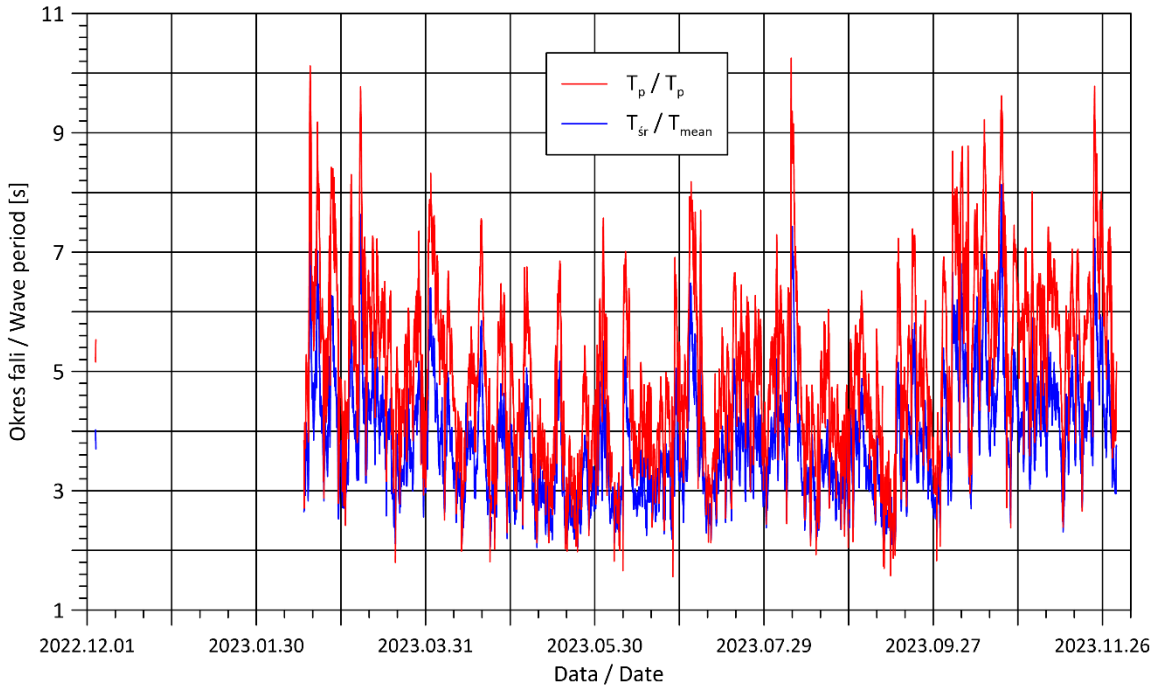


Figure 2.14. The peak wave periods Tp and mean wave periods T_{mean} measured at survey station B_MFW_3 throughout a measurement period of one full year

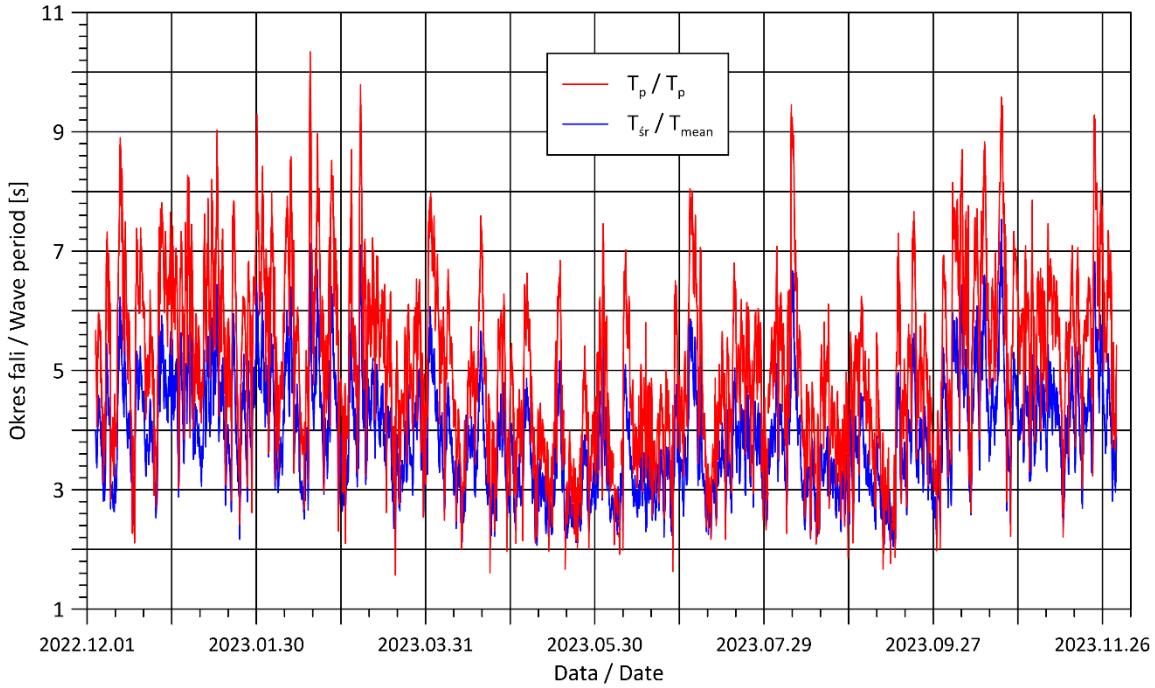


Figure 2.15. The peak wave periods Tp and mean wave periods T_{mean} measured at survey station B_MFW_4 throughout a measurement period of one full year

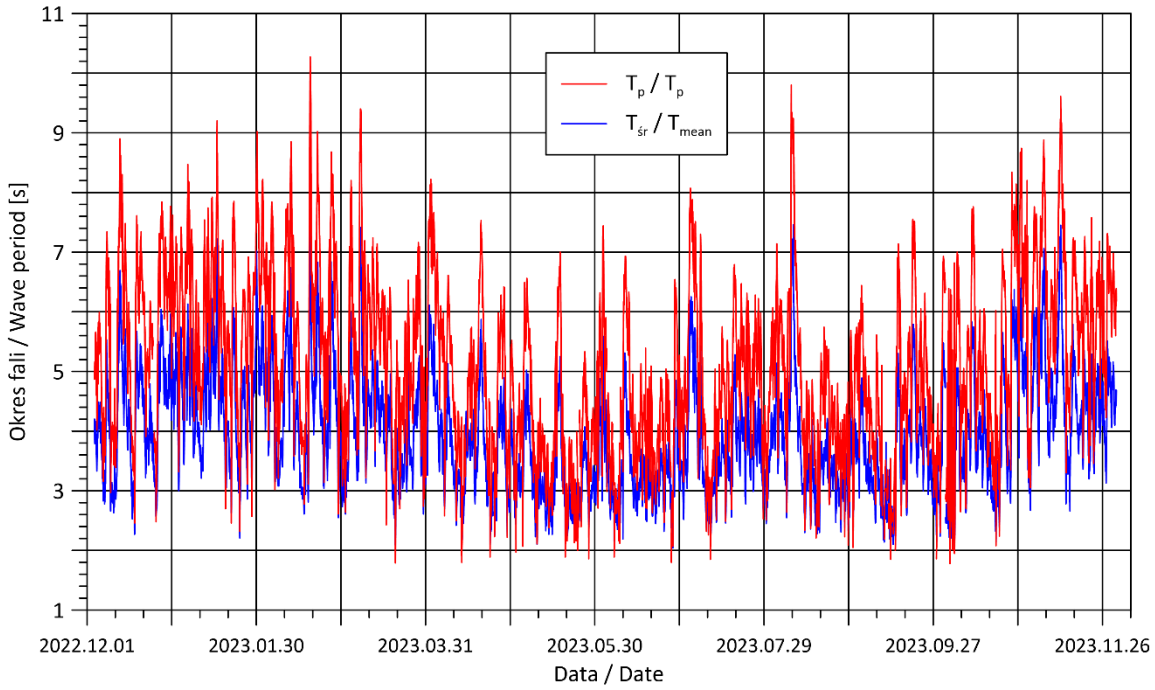


Figure 2.16. The peak wave periods Tp and mean wave periods T_{mean} measured at survey station B_MFW_5 throughout a measurement period of one full year

Figure 2.17–Figure 2.21 present the results compiled for the hourly measurements of the significant wave direction distribution (wave roses) at the survey stations located within the survey area: B_MFW_1, B_MFW_2, B_MFW_3, B_MFW_4, and B_MFW_5.

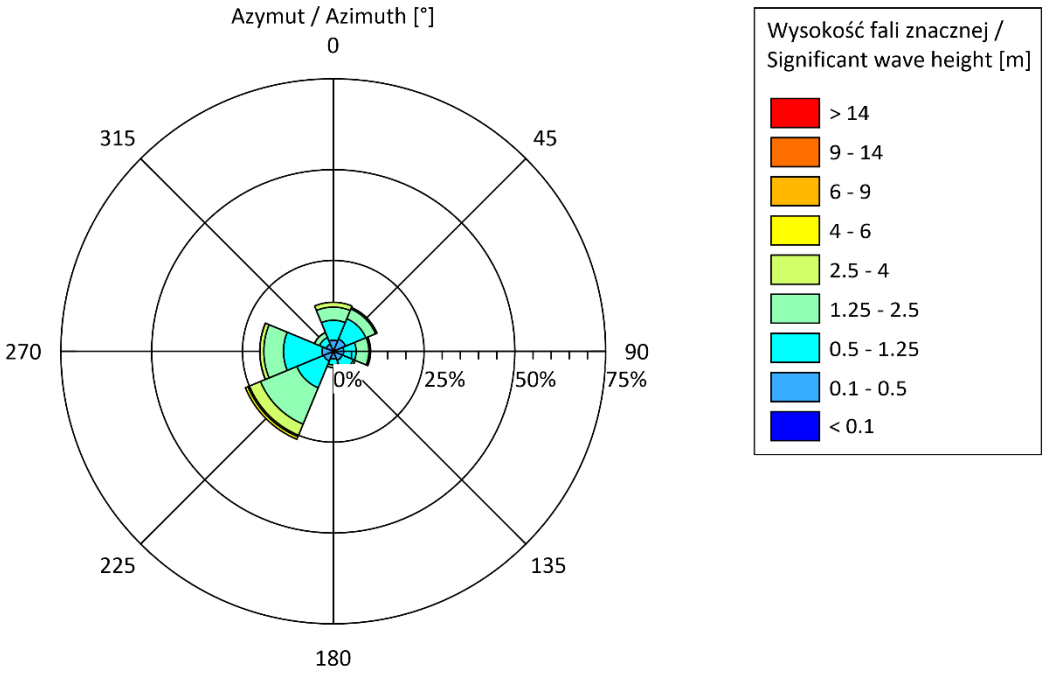


Figure 2.17. The wave rose diagram for the values measured at survey station B_MFW_1 throughout a measurement period of one full year

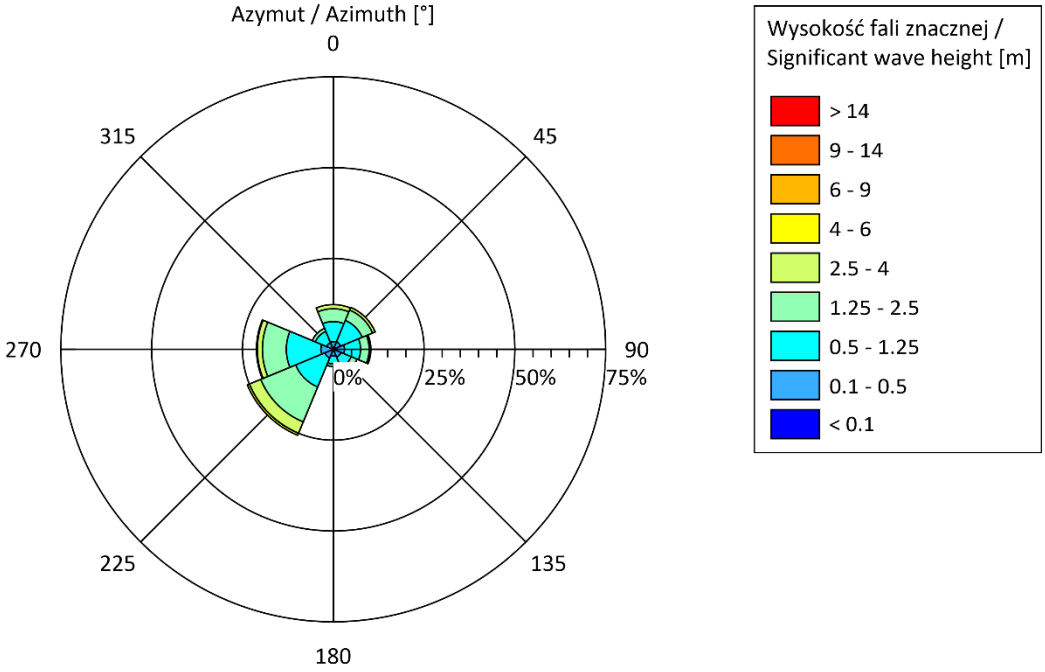


Figure 2.18. The wave rose diagram for the values measured at survey station B_MFW_2 throughout a measurement period of one full year

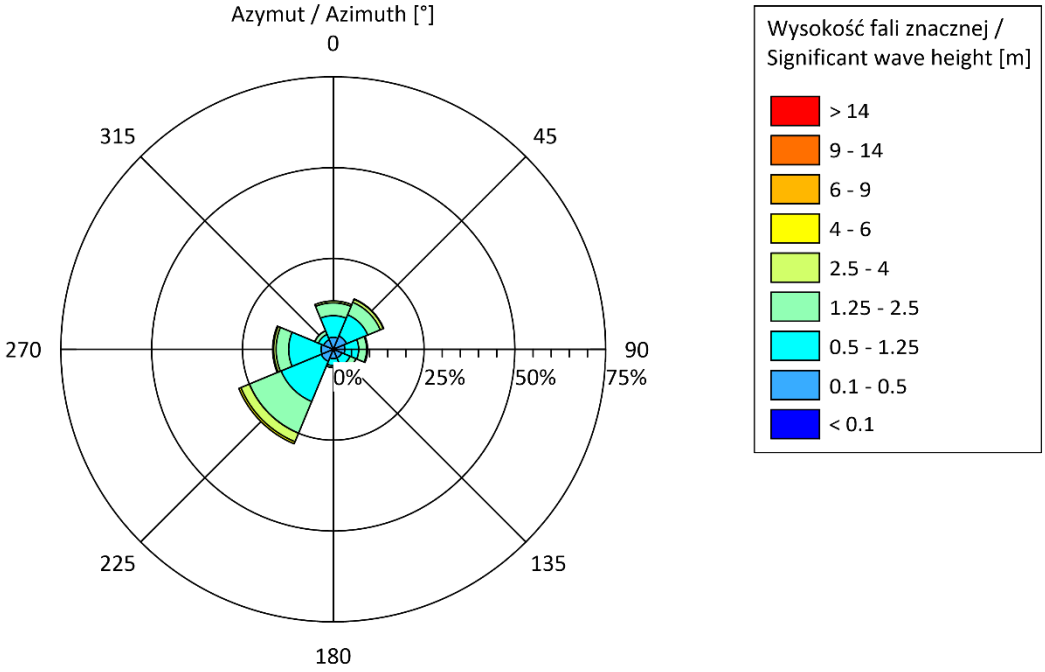


Figure 2.19. The wave rose diagram for the values measured at survey station B_MFW_3 throughout a measurement period of one full year

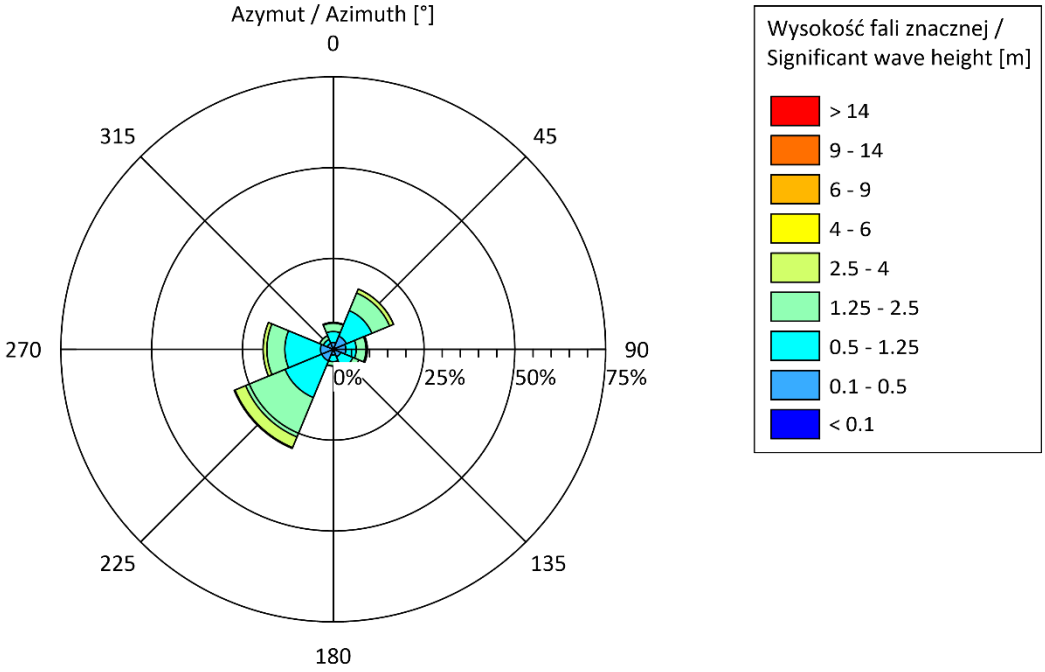


Figure 2.20. The wave rose diagram for the values measured at survey station B_MFW_4 throughout a measurement period of one full year

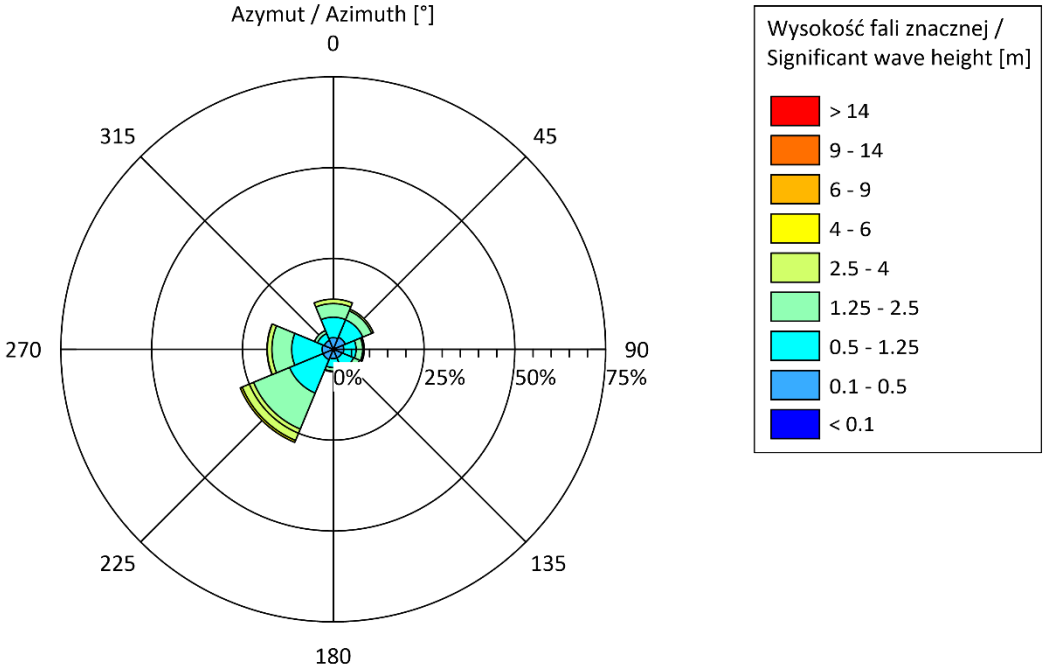


Figure 2.21. The wave rose diagram for the values measured at survey station B_MFW_5 throughout a measurement period of one full year

2.1.5.2.2 Water depth (thickness of the sea deep)

Figure 2.22–Figure 2.26 compare the changes in the height of the water column (water thickness) obtained from the recordings made using AWAC profilers at survey stations located in the survey area. It should be noted that for each service series (i.e. the period between the installation and retrieval of

the instruments from the seabed), the initial sea depth at the location of the apparatus may differ slightly. Hence, the graphs below illustrate the course of relative changes in the level of the free sea surface at the location and time of the recording.

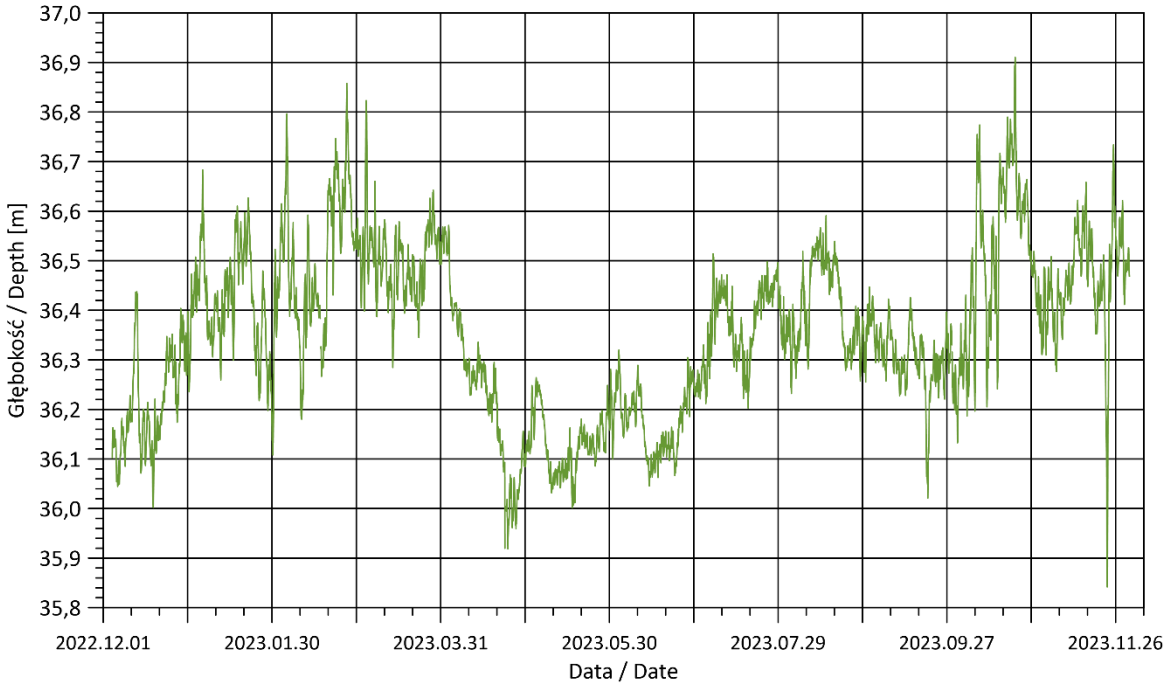


Figure 2.22. Changes in the sea depth (thickness of the water column) recorded at survey station B_MFW_1 throughout a measurement period of one full year

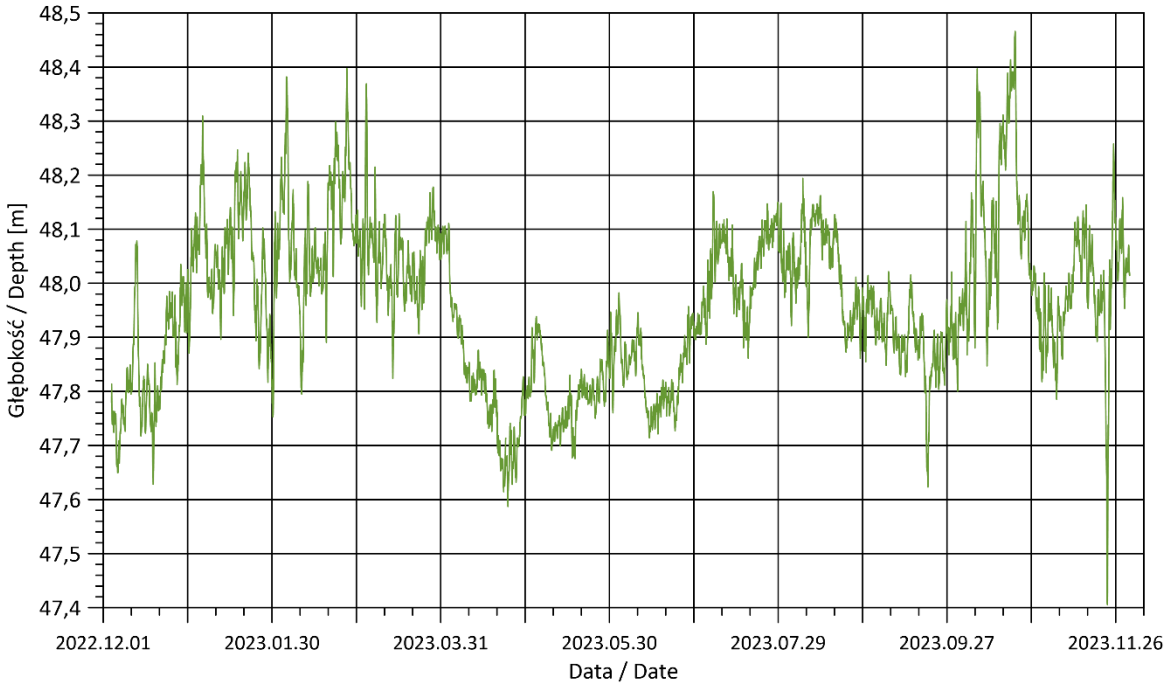


Figure 2.23. Changes in the sea depth (thickness of the water column) recorded at survey station B_MFW_2 throughout a measurement period of one full year

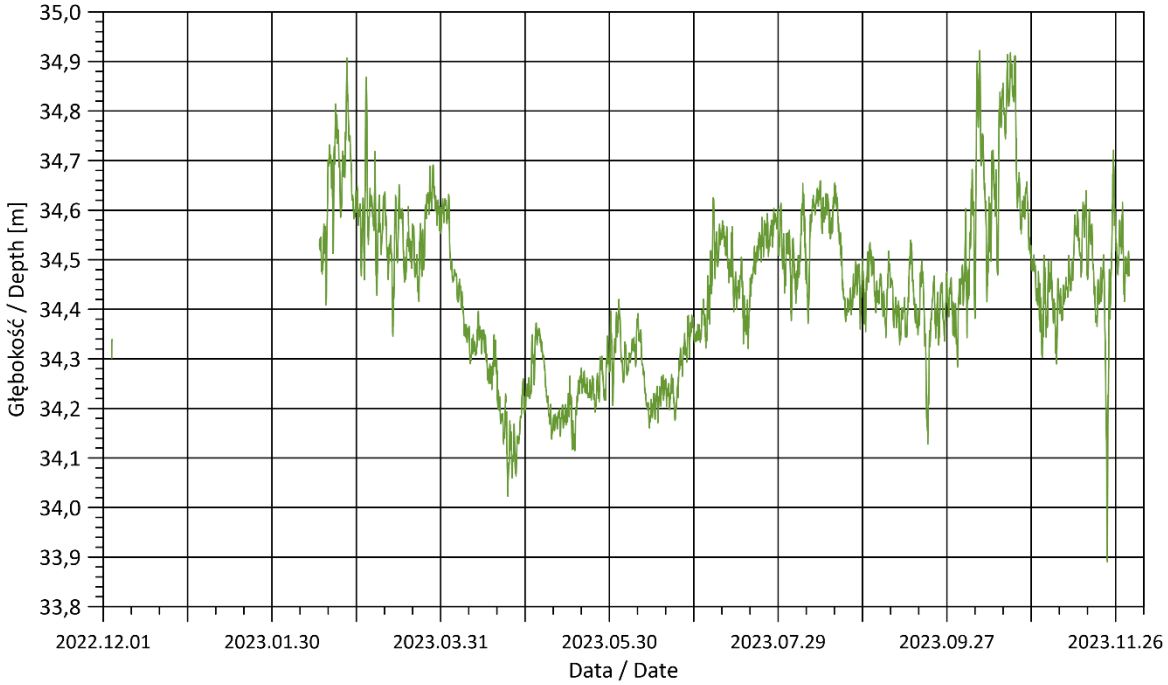


Figure 2.24. Changes in the sea depth (thickness of the water column) recorded at survey station B_MFW_3 throughout a measurement period of one full year

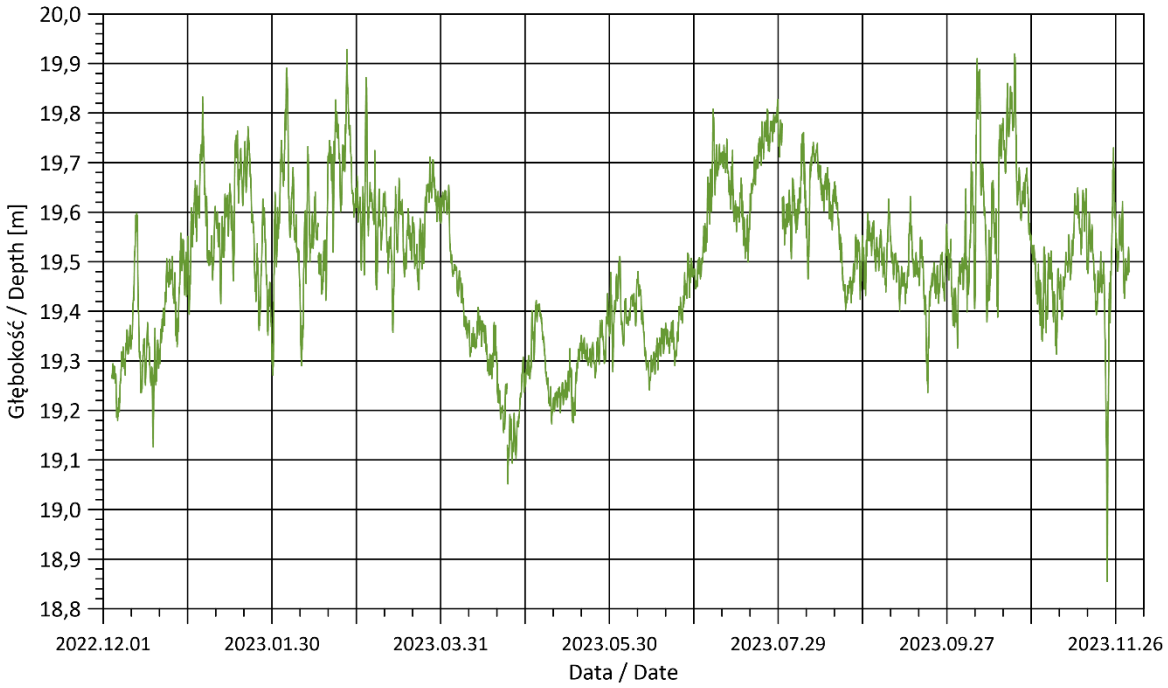


Figure 2.25. Changes in the sea depth (thickness of the water column) recorded at survey station B_MFW_4 throughout a measurement period of one full year

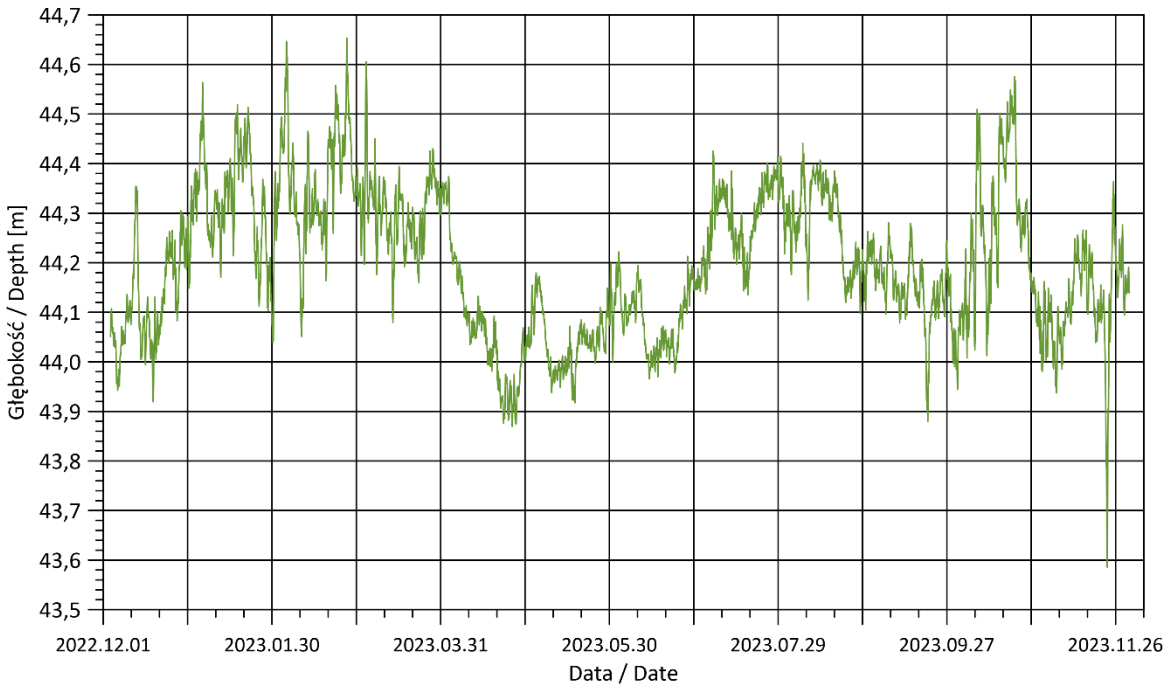


Figure 2.26. Changes in the sea depth (thickness of the water column) recorded at survey station B_MFW_5 throughout a measurement period of one full year

2.1.5.2.3 Water flow

The statistical parameters for the water flow measured at the two survey stations located within the survey area are presented in Table 2.10.

Table 2.10. The characteristics of the water flow measured across the water depth profile at the survey stations located within the survey area throughout a measurement period of one full year

Measurement point	Layer	Depth [m]	Water flow velocity [m·s^{-1}]			Standard deviation
			Mean	Minimum	Maximum	
B_MFW_1	Near-surface	1–4	0.12	0.00	0.57	0.07
	Middle	4–8	0.10	0.00	0.55	0.06
	Middle	8–12	0.10	0.00	0.52	0.06
	Middle	12–16	0.09	0.00	0.46	0.06
	Middle	16–20	0.09	0.00	0.41	0.06
	Middle	20–24	0.09	0.00	0.40	0.06
	Middle	24–28	0.09	0.00	0.39	0.06
	Middle	28–32	0.09	0.00	0.36	0.05
	Near-seabed	32–36	0.08	0.00	0.34	0.05
	The entire profile of the water depth	1–36	0.08	0.00	0.39	0.07
B_MFW_2	Near-surface	1–4	0.11	0.00	0.54	0.06
	Middle	4–8	0.10	0.00	0.52	0.06
	Middle	8–12	0.10	0.00	0.61	0.06
	Middle	12–16	0.09	0.00	0.59	0.06
	Middle	16–20	0.09	0.00	0.50	0.06

Measurement point	Layer	Depth [m]	Water flow velocity [m·s^{-1}]			Standard deviation
			Mean	Minimum	Maximum	
	Middle	20–24	0.09	0.00	0.58	0.06
	Middle	24–28	0.09	0.00	0.45	0.05
	Middle	28–32	0.08	0.00	0.51	0.05
	Middle	32–36	0.08	0.00	0.43	0.05
	Middle	36–40	0.08	0.00	0.47	0.05
	Middle	40–44	0.08	0.00	0.38	0.05
	Near-seabed	44–46	0.08	0.00	0.32	0.05
	The entire profile of the water depth	1–46	0.07	0.00	0.40	0.06
B_MFW_3	Near-surface	1–4	0.10	0.00	0.48	0.06
	Middle	4–8	0.09	0.00	0.51	0.06
	Middle	8–12	0.09	0.00	0.48	0.06
	Middle	12–16	0.09	0.00	0.46	0.06
	Middle	16–20	0.09	0.00	0.48	0.06
	Middle	20–24	0.08	0.00	0.40	0.06
	Middle	24–28	0.08	0.00	0.43	0.05
	Middle	28–32	0.08	0.00	0.36	0.05
	Near-seabed	30–33	0.07	0.00	0.44	0.05
	The entire profile of the water depth	1–33	0.07	0.00	0.42	0.06
B_MFW_4	Near-surface	1–4	0.11	0.00	0.55	0.07
	Middle	4–8	0.11	0.00	0.50	0.07
	Middle	8–12	0.10	0.00	0.49	0.06
	Middle	12–16	0.10	0.00	0.45	0.06
	Near-seabed	16–19	0.10	0.00	0.41	0.06
	The entire profile of the water depth	1–19	0.10	0.00	0.47	0.08
B_MFW_5	Near-surface	1–4	0.11	0.00	0.46	0.06
	Middle	4–8	0.09	0.00	0.44	0.05
	Middle	8–12	0.08	0.00	0.43	0.05
	Middle	12–16	0.08	0.00	0.43	0.05
	Middle	16–20	0.07	0.00	0.37	0.05
	Middle	20–24	0.07	0.00	0.36	0.04
	Middle	24–28	0.07	0.00	0.38	0.04
	Middle	28–32	0.07	0.00	0.37	0.04
	Middle	32–36	0.06	0.00	0.38	0.04
	Middle	36–40	0.06	0.00	0.37	0.04
	Near-seabed	40–44	0.06	0.00	0.38	0.04
	The entire profile of the water depth	1–44	0.06	0.00	0.36	0.05

The water movement velocities across the water depth profile were recorded with an AWAC acoustic current profiler as the averaged values from subsequent 1 m thick water layers. As the seawater flow dynamics are subject to complex fluctuations, to obtain information on the resultant velocity and direction of water masses movement in the survey area, a principle has been adopted for the water

movement velocity and direction analysis, taking into account the values averaged in the subsequent water layers with a thickness of 4 m, from the surface to the seabed (the "depth" column in Table 2.10). Due to the constant changes in the level of the free sea surface, which is also highly disturbed by wave motion, and the fact that the applied measurement performance method prevents the recording of water dynamics in the layers directly adjacent to the seabed (to the level from approx. 1 to 1.5 m above the seabed – the height of the tripod and the blank zone), data from these border layers of water are not included in the calculations.

Figure 2.27–Figure 2.31 present the courses of changes in the flow velocities obtained from the measurements conducted at the stations located within the survey area in three selected water layers of 4 m in thickness: near-surface, one of the middle layers of the water deep, and near-seabed layer.

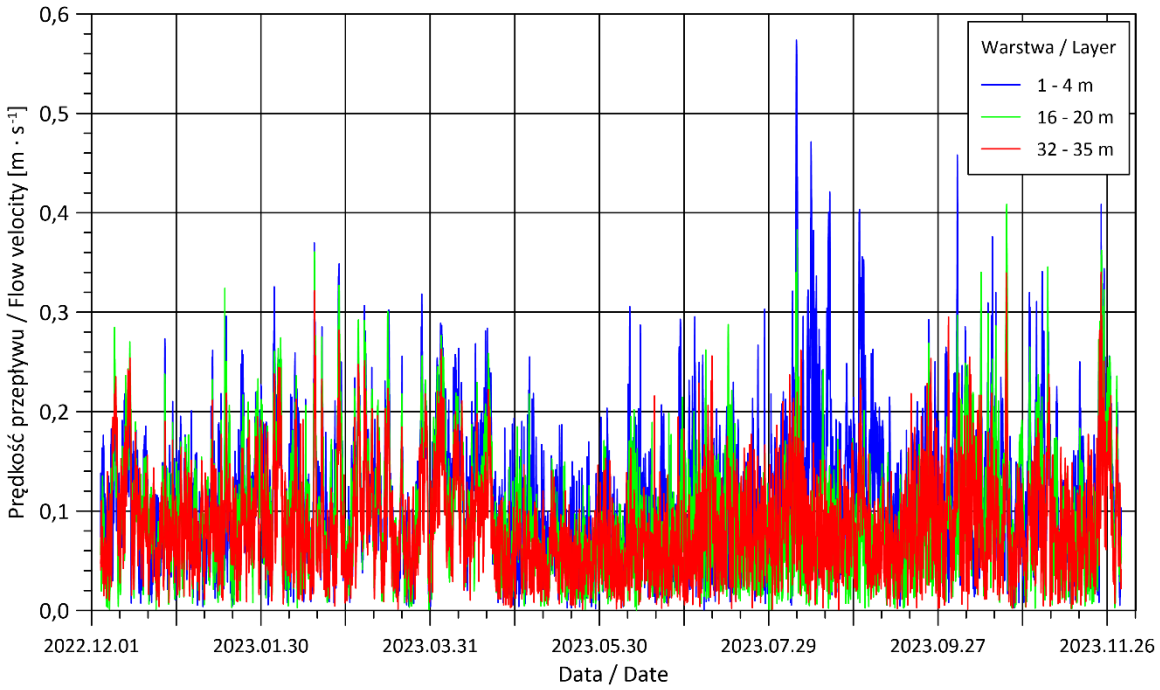


Figure 2.27. The water flow velocities measured at survey station B_MFW_1 throughout a measurement period of one full year

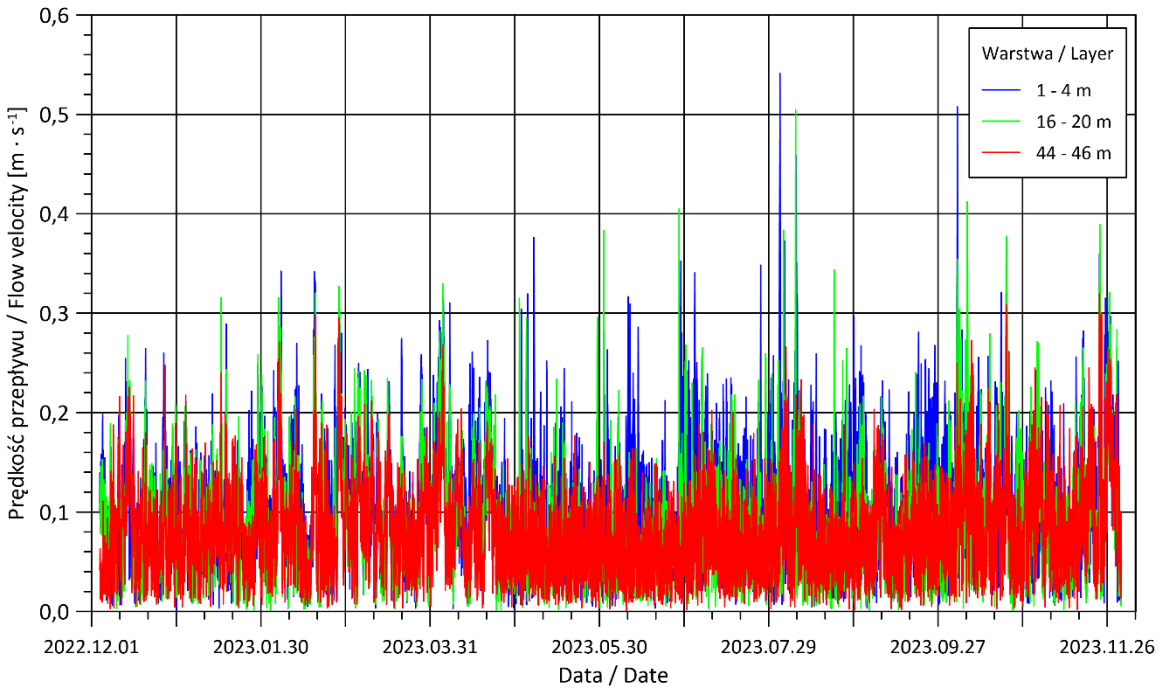


Figure 2.28. The water flow velocities measured at survey point B_MFW_2 throughout a measurement period of one full year

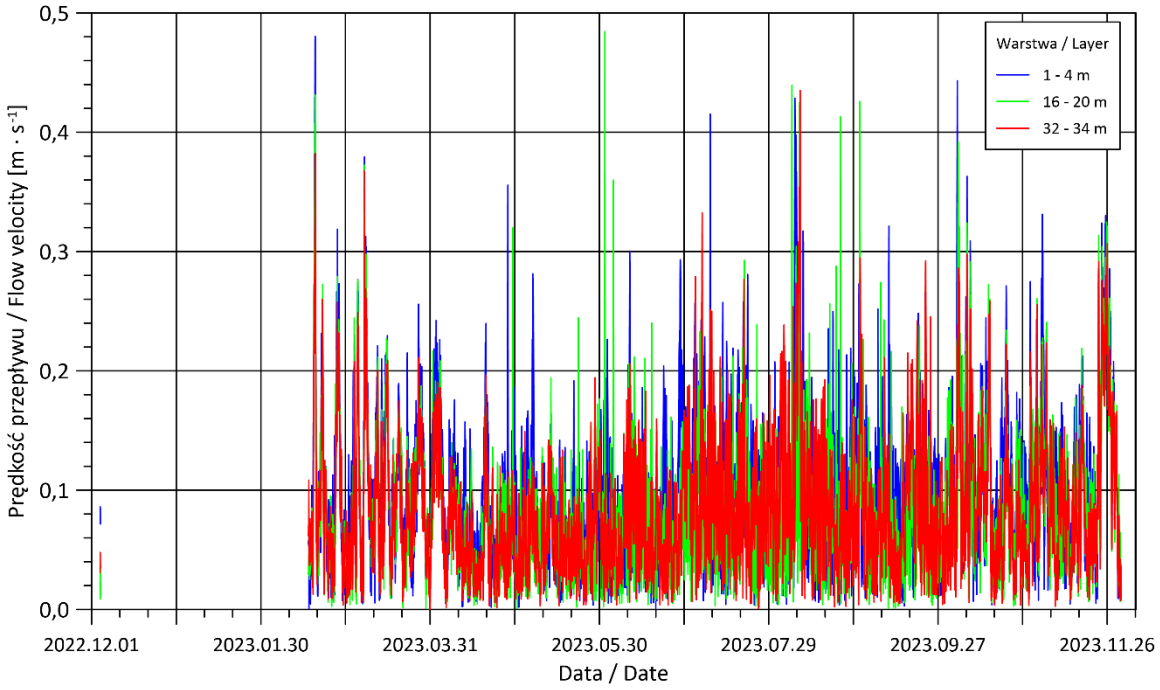


Figure 2.29. The water flow velocities measured at survey point B_MFW_3 throughout a measurement period of one full year

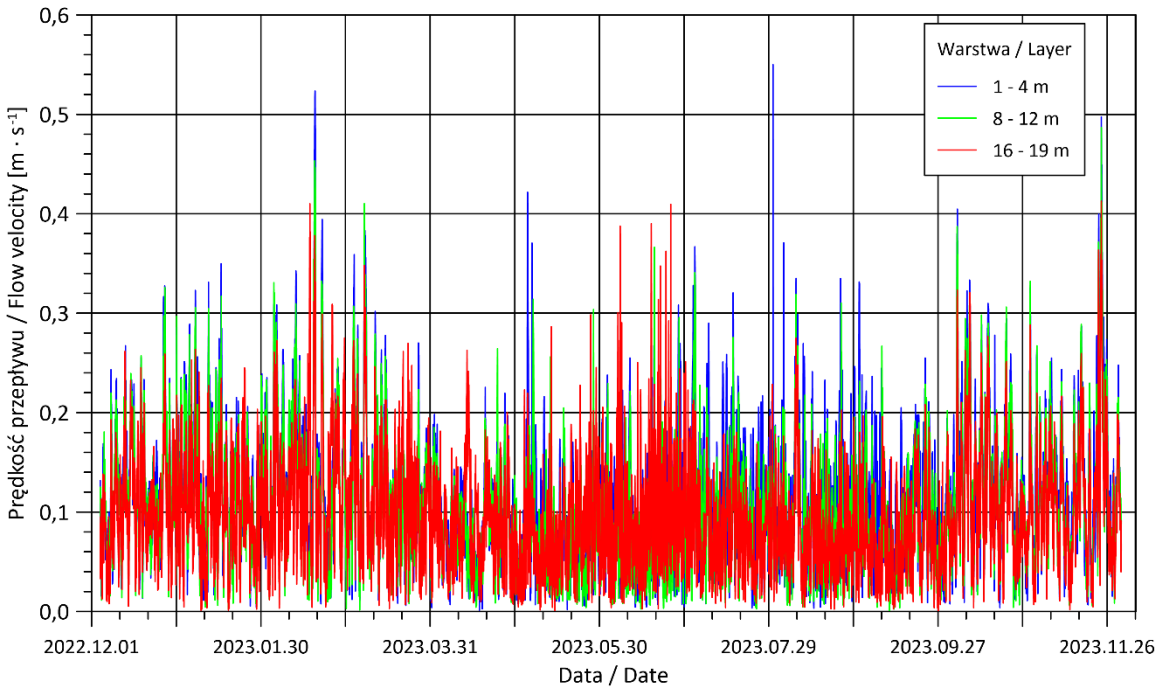


Figure 2.30. The water flow velocities measured at survey point B_MFW_4 throughout a measurement period of one full year

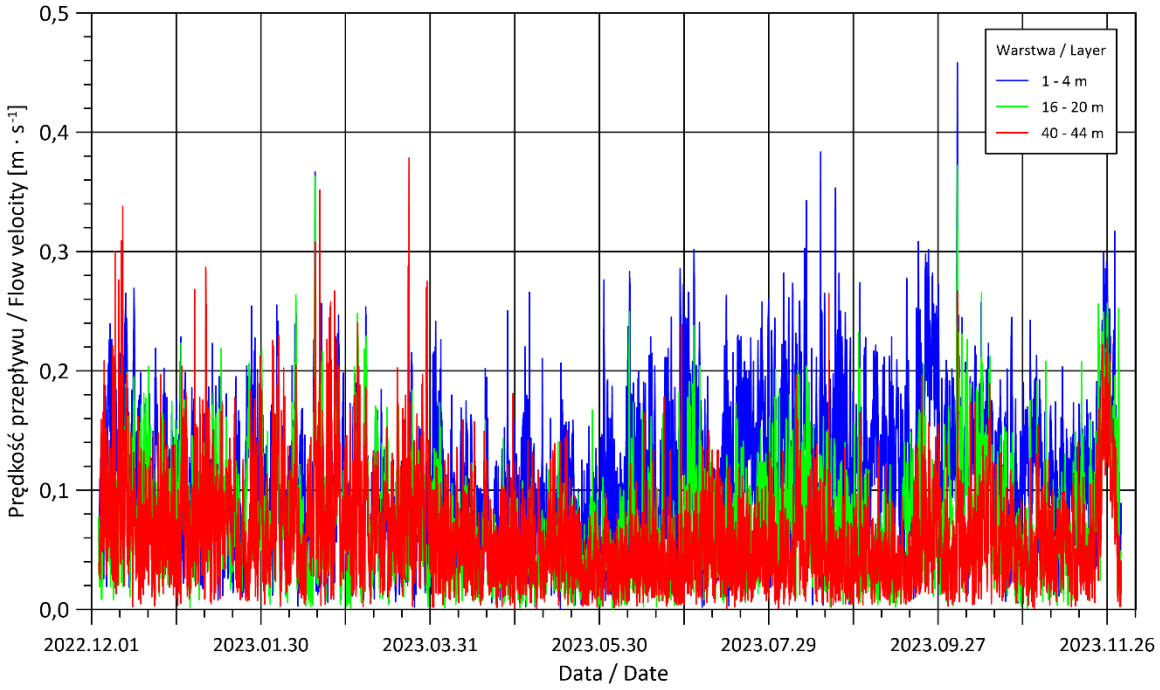


Figure 2.31. The water flow velocities measured at survey point B_MFW_5 throughout a measurement period of one full year

Subsequent charts [Figure 2.32–Figure 2.46] present the directional distribution of water flow velocities at the recording points in the three selected 4-m thick layers of water (Figure 2.27–Figure 2.31, respectively). The directions presented in the directional distributions of the velocities represent the directions in which the water flows.

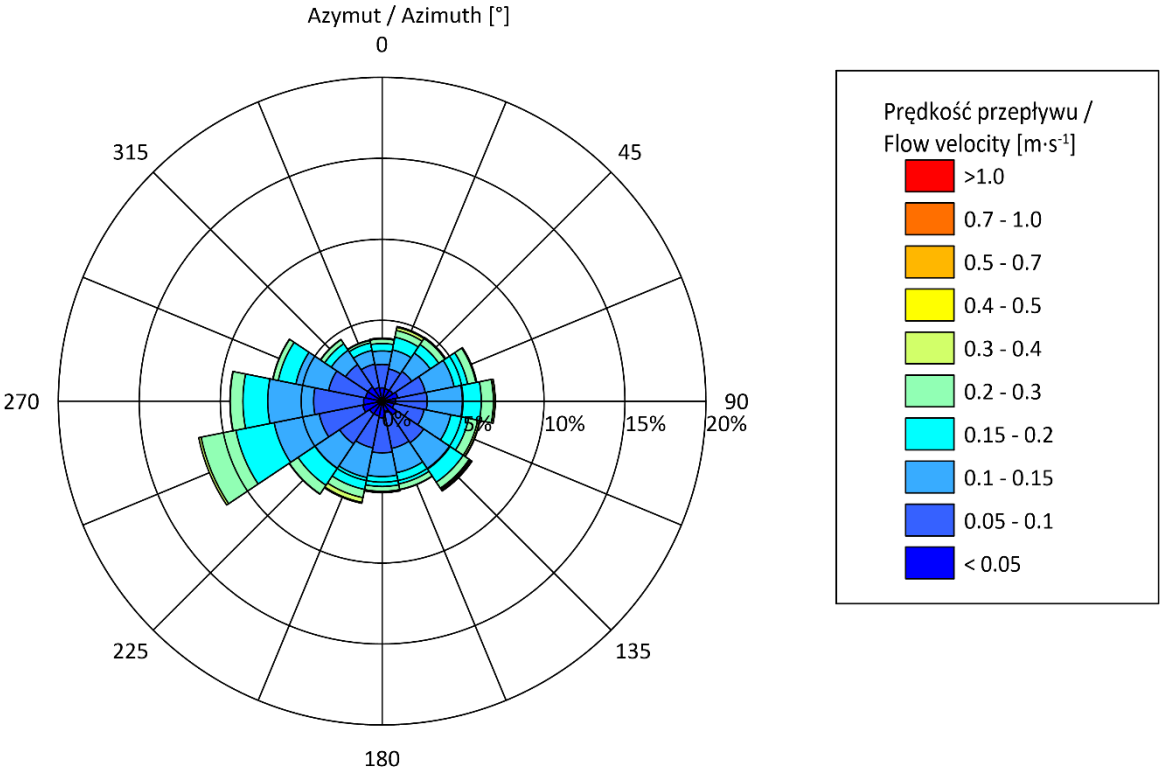


Figure 2.32. The directional distributions of the water flow velocities measured at survey station B_MFW_1 in the layer from the free sea surface to the depth of 4 m throughout a measurement period of one full year

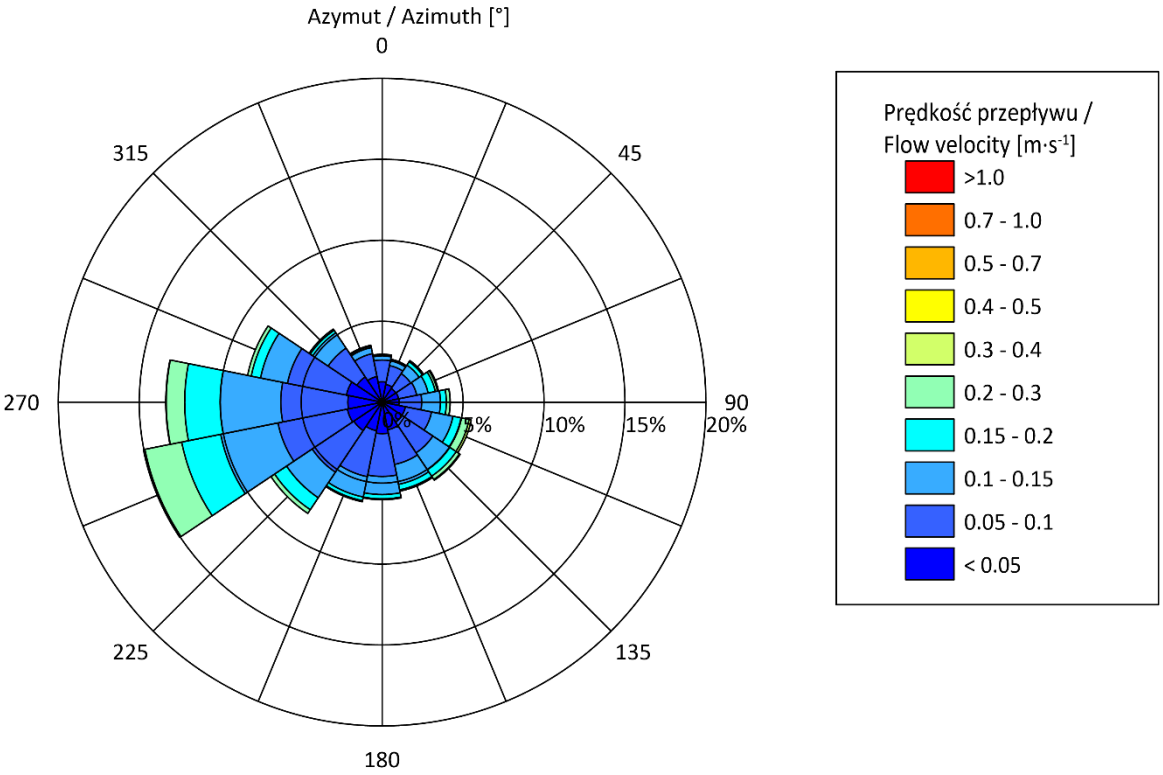


Figure 2.33. The directional distributions of the water flow velocities measured at survey station B_MFW_1 in the layer from the depth of 16 m to the depth of 20 m below the sea surface throughout a measurement period of one full year

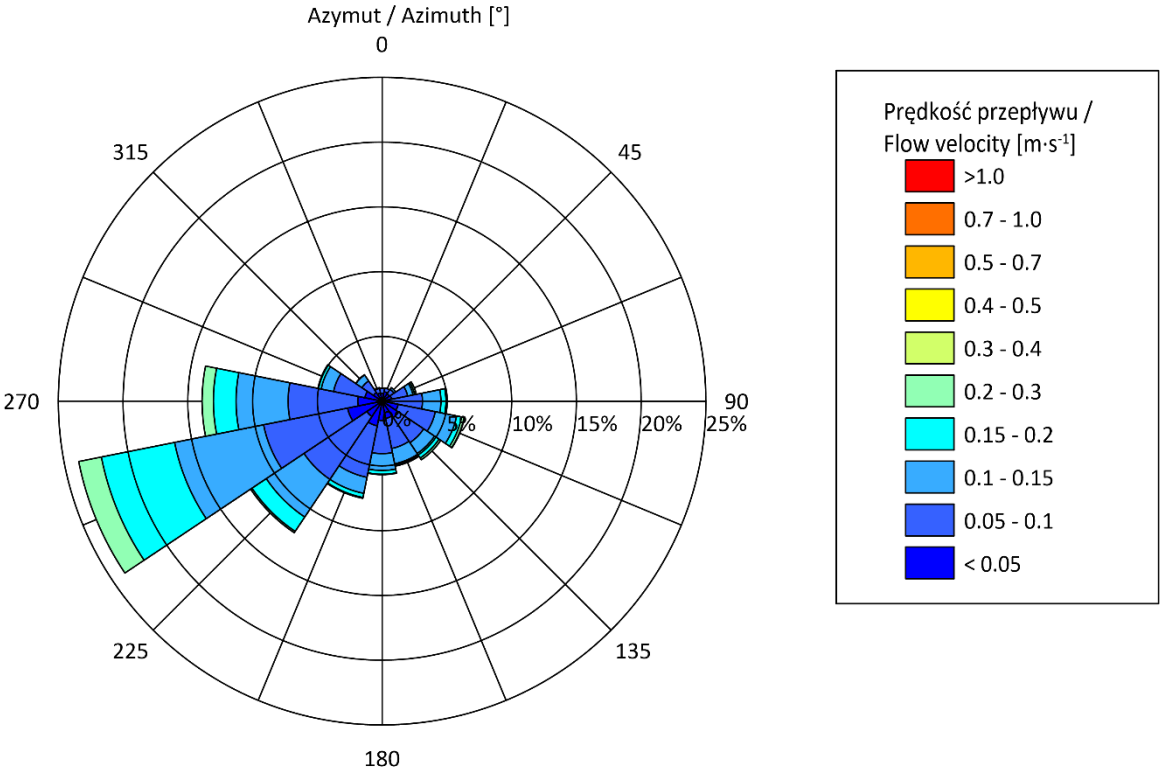


Figure 2.34. The directional distributions of the water flow velocities measured at survey station B_MFW_1 in the layer from the depth of 32 m to the seabed

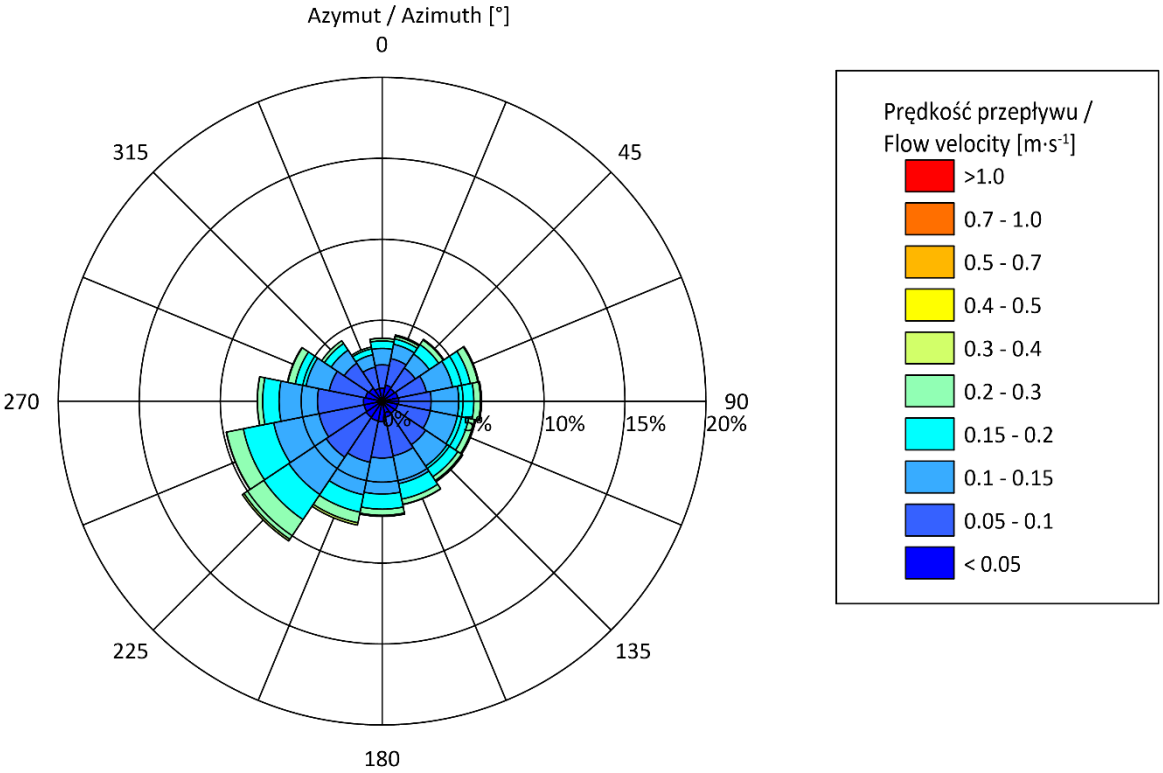


Figure 2.35. The directional distributions of the water flow velocities measured at survey station B_MFW_2 in the layer from the free sea surface to the depth of 4 m throughout a measurement period of one full year

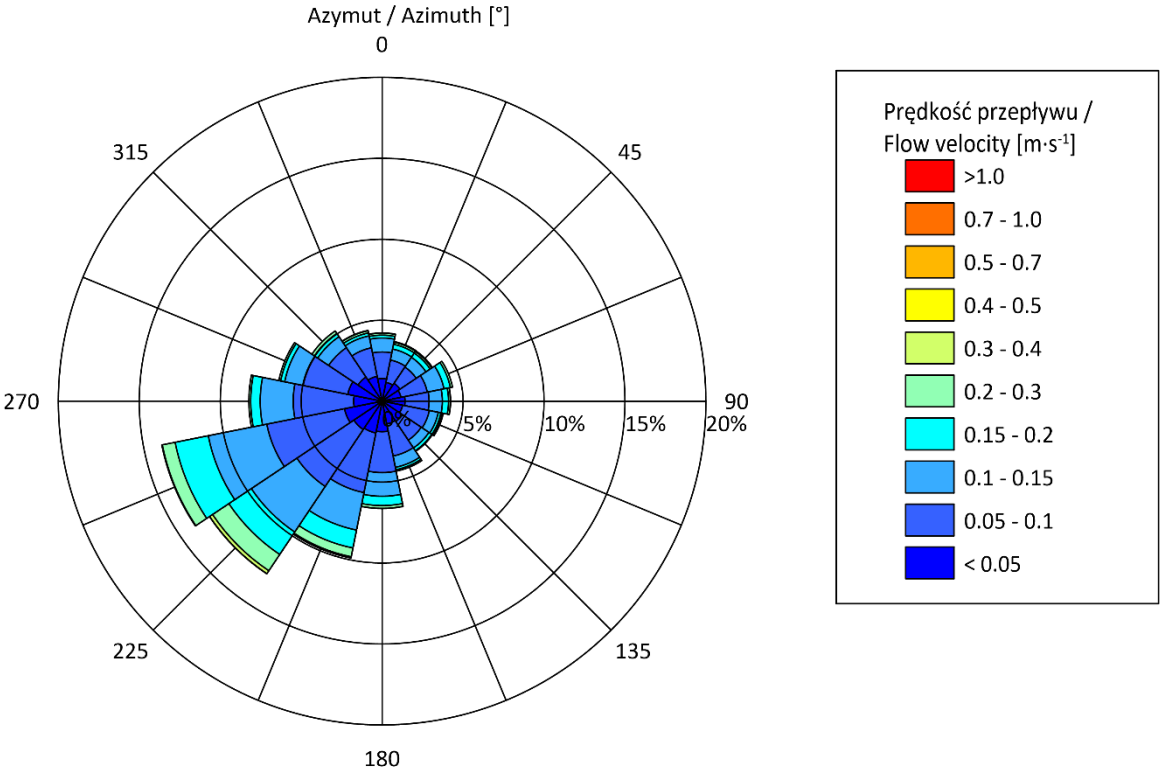


Figure 2.36. The directional distributions of the water flow velocities measured at survey station B_MFW_2 in the layer from the depth of 16 m to the depth of 20 m below the sea surface throughout a measurement period of one full year

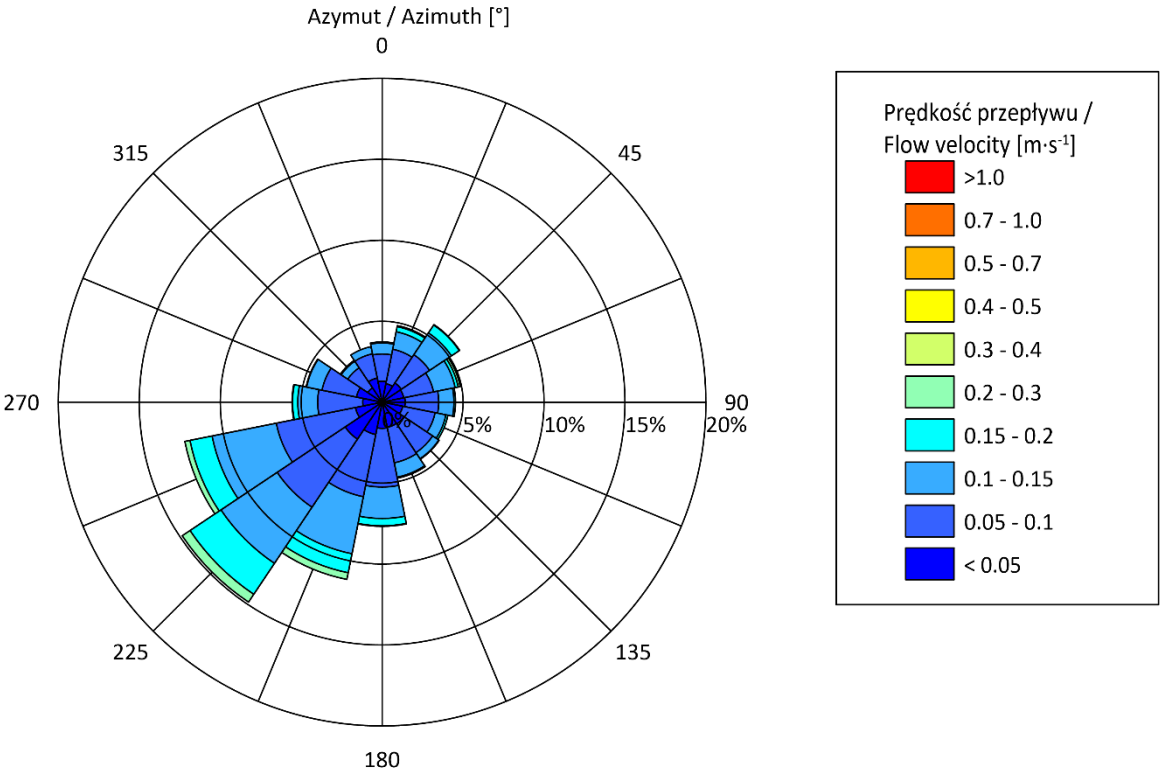


Figure 2.37. The directional distributions of the water flow velocities measured at survey station B_MFW_2 in the layer from the depth of 44 m to the seabed

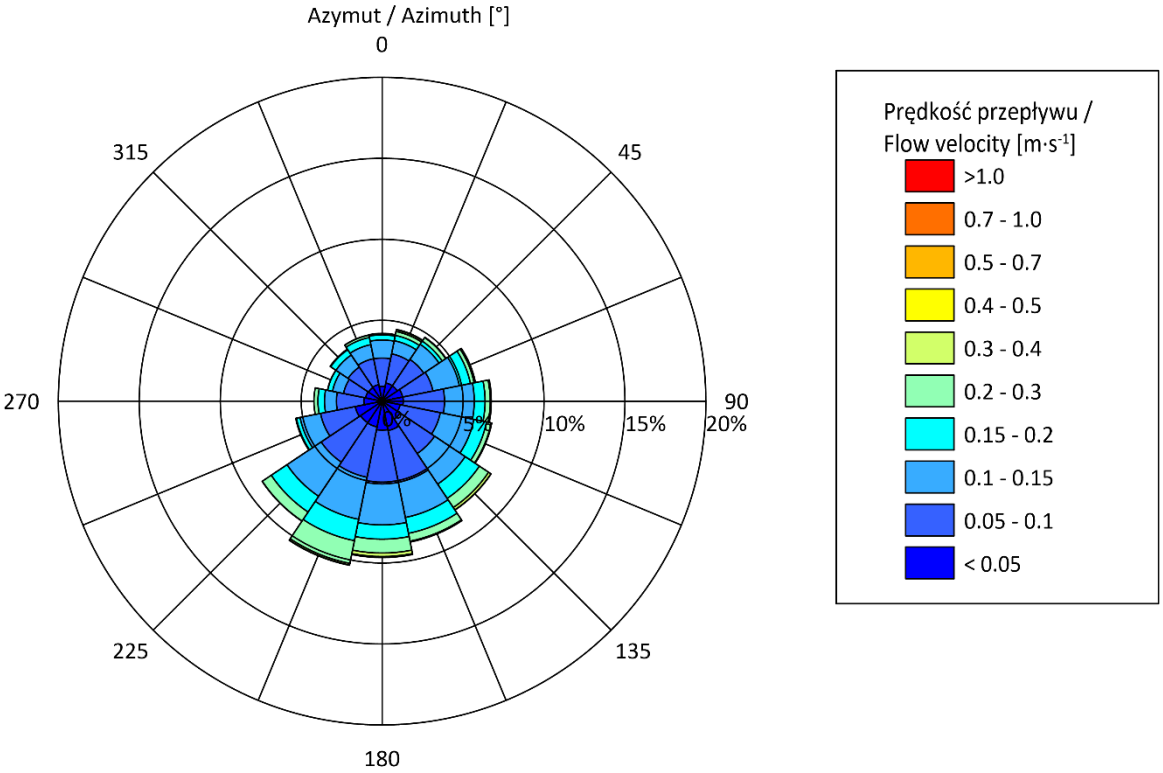


Figure 2.38. The directional distributions of the water flow velocities measured at survey station B_MFW_3 in the layer from the free sea surface to the depth of 4 m throughout a measurement period of one full year

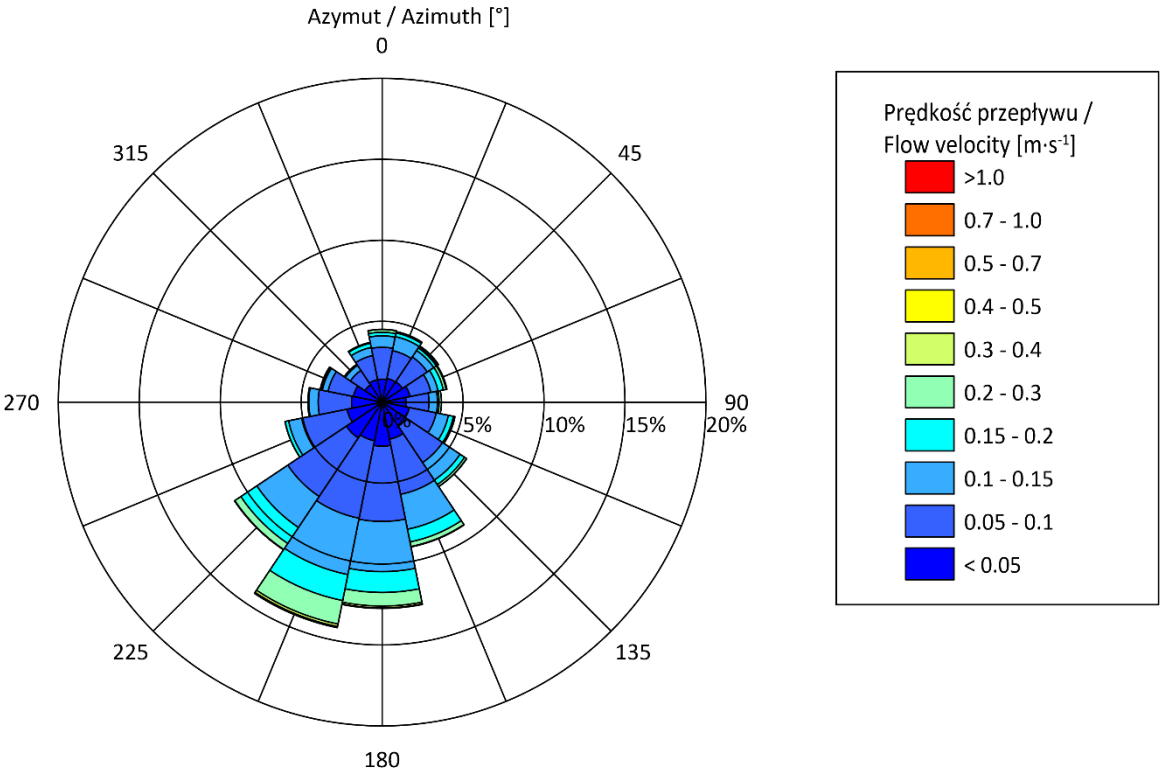


Figure 2.39. The directional distributions of the water flow velocities measured at survey station B_MFW_3 in the layer from the depth of 16 m to the depth of 20 m below the sea surface throughout a measurement period of one full year

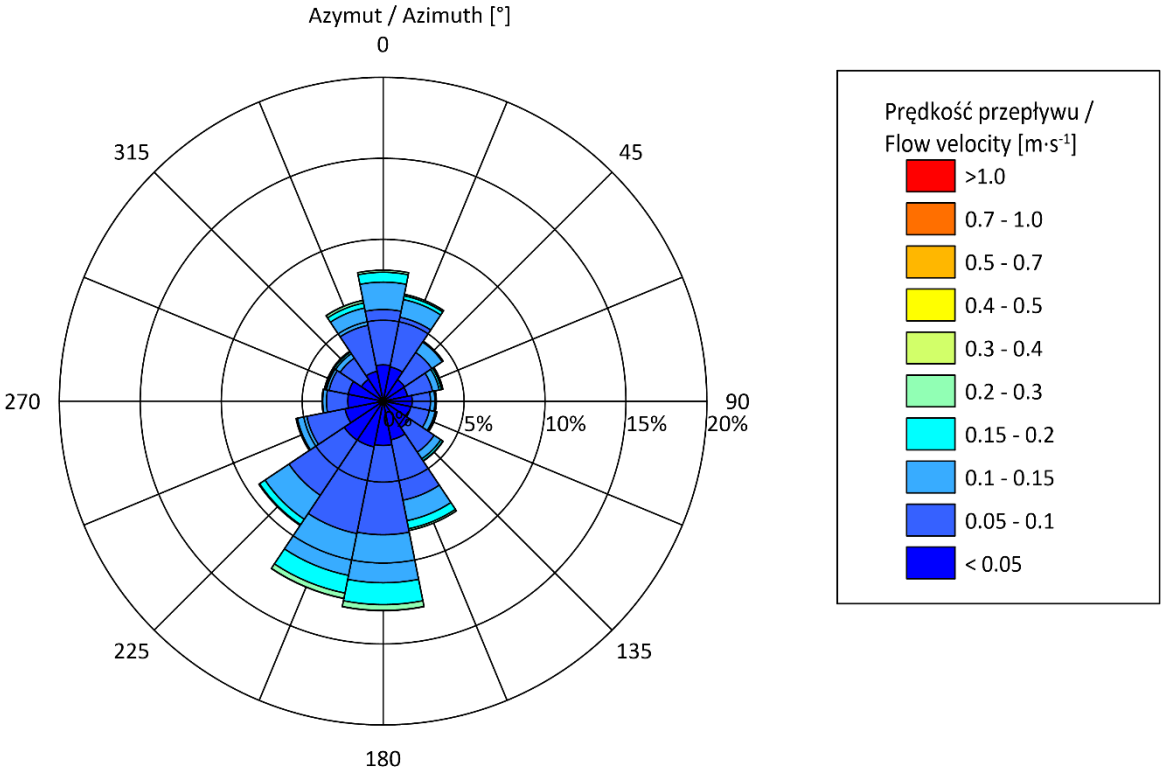


Figure 2.40. The directional distributions of the water flow velocities measured at survey station B_MFW_3 in the layer from the depth of 32 m to the seabed throughout a measurement period of one full year

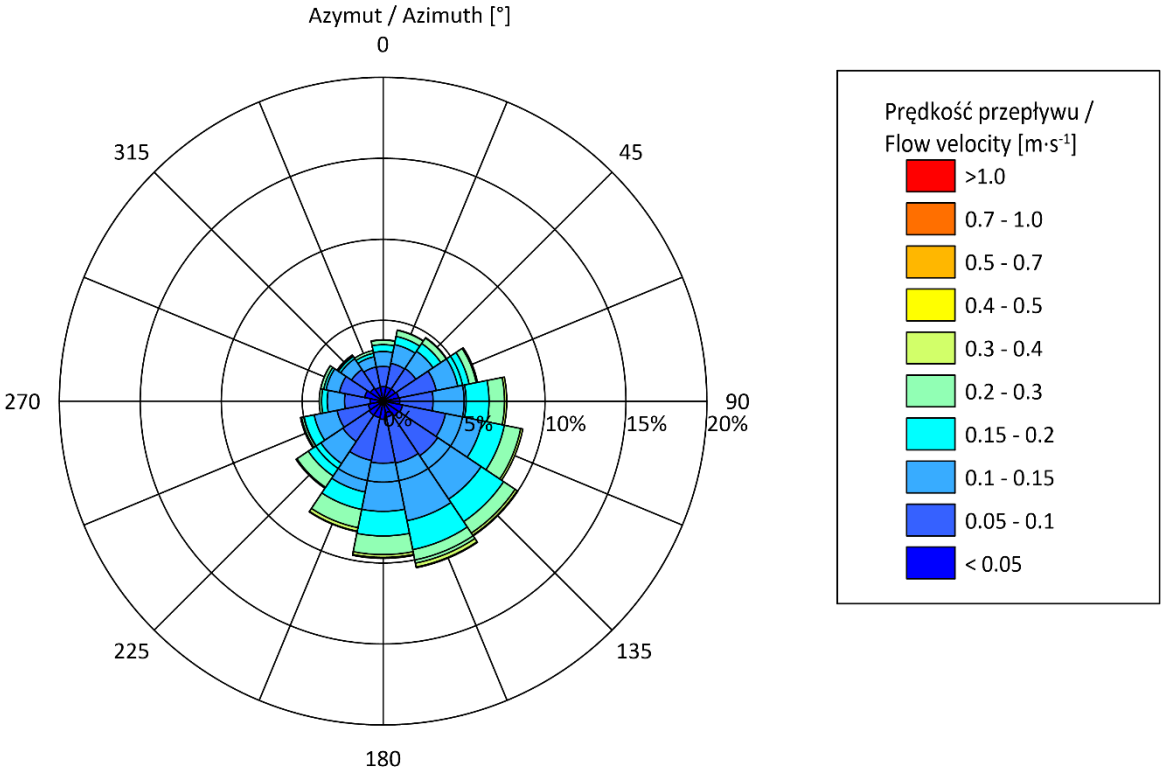


Figure 2.41. The directional distributions of the water flow velocities measured at survey station B_MFW_4 in the layer from the free sea surface to the depth of 4 m throughout a measurement period of one full year

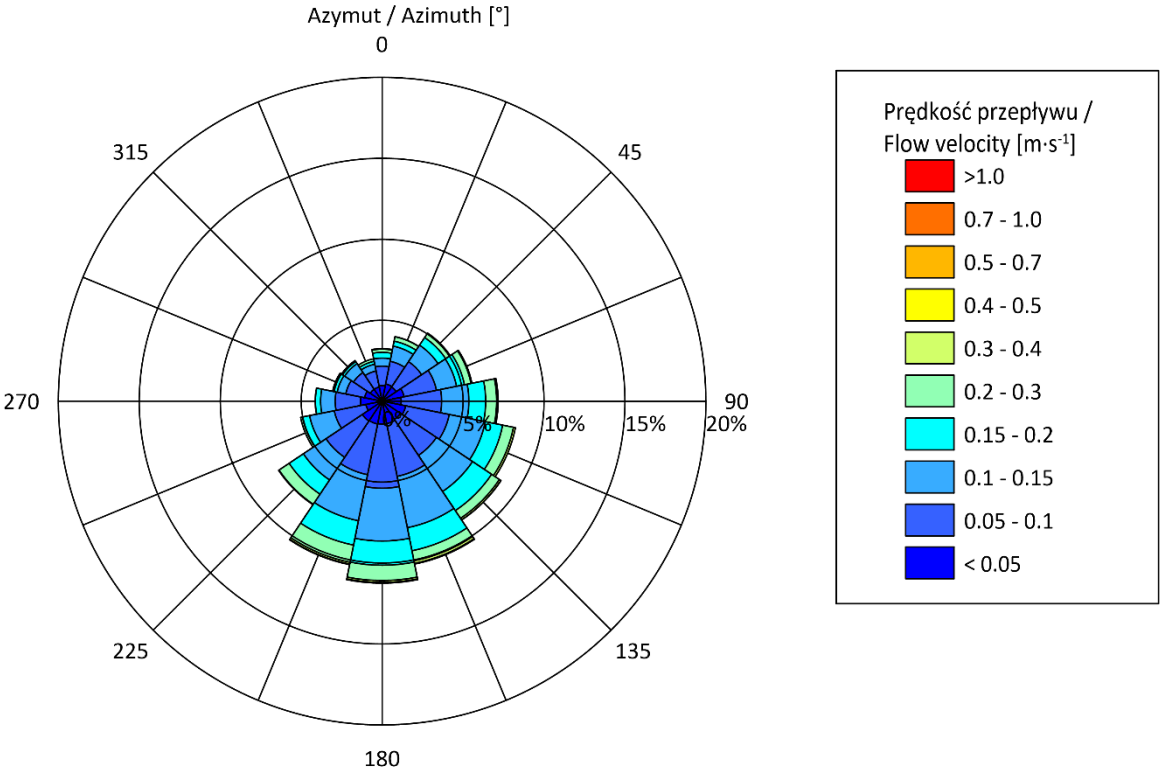


Figure 2.42. The directional distributions of the water flow velocities measured at survey station B_MFW_4 in the layer from the depth of 8 m to the depth of 12 m below the sea surface throughout a measurement period of one full year

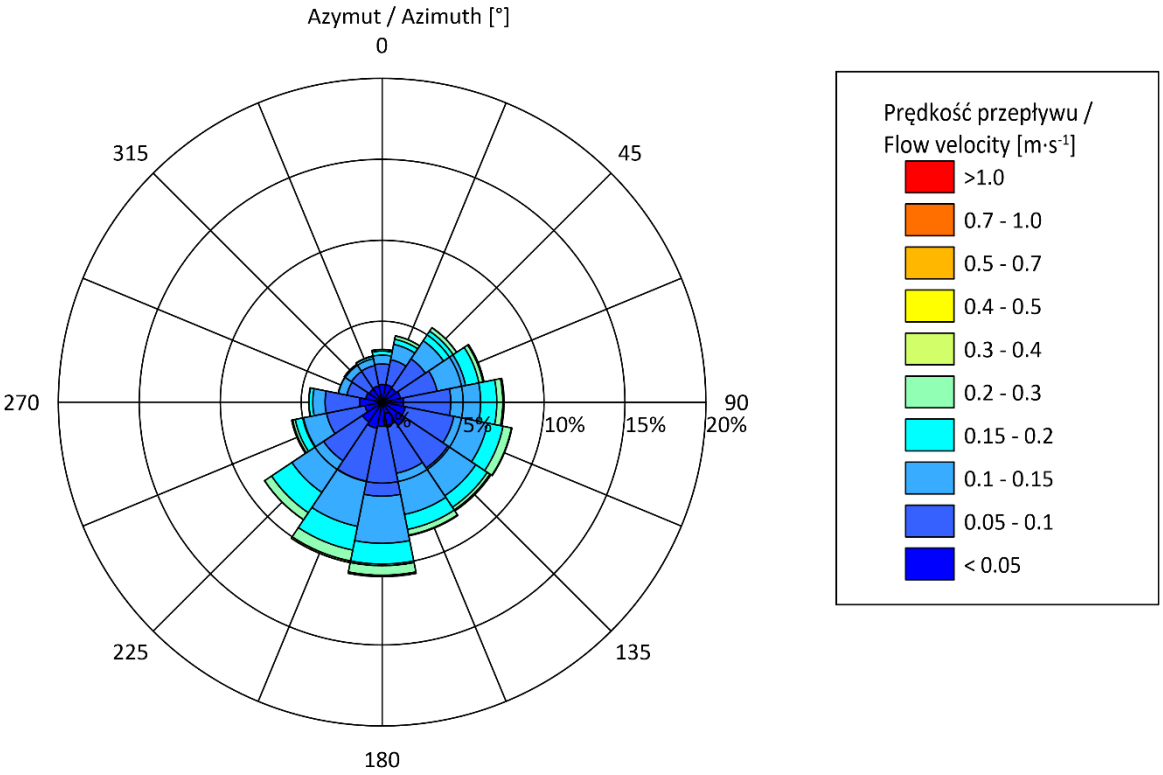


Figure 2.43. The directional distributions of the water flow velocities measured at survey station B_MFW_4 in the layer from the depth of 16 m to the seabed throughout a measurement period of one full year

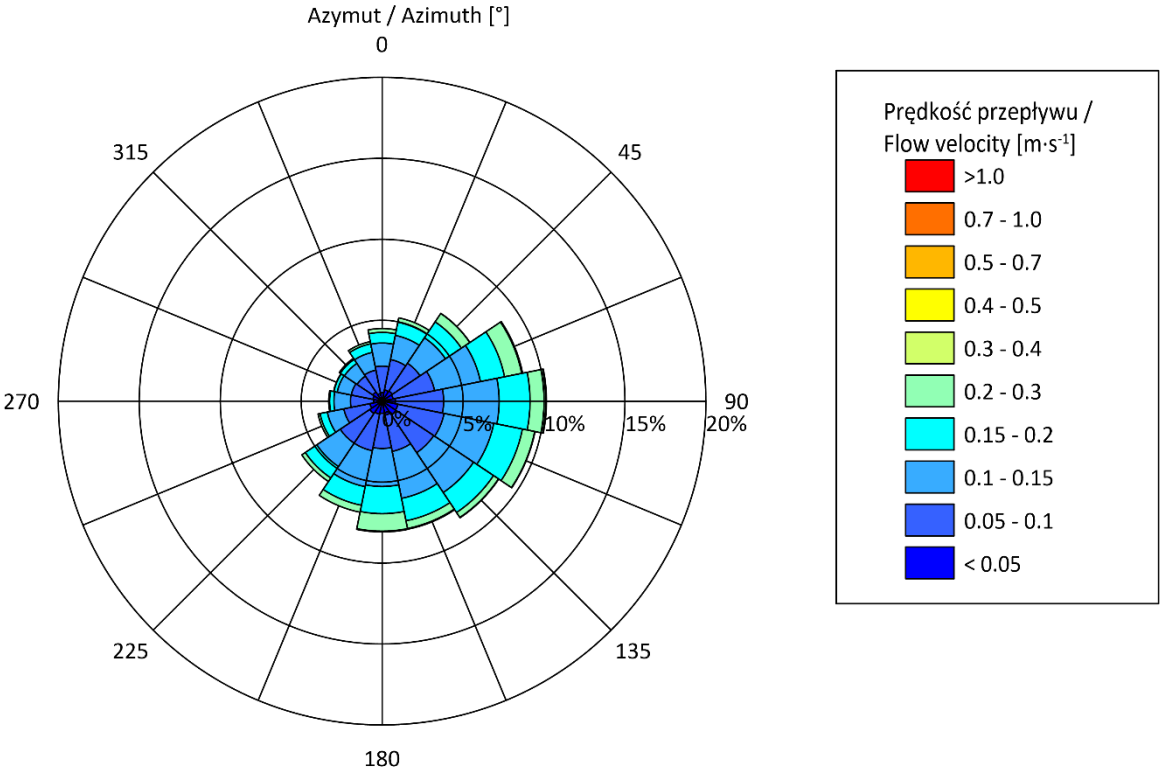


Figure 2.44. *The directional distributions of the water flow velocities measured at survey station B_MFW_5 in the layer from the free sea surface to the depth of 4 m throughout a measurement period of one full year*

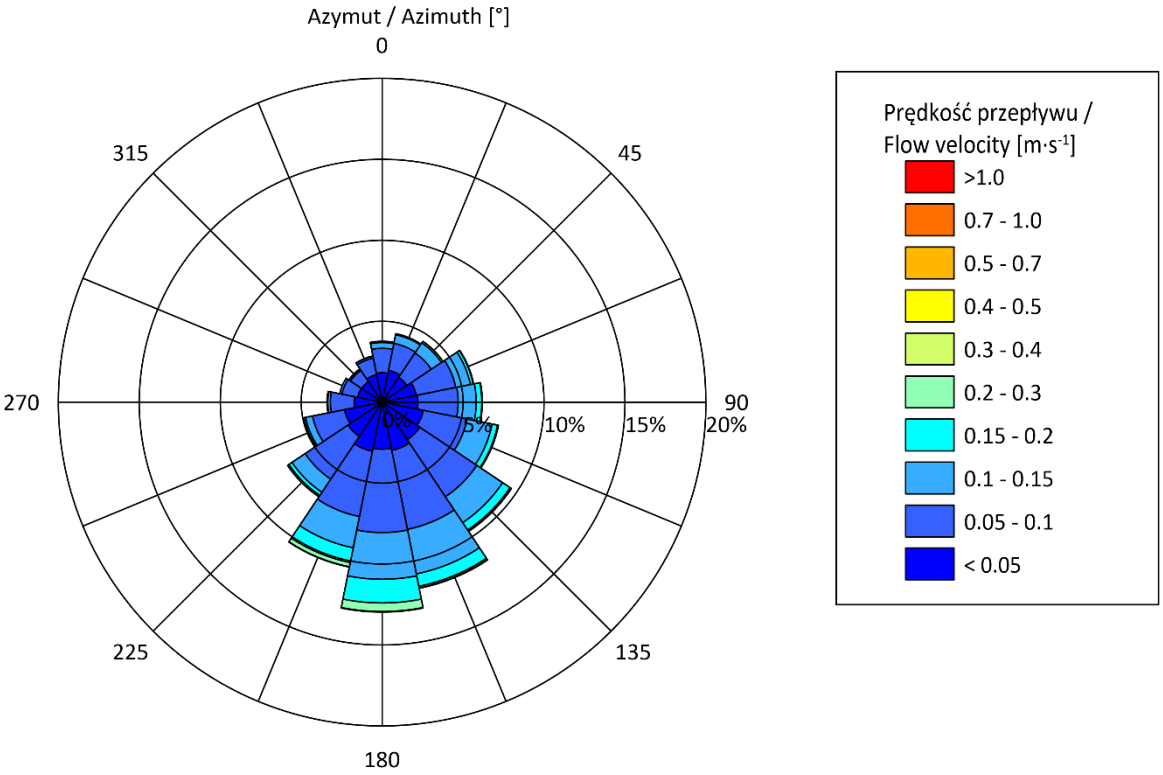


Figure 2.45. *The directional distributions of the water flow velocities measured at survey station B_MFW_5 in the layer from the depth of 16 m to the depth of 20 m below the sea surface throughout a measurement period of one full year*

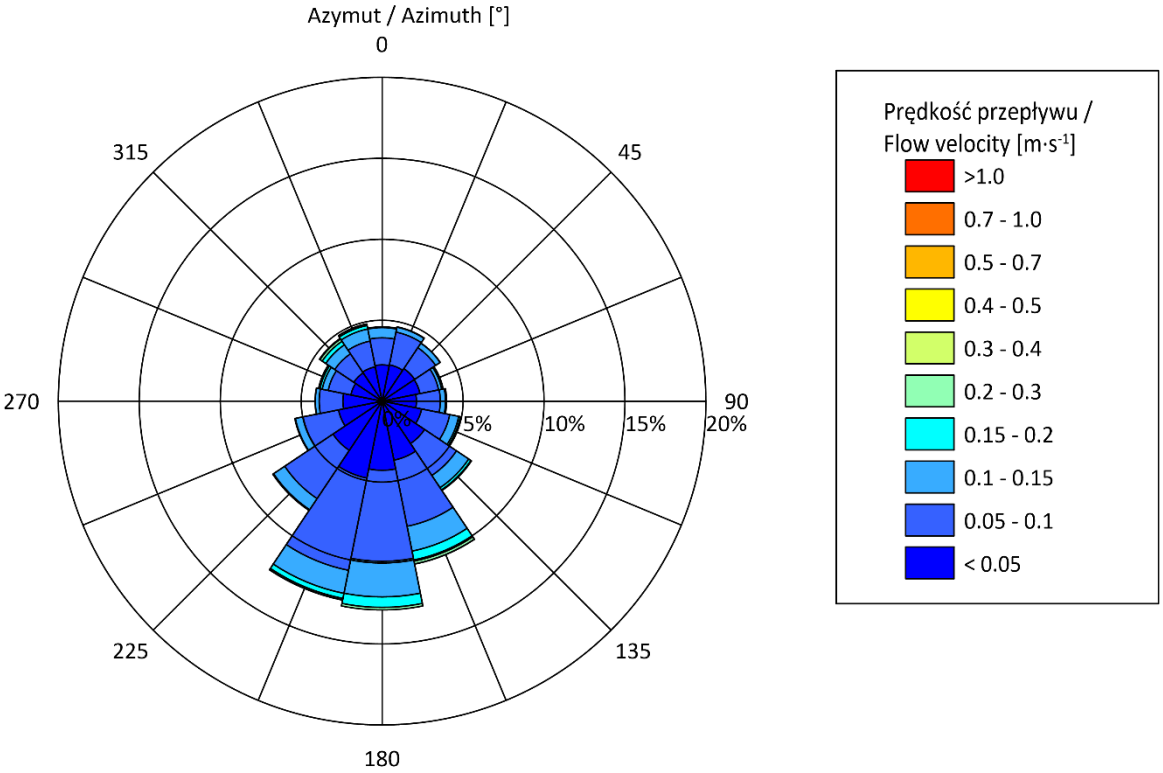


Figure 2.46. The directional distributions of the water flow velocities measured at survey station B_MFW_5 in the layer from the depth of 40 m to the seabed

2.1.5.3 Hydrophysical measurements

2.1.5.3.1 Continuous recordings

2.1.5.3.1.1 Water temperature

The water temperature was measured using the CTD probes at the survey stations located within the survey area: B_MFW_1, B_MFW_3 and B_MFW_5. At survey station B_MFW_3, the measurement was taken at five depths across the sea depth: 1 m, 4 m, 8 m, 16 m, and above the seabed. Whereas at survey stations B_MFW_1 and B_MFW_5, the measurement was taken at one depth – above the seabed. The statistical analysis of the water temperature measured is presented in Table 2.11.

Table 2.11. A statistical analysis of the water temperature measured at survey stations B_MFW_1, B_MFW_3, and B_MFW_5 located within the survey area throughout the entire measurement period

Measurement point	Depth [m]	Temperature [°C]			
		Mean	Minimum	Maximum	Standard deviation
B_MFW_1	Over the seabed	6.31	2.97	14.35	2.20
B_MFW_3	1	10.30	3.11	21.16	5.52
	4	9.66	3.10	19.22	5.26
	8	9.50	3.10	18.44	5.08
	16	9.56	3.09	18.76	4.98
	Over the seabed	6.13	3.09	14.14	2.04
B_MFW_5	Over the seabed	5.64	3.18	12.72	1.59

The values of water temperature have been presented in the following plots [Figure 2.47–Figure 2.49].

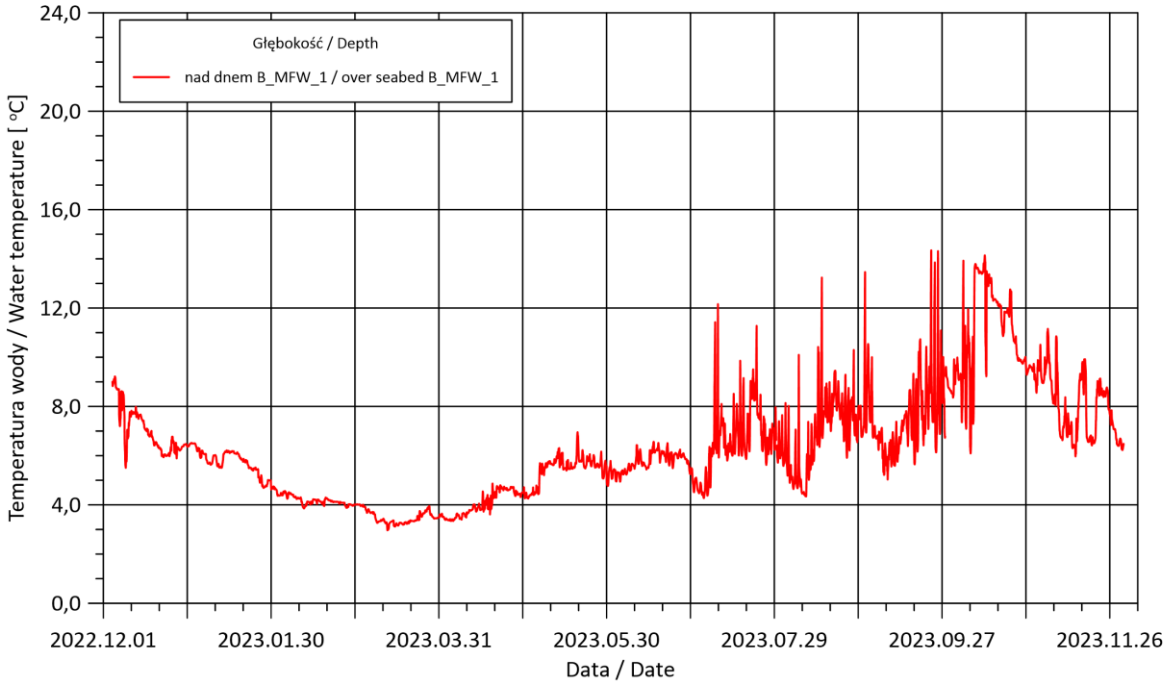


Figure 2.47. The water turbidity measured at survey station B_MFW_1 throughout the entire measurement period

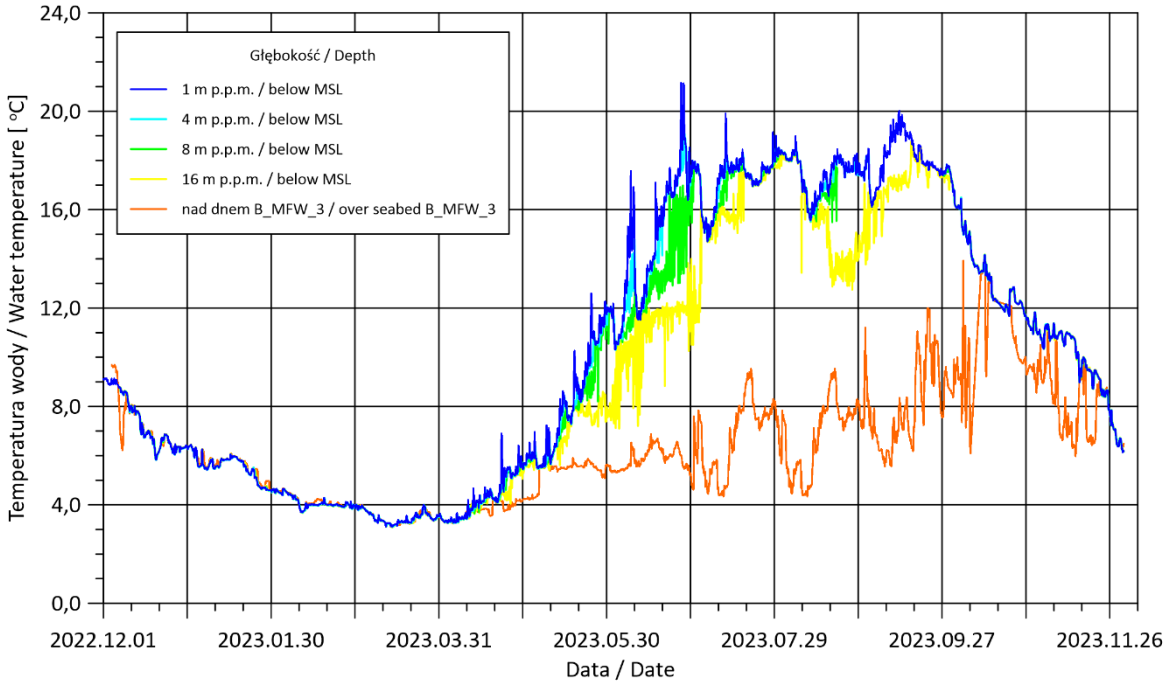


Figure 2.48. The water turbidity measured at survey station B_MFW_3 throughout the entire measurement period

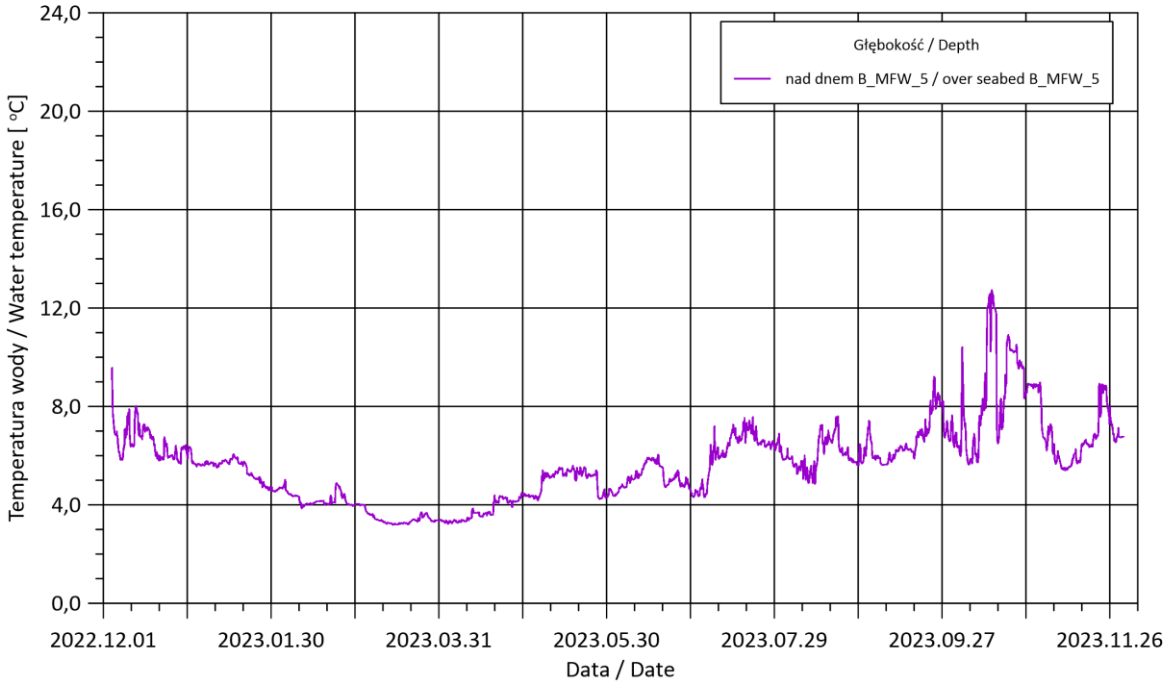


Figure 2.49. The water turbidity measured at survey station B_MFW_5 throughout the entire measurement period

2.1.5.3.1.2 Electrical conductivity of water

The electrical conductivity of water was measured using CTD probes at survey stations located within the survey area: B_MFW_1, B_MFW_3 and B_MFW_5. At survey station B_MFW_3, the measurement was taken at five depths across the sea depth: 1 m, 4 m, 8 m, 16 m, and above the seabed. Whereas at survey stations B_MFW_1 and B_MFW_5, the measurement was taken at one depth – above the seabed. A statistical analysis of the measured electrical conductivity of water is presented in Table 2.12.

Table 2.12. A statistical analysis of the electrical conductivity of water measured at survey stations B_MFW_1, B_MFW_3, and B_MFW_5 located within the survey area throughout the entire measurement period

Measurement point	Depth [m]	Electrical conductivity [S·m^{-1}]			
		Mean	Minimum	Maximum	Standard deviation
B_MFW_1	Over the seabed	8.44	7.51	10.45	0.59
B_MFW_3	1	8.97	7.43	11.78	1.20
	4	8.94	7.41	11.32	1.19
	8	8.90	7.46	11.19	1.13
	16	8.94	7.45	11.26	1.12
	Over the seabed	8.44	7.51	10.45	0.59
B_MFW_5	Over the seabed	8.34	7.44	10.05	0.50

The values of the electrical conductivity of water are presented in the charts below [Figure 2.50–Figure 2.52].

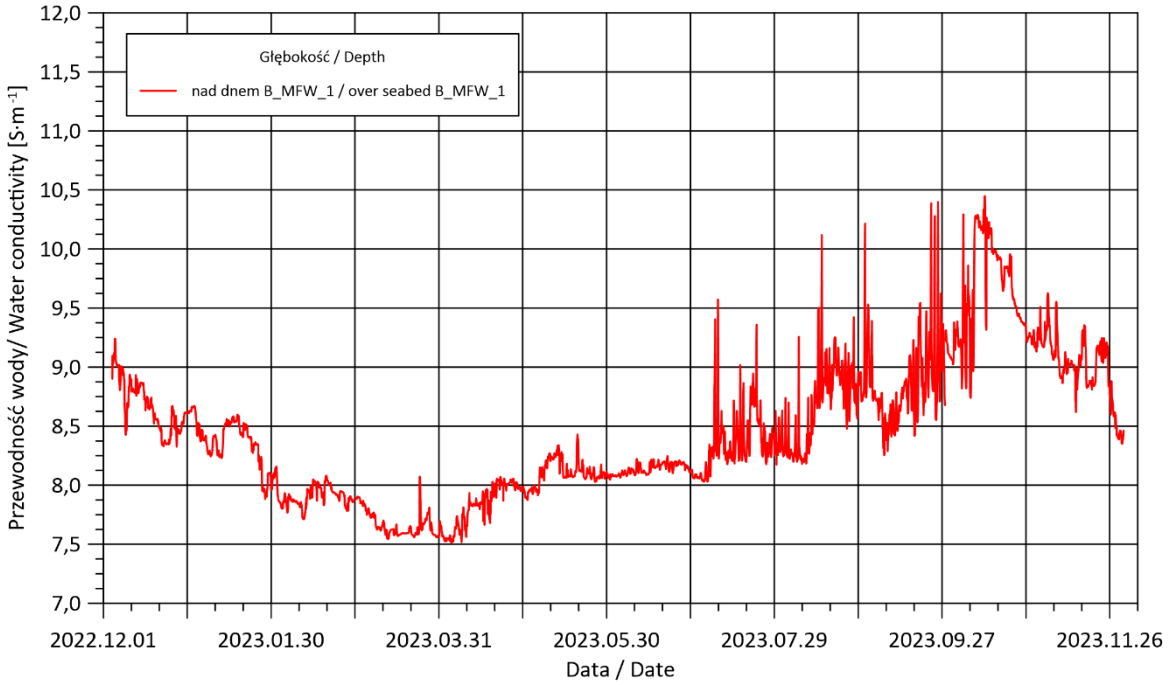


Figure 2.50. The electrical conductivity of water measured at survey station B_MFW_1 throughout the entire measurement period

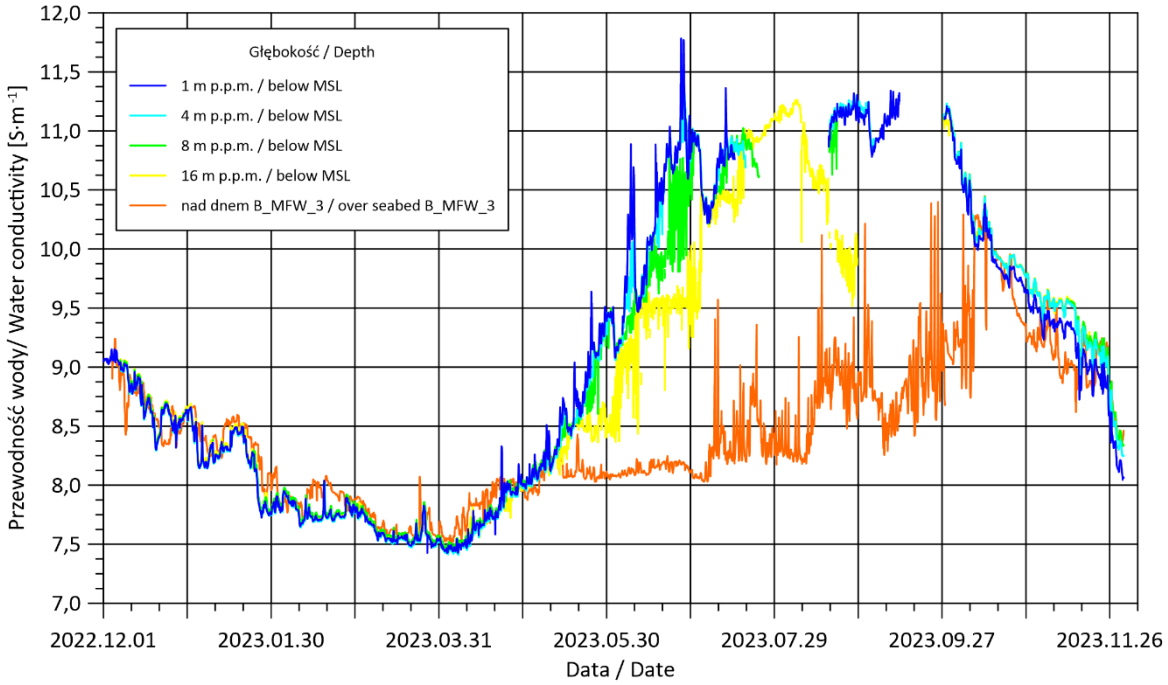


Figure 2.51. The electrical conductivity of water measured at survey station B_MFW_3 throughout the entire measurement period

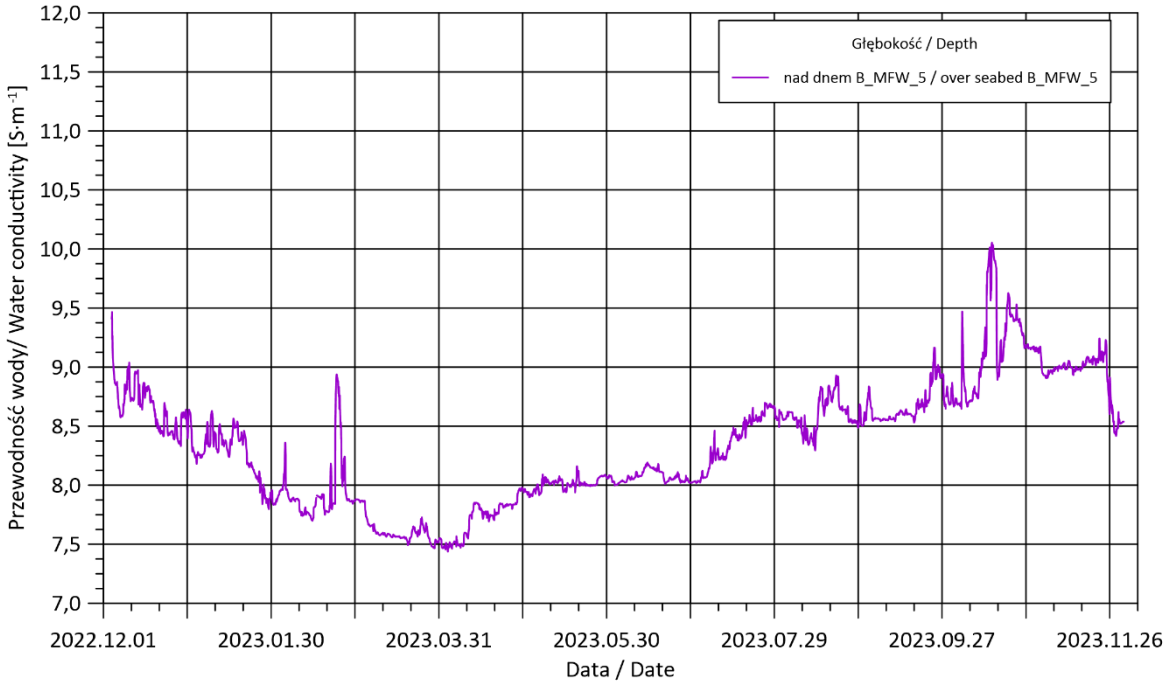


Figure 2.52. The electrical conductivity of water measured at survey station B_MFW_5 throughout the entire measurement period

2.1.5.3.1.3 Water salinity

Water salinity was measured with the use of CTD probes deployed at survey stations distributed within the survey area: B_MFW_1, B_MFW_3 and B_MFW_5. At survey station B_MFW_3, the measurement was taken at five depths across the sea depth: 1 m, 4 m, 8 m, 16 m, and above the seabed. Whereas at survey stations B_MFW_1 and B_MFW_5, the measurement was taken at one depth – above the seabed. A statistical analysis of water salinity is presented in Table 2.13.

Table 2.13. A statistical analysis of the water salinity calculated for the survey stations B_MFW_1, B_MFW_3 and B_MFW_5 located within the survey area for the entire measurement period

Measurement point	Depth [m]	Salinity [PSU]			
		Medium	Minimum	Maximum	Standard deviation
B_MFW_1	Over the seabed	7.50	7.24	8.07	0.14
B_MFW_3	1	7.38	7.11	7.70	0.12
	4	7.39	7.16	7.69	0.14
	8	7.40	7.20	7.75	0.12
	16	7.41	7.11	7.74	0.13
	Over the seabed	7.50	7.24	8.07	0.14
B_MFW_5	Over the seabed	7.56	7.20	8.34	0.21

The following plots present the salinity fluctuations recorded over time [Figure 2.53–Figure 2.55].

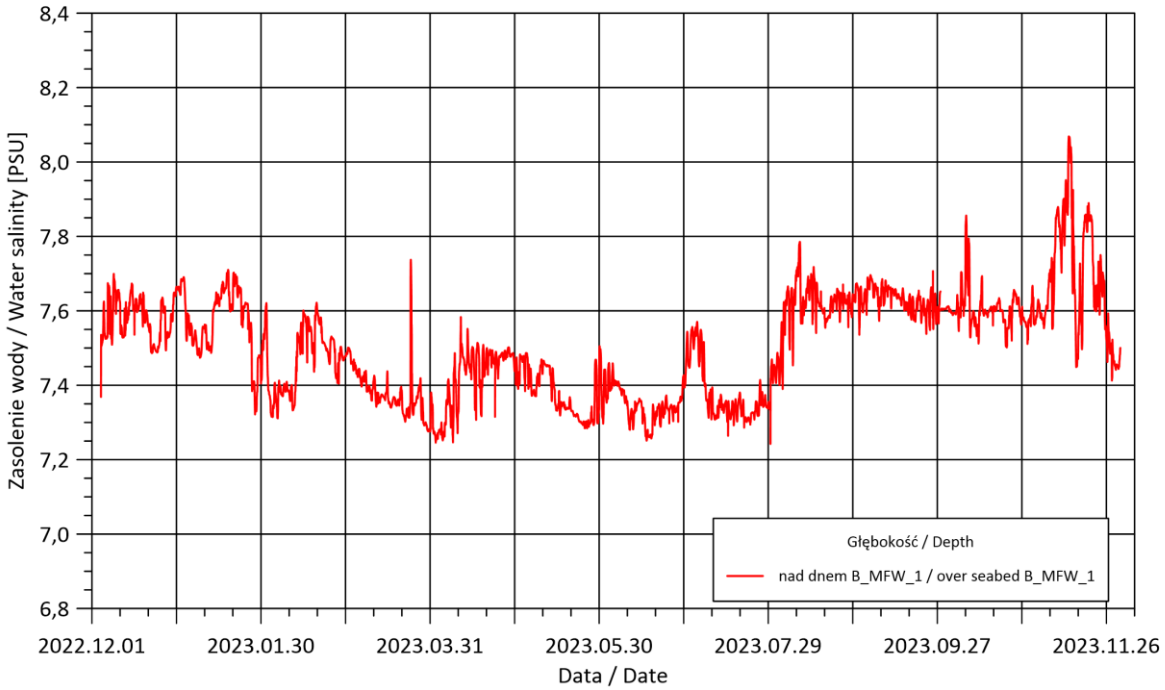


Figure 2.53. The water salinity calculated for survey station B_MFW_1 for the entire measurement period

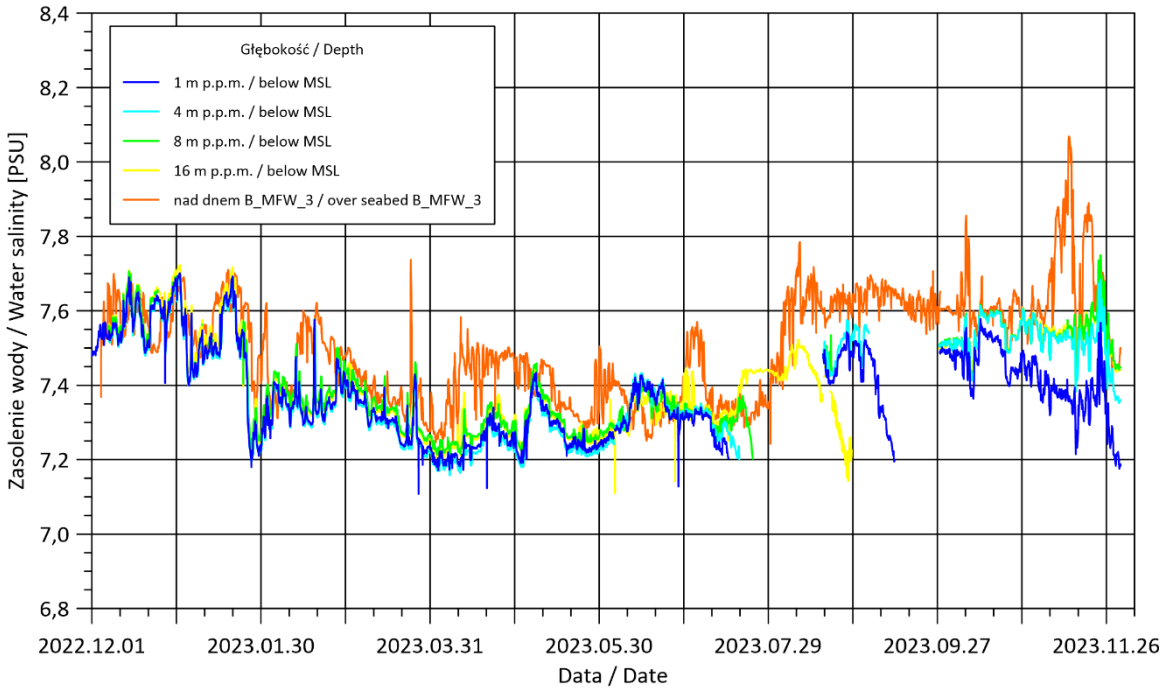


Figure 2.54. The water salinity calculated for survey station B_MFW_3 for the entire measurement period

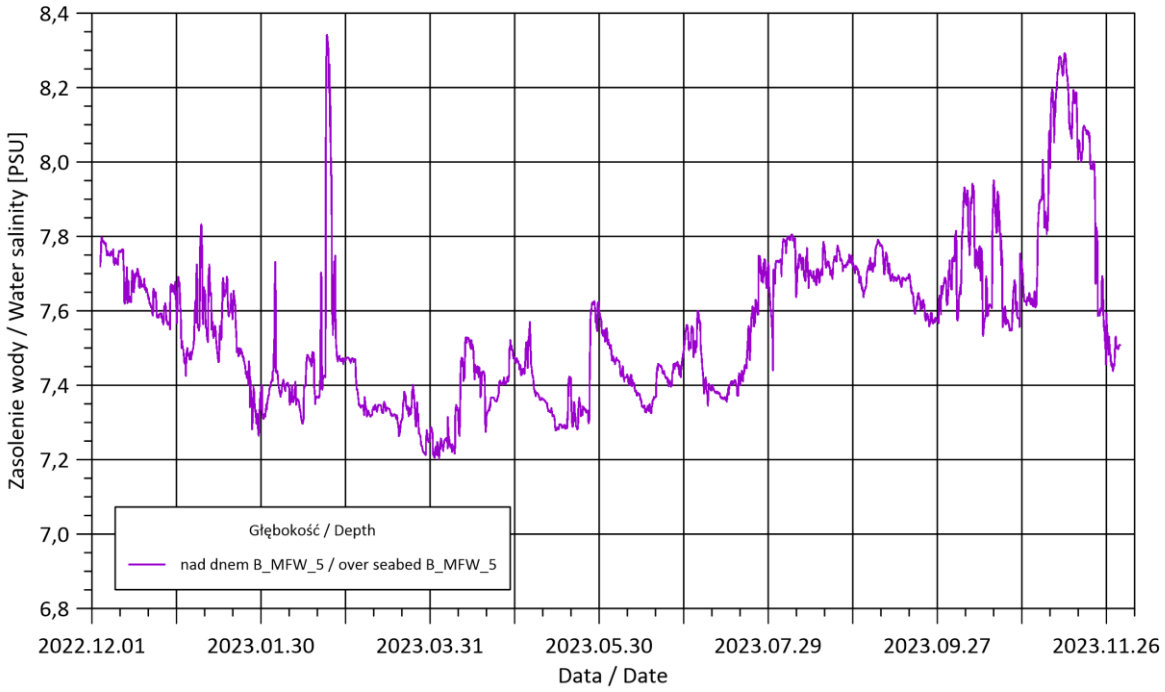


Figure 2.55. The water salinity calculated for survey station B_MFW_5 for the entire measurement period

2.1.5.3.1.4 Water turbidity

Water turbidity was measured at survey stations B_MFW_1, B_MFW_3, and B_MFW_5 with the use of CTD probes installed over the seabed. The statistical analysis of the turbidity measured has been presented in Table 2.14.

Table 2.14. A statistical analysis of the water turbidity measured at survey stations B_MFW_1, B_MFW_3, and B_MFW_5 located within the survey area for the entire measurement period

Measurement point	Depth [m]	Water turbidity [FTU]			
		Median	Minimum	Maximum	Standard deviation
B_MFW_1	Over the seabed	2.86	0.65	85.73	3.97
B_MFW_3	Over the seabed	1.94	0.41	139.89	6.37
B_MFW_5	Over the seabed	2.59	0.43	105.65	4.61

The results of water turbidity measurements have been presented in the following plots [Figure 2.56–Figure 2.58].

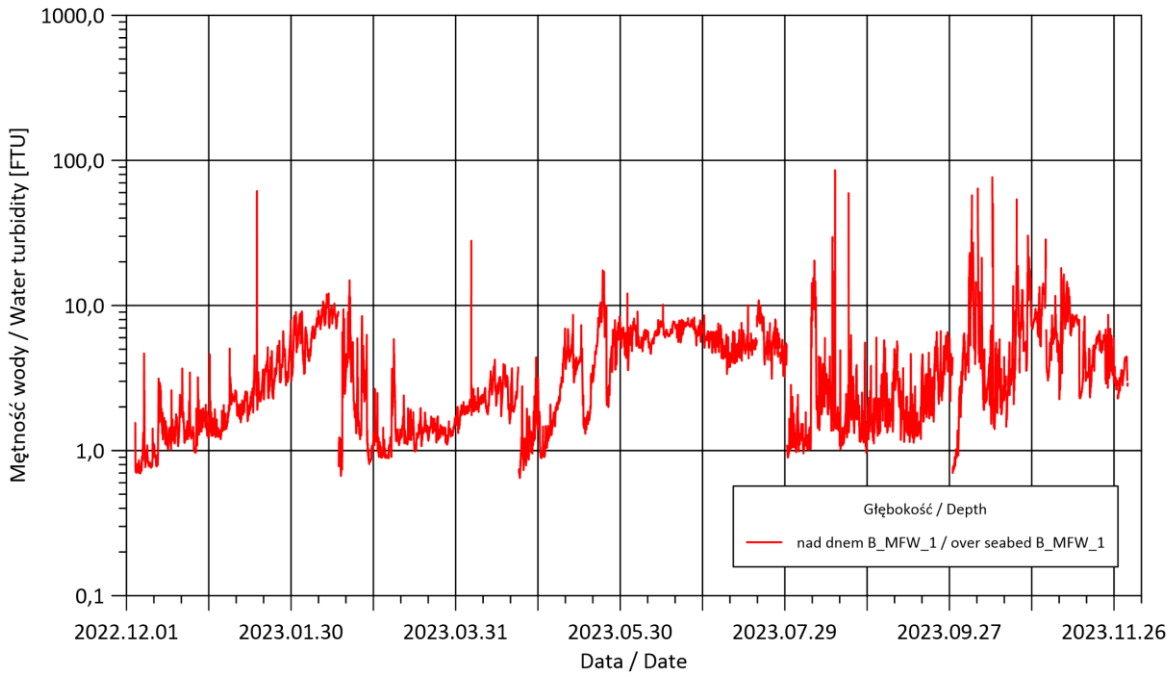


Figure 2.56. The water turbidity measured at survey point B_MFW_1 for the entire measurement period

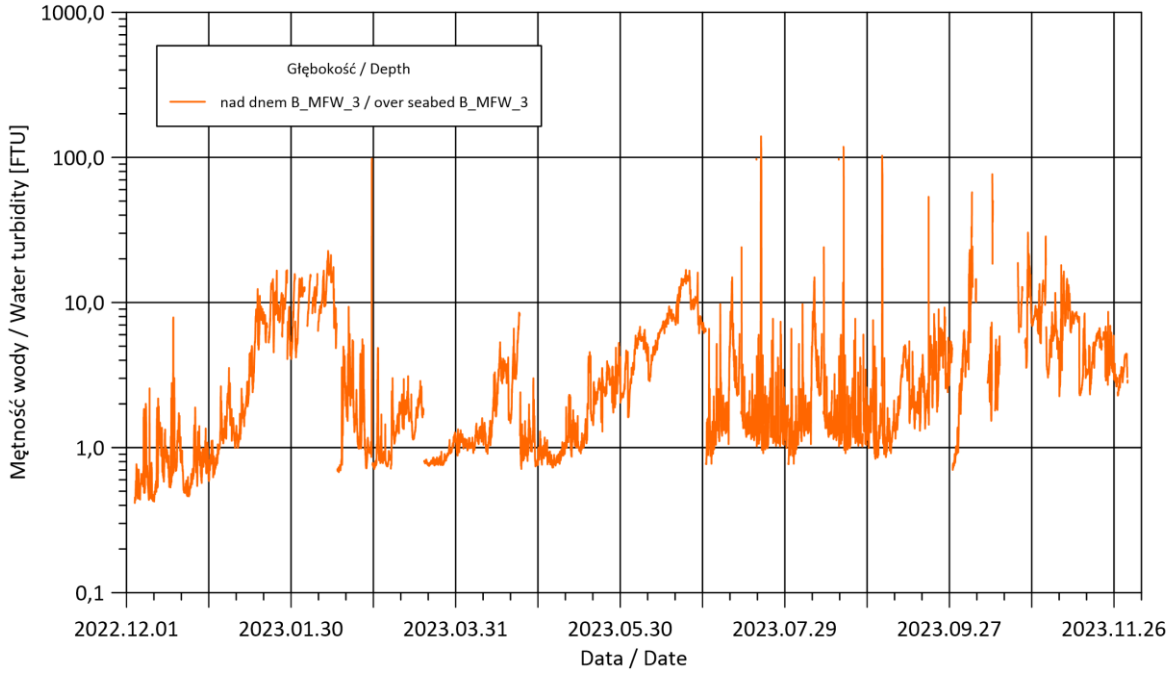


Figure 2.57. The water turbidity measured at survey point B_MFW_3 for the entire measurement period

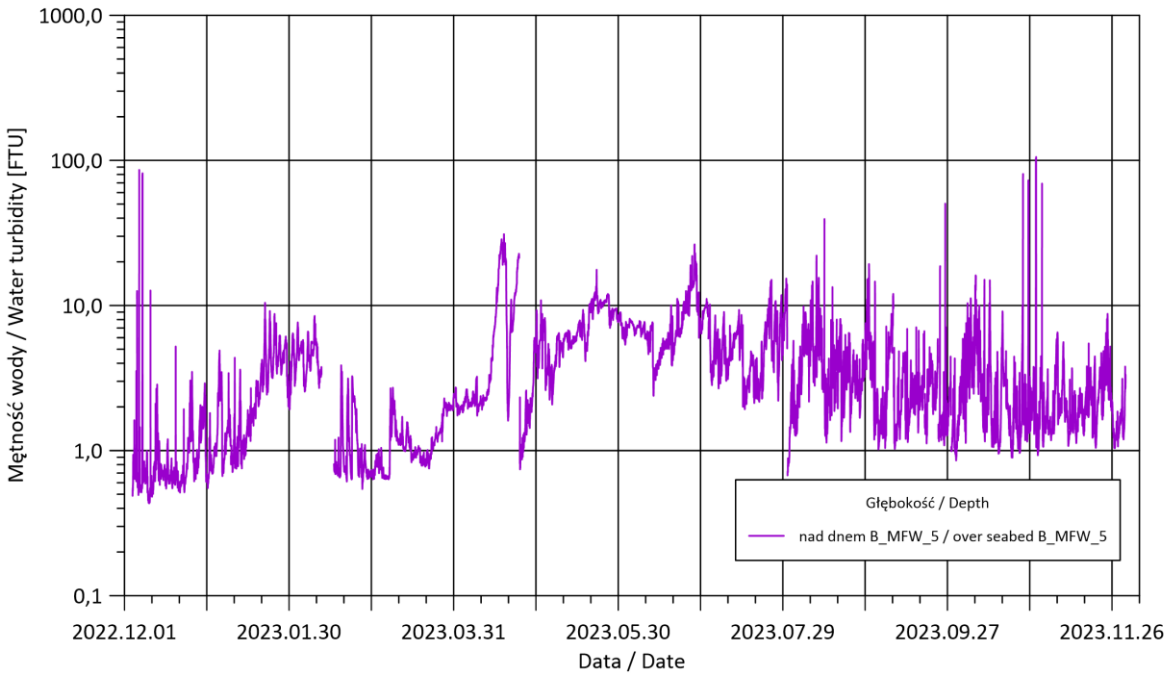


Figure 2.58. The water turbidity measured at survey point B_MFW_5 for the entire measurement period

2.1.5.3.2 CTD measurements performed during the water and sediment sampling

2.1.5.3.2.1 Water temperature

The statistical analysis of temperature measured during the water and sediment sampling has been presented in Table 2.15.

Table 2.15. A statistical analysis of water temperature measured during the water and sediment sampling throughout the entire measurement period

Survey campaign	Water temperature [°C]			
	Mean	Minimum	Maximum	Standard deviation
The first water sampling campaign	5.81	4.93	6.00	0.08
The second water sampling campaign	3.37	2.59	4.41	0.06
The third water sampling campaign	5.47	4.01	6.95	0.60
The fourth water sampling campaign	13.63	5.28	18.47	4.12
The fifth water sampling campaign	15.51	4.55	17.69	3.36
The sixth water sampling campaign	6.49	2.53	7.09	0.20
The first seabed sediment sampling campaign	4.16	2.43	9.66	0.59
The second seabed sediment sampling campaign	14.03	4.03	19.68	5.11

Figure 2.59 presents seasonal changes in the water temperature in the waters of the survey area under individual survey campaigns conducted from January to November 2023.

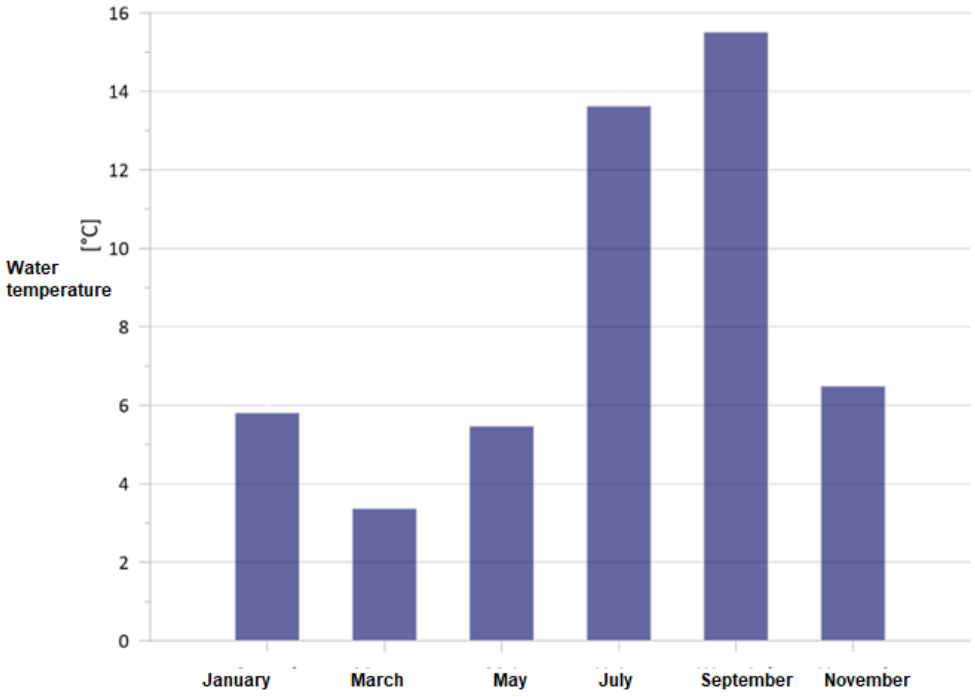


Figure 2.59. The mean water temperature values measured in the survey area during individual water sampling campaigns conducted from January to November 2023

2.1.5.3.2.2 Electrical conductivity of water

The statistical analysis of the electrical conductivity of water measured during the water and seabed sediment sampling has been presented in Table 2.16.

Table 2.16. A statistical analysis of the electrical conductivity of water measured during the water and seabed sediment sampling throughout the entire measurement period

Survey campaign	Electrical conductivity [S·m^{-1}]			
	Mean	Minimum	Maximum	Standard deviation
The first water sampling campaign	8.47	8.28	8.62	0.06
The second water sampling campaign	7.62	6.59	7.72	0.03
The third water sampling campaign	8.03	7.37	8.33	0.08
The fourth water sampling campaign	9.94	8.18	11.04	0.91
The fifth water sampling campaign	10.68	7.36	11.17	0.76
The sixth water sampling campaign	8.41	7.96	8.61	0.05
The first seabed sediment sampling campaign	8.15	6.97	16.32	0.79
The second seabed sediment sampling campaign	10.37	7.95	14.70	1.21

The figure below [Figure 2.60] presents seasonal changes in the electrical conductivity of the waters of the survey area during individual survey campaigns conducted from January to November 2023.

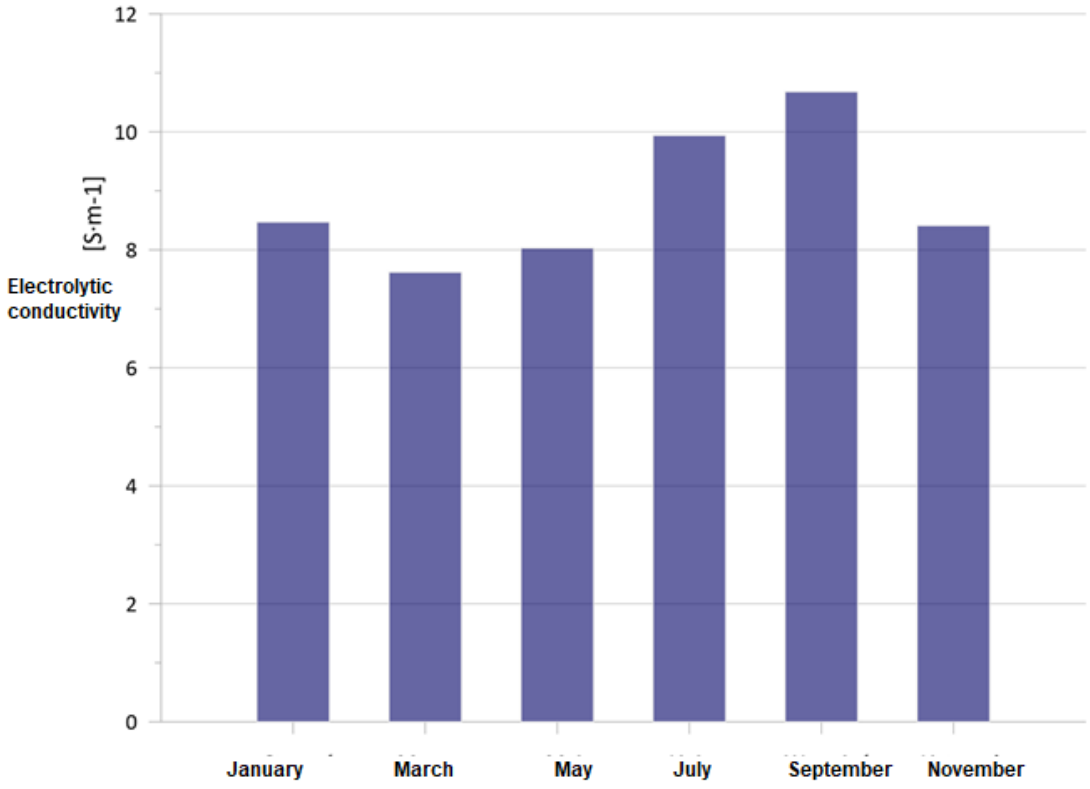


Figure 2.60. The mean values of electrical conductivity of water measured in the survey area during individual water sampling campaigns from January to November 2023

2.1.5.3.2.3 Water salinity

A statistical analysis of water salinity for the measurements conducted during individual water and seabed sediment sampling campaigns is presented in Table 2.17.

Table 2.17. A statistical analysis of water salinity calculated during the water and seabed sediment sampling throughout the entire measurement period

Survey campaign	Salinity [PSU]			
	Medium	Minimum	Maximum	Standard deviation
The first water sampling campaign	7.65	7.52	7.87	0.04
The second water sampling campaign	7.36	6.27	7.57	0.03
The third water sampling campaign	7.30	6.54	7.81	0.09
The fourth water sampling campaign	7.31	6.60	7.50	0.07
The fifth water sampling campaign	7.53	4.88	7.94	0.08
The sixth water sampling campaign	7.44	6.99	8.37	0.03
The first seabed sediment sampling campaign	7.70	6.57	13.92	0.61
The second seabed sediment sampling campaign	7.59	5.92	13.24	0.51

The seasonal variations of the water salinity in the survey area as measured waters during individual survey campaigns from January to November 2023 are presented in Figure 2.61.

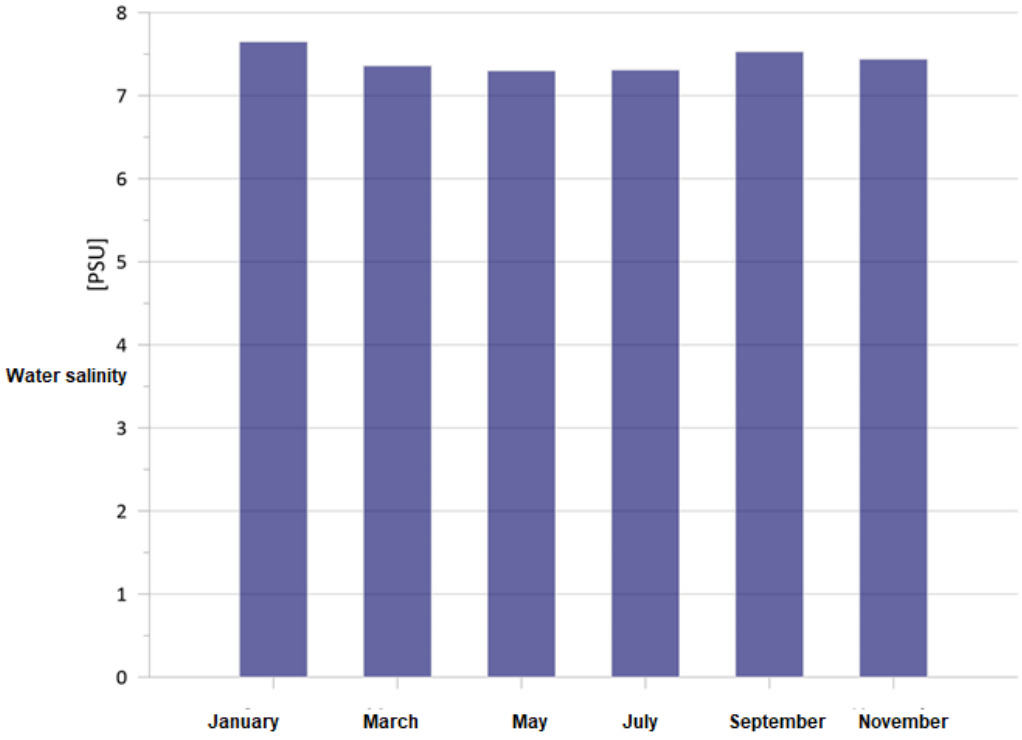


Figure 2.61. The mean values of water salinity calculated for the survey area during individual water sampling campaigns from January to November 2023

2.1.5.3.2.4 Water turbidity

A statistical analysis of water turbidity for measurements taken during the water and seabed sediment sampling is presented in Table 2.18.

Table 2.18. A statistical analysis of water turbidity measured during the water and seabed sediment sampling within the entire measurement period

Survey campaign	Water turbidity [FTU]			
	Mean	Minimum	Maximum	Standard deviation
The first water sampling campaign	0.74	0.35	9.63	0.36
The second water sampling campaign	1.01	0.25	8.06	0.35
The third water sampling campaign	0.85	0.19	11.75	0.26
The fourth water sampling campaign	1.21	0.81	11.00	0.44
The fifth water sampling campaign	0.77	0.34	359.49	4.01
The sixth water sampling campaign	1.32	1.13	150.44	1.63
The first seabed sediment sampling campaign	0.86	0.31	30.69	0.48
The second seabed sediment sampling campaign	0.67	0.01	22.54	0.38

The seasonal variations of water turbidity in the survey area during individual water sampling campaigns conducted from January to November 2023 are presented in Figure 2.62.

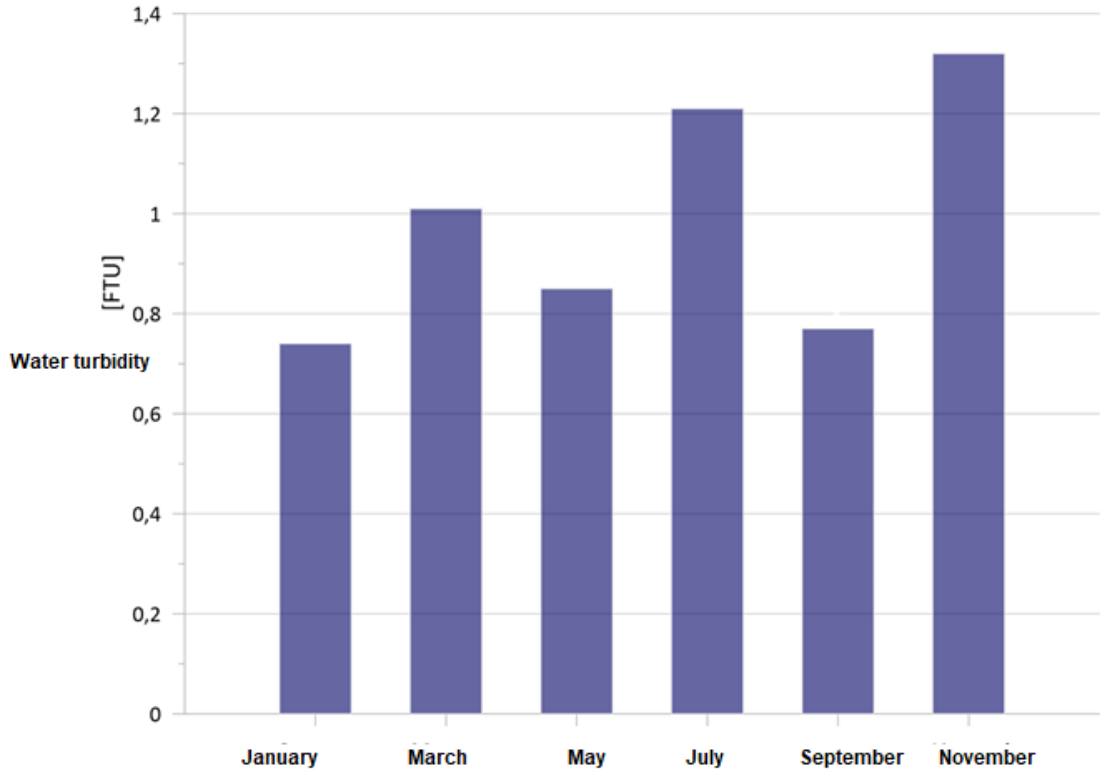


Figure 2.62. The mean values of water turbidity measured in the survey area during individual water sampling campaigns in the period from January to November 2023

2.1.5.3.2.5 Depth

A statistical analysis of water depth for measurements taken during the water and seabed sediment sampling is presented in Table 2.19.

Table 2.19. A statistical analysis of water depth measured during the water and seabed sediment sampling within the entire measurement period

Survey campaign	Depth [m]			Standard deviation
	Mean	Minimum	Maximum	
The first water sampling campaign	18.17	0.51	48.92	11.29
The second water sampling campaign	18.20	0.52	48.72	11.16
The third water sampling campaign	17.29	0.51	48.64	10.90
The fourth water sampling campaign	18.19	0.51	48.66	10.89
The fifth water sampling campaign	18.12	0.51	48.75	11.01
The sixth water sampling campaign	18.19	0.53	48.84	10.19
The first seabed sediment sampling campaign	24.91	0.51	83.64	17.91
The second seabed sediment sampling campaign	22.47	0.51	83.79	15.29

Figure 2.63 presents the changes in the water depth within the survey area recorded during individual water sampling survey campaigns conducted from January to November 2023.

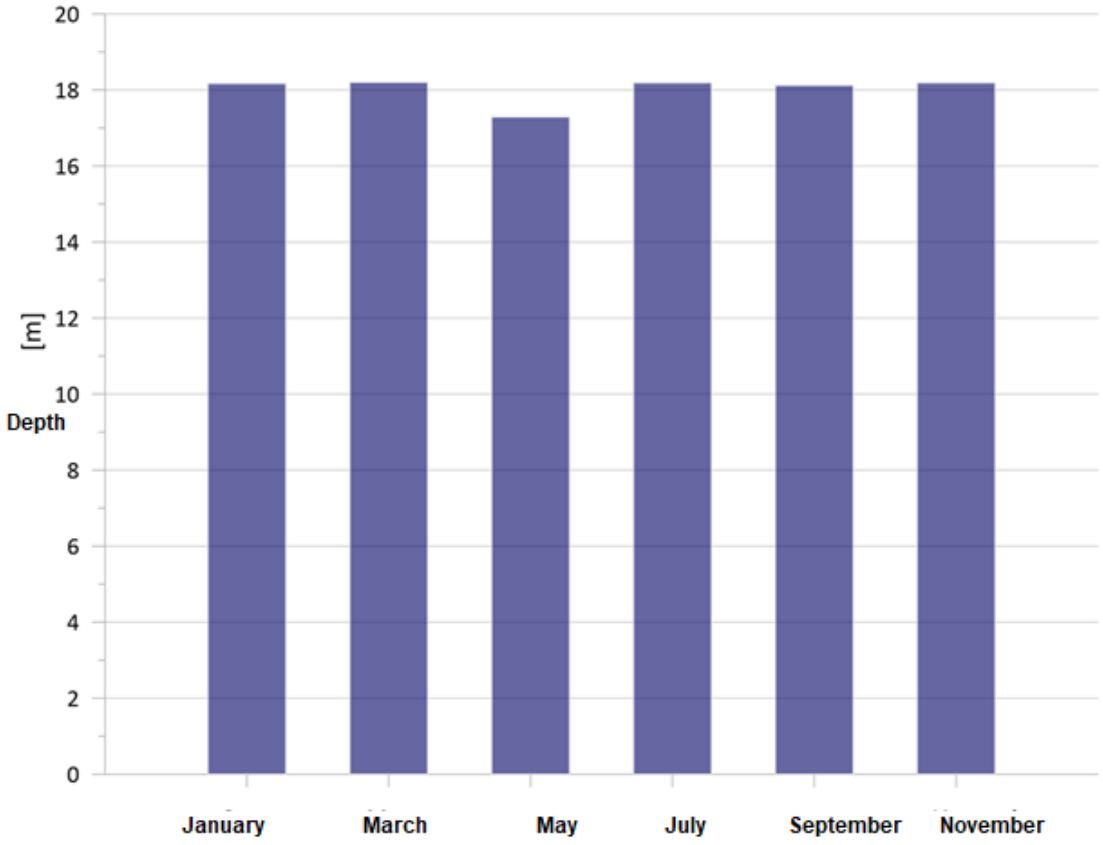


Figure 2.63. The mean values of water depth measured in the survey area during individual water sampling campaigns in the period from January to November 2023

2.1.5.4 Ice conditions

No direct registrations allowing assessment of ice conditions are conducted in the surveyed sea area. Information on the occurrence of specific forms of ice (drifting or in the form or a solid ice cover) has been obtained from a service devoted to ice conditions of the Baltic Sea, which is issued every week throughout the entire winter season by the IMWM-NRI (https://baltyk.imgw.pl//index.php?page=22&subpage=87) and the Swedish SMHI (https://www.smhi.se/oceanografi/istjanst/havsis_en.php).

During the annual reporting period from December 2022 to November 2023, no ice phenomena occurred in the surveyed sea area.

2.1.6 Summary of results and conclusions

2.1.6.1 Meteorological measurements

The recorded course of changes in meteorological parameters of the atmosphere in the near-water layer of the atmosphere at a large distance from the coast shows the variability of weather phenomena characteristic of the open sea areas of the Southern Baltic Sea. The presented wind data include the full range of wind conditions variability: from strong storms (with wind speeds exceeding 20 $m \cdot s^{-1}$ and gusts of 28 $m \cdot s^{-1}$ – such situations occurred, among others, on 18.02.2023 – which caused damage to the meteorological station on the buoy, and on 22.11.2023), to periods of calm (e.g. on 08.09.2023),

with an average wind speed of 7.28 $m \cdot s^{-1}$. Winds from the south-western sector clearly dominated (from SSW to WSW), although the share of directions from the north-eastern and eastern sectors (from NNE to ESE) is also noticeable. Significant changes in atmospheric pressure could be observed(approx. 980.0–1041.5 hPa; with an average for the period of 1012.87 hPa). Air temperature shows seasonal variability throughout the year, from -2.9°C (28.11.2023) to 23.3°C (08.09.2023), with an average for the period of 10.16°C. Air humidity varied from approx. 42 to 100%, with an average of 86%.

2.1.6.2 Hydrological measurements

2.1.6.2.1 Wave motion

The wave motion was characterised by variable intensity depending on the season. The highest waves were recorded in winter, while the spring and summer were the calmest. The maximum recorded wave was 9.51 m in height. Depending on the survey station, the mean wave motion height ranged from 0.64 m to 0.71 m. Wave motion from the west and south-west was dominant.

The characteristics of the wind-generated wave motion on the free sea surface at the two survey stations located within the survey area are similar.

2.1.6.2.2 Water depth (thickness of the sea deep)

The course of changes in the thickness of the water column for all locations in which recording was conducted is consistent with the annual hydrological cycle of sea level changes typical for the areas of the southern Baltic Sea. Long-term changes in water level are related primarily to changes in atmospheric circulation over the entire Baltic Sea area taking place during the year. Short-term fluctuations in water level are associated with the passage of active and deep cyclonic systems over the sea area, which appears particularly often in the autumn-winter season, and they are associated with a significant increase in wind speed and the occurrence of storm conditions at sea.

2.1.6.2.3 Water flows

The recorded values and directions of water flow in the surveyed sea area are conditioned by the current wind conditions on the one hand, the morphometric characteristics of the seabed, the depth of the sea at the registration point and its distance from the coast on the other. This is visible particularly well in the disparity in the dynamics of the two boundary layers (atmosphere–water and water–seabed) in relation to the dynamics of the intermediate layers of the water depth. The near-surface water layers, which are strongly influenced by wind and wind-generated wave motion, show greater differentiation in water flow directions (the influence of wind-generated wave motion is particularly visible here), while in the intermediate water layers, a clear flow dominance is established in specific directional sectors. In places with greater sea depths (over 40 m), an increase in the average water flow velocity is visible in deeper layers of the water column compared to layers closer to the surface. Certain differences are noticeable between the nature of water flows in relatively shallow, coastal areas of the sea (usually a two-way longitudinal flow occurs here), in shallow-water areas of the Middle Bank (where flows remain basically similar throughout the water column), and in places of the sea located in the area of the Słupsk Furrow, which is characterised by significant depths (the occurrence of a pycnocline is clearly visible here). A characteristic pattern of dominant flows in the southern and south-western sectors is visible in the area of the planned wind farm. The mean values of water flow velocities are similar for all surveyed locations, although they are slightly higher in the deep-water areas compared to the shallow-water areas – they generally remain within the range of

0.06 $m \cdot s^{-1}$ by the seabed to 0.12 $m \cdot s^{-1}$ near the surface. During strong storms, maximum water flow velocities can reach approx. 0.6 $m \cdot s^{-1}$.

2.1.6.3 Hydrophysical measurements

2.1.6.3.1 Continuous recordings

2.1.6.3.1.1 Water temperature

In the entire measurement period, the minimum value of water temperature was 2.97°C, while the maximum was 21.16°C.

The analysis of the course of changes in water temperature at all stations during the entire reporting period indicated a clear seasonality of this parameter resulting from the varying intensity of solar radiation. In winter, the water temperature dropped to the level of 2.97°C. This was due to reduced solar radiation and more intense storm conditions, which translated into cooling of the surface layer and deeper parts of the sea. In the spring and summer period, the water temperature in the near-surface layer increased rapidly, but only to a depth of several meters. Below, there was a thermocline. In the summer, the near-seabed conditions differed from the conditions by the surface. In the summer period, due to the increased intensity of solar radiation, water temperature reached values exceeding 21°C. The water temperature in the near-seabed layer was stable, unmodified by average dynamic phenomena in the water column and atmosphere.

2.1.6.3.1.2 Electrical conductivity of water

The values of electrical conductivity in the water at the survey stations ranged from 7.41 $S \cdot m^{-1}$ to 11.78 $S \cdot m^{-1}$.

The analysis of the electrical conductivity of water in the entire measurement period showed a seasonality of this parameter, which is linked to changes in the water temperature. Also, the values of this parameter were similar across the entire vertical profile. In summer, significant fluctuations of this parameter were observed.

2.1.6.3.1.3 Water salinity

The values of water salinity at the survey stations ranged from 7.11 to 8.34 PSU. The maximum, mean, and minimum values were similar across the entire vertical profile. An analysis of water salinity indicated low variability of this parameter within the entire measurement period. The maximum, mean, and minimum values were similar across the entire vertical profile. Water salinity was stable at all depths.

2.1.6.3.1.4 Water turbidity

The maximum measured value of turbidity was 139.89 FTU. The lowest value recorded in the measurement period discussed was 0.41 FTU. When analysing the water turbidity measurement at survey stations B_MFW_1, B_MFW_3, and B_MFW_5, clear fluctuations in the value of this parameter can be observed. In the survey area, the value of water turbidity in the near-seabed layer recorded was higher in the autumn period, which was due to conditions of an intensive mixing of the waters.

2.1.6.3.2 CTD measurements performed during the water and sediment sampling

2.1.6.3.2.1 Water temperature

Water temperature during water and sediment sampling depended on the season. The lowest temperature was recorded during the first campaign of seabed sediment sampling and was 2.43°C, while the highest temperature of 19.68°C was measured during the second campaign of seabed sediment sampling. Mean temperature values for all sampling sessions ranged from 3.37°C to 15.51°C.

2.1.6.3.2.2 Electrical conductivity of water

The measured electrical conductivity of water during the water and sediment sampling was quite uniform for all campaigns. The lowest conductivity was recorded during the second water sampling campaign and it was 6.59 $S \cdot m^{-1}$, while the highest conductivity of 15.32 $S \cdot m^{-1}$ was measured during the first seabed sediment sampling campaign. The mean values of electrical conductivity of water collected during all sampling sessions ranged from 7.62 $S \cdot m^{-1}$ to 10.68 $S \cdot m^{-1}$.

2.1.6.3.2.3 Water salinity

The measured average salinity of water during the water and sediment sampling was quite uniform for all campaigns. The lowest salinity level was recorded during the fifth water sampling campaign and it was 4.88 PSU, while the highest conductivity of 13.92 PSU was measured during the first seabed sediment sampling campaign. The mean water salinity values for all sampling sessions fell within the range of 7.30–7.70 PSU.

2.1.6.3.2.4 Water turbidity

The water turbidity levels measured during the collection of water and sediment samples were much varied. The lowest value of turbidity was recorded during the second sediment sampling campaign, and it was 0.01 FTU, while the highest turbidity of 359.49 FTU was measured during the fifth water sampling campaign. The mean values of water turbidity measured during all sampling sessions varied in the range of 0.67–1.32 FTU.

2.1.6.3.3 Water depth

The water depths for each of the stations at which hydrophysical parameters were recorded were similar throughout the measurement period. However, the water depth for individual stations at sea varied from approximately 13.7 m to approximately 51.8 m.

2.1.6.4 Ice conditions

No ice phenomena occurred in the surveyed sea areas throughout the survey period. Solid or drifting forms of ice can only appear during severe and very severe winters. However, the climate changes observed in recent decades also apply to the Baltic area, hence the possibility of such winters occurring is small.

2.1.7 Shortcomings and gaps in the state-of-the-art

The meteorological, wave motion, current, and hydrophysical parameters of the near-water layer of the atmosphere, as well as the waters covered by the surveys presented in this Report have still not been sufficiently examined in all parts of the Polish sea areas. So far, mainly expedition, monitoring, or short-term measurements have been conducted in selected locations near the coast and in the open waters. These surveys were related to scientific research, monitoring, and work performed for various

purposes of the maritime economy branch. As a result, annual reports on monitoring studies of the Baltic Sea performed by the IMWM-NRI are available. In addition, there are studies available in environmental impact reports developed for some areas related to planned offshore wind farms (e.g. Bałtyk II OWF, Bałtyk III OWF, Baltic Power OWF, FEW Baltic II OWF, and Baltica OWF). This information is fragmented and incomplete and it refers to different physical parameters and different periods of time, and the majority of commercial measurement data have never been published. Therefore, the expert knowledge gained so far on the subject of the Polish sea areas of the Baltic Sea does not ensure a clear picture of the phenomena occurring there and the in-depth characteristics of the discussed hydrological and meteorological parameters remain poorly determined. Moreover, in the area analysed, no such extensive and long-term surveys have ever been conducted, and no scientific or commercial reports have been developed, which is why it is impossible to compare the parameters measured and refer them to the results of any previous surveys. It would also be necessary to conduct appropriate climate studies and analyses for the sea areas related to the planned OWFs taking into account also the rapidly progressing climate changes in recent years.

2.2 SURVEYS OF PHYSICOCHEMICAL PROPERTIES OF WATER

2.2.1 Non-specialist summary

The surveys covered the sea basin designated for implementing the project consisting of the construction of the Baltica-1 OWF. The Baltica-1 OWF Area is located on the border of the Polish exclusive economic zone, at the level of the Łeba commune in the Pomeranian Voivodeship. The Baltica-1 OWF survey area is located on the southern slopes of the Middle Bank, approximately 80 km from the port in Łeba, in waters of 13.7–51.8 m in depth.

The purpose of the Report is to present the results of physical, chemical and physicochemical surveys of the marine environment conducted in 2023 within the survey area. The surveys were conducted from January to November 2023. Water samples for analyses were collected using bathometers (special instruments for sampling water at different depths) in a uniform measurement grid (1 station per 5 km^2). This evenly spaced grid of water sampling stations enables obtaining representative results for the area surveyed.

To obtain the overall characteristics of the seawater hydrochemical indicators, measurements and analyses of the following indicators were carried out: oxygen conditions [dissolved oxygen, five-day oxygen demand (BOD_5)], total organic carbon (TOC), acidification (pH) and alkalinity, nutrients [ammoniacal nitrogen, nitrate nitrogen, total nitrogen, mineral nitrogen (DIN), phosphates, total phosphorus] and suspended solids. Also, the analyses of the content of substances particularly harmful to the environment, such as mercury, nickel, lead, cadmium, arsenic, total chromium, chromium (VI), aluminium, phenols, cyanides, mineral oils, polycyclic aromatic hydrocarbons (16 PAHs), polychlorinated biphenyls (7 PCB congeners: 28, 52, 101, 118, 138, 153, 180), as well as the measurements of the radioactivity of caesium (^{137}Cs) and strontium (^{90}Sr) isotopes were carried out. The measurement and testing methods specified as the preferred ones in the implementing regulations and used in the monitoring carried out as part of the State Environmental Monitoring were applied.

The survey methods applied were characterised by sufficient precision and sensitivity in relation to the determinations of indicators included in the scope of work. The analytical techniques used are well described in the available literature, standardised and accredited, and the test results were subject to proper quality control measures.

The water parameters tested in the survey area generally reached the concentrations typical for the waters of the southern Baltic Sea. These waters were characterised by alkaline pH (approx. 8.0 pH), alkalinity of approx. 1.7 mmol·dm^{-3}, and relatively good oxygenation, with a seasonal variability characteristic of the southern Baltic Sea waters. The assessment of the quality of water in the survey area based on the oxygen content in the near-seabed layer in the summer period (July) indicates good condition (no oxygen deficit).

Within the entire survey period (January–November 2023), the average biochemical oxygen demand (BOD_5) in the water samples collected from the survey area in individual measurement periods was generally < 2.0 mg·dm^{-3}. Also, the suspended solids in individual measurement periods were at the level typical for the waters of the southern region of the Baltic Sea.

The concentration of nutrients [total nitrogen, mineral nitrogen (nitrates, nitrites, and ammonia), phosphates, and total phosphorus] in the water samples collected from the survey area indicated seasonal variability typical for the waters of the southern Baltic Sea. The lowest concentrations of the substances tested were found in May, July, and September. However, in the winter months (November–March), an increase in concentrations was observed in accordance with the seasonal trend of nutrient level restoration.

The waters of the region surveyed were characterised by low concentrations of particularly harmful substances. Polychlorinated biphenyls, free and bound cyanides, metals [Pb, Cd, Cr, Cr (VI), As, Ni, Hg], phenols, and the mineral oil index were present at trace levels. The waters tested were also characterised by low Al concentrations and low isotope activity values of ^{137}Cs and ^{90}Sr, typical of the southern Baltic Sea waters, which confirms the very slow trend of ^{90}Sr and ^{137}Cs concentration decrease in the Baltic Sea area.

PAH concentrations slightly higher than the ones specified by the data from literature were observed in survey area, which may be due to the differences at the stage of preparation of samples for the analysis (PAHs were determined in water without separation of suspended solids).

Comparing the results obtained from the water analyses with the limit values set out in the currently applicable implementing regulations regarding the classification of surface water quality, as well as the environmental quality standards for priority substances, the survey area can be included in water quality class 1 (very good status) due to the content of inorganic nitrogen compounds (in winter), total nitrogen, total phosphorus, and TOC (in summer), free and bound cyanides, phenol index of mineral oil and metals [arsenic (As), total chromium (TCr), chromium (VI) (Cr(VI)), copper (Cu) and aluminium (Al)]. No exceedance of the limit values of the water quality indicators for the average concentrations of polycyclic aromatic hydrocarbons, nor for cadmium (Cd), lead (Pb), mercury (Hg), and nickel (Ni) was found in the waters of the survey area.

In terms of dissolved oxygen concentration near the seabed in summer, the survey area can be classified as water quality class 1 (very good status).

However, due to the phosphate phosphorus content (the average concentration of which in the water column was 0.016 mg·dm^{-3}), the waters tested did not present good quality.

The comparison was also made between the values of the concentration obtained for all indicators tested and the available data published in literature concerning the area of the Baltic Sea covered by the surveys. Essentially, the results obtained do not differ from the data presented in the literature, data from the State Environmental Monitoring program, and data published by HELCOM. As a result of

this comparison, it was found that the data obtained were typical for the Baltic Sea areas discussed (the south-eastern part of the Gotland Basin).

2.2.2 Spatial scope of the surveys

The spatial scope of measurements of physicochemical properties of water was limited to the survey area covering the Baltica-1 OWF construction area, which is the area of construction of WTGs, OSSs, and cable lines (area A) and the area of construction of cable lines (area B) together with a zone of no less than 1 NM in width measured from the boundary of area A [Figure 2.64].

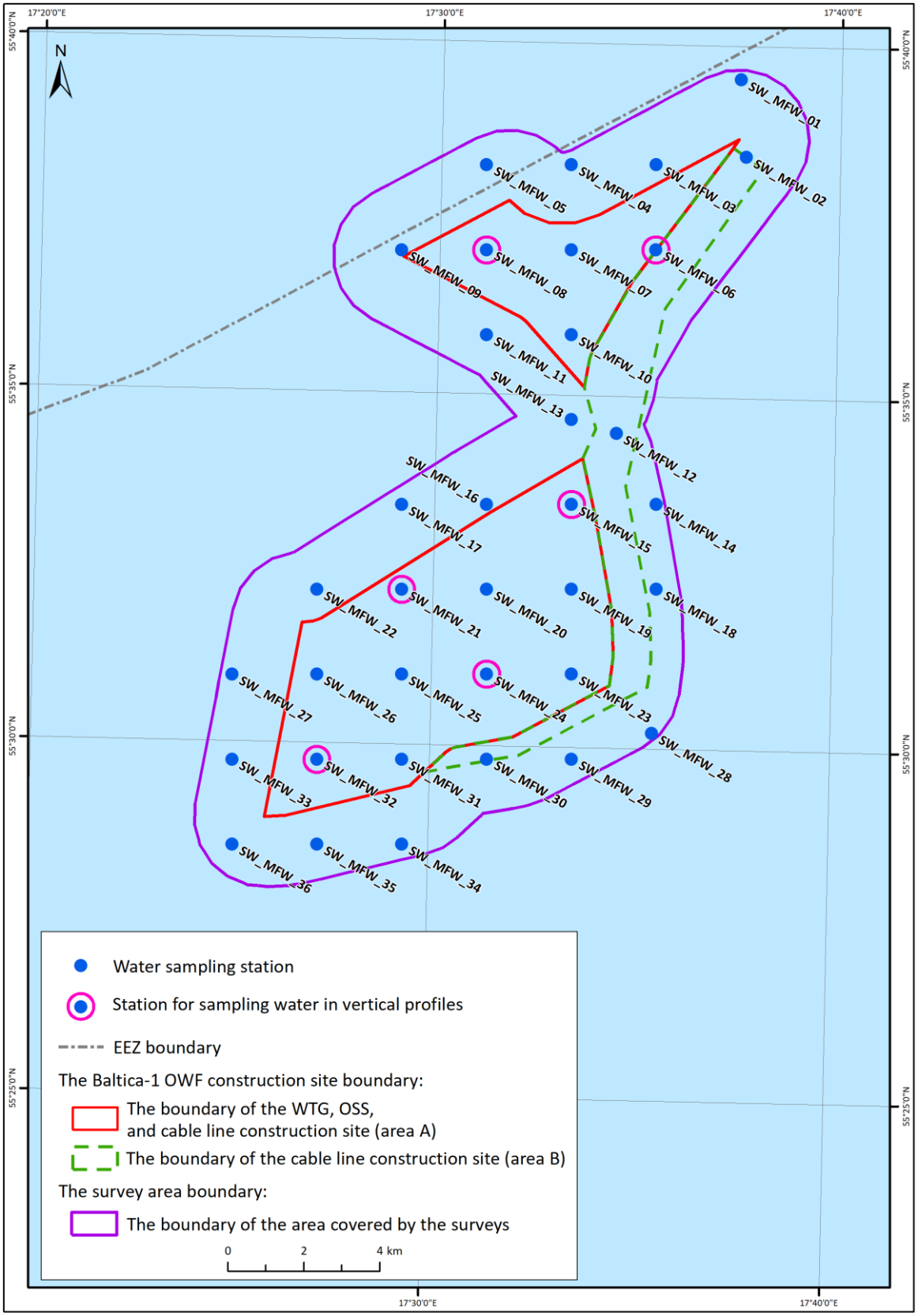


Figure 2.64. The location of the survey stations for water sampling within the survey area

2.2.3 Methodology

2.2.3.1 Survey methodology

The sampling of seawater for the purposes of surveys of the physicochemical properties of water was planned based on the recommendations contained in the Regulation of the Minister of Infrastructure of 13 July 2021 *on the forms and methods of monitoring surface and groundwater bodies* (Journal of Laws of 2021, item 1576).

The water samples were collected from a representative number of points (survey stations) from the near-surface and near-seabed layers of water, 6 times a year, within the survey area.

To characterise the physicochemical parameters of water, water samples were collected as part of six survey campaigns at 36 survey stations located within the survey area:

- 2 samples were collected at each of the 36 survey stations located within the survey area – from the near-surface and near-seabed layers. The near-seabed layer is understood as the layer at approx. 2 m in thickness above the seabed, while the near-surface layer is understood as a 0.5–1.0 m layer below the actual water surface (water table);
- at 6 survey stations within the survey area, samples were collected from the near-surface and the near-seabed layers in accordance with the definition above, and additionally, at the following levels: 2.5 m, 5 m, 10 m, 15 m, and next at an interval of 10 m down to the seabed. Profile survey stations were established at the following points:
    - SW_MFW_06 with intermediate sampling depths of: 2,5; 5; 10; 15; 25 m;
    - SW_MFW_08 with intermediate sampling depths of: 2,5; 5; 10; 15 m;
    - SW_MFW_15 with intermediate sampling depths of: 2,5; 5; 10; 15; 25 m;
    - SW_MFW_21 with intermediate sampling depths of: 2,5; 5; 10; 15 m;
    - SW_MFW_24 with intermediate sampling depths of: 2,5; 5; 10; 15; 25; 35 m;
    - SW_MFW_32 with intermediate sampling depths of: 2,5; 5; 10; 15; 25 m.

The water sampling was conducted in compliance with the following procedure:

- collecting all water samples at the designated survey stations in accordance with the standard PN-EN ISO 5667-9;
- performance of some of the laboratory tests and measurements during the vessel passages (directly after the water sampling) in the mobile laboratory located on the vessel from aboard where the sampling had been carried out. A number of analyses of hydrochemical parameters were conducted in this way, such as the analyses of dissolved oxygen, five-day oxygen demand (BOD_5), reaction (pH), alkalinity, ammoniacal nitrogen content, and total suspended solids content;
- transport of the samples to the laboratory for further testing in the conditions preventing changes in the analyte content – i.e. after they had been preserved, cooled or frozen, depending on the indicator tested, in accordance with the PN-EN ISO 5667-3 standard on water quality;
- analysis of specified indicators in water samples in line with the reference methods detailed in Annex 8 to the Regulation of the Minister of Infrastructure of 13 July 2021 *on the forms and methods of monitoring surface and groundwater bodies* (Journal of Laws of 2021, item 1576) regarding:

- aerobic conditions (dissolved oxygen, 5-day biochemical oxygen demand [BOD_5], total organic carbon [TOC]),
- acidification (pH), and alkalinity,
- nutrients (ammonia, nitrate nitrogen, nitrite nitrogen, total nitrogen, mineral nitrogen, phosphates, total phosphorus),
- total suspended solids,
- particularly harmful substances, such as mercury, nickel, lead, cadmium, arsenic, total chromium, chromium (VI), aluminium, phenols, cyanides, mineral oil, polycyclic aromatic hydrocarbons (PAHs), polychlorinated biphenyls (PCBs).

Additionally, at 6 survey stations, the following surveys were conducted:

- the activity of radioactive caesium isotopes (^{137}Cs) – using a gamma or radiochemical spectrometry method;
- the activity of radioactive strontium isotopes (^{90}Sr) – using the radiochemical method.

Some of the laboratory tests were carried out in the laboratory located on the vessel, from which the water sampling was performed (immediately after the sampling). In this way, the following hydrochemical parameters were analysed: dissolved oxygen, BOD_5, pH value, alkalinity, ammoniacal nitrogen, and total suspended solids. These parameters, in accordance with the standards and analytical procedures, must be tested directly after or shortly after water sampling.

The remaining analyses were conducted by the stationary laboratory of the Environment Protection Department at the Maritime Institute of the Gdynia Maritime University (EPD MI GMU). The water samples collected for testing were transported to the laboratory under conditions that prevent changes in the analyte content – after they had been frozen, in accordance with the water quality standard PN-EN ISO 5667-3.

During water sampling as part of all campaigns, measurements of temperature, electrical conductivity, pressure, and turbidity using CTDs were carried out at all survey stations. The measurements were taken in the entire vertical profile at intervals not greater than 0.5 m (detailed information is presented in Subsection 2.1.5).

A list of methods, techniques, and indicators of water sample tests carried out as part of all survey campaigns at the laboratory of EPD MI GMU is presented in Table 2.20. The methodology to be used for physicochemical testing of water is consistent with, or equivalent to, Annex 8 to the Regulation of the Minister of Infrastructure of 13 July 2021 *on the forms and methods of monitoring surface and groundwater bodies* (Journal of Laws of 2021, item 1576) except for radionuclides (^{137}Cs and ^{90}Sr), which are not mentioned in the regulation. All methods listed in the regulation ensure equal, comparable results.

Table 2.20. Methods and techniques applied in the in situ testing of water samples in the mobile and stationary laboratories

No.	Indicator	Testing place	Analytical method including the lower limit of quantification (LOQ)
1.	Water sampling	-	In accordance with the PN-ISO 5667-9:2005 standard
Physicochemical indicators			
2.	Total suspended solids	Mobile laboratory	Gravimetric method in accordance with the PN-EN 872:2007+Ap1:2007 standard (LOQ: 2.00 $mg \cdot dm^{-3}$)

No.	Indicator	Testing place	Analytical method including the lower limit of quantification (LOQ)
Oxygen conditions and organic pollutant indicators			
3.	Dissolved oxygen	Mobile laboratory	Optical method with the use of a sensor, in accordance with the Standard PN-EN 17289:2014 (LOQ: 0.5 $mg \cdot dm^{-3}$)
4.	Biochemical oxygen demand (BOD_5)	Mobile laboratory	Optical sensor method in accordance with the PN EN ISO 5815-1:2019-12 and ISO 17289:2014 standards (LOQ: 2.0 $mg \cdot dm^{-3}$)
5.	Total organic carbon (TOC)	Stationary laboratory	Infra-red spectrophotometry, analytical procedure in accordance with the PN-EN 1484:1999 standard (LOQ: 0.5 $mg \cdot dm^{-3}$)
Acidification indicators			
6.	pH	Mobile laboratory	Potentiometric method in accordance with the PN-EN ISO 10523:2012 standard (LOQ: pH 2.00)
7.	Alkalinity	Mobile laboratory	Titration method in accordance with the PN-EN ISO 9963-1:2001+Ap1:2004 standard (LOQ: 0.40 $mmol \cdot dm^{-3}$)
Indicators of nutrient conditions (nutrients)			
8.	Ammoniacal nitrogen ($N\text{-}NH^{+}_{4}$)	Mobile laboratory	Spectrophotometric method, analytical procedure PB-30, issue 5 of 06.05.2022 (Grasshoff et al., 1999) (LOQ: 0.003 $mg \cdot dm^{-3}$)
9.	Nitrate nitrogen ($N\text{-}NO^{-}_{3}$)	Stationary laboratory	Spectrophotometric method, PB28 analytical procedure, issue 6 of 06.05.2022 (HELCOM methodology acc. to Grasshoff et al., 1999) (LOQ: 0.003 $mg \cdot dm^{-3}$)
10.	Nitrite nitrogen ($N\text{-}NO^{-}_{2}$)	Stationary laboratory	Spectrophotometric method, analytical procedure PB-29, issue 6 of 06.05.2022 (HELCOM methodology acc. to Grasshoff et al., 1999) (LOQ: 0.003 $mg \cdot dm^{-3}$)
11.	Total nitrogen (TN)	Stationary laboratory	Spectrophotometric method after oxidation of organic nitrogen compounds using potassium persulphate in an alkaline medium (HELCOM methodology acc. to Grasshoff et al., 1999). Analytical procedure PB-27, issue 4 dated 25.02.2021 (LOQ: 0.07 $mg \cdot dm^{-3}$)
12.	Mineral nitrogen (DIN) ($N\text{-}NH_4$+ $N\text{-}NO_2$+ $N\text{-}NO_3$)	Stationary laboratory	Calculation method based on the determination of ammoniacal, nitrite and nitrate nitrogen (I-16, issue 2 of 15.03.2020) (LOQ: 0.003 $mg \cdot dm^{-3}$)
13.	Phosphate phosphorus ($P\text{-}PO_4^{-3}$)	Stationary laboratory	Spectrophotometric method, analytical procedure PB-32, issue 6 of 06.05.2022 (HELCOM methodology acc. to Grasshoff et al., 1999) (LOQ: 0.009 $mg \cdot dm^{-3}$)
14.	Total phosphorus (TP)	Stationary laboratory	Spectrophotometric method after oxidation of organic phosphorus compounds using potassium persulfate in an acidic medium (HELCOM methods, Grasshoff et al., 1999). Analytical procedure PB-31, issue 6 of 06.05.2022 (LOQ: 0.009 $mg \cdot dm^{-3}$)
Specific synthetic and non-synthetic pollutants and a group of chemical indicators characteristic for the occurrence of substances particularly harmful to aquatic environment and substances of priority importance in the water policy			
15.	Arsenic (As)	Stationary laboratory	Inductively coupled plasma mass spectrometry (ICP-MS) technique in accordance with the PN-EN ISO 17294-2:2016 standard (LOQ: 0.010 $\mu g \cdot dm^{-3}$)
16.	Chromium (VI)	Stationary laboratory	Spectrophotometric method in accordance with the PN-EN ISO 18412:2007 standard (LOQ: 0.005 $mg \cdot dm^{-3}$)
17.	Total chromium (TCr)	Stationary laboratory	Inductively coupled plasma mass spectrometry (ICP-MS) technique in accordance with the PN-EN ISO 17294-2:2016 standard (LOQ: 0.03 $\mu g \cdot dm^{-3}$)
18.	Petroleum hydrocarbons – mineral oil index	Stationary laboratory	Gas chromatography method (GC-FID) in accordance with the PN-EN ISO 9377-2:2003 standard (LOQ: 0.01 $mg \cdot dm^{-3}$)

No.	Indicator	Testing place	Analytical method including the lower limit of quantification (LOQ)
19.	Cadmium (Cd) and its compounds	Stationary laboratory	Inductively coupled plasma mass spectrometry (ICP-MS) technique in accordance with the PN-EN ISO 17294-2:2016 standard (LOQ: 0.01 µg·dm^{-3})
20.	Lead (Pb) and its compounds	Stationary laboratory	Inductively coupled plasma mass spectrometry (ICP-MS) technique in accordance with the PN-EN ISO 17294-2:2016 standard (LOQ: 0.01 µg·dm^{-3})
21.	Mercury (Hg) and its compounds	Stationary laboratory	Inductively coupled plasma mass spectrometry (ICP-MS) technique in accordance with the PN-EN ISO 17294-2:2016 standard (LOQ: 0.05 µg·dm^{-3}) Atomic absorption spectrometry (AAS) with amalgamation of mercury vapours technique, in accordance with analytical procedure PB-21, issue 6 of 06.05.2022 (LOQ: 0.05 µg·dm^{-3})
22.	Nickel (Ni) and its compounds	Stationary laboratory	Inductively coupled plasma mass spectrometry (ICP-MS) technique in accordance with the PN-EN ISO 17294-2:2016 standard (LOQ: 0.010 µg·dm^{-3})
23.	Aluminium (Al)	Stationary laboratory	Inductively coupled plasma mass spectrometry (ICP-MS) technique in accordance with the PN-EN ISO 17294-2:2016 standard (LOQ: 1.0 µg·dm^{-3})
24.	Volatile phenols – phenol index	Stationary laboratory	Spectrophotometric method in accordance with the PN-EN ISO 6439:1994 standard (LOQ: 0.001 mg·dm^{-3})
25.	Free and bound cyanides	Stationary laboratory	Colorimetric analysis in accordance with the PN-EN 27888:1980 standard (LOQ: 0.005 mg·dm^{-3})
26.	16 PAHs	Stationary laboratory	Gas chromatography – mass spectrometry (GC-MS) in accordance with the analytical procedure PB-02, issue 5 of 05.03.2021 (LOQ: benzo(a)pyrene and benzo(ghi)perylene – 0.00017 µg·dm^{-3}, the other ones – 0.001 µg·dm^{-3})
27.	7 PCBs	Stationary laboratory	Gas chromatography – mass spectrometry (GC-MS) in accordance with the test procedure PB-02, issue 5 of 05.03.2021 (LOQ: 0.001 µg·dm^{-3})
28.	Caesium 137 (^{137}Cs)	Stationary laboratory	Gamma spectrometry method. The measuring set includes a semi-conductive HPGe detector with an efficiency of 18% and a resolving power of 1.9 keV at 1332 keV energy, together with the analyser (LOQ: 2.3 Bq m^{-3})
29.	Strontium 90 (^{90}Sr)	Stationary laboratory	Radiochemical technique involving the obtaining of a radio-chemically pure preparation ^{90}Y, the concentration of which is equal to the concentration of ^{90}Sr after a secular equilibrium is established. The activity of ^{90}Y is measured using a low-level beta counter FHT 7700T (ESM Eberlin) (LOQ: 7 mBq m^{-3})

All physical, chemical and physicochemical tests (excluding radionuclides) were conducted by the accredited laboratory of the EPD MI GMU, holding the accreditation certificate no. AB 646 issued by the Polish Centre for Accreditation (PCA). Testing of concentrations of radioactive substances (radionuclides) was carried out by the Laboratory of the Institute of Meteorology and Water Management National Research Institute, Maritime Branch in Gdynia (IMWM-NRI).

2.2.3.2 Methodology for data post-processing

This Report includes the results of hydrochemical monitoring conducted throughout a single year, from January to November 2023. Water samples for hydrochemical surveys were collected in the survey area from 18 January to 29 November 2023 as part of six water sampling campaigns.

The tables with the results contain the information on the minimum, maximum, and mean values obtained for each indicator tested in the corresponding water layer, as well as the number of results falling below the limit of quantification of the survey method applied to test a given indicator in a particular survey period.

The minimum values are the lowest concentration value from the ones obtained at all survey stations in a given layer, taking into account the values below the limit of quantification (< LOQ) of the given analytical method.

The maximum values present the highest concentration value from the ones obtained at all survey stations in a given layer or, if all the concentration values obtained are below the LOQ, the maximum value is the value below the LOQ for a given indicator.

The average value is an arithmetic average of all the concentration results obtained for a particular indicator in a given layer at all survey stations located within the survey area. If a given sample provides results below the LOQ, the measurement result is adopted at a level of half of the LOQ value for the purpose of calculating the mean values. In the case when the calculated mean value of the measurement result was below the limit of quantification, the mean value has been determined as below the LOQ. Such presentation of the mean values is due to the technical specification concerning the analysis and monitoring of chemical status of water, published in the Commission Directive 2009/90/EC of 31 July 2009 (OJ EU L 201 of 01.08.2009).

The charts present the obtained test results on the physicochemical indicators in the survey area separately for the near-surface and near-surface layers of water and in the vertical profiles. Depending on the seabed topography, and thus also the relative depth, the near-seabed layer (SEABED) for various survey stations on the charts for vertical profiles means either 21 or 49 m.

The assessments of water quality status were conducted by comparing the results obtained for individual indicators with the limit values listed in the Regulation of the Minister for Infrastructure of 25 June 2021 *on the classification of ecological status, ecological potential and chemical status and on the method of classification of the state of surface water bodies and the environmental quality standards for priority substances* (Journal of Laws of 2021, item 1475) as well as by comparing all the results obtained with literature data.

All the results obtained were referenced to the data presented in the literature and the historical monitoring data (if possible).

2.2.4 Activities performed

During the survey period from January to November 2023, water samples were collected 6 times at 36 survey stations in the survey area. As a result of the activities performed in the course of all water sampling campaigns, a total of 216 water samples from the near-surface layer and 216 water samples from the near-seabed layer were collected (432 water samples in total).

At 6 survey stations (SW_MFW_06, SW_MFW_08, SW_MFW_15, SW_MFW_21, SW_MFW_24, SW_MFW_32), samples supplementing the vertical profiles were additionally collected (29 water samples altogether from the layers supplementing the profiles) during each water sampling campaign (174 water samples in total).

Throughout the entire survey period, 606 water samples were collected in the survey area for physicochemical analyses.

A full range of analyses was conducted for all the water samples collected, including: total suspended solids, dissolved oxygen, BOD_5, pH level, total alkalinity, TOC, ammoniacal nitrogen, nitrate nitrogen, nitrite nitrogen, total nitrogen, mineral nitrogen (DIN), phosphate phosphorus and total phosphorus. 101 water samples collected in July 2023 were also analysed for the presence of: arsenic, chromium (IV), total chromium, aluminium, crude oil derivative hydrocarbons (mineral oil index), cadmium and its compounds, lead and its compounds, mercury and its compounds, nickel and its compounds, volatile phenols (phenol index), free and bound cyanides, PAHs, and PCBs, while, 24 water samples collected from 6 vertical profiles were tested for the presence of radionuclides: caesium 137 (^{137}Cs) and strontium 90 (^{90}Sr). A detailed list of the activities performed is presented in Table 2.21 and Table 2.22.

Table 2.21. A list of activities conducted in relation to water sampling in the survey area

Campaign	Sampling date	Number of water samples collected	Survey station ID / Sample ID*
I	18–19.01.2023	101	SW_MFW_01, SW_MFW_02, SW_MFW_03, SW_MFW_04, SW_MFW_05, **SW_MFW_06**, SW_MFW_07, **SW_MFW_08**, SW_MFW_09, SW_MFW_10, SW_MFW_11, SW_MFW_12, SW_MFW_13, SW_MFW_14, **SW_MFW_15**, SW_MFW_16, SW_MFW_17, SW_MFW_18, SW_MFW_19, SW_MFW_20, **SW_MFW_21**, SW_MFW_22, SW_MFW_23, **SW_MFW_24**, SW_MFW_25, SW_MFW_26, SW_MFW_27, SW_MFW_28, SW_MFW_29, SW_MFW_30, SW_MFW_31, **SW_MFW_32**, SW_MFW_33, SW_MFW_34, SW_MFW_35, SW_MFW_36
II	09–10.03.2023	101	SW_MFW_01, SW_MFW_02, SW_MFW_03, SW_MFW_04, SW_MFW_05, **SW_MFW_06**, SW_MFW_07, **SW_MFW_08**, SW_MFW_09, SW_MFW_10, SW_MFW_11, SW_MFW_12, SW_MFW_13, SW_MFW_14, **SW_MFW_15**, SW_MFW_16, SW_MFW_17, SW_MFW_18, SW_MFW_19, SW_MFW_20, **SW_MFW_21**, SW_MFW_22, SW_MFW_23, **SW_MFW_24**, SW_MFW_25, SW_MFW_26, SW_MFW_27, SW_MFW_28, SW_MFW_29, SW_MFW_30, SW_MFW_31, **SW_MFW_32**, SW_MFW_33, SW_MFW_34, SW_MFW_35, SW_MFW_36
III	01–02.05.2023	101	SW_MFW_01, SW_MFW_02, SW_MFW_03, SW_MFW_04, SW_MFW_05, **SW_MFW_06**, SW_MFW_07, **SW_MFW_08**, SW_MFW_09, SW_MFW_10, SW_MFW_11, SW_MFW_12, SW_MFW_13, SW_MFW_14, **SW_MFW_15**, SW_MFW_16, SW_MFW_17, SW_MFW_18, SW_MFW_19, SW_MFW_20, **SW_MFW_21**, SW_MFW_22, SW_MFW_23, **SW_MFW_24**, SW_MFW_25, SW_MFW_26, SW_MFW_27, SW_MFW_28, SW_MFW_29, SW_MFW_30, SW_MFW_31, **SW_MFW_32**, SW_MFW_33, SW_MFW_34, SW_MFW_35, SW_MFW_36
IV	11–13.07.2023	101	SW_MFW_01, SW_MFW_02, SW_MFW_03, SW_MFW_04, SW_MFW_05, **SW_MFW_06**, SW_MFW_07, **SW_MFW_08**, SW_MFW_09, SW_MFW_10, SW_MFW_11, SW_MFW_12, SW_MFW_13, SW_MFW_14, **SW_MFW_15**, SW_MFW_16, SW_MFW_17, SW_MFW_18, SW_MFW_19, SW_MFW_20, **SW_MFW_21**, SW_MFW_22, SW_MFW_23, **SW_MFW_24**, SW_MFW_25, SW_MFW_26, SW_MFW_27, SW_MFW_28, SW_MFW_29, SW_MFW_30, SW_MFW_31, **SW_MFW_32**, SW_MFW_33, SW_MFW_34, SW_MFW_35, SW_MFW_36
V	25–26.09.2023	101	SW_MFW_01, SW_MFW_02, SW_MFW_03, SW_MFW_04, SW_MFW_05, **SW_MFW_06**, SW_MFW_07, **SW_MFW_08**, SW_MFW_09, SW_MFW_10, SW_MFW_11, SW_MFW_12, SW_MFW_13, SW_MFW_14, **SW_MFW_15**, SW_MFW_16, SW_MFW_17, SW_MFW_18, SW_MFW_19, SW_MFW_20, **SW_MFW_21**, SW_MFW_22, SW_MFW_23, **SW_MFW_24**, SW_MFW_25, SW_MFW_26, SW_MFW_27, SW_MFW_28, SW_MFW_29, SW_MFW_30,

Campaign	Sampling date	Number of water samples collected	Survey station ID / Sample ID*
			SW_MFW_31, **SW_MFW_32**, SW_MFW_33, SW_MFW_34, SW_MFW_35, SW_MFW_36
VI	29.11.2023	101	SW_MFW_01, SW_MFW_02, SW_MFW_03, SW_MFW_04, SW_MFW_05, **SW_MFW_06**, SW_MFW_07, **SW_MFW_08**, SW_MFW_09, SW_MFW_10, SW_MFW_11, SW_MFW_12, SW_MFW_13, SW_MFW_14, **SW_MFW_15**, SW_MFW_16, SW_MFW_17, SW_MFW_18, SW_MFW_19, SW_MFW_20, **SW_MFW_21**, SW_MFW_22, SW_MFW_23, **SW_MFW_24**, SW_MFW_25, SW_MFW_26, SW_MFW_27, SW_MFW_28, SW_MFW_29, SW_MFW_30, SW_MFW_31, **SW_MFW_32**, SW_MFW_33, SW_MFW_34, SW_MFW_35, SW_MFW_36

**Profile stations marked in bold*

Table 2.22. The scope of the tests conducted on the water samples collected as part of all six water sampling campaigns carried out in the survey area

Campaign	Sampling date	Number of water samples collected	Scope of the tests performed
I	18–19.01.2023	101	Analyses performed at the mobile laboratory: total suspended solids, dissolved oxygen, BOD_5, total alkalinity, ammoniacal nitrogen Analyses performed at the stationary laboratory: total organic carbon (TOC), nitrate nitrogen, nitrite nitrogen, total nitrogen, total phosphorus, mineral nitrogen (DIN)
II	09–10.03.2023	101	Analyses performed at the mobile laboratory: total suspended solids, dissolved oxygen, BOD_5, total alkalinity, ammoniacal nitrogen Analyses performed at the stationary laboratory: total organic carbon (TOC), nitrate nitrogen, nitrite nitrogen, total nitrogen, total phosphorus, mineral nitrogen (DIN)
III	01–02.05.2023	101	Analyses performed at the mobile laboratory: total suspended solids, dissolved oxygen, BOD_5, total alkalinity, ammoniacal nitrogen Analyses performed at the stationary laboratory: total organic carbon (TOC), nitrate nitrogen, nitrite nitrogen, total nitrogen, total phosphorus, mineral nitrogen (DIN)
IV	11–13.07.2023	101	Analyses performed at the mobile laboratory: total suspended solids, dissolved oxygen, BOD_5, total alkalinity, ammoniacal nitrogen Analyses performed at the stationary laboratory: nitrate nitrogen, total nitrogen, nitrite nitrogen, phosphate phosphorus, total phosphorus, dissolved inorganic nitrogen (DIN), total organic carbon (TOC), mercury, nickel, lead, cadmium, arsenic, total chromium, chromium (VI), aluminium, cyanides, phenol index, mineral oil index, polycyclic aromatic hydrocarbons (PAHs), and polychlorinated biphenyls (PCBs)
		24	Analyses performed at the stationary laboratory of the IMWM-NRI: caesium 137 (^{137}Cs), strontium 90 (^{90}Sr)

Campaign	Sampling date	Number of water samples collected	Scope of the tests performed
V	25–26.09.2023	101	Analyses performed at the mobile laboratory: total suspended solids, dissolved oxygen, BOD_5, total alkalinity, ammoniacal nitrogen Analyses performed at the stationary laboratory: total organic carbon (TOC), nitrate nitrogen, nitrite nitrogen, total nitrogen, total phosphorus, mineral nitrogen (DIN)
VI	29.11.2023	101	Analyses performed at the mobile laboratory: total suspended solids, dissolved oxygen, BOD_5, total alkalinity, ammoniacal nitrogen Analyses performed at the stationary laboratory: total organic carbon (TOC), nitrate nitrogen, nitrite nitrogen, total nitrogen, total phosphorus, mineral nitrogen (DIN)

2.2.5 Results

2.2.5.1 Physical state indicators (suspended solids)

The test results on the indicator characterising the physical state (suspended solids content) in the water samples collected from the near-surface and near-seabed layers in the survey area as part of six survey campaigns are presented in Table 2.23. Table 2.24 presents the results of analyses of this indicator in vertical water profiles sampled within the survey area.

Table 2.23. The mean, minimum, and maximum contents of total suspended solids in the water samples collected in the survey area

Indicator	Campaign	Depth	Number of detections	Value			Number of results < LOQ
				Mean	Minimum	Maximum	
Total suspended solids [mg·dm^{-3}]	I	SURFACE	36	2.61	< 2.00	8.1	13
		SEABED	36	2.41	< 2.00	5.3	14
	II	SURFACE	36	5.17	< 2.00	9.9	2
		SEABED	36	4.82	< 2.00	11.2	6
	III	SURFACE	36	5.61	3.80	9.60	0
		SEABED	36	5.79	3.50	11.80	0
	IV	SURFACE	36	3.62	< 2.00	6.70	4
		SEABED	36	2.75	< 2.00	8.40	20
	V	SURFACE	36	< 2.00	< 2.00	2.41	33
		SEABED	36	< 2.00	< 2.00	2.24	32
	VI	SURFACE	36	< 2.00	< 2.00	2.19	30
		SEABED	36	< 2.00	< 2.00	2.26	29

SURFACE – the near-surface layer; SEABED – the near-seabed layer; LOQ – the limit of quantification

Table 2.24. The mean, minimum, and maximum content of total suspended solids in the profile water samples collected in the survey area

Indicator	Campaign	Depth	Number of detections	Value			Number of results < LOQ
				Mean	Minimum	Maximum	
Total suspended solids [mg·dm^{-3}]	I	SURFACE	6	3.07	< 2.00	8.10	2
		2.5 m	6	2.91	< 2.00	5.00	1
		5 m	6	< 2.00	< 2.00	4.80	5

Indicator	Campaign	Depth	Number of detections	Value			Number of results < LOQ
				Mean	Minimum	Maximum	
		10 m	6	2.57	< 2.00	4.40	3
		15 m	6	3.09	< 2.00	5.30	1
		25 m	4	2.70	< 2.00	5.20	2
		35 m	1	< 2.00*	-	-	1
		SEABED	6	2.66	< 2.00	4.10	1
	II	SURFACE	6	5.11	3.04	7.70	0
		2.5 m	6	4.65	< 2.00	6.80	1
		5 m	6	5.57	2.74	8.60	0
		10 m	6	4.06	< 2.00	7.60	1
		15 m	6	4.19	< 2.00	6.90	1
		25 m	4	5.40	4.10	6.60	0
		35 m	1	4.20*	-	-	0
		SEABED	6	4.18	< 2.00	6.50	1
	III	SURFACE	6	5.22	4.40	5.60	0
		2.5 m	6	5.03	4.20	6.50	0
		5 m	6	4.63	4.00	5.90	0
		10 m	6	4.93	4.20	5.70	0
		15 m	6	4.70	2.50	5.50	0
		25 m	4	5.73	4.10	7.40	0
		35 m	1	3.24*	-	-	0
		SEABED	6	5.75	3.70	9.00	0
	IV	SURFACE	6	3.68	< 2.00	6.70	1
		2.5 m	6	3.86	< 2.00	5.60	1
		5 m	6	4.53	2.24	7.90	0
		10 m	6	4.25	2.00	7.10	0
		15 m	6	3.36	< 2.00	7.00	1
		25 m	4	3.37	< 2.00	5.60	1
		35 m	1	< 2.00*	-	-	1
		SEABED	6	2.92	< 2.00	8.40	4
	V	SURFACE	6	< 2.00	< 2.00	2.10	5
		2.5 m	6	< 2.00	< 2.00	< 2.00	6
		5 m	6	< 2.00	< 2.00	< 2.00	6
		10 m	6	< 2.00	< 2.00	< 2.00	6
		15 m	6	< 2.00	< 2.00	< 2.00	6
		25 m	4	< 2.00	< 2.00	< 2.00	4
		35 m	1	< 2.00*	-	-	1
		SEABED	6	< 2.00	< 2.00	< 2.00	6
	VI	SURFACE	6	< 2.00	< 2.00	< 2.00	6
		2.5 m	6	< 2.00	< 2.00	< 2.00	6
		5 m	6	< 2.00	< 2.00	2.00	5

Indicator	Campaign	Depth	Number of detections	Value			Number of results < LOQ
				Mean	Minimum	Maximum	
		10 m	6	< 2.00	< 2.00	2.07	5
		15 m	6	< 2.00	< 2.00	2.02	5
		25 m	4	< 2.00	< 2.00	2.08	2
		35 m	1	2.08*	-	-	0
		SEABED	6	< 2.00	< 2.00	2.15	5

SURFACE – the near-surface layer; SEABED – the near-seabed layer; LOQ – the limit of quantification
**a single result for a given depth*

2.2.5.2 Indicators of oxygen conditions

The value ranges for the concentrations of indicators characterising the oxygen conditions – dissolved oxygen concentration, biochemical oxygen demand (BOD_5) and total organic carbon (TOC) in the water samples collected from the near-surface and near-seabed layers in the survey area as part of six survey campaigns are presented in Table 2.25. The test results for these indicators in the vertical profiles of water collected for testing in the survey area are presented in Table 2.26.

Table 2.25. The mean, minimum, and maximum values of the content of dissolved oxygen, BOD_5, and TOC in the water samples collected in the survey area

Indicator	Campaign	Depth	Number of detections	Value			Number of results < LOQ
				Mean	Minimum	Maximum	
Dissolved oxygen [mg·dm^{-3}]	I	SURFACE	36	11.0	10.5	11.6	0
		SEABED	36	11.2	10.6	12.3	0
	II	SURFACE	36	11.73	10.9	12.3	0
		SEABED	36	11.65	10.9	12.2	0
	III	SURFACE	36	11.4	10.9	11.7	0
		SEABED	36	11.6	10.8	11.9	0
	IV	SURFACE	36	9.50	9.30	9.90	0
		SEABED	36	8.40	7.80	9.60	0
	V	SURFACE	36	8.71	8.50	8.90	0
		SEABED	36	8.08	7.10	9.00	0
	VI	SURFACE	36	10.61	10.00	11.20	0
		SEABED	36	10.64	10.30	11.00	0
BOD_5 [mg·dm^{-3}]	I	SURFACE	36	2.05	< 2.00	3.64	15
		SEABED	36	2.06	< 2.00	4.90	17
	II	SURFACE	36	< 2.00	< 2.00	< 2.00	36
		SEABED	36	< 2.00	< 2.00	< 2.00	36
	III	SURFACE	36	< 2.00	< 2.00	< 2.00	36
		SEABED	36	< 2.00	< 2.00	< 2.00	36
	IV	SURFACE	36	< 2.00	< 2.00	2.28	33
		SEABED	36	< 2.00	< 2.00	2.33	34
	V	SURFACE	36	< 2.00	< 2.00	< 2.00	36
		SEABED	36	< 2.00	< 2.00	< 2.00	36

Indicator	Campaign	Depth	Number of detections	Value			Number of results < LOQ
				Mean	Minimum	Maximum	
	VI	SURFACE	36	< 2.00	< 2.00	< 2.00	36
		SEABED	36	< 2.00	< 2.00	< 2.00	36
TOC [mg·dm^{-3}]	I	SURFACE	36	4.30	2.00	5.60	0
		SEABED	36	4.20	< 2.00	5.60	0
	II	SURFACE	36	3.85	2.20	5.50	0
		SEABED	36	3.94	1.50	5.40	0
	III	SURFACE	36	3.00	1.10	4.70	0
		SEABED	36	3.10	1.40	4.50	0
	IV	SURFACE	36	3.10	1.10	4.40	0
		SEABED	36	2.90	1.10	3.90	0
	V	SURFACE	36	3.22	1.50	4.30	0
		SEABED	36	3.00	1.60	4.20	0
	VI	SURFACE	36	3.19	1.90	4.50	0
		SEABED	36	3.18	2.00	4.60	0

SURFACE – the near-surface layer; SEABED – the near-seabed layer; LOQ – the limit of quantification

Table 2.26. The mean, minimum, and maximum content of dissolved oxygen, BOD_5, and TOC in the profile water samples collected in the survey area

Indicator	Campaign	Depth	Number of detections	Value			Number of results < LOQ
				Mean	Minimum	Maximum	
Dissolved oxygen [mg·dm^{-3}]	I	SURFACE	6	11.20	10.50	11.60	0
		2.5 m	6	11.40	11.30	11.50	0
		5 m	6	11.30	11.00	11.50	0
		10 m	6	11.40	11.10	11.50	0
		15 m	6	11.30	10.60	11.50	0
		25 m	4	11.50	11.30	11.60	0
		35 m	1	11.50*	-	-	0
		SEABED	6	11.20	11.00	11.40	0
	II	SURFACE	6	11.60	10.90	12.30	0
		2.5 m	6	12.10	11.90	12.20	0
		5 m	6	12.30	11.90	12.40	0
		10 m	6	12.20	11.80	12.40	0
		15 m	6	12.10	11.70	12.40	0
		25 m	4	12.20	11.70	12.40	0
		35 m	1	12.40*	-	-	0
		SEABED	6	11.60	10.90	11.90	0
	III	SURFACE	6	11.30	11.10	11.50	0
		2.5 m	6	11.60	11.00	11.90	0
		5 m	6	11.80	11.60	12.10	0
		10 m	6	11.90	11.70	12.20	0

Indicator	Campaign	Depth	Number of detections	Value			Number of results < LOQ
				Mean	Minimum	Maximum	
		15 m	6	12.00	11.90	12.20	0
		25 m	4	12.10	11.90	12.20	0
		35 m	1	12.10*	-	-	0
		SEABED	6	11.70	11.60	11.80	0
	IV	SURFACE	6	9.50	9.40	9.70	0
		2.5 m	6	9.60	9.30	9.80	0
		5 m	6	9.80	9.60	9.90	0
		10 m	6	9.60	9.30	9.90	0
		15 m	6	9.10	8.90	9.20	0
		25 m	4	8.80	8.30	9.20	0
		35 m	1	8.40*	-	-	1
		SEABED	6	8.40	8.10	9.10	0
	V	SURFACE	6	8.70	8.50	8.90	0
		2.5 m	6	8.90	8.50	9.00	0
		5 m	6	8.90	8.80	9.00	0
		10 m	6	8.80	8.80	9.00	0
		15 m	6	8.80	8.50	9.00	0
		25 m	4	8.100	7.60	8.50	0
		35 m	1	7.60*	-	-	0
		SEABED	6	8.10	7.10	9.00	0
	VI	SURFACE	6	10.70	10.20	11.00	0
		2.5 m	6	10.70	10.60	10.80	0
		5 m	6	10.80	10.60	10.90	0
		10 m	6	10.70	10.60	10.90	0
		15 m	6	10.70	10.70	10.80	0
		25 m	4	10.80	10.70	10.8	0
		35 m	1	10.80*	-	-	0
		SEABED	6	10.70	10.40	11.00	0
BOD_5 [$mg \cdot dm^{-3}$]	I	SURFACE	6	< 2.00	< 2.00	3.24	4
		2.5 m	6	2.10	< 2.00	3.17	2
		5 m	6	< 2.00	< 2.00	2.90	3
		10 m	6	2.43	< 2.00	3.36	2
		15 m	6	< 2.00	< 2.00	3.19	3
		25 m	4	< 2.00	< 2.00	2.90	2
		35 m	1	< 2.00*	-	-	1
		SEABED	6	2.19	< 2.00	3.54	2
	II	SURFACE	6	< 2.00	< 2.00	3.24	4
		2.5 m	6	2.10	< 2.00	3.17	2
		5 m	6	< 2.00	< 2.00	2.90	3

Indicator	Campaign	Depth	Number of detections	Value			Number of results < LOQ
				Mean	Minimum	Maximum	
		10 m	6	2.43	< 2.00	3.36	2
		15 m	6	< 2.00	< 2.00	3.19	3
		25 m	4	< 2.00	< 2.00	2.90	2
		35 m	1	< 2.00*	-	-	1
		SEABED	6	2.19	< 2.00	3.54	2
	III	SURFACE	6	< 2.00	< 2.00	< 2.00	6
		2.5 m	6	< 2.00	< 2.00	< 2.00	6
		5 m	6	< 2.00	< 2.00	< 2.00	6
		10 m	6	< 2.00	< 2.00	< 2.00	6
		15 m	6	< 2.00	< 2.00	< 2.00	6
		25 m	4	< 2.00	< 2.00	< 2.00	5
		35 m	1	< 2.00*	-	-	1
		SEABED	6	< 2.00	< 2.00	< 2.00	6
	IV	SURFACE	6	< 2.00	< 2.00	< 2.00	6
		2.5 m	6	< 2.00	< 2.00	< 2.00	6
		5 m	6	< 2.00	< 2.00	< 2.00	6
		10 m	6	< 2.00	< 2.00	< 2.00	6
		15 m	6	< 2.00	< 2.00	< 2.00	6
		25 m	4	< 2.00	< 2.00	< 2.00	4
		35 m	1	< 2.00*	-	-	1
		SEABED	6	< 2.00	< 2.00	< 2.00	6
	V	SURFACE	6	< 2.00	< 2.00	< 2.00	6
		2.5 m	6	< 2.00	< 2.00	< 2.00	6
		5 m	6	< 2.00	< 2.00	< 2.00	6
		10 m	6	< 2.00	< 2.00	< 2.00	6
		15 m	6	< 2.00	< 2.00	< 2.00	6
		25 m	4	< 2.00	< 2.00	< 2.00	4
		35 m	1	< 2.00*	-	-	1
		SEABED	6	< 2.00	< 2.00	< 2.00	6
	VI	SURFACE	6	< 2.00	< 2.00	< 2.00	6
		2.5 m	6	< 2.00	< 2.00	< 2.00	6
		5 m	6	< 2.00	< 2.00	< 2.00	6
		10 m	6	< 2.00	< 2.00	< 2.00	6
		15 m	6	< 2.00	< 2.00	< 2.00	6
		25 m	4	< 2.00	< 2.00	< 2.00	4
		35 m	1	< 2.00*	-	-	1
		SEABED	6	< 2.00	< 2.00	< 2.00	6
TOC [mg·dm^{-3}]	I	SURFACE	6	4.80	3.60	5.30	0
		2.5 m	6	4.60	3.60	5.40	0

Indicator	Campaign	Depth	Number of detections	Value			Number of results < LOQ
				Mean	Minimum	Maximum	
		5 m	6	4.90	3.60	5.50	0
		10 m	6	4.70	3.50	5.60	0
		15 m	6	5.10	4.00	5.50	0
		25 m	4	4.60	3.70	5.30	0
		35 m	1	3.30*	-	-	0
		SEABED	6	4.30	3.00	5.20	0
	II	SURFACE	6	3.80	3.10	4.90	0
		2.5 m	6	3.90	3.00	4.60	0
		5 m	6	3.60	2.70	4.50	0
		10 m	6	4.20	3.80	4.40	0
		15 m	6	3.80	2.50	4.40	0
		25 m	4	4.20	3.80	4.60	0
		35 m	1	4.80*	-	-	0
		SEABED	6	3.50	2.70	4.20	0
	III	SURFACE	6	3.70	2.50	4.70	0
		2.5 m	6	3.60	2.40	4.60	0
		5 m	6	2.90	2.10	4.60	0
		10 m	6	3.50	2.60	4.40	0
		15 m	6	3.40	1.90	4.50	0
		25 m	4	3.35	2.30	4.50	0
		35 m	1	2.00*	-	-	0
		SEABED	6	2.70	1.50	4.40	0
	IV	SURFACE	6	2.90	1.10	4.10	0
		2.5 m	6	3.20	2.40	4.10	0
		5 m	6	3.00	1.00	4.00	0
		10 m	6	2.90	1.40	4.00	0
		15 m	6	3.20	1.50	3.80	0
		25 m	4	3.00	2.60	3.30	0
		35 m	1	3.50*	-	-	1
		SEABED	6	2.80	2.00	3.50	0
	V	SURFACE	6	2.70	1.70	3.60	0
		2.5 m	6	3.50	2.40	4.00	0
		5 m	6	2.80	1.80	3.40	0
		10 m	6	3.20	2.30	4.30	0
		15 m	6	2.80	2.00	3.70	0
		25 m	4	2.90	2.00	3.90	0
		35 m	1	3.60*	-	-	0
		SEABED	6	3.10	2.30	4.20	0
	VI	SURFACE	6	2.90	2.00	4.00	0

Indicator	Campaign	Depth	Number of detections	Value			Number of results < LOQ
				Mean	Minimum	Maximum	
		2.5 m	6	3.90	2.60	4.20	0
		5 m	6	3.80	2.40	4.30	0
		10 m	6	3.10	2.60	4.00	0
		15 m	6	3.50	2.50	4.10	0
		25 m	4	3.10	2.30	4.20	0
		35 m	1	3.50*	-	-	0
		SEABED	6	2.90	2.00	4.00	0

SURFACE – the near-surface layer; SEABED – the near-seabed layer; LOQ – the limit of quantification
**a single result for a given depth*

2.2.5.3 Acidification indicators

The results of tests of the indicators characterising the acidification, i.e. the pH level and alkalinity, in the water samples collected from the near-surface and near-seabed layers in the survey area as part of six survey campaigns are presented in Table 2.27. The test results for these indicators in the vertical profiles of water collected in the survey area are presented in Table 2.28.

Table 2.27. The mean, minimum, and maximum value of reaction (pH) and alkalinity in water samples collected in the survey area

Indicator	Campaign	Depth	Number of detections	Value			Number of results < LOQ
				Mean	Minimum	Maximum	
pH	I	SURFACE	36	8.00	7.89	8.03	0
		SEABED	36	8.00	7.67	8.03	0
	II	SURFACE	36	8.00	7.85	8.05	0
		SEABED	36	8.00	7.89	8.05	0
	III	SURFACE	36	8.12	7.48	8.21	0
		SEABED	36	8.10	7.73	8.20	0
	IV	SURFACE	36	8.31	8.19	8.39	0
		SEABED	36	7.76	7.40	8.17	0
	V	SURFACE	36	8.19	8.01	8.25	0
		SEABED	36	7.95	7.67	8.22	0
	VI	SURFACE	36	7.88	7.60	7.93	0
		SEABED	36	7.88	7.49	7.93	0
Alkalinity [mmol·dm^{-3}]	I	SURFACE	36	1.68	1.64	1.78	0
		SEABED	36	1.72	1.66	1.80	0
	II	SURFACE	36	1.71	1.62	1.80	0
		SEABED	36	1.72	1.64	1.84	0
	III	SURFACE	36	1.71	1.60	1.80	0
		SEABED	36	1.76	1.72	1.80	0
	IV	SURFACE	36	1.69	1.60	1.82	0
		SEABED	36	1.66	1.58	1.78	0
	V	SURFACE	36	1.73	1.70	1.78	0

Indicator	Campaign	Depth	Number of detections	Value			Number of results < LOQ
				Mean	Minimum	Maximum	
		SEABED	36	1.75	1.70	1.80	0
	VI	SURFACE	36	1.67	1.58	1.82	0
		SEABED	36	1.69	1.62	1.92	0

SURFACE – the near-surface layer; SEABED – the near-seabed layer; LOQ – the limit of quantification

Table 2.28. The mean, minimum, and maximum value of reaction (pH) and alkalinity in the profile water samples collected in the survey area

Indicator	Campaign	Depth	Number of detections	Value			Number of results < LOQ
				Mean	Minimum	Maximum	
Reaction [pH]	I	SURFACE	6	8.00	7.99	8.01	0
		2.5 m	6	8.01	8.00	8.02	0
		5 m	6	8.01	7.99	8.02	0
		10 m	6	8.01	7.99	8.03	0
		15 m	6	8.01	7.99	8.03	0
		25 m	4	8.02	8.01	8.03	0
		35 m	1	8.02*	-	-	0
		SEABED	6	8.00	8.02	8.02	0
	II	SURFACE	6	8.01	7.99	8.03	0
		2.5 m	6	8.00	7.98	8.02	0
		5 m	6	7.99	7.97	8.02	0
		10 m	6	7.99	7.96	8.01	0
		15 m	6	7.99	7.98	8.01	0
		25 m	4	7.98	7.97	7.99	0
		35 m	1	7.99*	-	-	0
		SEABED	6	8.00	7.98	8.02	0
	III	SURFACE	6	8.14	8.10	8.17	0
		2.5 m	6	8.13	8.10	8.17	0
		5 m	6	8.13	8.12	8.17	0
		10 m	6	8.15	8.13	8.19	0
		15 m	6	8.15	8.12	8.18	0
		25 m	4	8.15	8.13	8.18	0
		35 m	1	8.10*	-	-	0
		SEABED	6	8.11	8.09	8.14	0
	IV	SURFACE	6	8.32	8.22	8.39	0
		2.5 m	6	8.32	8.21	8.40	0
		5 m	6	8.34	8.23	8.41	0
		10 m	6	8.29	8.20	8.35	0
		15 m	6	8.17	8.06	8.24	0
		25 m	4	7.88	7.54	8.10	0
		35 m	1	7.55*	-	-	1

Indicator	Campaign	Depth	Number of detections	Value			Number of results < LOQ
				Mean	Minimum	Maximum	
		SEABED	6	7.75	7.42	8.12	0
	V	SURFACE	6	8.20	8.18	8.22	0
		2.5 m	6	8.19	8.10	8.23	0
		5 m	6	8.22	8.18	8.25	0
		10 m	6	8.22	8.19	8.26	0
		15 m	6	8.22	8.19	8.25	0
		25 m	4	8.17	8.05	8.26	0
		35 m	1	7.81*	-	-	0
		SEABED	6	8.02	7.78	8.22	0
	VI	SURFACE	6	7.90	7.87	7.92	0
		2.5 m	6	7.89	7.85	7.94	0
		5 m	6	7.91	7.87	7.94	0
		10 m	6	7.91	7.87	7.94	0
		15 m	6	7.91	7.86	7.94	0
		25 m	4	7.93	7.92	7.93	0
		35 m	1	7.93*	-	-	0
		SEABED	6	7.90	7.86	7.92	0
Alkalinity [mmol·dm^{-3}]	I	SURFACE	6	1.66	1.64	1.70	0
		2.5 m	6	1.68	1.64	1.72	0
		5 m	6	1.68	1.66	1.72	0
		10 m	6	1.69	1.66	1.72	0
		15 m	6	1.70	1.68	1.72	0
		25 m	4	1.70	1.68	1.72	0
		35 m	1	1.70*	-	-	0
		SEABED	6	1.74	1.72	1.80	0
	II	SURFACE	6	1.71	1.68	1.72	0
		2.5 m	6	1.73	1.72	1.76	0
		5 m	6	1.70	1.64	1.76	0
		10 m	6	1.73	1.66	1.82	0
		15 m	6	1.72	1.66	1.76	0
		25 m	4	1.72	1.64	1.78	0
		35 m	1	1.70*	-	-	0
		SEABED	6	1.73	1.68	1.82	0
	III	SURFACE	6	1.71	1.66	1.80	0
		2.5 m	6	1.71	1.68	1.78	0
		5 m	6	1.71	1.68	1.74	0
		10 m	6	1.73	1.70	1.76	0
		15 m	6	1.74	1.72	1.76	0
		25 m	4	1.76	1.74	1.78	0

Indicator	Campaign	Depth	Number of detections	Value			Number of results < LOQ
				Mean	Minimum	Maximum	
		35 m	1	1.76*	-	-	0
		SEABED	6	1.76	1.72	1.80	0
	IV	SURFACE	6	1.68	1.60	1.80	0
		2.5 m	6	1.68	1.60	1.80	0
		5 m	6	1.69	1.58	1.80	0
		10 m	6	1.69	1.60	1.78	0
		15 m	6	1.64	1.60	1.78	0
		25 m	4	1.65	1.60	1.76	0
		35 m	1	1.64*	-	-	1
		SEABED	6	1.65	1.58	1.78	0
	V	SURFACE	6	1.74	1.70	1.76	0
		2.5 m	6	1.75	1.70	1.82	0
		5 m	6	1.71	1.66	1.80	0
		10 m	6	1.73	1.68	1.78	0
		15 m	6	1.76	1.72	1.80	0
		25 m	4	1.76	1.70	1.78	0
		35 m	1	1.78*	-	-	0
		SEABED	6	1.76	1.70	1.80	0
	VI	SURFACE	6	1.67	1.66	1.68	0
		2.5 m	6	1.67	1.64	1.68	0
		5 m	6	1.67	1.64	1.70	0
		10 m	6	1.67	1.64	1.70	0
		15 m	6	1.66	1.66	1.68	0
		25 m	4	1.68	1.64	1.70	0
		35 m	1	1.68*	-	-	0
		SEABED	6	1.68	1.64	1.70	0

SURFACE – the near-surface layer; SEABED – the near-seabed layer; LOQ – the limit of quantification
**a single result for a given depth*

2.2.5.4 Indicators of nutrient conditions

The concentration ranges for ammoniacal nitrogen,, nitrate nitrogen, nitrite nitrogen, total nitrogen, mineral nitrogen (DIN), phosphate phosphorus, and total phosphorus in the water samples collected from the near-surface and near-seabed layers in the survey area as part of six survey campaigns are presented in Table 2.29. Table 2.30 presents the results of analyses of nutrient content in vertical water profiles collected within the survey area.

Table 2.29. The mean, minimum, and maximum values of nitrogen and phosphorus compounds in the water samples collected in the survey area

Indicator	Campaign	Depth	Number of detections	Value			Number of results < LOQ
				Mean	Minimum	Maximum	
Ammoniacal nitrogen ($N\text{-}NH_4^+$) [$mg \cdot dm^{-3}$]	I	SURFACE	36	< 0.003	< 0.003	0.010	29
		SEABED	36	< 0.003	< 0.003	0.009	31
	II	SURFACE	36	< 0.003	< 0.003	< 0.003	36
		SEABED	36	< 0.003	< 0.003	0.003	34
	III	SURFACE	36	< 0.003	< 0.003	0.003	35
		SEABED	36	< 0.003	< 0.003	0.005	33
	IV	SURFACE	36	< 0.003	< 0.003	0.003	33
		SEABED	36	< 0.003	< 0.003	0.004	32
	V	SURFACE	36	< 0.003	< 0.003	0.003	33
		SEABED	36	< 0.003	< 0.003	0.003	32
	VI	SURFACE	36	< 0.003	< 0.003	0.012	23
		SEABED	36	< 0.003	< 0.003	0.012	25
Nitrite nitrogen ($N\text{-}NO_2^-$) [$mg \cdot dm^{-3}$]	I	SURFACE	36	< 0.003	< 0.003	< 0.003	36
		SEABED	36	< 0.003	< 0.003	< 0.003	36
	II	SURFACE	36	< 0.003	< 0.003	< 0.003	36
		SEABED	36	< 0.003	< 0.003	< 0.003	36
	III	SURFACE	36	< 0.003	< 0.003	< 0.003	36
		SEABED	36	< 0.003	< 0.003	< 0.003	36
	IV	SURFACE	36	< 0.003	< 0.003	< 0.003	36
		SEABED	36	< 0.003	< 0.003	< 0.003	36
	V	SURFACE	36	< 0.003	< 0.003	< 0.003	36
		SEABED	36	< 0.003	< 0.003	0.006	26
	VI	SURFACE	36	< 0.003	< 0.003	< 0.003	36
		SEABED	36	< 0.003	< 0.003	< 0.003	36
Nitrate nitrogen ($N\text{-}NO_3^-$) [$mg \cdot dm^{-3}$]	I	SURFACE	36	0.030	0.013	0.049	0
		SEABED	36	0.031	0.017	0.046	0
	II	SURFACE	36	0.027	0.009	0.052	0
		SEABED	36	0.028	0.004	0.048	0
	III	SURFACE	36	< 0.003	< 0.003	< 0.003	36
		SEABED	36	< 0.003	< 0.003	0.003	35
	IV	SURFACE	36	0.003	< 0.003	0.031	30
		SEABED	36	0.003	< 0.003	0.021	21
	V	SURFACE	36	< 0.003	< 0.003	< 0.003	36
		SEABED	36	0.006	< 0.003	0.016	14
	VI	SURFACE	36	0.011	< 0.003	0.024	2
		SEABED	36	0.013	0.004	0.024	0
	I	SURFACE	36	0.031	0.013	0.053	0
		SEABED	36	0.032	0.017	0.050	0

Indicator	Campaign	Depth	Number of detections	Value			Number of results < LOQ
				Mean	Minimum	Maximum	
Mineral nitrogen (DIN) ($N\text{-}NH_4^+$+ $N\text{-}NO_3^{-+}$+ $N\text{-}NO_2^-$) [mg·dm^{-3}]	II	SURFACE	36	0.027	0.009	0.052	0
		SEABED	36	0.028	0.004	0.048	0
	III	SURFACE	36	< 0.003	< 0.003	0.003	35
		SEABED	36	< 0.003	< 0.003	0.005	32
	IV	SURFACE	36	0.003	< 0.003	0.031	27
		SEABED	36	0.003	< 0.003	0.021	18
	V	SURFACE	36	< 0.003	< 0.003	0.003	33
		SEABED	36	0.007	< 0.003	0.018	13
	VI	SURFACE	36	0.013	< 0.003	0.025	1
		SEABED	36	0.015	0.008	0.024	0
Total nitrogen (TN-) [mg·dm^{-3}]	I	SURFACE	36	0.120	< 0.070	0.250	1
		SEABED	36	0.110	< 0.070	0.150	2
	II	SURFACE	36	0.100	< 0.070	0.150	3
		SEABED	36	0.100	< 0.070	0.160	4
	III	SURFACE	36	0.080	< 0.070	0.130	12
		SEABED	36	0.080	< 0.070	0.130	12
	IV	SURFACE	36	0.130	0.040	0.210	2
		SEABED	36	0.110	0.040	0.190	1
	V	SURFACE	36	0.090	< 0.070	0.210	7
		SEABED	36	0.080	< 0.070	0.150	13
	VI	SURFACE	36	0.120	< 0.070	0.390	12
		SEABED	36	0.120	< 0.070	0.420	11
Phosphorus phosphate ($P\text{-}PO_4^{3-}$) [mg·dm^{-3}]	I	SURFACE	36	0.014	< 0.009	0.019	3
		SEABED	36	0.014	< 0.009	0.019	4
	II	SURFACE	36	0.016	< 0.009	0.024	2
		SEABED	36	0.016	< 0.009	0.024	1
	III	SURFACE	36	0.013	< 0.009	0.016	1
		SEABED	36	0.014	< 0.009	0.026	1
	IV	SURFACE	36	< 0.009	< 0.009	0.012	31
		SEABED	36	0.017	< 0.009	0.030	4
	V	SURFACE	36	< 0.009	< 0.009	< 0.009	36
		SEABED	36	< 0.009	< 0.009	0.021	21
	VI	SURFACE	36	0.015	0.010	0.026	0
		SEABED	36	0.017	0.011	0.042	0
Total phosphorus (TP) [mg·dm^{-3}]	I	SURFACE	36	0.019	0.011	0.026	0
		SEABED	36	0.019	< 0.009	0.027	1
	II	SURFACE	36	0.025	0.017	0.034	0
		SEABED	36	0.026	0.017	0.036	0
	III	SURFACE	36	0.019	0.012	0.024	0

Indicator	Campaign	Depth	Number of detections	Value			Number of results < LOQ
				Mean	Minimum	Maximum	
		SEABED	36	0.021	0.014	0.034	0
	IV	SURFACE	36	0.017	0.011	0.024	0
		SEABED	36	0.027	0.014	0.036	0
	V	SURFACE	36	0.010	< 0.009	0.017	11
		SEABED	36	0.013	< 0.009	0.025	6
	VI	SURFACE	36	0.020	0.010	0.033	0
		SEABED	36	0.021	0.011	0.046	0

SURFACE – the near-surface layer; SEABED – the near-seabed layer; LOQ – the limit of quantification

Table 2.30. The mean, minimum, and maximum values of nitrogen and phosphorus compounds in the water samples collected in the survey area

Indicator	Campaign	Depth	Number of detections	Value			Number of results < LOQ
				Mean	Minimum	Maximum	
Ammoniacal nitrogen ($N\text{-}NH_4^+$) [$mg \cdot dm^{-3}$]	I	SURFACE	6	0.003	< 0.003	0.010	4
		2.5 m	6	< 0.003	< 0.003	0.006	4
		5 m	6	< 0.003	< 0.003	< 0.003	6
		10 m	6	< 0.003	< 0.003	0.003	4
		15 m	6	< 0.003	< 0.003	< 0.003	6
		25 m	4	< 0.003	< 0.003	< 0.003	4
		35 m	1	< 0.003*	-	-	1
		SEABED	6	< 0.003	< 0.003	0.004	5
	II	SURFACE	6	< 0.003	< 0.003	< 0.003	6
		2.5 m	6	< 0.003	< 0.003	< 0.003	6
		5 m	6	< 0.003	< 0.003	< 0.003	6
		10 m	6	< 0.003	< 0.003	< 0.003	6
		15 m	6	< 0.003	< 0.003	< 0.003	6
		25 m	4	< 0.003	< 0.003	< 0.003	5
		35 m	1	< 0.003*	-	-	1
		SEABED	6	< 0.003	< 0.003	0.003	5
	III	SURFACE	6	< 0.003	< 0.003	< 0.003	6
		2.5 m	6	< 0.003	< 0.003	0.005	4
		5 m	6	< 0.003	< 0.003	0.003	5
		10 m	6	< 0.003	< 0.003	< 0.003	6
		15 m	6	< 0.003	< 0.003	< 0.003	6
		25 m	4	< 0.003	< 0.003	< 0.003	4
		35 m	1	< 0.003*	-	-	1
		SEABED	6	< 0.003	< 0.003	0.003	5
	IV	SURFACE	6	< 0.003	< 0.003	< 0.003	6
		2.5 m	6	< 0.003	< 0.003	< 0.003	6
		5 m	6	< 0.003	< 0.003	< 0.003	6

Indicator	Campaign	Depth	Number of detections	Value			Number of results < LOQ
				Mean	Minimum	Maximum	
		10 m	6	< 0.003	< 0.003	< 0.003	6
		15 m	6	< 0.003	< 0.003	< 0.003	6
		25 m	4	< 0.003	< 0.003	< 0.003	4
		35 m	1	< 0.003*	-	-	1
		SEABED	6	< 0.003	< 0.003	< 0.003	6
	V	SURFACE	6	< 0.003	< 0.003	< 0.003	6
		2.5 m	6	< 0.003	< 0.003	0.003	5
		5 m	6	< 0.003	< 0.003	< 0.003	6
		10 m	6	< 0.003	< 0.003	0.003	4
		15 m	6	< 0.003	< 0.003	0.003	5
		25 m	4	< 0.003	< 0.003	< 0.003	4
		35 m	1	< 0.003*	-	-	1
		SEABED	6	< 0.003	< 0.003	0.003	5
	VI	SURFACE	6	0.004	< 0.003	0.012	3
		2.5 m	6	0.003	< 0.003	0.010	4
		5 m	6	0.003	< 0.003	0.011	4
		10 m	6	0.003	< 0.003	0.007	3
		15 m	6	0.004	< 0.003	0.010	3
		25 m	4	0.004	< 0.003	0.010	2
		35 m	1	< 0.003*	-	-	1
		SEABED	6	0.004	< 0.003	0.012	4
Nitrite nitrogen ($N\text{-}NO_2^-$) [$mg \cdot dm^{-3}$]	I	SURFACE	6	< 0.003	< 0.003	< 0.003	6
		2.5 m	6	< 0.003	< 0.003	< 0.003	6
		5 m	6	< 0.003	< 0.003	< 0.003	6
		10 m	6	< 0.003	< 0.003	< 0.003	6
		15 m	6	< 0.003	< 0.003	< 0.003	6
		25 m	4	< 0.003	< 0.003	< 0.003	4
		35 m	1	< 0.003	< 0.003	< 0.003	1
		SEABED	6	< 0.003	< 0.003	< 0.003	6
	II	SURFACE	6	< 0.003	< 0.003	< 0.003	6
		2.5 m	6	< 0.003	< 0.003	< 0.003	6
		5 m	6	< 0.003	< 0.003	< 0.003	6
		10 m	6	< 0.003	< 0.003	< 0.003	6
		15 m	6	< 0.003	< 0.003	< 0.003	6
		25 m	4	< 0.003	< 0.003	< 0.003	5
		35 m	1	< 0.003*	-	-	1
		SEABED	6	< 0.003	< 0.003	< 0.003	6
	III	SURFACE	6	< 0.003	< 0.003	< 0.003	6
		2.5 m	6	< 0.003	< 0.003	< 0.003	6

Indicator	Campaign	Depth	Number of detections	Value			Number of results < LOQ
				Mean	Minimum	Maximum	
		5 m	6	< 0.003	< 0.003	< 0.003	6
		10 m	6	< 0.003	< 0.003	< 0.003	6
		15 m	6	< 0.003	< 0.003	< 0.003	6
		25 m	4	< 0.003	< 0.003	< 0.003	4
		35 m	1	< 0.003*	-	-	1
		SEABED	6	< 0.003	< 0.003	< 0.003	6
	IV	SURFACE	6	< 0.003	< 0.003	< 0.003	6
		2.5 m	6	< 0.003	< 0.003	< 0.003	6
		5 m	6	< 0.003	< 0.003	< 0.003	6
		10 m	6	< 0.003	< 0.003	< 0.003	6
		15 m	6	< 0.003	< 0.003	< 0.003	6
		25 m	4	< 0.003	< 0.003	< 0.003	4
		35 m	1	< 0.003*	-	-	1
		SEABED	6	< 0.003	< 0.003	< 0.003	6
	V	SURFACE	6	< 0.003	< 0.003	< 0.003	6
		2.5 m	6	< 0.003	< 0.003	< 0.003	6
		5 m	6	< 0.003	< 0.003	< 0.003	6
		10 m	6	< 0.003	< 0.003	< 0.003	6
		15 m	6	< 0.003	< 0.003	< 0.003	6
		25 m	4	< 0.003	< 0.003	< 0.003	4
		35 m	1	0.005*	-	-	0
		SEABED	6	0.003	< 0.003	0.006	3
	VI	SURFACE	6	< 0.003	< 0.003	< 0.003	6
		2.5 m	6	< 0.003	< 0.003	< 0.003	6
		5 m	6	< 0.003	< 0.003	< 0.003	6
		10 m	6	< 0.003	< 0.003	< 0.003	6
		15 m	6	< 0.003	< 0.003	< 0.003	6
		25 m	4	< 0.003	< 0.003	< 0.003	4
		35 m	1	< 0.003*	-	-	1
		SEABED	6	< 0.003	< 0.003	< 0.003	6
Nitrate nitrogen ($N\text{-}NO_3^-$) [$mg \cdot dm^{-3}$]	I	SURFACE	6	0.032	0.016	0.043	0
		2.5 m	6	0.035	0.027	0.045	0
		5 m	6	0.035	0.023	0.047	0
		10 m	6	0.035	0.024	0.040	0
		15 m	6	0.039	0.036	0.042	0
		25 m	4	0.035	0.027	0.047	0
		35 m	1	0.027	0.027	0.027	0
		SEABED	6	0.031	0.021	0.038	0
	II	SURFACE	6	0.027	0.022	0.034	0

Indicator	Campaign	Depth	Number of detections	Value			Number of results < LOQ
				Mean	Minimum	Maximum	
		2.5 m	6	0.026	0.010	0.034	0
		5 m	6	0.030	0.019	0.039	0
		10 m	6	0.028	0.013	0.040	0
		15 m	6	0.027	0.016	0.040	0
		25 m	4	0.026	0.018	0.037	0
		35 m	1	0.021*	-	-	0
		SEABED	6	0.026	0.012	0.035	0
	III	SURFACE	6	< 0.003	< 0.003	< 0.003	6
		2.5 m	6	< 0.003	< 0.003	0.006	5
		5 m	6	< 0.003	< 0.003	< 0.003	6
		10 m	6	< 0.003	< 0.003	< 0.003	6
		15 m	6	< 0.003	< 0.003	< 0.003	6
		25 m	4	< 0.003	< 0.003	< 0.003	4
		35 m	1	< 0.003*	-	-	1
		SEABED	6	< 0.003	< 0.003	< 0.003	6
	IV	SURFACE	6	0.006	< 0.003	0.031	5
		2.5 m	6	< 0.003	< 0.003	< 0.003	6
		5 m	6	< 0.003	< 0.003	< 0.003	6
		10 m	6	< 0.003	< 0.003	< 0.003	6
		15 m	6	< 0.003	< 0.003	0.003	5
		25 m	4	< 0.003	< 0.003	< 0.003	4
		35 m	1	< 0.003*	-	-	1
		SEABED	6	0.003	< 0.003	0.011	5
	V	SURFACE	6	< 0.003	< 0.003	< 0.003	6
		2.5 m	6	< 0.003	< 0.003	< 0.003	6
		5 m	6	< 0.003	< 0.003	< 0.003	6
		10 m	6	< 0.003	< 0.003	< 0.003	6
		15 m	6	< 0.003	< 0.003	< 0.003	6
		25 m	4	< 0.003	< 0.003	< 0.003	4
		35 m	1	0.008*	-	-	0
		SEABED	6	0.004	< 0.003	0.009	3
	VI	SURFACE	6	0.010	0.007	0.016	0
		2.5 m	6	0.015	0.007	0.019	0
		5 m	6	0.017	0.007	0.024	0
		10 m	6	0.010	0.004	0.015	0
		15 m	6	0.016	0.006	0.030	0
		25 m	4	0.012	0.010	0.016	0
		35 m	1	0.014*	-	-	0
		SEABED	6	0.013	0.008	0.018	0

Indicator	Campaign	Depth	Number of detections	Value			Number of results < LOQ
				Mean	Minimum	Maximum	
Mineral nitrogen (DIN) ($N\text{-}NH_4^+ + N\text{-}NO_3^- + N\text{-}NO_2^-$) [$mg \cdot dm^{-3}$]	I	SURFACE	6	0.034	0.020	0.052	0
		2.5 m	6	0.037	0.030	0.051	0
		5 m	6	0.035	0.023	0.047	0
		10 m	6	0.036	0.027	0.041	0
		15 m	6	0.039	0.036	0.042	0
		25 m	4	0.035	0.027	0.047	0
		35 m	1	0.027	0.027	0.027	0
		SEABED	6	0.032	0.021	0.038	0
	II	SURFACE	6	0.027	0.022	0.034	0
		2.5 m	6	0.026	0.010	0.034	0
		5 m	6	0.030	0.019	0.039	0
		10 m	6	0.028	0.013	0.040	0
		15 m	6	0.027	0.016	0.040	0
		25 m	4	0.026	0.018	0.037	0
		35 m	1	0.021*	-	-	0
		SEABED	6	0.027	0.012	0.038	0
	III	SURFACE	6	< 0.003	< 0.003	< 0.003	6
		2.5 m	6	0.003	< 0.003	0.006	3
		5 m	6	< 0.003	< 0.003	0.003	5
		10 m	6	< 0.003	< 0.003	< 0.003	6
		15 m	6	< 0.003	< 0.003	< 0.003	6
		25 m	4	< 0.003	< 0.003	< 0.003	4
		35 m	1	< 0.003	< 0.003	< 0.003	1
		SEABED	6	< 0.003	< 0.003	0.003	5
	IV	SURFACE	6	0.006	< 0.003	0.031	5
		2.5 m	6	< 0.003	< 0.003	< 0.003	6
		5 m	6	< 0.003	< 0.003	< 0.003	6
		10 m	6	< 0.003	< 0.003	< 0.003	6
		15 m	6	< 0.003	< 0.003	0.003	5
		25 m	4	< 0.003	< 0.003	< 0.003	4
		35 m	1	< 0.003*	-	-	1
		SEABED	6	0.003	< 0.003	0.011	5
	V	SURFACE	6	< 0.003	< 0.003	< 0.003	6
		2.5 m	6	< 0.003	< 0.003	0.003	5
		5 m	6	< 0.003	< 0.003	< 0.003	6
		10 m	6	< 0.003	< 0.003	0.003	4
		15 m	6	< 0.003	< 0.003	0.003	5
		25 m	4	< 0.003	< 0.003	< 0.003	4
		35 m	1	0.013*	-	-	0

Indicator	Campaign	Depth	Number of detections	Value			Number of results < LOQ
				Mean	Minimum	Maximum	
		SEABED	6	0.007	< 0.003	0.014	2
	VI	SURFACE	6	0.013	0.007	0.019	0
		2.5 m	6	0.017	0.007	0.026	0
		5 m	6	0.019	0.007	0.035	0
		10 m	6	0.013	0.008	0.018	0
		15 m	6	0.019	0.006	0.034	0
		25 m	4	0.015	0.012	0.020	0
		35 m	1	0.014*	-	-	0
		SEABED	6	0.016	0.008	0.022	0
Total nitrogen (TN-) [mg·dm^{-3}]	I	SURFACE	6	0.120	0.080	0.140	0
		2.5 m	6	0.120	0.090	0.140	0
		5 m	6	0.130	0.100	0.180	0
		10 m	6	0.120	0.110	0.140	0
		15 m	6	0.130	0.120	0.160	0
		25 m	4	0.120	0.100	0.150	0
		35 m	1	0.100	0.100	0.100	0
		SEABED	6	0.120	0.120	0.130	0
	II	SURFACE	6	0.110	0.080	0.150	0
		2.5 m	6	0.100	0.080	0.110	0
		5 m	6	0.110	0.080	0.140	0
		10 m	6	0.090	< 0.070	0.120	1
		15 m	6	0.090	< 0.070	0.110	1
		25 m	4	0.100	0.070	0.120	0
		35 m	1	0.090*	-	-	0
		SEABED	6	0.090	< 0.070	0.120	1
	III	SURFACE	6	0.100	0.080	0.130	0
		2.5 m	6	0.080	< 0.070	0.110	1
		5 m	6	< 0.070	< 0.070	0.110	4
		10 m	6	0.080	< 0.070	0.110	2
		15 m	6	0.080	< 0.070	0.110	2
		25 m	4	0.090	< 0.070	0.130	1
		35 m	1	< 0.070*	-	-	1
		SEABED	6	0.070	< 0.070	0.120	3
	IV	SURFACE	6	0.130	< 0.070	0.200	1
		2.5 m	6	0.130	0.100	0.150	0
		5 m	6	0.120	0.080	0.140	0
		10 m	6	0.110	0.070	0.150	0
		15 m	6	0.120	< 0.070	0.150	1
		25 m	4	0.110	0.090	0.120	0

Indicator	Campaign	Depth	Number of detections	Value			Number of results < LOQ
				Mean	Minimum	Maximum	
		35 m	1	0.110*	-	-	0
		SEABED	6	0.090	< 0.070	0.130	1
	V	SURFACE	6	0.070	< 0.070	0.100	2
		2.5 m	6	0.110	0.080	0.140	0
		5 m	6	0.080	< 0.070	0.110	1
		10 m	6	0.110	0.090	0.170	0
		15 m	6	0.090	< 0.070	0.140	1
		25 m	4	< 0.070	< 0.070	0.100	2
		35 m	1	0.100*	-	-	0
		SEABED	6	0.090	< 0.070	0.150	1
	VI	SURFACE	6	0.080	< 0.070	0.140	2
		2.5 m	6	0.110	0.080	0.120	0
		5 m	6	0.110	0.090	0.130	0
		10 m	6	0.140	< 0.070	0.300	3
		15 m	6	0.160	< 0.070	0.300	1
		25 m	4	0.120	< 0.070	0.230	1
		35 m	1	0.100*	-	-	0
		SEABED	6	0.130	< 0.070	0.270	2
Phosphorus phosphate ($P\text{-}PO_4^{3-}$) [$mg \cdot dm^{-3}$]	I	SURFACE	6	0.015	0.011	0.018	0
		2.5 m	6	0.016	0.014	0.018	0
		5 m	6	0.016	0.014	0.018	0
		10 m	6	0.016	0.015	0.018	0
		15 m	6	0.017	0.015	0.018	0
		25 m	4	0.015	0.013	0.018	0
		35 m	1	0.014	0.014	0.014	0
		SEABED	6	0.015	0.009	0.017	0
	II	SURFACE	6	0.016	0.011	0.020	0
		2.5 m	6	0.016	0.010	0.020	0
		5 m	6	0.018	0.011	0.024	0
		10 m	6	0.019	0.014	0.024	0
		15 m	6	0.017	0.012	0.023	0
		25 m	4	0.015	< 0.009	0.019	1
		35 m	1	0.016*	-	-	0
		SEABED	6	0.016	0.009	0.024	0
	III	SURFACE	6	0.014	0.010	0.016	0
		2.5 m	6	0.013	0.010	0.015	0
		5 m	6	0.013	0.010	0.014	0
		10 m	6	0.013	0.011	0.015	0
		15 m	6	0.014	0.009	0.016	0

Indicator	Campaign	Depth	Number of detections	Value			Number of results < LOQ
				Mean	Minimum	Maximum	
		25 m	4	0.013	0.009	0.015	0
		35 m	1	0.010*	-	-	0
		SEABED	6	0.012	< 0.009	0.016	1
	IV	SURFACE	6	< 0.009	< 0.009	< 0.009	6
		2.5 m	6	< 0.009	< 0.009	< 0.009	6
		5 m	6	< 0.009	< 0.009	0.010	5
		10 m	6	< 0.009	< 0.009	0.010	5
		15 m	6	< 0.009	< 0.009	0.012	4
		25 m	4	0.010	< 0.009	0.018	2
		35 m	1	0.019*	-	-	0
		SEABED	6	0.018	< 0.009	0.030	1
	V	SURFACE	6	< 0.009	< 0.009	< 0.009	6
		2.5 m	6	< 0.009	< 0.009	< 0.009	6
		5 m	6	< 0.009	< 0.009	< 0.009	6
		10 m	6	< 0.009	< 0.009	< 0.009	6
		15 m	6	< 0.009	< 0.009	< 0.009	6
		25 m	4	< 0.009	< 0.009	< 0.009	4
		35 m	1	0.014*	-	-	0
		SEABED	6	< 0.009	< 0.009	0.011	4
	VI	SURFACE	6	0.014	0.010	0.017	0
		2.5 m	6	0.018	0.016	0.022	0
		5 m	6	0.017	0.015	0.019	0
		10 m	6	0.015	0.010	0.017	0
		15 m	6	0.017	0.015	0.020	0
		25 m	4	0.019	0.010	0.033	0
		35 m	1	0.015*	-	-	0
		SEABED	6	0.015	0.011	0.019	0
Total phosphorus (TP) [mg·dm^{-3}]	I	SURFACE	6	0.021	0.013	0.026	0
		2.5 m	6	0.018	0.015	0.022	0
		5 m	6	0.020	0.014	0.024	0
		10 m	6	0.021	0.015	0.027	0
		15 m	6	0.021	0.015	0.026	0
		25 m	4	0.019	0.014	0.026	0
		35 m	1	0.015	0.015	0.015	0
		SEABED	6	0.021	0.015	0.025	0
	II	SURFACE	6	0.025	0.018	0.033	0
		2.5 m	6	0.026	0.023	0.029	0
		5 m	6	0.027	0.021	0.032	0
		10 m	6	0.024	0.012	0.029	0

Indicator	Campaign	Depth	Number of detections	Value			Number of results < LOQ
				Mean	Minimum	Maximum	
		15 m	6	0.024	0.015	0.028	0
		25 m	4	0.025	0.020	0.031	0
		35 m	1	0.022*	-	-	0
		SEABED	6	0.024	0.017	0.028	0
	III	SURFACE	6	0.021	0.017	0.024	0
		2.5 m	6	0.019	0.011	0.024	0
		5 m	6	0.018	0.014	0.024	0
		10 m	6	0.019	0.017	0.021	0
		15 m	6	0.021	0.014	0.025	0
		25 m	4	0.021	0.015	0.024	0
		35 m	1	0.015*	-	-	0
		SEABED	6	0.019	0.014	0.023	0
	IV	SURFACE	6	0.017	0.013	0.022	0
		2.5 m	6	0.017	0.012	0.020	0
		5 m	6	0.016	0.011	0.022	0
		10 m	6	0.015	0.011	0.020	0
		15 m	6	0.017	0.010	0.023	0
		25 m	4	0.023	0.014	0.031	0
		35 m	1	0.033*	-	-	0
		SEABED	6	0.026	0.015	0.036	0
	V	SURFACE	6	0.009	< 0.009	0.014	2
		2.5 m	6	0.011	< 0.009	0.015	1
		5 m	6	< 0.009	< 0.009	0.011	2
		10 m	6	< 0.009	< 0.009	0.013	3
		15 m	6	0.009	< 0.009	0.022	3
		25 m	4	< 0.009	< 0.009	0.012	2
		35 m	1	0.015*	-	-	0
		SEABED	6	0.012	< 0.009	0.017	1
	VI	SURFACE	6	0.018	0.011	0.026	0
		2.5 m	6	0.023	0.017	0.026	0
		5 m	6	0.024	0.018	0.027	0
		10 m	6	0.019	0.010	0.025	0
		15 m	6	0.023	0.019	0.027	0
		25 m	4	0.023	0.013	0.041	0
		35 m	1	0.021*	-	-	0
		SEABED	6	0.018	0.013	0.028	0

SURFACE – the near-surface layer; SEABED – the near-seabed layer; LOQ – the limit of quantification

**a single result for a given depth*

2.2.5.5 Particularly harmful and priority substances

2.2.5.5.1 Metals and metalloids

The concentration ranges of metals in the water samples collected from the near-surface and near-seabed layers in the survey area, in July 2023 are presented in Table 2.31. Table 2.32 presents the results of tests of these indicators in the vertical profiles of water.

Table 2.31. The mean, minimum, and maximum concentration values of metals and metalloids in the water samples collected in summer 2023, in the survey area

Indicator	Campaign	Depth	Number of detections	Value			Number of results < LOQ
				Mean	Minimum	Maximum	
Arsenic (As) [mg·dm^{-3}]	IV	SURFACE	36	0.001828	0.001600	0.002400	0
		SEABED	36	0.001848	0.001640	0.002110	0
Chromium (VI) [mg·dm^{-3}]		SURFACE	36	< 0.005000	< 0.005000	< 0.005000	36
		SEABED	36	< 0.005000	< 0.005000	< 0.005000	36
Total chromium (TCr) [mg·dm^{-3}]		SURFACE	36	0.000030	< 0.000030	0.000340	32
		SEABED	36	0.000150	< 0.000030	0.003130	32
Cadmium and its compounds [µg·dm^{-3}]		SURFACE	36	0.020000	< 0.010000	0.220000	25
		SEABED	36	0.020000	< 0.010000	0.220000	20
Lead and its compounds [µg·dm^{-3}]		SURFACE	36	0.150000	< 0.010000	5.030000	34
		SEABED	36	< 0.010000	< 0.010000	< 0.010000	36
Nickel and its compounds [µg·dm^{-3}]		SURFACE	36	0.950000	0.530000	5.070000	0
		SEABED	36	0.950000	0.540000	3.060000	0
Aluminium (Al) [mg·dm^{-3}]		SURFACE	36	0.009000	< 0.001000	0.015000	1
		SEABED	36	0.010000	0.008000	0.017000	0
Mercury (Hg) [µg·dm^{-3}]		SURFACE	36	< 0.050000	< 0.050000	< 0.050000	36
		SEABED	36	< 0.050000	< 0.050000	< 0.050000	36

SURFACE – the near-surface layer; SEABED – the near-seabed layer; LOQ – the limit of quantification

Table 2.32. The mean, minimum, and maximum metal concentration values in the profile water samples collected in summer 2023 in the survey area

Indicator	Campaign	Depth	Number of detections	Value			Number of results < LOQ
				Mean	Minimum	Maximum	
Arsenic (As) [mg·dm^{-3}]	IV	SURFACE	6	0.001915	0.001680	0.002400	0
		2.5 m	6	0.001763	0.001680	0.001880	0
		5 m	6	0.001833	0.001710	0.001980	0
		10 m	6	0.001800	0.001660	0.001940	0
		15 m	6	0.001800	0.001730	0.001830	0
		25 m	4	0.001810	0.001690	0.001900	0
		35 m	1	0.001680*	-	-	0

Indicator	Campaign	Depth	Number of detections	Value			Number of results < LOQ
				Mean	Minimum	Maximum	
		SEABED	6	0.001868	0.001740	0.002080	0
Chromium (VI) [mg·dm^{-3}]		SURFACE	6	< 0.005000	< 0.005000	< 0.00500	6
		2.5 m	6	< 0.005000	< 0.005000	< 0.005000	6
		5 m	6	< 0.005000	< 0.005000	< 0.005000	6
		10 m	6	< 0.005000	< 0.005000	< 0.005000	6
		15 m	6	< 0.005000	< 0.005000	< 0.005000	6
		25 m	4	< 0.005000	< 0.005000	< 0.005000	4
		35 m	1	< 0.005000*	-	-	1
		SEABED	6	< 0.005000	< 0.005000	< 0.005000	6
Total chromium (TCr) [µg·dm^{-3}]		SURFACE	6	0.0000700	< 0.000030	0.000340	5
		2.5 m	6	< 0.000030	< 0.000030	< 0.000030	6
		5 m	6	< 0.000030	< 0.000030	< 0.000030	6
		10 m	6	< 0.000030	< 0.000030	< 0.000030	6
		15 m	6	< 0.000030	< 0.000030	< 0.000030	6
		25 m	4	< 0.000030	< 0.000030	< 0.000030	4
		35 m	1	0.000380*	-	-	0
		SEABED	6	0.000240	< 0.000030	0.001180	4
Cadmium and its compounds (Cd) [µg·dm^{-3}]		SURFACE	6	0.050000	< 0.010000	0.220000	3
		2.5 m	6	< 0.010000	< 0.010000	< 0.010000	6
		5 m	6	0.020000	< 0.010000	0.080000	3
		10 m	6	< 0.010000	< 0.010000	0.020000	3
		15 m	6	< 0.010000	< 0.010000	0.010000	5
		25 m	4	< 0.010000	< 0.010000	< 0.010000	4
		35 m	1	< 0.010000*	-	-	1
		SEABED	6	0.040000	< 0.010000	0.220000	3
Lead and its compounds (Pb) [µg·dm^{-3}]		SURFACE	6	< 0.010000	< 0.010000	< 0.010000	6
		2.5 m	6	< 0.010000	< 0.010000	< 0.010000	6
		5 m	6	< 0.010000	< 0.010000	< 0.010000	6
		10 m	6	< 0.010000	< 0.010000	< 0.010000	6
		15 m	6	< 0.010000	< 0.010000	< 0.010000	6
		25 m	4	< 0.010000	< 0.010000	< 0.010000	4
		35 m	1	< 0.010000*	-	-	1
		SEABED	6	< 0.010000	< 0.010000	< 0.010000	6
Nickel and its compounds (Ni) [µg·dm^{-3}]		SURFACE	6	1.550000	0.530000	5.070000	0
		2.5 m	6	1.450000	0.480000	4.660000	0
		5 m	6	0.700000	0.600000	0.790000	0
		10 m	6	0.630000	0.570000	0.670000	0
		15 m	6	0.670000	0.530000	1.030000	0
		25 m	4	0.680000	0.480000	0.920000	0

Indicator	Campaign	Depth	Number of detections	Value			Number of results < LOQ
				Mean	Minimum	Maximum	
		35 m	1	0.750000*	-	-	0
		SEABED	6	1.040000	0.540000	2.310000	0
Aluminium (Al) [mg·dm^{-3}]		SURFACE	6	0.010000	0.008000	0.015000	0
		2.5 m	6	0.010000	0.008000	0.020000	0
		5 m	6	0.010000	0.008000	0.016000	0
		10 m	6	0.014000	0.008000	0.025000	0
		15 m	6	0.010000	0.008000	0.015000	0
		25 m	4	0.010000	0.008000	0.013000	0
		35 m	1	0.009000*	-	-	0
		SEABED	6	0.010000	0.008000	0.013000	0
Mercury (Hg) [µg·dm^{-3}]		SURFACE	6	< 0.050000	< 0.050000	< 0.050000	6
		2.5 m	6	< 0.050000	< 0.050000	< 0.050000	6
		5 m	6	< 0.050000	< 0.050000	< 0.050000	6
		10 m	6	< 0.050000	< 0.050000	< 0.050000	6
		15 m	6	< 0.050000	< 0.050000	< 0.050000	6
		25 m	4	< 0.050000	< 0.050000	< 0.050000	4
		35 m	1	< 0.050000*	-	-	1
		SEABED	6	< 0.050000	< 0.050000	< 0.050000	6

SURFACE – the near-surface layer; SEABED – the near-seabed layer; LOQ – the limit of quantification
**a single result for a given depth*

2.2.5.5.2 Phenol index and cyanides (free and bound)

The concentration ranges of phenols and free and bound cyanides in the water samples collected from the near-surface and near-seabed layers in the survey area, in July 2023 are presented in Table 2.33. Table 2.34 presents the results of tests of these indicators in the vertical profiles of water.

Table 2.33. The mean, minimum, and maximum concentrations of phenols and free and bound cyanides in the water samples collected in July 2023 in the survey area

Indicator	Campaign	Depth	Number of detections	Value			Number of results < LOQ
				Mean	Minimum	Maximum	
Volatile phenols – phenol index [mg·dm^{-3}]	IV	SURFACE	36	< 0.001	< 0.001	< 0.001	36
		SEABED	36	< 0.001	< 0.001	< 0.001	36
Free cyanides [mg·dm^{-3}]		SURFACE	36	< 0.005	< 0.005	< 0.005	36
		SEABED	36	< 0.005	< 0.005	< 0.005	36
Bound cyanides [mg·dm^{-3}]		SURFACE	36	< 0.005	< 0.005	< 0.005	36
		SEABED	36	< 0.005	< 0.005	< 0.005	36

SURFACE – the near-surface layer; SEABED – the near-seabed layer; LOQ – the limit of quantification

Table 2.34. The mean, minimum, and maximum concentration values of phenols and free and bound cyanides in the profile water samples collected in summer 2023 in the survey area

Indicator	Campaign	Depth	Number of detections	Value			Number of results < LOQ
				Mean	Minimum	Maximum	
Volatile phenols – phenol index [mg·dm^{-3}]	IV	SURFACE	6	< 0.001	< 0.001	< 0.001	6
		2.5 m	6	< 0.001	< 0.001	< 0.001	6
		5 m	6	< 0.001	< 0.001	< 0.001	6
		10 m	6	< 0.001	< 0.001	< 0.001	6
		15 m	6	< 0.001	< 0.001	< 0.001	6
		25 m	4	< 0.001	< 0.001	< 0.001	4
		35 m	1	< 0.001*	-	-	1
		SEABED	6	< 0.001	< 0.001	< 0.001	6
Free cyanides [mg·dm^{-3}]		SURFACE	6	< 0.005	< 0.005	< 0.005	6
		2.5 m	6	< 0.005	< 0.005	< 0.005	6
		5 m	6	< 0.005	< 0.005	< 0.005	6
		10 m	6	< 0.005	< 0.005	< 0.005	6
		15 m	6	< 0.005	< 0.005	< 0.005	6
		25 m	4	< 0.005	< 0.005	< 0.005	4
		35 m	1	< 0.005*	-	-	1
		SEABED	6	< 0.005	< 0.005	< 0.005	6
Bound cyanides [mg·dm^{-3}]		SURFACE	6	< 0.005	< 0.005	< 0.005	6
		2.5 m	6	< 0.005	< 0.005	< 0.005	6
		5 m	6	< 0.005	< 0.005	< 0.005	6
		10 m	6	< 0.005	< 0.005	< 0.005	6
		15 m	6	< 0.005	< 0.005	< 0.005	6
		25 m	4	< 0.005	< 0.005	< 0.005	4
		35 m	1	< 0.005*	-	-	1
		SEABED	6	< 0.005	< 0.005	< 0.005	6

SURFACE – the near-surface layer; SEABED – the near-seabed layer; LOQ – the limit of quantification
**a single result for a given depth*

2.2.5.5.3 Mineral oil index

The concentration ranges of petroleum hydrocarbons (mineral oil index) in the water samples collected from the near-surface and near-seabed layers in the survey area in July 2023 are presented in Table 2.35. The results of tests of this indicator in the vertical profiles of water are presented in Table 2.36.

Table 2.35. The mean, minimum, and maximum concentration values of petroleum hydrocarbons (mineral oil index) in the water samples collected in July 2023 in the survey area

Indicator	Campaign	Depth	Number of detections	Value			Number of results < LOQ
				Mean	Minimum	Maximum	
Petroleum hydrocarbons – mineral oil index	IV	SURFACE	36	0.05	0.02	0.12	0
		SEABED	36	0.05	0.01	0.22	0

Indicator	Campaign	Depth	Number of detections	Value			Number of results < LOQ
				Mean	Minimum	Maximum	
[mg·dm^{-3}]							

SURFACE – the near-surface layer; SEABED – the near-seabed layer; LOQ – the limit of quantification

Table 2.36. The mean, minimum, and maximum concentration values of petroleum hydrocarbons (mineral oil index) in the profile water samples collected in summer 2023 in the survey area

Indicator	Campaign	Depth	Number of detections	Value			Number of results < LOQ
				Mean	Minimum	Maximum	
Petroleum hydrocarbons – mineral oil index [mg·dm^{-3}]	IV	SURFACE	6	0.04	0.02	0.08	0
		2.5 m	6	0.06	0.02	0.09	0
		5 m	6	0.08	0.03	0.18	0
		10 m	6	0.05	0.04	0.07	0
		15 m	6	0.07	0.03	0.14	0
		25 m	4	0.06	0.03	0.12	0
		35 m	1	0.04*	-	-	0
		SEABED	6	0.05	0.03	0.13	0

SURFACE – the near-surface layer; SEABED – the near-seabed layer; LOQ – the limit of quantification
**a single result for a given depth*

2.2.5.5.4 Polycyclic aromatic hydrocarbons (PAHs)

The concentration ranges of polycyclic aromatic hydrocarbons (PAHs) and the sum of 16 PAHs in the water samples collected from the near-surface and near-seabed layers in the survey area in July 2023 are presented in Table 2.37. The results of tests of these indicators in the vertical profiles of water are presented in Table 2.38.

Table 2.37. The mean, minimum, and maximum concentration values of the sum of 16 PAHs in the water samples collected in July 2023 in the survey area

Indicator	Campaign	Depth	Number of detections	Value			Number of results < LOQ
				Mean	Minimum	Maximum	
Naphthalene [µg·dm^{-3}]	IV	SURFACE	36	0.00200	< 0.00100	0.00700	20
		SEABED	36	0.00200	< 0.00100	0.00500	13
Acenaphthylene [µg·dm^{-3}]		SURFACE	36	< 0.00100	< 0.00100	< 0.00100	36
		SEABED	36	< 0.00100	< 0.00100	0.00100	35
Acenaphthene [µg·dm^{-3}]		SURFACE	36	< 0.00100	< 0.00100	0.00100	32
		SEABED	36	0.00100	< 0.00100	0.01700	34
Fluorene [µg·dm^{-3}]		SURFACE	36	0.00100	< 0.00100	0.00200	7
		SEABED	36	0.00100	< 0.00100	0.01500	3
Phenanthrene [µg·dm^{-3}]		SURFACE	36	0.00200	< 0.00100	0.00800	7
		SEABED	36	0.00200	< 0.00100	0.01200	6
Anthracene [µg·dm^{-3}]		SURFACE	36	< 0.00100	< 0.00100	< 0.00100	36
		SEABED	36	< 0.00100	< 0.00100	0.00300	32

Indicator	Campaign	Depth	Number of detections	Value			Number of results < LOQ
				Mean	Minimum	Maximum	
Fluoranthene [µg·dm^{-3}]		SURFACE	36	< 0.00100	< 0.00100	0.00400	20
		SEABED	36	0.00100	< 0.00100	0.00300	20
Pyrene [µg·dm^{-3}]		SURFACE	36	< 0.00100	< 0.00100	0.00200	28
		SEABED	36	< 0.00100	< 0.00100	0.00200	23
Benzo(a)anthracene [µg·dm^{-3}]		SURFACE	36	< 0.00100	< 0.00100	< 0.00100	36
		SEABED	36	< 0.00100	< 0.00100	< 0.00100	36
Chrysene [µg·dm^{-3}]		SURFACE	36	< 0.00100	< 0.00100	< 0.00100	36
		SEABED	36	< 0.00100	< 0.00100	0.00100	35
Benzo(b)fluoranthene [µg·dm^{-3}]		SURFACE	36	< 0.00100	< 0.00100	0.00100	35
		SEABED	36	< 0.00100	< 0.00100	0.00100	35
Benzo(k)fluoranthene [µg·dm^{-3}]		SURFACE	36	< 0.00100	< 0.00100	< 0.00100	36
		SEABED	36	< 0.00100	< 0.00100	< 0.00100	36
Benzo(a)pyrene [µg·dm^{-3}]		SURFACE	36	< 0.00017	< 0.00017	< 0.00017	36
		SEABED	36	< 0.00017	< 0.00017	< 0.00017	36
Indeno(1,2,3,-cd)pyrene [µg·dm^{-3}]		SURFACE	36	< 0.00100	< 0.00100	< 0.00100	36
		SEABED	36	< 0.00100	< 0.00100	< 0.00100	36
Dibenzo(a,h)anthracene [µg·dm^{-3}]		SURFACE	36	< 0.00100	< 0.00100	< 0.00100	36
		SEABED	36	< 0.00100	< 0.00100	< 0.00100	36
Benzo(g,h,i)perylene [µg·dm^{-3}]		SURFACE	36	< 0.00017	< 0.00017	0.00029	34
		SEABED	36	< 0.00017	< 0.00017	0.00033	34
Sum of PAHs [µg·dm^{-3}]		SURFACE	36	0.00500	< 0.00100	0.01600	4
		SEABED	36	0.00700	< 0.00100	0.04500	1

SURFACE – the near-surface layer; SEABED – the near-seabed layer; LOQ – the limit of quantification

Table 2.38. The mean, minimum, and maximum concentration values of PAHs and the sum of 16 PAHs in the profile water samples collected in summer 2023 in the survey area

Indicator	Campaign	Depth	Number of detections	Value			Number of results < LOQ
				Mean	Minimum	Maximum	
Naphthalene [µg·dm^{-3}]	IV	SURFACE	6	0.00100	< 0.00100	0.00400	4
		2.5 m	6	< 0.00100	< 0.00100	0.00100	4
		5 m	6	< 0.00100	< 0.00100	0.00100	4
		10 m	6	0.00200	< 0.00100	0.00500	2
		15 m	6	0.00100	< 0.00100	0.00300	3
		25 m	4	0.00100	< 0.00100	0.00200	2
		35 m	1	< 0.00100*	-	-	1
		SEABED	6	0.00300	< 0.00100	0.00500	1
Acenaphthylene [µg·dm^{-3}]		SURFACE	6	< 0.00100	< 0.00100	< 0.00100	6
		2.5 m	6	< 0.00100	< 0.00100	< 0.00100	6

Indicator	Campaign	Depth	Number of detections	Value			Number of results < LOQ
				Mean	Minimum	Maximum	
		5 m	6	< 0.00100	< 0.00100	< 0.00100	6
		10 m	6	< 0.00100	< 0.00100	< 0.00100	6
		15 m	6	< 0.00100	< 0.00100	< 0.00100	6
		25 m	4	< 0.00100	< 0.00100	< 0.00100	4
		35 m	1	< 0.00100*	-	-	1
		SEABED	6	< 0.00100	< 0.00100	< 0.00100	6
		SURFACE	6	< 0.00100	< 0.00100	< 0.00100	6
		2.5 m	6	< 0.00100	< 0.00100	0.00100	5
		5 m	6	< 0.00100	< 0.00100	< 0.00100	6
Acenaphthene [µg·dm^{-3}]		10 m	6	< 0.00100	< 0.00100	< 0.00100	6
		15 m	6	< 0.00100	< 0.00100	0.00100	4
		25 m	4	< 0.00100	< 0.00100	0.00100	3
		35 m	1	0.00100*	-	-	0
		SEABED	6	< 0.00100	< 0.00100	0.00100	5
		SURFACE	6	< 0.00100	< 0.00100	0.00100	4
		2.5 m	6	0.00100	< 0.00100	0.00200	2
		5 m	6	< 0.00100	< 0.00100	0.00200	3
Fluorene [µg·dm^{-3}]		10 m	6	< 0.00100	< 0.00100	0.00100	1
		15 m	6	0.00200	0.00100	0.00300	0
		25 m	4	0.00100	< 0.00100	0.00200	1
		35 m	1	0.00200*	-	-	0
		SEABED	6	0.00100	< 0.00100	0.00200	1
		SURFACE	6	< 0.00100	< 0.00100	0.00200	3
		2.5 m	6	0.00100	< 0.00100	0.00300	1
		5 m	6	0.00100	< 0.00100	0.00200	2
Phenanthrene [µg·dm^{-3}]		10 m	6	0.00100	< 0.00100	0.00200	1
		15 m	6	0.00200	< 0.00100	0.00600	1
		25 m	4	0.00200	< 0.00100	0.00300	1
		35 m	1	0.00200*	-	-	0
		SEABED	6	0.00200	< 0.00100	0.00500	1
		SURFACE	6	< 0.00100	< 0.00100	< 0.00100	6
		2.5 m	6	< 0.00100	< 0.00100	< 0.00100	6
		5 m	6	< 0.00100	< 0.00100	< 0.00100	6
Anthracene [µg·dm^{-3}]		10 m	6	< 0.00100	< 0.00100	< 0.00100	6
		15 m	6	< 0.00100	< 0.00100	0.00100	5
		25 m	4	< 0.00100	< 0.00100	< 0.00100	4
		35 m	1	< 0.00100*	-	-	1
		SEABED	6	< 0.00100	< 0.00100	< 0.00100	6
Fluoranthene		SURFACE	6	< 0.00100	< 0.00100	0.00200	4

Indicator	Campaign	Depth	Number of detections	Value			Number of results < LOQ
				Mean	Minimum	Maximum	
[µg·dm^{-3}]		2.5 m	6	0.00100	< 0.00100	0.00500	4
		5 m	6	< 0.00100	< 0.00100	0.00100	4
		10 m	6	0.00100	< 0.00100	0.00200	2
		15 m	6	< 0.00100	< 0.00100	0.00100	3
		25 m	4	< 0.00100	< 0.00100	< 0.00100	4
		35 m	1	0.00100*	-	-	0
		SEABED	6	< 0.00100	< 0.00100	0.00200	4
Pyrene [µg·dm^{-3}]		SURFACE	6	< 0.00100	< 0.00100	0.00200	5
		2.5 m	6	0.001000	< 0.00100	0.00300	4
		5 m	6	< 0.00100	< 0.00100	0.00100	5
		10 m	6	< 0.00100	< 0.00100	0.00100	4
		15 m	6	< 0.00100	< 0.00100	0.00100	3
		25 m	4	< 0.00100	< 0.00100	< 0.00100	4
		35 m	1	< 0.00100*	-	-	1
		SEABED	6	< 0.00100	< 0.00100	0.00100	4
Benzo(a)anthracene [µg·dm^{-3}]		SURFACE	6	< 0.00100	< 0.00100	< 0.00100	6
		2.5 m	6	< 0.00100	< 0.00100	< 0.00100	6
		5 m	6	< 0.00100	< 0.00100	< 0.00100	6
		10 m	6	< 0.00100	< 0.00100	< 0.00100	6
		15 m	6	< 0.00100	< 0.00100	< 0.00100	6
		25 m	4	< 0.00100	< 0.00100	< 0.00100	4
		35 m	1	< 0.00100*	-	-	1
		SEABED	6	< 0.00100	< 0.00100	< 0.00100	6
Chrysene [µg·dm^{-3}]		SURFACE	6	< 0.00100	< 0.00100	< 0.00100	6
		2.5 m	6	< 0.00100	< 0.00100	< 0.00100	6
		5 m	6	< 0.00100	< 0.00100	< 0.00100	6
		10 m	6	< 0.00100	< 0.00100	< 0.00100	6
		15 m	6	< 0.00100	< 0.00100	< 0.00100	6
		25 m	4	< 0.00100	< 0.00100	< 0.00100	4
		35 m	1	< 0.00100*	-	-	1
		SEABED	6	< 0.00100	< 0.00100	< 0.00100	6
Benzo(b)fluoranthene [µg·dm^{-3}]		SURFACE	6	< 0.00100	< 0.00100	< 0.00100	6
		2.5 m	6	< 0.00100	< 0.00100	< 0.00100	6
		5 m	6	< 0.00100	< 0.00100	< 0.00100	6
		10 m	6	< 0.00100	< 0.00100	< 0.00100	6
		15 m	6	< 0.00100	< 0.00100	< 0.00100	6
		25 m	4	< 0.00100	< 0.00100	< 0.00100	4
		35 m	1	< 0.00100*	-	-	1
		SEABED	6	< 0.00100	< 0.00100	< 0.00100	6

Indicator	Campaign	Depth	Number of detections	Value			Number of results < LOQ
				Mean	Minimum	Maximum	
Benzo(k)fluoranthene [µg·dm^{-3}]		SURFACE	6	< 0.00100	< 0.00100	< 0.00100	6
		2.5 m	6	< 0.00100	< 0.00100	< 0.00100	6
		5 m	6	< 0.00100	< 0.00100	< 0.00100	6
		10 m	6	< 0.00100	< 0.00100	< 0.00100	6
		15 m	6	< 0.00100	< 0.00100	< 0.00100	6
		25 m	4	< 0.00100	< 0.00100	< 0.00100	4
		35 m	1	< 0.00100*	-	-	1
		SEABED	6	< 0.00100	< 0.00100	< 0.00100	6
Benzo(a)pyrene [µg·dm^{-3}]		SURFACE	6	< 0.00017	< 0.00017	< 0.00017	6
		2.5 m	6	< 0.00017	< 0.00017	< 0.00017	6
		5 m	6	< 0.00017	< 0.00017	< 0.00017	6
		10 m	6	< 0.00017	< 0.00017	< 0.00017	6
		15 m	6	< 0.00017	< 0.00017	< 0.00017	6
		25 m	4	< 0.00017	< 0.00017	< 0.00017	4
		35 m	1	< 0.00017*	-	-	1
		SEABED	6	< 0.00017	< 0.00017	< 0.00017	6
Indeno(1,2,3,-cd)pyrene [µg·dm^{-3}]		SURFACE	6	< 0.00100	< 0.001	< 0.00100	6
		2.5 m	6	< 0.00100	< 0.001	< 0.00100	6
		5 m	6	< 0.00100	< 0.001	< 0.00100	6
		10 m	6	< 0.00100	< 0.001	< 0.00100	6
		15 m	6	< 0.00100	< 0.001	< 0.00100	6
		25 m	4	< 0.00100	< 0.001	< 0.00100	4
		35 m	1	< 0.00100*	-	-	1
		SEABED	6	< 0.00100	< 0.001	< 0.00100	6
Dibenzo(a,h)anthracene [µg·dm^{-3}]		SURFACE	6	< 0.00100	< 0.001	< 0.00100	6
		2.5 m	6	< 0.00100	< 0.001	< 0.00100	6
		5 m	6	< 0.00100	< 0.001	< 0.00100	6
		10 m	6	< 0.00100	< 0.001	< 0.00100	6
		15 m	6	< 0.00100	< 0.001	< 0.00100	6
		25 m	4	< 0.00100	< 0.001	< 0.00100	4
		35 m	1	< 0.00100*	-	-	1
		SEABED	6	< 0.00100	< 0.001	< 0.00100	6
Benzo(g,h,i)perylene [µg·dm^{-3}]		SURFACE	6	< 0.00017	< 0.00017	< 0.00017	6
		2.5 m	6	< 0.00017	< 0.00017	< 0.00017	6
		5 m	6	< 0.00017	< 0.00017	< 0.00017	6
		10 m	6	< 0.00017	< 0.00017	< 0.00017	6
		15 m	6	< 0.00017	< 0.00017	< 0.00017	6
		25 m	4	< 0.00017	< 0.00017	< 0.00017	4
		35 m	1	< 0.00017*	-	-	1

Indicator	Campaign	Depth	Number of detections	Value			Number of results < LOQ
				Mean	Minimum	Maximum	
		SEABED	6	< 0.00017	< 0.00017	< 0.00017	6
Sum of PAHs [µg·dm^{-3}]		SURFACE	6	0.00300	< 0.00100	0.00800	3
		2.5 m	6	0.00400	< 0.00100	0.01300	1
		5 m	6	0.00300	< 0.00100	0.00600	2
		10 m	6	0.00500	0.00300	0.00900	0
		15 m	6	0.00600	0.00200	0.01400	0
		25 m	4	0.00400	0.00100	0.00800	0
		35 m	1	0.00600*	-	-	0
		SEABED	6	0.00700	0.00200	0.01200	0

SURFACE – the near-surface layer; SEABED – the near-seabed layer; LOQ – the limit of quantification
**a single result for a given depth*

2.2.5.5.5 Polychlorinated biphenyls (PCBs)

The concentration ranges of the PCBs and the sum of seven PCB congeners (IUPAC no. 28, 52, 101, 118, 138, 153, 180) in the water samples collected from the near-surface and near-seabed layers in the survey area in July 2023 are presented in Table 2.39. The results of tests of these indicators in the vertical profiles of water are presented in Table 2.40.

Table 2.39. The mean, minimum, and maximum concentration values of the sum of 7 PCBs in the water samples collected in July 2023 in the survey area

Indicator	Campaign	Depth	Number of detections	Value			Number of results < LOQ
				Mean	Minimum	Maximum	
PCB 28 [µg·dm^{-3}]	IV	SURFACE	36	< 0.001	< 0.001	< 0.001	36
		SEABED	36	< 0.001	< 0.001	< 0.001	36
PCB 52 [µg·dm^{-3}]		SURFACE	36	< 0.001	< 0.001	< 0.001	36
		SEABED	36	< 0.001	< 0.001	< 0.001	36
PCB 101 [µg·dm^{-3}]		SURFACE	36	< 0.001	< 0.001	< 0.001	36
		SEABED	36	< 0.001	< 0.001	< 0.001	36
PCB 118 [µg·dm^{-3}]		SURFACE	36	< 0.001	< 0.001	< 0.001	36
		SEABED	36	< 0.001	< 0.001	< 0.001	36
PCB 138 [µg·dm^{-3}]		SURFACE	36	< 0.001	< 0.001	< 0.001	36
		SEABED	36	< 0.001	< 0.001	< 0.001	36
PCB 153 [µg·dm^{-3}]		SURFACE	36	< 0.001	< 0.001	< 0.001	36
		SEABED	36	< 0.001	< 0.001	< 0.001	36
PCB 180 [µg·dm^{-3}]		SURFACE	36	< 0.001	< 0.001	< 0.001	36
		SEABED	36	< 0.001	< 0.001	< 0.001	36
Total PCBs [µg·dm^{-3}]		SURFACE	36	< 0.001	< 0.001	< 0.001	36
		SEABED	36	< 0.001	< 0.001	< 0.001	36

SURFACE – the near-surface layer; SEABED – the near-seabed layer; LOQ – the limit of quantification

Table 2.40. The mean, minimum, and maximum concentration values of the sum of 7 PCBs in the profile water samples collected in summer 2023 in the survey area

Indicator	Campaign	Depth	Number of detections	Value			Number of results < LOQ
				Mean	Minimum	Maximum	
PCB 28 [µg·dm^{-3}]	IV	SURFACE	6	< 0.001	< 0.001	< 0.001	6
		2.5 m	6	< 0.001	< 0.001	< 0.001	6
		5 m	6	< 0.001	< 0.001	< 0.001	6
		10 m	6	< 0.001	< 0.001	< 0.001	6
		15 m	6	< 0.001	< 0.001	< 0.001	6
		25 m	4	< 0.001	< 0.001	< 0.001	4
		35 m	1	< 0.001*	-	-	1
		SEABED	6	< 0.001	< 0.001	< 0.001	6
PCB 52 [µg·dm^{-3}]		SURFACE	6	< 0.001	< 0.001	< 0.001	6
		2.5 m	6	< 0.001	< 0.001	< 0.001	6
		5 m	6	< 0.001	< 0.001	< 0.001	6
		10 m	6	< 0.001	< 0.001	< 0.001	6
		15 m	6	< 0.001	< 0.001	< 0.001	6
		25 m	4	< 0.001	< 0.001	< 0.001	4
		35 m	1	< 0.001*	-	-	1
		SEABED	6	< 0.001	< 0.001	< 0.001	6
PCB 101 [µg·dm^{-3}]		SURFACE	6	< 0.001	< 0.001	< 0.001	6
		2.5 m	6	< 0.001	< 0.001	< 0.001	6
		5 m	6	< 0.001	< 0.001	< 0.001	6
		10 m	6	< 0.001	< 0.001	< 0.001	6
		15 m	6	< 0.001	< 0.001	< 0.001	6
		25 m	4	< 0.001	< 0.001	< 0.001	4
		35 m	1	< 0.001*	-	-	1
		SEABED	6	< 0.001	< 0.001	< 0.001	6
PCB 118 [µg·dm^{-3}]		SURFACE	6	< 0.001	< 0.001	< 0.001	6
		2.5 m	6	< 0.001	< 0.001	< 0.001	6
		5 m	6	< 0.001	< 0.001	< 0.001	6
		10 m	6	< 0.001	< 0.001	< 0.001	6
		15 m	6	< 0.001	< 0.001	< 0.001	6
		25 m	4	< 0.001	< 0.001	< 0.001	4
		35 m	1	< 0.001*	-	-	1
		SEABED	6	< 0.001	< 0.001	< 0.001	6
PCB 138 [µg·dm^{-3}]		SURFACE	6	< 0.001	< 0.001	< 0.001	6
		2.5 m	6	< 0.001	< 0.001	< 0.001	6
		5 m	6	< 0.001	< 0.001	< 0.001	6
		10 m	6	< 0.001	< 0.001	< 0.001	6
		15 m	6	< 0.001	< 0.001	< 0.001	6
		25 m	4	< 0.001	< 0.001	< 0.001	4
		35 m	1	< 0.001*	-	-	1

Indicator	Campaign	Depth	Number of detections	Value			Number of results < LOQ
				Mean	Minimum	Maximum	
		SEABED	6	< 0.001	< 0.001	< 0.001	6
PCB 153 [µg·dm^{-3}]		SURFACE	6	< 0.001	< 0.001	< 0.001	6
		2.5 m	6	< 0.001	< 0.001	< 0.001	6
		5 m	6	< 0.001	< 0.001	< 0.001	6
		10 m	6	< 0.001	< 0.001	< 0.001	6
		15 m	6	< 0.001	< 0.001	< 0.001	6
		25 m	4	< 0.001	< 0.001	< 0.001	4
		35 m	1	< 0.001*	-	-	1
		SEABED	6	< 0.001	< 0.001	< 0.001	6
PCB 180 [µg·dm^{-3}]		SURFACE	6	< 0.001	< 0.001	< 0.001	6
		2.5 m	6	< 0.001	< 0.001	< 0.001	6
		5 m	6	< 0.001	< 0.001	< 0.001	6
		10 m	6	< 0.001	< 0.001	< 0.001	6
		15 m	6	< 0.001	< 0.001	< 0.001	6
		25 m	4	< 0.001	< 0.001	< 0.001	4
		35 m	1	< 0.001*	-	-	1
		SEABED	6	< 0.001	< 0.001	< 0.001	6
Total PCBs [µg·dm^{-3}]		SURFACE	6	< 0.001	< 0.001	< 0.001	6
		2.5 m	6	< 0.001	< 0.001	< 0.001	6
		5 m	6	< 0.001	< 0.001	< 0.001	6
		10 m	6	< 0.001	< 0.001	< 0.001	6
		15 m	6	< 0.001	< 0.001	< 0.001	6
		25 m	4	< 0.001	< 0.001	< 0.001	4
		35 m	1	< 0.001*	-	-	1
		SEABED	6	< 0.001	< 0.001	< 0.001	6

SURFACE – the near-surface layer; SEABED – the near-seabed layer; LOQ – the limit of quantification
**a single result for a given depth*

2.2.5.6 Radionuclides

The ranges of caesium (^{137}Cs) and strontium (^{90}Sr) radioactivity in the vertical profiles of water collected for testing in the survey area in July 2023 are presented in Table 2.41.

Table 2.41. The mean, minimum, and maximum values of the caesium (^{137}Cs) and strontium (^{90}Sr) radioactivity in the water samples collected in summer 2023 in the survey area

Indicator	Campaign	Depth	Number of detections	Value			Number of results < LOQ
				Mean	Minimum	Maximum	
^{137}Cs [Bq m^{-3}]	IV	SURFACE	6	17.27	16.80	17.82	0
		10 m	6	16.98	16.42	17.74	0
		25 m	6	16.13	15.60	16.51	0
		SEABED	6	16.77	15.54	18.42	0
^{90}Sr		SURFACE	6	4.74	4.41	5.38	0

Indicator	Campaign	Depth	Number of detections	Value			Number of results < LOQ
				Mean	Minimum	Maximum	
[Bq m^{-3}]		10 m	6	4.52	4.10	5.60	0
		25 m	6	4.58	3.80	5.18	0
		SEABED	6	4.32	4.02	5.01	0

SURFACE – the near-surface layer; SEABED – the near-seabed layer; LOQ – the limit of quantification

2.2.6 Summary of results and conclusions

2.2.6.1 Physical state indicators (suspended solids)

Suspended solids are defined as a fraction of particles larger than 0.45 µm, forming the suspended phase in the water (Salbu and Oughton, 1994; Stroomberg, 1995). They include organic and inorganic particles floating in the water masses. Suspended organic matter is composed of bacteria, small organisms or their fragments, and plant pollen transferred from the shore. Inorganic particles are composed, in contrast, of silty and clayey material, sand and rock particles, and the colloidal particles of various chemical compounds. The inorganic matter is transported by river waters, in the atmosphere, is lifted from the seabed of the basin or washed away from the shores (Maciejowski, 1995). Due to its high sorption properties, suspended matter is characterised by the ability to collect hydrophobic organic contaminants and trace amounts of metals. Sometimes, the values of the enrichment factor of these contaminants reach an order of several thousand or more (Aminot, 1995; Dojlido, 1995; Galer et al., 2001; Stroomberg, 1995).

The concentrations of suspended solids in the seawater samples from survey area collected from January to November 2023 under six survey campaigns were low.

The average concentration of suspension in waters from the survey area in various measurement periods is shown in Figure 2.65.

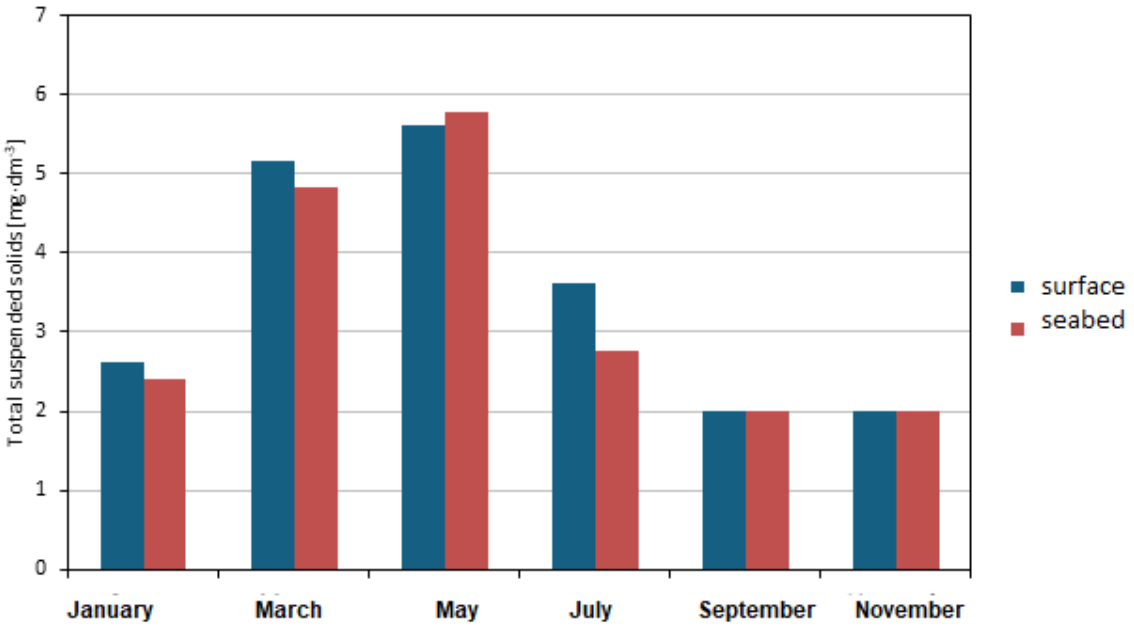


Figure 2.65. The mean concentration of suspended solids in the near-surface and near-seabed layers tested under individual survey campaigns

The lowest mean concentrations of suspended solids in the survey area were recorded in January, September, and November 2023 (the first, fifth, and sixth campaign, respectively) and were below or close to the lower limit of quantification of the analytical method used (i.e. 2.0 mg·dm^{-3}). The highest average concentration of suspended solids was observed in May 2023, as part of the third water sampling campaign – 5.61 mg·dm^{-3} in the near-surface water layer and 5.79 mg·dm^{-3} in the near-seabed water layer. The maximum concentration of suspended solids was achieved at survey station SW_MFW_10 (11.80 mg·dm^{-3}). Differences in the concentration of suspended solids in water can be explained by many factors. It may be the wind causing water mixing, which leads to the suspended solids rising from the seabed to the water column, which results in an increase in the concentration of suspended solids, but also an increase in water temperature, and in consequence, a period of increased biological activity in marine ecosystems. Phytoplankton begins to grow intensively in response to higher temperatures and more sunlight, which leads to an increase in the biomass of organic suspended matter in water. These processes can occur simultaneously.

The obtained results of the analyses of total suspended solids content do not indicate a significant change alongside the depth in any of the vertical profiles sampled in the survey area.

The concentration of suspended solids obtained for the survey area is typical for the waters of the Baltic Sea. By comparison, the concentration of suspended solids in the open waters of the Baltic Sea ranges from below 0.01 to 10.0 mg·dm^{-3}, reaching the highest concentrations of up to 45.7 mg·dm^{-3} in spring (Bernard et al., 1989; Burska et al., 2005; Chałacińska et al., 2014).

2.2.6.2 Indicators of oxygen conditions

2.2.6.2.1 Dissolved oxygen

Oxygen dissolved in water is a valuable index characterising the marine environment conditions and a sensitive indicator of biological and chemical processes taking place in the sea (Bolałek and Falkowska, 1999). Oxygen conditions of the sea depend mainly on the physical and biochemical processes. Oxygen dissolved in seawater is used in the process of respiration and microbiological oxidation. While its resources are renewed in the processes of photosynthesis, direct exchange with the atmosphere or by means of gas bubbles entering the water depth when waves are breaking on the sea surface (Bidleman et al., 2015; Bolałek and Falkowska, 1999). In addition to the temperature and salinity, dissolved oxygen is the most important component characterising the conditions of the marine environment.

Figure 2.66 presents seasonal changes in the oxygen dissolved in the waters of survey area under individual survey campaigns from January to November 2023.

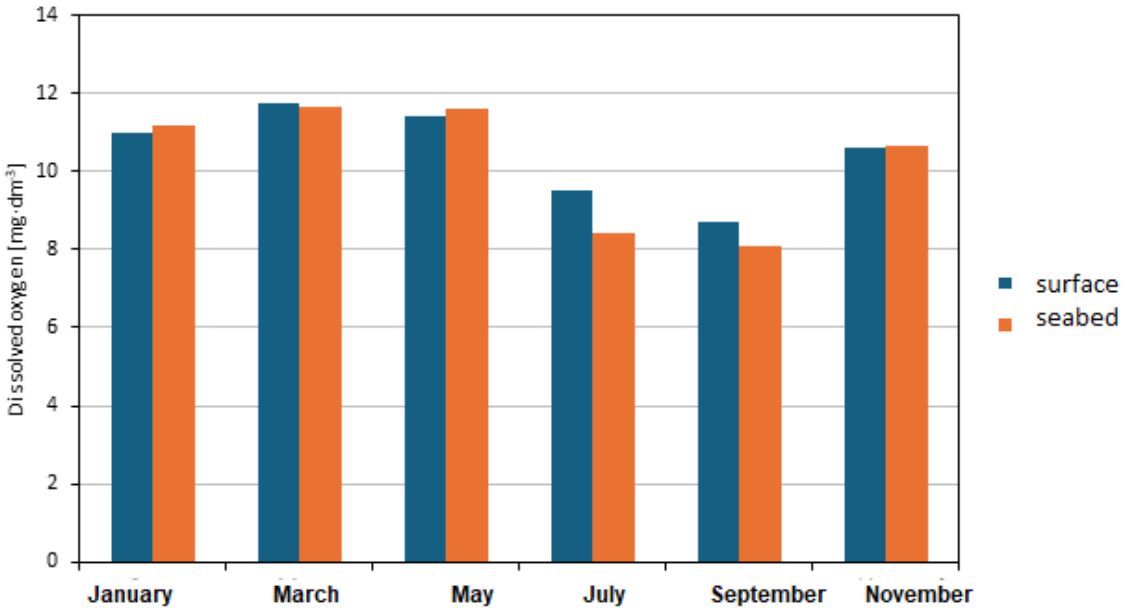


Figure 2.66. The mean concentration of dissolved oxygen in the near-surface and near-seabed layers of water from the survey area under individual survey campaigns

The analysis of the mean concentration of dissolved oxygen in the water of the survey area in individual survey campaigns indicated the lowest concentrations in this area in summer (July – the fourth campaign/ September – the fifth campaign), which was caused by an increased decomposition of organic matter in that period. In all survey months, small differences in the dissolved oxygen concentrations in the near-surface layer compared to the near-seabed layer were observed, which indicates their good mixing in the area surveyed.

The spatial analysis of the dissolved oxygen concentration distributions in the vertical profiles showed a uniform distribution of oxygen concentration in individual layers [Figure 2.67].

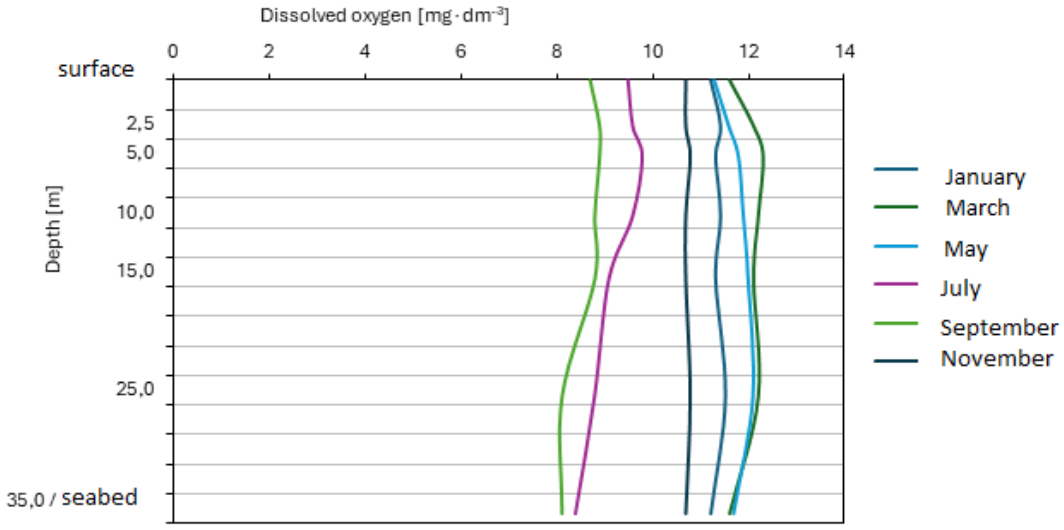


Figure 2.67. The diversification of the average dissolved oxygen concentration with depth from the six profiles surveyed in the survey area under individual survey campaigns

The spatial analysis of the distribution of dissolved oxygen concentration in the vertical water profiles from the survey area in individual survey periods demonstrated that the highest concentrations at all survey stations in that area were recorded in the winter-spring period, while the lowest concentrations were recorded in the summer-early-autumn period, which was caused by the increased decomposition of organic matter in that period. The waters surveyed were characterised by a uniform distribution of dissolved oxygen concentrations in individual survey layers. Only in July and September, little variation was observed in the vertical distribution of concentrations, i.e. lower concentrations in the near-seabed layer in relation to the near-surface layer, which is typical of that survey period.

The assessment of the quality of water in the survey area based on the oxygen content in the near-seabed layer in summer (July – the fourth campaign, September – the fifth campaign) indicates a good status (no oxygen deficit). The minimum concentration of dissolved oxygen in this period in the near-seabed layer reached values exceeding the limit value of 6.0 mg·dm^{-3} (Krzymiński, 2013) – from 7.1 to 7.8 mg·dm^{-3}.

The comparison of the results obtained for the near-seabed dissolved oxygen concentrations with the limit values set out in the Regulation of the Minister of Infrastructure of 25 June 2021 *on the classification of ecological status, ecological potential and chemical status and on the method of classifying the status of surface water bodies and the environmental quality standards for priority substances* (Journal of Laws of 2021, item 1475) indicates that the waters of the survey area analysed fall into Class 1 of water quality for the SWBs such as coastal waters (exclusively on the basis of the near-seabed dissolved oxygen concentration).

2.2.6.2.2 Biochemical oxygen demand (BOD_5)

Biochemical oxygen demand BOD_n is a conventional indicator that specifies the amount of oxygen consumed during the aerobic metabolism of organic compounds (with the participation of micro-organisms) in the temperature of 20°C and with the water or waste water volume unit and the

observation time specified. The course of oxygen consumption depends not only on the composition of biodegradable organic compounds and the type of microorganisms involved in the reaction, but also on temperature, the presence of toxic compounds and inhibitors of biochemical reactions.

The BOD_5 values observed in the survey area were relatively low, which may signify a low content of organic substances that can be biologically oxidised in the waters surveyed. The mean values of BOD_5 in all survey campaigns, both in the near-surface and near-seabed layer, were generally < 2.0 mg·dm^{-3}. Spatial analysis of concentration distribution of BOD_5 in vertical profiles revealed a uniform, to a large extent, distribution in individual layers.

Comparing the BOD_5 results obtained for the survey area to the literature data, it was found that these concentrations did not exceed typical values for waters of the central southern coast of the Baltic Sea in particular periods of measurement (Poleszczuk, 1996).

2.2.6.2.3 Total organic carbon content (TOC)

Total organic carbon is a summary indicator representing the total amount of carbon contained in the organic compounds of the matrix analysed (Zabiegała, 2002). The typical concentration of TOC in water can vary from below 1 µg·dm^{-3} (1 ppb) to over 1000 mg·dm^{-3} (1000 ppm) – in the case of waste water (Namieśnik, 2001).

The mean TOC concentration in the survey area under individual survey campaigns did not exceed 5 mg·dm^{-3}.

The seasonal variations of TOC in the survey area waters during individual survey campaigns from January to November 2023 are presented in Figure 2.68.

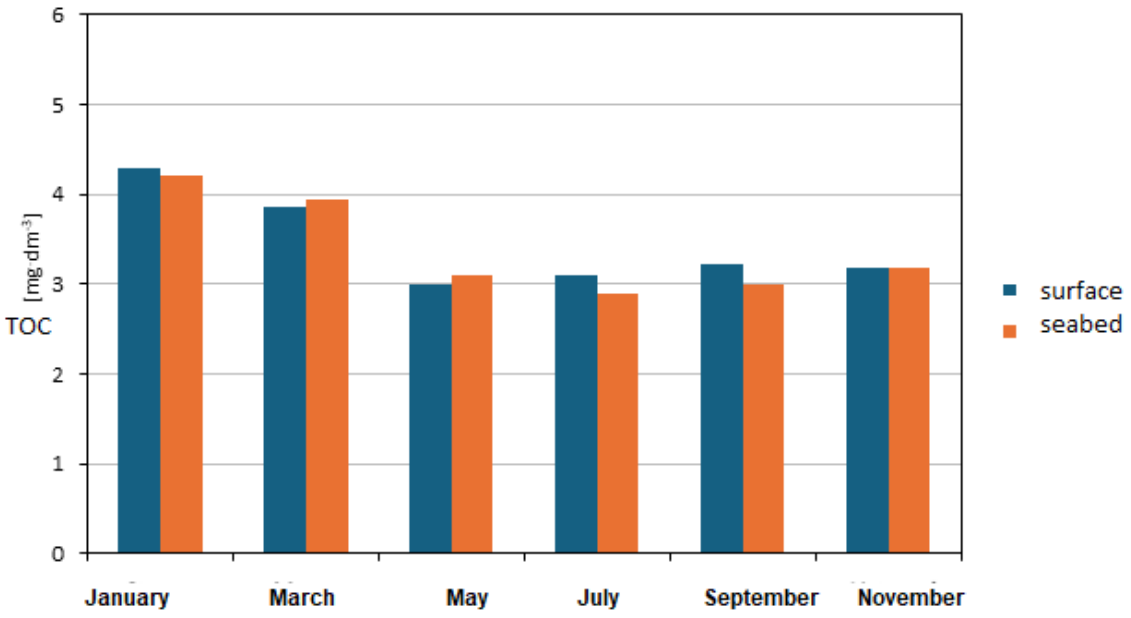


Figure 2.68. The mean concentration of TOC in the near-surface and near-seabed water layers from the survey area under individual survey campaigns

When analysing spatial distribution of TOC concentration in the surveyed waters of the survey area, no significant differences between the near-surface and near-seabed layers as well as vertical profiles were found [Figure 2.69].

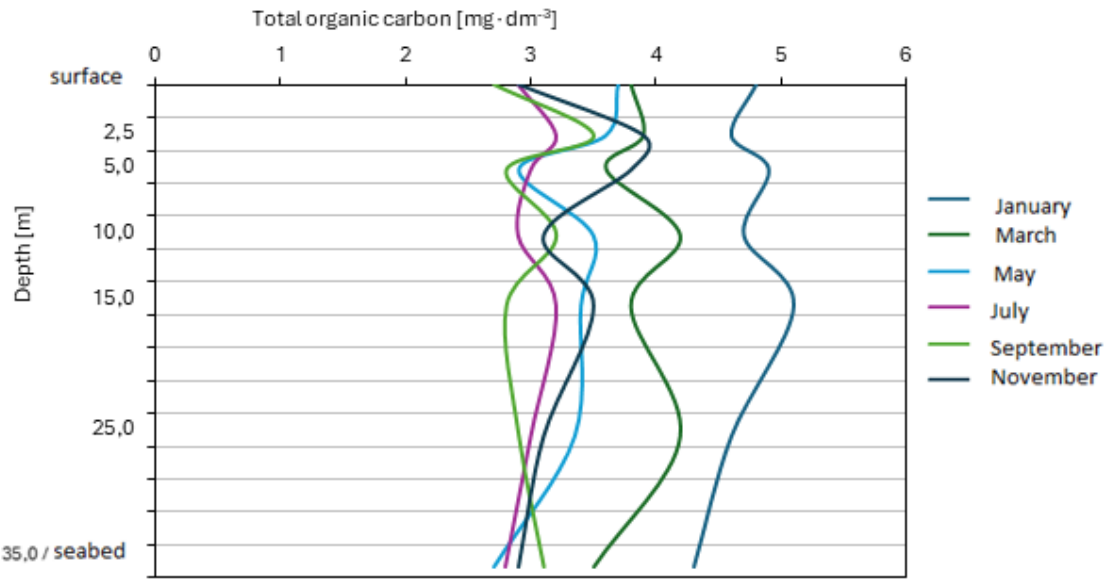


Figure 2.69. The diversification of the TOC concentrations with depth in the six profiles surveyed in the survey area under individual survey campaigns

Comparing the TOC results obtained from the survey area to the literature data, it was found that these concentrations did not exceed values typical for waters of the central southern coast of the Baltic Sea in particular periods of measurement (Pęcherzewski and Ławacz, 1975).

The average TOC concentrations recorded within the survey area do not exceed the limit value for water quality Class 1 (5 mg·dm^{-3}) and Class 2 (10 mg·dm^{-3}) set out in the Regulation of the Minister of Infrastructure of 25 June 2021 *on the classification of ecological status, ecological potential, chemical status and the method of classifying the status of surface water bodies as well as environmental quality standards for priority substances for the SWBs such as coastal waters* (Journal of Laws of 2021, item 1475) (based on the values measured from June to September, i.e. during the period of the most intense growth).

2.2.6.3 Acidification indicators

2.2.6.3.1 Reaction (pH)

The pH value of natural water depends on many factors:

- dissociation and hydrolysis of the compounds dissolved in the water;
- the carbonate system, i.e. the content of carbonates and CO_2; carbonate waters are alkaline and carbonate-poor waters are acidic; surface waters may owe their alkalinity to increased photosynthesis;
- the character of soil substratum which may contain acidic or alkaline compounds;
- contamination from sewage or precipitation, which can cause an increase in the amount of acid in the water.

Within the entire survey period between January and November 2023, the average pH value of water calculated from all the samples collected in the survey area and tested was 8.01 and was alkaline. An insignificant variability of this parameter was found out in the entire survey area. The survey results obtained are consistent with the multi-annual data from the literature on the Baltic Sea area surveyed, according to which the pH value equals approx. 8.00 (Brutemark et al., 2011; Ulfsbo et al., 2011).

This parameter was characterised by depth-dependent and season-dependent variability [Figure 2.70].

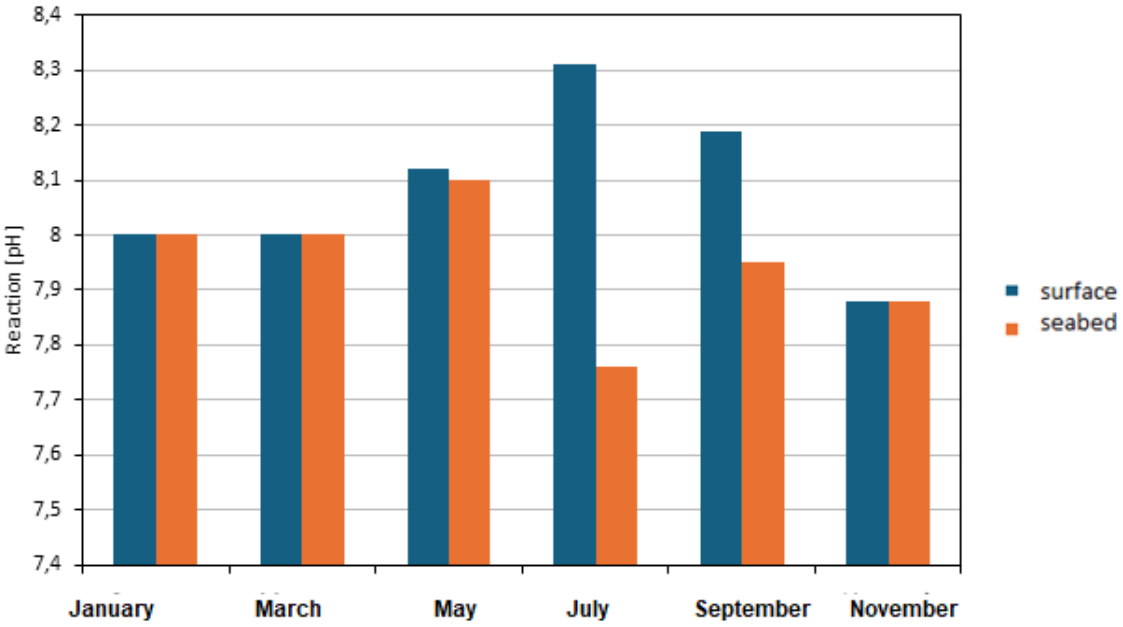


Figure 2.70. The mean pH value in the near-surface and near-seabed layer of water in the survey area in individual survey campaigns

The changes in the pH value with depth are noticeable, beginning in late spring until summer (from May to September), and fade away in autumn and winter (from November to March), which indicates a good mixing of water [Figure 2.71]. The difference in the mean water pH value between the surface layer and water obtained from greater depths results form the discrepancies in quality of mixing, salinity, or changes in meteorological conditions. Additionally, it is associated directly with the photosynthesis activity, which involves carbon dioxide. This process is the most intensive in the near-surface layer of water. In the process, carbon dioxide is absorbed and oxygen is released. A slight increase in the pH value in the warmer, near-surface water is a natural phenomenon and is compliant with the cycle of seasonal changes (Brutemark et al., 2011).

However, the similarity between the results obtained for various depths in the autumn and winter period (November–March) is attributed to good mixing and slight differences of water temperature between individual layers.

Figure 2.71 presents the change in the average pH value with the increase in depth in all vertical profiles collected in the survey area from January to November 2023. The differences are most distinct in July and September 2023.

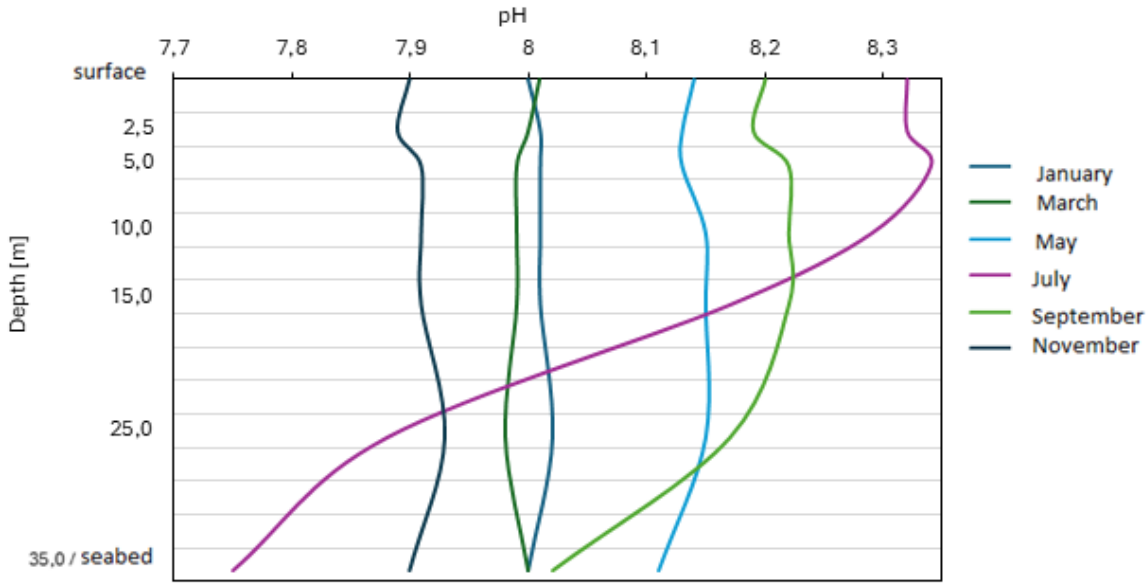


Figure 2.71. The mean pH value changing alongside the depth in the six profiles surveyed in the survey area under individual survey campaigns

The pH value results for the surface water samples collected within the survey area are confirmed by the data from literature, which indicate that the pH value for the Baltic Sea water increases systematically from January to May, stabilises in summer (until August), and then gradually falls (until December), remaining within a pH range of 7.5–8.5 throughout the year (Brutemark et al., 2011).

When comparing the results obtained with the limit values of the water quality indicators for the water quality Class 1 and 2, which apply to the SWBs such as coastal waters, set out in Annex 10 to the Regulation of the Minister of Infrastructure of 25 June 2021 *on the classification of ecological status, ecological potential, chemical status and the method of classifying the status of surface water bodies as well as environmental quality standards for priority substances* (Journal of Laws of 2021, item 1475), it was concluded that the limit values determined for mineral oil index (Class 1 ≥ 7.0–≤ 8.0 and Class 2 ≥ 7.0–≤ 8.8) were not exceeded in any of the samples collected.

2.2.6.3.2 Alkalinity

Alkalinity is understood as the ability of water to neutralise mineral acids. Water owes this property to the following chemicals present in it: bicarbonates, carbonates, and hydroxides, as well as silicates, borates, and phosphates, which are present in small quantities. Alkalinity is one of the parameters which characterise the acid-base balance of the marine waters. It specifies the sum of alkaline components in a sample (hydroxide, carbonate, bicarbonate and other buffering compounds) (Bolałek, Falkowska, 1999; Dojlido, 1995).

The summarised results of alkalinity tests indicate a lack of variability of this parameter in the surface layer of survey area and in the near-seabed layer of water sampled at the depths between 25 and 40 m, depending on the seabed relief. Changes in alkalinity values related to depth are negligible over the entire survey period (Figure 2.72). The difference in the mean water alkalinity values between the surface layer and the water obtained from greater depths in the survey area is insignificant.

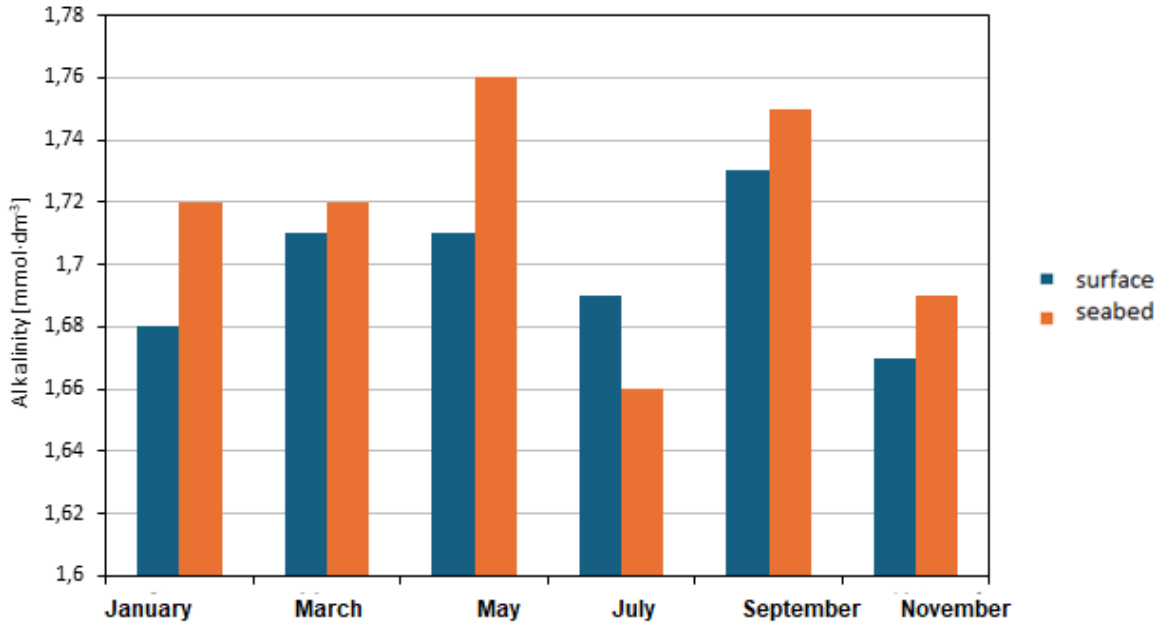


Figure 2.72. The mean alkalinity value in the near-surface and near-seabed layer of water in the survey area during the individual survey campaigns

The parameter that has the greatest impact on the variability of alkalinity of the waters of the southern Baltic Sea is water salinity. Alkalinity decreases with the decrease in salinity and is variable within individual basins of this sea (Hjalmarsson et al., 2008).

The obtained results of alkalinity tests in the surveyed periods do not show variability with depth in all vertical profiles obtained from the survey area. Figure 2.73 presents slight differences in the alkalinity test results obtained in individual layers in all vertical profiles sampled in survey area.

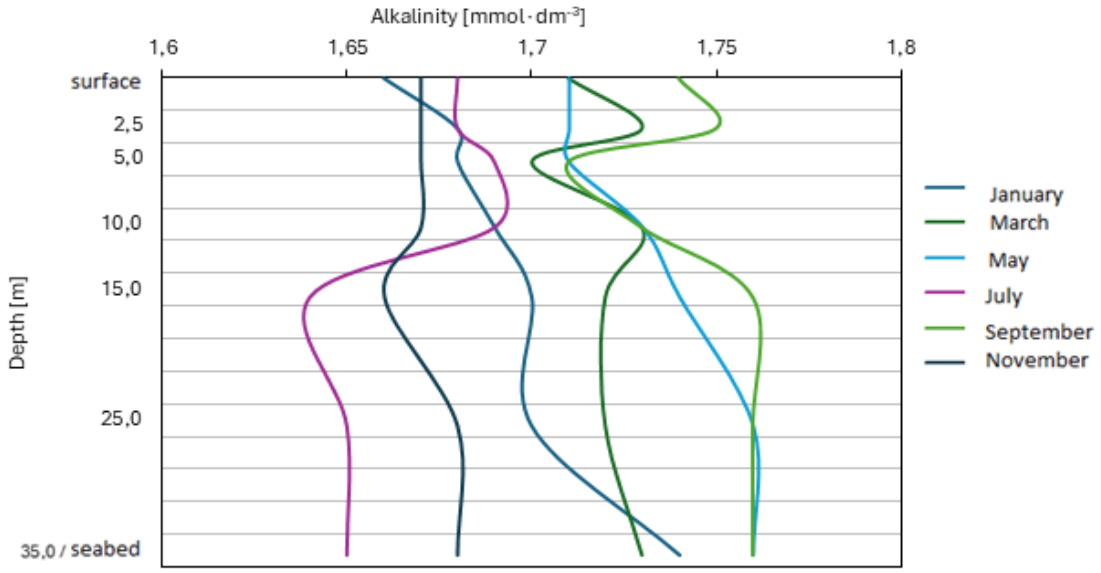


Figure 2.73. The diversification of the mean alkalinity value with depth in the six profiles surveyed in the survey area under individual survey campaigns

The mean of the results of alkalinity tested in the samples from the entire survey area during the entire survey period (1.7 mmol·dm^{-3}) is compliant with the multi-annual data from the literature on the Baltic Sea, according to which it equals approx. 1.7 mmol·dm^{-3} for the sampling location (Hjalmarsson et al., 2008; Ulfsbo et al., 2011).

2.2.6.4 Indicators of nutrient conditions (nutrients)

2.2.6.4.1 Nitrites

In the water samples collected from survey area in the measurement period from January to November 2023, occasional presence of small concentrations of nitrites was found. The mean concentration of nitrites in the entire survey period was below the LOQ of the method used (< 0.003 mg·dm^{-3}). The presence of nitrites was confirmed mainly for the fifth water sampling campaign (September), within a range from < 0.003 to 0.006 mg·dm^{-3}. When analysing the distribution of nitrite nitrogen concentrations with depth in the six profiles surveyed in the survey area, from January to November 2023, nitrites were found in the water samples collected near the seabed in September 2023.

2.2.6.4.2 Nitrates

Nitrates are the final product of nitrogen compounds oxidation. In the euphotic zone of numerous sea areas, nitrates determine the extent of primary production and, therefore, they are classified as substances limiting phytoplankton growth. When sunlight penetrates the water profile to a considerable depth, the processes of assimilation by phytoplankton are more intense than transportation of nitrates from deeper layers to the surface. Hence, the concentration of nitrates in the euphotic zone of numerous water areas is close to zero. The seasonal cycle of nitrates is characterised by high concentrations in autumn, winter and very early spring, and by low concentrations in late spring and summer (Andrulewicz et al., 2008). The level of nitrate concentrations in relation to temperature may be an indicator of upwellings, because in these areas, elevation of nitrates with deep waters proceeds faster than their assimilation, which means that even at times of the peak demand for biogenic salts, there is no shortage of nitrates in these areas.

The concentrations of nitrates in the water samples from the survey area collected in the survey period from January to November 2023 indicated a characteristic seasonal variability. In the period from May to July 2023, the average nitrate concentration in the water samples tested was low and within a range of < 0.003–0.003 mg·dm^{-3}. This state was resulted from an intensive phytoplankton growth in the spring-summer season. A gradual increase in nitrate nitrogen concentrations was observed from September (near-seabed water), through November, until the highest values were reached in the winter period (January–March) The average nitrate concentration values measured in the water samples from the survey area in winter were the highest in January (0.030 mg·dm^{-3} in the near-surface waters and 0.031 mg·dm^{-3} in the near-seabed layer). The increase in the concentrations of nitrates in the autumn and winter season in near-seabed waters was due to an organic matter falling down after the spring and summer phytoplankton bloom and the restoration of the nutrient pool. In March, the concentration decreased from 0.030 to 0.027 mg·dm^{-3} in near-surface water from 0.031 to 0.028 mg·dm^{-3} in near-seabed water, which indicates that the vegetation period was not started at the time of that the survey year. In May, however, there was a significant decrease in nitrate concentrations below the lower limit of detection of the applied method (i.e. below 0.003 mg·dm^{-3}), which indicates that the vegetation period was already developed [Figure 2.74]. The obtained results are consistent with the course of phytoplankton development observed in the entire Baltic Sea. It is characterised by

an intensive though short peak bloom of diatoms in spring, after which other algal blooms take place from mid-summer to autumn. Following the spring bloom, the concentration of nutrients in water decreases sharply. The level remains this low till autumn due to insignificant vertical water motion in summer. The winter inhibition of primary production (due to the insufficient amount of light and heat) enables full regeneration of nutrient supply in the euphotic zone (Andrulewicz et al., 2008). This tendency is also confirmed by the results of the nitrate nitrogen concentrations with the increase of depth in six profiles surveyed in the survey area from January to November 2023 [Figure 2.75]. The presence of nitrates in the deeper layers of water was already observed in September 2023. The concentrations of nitrate nitrogen in the entire surface-to-seabed profile were recorded in January, March, and November 2023, with the highest concentrations in January 2023.

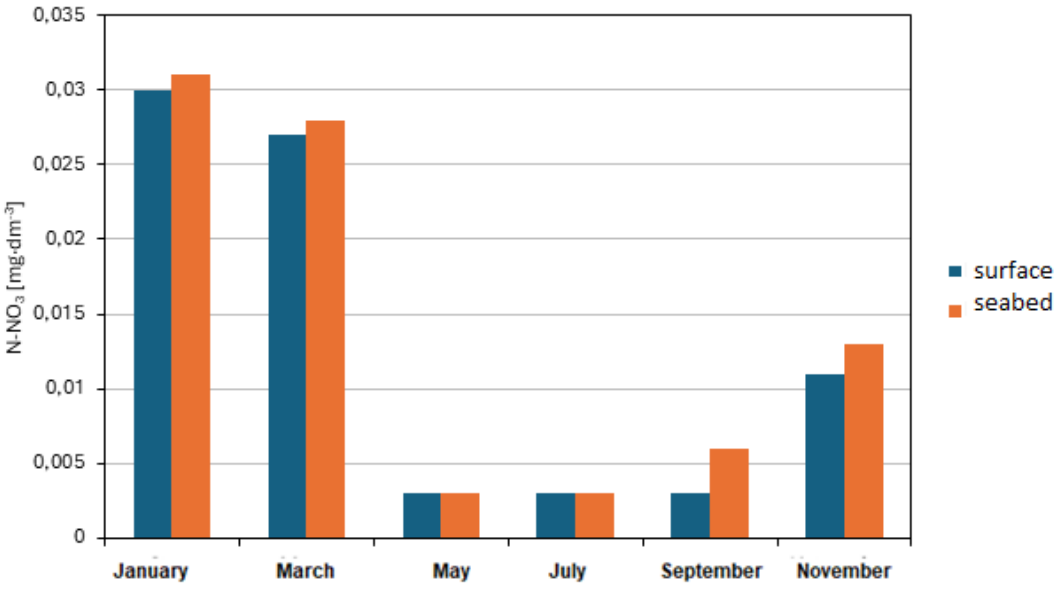


Figure 2.74. The mean nitrate nitrogen concentration values in the near-surface and near-seabed layers from the survey area under individual survey campaigns

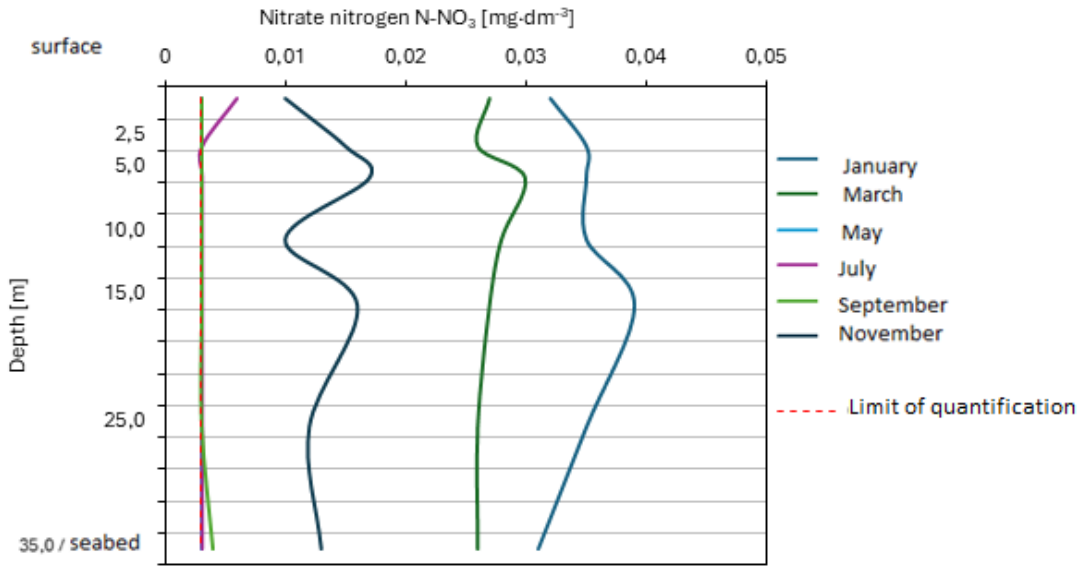


Figure 2.75. The diversification of the average nitrate nitrogen concentration value with depth in the six profiles surveyed in the survey area under individual survey campaigns

The Regulation of the Minister of Infrastructure of 25 June 2021 o*n the classification of ecological status, ecological potential, chemical status and the method of classifying the status of surface water bodies as well as environmental quality standards for priority substances* (Journal of Laws of 2021, item 1475) specifies the limit value of nitrates for the average value of the concentrations measured in the water column from January to March, i.e. in the period of nutrient pool regeneration in the water. The average content of nitrate nitrogen measured in the water samples collected from in the water column in the survey area in January and March 2023 was 0.031 mg·dm^{-3} and did not exceed the limit value (0.05 mg·dm^{-3}) specified for Class 1 of water quality for SWBs such as coastal waters.

2.2.6.4.3 Ammoniacal nitrogen (ammonia)

The concentrations of ammonia in oxygenated and unpolluted waters rarely exceed the value of 5 µmol·dm^{-3} (0.092 mg·dm^{-3}). However, when conditions are changing into anaerobic, ammonia concentration may be as high as 100 µmol·dm^{-3} (0.092 mg·dm^{-3}). In anaerobic conditions, a denitrification of nitrate ions takes place, which leads to the formation of ammonia and molecular nitrogen. Also, during bacterial sulphate reduction in the deep waters, apart from hydrogen sulphide, ammonia is also produced. In the marine environment, alongside ammonium ions, NH_3 is also present in the form of non-ionised molecules. The NH_3 concentration depends on changes in pH and temperature. At the pH of 8.2 and temperature of 5°C, only about 1.9% of ammonia occurs in form of undissociated NH_3, but at the same pH and temperature of 25°C of water the share of this form increases to 8.1%. The degree of proportion of individual ammonia forms is extremely important, because the NH_3 form is toxic, for example, to fish, in contrast to NH_4^+ (Falkowska et al., 1999).

In the seawater samples collected from survey area in the measurement period from January to November 2023, occasional presence of small concentrations of ammoniacal nitrogen was found. The mean concentration of ammonia in the entire survey period was below the LOQ of the method used (< 0.003 mg·dm^{-3}).

The Regulation of the Minister of Infrastructure of 25 June 2021 *on the classification of ecological status, ecological potential and chemical status and the method of classification of the status of surface water bodies and the environmental quality standards for priority substances* (Journal of Laws of 2019, item 1475) does not specify the limit value for ammoniacal nitrogen.

2.2.6.4.4 Mineral nitrogen (DIN)

Mineral nitrogen (DIN) denotes the sum of nitrites, nitrates and ammonium ions. In the seawater samples collected from survey area from January to November 2023, DIN included mainly nitrates. As in the case of nitrates, the DIN content in the water samples collected in the survey area was confirmed in all the samples collected in January, March and in the majority of samples collected in November 2023 [Figure 2.76]. The distribution of DIN concentrations in the vertical profiles is presented below on a graph [Figure 2.77].

The Regulation of the Minister of Infrastructure of 25 June 2021 *on the classification of ecological status, ecological potential, chemical status and the method of classifying the status of surface water bodies as well as environmental quality standards for priority substances* (Journal of Laws of 2021, item 1475) specify the limit value of DIN for the concentrations measured from January to March (as the mean from the water column), i.e. in the period of the nutrient pool reconstruction in water. The mean DIN concentration in the water column in the water samples from the survey area collected in January and March 2023, equalled 0.031 mg·dm^{-3} and did not exceed the limit value (0.06 mg·dm^{-3}), specified for water quality Class 1 of the SWBs such as coastal waters.

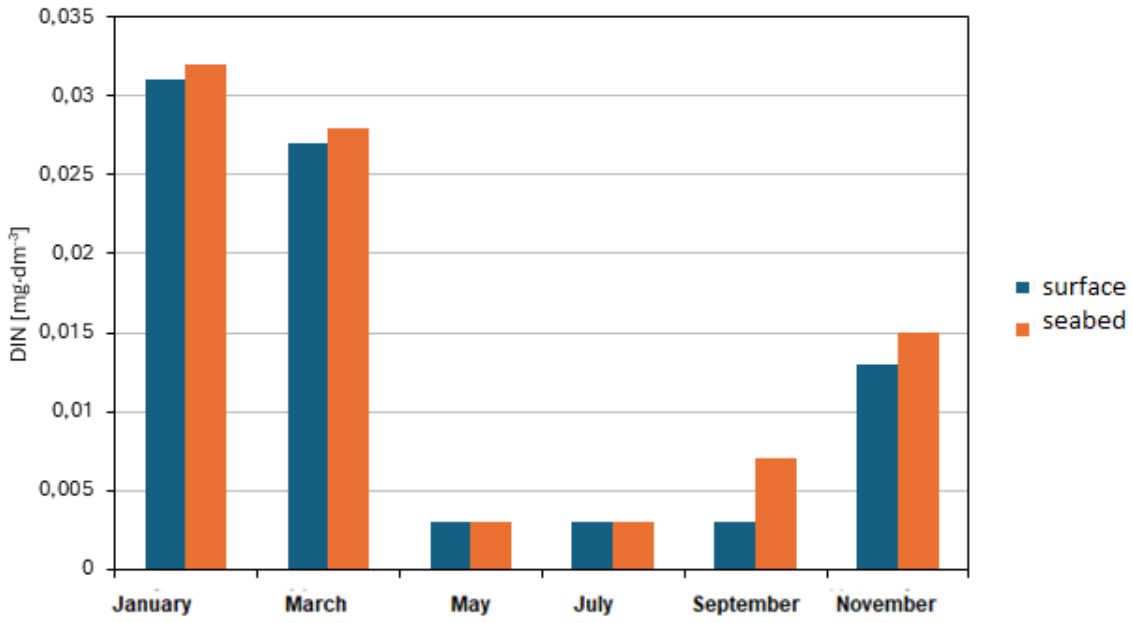


Figure 2.76. The mean values of the mineral nitrogen concentrations (DIN) in the near-surface and near-seabed water in the survey area in individual survey campaigns

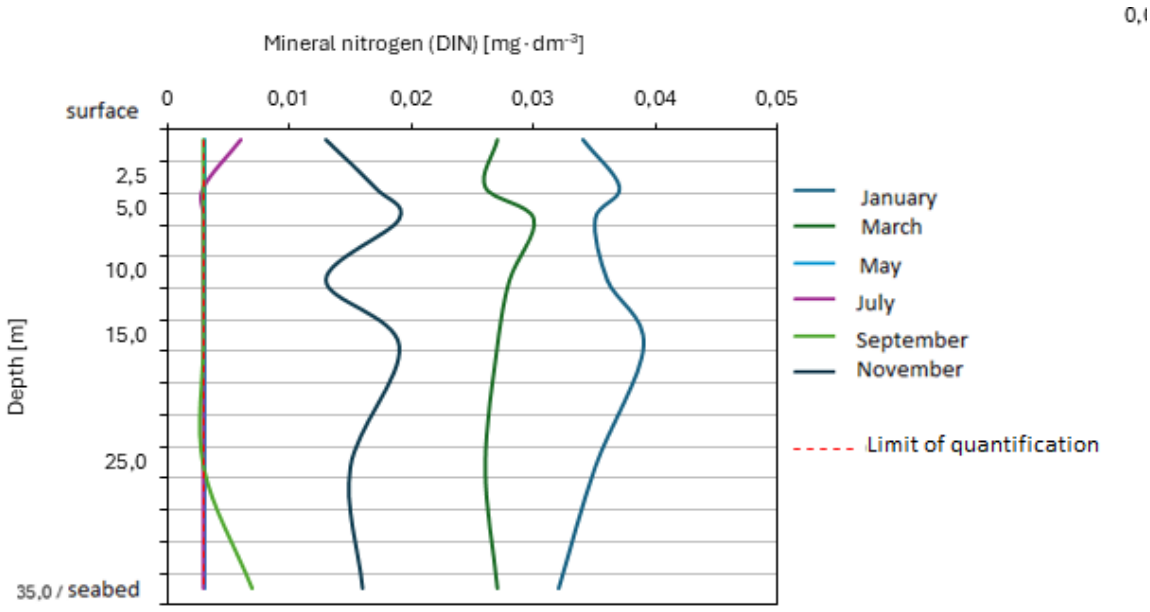


Figure 2.77. The diversification of the mean mineral nitrogen concentration (DIN) value with depth in the six profiles surveyed in the survey area under individual survey campaigns

2.2.6.4.5 Total nitrogen

In natural seawater, organic nitrogen compounds are present in dissolved or suspended forms. The suspended fraction consists of cells of living micro-organisms and dead organic matter. The concentration of organic nitrogen in suspended form ranges from trace amounts up to approx. 0.07 mg·dm^{-3}. The concentrations of dissolved organic nitrogen compounds may exceed the level of 1.4 mg·dm^{-3}. Almost half of this amount is the so-called nitrogen albumin, which consists of nitrogen of unsubstituted amino groups of numerous amino acids, polypeptides and proteins. Some of the dissolved organic nitrogen compounds are combinations containing nitrogen derived from animal excrement, and compounds released from detritus. Small amounts of nitrogen (approx. 0.03 mg·dm^{-3}) come from the urea, and even smaller from the humic substances (Falkowska et al., 1999).

The average concentration of the total nitrogen in the water samples collected in the survey area was similar in the entire survey period and fell within the range from 0.08 to 0.13 mg·dm^{-3} [Figure 2.78]. The highest total nitrogen concentration was observed in the fourth water sampling campaign.

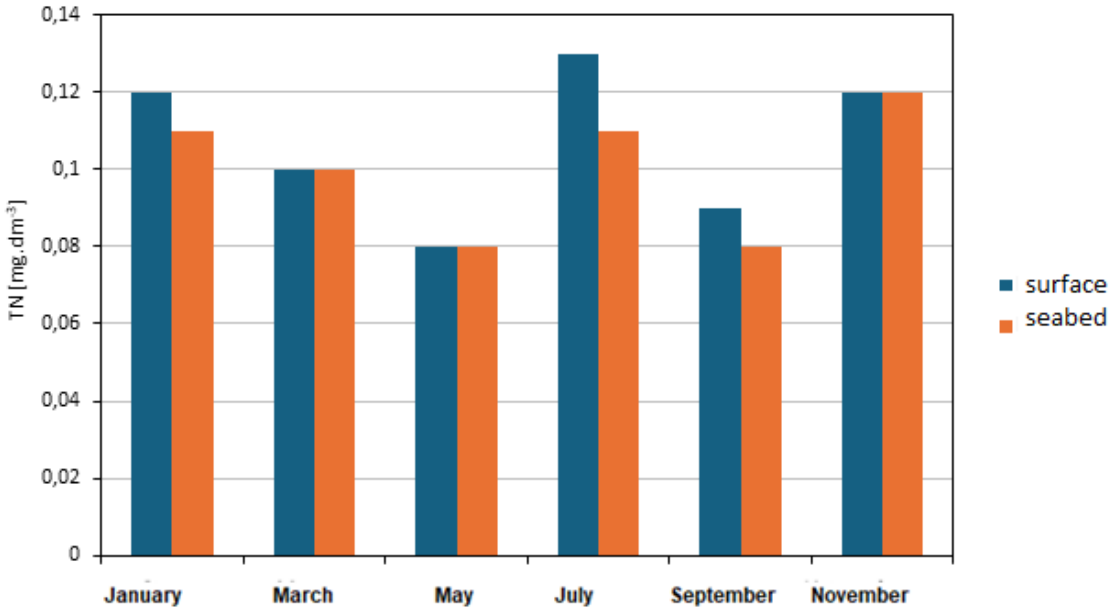


Figure 2.78. The mean total nitrogen concentration values in the near-surface and near-seabed layer of water in the survey area under individual survey campaigns

An analysis of total nitrogen concentrations distribution in vertical profiles in the survey period from January to November 2023 did not reveal any significant differences [Figure 2.79]. The vertical distribution of nutrient concentrations depends on the local hydrological conditions. Heterogeneity occurs in deeper regions of the Baltic Sea, where a clearly marked halocline appears. In general, haloclines are also "nutrient separators" dividing surface waters with lower concentrations of nutrients from near-seabed waters rich in these substances. Because the decomposition and mineralisation of a large part of the matter take place mainly in the deeper, near-seabed water and sediment layers, these environments constitute a reservoir of nutrients (Andrulewicz et al., 2008).

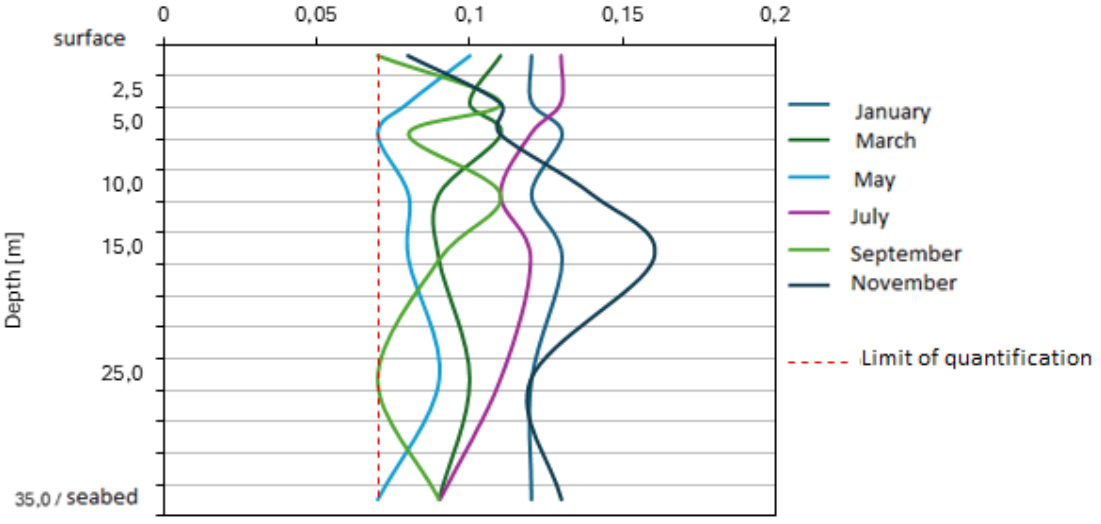


Figure 2.79. The diversification of the mean total nitrogen concentration value with depth in the six profiles surveyed in the survey area under individual survey campaigns

The results obtained for the total nitrogen indicate that the waters of the survey area analysed fall into Class 1 of water quality for the SWBs such as coastal waters (exclusively on the basis of the total nitrogen concentration). The Regulation of the Minister of Infrastructure of 25 June 2021 *on the classification of ecological status, ecological potential, chemical status and the method of classifying the status of surface water bodies as well as environmental quality standards for priority substances* (Journal of Laws, item 1475) specifies the limit value measured from June to September, i.e. during the period of the most intense growth. The limit value for water quality Class 1 is < 0.25 mg·dm^{-3}. The mean concentration of total nitrogen for samples collected from survey area in July and September was 0.10 mg·dm^{-3} (the mean calculated for the water column).

2.2.6.4.6 Phosphates

In the euphotic zone of numerous sea areas, in the case of the deficiency of nitrogen compounds, the phosphates may determine the extent of primary production and therefore, they are also classified as substances limiting the growth of phytoplankton. The suppression of phytoplankton growth by phosphorus plays a very important role in the northern area of the Gulf of Bothnia, and the eastern area of the Gulf of Riga, as well as locally in the remaining areas of the Baltic Sea (Andrulewicz et al., 2008). Phytoplankton development is similar in the entire area of the Baltic Sea and It is characterised by an intensive though short peak bloom of diatoms in spring, after which other algal blooms take place from mid-summer to autumn causing a decrease in the level of nutrients in the water. The winter inhibition of primary production (due to the insufficient amount of light and heat) enables full regeneration of nutrient supply in the euphotic zone (Andrulewicz et al., 2008).

Similar seasonal changes in the concentrations of phosphates were observed in water samples collected from survey area in the studied period from January to November 2023 [Figure 2.80]. During the autumn-winter period of the nutrient pool reconstruction (January–March and November 2023), the average phosphate concentration values measured in the water samples from the survey area, from the near-surface and near-seabed layers, were from 0.014 to 0.016 mg·dm^{-3} and did not indicate differences between the near-surface and near-seabed layer of the waters analysed. In the remaining months, the average values of phosphate concentrations decreased as a result of the phytoplankton growth to < 0.009–0.015 mg·dm^{-3} in the near-surface layer and to < 0.009–0.017 mg·dm^{-3} near the seabed.

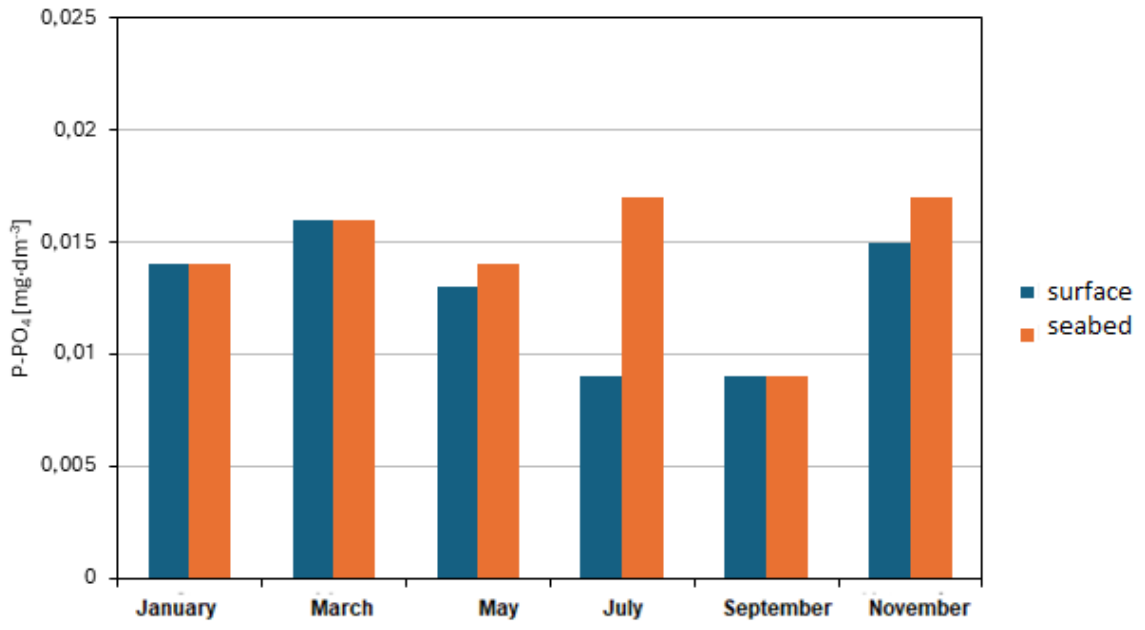


Figure 2.80. The mean total phosphorus concentration values in the surface and near-seabed layer of water in the survey area under individual survey campaigns

An analysis of phosphate concentrations distribution in vertical profiles in the survey period from January to November 2023 indicated an even concentration distribution in the water column. A slight increase in the total phosphorus concentrations near the seabed was observed in July 2023 [Figure 2.81]. The vertical distribution of nutrients concentrations depends on the local hydrological conditions. The diversification is present in the deeper regions of the Baltic Sea, where a distinct halocline can be observed. The vertical distribution of phosphorus compound concentrations is the same as in the case of nitrogen and is characterised by an increase in their concentration in the near-seabed layer with higher salinity (periodical influx of water from the deeper layers below the halocline). The anoxic environment also increases the phosphate content in the water (Andrulewicz et al., 2008).

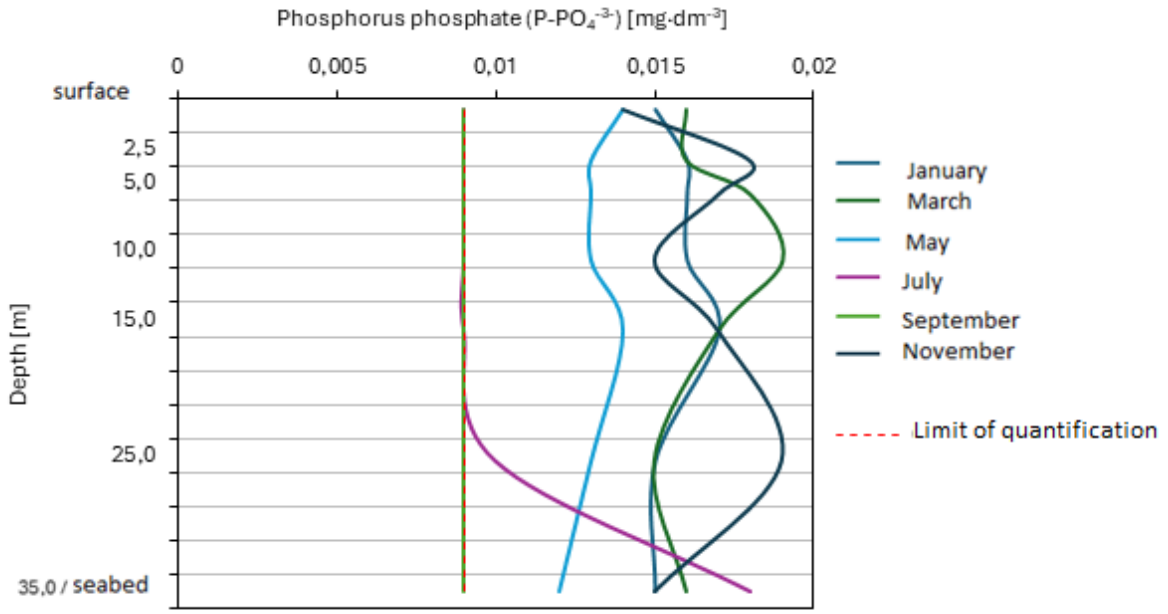


Figure 2.81. The diversification of the mean phosphate phosphorus concentration value with depth in the six profiles surveyed in the survey area under individual survey campaigns

The results obtained for phosphate concentrations in the water samples from the survey area exceed the limit value for Class 2 (< 0.015 mg·dm^{-3}) of the SWBs such as coastal waters, including highly modified surface water bodies, specified in the Regulation of the Minister of Infrastructure of 25 June 2021 *on the classification of ecological status, ecological potential, chemical status and the method of classifying the status of surface water bodies as well as environmental quality standards for priority substances* (Journal of Laws of 2021, item 1475). The mean concentration of phosphates found in the samples collected in January and March 2023 was 0.016 mg·dm^{-3} (the mean calculated for the water column).

2.2.6.4.7 Total phosphorus

The mean concentration of total phosphorus for samples collected in the survey area in winter (January and March 2023) fell within the range of 0.019–0.022 mg·dm^{-3} in the near-surface and near-seabed layers. A decrease in total phosphorus concentrations was observed in September 2023 (to 0.010 mg·dm^{-3} in the near-surface waters and to 0.013 mg·dm^{-3} in the near-seabed waters) [Figure 2.82].

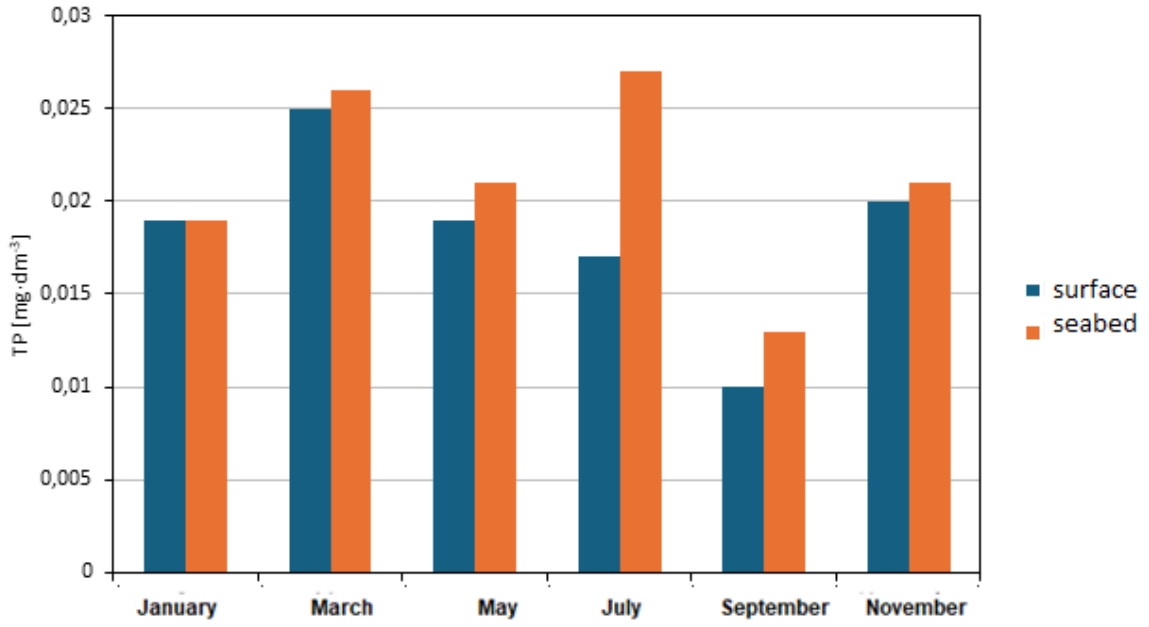


Figure 2.82. The mean total phosphorus concentration values in the surface and near-seabed layer of water in the survey area under individual survey campaigns

Vertical distributions of total phosphorus concentrations in the analysed period from January to November 2023 in the water samples collected from survey area show fairly uniform values from the surface to the seabed. An increase in the total phosphorus concentrations near the seabed were observed in July and September 2023 [Figure 2.83].

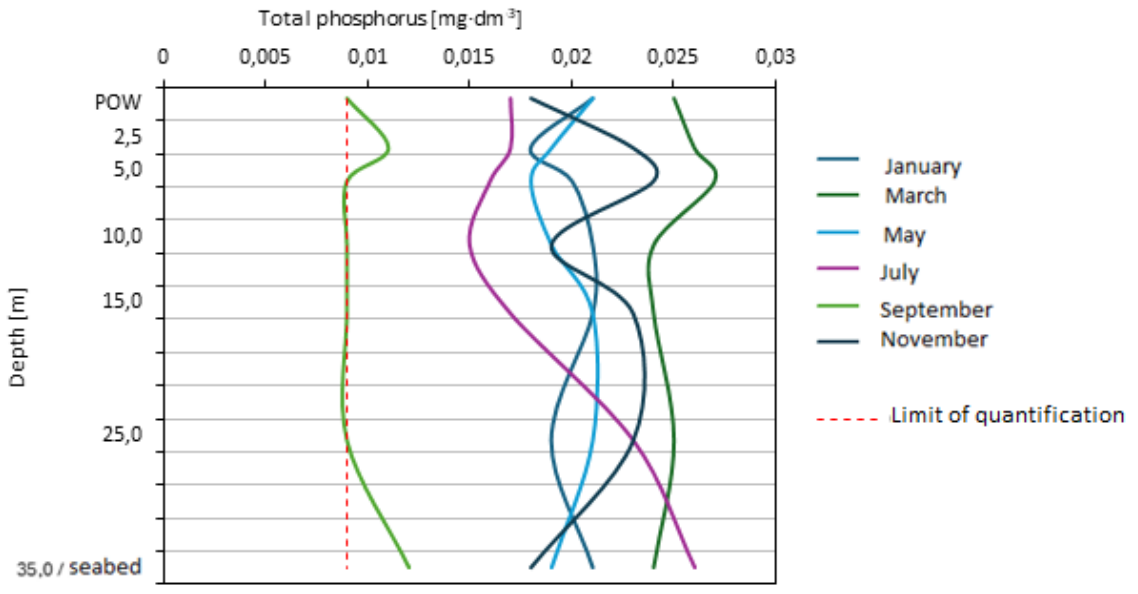


Figure 2.83. The diversification of the mean total phosphorus concentration value with depth in the six profiles surveyed in the survey area under individual survey campaigns

The mean concentration of total phosphorus in the water column in July and September was 0.016 mg·dm^{-3} and it did not exceed the limit value (< 0.020 mg·dm^{-3}) for Class 1 water quality specified in the Regulation of the Minister for Infrastructure of 25 June 2021 *on the classification of ecological*

status, ecological potential and chemical status and the method of classification of the status of surface water bodies and the environmental quality standards for priority substances (Journal of Laws of 2021, item 1475). This regulation specifies the limit values based on the months from June to September, i.e. in the period of the most intense growth.

2.2.6.5 Specific synthetic and non-synthetic contaminants and a group of chemical indicators characterising the presence of substances particularly harmful to the aquatic environment and the priority substances in the field of water policy

2.2.6.5.1 Metals and metalloids

The metals tested (Pb, Cd, Cr, TCr, Cr (VI), As, Ni, Hg, Al) were present in the waters of the survey area in very low concentrations. The mean concentrations in the near-surface and near-seabed layers were as follows: arsenic – 0.00015 mg·dm^{-3}, total chromium – 0.00003/0.00015 mg·dm^{-3}, cadmium – 0.02 µg·dm^{-3}, nickel – 0.95 µg·dm^{-3}, lead – 0.15/< 0.01 µg·dm^{-3}, aluminium – 0.009/0.010 mg·dm^{-3}, while the concentrations of mercury and chromium (IV) were below the lower LOQ, i.e. Cr (VI) < 0.005 mg·dm^{-3} and Hg < 0.05 µg·dm^{-3}.

The vertical distributions of concentrations of the elements analysed in the water samples collected from the survey area in July 2023, did not indicate a depth-dependant variability.

When comparing the results obtained for average metal concentrations in the waters of the survey area with the limit values of indicators for water quality applying to the SWBs such as coastal waters, set out in Annex 11 to the Regulation of the Minister of Infrastructure of 25 June 2021 *on the classification of ecological status, ecological potential, chemical status and the method of classifying the status of surface water bodies as well as environmental quality standards for priority substances* (Journal of Laws, item 1475), it was concluded that the average concentration values recorded within the survey area for individual metals did not exceed the allowable values which were the following: Cr (VI) – ≤ 0.02 mg·dm^{-3} and As – ≤ 0.05 mg·dm^{-3}.

When comparing the results obtained for average metal concentrations in the waters of the survey area with the limit values of indicators for water quality applying to the SWBs such as coastal waters, set out in Annex 11 to the Regulation of the Minister of Infrastructure of 25 June 2021 *on the classification of ecological status, ecological potential, chemical status and the method of classifying the status of surface water bodies as well as environmental quality standards for priority substances* (Journal of Laws, item 1475), it was concluded that none of the results obtained for Cd, Pb, Ni and Hg from the survey area exceeded the maximum allowable concentrations (MAC-EQS), which are the following: Cd – 1.5 µg·dm^{-3}, Pb – 14 µg·dm^{-3}, Ni – 34 µg·dm^{-3}, and Hg 0.07 – mg·dm^{-3}. For cadmium, the limit value assumed was the one for the water with the total hardness above 200 mg $CaCO_3$·dm^{-3}, since the water in the surveyed area has the hardness above 1100 mg $CaCO_3$·dm^{-3}. The following annual average values for Cd, Pb, and Ni, were also not exceeded in the seawater tested: Cd – 0.2 µg·dm^{-3}, Pb – 1.3 µg·dm^{-3}, and Ni – 8.6 µg·dm^{-3}.

The concentrations obtained for cadmium and lead are congruent with the data for the content of these indicators in the waters of the Eastern Gotland Basin, presented in the latest HELCOM report published in July 2023 [HELCOM, 2023 (Cd); HELCOM, 2023 (Pb)].

Since 1 January 2022, §24 and Annex 26 to the Regulation of the Minister of Infrastructure of 25 June 2021 o*n the classification of ecological status, ecological potential, chemical status and the method of classifying the status of surface water bodies as well as environmental quality standards for priority*

substances (Journal of Laws of 2021, item 1475), which set out the limit values for the surface water quality Class 2 based on the indicators such as total chromium and aluminium are no longer applicable. These were as follows: total chromium – 0.05 mg·dm^{-3} and aluminium – 0.4 mg·dm^{-3}. The current Annex 11 to the same regulation does not include these indicators, and thus, does not provide the current limit values for them. However, for illustrative purposes, after comparing the results obtained for the concentrations of total chromium and aluminium in the waters of the survey area to the no longer applicable limit values of indicators for water quality applying to the SWBs of all categories, set out in Annex 26, it was concluded that none of the indicators analysed exceeded the allowable values.

2.2.6.5.2 Phenol index and cyanides (free and bound)

In all the analysed water samples from the survey area, the contents of phenol index and free and bound cyanides were below the LOQ of the methods used (i.e., respectively: 0.001 mg·dm^{-3}, 0.005 mg·dm^{-3}, 0.005 mg·dm^{-3}).

Since 1 January 2022, §24 and Annex 26 to the Regulation of the Minister of Infrastructure of 25 June 2021 *on the classification of ecological status, ecological potential, chemical status and the method of classifying the status of surface water bodies as well as environmental quality standards for priority substances* (Journal of Laws of 2021, item 1475), which set out the limit values for surface water quality Class 2 based on the indicators such as free and bound cyanides and volatile phenols are no longer applicable. These were as follows: phenols – 0.1 mg·dm^{-3}, free cyanides – 0.05 mg·dm^{-3} and bound cyanides – 0.05 mg·dm^{-3}. The current Annex 11 to the same regulation does not include these indicators, and thus, does not provide the current limit values for them. However, for illustrative purposes, after comparing the results obtained for phenol and cyanide concentrations in the waters of the survey area to the no longer applicable limit values of indicators for water quality applying to the SWBs of all categories, set out in Annex 26, it was concluded that none of the indicators analysed exceeded the allowable values.

2.2.6.5.3 Mineral oil index

Crude oil, when spilt at sea, undergoes many processes which have a great influence on the distribution of its residues in the marine environment. The parameter which characterises this group of pollutants is the mineral oil index. Oil spillages pollute water by creating an oily layer on its surface. Depending on the quality of oil, the spillages may also mix or dissolve in the water. Currently, any discharges into the Baltic Sea of oil or diluted mixtures containing oil in any form including crude oil, fuel oil, oil sludge, or refined products are prohibited. This applies also to oily waters from the engine room of any ship, as well as from ballast or cargo tanks from oil tankers (HELCOM, 2006; HELCOM, 2012).

The mineral oil index tested in the water samples from the survey area in summer equalled 0.05 mg·dm^{-3} reaching the maximum value of 0.22 mg·dm^{-3} near the seabed in the sample collected at survey station SW_MFW_27.

The obtained results did not reveal differences between the surface and near-seabed water layers. Also, the analysis of mineral oil index concentrations distribution in vertical profiles did not reveal any significant differences.

When comparing the results obtained with the limit values of the water quality indicators for the water quality Class 1 and 2, which apply to the SWBs such as coastal waters, set out in Annex 11 to the Regulation of the Minister of Infrastructure of 25 June 2021 *on the classification of ecological status, ecological potential, chemical status and the method of classifying the status of surface water bodies*

as well as environmental quality standards for priority substances (Journal of Laws of 2021, item 1475), it was concluded that the limit value for mineral oil index (Classes 1 and 2 – ≤ 0.2 mg·dm^{-3}) was exceeded in one sample collected in the near-seabed layer (survey station SW_MFW_27). This exceedance is incidental, within the measurement uncertainty of the analytical method applied. On the other hand, the average concentration value of mineral oils in the water within the survey area is 0.05 mg·dm^{-3} and does not exceed the limit value.

2.2.6.5.4 Polycyclic aromatic hydrocarbons (PAHs)

The concentrations of the sum of PAHs found in the water samples collected in the survey area were slightly higher than the ones described in literature (HELCOM, 2002; Witt, 2002) and fell between the lower LOQ (0.001 µg·dm^{-3}) and 0.045 µg·dm^{-3}, which may result from the differences at the stage of sample preparation for testing (PAHs were determined in the water without the separation of suspended solids, in accordance with the reference methodology).

PAHs present in the water can undergo many changes as well as have significant impact on the environment. The scope of impact depends on the transformations that these compounds undergo. These can be abiotic processes such as sorption, elution, oxidation, photodegradation, reactions with other compounds, and biological processes, such as microbiological transformations. Polycyclic aromatic hydrocarbons may stimulate or inhibit the growth of microorganisms, have a phytotoxic or stimulating influence on the growth of plants as well as be toxic to fauna (Galer et al., 1997).

Multi-annual observations show that the concentration of PAHs in the Baltic Sea waters is characterised by a cycle of seasonal changes – the highest values are obtained in the winter months and decrease after the spring bloom of algae, dropping to the lowest levels in summer, to increase again in the late autumn months. Such a cycle is consistent with the changes in temperature, the amount of suspended solids in the water and the number of sources of such compounds in the environment (combustion) (Witt, 2002).

Vertical distributions of PAHs concentrations in the water samples collected from the survey area show quite even a distribution of concentrations with slight fluctuations in the content from the surface to the seabed [Figure 2.84].

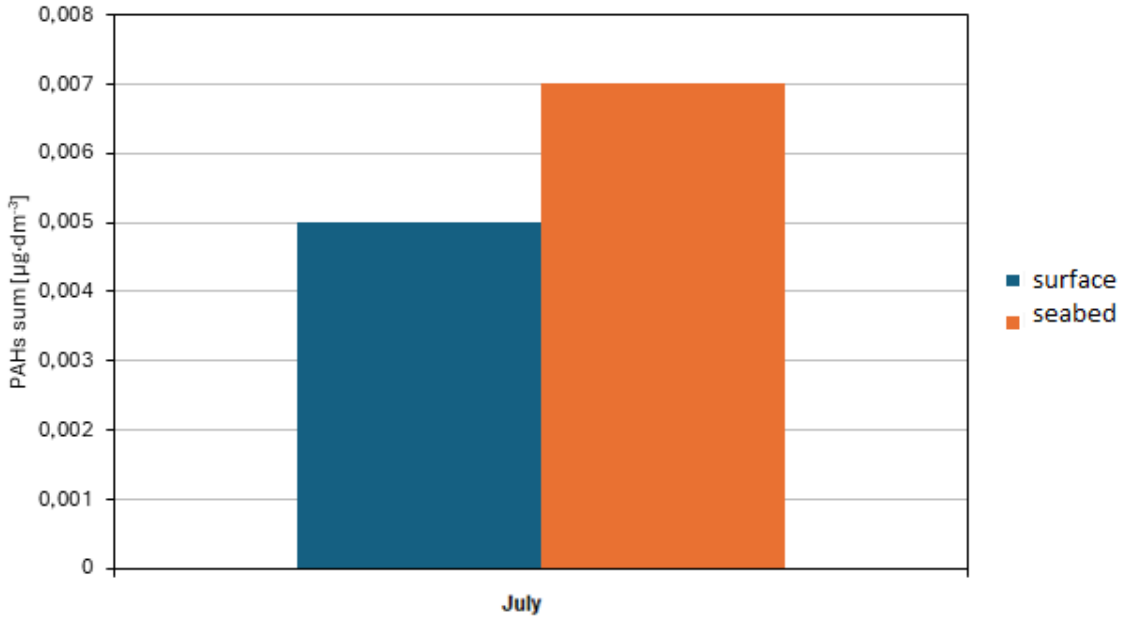


Figure 2.84. The change of the mean concentration values of PAHs in the water sampled in the survey area in August 2023

Comparing the results obtained with the limit values of indicators for the water quality applying to the SWBs such as coastal waters, specified in Annex 14 to the Regulation of the Minister of Infrastructure of 25 June 2021 o*n the classification of ecological status, ecological potential, chemical status and the method of classifying the status of surface water bodies as well as environmental quality standards for priority substances* (Journal of Laws of 2021, item 1475), it was concluded that specified concentration limits expressed as the maximum allowable concentrations for naphthalene (130 µg·dm^{-3}), anthracene (0.1 µg·dm^{-3}), fluoranthene (0.12 µg·dm^{-3}), benzo(a)pyrene (0.027 µg·dm^{-3}), benzo(b)fluoranthene and benzo(k)fluoranthene (0.017 µg·dm^{-3}) and benzo(g,h,i)perylene (limit value 0.00082 µg·dm^{-3}) were not exceeded in any of the water samples collected in the survey area.

2.2.6.5.5 Polychlorinated biphenyls (PCBs)

In all the water samples analysed from the survey area analysed, the content of the sum of 7 PCBs was below the LOQ of the analytical methods applied (i.e. 0.001 µg·dm^{-3}).

Many years of monitoring the concentrations of PCBs in the Baltic Sea demonstrated rather low concentrations of these compounds. For example, the concentration of PCB 153, one of the main congeners, was in the range from 10 to 24 pg·dm^{-3} (the mean values in the period of 1994–1998). The authors of this Report could not determine the time trends, because of the low concentration and the fact, that many of the samples tested were below the detection limit of the tests. Also, no evidence of geographical changes in concentration has been found, except for a general increase in concentration towards the coast. It has also been established, that due to their high lipophilicity, PCBs are enriched in suspended solids and in seabed sediment (HELCOM, 2002).

The test results obtained for the PCB concentrations in the water samples collected in the survey area in the summer period, do not deviate from the data from literature on the surface waters of the

Southern Baltic (Sapota, 2004; Kot-Wasik et al., 2004) and indicate a possible continuous decrease in the concentration of these pollutants.

The vertical distributions of PCBs concentrations in the analysed water samples taken in survey area cannot be analysed as the results obtained are below the limit of quantification of the method.

2.2.6.6 Radionuclides

The breakdown of the nuclear power plant in Chornobyl in 1986 significantly changed the level of pollution of the Baltic Sea. Most hazardous radioactive substances have undergone a fast decay (up to several months after the disaster). 1% of substances emitted in the atmosphere remained in the aquatic environment.

In the environment of the Baltic Sea, the contamination with ^{137}Cs, ^{90}Sr, ^{134}Cs proved to be the most significant. In 1986, the Bothnian Sea and Gulf of Finland were the most contaminated areas. 15% to 30% of the total load of ^{137}Cs received by the Baltic Sea waters reached the waters of the Baltic Proper.

The activity of radioactive substances in seawater in particular areas of the Baltic Sea has undergone a decrease and levelling since 1986, as a result of pass of time and hydrological phenomena such as movement of masses of water from one sea area to another. The radioactivity level in the Baltic Sea is still elevated in relation to the state from before 1986. It is estimated that with the maintenance of the hitherto trend of decrease in activity of radioactive substances in the marine environment, the state from before the disaster will have been recovered in 2035.

Concentrations of tested radionuclides in water samples collected from the survey area did not show differences between activity in surface waters and near-seabed waters. The average measured activity of ^{137}Cs in water was 16.79 Bq·m^{-3}, while the concentration values fell between 15.54 and 18.42 Bq·m^{-3}. On the other hand, the mean activity of ^{90}Sr in the water samples collected in the survey area oscillated at a level of 4.54 Bq·m^{-3} and the concentration values fell between 3.80 and 5.60 Bq·m^{-3}.

In the case of both ^{90}Sr as well as ^{137}Cs isotopes, no significant differences were observed in the activities of the isotopes analysed in the samples. The mean ^{90}Sr activities at individual levels were similar and fell between 5.0–5.6 Bq m^{-3} and the greatest range of activity was characteristic for the waters collected at a depth of 5 m (4.10–5.60 Bq·m^{-3}). In the case of ^{137}Cs as in the case of ^{90}Sr, the average activities at individual levels were similar and fell between 16.0 and 17.3 Bq·m^{-3}, while the greatest variation in radioactivity was found in the near-seabed waters (15.54–18.42 Bq·m^{-3}).

In compliance with the predictions, these values are lower than the concentrations recorded in 2010, when the average ^{137}Cs activity was recorded at a level of 32 Bq·m^{-3} in the near-surface water layer and at 34 Bq·m^{-3} in the near-seabed layer and the average activity recorded for ^{90}Sr was 8.5 Bq·m^{-3} on the surface and 9 Bq·m^{-3} near the seabed (Zalewska, Suplińska, 2013). The values were also lower than the results obtained in 2017 for ^{137}Cs in the range from 12.4 to 20.4 Bq·m^{-3}, and for ^{90}Sr in the range from 5 to 12 Bq·m^{-3} in the waters of the Southern Baltic and from the ones obtained in 2018 for ^{137}Cs in the range from 13.2 to 27.8 Bq·m^{-3}, and for ^{90}Sr in the range from 4.3 to 9.5 Bq·m^{-3} (Krzymiński, 2018; Zalewska, Kraśniewski, 2019). That downward trend of the ^{137}Cs concentration results is also confirmed by the latest HELCOM report published in July 2023 and the concentration values obtained are congruent with the data on the content of these indicators in the Eastern Gotland Basin (HELCOM, 2023 (Cs137)).

On the other hand, the results obtained were comparable with the results of the monitoring carried out in 2021 as part of the SEM by IMWM-NRI at 17 stations located in the Polish Exclusive Economic Zone in the Baltic Sea, where the mean radioactive concentration of ^{137}Cs in seawater was 15.6 Bq·m^{-3} and the mean radioactive concentration of ^{90}Sr was 4.9 Bq·m^{-3} (Zalewska, Kraśniewski, 2022).

2.2.6.7 A summary of results obtained for the survey area

The results of the physicochemical analyses carried out in the period discussed, characterising the water quality status are representative of the survey period analysed and can be used to assess the water quality in the survey area. No anomalous concentration values were reported for any of the indicators tested in the water samples analysed.

These waters had an alkaline reaction (approx. pH 8.1) and alkalinity of approx. 1.7 mmol·dm^{-3} and were relatively well-oxygenated. The mean content of dissolved oxygen in the survey area was always above the limit value of 6.0 mg·dm^{-3}.

Comparing the results obtained from the water surveys with the threshold values specified in the Regulation of the Minister of Infrastructure of 25 June 2021 *on the classification of ecological status, ecological potential, chemical status and the method of classifying the status of surface water bodies as well as environmental quality standards for priority substances* (Journal of Laws of 2021, item 1475), the survey area surveyed can be classified as water Class 1 (very good status) due to the concentrations of nitrate nitrogen, DIN as well as total nitrogen and total phosphorus. However, due to the phosphate phosphorus content (the average concentration of which in the water column was 0.016 mg·dm^{-3}), the waters tested did not present good quality.

The assessment of quality in terms of specific synthetic and non-synthetic pollutants as well as a group of chemical indicators characterising substances particularly harmful to the aquatic environment and priority substances in the field of water policy, i.e. metals (Pb – 14 µg·dm^{-3}, Cd – 0.45 µg·dm^{-3}, Cr (VI) – 0.02 mg·dm^{-3}, As – 0.05 mg·dm^{-3}, Ni – 34 µg·dm^{-3}, Hg – 0.07 µg·dm^{-3}), mineral oil index – 0.2 mg·dm^{-3}, and PAHs (naphthalene – 130 µg·dm^{-3}, anthracene – 0.1 µg·dm^{-3}, fluoranthene – 0.12 µg·dm^{-3}, benzo(a)pyrene – 0.027µg·dm^{-3}, benzo(b)fluoranthene and benzo(k)fluoranthene – 0.017 µg·dm^{-3}, benzo(g,h,i)perylene – limit value 0.00082 µg·dm^{-3}) carried out in the water samples collected in July 2023, indicated that the limit values were not exceeded in the water samples collected in the survey area. One exception is the mineral oil index with a value of 0.22 mg·dm^{-3} determined in a water sample from survey station SW_MFW_27 in the near-seabed water layer. This exceedance is incidental, within the measurement uncertainty of the analytical method applied. On the other hand, the average concentration value of mineral oils in the water within the survey area is 0.05 mg·dm^{-3} and does not exceed the limit value. Limit values are given in the units of measurement in which they are indicated in the regulation to which they are referenced (Journal of Laws of 2021, item 1475).

Since 1 January 2022, §24 and Annex 26 to the Regulation of the Minister of Infrastructure of 25 June 2021 *on the classification of ecological status, ecological potential, chemical status and the method of classifying the status of surface water bodies as well as environmental quality standards for priority substances* (Journal of Laws of 2021, item 1475), which set out the limit values for the surface water quality Class 2 based on the indicators such as total chromium, aluminium, free and bound cyanides, and volatile phenols, are no longer applicable. These were as follows: total chromium – 0.05 mg·dm^{-3}, aluminium – 0.4 mg·dm^{-3}, phenols – 0.01 mg·dm^{-3}, free cyanides – 0.05 mg·dm^{-3} and bound cyanides – 0.05 mg·dm^{-3}. The current Annex 11 to the same regulation does not include these indicators, and thus,

does not provide the current limit values for them. However, for illustrative purposes, after comparing the results obtained for the concentrations of total chromium, aluminium, phenols and cyanides in the waters of the survey area to the no longer applicable limit values of indicators for water quality applying to the SWBs of all categories, set out in Annex 26, it could be concluded that none of the indicators analysed exceeded the allowable values.

In all the water samples analysed from the survey area analysed, the content of the sum of 7 PCBs was below the LOQ of the analytical methods applied (i.e. 0.001 $\mu g \cdot dm^{-3}$).

The mean concentration of ^{137}Cs in the seawater collected in the OWF area was 16.79 $Bq \cdot m^{-3}$. In the case of ^{90}Sr, its mean activity in water was 4.54 $Bq \cdot m^{-3}$. The results obtained confirmed a successive decrease in radionuclide activity since the beginning of continuous monitoring in 2010/2011.

2.2.7 Shortcomings and gaps in the state-of-the-art

No shortcomings nor gaps in the state of the art were identified as part of the surveys of the physicochemical properties of water.

2.3 SEABED SEDIMENTS

2.3.1 Non-specialist summary

The surveys covered the sea area designated for the implementation of an investment consisting in the construction of an the Baltica-1 offshore wind farm. The survey area is located on the border of the Polish exclusive economic zone, at the level of the Łeba commune in the Pomeranian Voivodeship. The planned offshore wind farm is located on the southern slopes of the Middle Bank, approximately 80 km from the port in Łeba, in waters of 17–49 m in depth.

Most of the pollutants (heavy metals and toxic organic compounds of low solubility and difficult to degrade) introduced into the environment as a result of the human economic activity and reaching surface waters are retained in sediments. Sediments, however, are not only a place of deposition of persistent and toxic pollutants reaching the environment but also a place of existence, source of nourishment, and a place of reproduction and growth of numerous aquatic organisms. Processes determining the content of pollutants in the sediment depend also on physical factors such as wave motion and currents. If the sediments are disturbed, there is also the possibility that the pollutants deposited within it will return to the water column.

Many of these processes with various intensity will occur mainly during construction and operation of the Baltica-1 offshore wind farm. Therefore, it was extremely important to verify the status of sediments in the region of the Baltica-1 offshore wind farm planned construction. The surveys conducted will help to determine to what extent the disruption of sediments (connected with the construction, and in particular with the laying of foundations for WTGs) will influence the possible deterioration of water quality and, indirectly, also marine organisms.

Sediments constitute a very important element of the aquatic ecosystem of the Baltic Sea, which is a shallow sea, with limited water exchange and an area about 4 times smaller than its catchment area.

As part of the monitoring of the properties of seabed sediments, selected physicochemical indicators of the samples collected during the winter and summer sediment sampling carried out within the survey area in February 2023 and within the survey area in February and during the first days of March 2023 were analysed. The grain size analyses conducted using two methods (either dry sieve analysis or

areometric analysis, depending on the type of soil) indicate that coarse-grain soils are prevalent on the seabed of the survey area.

Physicochemical analyses were carried out on samples collected at 108 survey stations located within the survey area.

To obtain comprehensive characteristics of the physicochemical properties of sediments from the Baltica-1 OWF area, the following physicochemical indicators were selected for testing: moisture content, loss on ignition (LOI), total organic carbon (TOC), content of metals (Pb, Cu, Zn, Ni, Cd, Cr, As, Hg) and their labile form, polycyclic aromatic hydrocarbons (16 PAHs), polychlorinated biphenyls (7 PCB congeners: 28, 52, 101, 118, 138, 153, 180), mineral oils, radioactivity of ^{137}Cs, organic tin compounds (TBT, DBT, MBT) and twice a year (due to seasonal changes), the content of nutrients (total nitrogen and total phosphorus). Sediment samples for physicochemical testing as part of the summer and winter survey campaigns were collected in an evenly distributed measurement grid (1 sample per 1 km^2) from the sediment layer using a grab sampler (van Veen grab sampler).

Additionally, out of all the seabed sediment samples collected as part of the winter sampling campaign, 25 seabed sediment samples from the survey area and 20 samples from the survey area were analysed for the content of mineral oils, butyltin compounds, i.e. tributyltin (TBT), dibutyltin (DBT) and monobutyltin (MBT) as well as for ^{137}Cs radioactivity.

The analysed sediments from the survey area are inorganic sediments with organic matter content expressed with a loss on ignition of below 2%.

The concentration of nutrients (total nitrogen and total phosphorus) in the survey area did not exceed the values typical for the sediments of the southern Baltic Sea Concentrations of persistent organic pollutants (i.e. PAHs, PCBs, TBT) and harmful substances such as metals or mineral oils in the surveyed area were low and generally did not differ from the literature data for the sandy sediments of the southern Baltic Sea. The sediments tested were also characterised by low concentrations of the radioactive element ^{137}Cs, typical for sandy sediments.

For illustrative purposes, the results obtained for metals (labile form of Pb, Cu, Zn, Ni, Cd, Cr, As, Hg), PAHs, and PCBs were compared with the limit values specified in the implementing regulation (Regulation of the Minister of the Environment of 11 May 2015 o*n the recovery of waste outside the installations and facilities* [Journal of Laws of 2015, item 796]), below which the seabed sediments can be used in reclamation processes, i.e. indirectly determining their purity. On this basis, it was concluded that the concentration values obtained for the above-mentioned compound groups in the analysed sediments from the survey area were low and the sediments were not contaminated with the compounds of this group.

The entire surface of the survey area consists of sandy and sand and gravel soils.

2.3.2 Spatial scope of the surveys

The spatial scope of surface sediment surveys was limited to the survey area covering the Baltica-1 OWF construction area, which is the area of construction of WTGs, OSSs, and cable lines (area A) and the area of construction of cable lines (area B) [Figure 2.85].

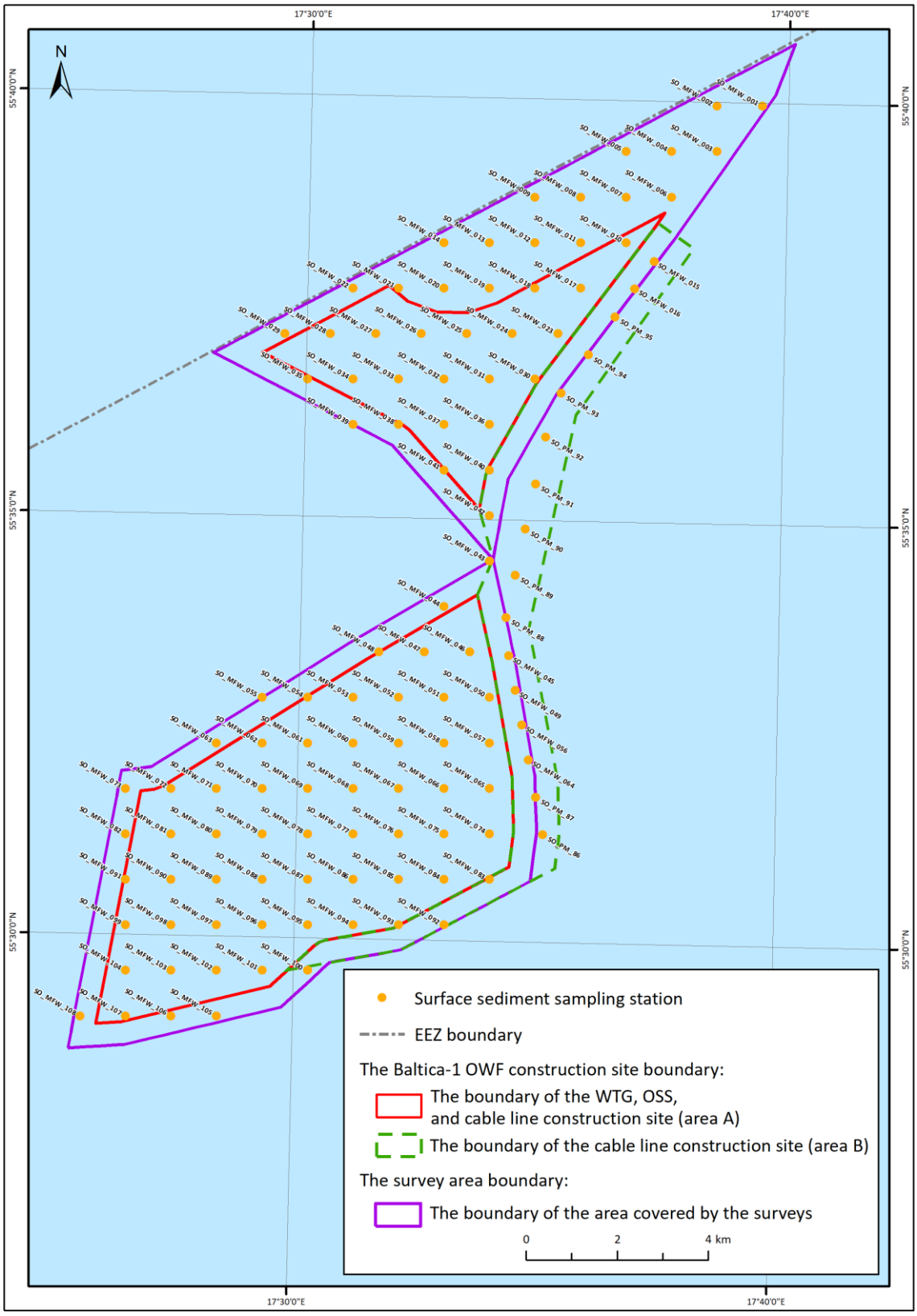


Figure 2.85. The location of the survey stations for core sampling within the survey area

2.3.3 Methodology

2.3.3.1 Survey methodology

The sediment samples were taken from the near-surface layer of the survey area using a van Veen grab sampler. At each survey station, one sample was collected. If the grab sampler was retrieved empty, one additional attempt to collect a sample at a given location after relocating by approx. 50 m was made. If sediment sampling failed at a given survey station during the first seabed sediment sampling, another sampling attempt was made during the second sampling campaign, while allowing the sampling location to be shifted by up to 200 m, taking into account the sonar data collected within the seabed area where the collection of a seabed sample was more likely.

As part of sediment sampling, water temperature, electrical conductivity, pressure and turbidity measurements were conducted using a CTD at all survey stations during each sediment sampling campaign. The measurement was made in the entire vertical profile at intervals not greater than 0.5 m (detailed information is presented in Subsection 2.1.5).

The samples were transported to the laboratory at the EPD MI GMU for physicochemical analyses and to the Geotechnical Laboratory of the MGD MI GMU for particle grain size analyses under conditions preventing the changes in the analyte content.

Seabed sediment samples intended for the determination of organic pollutants were transported in appropriate sealed glass containers, protected from light and heat (at a temperature of 4°C). Sediment samples intended for the determination of metals were transported in sealed containers made of appropriate plastic (string bags), protected from heat or light (at a temperature of -18°C). It was permissible for all analytes to pack and transport the samples in polyethene plastic bags (tight string bags) after immediate freezing in line with the PN-ISO 5667-19 and PN-EN ISO 5667-15 standards (at a temperature of -18°C).

Sediment samples intended for the grain size analysis were transported in plastic string bags at a temperature of 5–25°C.

For the physicochemical analyses, the sediment samples collected from the survey area were pre-treated in line with the PN-ISO 11464 standard, to obtain analytical samples.

As part of the first (winter) survey campaign, a grain size analysis was performed and the following indicators of the seabed sediment samples were tested:

- moisture content;
- loss on ignition (LOI);
- total organic carbon (TOC);
- content of heavy metals and their mobile forms (Pb, Cu, Zn, Ni, Cd, Cr, As, Hg, Al);
- polycyclic aromatic hydrocarbons (PAHs);
- polychlorinated biphenyls (PCBs).

The nutrient content (total nitrogen and total phosphorus) was tested as part of both campaigns.

Additionally, out of the total seabed sediment samples collected during the winter survey campaign, 22 seabed sediment samples from the survey area were analysed for the content of mineral oils, butyltin compounds, i.e. tributyltin (TBT), dibutyltin (DBT) and monobutyltin (MBT), as well as for ^{137}Cs radioactivity.

Table 2.42 presents the methods used for seabed sediment sampling and analysis of physicochemical indicators.

Table 2.42. The methods and techniques used for analysing seabed sediment samples with the indication of the limit of quantification of a particular method

No.	Test type	Method
1.	Seabed sediment sampling	In accordance with the PN-EN ISO 5667-19:2006 standard, samples from the surface sediment layer are taken with the use of a van Veen grab
2.	Loss on ignition (LOI)	Gravimetric analysis in accordance with the PN-EN 12879:2004 standard (LOQ: 0.1%)
3.	Moisture content	Gravimetric analysis in accordance with the PN-ISO 11465:1999 standard (LOQ: 0.1%)
4.	Total nitrogen	Titration method according to the standard PN-EN ISO 11261:2002 (LOQ: 200 $mg \cdot kg^{-1}$ DW)
5.	Total phosphorus	Inductively coupled plasma – optical emission spectrometry (ICP-OES) technique, procedure PB-10, issue 10 of 05.03.2021 (LOQ: 25 $mg \cdot kg^{-1}$ DW)
6.	Arsenic (As)	Inductively coupled plasma – optical emission spectrometry (ICP-OES) technique, procedure PB-10, issue 10 of 05.03.2021 (LOQ: 1.25 $mg \cdot kg^{-1}$ DW)
7.	Total chromium (TCr)	Inductively coupled plasma – optical emission spectrometry (ICP-OES) technique, procedure PB-10, issue 10 of 05.03.2021 (LOQ: 0.25 $mg \cdot kg^{-1}$ DW)
8.	Zinc (Zn)	Inductively coupled plasma – optical emission spectrometry (ICP-OES) technique, procedure PB-10, issue 10 of 05.03.2021 (LOQ: 0.25 $mg \cdot kg^{-1}$ DW)
9.	Copper (Cu)	Inductively coupled plasma – optical emission spectrometry (ICP-OES) technique, procedure PB-10, issue 10 of 05.03.2021 (LOQ: 0.25 $mg \cdot kg^{-1}$ DW)
10.	Cadmium (Cd) and its compounds	Inductively coupled plasma – optical emission spectrometry (ICP-OES) technique, procedure PB-10, issue 10 of 05.03.2021 (LOQ: 0.05 $mg \cdot kg^{-1}$ DW)
11.	Lead (Pb) and its compounds	Inductively coupled plasma – optical emission spectrometry (ICP-OES) technique, procedure PB-10, issue 10 of 05.03.2021 (LOQ: 0.25 $mg \cdot kg^{-1}$ DW)
12.	Mercury (Hg) and its compounds	Atomic absorption spectrometry with the amalgamation of mercury vapour (according to procedure PB-21, issue 6 of 06.05.2022) (LOQ: 0.01 $mg \cdot kg^{-1}$ DW)
13.	Nickel (Ni) and its compounds	Inductively coupled plasma – optical emission spectrometry (ICP-OES) technique, procedure PB-10, issue 10 of 05.03.2021 (LOQ: 0.25 $mg \cdot kg^{-1}$ DW)
14.	Aluminium (Al)	Inductively coupled plasma – optical emission spectrometry (ICP-OES) technique, procedure PB-10, issue 10 of 05.03.2021 (LOQ: 25 $mg \cdot kg^{-1}$ DW)
15.	Polycyclic aromatic hydrocarbons (PAHs)	Gas chromatography – mass spectrometry (GC-MS) method, procedure PB-09, issue 5 of 20.12.2021 (LOQ: 0.001 $mg \cdot kg^{-1}$ DW)
16.	Polychlorinated biphenyls (PCBs) (congeners: 28, 52, 101, 118, 138, 153, 180)	Gas chromatography – mass spectrometry (GC-MS) method, procedure PB-09, issue 5 of 20.12.2021 (LOQ: 0.0001 $mg \cdot kg^{-1}$ DW)
17.	Organotin compounds (TBT, DBT, MBT)	Gas chromatography – mass spectrometry (GC-MS) method in accordance with the PN-EN ISO 23161:2019:03 standard (LOQ respectively: 0.01 $mg \cdot kg^{-1}$ DW, 0.001 $mg \cdot kg^{-1}$ DW, 0.005 $mg \cdot kg^{-1}$ DW)
18.	Crude oil derivative hydrocarbons (mineral oils)	Gas chromatography with flame-ionisation detection method (GC-FID) in accordance with the PN-EN ISO 16703:2011-12 standard (LOQ: 5.0 $mg \cdot kg^{-1}$ DW)
19.	Caesium 137 (^{137}Cs)	Gamma spectrometry method. The measuring set includes a semi-conductive HPGe detector with an efficiency of 18% and a resolving power of 1.9 keV at 1332 keV energy, together with the analyser (LOQ: 0.84 $Bq \cdot kg^{-1}$ DW)

All the physicochemical analyses (excluding ^{137}Cs radionuclides) were performed by the accredited Laboratory of the Environment Protection Department at the Maritime Institute of the Gdynia Maritime University (EPD MI GMU), which holds the PCA certificate no. AB 646. The PCA accreditation scope (AB 646) includes the following testing activities: seabed sediment sampling, moisture content,

loss on ignition (LOI), total organic carbon (TOC), total phosphorus, total nitrogen, metals (Pb, Cu, Zn, Ni, Cd, Cr, As, Hg), aluminium (Al), PAHs, PCBs, mineral oils, and organotin compounds.

The radioactive concentration of ^{137}Cs in seabed sediment samples is determined by the laboratory of the IMWM-NRI in Gdynia.

As part of the grain size analyses, the sediment samples collected from the survey area were described macroscopically in accordance with the PN-EN ISO 14688-1:2018 and PN-EN ISO 14688-2:2018 standards and a photo documentation was prepared. The description included the identification of the fractions (taking into account additional components such as shell fragments, wood fragments, etc.), the determination of the degree of sediment sorting, colour, carbonate content as well as the cohesion or plasticity of the deposit depending on its type. Subsequently, the sediment samples were subjected to a sieve analysis in the case of coarse-grained sediments – sands and gravels – as well as a hydrometric analysis in the case of fine-grained sediments – silts and clays. The sediments were determined and classified consistently with the PN-EN ISO 14688-1:2018-05 standard.

As part of the sieve analysis, the determination of the grain size distribution of coarse-grained sediments was conducted by dry sieving. A standard set of sieves used for sieve analysis is presented in Table 2.43.

Table 2.43. A standard set of sieves for sieve analysis

Sieve number	Mesh aperture [mm]
1	63
2	32
3	16
4	6.3
5	4
6	2
7	1
8	0.5
9	0.2
10	0.125
11	0.063

A laboratory shaker was used for the analysis. Before the analysis, the samples were dried for 24 hours at a temperature of 105°C.

The areometric analysis was carried out on the samples which contained more than 10% of particles with an equivalent diameter below 0.063 mm. The test procedure was based on Stokes's law. Suspension was created from the sediment by mixing an appropriately sized sample with a water solution and a dispersant (e.g. sodium hexametaphosphate). The mixture was next strained through a sieve with a mesh aperture of 0.063 mm. The sediment that remained on the sieve was then dried and sieved, and the poured suspension was placed on the cylinder and read at appropriate intervals over a period of 24 hours. The density reading was taken using a suitably calibrated areometer. Changes in the suspension density occurred as a result of the particles falling. The equivalent particle diameters and the content of individual fractions were determined on the basis of Stokes's law.

2.3.3.2 Methodology of data post-processing

This Report includes the results of geochemical monitoring conducted as part of two sediment sampling campaigns, in February (winter campaign) and in July (summer campaign) 2023.

The tables with the results contain the information on the minimum, maximum and mean values obtained for each indicator tested as well as the number of results below the LOQ of the analytical method applied to test a given indicator in a particular survey period.

The minimum values are the lowest concentration values from the ones obtained at all survey stations in a given layer, taking into account the values below the limit of quantification (< LOQ) of the given analytical method.

The maximum values present the highest concentration value from the ones obtained at all survey stations in a given layer or, if all the concentration values obtained are below the LOQ, the maximum value is the value below the LOQ for a given indicator.

The mean value is an arithmetic mean of all the concentration results obtained for a particular indicator in a given layer at all survey stations located within the survey area for a particular indicator under both survey campaigns. Only for total nitrogen and total phosphorus, the mean value is calculated separately for individual survey campaigns, due to seasonal variation exhibited by these indicators. If a given sample provided results below the LOQ, the measurement result was adopted at a level of half of the LOQ value for the purpose of calculating the mean values. If the calculated mean value of the measurement results was below the limit of quantification, the mean value was determined as below the LOQ.

For illustrative purposes, the results obtained for the concentrations of metals (labile form), PAHs and PCBs in sediments were compared with the threshold values specified in the Regulation of the Minister of the Environment of 11 May 2015 o*n the recovery of waste outside the installations and facilities* (Journal of Laws of 2015, item 796), indicating the threshold values below which sediments can be used in reclamation processes, i.e. indirectly determining their purity. The results of this comparison are presented in this Report.

All the results obtained were referenced to the data presented in the literature and the historical monitoring data (if possible).

The results of macroscopic analyses of the sediments are presented in tabular form, whereas the results of the grain size analyses are presented in the form of grain size distribution curves derived from the sieve analyses as well as in the form of grain size distribution curves derived from the hydrometric and sieve analyses.

2.3.4 Activities performed

Physicochemical analyses were performed on samples collected at 118 survey stations.

As a result of the activities performed, 108 sediment samples were collected as part of the first campaign and 117 sediment samples were collected as part of the second campaign (no sample could be collected at station SO_PM_91 during the second campaign).

From among the sediment samples collected as part of the first (winter) campaign, 25 samples were selected, on which analyses of mineral oils, butyltin compounds (tributyltin, dibutyltin and monobutyltin) and caesium-137 were performed additionally. The sediment samples were collected at

the following survey stations: SO_MFW_001, SO_MFW_004, SO_MFW_010, SO_MFW_013, SO_MFW_022, SO_MFW_025, SO_MFW_029, SO_MFW_034, SO_MFW_036, SO_MFW_041, SO_MFW_048, SO_MFW_051, SO_MFW_055, SO_MFW_067, SO_MFW_069, SO_MFW_073, SO_MFW_083, SO_MFW_089, SO_MFW_091, SO_MFW_094_A, SO_MFW_105, SO_MFW_108, SO_PM_87, SO_PM_89, SO_PM_94.

The operations in winter conducted as part of the first sampling campaign, were carried out on 22–23 and 27–28 February 2023. Sampling was carried out at 118 survey stations. Material for laboratory analyses was obtained at all survey stations.

As part of the second (summer) campaign, sediment samples were collected in the survey area for total nitrogen and total phosphorus content analysis.

Under the summer campaign, the operations were conducted in the survey area on 28–29 July 2023. Sampling was carried out at 118 planned survey stations. 117 samples were taken for laboratory analyses (a sample was not taken from station SO_PM_91 because of the rocky seabed). Material for laboratory analyses was obtained at all survey stations.

A detailed list of the activities performed is presented in Table 2.44 and Table 2.45.

Table 2.44. A list of activities conducted as part of sediment sampling in the survey area

Campaign	Sampling date	Number of samples taken	Survey station*
I (winter)	22.02.2023	31	SO_MFW_001, SO_MFW_002, SO_MFW_003, SO_MFW_004, SO_MFW_005, SO_MFW_006, SO_MFW_007, SO_MFW_008, SO_MFW_009, SO_MFW_010, SO_MFW_011, SO_MFW_012, SO_MFW_013, SO_MFW_014, SO_MFW_015, SO_MFW_016, SO_MFW_017, SO_MFW_018, SO_MFW_019, SO_MFW_020, SO_MFW_021, SO_MFW_022, SO_MFW_023, SO_MFW_024, SO_MFW_025, SO_MFW_026, SO_MFW_027, SO_MFW_028, SO_MFW_029, SO_MFW_030, SO_MFW_031, SO_PM_93, SO_PM_94, SO_PM_95
	23.02.2023	3	SO_MFW_032, SO_MFW_033, SO_MFW_034
	27.02.2023	36	SO_MFW_035, SO_MFW_036, SO_MFW_037, SO_MFW_038, SO_MFW_039, SO_MFW_040, SO_MFW_041, SO_MFW_042, SO_MFW_043, SO_MFW_044, SO_MFW_045, SO_MFW_046, SO_MFW_047, SO_MFW_048, SO_MFW_049, SO_MFW_050, SO_MFW_051. SO_MFW_052, SO_MFW_053, SO_MFW_054, SO_MFW_055, SO_MFW_056, SO_MFW_057, SO_MFW_058, SO_MFW_059, SO_MFW_060, SO_MFW_061, SO_MFW_062, SO_MFW_063, SO_MFW_064, SO_MFW_065, SO_MFW_066, SO_MFW_067, SO_MFW_068, SO_MFW_069, SO_MFW_070, SO_PM_87, SO_PM_88, SO_PM_89, SO_PM_90, SO_PM_91, SO_PM_92
	28.02.2023	38	SO_MFW_071, SO_MFW_072, SO_MFW_073, SO_MFW_074, SO_MFW_075, SO_MFW_076, SO_MFW_077, SO_MFW_078, SO_MFW_079, SO_MFW_080, SO_MFW_081, SO_MFW_082, SO_MFW_083, SO_MFW_084, SO_MFW_085, SO_MFW_086, SO_MFW_087, SO_MFW_088, SO_MFW_089, SO_MFW_090, SO_MFW_091, SO_MFW_092, SO_MFW_093, SO_MFW_094, SO_MFW_095, SO_MFW_096, SO_MFW_097, SO_MFW_098, SO_MFW_099, SO_MFW_100, SO_MFW_101, SO_MFW_102,

Campaign	Sampling date	Number of samples taken	Survey station*
			SO_MFW_103, SO_MFW_104, SO_MFW_105, SO_MFW_106, SO_MFW_107, SO_MFW_108, SO_PM_86
II (summer)	28.07.2023	44	SO_MFW_001, SO_MFW_002, SO_MFW_003, SO_MFW_004, SO_MFW_005, SO_MFW_006, SO_MFW_007, SO_MFW_008, SO_MFW_009, SO_MFW_010, SO_MFW_011, SO_MFW_012, SO_MFW_013, SO_MFW_014, SO_MFW_015, SO_MFW_016, SO_MFW_017, SO_MFW_018, SO_MFW_019, SO_MFW_020, SO_MFW_021, SO_MFW_022, SO_MFW_023, SO_MFW_024, SO_MFW_025, SO_MFW_026, SO_MFW_027, SO_MFW_028, SO_MFW_029, SO_MFW_030, SO_MFW_031 SO_MFW_032, SO_MFW_033, SO_MFW_034, SO_MFW_035, SO_MFW_036, SO_MFW_037, SO_MFW_038, SO_MFW_039, SO_MFW_040, SO_MFW_041, SO_MFW_042, SO_MFW_043, SO_MFW_044
	29.07.2023	64	SO_MFW_045, SO_MFW_046, SO_MFW_047, SO_MFW_048, SO_MFW_049, SO_MFW_050, SO_MFW_051. SO_MFW_052, SO_MFW_053, SO_MFW_054, SO_MFW_055, SO_MFW_056, SO_MFW_057, SO_MFW_058, SO_MFW_059, SO_MFW_060, SO_MFW_061, SO_MFW_062, SO_MFW_063, SO_MFW_064, SO_MFW_065, SO_MFW_066, SO_MFW_067, SO_MFW_068, SO_MFW_069, SO_MFW_070, SO_MFW_071, SO_MFW_072, SO_MFW_073, SO_MFW_074, SO_MFW_075, SO_MFW_076, SO_MFW_077, SO_MFW_078, SO_MFW_079, SO_MFW_080, SO_MFW_081, SO_MFW_082, SO_MFW_083, SO_MFW_084, SO_MFW_085, SO_MFW_086, SO_MFW_087, SO_MFW_088, SO_MFW_089, SO_MFW_090, SO_MFW_091, SO_MFW_092, SO_MFW_093, SO_MFW_094, SO_MFW_095, SO_MFW_096, SO_MFW_097, SO_MFW_098, SO_MFW_099, SO_MFW_100, SO_MFW_101, SO_MFW_102, SO_MFW_103, SO_MFW_104, SO_MFW_105, SO_MFW_106, SO_MFW_107, SO_MFW_108, SO_PM_85, SO_PM_86, SO_PM_87, SO_PM_88, SO_PM_89, SO_PM_90, **SO_PM_91**, SO_PM_92, SO_PM_93, SO_PM_94, SO_PM_95

**Stations at which no sample could be collected despite making two sampling attempts and moving the originally planned sampling location by approx. 50 m, are marked in bold*

Table 2.45. The scope of the analyses of seabed sediment samples collected within the survey area

Campaign	Sampling date	Number of samples taken	Scope of the tests performed
I (winter)	22–28.02.2023	108*	Laboratory analyses: moisture content, loss on ignition (LOI), total organic carbon (TOC), total nitrogen, total phosphorus, metals and metalloids: arsenic (As), total chromium (TC), zinc (Zn), copper (Cu), cadmium (Cd), lead (Pb), nickel (Ni), aluminium (Al), mercury (Hg) and their labile forms, polychlorinated biphenyls (PCBs), polycyclic aromatic hydrocarbons (PAHs), organotin compounds (TBT, DBT, MBT), petroleum hydrocarbons, and radioactivity of ^{137}Cs
II (summer)	28, 29.07.2023	108	Laboratory analyses: total nitrogen, total phosphorus

**in the case of 25 out of 118 samples collected, additional analyses of mineral oils, butyltin compound (tributyltin, dibutyltin and monobutyltin), and caesium-137 were conducted*

2.3.5 Results

2.3.5.1 Indicators characterising the physicochemical properties of sediments (LOI, moisture content, TOC)

The test results for the indicators characterising the physicochemical properties (total organic carbon (TOC), moisture content and (LOI)) of the sediments, contained in the sediment samples collected within the survey area in the winter of 2023 are presented in Table 2.46.

Table 2.46. The mean, minimum, and maximum values of LOI, moisture content, and TOC in the sediment samples collected within the survey area

Indicator	Number of detections	Value			Number of results < LOQ
		Mean	Minimum	Maximum	
Loss on ignition (LOI) [%]	118	0.50	< 0.10	1.76	2
Moisture content [%]	118	22.7	4.8	32.5	0
Total organic carbon (TOC) [mg·kg^{-1} DW]	118	< 1000	< 1000	3226	96

LOQ – the limit of quantification

2.3.5.2 Nutrient indicators (total nitrogen, total phosphorus)

The test results for the indicators characterising eutrophication (total nitrogen, total phosphorus) in the sediment samples from the survey area in the winter and summer of 2023 are presented in Table 2.47.

Table 2.47. The mean, minimum, and maximum values of total nitrogen and total phosphorus concentrations in the sediment samples from the survey area

Indicator	Campaign	Number of detections	Value			Number of results < LOQ
			Mean	Minimum	Maximum	
Total nitrogen [mg·kg^{-1} DW]	Winter	118	131	< 200	423	97
	Summer	117	137	< 200	395	88
Total phosphorus [mg·kg^{-1} DW]	Winter	118	190	108	373	0
	Summer	117	193	104	396	0

LOQ – the limit of quantification

2.3.5.3 Specific synthetic and non-synthetic contaminants, as well as metals from the group of substances particularly harmful to the aquatic environment

2.3.5.3.1 Metals and metalloids

The test results for the concentrations of metals and their labile forms in the sediment samples from the survey area collected in the winter of 2023 are presented in Table 2.48.

Table 2.48. The mean, minimum, and maximum values of trace metal concentrations (total content and labile form) in the sediment samples from the survey area

Indicator	Number of detections	Value			Number of results < LOQ
		Mean	Minimum	Maximum	
Lead [mg·kg^{-1} DW]	118	3.30	1.20	7.70	0
Labile Pb [mg·kg^{-1} DW]	118	2.49	0.33	7.10	0
Copper [mg·kg^{-1} DW]	118	1.82	0.82	5.10	0

Indicator	Number of detections	Value			Number of results < LOQ
		Mean	Minimum	Maximum	
Labile Cu [mg·kg^{-1} DW]	118	1.01	< 0.25	3.13	9
Zinc [mg·kg^{-1} DW]	118	9.52	5.60	21.70	0
Labile Zn [mg·kg^{-1} DW]	118	7.01	3.60	16.40	0
Nickel [mg·kg^{-1} DW]	118	2.62	1.28	7.70	0
Labile Ni [mg·kg^{-1} DW]	118	1.09	< 0.25	3.60	1
Cadmium [mg·kg^{-1} DW]	118	< 0.05	< 0.05	0.12	108
Labile Cd [mg·kg^{-1} DW]	118	< 0.05	< 0.05	< 0.05	118
Arsenic [mg·kg^{-1} DW]	118	< 1.25	< 1.25	3.00	63
Labile As [mg·kg^{-1} DW]	118	< 1.25	< 1.25	2.10	116
Chromium [mg·kg^{-1} DW]	118	4.92	2.04	10.90	0
Labile Cr [mg·kg^{-1} DW]	118	1.00	< 0.25	2.08	1
Mercury [mg·kg^{-1} DW]	118	< 0.01	< 0.01	0.01	91
Labile Hg [mg·kg^{-1} DW]	118	< 0.01	< 0.01	0.01	1144
Aluminium [mg·kg^{-1} DW]	118	2467.00	1626.00	5476.00	0
Labile Al [mg·kg^{-1} DW]	118	593.00	162.00	1106.00	0

LOQ – the limit of quantification

2.3.5.3.2 A group of chemical indicators characterising the occurrence of substances harmful to the aquatic environment

2.3.5.3.2.1 Crude oil derivative hydrocarbons (mineral oils)

The test results for the mineral oil content in the sediment samples collected at 22 survey stations from the survey area in the winter of 2023 are presented in Table 2.49.

Table 2.49. The mean, minimum, and maximum values of mineral oil concentration in the sediment samples from the survey area

Indicator	Number of detections	Value			Number of results < LOQ
		Mean	Minimum	Maximum	
Mineral oils [mg·kg^{-1} DW]	25	7.0	< 5.0	15.2	12

LOQ – the limit of quantification

2.3.5.3.2.2 Polycyclic aromatic hydrocarbons (PAHs)

The test results for the PAH content in the sediment samples from the survey area collected in the winter and summer of 2023 are presented in Table 2.50.

Table 2.50. The mean, minimum, and maximum values of PAH concentrations in the sediment samples from the survey area

Indicator	Number of detections	Value			Number of results < LOQ
		Mean	Minimum	Maximum	
Naphthalene [mg·kg^{-1} DW]	118	< 0.001	< 0.001	0.004	87
Acenaphthylene [mg·kg^{-1} DW]	118	< 0.001	< 0.001	0.001	117
Acenaphthene [mg·kg^{-1} DW]	118	< 0.001	< 0.001	0.003	113
Fluorene [mg·kg^{-1} DW]	118	< 0.001	< 0.001	0.002	95

Indicator	Number of detections	Value			Number of results < LOQ
		Mean	Minimum	Maximum	
Phenanthrene [mg·kg^{-1} DW]	118	0.003	< 0.001	0.030	22
Anthracene [mg·kg^{-1} DW]	118	< 0.001	< 0.001	0.005	109
Fluoranthene [mg·kg^{-1} DW]	118	0.003	< 0.001	0.036	41
Pyrene [mg·kg^{-1} DW]	118	0.002	< 0.001	0.028	61
Benzo(a)anthracene [mg·kg^{-1} DW]	118	0.001	< 0.001	0.018	77
Chrysene [mg·kg^{-1} DW]	118	0.002	< 0.001	0.019	62
Benzo(b)fluoranthene [mg·kg^{-1} DW]	118	0.003	< 0.001	0.028	50
Benzo(k)fluoranthene [mg·kg^{-1} DW]	118	0.003	< 0.001	0.032	50
Benzo(a)pyrene [mg·kg^{-1} DW]	118	0.001	< 0.001	0.023	71
Indeno(1,2,3,-cd)pyrene [mg·kg^{-1} DW]	118	0.003	< 0.001	0.029	47
Dibenzo(a,h)anthracene [mg·kg^{-1} DW]	118	< 0.001	< 0.001	0.005	88
Benzo(ghi)perylene [mg·kg^{-1} DW]	118	0.003	< 0.001	0.033	49
Sum of 16 PAHs [mg·kg^{-1} DW]	118	0.024	< 0.001	0.280	14

LOQ – the limit of quantification

2.3.5.3.2.3 Polychlorinated biphenyls (PCBs)

The test results for the PCB content in the sediment samples from the survey area collected in the winter of 2023 are presented in Table 2.51.

Table 2.51. The mean, minimum, and maximum values of PCB concentrations in the sediment samples from the survey area

Indicator	Number of detections	Value			Number of results < LOQ
		Mean	Minimum	Maximum	
PCB 28 [mg·kg^{-1} DW]	118	< 0.0001	< 0.0001	0.0001	108
PCB 52 [mg·kg^{-1} DW]	118	< 0.0001	< 0.0001	0.0001	117
PCB 101 [mg·kg^{-1} DW]	118	< 0.0001	< 0.0001	0.0001	116
PCB 118 [mg·kg^{-1} DW]	118	< 0.0001	< 0.0001	0.0001	116
PCB 138 [mg·kg^{-1} DW]	118	< 0.0001	< 0.0001	0.0001	114
PCB 153 [mg·kg^{-1} DW]	118	< 0.0001	< 0.0001	0.0001	115
PCB 180 [mg·kg^{-1} DW]	118	< 0.0001	< 0.0001	< 0.0001	118
Sum of 7 PCB congeners [mg·kg^{-1} DW]	118	< 0.0001	< 0.0001	0.0006	105

LOQ – the limit of quantification

2.3.5.3.2.4 Organotin compounds (TBT, DBT, MBT)

The test results for the concentrations of organotin compounds in the sediment samples collected at 25 survey stations in the survey area in the winter of 2023 are presented in Table 2.52.

Table 2.52. The mean, minimum, and maximum concentrations of organotin compounds in the sediment samples from the survey area

Indicator	Number of detections	Value			Number of results < LOQ
		Mean	Minimum	Maximum	
TBT [mg·kg^{-1} DW]	25	< 0.01	< 0.01	< 0.01	25

Indicator	Number of detections	Value			Number of results < LOQ
		Mean	Minimum	Maximum	
DBT [mg·kg^{-1} DW]	25	< 0.001	< 0.001	< 0.001	25
MBT [mg·kg^{-1} DW]	25	< 0.005	< 0.005	< 0.005	25

LOQ – the limit of quantification

2.3.5.3.3 Radionuclides

The test results for caesium (^{137}Cs) radioactivity in the sediment samples collected at 25 survey stations in the survey area in the winter of 2023 are presented in Table 2.53.

Table 2.53. The mean, minimum, and maximum values of caesium (^{137}Cs) radioactivity in the sediment samples from the survey area

Indicator	Number of detections	Value			Number of results < LOQ
		Mean	Minimum	Maximum	
^{137}Cs [Bq·kg^{-1} DW]	25	3.55	< 0.84	8.87	2

LOQ – the limit of quantification

2.3.5.4 Grain size analysis

As part of the surveys, 118 sediment samples were collected from the survey area. Table 1.5 presents the results of the macroscopic analysis and grain size analysis of the sediment samples collected.

2.3.6 Summary of results and conclusions

2.3.6.1 Indicators characterising the physicochemical properties of sediments (LOI, moisture content, TOC)

The content of carbon and nutrients in sediments is shaped by comprehensively interacting biotic and abiotic factors. Benthic organisms limit the organic matter accumulation within the seabed, thus shaping the vertical and horizontal distribution of carbon and nutrients in sediments.

In the area of the Baltic Sea, which is a shallow sea, the seasonally variable wind-generated wave motion and the seabed topography have a significant influence on the dynamics of the near-seabed waters, and thus, also on the dynamics of the sediments ((Jönsson et al., 2005). The differences in the frequency and intensity of the near-seabed water mixing are reflected in the differences in sediment grain size analysis, sediment moisture content, organic matter content expressed as a loss on ignition (LOI), TOC, and the differences in the carbon and nutrient contents (Uścinowicz, 2011).

The sediments collected in the survey area and analysed belonged to the inorganic sediments with low organic matter content, expressed by the LOI indicator of < 2% and moisture content of 22.7%.

The results obtained for the total organic carbon (TOC) in the sediments analysed (< 1.0 g·kg^{-1} DW) were typical for sandy sediments and do not deviate from the data from literature. Total organic carbon in the sediments of the Baltic Sea falls within a wide range, from values close to zero in sandy sediments to more than 16% in silty sediments (Szczepańska, Uścinowicz, 1994; Uścinowicz, 2011).

2.3.6.2 Nutrient indicators (total nitrogen, total phosphorus)

2.3.6.2.1 Total nitrogen

In the Baltic Sea sediments, nitrogen occurs mainly in organic form and its regional variability is analogous to the variability of carbon (Carman, 2003). Usually, inorganic forms of nitrogen constitute

no more than 10% of the total nitrogen in the sediments. An increase in the proportion of inorganic nitrogen forms is possible in the erosion and transport zone of the sediments of fine particle dispersion.

The mean concentration values of total nitrogen confirmed for the winter (February 2023) and summer (July 2023) periods surveyed, in the majority of samples tested were below LOQ of the method applied (200 mg·kg^{-1} DW). The presence of total nitrogen was found only in 20 samples taken in winter (the maximum concentration of 423 mg·kg^{-1} DW) and in 30 samples taken in summer (the maximum concentration of 395 mg·kg^{-1} DW). The nitrogen content in the southern Baltic Sea sediments falls between 98–2604 mg N·kg^{-1} DW in sandy sediments, 1106–3094 mg N·kg^{-1} DW in sandy-clayey sediments, 1904–9506 mg N·kg^{-1} DW in clays, and 1694–4606 mg N·kg^{-1} DW in tills (Pęcherzewski, 1972). In the area of the coastal sands, nitrogen concentrations rarely exceed 700 mg N·kg^{-1} DW.

The Regulation of the Minister of the Environment of 11 May 2015 *on the recovery of waste outside the installations and facilities* (Journal of Laws of 2015, item 796) does not specify the limit values for total nitrogen.

2.3.6.2.2 Total phosphorus

Phosphorus in the seabed sediments is conventionally divided into labile and refractive phosphorus. The refractive phosphorus deposits in sediments and in this way is removed from the water body. The labile phosphorus, on the other hand, is the phosphorus contained in fresh organic matter, phosphates present in the interstitial waters, the combinations of phosphorus and Fe^{3+}, as well as phosphates loosely bound by adsorption with various elements of sediment. The labile forms easily return into the circulation of the water column due to the organic matter mineralisation and the dissolving of connections between phosphorus and Fe^{3+} as a result of a decrease in the value of the redox potential.

The presence of the total phosphorus was observed in all the seabed sediment samples collected in the survey area, both in winter (February 2023) and summer (July 2023). The mean concentration values of the total phosphorus obtained for the survey area were very similar within the entire survey period (on average, 190 mg·kg^{-1} DW in winter and 193 mg·kg^{-1} DW in summer). The maximum concentration of total phosphorus in the winter was 373 mg·kg^{-1} DW recorded at the survey station SO_MFW_092. In the summer, the maximum concentration of total phosphorus was 396 mg·kg^{-1} DW recorded at the survey station SO_MFW_001. At the station SO_MFW_092, the concentration of total phosphorus in the summer was 258 mg·kg^{-1} DW.

The Regulation of the Minister of the Environment of 11 May 2015 *on the recovery of waste outside the installations and facilities* (Journal of Laws of 2015, item 796) does not specify the limit values for total phosphorus.

These results do not diverge from the literature data. Concentrations of phosphorus in the Baltic Sea usually do not exceed 6180 mg P·kg^{-1} DW (Uścinowicz, 2011). The mean content of phosphorus in the surface layer of sediments in the Gdańsk Basin is 1607 mg P·kg^{-1} DW (Szczepańska, Uścinowicz, 1994). In the Baltic Proper, concentrations range from 414 mg P·kg^{-1} DW to 5407 mg P·kg^{-1} DW (Carman, Cederwall, 2001; Carman, Jonsson, 1991; Edlund, Carman, 2001).

2.3.6.3 Specific synthetic and non-synthetic contaminants, as well as metals from the group of substances particularly harmful to the aquatic environment

2.3.6.3.1 Metals and metalloids

2.3.6.3.1.1 Metal and metalloid content

Within the survey area, the mean concentrations of the elements tested in the sediments were relatively low (arsenic (As) – < 1.25 mg·kg^{-1} DW, chromium (Cr) – 4.92 mg·kg^{-1} DW, zinc (Zn) – 9.52 mg·kg^{-1} DW, copper (Cu) – 1.82 mg·kg^{-1} DW, cadmium (Cd) – < 0.05 mg·kg^{-1} DW, lead (Pb) – 3.3 mg·kg^{-1} DW, nickel (Ni) – 2.62 mg·kg^{-1} DW, and mercury (Hg) – < 0.01 mg·kg^{-1} DW). The concentration of aluminium (Al), which belongs to the macro elements, was also relatively low and equalled 2467 mg·kg^{-1} DW. The concentration values of the elements tested were more or less even within the entire survey area, with the exception of the north-eastern areas in the vicinity of stations SO_MFW_001, SO_MFW_002 and SO_MFW_003, where slightly elevated concentrations of the elements tested were observed, which resulted from the increased content of organic carbon in this region (2524–3226 mg·kg^{-1} DW).

The concentrations of metals (Pb, Cu, Zn, Ni, Cd, Cr, As, Al, Hg) tested in the sediments of the survey area, did not exceed the values typical for the sediments of the southern Baltic Sea (Uścinowicz, 2011; Szczepańska, Uścinowicz, 1994; Szefer, 2002; Dembska, 2003). The results obtained are also congruent with, and even lower than, the data on the concentrations of cadmium and lead from the Eastern Gotland Basin presented in the latest HELCOM report published in July 2023 [HELCOM, 2023 (Cd); HELCOM, 2023 (Pb)]. It can be added that the concentration values for none of the samples tested from the survey area exceeded the limit values for sediments determined by HELCOM as EQS values in the HOLAS 3 program for lead (< 120 mg·kg^{-1} DW) and cadmium (< 2.3 mg·kg^{-1} DW) [HELCOM, 2023 (Cd); HELCOM, 2023 (Pb)].

The Regulation of the Minister of the Environment of 11 May 2015 *on the recovery of waste outside the installations and facilities* (Journal of Laws of 2015, item 796) specifies only the limit values for labile metal content.

2.3.6.3.1.2 Content of labile metal form

The determination of the total element content in the sediment tested is insufficient to determine its properties, e.g. toxicity, bioavailability, migration, accumulation, or biomagnification. The characteristics of a given chemical element as well as its availability (ability to transfer to the water column), depend on the physicochemical form in which it occurs (Siepak, 1998; Savvides et al., 1995). Speciation analysis is helpful in distinguishing these physical and chemical forms, since it allows the identification and quantification of these forms in a particular material.

In terms of persistence and physicochemical connections, the method of binding metals with sediments can be divided into two main groups: the group of metals permanently bound in the crystal lattice – mainly aluminosilicates, and the mobile (labile) group of metals, susceptible to transition, in natural conditions, into the water depths. The sum of the labile metal forms in the sediments tested was obtained by mineralising the sediment in hydrochloric acid (1+4) (Luoma, Bryan, 1981; Dembska, 2003; Journal of Laws 2015 item 796).

The highest concentrations were recorded (similarly to the total content of the elements tested) in the north-eastern part of the survey area. In the remaining parts of the survey area, the concentrations of the labile form of the elements tested were more or less evenly distributed.

To determine the part of metals from seabed sediments from the survey area which can transfer into the water depth, the percentage share of the labile form of individual metals was calculated in relation to their total content. The obtained results are shown in Figure 2.86.

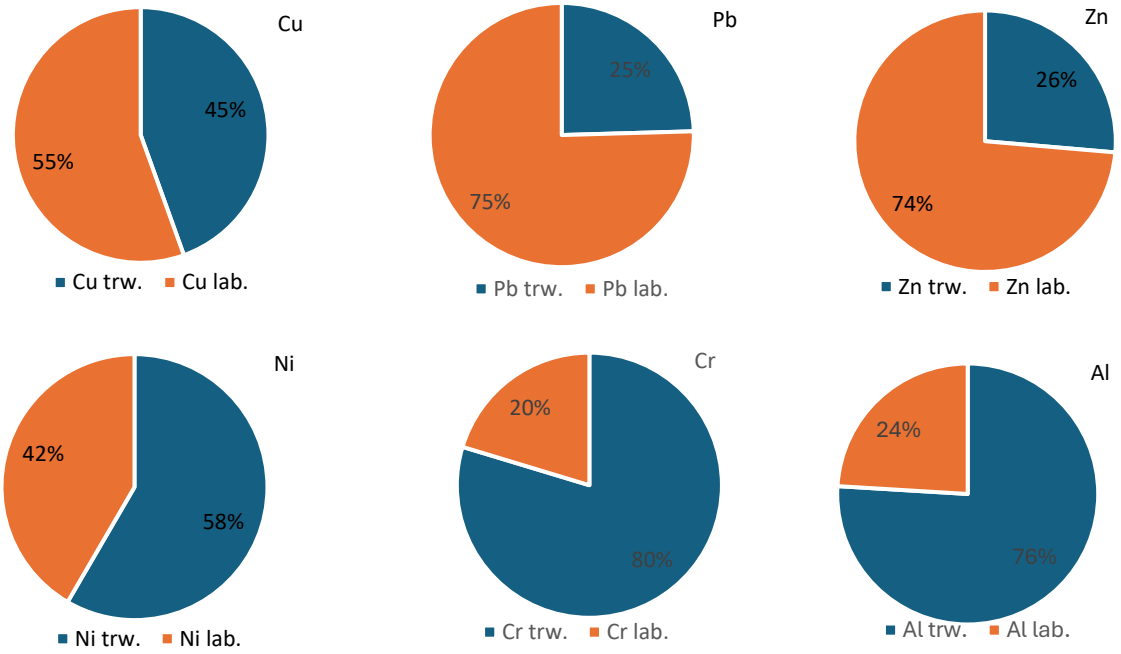


Figure 2.86. The proportion of metal labile forms (lab.) and forms permanently bound with the sediment (perm.) in the survey area

As a result of the surveys conducted, it was established that in the survey area, approx. 75% of lead, 74% of zinc, and 55% of copper present in the sediment analysed can, in favourable conditions, transfer from the sediment to the water column. Chromium, aluminium, and nickel present in the sediment surveyed are, in most cases, permanently bound with it. Only 20% of chromium, 24% of aluminium and 42% of nickel may, in favourable conditions, be transmitted from the sediment into the water.

For illustrative purposes only, the obtained results of metal labile form content in the surveyed parts of the survey area were compared with the normative values stipulated in the Regulation of the Minister of the Environment of 11 May 2015 o*n the recovery of waste outside the installations and facilities* (Journal of Laws 2015, item 796), which allows to classify sediment as clean in the context of practical application. Despite the limit values of heavy metals presented in this regulation do not apply to the sediment transported in the water, they may provide a basis for assessment of sediment contamination with chemical compounds.

None of the analysed sediment samples from the survey area exceeded the permissible values set for metals in the above-mentioned regulation. The limit values for individual metals in labile form (defined in the Regulation) are as follows: Hg – 1.0 $mg \cdot kg^{-1}$ DW, Pb – 200 $mg \cdot kg^{-1}$ DW, Cu – 150 $mg \cdot kg^{-1}$ DW, Zn – 1000 $mg \cdot kg^{-1}$ DW, Ni – 75 $mg \cdot kg^{-1}$ DW, Cd – 7.5 $mg \cdot kg^{-1}$ DW, Cr – 200 $mg \cdot kg^{-1}$ DW, and As – 30 $mg \cdot kg^{-1}$ DW.

The Regulation of the Minister of the Environment of 11 May 2015 o*n the recovery of waste outside the installations and facilities* (Journal of Laws 2015, item 796) does not specify limit values for aluminium.

The concentrations of labile forms of the analysed metals and metalloids (Pb, Cu, Zn, Ni, Cd, Cr, As, Al, Hg) in the sediments from the survey area did not exceed typical values for the sediments of the southern Baltic Sea (Bednarska et al., 2017; Opioła et al., 2020; Chałacińska et al., 2014; Chałacińska et al., 2015).

2.3.6.3.2 Polycyclic aromatic hydrocarbons (PAHs)

The relatively low concentrations of polycyclic aromatic hydrocarbons have been confirmed during the long-term monitoring of seabed sediments of the Baltic Sea. The data published in 2002 in HELCOM's "COMBINE monitoring programme" refer to the concentrations of the sum of PAHs. The highest concentrations of PAHs (from 4.5 to 35.2 mg·kg^{-1} DW) were found in the southernmost part of the Baltic Sea (the Gulf of Gdańsk, Gulf of Lübeck, Gulf of Mecklenburg, and Arkona Basin). Slightly lower concentrations (the sum of 15 PAHs) ranging from 0.01 to 7.0 mg·kg^{-1} DW (on average, 1.83 mg·kg^{-1} DW) were recorded in the Gulf of Gdańsk (HELCOM, 2002; Witt, 1995, Uścinowicz, 2011). The accumulation of PAHs in sediments is facilitated, among others, by a high percentage of silt and clay fractions with sediment particles with a size of < 0.063 mm, and characterised by a large specific surface area and a significant ability to adsorb hydrophobic pollutants and organic compounds of phosphorus, sulphur, and nitrogen. The extremely high pyrogenic durability of PAHs in sediments is caused by the occlusion of these chemical compounds in the very fine sediment particles (originally constituting volatile ash components) (Bolałek, 2010).

The content of PAHs in the uncontaminated sediments is very low, roughly 0.1 mg·kg^{-1}, while the sediments rich in organic matter, such as lake sediments, are often characterised by PAHs content close to 1 mg·kg^{-1}. The high values of PAHs, ranging from a few to a few dozen or even a few hundred mg·kg^{-1} of dry weight, are recorded in the areas more vulnerable to contamination, for example in ports, shipyards and areas of river estuaries (Głód, 1998; Guz et al., 2000).

In the survey area, the concentrations of the sum of PAHs in the sediments were relatively low, ranging from 0.001 to 0.280 mg·kg^{-1} DW with the mean value of 0.024 mg·kg^{-1} DW.

For illustrative purposes only, the results obtained for PAH content were compared with the normative values specified in the Regulation of the Minister of the Environment of 11 May 2015 o*n the recovery of waste outside the installations and facilities* (Journal of Laws of 2015, item 796), which allows classifying sediment as clean in the context of practical applications. Despite the limit values of PAHs specified therein do not refer to the sediment displaced within the waters, they may provide a basis for the assessment of the sediment contamination with chemical compounds.

The comparison performed indicates that the limit concentrations of PAHs mentioned in this regulation [i.e. benzo(a)anthracene – ≥ 1.5 mg·kg^{-1} DM, benzo(b)fluoranthene – ≥ 1.5 mg·kg^{-1} DM, benzo(k)fluoranthene – ≥ 1.5 mg·kg^{-1} DM, benzo(g,h,i)perylene – ≥ 1.0 mg·kg^{-1} DM, dibenzo(a,h)anthracene – ≥ 1.0 mg·kg^{-1} DM] were not exceeded in any of the samples taken. On this basis, it can be concluded that the concentration values obtained for the seabed sediments in the survey area are low and the sediments are not contaminated with the compounds of this group.

2.3.6.3.3 Polychlorinated biphenyls (PCBs)

Polychlorinated biphenyls have been recorded in the sediments of the Baltic Sea for many years. These are synthetic substances which do not occur naturally in the environment, but are emitted from anthropogenic sources only, and, as the ongoing surveys demonstrate, they pose a significant threat to the environment. PCBs are characterised by high durability and hydrophobic and lipophilic properties. These features determine their easy absorption by plants, crustaceans and fish. These substances, through synergistic cooperation with pesticides and arsenic compounds, also reduce the reproduction of aquatic organisms, increase larval mortality, and cause the reduction of thickness of bird egg shells. PCBs are also adsorbed on the surface of organic particles suspended in the water and get to the seabed sediments in the sedimentation process. Their accumulation in sediments is promoted by the high proportion of silt and clay fraction (< 0.063 mm) and the high content of organic matter (> 10%) (Niemirycz, Sapota, 2010).

In the survey area, the maximum concentration of the sum of 7 PAHs in the sediments was 0.0006 mg·kg^{-1} DW at survey station SO_MFW_059.

In the vast majority of surface seabed sediment samples collected in the survey area, the concentrations of the sum of seven PCB congeners (no. 28, 52, 101, 118, 138, 180) were below the LOQ of the method applied (i.e. 0.1 ng·kg^{-1}). The test results obtained for the PCBs do not diverge from the data from literature regarding the sediments of the southern Baltic Sea, but being in the lower range, these results indicate a decrease in the concentration of these compounds over time (Bogdaniuk et al., 2012; Konat, Kowalewska, 2001; Kowalewska, Konat, 1999; Sapota, 2006).

For illustrative purposes, the results obtained for the PCB content within the survey area were compared with the normative values stipulated in the Regulation of the Minister of the Environment of 11 May 2015 o*n the recovery of waste outside the installations and facilities* (Journal of Laws of 2015, item 796), which allows classifying sediment as clean in the context of practical applications. Although the limit values for PCBs specified therein do not refer to the sediment transferred in waters, they serve as the basis for assessing sediment contamination with chemical compounds.

This comparison has shown that the concentration of the sum of seven PCB congeners (no. 28, 52, 101, 118, 138, 153, 180) (<0.3 mg·kg^{-1} DW) was not exceeded for any of the samples taken.

2.3.6.3.4 Crude oil derivative hydrocarbons

Petroleum and petroleum products belong to contaminants that may accumulate in the sediments. The accumulation of petroleum products is caused by a high sorption capacity of the sediment components (Belkina, 2006). The time during which the oil components and the products of their degradation remain in the sediments depends on many factors, such as: type of sediment, temperature, type of oil, nutrient content, rate of biological decomposition, etc. (Nikanorov, Stradomskaya, 2003). The sorption strength of hydrocarbons in sediments varies depending on the type of hydrocarbon and the content of organic matter in the sediment.

In general, the content of mineral oils in the Polish part of the southern Baltic Sea is at a level from below 5 mg·kg^{-1} DW to 25 mg·kg^{-1} DW. The oil content in the sediments from Polish harbours equals 300–625 mg·kg^{-1} DW (Sapota et al., 2012).

In all the sediment samples selected in the survey area, the mean petroleum hydrocarbon concentration equals 7.0 mg·kg^{-1} DW, with the maximum concentration of this compound group being 15.2 mg·kg^{-1} DW.

Currently, there are no Polish legal standards specifying the limit value for the content of petroleum hydrocarbons (mineral oils) indicating sediment contamination. However, such regulations exist in the Baltic countries such as Estonia, Finland, Germany, Latvia, Lithuania, and Russia. Most of these countries specifies two limit values (the first limit and the second limit). If the content of hazardous substances in sediments does not exceed the first limit value, the sediments are considered to be clean and can be deposited in the sea. The content of hazardous substances in dredged sediments exceeding the second limit value indicates that the sediments are contaminated and cannot be deposited in the sea. If the pollution content is between the first and second threshold value, such sediments are defined as potentially polluted and the decision on its deposition can be made after additional tests are carried out (Sapota, 2011).

Exemplary limit values applicable for mineral oils e.g. in Latvia, are 100 mg·kg^{-1} DW (the first limit value) and 400 mg·kg^{-1} DW (the second limit value), while in Finland they are 50 mg·kg^{-1} DW (the first limit value) and 1500 mg·kg^{-1} DW (the second limit value) (Sapota et al., 2012). On this basis, it can be concluded that the concentration values obtained for the seabed sediments in the survey area are low and the sediments are not contaminated with the compounds of this group.

2.3.6.3.5 Organotin compounds (TBT, DBT, and MBT)

Tributyltin is considered to be a persistent pollutant of the marine environment. It is hazardous to numerous aquatic organisms, especially those living in the sediments. TBT was mainly used for producing anti-lichen paints used for coating ship hulls. Currently, the use of the majority of agents containing TBT has been prohibited. Tributyltin decays quite quickly in the marine environment, but is adsorbed on the sediment particles, where the processes of degradation are much slower and may take many years (Antizar-Ladislao, 2008).

TBT may, under favourable conditions, undergo subsequent degradation to dibutyltin (DBT), monobutyltin (MBT), and eventually to inorganic tin. These compounds, in such order, become gradually less toxic (Antizar-Ladislao, 2008).

TBT in particular is highly toxic to marine life, causing changes in oyster shells and interference in the female reproductive organs of the sea snail, an effect known as the "imposex", causing infertility in some sensitive species. TBT is bioaccumulated by marine organisms, causing deleterious effects that depend mainly on the level of final concentration in tissues. Bivalves are not able to degrade TBT via debutylation, such as, for example, fish and some sea snails (HELCOM, 2018).

The Regulation of the Minister of the Environment of 11 May 2015 *on the recovery of waste outside the installations and facilities* (Journal of Laws of 2015, item 796) does not specify the limit values for butyltin compounds (TBT, DBT, and MBT). At present, there are no Polish legal standards specifying the limit value for the TBT concentration indicating the contamination of the seabed sediments. Norway and Sweden also do not have such action levels or dredged material classification. In some Baltic countries, such as Denmark and Finland, there are legal regulations concerning an assessment of seabed sediment. In Finland, the level of seabed contamination is assessed only for purposes of relocation after dredging. In Denmark, the content of hazardous substances is taken into consideration as an essential element of the assessment of the manner of handling sediments and dredged material.

Exemplary limit values applicable for TBT e.g. in Latvia, are 0.007 mg·kg^{-1} DW (the first action limit value) and 0.2 mg·kg^{-1} DW (the second action limit value), while in Finland there are four classes of dredged sediment purity – < 0.005 mg·kg^{-1} DW (Class 1), 0.005–0.030 mg·kg^{-1} DW (Class 2), 0.030–0.100 mg·kg^{-1} DW (Class 3), and 0.100–0.150 mg·kg^{-1} DW (class 4) (Olsen et al., 2019). When the sediment samples collected from the survey area and analysed are compared to these limit values, they can be regarded as close to the first two purity classes in Finland and to the first limit value in Denmark.

The TBT, DBT, and MBT concentrations in all of the sediment samples collected in the survey area were below the LOQ of the analytical method applied (i.e. 0.010 mg·kg^{-1}, 0.001 mg·kg^{-1}, 0.005 mg·kg^{-1}, respectively). The concentrations of TBT and the products of its decomposition (DBT and MBT) obtained for the sediments from the survey area were below the LOQ and were typical for the sandy sediments of the southern Baltic Sea (HELCOM, 2002).

In the Arkona Basin, TBT was determined in the range from 0.003 mg·kg^{-1} to 0.006 mg·kg^{-1}, DBT – from 0.002 mg·kg^{-1} to 0.004 mg·kg^{-1}, and MBT – from 0.002 mg·kg^{-1} to 0.015 mg·kg^{-1} (Abraham et al., 2017).

2.3.6.4 Radionuclides

The radioactivity level in the Baltic Sea is shaped mainly by the presence of caesium-137 (^{137}Cs) and strontium-90 (^{90}Sr) isotopes. Currently, the Baltic Sea is still considered to be the sea most contaminated with ^{137}Cs in the world (International Atomic Energy Agency, 2005; HELCOM, 2009). Practically since 1989, a successive decrease in the ^{137}Cs average activity is observed in the coastal area. This decrease is of exponential character and is associated mostly with radioactive decay and the exchange of waters with the North Sea (Miętus, Sztobryn, 2011). The ^{137}Cs activity in the samples analysed was from < 0.84 to 8.87 Bq·kg^{-1} DW for the sediments collected in the survey area (with an average of 3.55 Bq·kg^{-1} DW).

The activity observed did not exceed the literature values for sandy sediments of the southern Baltic Sea. The differences in the observed activity of ^{137}Cs result directly from the fact that ^{137}Cs is accumulated mainly by organic matter (fauna and flora organisms) suspended in the water column, which is then transported to the seabed, thus forming further layers of seabed sediments along with the inorganic matter. In the case of the seabed sediment samples tested, ^{137}Cs is sorbed only on the surface of mineral particles, which results in its low activities (Saniewski et al., 2021; Saniewski, Zalewska, 2016; Zalewska, Suplińska, 2013).

To compare, in 2010 the radioactive concentration of ^{137}Cs in the surface layer of the seabed sediments in the area of the Gdańsk Deep exceeded 200 Bq·kg^{-1}, while in the Bornholm Deep it equalled approx. 50 Bq·kg^{-1} (Zalewska, Kraśniewski, 2019).

2.3.6.5 Grain size analysis

The grain size analysis of surface soil samples indicates the sandy and sand-gravel character of the sediments within the survey area. Locally, in the northern part of the survey area, higher contents of gravel fraction were observed (50% in sample SO_MFW_029).

An increased content of fine fractions (silt and clay) was observed in the south-eastern part of the survey area. Only one surface soil sample from the survey area (SO_MFW_075) had a fine-particle content of more than 10% (15.3%) and was classified as sand with silt.

2.3.6.6 Summary of the analysis results

The analysed sediments from the survey area belong to non-organic sediments with an organic matter content expressed with LOI < 2% and TOC concentration below 1.0 g·kg^{-1} DW. Sandy and sand and gravel sediments are predominant.

Sediments were characterised by a low nutrient content. In most of the analysed samples, concentrations of total nitrogen were below the LOQ of the method applied (200 mg·kg^{-1} DW). The mean concentrations of total phosphorus obtained in the survey area were, respectively, 190 mg·kg^{-1} DW in the winter and 193 mg·kg^{-1} DW in the summer. The concentrations of persistent organic pollutants (i.e. PAHs, PCBs, and TBT) and toxic substances such as metals and metalloids (Pb, Cu, Zn, Ni, Cd, As, Hg, Al) or petroleum hydrocarbons, in the survey area, were low and did not deviate substantially from the data from literature regarding sandy sediments of the southern Baltic Sea. The sediments tested were also characterised by low concentrations of the radioactive element ^{137}Cs typical for sandy sediments.

The results obtained for metals and metalloids (mobile form Pb, Cu, Zn, Ni, Cd, Cr, As, Hg), PAHs and PCBs were compared with the limit values specified in the Regulation of the Minister of the Environment of 11 May 2015 o*n the recovery of waste outside the installations and facilities* (Journal of Laws of 2015, item 796), below which the seabed sediments can be used in reclamation processes, i.e. the regulation indirectly determines the sediment purity. On this basis, it was concluded that the concentration values obtained for the above-mentioned compound groups in the sediments analysed from the survey area were low, and the sediments were not contaminated with the compounds of this group.

2.3.7 Shortcomings and gaps in the state-of-the-art

No shortcomings nor gaps in the state of the art were identified as part of the seabed sediment surveys.

2.4 AGGREGATES

2.4.1 Non-specialist summary

Based on the bathymetric and sonar data analysis and using the data from the analysis of surface sediment samples and core samples collected using a vibrocorer, as well as data from seismic and seismo-acoustic surveys, a preliminary characterisation of the survey area was commenced regarding the presence of sandy and sand and gravel covers. Data from literature were also analysed. It stems from these analyses that the survey area lies within the range of occurrence of sands and sands and gravels of various grain sizes. Fine- and medium-grained sands are deposited on the seabed, with medium- and coarse-grained sands as well as gravelly sands and sandy gravels in its northern part. The thickness of the sand and gravel sediments in the greater part of the survey area exceeds 1 m. Almost the entire survey area is identified as prospective in terms of the occurrence of aggregate resources. Furthermore, in the western part of the area, the "Southern Middle Bank" Southern Baltic mining site is located, which borders the WTG construction area to the west.

A map of surface sediments was drafted for the survey area. A map of the thickness of sandy and sand-gravel sediments and a map of boulder occurrence were also developed and analysed. The extent of the potential aggregate deposit was determined and sample geological cross-sections were prepared.

2.4.2 Spatial scope of the surveys

The spatial scope of the identification of potential mineral deposits is the survey area covered by geophysical surveys (Subsection 1.2).

2.4.3 Methodology

The occurrence of potential aggregate deposits in the survey area was determined based on the analysed results of geophysical data processing and on the basis of sediment geological surveys.

According to the Act of 9 June 2011 – *Geological and Mining Law* (Journal of Laws of 2022, No. 1072, item 981, as amended) and the Regulation of the Minister of the Environment of 1 July 2015 *on the geological documentation of mineral deposits, excluding hydrocarbon deposits* (Journal of Laws of 2015, item 987), a deposit should have a thickness of at least 2 m, the maximum overburden ratio should be 1, while the maximum mineral dust content may be 15% (the limit values of the parameters defining a deposit and its boundaries for individual minerals – gravel deposits, gravel-sand deposits and sand-gravel deposits with a sand point below 75%). It should be emphasised that the permissible values contained in the Regulation do not distinguish between terrestrial and marine mineral deposits. Since 1 January 2012, the same permissible values are applicable to terrestrial and marine mineral deposits.

These criteria do not fully correspond to the conditions of occurrence of deposits on the seabed. Therefore, the documentation of natural aggregate deposits in the Baltic Sea to date was based on the now-expired "Balance Criteria for Natural Aggregate Deposits in the Polish Baltic Area" (Ministry of Industry, Warsaw, 1988). According to the "Balance criteria…" quoted, a marine deposit must be characterised by the following parameters:

- it must not occur under the overburden;
- the minimum thickness of the deposit series: 0.3 m on sandy substrate or 0.5 m on till and clay substrate;
- the minimum surface area of the deposit field: 0.25 km^2;
- deposit depth (ordinate of the deposit series bottom): up to 30 m BSL.

During the preparation of the Geoenvironmental Map of the Polish Sea Areas at a scale of 1:250 000 (Kramarska et al., 2019), the following parameters were adopted for the delineation of prospective areas of sand and gravel deposition:

- sea depth of 30–40 m at a maximum;
- thickness of sandy sediments approximately greater than 1 m;
- median grain size of seabed surface sediments greater than 0.125 mm.

Given the above, the following limit values were adopted for the parameters defining a clastic deposit:

- the type of mineral – sands and gravels;
- the minimum deposit thickness – 2.0 m;
- the minimum surface area of the deposit field – 0.25 km^2;
- the maximum sea depth – 40 m.

Due to the high lithological diversity of the sediments and insufficient density of the sampling points for surface sediments and core samples, the grain size median and the mineral silt content were not accounted for.

2.4.4 Activities performed

The data collected were interpreted in terms of evaluation and characteristic of the survey area to identify prospective areas of occurrence of clastic deposits. In addition, literature data were analysed in terms of the occurrence of mineral resources in the survey area. Maps of surface sediments were prepared and maps of the thickness of sandy and sand-gravel sediments and a map of boulder occurrence were developed and analysed. The extent of the potential aggregate deposit was determined, sample geological cross-sections were prepared.

2.4.5 Results

According to the literature data, the area under analysis is located within the range of occurrence of sands and sands and gravels of various grain sizes (Pikies, 1990, 1995). Mainly fine- and medium-grained sands are deposited on the seabed surface and in the northern part of the area analysed – medium- and coarse-grained sands as well as gravelly sands and sandy gravels (Kramarska, 1995 a,b; Kramarska et al., 1995) [Figure 2.87]. These are mainly fluvioglacial sands and gravels as well as marine sands and gravels. In most part of the survey area, the thickness of the sand and gravel sediments is greater than 1 m (Kramarska, 1995a).

Nearly the entire survey area is identified as prospective in terms of sand and gravel resources occurrence (area V – Southern Middle Bank) (Kramarska et al., 2005, 2019) [Figure 2.88].

The western part of the survey area is adjacent to, while the survey area overlaps by a 1-NM wide strip with the mining site "Southern Middle Bank" Southern Baltic KN 6192 with a surface area of 8167 ha (Register No. 9/2/226/a,b,c; license validity date: 15 November 2031). Within this area, three mining areas have been indicated:

- Southern Middle Bank A with an area of 826 ha (Register No. 9/2/226/a; license validity date: 15 November 2031);
- Southern Middle Bank B with an area of 3360 ha (Register No. 9/2/226/b; license validity date: 15 November 2031);
- Southern Middle Bank C with an area of 702 ha (Register No. 9/2/226/c; license validity date: 15 November 2031) (igs.pgi.gov.pl; geolog.pgi.gov.pl).

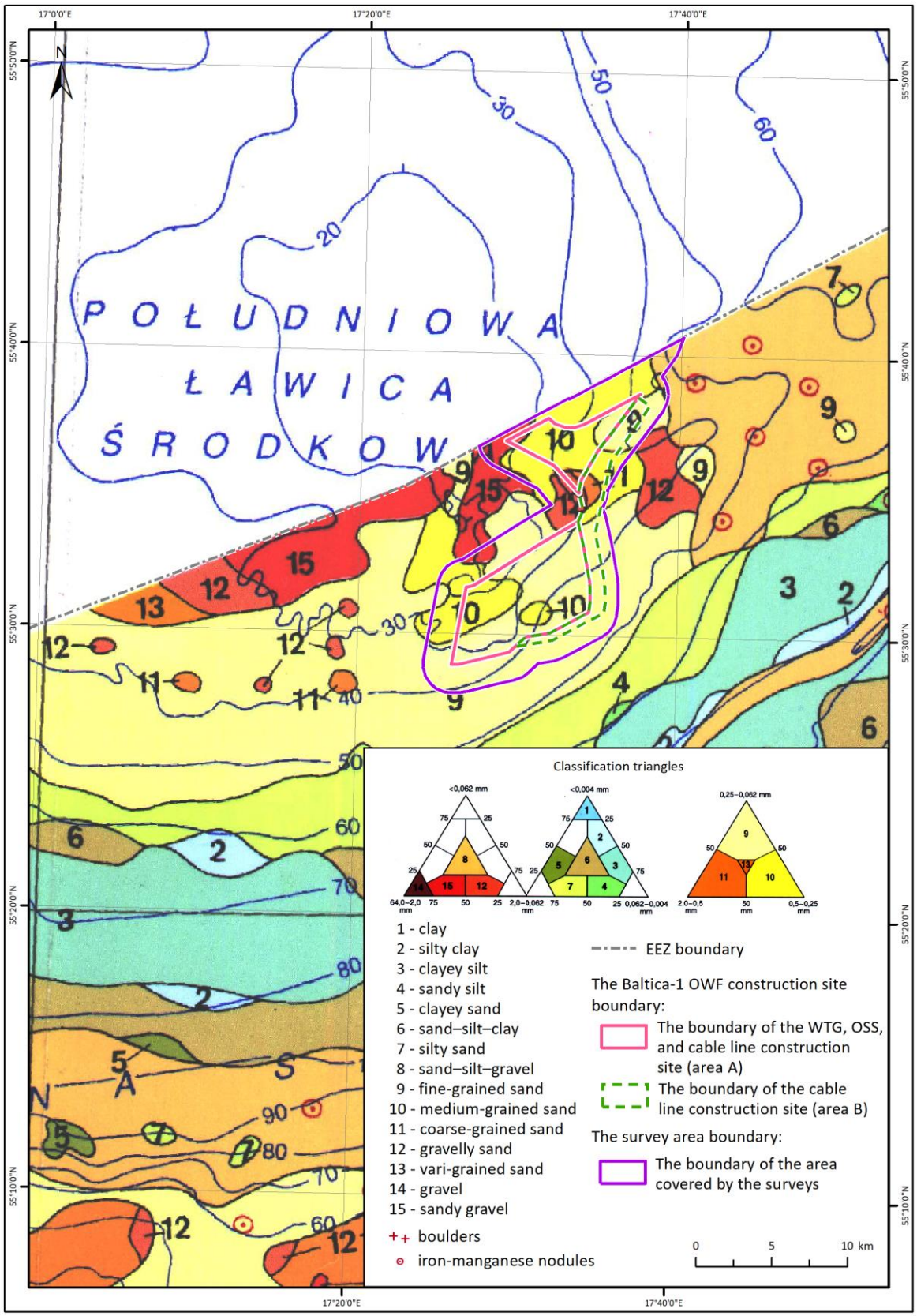


Figure 2.87. The survey area against the background of a fragment of the map of surface sediments [Source: internal materials based on Kramarska, 1995b]

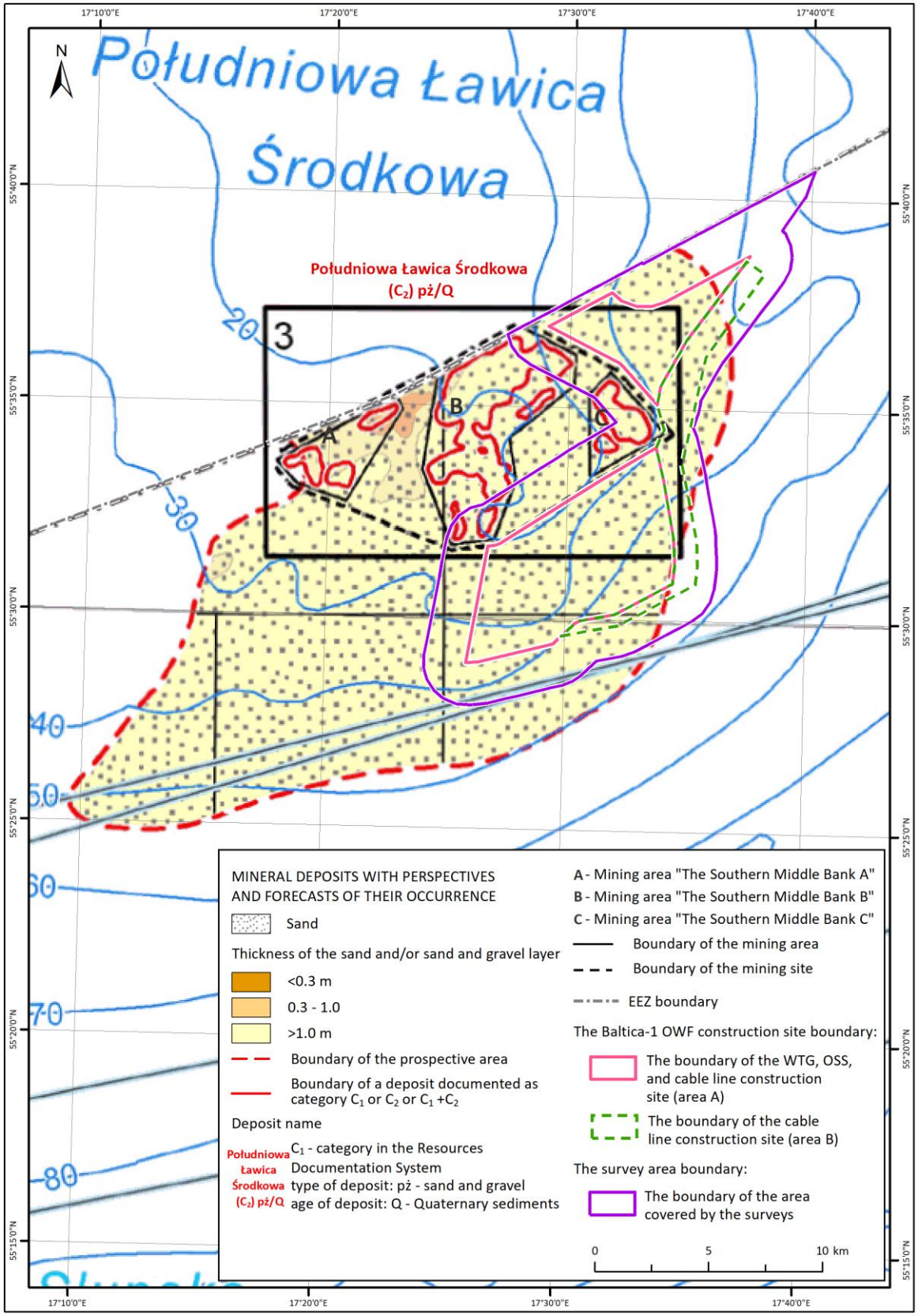


Figure 2.88. The survey area against the background of a fragment of the map of "Deposits and prospective areas of aggregate resources" [Source: internal materials based on Kramarska et al., 2005]

The results of the analyses of the grain size analysis of the surface sediment samples collected from the survey area indicate that at all the designated surface sediment sampling points, sand and sand and gravel sediments were identified.

The analysis of core samples collected using a vibrocorer confirms the presence of sandy and sand-gravel deposits over the majority of the survey area. In the northern end of the area, only a small layer of sand and sand-and-gravel cover was found, with a thickness of 0.1 to 0.3 m, underlain with cohesive sediments (clays with silt, sand and gravel). The proportion of sandy sediments in the borehole profiles increases towards the south. In the southern part of the survey area, the thickness of the sand and sand-gravel sediments reaches the limits of identification using a core (6 m).

Analyses of the grain size of the core samples from the survey area indicate a clear dominance of sands in the borehole profiles. Of all the samples from the survey area subjected to grain size analysis, 60% are coarse-grained soils (mainly sands and sands with gravel). The remaining samples (40%) are fine-grained soils (mainly clays with silt and sand as well as sands with silt). Gravels occur sporadically (in less than 3% of the samples).

Coarse-grained material occurring directly on the seabed within the survey area is prospective in the context of raw material management.

Maps of surface sediments and boulder occurrence developed for the survey area are included in Chapter 1.

A map of the extent and thickness of a potential deposit formed of sand and sand-gravel sediments identified based on seismic and seismo-acoustic data as unit IA [fine- and medium-grained sands, locally silty sands in some places coarse-grained sand and gravels (marine, fluvial and fluvioglacial)] and unit IB [fine- and medium-grained sands, locally sands with gravel (lagoon, fluvial, fluvioglacial)] is presented in Figure 2.89. Following the adopted methodology, there were delimited the areas with a minimum deposit thickness of – 2.0 m (taking into account the total thickness of sediments representing units IA and IB), an area with a minimum deposit field – 0.25 km^2, and areas with a maximum sea depth – 40 m. Example geological cross-sections were also prepared [Figure 2.90–Figure 2.94].

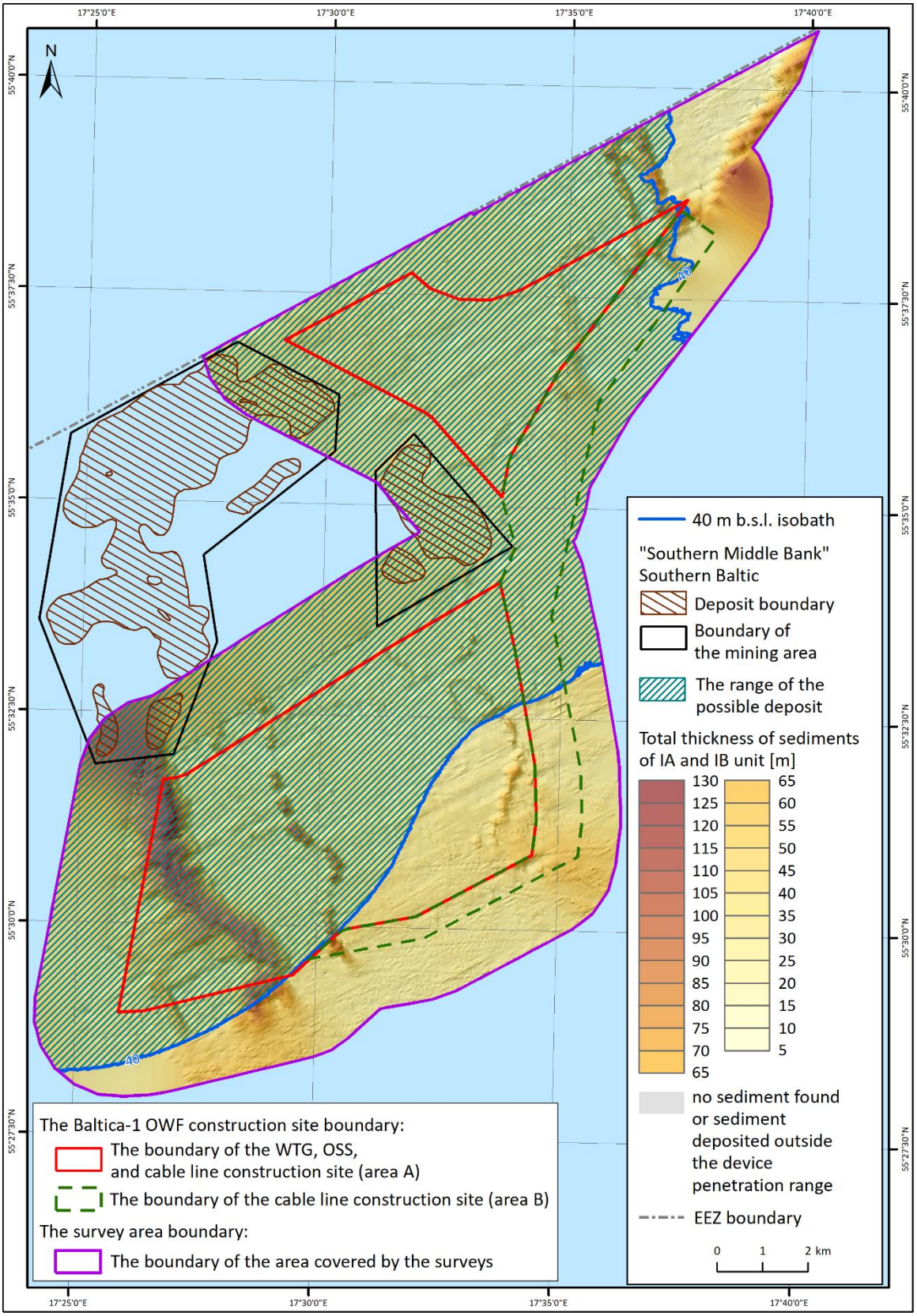


Figure 2.89. The extent and thickness of the potential aggregate deposit (with a thickness > 2 m) located in the survey area

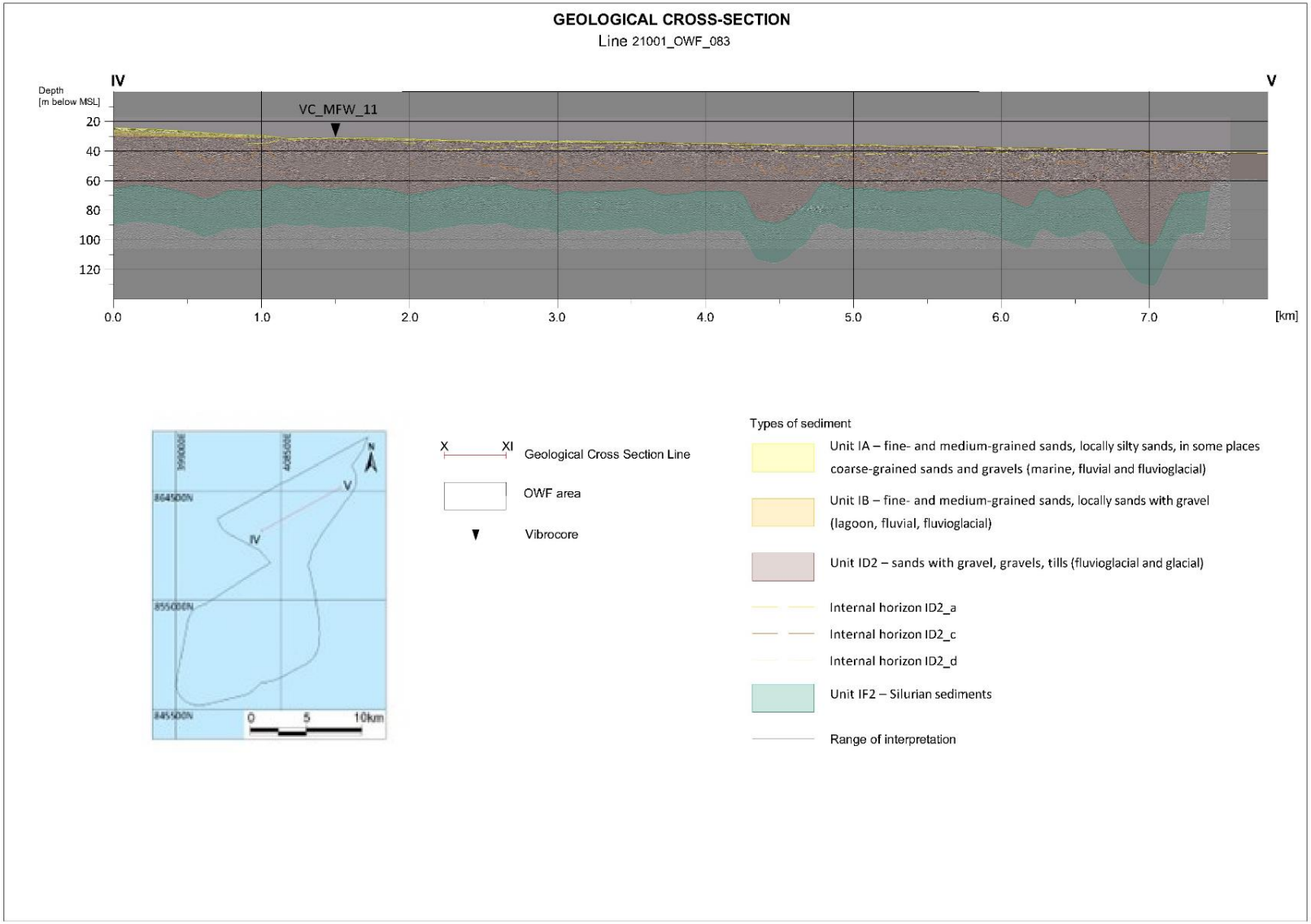


Figure 2.90. A geological cross-section along survey line 21001_OWF_083; the survey area

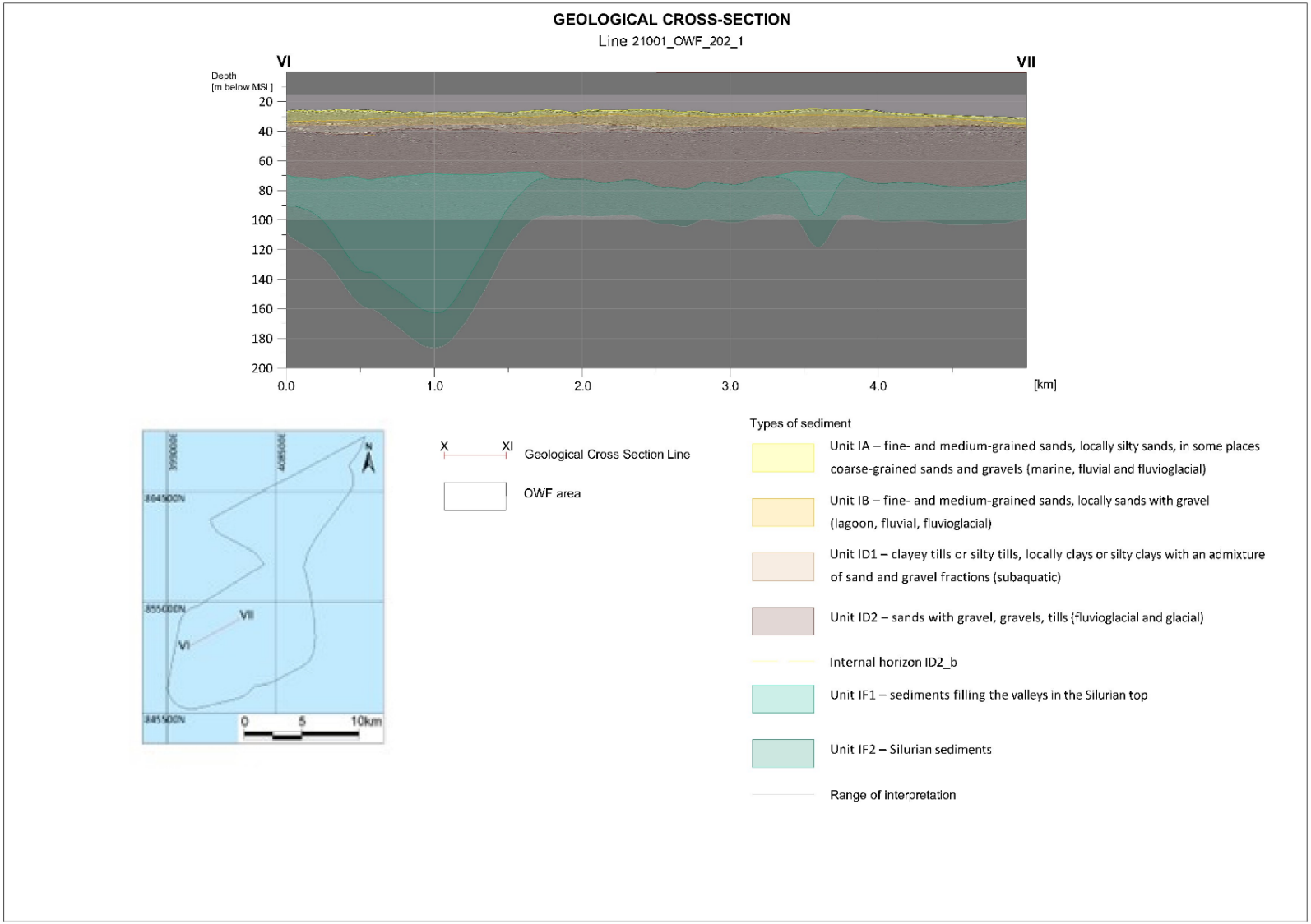


Figure 2.91. A geological cross-section along survey line 21001_OWF_202_1; the survey area

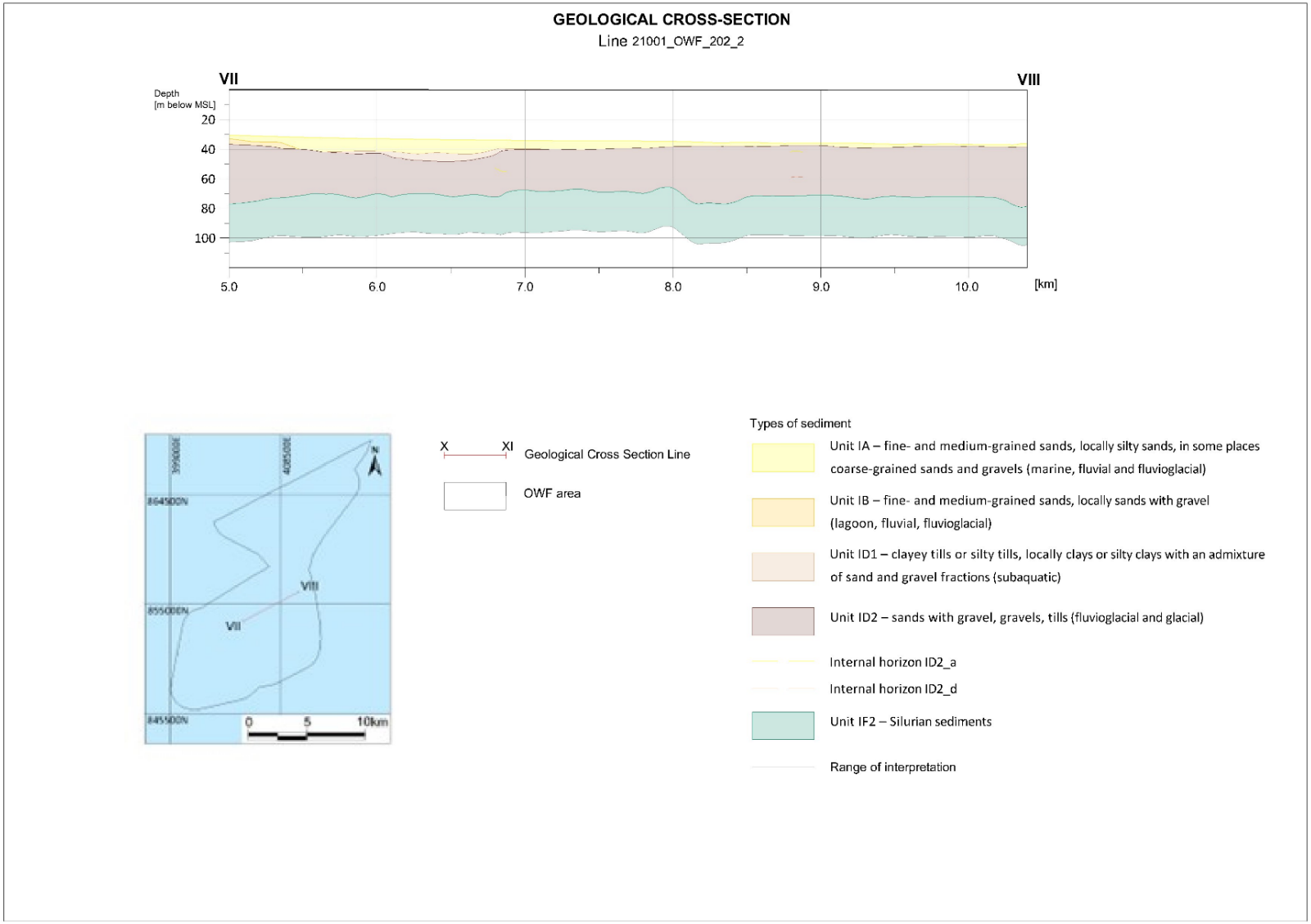


Figure 2.92. A geological cross-section along survey line 21001_OWF_202_2; the survey area

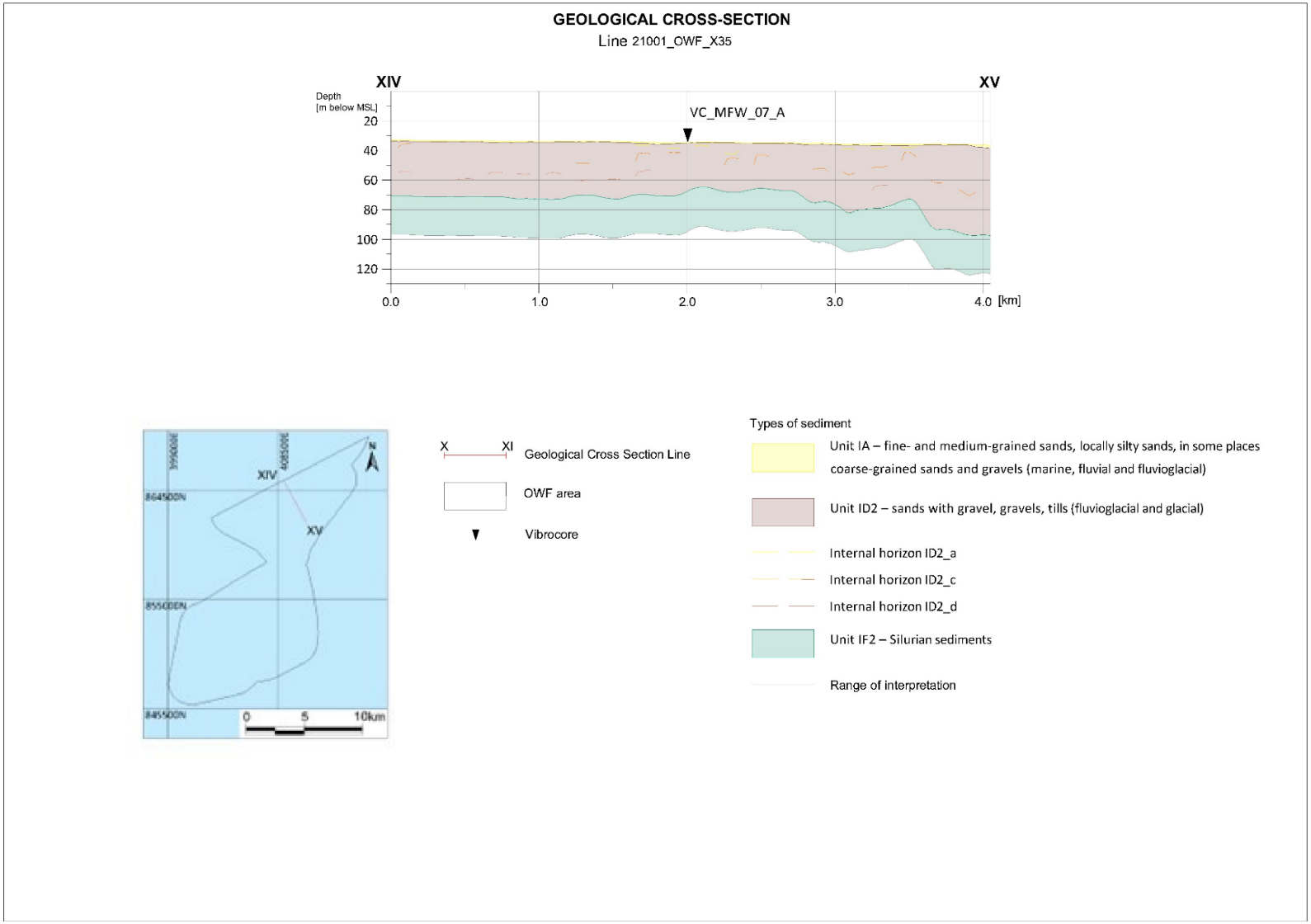


Figure 2.93. A geological cross-section along survey line 21001_OWF_X35; the survey area

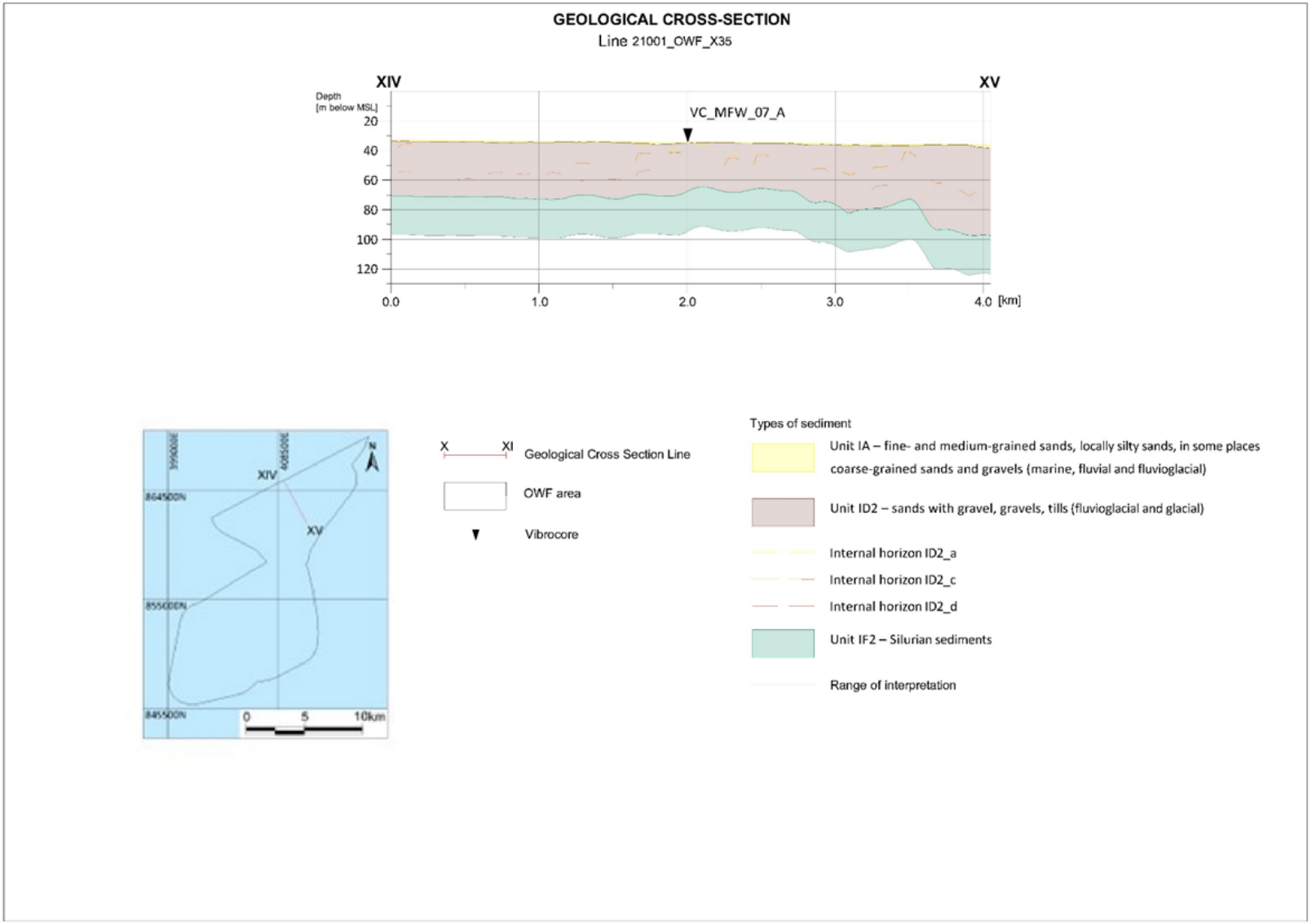


Figure 2.94. A geological cross-section along survey line 21001_OWF_X18; the survey area

2.4.6 Summary of results and conclusions

The survey area lies within the range of occurrence of sands and sands and gravels of various grain sizes. Fine- and medium-grained sands are deposited on almost the entire seabed surface, while in its northern part, additionally, there are medium- and coarse-grained sands as well as gravelly sands and sandy gravels.

The thickness of the sand and gravel sediments in the greater part of the survey area exceeds 1 m. Almost the entire survey area is identified as prospective in terms of the occurrence of aggregate resources. In the western part of the area, the mining site "Southern Middle Bank" Southern Baltic is located.

A map of surface sediments was drafted for the survey area. A map of the thickness of sandy and sand-gravel sediments and a map of boulder occurrence were also developed and analysed. The extent of the potential aggregate deposit was determined and sample cross-sections were prepared.

As part of the marine aggregate surveys, no project constraints were identified that would result from the environmental surveys conducted so far, including the classification of a part of the survey area as an area prospective for the occurrence of clastic deposits.

In accordance with the provisions of the Regulation of the Council of Ministers of 14 April 2021 *on the adoption of the spatial development plan for the internal sea waters, the territorial sea and the exclusive economic zone at the scale of 1:200 000* (Journal of Laws of 2021, item 935, as amended) for the sea basin POM.60.E in which the Project area is located, the basic function is "renewable energy acquisition". A permissible function is the "exploration and prospecting of mineral resources and extraction of minerals from deposits", which is described further on in the sea basin sheet: "*in the entire sea basin, the function of (prospecting and exploration of mineral resources and extraction of minerals from deposits) shall be limited to methods which do not disturb linear elements of technical infrastructure; do not jeopardise the ecological function of spawning grounds and the survival of the early development stages (eggs and larvae) of commercial species; in the entire sea basin the extraction of minerals from deposits is limited to projects agreed upon with the relevant project owners of offshore wind farms*." Due to the indication of the superior function for the sea basin POM.60.E – acquisition of renewable energy, the topic of exploration and prospecting of mineral resources, as well as extraction of minerals from deposits should be considered a secondary issue.

2.4.7 Shortcomings and gaps in the state-of-the-art

No shortcomings or gaps in the current knowledge were identified during the surveys.

2.5 ACOUSTIC BACKGROUND

2.5.1 Non-specialist summary

In an aquatic environment, sound waves are a very effective and irreplaceable way to transfer information. Perfect propagation conditions – sound propagates relatively quickly and far in water – mainly caused by a much lower attenuation of sound waves in water unlike electromagnetic waves. This allows information to be provided “by sound” in much larger spatial scales (ranges) compared to other sensory stimuli, such as light or smell.

Most of the marine organisms use sound as a sensory tool to study the surrounding marine environment, and for fundamental life functions. For mammals, some fish, and invertebrates, sound is

used for spatial orientation and navigation under water, for searching of food or avoiding predators, for intraspecific communication, and for displaying certain behaviours (including of mating and reproduction), for informing about danger, as well as for parental care.

Noise of anthropogenic origin has been recognised on a global scale as a pollutant for years, and it is assumed that it is one of the most harmful forms of pollution, ubiquitous in both terrestrial and underwater ecosystems. As measurement and observation techniques advance, there is increasing evidence of the negative effects of anthropogenic noise on marine life. This noise is a major stress factor for marine organisms, causing changes, for example in the hearing threshold (auditory ability), as well as causing behavioural and physiological changes in them.

In legal terms, in 2008, the Marine Strategy Framework Directive (MSFD) was adopted in the EU, which defines the main legal conditions regarding underwater noise. In this document, under the law, underwater noise was recognised as a significant pollutant of the marine environment, adversely affecting the welfare of animals and potentially threatening their life. It also emphasised that the level of noise emissions should be limited, and one of the basic tasks is to protect European seas, including – achieving the so-called Good Environmental Status (GES). In the guidelines of the MSFD directive with regard to the continuous noise, it is recommended to monitor underwater noise throughout the year and determine noise levels in the 1/3-octave frequency bands with the central frequencies of 63 Hz and 125 Hz (descriptor 11.2), as well as performing calculations of the basic physical characteristics of underwater noise in a wide frequency range, i.e. at least up to 10 kHz (Van der Graaf et al., 2012).

The aim of the monitoring surveys was to conduct pre-investment measurements of the underwater noise field in the survey area. The main priority was to determine the base situation ("zero point") in relation to the noise level to obtain the possibility of identifying potential changes in the marine environment caused by anthropogenic activity during the construction, operation, and decommissioning phase of the investment project.

This Report presents the results of the acoustic background noise research conducted in the survey area in the period of December 2022–February 2024 for further use in the environmental impact assessment (EIA).

The acoustic data were collected in accordance with international standards and recommendations for the best practices in underwater noise field measurements. The basic element of the monitoring survey was the recording of underwater ambient noise with the use of the autonomous noise recorder SM4M Submersible (Wildlife Acoustics, USA) equipped with the omnidirectional ultrasonic hydrophone HTI-96. In the study discussed, acoustic data were analysed in detail in the frequency range of individual 1/3 octave bands with central frequencies from 20 Hz to 20 kHz. It is fully compliant with the latest recommendations of the HELCOM EN-Noise Expert Group (HELCOM, 2021). This scope covers the majority of anthropogenic noises caused by human activities at sea, including in particular: shipping noise, sounds emitted by seismic research devices, noise generated during the pile-driving process as well as during underwater explosions.

The methodology of data post-processing was in line with international standards of many organisations and recommendations of the expert groups (EU TG-Noise, HELCOM EN-Noise) in the field of acoustic data analysis of the underwater noise field, widely used also in international research projects. All recorded data obtained in individual measurement campaigns were analysed. The results are presented divided by seasons, in accordance with the observed sound propagation conditions in

the survey area, obtained based on the measurements of the vertical temperature and salinity profiles performed during individual services of research instruments.

The results of the background noise monitoring in the survey area showed that the ambient noise levels (and ranges of variability) show values which are characteristic of the southern Baltic Sea area. In the time series of the sound pressure level SPL, a significant contribution to the underwater ambient noise is caused by the anthropogenic component related mainly to shipping as well as operations of seismo-acoustic devices (e.g. sparker, boomer, sub-bottom profiler) is observed. In regards to the sounds of natural origin, there are significant fluctuations in the noise level (single peaks), reaching values in the order of 20–25 dB.

2.5.2 Spatial scope of the surveys

The spatial scope of acoustic noise measurements was limited to the survey area covering the Baltica-1 OWF construction area, which is the area of construction of WTGs, OSSs, and cable lines (area A) and the area of construction of cable lines (area B) together with a zone of no less than 40 km in width measured from the boundary of area A [Figure 2.95].

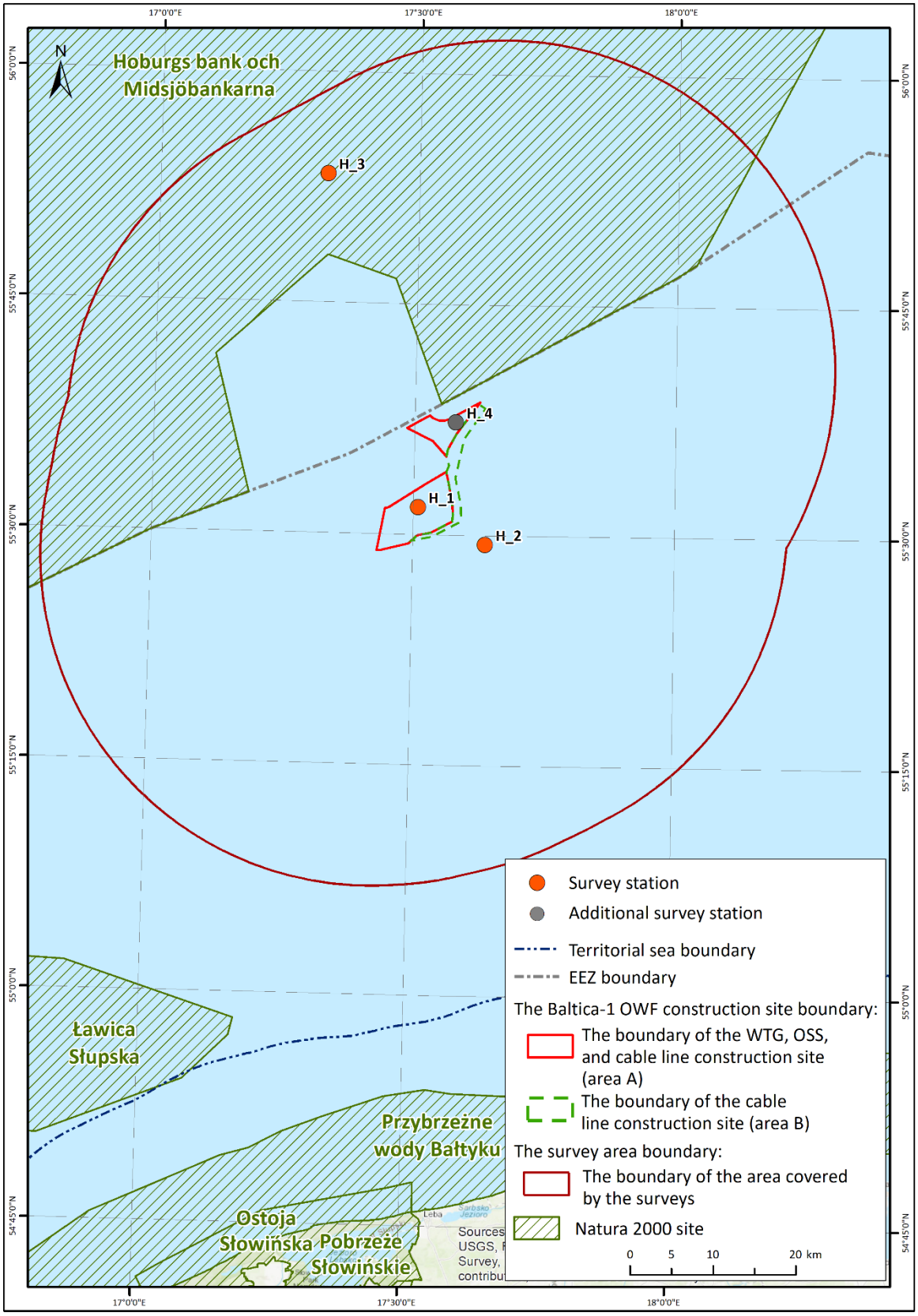


Figure 2.95. The deployment locations of the SM4M noise recorders in the survey area

2.5.3 Methodology

Acoustic data were collected in line with the international standards and recommendations of the Expert Group on the acoustic noise operating within the framework of the Marine Strategy Framework Directive (BSH, 2011; Dekeling et al., 2014a, b, c; Van der Graaf et al., 2012).

The primary element of the monitoring was a registration of ambient underwater noise using an autonomous noise recorder SM4M Submersible Wildlife Acoustics equipped with an omnidirectional ultrasonic hydrophone HTI-96 allowing the registration of ambient noise in the frequency range from 2 Hz up to 192 kHz. According to the manufacturer's data, the sensitivity of the hydrophone at the preamplifier output is approximately -165 dB re 1V μPa^{-1} in frequency range 200 Hz – 1.6 kHz.

The SM4M noise recorders were deployed in water column approximately 5 m above the seabed in compliance with the deployment scheme presented in Figure 2.96. It should be mentioned that only flexible elements (composite ropes) were used in the anchoring system, i.e. there were no metal elements (e.g. chains), which could have caused unwanted interferences.



Figure 2.96. Noise recorder SM4M Submersible (Wildlife Acoustics, USA) with a single HTI-96 hydrophone (on the left) and the measuring instrument deployment scheme (on the right)

In the surveys discussed, ambient noise was registered, in general, in the frequency range from 2 Hz up to 96 kHz. The upper limit of this frequency range resulted from the fact that the sampling frequency *Fs = 192 kHz* was chosen for the survey conducted with the use of SM4M recorders (which is the minimum available frequency in survey instruments of such type), and following the Nyquist rule, *Fs/2 = 96kHz*. However, a detailed analysis was performed for acoustic data in the frequency range from 20 Hz up to 20 kHz – these frequencies indicate the central frequencies of the 1/3-octave bands (HELCOM, 2021). The HELCOM document underlines also that to fully cover all the 1/3-octave frequency bands in the range of 20 Hz–20 kHz (34 bands in total), the acoustic data should be recorded in the frequency range from 17.8 Hz up to 22.39 kHz [Table 1 in HELCOM (2021)]. Due to the "elevated" frequency sampling, the noise data in the range of very high frequencies (i.e. nominal frequencies of over 22.39 kHz) are treated as a "excess". Moreover, it should be noted that there are no any underwater sounds of natural origin (including biosounds) as well as noise of anthropogenic origin with the frequencies consistent with the frequency range of interest, and which could cause any significant changes in the ambient noise spectrum – taking into account also the fact that, in context of the investment analysed, the main part of acoustic energy is (or is emitted) in a frequency range of up to several kHz during the WTG construction phase.

In general, SM4M noise recorders allow recording survey data in digital format (wav-files) with a 16-bit quantisation and the chosen sampling frequency in the range of 192 kHz–384 kHz (for the surveys discussed, sampling frequency F_s = 192 kHz was chosen). To increase the effectiveness of survey data recording, including minimising the risk of power off due to drained batteries and reaching the data storage limits, a data recording scheme with a duty cycle of 1-minute recording and 9-minute pause was introduced (which means 6 records per 1 h, i.e. 10% day cycle).

Ambient noise signals were recorded on SD memory cards. Next, a data analysis was performed using specific scripts developed specifically for this purpose in MATLAB® (MathWorks Inc., USA) software.

All data registered were subjected to the analysis. At the first stage of the ambient noise data analysis, fragments of time series with acoustic signal clipping (oversaturation) were eliminated from further analysis. The main reason of acoustic signal clipping is noise from vessels passing at a very small distance from the recorder and/or high-energy impulse noise from operating seismoacoustic survey instruments. In this case, some of survey data samples exceed the dynamic range of the noise recorder causing signal clipping. A simple algorithm was used to scan the entire signal of a sample meeting the threshold value (limited by the dynamic range of the noise recorder). A time series was considered unrepresentative if the number of samples with clippings was at least 0.1%. It complies with the signal processing scheme proposed in the BIAS project (Betke et al., 2015).

The spectral analysis of noise signals was conducted with the use of the Fourier Transform, which is widely used in practice. An algorithm known as the Fast Fourier Transform (FFT) was applied. The algorithm, which is based on the mathematical properties of the Fourier Transform, optimises its computational process.

The instantaneous spectra were calculated for fragments of noise signals with the length of $N = 4*2^{14} = 4*16\,384 = 65536$ samples (with a duration of $\tau = 341.3$ ms) and then averaged over 1-minute sections. The use of the averaging time T_{ave} = 1 min complies with the recommendations of the European TG-Noise Expert Group (Ainslie, Dekeling, 2018).

The power spectral density (PSD) was calculated using the spectrogram function (which is provided in the MATLAB Signal Processing Toolbox), with the use of a non-overlapping rectangular window of N length equal to the length of the analysed fragments of the noise signal (with no overlapping of subsequent sub-samples). The noise spectra were calculated in 1 Hz frequency bands and thirds (1/3-octave frequency bands). In addition to, the sound pressure levels (SPL) in 1/3-octave frequency bands with central frequencies of 63 Hz and 125 Hz were calculated, which, are mentioned in the MSFD as descriptors of background noise in marine environment (Dekeling et al., 2014a, b, c). The broadband SPL in the frequency range from 20 Hz up to 20 kHz was calculated as well (in line with HELCOM, 2021).

The central frequencies of the 1/3-octave frequency bands (thirds) were defined in accord with the standards of the American National Standards Institute (ANSI, 2009) and the International Electrotechnical Commission (IEC 61260-1, 2014).

Additionally, during the maintenance services of the survey devices the vertical temperature and salinity profiles were measured at each survey station with the use of the Valeport Monitor CTD+ probe. The sound velocity was calculated based on the measured values of temperature, salinity (conductivity), and pressure (depth) with the application of a commonly used empirical equation proposed by Chen and Millero, known in the literature as the UNESCO algorithm (Chen, Millero, 1977). In determinations of sound velocity in water, this algorithm implies little derogation from the

measurement data in a wide range of individual parameters included in the equation: temperature in the range of 0–40°C, salinity from 0 to 40 PSU, and hydrostatic pressure from 0 to 100 MPa (i.e. to the depth of approximately 10 km).

2.5.4 Activities performed

The acoustic noise measurements were carried out in the period from December 2022 to February 2024. The measuring devices at survey stations H_1, H_2 and H_4 (an additional station) were deployed on 3 December 2022. At survey station H_3, the device was deployed on 15 February 2023, after an e-mail confirmation had been received from the Swedish side that there was no need to apply for a permit to conduct monitoring in the Swedish EEZ.

A compilation of survey data obtained is presented in Table 2.54.

Table 2.54. A summary of the obtained survey data

Survey station	Measurement period		Data yield percentage in the measurement period [%]	Total number of samples containing data/the number of samples analysed	Comments	Type of data delivered
	Survey gear deployment date	Data reading date				
H_1	03.12.2022	07.02.2023	100	9455 / 9439	-	Raw data in *.wav format; Processed data in *.mat format: • the mean power spectrum density PSD [dB re 1 µPa^2·Hz^{-1}] in 1/3-octave bands (in the frequency range of 20 Hz–20 kHz); • time series of the sound pressure level SPL [dB re 1 µPa] in 1/3-octave frequency bands (in the frequency range of 20 Hz–20 kHz); • time series of broadband $SPL_{20Hz\text{-}20kHz}$
	07.02.2023	24.04.2023	100	10946 / 10945	-	
	24.04.2023	13.08.2023	100	15977 / 15435	-	
	13.08.2023	12.11.2023	100	13147 / 13141	-	
	12.11.2023	03.12.2023	100	3070 / 3067	-	
H_2	03.12.2022	-	0	-	Disappearance of the survey device was noted on 7.02.2023, during a service vessel passage. No data available. As data obtained at stations H_1 and H_4 are representative for the survey area (in terms of acoustics, this is the same area), the lack of data from station H_2 does not affect the conducted environmental impact assessment	
	16.02.2023	29.04.2023	100	10411 / 10399	-	
	29.04.2023	12.08.2023	0	-	Damage to the measurement buoy. No data available. As data obtained at stations H_1, H_3, and H_4 are representative of the survey area (in terms of acoustics, this is the same area), the lack of data from station H_2 does not affect the conducted environmental impact assessment	
	12.08.2023	13.11.2023	0	-	Damage to the measurement buoy. No data available. As data obtained at stations H_1, H_3, and H_4 are representative of the survey area (in terms of acoustics, this is the same area), the lack of data from station H_2 does not affect the conducted environmental impact assessment	
	14.11.2023	15.02.2024	100	13444 / 13436	-	
H_3	15.02.2023	30.04.2023	100	10744 / 10668	-	

Survey station	Measurement period		Data yield percentage in the measurement period [%]	Total number of samples containing data/the number of samples analysed	Comments	Type of data delivered
	Survey gear deployment date	Data reading date				
	30.04.2023	12.08.2023	100	14941 / 14934	-	
	12.08.2023	13.11.2023	100	13486 / 13477	-	
	13.11.2023	15.02.2024	100	13485 / 13483	-	
H_4	03.12.2022	07.02.2023	100	9505 / 9498	An additional survey station	
	07.02.2023	24.04.2023	100	10879 / 10622		
	24.04.2023	13.08.2023	100	15959 / 15951		
	13.08.2023	12.11.2023	100	13166 / 13141		
	12.11.2023	03.12.2023	100	3097 / 3096		

2.5.5 Results

The conditions of sound wave propagation in seawater are evaluated on the basis of the vertical sound velocity profile, which, in turn, is determined based on the thermohaline conditions (temperature and salinity distribution). For the Baltic Sea, it is characteristic that the sound velocity profiles indicate both spatial and temporal variability. Spatial variability is observed with an increasing distance from the Arkona Deep in the eastern and north-eastern directions. In turn, the temporal variability depends essentially on the seasonal changes of temperature and salinity distribution, which result in the formation of a near-surface acoustic channel (waveguide), and in the summer time – a deep-water acoustic waveguide (Klusek, 1990; Klusek and Lisimenka, 2016).

The changes in the sound propagation conditions in the survey area are presented in the form of the vertical profiles of temperature, salinity, and sound speed measured at individual survey stations – H_1, H_2, H_3, and H_4. The vertical profiles of temperature and salinity were obtained during the deployment and servicing of the survey equipment [Table 2.54] with the use of a Valeport Monitor CTD+ probe and the sound velocity profile calculated [Figure 2.97–Figure 2.100]. For clarity, each figure also illustrates the results from the previous measurements taken at each survey station.

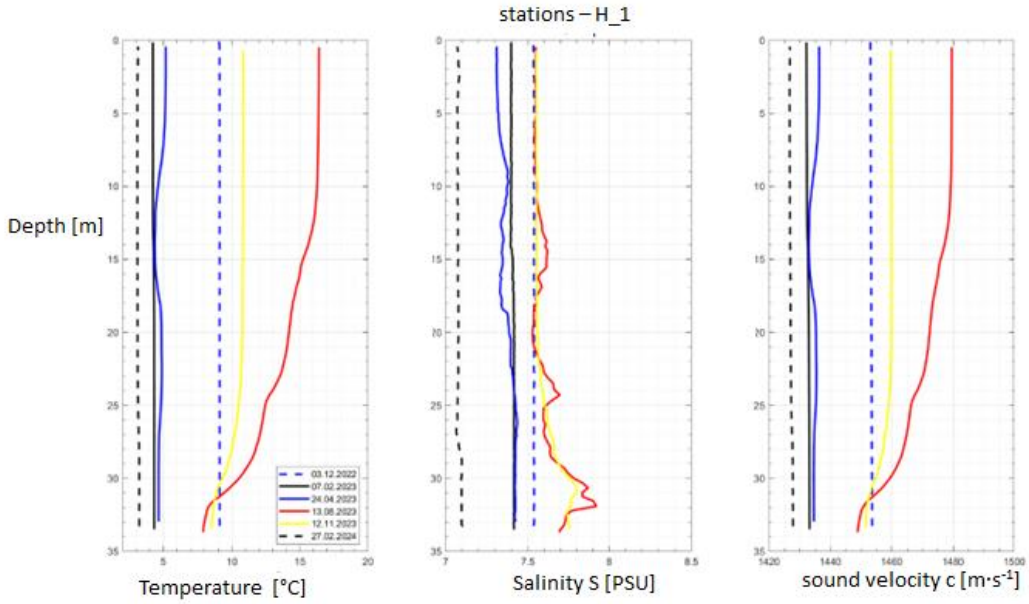


Figure 2.97. The vertical profiles of temperature T [°C], salinity S [PSU], and sound velocity c [m·s^{-1}] recorded at survey station H_1 on 3 December 2022 (dashed blue curves), 7 February 2023, 24 April 2023, 13 August 2023, 12 November 2023 (respectively, solid black, blue, red, and yellow curves) and 27 February 2024 (dashed black curves)

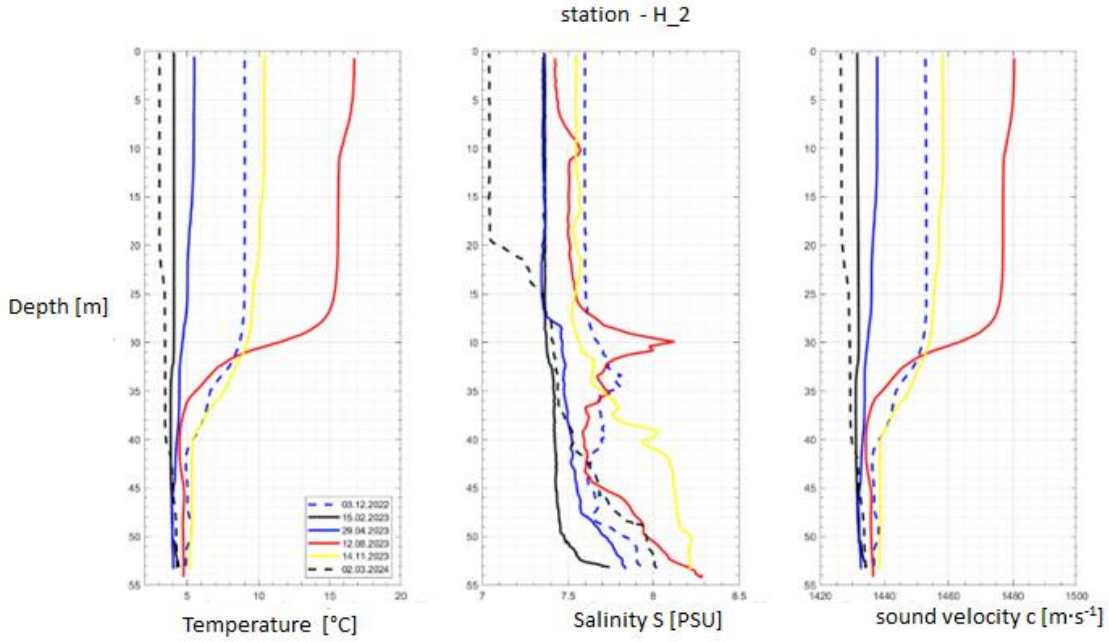


Figure 2.98. The vertical profiles of temperature T [°C], salinity S [PSU], and sound velocity c [m·s^{-1}] recorded at survey station H_2 on 3 December 2022 (dashed blue curves), 15 February 2023, 29 April 2023, 12 August 2023, 12 November 2023 (respectively, solid black, blue, red, and yellow curves) and 2 March 2024 (dashed black curves)

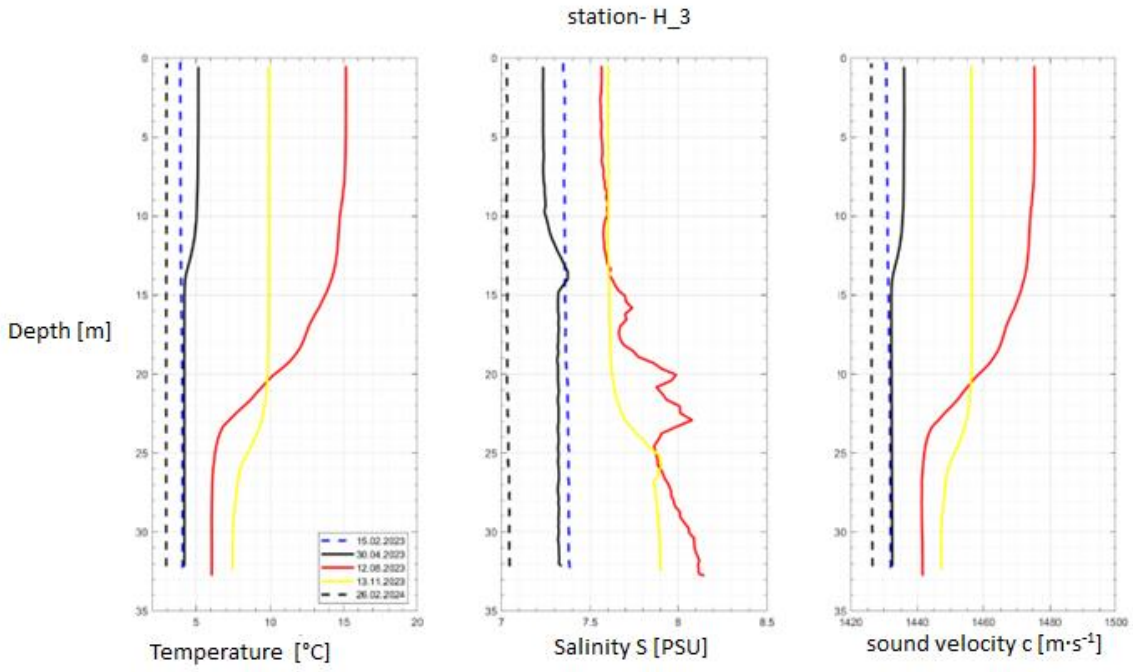


Figure 2.99. The vertical profiles of temperature T [°C], salinity S [PSU], and sound velocity c [m·s^{-1}] recorded at survey station H_3 on 15 February 2022 (dashed blue curves), 30 April 2023, 12 August 2023, 13 November 2023 (respectively, solid black, blue, red, and yellow curves) and 26 February 2024 (dashed black curves)

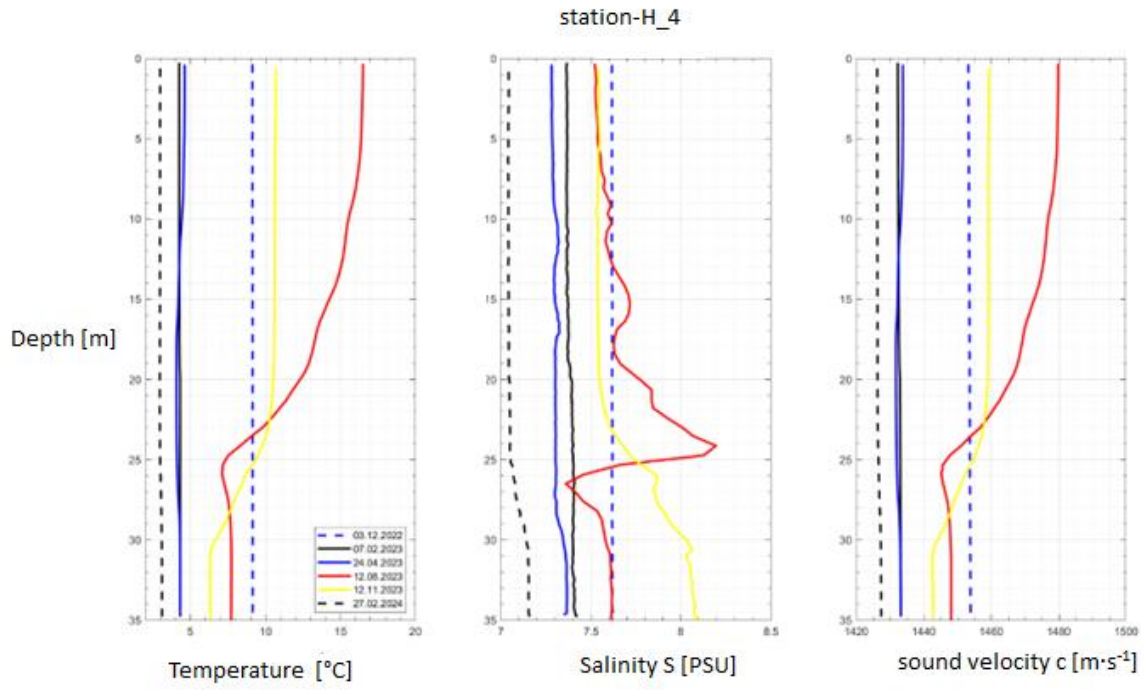


Figure 2.100. The vertical profiles of temperature T [°C], salinity S [PSU], and sound velocity c [m·s^{-1}] recorded at survey station H_4 on 3 December 2022 (dashed blue curves), 7 February 2023, 24 April 2023, 12 August 2023, 12 November 2023 (respectively, solid black, blue, red, and yellow curves) and 27 February 2024 (dashed black curves)

The results obtained revealed that the thermohaline conditions at all survey stations share similar characteristics. Namely, all of them present a well-mixed isothermal water layer with a temperature of approximately T ≈ 3–5°C and salinity S ≈ 7–8 PSU in the whole water column is observed (in the winter season) and the occurrence of a temperature drop (in the water layer below 15–25 m), i.e. the occurrence of a thermocline with the temperature decreasing to approximately ΔT ≈ 10°C in comparison to values observed in the near-surface layer.

In this way, during the winter season, a sound velocity profile is formed throughout the water column with characteristic velocities of approximately c = 1430–1435 m·s^{-1}. In turn, during the summer season, the phenomena of so-called negative refraction are observed, when the sound velocity in the near-surface layer (c ≈ 1475–1480 m·s^{-1}) resents higher values in comparison to values observed in the near-seabed layer (c = 1435–1450 m·s^{-1}).

As an example, Figure 2.101 shows the time course of the sound pressure changes of a noise signal with the execution time τ = 1 min (left) together with its spectrum averaged over 1 min (right), the so-called power spectral density PSD [dB re 1 μPa2·Hz^{-1}], in the entire measured frequency range limited by the Nyquist frequency $F_s/2$ = 192 kHz /2 = 96 kHz.

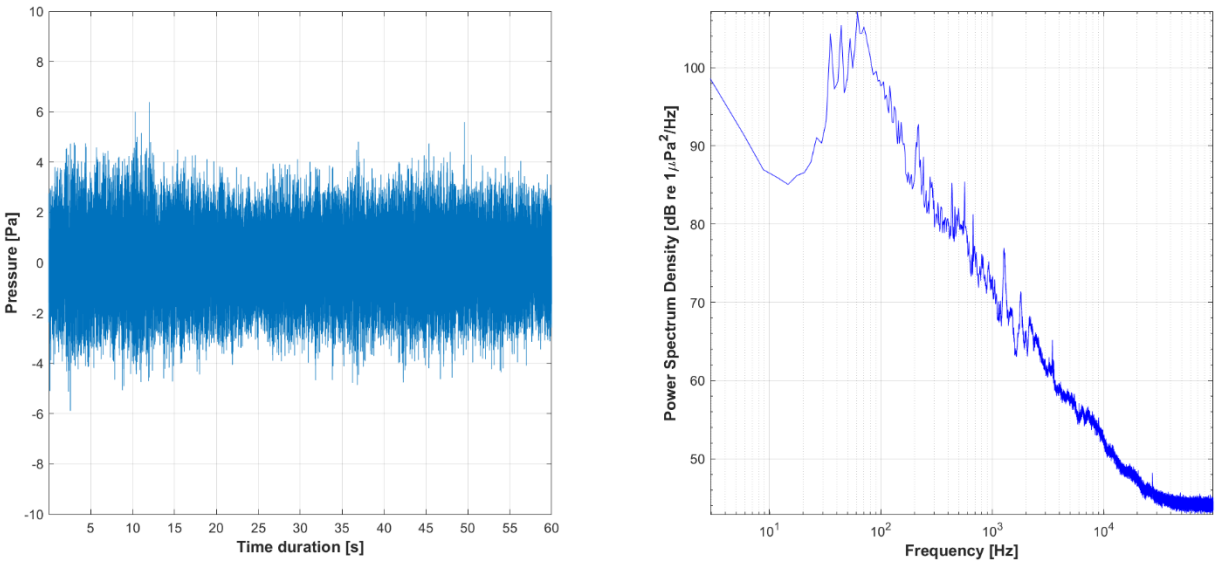


Figure 2.101. A sample time series of ambient noise signals with a time duration of 1 min. (left) and its PSD levels [dB re 1 μPa²·H⁻¹] (right)

In the ambient noise spectrum with frequencies of below 40–70 Hz, there is a significant decrease in the PSD level. The observed phenomenon is associated with the low-frequency cutoff in "shallow" natural waveguide, limited by the sea depth, i.e. the two boundaries in the form of the sea surface and seabed (Urick, 1984; Medwin and Clay, 1998). For example, with the sea depth of approximately z = 35 mm and in the sound propagation conditions typical for the winter season (sound velocity of approximately c = 1435 m/s), the "cutoff" is observed for frequencies below 20 Hz or so [Figure 2.102, blue curve].

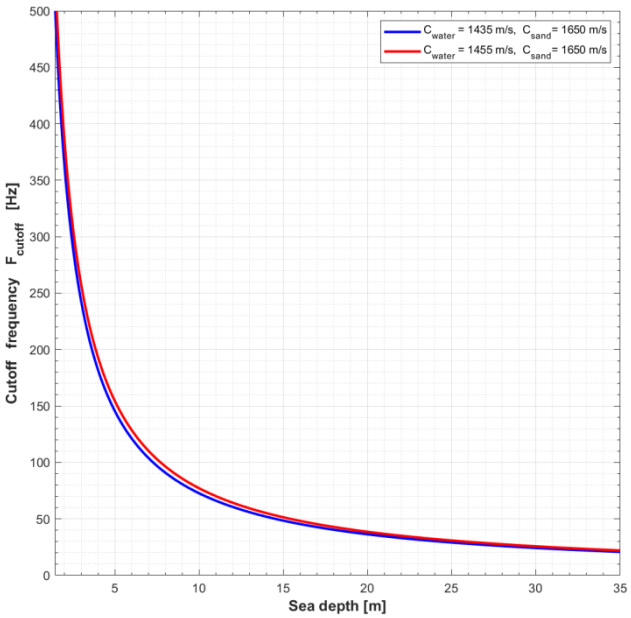


Figure 2.102. The low frequency "cutoff" phenomenon in shallow waters. The vertical axis Y – the "cutoff" frequency [Hz]; the horizontal axis X – sea depth [m]

For this reason, at further stages of signal processing, a detailed analysis of ambient noise data was performed in the frequency range from 20 Hz up to 20 kHz. It is fully compliant with the latest recommendations of the HELCOM EN-Noise Expert Group (HELCOM, 2021).

The power spectral density (PSD) of the background noise was calculated in 1/3-octave frequency bands with the central frequencies F_{centr} of the bands (between 20 Hz and 20 kHz). The results of the mean PSD levels calculations [dB re 1 $\mu Pa^2 \cdot Hz^{-1}$] in individual 1/3-octave frequency bands are presented in the form of boxplots (boxplot function, MATLAB®), which reflect the general information on the statistics of the measured ambient noise data [Figure 2.103–Figure 2.106]. The results in graphic form are presented in compliance with the numbers of individual survey stations H_1–H_4 and in chronological order of data reading during the service vessel passages [Table 2.54].

Physically, boxplots should be interpreted as follows – the central red line marks the median value in each “box” (i.e. rectangle) the bottom and upper limits of which mark, respectively, the first quartile Q1 and third quartile Q3 (i.e. the percentiles 25 and 75). According to the definition, the so-called interquartile range (IQR), i.e. the distance between Q1 and Q3, comprises half of all observations. The values of so-called whiskers are determined by default as 1.5 of the interquartile range, i.e. $\Delta Q = 1.5*IQR$. If the observed minimum is higher than the value of the bottom whisker $Q1-\Delta Q$ and/or the observed maximum is lower than the upper whisker $Q3+\Delta Q$, the length of the whiskers is limited by the observed extreme values accordingly. All the observations outside the whiskers are considered outliers and they are marked individually using colourful signs (here, red pluses were used).

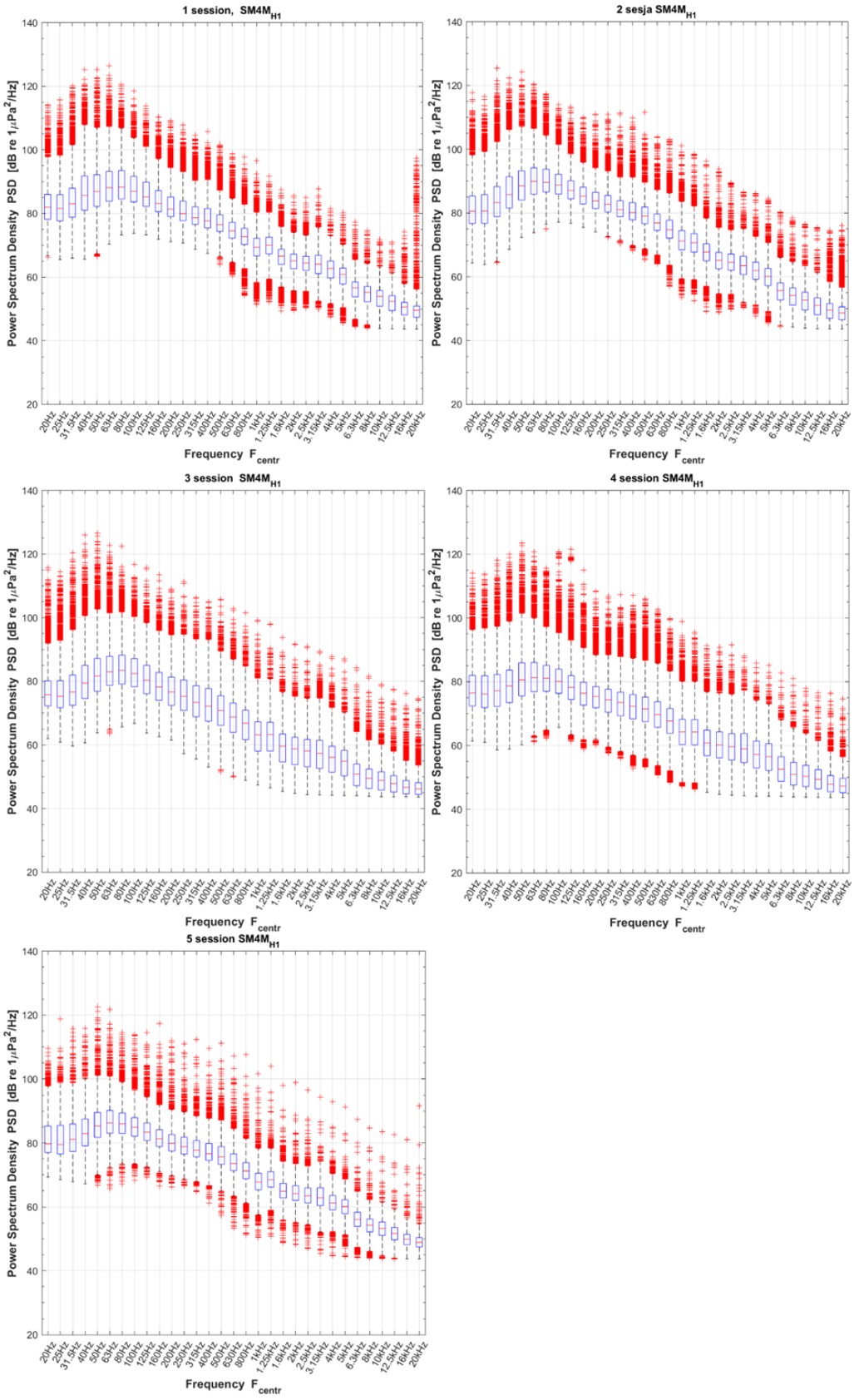


Figure 2.103. Survey station H_1. The statistical distribution of the averaged power spectral density (PSD) [dB re 1 µPa2·Hz^{-1}] values of the ambient noise in 1/3-octave bands. The central frequencies F_{centr} of individual bands are marked on the horizontal axis

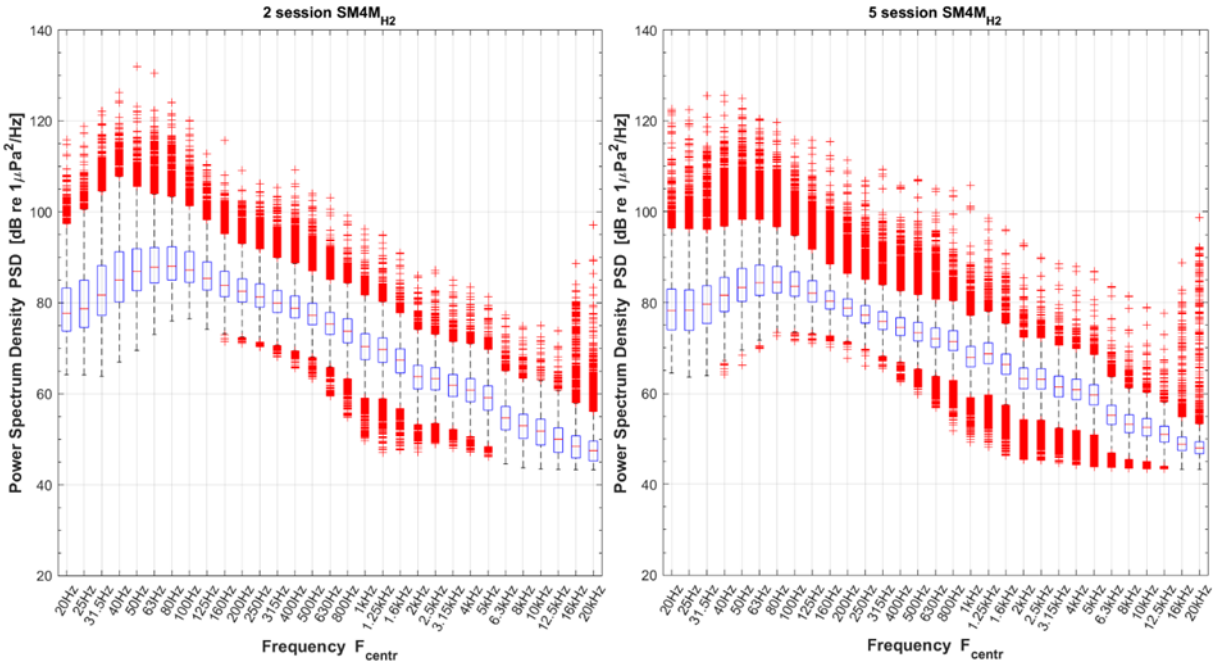


Figure 2.104. Survey station H_2. The statistical distribution of the averaged power spectral density (PSD) [dB re 1 µPa2·Hz^{-1}] values of the ambient noise in 1/3-octave bands. The central frequencies F_{centr} of individual bands are marked on the horizontal axis

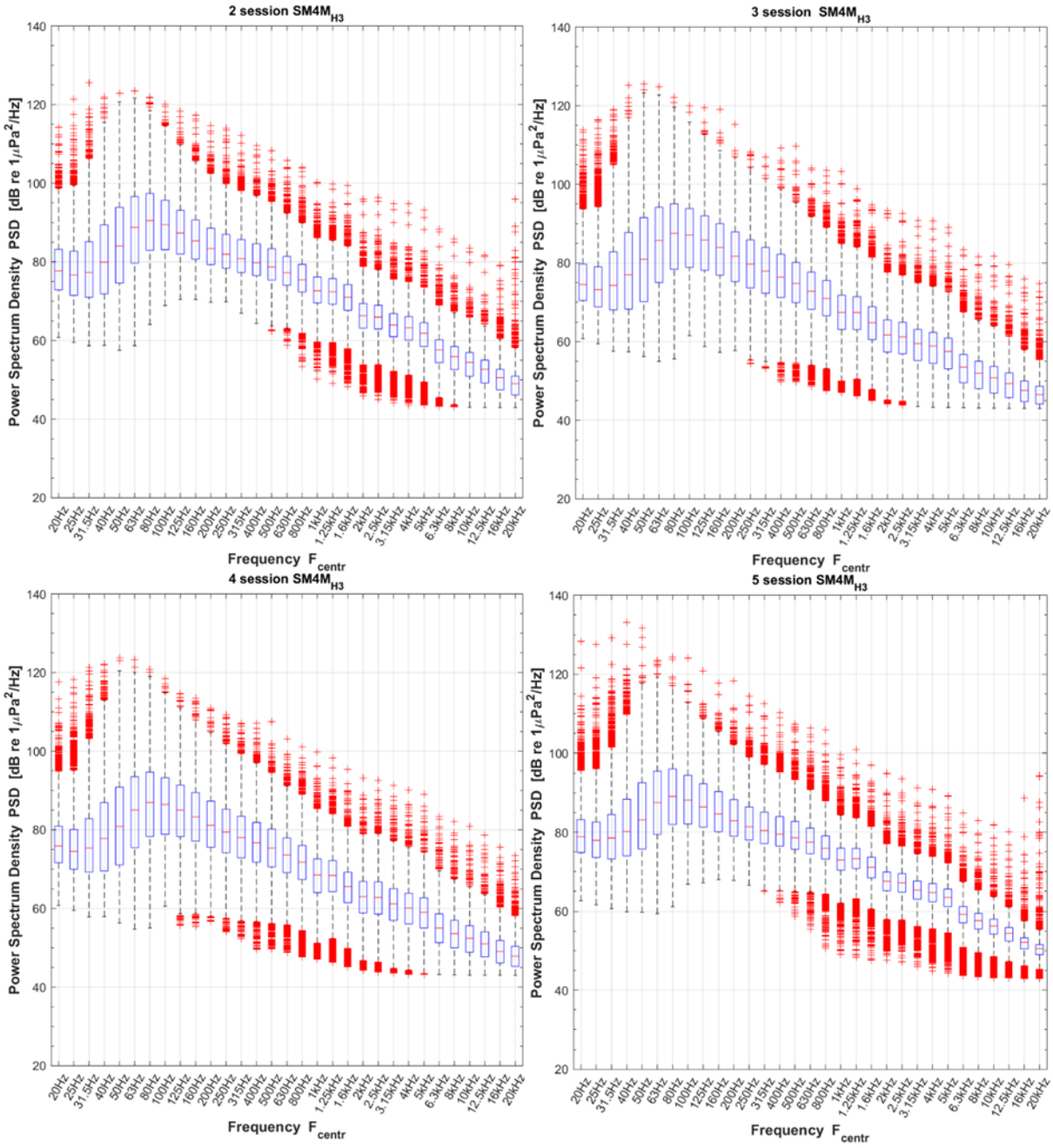


Figure 2.105. Survey station H_3. The statistical distribution of the averaged power spectral density (PSD) [dB re 1 µPa2·Hz^{-1}] values of the ambient noise in 1/3-octave bands. The central frequencies F_{centr} of individual bands are marked on the horizontal axis

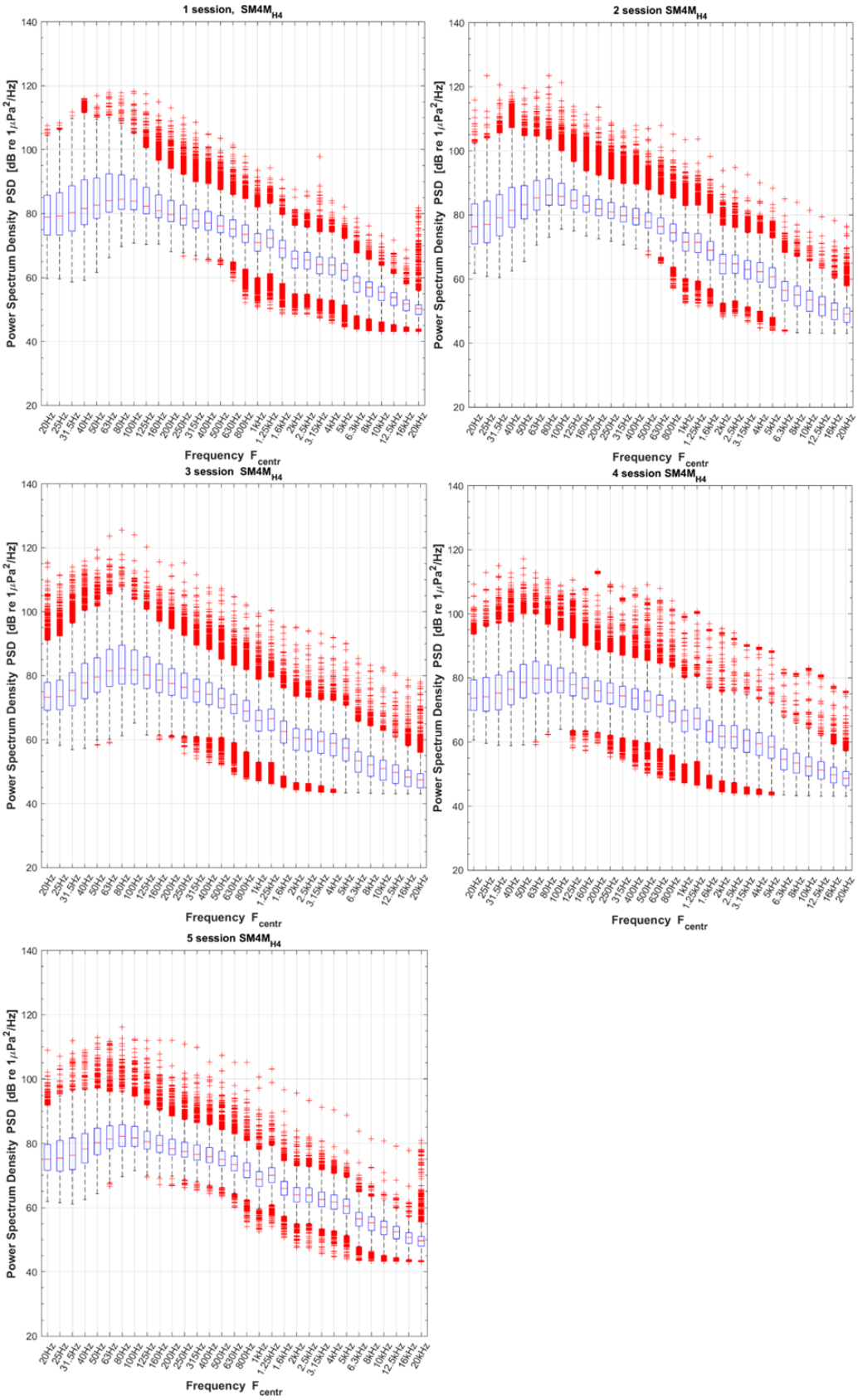


Figure 2.106. Survey station H_4. The statistical distribution of the averaged power spectral density (PSD) [dB re 1 µPa2·Hz^{-1}] values of the ambient noise in 1/3-octave bands. The central frequencies F_{centr} of individual bands are marked on the horizontal axis

In the next step, the mean values of the power spectrum density $PSD_{1/3\ oct}$ in the 1/3-octave bands [Figure 2.107–Figure 2.110] are calculated for different percentiles (p = 0.05; 0.10; 0.25; 0.50; 0.75; 0.90; 0.95). For example, percentile L05 means that the noise level is larger than the L05 threshold (known as “the loudest sounds”) for 5% of the observation time. In turn, percentile L95 corresponds to „the softest sounds”. Naturally, percentile L50 is the median value.

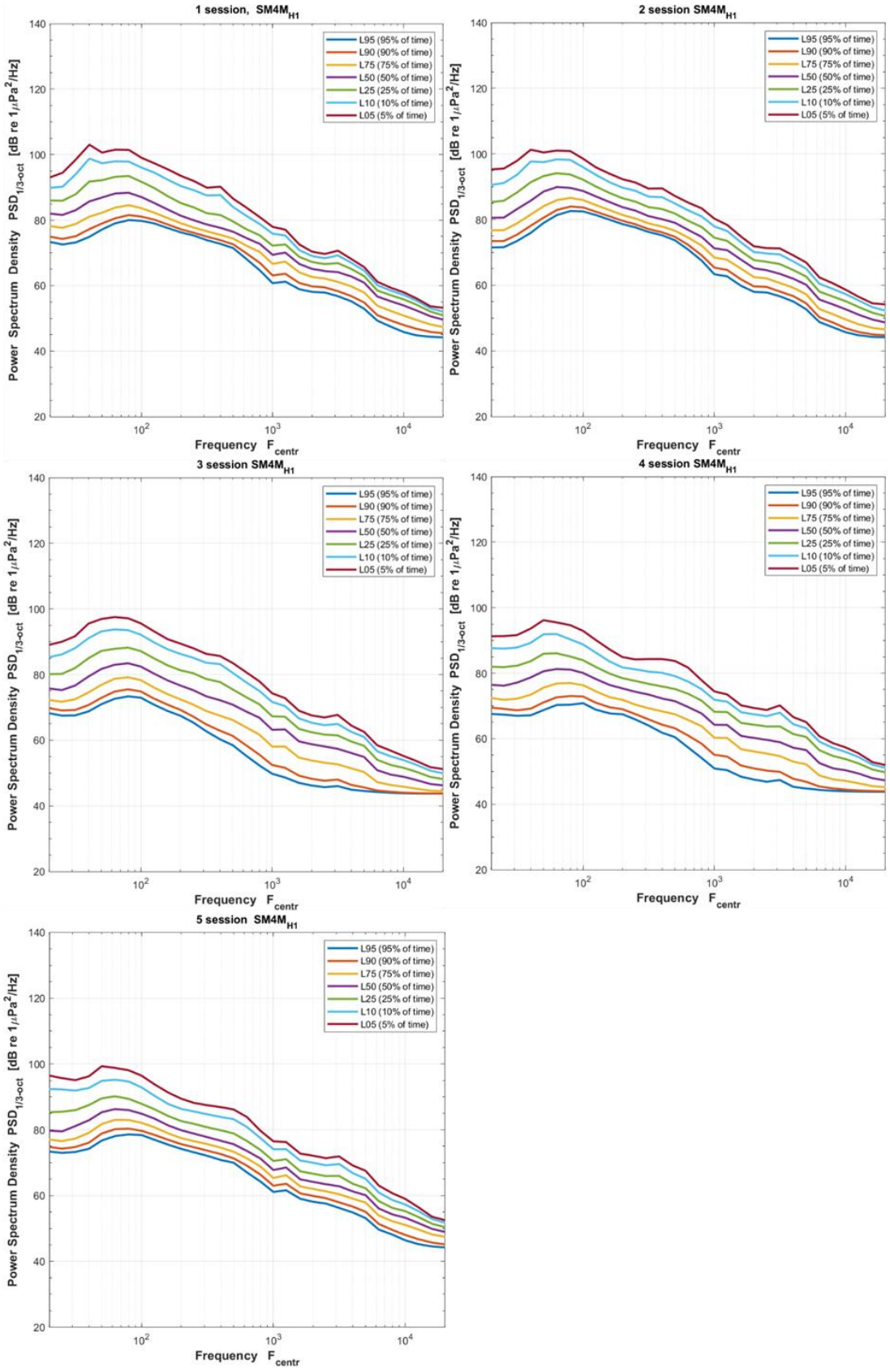


Figure 2.107. Survey station H_1. The mean values of the power spectrum density levels of the ambient noise in 1/3-octave bands PSD1/3 oct [dB re 1 µPa^2·Hz^{-1}] calculated for individual percentiles

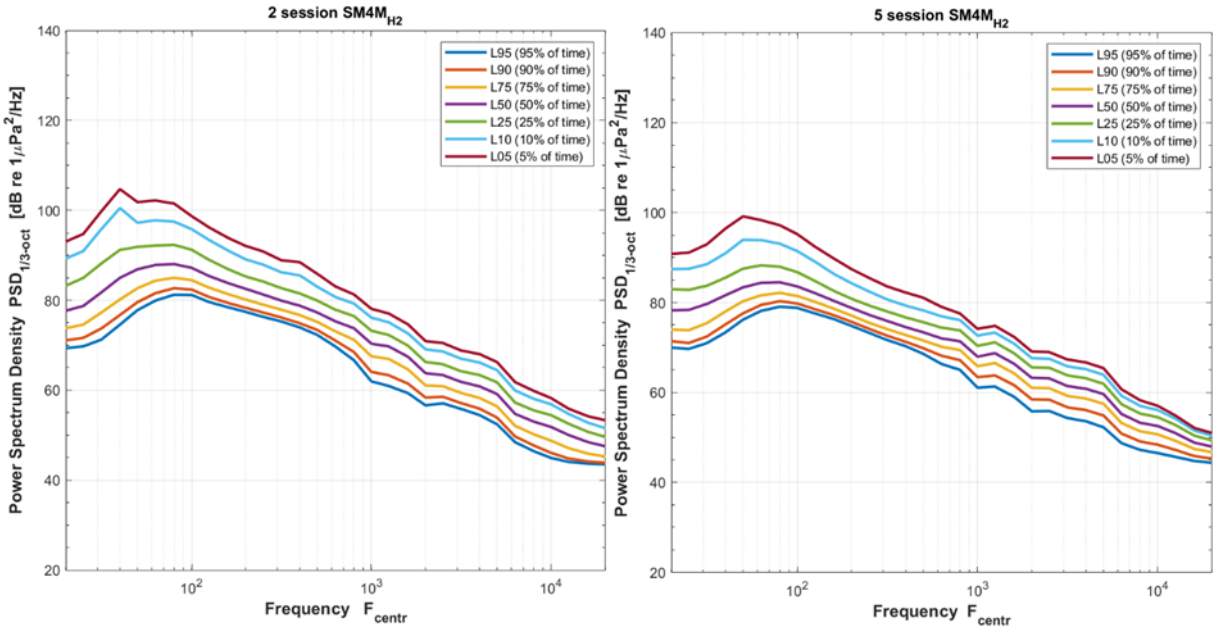


Figure 2.108. Survey station H_2. The mean values of the power spectrum density levels of the ambient noise in 1/3-octave bands $PSD_{1/3\,oct}$ [dB re 1 µPa^2·Hz^{-1}] calculated for individual percentiles

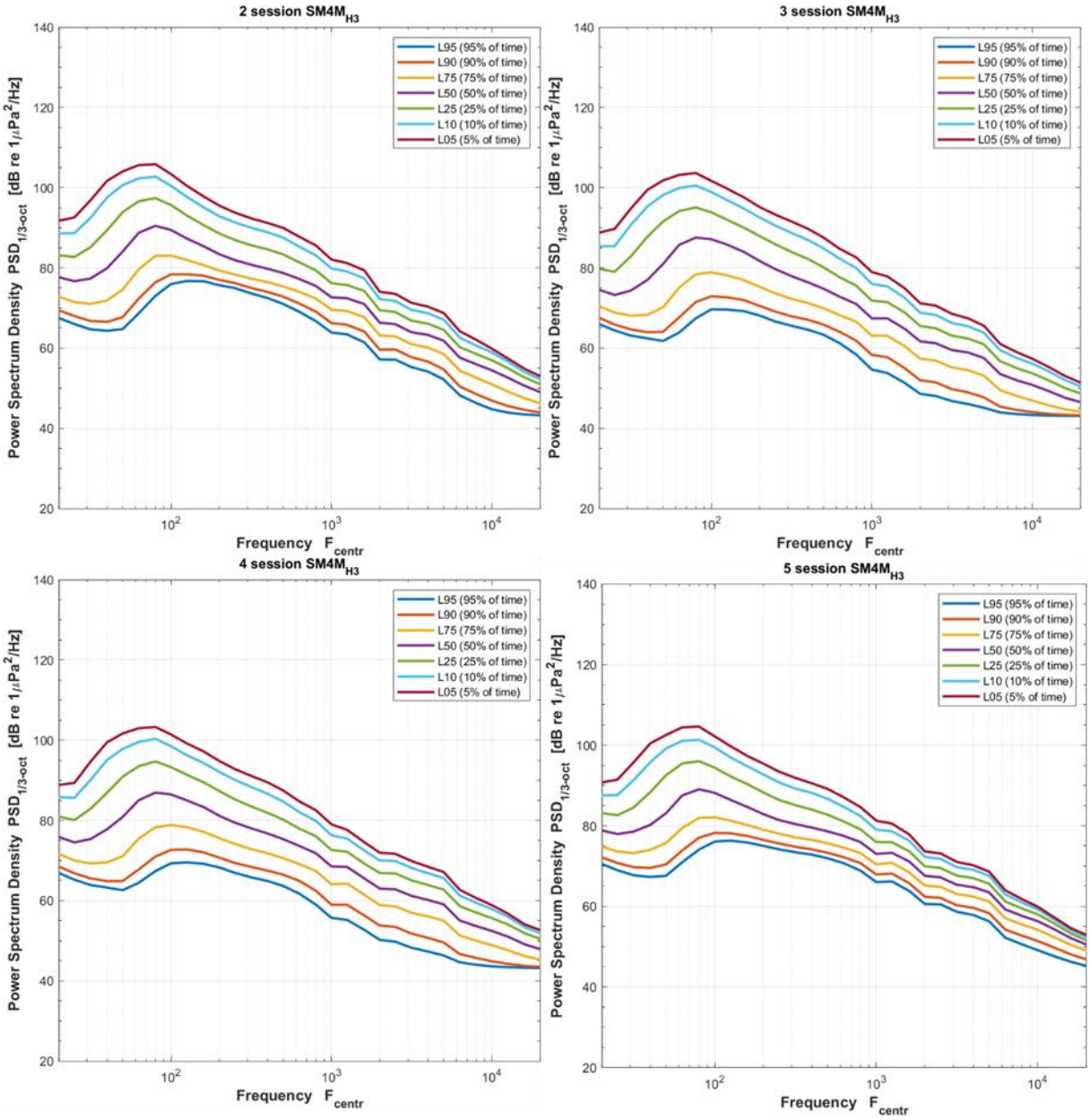


Figure 2.109. Survey station H_3. The mean values of the power spectrum density levels of the ambient noise in 1/3-octave bands $PSD_{1/3\,oct}$ [dB re 1 µPa^2·Hz^{-1}] calculated for individual percentiles

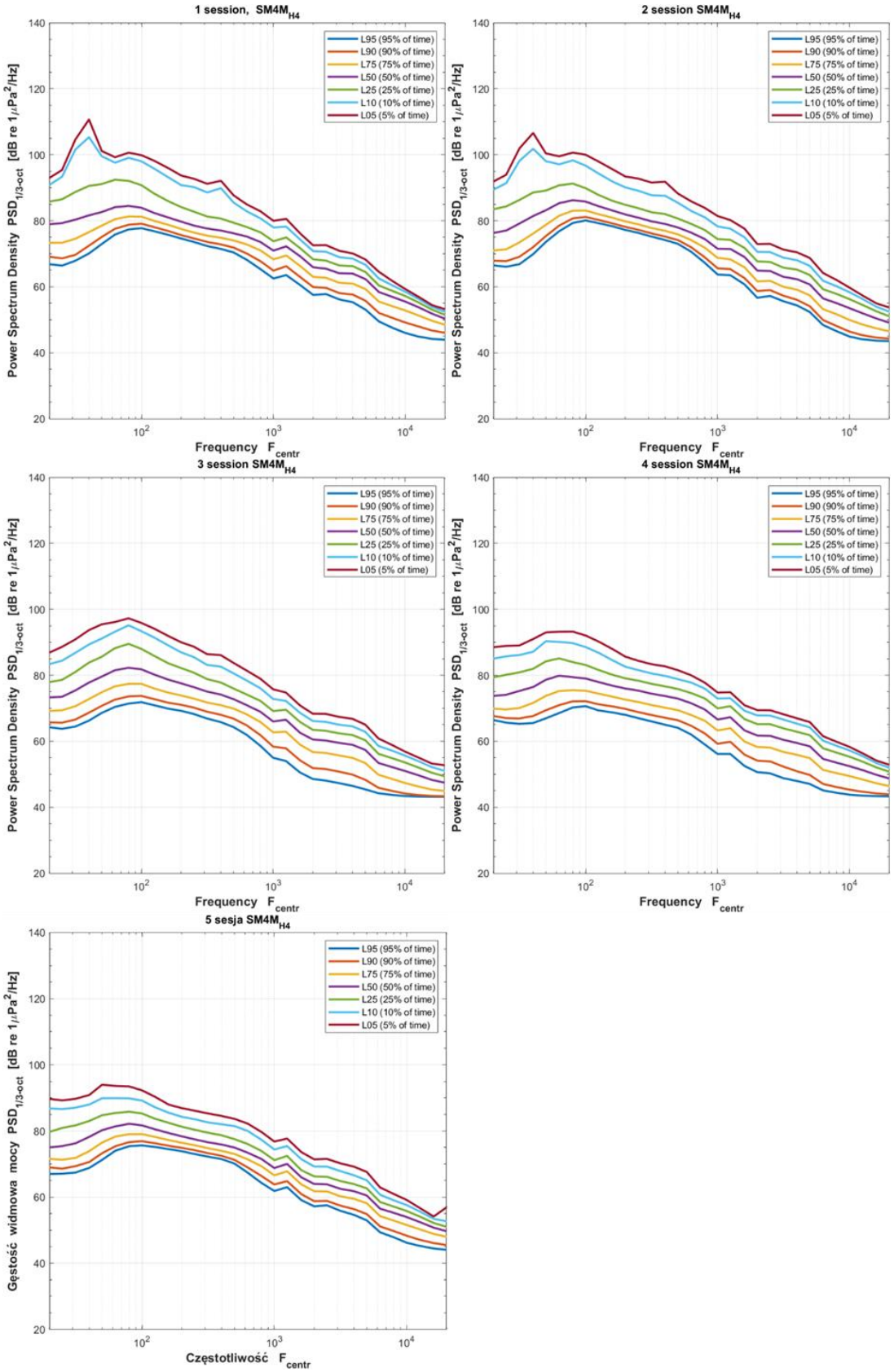


Figure 2.110. Survey station H_4. The mean values of the power spectrum density levels of the ambient noise in 1/3-octave bands $PSD_{1/3\,oct}$ [dB re 1 µPa^2·Hz^{-1}] calculated for individual percentiles

At a further step of data analysis, there were calculated the mean values of sound pressure levels SPL [dB re 1 µPa] in the two 1/3-octave bands with the central frequencies of 63 Hz and 125 Hz including the broadband SPL estimated for the 20 Hz–20 kHz band (HELCOM, 2021). The primary statistical values, i.e. the mean, median, and mode (dominant) values were calculated. The mean and median values were calculated in the linear scale, i.e. based on the absolute values. In turn, the mode value was obtained on the basis of the histogram of the acoustic pressure values SPL [dB re 1 µPa], by finding the most frequent value in the statistical distribution. The above-mentioned results are illustrated in Figure 2.111–Figure 2.126.

The detailed statistical information is obtained based on all the survey sessions presented in Table 2.55–Table 2.59.

Table 2.55. Survey campaign no. 1. The statistical values of the sound pressure level values SPL [dB re 1 µPa] in two 1/3-octave frequency bands with central frequencies of 63 Hz and 125 Hz and in the 20–20 000 Hz broadband

Survey station	Frequency band	Sound pressure level (SPL) [dB re 1 µPa]				
		Mean	Median	Mode	5%-percentile SPL_{L05}	95%-percentile SPL_{L95}
H_1	63 Hz (1/3 oct.)	110.0	99.8	97.5	113.1	90.7
	125 Hz (1/3 oct.)	106.4	99.9	98.4	112.0	93.6
	20–20,000 Hz	118.3	111.3	109.5	123.5	105.5
H_4	63 Hz (1/3 oct.)	105.8	95.7	94.9	110.9	87.4
	125 Hz (1/3 oct.)	106.4	97.0	95.9	112.8	91.4
	20–20,000 Hz	117.90	109.8	108.3	124.9	104.2

Table 2.56. Survey campaign no. 2. The statistical values of the sound pressure level values SPL [dB re 1 µPa] in two 1/3-octave frequency bands with central frequencies of 63 Hz and 125 Hz and in the 20–20 000 Hz broadband

Survey station	Frequency band	Sound pressure level (SPL) [dB re 1 µPa]				
		Mean	Median	Mode	5%-percentile SPL_{L05}	95%-percentile SPL_{L95}
H_1	63 Hz (1/3 oct.)	108.9	101.5	98.1	101.0	81.3
	125 Hz (1/3 oct.)	105.9	101.7	99.3	96.0	81.4
	20–20,000 Hz	118.0	113.0	111.7	122.5	107.6
H_2	63 Hz (1/3 oct.)	110.0	99.5	98.1	102.2	80.0
	125 Hz (1/3 oct.)	105.3	100.0	98.4	96.2	79.6
	20–20,000 Hz	118.0	111.7	110.5	123.0	106.4
H_3	63 Hz (1/3 oct.)	111.2	100.4	103.9	105.6	68.7
	125 Hz (1/3 oct.)	109.2	102.0	98.3	100.5	76.7
	20–20,000 Hz	120.0	113.5	108.8	126.1	104.7
H_4	63 Hz (1/3 oct.)	105.4	97.0	94.8	99.5	76.8
	125 Hz (1/3 oct.)	105.8	99.0	98.5	98.0	79.3
	20–20,000 Hz	117.3	111.0	110.5	124.2	105.8

Table 2.57. Survey campaign no. 3. The statistical values of the sound pressure level values SPL [dB re 1 µPa] in two 1/3-octave frequency bands with central frequencies of 63 Hz and 125 Hz and in the 20–20 000 Hz broadband

Survey station	Frequency band	Sound pressure level (SPL) [dB re 1 µPa]				
		Mean	Median	Mode	5%-percentile SPL_{L05}	95%-percentile SPL_{L95}
H_1	63 Hz (1/3 oct.)	106.1	94.6	93.6	109.1	84.2
	125 Hz (1/3 oct.)	102.4	95.0	94.9	107.9	85.5
	20–20,000 Hz	114.6	106.7	102.7	118.8	97.8
H_2	63 Hz (1/3 oct.)	-	-	-	-	-
	125 Hz (1/3 oct.)	-	-	-	-	-
	20–20,000 Hz	-	-	-	-	-
H_3	63 Hz (1/3 oct.)	109.0	97.4	99.5	114.8	75.5
	125 Hz (1/3 oct.)	108.3	100.5	104.6	114.4	84.2
	20–20,000 Hz	118.3	110.9	105.3	124.3	99.0
H_4	63 Hz (1/3 oct.)	103.9	93.1	91.6	107.8	82.0
	125 Hz (1/3 oct.)	103.7	94.6	92.7	108.8	85.5
	20–20,000 Hz	114.1	107.1	104.1	119.1	100.2

Table 2.58. Survey campaign no. 4. The statistical values of the sound pressure level values SPL [dB re 1 µPa] in two 1/3-octave frequency bands with central frequencies of 63 Hz and 125 Hz and in the 20–20 000 Hz broadband

Survey station	Frequency band	Sound pressure level (SPL) [dB re 1 µPa]				
		Mean	Median	Mode	5%-percentile SPL_{L05}	95%-percentile SPL_{L95}
H_1	63 Hz (1/3 oct.)	105.3	92.9	72.7	107.1	81.9
	125 Hz (1/3 oct.)	106.1	92.9	75.9	104.8	83.5
	20–20,000 Hz	114.8	106.0	107.2	117.7	97.5
H_2	63 Hz (1/3 oct.)	-	-	-	-	-
	125 Hz (1/3 oct.)	-	-	-	-	-
	20–20,000 Hz	-	-	-	-	-
H_3	63 Hz (1/3 oct.)	109.3	96.7	66.1	114.6	76.1
	125 Hz (1/3 oct.)	107.8	99.6	68.9	113.9	84.2
	20–20,000 Hz	118.1	110.8	110.4	124.1	99.4
H_4	63 Hz (1/3 oct.)	99.1	91.5	70.6	104.8	80.2
	125 Hz (1/3 oct.)	99.6	92.6	72.3	104.9	84.0
	20–20,000 Hz	112.7	106.3	106.7	116.0	99.3

Table 2.59. Survey campaign no. 5. The statistical values of the sound pressure level values SPL [dB re 1 µPa] in two 1/3-octave frequency bands with central frequencies of 63 Hz and 125 Hz and in the 20–20,000 Hz broadband

Survey station	Frequency band	Sound pressure level (SPL) [dB re 1 µPa]				
		Mean	Median	Mode	5%-percentile SPL_{L05}	95%-percentile SPL_{L95}
H_1	63 Hz (1/3 oct.)	107.3	97.9	97.4	110.4	89.7

Survey station	Frequency band	Sound pressure level (SPL) [dB re 1 µPa]				
		Mean	Median	Mode	5%-percentile SPL_{L05}	95%-percentile SPL_{L95}
	125 Hz (1/3 oct.)	104.5	98.0	99.1	108.5	91.6
	20–20,000 Hz	116.7	109.7	109.4	120.3	104.7
H_2	63 Hz (1/3 oct.)	106.4	96.0	94.1	109.9	89.8
	125 Hz (1/3 oct.)	102.6	96.7	95.3	107.1	92.2
	20–20,000 Hz	115.1	108.5	106.6	118.8	104.6
H_3	63 Hz (1/3 oct.)	110.4	99.2	102.7	116.1	82.6
	125 Hz (1/3 oct.)	108.4	101.1	95.9	114.4	90.9
	20–20,000 Hz	119.5	112.9	110.8	125.1	105.2
H_4	63 Hz (1/3 oct.)	102.3	93.0	90.8	105.2	85.7
	125 Hz (1/3 oct.)	102.1	95.1	92.9	105.0	89.8
	20–20,000 Hz	113.4	108.1	108.2	117.1	103.6

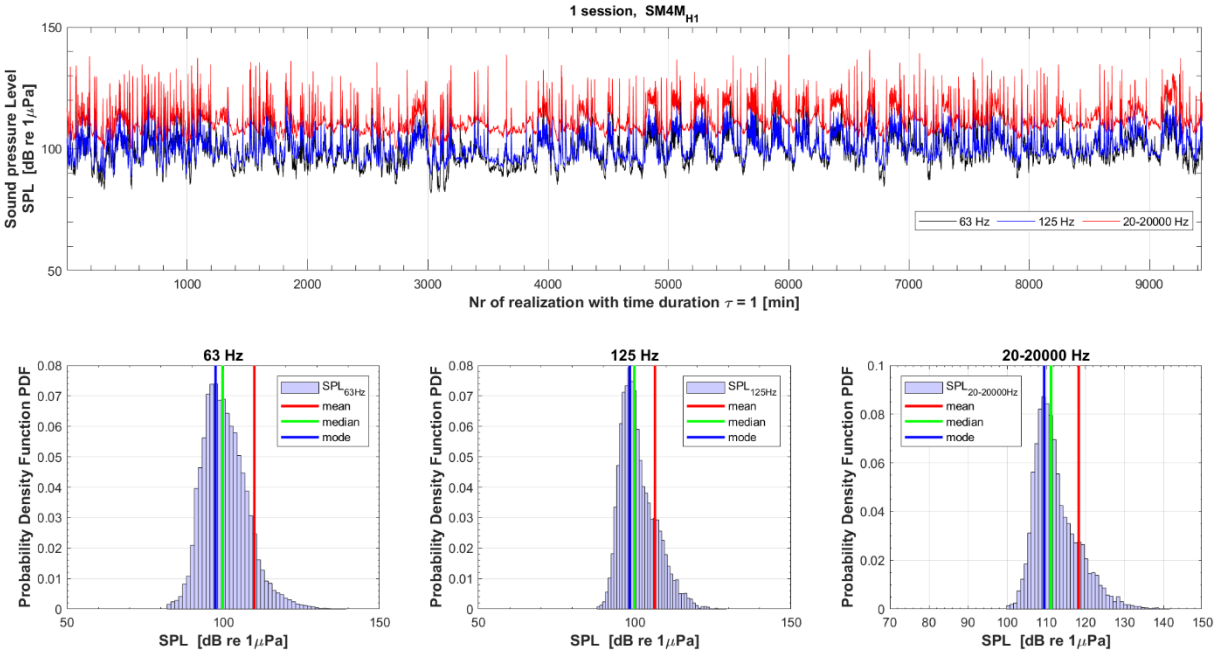


Figure 2.111. Survey station H_1. The time series of the sound pressure level SPL [dB re 1 µPa] in 1/3-octave bands of 63 Hz and 125 Hz (black and blue curves, respectively) and the 20–20 000 Hz broadband (red curve) – upper panel. The histograms of the sound pressure levels $SPL_{63\,Hz}$, $SPL_{125\,Hz}$ and $SPL_{20–20\,000\,Hz}$ – bottom panel. Red line – the mean SPL value, green line – the median SPL value, blue line – the mode SPL value. Survey session no. 1 (03.12.2022–07.02.2023)

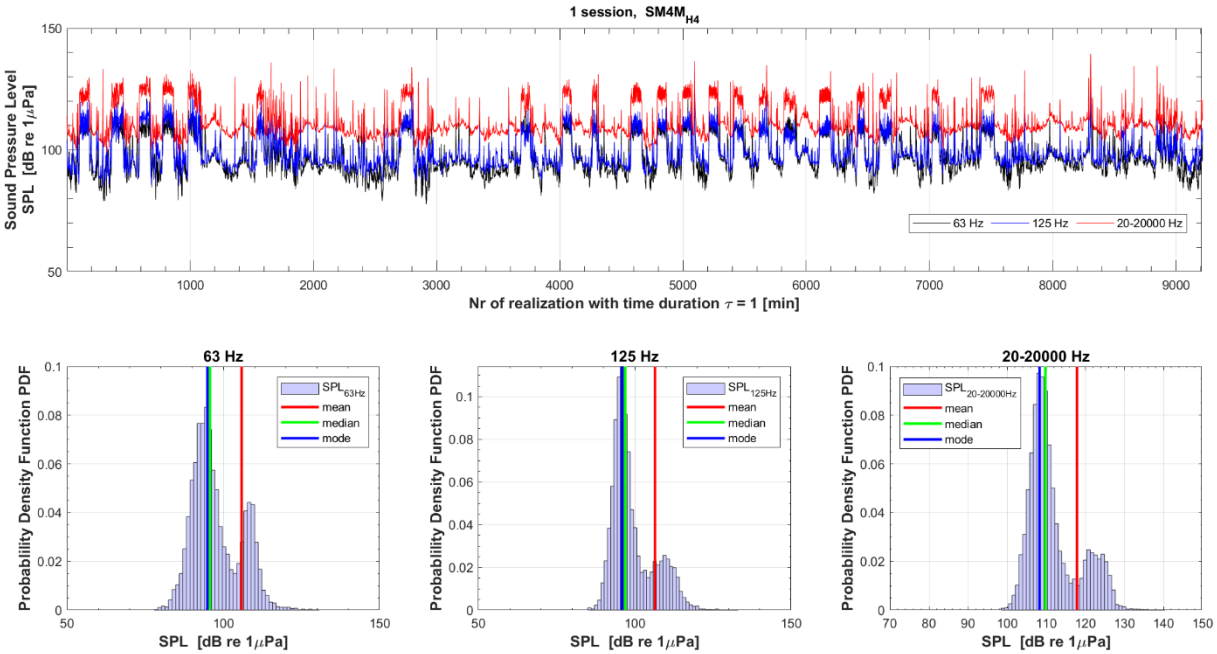


Figure 2.112. Survey station H_4. The time series of the sound pressure level SPL [dB re 1 µPa] in 1/3-octave bands of 63 Hz and 125 Hz (black and blue curves, respectively) and the 20–20 000 Hz broadband (red curve) – upper panel. The histograms of the sound pressure levels $SPL_{63\,Hz}$, $SPL_{125\,Hz}$, and $SPL_{20–20\,000\,Hz}$ – bottom panel. Red line – the mean SPL value, green line – the median SPL value, blue line – the mode SPL value. Survey session no. 1 (03.12.2022–07.02.2023)

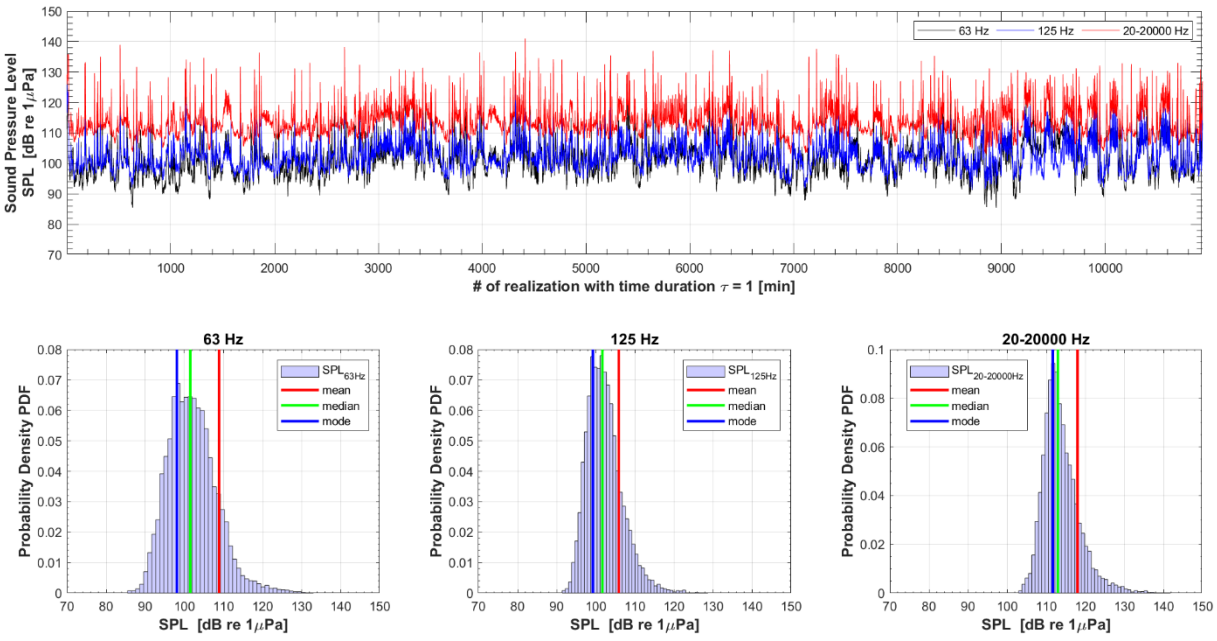


Figure 2.113. Survey station H_1. The time series of the sound pressure level SPL [dB re 1 µPa] in 1/3-octave bands of 63 Hz and 125 Hz (black and blue curves, respectively) and the 20–20 000 Hz broadband (red curve) – upper panel. The histograms of the sound pressure levels $SPL_{63\,Hz}$, $SPL_{125\,Hz}$ and $SPL_{20–20\,000\,Hz}$ – bottom panel. Red line – the mean SPL value, green line – the median SPL value, blue line – the mode SPL value. Survey session no. 2 (07.02.2023–24.04.2023)

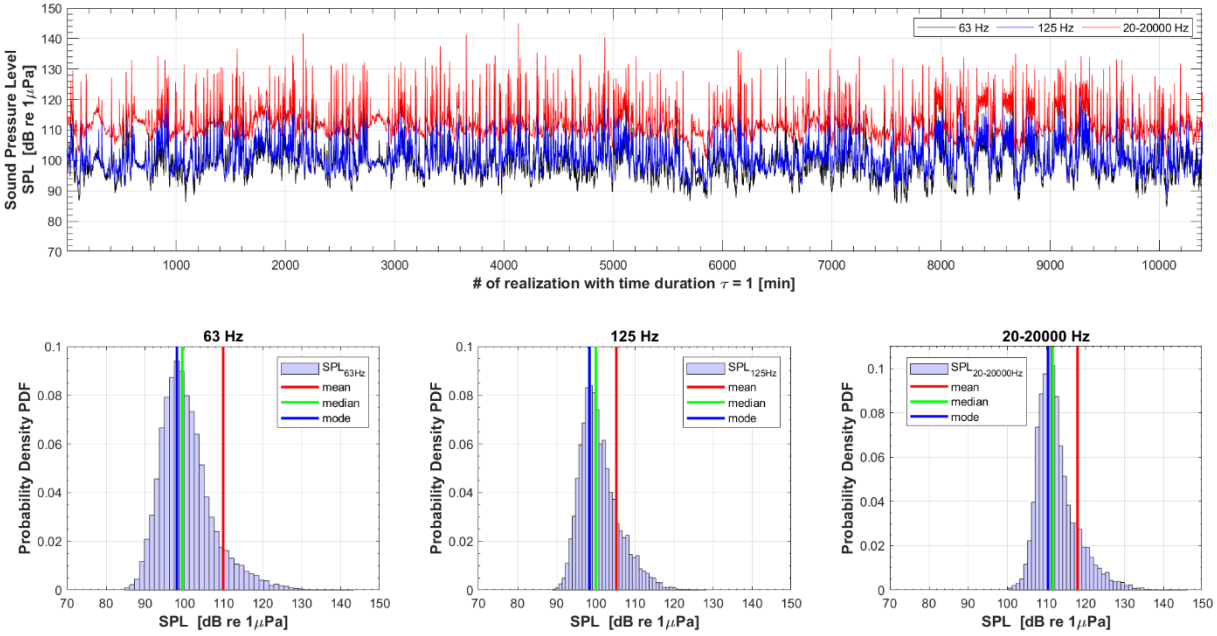


Figure 2.114. Survey station H_2. The time series of the sound pressure level SPL [dB re 1 µPa] in 1/3-octave bands of 63 Hz and 125 Hz (black and blue curves, respectively) and the 20–20 000 Hz broadband (red curve) – upper panel. The histograms of the sound pressure levels $SPL_{63\,Hz}$, $SPL_{125\,Hz}$ and $SPL_{20–20\,000\,Hz}$ – bottom panel. Red line – the mean SPL value, green line – the median SPL value, blue line – the mode SPL value. Survey session no. 2 (16.02.2023–29.04.2023)

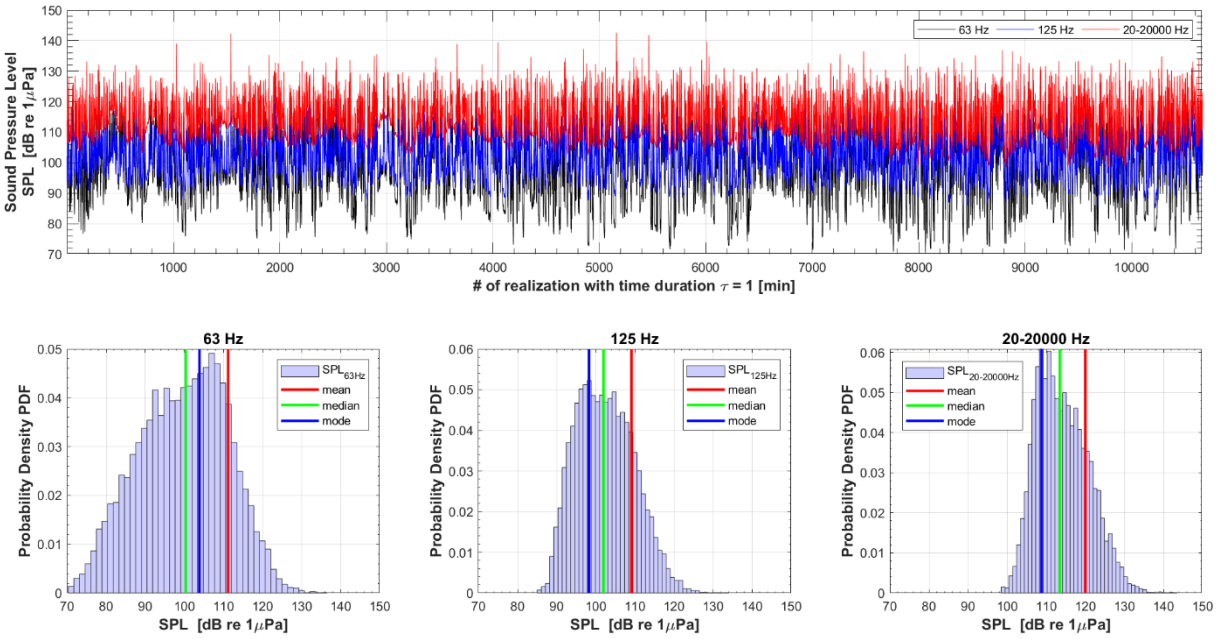


Figure 2.115. Survey station H_3. The time series of the sound pressure level SPL [dB re 1 µPa] in 1/3-octave bands of 63 Hz and 125 Hz (black and blue curves, respectively) and the 20–20 000 Hz broadband (red curve) – upper panel. The histograms of the sound pressure levels $SPL_{63\,Hz}$, $SPL_{125\,Hz}$ and $SPL_{20–20\,000\,Hz}$ – bottom panel. Red line – the mean SPL value, green line – the median SPL value, blue line – the mode SPL value. Survey session no. 2 (15.02.2023–30.04.2023)

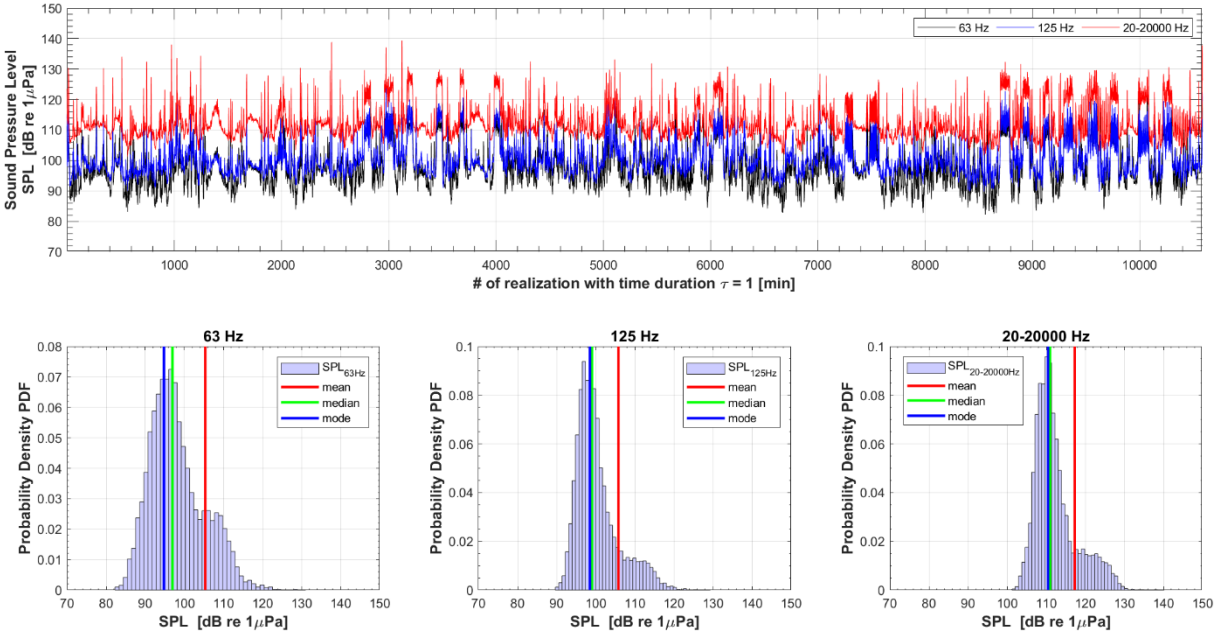


Figure 2.116. Survey station H_4. The time series of the sound pressure level SPL [dB re 1 µPa] in 1/3-octave bands of 63 Hz and 125 Hz (black and blue curves, respectively) and the 20–20 000 Hz broadband (red curve) – upper panel. The histograms of the sound pressure levels $SPL_{63\,Hz}$, $SPL_{125\,Hz}$ and $SPL_{20–20\,000\,Hz}$ – bottom panel. Red line – the mean SPL value, green line – the median SPL value, blue line – the mode SPL value. Survey session no. 2 (07.02.2023–24.04.2023)

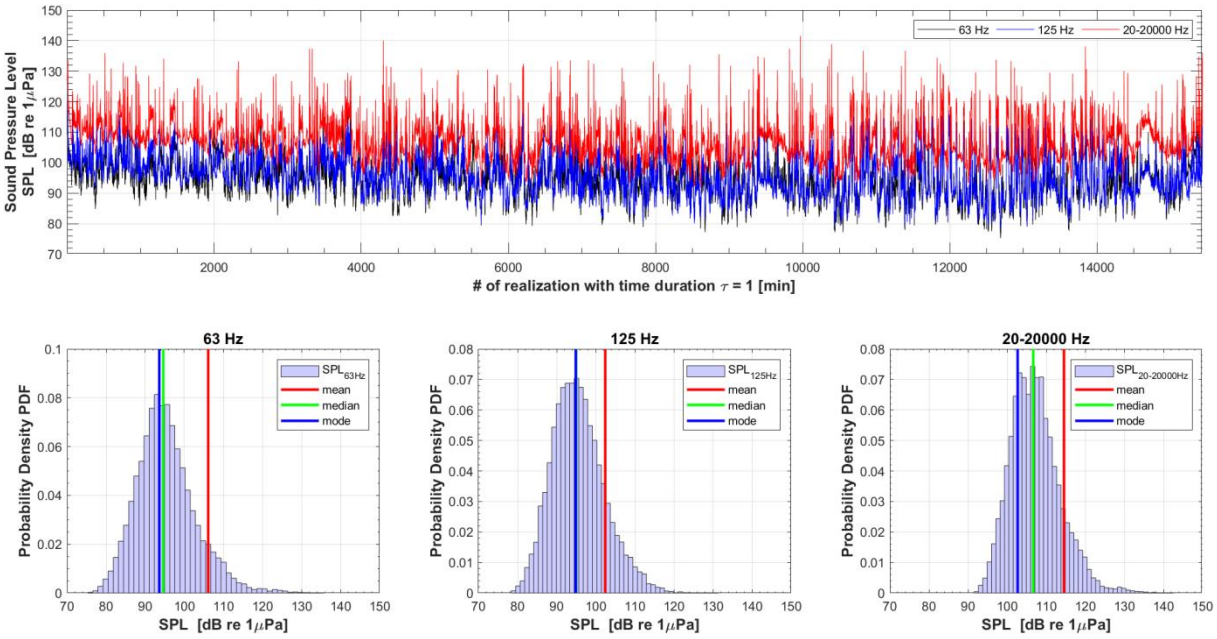


Figure 2.117. Survey station H_1. The time series of the sound pressure level SPL [dB re 1 µPa] in 1/3-octave bands of 63 Hz and 125 Hz (black and blue curves, respectively) and the 20–20 000 Hz broadband (red curve) – upper panel. The histograms of the sound pressure levels $SPL_{63\,Hz}$, $SPL_{125\,Hz}$ and $SPL_{20–20\,000\,Hz}$ – bottom panel. Red line – the mean SPL value, green line – the median SPL value, blue line – the mode SPL value. Survey session no. 3 (24.04.2023–13.08.2023)

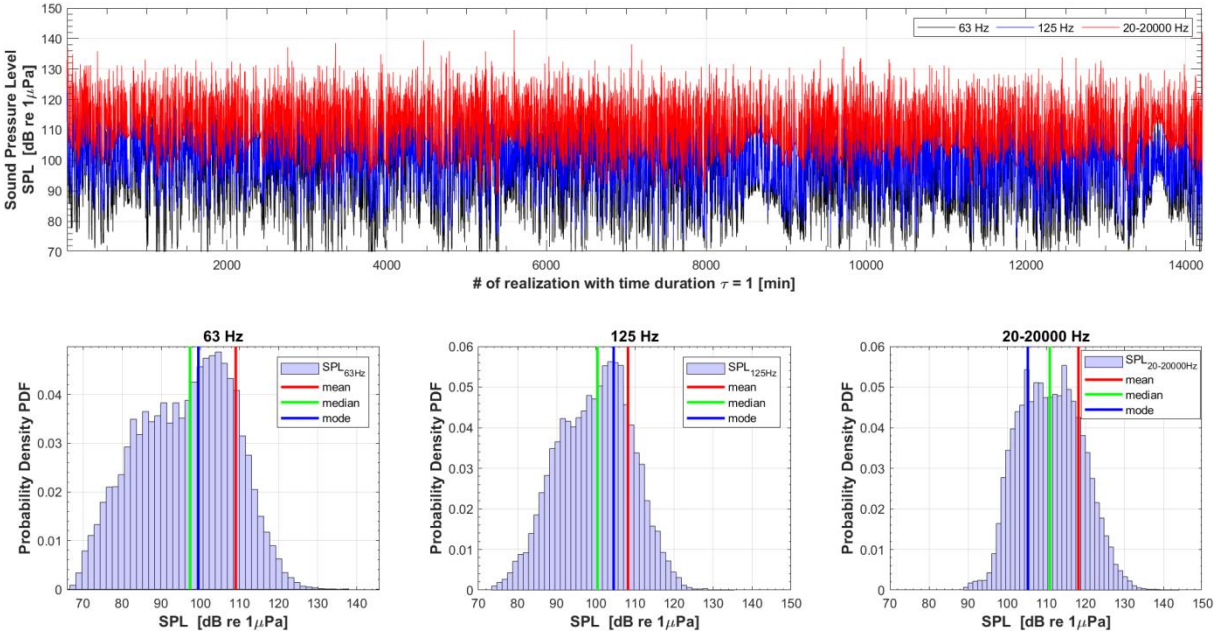


Figure 2.118. Survey station H_3. The time series of the sound pressure level SPL [dB re 1 µPa] in 1/3-octave bands of 63 Hz and 125 Hz (black and blue curves, respectively) and the 20–20 000 Hz broadband (red curve) – upper panel. The histograms of the sound pressure levels $SPL_{63\,Hz}$, $SPL_{125\,Hz}$ and $SPL_{20–20\,000\,Hz}$ – bottom panel. Red line – the mean SPL value, green line – the median SPL value, blue line – the mode SPL value. Survey session no. 3 (30.04.2023–12.08.2023)

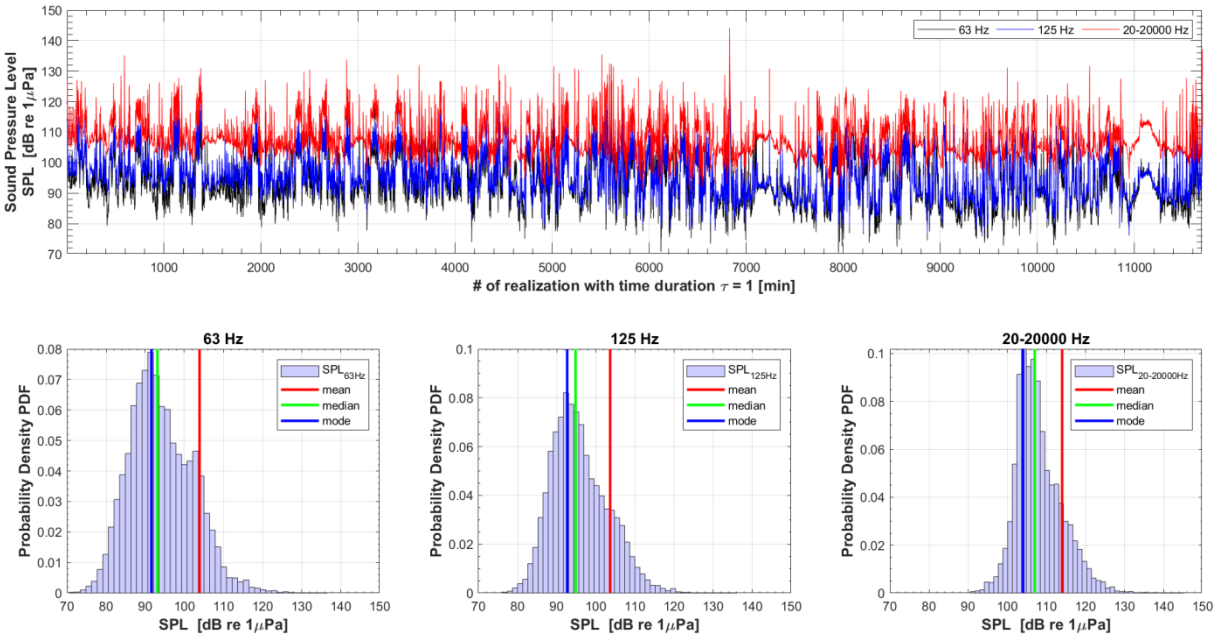


Figure 2.119. Survey station H_4. The time series of the sound pressure level SPL [dB re 1 µPa] in 1/3-octave bands of 63 Hz and 125 Hz (black and blue curves, respectively) and the 20–20 000 Hz broadband (red curve) – upper panel. The histograms of the sound pressure levels $SPL_{63\,Hz}$, $SPL_{125\,Hz}$ and $SPL_{20–20\,000\,Hz}$ – bottom panel. Red line – the mean SPL value, green line – the median SPL value, blue line – the mode SPL value. Survey session no. 3 (24.04.2-23–13.08.2023)

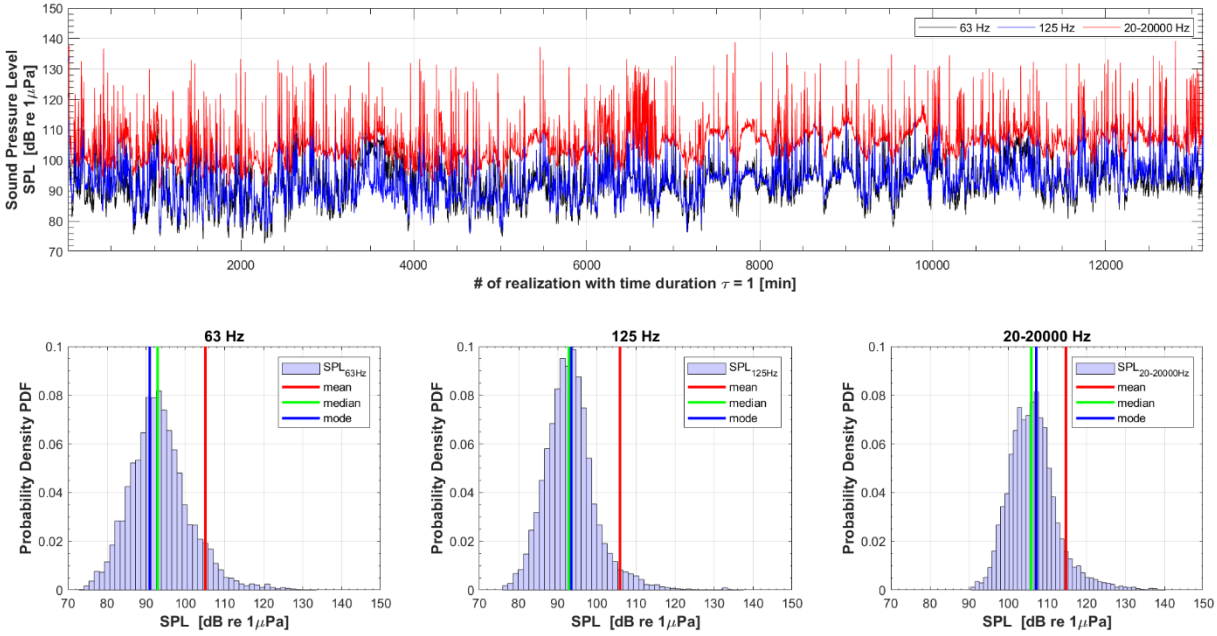


Figure 2.120. Survey station H_1. The time series of the sound pressure level SPL [dB re 1 µPa] in 1/3-octave bands of 63 Hz and 125 Hz (black and blue curves, respectively) and the 20–20 000 Hz broadband (red curve) – upper panel. The histograms of the sound pressure levels $SPL_{63\,Hz}$, $SPL_{125\,Hz}$ and $SPL_{20–20\,000\,Hz}$ – bottom panel. Red line – the mean SPL value, green line – the median SPL value, blue line – the mode SPL value. Survey session no. 4 (13.08.2023–12.11.2023)

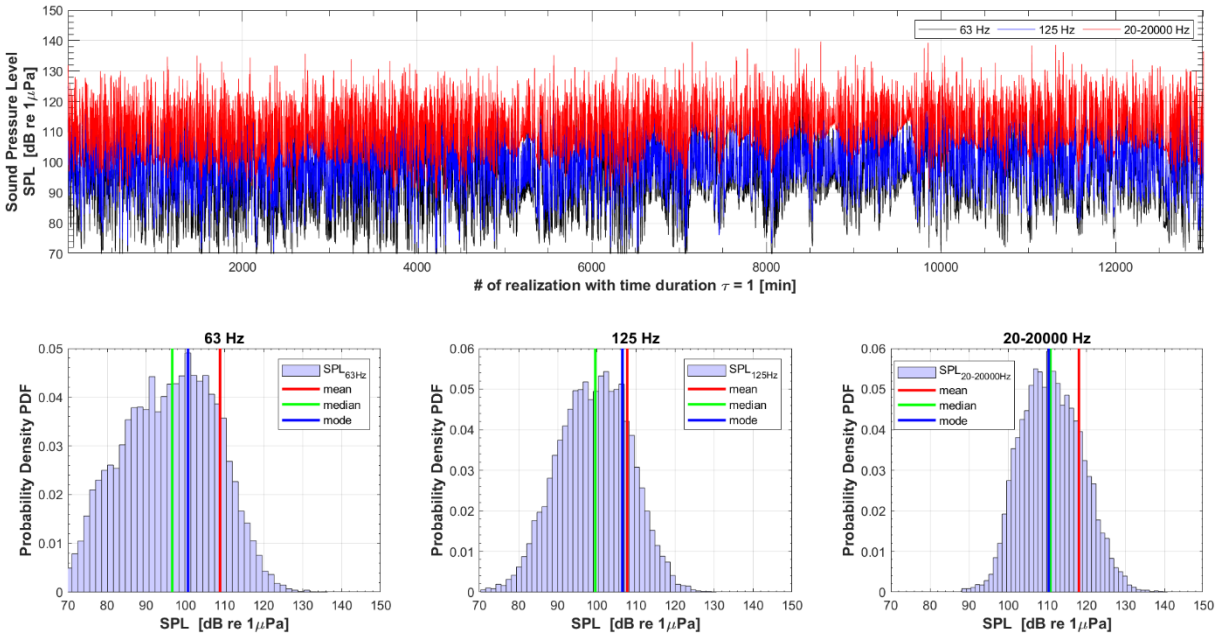


Figure 2.121. Survey station H_3. The time series of the sound pressure level SPL [dB re 1 µPa] in 1/3-octave bands of 63 Hz and 125 Hz (black and blue curves, respectively) and the 20–20 000 Hz broadband (red curve) – upper panel. The histograms of the sound pressure levels $SPL_{63\,Hz}$, $SPL_{125\,Hz}$ and $SPL_{20–20\,000\,Hz}$ – bottom panel. Red line – the mean SPL value, green line – the median SPL value, blue line – the mode SPL value. Survey session no. 4 (12.08.2023–13.11.2023)

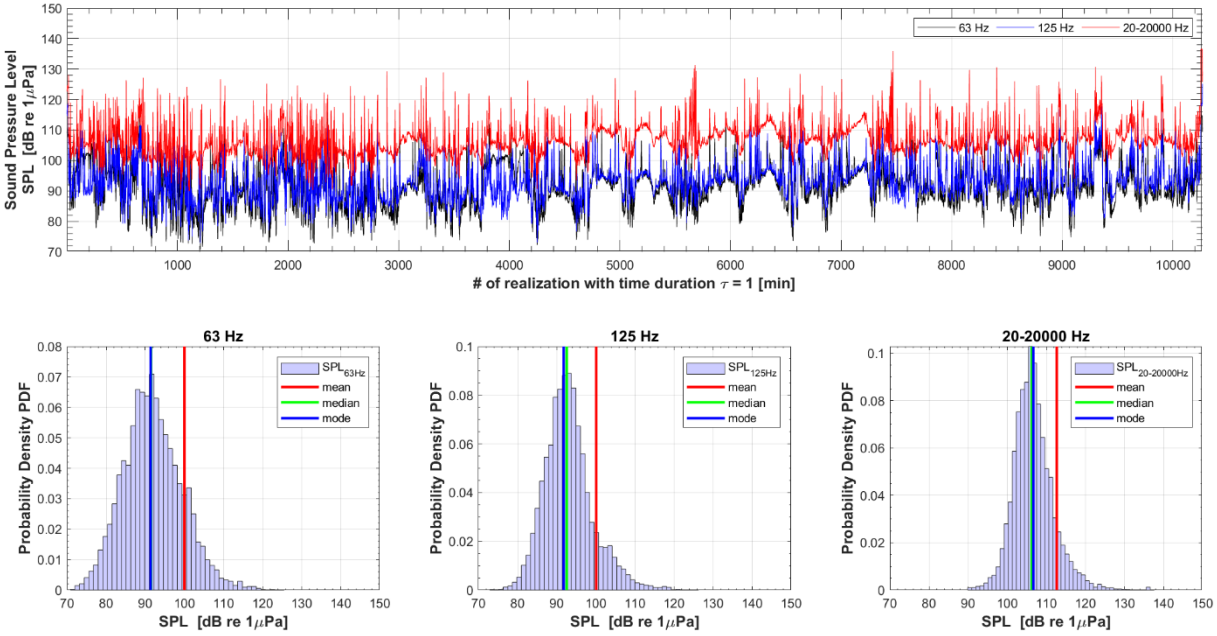


Figure 2.122. Survey station H_4. The time series of the sound pressure level SPL [dB re 1 µPa] in 1/3-octave bands of 63 Hz and 125 Hz (black and blue curves, respectively) and the 20–20 000 Hz broadband (red curve) – upper panel. The histograms of the sound pressure levels $SPL_{63\ Hz}$, $SPL_{125\ Hz}$ and $SPL_{20–20\ 000\ Hz}$ – bottom panel. Red line – the mean SPL value, green line – the median SPL value, blue line – the mode SPL value. Survey session no. 4 (13.08.2023–12.11.2023)

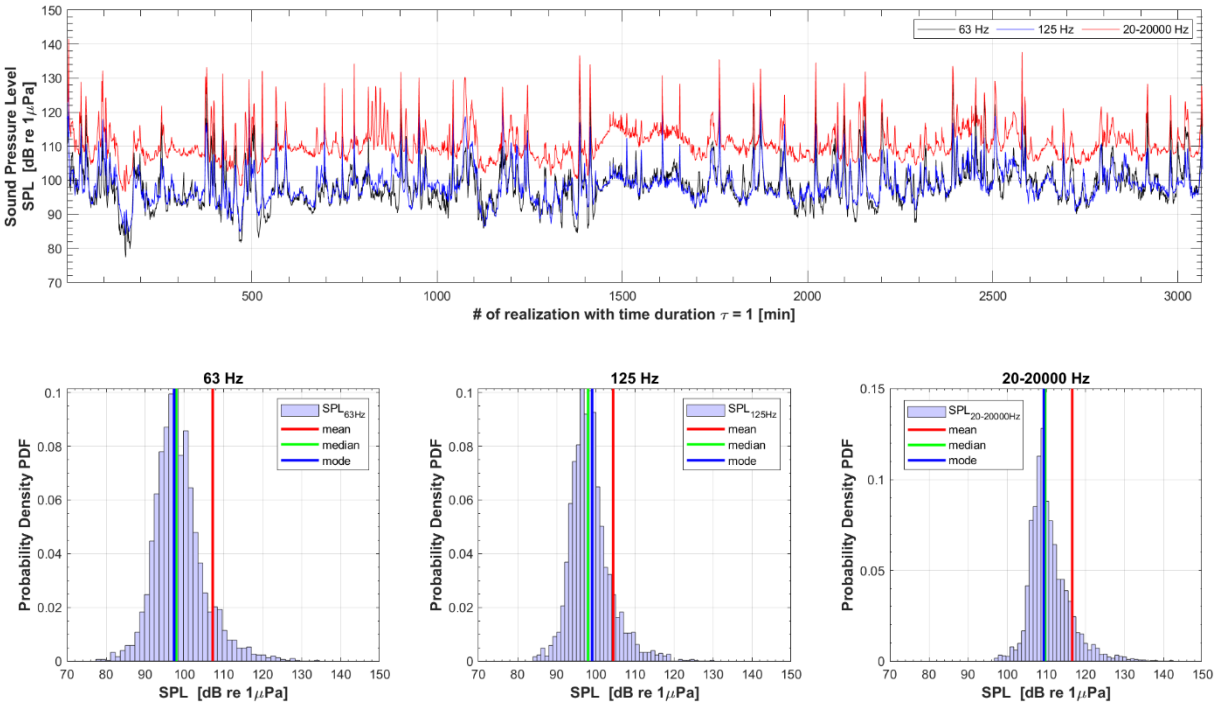


Figure 2.123. Survey station H_1. The time series of the sound pressure level SPL [dB re 1 µPa] in 1/3-octave bands of 63 Hz and 125 Hz (black and blue curves, respectively) and the 20–20 000 Hz broadband (red curve) – upper panel. The histograms of the sound pressure levels $SPL_{63\ Hz}$, $SPL_{125\ Hz}$ and $SPL_{20–20\ 000\ Hz}$ – bottom panel. Red line – the mean SPL value, green line – the median SPL value, blue line – the mode SPL value. Survey session no. 5 (12.11.2023–03.12.2023)

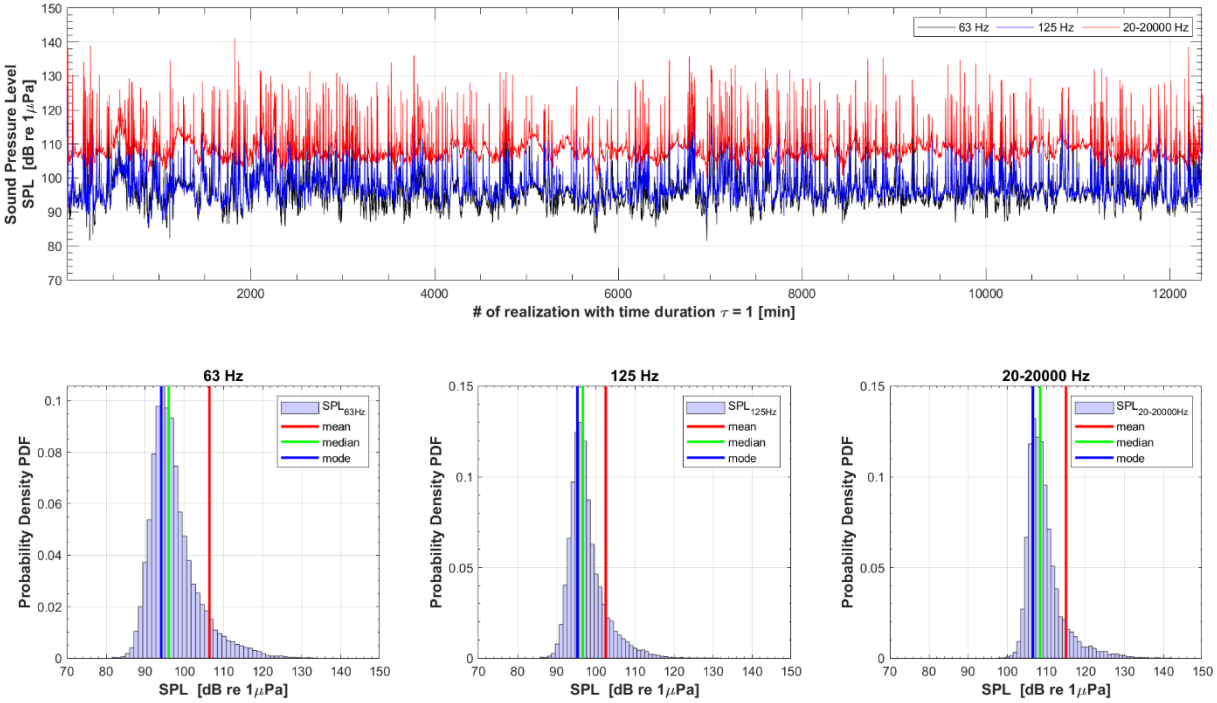


Figure 2.124. Survey station H_2. The time series of the sound pressure level SPL [dB re 1 µPa] in 1/3-octave bands of 63 Hz and 125 Hz (black and blue curves, respectively) and the 20–20 000 Hz broadband (red curve) – upper panel. The histograms of the sound pressure levels $SPL_{63\,Hz}$, $SPL_{125\,Hz}$ and $SPL_{20–20\,000\,Hz}$ – bottom panel. Red line – the mean SPL value, green line – the median SPL value, blue line – the mode SPL value. Survey session no. 5 (12.11.2023–15.02.2024)

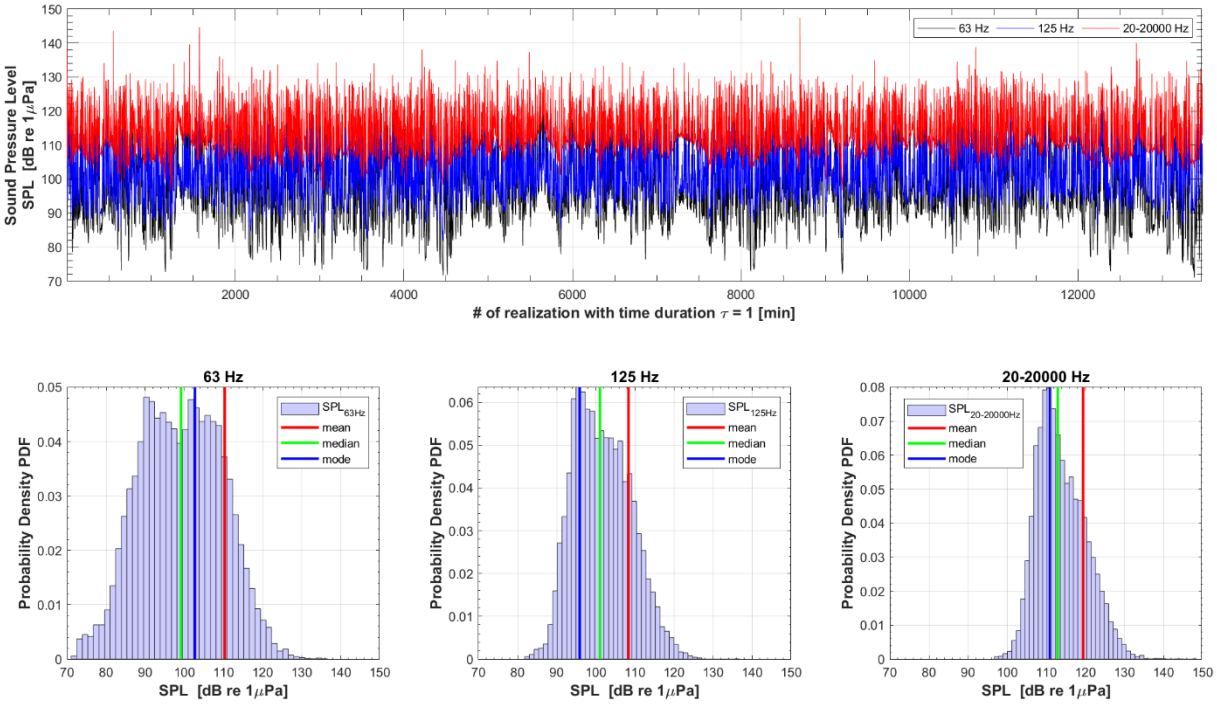


Figure 2.125. Survey station H_3. The time series of the sound pressure level SPL [dB re 1 µPa] in 1/3-octave bands of 63 Hz and 125 Hz (black and blue curves, respectively) and the 20–20 000 Hz broadband (red curve) – upper panel. The histograms of the sound pressure levels $SPL_{63\,Hz}$, $SPL_{125\,Hz}$ and $SPL_{20–20\,000\,Hz}$ – bottom panel. Red line – the mean SPL value, green line – the median SPL value, blue line – the mode SPL value. Survey session no. 5 (12.11.2023–15.02.2024)

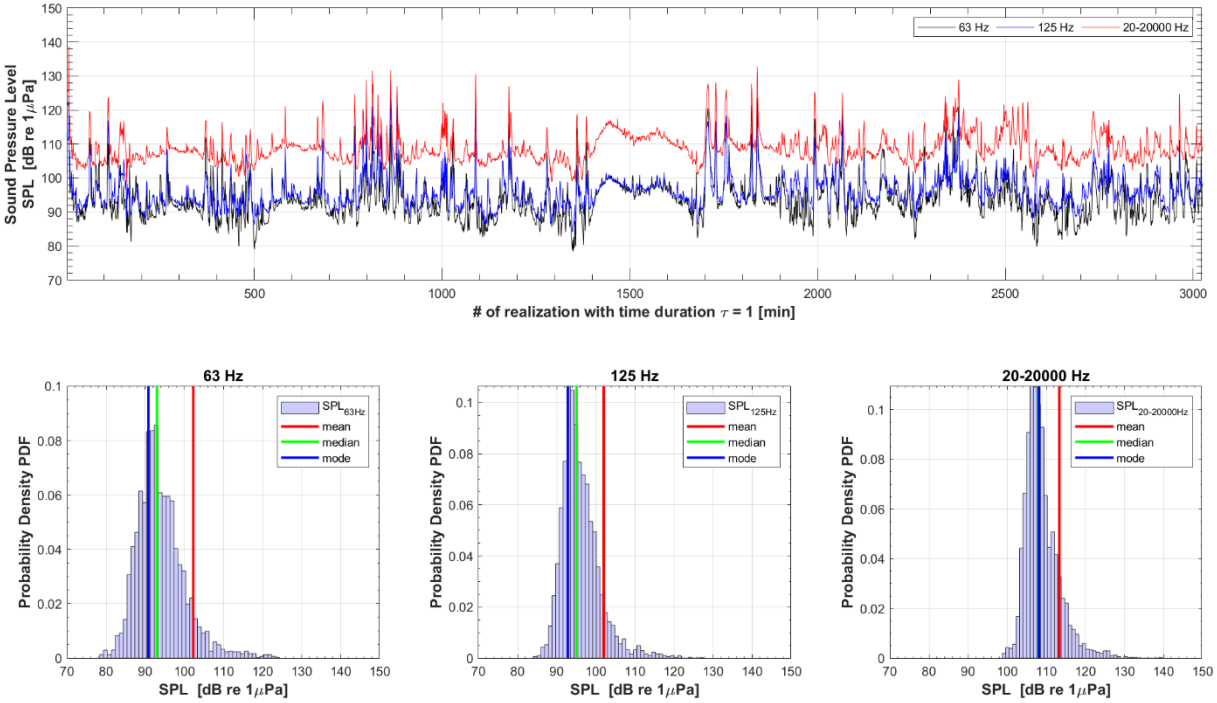


Figure 2.126. Survey station H_4. The time series of the sound pressure level SPL [dB re 1 µPa] in 1/3-octave bands of 63 Hz and 125 Hz (black and blue curves, respectively) and the 20–20 000 Hz broadband (red curve) – upper panel. The histograms of the sound pressure levels $SPL_{63\ Hz}$, $SPL_{125\ Hz}$ and $SPL_{20–20\ 000\ Hz}$ – bottom panel. Red line – the mean SPL value, green line – the median SPL value, blue line – the mode SPL value. Survey session no. 5 (12.11.2023–03.12.2023)

To perform a roughly estimate the occurrence frequency anthropogenic noise, a simple algorithm was developed to flag the broadband sound pressure level values SPL (20 Hz–20 kHz) with values exceeding the threshold of the "median value L50+3dB". The corresponding median values obtained at individual survey stations are presented in tabular form [Table 2.55–Table 2.59]. The application of the above-mentioned threshold criterion could be explained by the fact that, in underwater acoustics, the median value (so-called L50, the 50% percentile) is considered to be a characteristic indicator corresponding to the level of natural noise, i.e. noise of hydrodynamic origin, including mainly the noise caused by wind (e.g., scientific projects like BIAS and JOMOPANS on the monitoring of underwater ambient noise in the Baltic Sea and in the North Sea, respectively). In turn, it is well known that in the logarithmic scale, the value of "+3 dB" equals to double (2x) the value in linear scale, and it is frequently used in the determination of the uncertainty factor. The result of the analysis performed indicated that based on the (arbitrarily) chosen threshold criterion, the presence of noise of the anthropogenic origin is observed for from approximately 20% up to approximately 35% of the observation time in general.

At the next step, according to the recommendations of Bundesamt für Seeschifffahrt und Hydrographie (BSH, 2011), an analysis of the dependence between the sound pressure level SPL and wind speed/sea state was performed. The wind data were obtained from the LUFFT WS500-UMB meteorological station located on a survey buoy deployed at the surveys station B_MFW_3.

The time series of sound pressure level SPL (in the appropriately selected frequency bands) and the wind speed levels [$m \cdot s^{-1}$] were analysed. Their interdependency is illustrated in the form of a "point cloud" consisting of individual realizations [Figure 2.127–Figure 2.142]. At the next step, statistical values – the mean and median values of the SPL in the appropriate frequency bands (63 Hz, 125 Hz,

and in the 20–20,000 Hz broadband) and in individual wind speed classes according to the Beaufort scale were calculated. The statistical information is presented in tables [Table 2.60–Table 2.75].

Table 2.60. Survey station H_1. The statistical values of the sound pressure level values (SPL) [dB re 1 µPa] in two 1/3-octave bands with central frequencies of 63 Hz and 125 Hz and in the 20–20,000 Hz broadband in individual wind speed classes according to the Beaufort scale [°B] Survey session no. 1 (03.12.2022–07.02.2023)

Season	Wind speed [°B]	Wind speed [m·s^{1}]	Sea state	Percentage share in the wind conditions observed [%]	Number of analysed samples	Sound pressure level (SPL) [dB re 1 µPa]					
						63 Hz (1/3 oct.)		125 Hz (1/3 oct.)		20–20,000 Hz	
						mean	median	mean	median	mean	median
1	0–1	0–1.5	1	1.7	162	101.6	100.1	102.0	101.8	112.5	111.3
	2	1.6–3.3	2	6.2	588	101.2	100.7	102.6	101.7	113.2	111.9
	3	3.4–5.5		10.9	1031	101.0	101.7	101.6	101.0	112.4	111.9
	4	5.6–7.9	3	21.2	1998	100.9	100.8	102.0	101.2	112.8	111.6
	5	8.0–10.7	4	27.8	2627	99.4	98.2	100.0	98.6	111.6	109.8
	6	10.8–13.8	5	26.4	2495	100.9	99.5	100.7	99.3	112.9	111.2
	7	13.9–17.1	6	5.5	521	101.5	100.5	101.6	100.4	114.1	113.2
	8*	17.1–20.7	7	0.2	17	102.4	102.0	101.7	101.3	115.2	114.7

**due to a low number of samples representing a given wind class, the values are presented for the demonstrative purpose only*

Table 2.61. Survey station H_4. The statistical values of the sound pressure level values (SPL) [dB re 1 µPa] in two 1/3-octave bands with central frequencies of 63 Hz and 125 Hz and in the 20–20,000 Hz broadband in individual wind speed classes according to the Beaufort scale [°B] Survey session no. 1 (03.12.2022–07.02.2023)

Season	Wind speed [°B]	Wind speed [m·s^{1}]	Sea state	Percentage share in the wind conditions observed [%]	Number of analysed samples	Sound pressure level (SPL) [dB re 1 µPa]					
						63 Hz (1/3 oct.)		125 Hz (1/3 oct.)		20–20,000 Hz	
						mean	median	mean	median	mean	median
1	0–1	0–1.5	1	1.7	156	99.2	97.2	101.8	99.3	113.2	110.4
	2	1.6–3.3	2	6.2	567	97.4	95.4	99.9	97.9	110.9	108.8
	3	3.4–5.5		10.8	999	99.1	97.3	100.6	97.9	112.7	110.2
	4	5.6–7.9	3	21.4	1970	97.5	95.5	99.4	96.8	111.7	109.1
	5	8.0–10.7	4	28.1	2591	98.2	96.0	99.7	97.0	112.4	110.0
	6	10.8–13.8	5	26.2	2414	96.8	95.1	97.9	96.4	111.2	109.7
	7	13.9–17.1	6	5.5	503	98.2	96.6	98.8	97.3	112.0	110.9

Season	Wind speed [°B]	Wind speed [m·s^{1}]	Sea state	Percentage share in the wind conditions observed [%]	Number of analysed samples	Sound pressure level (SPL) [dB re 1 µPa]					
						63 Hz (1/3 oct.)		125 Hz (1/3 oct.)		20–20,000 Hz	
						mean	median	mean	median	mean	median
	8*	17.1–20.7	7	0.2	15	96.2	96.9	96.9	96.7	110.6	111.1

**due to a low number of samples representing a given wind class, the values are presented for the demonstrative purpose only*

*Table 2.62. Survey station H_1. The statistical values of the sound pressure level values (SPL) [dB re 1 µPa] in two 1/3-octave bands with central frequencies of 63 Hz and 125 Hz and in the 20–20,000 Hz broadband in individual wind speed classes according to the Beaufort scale [°B] Survey campaign no. 2 (19.03.2023– –24.04.2023)**

Season	Wind speed [°B]	Wind speed [m·s^{1}]	Sea state	Percentage share in the wind conditions observed [%]	Number of analysed samples	Sound pressure level (SPL) [dB re 1 µPa]					
						63 Hz (1/3 oct.)		125 Hz (1/3 oct.)		20–20,000 Hz	
						mean	median	mean	median	mean	median
2	0–1	0–1.5	1	2.9	148	103.3	103.6	102.6	100.8	114.5	112.5
	2	1.6–3.3	2	13.2	679	103.5	104.3	103.3	102.3	114.7	113.8
	3	3.4–5.5		23.7	1219	102.5	103.1	102.5	102.4	113.8	113.2
	4	5.6–7.9	3	32.2	1661	102.9	102.3	102.8	102.3	113.9	113.2
	5	8.0–10.7	4	16.6	856	102.8	103.0	102.8	102.6	114.1	113.7
	6	10.8–13.8	5	11.4	587	101.3	100.8	100.5	99.6	112.7	111.7
	7**	13.9–17.1	6	0.1	4	95.1	95.2	96.0	96.1	110.2	110.2

**due to the damage to the meteorological station, the wind-noise dependence analysis was performed for the measurement data obtained after 19 March 2023;*
*** due to a low number of samples representing a given wind class, the values are presented for the demonstrative purpose only*

*Table 2.63. Survey station H_2. The statistical values of the sound pressure level values (SPL) [dB re 1 µPa] in two 1/3-octave bands with central frequencies of 63 Hz and 125 Hz and in the 20–20,000 Hz broadband in individual wind speed classes according to the Beaufort scale [°B] Survey session no. 2 (19.03.2023–24.04.2023)**

Season	Wind speed [°B]	Wind speed [m·s^{1}]	Sea state	Percentage share in the wind conditions observed [%]	Number of analysed samples	Sound pressure level (SPL) [dB re 1 µPa]					
						63 Hz (1/3 oct.)		125 Hz (1/3 oct.)		20–20,000 Hz	
						mean	median	mean	median	mean	median
2	0–1	0–1.5	1	2.8	167	100.8	100.4	102.3	101.7	114.1	112.7
	2	1.6–3.3	2	12.4	728	100.8	100.5	102.1	101.0	113.4	112.0

Season	Wind speed [°B]	Wind speed [m·s^{1}]	Sea state	Percentage share in the wind conditions observed [%]	Number of analysed samples	Sound pressure level (SPL) [dB re 1 µPa]					
						63 Hz (1/3 oct.)		125 Hz (1/3 oct.)		20–20,000 Hz	
						mean	median	mean	median	mean	median
	3	3.4–5.5		23.0	1352	100.2	99.0	101.2	100.6	112.6	111.7
	4	5.6–7.9	3	32.1	1887	100.2	99.2	101.3	100.7	112.5	111.5
	5	8.0–10.7	4	19.6	1151	99.7	98.6	100.4	99.6	112.1	110.7
	6	10.8–13.8	5	10.1	591	99.7	99.0	98.8	97.9	111.7	110.8
	7**	13.9–17.1	6	0.1	3	95.5	95.4	95.7	95.8	110.0	110.0

**due to the damage to the meteorological station, the wind-noise dependence analysis was performed for the measurement data obtained after 19 March 2023;*
*** due to a low number of samples representing a given wind class, the values are presented for the demonstrative purpose only*

*Table 2.64. Survey station H_3. The statistical values of the sound pressure level values (SPL) [dB re 1 µPa] in two 1/3-octave bands with central frequencies of 63 Hz and 125 Hz and in the 20–20,000 Hz broadband in individual wind speed classes according to the Beaufort scale [°B] Survey session no. 2 (19.03.2023–24.04.2023)**

Season	Wind speed [°B]	Wind speed [m·s^{1}]	Sea state	Percentage share in the wind conditions observed [%]	Number of analysed samples	Sound pressure level (SPL) [dB re 1 µPa]					
						63 Hz (1/3 oct.)		125 Hz (1/3 oct.)		20–20,000 Hz	
						mean	median	mean	median	mean	median
2	0–1	0–1.5	1	2.9	173	101.5	103.9	104.6	105.2	115.5	116.4
	2	1.6–3.3	2	12.3	736	99.0	101.4	103.1	103.1	113.6	113.8
	3	3.4–5.5		23.1	1387	99.0	100.6	102.7	102.7	113.6	113.5
	4	5.6–7.9	3	31.7	1898	99.0	100.1	102.2	101.8	113.5	112.6
	5	8.0–10.7	4	20.2	1211	100.1	100.5	102.3	101.8	114.3	113.0
	6	10.8–13.8	5	9.8	588	102.0	101.7	102.6	101.6	115.3	114.1
	7**	13.9–17.1	6	0.1	3	93.4	93.9	99.3	99.2	111.9	111.7

**due to the damage to the meteorological station, the wind-noise dependence analysis was performed for the measurement data obtained after 19 March 2023;*
*** due to a low number of samples representing a given wind class, the values are presented for the demonstrative purpose only*

*Table 2.65. Survey station H_4. The statistical values of the sound pressure level values (SPL) [dB re 1 µPa] in two 1/3-octave bands with central frequencies of 63 Hz and 125 Hz and in the 20–20,000 Hz broadband in individual wind speed classes according to the Beaufort scale [°B] Survey session no. 2 (19.03.2023–24.04.2023)**

Season	Wind speed [°B]	Wind speed [m·s^{1}]	Sea state	Percentage share in the wind conditions observed [%]	Number of analysed samples	Sound pressure level (SPL) [dB re 1 µPa]					
						63 Hz (1/3 oct.)		125 Hz (1/3 oct.)		20–20,000 Hz	
						mean	median	mean	median	mean	median
2	0–1	0–1.5	1	2.9	148	98.3	97.4	101.0	98.8	113.2	111.2
	2	1.6–3.3	2	12.9	658	99.0	97.4	101.5	99.7	113.3	111.1
	3	3.4–5.5		23.5	1197	97.0	95.8	99.8	98.8	111.0	109.8
	4	5.6–7.9	3	32.5	1653	98.1	96.9	100.7	99.1	112.2	110.3
	5	8.0–10.7	4	16.6	846	99.0	97.5	100.9	99.6	113.2	111.1
	6	10.8–13.8	5	11.5	585	99.5	97.8	100.0	98.6	112.7	111.3
	7**	13.9–17.1	6	0.1	4	103.1	103.1	102.4	101.8	114.1	113.5

**due to the damage to the meteorological station, the wind-noise dependence analysis was performed for the measurement data obtained after 19 March 2023;*
*** due to a low number of samples representing a given wind class, the values are presented for the demonstrative purpose only*

Table 2.66. Survey station H_1. The statistical values of the sound pressure level values (SPL) [dB re 1 µPa] in two 1/3-octave bands with central frequencies of 63 Hz and 125 Hz and in the 20–20,000 Hz broadband in individual wind speed classes according to the Beaufort scale [°B] Survey session no. 3 (24.04.2023–12.08.2023)

Season	Wind speed [°B]	Wind speed [m·s^{1}]	Sea state	Percentage share in the wind conditions observed [%]	Number of analysed samples	Sound pressure level (SPL) [dB re 1 µPa]					
						63 Hz (1/3 oct.)		125 Hz (1/3 oct.)		20–20,000 Hz	
						mean	median	mean	median	mean	median
3	0–1	0–1.5	1	3.4	521	95.2	94.9	95.6	94.9	106.5	106.2
	2	1.6–3.3	2	15.3	2367	95.2	94.7	95.2	94.5	106.4	105.3
	3	3.4–5.5		26.5	4093	96.0	95.3	96.1	95.8	107.3	106.8
	4	5.6–7.9	3	28.8	4438	95.3	94.5	95.7	95.1	107.3	106.9
	5	8.0–10.7	4	20.2	3123	94.9	93.7	95.2	94.5	107.5	107.2
	6	10.8–13.8	5	4.6	717	94.5	93.3	94.2	93.1	107.1	106.3
	7	13.9–17.1	6	0.6	94	96.4	96.0	94.7	94.6	110.7	110.7
	8*	17.1–20.7	7	0.5	78	97.8	97.6	96.9	96.7	113.2	113.2

**due to a low number of samples representing a given wind class, the values are presented for the demonstrative purpose only*

Table 2.67. Survey station H_3. The statistical values of the sound pressure level values (SPL) [dB re 1 µPa] in two 1/3-octave bands with central frequencies of 63 Hz and 125 Hz and in the 20–20,000 Hz broadband in individual wind speed classes according to the Beaufort scale [°B] Survey session no. 3 (30.04.2023–12.08.2023)

Season	Wind speed [°B]	Wind speed [m·s^{1}]	Sea state	Percentage share in the wind conditions observed [%]	Number of analysed samples	Sound pressure level (SPL) [dB re 1 µPa]					
						63 Hz (1/3 oct.)		125 Hz (1/3 oct.)		20–20,000 Hz	
						mean	median	mean	median	mean	median
3	0–1	0–1.5	1	3.4	490	95.6	96.4	99.5	100.8	110.0	110.3
	2	1.6–3.3	2	15.9	2253	97.1	98.8	100.8	101.8	111.3	111.7
	3	3.4–5.5		26.9	3824	96.8	98.3	100.7	101.6	111.4	111.7
	4	5.6–7.9	3	28.6	4056	95.5	96.7	99.3	99.9	110.6	110.3
	5	8.0–10.7	4	19.0	2705	95.5	95.2	98.8	98.9	110.9	109.8
	6	10.8–13.8	5	5.0	708	97.4	96.9	99.4	98.9	112.1	110.7
	7	13.9–17.1	6	0.6	92	100.6	98.8	100.1	98.9	114.5	113.9
	8*	17.1–20.7	7	0.5	77	102.1	101.9	100.7	99.8	115.7	115.3

**due to a low number of samples representing a given wind class, the values are presented for the demonstrative purpose only*

Table 2.68. Survey station H_4. The statistical values of the sound pressure level values (SPL) [dB re 1 µPa] in two 1/3-octave bands with central frequencies of 63 Hz and 125 Hz and in the 20–20,000 Hz broadband in individual wind speed classes according to the Beaufort scale [°B] Survey session no. 3 (24.04.2023–12.08.2023)

Season	Wind speed [°B]	Wind speed [m·s^{1}]	Sea state	Percentage share in the wind conditions observed [%]	Number of analysed samples	Sound pressure level (SPL) [dB re 1 µPa]					
						63 Hz (1/3 oct.)		125 Hz (1/3 oct.)		20–20,000 Hz	
						mean	median	mean	median	mean	median
3	0–1	0–1.5	1	3.3	389	93.6	92.0	94.5	93.7	106.8	105.8
	2	1.6–3.3	2	15.4	1807	94.8	94.2	96.5	95.4	108.4	107.2
	3	3.4–5.5		26.6	3109	95.0	93.9	96.7	95.5	108.6	107.5
	4	5.6–7.9	3	28.5	3339	93.6	92.9	95.4	94.7	107.6	106.6
	5	8.0–10.7	4	20.3	2375	93.6	92.4	95.8	94.8	108.2	107.1
	6	10.8–13.8	5	4.7	549	92.4	91.4	93.1	92.0	106.9	106.4
	7	13.9–17.1	6	0.6	69	93.0	92.4	93.0	92.2	109.0	108.7
	8*	17.1–20.7	7	0.5	60	94.7	95.0	95.0	95.1	111.2	111.4

**due to a low number of samples representing a given wind class, the values are presented for the demonstrative purpose only*

Table 2.69. Survey station H_1. The statistical values of the sound pressure level values (SPL) [dB re 1 µPa] in two 1/3-octave bands with central frequencies of 63 Hz and 125 Hz and in the 20–20,000 Hz broadband in individual wind speed classes according to the Beaufort scale [°B] Survey session no. 4 (13.08,2023–12.11.2023)

Season	Wind speed [°B]	Wind speed [m·s^{1}]	Sea state	Percentage share in the wind conditions observed [%]	Number of analysed samples	Sound pressure level (SPL) [dB re 1 µPa]					
						63 Hz (1/3 oct.)		125 Hz (1/3 oct.)		20–20,000 Hz	
						mean	median	mean	median	mean	median
4	0–1	0–1.5	1	1.9	246	93.6	94.1	92.1	90.3	104.4	102.8
	2	1.6–3.3	2	7.4	971	92.3	92.2	91.8	91.3	103.9	102.9
	3	3.4–5.5		15.6	2054	93.5	93.0	93.1	92.5	105.6	104.2
	4	5.6–7.9	3	24.7	3241	92.5	91.3	91.8	91.1	105.0	103.7
	5	8.0–10.7	4	24.4	3206	92.4	91.2	92.6	91.4	105.9	104.6
	6	10.8–13.8	5	15.9	2090	95.0	93.2	95.1	94.0	108.5	107.4
	7	13.9–17.1	6	7.9	1041	97.1	95.8	96.3	95.2	110.6	109.8
	8	17.1–20.7	7	2.1	278	98.4	97.4	97.7	97.1	112.7	112.2

Table 2.70. Survey station H_3. The statistical values of the sound pressure level values (SPL) [dB re 1 µPa] in two 1/3-octave bands with central frequencies of 63 Hz and 125 Hz and in the 20–20,000 Hz broadband in individual wind speed classes according to the Beaufort scale [°B] Survey session no. 3 (12.08.2023–13.11.2023)

Season	Wind speed [°B]	Wind speed [m·s^{1}]	Sea state	Percentage share in the wind conditions observed [%]	Number of analysed samples	Sound pressure level (SPL) [dB re 1 µPa]					
						63 Hz (1/3 oct.)		125 Hz (1/3 oct.)		20–20,000 Hz	
						mean	median	mean	median	mean	median
4	0–1	0–1.5	1	1.9	247	95.8	95.2	100.3	100.6	111.0	111.3
	2	1.6–3.3	2	7.4	966	95.3	96.2	99.2	99.8	110.2	110.0
	3	3.4–5.5		15.7	2043	96.4	97.6	99.8	100.4	110.8	110.8
	4	5.6–7.9	3	25.1	3269	94.8	96.0	98.9	99.5	110.3	110.1
	5	8.0–10.7	4	24.5	3185	96.2	96.7	99.4	99.7	111.4	110.7
	6	10.8–13.8	5	15.5	2020	97.0	97.3	99.5	99.4	112.2	111.6
	7	13.9–17.1	6	7.7	1000	97.4	96.5	99.4	98.8	112.5	111.9
	8	17.1–20.7	7	2.1	269	97.3	96.8	99.9	98.8	112.6	111.1

Table 2.71. Survey station H_4. The statistical values of the sound pressure level values (SPL) [dB re 1 µPa] in two 1/3-octave bands with central frequencies of 63 Hz and 125 Hz and in the 20–20,000 Hz broadband in individual wind speed classes according to the Beaufort scale [°B] Survey session no. 4 (13.08,2023–12.11.2023)

Season	Wind speed [°B]	Wind speed [m·s^1]	Sea state	Percentage share in the wind conditions observed [%]	Number of analysed samples	Sound pressure level (SPL) [dB re 1 µPa]					
						63 Hz (1/3 oct.)		125 Hz (1/3 oct.)		20–20,000 Hz	
						mean	median	mean	median	mean	median
4	0–1	0–1.5	1	1.9	192	89.8	88.4	91.6	90.4	105.6	105.0
	2	1.6–3.3	2	7.3	749	90.6	89.9	92.0	91.1	105.5	104.8
	3	3.4–5.5		15.7	1613	91.3	91.2	92.6	92.0	105.9	105.5
	4	5.6–7.9	3	24.7	2531	91.6	91.0	92.5	92.0	106.3	105.6
	5	8.0–10.7	4	24.5	2519	92.6	91.9	93.0	92.3	106.8	106.2
	6	10.8–13.8	5	15.9	1636	92.5	91.7	94.6	93.5	107.7	107.0
	7	13.9–17.1	6	7.9	806	92.7	92.5	94.5	94.0	108.5	108.4
	8	17.1–20.7	7	2.1	216	93.7	92.7	95.1	94.1	109.3	109.2

Table 2.72. Survey station H_1. The statistical values of the sound pressure level values (SPL) [dB re 1 µPa] in two 1/3-octave bands with central frequencies of 63 Hz and 125 Hz and in the 20–20,000 Hz broadband in individual wind speed classes according to the Beaufort scale [°B] Survey session no. 4 (12.11,2023–03.12.2023)

Season	Wind speed [°B]	Wind speed [m·s^1]	Sea state	Percentage share in the wind conditions observed [%]	Number of analysed samples	Sound pressure level (SPL) [dB re 1 µPa]					
						63 Hz (1/3 oct.)		125 Hz (1/3 oct.)		20–20,000 Hz	
						mean	median	mean	median	mean	median
5	0–1	0–1.5	1	2.0	60	97.3	96.6	99.8	99.4	112.7	110.8
	2	1.6–3.3	2	3.7	113	100.0	99.7	100.5	100.1	112.6	112.5
	3	3.4–5.5		7.9	241	99.5	99.2	100.0	99.4	110.8	109.8
	4	5.6–7.9	3	17.0	520	98.9	98.7	98.9	98.7	110.5	109.6
	5	8.0–10.7	4	35.6	1091	98.7	97.4	98.3	97.2	110.3	108.8
	6	10.8–13.8	5	20.4	624	97.5	96.4	97.6	96.8	110.1	109.0
	7	13.9–17.1	6	9.0	276	99.0	98.0	98.7	97.7	111.8	110.9
	8	17.1–20.7	7	4.0	123	100.4	100.0	100.0	99.4	114.4	114.1
	9*	20.7–24.4	8	0.6	18	102.3	102.1	101.8	101.5	116.9	116.7

**due to a low number of samples representing a given wind class, the values are presented for the demonstrative purpose only*

Table 2.73. Survey station H_2. The statistical values of the sound pressure level values (SPL) [dB re 1 µPa] in two 1/3-octave bands with central frequencies of 63 Hz and 125 Hz and in the 20–20,000 Hz broadband in individual wind speed classes according to the Beaufort scale [°B] Survey session no. 4 (12.11.2023–15.02.2024)

Season	Wind speed [°B]	Wind speed [m·s^{1}]	Sea state	Percentage share in the wind conditions observed [%]	Number of analysed samples	Sound pressure level (SPL) [dB re 1 µPa]					
						63 Hz (1/3 oct.)		125 Hz (1/3 oct.)		20–20,000 Hz	
						mean	median	mean	median	mean	median
5	0–1	0–1.5	1	0.9	111	97.9	97.3	99.3	98.5	110.3	109.6
	2	1.6–3.3	2	1.9	239	99.0	97.5	99.4	98.6	110.3	108.6
	3	3.4–5.5		5.6	694	98.4	97.6	98.9	98.3	109.7	108.6
	4	5.6–7.9	3	15.0	1851	97.4	95.9	98.1	97.3	109.3	107.8
	5	8.0–10.7	4	28.3	3492	97.3	95.8	97.5	96.6	109.1	107.8
	6	10.8–13.8	5	30.0	3704	97.3	95.9	97.5	96.5	109.6	108.5
	7	13.9–17.1	6	14.9	1844	96.7	95.5	97.2	96.2	109.8	109.1
	8	17.1–20.7	7	3.2	401	97.6	97.0	98.0	97.4	111.2	111.2
	9*	20.7–24.4	8	0.2	20	97.9	97.8	97.1	97.1	111.9	111.9

**due to a low number of samples representing a given wind class, the values are presented for the demonstrative purpose only*

Table 2.74. Survey station H_3. The statistical values of the sound pressure level values (SPL) [dB re 1 µPa] in two 1/3-octave bands with central frequencies of 63 Hz and 125 Hz and in the 20–20,000 Hz broadband in individual wind speed classes according to the Beaufort scale [°B] Survey session no. 4 (12.11.2023–15.02.2024)

Season	Wind speed [°B]	Wind speed [m·s^{1}]	Sea state	Percentage share in the wind conditions observed [%]	Number of analysed samples	Sound pressure level (SPL) [dB re 1 µPa]					
						63 Hz (1/3 oct.)		125 Hz (1/3 oct.)		20–20,000 Hz	
						mean	median	mean	median	mean	median
5	0–1	0–1.5	1	0.9	120	102.9	102.8	104.3	104.7	115.3	115.8
	2	1.6–3.3	2	2.0	270	96.7	97.8	101.8	101.2	112.6	112.6
	3	3.4–5.5		5.6	756	98.4	100.1	102.6	102.5	113.7	113.8
	4	5.6–7.9	3	15.0	2022	97.8	99.1	101.5	101.4	112.9	112.1
	5	8.0–10.7	4	28.3	3815	98.7	99.0	101.7	101.4	113.5	112.5
	6	10.8–13.8	5	29.9	4032	99.3	98.9	101.5	100.8	114.0	112.5
	7	13.9–17.1	6	14.9	2007	100.3	98.5	101.5	99.8	114.9	113.2

Season	Wind speed [°B]	Wind speed [m·s^{1}]	Sea state	Percentage share in the wind conditions observed [%]	Number of analysed samples	Sound pressure level (SPL) [dB re 1 µPa]					
						63 Hz (1/3 oct.)		125 Hz (1/3 oct.)		20–20,000 Hz	
						mean	median	mean	median	mean	median
	8	17.1–20.7	7	3.2	434	103.8	102.3	102.3	101.4	116.8	115.7
	9*	20.7–24.4	8	0.2	21	102.3	101.9	101.8	101.6	117.9	117.9

**due to a low number of samples representing a given wind class, the values are presented for the demonstrative purpose only*

Table 2.75. Survey station H_4. The statistical values of the sound pressure level values (SPL) [dB re 1 µPa] in two 1/3-octave bands with central frequencies of 63 Hz and 125 Hz and in the 20–20,000 Hz broadband in individual wind speed classes according to the Beaufort scale [°B] Survey session no. 4 (12.11,2023–03.12.2023)

Season	Wind speed [°B]	Wind speed [m·s^{1}]	Sea state	Percentage share in the wind conditions observed [%]	Number of analysed samples	Sound pressure level (SPL) [dB re 1 µPa]					
						63 Hz (1/3 oct.)		125 Hz (1/3 oct.)		20–20,000 Hz	
						mean	median	mean	median	mean	median
5	0–1	0–1.5	1	2.0	61	93.4	92.2	98.4	96.6	109.8	108.4
	2	1.6–3.3	2	3.6	110	95.7	95.5	98.8	98.6	111.3	111.4
	3	3.4–5.5		7.7	233	94.8	93.5	97.1	96.6	109.2	108.0
	4	5.6–7.9	3	17.3	523	94.4	93.5	97.1	96.0	108.7	107.2
	5	8.0–10.7	4	35.7	1079	92.5	91.3	95.1	94.1	107.8	106.8
	6	10.8–13.8	5	20.1	609	94.2	92.7	95.3	94.3	109.0	108.1
	7	13.9–17.1	6	9.0	272	95.1	94.0	96.1	95.0	110.3	109.5
	8	17.1–20.7	7	4.0	120	97.4	97.2	97.8	97.6	112.8	112.5
	9*	20.7–24.4	8	0.6	18	98.5	98.6	98.8	98.7	114.7	114.5

**due to a low number of samples representing a given wind class, the values are presented for the demonstrative purpose only*

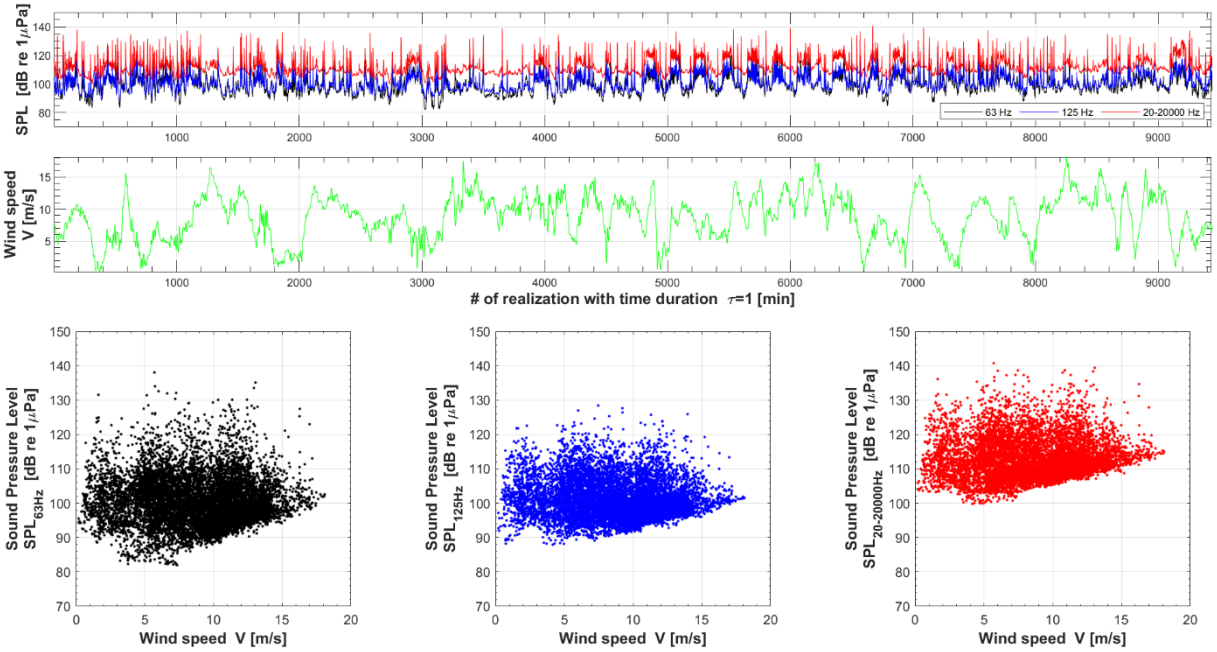


Figure 2.127. Survey station H_1. The time series of the sound pressure levels (SPL) [dB re 1 µPa] in 1/3-octave bands of 63 Hz and 125 Hz (black and blue curves, respectively) and in the 20–20,000 Hz broadband (red curve) – upper panel. The time series of wind velocity V [m·s^{-1}] – middle panel. The dependence of sound pressure levels $SPL_{63\ Hz}$, $SPL_{125\ Hz}$, and $SPL_{20–20\,000\ Hz}$ on the wind velocity – bottom panel. Survey session no. 1 (03.12.2022–07.02.2023)

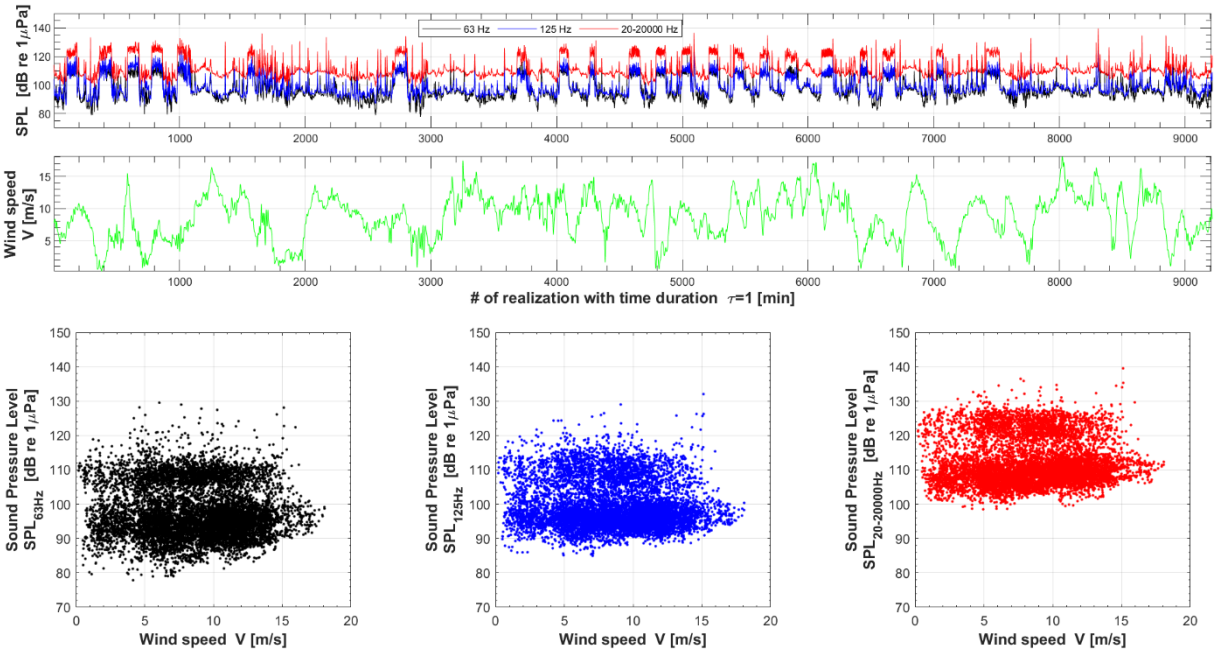


Figure 2.128. Survey station H_4. The time series of the sound pressure levels (SPL) [dB re 1 µPa] in 1/3-octave bands of 63 Hz and 125 Hz (black and blue curves, respectively) and in the 20–20,000 Hz broadband (red curve) – upper panel. The time series of wind velocity V [m·s^{-1}] – middle panel. The dependence of sound pressure levels $SPL_{63\ Hz}$, $SPL_{125\ Hz}$, and $SPL_{20–20\,000\ Hz}$ on the wind velocity – bottom panel. Survey session no. 1 (03.12.2022–07.02.2023)

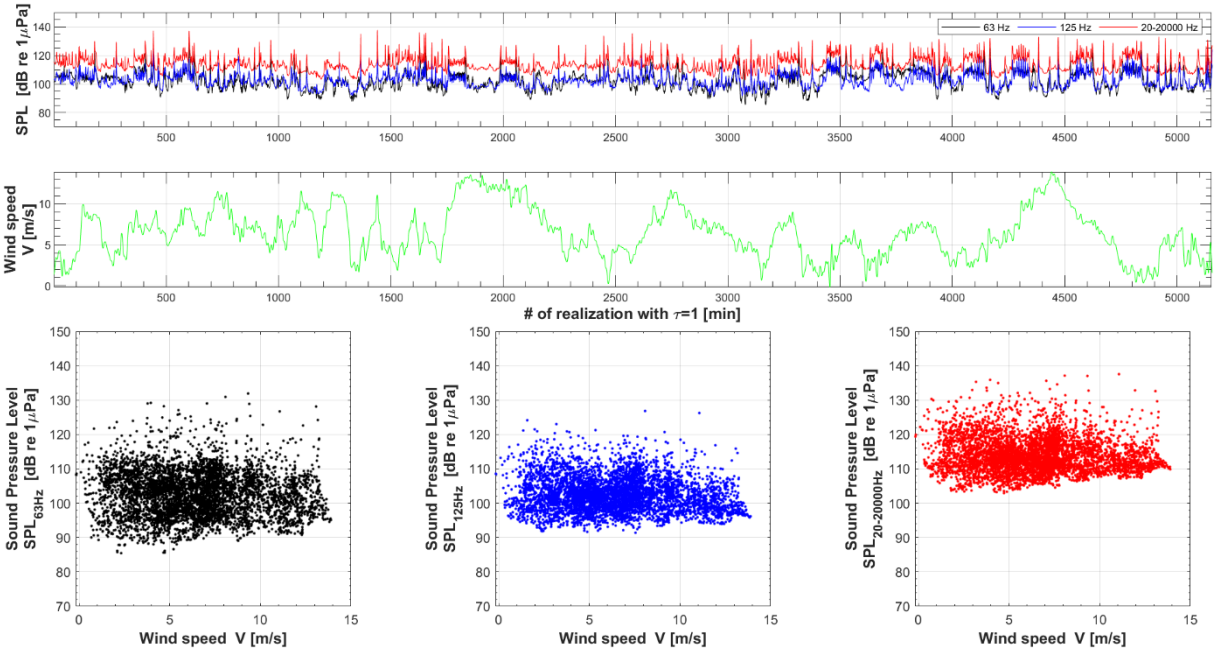


Figure 2.129. Survey station H_1. The time series of the sound pressure levels (SPL) [dB re 1 µPa] in 1/3-octave bands of 63 Hz and 125 Hz (black and blue curves, respectively) and in the 20–20,000 Hz broadband (red curve) – upper panel. The time series of wind velocity V [m·s^{-1}] – middle panel. The dependence of sound pressure levels $SPL_{63\ Hz}$, $SPL_{125\ Hz}$, and $SPL_{20–20\,000\ Hz}$ on the wind velocity – bottom panel. Survey session no. 2 (19.03.2023–24.04.2023)

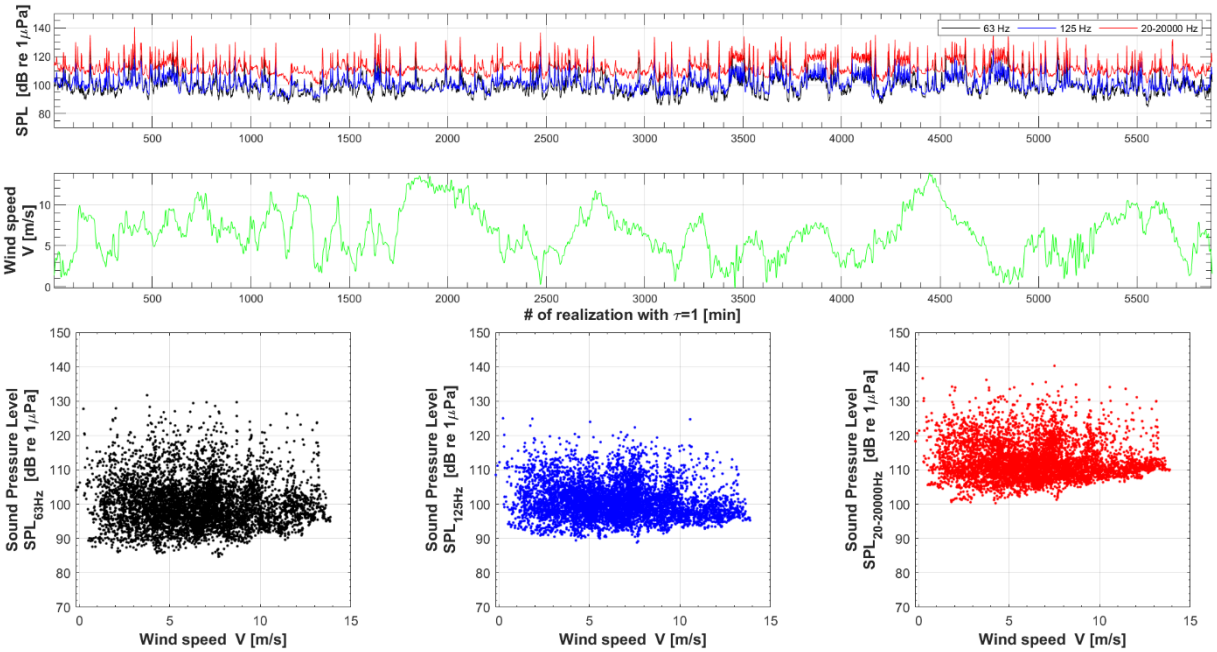


Figure 2.130. Survey station H_2. The time series of the sound pressure levels (SPL) [dB re 1 µPa] in 1/3-octave bands of 63 Hz and 125 Hz (black and blue curves, respectively) and in the 20–20,000 Hz broadband (red curve) – upper panel. The time series of wind velocity V [m·s^{-1}] – middle panel. The dependence of sound pressure levels $SPL_{63\ Hz}$, $SPL_{125\ Hz}$, and $SPL_{20–20\,000\ Hz}$ on the wind velocity – bottom panel. Survey session no. 2 (19.03.2023–29.04.2023)

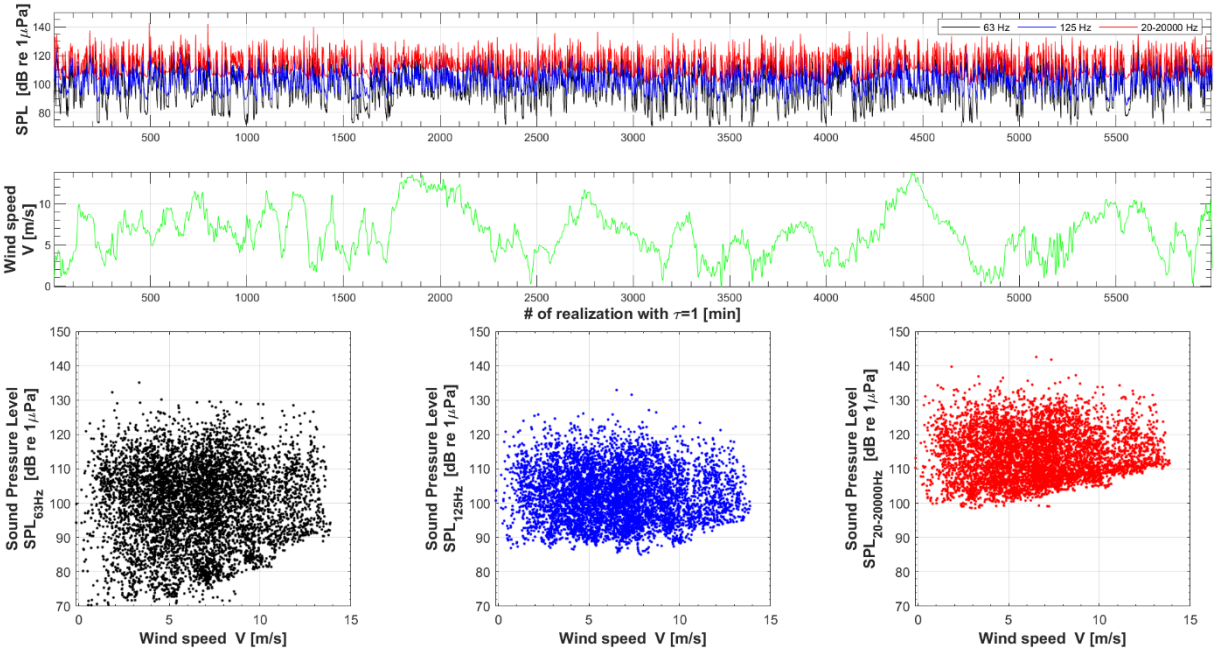


Figure 2.131. Survey station H_3. The time series of the sound pressure levels (SPL) [dB re 1 µPa] in 1/3-octave bands of 63 Hz and 125 Hz (black and blue curves, respectively) and in the 20–20,000 Hz broadband (red curve) – upper panel. The time series of wind velocity V [m·s^{-1}] – middle panel. The dependence of sound pressure levels $SPL_{63\ Hz}$, $SPL_{125\ Hz}$, and $SPL_{20–20\,000\ Hz}$ on the wind velocity – bottom panel. Survey session no. 2 (19.03.2023–30.04.2023)

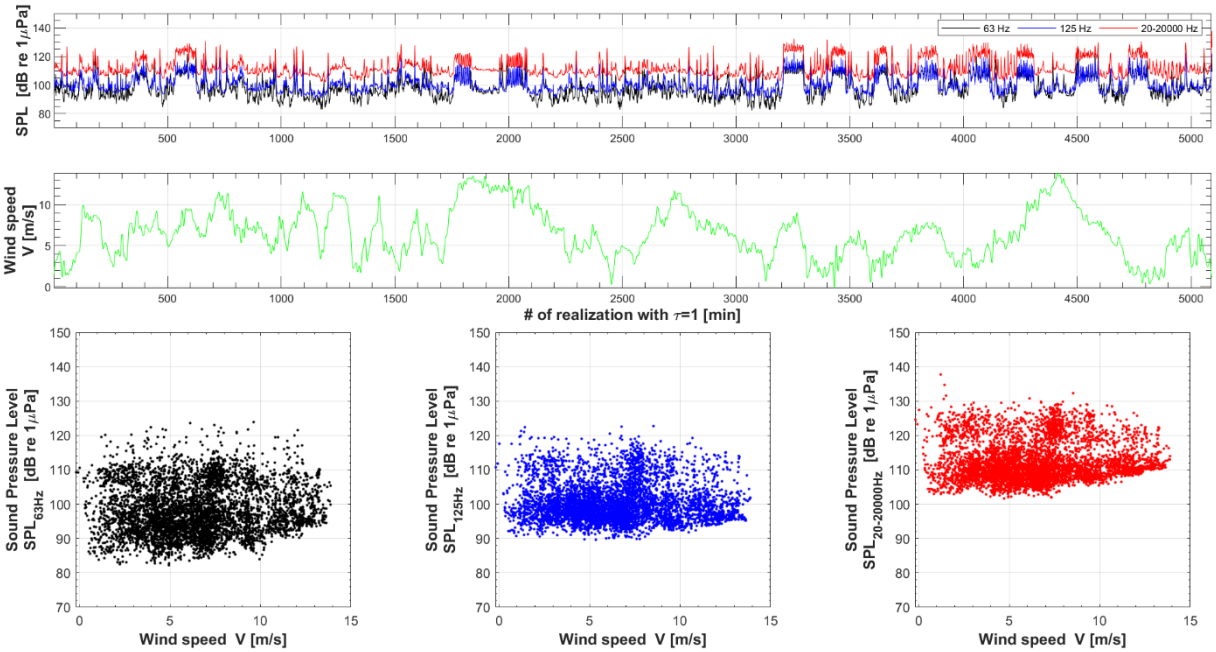


Figure 2.132. Survey station H_4. The time series of the sound pressure levels (SPL) [dB re 1 µPa] in 1/3-octave bands of 63 Hz and 125 Hz (black and blue curves, respectively) and in the 20–20,000 Hz broadband (red curve) – upper panel. The time series of wind velocity V [m·s^{-1}] – middle panel. The dependence of sound pressure levels $SPL_{63\ Hz}$, $SPL_{125\ Hz}$, and $SPL_{20–20\,000\ Hz}$ on the wind velocity – bottom panel. Survey session no. 2 (19.03.2023–24.04.2023)

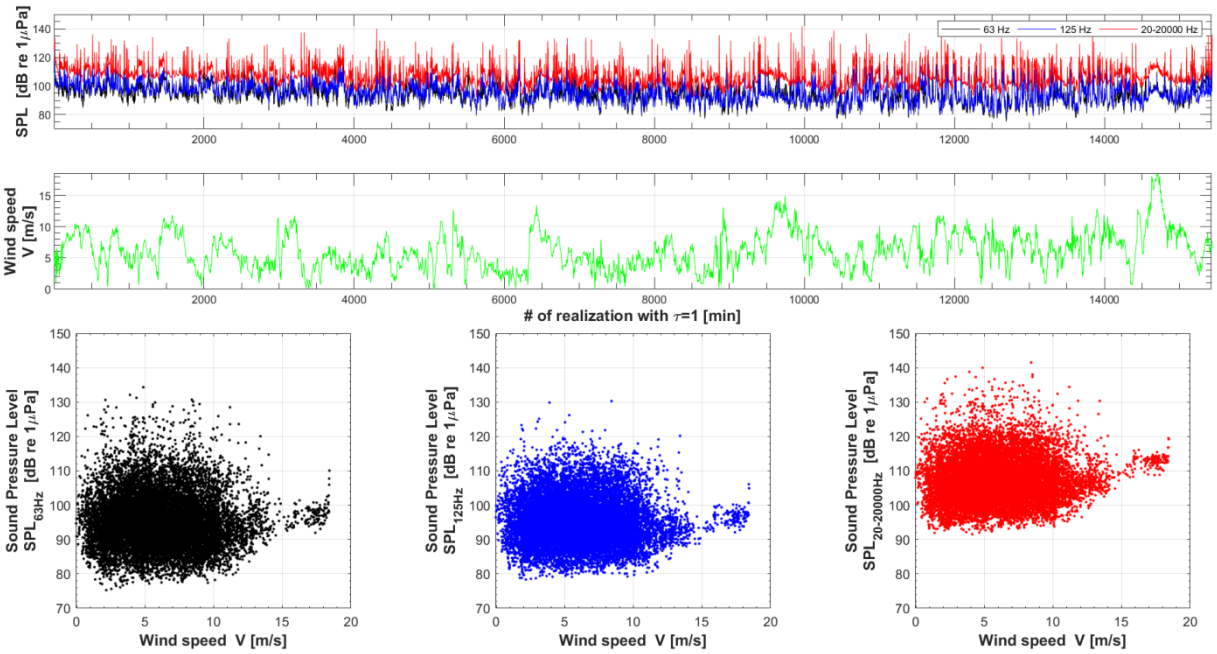


Figure 2.133. Survey station H_1. The time series of the sound pressure levels (SPL) [dB re 1 µPa] in 1/3-octave bands of 63 Hz and 125 Hz (black and blue curves, respectively) and in the 20–20,000 Hz broadband (red curve) – upper panel. The time series of wind velocity V [m·s^{-1}] – middle panel. The dependence of sound pressure levels $SPL_{63\ Hz}$, $SPL_{125\ Hz}$, and $SPL_{20–20\,000\ Hz}$ on the wind velocity – bottom panel. Survey session no. 3 (24.04.2023–12.08.2023)

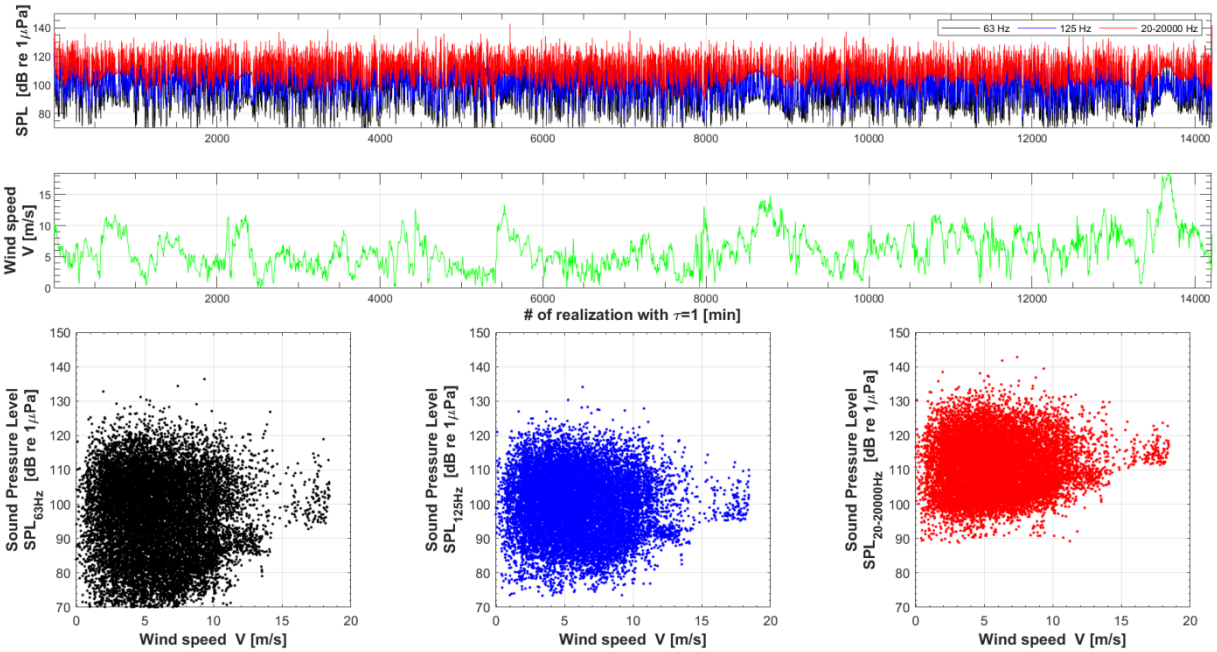


Figure 2.134. Survey station H_3. The time series of the sound pressure levels (SPL) [dB re 1 µPa] in 1/3-octave bands of 63 Hz and 125 Hz (black and blue curves, respectively) and in the 20–20,000 Hz broadband (red curve) – upper panel. The time series of wind velocity V [m·s^{-1}] – middle panel. The dependence of sound pressure levels $SPL_{63\ Hz}$, $SPL_{125\ Hz}$, and $SPL_{20–20\,000\ Hz}$ on the wind velocity – bottom panel. Survey session no. 3 (30.04.2023–12.08.2023)

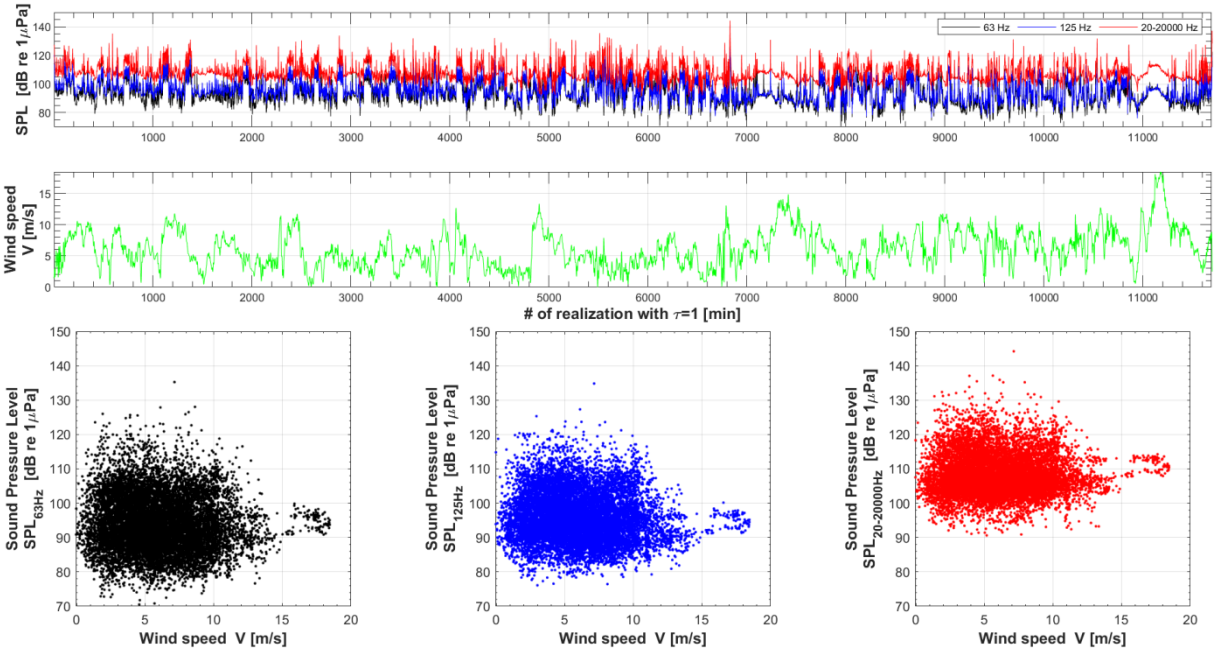


Figure 2.135. Survey station H_4. The time series of the sound pressure levels (SPL) [dB re 1 µPa] in 1/3-octave bands of 63 Hz and 125 Hz (black and blue curves, respectively) and in the 20–20,000 Hz broadband (red curve) – upper panel. The time series of wind velocity V [m·s^{-1}] – middle panel. The dependence of sound pressure levels $SPL_{63\ Hz}$, $SPL_{125\ Hz}$, and $SPL_{20–20\,000\ Hz}$ on the wind velocity – bottom panel. Survey session no. 3 (24.04.2023–12.08.2023)

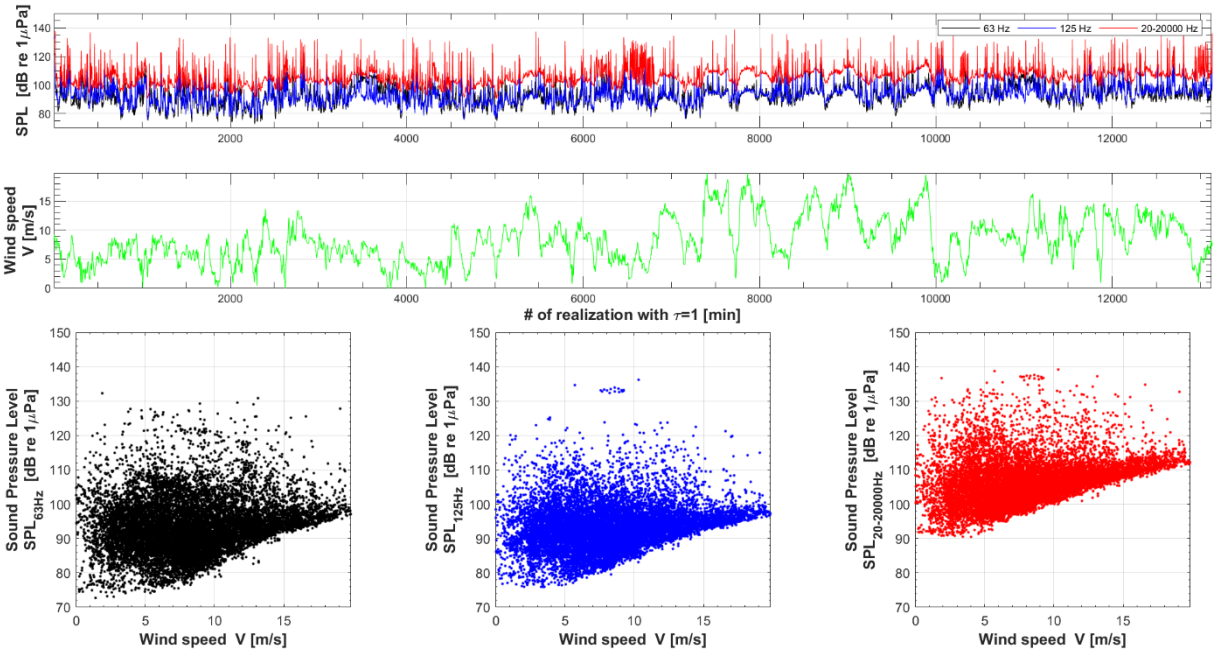


Figure 2.136. Survey station H_1. The time series of the sound pressure levels (SPL) [dB re 1 µPa] in 1/3-octave bands of 63 Hz and 125 Hz (black and blue curves, respectively) and in the 20–20,000 Hz broadband (red curve) – upper panel. The time series of wind velocity V [m·s^{-1}] – middle panel. The dependence of sound pressure levels $SPL_{63\ Hz}$, $SPL_{125\ Hz}$, and $SPL_{20–20\,000\ Hz}$ on the wind velocity – bottom panel. Survey session no. 4 (13.08.2023–12.11.2023)

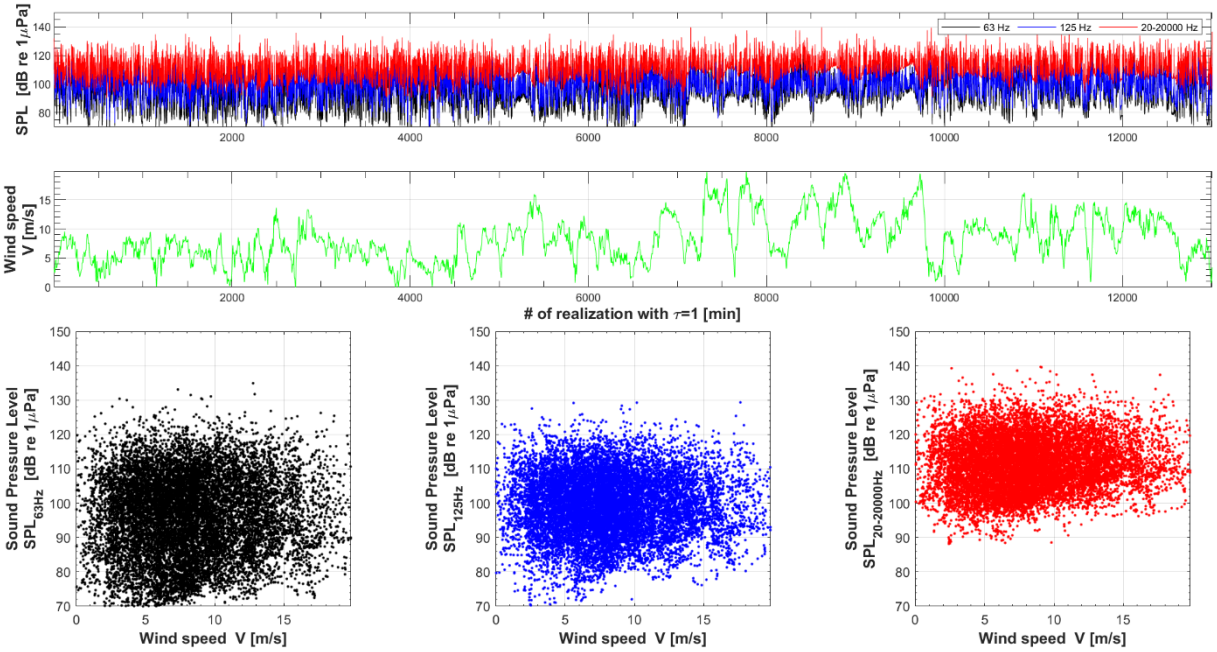


Figure 2.137. Survey station H_3. The time series of the sound pressure levels (SPL) [dB re 1 µPa] in 1/3-octave bands of 63 Hz and 125 Hz (black and blue curves, respectively) and in the 20–20,000 Hz broadband (red curve) – upper panel. The time series of wind velocity V [m·s^{-1}] – middle panel. The dependence of sound pressure levels $SPL_{63\ Hz}$, $SPL_{125\ Hz}$, and $SPL_{20–20\,000\ Hz}$ on the wind velocity – bottom panel. Survey session no. 4 (12.08.2023–13.11.2023)

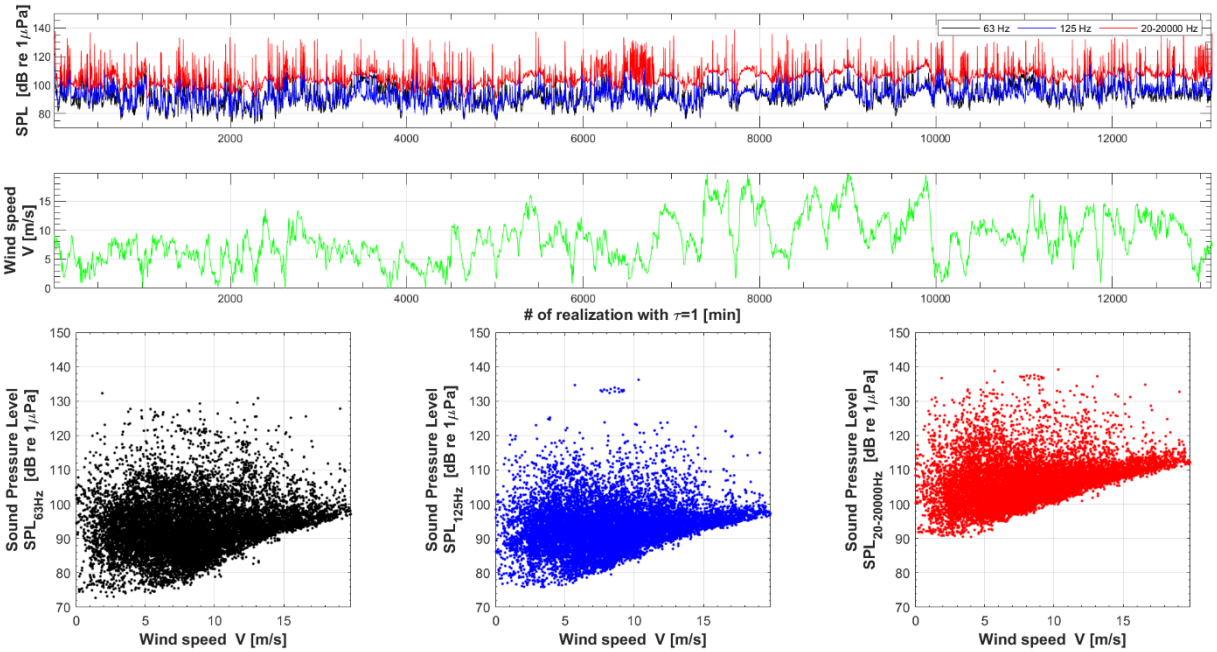


Figure 2.138. Survey station H_4. The time series of the sound pressure levels (SPL) [dB re 1 µPa] in 1/3-octave bands of 63 Hz and 125 Hz (black and blue curves, respectively) and in the 20–20,000 Hz broadband (red curve) – upper panel. The time series of wind velocity V [m·s^{-1}] – middle panel. The dependence of sound pressure levels $SPL_{63\ Hz}$, $SPL_{125\ Hz}$, and $SPL_{20–20\,000\ Hz}$ on the wind velocity – bottom panel. Survey session no. 4 (13.08.2023–12.11.2023)

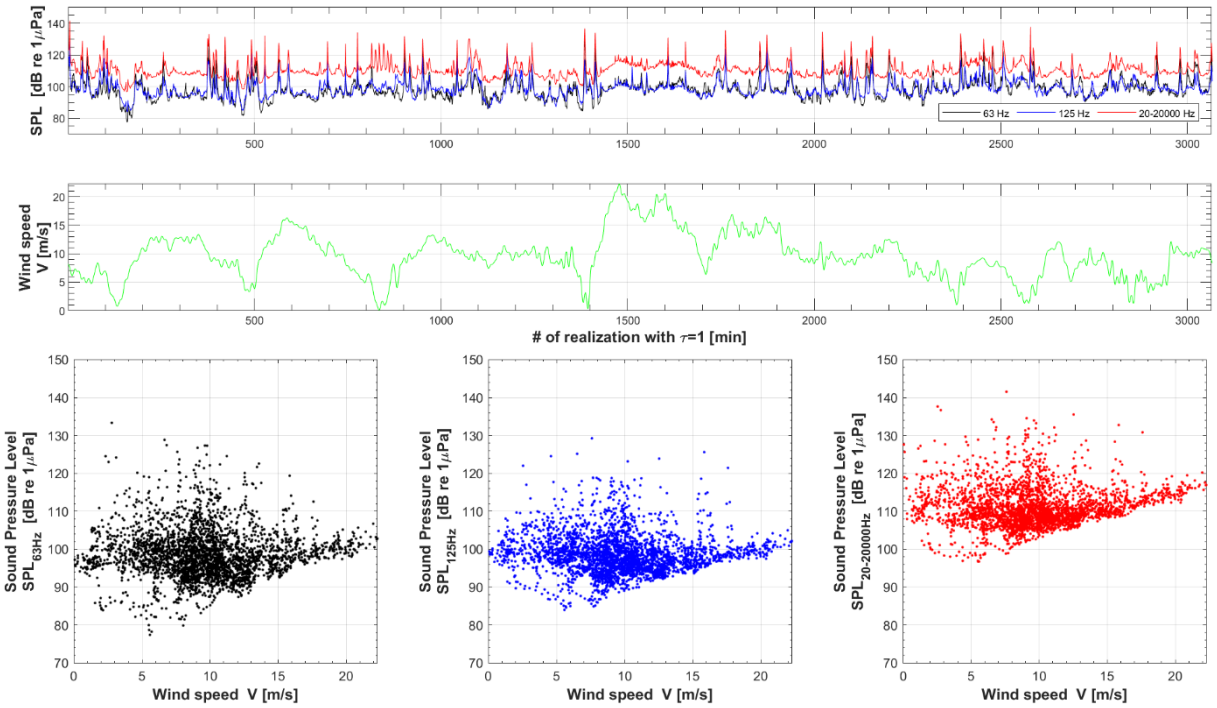


Figure 2.139. Survey station H_1 The time series of the sound pressure levels (SPL) [dB re 1 μPa] in 1/3-octave bands of 63 Hz and 125 Hz (black and blue curves, respectively) and in the 20–20,000 Hz broadband (red curve) – upper panel. The time series of wind velocity V [m·s^{-1}] – middle panel. The dependence of sound pressure levels $SPL_{63\ Hz}$, $SPL_{125\ Hz}$, and $SPL_{20–20\,000\ Hz}$ on the wind velocity – bottom panel. Survey session no. 5 (12.11.2023–03.12.2023)

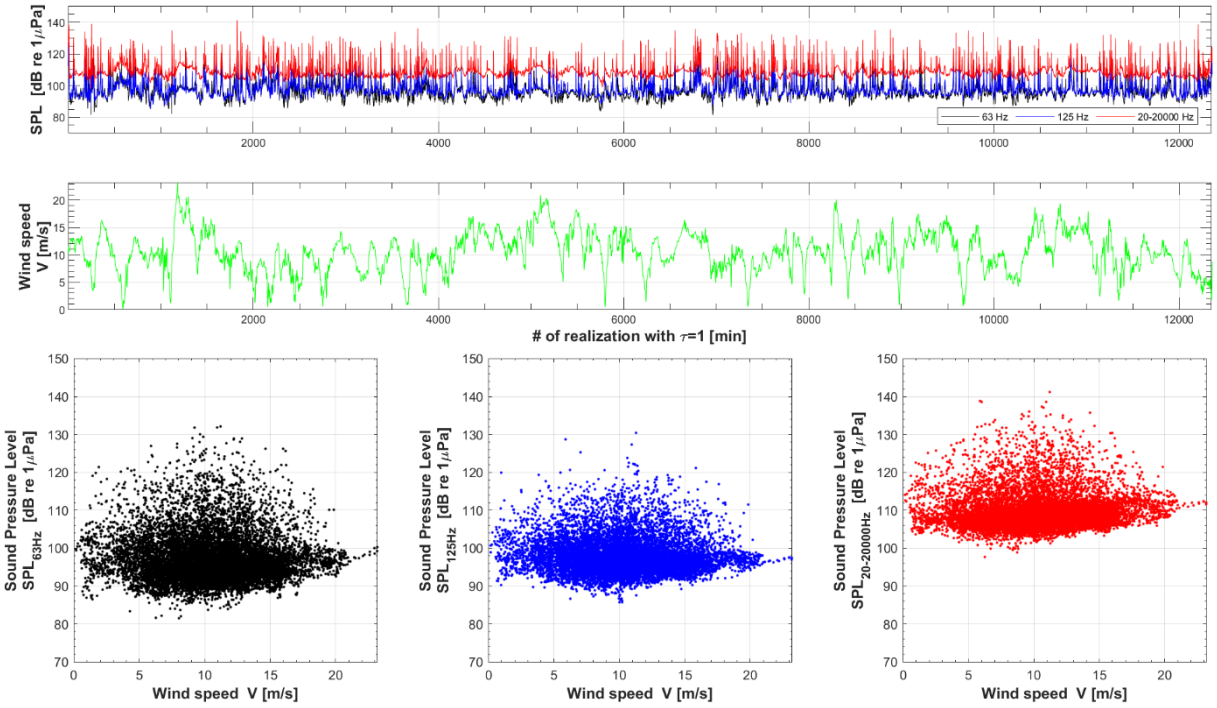


Figure 2.140. Survey station H_2. The time series of the sound pressure levels (SPL) [dB re 1 μPa] in 1/3-octave bands of 63 Hz and 125 Hz (black and blue curves, respectively) and in the 20–20,000 Hz broadband (red curve) – upper panel. The time series of wind velocity V [m·s^{-1}] – middle panel. The dependence of sound pressure levels $SPL_{63\ Hz}$, $SPL_{125\ Hz}$, and $SPL_{20–20\,000\ Hz}$ on the wind velocity – bottom panel. Survey session no. 5 (12.11.2023–15.02.2024)

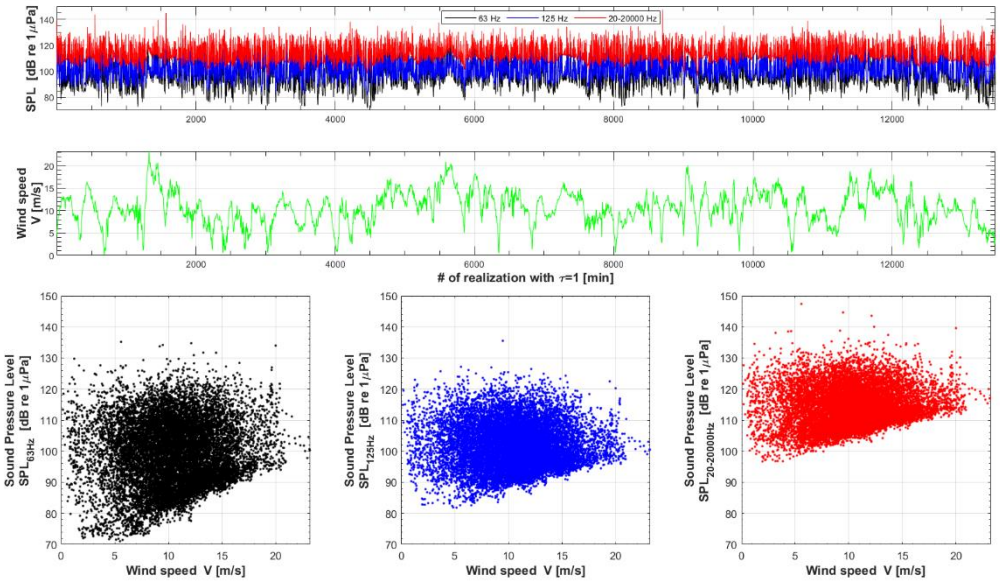


Figure 2.141. Survey station H_3. The time series of the sound pressure levels (SPL) [dB re 1 µPa] in 1/3-octave bands of 63 Hz and 125 Hz (black and blue curves, respectively) and in the 20–20,000 Hz broadband (red curve) – upper panel. The time series of wind velocity V [m·s^{-1}] – middle panel. The dependence of sound pressure levels $SPL_{63\ Hz}$, $SPL_{125\ Hx}$, and $SPL_{20–20\,000\ Hz}$ on the wind velocity – bottom panel. Survey session no. 5 (12.11.2023–15.02.2024)

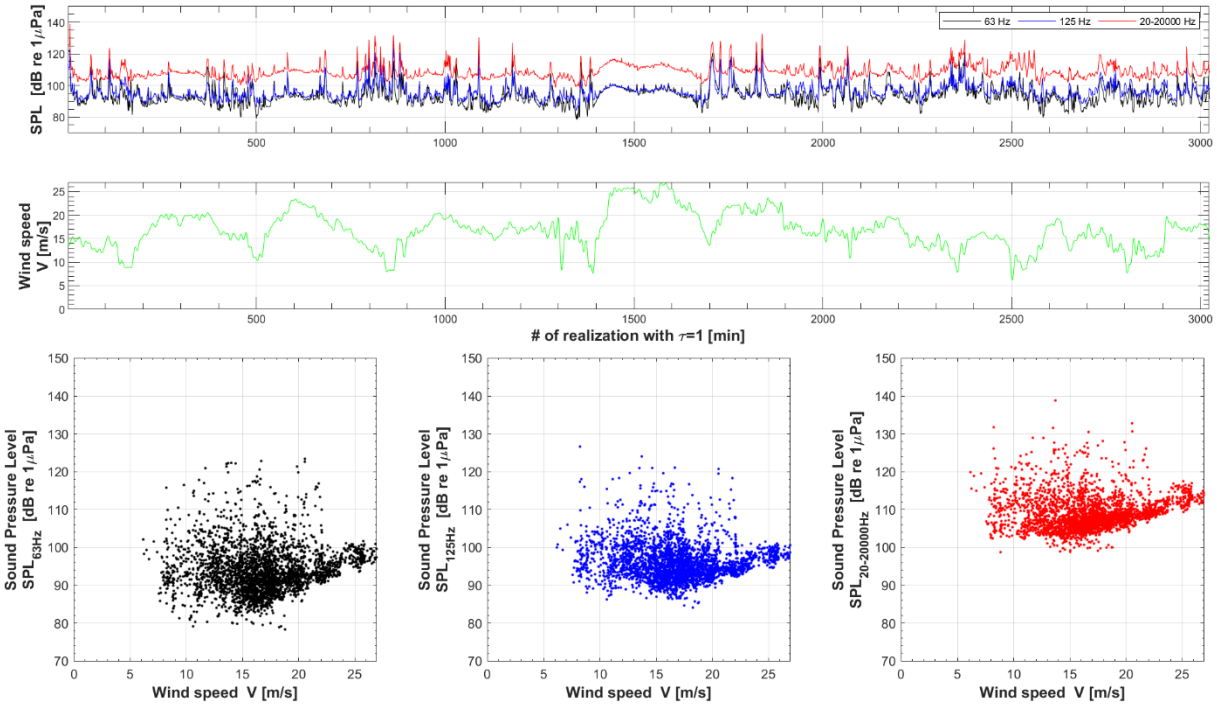


Figure 2.142. Survey station H_4. The time series of the sound pressure levels (SPL) [dB re 1 µPa] in 1/3-octave bands of 63 Hz and 125 Hz (black and blue curves, respectively) and in the 20–20,000 Hz broadband (red curve) – upper panel. The time series of wind velocity V [m·s^{-1}] – middle panel. The dependence of sound pressure levels $SPL_{63\ Hz}$, $SPL_{125\ Hz}$, and $SPL_{20–20\,000\ Hz}$ on the wind velocity – bottom panel. Survey session no. 5 (12.11.2023–03.12.2023)

2.5.6 Summary of results and conclusions

The results of the acoustic background monitoring conducted in the survey area from December 2022 to November 2023 indicate that the underwater ambient noise levels (and their dynamic ranges), have values characteristic for the southern Baltic Sea (Lisimenka, 2007; Klusek and Lisimenka, 2016; Mustonen et al., 2019).

The ambient noise levels vary over time, depending on the sound propagation conditions changing seasonally in the Baltic Sea, which are, in turn, dependent on the thermohaline conditions. The observed ambient noise levels show higher values under favourable sound propagation conditions characteristic for the winter season (survey session no. 2) with positive sound refraction (directed towards the sea surface) compared to the unfavourable sound propagation conditions characteristic for the summer season (survey session no.2) with negative refraction (directed towards the seabed). This is consistent with the previous results of numerical simulations (Klusek 1977a,b; 2000), as well as the results of *in situ* observations carried out in the Baltic Sea in the 1980s (Wille and Geyer, 1984; Wagstaff and Newcomb, 1987) and currently (The BIAS project, 2012–2015; Klusek and Lisimenka, 2016; Mustonen et al., 2019).

A comparative analysis of the ambient noise levels calculated in a broadband frequency range (20–20,000 Hz) for different seasons showed that in the winter season (survey session no. 2), the ambient noise levels are higher by several decibels (2–7 dB) than in the other seasons [Table 2.55–Table 2.58]. For example, at survey station H_1, the median SPL values obtained in the analysed broadband frequency range in the winter season $SPL_{20–20\,000\,Hz}$ = 113.0 dB re 1µPa are higher by 7 dB compared to the SPL values obtained in the summer season $SPL_{20–20\,000\,Hz}$ = 106.0 dB re 1µPa (during survey sessions no. 2 and 4, respectively).

In general, the time series of the sound pressure level SPL show significant fluctuations in the ambient noise level (single peaks), reaching values in the order of 20–25 dB against the background of natural noise. This can be interpreted as a significant contribution of the anthropogenic component related primarily to vessel traffic and, occasionally, to the emission of low-frequency sounds during seismoacoustic surveys of the seabed [e.g. Figure 2.121, upper panel]. To estimate roughly the frequency of anthropogenic event occurrence, a simple algorithm was developed to find samples of broadband sound pressure level SPL (20 Hz–20 kHz) exceeding the threshold of "SPL_{median} + 3 dB". In general (for all seasons) the result of such assessment showed that sounds of anthropogenic origin occur for up to approximately 1/3 of the observation time.

It should be noted that due to the significant contribution of the anthropogenic component to the ambient noise field, regardless of the season, the sound pressure level SPL is practically permanently above the hearing threshold of the clupeids [Figure 2.143, dark blue curve], amounting to approximately 75–80 dB re 1 µPa in the frequency range below 1000 Hz (Enger, 1967; Andersson, 2011). In the case of the Baltic Sea, this applies to herring (*Clupea harengus*) and sprat (*Sprattus sprattus*) – these species are among the most noise-sensitive fishes, in which the response to sound manifests itself in the low-frequency range from several dozen Hz to 3–4 kHz (with the highest sensitivity observed of the level of approximately 100 Hz). This may also partially apply to cod, which has limited hearing in the frequency range above 500 Hz or so.

It is also probable that some sounds could be heard by seals, which show better audible perception in the low-frequency range in comparison to harbour porpoises.

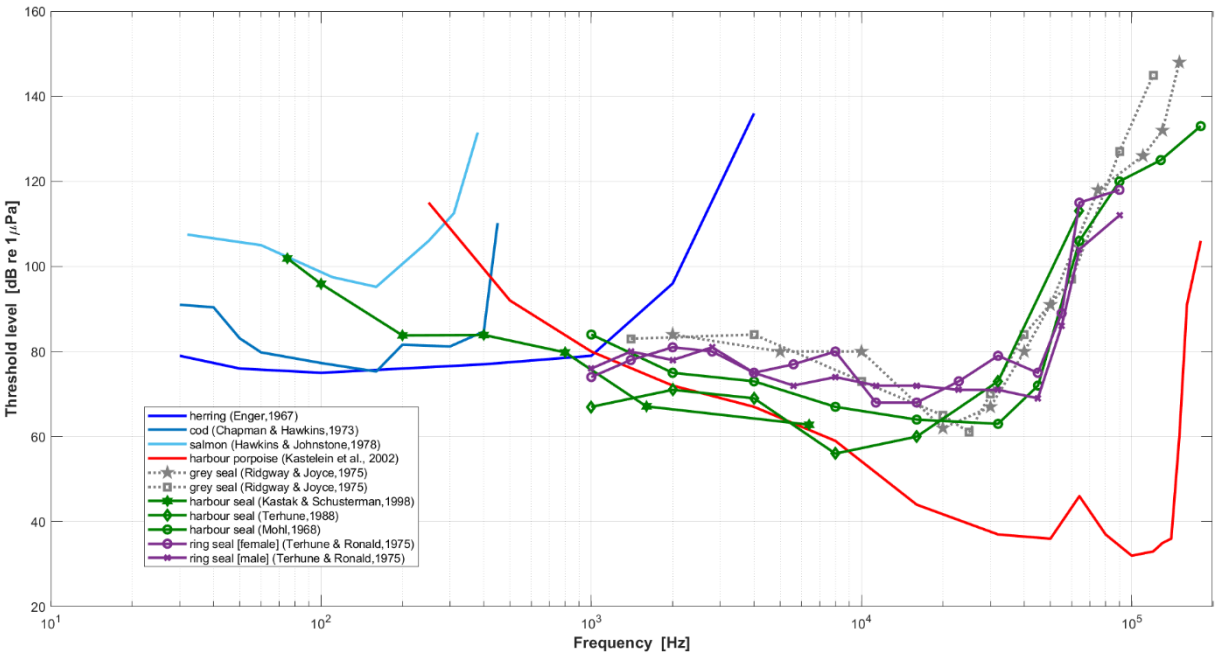


Figure 2.143. The hearing thresholds of selected fish and mammal species occurring in the Baltic Sea [Source: herring (Enger, 1967); cod (Chapman and Hawkins, 1973); salmon (Hawkins and Johnstone, 1978); harbour porpoise (Kastelein et al., 2002); grey seal (Ridgway and Joyce, 1975); harbour seal (Kastak and Schusterman, 1998; Terhune, 1988; Møhl, 1968); ringed seal (Terhune and Ronald, 1975)]

In principle, the analysis of the noise-wind dependence (SPL vs wind speed) in the analysed 1/3-octave bands of 63 Hz and 125 Hz reveal lack of correlation [Figure 2.127–Figure 2.138]. The lack of increase in SPL with increasing wind speed in the low frequency range is related to primarily the contribution of the anthropogenic component (noise from vessels, operation of seismoacoustic survey devices) compared to noise of hydrodynamic origin (especially for low sea states). In turn, the noise-wind correlation is relatively stronger in the broadband frequency range 20–20,000 Hz. This results from the fact that in higher frequency bands (of over approximately 1–2 kHz), the ambient noise from the local sound sources located on the sea surface (from acoustically active air bubbles generated by the wave breaking) becomes dominant.

2.5.7 Shortcomings and gaps in the state-of-the-art

Despite the fact that, in recent years, the adverse impact of anthropogenic noise on marine animals, primarily on mammals, fish, and invertebrates (Shannon et al., 2016), as well as on zooplankton (McCauley et al., 2017) has been recognised and documented in the scientific literature, there are still no threshold values for the ambient noise level corresponding to the Good Environmental Status (GES).

Highly intensive underwater noise of anthropogenic origin, especially noise in the low-frequency range, has an adverse environmental impact on the following aspects in relation to marine organisms:

- development – including underdevelopment/body deformation, higher egg and/or juvenile mortality, and decreased growth rate (Aguilar de Soto et al., 2013; Nedelec et al., 2014; 2015);
- anatomy – hearing loss, extensive internal trauma, and disorientation (Hastings et al., 1996; McCauley et al., 2003; André et al., 2011; Solé et al., 2017);
- physiology – including an increase in stress hormones, metabolism, and oxygen consumption (Wysocki et al., 2006; Anderson et al., 2011; Nichols et al., 2015; Spiga et al., 2016);

- behaviour – e.g. increased aggression, decreased defensive behaviour and feeding habits, and distraction (Kastelein et al., 2008; Fewtrell and McCauley, 2012; La Manna et al., 2016; Nedelec et al., 2017);
- masking (acoustic jamming) of echolocation sounds used by marine animals for their fundamental life functions (amongst others Thomsen et al., 2006; Codarin et al., 2009).

In the literature, there are also no defined reliable indicators of individual harmful pressures and the threshold values of the noise level determining the relevant negative reactions of marine organisms to sound. This applies to behavioural reactions (e.g. escape) as well as physiological (e.g. pain or, in extreme cases, lethal impact). There are also no long-term *in situ* studies conducted to determine the spatial scale of various harmful pressures under the most realistic scenarios.

3 BIOTIC ELEMENTS IN MARINE SURVEYS – THE BASIC SCOPE OF SURVEYS CONTRACTED

3.1 PHYTOBENTHOS

3.1.1 Non-specialist summary

The phytobenthos surveys in the survey area were performed in June 2023. Seabed filming was performed with an underwater Falcon ROV remotely operated from aboard a vessel, along two transects, each at least 100 m long.

In the survey area, the inspection was carried out along two transects on a stony seabed within the depth range from 24.4 to 27.5 m. No macroalgae were found. The analysis of the video footage showed that the boulders and cobbles present on the seabed were only covered with dense colonies of mussels, i.e. the bivalves of the *Mytilus trossulus* species.

This element will not determine the feasibility of the proposed project and will not affect the environmental impact assessment.

3.1.2 Spatial scope of the surveys

The spatial range of phytobenthos surveys was limited to the survey area covering the Baltica-1 OWF construction area, which is the area of construction of WTGs, OSSs, and cable lines (area A) and the area of construction of cable lines (area B) together with a zone of no less than 1 NM in width measured from the boundary of area A [Figure 3.1].

3.1.3 Methodology

Based on the analysis of the literature and the data available on the depth range of phytobenthos in the Polish sea areas, it was determined that the maximum range of macroalgae occurrence (with the seabed coverage of at least 10%) on the hard bottom (e.g. boulders and cobbles) is approximately 22 m, while the maximum range of occurrence of plants rooted in the sandy seabed is 10 m (Kruk-Dowgiałło et al., 2011; Błeńska et al., 2014; Błeńska et al., 2015a and b; SEM 2002–2022; Michałek et al., 2020; Brzeska-Roszczyk and Kruk-Dowgiałło, 2017; Michałek et al., 2020; Brzeska-Roszczyk et al., 2021; Barańska et al., 2020). In the deeper parts of the Polish zone of the Baltic Sea, at depths between 20 and 26 m, only single, small specimens of macroalgae occur (Błeńska et al., 2014; Błeńska et al., 2015a and b; Brzeska-Roszczyk et al., 2021). Taking the above conditions into account, the transects for video inspection were selected in the shallowest regions of the survey area where stony seabed occurred (2 transects to confirm the occurrence of macroalgae) [Figure 3.1].

Table 3.1 contains the coordinates of the transects along which the seabed was inspected for phytobenthos occurrence.

The seabed filming was performed with the Falcon ROV operated remotely from aboard a vessel, along two transects, each at least 100 m long. The surveys were conducted by a phytobenthos specialist who supervised the process of seabed filming and by qualified ROV operators who were responsible for its maintenance.

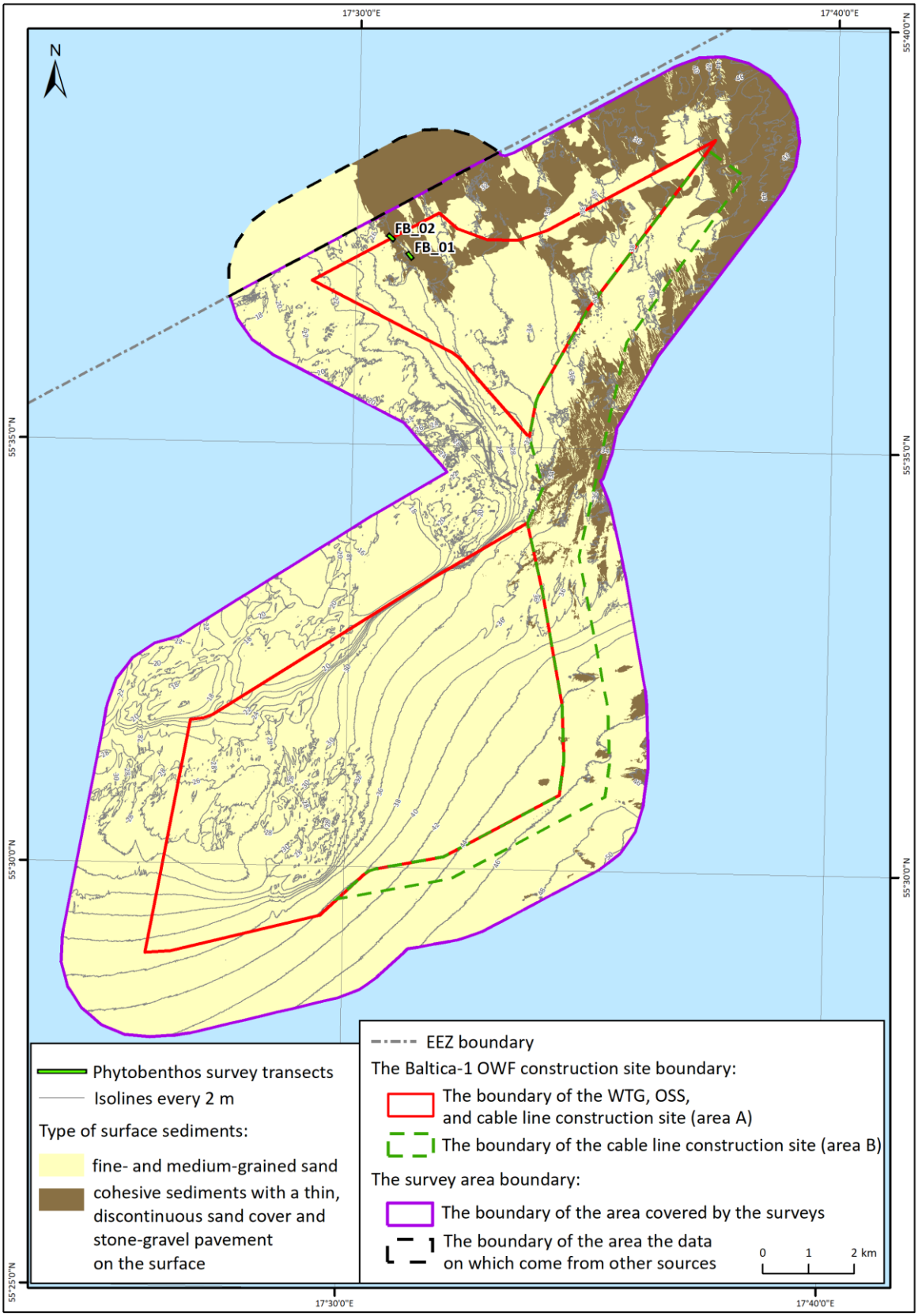


Figure 3.1. The locations of the survey transects within the survey area on the surface sediment types basemap

Table 3.1. Coordinates of the transects along which the seabed inspection was conducted to establish the phytobenthos occurrence within the survey area

Transect	Two-dimensional Cartesian coordinate system PL-1992 [m]			
	Transect beginning		Transect end	
	y	x	y	x
FB_01	406766.76	862976.39	406701.55	863062.67
FB_02	406360.84	863381.71	406278.12	863454.06

Video documentation obtained along each transect was analysed in terms of:

- seabed description (sediment type);
- identification of the areas of phytobenthos occurrence;
- assessment of the seabed coverage with phytobenthos [%];
- identification of taxonomic composition to the lowest possible rank.

Photo-documentation of the seabed (freeze-frames) was also prepared.

Due to the low seabed coverage with phytobenthos (below 10%), no survey stations were established for phytobenthos sampling in the survey area.

3.1.4 Activities performed

The activities carried out as part of the phytobenthos surveys are compiled in Table 3.2. The environmental surveys of phytobenthos in the survey area involving seabed filming along the transects were carried out on 18 June 2023 from aboard the Northern Karoline vessel. The analysis of video footage was conducted in August 2023.

Table 3.2. List of activities conducted as part of phytobenthos surveys in the survey area

Type of work	Scope of work	Date	Result
Preparations for surveys	Analysis of sonar and bathymetric data for the areas	13.06.2023	2 transects were delineated on the stony seabed
Environmental surveys	Video inspections of the seabed along the transects	16–18.06.2023	2 video footages from 2 transects on the stony seabed
Analyses of the video footage	Identification of phytobenthos occurrence locations along with an assessment of the degree of seabed coverage with phytobenthos, macroscopic description of the seabed	02–29.08.2023	Characteristics of the seabed and the phytobenthos on the transects

3.1.5 Results

The seabed filming for phytobenthos occurrence was performed within the depth range from 24.4 to 27.5 m, i.e. in the shallowest area of the stony seabed, which was located in the north-western part of the survey area [Figure 3.1, Table 3.3]. The inspection performed with an ROV showed no subsea vegetation along both transects. Boulders and cobbles lying on the stony seabed were covered with dense colonies of mussels, i.e. the bivalves of the *Mytilus trossulus* species [Table 3.3, Figure 3.2, Figure 3.3]. The results of the video footage analysis are included in Table 3.3.

Table 3.3. Characteristics of the transects along which the seabed inspection was conducted to establish the phytobenthos occurrence in the survey area

Transect	Video recording date	Transect depth [m]		Transect length [m]	Description of the seabed along the transect [%]	Phytobenthos coverage of the seabed along the transect [%]
		Initial	Final			
FB_01	18.06.2023	27.5	27.0	108	Hard bottom (boulders and cobbles covered with mussels) 95% Sandy seabed 5%	0
FB_02	18.06.2023	24.4	24.5	109	Hard bottom (boulders and cobbles covered with mussels) 95% Sandy seabed 5%	0

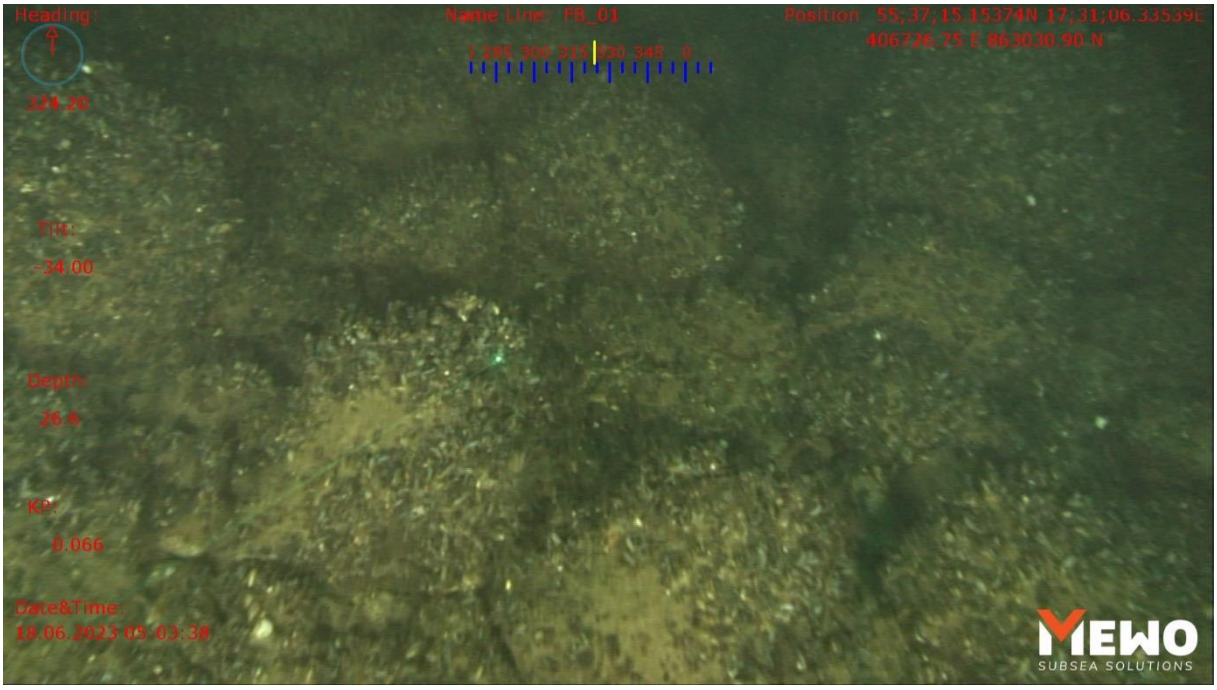


Figure 3.2. Image of the stony seabed along transect FB_01 in the survey area

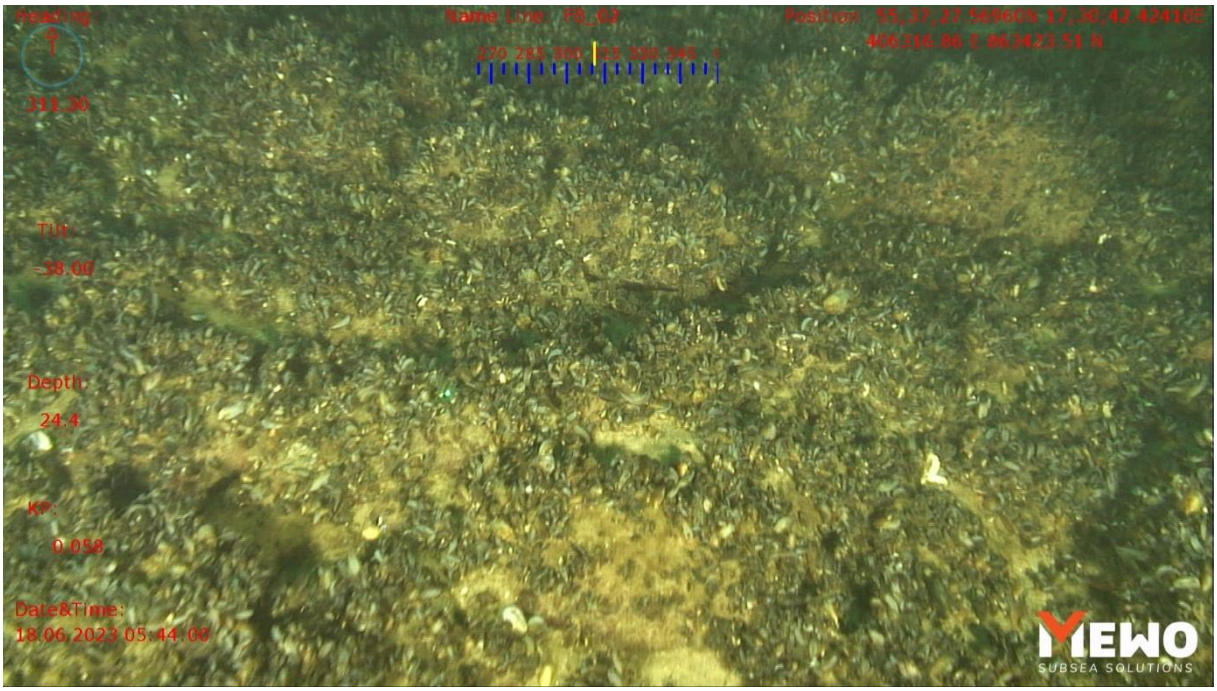


Figure 3.3. Image of the stony seabed along transect FB_02 in the survey area

3.1.6 Summary of results and conclusions

The environmental surveys of phytobenthos in the survey area were carried out in June 2023, along two transects on a stony seabed within the depth range from 24.4 to 27.5 m. No macroalgae were found within the survey area. The inspection carried out using an ROV showed that the boulders and cobbles on the seabed were covered only with dense colonies of mussels, i.e. the bivalves of the *Mytilus trossulus* species.

The stony seabed, which may constitute a substrate for the development of underwater vegetation, is located at depths beyond the range of phytobenthos occurrence. Consequently, this element will not determine the feasibility of the proposed project and will not affect the environmental impact assessment.

3.1.7 Shortcomings and gaps in the state-of-the-art

No technological shortcomings nor gaps in the state of the art were found regarding the phytobenthos surveys.

3.2 MACROZOOBENTHOS

3.2.1 Non-specialist summary

In 2023, field studies of macrozoobenthos were carried out in the survey area. The field surveys included collecting macrozoobenthos samples on the soft bottom (mainly sandy and sandy-gravelly seabed) using a van Veen grab sampler as well as collecting periphytic fauna and associated fauna complex on the hard (stony) bottom using a Cougar ROV equipped with a pipe for collecting macrozoobenthos from a specified surface. A total of 168 samples of macrozoobenthos were collected in the survey area.

Having completed the laboratory tests of the macrozoobenthos samples collected, the characteristics of the survey area were prepared with the results presented taking into account the division into soft bottom and hard bottom.

On the soft bottom in the survey area, where sampling was conducted in the depth range of 14.7–49.5 m, the occurrence of 29 macrozoobenthos taxa was confirmed. Commonly found there were the psammophilous polychaete *Pygospio elegans* which dominated the total abundance structure of this macrozoobenthos community, and one bivalve taxon, the Baltic clam *Macoma balthica,* which dominated in terms of biomass. The average abundance of the macrozoobenthos from the samples analysed was 2388±1815 ind.·m^{-2}, while the average biomass was 26.8±38.6 g WW·m^{-2}. The presence of the following four bivalve species was confirmed in the soft bottom samples: the Baltic clam *Macoma balthica*, the bay mussel *Mytilus trossulus*, the soft-shell clam *Mya arenaria* and the lagoon cockle *Cerastoderma glaucum*. In the case of *Macoma balthica*, the most numerous were the young individuals (1–5 mm), while in terms of biomass, the 11 to 15 mm long individuals dominated (over 1800 g WW·m^{-2}). The average value of index B was 3.00±0.62, which indicates a moderate status of the seabed fauna community inhabiting the area discussed. Only seven taxa were found in the two analysed macrozoobenthos samples collected from the hard bottom within the depth range of 26.3–38.6 m occurring in points in the northern part of the survey area. The bay mussel *Mytilus trossulus* dominated at both stations in terms of abundance and biomass. Juvenile bay mussels from the 1–5 mm size class were by far the most abundant. At one station, the quality status of this macrozoobenthos community was classified as good and at the other station as poor.

3.2.2 Spatial scope of the surveys

The spatial range of macrozoobenthos surveys was limited to the survey area covering the Baltica-1 OWF construction area, which is the area of construction of WTGs, OSSs, and cable lines (area A) and the area of construction of cable lines (area B) together with a zone of no less than 1 NM in width measured from the boundary of area A.

The distribution of the macrozoobenthos sampling stations in the survey area is presented in Figure 3.4.

3.2.3 Methodology

The survey stations for macrozoobenthos sampling were established both on the soft bottom and on the hard bottom within the survey area. The macrozoobenthos stations were established after the abiotic conditions had been identified, in accordance with the survey strategy allowing for the delimitation of seabed habitats and the type of seabed sediments, on the basis of a map of surface sediments and a bathymetric map of the survey area.

Therefore, 168 macrozoobenthos samples were collected on the soft bottom in the survey area (excluding 7 planned stations located in the buffer zone on the Swedish waters, where an exploration permit is awaited for the surveys to be conducted in the Swedish EEZ). An average of one survey station was designated per one square kilometre of the survey area. In total, 168 macrozoobenthos samples were collected on the soft bottom of the survey area [Figure 3.4].

Quantitative macrozoobenthos samples from the soft bottom (sand, gravel) were collected using a standard van Veen grab sampler with a sampling surface area of 0.1 m^2 and a mass of approximately 60 kg. In the case of an incorrectly collected sample (buckets open, stone between the jaws, buckets empty), sampling at a given station was repeated up to two times. After the second failed sampling

attempt, it was allowed to discontinue sampling at the relevant station. The habitat approach adopted in the surveys in question takes into account the possibility that a lower number of samples collected than the one assumed in the plan (if sampling at a given station is technically unfeasible) provides a sufficient amount of biological material to conduct an inventory survey of the qualitative and quantitative structure of the habitat surveyed. At each survey station, one macrozoobenthos sample was collected and rinsed on board a vessel using a washer and a bucket with a sieve of 1 mm mesh size, and then transferred to the marked containers and preserved with a 4% formaldehyde solution (Osowiecki and Błeńska, 2020).

In the survey area, survey stations were also designated on the hard bottom (boulders, pebbles, stone pavement). Samples of periphytic fauna and associated fauna complex were collected at two stations. The survey stations where macrozoobenthos samples were collected on the hard bottom are presented in Figure 3.4.

A remotely operated vehicle ROV Cougar fitted with a pipe for collecting macrozoobenthos from a specified, i.e.153.86 cm^2 hard substrate surface was used to collect periphytic fauna and associated fauna complex (Nowak et al., 2017). Videos of the seabed at the locations of sampling were also recorded. Next, the sample collected was transferred to the marked containers and preserved with a 4% formaldehyde solution.

The macrozoobenthos sampling on the soft and hard bottom was conducted according to the method described in the *Manual for Marine Monitoring in the COMBINE Programme* – HELCOM (2021). *Part C. Programme for monitoring of eutrophication and its effects. Annex C-8. Soft-bottom macrozoobenthos*, as well as in *Przewodnik do monitoringu elementów biologicznych i klasyfikacji stanu ekologicznego wód powierzchniowych. Aktualizacja metod. Makrozoobentos w wodach przejściowych i przybrzeżnych* (Manual for monitoring of biological elements and classification of the ecological status of surface waters. Update of methods. Macrozoobenthos in transitional and near-shore waters) (Osowiecki and Błeńska, 2020).

The macrozoobenthos samples collected underwent laboratory analyses which included:

- qualitative analysis of the species composition. For taxonomic identification, names were used in accordance with the current nomenclature in the World Register of Marine Species (WoRMS, www.marinespecies.org);
- abundance analysis, involving counts of individuals of all the taxa identified except for the species of Gymnolaemata, Thecostraca, and Hydrozoa;
- analysis of the biomass expressed as grams of wet weight per square metre (g $WW \cdot m^{-2}$; with an accuracy of 0.001 g);
- measurement of bivalve lengths in 0.5 cm ranges and biomasses in individual intervals.

The methods for laboratory analyses of macrozoobenthos samples are based on the guidelines contained in the *Manual for Marine Monitoring in the COMBINE Programme of HELCOM* – HELCOM (2021). *Part C. Programme for monitoring of eutrophication and its effects. Annex C-8. Soft-bottom macrozoobenthos*, as well as in *Przewodnik do monitoringu elementów biologicznych i klasyfikacji stanu ekologicznego wód powierzchniowych. Aktualizacja metod. Makrozoobentos w wodach przejściowych i przybrzeżnych* (Manual for monitoring of biological elements and classification of the ecological status of surface waters. Update of methods. Macrozoobenthos in transitional and near-shore waters) (Osowiecki and Błeńska, 2020).

The data were processed regarding the following indices:

- constancy index C (Odum 1982, Trojan 1980) – quantitative structure of the macrozoobenthos communities identified;
- dominance index D (Odum 1982, Trojan 1980) – quantitative structure of the macrozoobenthos communities identified;
- multimetric index B (Osowiecki et al., 2012) – assessment of the ecological quality of the survey area based on macrozoobenthos (soft bottom);
- Index of typical species presence (TSP) on the hard bottom (CIEP, 2018) – assessment of the ecological quality of the survey area on the basis of macrozoobenthos (hard bottom).

Multimetric index B

$$B = \frac{\sum_{i=1}^{3}(w_i Q_i sn_i)}{\sum_{i=1}^{3} D_i} - log\left(1 + \sum_{i=1}^{3} D_i\right)$$

where:

w_i – weighting of dominance classes:
w_1 = 3 for dominance class D1 (proportion >10%);
w_2 = 2 for dominance class D2 (5% ≤ proportion ≤ 10%)
w_3 = 1 for dominance class D3 (proportion <5%);

D_i – number of taxa belonging to each dominance class D1, D2, D3;

$sn_i = \Sigma sens_i$

Index Q_i = 0 if D_i = 0; Q_i = 1 if $D_i \neq 0$

$sens_i$ – coefficient of sensitivity/tolerance of taxa to the stress caused by human pressure:
$Sens_i$ = 3 – sensitive taxa with a narrow range of tolerance, so-called clean seabed indicator species;
$Sens_i$ = 2 – intermediate taxa, the occurrence of which is not strictly correlated with the organic matter content of the seabed sediments;
$Sens_i$ = 1 – tolerant taxa, able to withstand significant organic matter content in the sediment.

In its algorithm, the multimetric index B (Osowiecki et al., 2012) includes the most relevant criteria for assessing the qualities of the community, i.e. the taxonomic diversity expressed in the number of taxa identified and the abundance of individuals representing individual taxa, as well as qualitative information on the ecological sensitivity/tolerance of individual taxa. The higher the taxonomic diversity, and the more even the proportion of sensitive taxa as well as the proportion of taxa in the total abundance structure, the higher the index values. The sensitivity of examples of zoobenthic taxa is presented in Table 3.4.

*Table 3.4. A compilation of examples of zoobenthos taxa sensitivity used to calculate index B**

Sensitive taxa ($Sens_i$ = 3)	**Intermediate taxa ($Sens_i$ = 2)**	**Tolerant taxa ($Sens_i$ = 1)**
Pygospio elegans	*Halicryptus spinulosus*	*Bylgides sarsi*
Bathyporeia pilosa	Nemertea	*Hediste diversicolor*
Heterotanais oerstedii	*Diastylis rathkei*	*Marenzelleria* spp.
Monoporeia affinis	*Gammarus salinus*	*Scoloplos armiger*
Pontoporeia femorata	*Gammarus zaddachi*	Oligochaeta
Cerastoderma glaucum	Hydrobiidae	*Gammarus tigrinus*

Sensitive taxa ($Sens_i$ = 3)	Intermediate taxa ($Sens_i$ = 2)	Tolerant taxa ($Sens_i$ = 1)
-	*Mytilus trossulus*	*Saduria entomon*
-	-	*Macoma balthica*
-	-	*Mya arenaria*

**taxa names from the World Register of Marine Species, http://www.marinespecies.org, accessed on: 2023.01.12*

The soft-bottom zoobenthos evaluation (ecological quality classification) assessed with index B is determined by a five-point scale compliant with the Regulation of the Minister of Infrastructure of 25 June 2021 on the classification of ecological status, ecological potential and chemical status and the method of classifying the status of surface water bodies and the environmental quality standards for priority substances (Journal of Laws of 2021, item 1475) and the classification used in the Water Framework Directive (WFD), according to which zoobenthos is one of the elements for assessing the seabed quality status [Table 3.5].

Table 3.5. The limit values of index B used for the assessment of the ecological status of the soft-bottom zoobenthos

B index value	Ecological quality class (Journal of Laws of 2021, item 1475)	Quality status of the soft-bottom zoobenthos communities according to WFD
< 1.91	V	Bad
≥1.91	IV	Poor
≥2.70	III	Moderate
≥3.18	II	Good
>3.72	I	Very good

For the evaluation of periphytic fauna and the associated fauna of the hard bottom, the methodology used in the assessment of habitat 1170 – Reefs for the purpose of the Habitats Directive (Council Directive 92/43/EEC of 21 May 1992) was adopted (CIEP 2018). The index is based on the survey of the presence of 4 zoobenthic taxa typical of a stony seabed. These are: *Amphibalanus improvisus*, *Einhornia crustulenta*, *Mytilus trossulus* and scuds of the genus Gammarus. In each sample analysed, the typical species presence (TSP) index may represent values corresponding to the number of typical species, i.e. from 0 to 4. Based on the TSP index, the status of the hard-bottom zoobenthos communities is determined [Table 3.6].

Table 3.6. The limit values of the TSP index used for the assessment of the quality status of the hard-bottom macrozoobenthos communities

Number of typical species	Quality status of zoobenthos communities on the hard bottom
0	Bad
1	Poor
2	Moderate
3	Good
4	Very good

The Kriging interpolation method in Surfer was used to create the distribution maps of macrozoobenthos abundance and biomass. In the case of the map for indicator B, the IDW (*Inverse Distance Weighted*) method was used in ArcGIS. The quantitative results of macrozoobenthos in terms of abundance, biomass, and ecological quality were extrapolated to the survey area onto a fragment

of the seabed located within the boundaries of Swedish marine waters, taking into account the fact that the habitat types there are generally the same as in the Polish sea areas, which are mainly sands and coarse-grained sediments of the infralittoral zone and sands and coarse-grained sediments of the circalittoral zone (https://www.emodnet-sea-bedhabitats.eu/). Therefore, the results from stations near the Swedish waters can be used to characterise the entire area of individual habitats and the macrozoobenthic communities inhabiting them.

3.2.4 Activities performed

In 2023, macrozoobenthos field surveys were conducted in the survey area, excluding a part of the buffer zone on the Swedish side (a permit to conduct surveys within the Swedish EEZ is awaited to be issued). Despite this, the characterisation of macrozoobenthos communities in Swedish waters was based on a review of available literature, EUSeaMap 2021 mapping data, and results from stations adjacent to Swedish waters based on their extrapolation to the above-mentioned region. The macrozoobenthos environmental surveys were conducted in accordance with the methodology and as-planned schedule. The surveys conducted in the period discussed included the collection of macrozoobenthos samples on the soft bottom using a van Veen grab sampler as well as the collection of periphytic fauna and associated fauna complex on the hard bottom using a Cougar ROV equipped with a pipe for collecting zoobenthos from a specified surface.

Summary information on the environmental surveys conducted in 2023 regarding macrozoobenthos is presented in Table 3.7 and in Figure 3.4.

Table 3.7. The list of fieldwork activities conducted as part of the macrozoobenthos surveys in the survey area in 2023 on soft bottom and hard bottom

Type of sediment	**Survey dates**	**Scope of environmental surveys**	**Total number of stations surveyed in the survey area [Number of samples collected/Number of unsuccessful attempts]**
Soft bottom	2023.05.28–2023.05.31	Macrozoobenthos sampling using a van Veen grab sampler	173 [166/7]
	2023.06.04–2023.06.06	Macrozoobenthos sampling using a van Veen grab sampler	2 [2/0]
Hard bottom	2023.06.16–2023.06.19	Periphytic fauna and associated fauna complex sampling using an ROV fitted with a pipe for collecting zoobenthos from a specified hard substrate surface	2 [2/0]

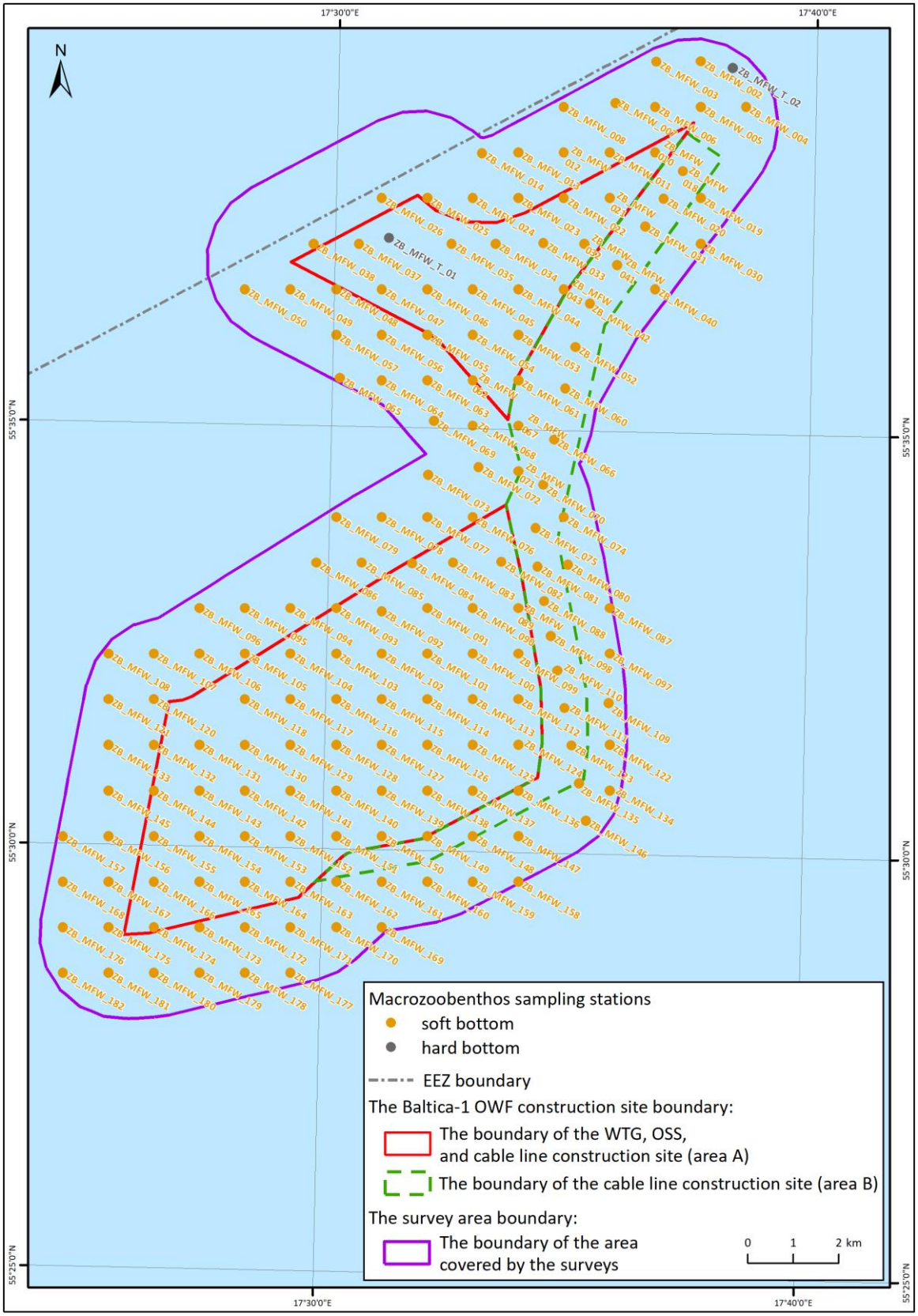


Figure 3.4. The location of the survey stations at which macrozoobenthos samples were collected in 2023 on soft bottom and hard bottom in the survey area

In total, 177 macrozoobenthos stations were surveyed during 3 environmental survey campaigns, while 170 macrozoobenthos samples were collected and analysed in accordance with the survey methodology and the schedule planned. The number of samples collected is representative and enabled the determination of the qualitative and quantitative structure of the soft-bottom and hard-bottom zoobenthos habitat following the strategy of including the delimitation of seabed habitats in the surveys.

Summary information on the laboratory tests conducted in 2023 is presented in Table 3.8.

Table 3.8. The list of activities conducted as part of the laboratory tests of macrozoobenthos sampled in the survey area in 2023

Period of laboratory tests	Scope of laboratory tests	Number of samples analysed from the soft bottom in the survey area	Number of samples analysed from the hard bottom in the survey area	Total number of samples tested
2023.06.12–2023.10.10	Taxonomic composition, abundance, biomass, measurements of bivalve lengths in size classes	168	2	170

3.2.5 Results

The results are presented with a division into soft bottom and hard bottom.

3.2.5.1 Soft bottom

3.2.5.1.1 Taxonomic composition

In the 168 macrozoobenthos samples from the soft bottom (sandy, gravelly) of the survey area, the presence of 29 taxa belonging to the Nemertea and Priapulida phyla and the 7 classes of Hydrozoa, Polychaeta, Clitellata, Malacostraca, Hexapoda, Gastropoda, and Bivalvia was confirmed [Table 3.9].

Table 3.9. The taxonomic composition in macrozoobenthos samples from the soft bottom in the survey area

No.	Taxon	Class	Phylum
1.	*Cordylophora caspia*	Hydrozoa	Cnidaria
2.	*Gonothyraea loveni*		
3.	Hydrozoa non det.		
4.	*Halicryptus spinulosus*	-	Priapulida
5.	Nemertea	-	Nemertea
6.	*Bylgides sarsi*	Polychaeta	Annelida
7.	*Hediste diversicolor*		
8.	*Marenzelleria* spp.		
9.	*Pygospio elegans*		
10.	Polychaeta non det.		
11.	Oligochaeta	Clitellata	Annelida
12.	*Bathyporeia pilosa*	Malacostraca	Arthropoda
13.	*Crangon crangon*		

No.	Taxon	Class	Phylum
14.	*Diastylis rathkei*		
15.	*Gammarus juvenes*		
16.	*Gammarus salinus*		
17.	*Gammarus zaddachi*		
18.	*Idotea balthica*		
19.	*Monoporeia affinis*		
20.	*Mysis mixta*		
21.	*Pontoporeia femorata*		
22.	*Saduria entomon*		
23.	Chironomidae	Hexapoda	
24.	Hydrobiidae	Gastropoda	
25.	*Cerastoderma glaucum*	Bivalvia	Mollusca
26.	*Macoma balthica*		
27.	*Mya arenaria*		
28.	*Mytilus trossulus*		
29.	*Einhornia crustulenta*	Gymnolaemata	Bryozoa

At station ZB_MFW_072, no benthic organisms were recorded at all, while at station ZB_MFW_015, there were 14 taxa, which is the maximum number of macrozoobenthos taxa at a single station. On average, about 7 macrozoobenthos taxa occurred at the soft-bottom stations surveyed. The most common taxa (absolutely constant – present at over 75% of the stations surveyed) were the psammophilous polychaete *Pygospio elegans* and the bivalve *Macoma balthica*. The taxa occurring commonly (constant – at over 50% of the stations surveyed) were both the polychaetes: *Marenzelleria* spp., *Diastylis rathkei*, *Bylgides sarsi* and *Monoporeia affinis*, as well as the oligochaetes (Oligochaeta), the priapulid *Halicryptus spinulosus* and the bivalve *Mytilus trossulus* [Table 3.10].

Table 3.10. The constancy of macrozoobenthos taxa presence in the samples from the soft bottom in the survey area

Constancy type of a given taxon (acc. to Trojan 1980)	Taxon	The constancy of occurrence [%]
Absolutely constant	*Pygospio elegans*	97.02
	Macoma balthica	79.17
Constant	*Marenzelleria* spp.	62.50
	Oligochaeta	61.31
	Diastylis rathkei	60.12
	Mytilus trossulus	59.52
	Halicryptus spinulosus	56.55
	Bylgides sarsi	56.55
	Monoporeia affinis	52.98
Accessory	*Pontoporeia femorata*	29.17
	Bathyporeia pilosa	26.19
Random	*Saduria entomon*	13.69
	Mya arenaria	13.10
	Cerastoderma glaucum	8.33
	Gonothyraea loveni	6.55
	Gammarus salinus	3.57
	Mysis mixta	2.98
	Hydrozoa non det.	2.38
	Nemertea	2.38
	Polychaeta non det.	2.38
	Hydrobiidae	2.38
	Hediste diversicolor	1.79
	Gammarus juvenes	1.79
	Einhornia crustulenta	1.79
	Crangon crangon	1.19
	Cordylophora caspia	0.60
	Gammarus zaddachi	0.60
	Idotea balthica	0.60
	Chironomidae	0.60

3.2.5.1.2 Macrozoobenthos abundance

The abundance of macrozoobenthos found in the analysed samples from the soft bottom in the survey area ranged from 30 ind.·m^{-2} (station ZB_MFW_069), excluding station ZB_MFW_072 at which no organisms were found at all, to 8240 ind.·m^{-2} (station ZB_MFW_116). Average abundance of macrozoobenthos in the survey area was 2402±1811 ind.·m^{-2}.

Out of 29 taxa found on the soft bottom in the survey area, 24 taxa underwent quantitative assessment. In the dominance structure of the macrozoobenthos abundance on the soft bottom, the greatest proportion belonged to the tiny psammophilous polychaete *Pygospio elegans* (58.72%). The bivalve *Macoma balthica* constituted 21.57% of the abundance. The other taxa (*Monoporeia affinis*, *Mytilus trossulus*, Oligochaeta, *Diastylis rathkei*, *Bylgides sarsi*, *Marenzelleria* spp., *Halicryptus spinulosus*)

accounted for less than 10% of the total abundance. The taxa, the proportion of which did not exceed 1% in the macrozoobenthos abundance structure and which had a joint proportion of 1.42% (15 taxa) are included in the group "varia" [Figure 3.5].

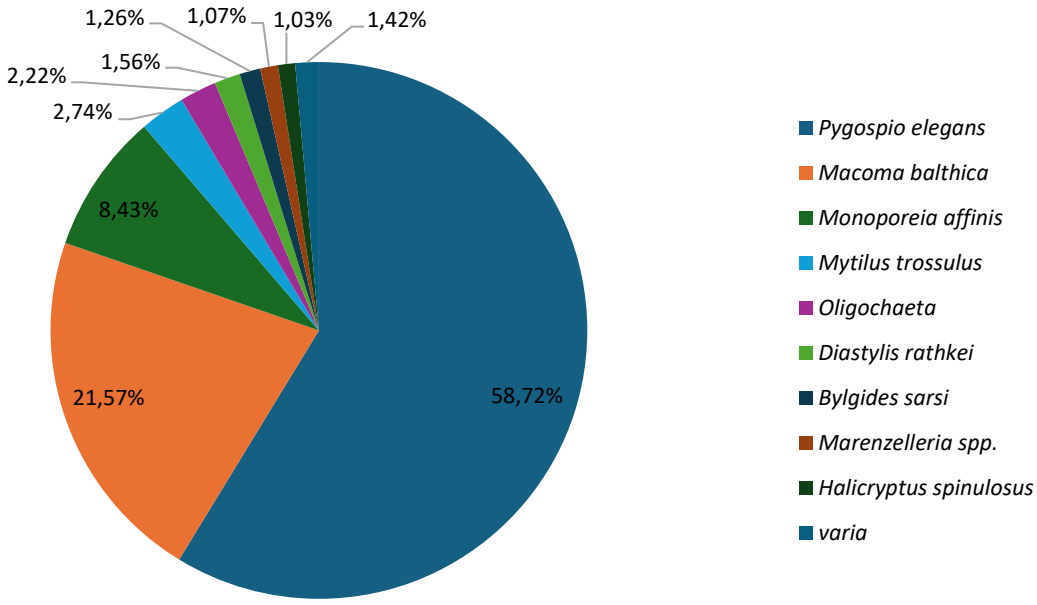


Figure 3.5. The dominance structure in the total abundance of the macrozoobenthos from the soft-bottom stations in the survey area

3.2.5.1.3 Macrozoobenthos biomass

Macrozoobenthos biomass recorded at soft-bottom stations in the survey area ranged from 0.05 g WW·m^{-2} (station ZB_MFW _069), excluding station ZB_MFW_072 at which no benthic organisms were found at all, to 86.99 g WW·m^{-2} (station ZB_MFW _116). The average macrozoobenthos biomass at the soft-bottom stations was 27.00±20.87 g WW·m^{-2}.

The species with the largest proportion in the total macrozoobenthos biomass in the survey area was the Baltic clam *Macoma balthica* (72.51%). The proportion of the remaining taxa did not exceed 10% of the total biomass, with the polychaete *Pygospio elegans* constituting 7.03% of the biomass. The taxa, the proportion of which did not exceed 1% in the macrozoobenthos biomass structure, are included in the group "varia" and these constituted in total 3.80% (17 taxa) [Figure 3.6].

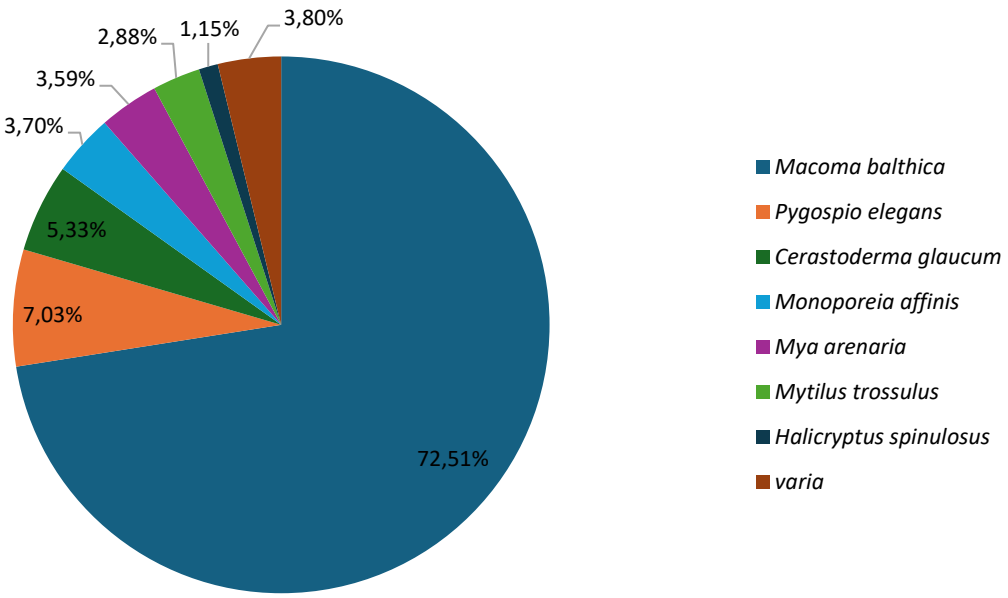


Figure 3.6. The dominance structure in the total macrozoobenthos biomass from the soft-bottom stations in the survey area

3.2.5.1.4 Bivalve size structure

The presence of the following 4 bivalve species was confirmed in 168 analysed samples from the soft bottom in the survey area: the Baltic clam *Macoma balthica*, the bay mussel *Mytilus trossulus*, the soft-shell clam *Mya arenaria*, and the lagoon cockle *Cerastoderma glaucum*. The measurements of the bivalve shells were performed in 5 mm size classes.

The bivalve *Macoma balthica* definitely dominated in terms of biomass in the survey area. Taking into account data from all the stations at which the Baltic clam occurred, on the basis of the measurement of 8660 individuals a size distribution in 5 mm size classes was prepared. The bivalve *Macoma balthica* was characterised by a length ranging from 1 to 25 mm. The distribution of the shell lengths of this bivalve is right-skewed, with juveniles (1–5 mm) constituting the largest group, and adults constituting the smallest group, reaching the maximum size in the 21–25 mm size class [Figure 3.7].

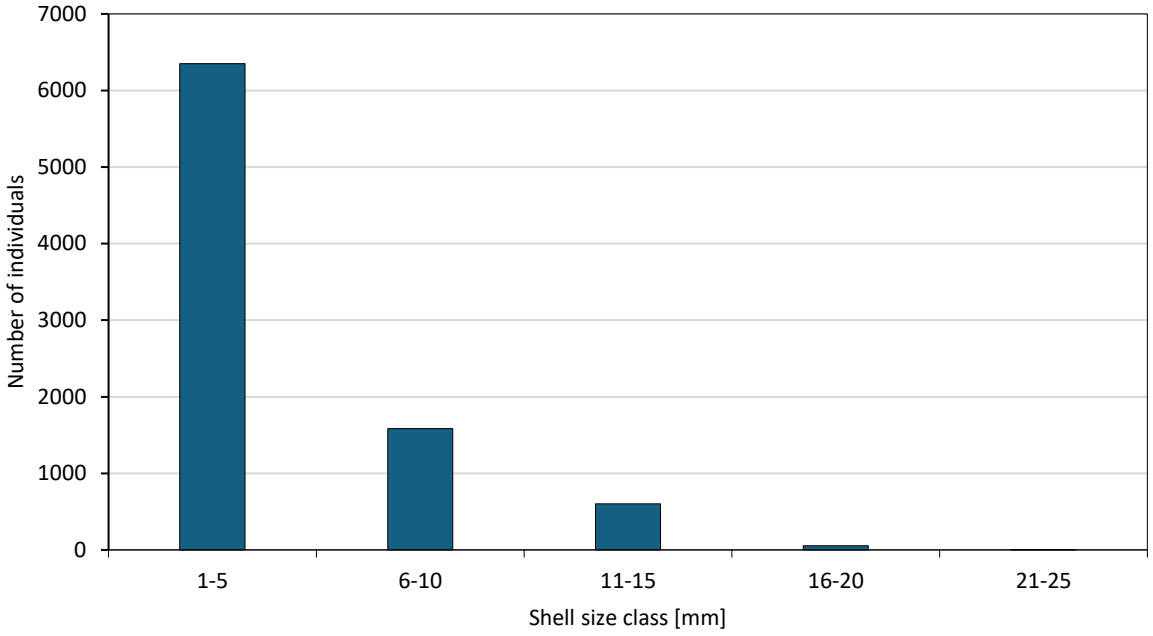


Figure 3.7. The distribution of Macoma balthica shell lengths in 5 mm size classes on the soft bottom in the survey area (N = 8660)

On the other hand, the *Macoma balthica* biomass distribution in 5 mm size classes indicates clearly that in terms of biomass, individuals from 11 to 15 mm long dominated (over 1800 g WW·m^{-2}), while the bivalves of these species of 6–10 mm long had slightly lower proportion in the biomass (approximately 800 g WW·m^{-2}). The remaining Baltic clam individuals (the smallest and the largest) had a much lower proportion in this species biomass [Figure 3.8].

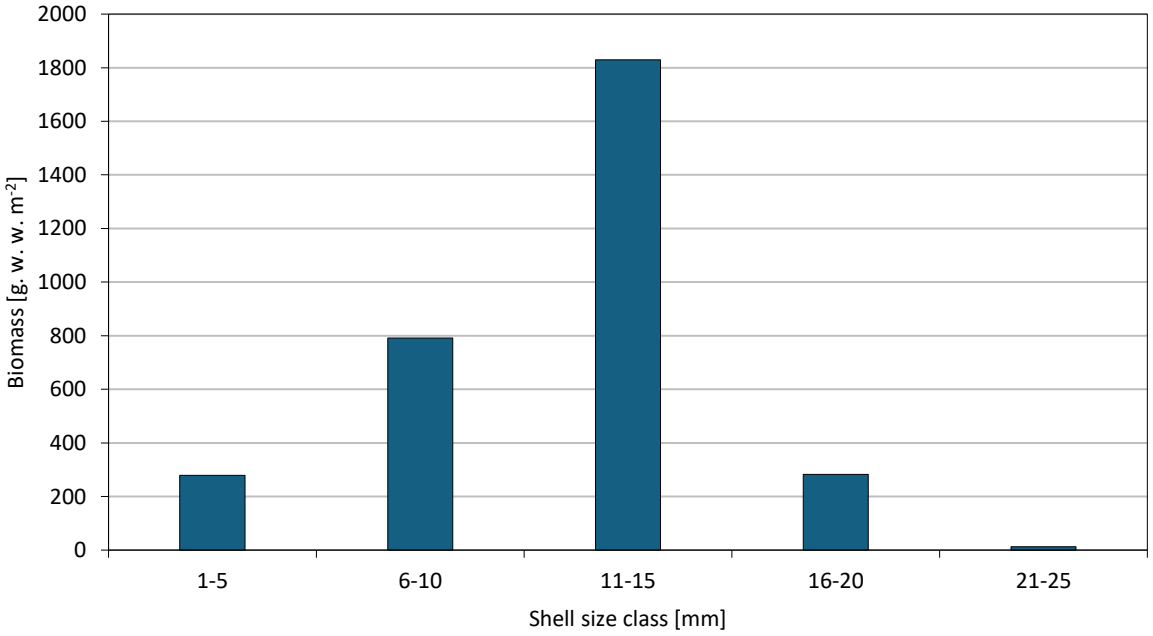


Figure 3.8. The distribution of Macoma balthica biomass in 5 mm size classes on the soft bottom in the survey area (N = 8660)

The size structure of the remaining species of bivalves, *Mytilus trossulus, Mya arenaria* and *Cerastoderma glaucum*, occurring on the soft bottom in the survey area, whose proportion in biomass was much smaller than that of *Macoma balthica*, is shown in the chart below [Figure 3.9]. In the case of *Mytilus trossulus* and *Cerastoderma glaucum*, juvenile individuals, 1–5 mm long, dominated, while in the case of *Mya arenaria*, individuals from the 6–10 mm size class were the most numerous. The largest sizes of few individuals of *Mya arenaria* and *Mytilus trossulus* were 31–35 mm, while the lagoon cockle *Cerastoderma glaucum* reached the maximum sizes in the size class 16–20 mm.

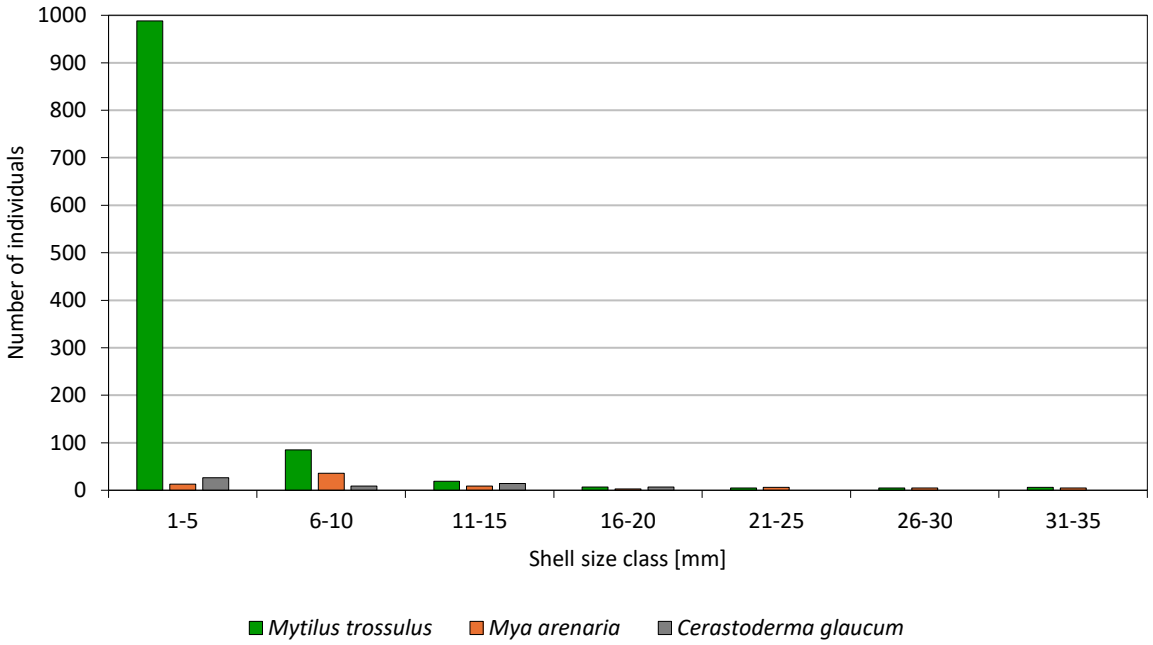


Figure 3.9. *The shell length distribution of Mytilus trossulus, Mya arenaria and Cerastoderma glaucum in 5-mm size classes on the soft bottom in the survey area (Mytilus trossulus N = 1103; Mya arenaria N = 68; Cerastoderma glaucum N = 57)*

The biomass distribution of both *Mytilus trossulus* and *Mya arenaria* in 5-mm size classes is bimodal. In both cases, in terms of biomass, the smallest individuals dominate due to their high abundance (*Mytilus trossulus* in the 1–5 mm size class; *Mya arenaria* in the 6–10 mm size class) and the largest individuals dominate due to their size (the 31–35 mm size class for both species of bivalves). On the other hand, *Cerastoderma glaucum* is characterised by a left-skewed biomass distribution with the highest share of biomass of the largest individuals with sizes ranging from 11 to 20 mm. The highest biomass of *Cerastoderma glaucum* in the 11–15 mm size class (over 100 g WW·m^{-2}) was 5 times higher than the highest biomass of *Mytilus trossulus* (in the 1–5 mm size class) or *Mya arenaria* (in the 6–10 mm size class) [Figure 3.10].

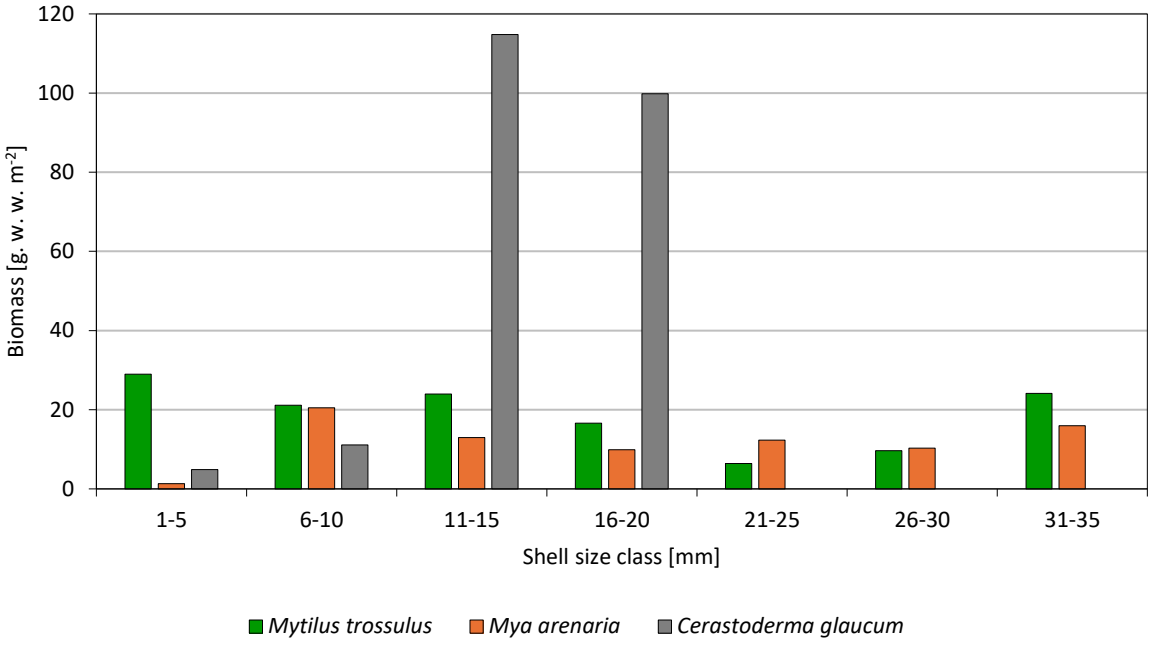


Figure 3.10. The biomass distribution of Mytilus trossulus, Mya arenaria and Cerastoderma glaucum in 5 mm size classes on the soft bottom in the survey area (Mytilus trossulus N = 1103; Mya arenaria N = 68; Cerastoderma glaucum N = 57)

3.2.5.1.5 B index

The values of index B calculated for the 168 individual stations located on the soft bottom in the survey area ranged from 0.90 (station ZB_MFW_079, poor status) to 4.67 (station ZB_MFW_056, very good status). The average value of index B was 3.00±0.62 (moderate status according to WFD), which corresponds to class 3 of water quality on a five-point scale compliant with the Regulation of the Minister for Infrastructure of 25 June 2021 on the classification of ecological status, ecological potential and chemical status and the method of classifying the status of surface water bodies as well as the environmental quality standards for priority substances (Journal of Laws of 2021, item 1475).

3.2.5.2 Hard bottom

3.2.5.2.1 Taxonomic composition

In the two macrozoobenthos samples analysed (of the periphytic fauna and associated fauna complex) which were collected from the hard bottom (from the surface of stones) in the survey area, the presence of only seven taxa representing five classes of Hydrozoa, Polychaeta, Thecostraca, Malacostraca and Bivalvia was confirmed [Table 3.11].

Table 3.11. The taxonomic composition in two macrozoobenthos samples from the hard bottom in the survey area

No.	Taxon	Class	Phylum
1.	*Gonothyraea loveni*	Hydrozoa	Cnidaria
2.	*Bylgides sarsi*	Polychaeta	Annelida
3.	*Amphibalanus improvisus*	Thecostraca	Arthropoda
4.	*Gammarus salinus*	Malacostraca	
5.	*Gammarus juvenes*		

No.	Taxon	Class	Phylum
6.	*Jaera* spp.		
7.	*Mytilus trossulus*	Bivalvia	Mollusca

3.2.5.2.2 Macrozoobenthos abundance

The macrozoobenthos abundance found in two samples from the hard bottom in the survey area ranged from a minimum of 7344 ind.·m^{-2} (station ZB_MFW_T_2) to a maximum of 25 543 ind.·m^{-2} (station ZB_MFW_T_1).

At both stations, the bivalve *Mytilus trossulus* dominated in terms of abundance (91.70%) [Figure 3.11].

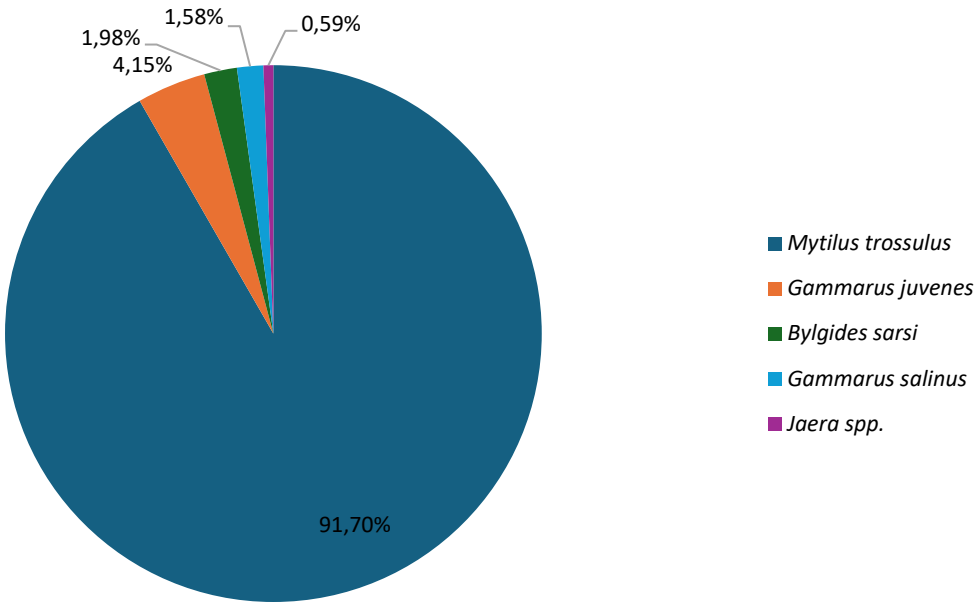


Figure 3.11. The dominance structure in the total macrozoobenthos abundance from the hard-bottom stations in the survey area

3.2.5.2.3 Macrozoobenthos biomass

The biomass of the benthic fauna of the hard bottom in the survey area ranged from 278.28 g WW·m^{-2} (station ZB_MFW_T_2) to 1398.95 g WW·m^{-2} (station ZB_MFW_T_1).

At both stations, the bivalve *Mytilus trossulus* dominated in terms of biomass (99.64%) [Figure 3.12].

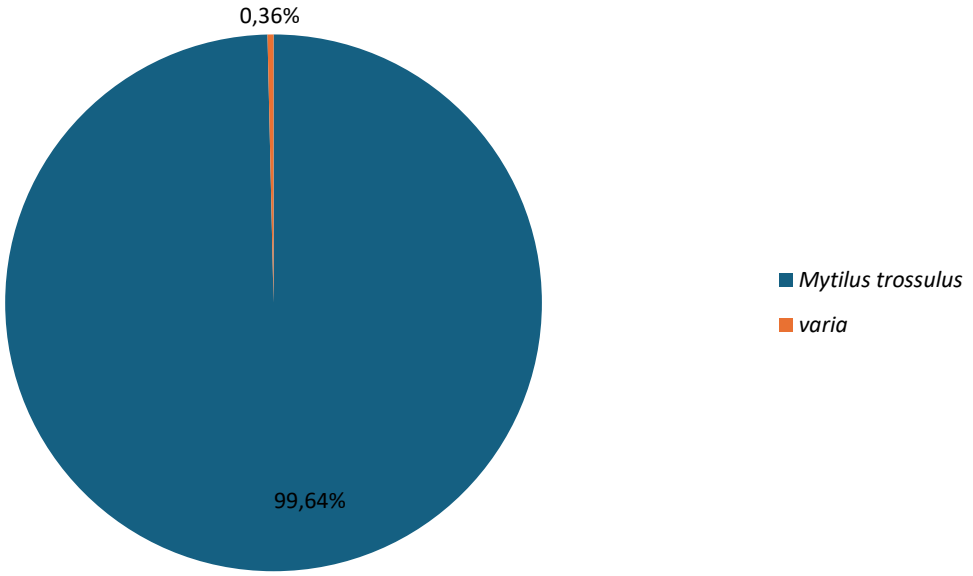


Figure 3.12. The dominance structure in the total macrozoobenthos biomass from the hard-bottom stations in the survey area

3.2.5.2.4 Bivalve size structure

In the case of the stony seabed in the survey area, on the basis of the length measurements of 464 *Mytilus trossulus* individuals, juvenile individuals from the size class 1–5 mm clearly dominated in terms of abundance. The right-skewed bay mussel length distribution indicates that the largest bay mussels were in the length range of 26–30 mm and were the least numerous [Figure 3.13].

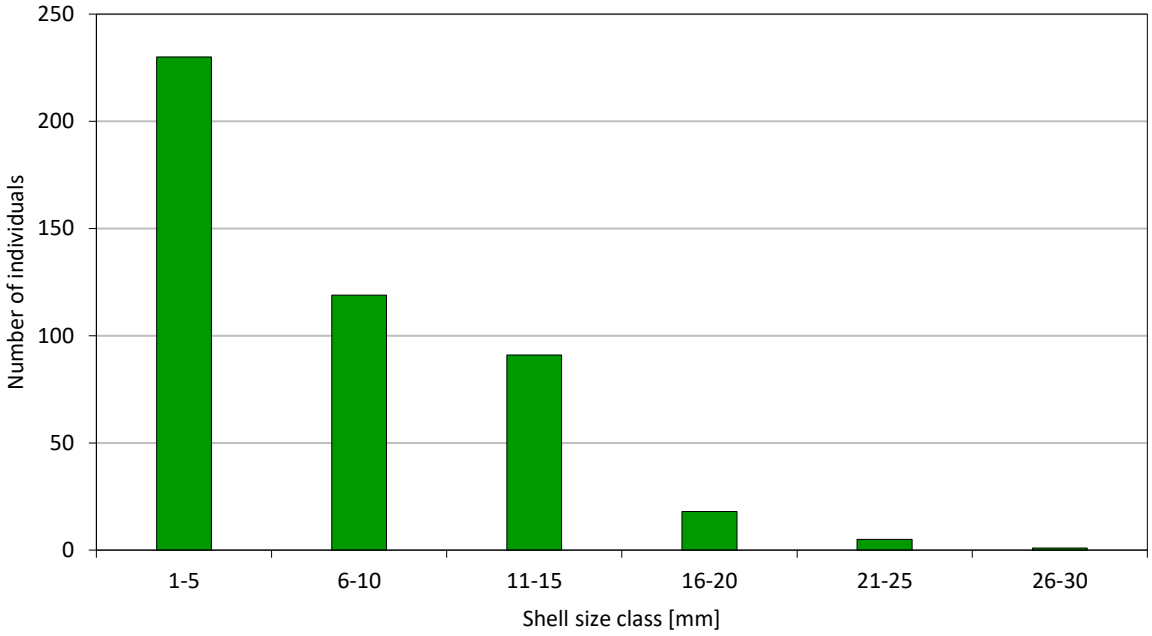


Figure 3.13. The distribution of Mytilus trossulus shell lengths in 5 mm size classes on the hard bottom in the survey area (N = 464)

The biomass distribution of *Mytilus trossulus* is unimodal with a clear dominance of individuals from the shell length range from 11 to 15 mm, reaching over 600 g WW·m^{-2} in that size class [Figure 3.14].

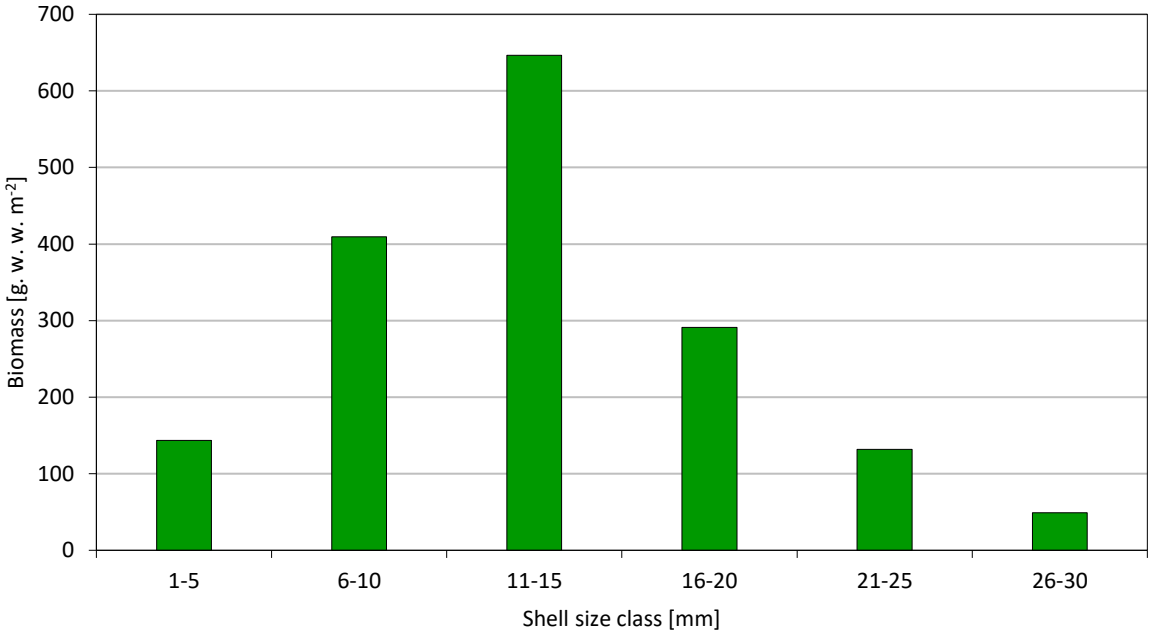


Figure 3.14. The distribution of Mytilus trossulus biomass in 5 mm size classes on the hard bottom in the survey area (N = 464)

3.2.5.2.5 TSP index

At station ZB_MFW_T_1, three typical taxa were found, which classifies the quality status of that macrozoobenthos community as good. On the other hand, the only typical taxon found at station ZB_MFW_T_2 was the bay mussel *Mytilus trossulus*, which maximally reduces the value of the TSP index to a poor status of this region.

3.2.6 Summary of results and conclusions

As a result of the inventory surveys conducted in 2023 including the analysis of macrozoobenthos samples collected in the survey area, comprehensive data were obtained to conduct a qualitative and quantitative analysis of benthic invertebrate communities in the planned project area and to assess the ecological status of the seabed habitats.

The compilation of the results of macrozoobenthos surveys both on the soft bottom as well as on the hard bottom in the survey area is presented in Table 3.12.

Based on the data obtained from the 168 samples analysed, the occurrence of 29 macrozoobenthos taxa on the soft bottom in the survey area was confirmed. The most common taxa (absolutely constant – present at over 75% of the stations surveyed) were the tiny, psammophilous polychaete *Pygospio elegans* and one bivalve species – *Macoma balthica*. In the dominance structure of the macrozoobenthos abundance on the soft bottom, the greatest proportion had the polychaete *Pygospio elegans* (58.72%). The average abundance of the macrozoobenthos from the samples analysed was 2388±1815 ind.·m^{-2}, while the average biomass was 26.8±38.6 g WW·m^{-2}. The species with the largest proportion in the total macrozoobenthos biomass in the survey area was the Baltic clam *Macoma balthica* (72.51%). The presence of the following three bivalve species was confirmed in the samples:

the bay mussel *Mytilus trossulus*, the soft-shell clam *Mya arenaria* and the lagoon cockle *Cerastoderma glaucum*. In the case of *Macoma balthica*, the most numerous were young individuals (1–5 mm), and adult individuals reaching the maximum size in the 21 to 25 mm size class accounted for the smallest proportion. On the other hand, the *Macoma balthica* biomass distribution in 5 mm size classes indicates clearly that in terms of biomass, individuals from 11 to 15 mm long dominated (over 1800 g WW·m^{-2}). The largest sizes of few individuals of *Mya arenaria* and *Mytilus trossulus* were 31–35 mm, while the lagoon cockle *Cerastoderma glaucum* reached the maximum sizes in the size class 16–20 mm. The highest biomass of *Cerastoderma glaucum* in the 11–15 mm size class (over 100 g WW·m^{-2}) was 5 times higher than the highest biomass of *Mytilus trossulus* (in the 1–5 mm size class) or *Mya arenaria* (in the 6–10 mm size class). The taxonomic composition, abundance and biomass established for the macrozoobenthos of this area indicate that the area is inhabited by quite diverse benthic macrofauna consisting of taxa characteristic for this depth range. The average value of index B was 3.00±0.62, which indicates only a moderate status of the seabed fauna community inhabiting the area described.

In the macrozoobenthos samples analysed (of the periphytic fauna and the associated fauna complex) collected from the hard bottom (from the surface of stones) in the survey area, the presence of only seven taxa was confirmed, which indicates a poor qualitative-quantitative composition of this community. The macrozoobenthos abundance found in two samples from the hard bottom in the survey area ranged from a minimum of 7344 ind.·m^{-2} (station ZB_MFW_T_2) to a maximum of 25,543 ind.·m^{-2} (station ZB_MFW_T_1). The biomass of the benthic fauna from the hard bottom in the survey area ranged from 278.3 g WW·m^{-2} (station ZB_MFW_T_2) to 1398.9 g WW·m^{-2} (station ZB_MFW_T_1). The bay mussel *Mytilus trossulus* dominated at both stations in terms of abundance and biomass. Juvenile bay mussels from the 1–5 mm size class were by far the most abundant. At one station, the quality status of this macrozoobenthos community was classified as good and at the other station as poor.

Table 3.12. Compilation of the results of macrozoobenthos surveys in the survey area

Parameter	Soft bottom	Hard bottom
Number of stations	168	2
Depth [m]	14.7–49.5	26.3–38.6
Number of taxa: total	29	7
Number of taxa: range at stations	0–14	2–7
Abundance [ind.·m^{-2}]: average±SD	2388±1815	16433
Abundance [ind.·m^{-2}]: range	0–8240	7344–25,543
Biomass [g WW·m^{-2}]: average±SD	27.00±20.87	838.62
Biomass [g WW·m^{-2}]: range	0–86.99	278.15–1393.00
B index: average±SD	3.00±0.62	-
B index: range	0.90–4.67	-
TSP index: average±SD	-	2
TSP index: range	-	1–3
Macrozoobenthos quality status	moderate	poor
Absolutely constant species	*Pygospio elegans*	-
	Macoma balthica	-
Dominant bivalve species	*Macoma balthica*	*Mytilus trossulus*

The areal distribution of the macrozoobenthos abundance in the survey area is presented in Figure 3.15. The majority of the survey area is dominated by sandy and gravelly sediments. In the southern part of the survey area, the total abundance of macrozoobenthos was slightly higher than in the northern part, where it did not exceed 2000 ind.·m^{-2}. Only in the north-western part of the survey area and in the north-eastern part of the area of the construction of WTGs, OSSs and cable lines (area A), in a small area relative to the soft bottom, the macrozoobenthos abundance was much higher (from approx. 7300 to 25 500 ind.·m^{-2}), which was related to the occurrence of the bay mussel *Mytilus trossulus* aggregations on the stony seabed. In the southern part of the survey area, the macrozoobenthos abundance values were up to a maximum of 6000 ind.·km^{-2}.

The total macrozoobenthos biomass was low and even across the entire survey area, not exceeding 80 g WW·m^{-2} except for point locations in the north-eastern (the area of the construction of WTGs, OSSs and cable lines – the so-called area A) as well as north-western part of the survey area, where the stony seabed occurred and thus, the macrozoobenthos biomass reached ranged from over 200 to approx. 14 000 g WW·m^{-2} there [Figure 3.16].

The figure below [Figure 3.17], presents the areal distribution of *Macoma balthica* biomass – a bivalve, which dominated in terms of abundance and biomass among all the species of bivalves identified there. *Macoma balthica* inhabited the seabed in the survey area mainly in its southern as well as north-eastern parts, with slightly higher values of this species biomass (approximately 50 g WW·m^{-2}) occurring in the southern part of the survey area. The northern part of the survey area was characterised by *Macoma balthica* biomass lower than 10 g WW·m^{-2}.

Mytilus trossulus, on the other hand, which had a proportion of 2.74% and 2.88% respectively, in the abundance and biomass in the survey area, occurred mainly in the southern part of the area surveyed not exceeding 10 g WW·m^{-2} on the sandy-gravelly seabed. However, it needs to be underlined, that the biomass of this species locally reached more than 300 g WW·m^{-2} which is related to the bay mussel aggregations in the northern part of the survey area [Figure 3.18].

The areal distribution of the ecological status based on macrozoobenthos, within the boundaries of the survey area, has a mosaic character. Most of the area indicated is covered by a sandy and sandy-gravelly seabed inhabited by macrozoobenthos representing poor and moderate status. Areas with higher values (good status) occur mainly in the southern strip of the survey area, as well as in the area of the construction of WTGs, OSSs and cable lines (area A). The valorisation in the point locations of the stony seabed occurrence indicates that this is not a valuable habitat area, because the status of the macrozoobenthos community inhabiting the stony seabed fragments was determined as poor in one place and good in another [Figure 3.19].

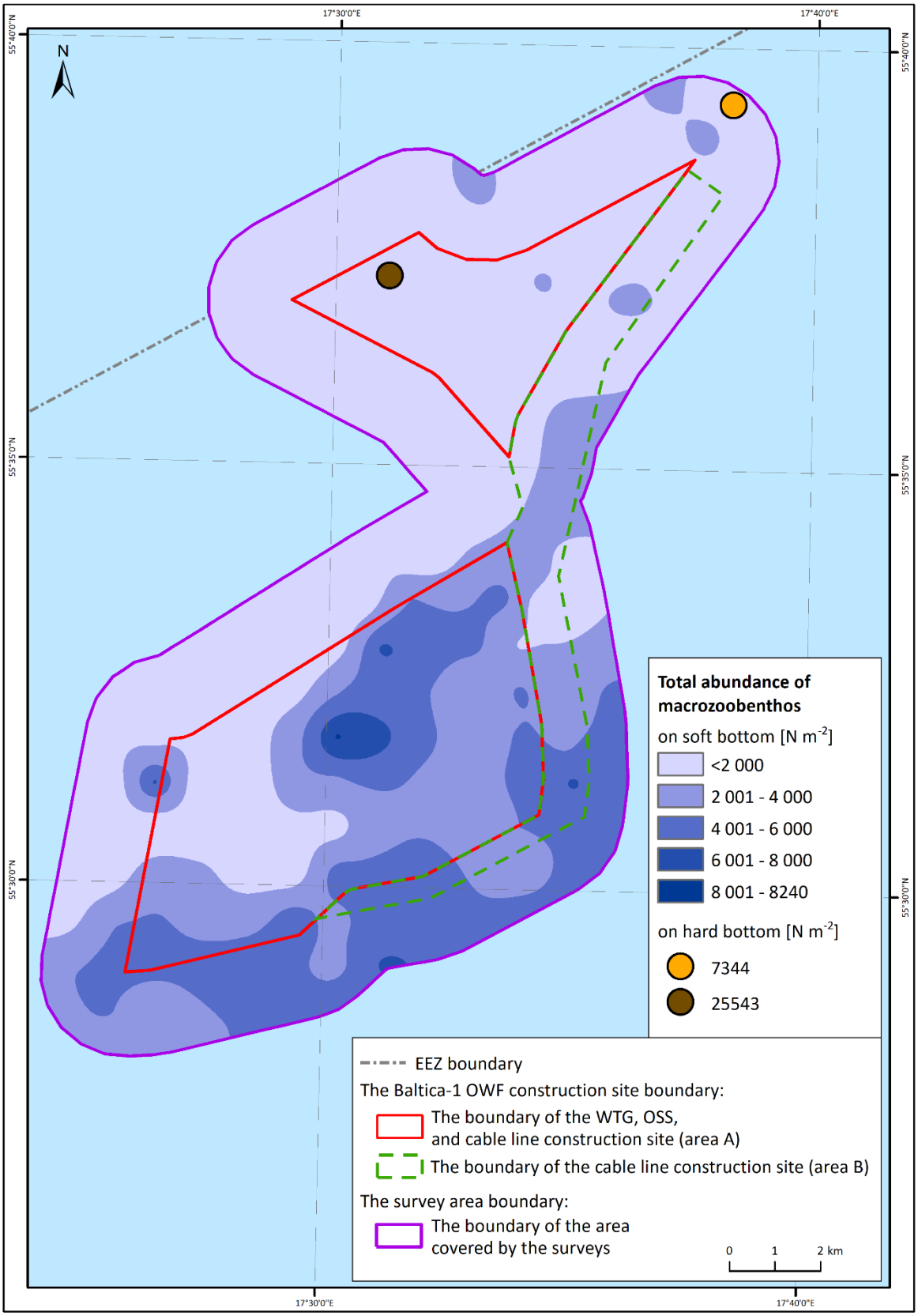


Figure 3.15. The macrozoobenthos abundance distribution in the survey area

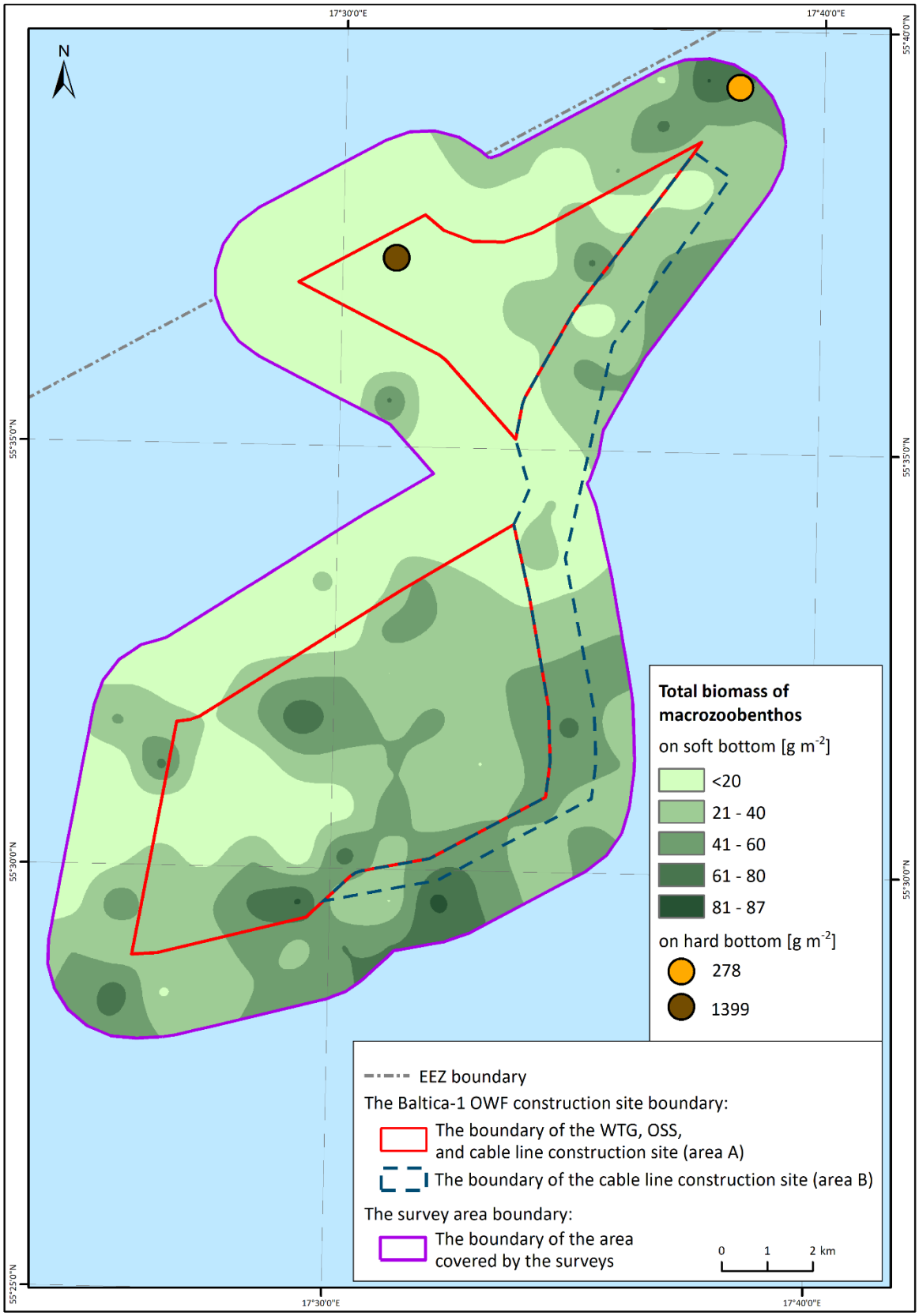


Figure 3.16. The macrozoobenthos biomass distribution in the survey area

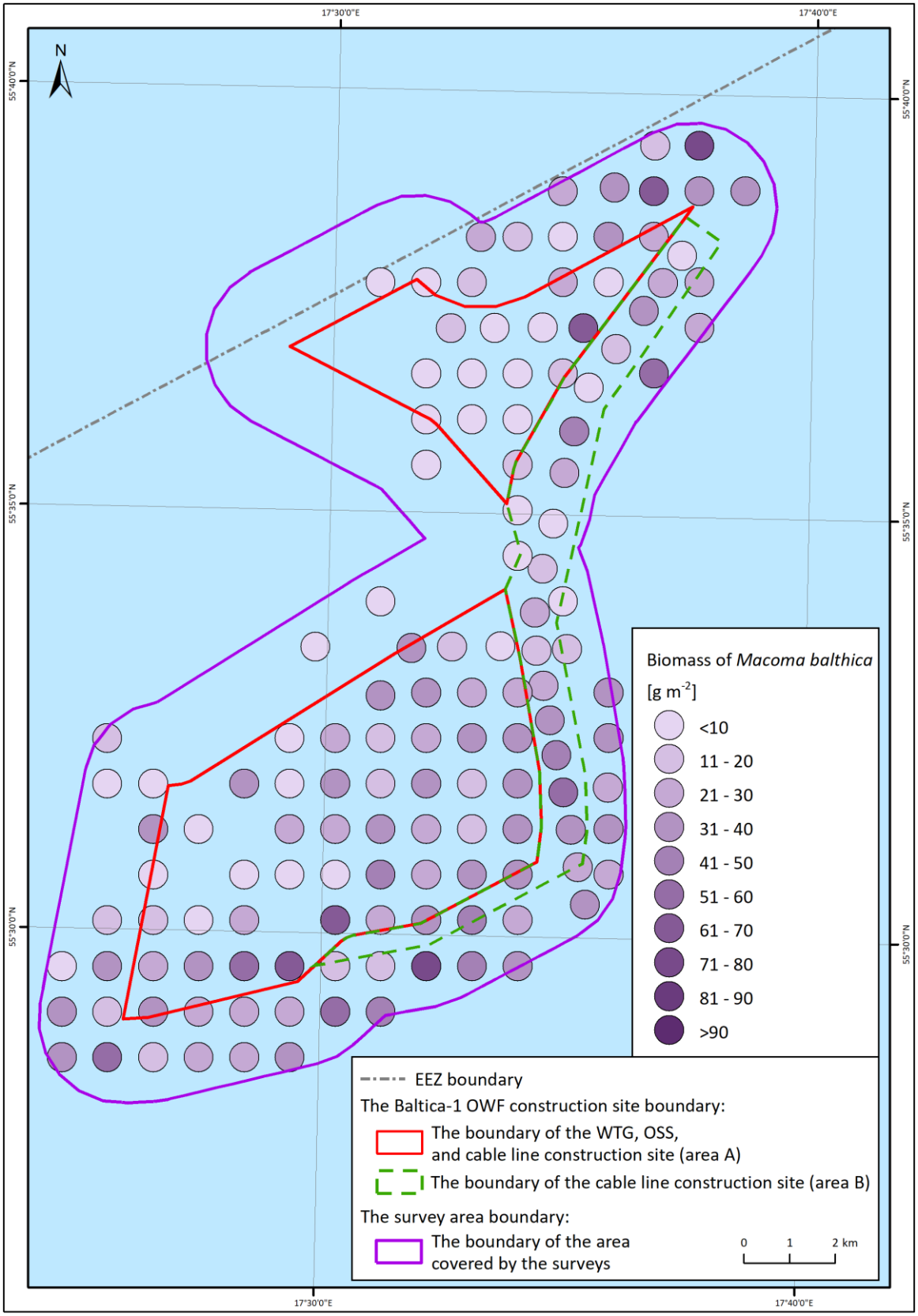


Figure 3.17. The Macoma balthica biomass distribution in the survey area

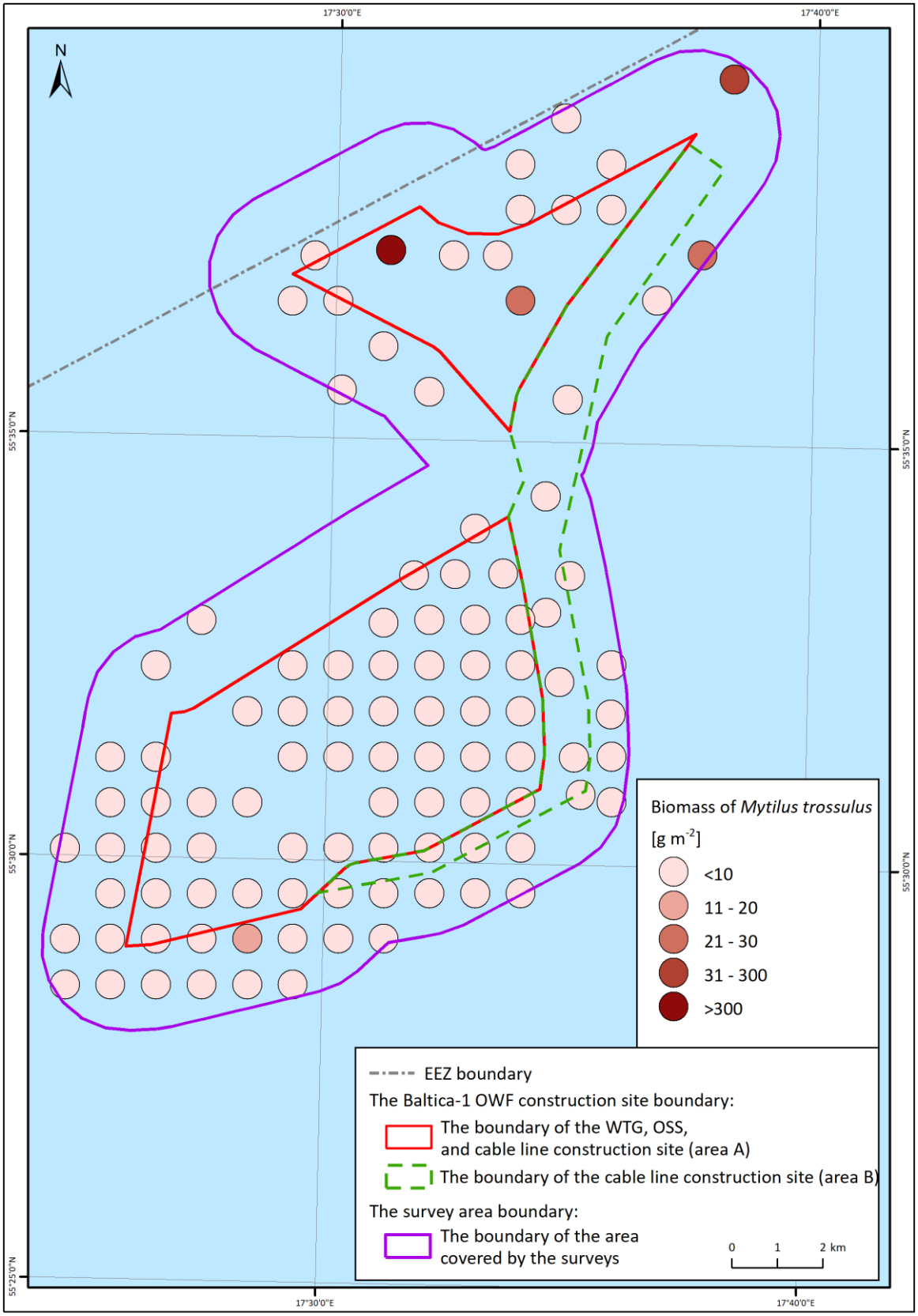


Figure 3.18. The Mytilus trossulus biomass distribution in the survey area

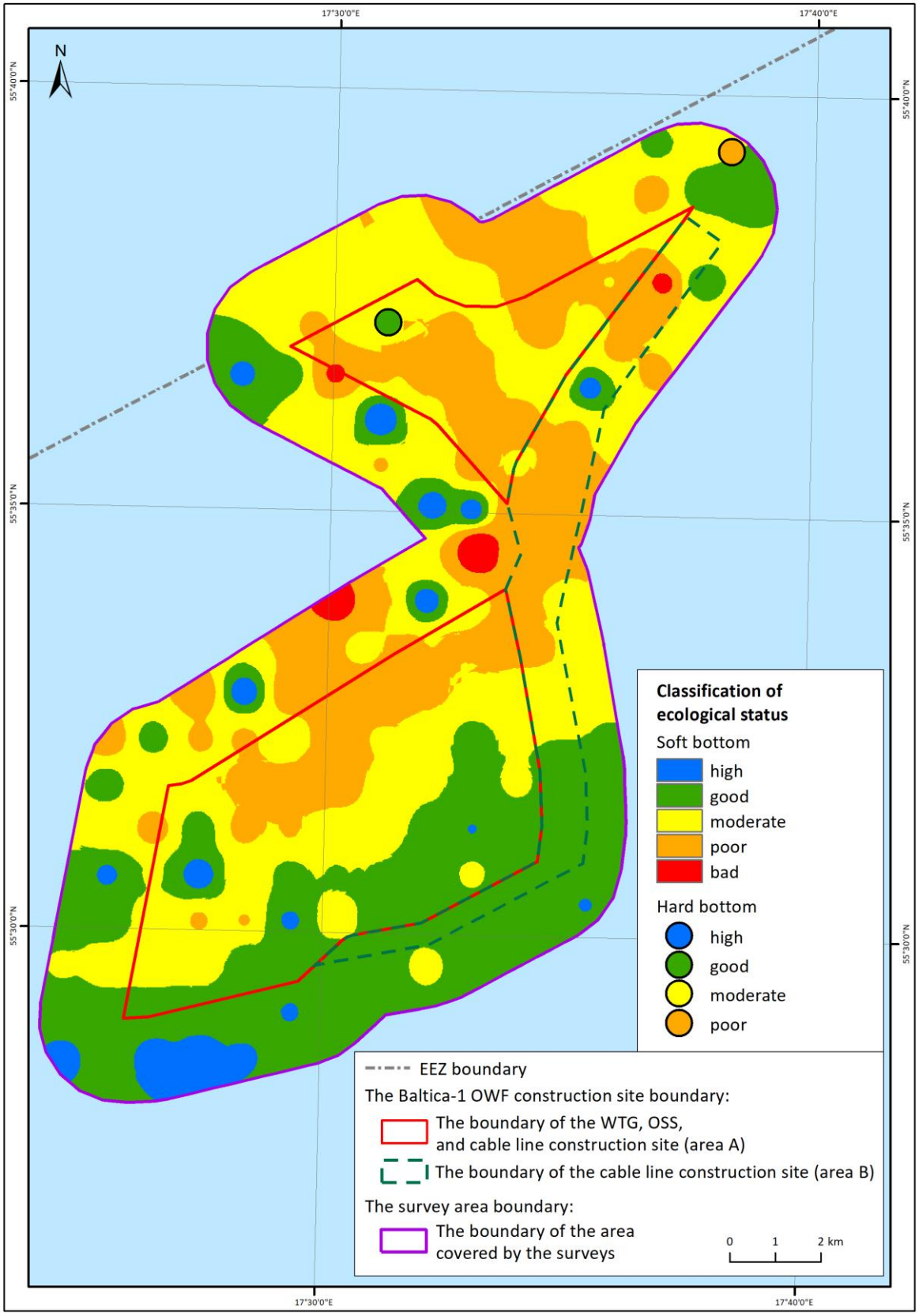


Figure 3.19. The ecological status distribution in the survey area based on macrozoobenthos quality status assessment

Additionally, it should be noted that no protected species of macrozoobenthos were found in the entire survey area.

3.2.7 Shortcomings and gaps in the state-of-the-art

No shortcomings nor gaps in the current knowledge were identified as part of the macrozoobenthos surveys. Despite the lack of permission for surveys in the Swedish EEZ, the characterisation of macrozoobenthos communities covered the entire survey area together with a fragment of the seabed located within the boundaries of Swedish sea waters, based on extrapolation of data to this part of the survey area.

3.3 ICHTHYOFAUNA

3.3.1 Non-specialist summary

The surveys of ichthyofauna were conducted in an annual cycle mode including four survey cycles covering all seasons of the year. The spatial scope of the ichthyofauna surveys was the survey area covering the Baltica-1 OWF construction area, which is the area of construction of the WTGs, OSSs, and cable lines (area A) and the area of construction of cable lines (area B) together with a zone of no less than 4 km in width measured from the boundary of area A.

Based on the results of the above surveys and literature knowledge, potential spawning sites, foraging grounds, migration routes and the distribution of fry within the survey area were also determined.

The taxonomic diversity of ichthyoplankton (larvae belonging to eight fish taxa) in the survey area was low in comparison with what is usually observed in the Southern Baltic surveys. Due to the low salinity of the area, the early-spring spawning of sprat does not take place there. The larvae caught during that period probably came from the spawning taking place in the Słupsk Furrow. The absence of larvae in summer might have resulted from the timing of sampling coinciding with the final period of the summer shallow-water spawning.

The salinity of the survey area is too low for the reproduction of the flounder and the fourbeard rockling to take place there. The larvae caught in the survey area came from the spawning taking place in the Słupsk Furrow. The ammodytid larvae caught in the survey area probably came from the spawning taking place in the shallow regions of the Middle Bank, including the shallowest part of the survey area in the Southern Middle Bank. The too great depth of the survey area eliminates the possibility that the goby larvae caught came from the spawning taking place in that region. Their reproduction probably took place in the coastal waters of the Stilo Bank, the Czołpino Shallows, the Słupsk Bank or in the shallowest part of the Middle Bank. The larvae of the autumn-spawning herring caught in October and March may have originated from the spawning taking place in the Słupsk Bank and the Middle Bank area, including the section of the area surveyed located in the shallowest part of the Southern Middle Bank. The few common seasnail and rock gunnel larvae caught in the survey area may have originated from the spawning taking place either in the shallowest part of the survey area, in the Słupsk Bank or in the coastal area.

The efficiency analysis of the survey gillnet gear demonstrated that the peak of fish density occurred in summer and autumn, due to the fact that the shallower waters of the survey area serve as foraging grounds during those seasons. In other periods, fish densities were similar, while the lowest efficiencies were recorded in winter.

In February 2023, the sprat started the first phase of spawning in the water depth of the Baltic Sea, i.a. in the survey area monitored. The process intensified on a large scale in May, then gradually declined in the second half of summer.

The analyses of stomach content confirm the more intense feeding of the herring in spring and summer. The high proportion of fish with empty stomachs in winter and autumn indicates the occurrence of low intensity feeding in the planned project area, possibly related to the low availability of the preferred zooplankton groups.

In the planned project area, mature herrings can migrate towards Swedish or Polish coasts, however the planned project area alone is not a significant spawning ground for the herring due to its depth, lack of suitable substrate and the distance from the shore. The observed concentrations of spring shoals are represented by the fish that had already spawned in the coastal regions.

The results of cod abundance surveys conducted during individual survey seasons indicate a low occurrence of these fish in winter and spring. The abundant occurrence of the cod was recorded in the potential area of the offshore wind farm location in summer and autumn. The above-mentioned results of cod abundance surveys might, therefore, indicate that the planned project area constitutes a less significant habitat for fish of this species in the winter-spring season than it does in summer and autumn.

Seasonal changes in the length composition of the cod recorded in the area of the planned project resulted from the biological characteristics of these fish. These are manifested by spawning migrations from the shore towards the depths, where cod spawning grounds are situated, and feeding migrations from the depths towards the shores. The planned project area lies on the path of the above-mentioned migrations.

In spring, cods preparing for spawning, i.e. larger and older individuals, migrate towards spawning grounds outside of the planned project area. A similar situation took place in the planned offshore wind farm area in summer when most adult cods spawned in the depths of the Baltic Sea. Whereas in autumn, the proportion of the shortest cods was the smallest, while the proportion of longer fish increased, as a result of the individuals returning to the feeding grounds after spawning. The fish migrated towards the shore, also through the planned project area. The food in the survey area was available for cods of a wide range of lengths.

The survey area served as a habitat mainly for adult flounders. They were the most abundant in summer and the least abundant in autumn.

Considering the prevailing hydrological conditions unfavourable to the reproduction of the European flounder (*Platichthys flesus*), it may be assumed that the fish from the survey area moved to the nearby Słupsk Furrow or to the Gdańsk Deep to spawn.

Four of the taxa recorded within the survey area, i.e. gobies, the common seasnail, the fourhorn sculpin and the twaite shad, belong to partially protected species under the Regulation of the Minister of the Environment of 16 December 2016 *on the protection of animal species* (Journal of Laws of 2016, item 2183, as amended).

According to the assessment of significance as a foraging and spawning ground as well as in terms of migration routes occurrence, the Baltica-1 OWF area was considered to be of average value.

3.3.2 Spatial scope of the surveys

The spatial scope of the ichthyofauna surveys was the survey area covering the Baltica-1 OWF construction area, which is the area of construction of the WTGs, OSSs, and cable lines (area A) and the area of construction of cable lines (area B) together with a zone of no less than 4 km in width measured from the boundary of area A.

The collection of ichthyoplankton samples, catches using gillnet sets, surveys involving the use of herring gillnets took place at the established survey stations, whereas hydro-acoustic surveys were conducted along the established transects. Pelagic catches were carried out in locations with increased values of echo integration (fish concentrations) at the echosounder.

The locations of the hydroacoustic transects and the survey stations at which the ichthyoplankton catches were carried out as well as the locations of the gillnet deployment were planned so as to cover each survey area evenly and provide representative data.

Due to the lack of permits from Sweden, the surveys were completed only within the PSA. This applies to the ichthyoplankton catches, pelagic fish and demersal fish community surveys as well as herring concentration surveys.

3.3.3 Methodology

3.3.3.1 Ichthyoplankton

In the survey area, ichthyoplankton samples were collected at 8 survey stations (the area coverage density was one station per 38 km^2) [Figure 3.20]. Ichthyoplankton are organisms passively drifting in the water column; therefore, the analysis of their occurrence required area-based rather than spot-oriented data interpretation. Consequently, the indicated location of the survey stations is only a navigational reference, and hauling is carried out in the immediate vicinity of the established station.

Samples were collected from 5 m above the seabed to the surface level using a 300 µm mesh size Bongo net equipped with a depth gauge to control the depth of the gear immersion. The hauls were carried out at a vessel speed of approximately 2–3 kn. The volume of water filtered during the haul was measured using a flowmeter. The biological material collected was preserved in 4% formaldehyde solution.

At each survey station, hydrological parameters (salinity and temperature) were measured throughout the water column using a CTD.

The ichthyoplankton samples collected were examined under a stereo microscope at a laboratory. All ichthyoplankton components were subjected to quantitative and qualitative analyses. In the case of very high abundance of ichthyoplankton (eggs or larvae/fry), a subsample was analysed taxonomically. The samples were identified to the lowest possible taxonomic unit (in most cases to the species).

The lengths of larvae/fry (all individuals or a subsample of 50 individuals, if the number of larvae in the sample exceeded this value) were measured using a digital image analysis system, involving NIS Elements software. Larval lengths were expressed as the standard length (SL), i.e. the distance from the tip of the head (with the snout shut) to the end of the notochord/urostyle in the case of larvae, or to the base of the caudal fin in the case of fry.

The material collected was used to determine the species composition and ichthyoplankton abundance (per 10 m^2 of the water surface) within the areas surveyed.

Ichthyoplankton surveys were carried out in accordance with the methodology adopted by ICES (2010; 2012) and FAO (Smith and Richardson, 1977).

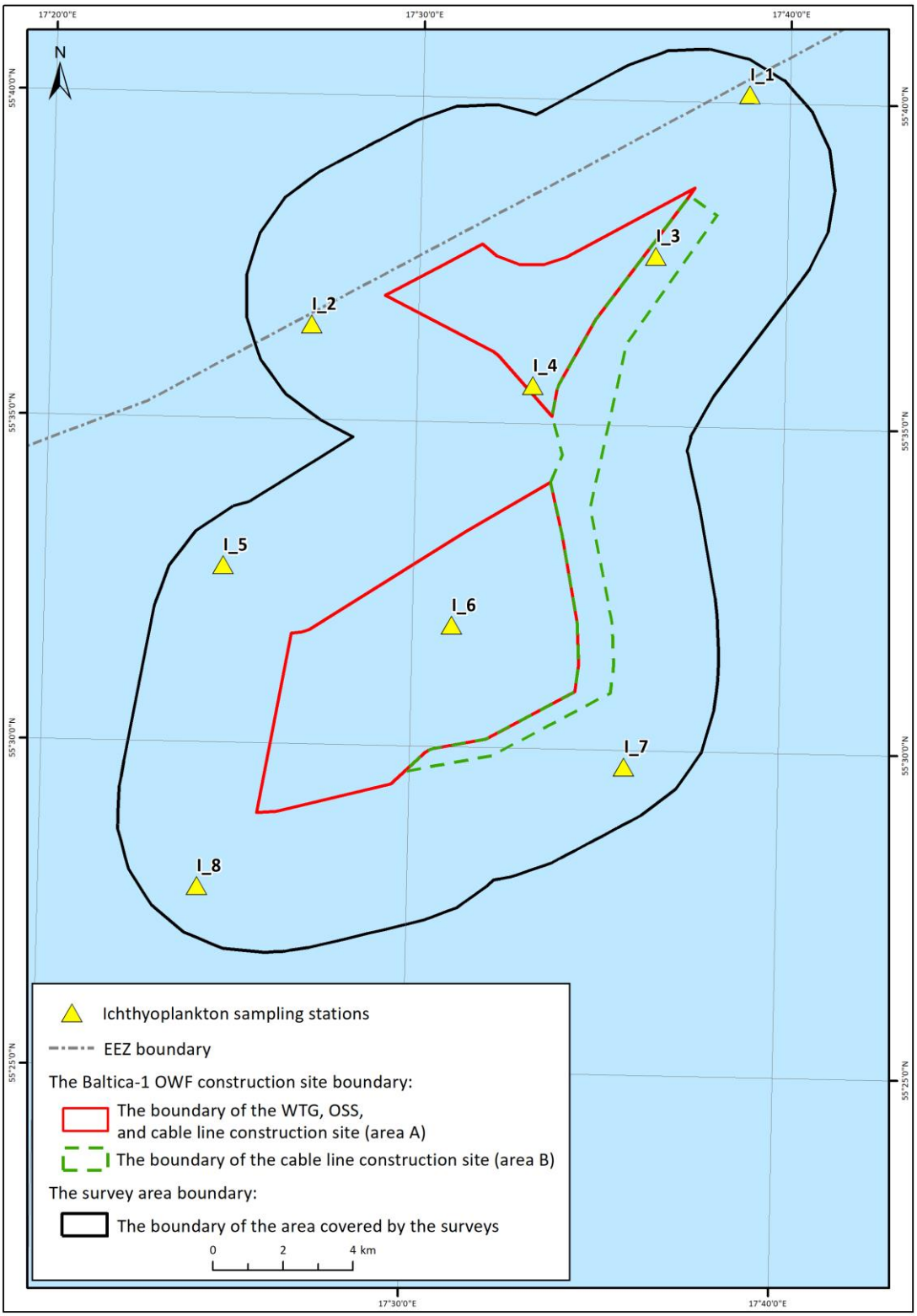


Figure 3.20. The locations of the survey stations for ichthyoplankton sampling within the survey area

3.3.3.2 Hydroacoustic surveys and pelagic hauls

The analysis of the density and characteristics of the pelagic fish community within the survey area was conducted using complementary hydroacoustic survey methods and pelagic control hauls.

To determine the pelagic fish areal biomass distribution and density, the acoustic method was used in accordance with the international standards adopted by the Baltic International Fish Survey Working Group (WGBIFS) of the International Council for the Exploration of the Sea (ICES), included in the Manual for the International Baltic Acoustic Survey (IBAS) [ICES, 2017]. For the purpose of acoustic monitoring of fish in the water column, a SIMRAD EK80 survey echosounder with a transducer operating at 38 kHz was used. Technical parameter settings of the echosounder were consistent with the above-mentioned document, while the calibration procedures were performed in accordance with the echosounder manufacturer's instructions (SIMRAD). The echo sounding was conducted at a vessel speed of approx. 7 kn. The hydro-acoustic profile grid was planned to cover the survey area (the total transect length was 132 km) [Figure 3.21]. The proposed grid of hydro-acoustic transects allowed correct interpolation and interpretation of the inventory results for the survey area. EchoView software from Myriax was used to analyse the echo-integration results.

Pelagic control hauls were carried out in order to determine the species composition as well as the proportion of fish in individual length classes, and afterwards, following the biological analysis, to determine the biomass of fish of individual species. The hauls were conducted after recording fish concentrations along the hydroacoustic transect. It should be noted that pelagic hauls do not have to be carried out exactly along the echo sounding route and the choice of the haul location may also be influenced by such factors as insufficient depth, wind and wave direction, presence of fishing nets or traffic of other vessels. In each case, the decision regarding the location of a pelagic haul was taken by people with many years of experience.

A WP53/64x4 type pelagic trawl with a fine-mesh liner (6 mm mesh size) in the cod-end, with an average horizontal opening of 18 m and a vertical opening of 15 m, was deployed for control catches. The assumed trawling time was 30 minutes per each haul, at a vessel speed of approx. 3 kn. In the case when high concentrations of fish were observed during a haul, the trawling time could be reduced to 15 minutes. For each haul, basic operating data were recorded, including the information on catch time, location and progress. For each haul, hydrological parameters (salinity, temperature and seawater oxygen concentration) were measured throughout the water column.

The operational procedure applied to the catch included:

- sorting fish by species;
- determining the weight of fish of individual species;
- measuring the total length (LT, *longitudo totalis*) of each fish species;
- ichthyological analyses of commercial fish species dominant in the catches.

The ichthyological analysis procedure included:

- measurements of individual length and wet weight (with precision of 1 g);
- determining sex and sexual maturity (gonad maturity stages) according to the revised 9-stage Maier’s scale;

- assessing fish stomach fullness (the 5-point scale adopted in Polish ichthyological surveys was used: 0 – empty stomachs, 1 – 1/4 full stomach, 2 – 1/2 full stomach, 3 – 3/4 full stomach, 4 – stomach completely full or distended with food);
- collecting otoliths to determine the age of a given fish – fish ages were determined after the vessel passage at the NMFRI laboratory.

The process of determining pelagic fish age involves counting winter annuli on the otolith surface under a stereo microscope in reflected light, using magnification appropriate for the herring and the sprat (Aps et al., 1992; Grygiel 2006a, b).

The ichthyological analysis focused on commercial species – the herring and the sprat.

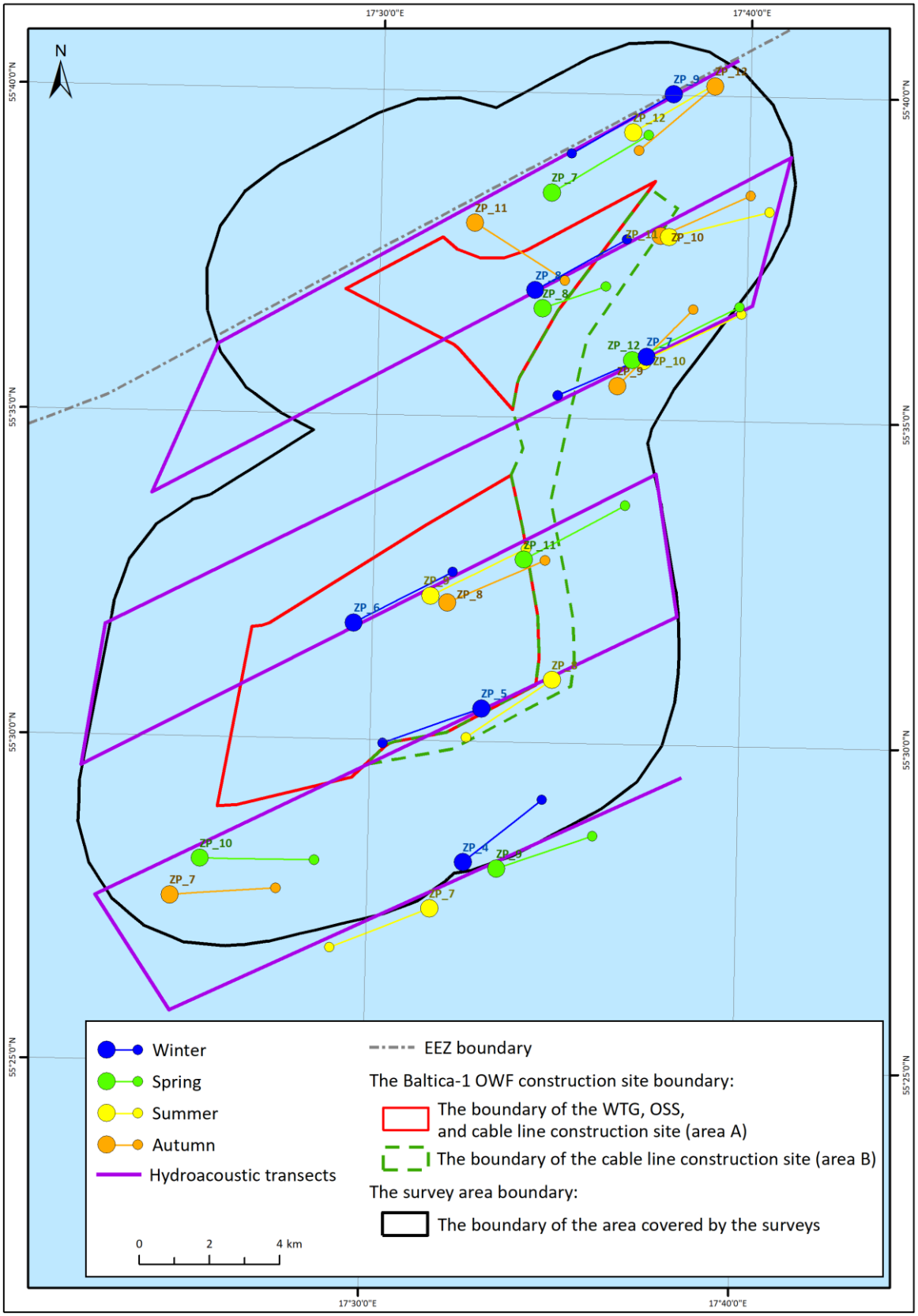


Figure 3.21. The routes of the hydroacoustic transect and pelagic hauls within the survey area

3.3.3.3 Demersal fish surveys

According to the survey methodology applied to demersal fish communities for EIA purposes so far, demersal fish catches were carried out using gillnet sets, including multi-mesh gillnets and nets used in commercial fishing.

Within the survey area [Figure 3.22], 10 survey stations were established for the deployment of the nets. The locations indicated served only as a navigational reference and the actual deployment of nets did not need to be at the exact location indicated.

Salinity and temperature measurements were conducted throughout the water column at the net deployment site.

The design of the gillnet sets accounted for the necessity of non-selective catching of all demersal fish occurring within the area surveyed and the need for assessment of the biological characteristics of the dominant fish species (the cod and flatfish).

Each survey set comprised the following elements:

- 4 standard Nordic coastal multi-mesh gillnet [IEP-NRI, 2020] with a length of 45 m and a height of 1.80 m each, with various mesh sizes in individual panels;
- standard cod fishing nets, with a total length of 165 m, a height of 3.5 m and a 55 mm mesh size;
- standard (scarp) fishing nets designed to catch flat fish (flounder, plaice, scarp), with a total length of 260 m, a height of 1 m and a 130 mm mesh size.

The total length of each survey set was 605 m.

The deployment duration of a single survey set was a minimum of 12 hours, including dusk and dawn hours, which are of particular significance for daily migrations of demersal fish. The catch efficiency (the number and weight of fish caught with each survey set) was calculated for 24 hours of catching time. Such standardisation ensured comparability of results obtained during observations conducted in other survey areas and periods.

At each survey station, surveys were conducted twice.

For each catch location, the following data were recorded:

- date and time of deploying and retrieving the gear;
- geographical position of gear deployment points (longitude and latitude in the GPS format);
- depth at the beginning and end of the gear set;
- conditions during the catch.

The operational procedure applied to the catch included:

- taking fish out from the multi-mesh survey nets;
- sorting fish by species;
- determining the weight of fish of individual species (separately for each type of gear);
- measuring the length of fish of individual species (separately for each type of gear);
- ichthyological analysis of the fish species predominant in the catch and target fish species.

Fish length measurements were conducted with an accuracy of up to 1.0 cm (rounded down), except for clupeids and ammodytids, for which the length measurement accuracy was up to 0.5 cm.

The ichthyological analysis procedure included:

- measurements of individual length and wet weight (with precision of 1 g);
- determining sex and sexual maturity (gonad maturity stages) according to the revised 9-stage Maier's scale;
- assessing fish stomach fullness (the 5-point scale adopted in Polish ichthyological surveys was used: 0 – empty stomachs, 1 – 1/4 full stomach, 2 – 1/2 full stomach, 3 – 3/4 full stomach, 4 – stomach completely full or distended with food);
- collecting otoliths to determine the age of a given fish – fish ages were determined after the vessel passage at the NMFRI laboratory.

Ages of demersal fish were determined at the NMFRI laboratory. For the cod, the reading was conducted on a sectioned otolith, and for flat fish, the reading was conducted on stained, thin otolith sections cut out from its core. In both cases, the age was determined by counting the annual rings of the otoliths in two different directions, using stereo microscopes and an appropriate magnification. The age reading for other species was carried out with a binocular microscope using reflected light, which will not require the otoliths to be prepared in the manner described above.

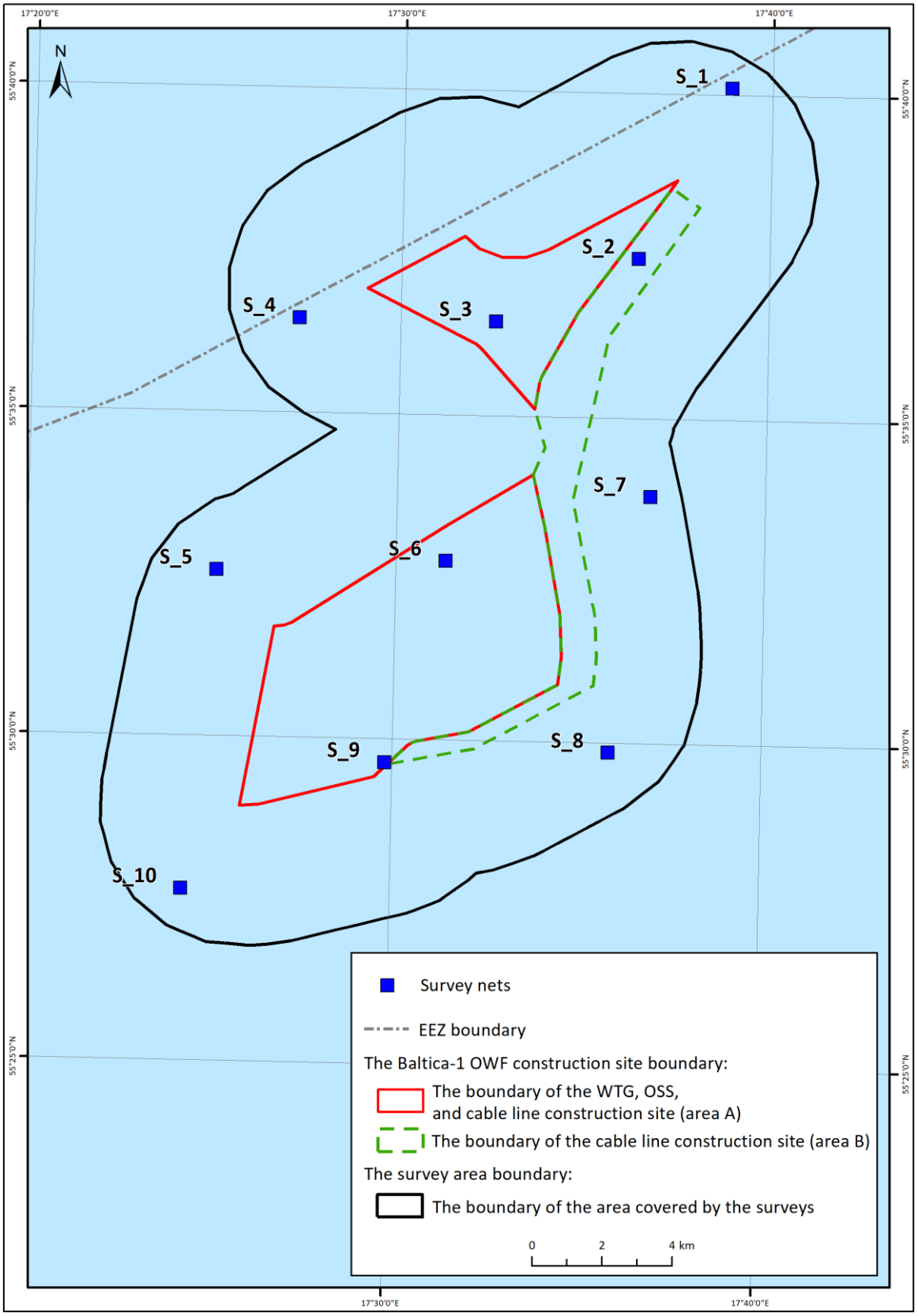


Figure 3.22. The locations of the survey stations for gillnet deployment within the survey area

3.3.3.4 Herring concentration surveys

Herring concentration surveys were carried out using survey nets including nets used in commercial herring fishing and multi-mesh nets (herring gillnets). To capture the relationship between the occurrence of herring and bird feeding, 12 vessel passages were conducted in March, April, August, September, October, and November 2023. Initially, it was planned to conduct 2 vessel passages in each of the above-mentioned months, but weather conditions allowed only 1 series of studies to be conducted in October. Hence, an additional vessel passage was conducted in November. The dates of the vessel passages coincided with the dates of the avifauna surveys. The surveys were conducted at seven survey stations located along the observation transects along which bird counts were conducted from vessels [Figure 3.23].

Each survey set comprised the following elements:

- 1 standard Nordic coastal multi-mesh gillnet [IEP-NRI, 2014] with a length of 45 m and a height of 1.80 m each, with various mesh sizes in individual panels;
- standard herring nets, with a total length of 150 m, a height of 2.2 m and a 35 mm mesh size.

The total length of each set was 195 m.

The operational procedure applied to the catch included:

- sorting fish by species;
- determining the weight of fish of individual species;
- measuring the total length (LT, *longitudo totalis*) of each fish species.

Furthermore, an ichthyological analysis of herrings was performed to determine the gonad maturity stages and possible spawning activity.

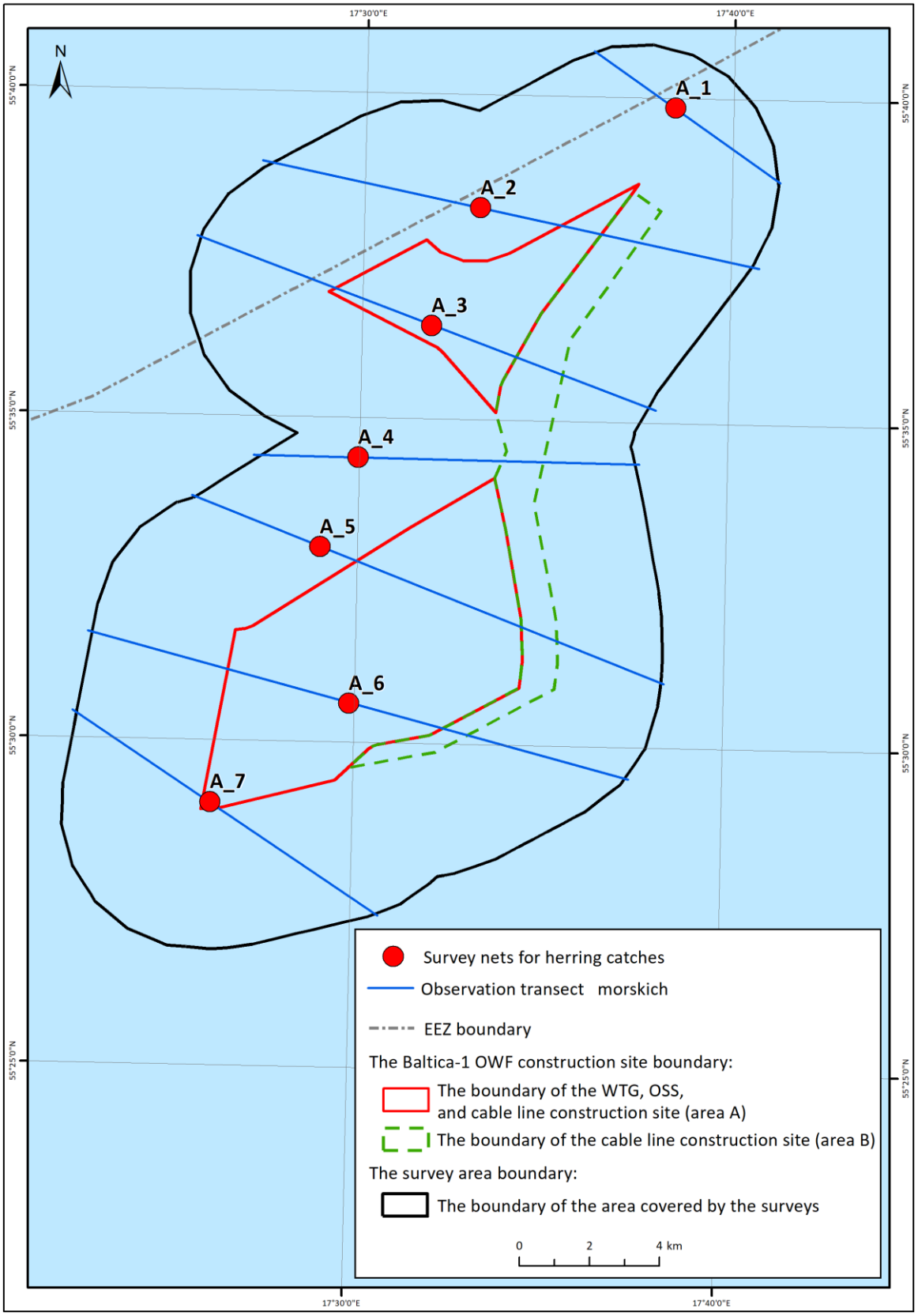


Figure 3.23. The locations of survey stations for the deployment of nets used in commercial herring fishing, together with multi-mesh nets, within the survey area

3.3.4 Activities performed

3.3.4.1 Ichthyoplankton

As part of the surveys, ichthyoplankton catches were conducted at eight survey stations [Table 3.13]. The surveys were carried out between March and October 2023 from aboard the fishing boat UST-204.

Table 3.13. A compilation of the ichthyoplankton catches conducted in the survey area

Survey campaign	Survey station	Two-dimensional Cartesian coordinate system PL-1992 [m]		Depth [m]	Haul duration [min]	Sampling date
		y	x			
Winter	I_1	415211.33	867731.41	50	24	09.03.2023
	I_2	402674.17	861324.50	18	16	09.03.2023
	I_3	412446.07	863059.90	42	20	09.03.2023
	I_4	409189.29	859323.90	32	15	09.03.2023
	I_5	400197.92	854223.83	23	16	09.03.2023
	I_6	406504.51	852495.12	38	19	09.03.2023
	I_7	411566.36	848680.51	54	24	09.03.2023
	I_8	399337.14	845117.09	44	21	09.03.2023
Spring	I_1	414521.99	868143.65	50	20	28.04.2023
	I_2	402363.97	861541.03	18	15	28.04.2023
	I_3	412037.50	863567.06	41	16	28.04.2023
	I_4	408632.33	859767.68	32	16	28.04.2023
	I_5	399929.60	854864.34	21	16	28.04.2023
	I_6	406502.25	853572.85	37	18	28.04.2023
	I_7	411399.64	849028.86	53	19	28.04.2023
	I_8	399159.98	845711.02	44	16	28.04.2023
Summer	I_1	415268.47	868309.00	50	21	14.08.2023
	I_2	402431.34	861830.75	19	15	14.08.2023
	I_3	412471.15	863630.69	41	19	14.08.2023
	I_4	408971.69	860074.08	33	26	14.08.2023
	I_5	400225.09	854770.42	22	16	14.08.2023
	I_6	406506.85	853097.90	37	17	14.08.2023
	I_7	411305.06	849193.99	53	31	14.08.2023
	I_8	399211.33	845652.34	43	15	14.08.2023
Autumn	I_1	415002.56	868219.58	49	21	22.10.2023
	I_2	402564.49	861727.62	17	15	22.10.2023
	I_3	412298.46	863700.93	41	19	22.10.2023
	I_4	408809.83	859917.93	30	18	22.10.2023
	I_5	399968.32	854809.67	21	15	22.10.2023
	I_6	406346.52	852930.68	37	18	22.10.2023
	I_7	411426.48	849054.29	50	25	22.10.2023
	I_8	399250.64	845619.91	43	19	22.10.2023

3.3.4.2 Hydroacoustic surveys and pelagic hauls

Pelagic trawl catches were conducted at 24 survey stations as part of the one-year-long campaign [Table 3.14]. The surveys were carried out from February to November 2023 from aboard UST-204.

Table 3.14. A compilation of pelagic trawl hauls conducted in the survey area

Survey campaign	Survey station	Two-dimensional Cartesian coordinate system PL-1992 [m]				Depth [m]	Catch duration [min]	Sampling date
		Start		End				
		x	y	x	y			
Winter	ZP_4	407930.25	846121.38	410189.72	847892.33	52.0	30	14.02.2023
	ZP_5	408453.72	850506.40	405643.15	849527.21	45.0	30	14.02.2023
	ZP_6	404822.63	852957.93	407641.02	854400.09	36.0	30	15.02.2023
	ZP_7	413178.97	860537.57	410636.08	859438.79	37.0	30	15.02.2023
	ZP_8	410004.52	862438.05	412615.86	863887.47	39.0	30	16.02.2023
	ZP_9	413946.40	868034.40	411049.59	866330.39	45.0	30	16.02.2023
Spring	ZP_7	410476.92	865224.36	413236.42	866866.60	36.0	30	31.05.2023
	ZP_8	410206.45	861918.99	412015.47	862539.70	36.0	20	31.05.2023
	ZP_9	408885.83	845937.23	411628.64	846859.77	54.0	30	04.06.2023
	ZP_10	400424.63	846242.79	403689.26	846187.39	42.0	30	04.06.2023
	ZP_11	409673.17	854747.47	412567.15	856296.11	38.0	30	04.06.2023
	ZP_12	412757.04	860438.16	415832.86	861943.80	36.0	30	04.06.2023
Summer	ZP_7	406978.81	844804.44	404122.90	843692.21	52.0	30	11.08.2023
	ZP_8	410468.78	851317.49	408022.90	849678.51	46.0	30	11.08.2023
	ZP_9	407010.93	853720.62	409734.80	855061.30	37.0	30	11.08.2023
	ZP_10	413067.47	860412.17	415890.04	861737.49	36.0	30	11.08.2023
	ZP_11	413813.03	863948.26	416689.69	864653.84	43.0	30	12.08.2023
	ZP_12	412789.51	866937.61	415181.11	868339.26	45.0	30	12.08.2023
Autumn	ZP_7	399572.08	845204.46	402580.06	845389.04	43.0	30	12.11.2023
	ZP_8	407487.92	853524.11	410272.72	854725.66	39.0	30	13.11.2023
	ZP_9	412340.03	859706.65	414506.45	861883.96	37.0	30	12.11.2023
	ZP_10	413575.73	863977.81	416144.38	865120.37	42.0	30	18.11.2023
	ZP_11	408282.44	864365.83	410851.07	862717.48	34.0	30	18.11.2023
	ZP_12	415135.25	868250.38	412961.27	866421.69	45.0	30	18.11.2023

3.3.4.3 Demersal fish surveys

As part of the winter campaign, catches with bottom-set gillnets were conducted at 10 survey stations. The surveys were carried out from February to November 2023 from aboard the fishing boats UST-52 and UST-125 [Table 3.15].

Table 3.15. A compilation of the catches with bottom-set gillnets conducted in the survey area

Survey campaign	Survey station	Re-run	Two-dimensional Cartesian coordinate system PL-1992 [m]				Depth [m]	Sampling date
			Start		End			
			X	Y	X	Y		
Winter	S_1	1	415048.52	868157.47	415590.16	868139.54	50	15.02.2023
	S_2	1	412338.88	863262.37	412850.89	863359.71	40	15.02.2023
	S_3	1	408306.72	861471.71	408824.87	861596.27	33	15.02.2023
	S_4	1	402677.36	861656.47	403185.96	861721.23	18	15.02.2023
	S_5	1	400160.18	854460.27	400707.42	854520.18	25	15.02.2023
	S_6	1	406793.71	854664.73	407281.19	854691.48	35	15.02.2023
	S_7	1	412532.70	856521.78	413032.82	856563.76	42	15.02.2023
	S_8	1	411383.20	849205.40	411876.62	849238.13	53	15.02.2023
	S_9	1	404912.79	848960.54	405303.57	848965.07	41	15.02.2023
	S_10	1	398976.82	845353.51	399492.21	845399.20	44	15.02.2023
	S_1	2	415040.18	868159.49	415591.97	868124.67	49	16.02.2023
	S_2	2	412334.76	863266.17	412906.78	863267.71	41	16.02.2023
	S_3	2	408298.99	861503.40	408858.46	861545.49	33	16.02.2023
	S_4	2	402656.11	861692.19	403190.22	861676.61	18	16.02.2023
	S_5	2	400191.13	854479.97	400786.09	854510.97	25	16.02.2023
	S_6	2	406824.43	854675.21	407343.99	854677.17	35	16.02.2023
	S_7	2	412573.79	856526.53	413068.93	856529.65	41	16.02.2023
	S_9	2	411395.30	849231.12	411951.95	849214.36	53	16.02.2023
	S_9	2	404806.56	848966.55	405266.13	848938.06	41	16.02.2023
	S_10	2	399015.07	845321.10	399461.20	845425.88	44	16.02.2023
Spring	S_1	1	414707.92	868216.05	415227.43	868192.94	47.81	19.05.2023
	S_2	1	411976.52	863301.19	412492.75	863294.53	37	19.05.2023
	S_3	1	407997.27	861535.71	408496.92	861528.93	31	19.05.2023

Survey campaign	Survey station	Re-run	Two-dimensional Cartesian coordinate system PL-1992 [m]				Depth [m]	Sampling date
			Start		End			
			X	Y	X	Y		
	S_4	1	402374.40	861631.69	402925.33	861663.94	17	19.05.2023
	S_5	1	400541.96	854459.00	400040.55	854472.27	22	19.05.2023
	S_6	1	407089.95	854649.16	406613.82	854711.22	33	19.05.2023
	S_7	1	412858.05	856496.75	412370.13	856539.87	39	19.05.2023
	S_8	1	411188.56	849264.98	411691.32	849186.21	49	19.05.2023
	S_9	1	405473.51	848983.67	404841.34	848967.65	37	19.05.2023
	S_10	1	399069.98	845325.40	399473.30	845494.24	41	19.05.2023
	S_1	2	415381.36	868184.39	414801.18	868214.23	47	20.05.2023
	S_2	2	412573.27	863331.87	412081.47	863300.93	38	20.05.2023
	S_3	2	408578.67	861521.66	408054.49	861560.47	32	20.05.2023
	S_4	2	403079.65	861662.37	402542.26	861672.46	17	20.05.2023
	S_5	2	400585.56	854480.27	399913.19	854514.13	19	20.05.2023
	S_6	2	407068.74	854690.42	406490.99	854721.26	33	20.05.2023
	S_7	2	412868.10	856526.23	412279.92	856549.10	39	20.05.2023
	S_8	2	411754.01	849214.62	411112.37	849246.12	50	20.05.2023
	S_9	2	405489.10	848974.06	404947.03	848985.76	39	20.05.2023
	S_10	2	399392.05	845444.16	398809.12	845394.47	42	20.05.2023
Summer	S_1	1	414783.81	868011.65	415159.31	868258.82	23	17.08.2023
	S_2	1	412214.81	863193.83	412600.49	863433.90	40	17.08.2023
	S_3	1	407926.20	861686.15	408388.98	861513.94	32	17.08.2023
	S_4	1	402398.68	861567.15	402827.15	861743.84	18	17.08.2023
	S_5	1	400459.50	854477.57	399980.10	854501.10	25	17.08.2023
	S_6	1	407013.83	854714.59	406542.64	854737.04	33	17.08.2023
	S_7	1	412929.27	856547.27	412490.85	856531.89	40	17.08.2023

Survey campaign	Survey station	Re-run	Two-dimensional Cartesian coordinate system PL-1992 [m]				Depth [m]	Sampling date
			Start		End			
			X	Y	X	Y		
	S_8	1	411103.83	849229.78	411591.19	849207.51	50	17.08.2023
	S_9	1	404816.44	848786.04	405275.51	848992.02	39	17.08.2023
	S_10	1	399395.57	845372.10	398967.04	845487.66	42	17.08.2023
	S_1	2	414753.24	868143.02	415248.34	868179.18	48	07.09.2023
	S_2	2	412011.25	863269.33	412502.38	863308.62	40	07.09.2023
	S_3	2	407821.82	861541.07	408308.71	861536.21	31	07.09.2023
	S_4	2	402335.60	861638.86	402818.13	861635.90	18	07.09.2023
	S_5	2	400516.31	854469.05	400028.05	854454.56	19	07.09.2023
	S_6	2	407055.36	854728.91	406560.11	854683.06	32	07.09.2023
	S_7	2	412901.68	856512.95	412414.51	856525.07	39	07.09.2023
	S_8	2	411116.21	849206.90	411596.17	849208.90	51	07.09.2023
	S_9	2	404764.56	848957.63	405265.02	848969.61	39	07.09.2023
	S_10	2	398986.29	845371.29	399497.58	845366.80	42	07.09.2023
Autumn	S_1	1	415071.72	868164.44	414610.75	868179.00	48	28.10.2023
	S_2	1	412375.75	863269.05	411880.61	863280.87	38	28.10.2023
	S_3	1	408343.89	861491.33	407823.16	861494.86	30	28.10.2023
	S_4	1	402705.68	861702.21	402178.70	861708.41	17	28.10.2023
	S_5	1	400227.51	854460.59	399711.13	854463.10	19	28.10.2023
	S_6	1	406825.25	854664.06	406354.28	854672.24	32	28.10.2023
	S_7	1	412573.82	856528.38	412093.76	856543.56	39	28.10.2023
	S_8	1	411450.04	849178.08	411020.77	849194.18	50	28.10.2023
	S_9	1	405252.96	848962.46	404793.08	848976.11	39	28.10.2023
	S_10	1	399237.48	845367.93	398783.11	845363.53	42	28.10.2023
	S_1	2	415071.72	868164.44	414610.75	868179.00	48	28.10.2023

Survey campaign	Survey station	Re-run	Two-dimensional Cartesian coordinate system PL-1992 [m]				Depth [m]	Sampling date
			Start		End			
			X	Y	X	Y		
	S_2	2	412375.75	863269.05	411880.61	863280.87	38	28.10.2023
	S_3	2	408343.89	861491.33	407823.16	861494.86	30	28.10.2023
	S_4	2	402705.68	861702.21	402178.70	861708.41	17	28.10.2023
	S_5	2	400227.51	854460.59	399711.13	854463.10	19	28.10.2023
	S_6	2	406825.25	854664.06	406354.28	854672.24	32	28.10.2023
	S_7	2	412573.82	856528.38	412093.76	856543.56	39	28.10.2023
	S_8	2	411450.04	849178.08	411020.77	849194.18	50	28.10.2023
	S_9	2	405252.96	848962.46	404793.08	848976.11	39	28.10.2023
	S_10	2	399237.48	845367.93	398783.11	845363.53	42	28.10.2023

3.3.4.4 Herring concentration surveys

Herring concentration studies were conducted from the UST-52 and UST-125 cutters in March, April, August, September, October and November 2023. Initially, 2 vessel passages were planned for each of the above-mentioned months, but weather conditions allowed only 1 series of studies to be conducted in October. Hence, an additional vessel passage was conducted in November. In each vessel passage, catches were conducted at seven survey stations situated along the seabird observation transects. The Vessel passage dates coincided with the dates of seabird surveys [Table 3.16].

Table 3.16. A list of the catches with herring gillnets carried out as part of the herring concentration surveys within the survey area

Month	Survey station	Deployment no.	Two-dimensional Cartesian coordinate system PL-1992 [m]				Depth [m]	Sampling date
			Start		End			
			x	Y	x	y		
March	A_1	1	414356.29	867712.87	414577.86	867730.78	48	01.03.2023
	A_2	1	408762.24	864880.71	408982.63	864883.53	40	01.03.2023
	A_3	1	407262.10	861577.21	407515.57	861547.73	29	01.03.2023
	A_4	1	405228.17	857792.29	405454.10	857791.11	20	01.03.2023
	A_5	1	403908.53	855220.46	404136.93	855230.29	20	01.03.2023
	A_6	1	404889.10	850782.55	405124.89	850783.01	31	01.03.2023
	A_7	1	400938.78	847946.57	401154.18	847969.54	38	01.03.2023
	A_1	2	414468.68	867669.86	414697.58	867687.63	48	21.03.2023
	A_2	2	408945.80	864878.74	408923.23	864903.32	40	21.03.2023
	A_3	2	407500.17	861514.66	407542.31	861521.19	29	21.03.2023
	A_4	2	405426.79	857743.47	405443.80	857752.38	20	21.03.2023
	A_5	2	404342.98	855179.42	404539.00	855151.03	20	21.03.2023
	A_6	2	405043.57	850721.70	405202.08	850701.58	31	21.03.2023
	A_7	2	401174.15	847920.87	401329.97	847917.36	37	21.03.2023
April	A_1	3	414377.54	867727.29	414615.04	867702.23	49	06.04.2023
	A_2	3	408825.24	864883.11	409051.92	864835.72	35	06.04.2023
	A_3	3	407277.04	861489.71	407505.07	861497.87	29	06.04.2023
	A_4	3	405266.48	857765.49	405469.41	857770.38	20	06.04.2023
	A_5	3	404114.29	855204.82	404321.68	855215.13	20	06.04.2023
	A_6	3	404947.78	850721.92	405159.54	850730.32	30	06.04.2023
	A_7	3	400878.60	847986.89	401093.62	847993.17	38	06.04.2023
	A_1	4	414490.36	867706.53	414253.51	867711.18	48	22.04.2023
	A_2	4	408911.08	864873.90	408667.62	864871.56	33	22.04.2023

Month	Survey station	Deployment no.	Two-dimensional Cartesian coordinate system PL-1992 [m]				Depth [m]	Sampling date
			Start		End			
			x	Y	x	y		
	A_3	4	407522.53	861529.03	407299.14	861541.18	29	22.04.2023
	A_4	4	405438.43	857746.93	405223.29	857760.86	15	22.04.2023
	A_5	4	404367.56	855197.43	404148.05	855209.65	19	22.04.2023
	A_6	4	405193.69	850751.84	404976.83	850750.97	31	22.04.2023
	A_7	4	401168.04	847930.28	400946.66	847922.28	37	22.04.2023
August	A_1	5	414344.65	867707.53	414583.97	867721.39	46	05.08.2023
	A_2	5	408753.11	864845.66	409031.03	864839.86	33	05.08.2023
	A_3	5	406982.05	861393.96	407212.51	861466.97	28	05.08.2023
	A_4	5	405176.79	857748.88	405387.76	857785.13	16	05.08.2023
	A_5	5	404080.21	855088.71	404312.82	855146.69	19	05.08.2023
	A_6	5	404979.97	850652.59	405194.27	850681.35	28	05.08.2023
	A_7	5	401063.39	847960.46	401250.96	847963.66	36	05.08.2023
	A_1	6	414466.65	867673.61	414701.49	867672.72	47	14.08.2023
	A_2	6	408907.47	864851.71	409143.36	864843.09	33	14.08.2023
	A_3	6	407534.89	861517.64	407809.05	861522.98	30	14.08.2023
	A_4	6	405424.04	857762.08	405670.66	857745.63	15	14.08.2023
	A_5	6	404353.81	855194.02	404587.47	855203.76	19	14.08.2023
	A_6	6	405185.27	850752.03	405440.90	850744.65	32	14.08.2023
	A_7	6	401173.43	847935.72	401417.39	847917.25	37	14.08.2023
September	A_1	7	414452.14	867676.49	414716.74	867712.67	47	08.09.2023
	A_2	7	408805.88	864830.09	409022.35	864841.16	33	08.09.2023
	A_3	7	407513.87	861377.67	407530.32	861584.70	27	08.09.2023
	A_4	7	405390.97	857622.57	405431.13	857822.59	16	08.09.2023
	A_5	7	404196.72	855146.26	404391.85	855216.56	17	08.09.2023

Month	Survey station	Deployment no.	Two-dimensional Cartesian coordinate system PL-1992 [m]				Depth [m]	Sampling date
			Start		End			
			x	Y	x	y		
	A_6	7	405058.03	850694.31	405280.40	850745.70	28	08.09.2023
	A_7	7	401043.58	847964.80	401261.19	847983.27	36	08.09.2023
	A_1	8	414755.87	867810.77	414587.26	867712.98	47	26.09.2023
	A_2	8	409079.15	864939.03	408880.48	864900.69	33	26.09.2023
	A_3	8	407732.23	861524.97	407539.75	861459.66	29	26.09.2023
	A_4	8	405614.90	857859.80	405417.44	857811.38	15	26.09.2023
	A_5	8	404516.01	855273.40	404327.60	855216.48	19	26.09.2023
	A_6	8	405208.28	850905.67	405235.00	850680.65	29	26.09.2023
	A_7	8	401356.27	848009.52	401151.81	847962.55	36	26.09.2023
October	A_1	10	414558.12	867686.65	414321.48	867702.42	48	22.10.2023
	A_2	10	409043.53	864885.98	408845.32	864890.11	33	22.10.2023
	A_3	10	407613.81	861575.33	407434.08	861467.84	30	22.10.2023
	A_4	10	405564.35	857786.88	405366.16	857709.54	16	22.10.2023
	A_5	10	404361.05	855332.98	404353.25	855119.84	19	22.10.2023
	A_6	10	405202.74	850829.55	405286.87	850631.12	29	22.10.2023
	A_7	10	401287.01	847927.60	401089.89	847920.91	37	22.10.2023
November	A_1	11	414501.67	867695.18	414758.48	867692.01	46	11.11.2023
	A_2	11	408850.84	864852.90	409092.20	864855.28	33	11.11.2023
	A_3	11	407499.16	861516.54	407738.77	861526.32	29	11.11.2023
	A_4	11	405430.35	857761.95	405647.59	857747.98	17	11.11.2023
	A_5	11	404345.93	855218.31	404653.69	855202.32	19	11.11.2023
	A_6	11	405195.80	850751.80	405427.26	850746.80	31	11.11.2023
	A_7	11	401183.75	847926.22	401416.47	847922.84	38	11.11.2023
	A_1	12	414297.23	867695.48	414513.13	867691.24	47	29.11.2023

Month	Survey station	Deployment no.	Two-dimensional Cartesian coordinate system PL-1992 [m]				Depth [m]	Sampling date
			Start		End			
			x	Y	x	y		
	A_2	12	408800.54	864855.80	409016.11	864879.13	33	29.11.2023
	A_3	12	407408.33	861540.72	407638.17	861535.86	27	29.11.2023
	A_4	12	405300.25	857772.18	405536.64	857768.93	17	29.11.2023
	A_5	12	404478.45	855219.12	404245.96	855214.93	20	29.11.2023
	A_6	12	405285.07	850742.45	405071.32	850787.88	30	29.11.2023
	A_7	12	401345.75	847963.38	401124.50	847914.56	37	29.11.2023
	A_1	9	414256.52	867757.49	414495.17	867684.18	47	30.11.2023
	A_2	9	408731.94	864936.99	408960.18	864863.60	33	30.11.2023
	A_3	9	407350.56	861540.09	407583.83	861548.14	27	30.11.2023
	A_4	9	405285.18	857804.04	405494.79	857729.02	17	30.11.2023
	A_5	9	404181.00	855273.85	404399.70	855176.32	20	30.11.2023
	A_6	9	404992.41	850741.36	405180.13	850757.70	29	30.11.2023
	A_7	9	401277.07	847953.80	401105.34	847905.72	35	30.11.2023

3.3.5 Results

3.3.5.1 Ichthyoplankton

No presence of pelagic eggs was recorded throughout the entire survey period, while the larvae of eight taxa of fish were caught. None of the taxa identified occurred in all survey periods. The larvae of gobies, the common seasnail, the herring and the fourbeard rockling were recorded in two survey seasons. The larvae of the remaining taxa, the sprat, ammodytids, the flounder and the rock gunnel, were observed only in one season. Two out of the taxa recorded, i.e. gobies and the common seasnail, belong to partially protected species pursuant to the Regulation of the Minister of the Environment of 16 December 2016 on the protection of animal species (Journal of Laws of 2016, item 2183, as amended). Although gobies were not identified to species, on the basis of the knowledge from literature, it can be assumed that the dominant species in the samples collected was the sand goby (Horackiewicz and Skóra, 1996; 1998).

Gobies were among the most common taxa caught (28.1% of samples collected) among the larvae observed in two survey seasons. Comparable frequency (25.0% of samples) was observed for sprat and flounder larvae which occurred in one survey period. Lower frequency was recorded for the larvae of the common seasnail (18.8% of samples) that was observed in one survey season only. The frequency of the larvae of the herring, the fourbeard rockling and ammodytids occurring in two survey seasons was 9.4%. The rock gunnel, observed only in one survey season, was the least frequent species (3.1% of samples) [Table 3.17].

Table 3.17. Frequency of larvae occurrence in the samples and the number of survey periods, in which they were found in the survey area

Taxon	Frequency* [%]	Number of periods with the taxon occurrence
Gobies *Gobiidae*	28.1	2
Sprat *Sprattus sprattus*	25.0	1
Flounder *Platichthys flesus*	25.0	1
Common seasnail *Liparis liparis*	18.8	2
Herring *Clupea harengus*	9.4	2
Fourbeard rockling *Enchelyopus cimbrius*	9.4	2
Sand lances *Ammodytidae*	9.4	2
Rock gunnel *Pholis gunnellus*	3.1	1

**the number of samples with the taxon occurrence/number of all samples collected (32)*

350 fish larvae were caught during the surveys, of which sprat larvae comprised the largest proportion (139 ind.; 39.7% of the total abundance of the larvae caught). The share of sand ammodytid larvae was also significant (112 individuals, 32.0%). The larvae of the flounder (49 ind.; 14.0%) and gobies (32 ind.; 9.1%) were observed much less abundantly. The remaining species occurred sparsely and their share in the total abundance of the larvae caught did not exceed 3% [Figure 3.24].

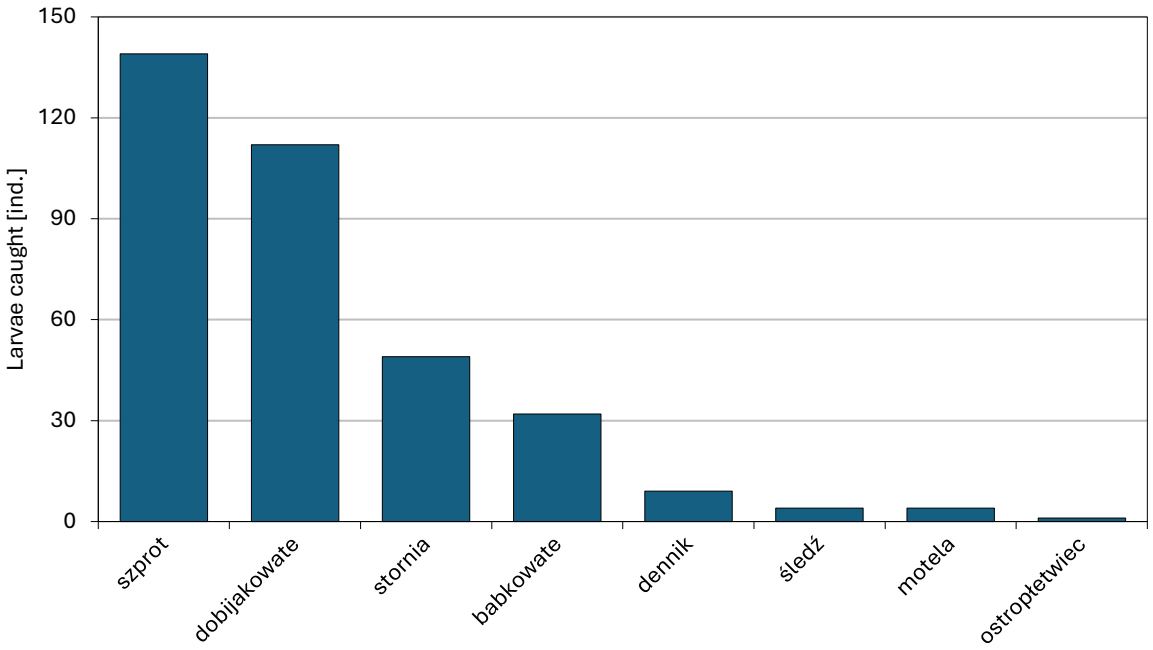


Figure 3.24. Number of larvae caught during the entire survey period in the survey aread

3.3.5.1.1 Ichthyoplankton species composition and abundance in individual survey seasons

3.3.5.1.1.1 Winter

During the surveys conducted in March 2023, no pelagic eggs were found, whereas five larvae belonging to three taxa: the common seasnail (three larvae), the herring and the rock gunnel (one larva each) were caught in the survey area The first taxon mentioned above is partially protected under the Regulation of the Minister of the Environment of 16 December 2016 on the protection of animal species (Journal of Laws of 2016, item 2183 as amended).

The presence of the common seasnail larvae was recorded at three stations. Their abundances ranged from 0.56 ind.·10 m^{-2} at station I_5 to 0.89 ind.·10 m^{-2} at station I_8. The lengths of the specimens ranged from 4.7 to 5.5 mm SL.

A herring larva was caught at station L_6 (abundance – 0.56 ind.·10 m^{-2}, length – 31.3 mm SL). A rock gunnel larva was found at station L_1 (abundance – 0.98 ind.·10 m^{-2}, length – 14.4 mm SL).

The abundance and the average lengths (SL) of the larvae collected at individual stations are presented in the tables below [Table 3.18, Table 3.19].

Table 3.18. Abundance of larvae [ind.·10 m^{-2}] of individual fish taxa at survey stations located in the survey area in winter

Survey station	Sampling date	Abundance [ind.·10 m^{-2}]		
		Herring	Common seasnail	Rock gunnel
I_1	09.03.2023			0.98
I_2	09.03.2023			
I_3	09.03.2023			
I_4	09.03.2023			
I_5	09.03.2023	0.56	0.56	

Survey station	Sampling date	Abundance [ind.·10 m^{-2}]		
		Herring	Common seasnail	Rock gunnel
I_6	09.03.2023		0.83	
I_7	09.03.2023			
I_8	09.03.2023		0.89	

Table 3.19. Average larval length [mm SL] of individual fish taxa at survey stations located in the survey area in winter

Survey station	Sampling date	Average length [mm SL]		
		Herring	Common seasnail	Rock gunnel
I_1	09.03.2023			14.4
I_2	09.03.2023			
I_3	09.03.2023			
I_4	09.03.2023			
I_5	09.03.2023	31.3	5.2	
I_6	09.03.2023		4.7	
I_7	09.03.2023			
I_8	09.03.2023		5.5	

3.3.5.1.1.2 Spring

During the surveys conducted in April 2023, no pelagic eggs were found, whereas 194 larvae belonging to three species, the sprat (139 larvae), the flounder (49 larvae) and the common seasnail (6 larvae), were caught. The last taxon mentioned above is partially protected under the Regulation of the Minister of the Environment of 16 December 2016 on the protection of animal species (Journal of Laws 2016, item 2183).

The sprat and flounder larvae were caught at all stations. Sprat abundance ranged from 0.38 ind.·10 m^{-2} (station I_2) to 74.88 ind.·10 m^{-2} at station I_7, while flounder abundance ranged from 0.75 ind.·10 m^{-2} at station I_2 to 21.74 ind.·10 m^{-2} at station I_7. The length of sprat larvae varied from 4.2 to 15.8 mm SL. The length of flounder larvae varied from 4.0 to 8.0 mm SL.

The common seasnail was identified at three stations, reaching the abundances between 1.05 and 1.64 ind.·10 m^{-2}. The length of the larvae measured was within the range 4.5–11.4 mm SL.

The abundance and the average lengths (SL) of the larvae collected at individual stations are presented in the tables below [Table 3.20, Table 3.21].

Table 3.20. Abundance of larvae [ind.·10 m^{-2}] of individual fish taxa at survey stations located in the survey area in spring

Survey station	Sampling date	Abundance [ind.·10 m^{-2}]		
		Sprat	Flounder	Common seasnail
I_1	28.04.2023	13.58	10.45	
I_2	28.04.2023	0.38	1.13	
I_3	28.04.2023	10.54	2.11	1.05
I_4	28.04.2023	2.98	0.75	
I_5	28.04.2023	0.41	1.23	1.64

Survey station	Sampling date	Abundance [ind.·10 m^{-2}]		
		Sprat	Flounder	Common seasnail
I_6	28.04.2023	4.24	2.54	
I_7	28.04.2023	74.88	21.74	1.21
I_8	28.04.2023	48.03	10.05	

Table 3.21. Average larval length [mm SL] of individual fish species at survey stations located in the survey area in spring

Survey station	Sampling date	Average length [mm SL]		
		Sprat	Flounder	Common seasnail
I_1	28.04.2023	10.0	5.7	
I_2	28.04.2023	8.6	5.6	
I_3	28.04.2023	10.3	6.9	7.8
I_4	28.04.2023	10.5	6.4	
I_5	28.04.2023	13.5	6.2	6.0
I_6	28.04.2023	9.8	6.4	
I_7	28.04.2023	7.8	5.7	11.4
I_8	28.04.2023	8.5	5.6	

3.3.5.1.1.3 Summer

During the surveys conducted in August 2023, no pelagic eggs were found, whereas 33 larvae belonging to three taxa, gobies (30 larvae), the fourbeard rockling (2 larvae) and ammodytids (1 larva), were caught.

The larvae of gobies occurred at all survey stations, with the exception of survey station I_5. Their abundance ranged from 0.36 ind.·10 m^{-2} (station I_2) to 5.84 ind.·10 m^{-2} at station I_4. The length of the larvae measured was within the range 3.5–8.7 mm SL.

The larvae of the fourbeard rockling were found only at station I_7 with an abundance of 1.64 ind.·10 m^{-2} (length of larvae 5.2- and 6.3-mm SL).

An ammodytid larva was found at station I_3 (abundance – 0.92 ind.·10 m^{-2}, length – 4.3 mm SL).

The abundance and the average lengths (SL) of the larvae collected at individual stations are presented in the tables below [Table 3.22, Table 3.23].

Table 3.22. Abundance of larvae [ind.·10 m^{-2}] of individual fish taxa at survey stations located in the survey area in summer

Survey station	Sampling date	Abundance [ind.·10 m^{-2}]		
		Gobies	Ammodytids	Fourbeard rockling
I_1	14.08.2023	2.19		
I_2	14.08.2023	0.36		
I_3	14.08.2023	5.50	0.92	
I_4	14.08.2023	5.84		
I_5	14.08.2023			
I_6	14.08.2023	5.76		1.64
I_7	14.08.2023	2.34		

Survey station	Sampling date	Abundance [ind.·10 m^{-2}]		
		Gobies	Ammodytids	Fourbeard rockling
I_8	14.08.2023	3.46		

Table 3.23. Average larval length [mm SL] of individual fish species at survey stations located in the survey area in summer

Survey station	Sampling date	Average length [mm SL]		
		Gobies	Ammodytids	Fourbeard rockling
I_1	14.08.2023	5.9		
I_2	14.08.2023	6.7		
I_3	14.08.2023	5.9	4.3	
I_4	14.08.2023	5.4		
I_5	14.08.2023			
I_6	14.08.2023	6.1		5.7
I_7	14.08.2023	6.3		
I_8	14.08.2023	5.9		

3.3.5.1.1.4 Autumn

During the surveys conducted in August 2023, no pelagic eggs were found, whereas eight larvae belonging to four species, the herring (3 individuals), gobies (2 individuals), the fourbeard rockling (2 individuals) and ammodytids (1 individual), were caught.

Herring, gobies and fourbeard rockling larvae occurred at two stations. The abundance of the first taxon was 1.03 ind.·10 m^{-2} at station I_8 and 2.30 ind.·10 m^{-2} at station I_1. Their length ranged from 9.6 to 15.2 mm SL.

The occurrence of gobies was recorded at stations I_1 (1.15 ind.·10 m^{-2}) and I_3 (0.98 ind.·10 m^{-2}). The lengths of the individuals caught ranged from 3.7 to 8.7 mm SL.

The larvae of the fourbeard rockling occurred at stations I_1 and I_2 reaching an abundance of 0.40 ind.·10 m^{-2} and 1.03 ind.·10 m^{-2}, respectively (length range of 5.3 – 6.7 mm SL).

A larva of the greater sand eel with a length of 16.9 mm SL was caught at station I_7 (abundance – 0.91 ind.·10 m^{-2}).

No ichthyoplankton occurrence was recorded at stations I_4, I_5 and I_6.

The abundance and the average lengths (SL) of the larvae collected at individual stations are presented in the tables below [Table 3.24, Table 3.25].

Table 3.24. Abundance of larvae [ind.·10 m^{-2}] of individual fish taxa at survey stations located in the survey area in autumn

Survey station	Sampling date	Abundance [ind.·10 m^{-2}]			
		Herring	Gobies	Fourbeard rockling	Ammodytids
I_1	22.10.2023	2.30	1.15		
I_2	22.10.2023			0.40	
I_3	22.10.2023		0.98		

Survey station	Sampling date	Abundance [ind.·10 m^{-2}]			
		Herring	Gobies	Fourbeard rockling	Ammodytids
I_4	22.10.2023				
I_5	22.10.2023				
I_6	22.10.2023				
I_7	22.10.2023				0.91
I_8	22.10.2023	1.03		1.03	

Table 3.25. Average larval length [mm SL] of individual fish species at survey stations located in the survey area in autumn

Survey station	Sampling date	Average length [mm SL]			
		Herring	Gobies	Fourbeard rockling	Ammodytids
I_1	22.10.2023	11.6	3.7		
I_2	22.10.2023			6.7	
I_3	22.10.2023		8.7		
I_4	22.10.2023				
I_5	22.10.2023				
I_6	22.10.2023				
I_7	22.10.2023				16.9
I_8	22.10.2023	15.2		5.3	

3.3.5.1.2 Variability of ichthyoplankton species composition and abundance between seasons

Fish larvae were recorded during all survey periods. The highest number of taxa was recorded in autumn (four taxa), while in the remaining seasons there were three taxa each [Figure 3.25].

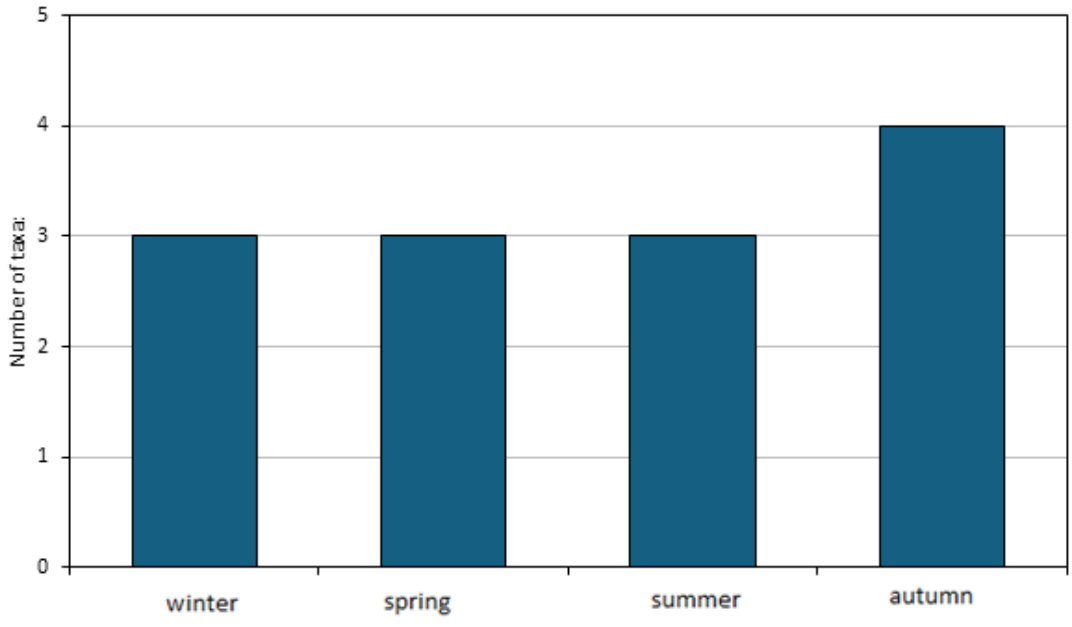


Figure 3.25. Number of ichthyoplankton taxa during individual survey periods in the survey area

The highest total abundance of fish larvae (average for the entire survey area) was recorded in spring at 26.12 ind.·10 m^{-2}. In summer, the total abundance of larvae was lower and equalled 18.58 ind.·10 m^{-2}. Much lower average abundances were recorded in winter and in autumn at 0.48 and 0.97 ind.·10 m^{-2}, respectively [Figure 3.26].

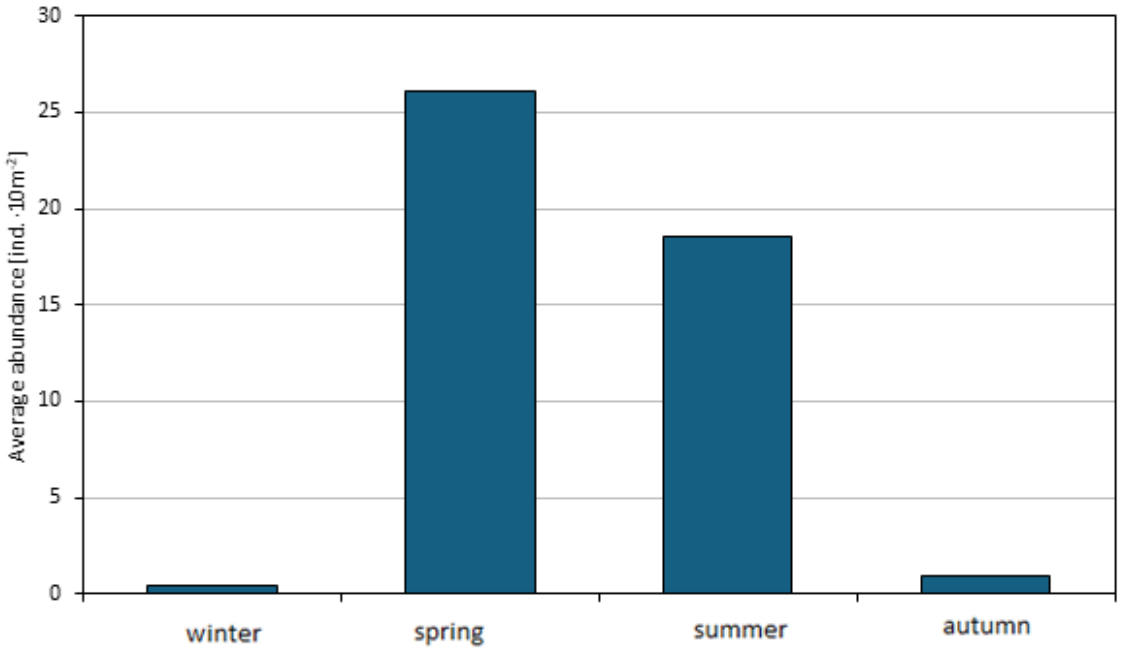


Figure 3.26. Average abundance of fish larvae [ind.·10 m^{-2}] during individual survey periods in the survey area

In winter, the dominance of the common seasnail larvae was recorded, which accounted for 59.7% of the total larvae abundance. The proportion recorded for the rock gunnel larvae was more than twice lower (25.7%), while the lowest proportion was observed for the flounder larvae (14.7%).

In spring, the most important taxa in terms of abundance were the sprat (74.2%) and gobies (23.9%).

In summer, ichthyoplankton was almost completely dominated by ammodytid larvae (81.8%). A significantly lower proportion was observed for the larvae of gobies (17.1%).

In autumn, the significance of goby larvae increased substantially (27.3%); nevertheless, the herring larvae were the most significant component (42.7%). A high proportion in the total ichthyoplankton abundance was also observed for the fourbeard rockling (18.4%) and ammodytid (11.7%) larvae [Figure 3.27].

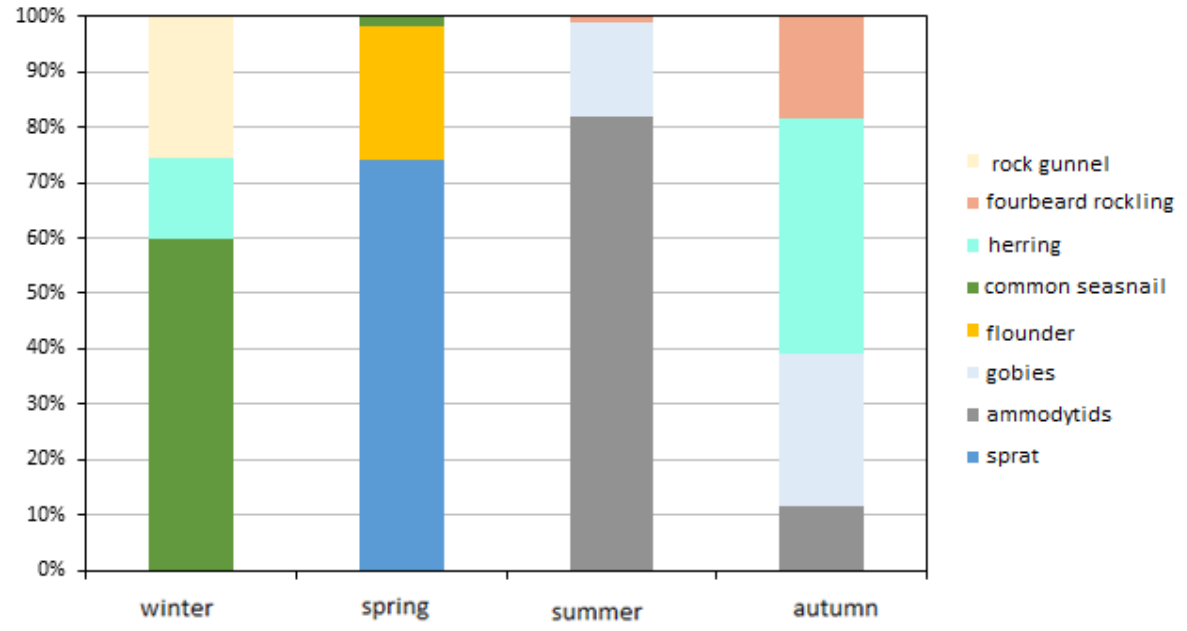


Figure 3.27. The proportion of individual taxa of fish larvae in the average total larval abundance in the survey area during individual survey periods

The sprat, the most important taxon in terms of abundance, only occurred in spring reaching the average abundance of 19.42 ind.·10 m^{-2} in the entire survey area.

Ammodytid larvae, the second taxon in terms of abundance, were the most numerous in summer, while their abundance in autumn was much lower (15.2 ind.·10 m^{-2} and 0.11 ind.·10 m^{-2}, respectively).

The occurrence of flounder larvae was only observed in spring when their abundance reached 6.2 ind.·10 m^{-2}.

Gobies were recorded in summer and autumn, reaching a markedly higher abundance (3.2 ind.·10 m^{-2}) in the first of the seasons.

Common seasnail larvae were found in samples collected in winter and spring. Their abundance reached 0.3 and 0.52 ind.·10 m^{-2}, respectively.

Herring larvae were present in autumn and, very sparsely, in winter (abundance of 0.41 and 0.1 ind.·10 m^{-2}, respectively). Fourbeard rockling larvae were observed in two survey periods – summer and autumn. Their abundance was at a similar level in both seasons (0.2 ind.·10 m^{-2}). The rock gunnel only occurred in winter (abundance of 0.1 ind.·10 m^{-2}) [Figure 3.28].

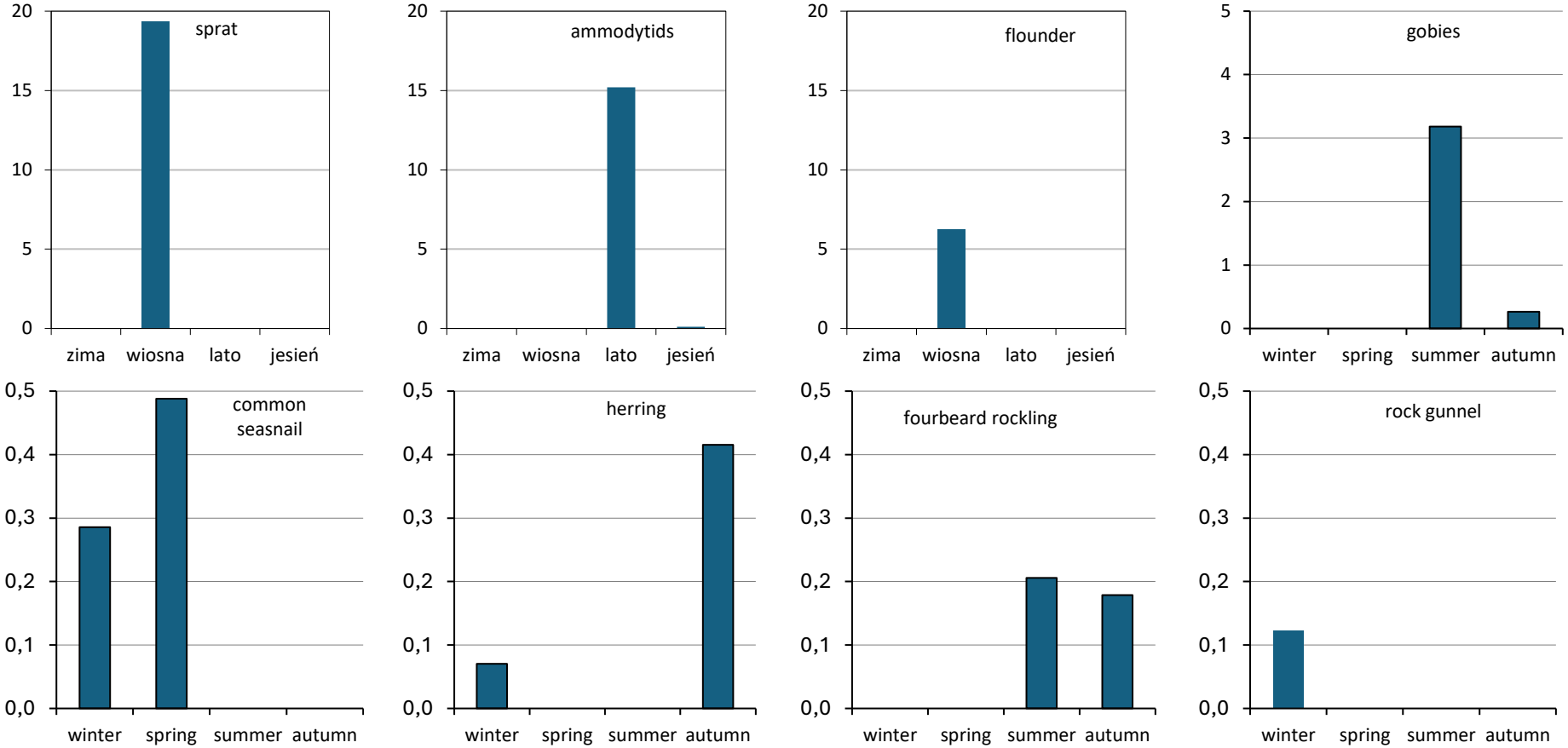


Figure 3.28. Abundance of larvae [ind.·10 m^{-2}] of individual fish species (average for the entire area) in the survey area during individual survey periods

The number of larvae and eggs caught for individual fish taxa, their average abundance for the entire area as well as the average standard length (SL) in particular survey periods are presented in Table 3.26.

Table 3.26. The number of individuals caught [pcs], abundance [pcs/ind.·10 m^{-2}] (average for the entire survey area) and the average standard length [mm SL] of the larvae of individual taxa in the annual cycle for the survey area

Taxon	Season	Number of individuals [pcs]	Abundance [pcs/ind.·10 m^{-2}]	Average standard length [mm SL]
Sprat *Sprattus sprattus*	Winter	-	-	-
	Spring	139	19.38	8.7
	Summer	-	-	-
	Autumn	-	-	-
Ammodytids* *Ammodytids*	Winter	-	-	-
	Spring	-	-	-
	Summer	111	15.19	4.3
	Autumn	1	0.11	16.9
Flounder *Platichthys flesus*	Winter	-	-	-
	Spring	49	6.25	5.8
	Summer	-	-	-
	Autumn	-	-	-
Gobies** *Gobiidae*	Winter	-	-	-
	Spring	-	-	-
	Summer	30	3.18	5.9
	Autumn	2	0.26	6.2
Common seasnail *Liparis liparis*	Winter	3	0.28	5.1
	Spring	6	0.49	7.2
	Summer	-	-	-
	Autumn	-	-	-
Herring *Clupea harengus*	Winter	1	0.07	31.3
	Spring	-	-	-
	Summer	-	-	-
	Autumn	3	0.41	12.8
Fourbeard rockling *Enchelyopus cimbrius*	Winter	-	-	-
	Spring	-	-	-
	Summer	2	0.20	5.7
	Autumn	2	0.18	6.0
Rock gunnel *Pholis gunnellus*	Winter	1	0.12	14.4
	Spring	-	-	-
	Summer	-	-	-
	Autumn	-	-	-

3.3.5.1.3 Spatial distribution

Taking into account the characteristics of the organisms surveyed (larvae drifting in the water column and being dispersed over great distances in a short time) and the relatively small surface of the area surveyed, not too much emphasis should be placed on the differences in the larval spatial distribution.

The key issue might be whether the larvae of a given species occurred occasionally at 1–2 stations, or whether they were observed at the majority of or at all stations. A certain indicator of the spawning ground locations, from which the larvae found within the survey area originate, is the difference in the abundance of the individuals belonging to a given species observed at shallow stations (in the vicinity of banks) in relation to deep stations (e.g., within the Słupsk Furrow, which is located the closest).

The occurrence of sprat larvae was observed at all survey stations only in spring. The highest abundances were observed in the southern part of the survey area, adjacent to the Słupsk Furrow [Figure 3.29].

In summer, ammodytid larvae occurred at two stations, reaching the highest abundance at the most northward sampling point. Only one larva was caught in autumn [Figure 3.30].

Flounder larvae were recorded throughout the entire survey area only in spring. The highest abundances were recorded at deep stations in the southern part of the area [Figure 3.31].

Goby larvae were present in two survey seasons. They were much more abundant in summer, when their presence was recorded at 7 out of 8 stations surveyed. In autumn, the presence of gobies was limited to the two most northward survey stations [Figure 3.32].

Common seasnail larvae were found at three survey stations, both in winter and in spring. In winter, their presence was recorded in the southern and western parts of the survey area, whereas in spring, the larvae were dispersed [Figure 3.33].

Fourbeard rockling larvae only occurred at one of the stations in summer and at two stations in winter. Therefore, there are no grounds for the analysis of their spatial distribution Figure 3.34].

In the case of the herring larvae, which occurred at one of the stations in winter and at two in autumn [Figure 3.35], there were no grounds for the analysis of their spatial distribution in the survey area.

Rock gunnel larvae occurred only in winter at one, most northward survey station [Figure 3.36].

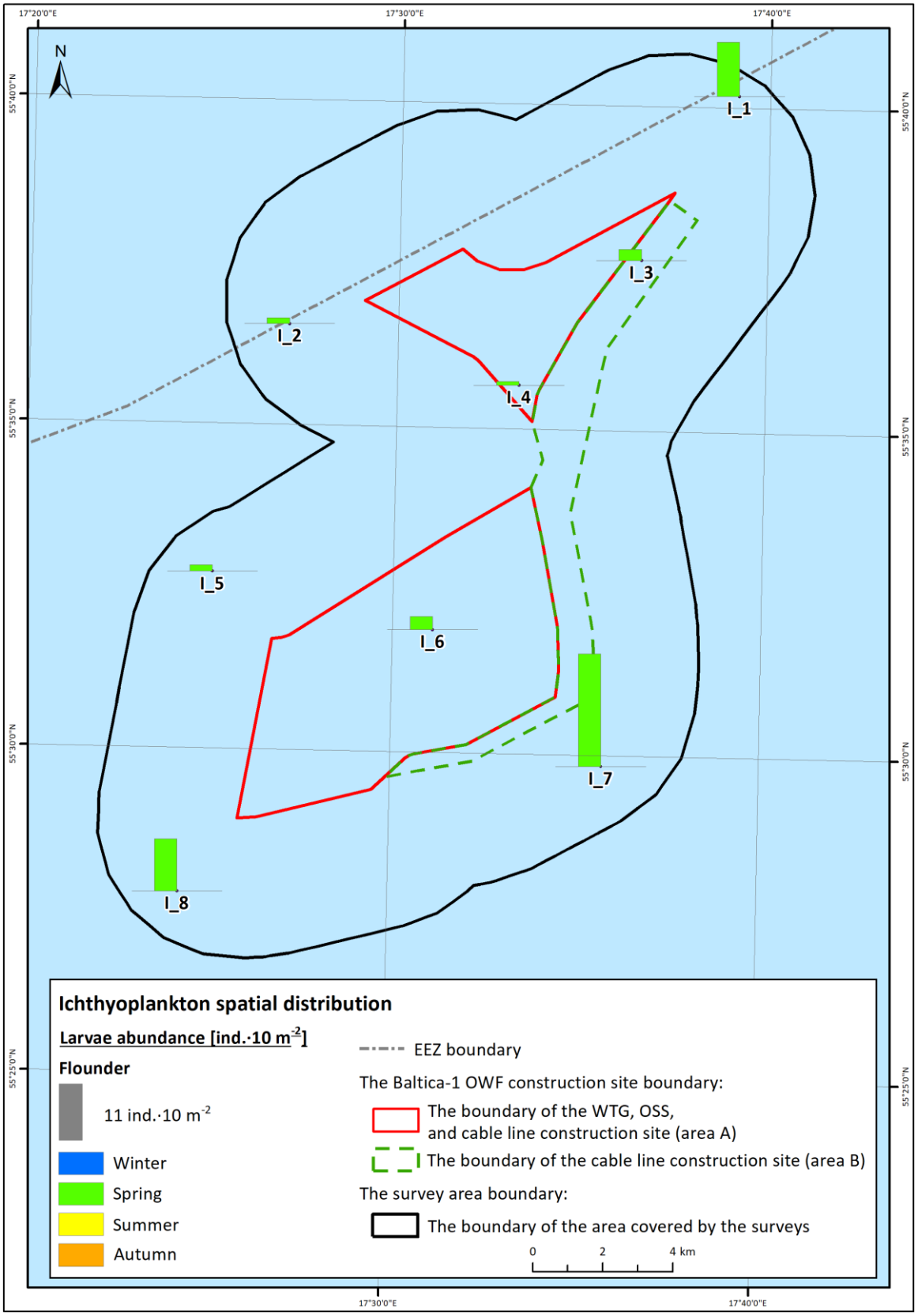


Figure 3.29. Spatial distribution of sprat larvae in the annual cycle within the survey area

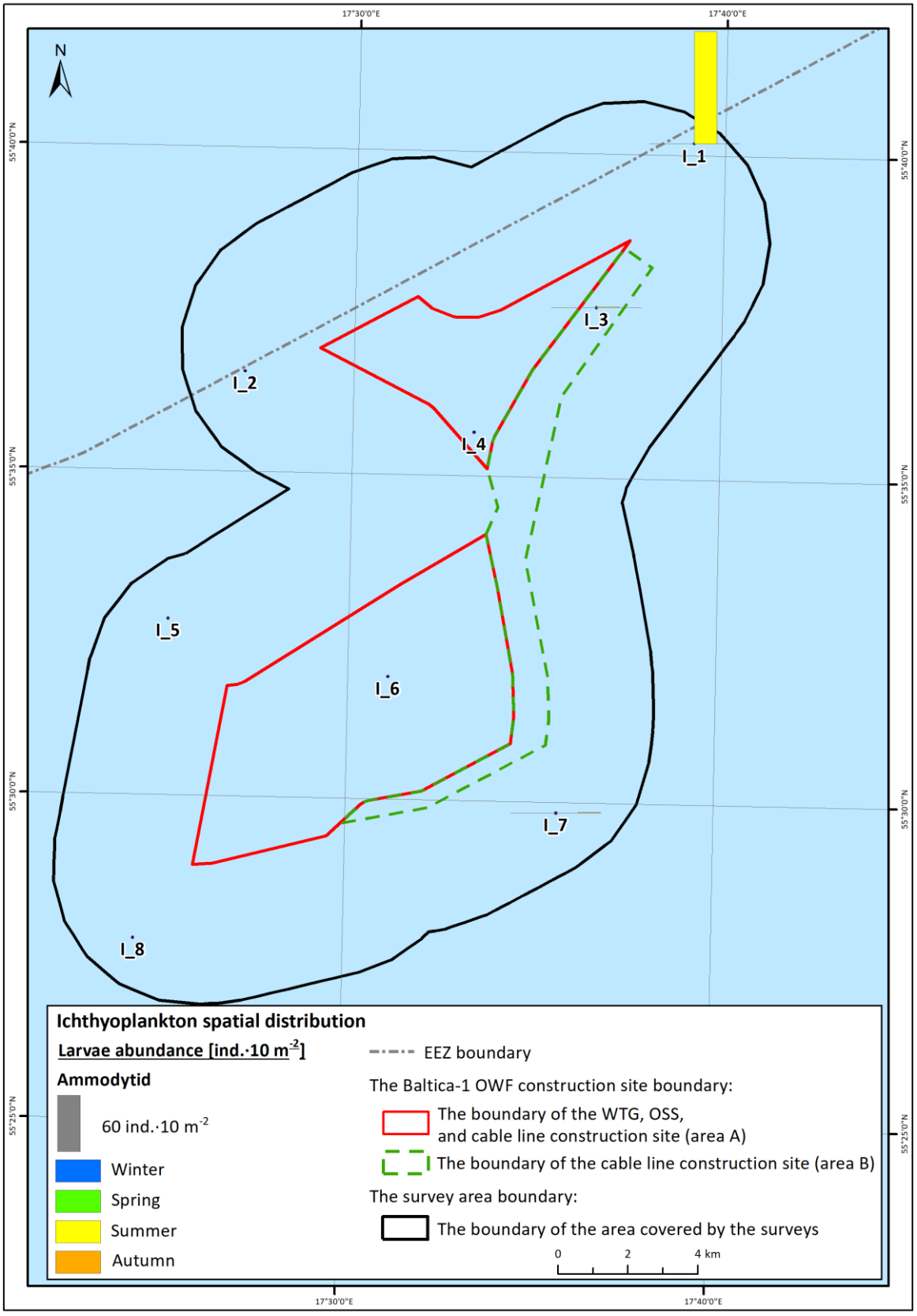


Figure 3.30. Spatial distribution of ammodytid larvae in the annual cycle within the survey area

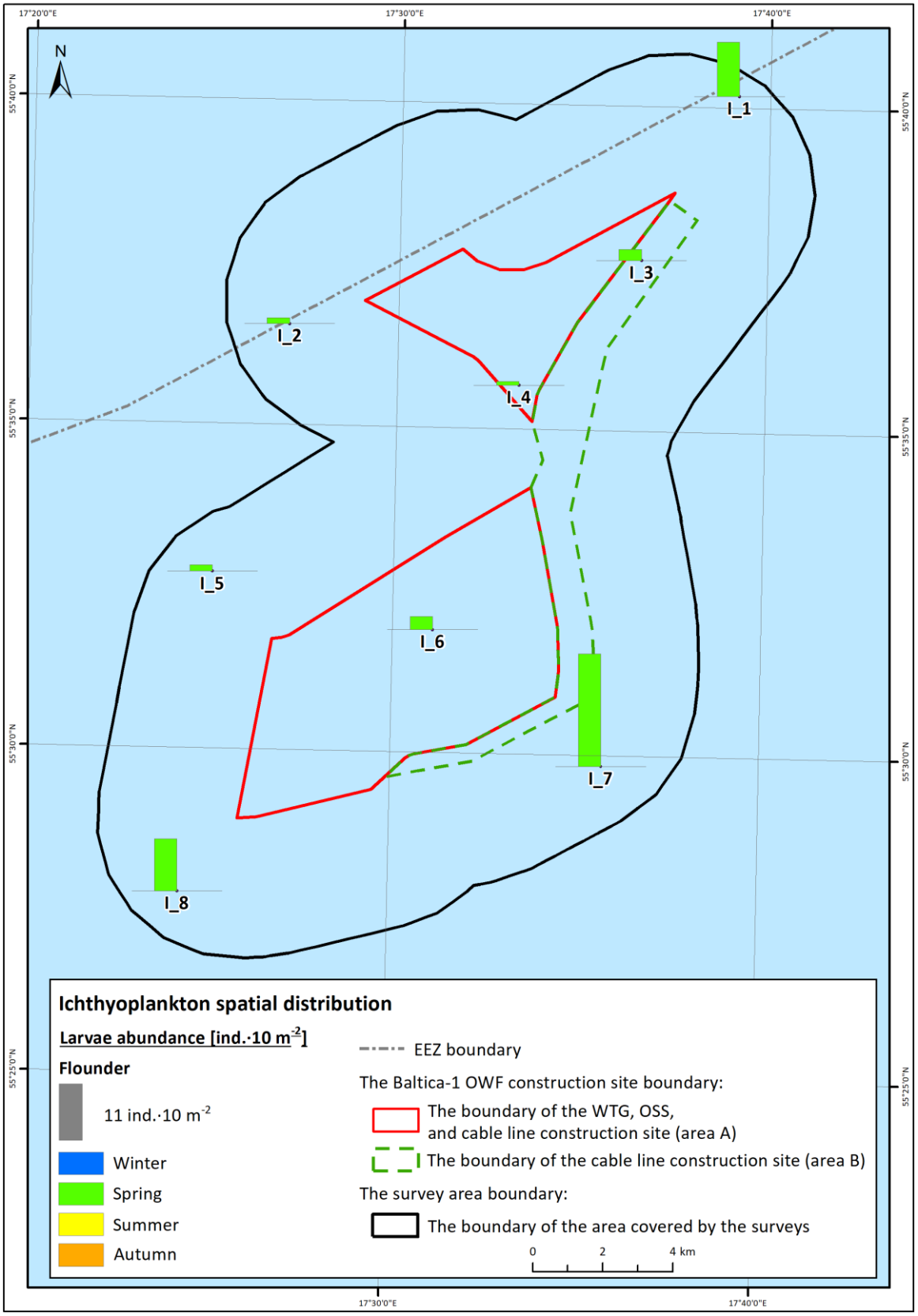


Figure 3.31. Spatial distribution of flounder larvae in the annual cycle within the survey area

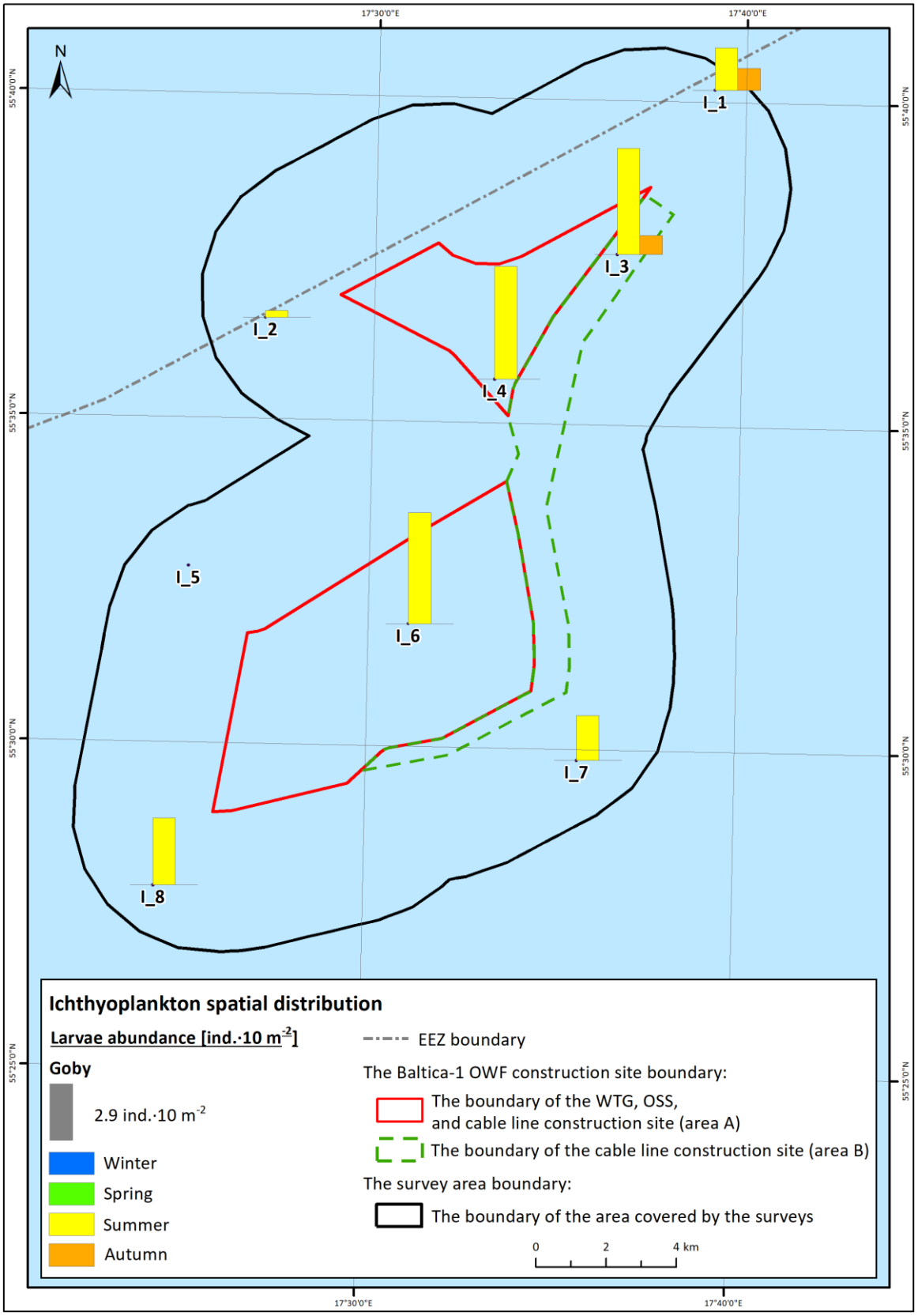


Figure 3.32. Spatial distribution of goby larvae in the annual cycle within the survey area

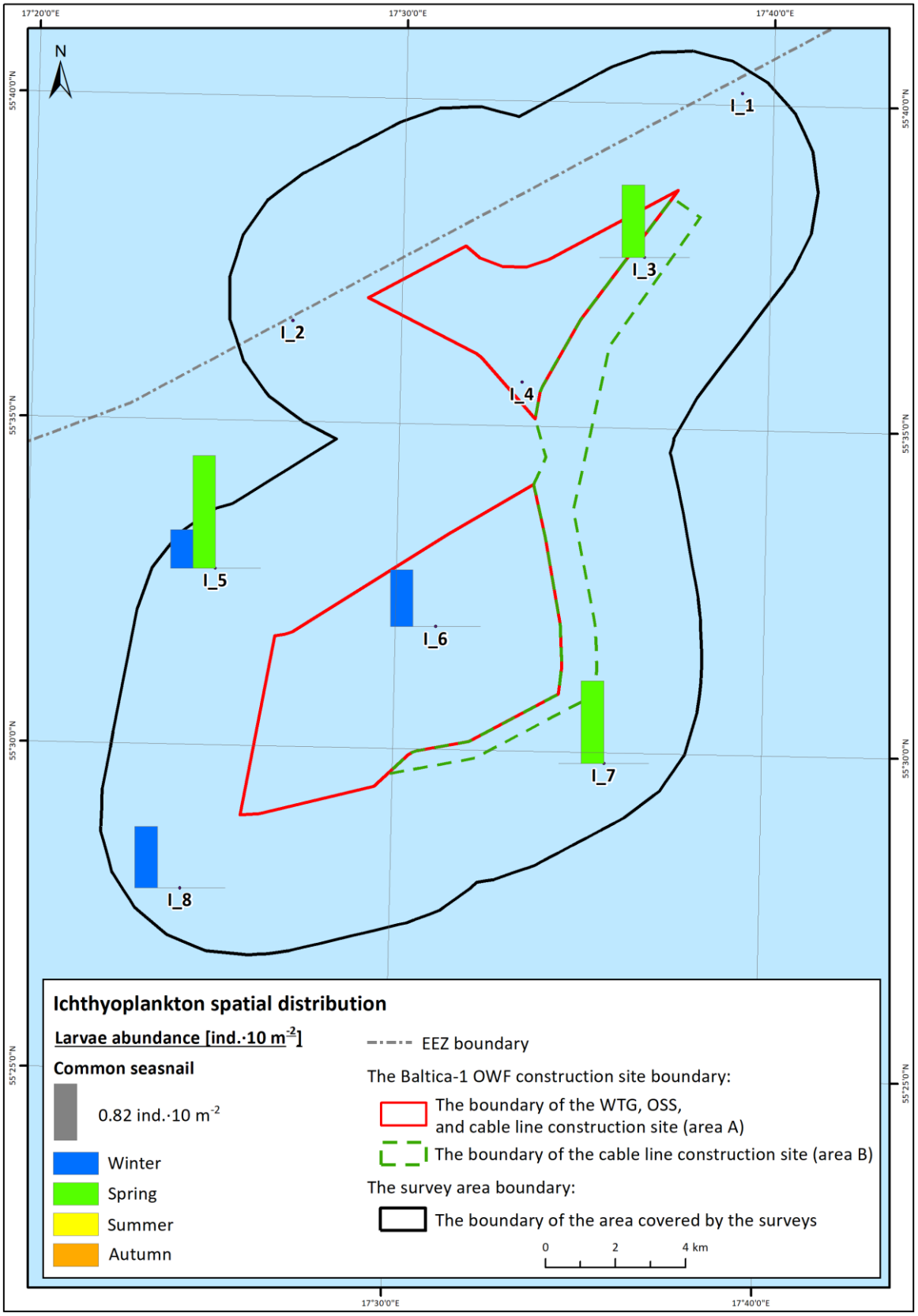


Figure 3.33. Spatial distribution of common seasnail larvae in the annual cycle within the survey area

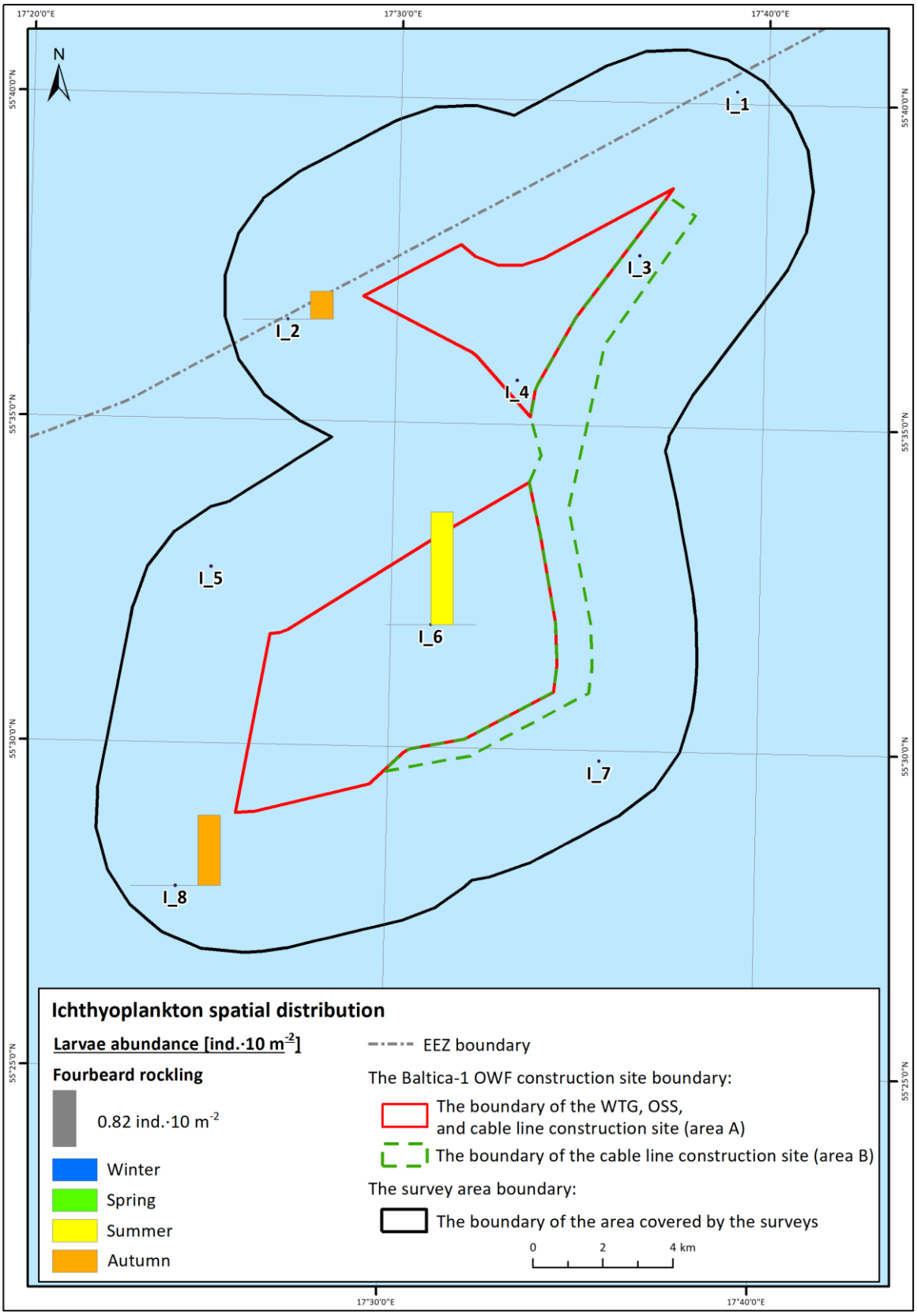


Figure 3.34. Spatial distribution of fourbeard rockling larvae in the annual cycle in the survey area

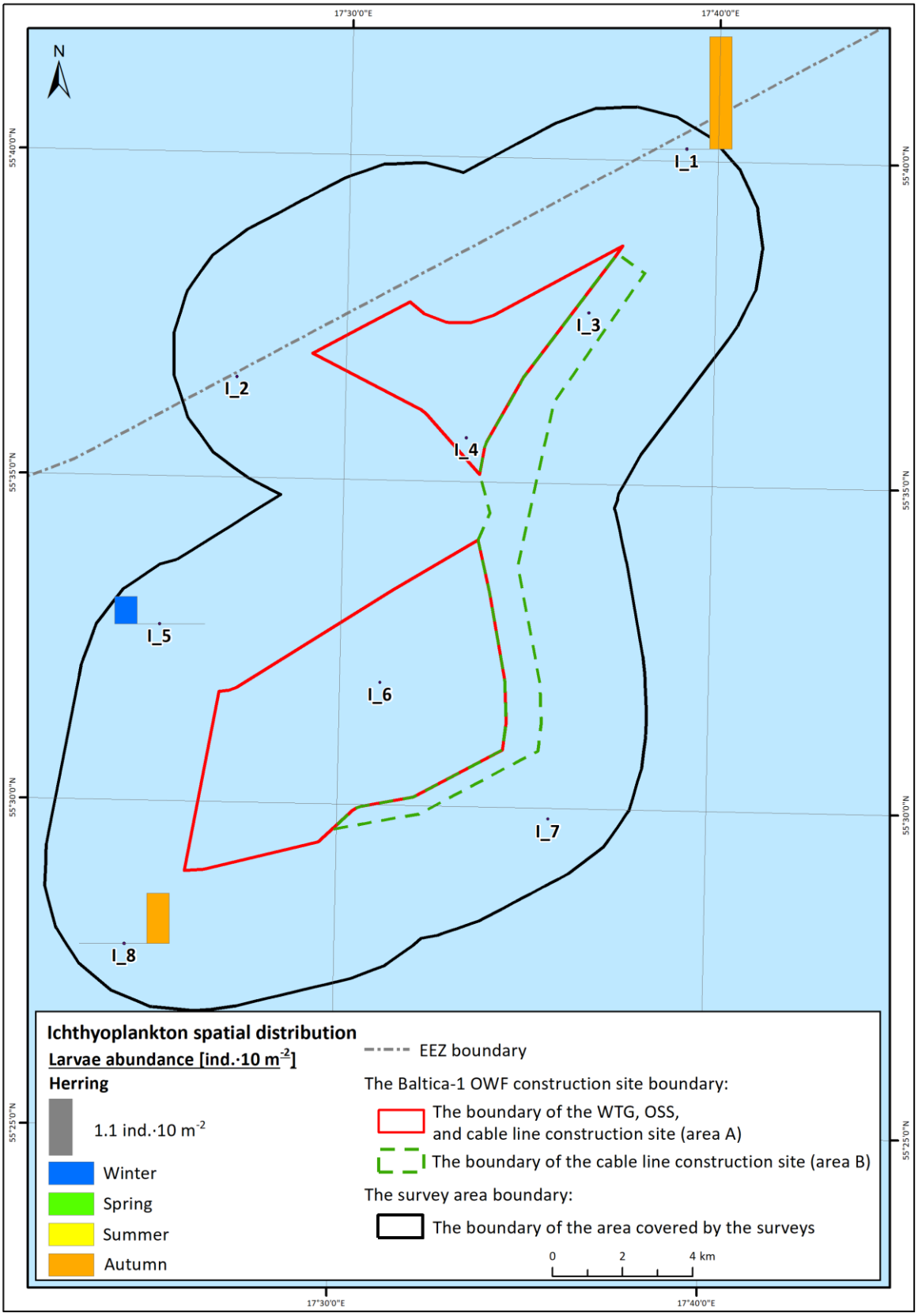


Figure 3.35. The spatial distribution of herring larvae in the annual cycle within the survey area

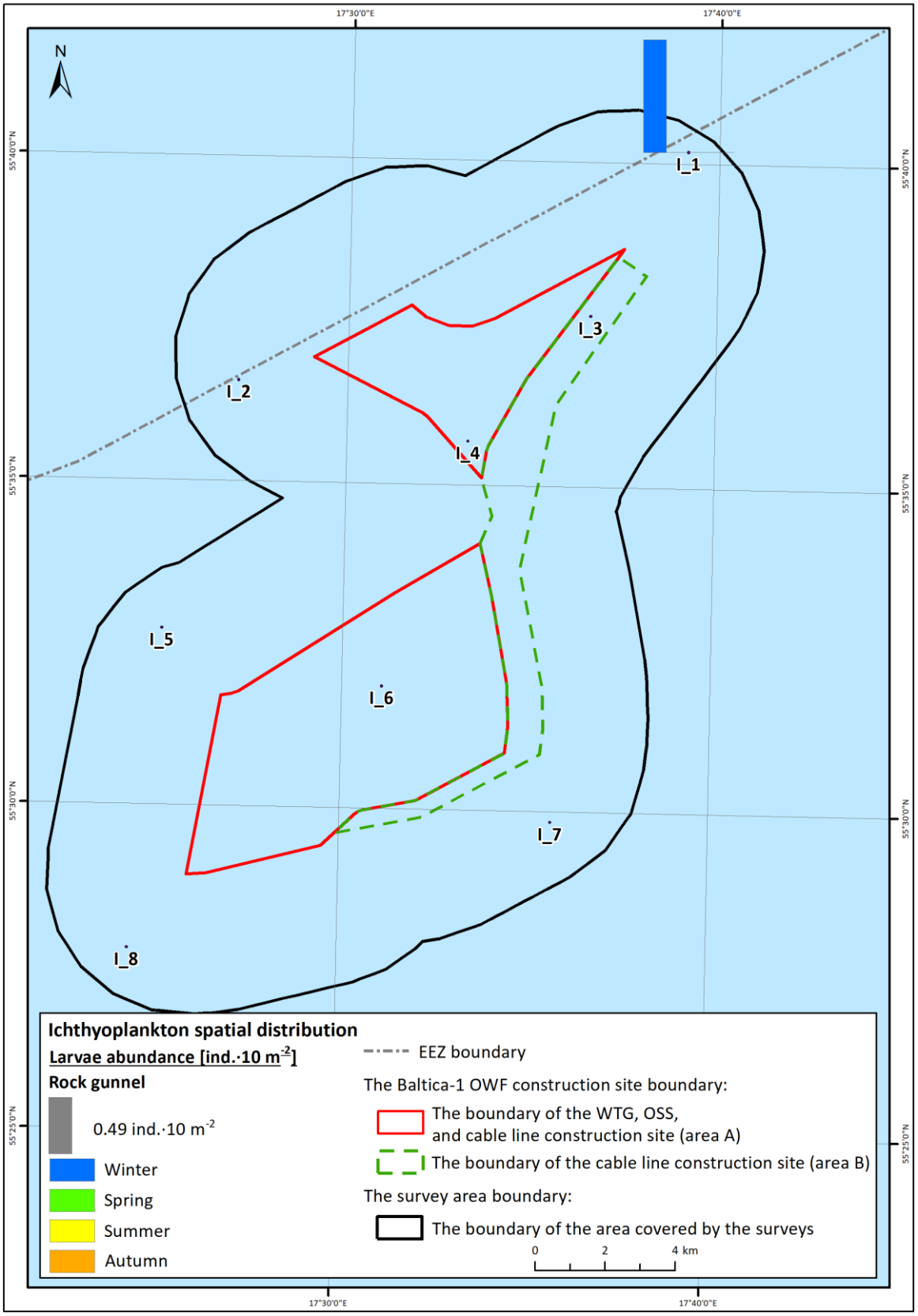


Figure 3.36. The spatial distribution of rock gunnel larvae in the annual cycle in the survey area

3.3.5.2 Hydroacoustic surveys and pelagic hauls

The table below [Table 3.27] presents the acoustic parameters obtained as a result of hydroacoustic surveys conducted in the survey area as part of four survey campaign in 2023. The parameters were calculated in accordance with the SISP Manual of International Baltic Acoustic Surveys. The area covered by acoustic echo sounding equalled 99.3 NM^2.

Table 3.27. The acoustic parameters for the survey area

Survey campaign	NASC [$m^2 \cdot NM^{-2}$]	EDSU [NM]	<σ> [m^2 10^{-4}]
February	9.8	71	1.7
May/June	232.3	71	1.47
August	115.3	71	2.24
November	16.3	71	3.86

NASC – Nautical Area Scattering Coefficient, also known as SA
EDSU – Elementary Distance Sampling Unit – an elementary integration unit, normally equal to 1 NM, not included directly in the calculations, but indicating the survey area coverage
<σ> – the average scattering cross-section, calculated taking into consideration the species composition and length distribution of individuals of particular species obtained based on control hauls

Six survey catches were carried out within the survey area during each campaign. In the summer and autumn campaigns, the results of only four hauls were included in the analyses; the hauls rejected were deemed unrepresentative due to a very low catch volume. In the spring campaign, all hauls were considered representative, while during the winter campaign, one haul was empty. The percentage of individual species in the total abundance [Table 3.28] was calculated as the average value of the percentages found in individual survey hauls carried out in individual campaigns. In addition to the main pelagic fish species (herring and sprat), the analysis accounts for the cod – because of its strong dispersal properties – as well as species with an average proportion of more than 1% in pelagic hauls (i.e. the three-spined stickleback, the nine-spined stickleback and the lumpfish during the winter campaign, and the greater sand eel during the summer campaign).

Table 3.28. The abundance proportions and average weights of the herring and the sprat determined based on the survey hauls carried out during four survey campaigns in the survey area

Survey campaign	Herring		Sprat	
	Average mass [g]	Proportion [%]	Average mass [g]	Proportion [%]
February	50.8	32.0	13.4	5.0
May/June	33.1	2.2	11.9	97.8
August	30.4	39.5	16.2	59.0
November	53.1	98.9	15.7	1.1

The stock estimation conducted using hydroacoustic methods taking into consideration the abundance proportions of the herring and the sprat [Table 3.28] allowed the determination of abundance, biomass and areal biomass density of pelagic fish species [Table 3.29].

Table 3.29. The abundance, biomass and areal biomass density of pelagic fish determined using acoustic methods

Survey campaign	Abundance [M ind.]		Biomass [t]		Areal biomass density [t·NM^{-2}]	
	Herring	Sprat	Herring	Sprat	Herring	Sprat
February	1.83	0.29	93.21	3.84	0.94	0.04
May/June	3.37	153.18	111.63	1815.29	1.12	18.29
August	20.19	30.17	611.91	487.26	6.16	4.91
November	4.15	0.05	214.41	0.71	2.16	0.01

The distribution of herring areal biomass density obtained on the basis of the seasonal acoustic surveys is presented in the figures [Figure 3.37 –Figure 3.40], while that of sprat areal biomass density in Figure 3.41–Figure 3.44.

The distributions presented were obtained by interpolating the areal biomass density of the herring and the sprat determined for one-mile sections (EDSU) of the hydroacoustic transect routed within the area.

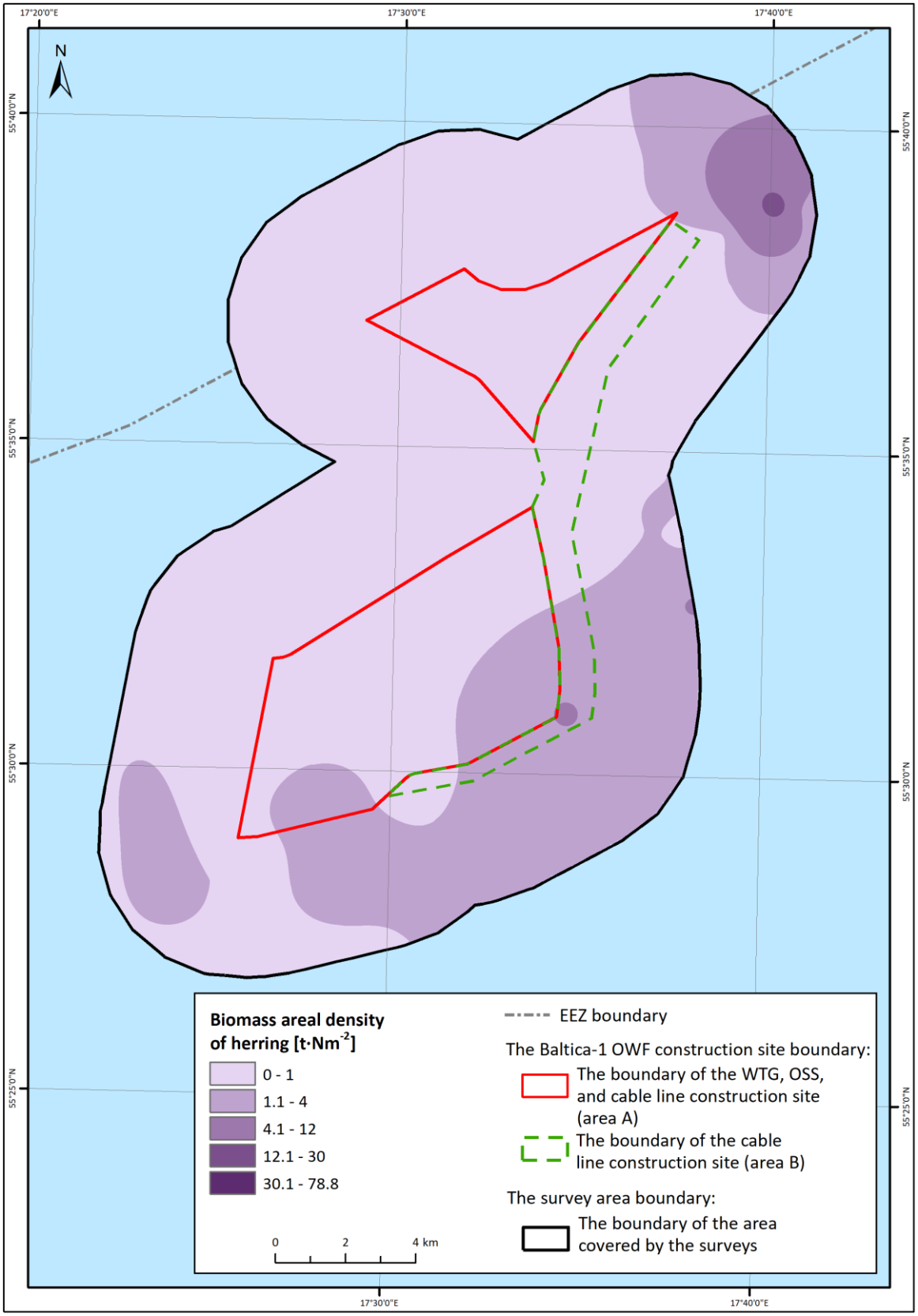


Figure 3.37. Herring areal biomass density [t·NM^{-2}] based on hydroacoustic surveys conducted in the survey area during the winter campaign

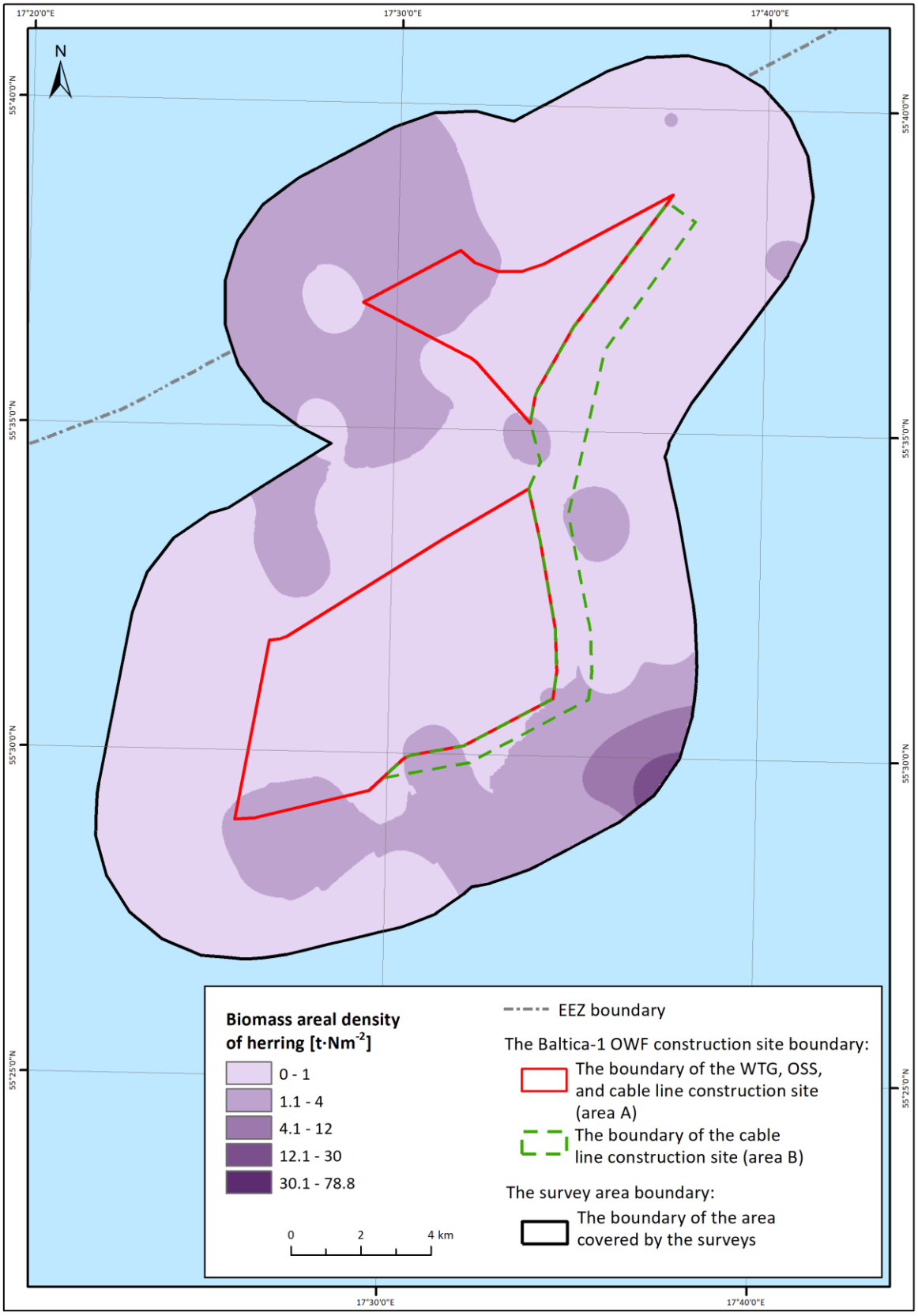


Figure 3.38. Herring areal biomass density [t·NM^{-2}] based on hydroacoustic surveys conducted in the survey area during the spring campaign

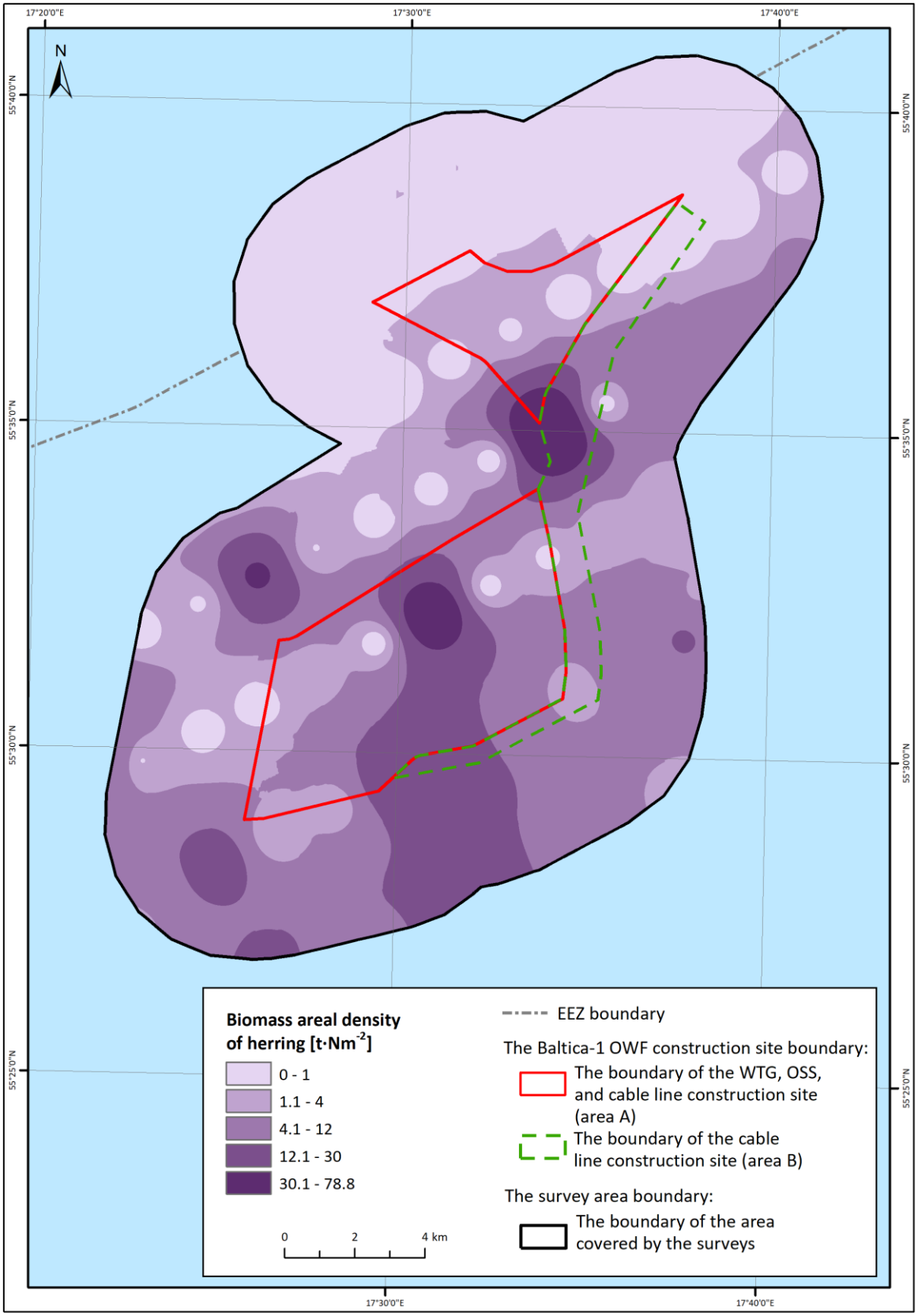


Figure 3.39. Herring areal biomass density [t·NM^{-2}] based on hydroacoustic surveys conducted in the survey area during the summer campaign

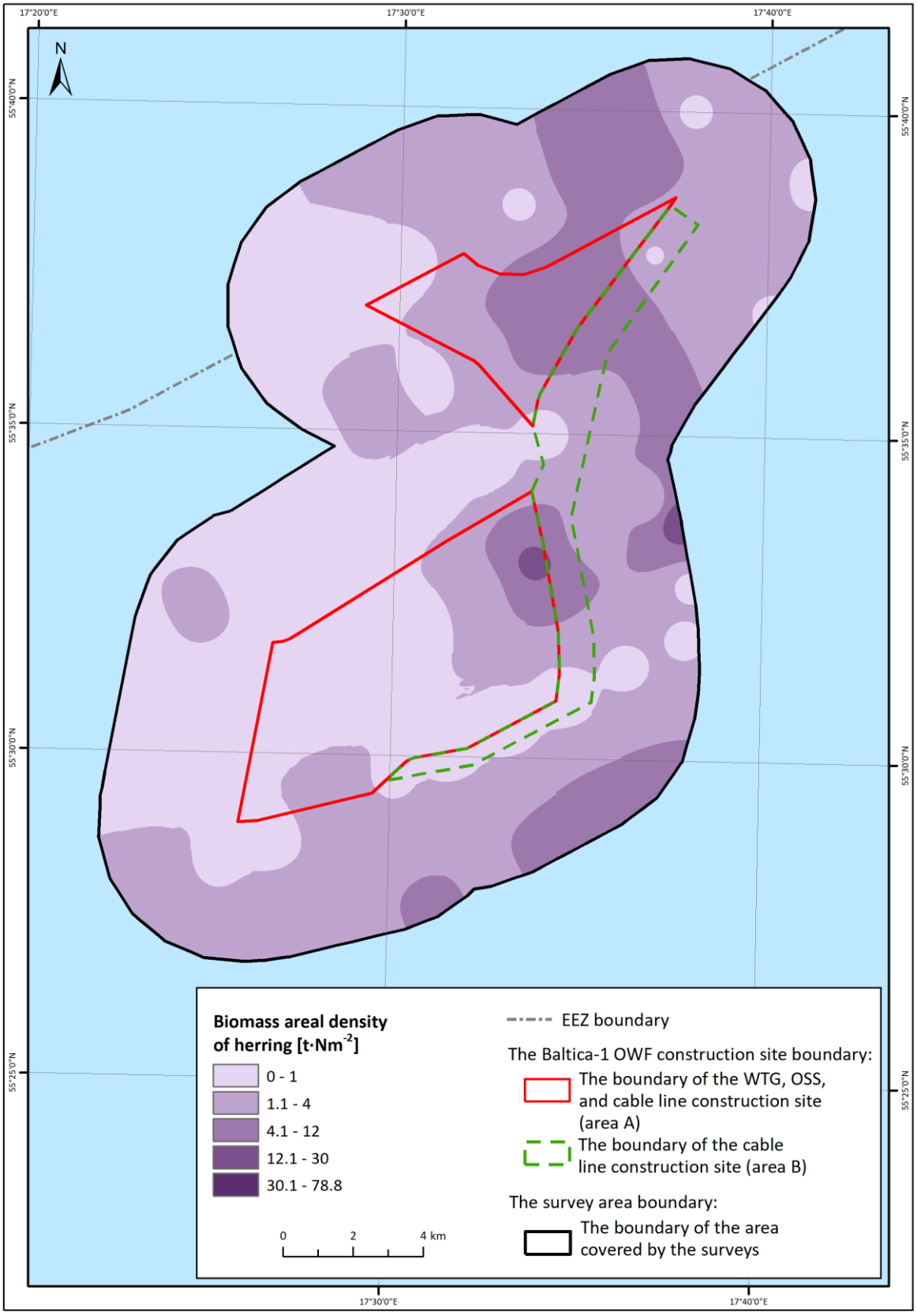


Figure 3.40. Herring areal biomass density [t·NM^{-2}] based on hydroacoustic surveys conducted in the survey area during the autumn campaign

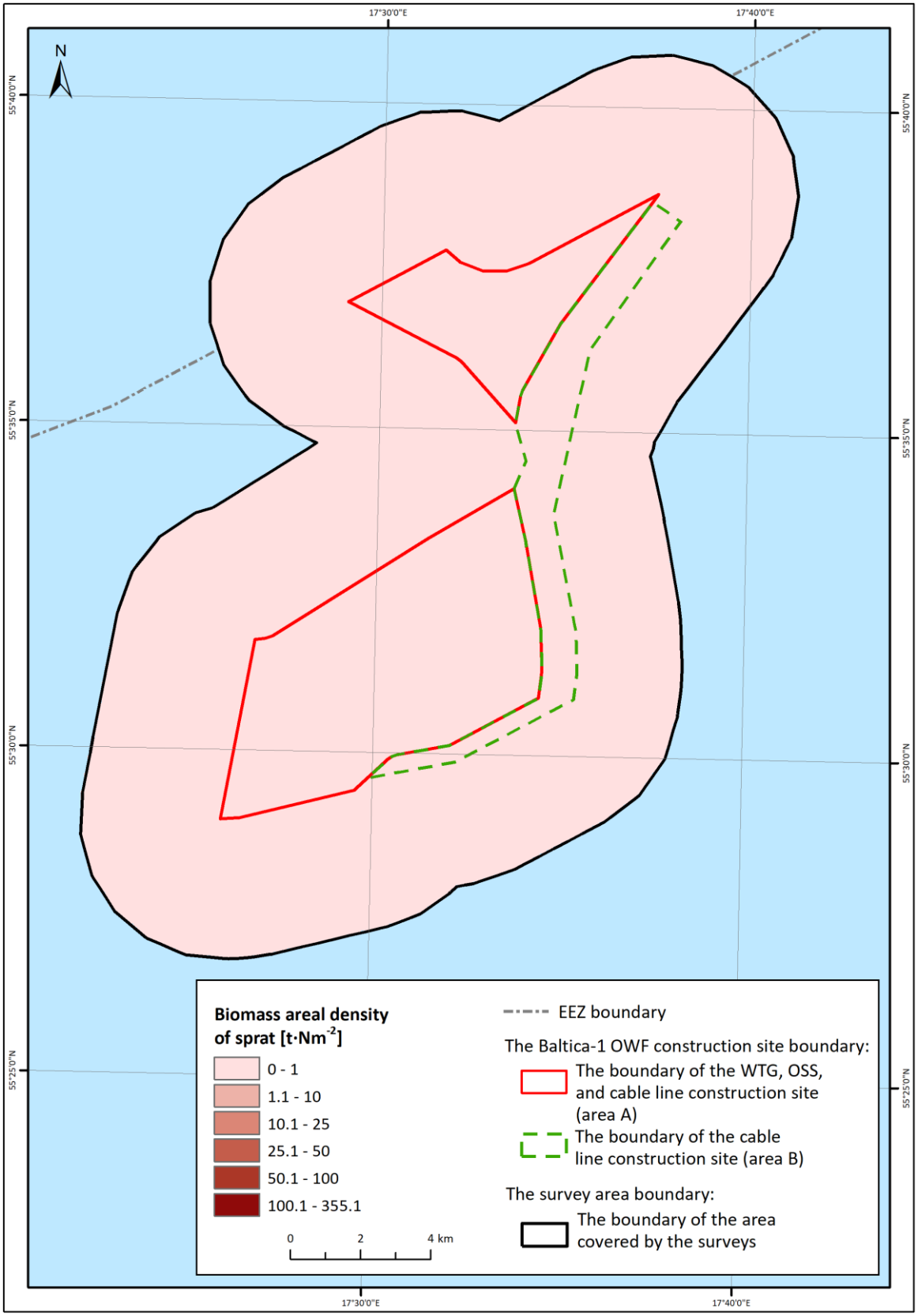


Figure 3.41. Sprat areal biomass density [t·NM^{-2}] based on hydroacoustic surveys conducted in the survey area during the winter campaign

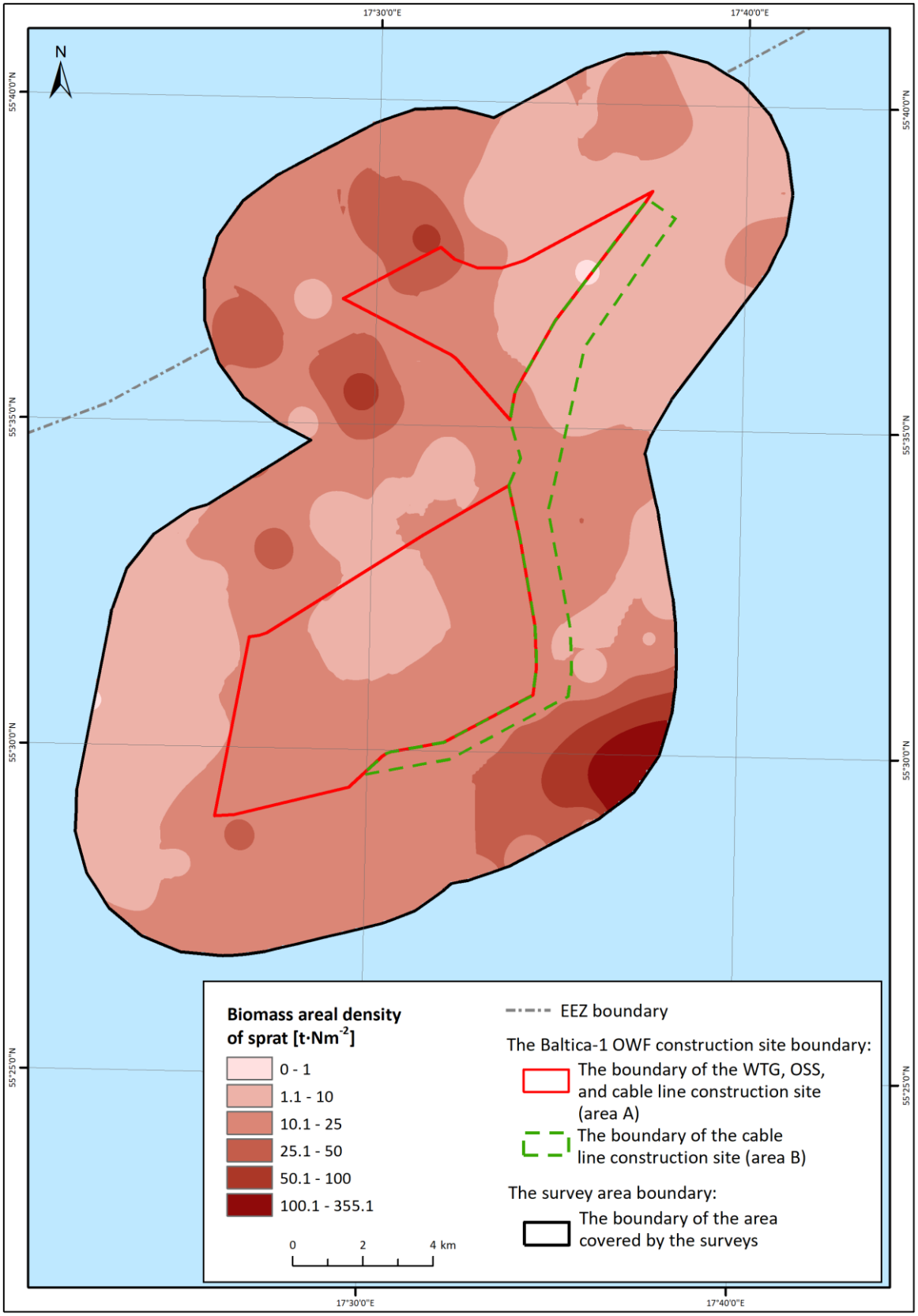


Figure 3.42. Sprat areal biomass density [t·NM^{-2}] based on hydroacoustic surveys conducted in the survey area during the spring campaign

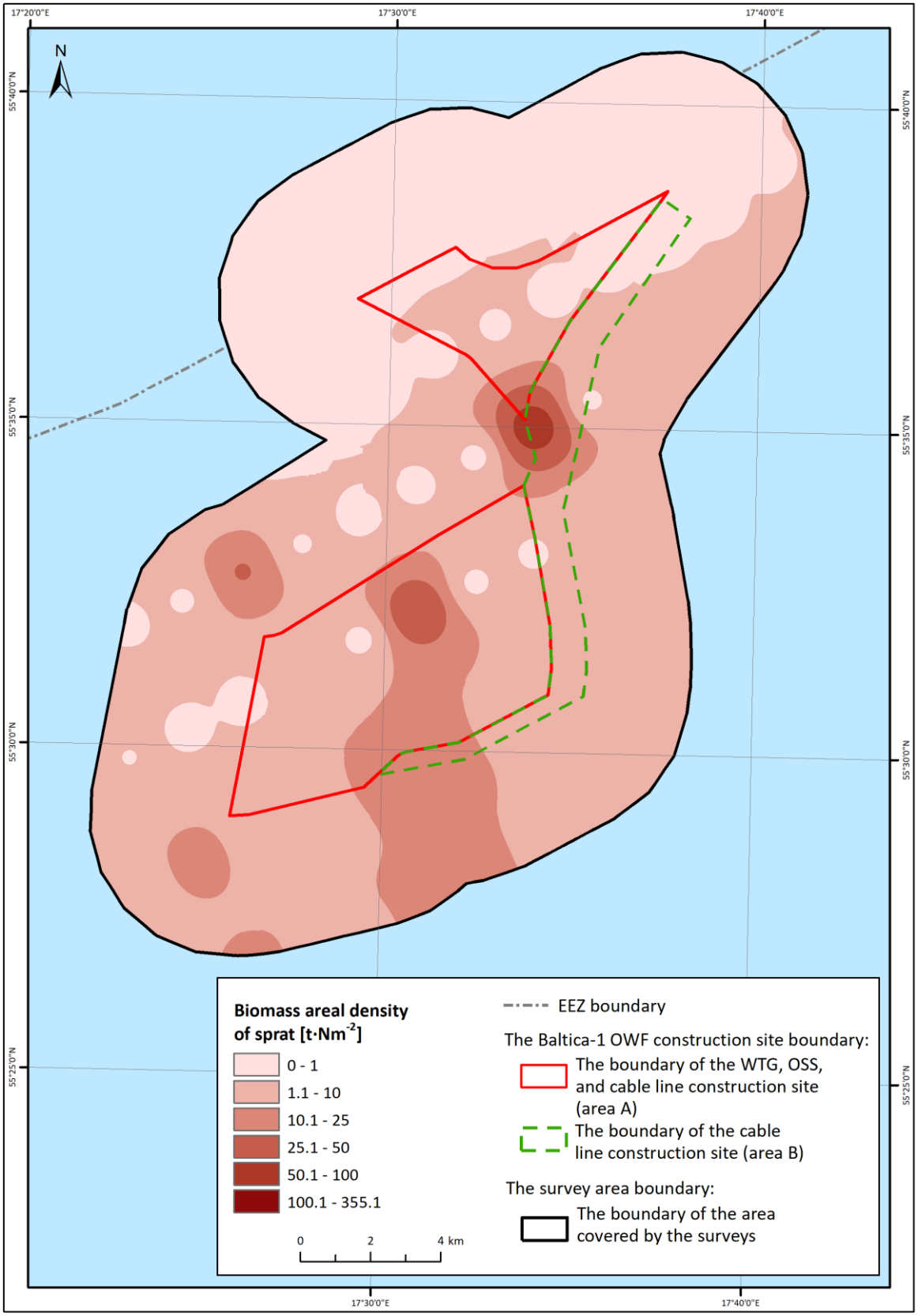


Figure 3.43. Sprat areal biomass density [t·NM^{-2}] based on hydroacoustic surveys conducted in the survey area during the summer campaign

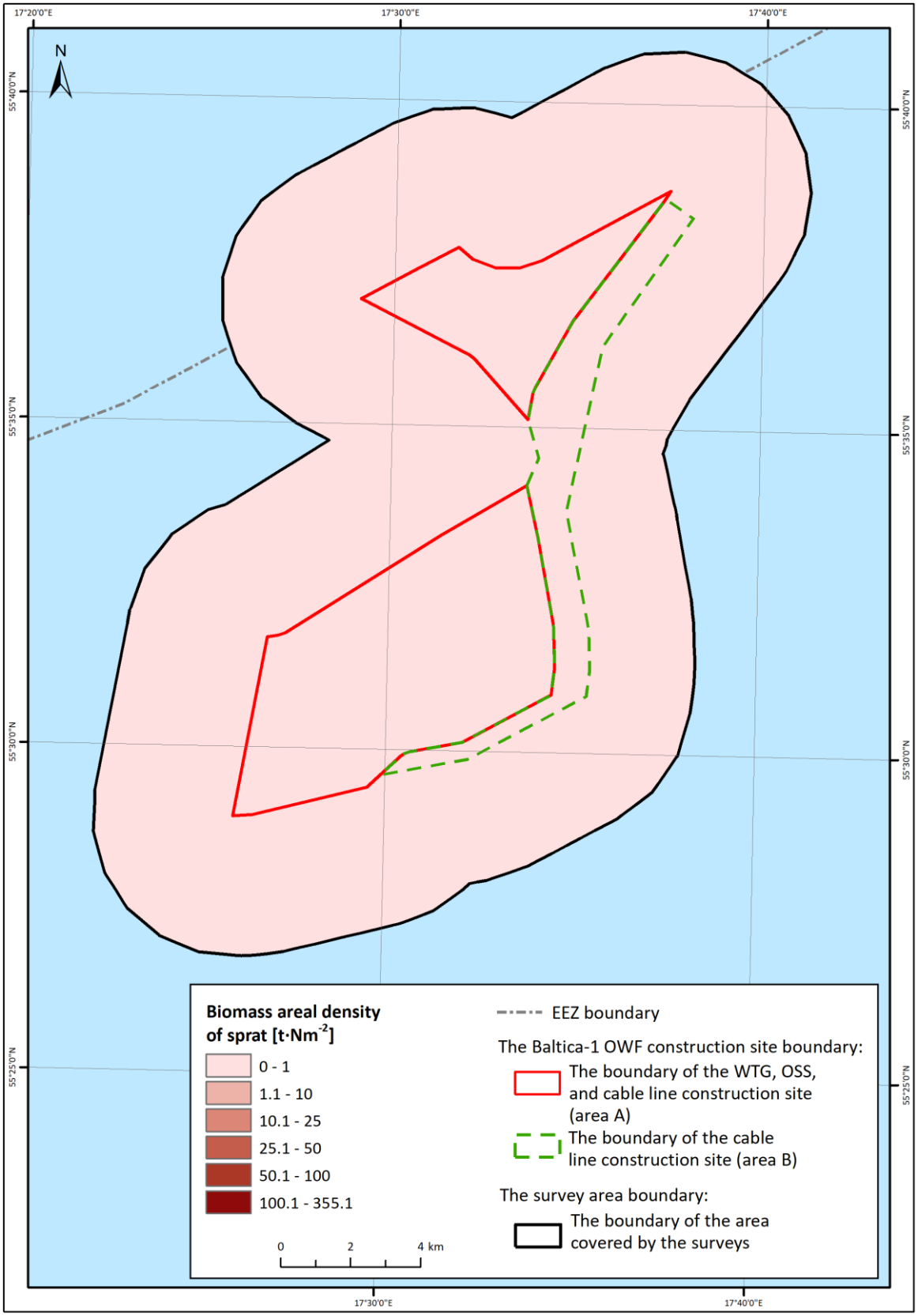


Figure 3.44. Sprat areal biomass density [t·NM^{-2}] based on hydroacoustic surveys conducted in the survey area during the autumn campaign

3.3.5.3 Demersal fish surveys

The weight and abundance of individual species caught in the survey area at ten survey stations are presented in Table 3.30 and Table 3.31.

Table 3.30. The weight of individual species of fish caught in bottom-set gillnet sets within the survey area during all survey campaigns

Species	Biomass [g]				
	Winter	Spring	Summer	Autumn	Total
Greater sand eel		16	399	32	447
Cod	128893	89879	324437	355771	898980
Plaice	1536	4855	7379	654	14424
Shorthorn sculpin	46226	29279	37548	18278	131331
Pogge	57				57
Mackerel			3529		3529
Twait shad				2916	2916
Turbot		2744	3064	381	6189
Flounder	20344	131158	172864	11423	335789
Sprat	59			17	76
Herring	16219	1655	3259	5428	26561
Lumpfish	1097	161			1258
Lesser sand eel	26				26
Viviparous eelpout			290		
Total	214457	259747	552769	394900	1421873

Table 3.31. The abundance of individual species of fish caught in bottom-set gillnet sets within the survey area during all survey campaigns

Species	Abundance [ind.]				
	Winter	Spring	Summer	Autumn	Total
Greater sand eel		1	18	1	20
Cod	504	428	1538	1537	4007
Plaice	8	29	37	4	78
Shorthorn sculpin	242	168	224	92	726
Pogge	2				2
Mackerel			6		6
Twait shad				9	9
Turbot		9	10	2	21
Flounder	89	652	720	54	1515
Sprat	4			1	5
Herring	304	33	58	86	481
Lumpfish	5	1			6
Lesser sand eel	1				1
Viviparous eelpout			3		3
Total	1159	1321	2614	1786	6880

1421.9 kg of fish belonging to 14 taxa were caught in total. The cod and the flounder dominated. The remaining species (greater sand eel, plaice, shorthorn sculpin, pogge, mackerel, twaite shad, turbot, sprat, herring, lumpfish, lesser sand eel and viviparous eelpout) constituted by-catches. Information on the species composition and the percentage of the catch weight in individual survey seasons is presented below.

In winter, nine fish species with a total weight of 214.4 kg were recorded. The predominant species was the cod, the weight percentage of which constituted 60% of the total fish catch mass. Among the remaining species, the shorthorn sculpin accounted for 21%, the flounder – 9.5% and the herring – 7.6%. In addition, the plaice, the pogge, the sprat, the lumpfish and the lesser sand eel were represented in small numbers.

In spring, eight fish species with a total weight of 259 kg were recorded in the catches. The flounder, the proportion of which accounted for 50% in the total catch weight, dominated, followed by the cod, which constituted 35% of the catch weight and the shorthorn sculpin (11%). The remaining species were represented by a smaller number of individuals. They included the greater sand eel, the plaice, the turbot, the herring and the lumpfish.

In summer, nine species of fish with a total weight of 552 kg were recorded, of which the cod accounted for 59%, the flounder – 31%, the shorthorn sculpin – 7% and the remaining 3% of the catch weight was made up of such species as the great sand eel, the plaice, the mackerel, the herring and the viviparous eelpout.

In autumn, nine fish species with a total weight of 395 kg were recorded in the catches. The predominant species was the cod, the weight percentage of which constituted 90% of the total fish catch mass. The remaining species were represented in smaller numbers – those included the greater sand eel, the plaice, the shorthorn sculpin, the twaite shad, the turbot, the flounder, the sprat and the herring.

The figure below [Figure 3.45] illustrates catch rates during successive survey campaigns at the survey stations located in the survey area.

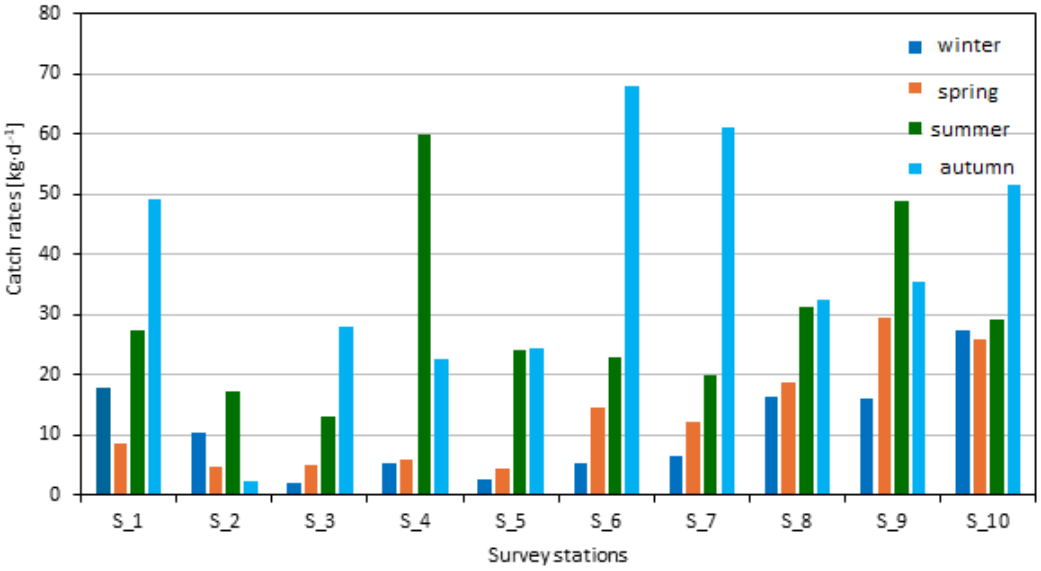


Figure 3.45. The average daily catch rates reported for the catches conducted using bottom-set gillnet sets during successive survey campaigns in the survey area

In winter, the catch rates ranged from 1.95 kg·d.$^{-1}$ at deployment point S_3 to 27.25 kg·d.$^{-1}$ at deployment point S_10. The average catch rate in the survey area was 10.91 kg·d.$^{-1}$ of fish per day of the survey gear deployment.

In spring, the catch rates ranged from 4.29 kg·d.$^{-1}$ at deployment point S_5 to 29.52 kg·d.$^{-1}$ at deployment point S_9. The average catch rate in the survey area was 12.90 kg·d.$^{-1}$ of fish per day of the survey gear deployment.

In summer, the catch rates ranged from 13.6 kg·d.$^{-1}$ at deployment point S_3 to 59.99 kg·d.$^{-1}$ at deployment point S_4. The average catch rate in the survey area was 29.38 kg·d.$^{-1}$ of fish per day of the survey gear deployment.

In autumn, the catch rates ranged from 2.27 kg·d.$^{-1}$ at deployment point S_2 to 67.90 kg·d.$^{-1}$ at the deployment point S_6. The average catch rate within the survey area was 37.48 kg of fish per day of the survey gear deployment.

3.3.5.4 Herring concentration surveys

The weight and abundance of individual species caught in the survey area at seven survey stations are presented in the tables [Table 3.32, Table 3.33].

Table 3.32. The weight of individual species of fish caught in herring gillnets in the survey area during all survey campaigns

Species	Biomass [g]				
	Winter	Spring	Summer	Autumn	Total
Greater sand eel		14	51		65
Cod	23123	23894	226095	199551	472663

Species	Biomass [g]				
	Winter	Spring	Summer	Autumn	Total
Plaice		250	877		1127
Shorthorn sculpin	5936	7287	12689	20527	46439
Fourhorn sculpin	134				134
Pogge				35	35
Mackerel		66	7669		7735
Twait shad			507	821	1328
Turbot			877	243	1120
Flounder	624	1979	24875	6845	34323
Sprat	12				12
Herring	13759	22484	33219	84643	154105
Lumpfish	176	234			410
Lesser sand eel			43		43
Viviparous eelpout				12	12
Total	43764	56208	306902	312677	719551

Table 3.33 Abundance of individual species of fish caught in herring gillnets in the survey area during all survey campaigns

Species	Abundance [ind.]				
	Winter	Spring	Summer	Autumn	Total
Greater sand eel		1	2		3
Cod	749	152	1281	1336	3518
Plaice		1	3		4
Shorthorn sculpin	55	43	78	111	287
Fourhorn sculpin	1				1
Pogge				1	1
Mackerel		1	14		15
Twait shad			2	3	5
Turbot			3	1	4
Flounder	3	7	115	32	157
Sprat	1				1
Herring	201	320	436	1198	2155
Lumpfish	1	1			2
Lesser sand eel			2		2
Viviparous eelpout				1	1
Total	1011	526	1936	2683	6156

719 kg of fish belonging to 15 taxa were caught in total. The cod and the herring prevailed.

To analyse the correlation between the occurrence of herrings and piscivorous birds, the results of herring catch rates (kg/day) were compared with the average densities of razorbills, guillemots and divers in the survey area [Table 3.34].

Table 3.34. A comparison of daily herring catch rates and densities of piscivorous birds on seabird observation days in the survey area

Observation date	Catch rate (kg/day)	Average density (razorbills, guillemots, divers)
01.03.2023	2.57	0.57
21.03.2023	0.85	1.10
06.04.2023	1.48	0.90
22.04.2023	3.79	4.94
05.08.2023	1.52	1.34
14.08.2023	2.67	0.91
08.09.2023	2.95	1.31
26.09.2023	1.05	0.00
22.10.2023	2.42	0.92
11.11.2023	3.61	0.68
29.11.2023	4.40	0.72
30.112.2023	7.60	0.42

The Pearson correlation test performed showed that there was no significant correlation between the average density of birds (razorbills, guillemots, divers) and the average herring catch rates (R^2 = 0.004; p = 0.84) [Figure 3.46].

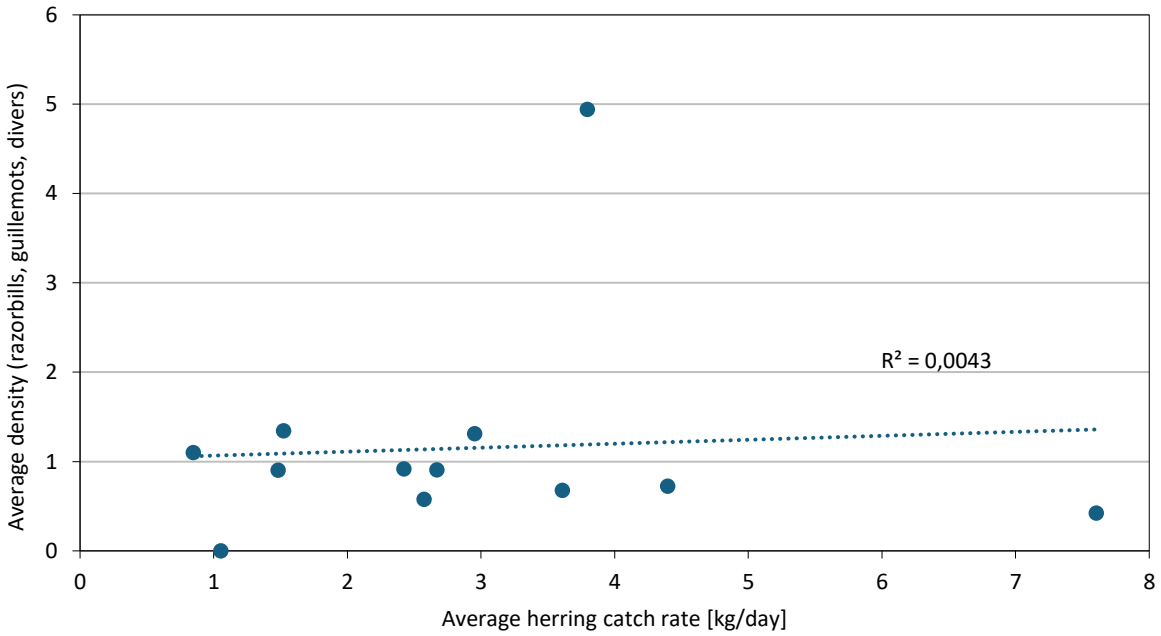


Figure 3.46. The correlation between herring occurrence and the average density of piscivorous birds in the survey area

Assuming that piscivorous birds may prey on fish of other species, an analysis of the correlation between the total catch rate and the density of razorbills, guillemots and divers was performed. The Pearson correlation test showed that those parameters were not significantly correlated (R^2 = 0.034; p = 0.57) [Figure 3.47].

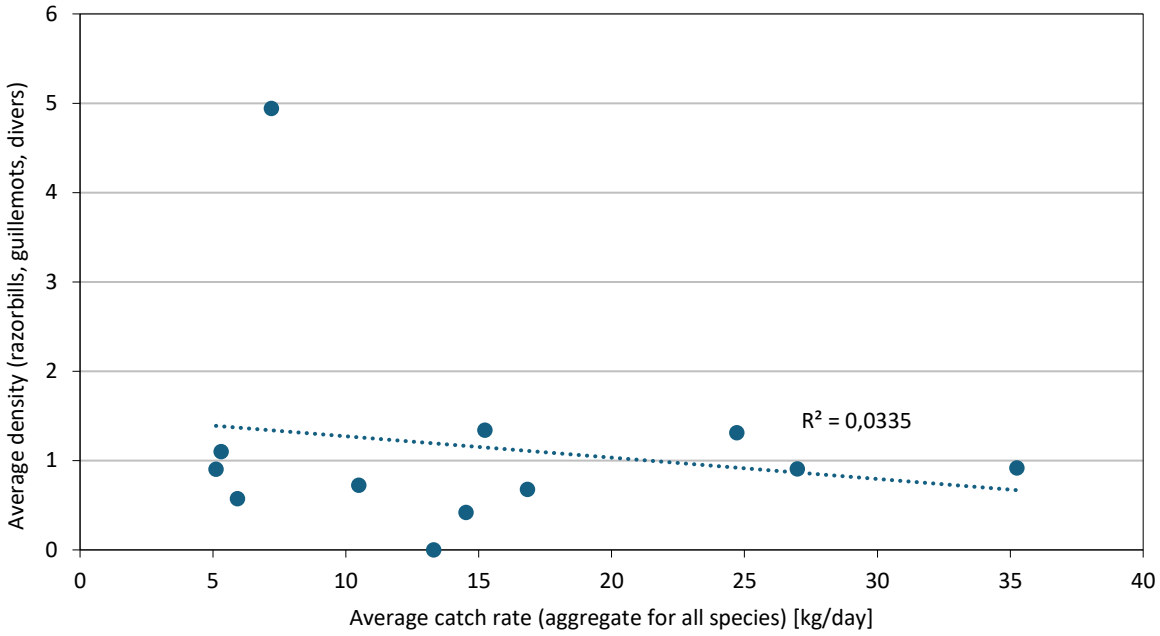


Figure 3.47. A correlation between the occurrence of all fish species and the average density of piscivorous birds in the survey area

3.3.5.5 Biological survey results

3.3.5.5.1 Sprat

Both the length range, as well as the modal length of sprats present in the samples from pelagic trawl (PT), catches differed depending on the survey season [Figure 3.48]. Samples collected in winter, spring, summer and autumn contained sprats in the following length classes: 10.5–14.5, 9.5–14.5, 11.5–15.0, and 8.5–14.5 cm, respectively. The length distribution of the above-mentioned fish in 0.5-cm classes, in the winter and summer samples, took the shape of an unimodal function with the maximum relative abundance proportion of 30.0 and 29.5%, respectively, marked accordingly in the 12.0 and 13.5 cm classes. The same type of variable developed based on materials collected in spring and autumn had the shape of a bimodal function and a broken curve, respectively [Figure 3.48]. The maximum proportion of sprat, i.e. 25.0% – in spring and 24.4% – in autumn, was marked adequately in the 12.0 and 14.0 cm classes. In spring and autumn, contrary to the data from the other seasons, the samples contained small sprat ("undersized"), smaller than the minimum technological standard/landing size in force in Poland, i.e. 10.0 cm. The proportion of sprat from the above-mentioned size fraction was on average 6.9% (in spring) and 6.6% (in autumn). A tendency towards a seasonal increase in the proportion of small, young sprat from the new generation was noted often also in previous years, but mainly in the first and fourth quarters and in coastal waters [Grygiel, 1987b, 1997, 1999, 2015; Grygiel et al., 2016; Grygiel and Radtke, 2017].

Sprat representing samples from pelagic trawl catches were identified as belonging to the following age groups and year classes depending on the season [Figure 3.49]:

- winter – age groups 2–9, year classes 2021–2014, with the dominance in the abundance of fish from age group 4 (average proportion = 41.7%);
- spring – age groups 1–9, year classes 2022–2014, with the dominance in the abundance of fish from age group 4 (27.2% proportion);

- summer – age groups 1–8, year classes 2022–2015, with the dominance in the abundance of fish from age group 3 (35.4% proportion);
- autumn – age groups 0–8, year classes 2023–2015, with the dominance in the abundance of fish from age groups 4 and 5 (34.2% and 29.6% proportion, respectively).

Distinguished by their sample proportion, sprat from age groups 3, 4, and 5, equated with fish belonging to year classes of 2020, 2019 and 2018, respectively, on the scale of the entire Baltic stock are classified as year classes 17% and 23% more numerous and 37% less numerous, respectively, than the long-term average abundance of recruiting year classes of 1973–2022, amounting to 81.3 million individuals (based on WGBFAS-ICES, 2022).

The histogram of the seasonal sprat proportion distribution (both males and females) in the samples according to Maier's 8-stage scale of gonad maturity (Maier, 1908; Mańkowski, 1951) is presented in Figure 3.50.

In the samples collected during the pelagic trawl catches, sprat were represented by gonads that were at the following stages of maturity in the individual survey periods of 2023 [Figure 3.50]:

- winter – stage 7 (spent; fish at the end of their spawning process) with an average proportion of 83.3% as well as stage 8 (resting; recently finished breeding) and stage 2 (maturing virgin) – with an equal proportion of 8.3%;
- spring – fish taking part in the breeding process, i.e. at stage 5 (gravid), stage 6 (spawning) and stage 7, with a total proportion of 57.5% as well as at stage 2 (21.7%) – will take part in spawning in the following year and stage 8 (3.3%);
- summer – stage 2 (73.5%) and stage 3 (developing; 7.4%) – most of the fish will take part in spawning in the following year, stage 7 (1.5%) and stage 8 (17.6%);
- autumn – stages 2 (59.1%) and 3 (29.5) – the fish will take part in spawning in the following year as well as stage 7 (4.5%) and stage 8 (6.8%) – sparse number of individuals which participated in the final phase of spawning or had just completed that process.

The biological data summarised above confirm the previous survey results for Baltic sprat concerning the changes in the physiological development of these fish throughout the year. In February 2023, sprat started the first phase of spawning in the water depth of the Baltic Sea (at a water depth of 50–90 m). The process intensified on a large scale in May, then gradually died out in the second half of summer. Exceptionally, in October-November, there were a few sprats present in the samples, which were involved in the final phase of spawning or had just completed that process. Sprat spawning extended over time (2023) has so far been recorded quite rarely and for a small proportion of the population of these fish.

One of the further biological traits of sprat analysed was the seasonal changes in stomach fullness degree. The stomach fullness degree was determined macroscopically according to a conventional five-point scale, i.e. from 0 – empty stomachs to 4 – stomachs completely filled with food. The results of the analysis of sprat samples collected in 2023 using a pelagic trawl in the area of the planned project indicate the following distribution of average relative proportion according to the scale mentioned [Figure 3.51]:

- in winter, fish with empty stomachs (non-feeding) dominated with a 100% proportion;

- in spring, fish with empty stomachs also dominated, with a proportion of 98.9%, while the supplement to the samples (1.1%) constituted moderately feeding sprat, i.e. with 1/2 full stomachs;
- in summer, also a relatively large number of sprats had empty stomachs (proportion = 54.4%), while the other were feeding with varying intensity, i.e. poorly-feeding (proportion = 29.4%), moderately-feeding (proportion = 8.8%) and fairly intensively-feeding (proportion = 7.4%) – the stomachs of these fish were filled with food in 1/4, 1/2 and 3/4 respectively;
- in autumn, quite similar to summer, a large number of sprats had empty stomachs (proportion = 72.7%), and the remaining ones were poorly feeding (proportion = 13.6%), moderately feeding (proportion = 6.8%) and fairly intensively feeding (proportion = 6.8%).

The process of mass feeding of sprat usually intensifies once the spawning ends, particularly at the turn of summer and autumn and then gradually fades away to a minimum (starving state) at the beginning of winter. In spring, that process is of an accidental nature and concerns only a few individuals (Mańkowski 1947; Khanh et al., 1972; Birjukov 1980; Kostrichkina et al., 1980; Shvetsov and Rudneva 1994; Grygiel 2016).

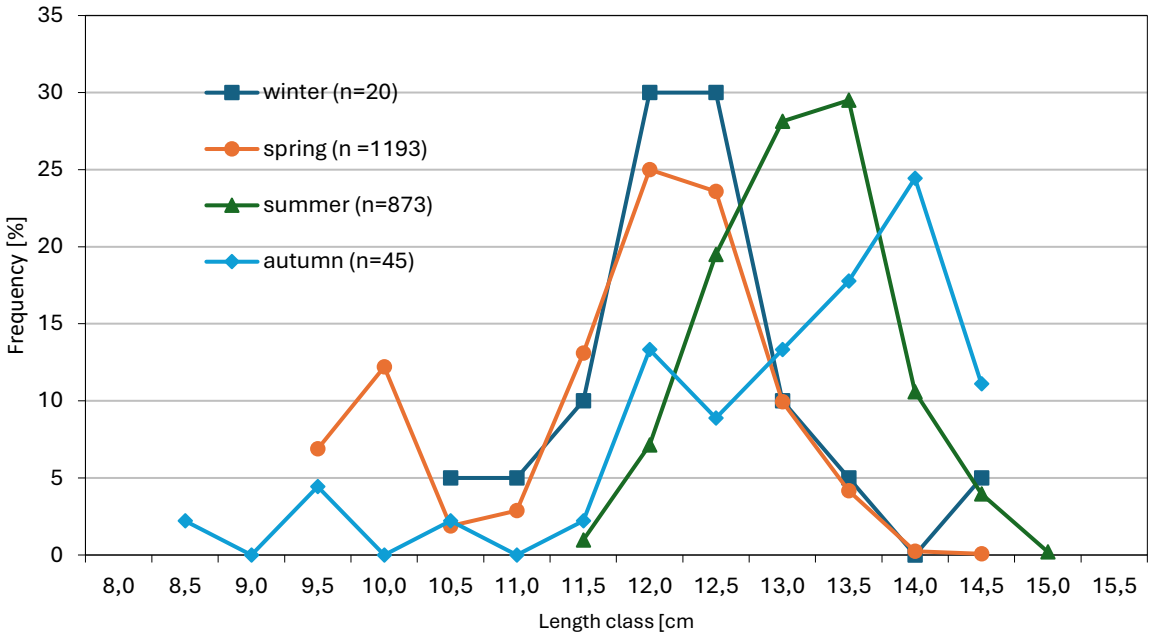


Figure 3.48. The length distribution of sprat caught in pelagic trawl in the survey area, by the season of 2023

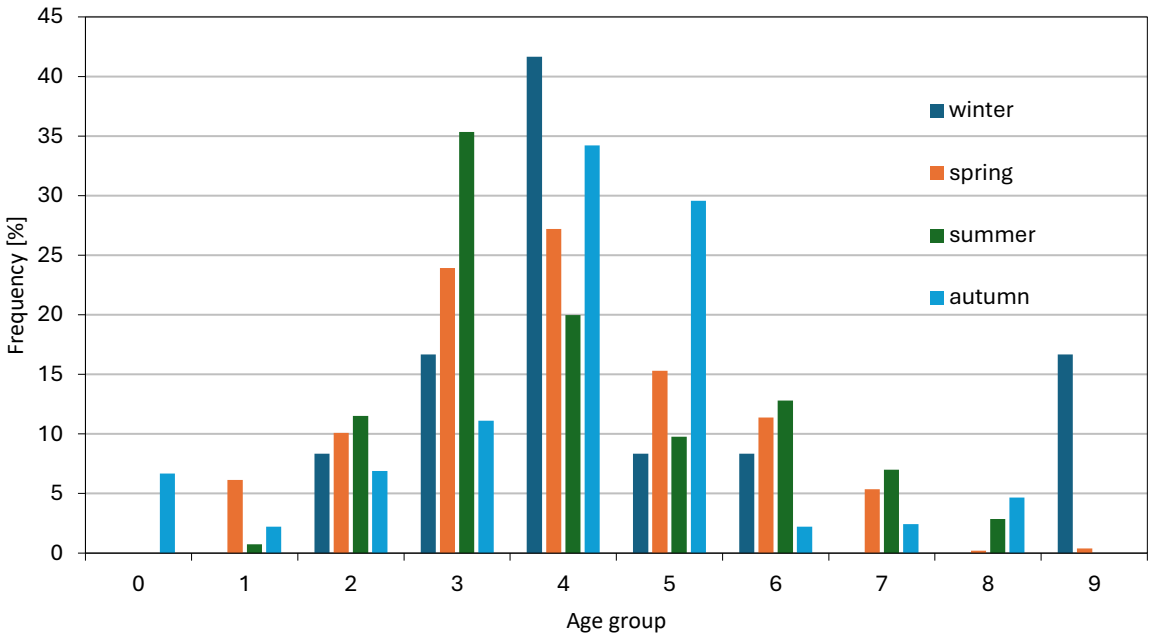


Figure 3.49. The age structure of sprat caught in pelagic trawl in the survey area, by the season of 2023

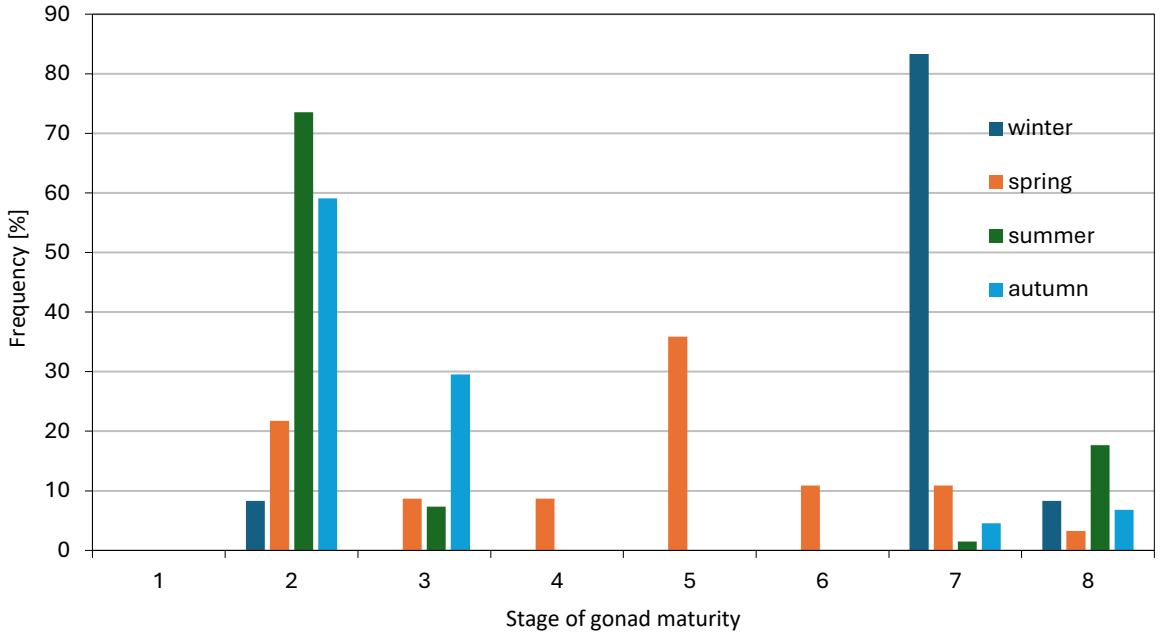


Figure 3.50. The distribution of gonad maturity stages of sprat caught in pelagic trawl in the survey area, by the season of 2023

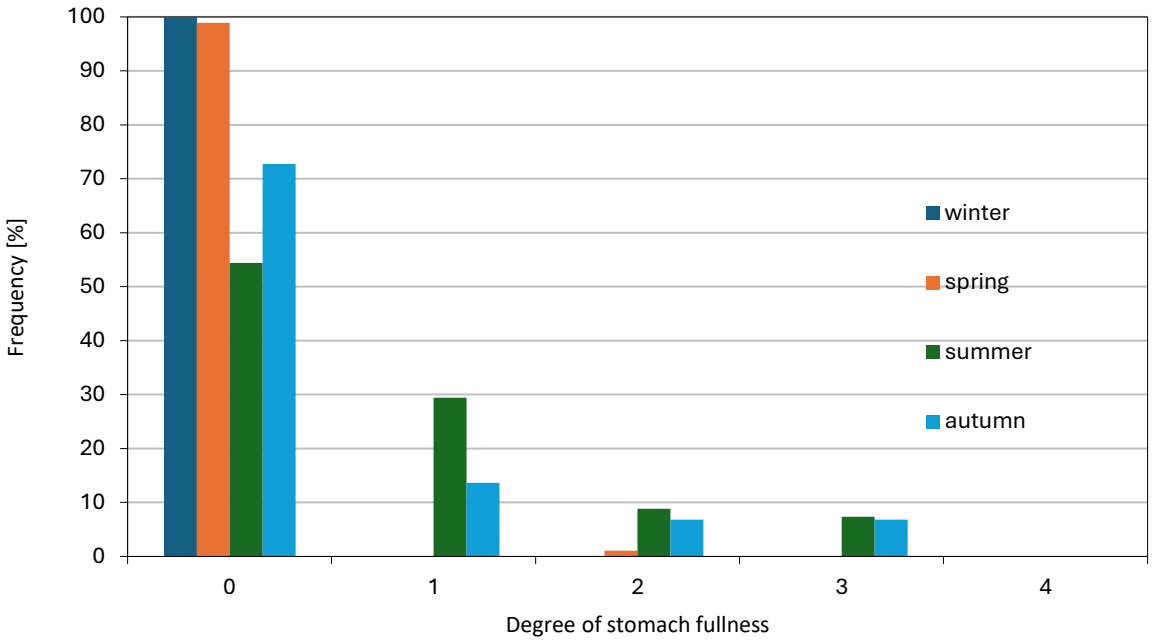


Figure 3.51. The distribution of stomach fullness degrees of sprat caught in pelagic trawl in the survey area, by the season of 2023

3.3.5.5.2 Herring

The analyses of the distribution and biological parameters of herring within the survey area were based on the results of pelagic trawl survey catches. The surveys were conducted from aboard the UST-204 fishing vessel in February, May, June, August and November 2023. The catches took place in the water column, in areas with an average depth of 34–54 m. In individual seasons (winter, spring, summer and autumn), the species discussed was present in 33%, 100%, 100% and 67% of the pelagic trawl hauls, respectively. It was most abundant in the summer catches, when 4643 fish were caught. They were less abundant in the autumn catches (3120 individuals), in spring (729 individuals) and the least abundant in winter (82 individuals). In individual seasons (winter, spring, summer and autumn), they constituted 74.6, 1.2 (98.7% of sprat), 10.5 (89.1% of sprat), 96.5% of the entire mass of all the fish caught using that type of gear. Herring were also observed in gillnet catches.

In the area surveyed, the length of herring caught [Figure 3.52] with pelagic trawls ranged from 12 cm to 24.5 cm. Herring length distribution varied between seasons. In winter, the largest individuals were caught, and the length distribution was unimodal with a clearly dominant group of fish of 20.5 cm in length. In spring, the distribution was also unimodal with a dominant group of fish of 16.5–19.5 cm in length. Fish caught in this period were smaller than those caught in the winter season. In summer, the herring length distribution was also bimodal with dominant groups of fish of 14–14.5 cm and 17–18 cm in length. On the other hand, in autumn, mainly herring similar in length to the fish caught in winter (with a dominant group of fish in the 19.0–20.5 cm length range) were recorded.

In the population structure of that species, mainly sprat belonging to the spring-spawning population from the northern areas of the Baltic Sea were observed [Figure 3.53]. These fish migrate to the Southern Baltic regions in search of feeding grounds, where they mostly winter, after which they usually return to their spawning grounds situated off the southern and eastern coasts of Sweden in spring. The proportion of the local population of spring-spawning herring was lower, whereas the autumn-

spawning herring was not recorded in the pelagic trawl survey catches within the survey area. The age composition of the spring-spawning herring – migrating from the north – was dominated by older fish between 2 and 9 years of age, with a dominant group of fish from the 2019-year class (individuals aged 4 years). Among the local spring-spawning herring (of the Southern Baltic), individuals aged 1–5 years were observed, with a distinct dominance of 1-year-old juvenile fish in summer.

The majority of herring had gonads at an early stage of development (stages 2–4). Only in spring, a small percentage (6%) of fish with gonads at the gravid stage and 6% of fish with gonads at the spent stage was recorded. Moreover, in spring, summer and autumn, fish with gonads at the resting stage (stage 8) were also recorded [Figure 3.54].

Herring stomach fullness was at a low level in all fishing seasons [Figure 3.55]. The vast majority of individuals (from 59% to 96%) in each season had empty stomachs (degree 0). Stomachs slightly filled with food (degree 1) were recorded in individuals constituting not more than 32% in each season. A small number of individuals with stomachs filled up to degrees 2 and 3 were observed only in spring and summer, but these constituted not more than 10% in total.

The catches focused on identifying the food source of avifauna in winter contained herring in length classes ranging from 18.5 cm to 25.0 cm, aged 3–14 years, while in the spring there were smaller (16.5 cm to 19.5 cm) and younger fish (aged 2–6 years). In the summer catches, herring in length classes from 17.0 cm to 27.0 cm, aged 7–16 years, were observed and in autumn, fish with a body length from 16 cm to 28 cm, aged 2–14 years. In all the seasons, the catches were dominated by fish from the northern coast of the Baltic Sea, which migrate to the survey area and mix with the populations of the Southern Baltic. In the first three fishing seasons (winter, spring, summer), the individuals caught had gonads mostly at the early maturity stages (stages 2–4). Only in autumn, herring in the spawning phase were recorded (approx. 14% of the fish had gonads at the spawning or spent stages), which suggests that those could be individuals from the autumn-spawning population, however, this was not confirmed by the otolith macrostructure analysis. The highest herring feeding intensity was recorded in winter, when 62.4% of individuals demonstrated low to medium stomach fullness degrees (degrees 1–3), while the remaining 37.6% had empty stomachs. In all the remaining seasons, fish were poorly feeding and their stomachs were mostly empty or slightly filled with food.

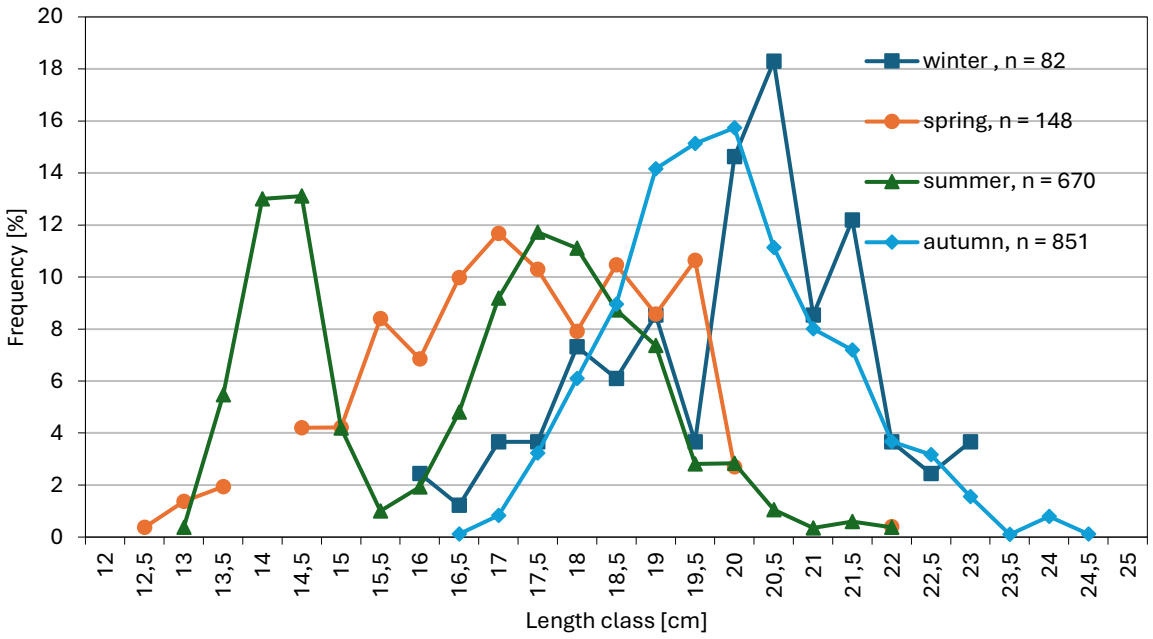


Figure 3.52. The length distribution of herring caught in pelagic trawls in the survey area, by the season of 2023

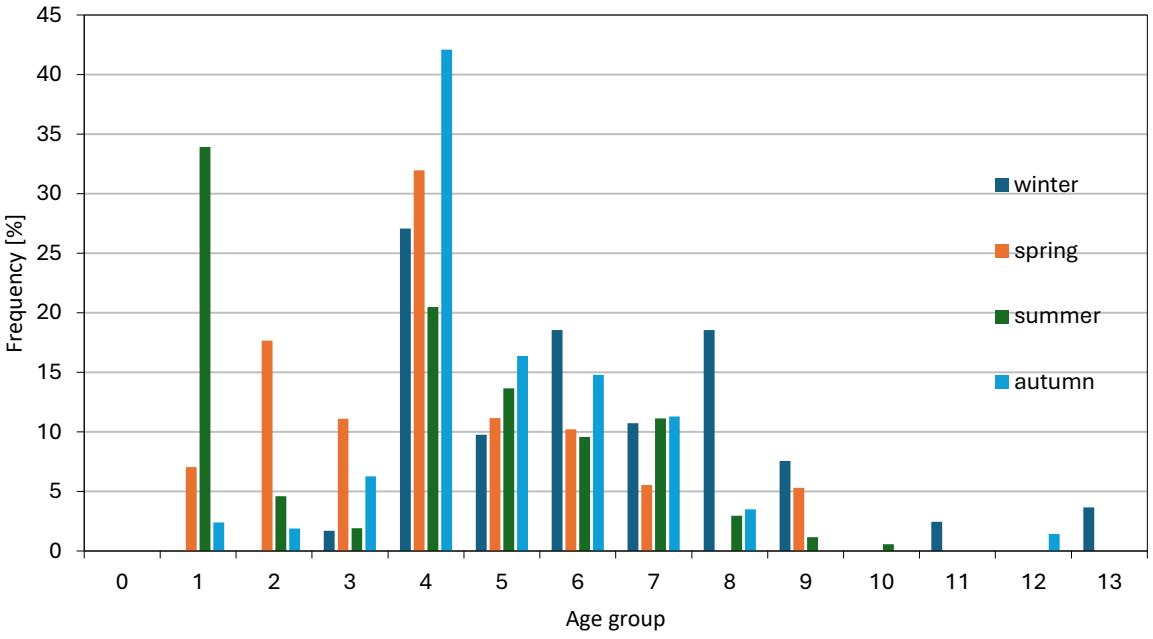


Figure 3.53. The age structure of herring caught in pelagic trawls in the survey area, by the season of 2023

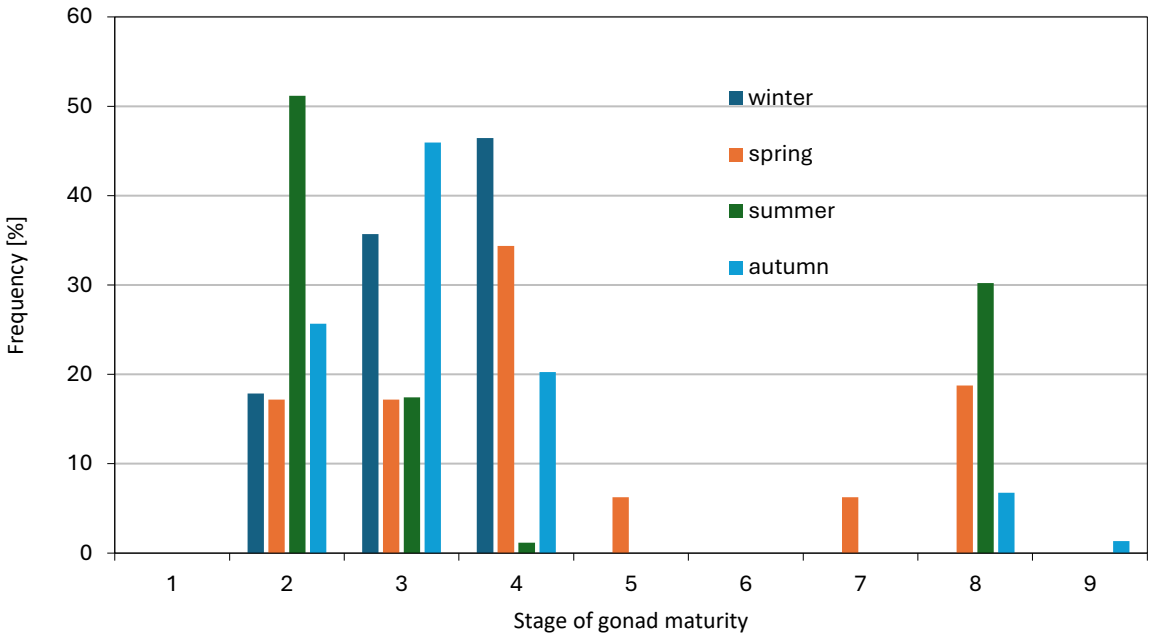


Figure 3.54. The distribution of gonad maturity stages of herring caught in pelagic trawls in the survey area, by the season of 2023

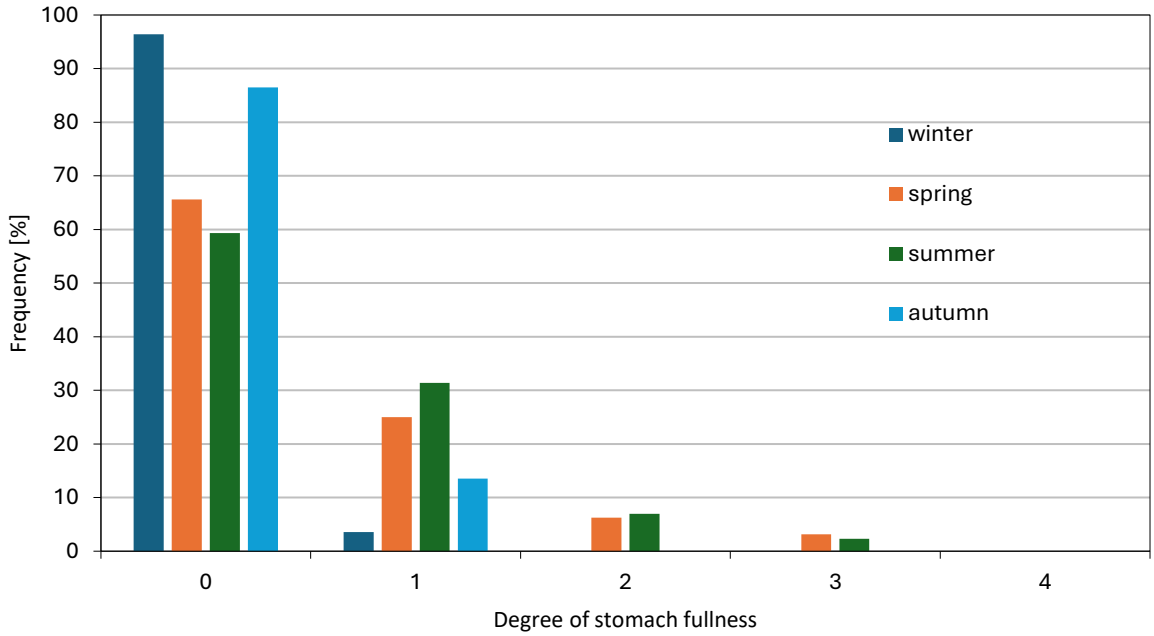


Figure 3.55. The distribution of stomach fullness degrees of herring caught in pelagic trawls in the survey area, by the season of 2023

3.3.5.5.3 Cod

Cod survey catches within the survey area were conducted in the winter, spring, summer and autumn of 2023 using survey bottom-set gillnets. The presence of cod was confirmed in each survey season. The smallest number of cods was recorded in spring – 428 ind., followed by winter – 504 ind. In summer

and autumn, significantly more cod were observed in the catches, with similar numbers of 1518 and 1536, respectively. In pelagic catches, cod were recorded only in winter (one individual) and in summer (four cod). During the catches conducted in summer using gillnets (herring gillnets and Nordic type fishing nets), aimed at investigating the avifauna, there was quite a significant by-catch of cod, the number of which amounted to 382 individuals.

The lengths of cod caught within the survey area and the distribution of their lengths varied on a seasonal basis, however, not significantly. In the catches conducted in winter and spring, the length range equalled from 16 cm to 62 cm and from 13 cm to 45 cm, respectively; whereas, in summer and autumn, the length ranges were almost identical and equalled from 13 cm to 55 cm and from 14 cm to 55 cm, respectively [Figure 3.56]. In winter, cod from the length classes from 22 cm to 30 cm constituted the most abundant fraction of fish with a proportion of 63.9%. In spring, cod from the range between 22 cm and 27 cm (63.1%) were predominant, while in summer, the length fraction of cod ranging from 21 cm to 33 cm clearly dominated in the catches with a proportion of 82.6%. In autumn, on the other hand, the catches were dominated by cod with a length of 25–32 cm, the proportion of which equalled 61.7%. From the length distribution analysis presented, it follows that the cod catches were characterised by a very high proportion of small fish from that species (< 35 cm), which clearly dominated in all the survey seasons. In winter, that proportion equalled 87.7%, while in spring, summer and autumn it was almost identical and accounted for a proportion of 91.4%, 90.6% and 90.0%, respectively.

The cod age structure within the survey area was characterised by a significant predominance of fish from age group 2 in all the survey seasons. In winter, the proportion of that age group was the highest and equalled 79.0%, and in the following survey seasons decreased slightly and in spring, summer and autumn equalled 66.9%, 65.6% and 63.8, respectively [Figure 3.57]. The range of cod age groups represented in the catches was small and slightly fluctuated depending on the survey season. In winter, it included five age groups – from age group 1 to six, with the exception of age group 5. In spring and autumn, cod from the narrowest age group range (from group 1 to 4) were recorded and cod from the age groups 1 to 5 were confirmed in summer.

The analysis of cod gonad maturity according to Maier's 8-stage scale indicated that in none of the survey seasons, cod characterised by gonads at stage 6 (spawning) were recorded within the area of the wind farm potential location [Figure 3.58]. In the summer and autumn survey seasons, cod with gonads at stage 2 (maturing virgin) accounted for the highest proportions of 84.4 and 76.2%, respectively. On the other hand, in spring and winter, the highest degree of gonad maturity for spawning was recorded, which is confirmed by the highest proportion (13.5% in each season) of cod with gonads at stage 5 (gravid), Which directly precedes reproduction. Cod with gonads at stage 8 (resting) were recorded in the catches in the survey area mainly in autumn and, to a lesser degree, in summer – 15.2% and 11.4%, respectively.

The degree of cod stomach fullness in spring, summer and autumn was characterised by the predominance of individuals with empty stomachs, 55.9%, 55.1% and 76.2%, respectively [Figure 3.59]. In winter, on the other hand, individuals with stomachs filled to a varying degree were predominant (55.6%) [Figure 3.59]. The composition of cod food was characterised by significant taxonomic diversity. The food of cod, both smaller and larger, included crustaceans such as common shrimps (*Crangon crangon*), *Saduria entomon*, mysids (Mysidacea), Gammarus, and also smaller fish, three-spined stickleback and round goby. Apart from crustaceans, the stomachs of larger individuals also contained

fish, mainly herring, sprat, greater sand eel and shorthorn sculpin, and in individual cases, also cod and fish eggs were found in the stomach.

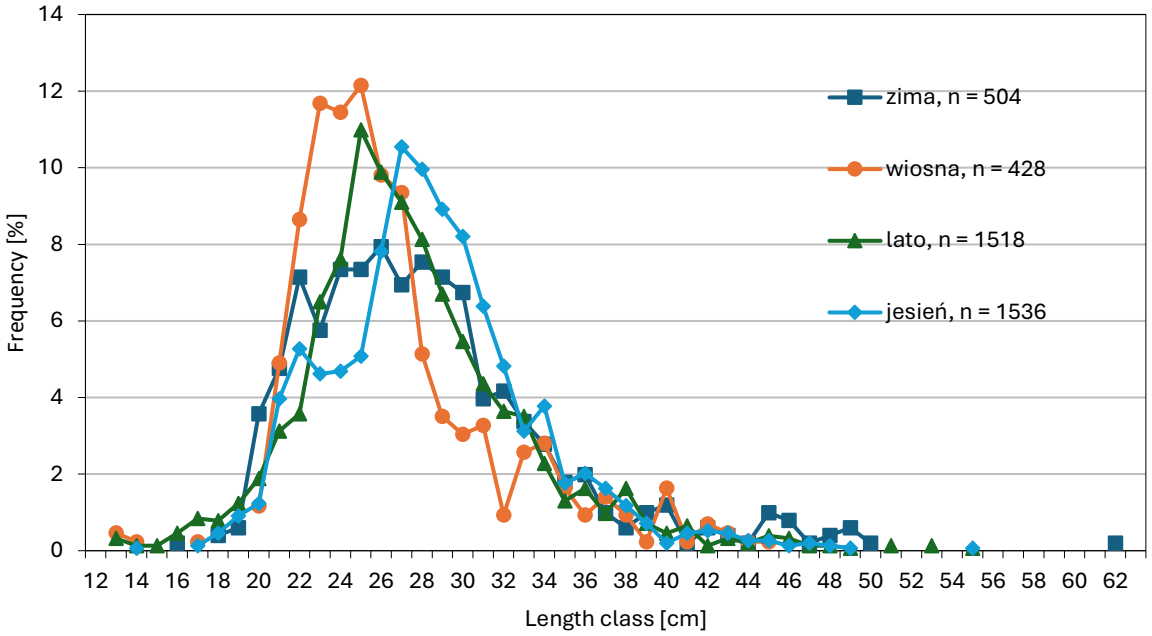


Figure 3.56. The length distribution of cod caught in gillnets in the survey area, by the season of 2023

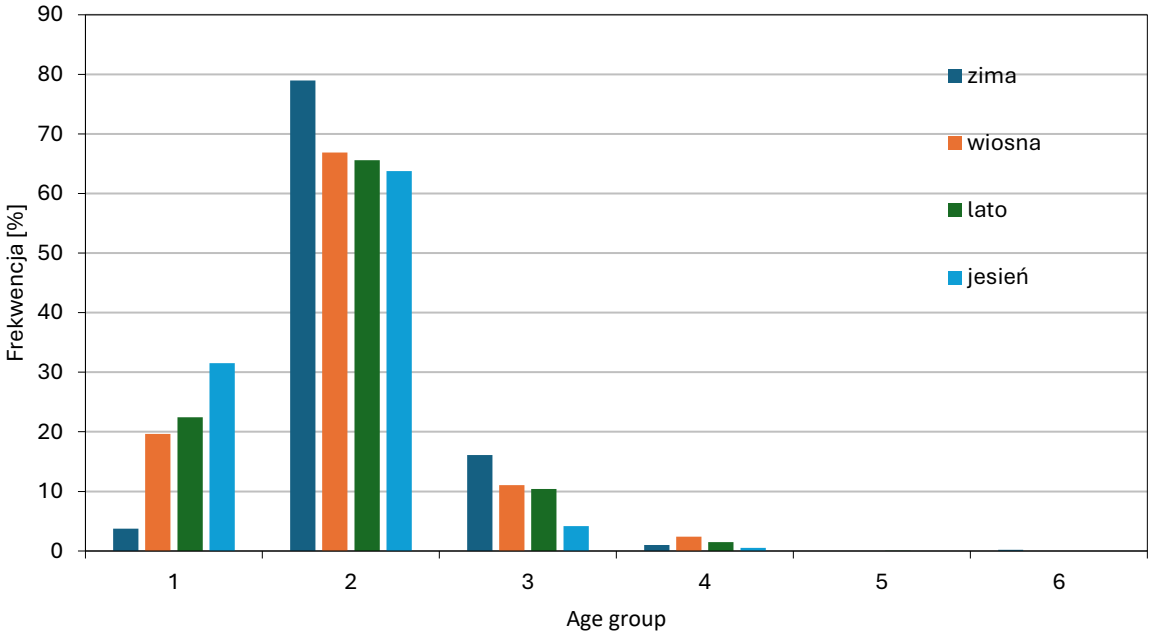


Figure 3.57. The age structure of cod caught in gillnets in the survey area, by the season of 2023

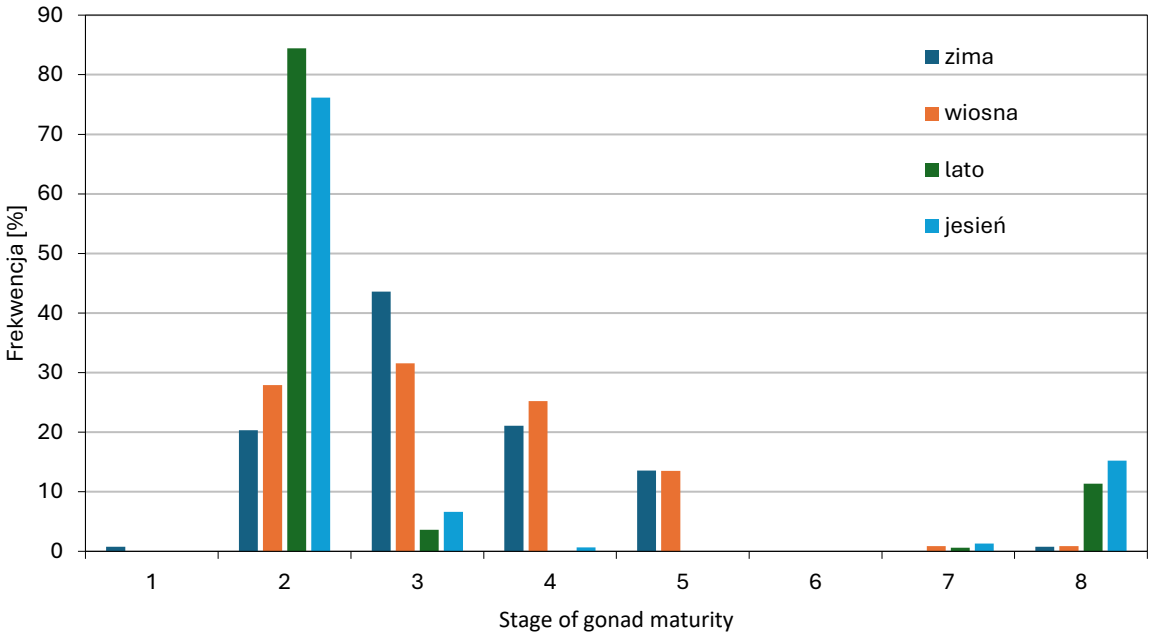


Figure 3.58. The distribution of gonad maturity stages of cod caught in gillnets in the survey area, by the season of 2023

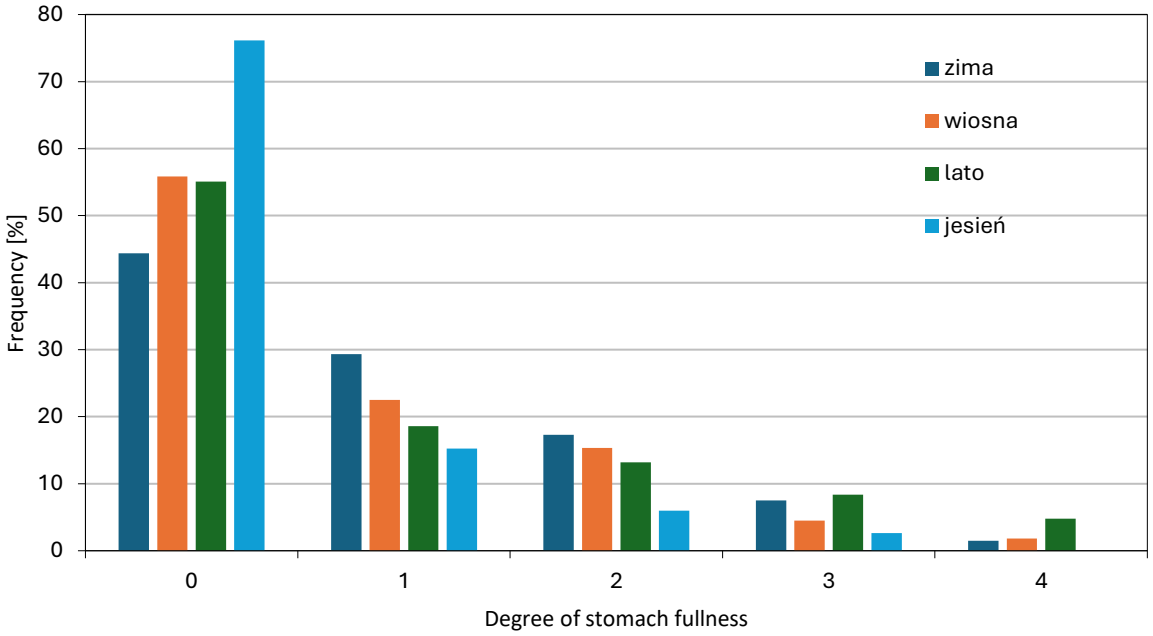


Figure 3.59. The distribution of stomach fullness degrees of cod caught in gillnets in the survey area, by the season of 2023

3.3.5.5.4 Flounder

Survey catches in the survey area were conducted using gillnets from the winter to the autumn of 2023. Flounder occurred in the survey area all year round. The lowest abundances of this species were recorded in autumn (54 individuals in a catch) and the highest (720 individuals) in summer.

The material obtained during the catches allowed describing the basic biological characteristics of flounder, such as length, age composition, gonad maturity stage in males and females and stomach fullness degree.

The length range of the flounder from the survey catches did not differ between the seasons. Most often caught were the adult individuals representing 24 to 28 cm length classes [Figure 3.60]. The individuals caught in the winter ranged from 20 to 36 cm, in the spring – from 18 to 42 cm, in the summer – from 17 to 37 cm, whereas in the autumn – from 20 to 31 cm. The individuals below the minimum landing size (23 cm) accounted for an abundance of 5.6% in the winter to an abundance of 9.8% in the summer. The peak of the length frequency distribution fell at 26 cm in winter (20.2% of the abundance proportion), 27 cm in spring (12.1% of the abundance proportion), 25 cm in summer (14.0% of the abundance proportion) and 24 cm in autumn (22.2% of the abundance proportion).

Fish aged between 1 to 24 years were caught within the area surveyed [Figure 3.61]. The proportions of individual age groups, as in the case of length distributions, did not differ significantly between the seasons. In winter and autumn, individuals from age group 4 were caught most often; they constituted 29.0 and 25.1% of the abundance proportion, respectively. Flounder from age group 6 (21.3% of the abundance proportion) dominated in spring, while in summer, from age group 7 (23.5% of the abundance proportion). Juvenile individuals, from age group 2, occurred in the survey area only in spring and summer, accounting for an abundance proportion of 0.2 and 1.0%, respectively. Fish from age group 11 and older were caught sparsely and in individual seasons accounted for a total abundance from 7.3% in spring to 11.6% in winter.

The analysis of gonad maturity stages conducted on males and females in the survey area indicated the presence of flounder spawning in winter. A proportion of individuals with gonads at the spawning stage (stage 6; 13.5% proportion) and at the spent stage (stage 7; 5.8% proportion) was recorded then. The most abundant were the individuals with gonads at the gravid stage (stage 5; 52.0% of the abundance proportion) [Figure 3.62]. Also present were flounder with gonads at the developing (stage 3) and developed (stage 4) stages, the joint abundance proportion of which was 26.9%. In spring, gonads at the maturing virgin stage dominated (stage 2; 64.8% of the abundance proportion). Also, fish with gonads at the resting stage (stage 8; 28.4% of the abundance proportion) were present in large numbers. Stages 3, 4 and 7 of the gonad maturity were observed in small proportions (up to 3.4%). In summer, similarly as in spring, the most abundant were the individuals with gonads at the maturing virgin stage (stage 2; 60.7% of the abundance proportion) and at the resting stage (stage 8; 21.4%). In autumn, individuals with gonads at the developed stage (stage 4) and at the developing stage (stage 3) prevailed, with the abundance proportion of 52.3 and 38.6%, respectively.

The results of the analyses of the stomach fullness degree of flounder showed that in the survey area, the fish fed most intensively in spring and summer. They fed least intensively in winter, when empty stomachs were observed in 84.6% of the individuals analysed [Figure 3.63]. In spring, the stomachs of 50.0% of the individuals were full. Among them, 1/4 and 1/2 full stomachs (degrees 1 and 2) were observed in 10.2 and 17.1% of fish, respectively. The individuals with full stomachs (degree 4) and with

3/4 full stomachs (degree 3) constituted 11.4% of the abundance proportion each. In summer, the feeding activity of flounder was the highest. Empty stomachs were observed in 45.2% of individuals. Among the individuals with stomachs filled with food, there were fish with stomachs 1/4 full and 1/2 full (degree 1 and 2, respectively) constituting 23.8 and 21.4% of the abundance proportion, respectively. The remaining flounder (9.5% of the abundance) had full stomachs (degree 4) and 3/4 full stomachs (degree 3). In autumn, flounder were feeding less intensively than in summer. Foraging individuals, with 1/4 full (degree 1), 1/2 full (degree 2) and 3/4 full stomachs (degree 3) accounted for 13.6, 6.8, and 11.4% of the abundance proportion, respectively. The flounder food content included mainly bivalves (with Baltic clams and bay mussels prevailing).

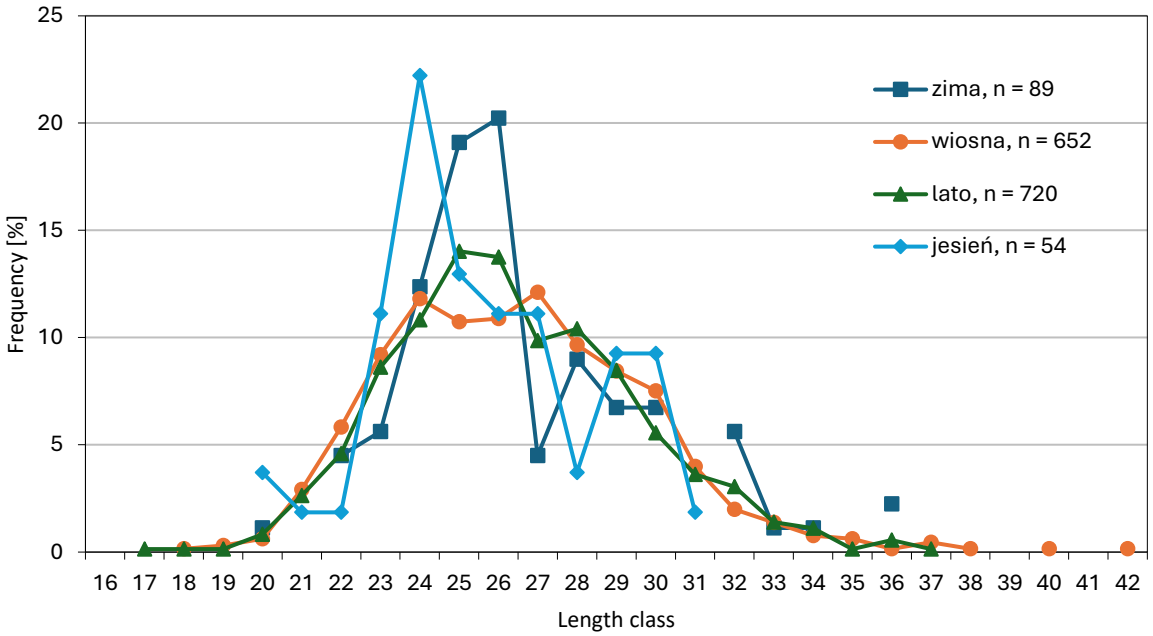


Figure 3.60. The length distribution of flounder caught in gillnets in the survey area, by the season of 2023

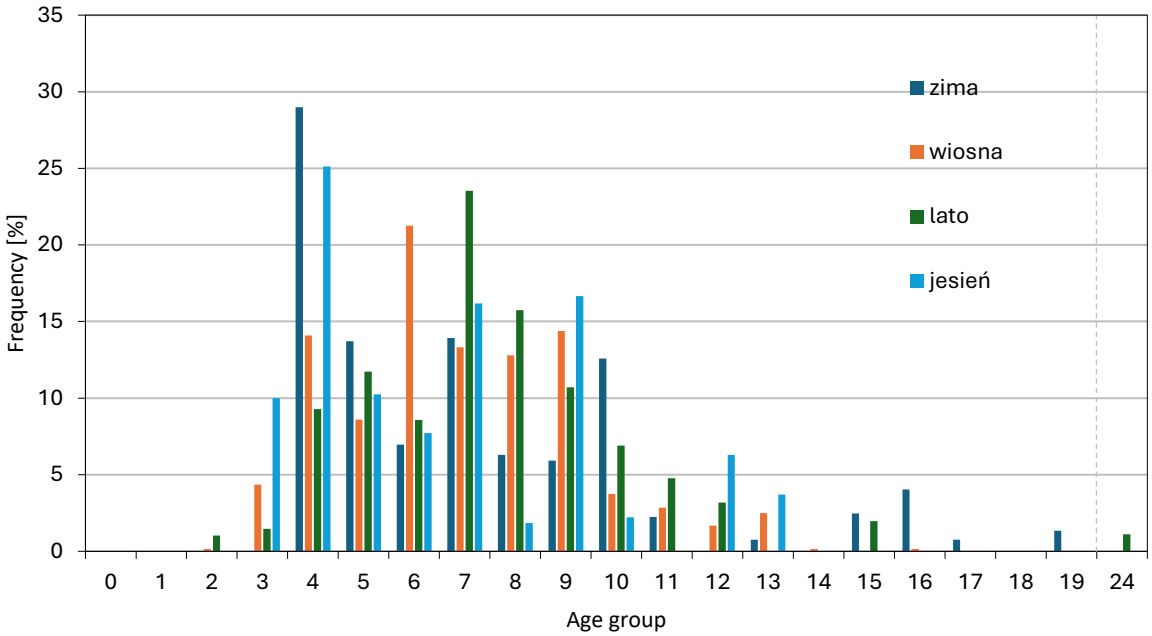


Figure 3.61. The age structure of flounder caught in gillnets in the survey area, by the season of 2023

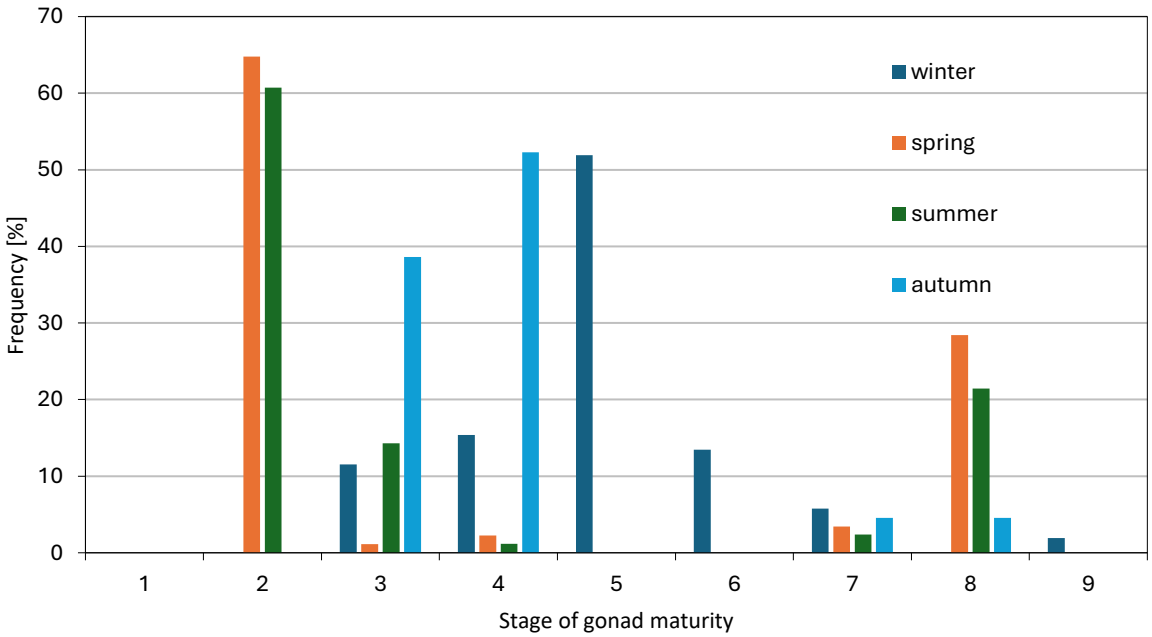


Figure 3.62. The distribution of gonad maturity stages of flounder caught in gillnets in the survey area, by the season of 2023

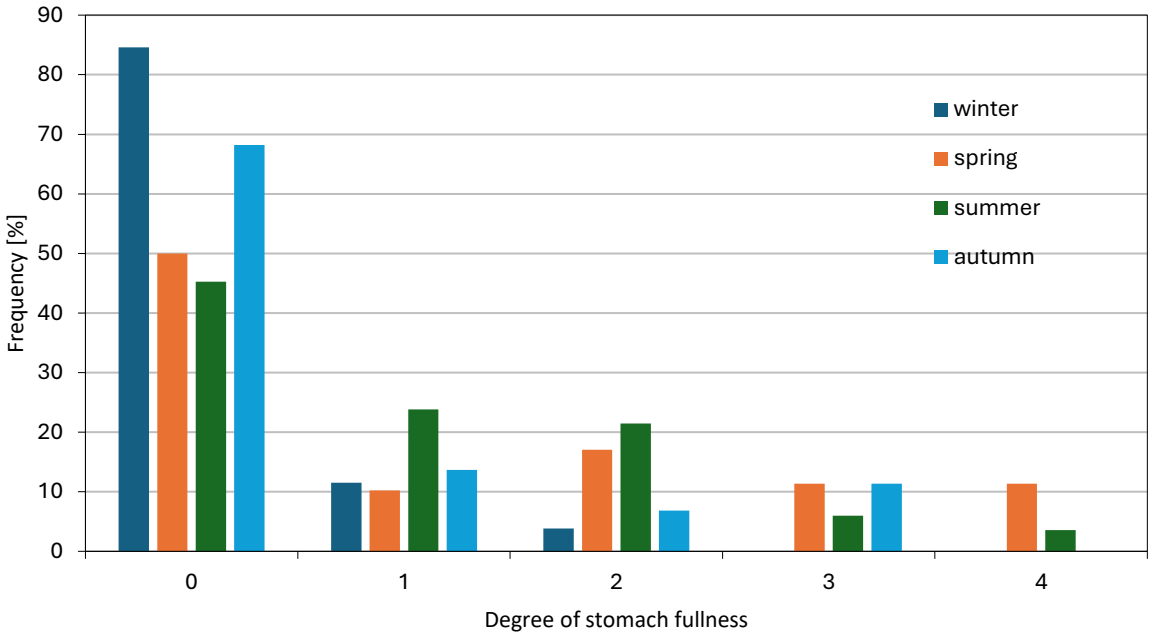


Figure 3.63. The distribution of stomach fullness degrees of flounder caught in gillnets in the survey area, by the season of 2023

3.3.6 Summary of results and conclusions

3.3.6.1 Ichthyoplankton

No pelagic eggs were caught during the ichthyoplankton surveys carried out in the survey area in winter, spring, summer or autumn; there were however records of fish larvae belonging to 8 taxa: sprat, ammodytids, flounder, gobies, common seasnail, herring, fourbeard rockling and rock gunnel.

The occurrence of larvae belonging to three species, common seasnail, herring and rock gunnel was observed in winter. The taxonomic diversity found was slightly lower than the one usually reported in the literature for the Southern Baltic in that season (4 taxa) (Herra, 1988). In spring, the larvae of fish belonging to three species, sprat, flounder and common seasnail, were caught. The number was lower than the one reported in literature for that period of the year (between 5 and 10 taxa) (Herra, 1988). In summer, also the larvae of fish representing three taxa, gobies, ammodytids and fourbeard rockling, were recorded. The taxonomic diversity found was much lower than the one usually observed in the Southern Baltic in in that season (10–11 taxa) (Herra, 1988). The occurrence of fish larvae belonging to four taxa, ammodytids, gobies, herring and fourbeard rockling, was recorded in autumn. Similarly as in the case of the other seasons, the diversity was lower than the one reported in literature for that period of the year (6 taxa) (Herra, 1988).

Throughout the entire survey period, sprat and ammodytid larvae represented the highest proportion (39.7% and 32%, respectively) in the total abundance of fish larvae, followed by flounder (14.0%) and gobies (9.14%). The remaining species collectively accounted for 5.14%.

The occurrence of sprat larvae was only recorded in spring in the average abundance of 19.38 ind.·10 m^{-2}. The most common date reported in literature for the beginning of the sprat

reproduction is February (Ojaveer and Kalejs, 2010), however, a low-intensity spawning was also recorded in January (Haslob et al., 2013).

The abundances of sprat observed in the survey area in April 2023 were higher than those observed in the same month of 2012 at the planned Bałtyk II OWF and Bałtyk III OWS areas (2.3 to 10.1 ind.·10 m^{-2}), which are located at similar depths (Drgas et al., 2014; Drgas et al., 2015). They were, however, within the range of the abundances recorded in the years 2006–2008 in the Southern Baltic at a similar depth range (1.7–55.4 ind.·10 m^{-2}) (Margoński et al., 2006; 2008).

In the years 2006–2008, the values observed at the spawning grounds in the Słupsk Furrow were in the lower part of the abundance range (1.4–1566.7 ind.·10 m^{-2}) (Margoński et al., 2006; 2008).

The early-spring sprat spawning does not take place there because of the too low water salinity. The spatial distribution of larvae (notably higher abundances at stations in the southern part of the survey area) indicated their origin from the spawning grounds in the Słupsk Furrow, where the salinity required for deep-water spawning reaches at least 9 PSU in spring.

The second most abundant taxon were the ammodytid larvae which occurred in two survey seasons, reaching their highest abundance in August (15.19 ind.·10 m^{-2}). Their abundance in October was several times lower. The occurrence of the larvae of this taxon was limited to two stations in summer and one in autumn. The ammodytid spawning occurs from May to November, in the shallow waters at depths of up to 20 m, on a seabed covered with a sandy or gravelly sediment, onto which the eggs are spawned. Ammodytids can spawn in the shallow waters of the Middle Bank, including the shallowest part of the survey area located within the Southern Middle Bank.

The third most abundant species of fish larvae in the survey area was flounder, occurring only in spring with the abundance of 6.25 ind.·10 m^{-2}. This value is within the range of the abundances recorded in the years 1983–1985 in the waters with a depth of up to 40 m (from 0 to 27.00 ind.·10 m^{-2}) (Herra, 1983; 1988). The abundance of flounder larvae in the survey area, on the other hand, was lower than the values observed for regions with similar depths, such as the planned Bałtyk II OWF and Bałtyk III OWF in 2012 (between 9.4–48.8 ind.·10 m^{-2}) (Drgas et al., 2014; Drgas et al., 2015] and the waters of the southern Baltic Sea in the years 2006–2007 (7.8–234.9 ind.·10 m^{-2}) (Margoński et al., 2006; 2008).

The spawning of flounder occurs in the near-seabed layers of the Arkona Deep, the Bornholm Deep, the Gdańsk Deep and the Słupsk Furrow at a depth of 40–80 m, where water salinity is within the range of 10.7–11.7 PSU (Nissling et al., 2002). Spawning of this species is precluded in the survey area by the water salinity being too low. The spawning grounds in the Słupsk Furrow were the probable place of origin of the larvae caught in the survey area. The spatial distribution of the abundance of larvae in April 2023 (values decreasing with the distance from the Słupsk Furrow) is a result of the process of multi-directional dispersion of larvae from their place of spawning.

The occurrence of goby larvae in the survey area was recorded in the highest abundance in summer (3.18 ind.·10 m^{-2}), as well as in autumn, in small abundances. The value recorded in August 2023 was within the lower range of the abundance scope observed in summer in the years 2006–2023 in the Southern Baltic within a depth range of 27–50 m (0.4–84.6 ind.·10 m^{-2}) (Margoński et al., 2006; 2007; 2008; 2009; 2010; 2011, 2012; 2013; 2014; 2016; 2017; 2018; 2019; 2020). However, the abundance recorded for the survey area exceeded the values for the areas of the planned offshore wind farms Bałtyk II OWF and Bałtyk III OWF (depth range of 22–52 m) recorded in summer 2012 (from 0.7 to 1.1 ind.·10 m^{-2}) (Drgas et al., 2014; Drgas et al., 2015).

The spawning of gobies takes place in summer in the shallow waters at depths between 2−10 m. The too great depth of the survey area excludes the possibility that the larvae caught came from the spawning taking place in that region. Their reproduction probably took place in the coastal waters of the Stilo Bank, the Czołpino Shallows, the Słupsk Bank or in the shallowest part of the Middle Bank. The larvae of gobies disperse widely in the water depth after spawning; therefore, it is safe to assume that the larvae caught were transported to the survey area with the sea currents. The even spatial distribution of the larvae caught within the entire area indicates that they originated from many potentially available places with favourable substrate required for spawning.

Few larvae of herring were observed in two survey periods, in autumn (0.41 ind.·10 m^{-2}) and in winter (0.07 ind.·10 m^{-2}) (the autumn-spawning herring). The abundances observed in the survey area were lower than those recorded in these seasons in the years 2012–2013 in the Bałtyk II OWF and Bałtyk III OWF areas, at the depths from 22 to 52 m (from 0.7 to 2.5 ind.·10 m^{-2} and from 0.7 to 0.9 ind.·10 m^{-2}, respectively) (Drgas et al., 2015 a and b). The larvae caught in the survey area may have originated from the spawning taking place on the bank slopes to a depth of 25 m. It may have taken place in the Słupsk Bank and the Middle Bank area, including the section of the area surveyed located in the shallowest part of the Southern Middle Bank.

The larvae of fourbeard rockling were recorded in two survey periods, in summer and autumn. They originated from the deep-water spawning grounds located in the Słupsk Furrow, where the salinity required for proper reproduction of 10–11 PSU can be found (Horbowa and Fey, 2013).

Few larvae of common seasnail were recorded in winter and spring, while the rock gunnel was only recorded in winter. The occurrence of these species in the survey area may result from the transfer of larvae from their spawning grounds in the Middle Bank, in the Słupsk Bank or in the coastal regions. However, it cannot be ruled out that they originated from the spawning occurring directly in the shallowest part of the survey area.

Two out of the taxa of fish larvae recorded, i.e. gobies and common seasnail, belong to partially protected species under the Regulation of the Minister of the Environment of 16 December 2016 on the protection of animal species (Journal of Laws of 2016, item 2183, as amended). During the surveys discussed, the presence of gobies was recorded in summer and in autumn, and of common seasnail in spring. Gobies were not identified to species, however, based on the knowledge from the literature, it can be assumed that the dominant species in the samples collected was sand goby (Horackiewicz and Skóra, 1996; 1998).

3.3.6.2 Hydroacoustic surveys and pelagic hauls

The areal biomass density of herring and sprat was referenced to the average areal biomass density of these species determined based on data from the spring SPRAS (Sprat Acoustic Survey) vessel passages and autumn BIAS (Baltic International Acoustic Survey) vessel passages in the corresponding ICES statistical rectangles in the years 2017–2021 [Table 3.35].

The highest areal biomass density of herring in the survey area, 6.16 t·NM^{-2}, was estimated for the summer survey campaign when it was two times higher than the average value of this parameter determined based on spring SPRAS vessel passages as well as more than two times lower than the average from the BIAS vessel passages in the years 2017–2021. Also, the areal biomass density of herring recorded during the autumn campaign, 2.16 t·NM^{-2}, was lower than the average from the autumn BIAS vessel passages calculated for the reference period. The areal biomass density of herring

recorded during the spring campaign, 1.12 t·NM^{-2}, was lower than the average from the May SPRAS vessel passages calculated for the reference period. The lowest value of the areal biomass of herring, 0.94 t·NM^{-2}, was recorded during the February campaign.

The highest areal biomass density of sprat in the survey area, 18.29 t·NM^{-2}, was estimated for the spring survey campaign; however, it was more than two times lower than the average value of this parameter defined based on the May SPRAS vessel passages in the years 2017–2021. Also, the areal biomass density of sprat recorded during the August campaign, 4.91 t·NM^{-2}, was lower than the average from the autumn BIAS vessel passages calculated for the reference period. The areal biomass densities of sprat estimated during the autumn and winter campaigns remained at a very low level of 0.01 and 0.04 t·NM^{-2}, respectively.

Table 3.35. The areal biomass density of pelagic fish, determined using acoustic methods based on SPRAS and BIAS vessel passages conducted in the years 2017–2021

ICES rectangle	Areal biomass density from the period 2017–2021 [t·NM^{-2}]			
	Herring		Sprat	
	SPRAS	BIAS	SPRAS	BIAS
39G7/40G7	2.77	14.91	41.50	10.63

3.3.6.3 Results of catches and biological analyses

The analysis of the results of catches and catch rates of the fish community inhabiting the survey area demonstrates that this area is typical in terms of species diversity compared with the waters of similar depth, with a distinct prevalence of cod and flounder in demersal catches and herring and sprat in pelagic catches.

A fish community is treated as a biocenosis – all living components comprising an ecosystem. A community is an integrated, local grouping of fish characterized by repeatability of its species composition. Fish, contrary to plant assemblages, are not permanently tied to a specific location – they migrate within the boundaries of the conditions optimal for them. Depending on their aim, these trips are called spawning or feeding migrations. It is an open system, in which persistence and accurate determination of geographic location boundaries for a fish community considered as a separate ichthyocenosis is difficult.

As a result of demersal catches using fixed nets in the survey area, 1421.9 kg of fish belonging to 14 taxa were caught. Cod and flounder dominated. The remaining species (greater sand eel, plaice, shorthorn sculpin, pogge, mackerel, twaite shad, turbot, sprat, herring, lumpfish, lesser sand eel and viviparous eelpout) constituted by-catches. In the case of herring gillnet catches, the same taxonomic composition (also recorded was the fourhorn sculpin) as in the case of multi-mesh gillnets was recorded.

Fish belonging to 24 taxa were caught in all the survey gear in the survey area [Table 3.36].

Table 3.36. All taxa recorded during the survey catches conducted within the survey area

No.	Taxon	Pelagic catches	Demersal catches	Ichthyoplankton catches
1.	Gobies			X
2.	Garfish	X		
3.	Nine-spined stickleback	X		
4.	Three-spined stickleback	X		

No.	Taxon	Pelagic catches	Demersal catches	Ichthyoplankton catches
5.	Common seasnail			X
6.	Greater sand eel	X	X	X
7.	Cod	X	X	
8.	Plaice		X	
9.	Shorthorn sculpin		X	
10.	Fourhorn sculpin		X	
11.	Pogge		X	
12.	Atlantic salmon	X		
13.	Mackerel	X	X	
14.	Fourbeard rockling			X
15.	Rock gunnel			
16.	Twait shad		X	
17.	Anchovy	X		
18.	Turbot	X	X	
19.	Flounder	X	X	X
20.	Sprat	X	X	X
21.	Herring	X	X	X
22.	Lumpfish	X	X	
23.	Lesser sand eel		X	
24.	Viviparous eelpout		X	

The efficiency analysis of the survey gillnet gear demonstrated that the peak of fish density occurred in summer and autumn because the shallower waters of the survey area serve as foraging grounds during those seasons. In other periods, fish densities were similar, while the lowest efficiencies were recorded in winter.

Both the length range as well as the modal length of sprat present in the samples from pelagic trawl catches differed depending on the survey season. The samples collected in the winter, spring, summer and autumn of 2023 contained sprat in the following length classes: 10.5–14.5, 9.5–14.5, 11.5–15.0, and 8.5–14.5 cm, respectively. In spring and autumn, unlike in the remaining seasons, the presence of small sprat, <10.0 cm, was found in the samples. The proportion of sprat from the above-mentioned size fraction was on average 6.9% (in spring) and 6.6% (in autumn).

Distinguished by their sample proportion, sprat from age groups 3, 4 and 5, equated with fish belonging to year classes of 2020, 2019 and 2018, respectively, on the scale of the entire Baltic stock are classified as year classes 17% and 23% more numerous and 37% less numerous, respectively, than the long-term average abundance of recruiting year classes of 1973–2022, amounting to 81.3 million individuals (based on WGBFAS-ICES, 2022).

In February 2023, as in previous years, sprat started the first phase of spawning in the water depth of the Baltic Sea, in waters deeper than the survey area. The process intensified on a large scale in May, then gradually declined in the second half of summer. Exceptionally, in October-November, there were a few sprats present in the samples, which were involved in the final phase of spawning or had just

completed that process. Sprat spawning extended over time (2023) has so far been recorded quite rarely and for a small proportion of the population of these fish.

The process of mass feeding of sprat intensifies once the spawning ends, particularly at the turn of summer and autumn, and then gradually declines to a minimum (starving state) at the beginning of winter, while in spring it is of an accidental nature and concerns only a few individuals.

Being a widespread species, herring occurs in the entire Polish area of the Baltic Sea (Fey et al., 2014). Ichthyofauna surveys carried out in 2023 demonstrated a moderate abundance of herring in the potential project location. The highest abundances of this species were recorded in summer, when the foraging shoals of herring or groups of herring searching for grounds with greater food availability were observed (Aro 1989, 2002). The analyses of stomach content confirm the more intense feeding of herring in summer. The high proportion of fish with empty stomachs in winter and autumn indicates the occurrence of low intensity feeding in the planned project area, possibly related to the low availability of preferred zooplankton groups (Casini et al., 2004; Ojaveer et al., 2018) or a periodic decrease in physiological activity.

The age structure of the fish caught reflects the typical age of herring in the Central Baltic stock, with the prevalence of the year class 2019 (ICES, 2023). The catches indicate the periodical occurrence of juvenile fish, particularly in summer, although herring with a length of less than 15 cm (age group 0 mostly) are rare, suggesting that the area is not a site of key significance for juvenile fish.

In winter, fish from the spring-spawning population migrate to spawning areas, where mature individuals spawn and juvenile forms develop (Seitz et al., 2014). The migrations mainly take place towards nearshore zones with smaller depths. In the planned project area, adult herring can migrate towards Swedish or Polish coasts, however the planned project area alone is not a significant spawning ground for herring due to its depth, lack of suitable substrate and the distance from the shore. According to the model studies performed by the Baltic Marine Environment Protection Commission, herring spawning might occur in numerous places along the coasts of both countries (HELCOM, 2021), including the Vistula Lagoon, where annual, high spawning concentrations of herring are observed (Krasovskaya 2003; Fey et al., 2014). Favourable spawning conditions can also be found in the Bay of Puck and the Bay of Pomerania (Ojaveer et al., 1981).

The herring spawning period is subject to phenological variation due to the year-to-year variability of hydrological conditions in the Baltic Sea. The period of the greatest activity can vary between years, depending on the thermal conditions or the icing of water bodies, as it is the case in the Vistula Lagoon (Krasovskaya, 2003). The highest intensity of herring spawning usually takes place from March to May. The surveys carried out in the planned project area showed that herring had gonads at the most developed stage in winter and spring, which indicates their preparation for reproduction. The low abundances of this species in the February (winter season) and May/June (spring season) catches confirm that the proposed project area does not play a significant role in the spawning of this species. Herring probably already gathers in the shallow spawning grounds at that time.

The results of cod abundance surveys conducted during individual survey seasons indicate a low occurrence of these fish in winter and spring. The abundant occurrence of cod was recorded in the potential area of the offshore wind farm location in summer and autumn. The above-mentioned results of cod abundance surveys might, therefore, indicate that the planned project area constitutes a less significant habitat for fish of this species in the winter-spring season than it does in summer and

autumn. The cod length composition within the survey area was characterised by substantial predominance of small fish (< 35 cm) in all survey seasons. The prevalence of small cod in the survey area was largely due to the shallow-water character of the sea area surveyed (from 18 to 52 m). Shallower waters are generally inhabited by smaller individuals (Orio et al., 2019). In addition, the long-observed status of the Eastern Baltic cod stocks is characterised by a considerable proportion of smaller fish due to overfishing (ICES, 2023; Svedäng and Hornborg, 2017), but also results from a more abundant hatching of these fish in the Bornholm Basin and their eastward expansion, causing the increased proportion of small cod in the catches (ICES, 2023; Radtke et al., 2023). Seasonal fluctuations in the dominant ranges of cod length classes were found within length classes of less than 35 cm. The shift of the length distribution curves within the dominant length classes to the right on the horizontal axis was observed also in the successive survey seasons, beginning in spring. Seasonal changes in the length composition of cod recorded in the area of the planned project resulted from the biological characteristics of these fish. These are manifested by spawning migrations from the shore towards the depths, where cod spawning grounds are situated and feeding migrations from the depths towards the shores. The planned project area lies on the path of the above-mentioned migrations (Aro, 1989; Lundgren et al., 2022; Więcaszek, 2010]. In spring, the cod preparing for spawning, i.e. larger and older individuals, migrate towards spawning grounds outside of the planned project area. A similar situation took place in the planned offshore wind farm area in summer when most adult cods spawned in the depths of the Baltic Sea. Whereas in autumn, the proportion of the shortest cods was the smallest, while the proportion of longer fish increased, as a result of the individuals returning to the feeding grounds after spawning. The fish migrated towards the shore, also through the planned project area. The clear dominance of cod within the 20–30 cm range observed in all the survey seasons was the result of the above-mentioned more abundant hatching of these fish in the Bornholm Basin. Literature data confirm that a noticeable increase in the proportion of smaller cod occurs especially when the abundance of a new year class is relatively high (Bagge et al., 1993; Eero, 2008). The age structure of the cod caught shows the prevalence of fish from age group 2 in all survey seasons, which is also confirmed by the results of the length measurements mentioned above, indicating the prevalence of cod within the 20–30 cm range. The area of the potential offshore wind farm location was thus characterised by the evident prevalence of juvenile cod, including age groups 0–2 and small fish, in all survey seasons. The results of gonad maturity stage analysis, which showed a lack of individuals with gonads at stage 6 (spawning) indicate that the area monitored is not a spawning ground for cod. The occurrence of cod after spawning (11.4 and 15.2% of cod with gonads at stage 8 – resting) in the survey area in autumn and summer complements the findings on cod migration taking place in the planned project area or through that area towards the shore after spawning – for feeding. The prevalence of cod with empty stomachs was recorded in the cod stomach fullness surveys in spring, summer and autumn (55.9, 55.1 and 76.2%, respectively). Cod that were found with stomachs filled with food were only dominant in winter at 55.6%. The above results indicate low food availability for cod during most of the survey seasons. However, the aforementioned considerable diversity of food components recorded in the stomachs of cod clearly indicates that the proposed project area is favourable for cod of different sizes, in terms of food composition. Crustaceans are eaten by larger cod but are primarily a major component of the diet of smaller cod up to 30 cm (Pachur and Horbowy, 2013; Pachur and Pawlak, 2016). Thus, it can be concluded that there was food in the survey area, available for cod of a wide length range. This is because food selection by cod is determined by their length (Pachur and Horbowy, 2013).

The survey area served as a habitat mainly for adult flounders. Flounder were most abundant there in summer and least abundant in autumn (720 and 54 individuals, respectively). The length distributions did not differ significantly between the seasons. Juvenile individuals, represented by age group 2, occurred in spring and summer with a proportion of up to 1.0% in summer.

The stages of gonad maturity recorded in winter flounder catches indicated the ongoing spawning of this species. The gravid stage of gonad maturity dominated. The occurrence of individuals with gonads at the spawning and spent stages was also recorded. The maturing virgin stage dominated in spring, which may be indicative of the completed spawning. Individuals with gonads at the resting and the maturing virgin stages dominated in summer. In autumn, when individuals with gonads at the developing stage were dominant, flounder began entering the preparatory phase for the next spawning.

Considering the hydrological conditions prevailing in the area (the maximum salinity of < 10 PSU) which are not favourable for the reproduction of the European flounder (*Platichthys flesus*) occurring in the survey area (Momigliano et al., 2018), it is safe to assume that the fish migrated from the area surveyed to the nearby Słupsk Furrow or the Gdańsk Deep to spawn. The results of the ichthyoplankton catches that were carried out in the area surveyed and in which flounder eggs were not recorded, may confirm that assumption. However, the occurrence of flounder larvae was recorded in the winter and spring catches, probably as a result of their drifting into the area from the spawning grounds located in the above-mentioned Baltic depths.

In spring and summer, flounder occurred most abundantly and were feeding most intensively in the survey area. In autumn, their abundance decreased significantly compared to summer (more than 13 times) and the individuals that remained in the area surveyed were foraging less intensively. Therefore, it can be assumed that in autumn, some of the flounder started migrating in search of spawning grounds. In winter, the feeding activity of the individuals that remained in the survey area stopped completely, while their abundance was similar to the one recorded in autumn. The low feeding activity of flounder was typical for this time of year – during spawning, flounder devote all their energy to reproduction and only replenish their energy losses after spawning. The individuals of this species started feeding intensively only in spring, and their abundance increased, indicating that a suitable food supply in or near the survey area is available.

3.3.6.4 Conclusions

The conclusions from the ichthyofauna surveys carried out in the survey area are listed below:

- The taxonomic diversity of ichthyoplankton (larvae belonging to 8 fish taxa) in the survey area was low in comparison with what is usually observed in the Southern Baltic surveys.
- Due to the low salinity of the area, the early-spring spawning of sprat does not take place there. The larvae caught during that period probably came from the spawning taking place in the Słupsk Furrow. The absence of larvae in summer might have resulted from the timing of sampling coinciding with the final period of the summer shallow-water spawning.
- The salinity of the survey area is too low for the reproduction of flounder and fourbeard rockling to take place there. The larvae caught in the survey area came from the spawning taking place in the Słupsk Furrow.

- The ammodytid larvae caught in the survey area probably came from the spawning taking place in the shallow regions of the Middle Bank, including the shallowest part of the survey area in the Southern Middle Bank.
- The too great depth of the survey area eliminates the possibility that the goby larvae caught came from the spawning taking place in that region. Their reproduction probably took place in the coastal waters of the Stilo Bank, the Czołpino Shallows, the Słupsk Bank or in the shallowest part of the Middle Bank.
- The larvae of the autumn-spawning herring caught in October and March may have originated from the spawning taking place in the Słupsk Bank and the Middle Bank area, including the section of the area surveyed located in the shallowest part of the Southern Middle Bank.
- The few common seasnail and rock gunnel larvae caught in the survey area may have originated from the spawning taking place either in the shallowest part of the survey area, in the Słupsk Bank or the coastal area.
- Two out of the taxa recorded in the survey area, i.e. gobies and common seasnail, belong to partially protected species under the Regulation of the Minister of the Environment of 16 December 2016 *on the protection of animal species* (Journal of Laws of 2016, item 2183, as amended).
- The survey area is typical in terms of species diversity among the waters of similar depth, with a clear predominance of cod and flounder in demersal catches, and herring and sprat in pelagic catches. Fish belonging to 24 taxa were caught in all the survey gear in the OWF area.
- The highest areal biomass density of sprat in the survey area was estimated for the spring survey campaign; however, it was more than two times lower than the average value of this parameter determined on the basis of the May SPRAS vessel passages in the years 2017–2021.
- The highest areal biomass density of herring was estimated for the summer survey campaign when it was two times higher than the average value of this parameter determined on the basis of spring SPRAS vessel passages as well as more than two times lower than the average from the BIAS vessel passages in the years 2017–2021.
- The efficiency analysis of the survey gillnet gear demonstrated that the peak of fish density occurred in summer and autumn since the shallower waters of the survey area serve as foraging grounds during those seasons. In other periods, fish densities were similar, while the lowest efficiencies were recorded in winter.
- In February 2023, as in the previous years, sprat started the first phase of spawning in the water depth of the Baltic Sea, in the areas deeper than the survey area. The process intensified on a large scale in May, then gradually declined in the second half of summer.
- The process of mass feeding of sprat intensifies once the spawning ends, particularly at the turn of summer and autumn, and then gradually declines to a minimum (starving state) at the beginning of winter, while in spring it is of an accidental nature and concerns only a few individuals.
- The analyses of stomach content confirm the more intense feeding of the herring in spring and summer. The high proportion of fish with empty stomachs in winter and autumn indicates the occurrence of low-intensity feeding in the planned project area, possibly related to the low availability of preferred zooplankton groups.
- The age structure of the fish caught reflects the typical age of herring in the Central Baltic stock, with the prevalence of the year class 2019 (ICES, 2023). The catches indicate the periodical

occurrence of juvenile fish, particularly in autumn, although herring with a length of less than 15 cm (age group 0 mostly) are rare, which suggests that the area is not a site of key significance for juvenile fish.

- In the planned project area, mature herrings can migrate towards Swedish or Polish coasts, however, the planned project area alone is not a significant spawning ground for the herring due to its depth, lack of suitable substrate and the distance from the shore. The observed concentrations of spring shoals are represented by the fish that had already spawned in the coastal regions.
- The results of cod abundance surveys conducted during individual survey seasons indicate a low occurrence of these fish in winter and spring. The abundant occurrence of cod was recorded in the potential area of the offshore wind farm location in summer and autumn. The above-mentioned results of cod abundance surveys might, therefore, indicate that the planned project area constitutes a less significant habitat for fish of this species in the winter-spring season than it does in summer and autumn.
- Seasonal changes in the length composition of the cod recorded in the area of the planned project resulted from the biological characteristics of these fish. These are manifested by spawning migrations from the shore towards the depths, where cod spawning grounds are situated, and feeding migrations from the depths towards the shores. The planned project area lies on the path of the above-mentioned migrations.
- In spring, the cod preparing for spawning, i.e. larger and older individuals, migrate towards spawning grounds outside of the planned project area. A similar situation took place in the planned offshore wind farm area in summer when most adult cods spawned in the depths of the Baltic Sea. Whereas in autumn, the proportion of the shortest cod was the smallest, while the proportion of longer fish increased, as a result of the individuals returning to the feeding grounds after spawning. The fish migrated towards the shore, also through the planned project area.
- The food in the survey area was available for cods of a wide range of lengths.
- The survey area served as a habitat mainly for adult flounders. They were the most abundant in summer and the least abundant in autumn.
- The stages of gonad maturity recorded in winter flounder catches indicated the ongoing spawning of this species. The gravid stage of gonad maturity dominated. The occurrence of individuals with gonads at the spawning and spent stages was also recorded. Considering the hydrological conditions prevailing in the area (the maximum salinity of < 10 PSU) which are not favourable for the reproduction of the European flounder (*Platichthys flesus*) occurring in the survey area (Momigliano et al., 2018), it is safe to assume that the fish migrated from the area surveyed to the nearby Słupsk Furrow or the Gdańsk Deep to spawn. The results of the ichthyoplankton catches that were carried out in the area surveyed and in which flounder eggs were not recorded, may confirm that assumption. However, the occurrence of flounder larvae was recorded in the winter and spring catches, probably as a result of their drifting into the area from the spawning grounds located in the above-mentioned Baltic depths.
- According to the Spatial Development Plan for the Polish Sea Areas, the sea area POM.60.E "presents good habitat and hydrological conditions for successful spawning of autumn-spawning herring population and, to a lesser extent, of the spring-spawning herring population". However, in recent years, the autumn population of herring has constituted a very small part of all fish of this species occurring in the Baltic Sea. This is also confirmed by detailed

ichthyological analyses of adult specimens carried out in the investment area, indicating high development of their gonads in winter and spring. This is a biological parameter that is the basis for identifying fish belonging to the spring-spawning population. It can therefore be assumed that despite the good environmental conditions indicated in the aforementioned document, autumn spawning of herring in the survey area does not take place or is of marginal importance. In turn, herrings of the spring population prefer areas with shallower depths for spawning than those observed in the survey area located in the deeper part of the water basin. For this reason, the potential of environmental conditions indicated in the Spatial Development Plan for the Polish Sea Areas does not translate into the importance of the investment area as a spawning ground for this population.

- The data form on the POM.60.E water basin also states that in the part of its area adjacent to the survey area "there are optimal conditions for effective spawning of turbot". No larvae of this species were noted in catches in the course of the environmental surveys conducted. This species occurred rarely also in the catches of adult fish. The conditions in which turbots spawn (depth range 5–40 m, salinity 6–7 PSU, on sandy, gravel, and silty seabed) occur in relatively extensive areas of the Baltic Sea. It can therefore be assumed that the area of the planned investment is not a key spawning ground for this species.

3.3.7 Shortcomings and gaps in the state-of-the-art

No ichthyoplankton surveys have been carried out in the survey area so far. The only source of information which can be used to compare the results obtained is the data collected during the one-year-long ichthyofauna monitoring conducted within the areas of the planned offshore wind farms located at similar depths. The scarce amount of data for the shallower areas of the Southern Baltic results from the fact that this region is located outside the network of survey stations at which the NMFRI conducts standard plankton surveys. The network is designed to ensure that it covers spawning areas of most commercial fish species while leaving out the shallower areas. Information on non-commercial fish species, early development stages of which inhabit both the deep-water and the coastal zones, is scarce, often outdated, and it does not apply directly to the survey area.

In the case of the deeper parts of the survey area located in the Słupsk Furrow region, it is possible to compare the data obtained with the data collected in recent years during NMFRI survey vessel passages. However, since the vessel passages take place only during summer, the data comparison can only be carried out for one season.

The scarce information from literature on the spatial distribution of ichthyoplankton in the coastal zone of the Baltic Sea of up to 40 m in depth is fragmentary and limited to single stations along the open Polish coast, with some of them concentrated in the Gulf of Gdańsk or in the Bay of Pomerania. This data is usually limited to one survey season.

As far as ichthyofauna and the cyclostomata are concerned, there is a problem with the efficiency of lamprey and eel catches in the sea. Since this group of organisms is found within the open sea waters in very low concentrations, the trawl methods appear to be the only theoretically effective means of gathering data; however, it should be based on long-term data series and the values of fishing effort which are virtually impossible to obtain.

Regarding ichthyofauna, no research methods can guarantee that the obtained results are each time 100 per cent representative of the surveyed area due to the occurrence of objective local difficulties

generated by the extreme hydrological conditions (upwelling, shifting sea currents), climate (radically different weather conditions characterising subsequent years) or factors altering the selectivity of survey tools (by-catching of material brought by sea currents or of organisms such as jellyfish). Despite this fact, the authors of this Report consider the applied survey methods to be adequate to the environmental conditions (e.g. characteristics of the seabed, hydrometeorological conditions, usage in fisheries) prevailing in the survey area. Moreover, the application of standard methods for the analyses of catches and biological analyses guarantees the comparability of the data collected and analysed.

3.4 MARINE MAMMALS

3.4.1 Non-specialist summary

Marine mammal monitoring conducted in the scope of the Baltica-1 OWF project included studies of the harbour porpoise and three species of seals – the grey, harbour, and ringed seal. The monitoring aimed to investigate to what extent the investment area was used by the animals and what the seasonality of their occurrence was.

The surveys were conducted with the use of passive acoustic monitoring (harbour porpoise) and visual methods (porpoise and seals), including observations from an airplane and from a boat. This report summarizes works conducted in the period between December 2022 and February 2024.

Passive acoustic monitoring was conducted with the use of F-POD detectors. Seventeen base monitoring stations were placed in total within the Baltica-1 OWF construction area and the buffer zone expanding up to 40 km from the area of construction of WTGs, OSSs and cable lines (area A). The buffer zone included Polish and Swedish waters. Moreover, four additional stations are deployed within the study area, serving as back-up stations in case of data loss. At the stations located in Polish waters, acoustic monitoring started on 3–4 December 2022, while at the Swedish locations – on 14 February 2023. Data were recorded continuously and collected during the service vessel passages. Within scope of the report, five sets of acoustic recordings have been analysed, including period between beginning of the monitoring and 28 February 2024. Data collected in the Polish locations covered over one year, providing a representative source of information on all seasons, including two winter seasons (winter 2022/2023 – winter 2023/2024). Due to a delayed start of measurements in Sweden, recordings obtained from the Swedish locations for winter covered shorter period however included all seasons (winter 2023 – winter 2023/2024). Recordings collected up to date were of a good quality and provided a good time coverage – data yield was over 90%, both for the Polish and Swedish locations. Analyses of the obtained acoustic recordings showed that harbour porpoises occurred in the study area along the year and their activity differed both regionally and seasonally. The highest detection rates were recorded in the Swedish buffer zone (5.9% DPD out of all recording days), especially at the most northern stations SM_14 and SM_15. Within Polish EEZ Poland, detection rates differed between the two study areas and were higher within the Baltica-1 OWF construction area (1.6% DPD out of all recording days). Regarding seasonality, both in Sweden and within the OWF area, the highest porpoise occurrence was found in the summer months, especially in August. In autumn, frequency of the animal occurrence was decreasing – from September within the B1 OWF area and from October in Sweden. In the Polish buffer zone, detection rates were low all the year round (0.4% DPD out of all recording days), at all the survey stations. At station SM_08, animals were not registered at all. The highest numbers of DPD in the buffer zone in Poland were found in November. Clear differences in the frequency of porpoise occurrence between Polish and Swedish locations were found over spring. At the Swedish locations, animals were recorded frequently, while in Poland, detection rates were low and limited to

two stations within the OWF – SM_04 and SM_05. During the winter season, porpoises occurred with low frequency throughout the survey area.

The results obtained in the acoustic monitoring are in line with available knowledge on the harbour porpoise occurrence in the Baltic Sea. The Swedish part of the survey area is located within the Natura 2000 site Hoburgs bank och Midsjöbakarna, where porpoises are of conservation concern. In this region, the species is found to occur frequently and aggregate during the reproduction period. The high detection rates, peaking over summer months, recorded during the monitoring in the Swedish area, seem to reflect activity of the animals for breeding purposes. In the Polish part of the survey area, the occurrence of porpoises within the survey area was found to be higher than in the case of other offshore regions of the Polish EEZ, for which data is available. The summer peak in the detections rates, decreasing over autumn, was similar as at the Swedish locations. Such results indicate that within the planned OWF area, the activity of porpoises is highly related to the proximity of the Swedish Natura 2000 site. In contrast with the stations within the Baltica-1 OWF construction area and in Sweden, within the Polish buffer zone, the activity of the species seems to increase at the end of the breeding season, when it is recognised to disperse in the Baltic Sea. The low detection levels recorded in the winter season throughout the survey area may confirm the scattered occurrence of porpoises in the Baltic Sea.

During the period covered by the monitoring, aerial observations were conducted along five transects. The transects covered the construction area of the Baltica-1 OWF, as well as the adjacent area, including Polish and Swedish waters. Within the reporting period, seven visual surveys from an airplane were performed. Flights took place in February, April, May, July, August and September 2023, which provided data for winter, spring, summer and autumn season. Observations of marine mammals were made only during the spring flights – in April and May. Two grey seals and one seal individual of unidentified species were recorded.

In the reporting time scope, visual surveys of marine mammals were also conducted from a vessel, during the studies of seabirds. Observation campaigns were carried out along the designated transects, covering the Baltica-1 OWF construction area, which is the area of construction of WTGs, OSSs, and cable lines (area A) and the area of construction of cable lines (area B) together with a zone of no less than 4 km in width measured from the boundary of area A, as well as a reference area located in Swedish waters. In the survey period, between December 2022 – December 2023, vessel surveys were conducted in every month, 39 times in total. Representative data for each season of the year was provided. Records of marine mammals included a total of 27 seal observations, out of which 23 observations concerned the grey seal (*Halichoerus grypus*) and four – seal individuals of an unidentified species (Phocidae). Animals were registered in all seasons, with the highest number of records made in winter.

In conclusion, visual monitoring conducted between December 2022 – December 2023 showed occurrence of seals in the survey area throughout the year. Animals were observed from an airplane and from a vessel. The observations covered the OWF area and the reference area. The only species identified during the monitoring was the grey seal. Some recorded individuals were of an unidentified species. In total, 30 seal observations were made during the survey period. The recorded occurrence of animals differed both regionally and seasonally. Seals were mostly observed within Baltica-1 OWF construction area. In the entire survey area, the highest number of records was made during the winter

season, especially in December (11 observations). Animals were observed with the lowest frequency in summer. In spring and autumn, the observation rate was similar.

Comparison of the obtained results with literature data on seal activity within Polish EEZ, confirmed that they grey seal is the most frequently occurring species in the southern part of the Baltic. The lowest observation rates recorded during summer months of the monitoring, most probably result from increased seal activity in the area of Vistula mouth in the moulting period. Due to differences in the methodology, the Baltica-1 OWF monitoring data cannot be directly compared to available information from other planned OWF surveys.

To sum up, the monitoring of marine mammals conducted between December 2022 and February 2024 showed that marine mammals are present in the survey area throughout the year. The activity of porpoises was found to be the highest in the summer season, while seals were most frequently observed in winter. The recorded animal activity differs depending on the part of the Baltic-1 OWF survey area, but both porpoises and seals are present within the planned OWF borders.

3.4.2 Spatial scope of the surveys

The spatial range of marine mammal monitoring was the survey area covering the Baltica-1 OWF construction area, which is the area of construction of WTGs, OSSs, and cable lines (area A) and the area of construction of cable lines (area B) together with a zone of no less than 40 km in width measured from the boundary of area A [Figure 3.64].

Due to variability of methods used during the surveys, the monitored regions differ depending on the type of the conducted surveys. The survey periods are also varied.

3.4.2.1 Passive acoustic monitoring

For the passive acoustic monitoring, 17 F-POD detectors were used, which were situated at the base survey stations. The stations were located within the Baltica-1 OWF construction area (SM_01–SM_05), as well as in the buffer zone expanding up to 4 km from the boundary of area A (SM_06–SM_17). The buffer zone includes both Polish (SM_06–SM_11) and Swedish (SM_12–SM_17) waters of the Baltic Sea. The Swedish locations are within the Natura 2000 site Hoburgs bank och Midsjöbakarna. Moreover, four additional survey stations were deployed within the survey area (SM_18–SM_21), serving as back-up stations in case of data loss [Table 3.37, Figure 3.64].

At the survey stations located within the Polish waters (SM_01–SM_11, SM_18–SM_20), acoustic monitoring started on 3–4 December 2022, while at the Swedish locations (SM_12–SM_17, SM_21) – on 14 February 2023 [Table 3.37]. At each of the stations, one F-POD detector was deployed to continuously record of acoustic data.

Table 3.37. The coordinates of the survey stations for the passive acoustic monitoring of porpoises in the survey area

Station	Two-dimensional Cartesian coordinate system PL-1992 [m]		Location	Station type	Start of the monitoring
	Y	X			
SM_01	403411.80	849719.29	Baltica-1 OWF construction area	Base stations	03.12.2022
SM_02	405925.34	852861.23			
SM_03	408637.33	852762.01			
SM_04	407711.28	862320.10			

Station	Two-dimensional Cartesian coordinate system PL-1992 [m]		Location	Station type	Start of the monitoring
	Y	X			
SM_05	410522.49	863113.85			
SM_06	435734.24	870706.86	Buffer zone 40 km from area A boundary, Poland		
SM_07	437565.04	850512.76			
SM_08	427301.57	833374.15			04.12.2022
SM_09	407140.98	821845.60			
SM_10	388127.58	826786.35			
SM_11	378348.58	842574.53			
SM_12	371770.17	858295.62	Buffer zone 40 km from area A boundary, Sweden, Natura 2000 site Hoburgs bank och Midsjöbakarna		14.02.2023
SM_13	377273.67	879578.82			
SM_14	395152.83	893207.94			
SM_15	412371.20	897003.93			
SM_16	432267.11	894961.93			
SM_17	426285.82	881962.04			
SM_18	406938.70	851532.80	Baltica-1 OWF construction area	Additional stations	03.12.2022
SM_19	412284.79	864512.77			
SM_20	417273.94	837963.25	Buffer zone 40 km from area A boundary, Poland		04.12.2022
SM_21	409598.91	892638.73	Buffer zone 40 km from area A boundary, Sweden, Natura 2000 site Hoburgs bank och Midsjöbakarna		14.02.2023

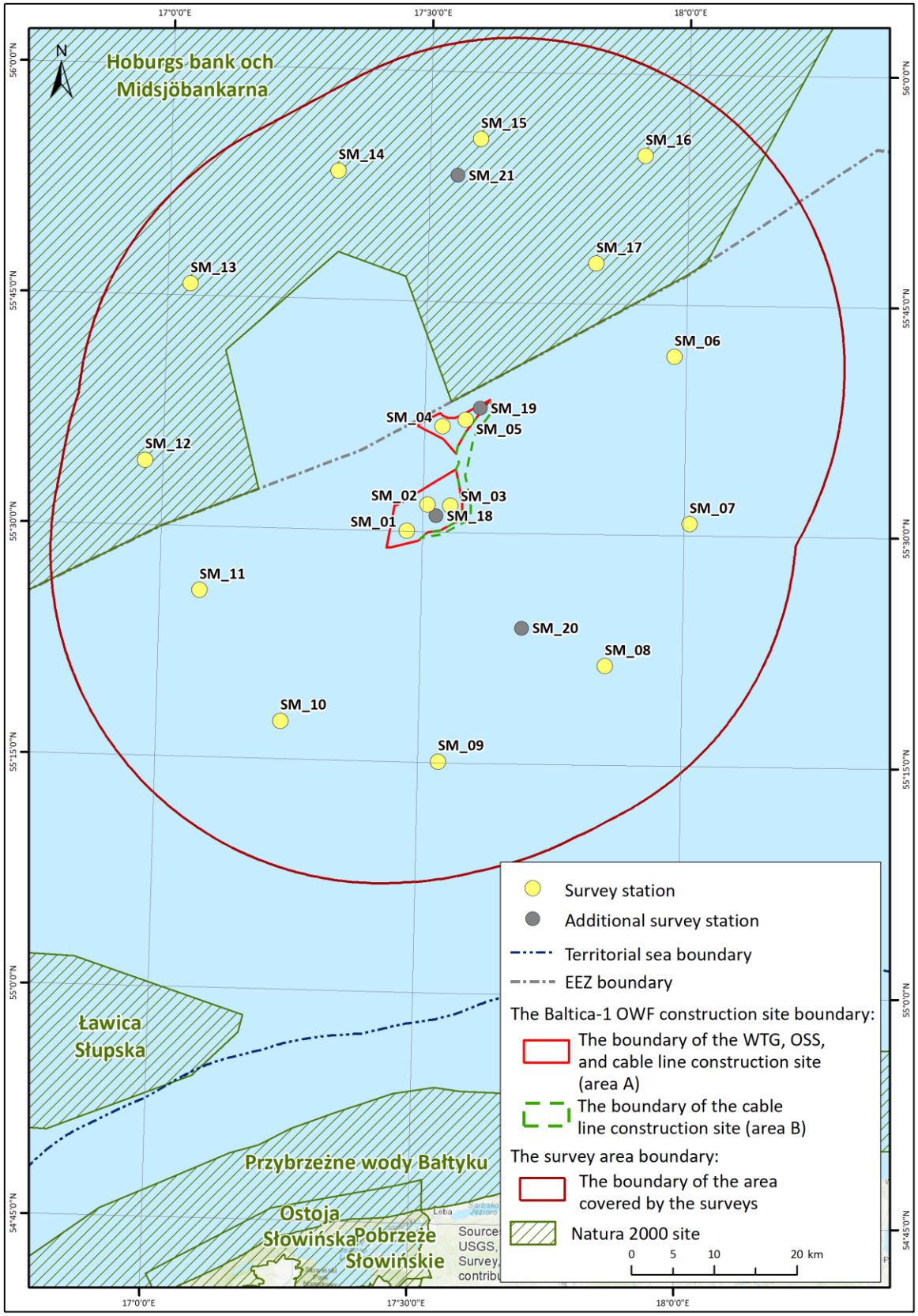


Figure 3.64. The locations of survey stations for passive acoustic monitoring in the survey area

3.4.2.2 Aerial visual monitoring

Visual surveys conducted from the aircraft followed five designated transects covering the construction area of the Baltica-1 OWF, as well as the adjacent area, including Polish and Swedish waters. Five parallel transects, with a total length of 50 km each were designated [Table 3.38, Figure 3.65]. The distance between the transect lines is approximately 8 km to avoid counting the same individuals several times (Hammond et al., 2002; Thomsen et al., 2004; SCANS, 2006; BSH, 2013).

Table 3.38. The coordinates of observation transects during the monitoring of marine mammals from the plane in the survey area

Transect	**Two-dimensional Cartesian coordinate system PL-1992 [m]**				**Length [km]**
	Transect beginning		**Transect end**		
	Y	**X**	**Y**	**X**	
Transekt_01	402665.5	828271.7	381448.6	873561.9	50
Transekt_02	409910.0	831665.5	388693.0	876955.7	50
Transekt_03	417154.5	835059.3	395937.5	880349.5	50
Transekt_04	424398.9	838453.1	403181.9	883743.3	50
Transekt_05	431643.4	841846.9	410426.4	887137.1	50

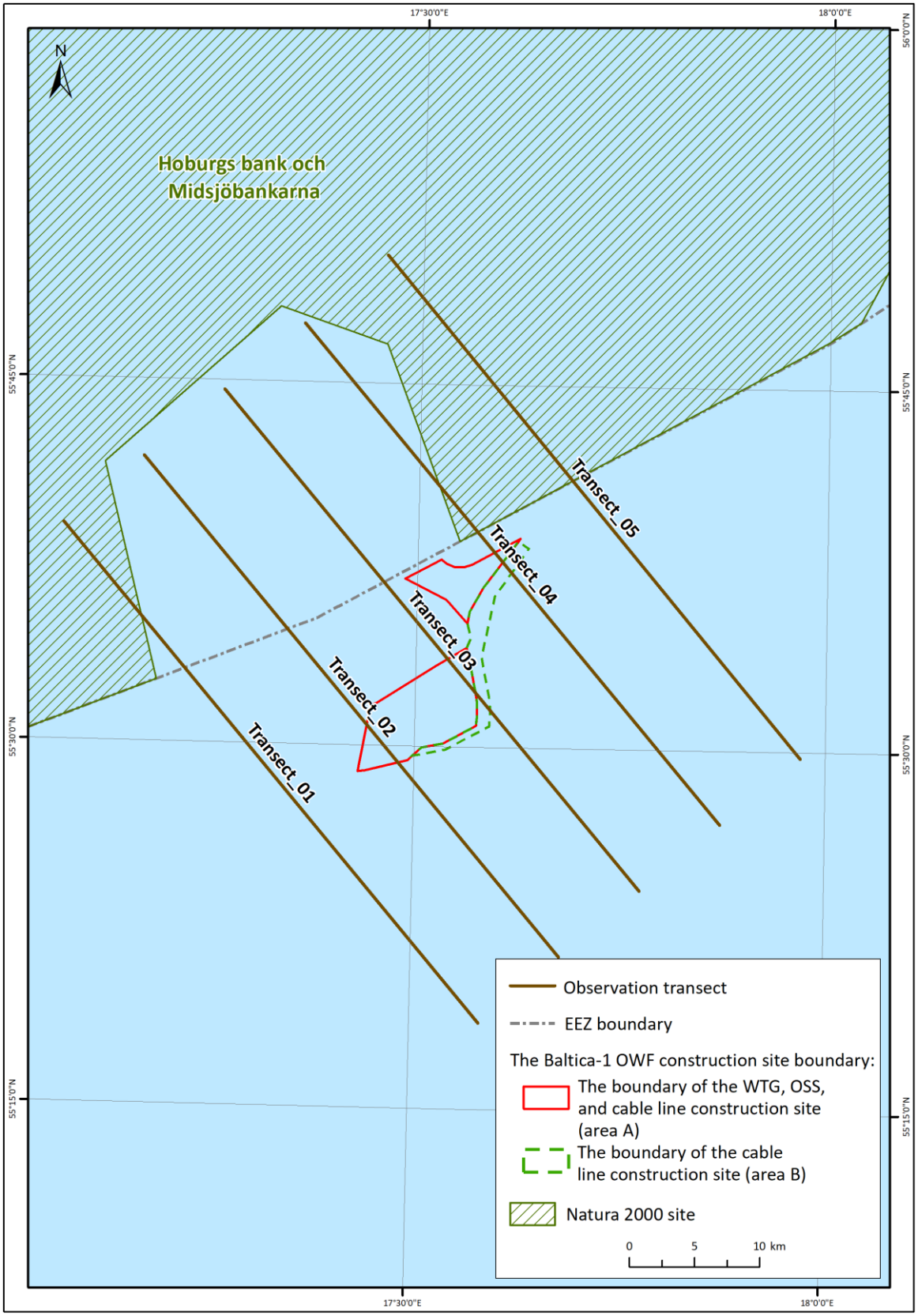


Figure 3.65. The location of the observation transects during the monitoring of marine mammals from the plane, in the survey area

3.4.2.3 Visual observations (marine mammal counting) during seabird surveys

Similarly, to airplane surveys, visual observations of marine mammals from aboard a vessel during seabird surveys were carried out along pre-defined transects. The transects covered the survey area constituting the Baltica-1 OWF construction area, including the area of construction of WTGs, OSSs, and cable lines (area A) and the area of construction of cable lines (area B) together with a zone of no less than 4 km in width measured from the boundary of area A, as well as a reference area located in Swedish waters (north of the Baltica-1 OWF area), mainly within the boundaries of the Natura 2000 site *Hoburgs bank och Midsjöbankarna* (SE0330308) [Figure 3.89].

3.4.3 Methodology

3.4.3.1 Passive acoustic monitoring

As part of the project, passive acoustic monitoring was conducted with F-POD detectors (Chelonia Limited, online).

F-POD data logger is a fully automated recorder of narrow-band ultrasonic sounds in the range of 20–160 kHz. Harbour porpoises emit sounds in a very narrow frequency range with the highest energy at around 130 kHz. Therefore, the waveform of the signal is characteristic and hence, F-PODs can be effectively used to detect sounds emitted by these animals (Chelonia Limited, online). For porpoises, the detection range of the device is approx. 400 m (Thomsen et al., 2004; Gauger et al., 2012; Chelonia Limited, online).

At each survey station, one F-POD was located [Chapter 3.4.2.1, Figure 3.64]. Locations of the survey stations were selected so as to allows for collection of suitable data on the animals' presence, with simultaneous avoidance of multiple recordings of the same clicks. The detectors were deployed 5 m above the seabed, with an anchoring system shown in Figure 3.66.

From the start of the monitoring, F-PODs collected acoustic recordings continuously. The recorded data was retrieved during the service vessel passages, with assumption of time intervals minimizing the risk of significant data loss due to trawling or loosing equipment during adverse weather conditions.

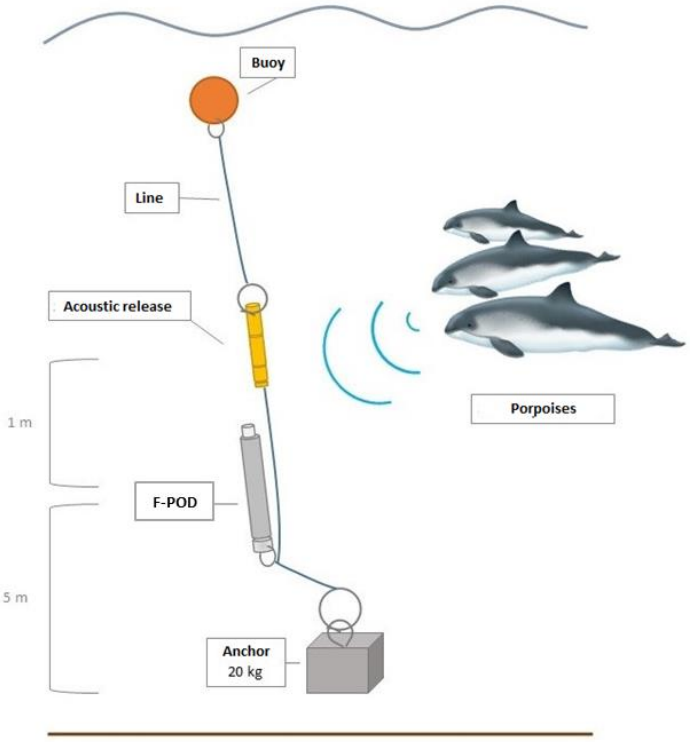


Figure 3.66. The anchoring system used for the deployment of F-POD detectors at the seabed

Acoustic data collected with F-PODs was processed using FPOD.exe software (Chelonia Limited, online). By an automated algorithm – KERNO-F, the software identifies series of acoustic clicks and classifies them into different sound categories, as follows:

- sound sources: 1) NBHF (porpoise), 2) other cetaceans, 3) side scan sonar and 4) unknown;
- quality of data recorded: 1) high, 2) medium, 3) low, 4) questionable.

For the analyses of porpoise detections, only clicks classified as high and medium quality were used (Chelonia Limited, online).

In the next step, clicks marked by the KERNO-F algorithm as coming from porpoises were visually validated, in order to confirm the correctness of automatic classification.

The results of the analyses were presented as the number and percentage of days of positive detection of the porpoise (DPD – detection positive days) and minutes of positive detection (DPM – detection positive minutes). DPD means the day in which at least one detection of the porpoise was recorded, while DPM – the minute in which the porpoise was recorded. The number of DPD and DPM is calculated in relation to the total number of days/minutes of data collection at the station, on a monthly, seasonal and annual basis and presented as a percentage of DPD/DPM.

As the main source of information from acoustic monitoring, recordings collected at the base F-POD stations (SM_01–SM_17) were considered. It was however agreed that as part of the project, the acoustic data coverage should be at least 90% of the monitoring time (excluding the time required for equipment maintenance). Therefore, in case of higher data losses, it was assumed that data from additional stations should be considered.

3.4.3.2 Aerial visual monitoring

Visual surveys from an airplane were conducted to provide additional information on marine mammal occurrence in the survey area. Such a method can serve as a potential source of data on the occurrence of harbour porpoise adults and calves.

Aerial observations were conducted along five designated transects [Figure 3.65], from a Vulcanair P-68 Observer 2 aircraft. The surveys took place under favourable weather conditions, which are:

- sea state below 3;
- absence of heavy precipitation;
- good visibility during observations (minimum 5 km).

During the observations, data was collected by two experienced observers, from two opposite sides of the aircraft and with the use of spherical "bubble" windows from an altitude of approximately 600 ft (approx. 183 m). The plane moved with a speed of approximately 100 knots (185 $km \cdot h^{-1}$, 115 mph). The flight route was recorded continuously by two GPS units, at at least 5-second intervals. Meteorological data (sea state, glare, cloud reflectivity, cloud coverage, precipitation and water turbidity) was recorded by each observer on a voice recorder at the beginning of each transect, the moment weather conditions changed and whenever a marine mammal was observed. In the event of recording the occurrence of a marine mammal, the observers specified its location relative to the transect, swimming direction, distance from the transect, as well as the time of recording (date; hour; minute; second relative to local time).

The project included eight observation flights, carried out within a year, according to the following schedule:

- 1 winter flight, between December and February;
- 2 flights in spring, from March to June;
- 3 flights in summer, in July–August;
- 2 flights in autumn, between September and November.

Potential changes in the assumed schedule could be introduced in the event of unfavourable weather conditions.

3.4.3.3 Visual observations (marine mammal counting) during seabird surveys

Observations of marine mammals from aboard a vessel were conducted during the surveys dedicated to seabirds. As part of the project, observations from aboard a vessel were scheduled for one year. Surveys were carried out along designated transects [Figure 3.89], according to the methodology described in Chapter 3.5.1.3. Observations were conducted on an opportunistic basis to provide information on marine mammal presence and the seasonality of their occurrence in the survey area. This method was mostly used as a source of data about seals.

3.4.4 Activities performed

3.4.4.1 Passive acoustic monitoring

Passive acoustic monitoring with F-PODs started on 3–4 December 2022 at the survey stations located in Poland (vessel passage 1A) [Table 3.39]. In Sweden, due to delays in obtaining necessary permits, acoustic measurements began on 14 February 2023 (vessel passage 2B). From the onset of the monitoring, F-POD recordings were performed continuously. Acoustic detectors were maintained, and

data was collected during the service vessel passages. In the reporting period, four maintenance vessel passages were conducted (2B–5E). The last maintenance took place on 16 and 25–28 February 2024, depending on the station. The summary of the activities performed has been presented in Table 3.39.

Table 3.39. A summary of activities performed during the reporting period as part of acoustic monitoring of marine mammals in the survey area

Vessel passage no.	Vessel passage date	Scope of work	Comments
1A	03.12.2022	Deployment of F-POD detectors at the stations SM_1–SM_7 and SM_18–SM_19, located in Poland	-
	04.12.2022	Deployment of F-POD detectors at the stations SM_8–SM_11 and SM_20, located in Poland	-
2B	06.02.2023	Service of F-POD detectors at the stations SM_06–SM_11 and SM_20	F-POD detector lost at station SM_10; new device deployed during another vessel passage
	07.02.2023	Service of F-POD detectors at the stations SM_01–SM_05 and SM_18–SM_19	Data collected
	14.02.2023	Deployment of F-POD detectors at the stations SM_12–SM_17 and SM_21, located in Sweden	-
	16.02.2023	Deployment of a new F-POD detector at the station SM_10	-
3C	24.04.2023	Service of F-POD detectors at the stations SM_01–SM_05, SM_10–SM_11, SM_18–SM_19	Data collected
	25.04.2023	Service of F-POD detectors at the stations SM_08–SM_09, SM_20	Data collected
	29.04.2023	Service of F-POD detectors at the stations SM_06–SM_07, SM_16–SM_17	Data collected
	30.04.2023	Service of F-POD detectors at the stations SM_12–SM_15, SM_21	Data collected
4D	2023-08-11	Service of F-POD detectors at the stations SM_09–SM_13	Data collected
	12.08.2023	Service of F-POD detectors at the stations SM_05–SM_08, SM_14–SM_17, SM_19–SM_21	Data collected
	13.08.2023	Service of F-POD detectors at the stations SM_01–SM_04, SM_18	Data collected
5E	12.11.2023	Service of F-POD detectors at the stations SM_01–SM_05	Data collected
	13.11.2023	Service of F-POD detectors at the stations SM_06–SM_08, SM_12–SM_15, SM_17–SM_21	Data collected
	13.11.2023	Deployment of a new detector at the station SM_16	F-POD detector lost at the station SM_16, data not collected
	18.11.2023	Service of F-POD detectors at the stations SM_09–SM_11	Data collected
6F	16.02.2024	Service of F-POD detectors at the stations SM_10–SM_12	Data collected

Vessel passage no.	Vessel passage date	Scope of work	Comments
	25.02.2024	Service of F-POD detectors at the station SM_09	Data collected
	26.02.2024	Service of F-POD detectors at the stations SM_06–SM_08, SM_14–SM_17, SM_20–SM_21	Data collected
	27.02.2024	Service of F-POD detectors at the stations SM_02-SM_05, SM_13, SM_18-SM_19	Data collected
	28.02.2024	Service of F-POD detectors at the station SM_01	Data collected

3.4.4.2 Aerial visual monitoring

Visual monitoring from an aircraft was carried out for one year. In total, seven observation flights were conducted. One of the flights planned for the autumn season between September and November 2023 was not performed due to long-term bad weather conditions (sea state > 3, heavy precipitation, no good visibility).

The observation flights conducted during the monitoring campaign are summarized in Table 3.40.

Table 3.40. A summary of the observation flights performed within the reporting period

Time range	Season	Date of the flight
December 2022 –February 2023	Winter	28.02.2023
March – June 2023	Spring	22.04.2023
		22.05.2023
July – August 2023	Summer	23.07.2023
		05.08.2023
		24.08.2023
September – November 2023	Autumn	28.09.2023

3.4.4.3 Visual observations (marine mammal counting) during seabird surveys

In the period from December 2022 to November 2023, a total of 39 seabird survey vessel passages were conducted, during which data on marine mammal observations was collected.

3.4.5 Results

In the following sub-chapters, results of the acoustic and visual monitoring of marine mammals are presented. Acoustic measurements showed the activity of harbour porpoises in the survey area, while visual surveys – the occurrence of grey seals.

3.4.5.1 Passive acoustic monitoring

Since the beginning of the monitoring, five acoustic datasets were collected. Due to the schedule of the service vessel passages, constrained by the substantial size of the study area, as well as by the weather conditions, the dates of data collection differed depending on the station [Table 3.41]. Overall, in the reporting period, data obtained for the survey stations located in Poland covered a period between 3 December 2022 and 28 February 2024, while for the stations in Sweden – from 14 February to 27 February 2024. For most of the stations, the obtained recordings were complete, covering the full range of data collection time. Minor gaps in the recordings were found for the stations SM_02 and SM_12 in February and March 2023, which were caused by technical problems. In the case of two

stations, data losses occurred due to the equipment loss, which concerned the station SM_10 (first dataset, December 2022/February 2023) and the station SM_16 (fourth dataset, August/November 2023). However, overall, very good coverage of data was obtained, including over 90% of the monitoring time (average for the base survey stations). A summary of the collected acoustic recordings is presented in Table 3.41 and Table 3.42. Due to the high data yield at the base stations both in Poland and Sweden, it was not necessary to include recordings from the additional stations in the analyses.

It is worth noting that during the reporting period, data collected from locations in Poland covered over a year of research, taking into account two winter seasons (winter 2022/2023 – winter 2023/2024). In the case of the location in Sweden, due to the delay in starting monitoring, the obtained recordings covered a shorter period and did not include winter 2022/2023. At the beginning of 2023, data was only collected for two weeks in February. Despite the delay, the obtained recordings cover the entire year and are a representative source of information about all seasons (winter 2023 – winter 2023/2024).

Table 3.41. A summary of acoustic data obtained from passive acoustic monitoring conducted in the survey area. Data have been divided into sets collected during five service vessel passages

Passage date	Station type	Station	Amount of data	Scope of data		Comments
				Start	End	
2023.02.06–2023.02.07	Base station, Baltica-1 OWF construction area	SM_01	65 d 10 h 39 min	03.12.2022	07.02.2023	Data complete
		SM_02	65 d 16 h 05 min	03.12.2022	07.02.2023	
		SM_03	65 d 13 h 36 min	03.12.2022	07.02.2023	
		SM_04	65 d 25 h 15 min	03.12.2022	07.02.2023	
		SM_05	66 d 00 h 48 min	03.12.2022	07.02.2023	
	Base station, Poland, buffer zone 40 km from the boundary of area A	SM_06	65 d 01 h 17 min	03.12.2022	06.02.2023	Data complete
		SM_07	65 d 04 h 36 min	03.12.2022	06.02.2023	
		SM_08	64 d 06 h 09 min	04.12.2022	06.02.2023	
		SM_09	64 d 11 h 04 min	04.12.2022	06.02.2023	
		SM_10	-			Device lost, no data
		SM_11	64 d 20 h 13 min	03.12.2022	06.02.2023	Data complete
	Base station, Sweden, 40 km buffer zone from the boundary of area A, Natura 2000 site Hoburgs bank och Midsjöbakarna	SM_12	-			Station deployed at a later date; data not collected
		SM_13				
		SM_14				
		SM_15				
		SM_16				

Passage date	Station type	Station	Amount of data	Scope of data		Comments
				Start	End	
		SM_17				
	Additional station, Baltica-1 OWF construction area	SM_18	50 d 06 h 12 min 15 d 06 h 06 min	03.12.2022	07.02.2023	Data complete
		SM_19	65 d 23 h 25 min	03.12.2022	07.02.2023	
		SM_20	64 d 08 h 45 min	04.12.2022	06.02.2023	
	Additional station, Sweden, 40 km buffer zone from the boundary of area A, Natura 2000 area Hoburgs bank och Midsjöbakarna	SM_21	-			Station deployed at a later date; data not collected
24.04.2023–25.04.2023, 29.04.2023–30.04.2023	Base station, Baltica-1 OWF construction area	SM_01	76 d 09 h 26 min	07.02.2023	24.04.2023	Missing data for the station SM_02, no recordings for 07–16.02.2023; Data complete for the stations SM_01, SM_03–SM_05
		SM_02	67 d 11 h 43 min	16.02.2023	24.04.2023	
		SM_03	76 d 00 h 16 min	07.02.2023	24.04.2023	
		SM_04	75 d 13 h 48 min	07.02.2023	24.04.2023	
		SM_05	75 d 12 h 09 min	07.02.2023	24.04.2023	
	Base station, Poland, 40 km buffer zone from the boundary of area A	SM_06	82 d 06 h 39 min	06.02.2023	29.04.2023	Data complete
		SM_07	81 d 16 h 51 min	06.02.2023	29.04.2023	
		SM_08	77 d 14 h 19 min	06.02.2023	25.04.2023	
		SM_09	77 d 05 h 19 min	06.02.2023	25.04.2023	
		SM_10	67 d 11 h 43 min	16.02.2023	24.04.2023	
		SM_11	76 d 17 h 35 min	07.02.2023	24.04.2023	

Passage date	Station type	Station	Amount of data	Scope of data		Comments
				Start	End	
	Base station, Sweden, 40 km buffer zone from the boundary of area A, Natura 2000 site Hoburgs bank och Midsjöbakarna	SM_12	52 d 07 h 06 min	08.03.2023	30.04.2023	Missing data for the station SM_12, no recordings for 2023.02.14–2023.03.07; Data complete for the stations SM_13–SM_17
		SM_13	74 d 17 h 55 min	14.02.2023	30.04.2023	
		SM_14	74 d 03 h 20 min	14.02.2023	30.04.2023	
		SM_15	74 d 01 h 27 min	14.02.2023	30.04.2023	
		SM_16	73 d 23 h 44 min	14.02.2023	29.04.2023	
		SM_17	73 d 22 h 41 min	14.02.2023	29.04.2023	
	Additional station, Baltica-1 OWF construction area	SM_18	75 d 30 h 18 min	22.01.2023	24.04.2023	Data complete
		SM_19	76 d 12 h 14 min	07.02.2023	24.04.2023	
		SM_20	77 d 13 h 35 min	06.02.2023	24.04.2023	
	Additional station, Sweden, 40 km buffer zone from the boundary of the area, Natura 2000 site Hoburgs bank och Midsjöbankarna.	SM_21	74 d 07 h 34 min	14.02.2023	30.04.2023	Data complete
2023.08.11–2023.08.13	Base station, Baltica-1 OWF construction area	SM_01	110 d 12 h 04 min	24.04.2023	13.08.2023	Data complete
		SM_02	110 d 20 h 28 min	24.04.2023	13.08.2023	
		SM_03	110 d 22 h 58 min	24.04.2023	13.08.2023	
		SM_04	110 d 20 h 49 min	24.04.2023	13.08.2023	
		SM_05	110 d 18 h 07 min	24.04.2023	12.08.2023	
	Base station, Poland, 40 km buffer zone from the boundary of area A	SM_06	104 d 17 h 12 min	29.04.2023	12.08.2023	Data complete
		SM_07	105 d 05 h 20 min	29.04.2023	12.08.2023	

Passage date	Station type	Station	Amount of data	Scope of data		Comments
				Start	End	
		SM_08	109 d 09 h 07 min	25.04.2023	12.08.2023	
		SM_09	108 d 07 h 34 min	25.04.2023	11.08.2023	
		SM_10	108 d 12 h 47 min	25.04.2023	11.08.2023	
		SM_11	108 d 19 h 09 min	24.04.2023	11.08.2023	
	Base station, Sweden, 40 km buffer zone from the boundary of area A, Natura 2000 site Hoburgs bank och Midsjöbakarna	SM_12	103 d 03 h 09 min	30.04.2023	11.08.2023	
		SM_13	103 d 09 h 33 min	30.04.2023	11.08.2023	
		SM_14	103 d 15 h 43 min	30.04.2023	12.08.2023	
		SM_15	104 d 03 h 26 min	30.04.2023	12.08.2023	Data complete
		SM_16	104 d 08 h 47 min	29.04.2023	12.08.2023	
		SM_17	104 d 12 h 50 min	29.04.2023	12.08.2023	
	Additional station, Baltica-1 OWF construction area	SM_18	101 d 10 h 02 min	24.04.2023	13.08.2023	
		SM_19	110 d 19 h 47 min	24.04.2023	12.08.2023	Data complete
		SM_20	109 d 08 h 57 min	25.04.2023	12.08.2023	
	Additional station, Sweden, 40 km buffer zone from the boundary of area A, Natura 2000 area Hoburgs bank och Midsjöbakarna	SM_21	104 d 00 h 12 min	30.04.2023	12.08.2023	Data complete
2023.11.12–2023.11.13, 2023.11.18	Base station, Baltica-1 OWF construction area	SM_01	91 d 15 h 02 min	13.08.2023	12.11.2023	
		SM_02	91 d 03 h 52 min	13.08.2023	12.11.2023	Data complete
		SM_03	91 d 10 h 56 min	13.08.2023	12.11.2023	

Passage date	Station type	Station	Amount of data	Scope of data		Comments
				Start	End	
		SM_04	85 d 20 h 15 min 05 d 13 h 46 min	13.08.2023	12.11.2023	
		SM_05	91 d 06 h 45 min	12.08.2023	12.11.2023	
	Base station, Poland, 40 km buffer zone from the boundary of area A	SM_06	92 d 19 h 04 min	12.08.2023	13.11.2023	Data complete
		SM_07	92 d 13 h 48 min	12.08.2023	13.11.2023	
		SM_08	92 d 09 h 12 min	12.08.2023	13.11.2023	
		SM_09	99 d 02 h 50 min	11.08.2023	18.11.2023	
		SM_10	98 d 21 h 56 min	11.08.2023	18.11.2023	
		SM_11	98 d 16 h 54 min	14.02.2023	18.11.2023	
	Base station, Sweden, 40 km buffer zone from the boundary of area A, Natura 2000 site Hoburgs bank och Midsjöbakarna	SM_12	94 d 04 h 19 min	11.08.2023	13.11.2023	Data complete
		SM_13	93 d 22 h 43 min	11.08.2023	13.11.2023	
		SM_14	93 d 13 h 58 min	12.08.2023	13.11.2023	
		SM_15	93 d 07 h 19 min	12.08.2023	13.11.2023	
		SM_16	-			Device lost, no data
		SM_17	92 d 22 h 48 min	12.08.2023	13.11.2023	Data complete
	Additional station, Baltica-1 OWF construction area	SM_18	83 d 17 h 37 min 07 d 19 h 20 min	13.08.2023	12.11.2023	Data complete
		SM_19	91 d 07 h 21 min	12.08.2023	12.11.2023	

Passage date	Station type	Station	Amount of data	Scope of data		Comments
				Start	End	
		SM_20	92 d 05 h 34 min	12.08.2023	12.11.2023	
	Additional station, Sweden, 40 km buffer zone from the boundary of area A, Natura 2000 area Hoburgs bank och Midsjöbakarna	SM_21	93 d 09 h 59 min	12.08.2023	13.11.2023	Data complete
2024.02.16, 2024.02.25 – 2024.02.28	Base station, Baltica-1 OWF construction area	SM_01	107 d 3 h 38 min	12.11.2023	28.02.2024	Data complete
		SM_02	107 d 3 h 29 m	12.11.2023	27.02.2024	Data complete
		SM_03	107 d 14 min	12.11.2023	27.02.2024	Data complete
		SM_04	107 d 2 h 13 min	12.11.2023	27.02.2024	Data complete
		SM_05	106 d 20 h 39 min	12.11.2023	27.02.2024	Data complete
	Base station, Poland, 40 km buffer zone from the boundary of area A	SM_06	105 d 5 h 12 min	13.11.2023	26.02.2024	Data complete
		SM_07	105 d 5 h 5 min	13.11.2023	26.02.2024	Data complete
		SM_08	105 d 2 h 17 min	13.11.2023	26.02.2024	Data complete
		SM_09	99 d 9 h 25 min	18.11.2023	25.02.2024	Data complete
		SM_10	90 d 5 h 28 min	18.11.2023	16.02.2024	Data complete
		SM_11	90 d 5 h 8 min	18.11.2023	16.02.2024	Data complete
	Base station, Sweden, 40 km buffer zone from the boundary of area A, Natura 2000 site Hoburgs bank och Midsjöbakarna	SM_12	94 d 12 h 22 min	13.11.2023	16.02.2024	Data complete
		SM_13	105 d 6 h 25 min	13.11.2023	27.02.2024	Data complete
		SM_14	105 d 5 h 20 min	13.11.2023	26.02.2024	Data complete
		SM_15	105 d 5 h 3 min	13.11.2023	26.02.2024	Data complete

Passage date	Station type	Station	Amount of data	Scope of data		Comments
				Start	End	
		SM_16	105 d 4 h 59 min	13.11.2023	26.02.2024	Data complete
		SM_17	105 d 5 h 8 min	13.11.2023	26.02.2024	Data complete
	Additional station, Baltica-1 OWF construction area	SM_18	107 d 8 min	12.11.2023	27.02.2024	Data complete
		SM_19	107 d 55 min	12.11.2023	27.02.2024	Data complete
		SM_20	105 d 6 h 33 min	12.11.2023	26.02.2024	Data complete
	Additional station, Sweden, 40 km buffer zone from the boundary of the area, Natura 2000 site Hoburgs bank och Midsjöbankarna.	SM_21	105 d 5 h 31 min	13.11.2023	26.02.2024	Data complete

Table 3.42. Data obtained during the passive acoustic monitoring conducted in the survey area

Station type	Station	Data collection period	Missing data	Data yield [%]					
				Service A	Service B	Service C	Service D	Service E	Service A-E*
Poland basic stations	SM_01	03.12.2022 – 28.02.2024	-	100	100	100	100	100	100
	SM_02	03.12.2022 – 27.02.2024	08–15.02.2023	100	88	100	100	100	98
	SM_03	03.12.2022 – 27.02.2024	-	100	100	100	100	100	100
	SM_04	03.12.2022 – 27.02.2024	-	100	100	100	100	100	100
	SM_05	03.12.2022 – 27.02.2024	-	100	100	100	100	100	100
	SM_06	03.12.2022 – 26.02.2024	-	100	100	100	100	100	100
	SM_07	03.12.2022 – 26.02.2024	-	100	100	100	100	100	100
	SM_08	04.12.2022 – 26.02.2024	-	100	100	100	100	100	100
	SM_09	04.12.2022 – 25.02.2024	-	100	100	100	100	100	100
	SM_10	04.12.2022 – 16.02.2024	04.12.2022 – 15.02.2023	0	100	100	100	100	83
	SM_11	03.12.2022 – 15.02.2024	-	100	100	100	100	100	100

Station type	Station	Data collection period	Missing data	Data yield [%]					
				Service A	Service B	Service C	Service D	Service E	Service A-E*
Sweden basic stations	SM_12	14.02.2023 – 16.02.2024	14.02 – 7.03.2023	-	70	100	100	100	93
	SM_13	14.02.2023 – 27.02.2024	-		100	100	100	100	100
	SM_14	14.02.2023 – 26.02.2024	-		100	100	100	100	100
	SM_15	14.02.2023 – 26.02.2024	-		100	100	100	100	100
	SM_16	14.02.2023 – 26.02.2024	13.08 – 13.11.2023		100	100	0	100	75
	SM_17	14.02.2023 – 26.02.2024	-		100	100	100	100	100
All stations**				97					

**ratio of the time of collected recordings to the total period of data collection at a given survey station*

***ratio of the time of collected recordings to the total period of data collection at all survey stations*

Analyses of the acoustic recordings were conducted for five datasets, covering the period between 3 December 2023 and 28 February 2024. Analyses were conducted for the base survey stations in Poland (SM_01 – SM_11) and in Sweden (SM_12 – SM_17), with consideration given to DPD and DPM, regarded in relation to the data collection time.

The obtained results showed that harbour porpoises were present in the survey area in all the seasons, both in Poland and in Sweden. Detailed information on the acoustic detections recorded over the reporting period is included in the table [Table 3.43]. Porpoises occurred at all the survey stations, except for station SM_08. The recorded occurrence showed both seasonal and regional trends. With regard to regional differences, the number of detections was much higher at the stations located in Sweden than in Poland. It concerned both number of days when animals were recorded (DPD) and the length of time when they were recorded (DPM) [Figure 3.67-Figure 3.68]. The highest rate of DPD was found at the stations SM_14 and SM_15, located in the northern part of the survey area (9.3% and 8.5% DPD, respectively) [Figure 3.69, Figure 3.70]. The overall time of porpoise registrations (rate of DPM) was the highest at the station SM_14 (ca. 0.02% DPM) [Figure 3.67]. At the stations SM_12, SM_13 and SM_15 animals were also recorded at long time intervals, with similar overall number of DPM obtained over the measurement time (up to ca. 0.01–0.02% DPM). The number of detections was visibly lower at the Swedish locations SM_16–SM_17 (up to 0.01% DPM) [Figure 3.67-Figure 3.69]. With regards to Poland, porpoises were detected more frequently within the B1 OWF construction area than in the buffer zone [Figure 3.67-Figure 3.69]. Within the OWF area, the overall number of DPD was similar for the stations SM_01–SM_05 (between 1.3% and 1.8% DPD). In the Polish buffer zone, the detection rate was low across the locations (below 1% DPD).

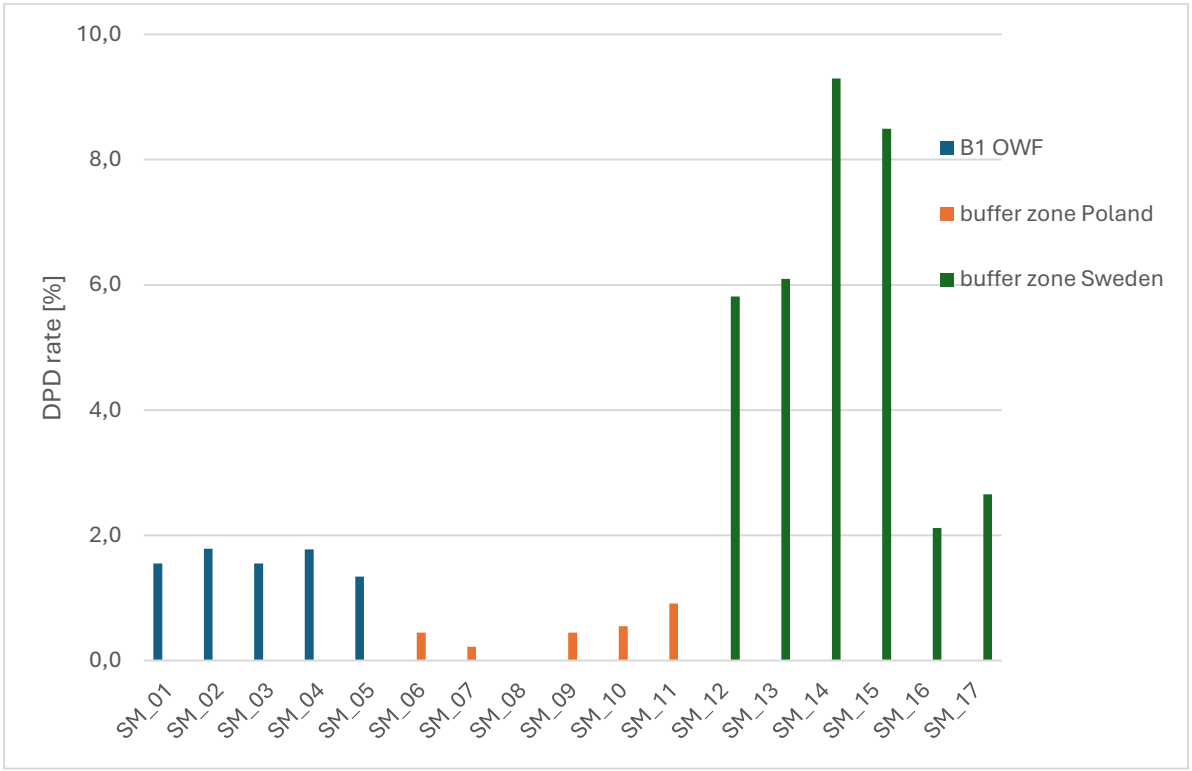


Figure 3.67. The harbour porpoise occurrence recorded at different survey stations during the acoustic monitoring in the survey area between 3 December 2022 (stations in Poland)/14 February 2023 (stations in Sweden) and 28 February 2024. Data is shown as a percentage of DPD recorded over all the recording days per survey station

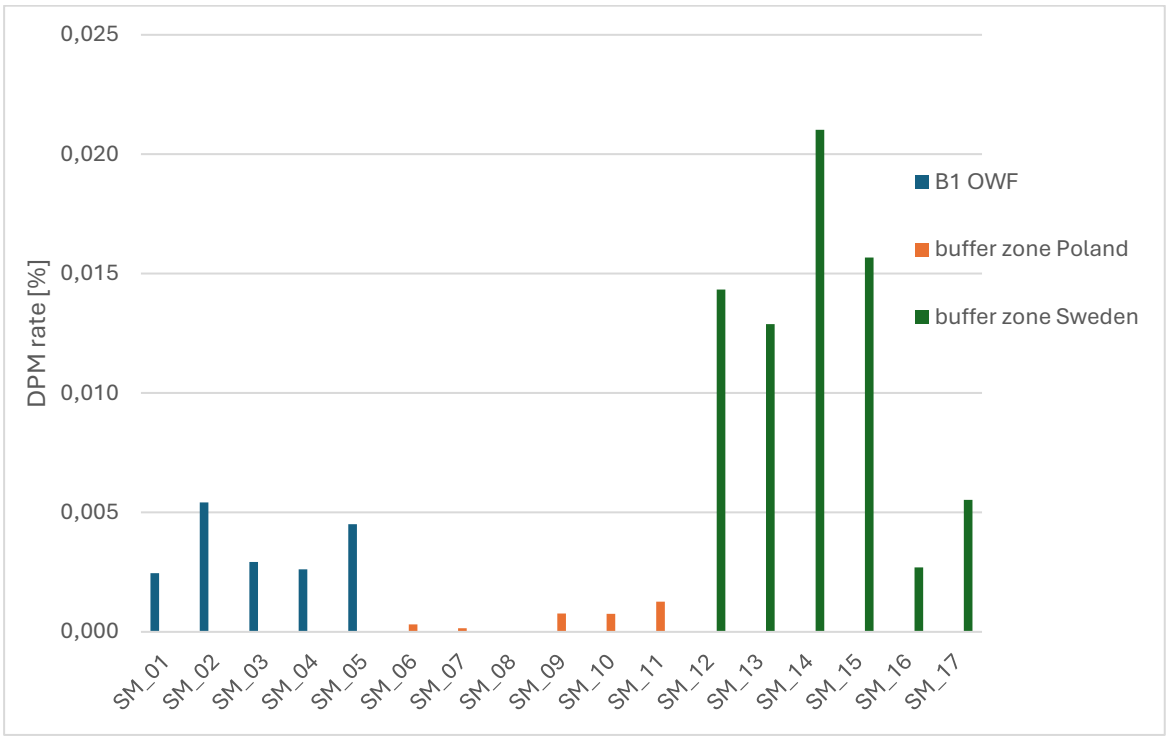


Figure 3.68. The harbour porpoise occurrence recorded at different survey stations during the acoustic monitoring in the survey area between 3 December 2022 (stations in Poland)/14 February 2023 (stations in Sweden) and 28 February 2024. Data is shown as a percentage of DPM recorded over all the recording minutes per survey station

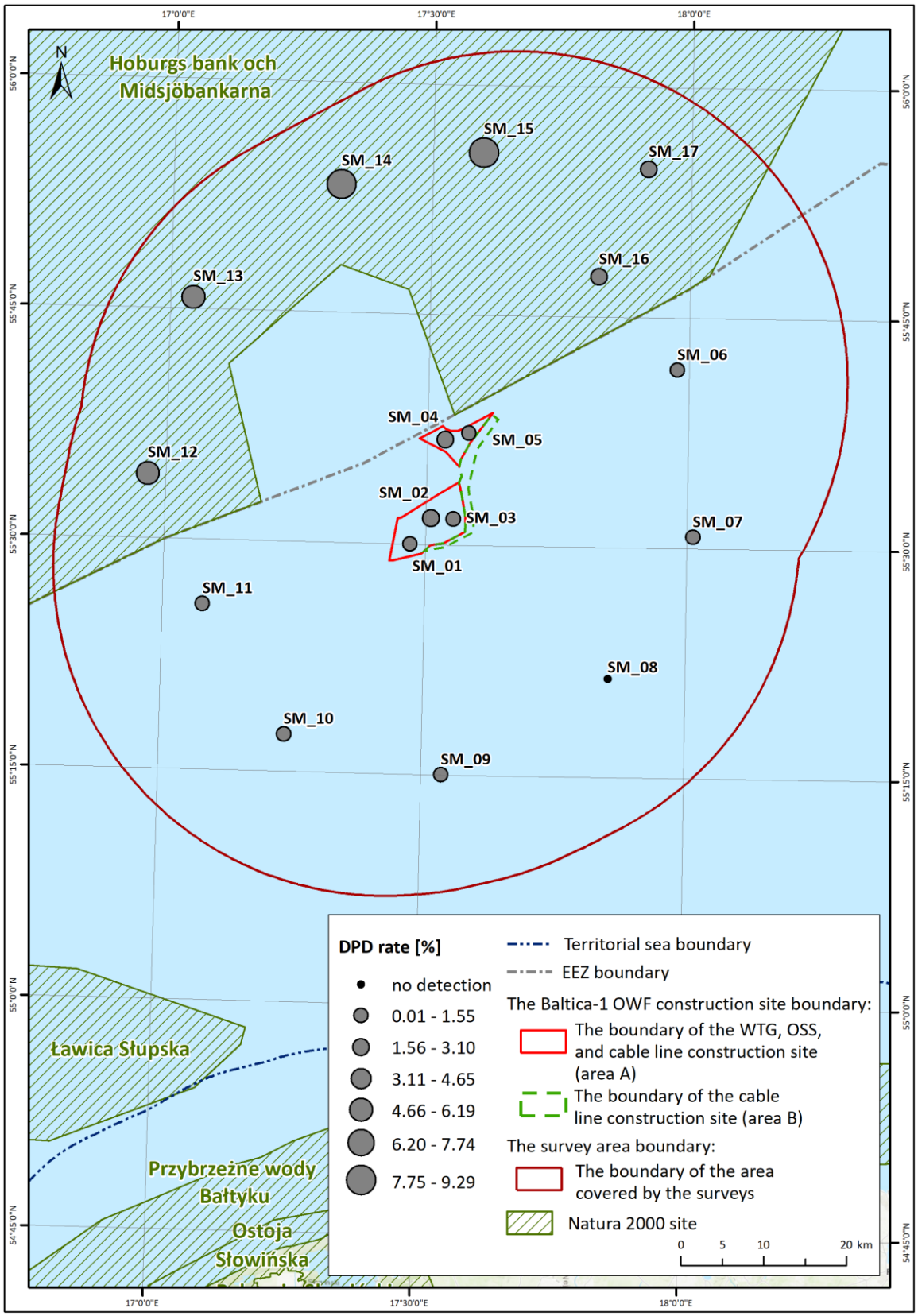


Figure 3.69. The harbour porpoise occurrence recorded at different survey stations during the acoustic monitoring in the survey area between 3 December 2022 (stations in Poland)/14 February 2023 (stations in Sweden) and 28 February 2024. Data is shown as a percentage of DPD recorded over all the recording days per survey station

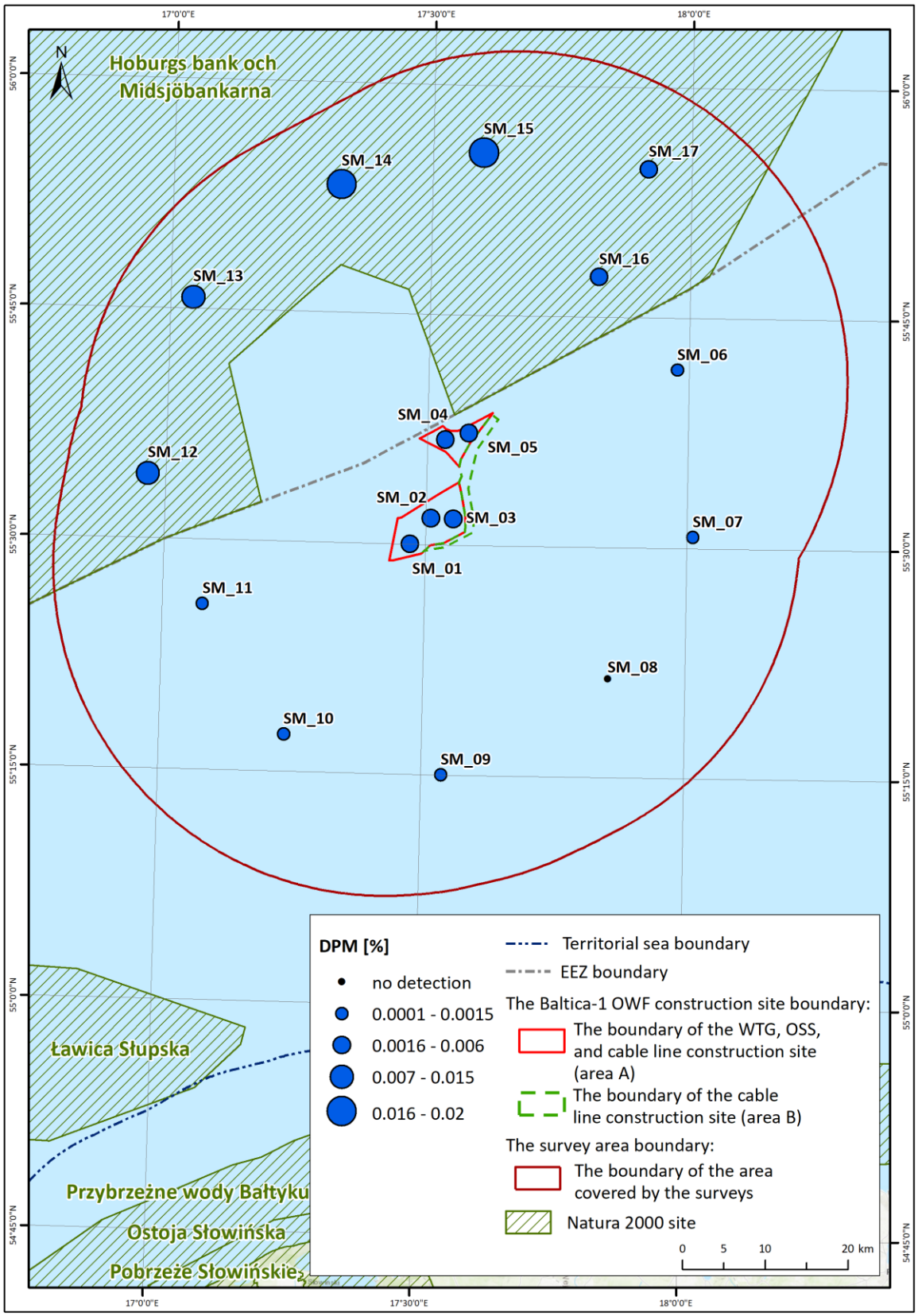


Figure 3.70. The harbour porpoise occurrence recorded at different survey stations during the acoustic monitoring in the survey area between 3 December 2022 (stations in Poland)/14 February 2023 (stations in Sweden) and 28 February 2024. Data is shown as a percentage of DPM recorded over all the recording days per survey station

Considering seasonality, trends in porpoise occurrence throughout the year were found both for the Polish and Swedish locations. Within the OWF area and in the buffer zone in Sweden, number of days with porpoise occurrence was the highest in summer and decreased over. In both survey regions, the highest rate of DPD was registered in August (15.1% DPD in Sweden, 5.8% DPD in Poland) [Figure 3.73]. Within the buffer zone in Poland, detection rate was generally low throughout the year and thus, trends in porpoise presence were not so visible [Figure 3.71]. With regards to the overall time of the species recordings, at the locations in Sweden, the rate of DPM increased from spring to summer (up to ca. 0.02% DPM) and decreased in autumn [Figure 3.71, Figure 3.72]. On a monthly basis, porpoises were detected for the longest time in August and September (c.a. 0.03% DPM) and the shortest – in November 2023 and February 2024 (below 0.01% DPM). In January 2024, animals were not recorded [Figure 3.74]. In case of the stations within OWF area, overall DPM rate was similar in winter 2022/ 2023 and autumn (below 0.01% DPM), and slightly higher during summer (ca. 0.01% DPM) [Figure 3.73]. The shortest time of the species recording was found in spring. On a monthly basis, the highest rate of DPM was found in August (ca. 0.02% DPM) [Figure 3.74]. DPM values were also higher in September (approx. 0.01% DPM). In March and October, no animals were recorded. It should be noted that the data presented for the winter of 2022/2023 are representative only for survey stations in Poland. In the case of Sweden, the recordings cover only two weeks of February and for this reason, the data for this period are not sufficient. The recordings for the winter season of 2023/2024 are complete for both Poland and Sweden. Taking into account the results for the two winter periods in Poland, similar trends in the occurrence of porpoises were found, both in terms of the number of detections and in spatial terms. In the buffer zone, animals appeared very rarely – approx. 0.2% DPD. In the OWF area, the number of detections was higher, but animals appeared occasionally. The detection levels were 1.4% DPD and 1.13% DPD, respectively for the subsequent winters [Figure 3.71]. Taking into account the DPM values, it can be seen that within the OWF area the total recording time of harbour porpoises was longer in winter 2022/2023 (0.004% DPM) than in winter 2023/2024 (less than 0.001% DPM) [Figure 3.72].

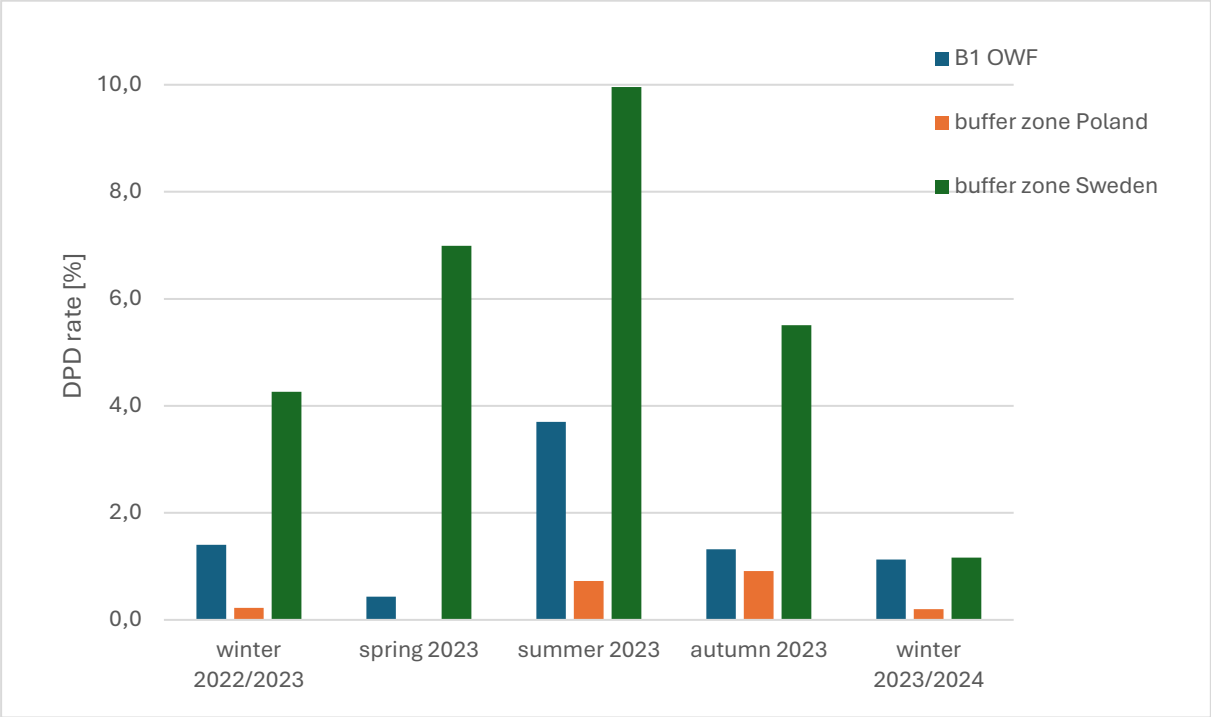


Figure 3.71. *The harbour porpoise occurrence recorded seasonally at the survey stations during the acoustic monitoring in the survey area between 3 December 2022 (stations in Poland)/ 14 February 2023 (stations in Sweden) – 28 February 2024. Data is shown as a percentage of DPD recorded over all the recording days within a season, obtained at a given station**

**The monitoring period during winter 2022/2023 differs between Poland (three months) and Sweden (two weeks)*

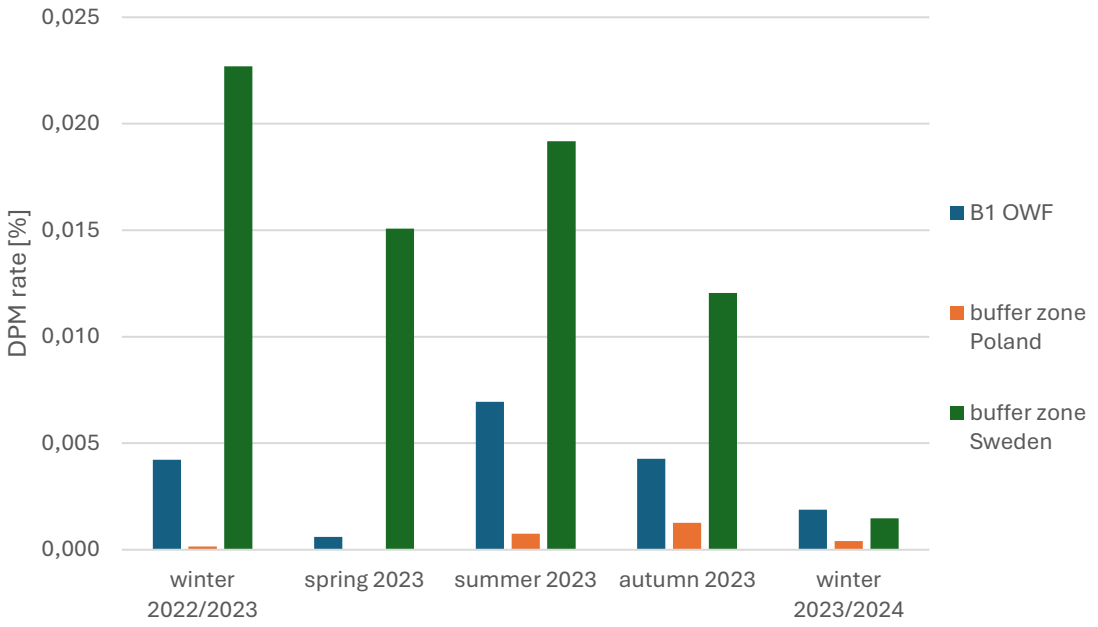


Figure 3.72. *The harbour porpoise occurrence recorded seasonally at the survey stations during the acoustic monitoring in the survey area between 3 December 2022 (stations in Poland)/ 14 February 2023 (stations in Sweden) and 28 February 2024. Data is shown as a percentage of DPM recorded over all the recording minutes within a season, obtained at a given station**

**The monitoring period during winter 2022/2023 differs between Poland (three months) and Sweden (two weeks)*

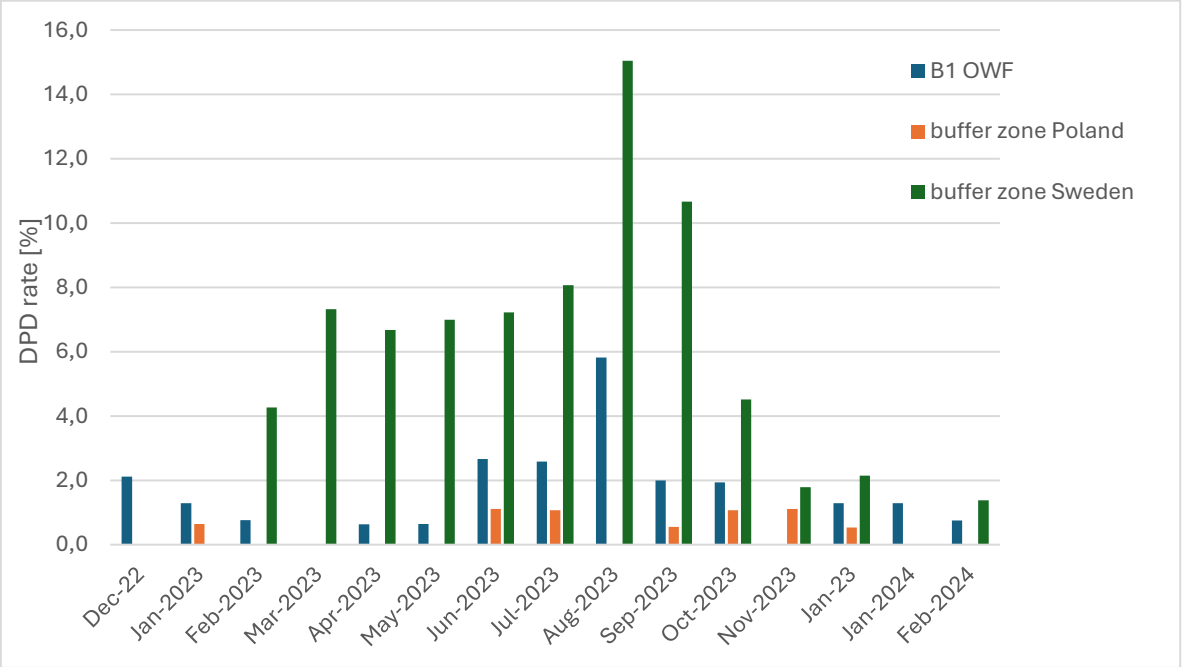


Figure 3.73. *The harbour porpoise occurrence recorded monthly at the survey stations during the acoustic monitoring in the survey area between 3 December 2022 (stations in Poland)/ 14 February 2023 (stations in Sweden) and 28 February 2024. Data is shown as a percentage of DPD recorded over all the recording days within a month, obtained at a given station**

**The monitoring period differs between Poland and Sweden*

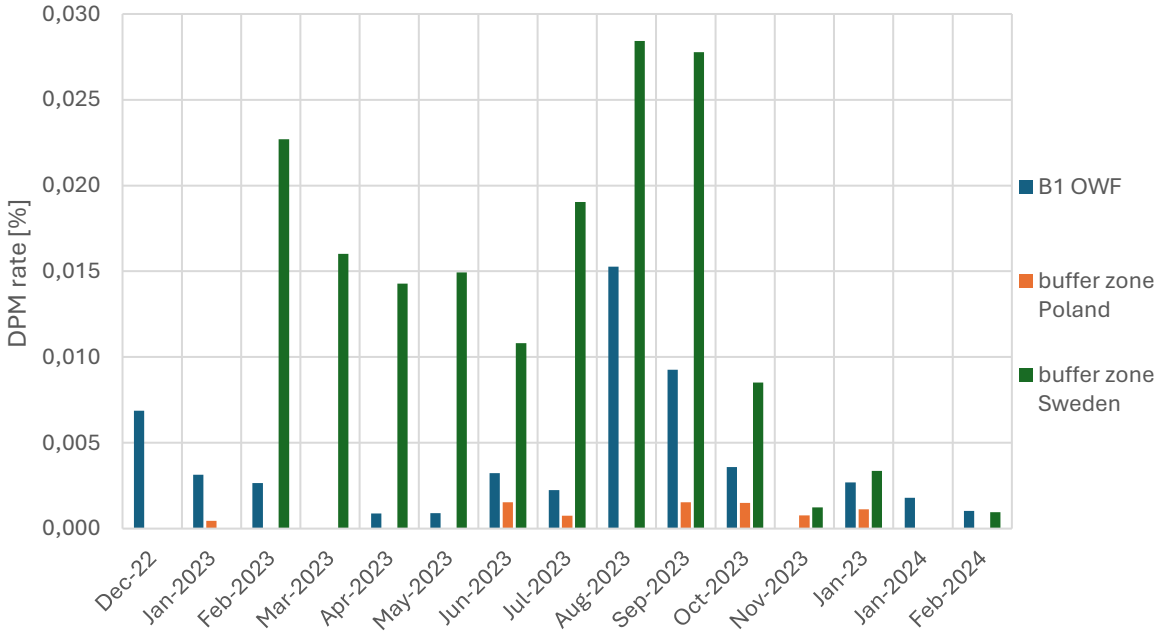


Figure 3.74. *The harbour porpoise occurrence recorded monthly at the survey stations during the acoustic monitoring in the survey area between 3 December 2022 (stations in Poland)/ 14 February 2023 (stations in Sweden) and February 2024. Data is shown as a percentage of DPM recorded over all the recording minutes within a month, obtained at a given station**

**The monitoring period differs between Poland and Sweden*

With regards to seasonal differences between survey stations, it was found that in Poland, porpoises occurred throughout the year mostly at the locations within the B1 OWF area [Figure 3.75Figure 3.75, Figure 3.77]. In the buffer zone, animals were recorded mostly in autumn. It was also noted that during spring, porpoises were only recorded at two stations within the OWF area – SM_04 and SM_05. Seasons when animals occurred in the widest part of the Polish survey area were summer (eight stations) and autumn (seven stations). The highest rates of DPD during these seasons were found at station SM_01 (5.4% DPD in summer) and SM_05 (3.3% DPD in autumn). Over winter periods, animals were registered mostly within the OWF area and at single locations in the buffer zone (SM_06 and SM_11) [Figure 3.75]. In the case of the Swedish buffer zone, porpoises occurred in the entire survey area in all seasons [Figure 3.75,Figure 3.77]. Throughout the survey period, detection rates were visibly lower at stations SM_16 and SM_17. In the summer, DPD rates were high across locations SM_12 – SM_15 (between 10.9% – 15.2% DPD). In spring, porpoises occurred most frequently at the station SM_15 (13.1% DPD), while in autumn – at the station SM_14 (12.1% DPD). In winter, detection levels were low across the stations. Concerning the overall time of the species recordings, in Poland, the longest detections were registered at the location SM_05 in autumn (ca. 0.02% DPM)) [Figure 3.67]. In summer, animals were recorded for the longest time at station SM_02. In Sweden, in spring and summer, DPM rates were highest at the stations SM_12 (up to 0.04% DPM in spring) and SM_14 (up to 0.03% DPM in autumn) [Figure 3.36]. It should be noted that data covering winter 2023 includes only two weeks of February and therefore, the obtained DPD and DPM rates are not representative – the values presented in the plots are inflated in comparison with other seasons [Figure 3.75, Figure 3.76].

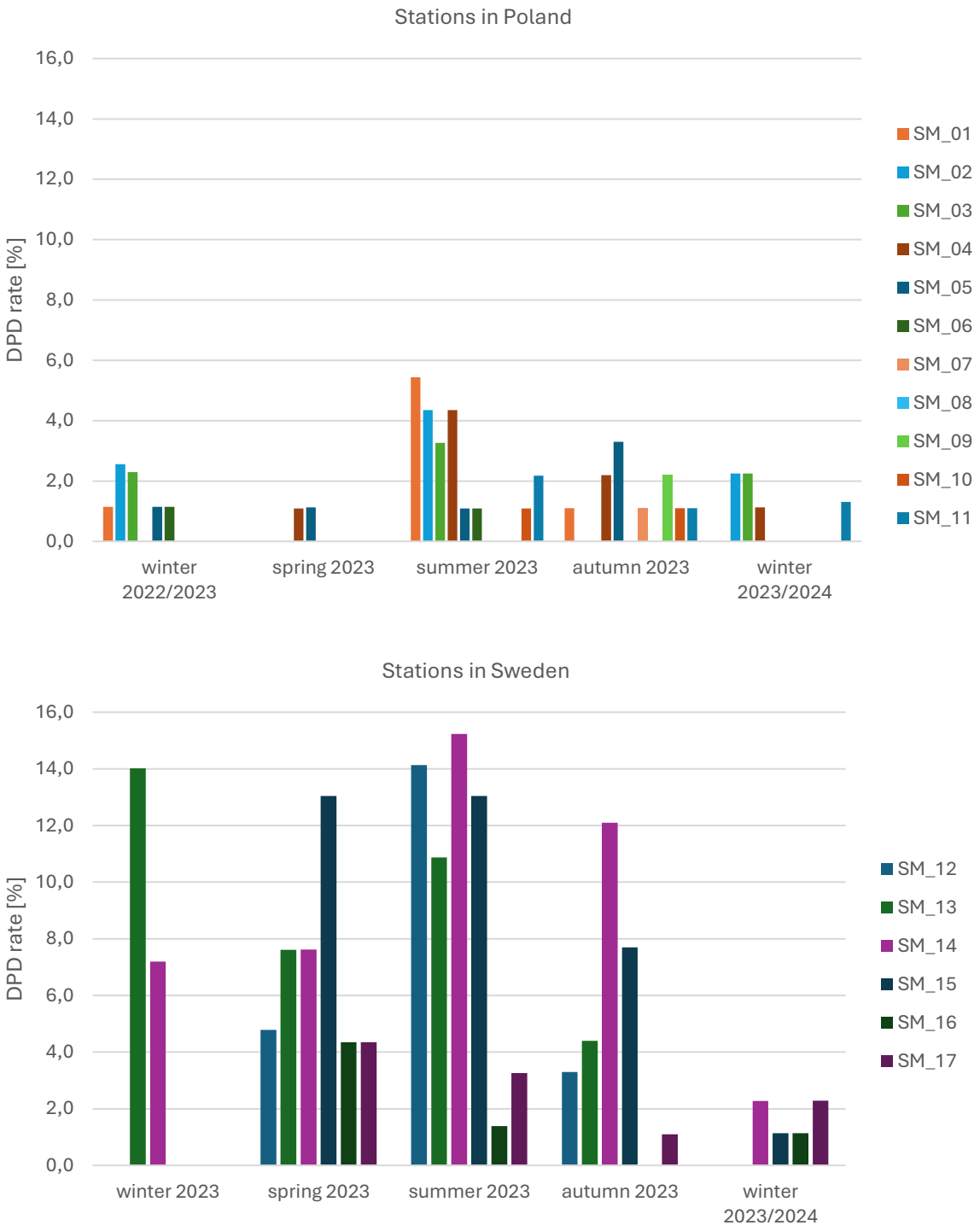


*Figure 3.75. The harbour porpoise occurrence recorded seasonally during the acoustic monitoring in the survey area between 3 December 2022 (stations in Poland)/ 14 February 2023 (stations in Sweden) and 28 February 2024. Data is shown as a percentage of DPD recorded over all the recording days within a season, obtained at a given station**

**The monitoring period during winter 2023 in Sweden covers only two weeks of February*

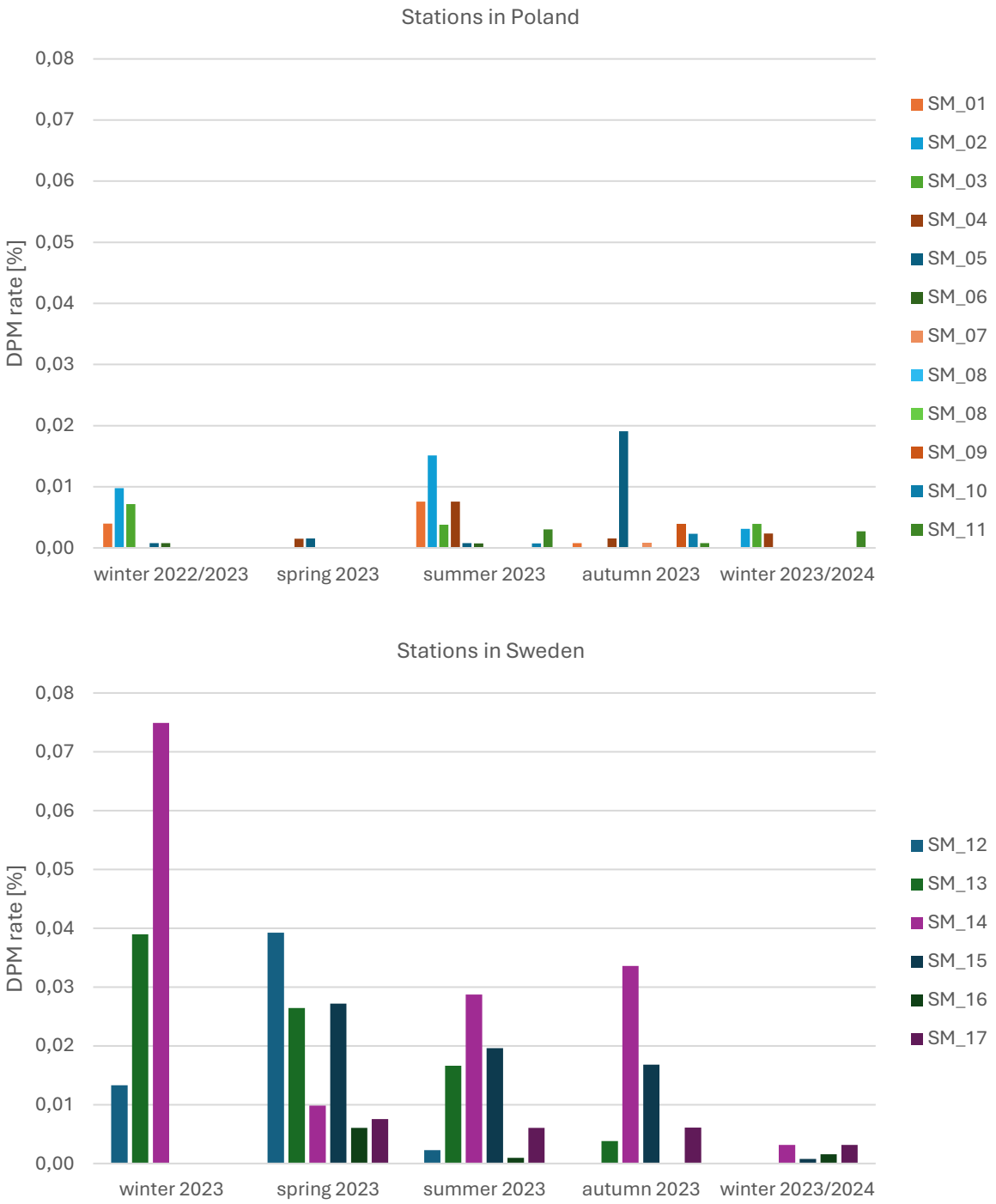


*Figure 3.76. The harbour porpoise occurrence recorded seasonally during the acoustic monitoring in the survey area between 3 December 2022 (stations in Poland)/ 14 February 2023 (stations in Sweden) and 28 February 2024. Data is shown as a percentage of DPM recorded over all the recording minutes within a season, obtained at a given station**

**The monitoring period during winter 2023 in Sweden covers only two weeks of February*

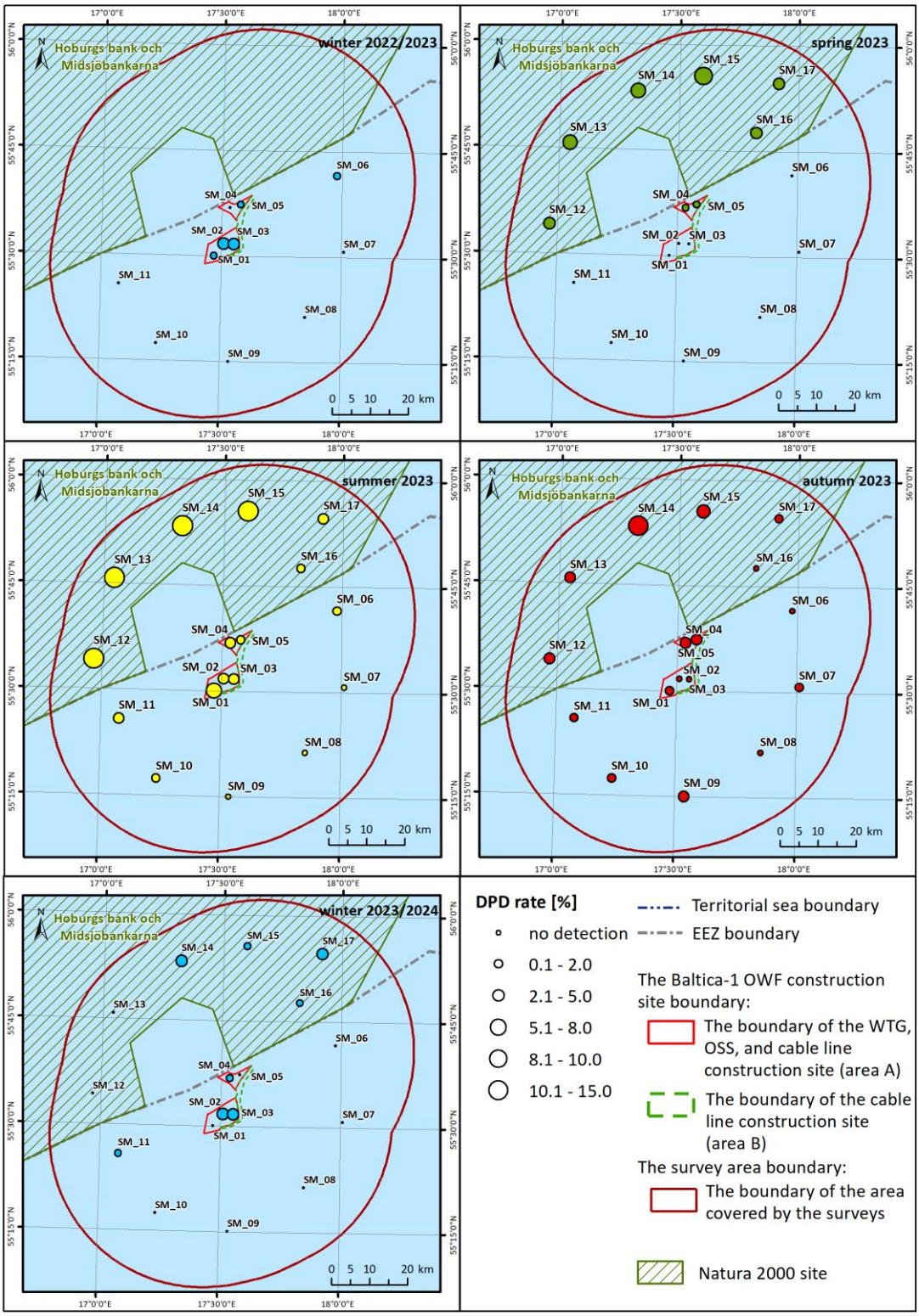


*Figure 3.77. The harbour porpoise occurrence recorded seasonally during the acoustic monitoring in the survey area between 3 December 2022 (stations in Poland)/ 14 February 2023 (stations in Sweden) – 28 February 2024. Data is shown as a percentage of DPD recorded over all the recording days within a season, obtained at a given station**

**The monitoring period during winter differs between Poland (two winter seasons) and Sweden (one season and additional two weeks)*

Table 3.43. A summary of harbour porpoise detections obtained during the acoustic monitoring in the OWF Baltica 1 survey area, between 3 December 2022 and 28 February 2024. Results are shown as days (DPD) and minutes (DPM) of porpoise positive detections, obtained with the use of the KERNO-F classifier and followed by a visual validation

Station	Month	Number of DPD	Number of DPM	Detection date	Comments
SM_01	December 2022	0	0	-	Scope of data: 03.12.2022–07.02.2023 (I) 07.02.2023–24.04.2023 (II) 24.04.2023–13.08.2023 (III) 13.08.2023–12.11.2023 (IV) 12.11.2023–28.02.2024 (V)
	January 2023	1	5	06.01.2023	
	February 2023	0	0	-	
	March 2023	0	0	-	
	April 2023	0	0	-	
	May 2023	0	0	-	
	June 2023	3	6	09.06.2023, 13.06.2023, 29.06.2023	
	July 2023	0	0	-	
	August 2023	2	4	08.08.2023, 21.08.2023	
	September 2023	0	0	-	
	October 2023	1	1	31.10.2023	
	November 2023	0	0	-	
	December 2023	0	0	-	
	January 2024	0	0	-	
	February 2024	0	0	-	
	IN TOTAL	**7**	**16**	-	
SM_02	December 2022	1	9	19.12.2022	Scope of data: 03.12.2022–07.02.2023 (I) 16.02.2023–24.04.2023 (II) 24.04.2023–13.08.2023 (III) 13.08.2023–12.11.2023 (IV) Missing data for the period: 07.02.2023–16.02.2023 Scope of data: 03.12.2022–07.02.2023 (I) 07.02.2023–24.04.2023 (II) 24.04.2023–13.08.2023 (III) 13.08.2023–12.11.2023 (IV) 12.11.2023–27.02.2023 (V)
	January 2023	1	2	06.01.2023	
	February 2023	0	0	-	
	March 2023	0	0	-	
	April 2023	0	0	-	
	May 2023	0	0	-	
	June 2023	1	1	22.06.2023	
	July 2023	1	2	27.07.2023	
	August 2023	2	17	08.08.2023, 16.08.2023	
	September 2023	0	0	-	
	October 2023	0	0	-	
	November 2023	0	0	-	
	December 2023	0	0	-	
	January 2024	2	4	04.01.2024, 26.01.2024	
	February 2024	0	0	-	
	IN TOTAL	**8**	**35**		
SM_03	December 2022	1	4	10.12.2022	
	January 2023	0	0	-	

Station	Month	Number of DPD	Number of DPM	Detection date	Comments
	February 2023	1	5	25.02.2023	
	March 2023	0	0	-	
	April 2023	0	0	-	
	May 2023	0	0	-	
	June 2023	0	0	-	
	July 2023	0	0	-	
	August 2023	3	5	08.08.2023, 16.08.2023, 29.08.2023	
	September 2023	0	0	-	
	October 2023	0	0	-	
	November 2023	0	0	-	
	December 2023	1	3	22.12.2023	
	January 2024	0	0	-	
	February 2024	1	2	10.02.2024	
	IN TOTAL	**7**	**14**		
SM_04	December 2022	0	0	-	Scope of data: 03.12.2022–07.02.2023 (I) 07.02.2023–24.04.2023 (II) 24.04.2023–13.08.2023 (III) 13.08.2023–12.11.2023 (IV) 12.11.2023–27.02.2023 (V)
	January 2023	0	0	-	
	February 2023	0	0	-	
	March 2023	0	0	-	
	April 2023	1	2	21.04.2023	
	May 2023	0	0	-	
	June 2023	0	0	-	
	July 2023	2	2	10.07.2023, 20.07.2023	
	August 2023	2	8	10.08.2023, 18.08.2023	
	September 2023	1	1	13.09.2023	
	October 2023	1	1	07.10.2023	
	November 2023	0	0	-	
	December 2023	1	3	28.12.2023	
	January 2024	0	0	-	
	February 2024	0	0	-	
	IN TOTAL	**8**	**17**		
SM_05	December 2022	1	1	11.12.2022	Scope of data: 03.12.2022–07.02.2023 (I) 07.02.2023–24.04.2023 (II) 24.04.2023–12.08.2023 (III) 12.08.2023–12.11.2023 (IV) 13.11.2023–26.02.2024 (V)
	January 2023	0	0	-	
	February 2023	0	0	-	
	March 2023	0	0	-	
	April 2023	0	0	-	
	May 2023	1	2	20.05.2023	
	June 2023	0	0	-	
	July 2023	1	1	12.07.2023	

Station	Month	Number of DPD	Number of DPM	Detection date	Comments
	August 2023	0	0	-	
	September 2023	2	19	14.09.2023, 15.09.2023	
	October 2023	1	6	06.10.2023	
	November 2023	0	0	-	
	December 2023	0	0	-	
	January 2024	0	0	-	
	February 2024	0	0	-	
	IN TOTAL	**6**	**29**		
SM_06	December 2022	0	0	-	Scope of data: 03.12.2022–06.02.2023 (I) 06.02.2023–29.04.2023 (II) 29.04.2023–12.08.2023 (III) 12.08.2023–13.11.2023 (IV) 13.11.2023–26.02.2024 (V)
	January 2023	1	1	14.01.2023	
	February 2023	0	0	-	
	March 2023	0	0	-	
	April 2023	0	0	-	
	May 2023	0	0	-	
	June 2023	0	0	-	
	July 2023	1	1	04.12.2022	
	August 2023	0	0	-	
	September 2023	0	0	-	
	October 2023	0	0	-	
	November 2023	0	0	-	
	December 2023	0	0	-	
	January 2024	0	0	-	
	February 2024	0	0	-	
	IN TOTAL	**2**	**2**	-	
SM_07	December 2022	0	0	-	Scope of data: 03.12.2022–06.02.2023 (I) 06.02.2023–29.04.2023 (II) 29.04.2023–12.08.2023 (III) 29.04.2023–12.08.2023 (IV) 13.11.2023–26.02.2024 (V)
	January 2023	0	0	-	
	February 2023	0	0	-	
	March 2023	0	0	-	
	April 2023	0	0	-	
	May 2023	0	0	-	
	June 2023	0	0	-	
	July 2023	0	0	-	
	August 2023	0	0	-	
	September 2023	0	0	-	
	October 2023	0	0	-	
	November 2023	1	1	11.11.2023	
	December 2023	0	0	-	
	January 2024	0	0	-	
	February 2024	0	0	-	
	IN TOTAL	**1**	**1**	-	

Station	Month	Number of DPD	Number of DPM	Detection date	Comments
SM_08	December 2022	0	0	-	Scope of data: 04.12.2022–06.02.2023 (I) 06.02.2023–25.04.2023 (II) 25.04.2023–12.08.2023 (III) 12.08.2023–13.11.2023 (IV) 13.11.2023–26.02.2024 (V)
	January 2023	0	0	-	
	February 2023	0	0	-	
	March 2023	0	0	-	
	April 2023	0	0	-	
	May 2023	0	0	-	
	June 2023	0	0	-	
	July 2023	0	0	-	
	August 2023	0	0	-	
	September 2023	0	0	-	
	October 2023	0	0	-	
	November 2023	0	0	-	
	December 2023	0	0	-	
	January 2024	0	0	-	
	February 2024	0	0	-	
	IN TOTAL	**0**	**0**	-	
SM_09	December 2022	0	0	-	Scope of data: 04.12.2022–06.02.2023 (I), 06.02.2023–25.04.2023 (II) 25.04.2023–11.08.2023 (III) 11.08.2023–18.11.2023 (IV) 18.11.2023–26.02.2024 (V)
	January 2023	0	0	-	
	February 2023	0	0	-	
	March 2023	0	0	-	
	April 2023	0	0	-	
	May 2023	0	0	-	
	June 2023	0	0	-	
	July 2023	0	0	-	
	August 2023	0	0	-	
	September 2023	1	4	13.09.2023	
	October 2023	1	1	08.10.2023	
	November 2023	0	0	-	
	December 2023	0	0	-	
	January 2024	0	0	-	
	February 2024	0	0	-	
	IN TOTAL	**2**	**5**	-	
SM_10	December 2022	No data			F-POD lost, no data for the period 04.12.2022–16.02.2023 (I)
	January 2023				
	February 2023				
	March 2023	0	0	-	Scope of data: 16.02.2023–24.04.2023 (II) 25.04.2023–11.08.2023 (III) 11.08.2023–18.11.2023 (IV) 18.11.2023–16.02.2024 (V)
	April 2023	0	0	-	
	May 2023	0	0	-	
	June 2023	0	0	-	
	July 2023	1	1	27.07.2023	
	August 2023	0	0	-	

Station	Month	Number of DPD	Number of DPM	Detection date	Comments
	September 2023	0	0	-	
	October 2023	1	3	29.10.2023	
	November 2023	0	0	-	
	December 2022	0	0	-	
	December 2023	0	0	-	
	January 2024	0	0	-	
	February 2024	0	0	-	
	IN TOTAL	**2**	**4**	-	
SM_11	December 2022	0	0	-	Scope of data: 03.12.2022–06.02.2023 (I) 06.02.2023–23.04.2023 (II) 24.04.2023–11.08.2023 (III) 11.08.2023–17.11.2023 (IV) 18.11.2023–16.02.2024 (V)
	January 2023	0	0	-	
	February 2023	0	0	-	
	March 2023	0	0	-	
	April 2023	0	0	-	
	May 2023	0	0	-	
	June 2023	2	4	26.06.2023, 28.06.2023	
	July 2023	0	0	-	
	August 2023	0	0	-	
	September 2023	0	0	-	
	October 2023	0	0	-	
	November 2023	1	1	02.11.2023	
	December 2023	1	3	16.12.2023	
	January 2024	0	0	-	
	February 2024	0	0	-	
	IN TOTAL	**3**	**5**		
SM_12	February 2023	No data			The device deployed in a wrong position
	March 2023	2	5	17.03.2023, 18.03.2023	Scope of data: 08.03.2023–30.04.2023 (II) 30.04.2023–11.08.2023 (III) 11.08.2023–13.11.2023 (IV) 13.11.2023–16.02.2024 (V)
	April 2023	2	11	26.04.2023, 27.04.2023	
	May 2023	0	0	-	
	June 2023	1	3	18.06.2023	
	July 2023	7	33	12.07.2023, 13.07.2023, 16.07.2023, 23.07.2023, 25.07.2023, 30.07.2023, 31.07.2023	
	August 2023	5	16	01.08.2023, 18.08.2023, 23.08.2023,	

Station	Month	Number of DPD	Number of DPM	Detection date	Comments
				24.08.2023, 31.08.2023	
	September 2023	1	1	13.09.2023	
	October 2023	1	1	26.10.2023	
	November 2023	1	1	11.11.2023	
	December 2023	0	0	-	
	January 2024	0	0	-	
	February 2024	0	0	-	
	IN TOTAL	**20**	**71**		
SM_13	February 2023	2	8	21.02.2023, 27.02.2023	Scope of data: 14.02.2023–30.04.2023 (II) 30.04.2023–11.08.2023 (III) 11.08.2023–13.11.2023 (IV) 13.11.2023–27.02.2024 (V)
	March 2023	4	22	14.03.2023, 18.03.2023, 20.03.2023, 25.03.2023	
	April 2023	2	9	08.04.2023, 25.04.2023	
	May 2023	1	4	16.05.2023	
	June 2023	4	8	08.06.2023, 17.06.2023, 21.06.2023, 30.06.2023	
	July 2023	2	3	12.07.2023, 17.07.2023	
	August 2023	4	11	13.08.2023, 16.08.2023, 25.08.2023, 26.08.2023	
	September 2023	2	2	01.09.2023, 15.09.2023	
	October 2023	1	2	31.10.2023	
	November 2023	1	1	01.11.2023	
	December 2023	0	0	-	
	January 2024	0	0	-	
	February 2024	0	0	-	
	IN TOTAL	**23**	**70**	-	
SM_14	February 2023	1	15	23.02.2023	Scope of data: 14.02.2023–30.04.2023 (II) 30.04.2023–12.08.2023 (III) 12.08.2023–13.11.2023 (IV) 13.11.2023–26.02.2024 (V)
	March 2023	2	2	15.03.2023, 16.03.2023	
	April 2023	1	1	11.04.2023	
	May 2023	4	10	04.05.2023, 12.05.2023, 19.05.2023, 20.05.2023	

Station	Month	Number of DPD	Number of DPM	Detection date	Comments
	June 2023	3	7	13.06.2023, 17.06.2023, 29.06.2023	
	July 2023	4	10	05.07.2023, 06.07.2023, 19.07.2023, 23.07.2023	
	August 2023	7	21	10.08.2023, 14.08.2023, 16.08.2023, 21.08.2023, 27.08.2023, 30.08.2023, 31.08.2023	
	September 2023	7	29	01.09.2023, 03.09.2023, 10.09.2023, 11.09.2023, 13.09.2023, 17.09.2023, 21.09.2023	
	October 2023	4	15	06.10.2023, 14.10.2023, 27.10.2023, 31.10.2023	
	November 2023	0	0	-	
	December 2023	1	3	17.12.2023	
	January 2024	0	0	-	
	February 2024	1	1	18.02.2024	
	IN TOTAL	**35**	**114**	-	
SM_15	February 2023	0	0	-	Scope of data: 14.02.2023–30.04.2023 (II) 30.04.2023–12.08.2023 (III) 12.08.2023–13.11.2023 (IV) 13.11.2023–26.02.2024 (V)
	March 2023	3	6	17.03.2023, 25.03.2023, 31.03.2023	
	April 2023	3	6	01.04.2023, 26.04.2023, 27.04.2023	
	May 2023	6	24	01.05.2023, 04.05.2023, 05.05.2023, 11.05.2023, 15.05.2023, 30.05.2023	
	June 2023	4	9	16.06.2023, 20.06.2023, 24.06.2023, 30.06.2023	
	July 2023	1	1	29.07.2023	

Station	Month	Number of DPD	Number of DPM	Detection date	Comments
	August 2023	7	16	03.08.2023, 04.08.2023, 06.08.2023, 13.08.2023, 15.08.2023, 21.08.2023, 30.08.2023	
	September 2023	5	20	05.09.2023, 11.09.2023, 13.09.2023, 18.09.2023, 19.09.2023	
	October 2023	1	1	31.10.2023	
	November 2023	1	1	06.11.2023	
	December 2023	0	0	-	
	January 2024	0	0	-	
	February 2024	1	1	23.02.2024	
	IN TOTAL	**32**	**85**	-	
SM_16	February 2023	0	0	-	Scope of data: 14.02.2023–29.04.2023 (II) 29.04.2023–12.08.2023 (III)
	March 2023	0	0	-	
	April 2023	3	7	03.04.2023, 04.04.2023, 14.04.2023	
	May 2023	1	1	16.05.2023	
	June 2023	1	1	15.06.2023	
	July 2023	0	0	-	
	August 2023	0	0	-	
	August 2023	No data			F-POD lost, no data for the period 12.08.2023–13.11.2023 (IV)
	September 2023				
	October 2023				
	November 2023				
	December 2023	1	2	29.12.2023	Scope of data: 13.11.2023–26.02.2024 (V)
	January 2024	0	0	-	
	February 2024	0	0	-	
	IN TOTAL	**6**	**11**		
SM_17	February 2023	0	0	-	Scope of data: 14.02.2023–29.04.2023 (II) 29.04.2023–12.08.2023 (III) 12.08.2023–13.11.2023 (IV) 13.11.2023–26.02.2024 (V)
	March 2023	2	6	28.03.2023, 31.03.2023	
	April 2023	1	3	26.04.2023	
	May 2023	1	1	06.05.2023	
	June 2023	0	0	-	
	July 2023	1	4	07.07.2023	
	August 2023	2	4	15.08.2023, 18.08.2023	

Station	Month	Number of DPD	Number of DPM	Detection date	Comments
	September 2023	1	8	04.09.2023	
	October 2023	0	0	-	
	November 2023	0	0	-	
	December 2023	2	4	17.12.2023, 28.12.2023	
	January 2024	0	0	-	
	February 2024	0	0	-	
	IN TOTAL	**10**	**30**	-	
In total	-	**173**	**517**	**-**	**The sum of DPD/DPM at all the stations**

3.4.5.2 Aerial visual monitoring

During the visual monitoring from an aircraft, seven flights were performed. However, on an annual basis, data from the aircraft surveys was collected for every season of the year.

During the winter season, visual monitoring from an aircraft was conducted on 28 February 2023. Marine mammals were not observed.

In the spring season, observation flights were carried out on 22 April and 22 May 2023. A total of three seal observations were reported – two grey seals during the first flight and one undetermined species during the second flight [Figure 3.78, Figure 3.79].

Three observation campaigns were carried out in the summer from an aircraft: on 23 July, 5, and 24 August 2023, during which marine mammals were not observed.

During the flight conducted in autumn, on 28 September 2023, marine mammals were also not observed.

Maps showing the flight routes and seal observations are shown in Figure 3.78, Figure 3.79.

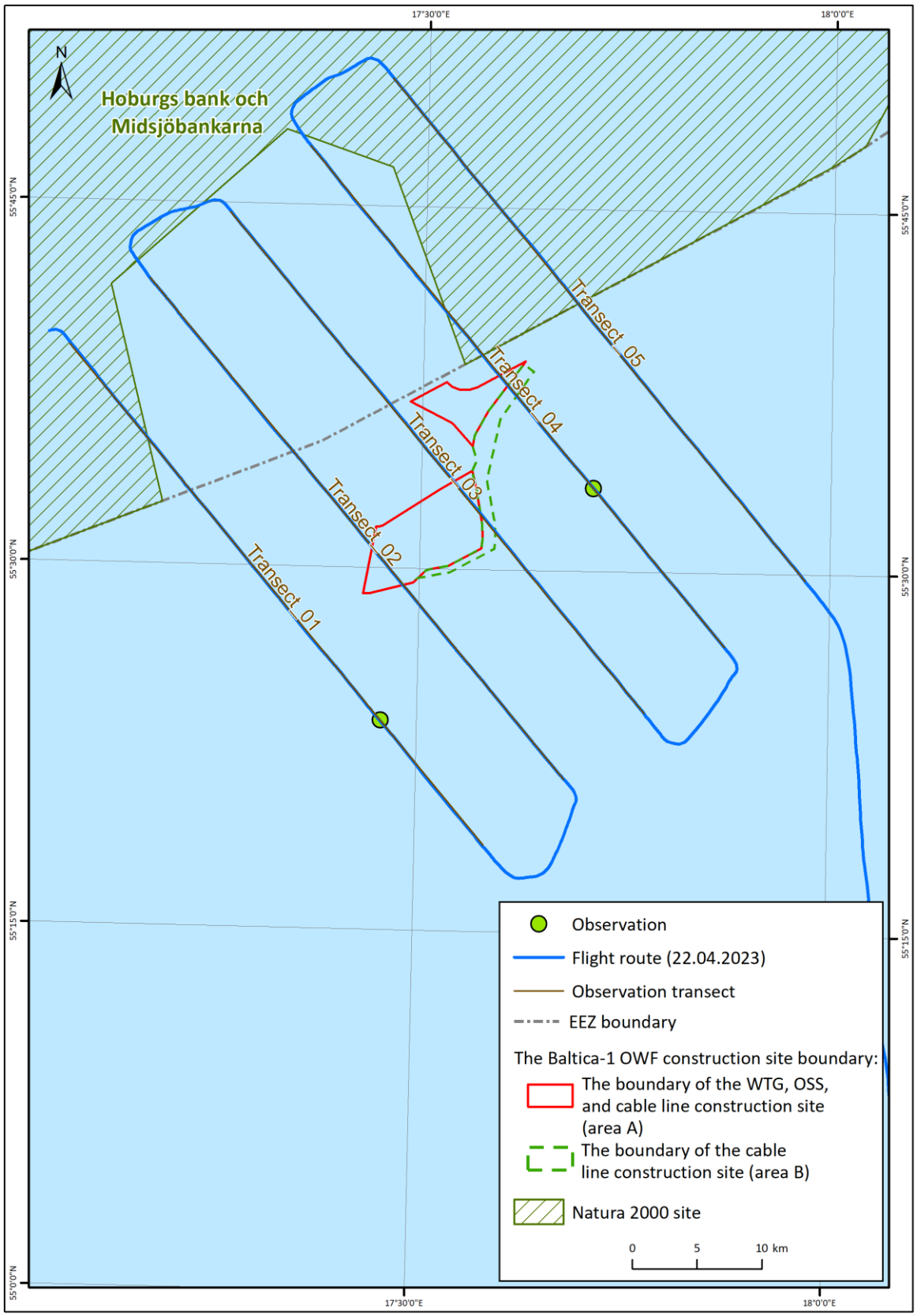


Figure 3.78. The flight route and seal observations during the aerial visual monitoring conducted on 22 April 2023 in the survey area

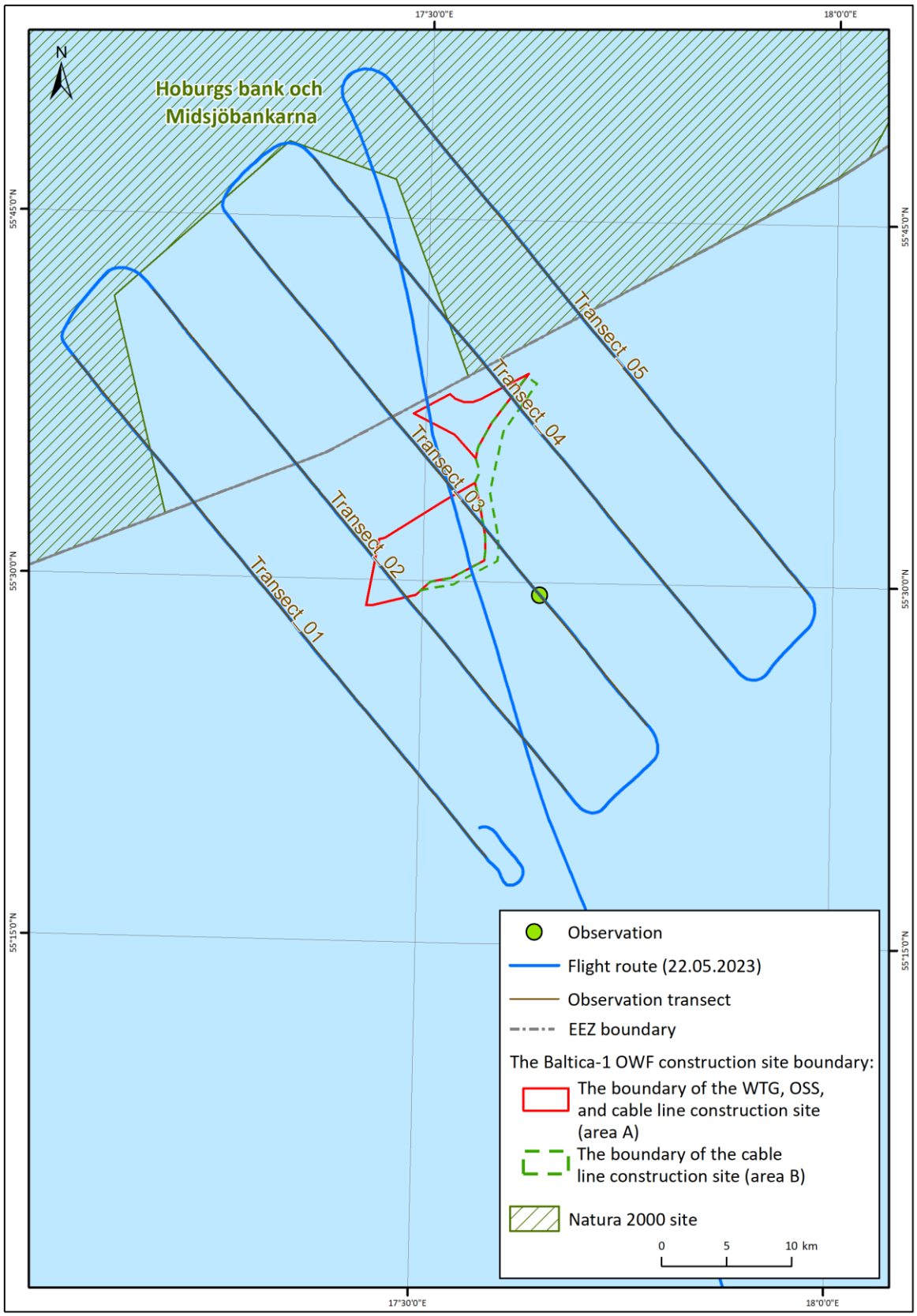


Figure 3.79. The flight route and seal observations during the aerial visual monitoring conducted on 22 May 2023 in the survey area

3.4.5.3 Visual observations (marine mammal counting) during seabird surveys

Visual observations of marine mammals from a ship were conducted from December 2022 to November 2023 in the survey area and the reference area. Mammal records made during the surveys included a total of twenty-seven seal observations, out of which twenty-three observations concerned the grey seal (*Halichoerus grypus*) and four – seal individuals of an unidentified species (Phocidae) [Table 3.44]. Animals were recorded both in the construction area of the Baltica-1 OWF (sixteen observations) and in the reference area (eleven observations). The presence of seals was recorded on 6 and 16 December 2022, 7 and 22 February 2023, 22 April 2023, 28 July 2023, 14 August 2023, 8 September 2023, 22 October 2023, 11 and 29 November 2023 [Table 3.44].

Table 3.44. A summary of marine mammal observations recorded during the seabird survey vessel passages, in the survey area and the reference area

Observation date	Area	Transect number	Section number	Transect zone	Species	Number of animals
06.12.2022	Reference area	02	6	4	Phocidae	1
		03	10	Out of the transect zone	Phocidae	1
	Baltica-1 OWF construction area	02	26	Out of the transect zone	*Halichoerus grypus*	1
		03	9	1	Phocidae	1
		03	9	4	*Halichoerus grypus*	1
		04	22	3	*Halichoerus grypus*	1
		04	13	4	*Halichoerus grypus*	1
		05	9	4	*Halichoerus grypus*	1
		05	24	1	*Halichoerus grypus*	1
16.12.2022	Reference area	03	11	4	*Halichoerus grypus*	1
		03	1	4	*Halichoerus grypus*	1
07.02.2023	Baltica-1 OWF construction area	07	20	4	*Halichoerus grypus*	1
22.02.2023	Reference area	01	5	Out of the transect zone	*Halichoerus grypus*	1
22.04.2023	Reference area	3	14	Out of the transect zone	*Halichoerus grypus*	1
	Baltica-1 OWF construction area	4	7	3	*Halichoerus grypus*	1
		4	21	Out of the transect zone	Phocidae	1
		6	17	2	*Halichoerus grypus*	1
28.07.2023	Baltica-1 OWF construction area	5	15	4	*Halichoerus grypus*	1
14.08.2023	Reference area	3	8	Out of the transect zone	Phocidae	1

Observation date	Area	Transect number	Section number	Transect zone	Species	Number of animals
		3	19	1	*Halichoerus grypus*	1
08.09.2023	Reference area	3	22	1	*Halichoerus grypus*	1
	Baltica-1 OWF construction area	6	11	Out of the transect zone	*Halichoerus grypus*	1
		7	20	Out of the transect zone	*Halichoerus grypus*	1
22.10.2023	Reference area	3	9	1	*Halichoerus grypus*	1
	Baltica-1 OWF construction area	7	20	3	*Halichoerus grypus*	1
11.11.2023	Reference area	4	3	Out of the transect zone	*Halichoerus grypus*	1
29.11.2023	Baltica-1 OWF construction area	1	13	1	*Halichoerus grypus*	1
Total						27

3.4.5.4 Summary of the visual monitoring results

Between December 2022 and November 2023, visual observations of marine mammals were conducted from an aircraft and from a vessel. The monitoring revealed occurrence of seals in the survey area. Porpoises were not observed during neither of the conducted surveys.

The presence of seals was recorded in all seasons in the Baltica-1 OWF survey area and the reference area [Figure 3.81]. The only species observed during the monitoring was the grey seal. Some seal individuals were not identified to the species level. Regional differences were found in the frequency of animal records. The number of observations was much higher within the B1 OWF survey area (19 observations), compared to the reference area (11 observations) [Figure 3.80]. Seals were most frequently observed during December 2022, followed by April 2023 and September 2023. No animals were recorded in January, March, and June 2023 [Figure 3.80]. The most abundant occurrence of seals was recorded in winter, and the least abundant in summer. The numbers of spring and autumn observations were similar [Figure 3.81].

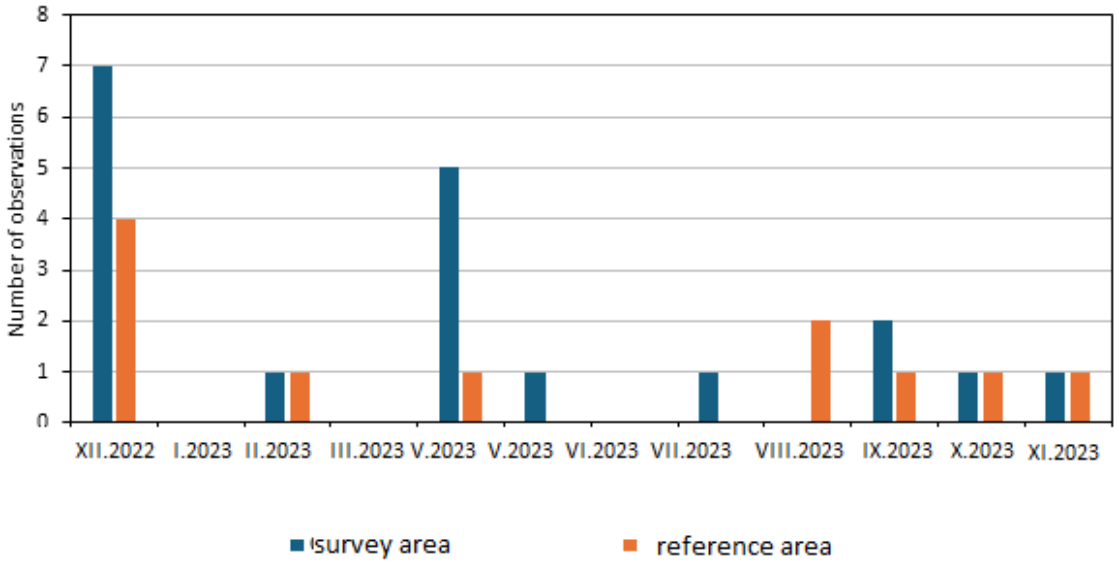


Figure 3.80. The number of seal observations recorded in individual months of the visual monitoring between December 2022 and November 2023 in the OWF Baltica-1 survey area and the reference area

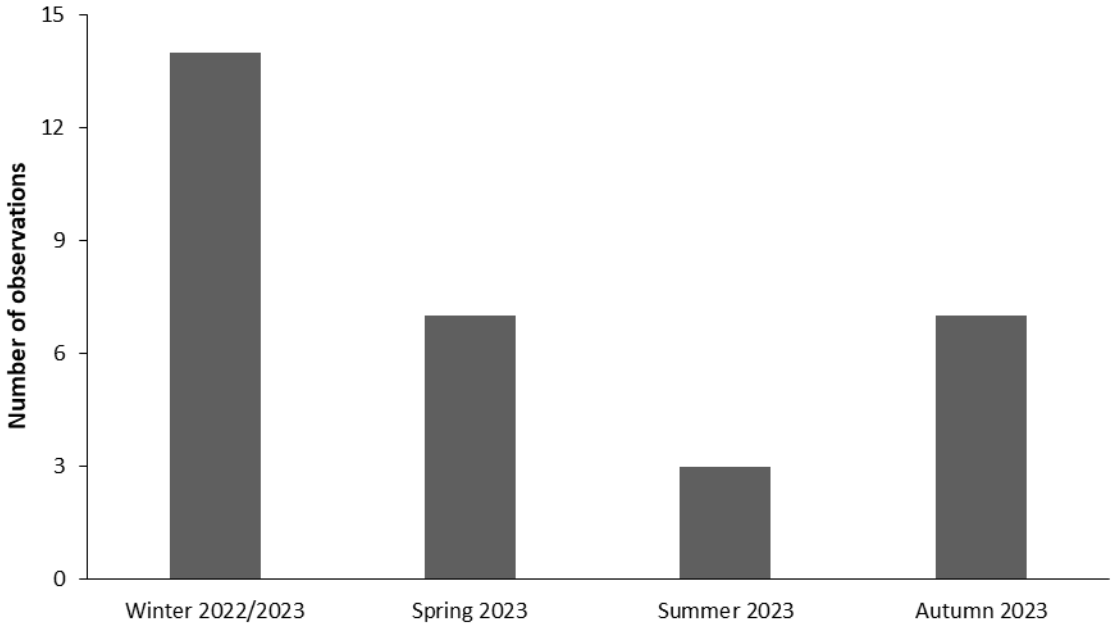


Figure 3.81. The number of seal observations recorded in individual seasons of the visual monitoring between December 2022 and November 2023 in the survey area

3.4.6 Summary of results and conclusions

3.4.6.1 Harbour porpoise

The conducted monitoring showed clear differences in the occurrence of harbour porpoises in different parts of the survey area. The number of animal detections was much higher at the locations within the Swedish EEZ than in the Polish waters. Moreover, in Poland, animals occurred more frequently within the Baltica-1 OWF construction area than in the adjacent buffer zone. In the Polish buffer zone, detection rates were low across all survey stations. The animal activity was mainly recorded in summer and autumn. At one of the stations (SM_08), animals were not recorded throughout the monitoring period. On the other hand, both within the B1 OWF area and in the Swedish buffer zone, porpoises occurred throughout the year, in all seasons. In these two survey areas, the number of detections reached the highest values during summer and decreased over autumn. In Poland, a substantial decrease in detection rates started in September, while in Sweden – it was most visible a month later, in October. In case of the Polish stations, the frequency of porpoise occurrence was lowest over spring – animals were recorded on few days, at two neighbouring stations within the Baltica-1 OWF construction area (SM_04, SM_05). In Sweden, spring detections were frequent and recorded all over the survey area. During winter, the porpoise occurred rarely in the whole Swedish buffer zone. Within the Baltica-1 OWF construction area, detection rates found for winter were similar as during autumn, while in the Polish buffer zone, animals were recorded only at the stations SM_06 and SM_11. In the monitoring period, the highest rates of DPD were registered for the stations SM_14 and SM_15, located in the most northward part of the Swedish buffer zone. Moreover, within the Swedish survey area, regional differences were found. Across seasons, porpoises occurred much less frequently at the locations SM_16 and SM_17, in the eastern part of the monitored area. In Poland, detection rates throughout the year were similar at the stations within the Baltica-1 OWF construction area and similar between the locations in the buffer zone. Analyses of acoustic data with regards to DPM rates showed that animal recordings were very long on certain days, especially in Sweden. Within the Swedish buffer zone, porpoise recordings were up to 40 minutes per day at a single station. Due to long records per day, trends found for monthly changes in DPM rates were slightly different that for DPD.

The results obtained in the acoustic monitoring are in line with available knowledge on the harbour porpoise occurrence in the Baltic Proper. The Swedish part of the survey area is located within the Natura 2000 site Hoburgs bank och Midsjöbakarna, where porpoises are protected. This region is recognized as the area of highest porpoise occurrence in the Baltic Proper, as well as a presumed breeding site of the species (SAMBAH, 2016; Carlen et al., 2018; Owen et al., 2021). The high rates of acoustic detections within the Hoburgs bank och Midsjöbakarna, in comparison to other parts of the eastern Baltic, were reported in two long-term monitoring projects – SAMBAH (Static Acoustic Monitoring of the Baltic Sea Harbour Porpoises) and the Swedish National Monitoring Program (SNMP). The SAMBAH project (April 2011 – July 2013) showed that porpoises from the Baltic Proper subpopulation aggregate in the region between May and October, which coincides with their reproduction period (SAMBAH, 2016; Carlen et al., 2018) [Figure 3.82]. The SNMP surveys (April 2017 – March 2020) confirmed these results, showing increased detection rates between the end of spring and the beginning of autumn (Owen et al., 2021). The project also revealed that porpoise occurrence is most frequent within the Northern Middle Bank, in the northern part of the Natura 2000 site [Figure 3.83]. The overall detection rates recorded during the SAMBAH and SNMP monitoring programs were 6.9% DPD (444 DPD out of 6422 recording days) and 9.1% DPD (737 DPD out of 8117 recording days),

respectively, indicating an upward trend in the species occurrence within Hoburgs bank och Midsjöbakarna.

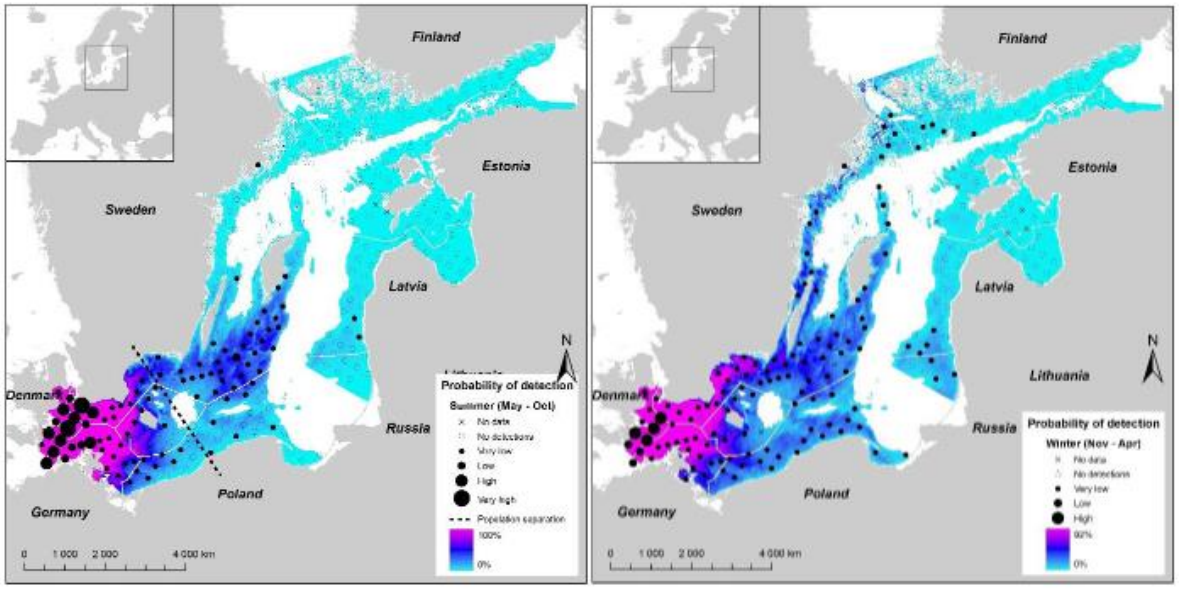


Figure 3.82. The probability of detecting porpoises in two seasons: May–October (left) and November–April, demonstrated during the SAMBAH project (2011–2013) (source: own study based on SAMBAH data]

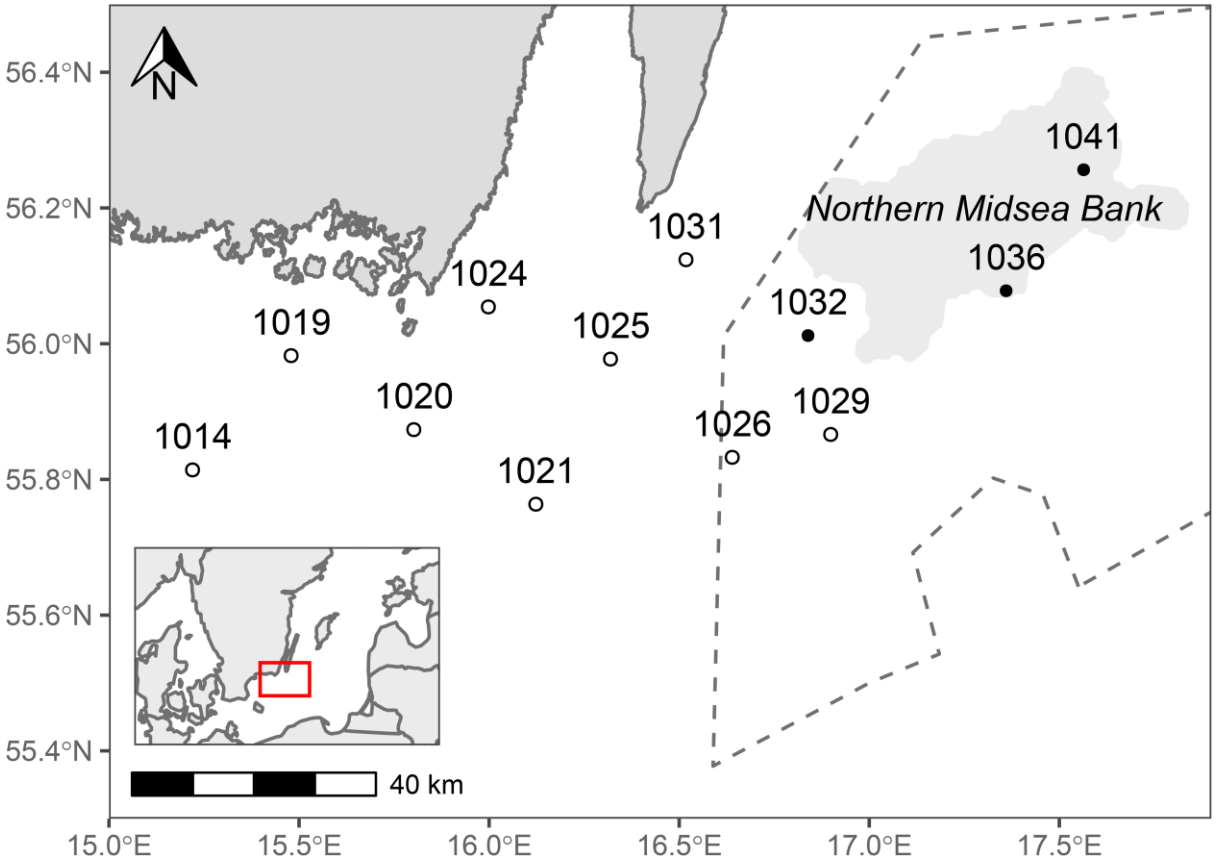


Figure 3.83. The location of survey stations during the acoustic monitoring under the SNMP projects (2017–2020). Black denotes stations with the highest porpoise detection rates during the project. Dashed lines denote the boundaries of the Natura 2000 site Hoburgs bank och Midsjöbakarna. The

locations of the monitoring stations under the SNMP program were the same as those under the SAMBAH project [Source: Owen et al., 2021]

In comparison, the overall detection rate found for the Swedish buffer zone of the Baltica-1 OWF survey area up to date was around 6% DPD (126 DPD out of 2135 recording days). Such value is similar to the results obtained in the SAMBAH project. Moreover, seasonal trends found during this project reflect well the survey results under the SAMBAH and SNMP projects. The high detection rates recorded between spring and summer at the Swedish locations indicate potential porpoise aggregation for breeding. On the other hand, a clear decrease in in the number of records in autumn and winter, suggests dispersion of the species to other regions of the Baltic. It seems to be confirmed by more frequent animal occurrence in the Polish buffer zone during autumn months. Moreover, a northward increase in the detection rates across the Baltica-1 OWF survey area (with the highest values found for the stations SM_14 and SM_15), is also in line with SAMBAH and SNMP, indicating the varying importance of different parts of the monitoring region for porpoises.

The recorded frequency of porpoise occurrence during summer and autumn showed similar trends within the Baltica-1 OWF construction area and in the Swedish buffer zone. As the planned OWF area borders on the Hoburgs bank och Midsjöbakarna, such results are well explainable. In contrast, detection patterns found in the Polish buffer zone, further away from the Swedish EEZ, differed from the ones obtained for the Swedish waters. In this part of the survey area, the detection rate was low throughout year (overall DPD rate around 0.4%) and animals were not detected during spring months. Most of the detections were made in November, after the period of increased porpoise activity in the Swedish waters. These results support the conclusions reached by the SAMBAH project, that after the reproduction season (from November) porpoises disperse within the Baltic Proper.

The results obtained for the Baltica-1 OWF area can also be compared to available data from acoustic monitoring programs conducted for other planned offshore wind farms. The data from this type of research are currently available, among others, for the locations of the Baltica OWF, Bałtyk II OWF, Bałtyk III OWF, Baltic Power OWF, BC-Wind OWF and Bałtyk I OWF. Based on the comparative analysis, it can be stated that the area within the planned Baltica-1 OWF is characterized by higher levels of porpoise detection (1.6% DPD) than in the case of investments located to the south – including the Bałtyk II OWF, Bałtyk III OWF, Baltic Power OWF(0.6% DPD), and BC-Wind OWF (0.6% DPD) (Plichta et al., 2014; 2015; Opioła et al., 2020; Gajewski et al., 2021). The studies conducted for the Bałtyk II OWF (formerly Bałtyk Środkowy II) and Bałtyk III OWF (formerly Bałtyk Środkowy III) – areas located southwest/south of the Baltica-1 OWF – showed a much lower frequency of porpoise occurrence than in the analyses in question. In both monitoring programs, only single detections of animals were recorded during the year, primarily in the summer–winter period (Plichta et al., 2014; 2015). The acoustic monitoring conducted for the Baltic Power OWF (2018–2019) showed rare occurrence of porpoises in the survey area. The overall frequency of detection days was found at 0.6% DPD. Animals were recorded in most of the study months, except for February, April, July and November, with the highest DPM level in the autumn season (Opioła et al., 2020). The monitoring carried out for the nearby BC Wind OWF (2019–2021) also indicated occasional occurrence of porpoises in the analysed area. The overall detection level was 0.6% DPD, with the highest number of animal records in the summer season (Gajewski et al., 2021).

In contrast to the stations within Baltica-1 OWF construction area, porpoise activity recorded in the Polish part of the survey area (0.4% DPD) seems to be similar to areas in the central part of the open waters of the Polish EEZ. In these areas, animals appear occasionally, at different times of the year.

Comparing the results obtained for the Baltica-1 OWF(locations within the Baltica-1 OWF construction area) with data from the nearby Bałtyk I OWF, similar trends in the occurrence of porpoises are observed. In both of these areas, animals were recorded more frequently than in the central part of the Polish sea areas. The overall detection level found for the Bałtyk I OWF was 2.9% DPD, which is even higher than in the case of this project (Brocławik et al., 2022). In relation to seasonal changes, in the area of both wind farms, porpoises appeared with the highest frequency in the summer, while in the autumn season the number of detections began to decrease. These results indicate that in the area of both Baltica-1 OWF and Bałtyk I OWF the occurrence of the species is largely related to the proximity of the Swedish Natura 2000 site.

In comparison with another offshore area within the Polish EEZ for which data on porpoise occurrence is available – the Stilo Bank (south-west the Baltica-1), it is also concluded that the Polish part of the Baltica-1 OWF survey area is characterized by a higher frequency of the species occurrence. The overall detection rate found for the Stilo Bank between June 2016 – April 2018, during the first part of the National Monitoring Program, was around 0.3% DPD (CIEP, 2018). The second part of the national monitoring confirmed the low porpoise occurrence in this region (CIEP, 2022).

In conclusion, the acoustic monitoring conducted for the planned Baltica-1 OWF project showed that porpoise occurrence within the planned OWF area is higher than in case of other offshore regions of the Polish EEZ, for which data is available. This result is related to the location of Baltica-1 OWF at the border with the Swedish Natura 2000 site Hoburgs bank och Midsjöbakarna, where frequent activity of porpoises coincides with the reproduction period (Carlen et al., 2018). Seasonal changes in the species occurrence within the planned OWF area seem to be related to its breeding activity in Sweden.

3.4.6.2 Seals

There are three species of seals in the Baltic Sea, which include the grey seal (*Halichoerus grypus*), the common seal (*Phoca vitulina*) and the ringed seal (*Pusa hispida*) (Cichocki et al., 2015). The most commonly observed species in the Polish EEZ, especially in the Vistula estuary region, is the grey seal (WWF, 2023a; WWF, 2023b). In contrast, according to HELCOM data, the probability of the occurrence of the other two species in the Southern Baltic Sea is assessed as low (HELCOM, 2018).

The results of the visual monitoring of marine mammals performed for the Baltica-1 OWF project can be compared to available data on the seal occurrence along the Polish coast, collected by WWF Poland Foundation and SMIOUG, in the years 2020–2023. The report on the project “Protection of marine mammals and seabirds – continuation” shows that the most numerous seal observations from the shore were on grey seals (1390 observations), followed by common seals (40 observations) and ringed seals (8 observations) (WWF, 2023a). During the monitoring conducted, only grey seals were sighted, which also reflects higher abundance of this species within the Polish EEZ. It is worth noting that, according to WWF data, grey seals were most often recorded to the east of Łeba [Figure 3.84, Figure 3.85, Figure 3.86, Figure 3.87].

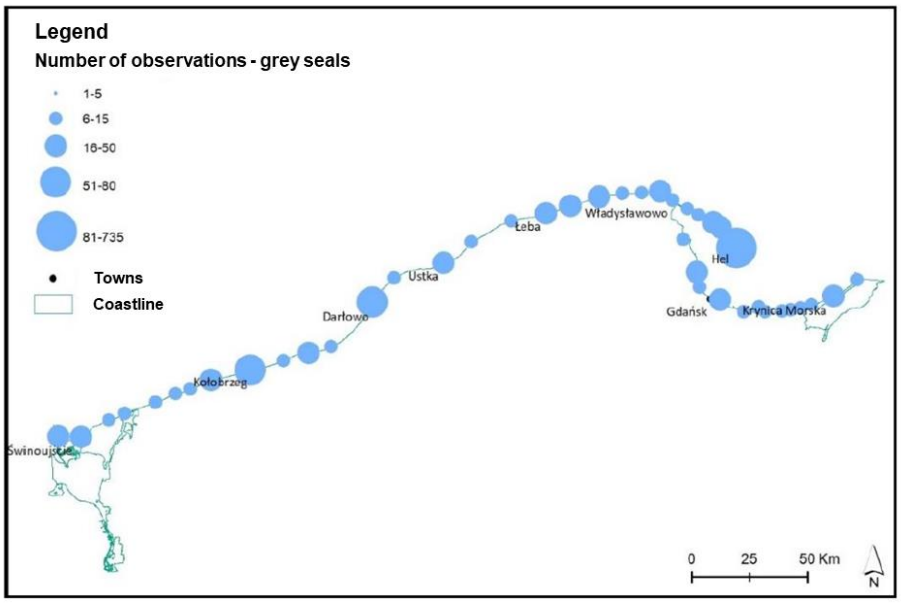


Figure 3.84. The observations of live grey seals in 2020–2023 [Source: WWF, 2023a]

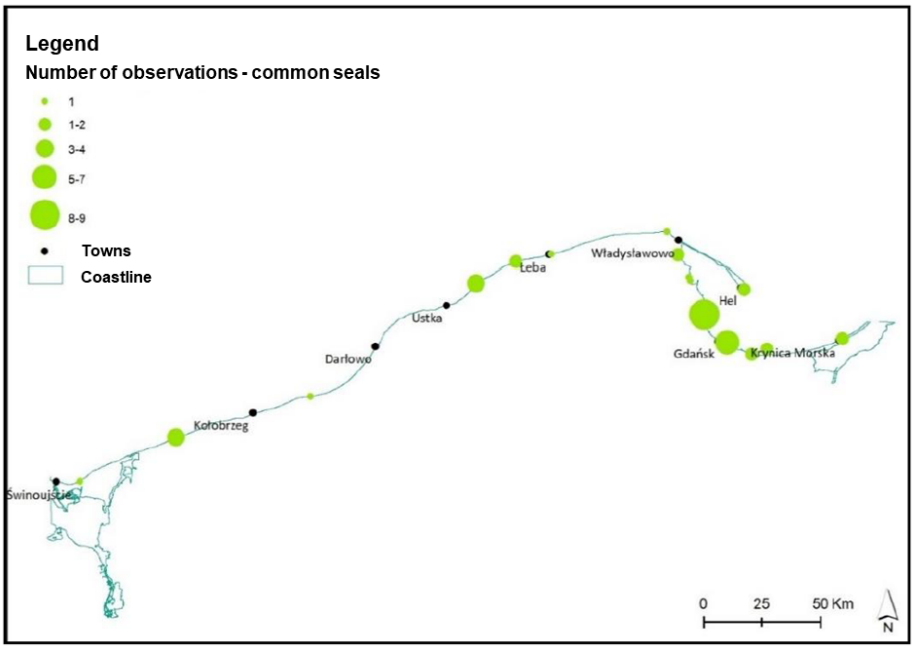


Figure 3.85. The observations of live harbour seals in 2020–2023 [Source: WWF, 2023a]

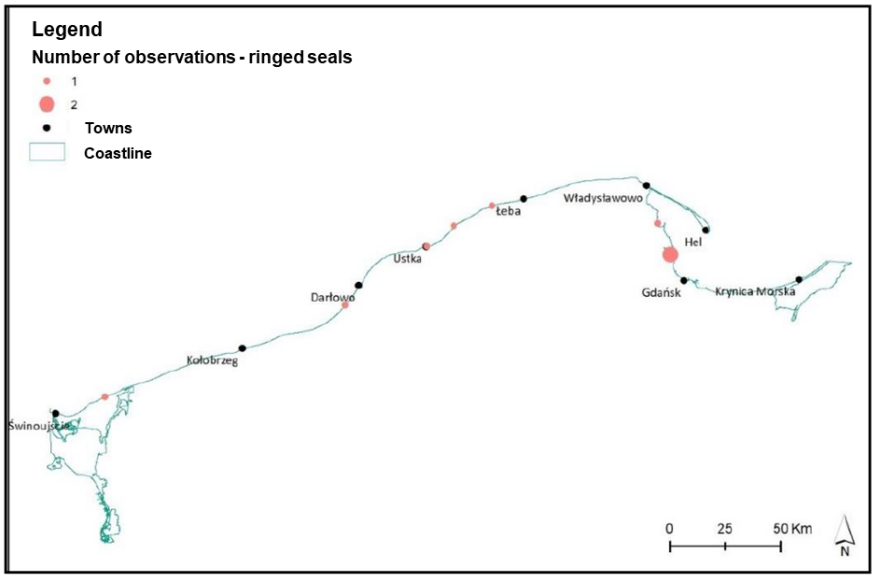


Figure 3.86. The observations of live ringed seals in 2020–2023 [Source: WWF, 2023a]

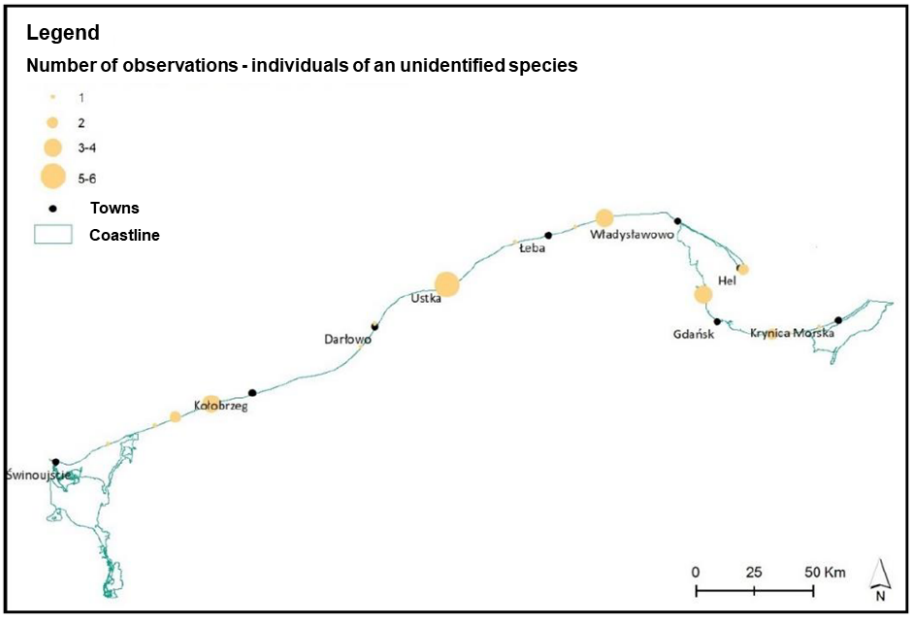


Figure 3.87. The observations of live unidentified seal species in 2020–2023 [Source: WWF, 2023a]

It should also be noted that in the Baltic Sea, seals migrate for exploration, feeding and breeding (Sjöberg and Ball, 2000), even over long distances of up to 100 km per day (WWF, 2019; WWF, 2020). Data on seal migration in the Baltic Sea comes from tagging individuals with satellite transmitters. Migration maps based on transmitter results show that seals use the entire Polish Baltic Sea area (WWF, 2019; WWF, 2020) [Figure 3.88]. On this basis, it can be assumed that individuals which are observed on the coast might also travel to the Baltica-1 OWF area.

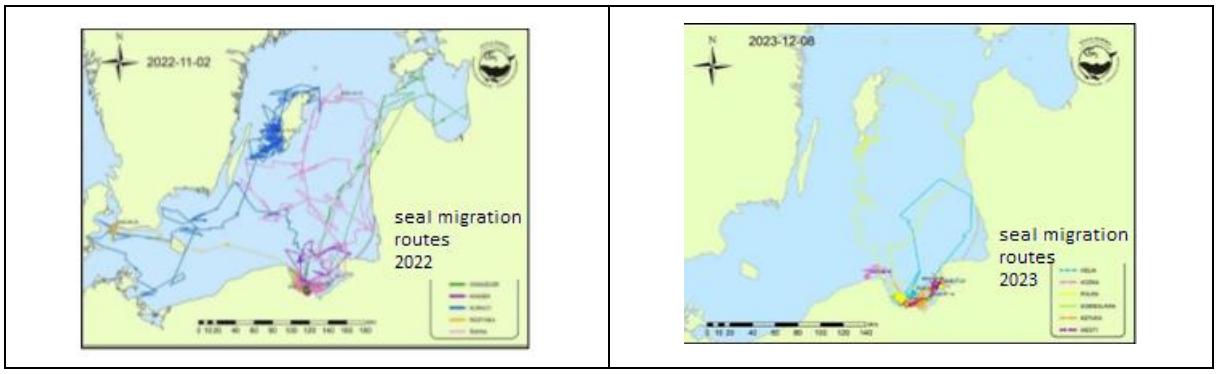


Figure 3.88. Migration routes of young grey seals for 2022 and 2023 [SMIOUG press materials available online]

Based on the data from the National Monitoring Project: "Pilot Implementation of Monitoring of Marine Species and Habitats 2015–2018" and data available in WWF Poland database, it was shown that there is a seal colony site within the Polish sea areas. The haul out site is located in the area of the Vistula Przekop estuary. In the years 2016–2017, it was found that the seal stock occurring in this region during the moulting period (summer season) was of about 200 individuals (Opioła et al., 2017). The planned area of the Baltica-1 OWF is located about 160 km in a straight line from the haul-out site. The results obtained during the project showed that occurrence of seals in the analysed region is the lowest during summer. This observation might be related to increased activity of seals around the Vistula mouth, in the months when moulting takes place. It could be presumed that in summer seals aggregate in the haul-out site and their migration to the northern parts of Polish EEZ decreases.

The results obtained for the Baltica-1 OWF area can also be compared with available data from the surveys conducted for other planned offshore wind farms, including the Bałtyk II OWF (2013–2014), Bałtyk III OWF (2012–2013), Baltic Power OWF (2018–2019), BC-Wind OWF (2020–2021) and Bałtyk I OWF (2020–2022). The monitoring studies conducted for these investments show that the open waters of the EEZ are used by grey seals throughout the year. The frequency of animal occurrence and their seasonal activity differs between the areas and years of research (Plichta et al., 2014; 2015; Opioła et al., 2020; Gajewski et al., 2021; Brocławik et al., 2022). During the visual monitoring from aboard a vessel carried out for the nearby Bałtyk I OWF (west of Baltica-1 OWF, 2020–2022), nine observations of grey seals were recorded, mostly in the autumn season and to a lesser extent in the summer (Brocławik et al., 2022). During the visual surveys from aboard a vessel carried out for the Baltic Power OWF (2018–2019), seals were recorded in all seasons, a total of ten times. Grey seals, harbour seals and individuals unidentified to species were recorded (Opioła et al., 2020). The presence of seals was also recorded during the monitoring conducted from aboard a ship for the BC-Wind OWF (2020–2021). A total of 28 observations were made in different periods of the year, of which 21 concerned grey seals, and the rest – individuals unidentified to species (Gajewski et al., 2021). As part of the Bałtyk II (2012–2013) and Bałtyk III (2013–2014) projects, during visual monitoring conducted from an aircraft, few seal observations were recorded in the spring and autumn seasons. Grey seals, harbour seals and individuals unidentified to species were recorded (Plichta et al., 2014; 2015).

Considering the large migration possibilities of grey seals, mainly related to searching for an appropriate food base, it is likely that the differences recorded during individual studies result from the availability of food. The total number of seal observations recorded during the year in the Baltica-1 OWF survey area (within the OWF area and the reference area) was the closest to the value recorded

in the monitoring conducted in the BC-Wind OWF area, located in the central part of the Polish EEZ, to the south of the Baltica-1 OWF. During the monitoring conducted from aboard a ship for these projects, 23 and 21 observations of grey seals were recorded, respectively.

In conclusion, literature data indicates that grey seals use the area of the Polish EEZ more frequently than common and ringed seals, which was also found during the monitoring conducted for the Baltica-1 OWF project. The pre-investment studies conducted for the planned offshore wind farms located in the open waters of the Polish EEZ indicate that grey seals appear in the area throughout the year, and the seasonality of their occurrence differs between locations and years of study. In the area of the Baltica-1 OWF and in adjacent waters, animals were observed most often in winter, and they were the least abundant in summer. It can be assumed that the reduced activity of seals in the monitored area in summer (moulting time) is related to the high aggregation of animals around the haul-out site, in the area of the Vistula River mouth.

3.4.7 Shortcomings and gaps in the state-of-the-art

Considering the nature of the surveys conducted at sea, deviations from the methodological assumptions may always occur. In the reporting time scope, most of the project activities related to marine mammal investigations were performed according to the plan. Good quality data was collected both during the acoustic measurements and the visual observations. In case of the acoustic monitoring, gaps found in the recordings were mostly related to losses or failures of the equipment. However, overall, data obtained for the base survey stations covered over 90% of the recording time, which is a very good result considering the high number of survey locations. In the case of visual observations, the performance of one of the autumn flights was not possible due to the weather constraints. Yet, visual surveys from aboard a ship were carried out according to plan, which allowed obtaining the necessary data for the autumn season. Overall, representative information on the occurrence of porpoises and seals in different seasons of the year was obtained.

3.5 AVIFAUNA

3.5.1 Bird counts from aboard vessels (seabirds)

3.5.1.1 Non-specialist summary

3.5.1.1.1 Subject matter and objective of the project

The aim of the marine avifauna surveys was to obtain data on species composition, abundance and distribution of birds associated with marine environment in the sea area including the area intended for the Baltica-1 OWF and the reference area, which was established for the purposes of comparisons with the area intended for the investment implementation. The surveys were conducted throughout the year, which enabled tracing changes in the grouping of seabirds in subsequent phenological periods: the wintering period, the spring migration period, the summer period and the autumn migration period.

3.5.1.1.2 Survey methods

In the survey area and the reference area, birds were counted during vessel passages from aboard vessels, following the survey methodology described in the methodological manual issued by the General Directorate for Environmental Protection "*Monitoring ptaków wodno-błotnych w okresie wędrówek*" ["Monitoring of wetland birds during migrations"]. The route of the vessel passages ran along the delineated sections, the so-called transects, that have been designated in such a way that

the results obtained were representative of the conditions changing with the depth changes. All birds in flight and sitting on the water were counted, including the separate recording of birds located within a 600 m wide strip (300 m on each vessel side) and outside of it. The transect strip was divided into four zones counted from the vessel side (up to 50, 50–100, 100–200 and 200–300 m) and during the counting, it was marked in which zone an individual was located. Consequently, in the analyses, it was possible to take into account the correction for the decreasing detection of birds with the increasing distance from the vessel side. During the vessel passages, also birds in flight were recorded, with the zone of their flight altitude marked:

- A – up to 30 m (below the range of rotors of future WTGs);
- B – from 30 to 150 m (potential lower rotor range of the future turbines);
- C – from 150 to 300 m (potential upper rotor range of the future turbines);
- D – above 300 m (above the range of rotors of future WTGs).

These results only supplement the radar surveys and allowed determining the species composition of birds flying during the day in the vicinity of the planned project, the intensity of such flights in subsequent phenological periods and the most common altitudes of these passages.

Bird distribution in the surveyed sea area is presented in the form of maps, where areas characterised by similar density values are marked with the same colour. The maps were drawn using the interpolation method. This allowed the estimation of the density distribution over the entire vast sea area crossed by the transects, on the basis of the data obtained in the course of a direct bird count within the transect strip.

3.5.1.1.3 Survey results

Year-round, the long-tailed duck was the most abundant species in all the areas surveyed. Apart from the long-tailed duck, other sea ducks (the velvet scoter and the common scoter) were very scarce in the planned survey area and in the reference area. In the survey area and in the reference area, in the summer and during the autumn migration period, a very high proportion of piscivorous species (ichthyophagous birds) was recorded, namely the common guillemot and the razorbill, which together accounted for 29.5 to 53.3% of the seabird grouping in the survey area as well as 65.1% and 45.3% in the reference area, respectively. During the wintering period, the razorbill was exceptionally abundant within survey area during one of the survey campaigns, and in the spring – the black-throated diver. These results indicate the great importance of both sea areas for piscivorous birds and particularly for the common guillemot, which was observed there in large numbers in the summer, i.e. the period when adult birds leave the breeding colonies with their fledglings. The occurrence of piscivorous species is not significantly affected by the depth of the sea area, as they concentrate in areas where pelagic fish are abundant. It can, therefore, be assumed that they found an abundant food supply there. In all the areas surveyed, there was also a fairly high proportion of the European herring gull, which aggregates in greater numbers away from the coast, in fishing areas, where it accompanies fishing boats.

In the survey area and in the reference area, the average densities of the entire seabird grouping and of individual species were not very high, except for the shallowest part of the planned project area, where the average density of the long-tailed duck exceeded 100 ind.·km^{-2} during spring and autumn migration periods. The very high concentrations of the long-tailed duck were only encountered during one survey campaign. In the spring, also the black-throated diver appeared very abundantly in the

survey area, together with the long-tailed duck. Such high concentrations of long-tailed ducks and black-throated divers were not observed in the reference area. The low abundance of seabird groupings in the remaining part of the survey area and the reference area is related to the significant depths, which make it difficult for birds from the most abundant group of diving benthophages species, such as the long-tailed duck, to reach food. Such a relationship between the sea area depth and abundance was not found in the case of piscivorous birds, their distribution being dependent on the presence of food supply, which is mainly pelagic fish.

The results of the avifauna observations covering four phenological periods indicated that most of the survey area is not a place of high aggregations of seabirds. Very high concentrations of the long-tailed duck were recorded during both migration periods only in its shallowest north-western part. High concentrations of two piscivorous species, namely the common guillemot and the razorbill, were found in the survey area and in the reference area. In terms of abundance, the common guillemot was the dominant species in the survey area and in the reference area during the summer, its proportion in the grouping amounting to 53.0% and 61.0%, respectively. In the summer, common guillemots occurred there after the breeding season when adult birds stay together with the young as the latter become independent. The razorbill, on the other hand, was more abundant in the winter, when its proportion in the entire seabird grouping was 8.9% in the survey area and 6.5% in the reference area.

Without repeating the survey over one more season, it is impossible to state unambiguously whether the shallowest part of the survey area is a regularly used stopover site for the long-tailed duck and the black-throated diver during their migration towards breeding grounds, or whether their concentrations observed on one occasion were caused by weather conditions that forced the birds to temporarily stop their migration. Before formulating the environmental impact assessment, it would also be necessary to confirm whether the survey area is a permanent site of post-breeding concentrations of the common guillemot. In this species, as in other species of the auk family, juvenile birds leaving the breeding colonies are not yet prepared for independent life and require a long period under the care of adult birds. What is of key importance are sea areas with a sufficiently abundant food supply, where the young learn to feed themselves.

The conducted observations of birds flying above the studied sea area are solely of ancillary nature, and they supplement the results obtained in the surveys with the use of radars. The vast majority of bird flights recorded during the survey vessel passages were below the limit of 30 m above the surface of the water, and thus also below the assumed minimum location of operating rotors of the wind turbines. Among the species observed in great numbers, flights at collision heights (30–300 m) concerned mainly herring gulls, which often fly above the sea at a higher altitude than other species of seabirds, and the geese of the genus Anser during the migration periods. The flights of birds of terrestrial environments over the sea area surveyed were very infrequent, but it should be noted that their movements over sea areas take place mainly at night and only the results of surveys carried out with the use of radars can provide a basis for describing the flight intensity of this group of birds.

3.5.1.2 Spatial scope of the surveys

Bird observations were carried out in the survey area covering the Baltica-1 OWF construction area, which is the area of construction of WTGs, OSSs, and cable lines (area A) and the area of construction of cable lines (area B) together with a zone of no less than 4 km in width measured from the boundary of area A and in the reference area, located northwest of the Baltica-1 OWF, within the Swedish EEZ [Figure 3.89].

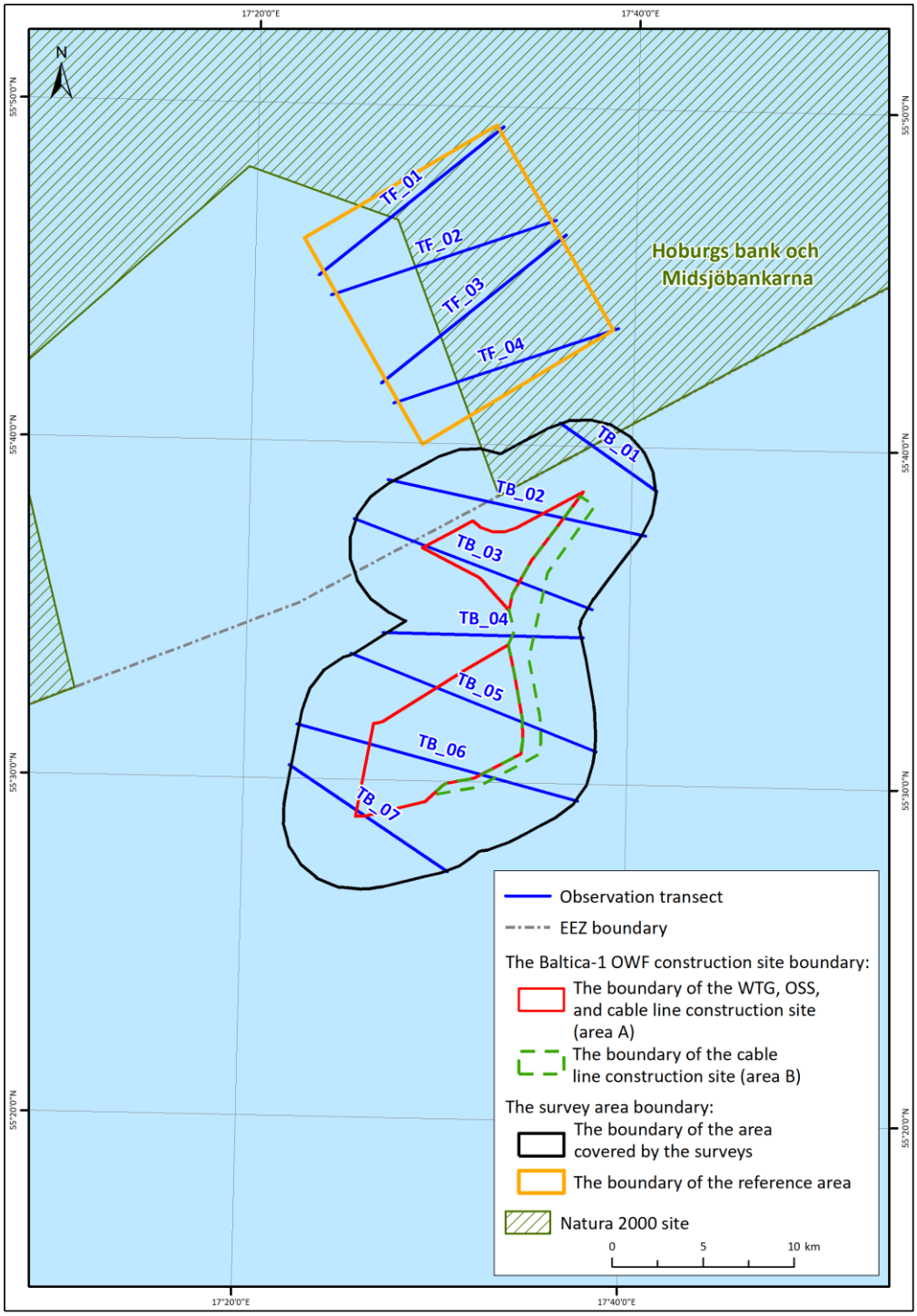


Figure 3.89. The location of observation transects along which seabird counts were conducted in the survey area and the reference area

3.5.1.3 Methodology

The results of the counts of seabirds identified during the surveys in the survey area and in the reference area, which are located in the open sea zone, are presented per three groups of species:

- seabirds which usually remain on sea waters outside their breeding period, reaching the highest abundances in the offshore zone, located over 1 km from the shore. Gulls which

accompany fishing boats to fishing grounds are an exception and their occurrence in the open sea is strongly conditioned by human activity. From among seagulls, the black-headed gull and common gull were excluded from the seabird group, as they very rarely remain in the open sea;

- the waterbirds which are related mainly to inland surface waters and appear only very close to the shores when at sea, mainly at river mouths, bays and sea lagoons;
- birds related only to land environments which only fly above the survey area and are not able to remain on water.

Observations of seabirds were carried out along the transects designated so as to make the counts cover not less than 10% of the sea area surface and to make the obtained results representative of the conditions changing as a result of depth level changes. Seven observation transects were delineated in the survey area and 4 transects in the reference area [Figure 3.89]. The length of the observation transects within the survey area and the reference area was 87 km and 52 km, respectively, while their surface area was approx. 50.9 km^2 and 29.6 km^2, respectively, accounting for 15% of the survey area and 18.6% of the reference area.

As in other pre-investment monitoring activities related to the construction of offshore wind farms (Meissner, 2014a, 2014b, 2015; Antczak and Meissner, 2018), the surveys followed a standard methodology (Komdeur et al., 1992), described in a manual published by the General Directorate for Environmental Protection (Meissner, 2011). Transects in the survey areas were designated in such a way that the results obtained were representative of the conditions changing with the depth changes. Each transect was divided into smaller sections of 500 m in length. Birds were counted separately for each section. Counting was performed simultaneously by two people standing close to each other at both vessel sides, each one counting the birds on one side of the vessel. A third member of the team monitored the position and speed of the ship using a GPS device, at the same time recording the depth of the sea area on the basis of the echosounder readings as well as the weather conditions. The position, speed and course of the vessel were continuously monitored using a GPS device. To minimise the likelihood of counting the same individuals twice, a gap of 0.6–2.6 km between adjacent transects was planned. The vessel navigated along a route delineated by the transect line. During the count, a constant speed of 8–10 knots was maintained, depending on the vessel and the weather conditions.

In the case of bird counts carried out at sea, weather conditions can be significant in determining species affiliation, abundance of birds and the distance from the vessel side at which the birds are recorded (Meissner, 2011). This is why the dates of survey vessel passages were carefully planned, accounting for weather forecasts from various sources, in order to avoid bird counts in conditions which might significantly influence the results obtained. During the counting, weather conditions were recorded at the beginning of each section forming a transect and at the end of the transect. It is recommended that bird observations at sea be carried out during low, or at most moderate, wave motion not exceeding sea state 3 according to the Douglas sea scale (Komdeur et al., 1992). At higher wave motion, and with precipitation reducing visibility, the detectability of birds at sea decreases, which leads to an underestimation of the number of birds present in a given area.

All birds in flight and sitting on the water were counted, including the separate recording of birds occurring within a 600 m wide transect strip (300 m on each vessel side) and those outside of it. The transect strip was divided into four zones counted from the vessel side (up to 50, 50–100, 100–200 and 200–300 m) and during the counting, it was marked in which zone an individual was located. This

allowed for a correction for decreasing bird detection with increasing distance from the vessel side to be taken into account when mapping bird densities, which is a standard procedure in the surveys of bird abundance and distribution at sea (Hoekman et al., 2011; Ronconi and Burger, 2009; Spurr et al., 2012), as well as in pre-investment monitoring in the Polish zone of the Baltic Sea (Meissner, 2014a, 2014b, 2015; Antczak and Meissner, 2018). The numbers of birds sitting on the water within the transect zones, after corrections for the detectability decreasing with distance from the vessel's side, were used to prepare density maps. Other analyses of species composition and changes in numbers were based on the results of counting birds sitting on the water in and outside the transect zones. During the survey vessel passages in the survey area and the reference area, also birds in flight were recorded, marking the zone of their flight altitude:

- A – up to 30 m (below the range of rotors of future WTGs);
- B – from 30 to 150 m (potential lower rotor range of the future turbines);
- C – from 150 to 300 m (potential upper rotor range of the future turbines);
- D – above 300 m (above the range of rotors of future WTGs).

Birds in flight were counted within the observer's eye reach irrespective of whether they were within the transect strip or outside of it. Counting birds in flight and breaking down their movements by altitude zones was also applied in the observations of birds flying over the reference area, although wind turbines are not to be installed there. The results concerning birds in flight over the sea area surveyed only supplement the radar surveys conducted as part of migratory bird observations and allow determining the species composition of birds flying in the vicinity of the planned project, the intensity of such flights in subsequent phenological periods and the most common altitudes of these passages.

In addition, birds in flight were counted using a "snapshot" technique (taking snapshots of the flying birds which are within the transect strip at the given moment). According to the valid methodology (Komdeur et al., 1992; Meissner, 2011), birds accompanying the vessel are not accounted for, as this would overstate their numbers by counting the same individuals multiple times. The frequency of bird counts using the "snapshot" technique depends on the speed of the vessel. It is calculated from the following formula:

$$N = \frac{0.309\mathrm{V}}{\mathrm{D}}$$

where:

N – the number of counts using the "snapshot" technique over 10 minutes;

V – vessel speed in knots;

D – the maximum distance from which birds flying in front of the vessel are identified to the level of species (expressed in km). Usually it is 0.8 km but at lower visibility this distance is reduced.

Counting with the use of the "snapshot" technique allows for the recording and inclusion in the later calculations of birds in flight, which were previously sitting on the water in the sea area surveyed. This type of sampling reduces the error of underestimating the number of birds caused by their movement (Komdeur et al., 1992). It should be noted that only a small fraction of the birds observed in flight are thus included in the computation of densities and the number of snapshots is always referred to the speed of the vessel.

The assessment of the distance from the side of the vessel was carried out according to the procedure presented by Heinemann (1981) and described in the GDEP methodological manual (Meissner, 2011), which is based on the relationship describing the distance from the horizon in relation to the height at which the observer's eye is located [Figure 3.90]. Observations were carried out from a height of approximately 2.5–5 m above the sea surface (the height of the observer's eye above the water surface). To determine the width of the transect strip, a calliper kept at a constant distance from the eye of the observer was used.

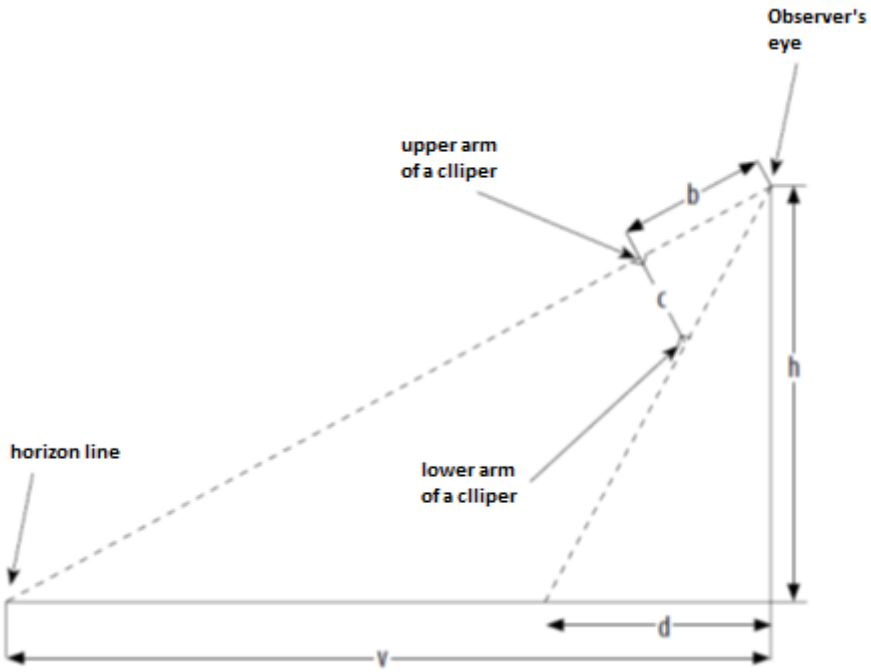


Figure 3.90. A diagram illustrating the method of determining the distance from the horizon; b – distance of the calliper from the eye of the observer (cm), c – opening of the calliper (cm), d – width of the transect on one side of the vessel (m), h – height of the observer's eye above the water surface (m), v – distance of the observer from the horizon, which is calculated using the formula: $v = 3838 (h^{0,5})$

In accordance with the methodology adopted, it was assumed that in the case of adverse weather conditions occurring for an entire month and preventing the completion of a second observation campaign (inspection), conducting only one observation campaign per month was allowed, which remains in line with the methodological manual (Meissner, 2011). However, in the event that two observation campaigns (inspections) are not carried out in a month, measures will be taken to conduct the non-performed campaign at the beginning of the following month, in addition to the two observation campaigns already scheduled in that month. To reduce the risk of such situations, the first inspections in a given month were planned, if possible, in the first favourable weather window forecast.

The results of bird counts were presented separately for the birds staying in the sea area surveyed and for the birds flying over it. The results are shown in the form of tables with abundances of all taxa found during subsequent survey campaigns.

Only specimens spotted in transect strip area and during ‘snapshot’ counting were included in calculation of bird concentration. Consequently, in the analyses, it was possible to take into account the correction for the decreasing detection of birds with the increasing distance from the vessel side.

Such a correction was carried out using the Distance 6.0 software (Thomas et al., 2010), which has recently become a standard tool in the analyses of bird distribution based on counts along transects. The most suitable model describing reduction of bird spotting rate was based on Akaike's criterion (Burnham and Anderson, 2002).

The so-called effective strip width (ESW) for a transect was calculated on the basis of the course of the function of detection decreasing with the increasing distance from the ship. It is a distance from one side of the ship, which divides a transect with a width of 300 meters into two parts in such a way that the number of birds sighted in the farther zone is equal to the number of birds unrecorded in the nearer zone (Thomas et al., 2010) [Figure 3.91].

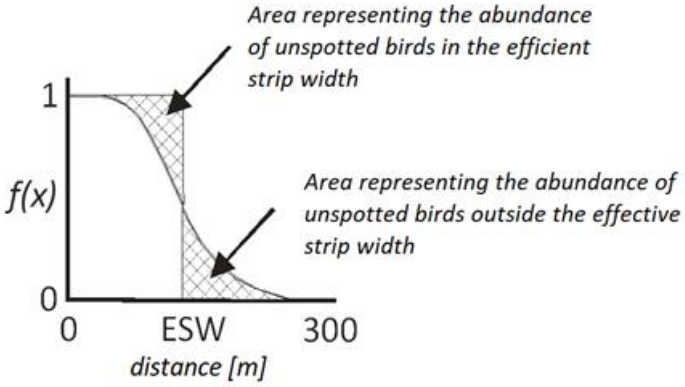


Figure 3.91. The scheme of an exemplary boundary of the transect effective strip width (ESW) in a 300-m wide strip of bird-counting

The abundances obtained during the counting along the transect strip were corrected on the basis of the ESW value. For example, when the ESW value was 250 m, and in the 300 m transect strip 200 birds were seen, the new, corrected abundance value was calculated as: 200 individuals × 300 m/250 m = 240 birds.

The functions describing the decline in bird detectability were determined for the most abundant species: the long-tailed duck, the velvet scoter, the razorbill, the common guillemot, the European herring gull and for the entire grouping of waterbirds. The ESW values calculated for various bird species and for the whole grouping fell between 159.22 and 213.15 [Table 3.45]. Low values of standard errors and coefficients of variation indicate high reliability of the estimated ESW value.

Table 3.45. The transect effective strip width (ESW) values for calculated for individual species and for the entire group of waterbirds staying in the survey area

Species or group of species	Effective strip width	Standard error	Coefficient of variation	Function parameters
Long-tailed duck *Clangula hyemalis*	204.91	6.49	< 18.14%	Half-normal distribution, cosine adjustment function
Razorbill *Alca torda*	161.26	9.15	< 10.03%	Half-normal distribution, cosine adjustment function
European herring gull *Larus argentatus*	196.66	6.27	< 10.12%	Half-normal distribution, polynomial adjustment function
All waterbirds	189.59	5.11	< 10.78%	Half-normal distribution, cosine adjustment function

Bird distribution in the surveyed sea area is presented in the form of maps, where areas characterised by similar density values are marked with the same colour. The bird densities on the maps are the result of data interpolation in the Surfer program using the co-kriging method.

For each of the phenological periods distinguished, density maps were produced for the entire grouping of birds and for the most abundant species. Each time, the spatial distribution of average densities in the survey area and in the reference area was presented on a single map, as it facilitates direct comparison of the results obtained for both sea areas. Maps covering the entire 12-month survey period were produced excluding those inspections during which a particular species was not recorded in a particular sea area, as this type of density mapping is intended to indicate locations within which birds are most likely to be found.

The analyses of species composition and changes in bird abundances were conducted separately for the survey area and the reference area based on data concerning all the birds sitting on the water within the transect strip and outside of it. To compare the number of birds in individual sea areas, the abundance index was used, which relates the number of individuals observed to the length of the transect or the shoreline length monitored (average number of birds/10 km of the transect or shoreline):

$$abundance\ index = \frac{total\ number\ of\ birds}{total\ length\ of\ the\ transects\ or\ coastline} * 10$$

Graphs of abundance changes were presented each time for the entire bird grouping as well as for the most abundant species, the average abundance of which exceeded 50 individuals observed during one survey campaign. The average number of 100 individuals per one survey campaign, or an average abundance factor of 10, was adopted as the minimum which allows considering a given species as abundant. However, the summer period, when bird abundance at sea is very low, was omitted here. As in other surveys concerning the abundance of various bird species (e.g. Tomiałojć and Stawarczyk, 2003), the above threshold was adopted arbitrarily, based on the total abundance of all the species recorded. For the survey area and the reference area, graphs of changes in abundance are presented for the same set of species, which makes it possible to compare their phenology in both these areas. However, it should be remembered that in the case of bird counts carried out from ships along transects it is impossible to count all the individuals present in the survey area, and the abundance figures obtained concern only a small fragment of a given area (Meissner, 2011).

The seabird groups were compared between the survey area and the reference area. This is because the reference area was delineated specifically to relate the results obtained to the sea area intended for the project development. It was assumed that if the difference in abundance index values for the sea areas compared exceeds 30%, the species is considered more abundant in one of them. The abundance values of low-abundance species were not compared when their abundance indices were below 1 in both areas.

For each seabird species found, the following information was provided: its conservation status in Poland [according to the Regulation of the Minister of the Environment of 16 December 2016 on the protection of animal species (Journal of Laws of 2016, item 2183)], the presence in Annex I of the EU Birds Directive (Directive 2009/147/EC of the European Parliament and of the Council of 30 November 2009 on the conservation of wild birds) and the threat category according to the International Union for Conservation of Nature and Natural Resources – IUCN (IUCN *Red List of Threatened Species*, Version 2021). Additionally, the SPEC (*Species of European Conservation Concern*) status assigned to a given

species by BirdLife International, which takes into account the threat category and the nature of the species occurrence in Europe and in the world was provided (BirdLife International, 2017). The threat categories developed by HELCOM for the Baltic Sea were also presented (HELCOM *Red List of Baltic Sea species in danger of becoming extinct*, 2013). Species that were found extremely sparse in a given phenological period, when their abundance index did not exceed 0.1 ind. in any of the sea areas inspected, were omitted from this compilation.

During the observations, the presence of other vessels in the transect zone, within a given section, was monitored and their impact on the behaviour of the birds was recorded (scaring them away, when a moving vessel startled birds sitting on the water, or attracting, when birds gather in close proximity to a vessel – this concerns primarily fishing vessels).

3.5.1.4 Activities performed

The surveys within the survey area and the reference area were conducted in accordance with the methodology adopted, providing sufficient data to characterise the grouping of seabirds using these areas.

3.5.1.4.1 Survey area

24 survey campaigns consisting of one vessel passage, or two vessel passages on one occasion, were carried out in the survey area, each time covering all six transects [Table 3.46]. One bird count lasted from 5 hours 36 minutes to 7 hours 39 minutes [Table 3.46]. During the 12-month survey period, the total time devoted to bird counting in the survey area was 166 hours and 51 minutes. Due to prolonged adverse weather conditions, it was impossible to carry out two survey campaigns planned for October 2023. In such a situation, the methodology of bird observation at sea (Meissner, 2011) as well as the methodology adopted in the surveys discussed herein allows for adopting the results of one vessel passage as representative for a given month. However, it was decided to conduct the missing vessel passage at a later date, on 30 November 2023 (Table 3.46: survey campaign 24), one day after the last survey campaign scheduled for the autumn migration period. Performing bird counts on two consecutive days and including them in the characterisation of the avifauna in a given period is not recommended because there is an extremely high chance of counting the same grouping of birds twice, so data from one part of the month are over-represented in the sample analysed. This phenomenon is particularly significant when there are few days of observation. This is the reason why it was assumed in the survey methodology adopted for the survey area that the minimum interval between consecutive survey vessel passages must be at least 7 days. Therefore, the results from the two survey vessel passages carried out on 29 and 30 November 2023 were not included in the report, whereas the average bird abundance from these two survey campaigns was taken into account. Three survey campaigns were carried out in February, including one in place of a survey vessel passage that was not undertaken in January due to adverse weather conditions. However, in that month, the interval between survey campaigns was at least 7 days, which is in line with the methodology adopted and the results from the three vessel passages conducted in February were included in the subsequent analysis.

Table 3.46. A list of dates of seabird observations in the survey area, including the names of people conducting the observations and the vessel used

Campaign no.	Vessel passage date	Vessel	Observers	Vessel passage beginning	Vessel passage end	Vessel passage duration
1	06.12.2022	Admirał II	Andrzej Kośmicki, Helena Trzeciak, Michał Barcz	07:06	14:11	07:05
2	16.12.2022	Admirał II	Krzysztof Stępniewski, Dominik Marchowski, Łukasz Wardecki	07:10	14:27	07:17
3	19.01.2023	Admirał II	Adam Janczyszyn, Samuel Sosnowski, Jan Rapczyński	06:51	14:21	07:30
4	06–07.02.2023	Admirał II	Krzysztof Stępniewski, Justyna Ciemińska, Michał Jasiński	12:54 06:26	13:19 12:51	0:25 06:25 06:50
5	15.02.2023	Admirał II	Krzysztof Stępniewski, Małgorzata Knitter, Maciej Przybysz	10:13	15:49	05:36
6	22.02.2023	Admirał II	Samuel Sosnowski, Justyna Ciemińska, Jakub Typiak	08:19	15:07	06:48
7	01.03.2023	Admirał III	Jakub Typiak, Krzysztof Stępniewski, Szymon Bzoma	06:03	13:21	07:18
8	21.03.2023	Admirał III	Grzegorz Zaniewicz, Łukasz Janocha, Samuel Sosnowski	09:30	15:42	06:12
9	06.04.2023	Admirał III	Adam Janczyszyn, Sabina Buczyńska, Andrzej Kośmicki	09:46	16:52	07:06
10	22.04.2023	Admirał III	Jakub Typiak, Katarzyna Stępniewska, Samuel Sosnowski	04:02	11:41	07:39
11	12.05.2023	Admirał III	Jakub Typiak, Adam Janczyszyn, Piotr Zientek	02:47	10:01	07:14
12	20.05.2023	Admirał III	Jakub Typiak, Cezary Wójcik, Samuel Sosnowski	02:26	09:59	07:33
13	08.06.2023	Admirał II	Adam Janczyszyn, Katarzyna Stępniewska, Szymon Bzoma	06:55	13:55	07:00
14	16.06.2023	Admirał II	Adam Janczyszyn, Grzegorz Zaniewicz, Marcin Sowa	07:24	14:20	06:56
15	10.07.2023	Admirał II	Adam Janczyszyn, Małgorzata Knitter, Piotr Zientek	07:28	14:47	07:19
16	28.07.2023	Admirał II	Krzysztof Stępniewski, Katarzyna Stępniewska, Jan Rapczyński	07:07	14:13	07:06
17	05.08.2023	Admirał II	Jakub Typiak, Cezary Wójcik, Maciej Kozakiewicz	10:54	18:00	07:06

Campaign no.	Vessel passage date	Vessel	Observers	Vessel passage beginning	Vessel passage end	Vessel passage duration
18	14.08.2023	Admirał III	Katarzyna Stępniewska, Justyna Ciemińska, Samuel Sosnowski	09:39	17:06	07:27
19	08.09.2023	Admirał II	Katarzyna Stępniewska, Marcin Dyduch, Marcin Sowa	08:30	15:24	06:54
20	26.09.2023	Admirał III	Jakub Typiak, Andrzej Kośmicki, Piotr Zientek	10:06	16:23	06:17
21	22.10.2023	Admirał II	Justyna Ciemińska, Mateusz Ściborski, Szymon Bzoma	09:23	15:32	06:09
22	11.11.2023	Admirał III	Grzegorz Zaniewicz, Katarzyna Stępniewska, Łukasz Janocha	05:56	13:20	07:24
23	29.11.2023	Admirał III	Katarzyna Stępniewska, Paweł Stańczak, Jan Rapczyński	07:23	14:00	06:37
24	30.11.2023	Admirał III	Maciej Kozakiewicz, Piotr Zientek, Jan Rapczyński	07:30	13:58	06:28

3.5.1.4.1.1 Weather conditions

Most counts in the survey area was carried out at sea states 0 and 1 (according to the Douglas sea scale), which occurred on 63.0% of sections in total [Figure 3.92]. Sea state 2 was recorded at 26.0% of the sections surveyed, while wave motion reaching 3 degrees on the Douglas sea state scale, which can slightly hinder bird counts at sea, was recorded at 11.0% of the sections. That increased wave motion occurred during the summer (6 sea states recorded) and during the autumn migration period (112 sea states recorded on 29 November 2023). During summer, bird abundances in sea areas are very low and increased wave motion during that period did not affect the quality of the data obtained. In autumn, bird abundance increases, and larger waves make it more difficult to spot all individuals, especially those belonging to species with cryptic colouration (razorbills, guillemots, grebes, divers). It should, therefore, be concluded that the results obtained for the autumn period for these species may be slightly underestimated. However, this effect was reduced by averaging the results from the vessel passage performed on 29 November 2023, when the wave motion was slightly higher, with the results from the following day, when a survey campaign was conducted to compensate for the earlier lacking vessel passage in October. The vessel passage on the following day (30 November 2023) was carried out at sea state of 1–2, and only 7 razorbills, 3 guillemots and 1 black-throated diver were recorded within the area surveyed. This indicates that the abundance of species that were difficult to spot at sea during the increased wave motion on the previous day was low. Therefore, it can be assumed that the results obtained for the survey area are also representative for the autumn migration period, as the possible error related to increased wave motion could not be significant.

During the vessel passages, precipitation in the form of drizzle was recorded only in the case of 0.3% of all the weather conditions registered [Figure 3.93]. Hence, precipitation did not have any influence on quality of obtained results.

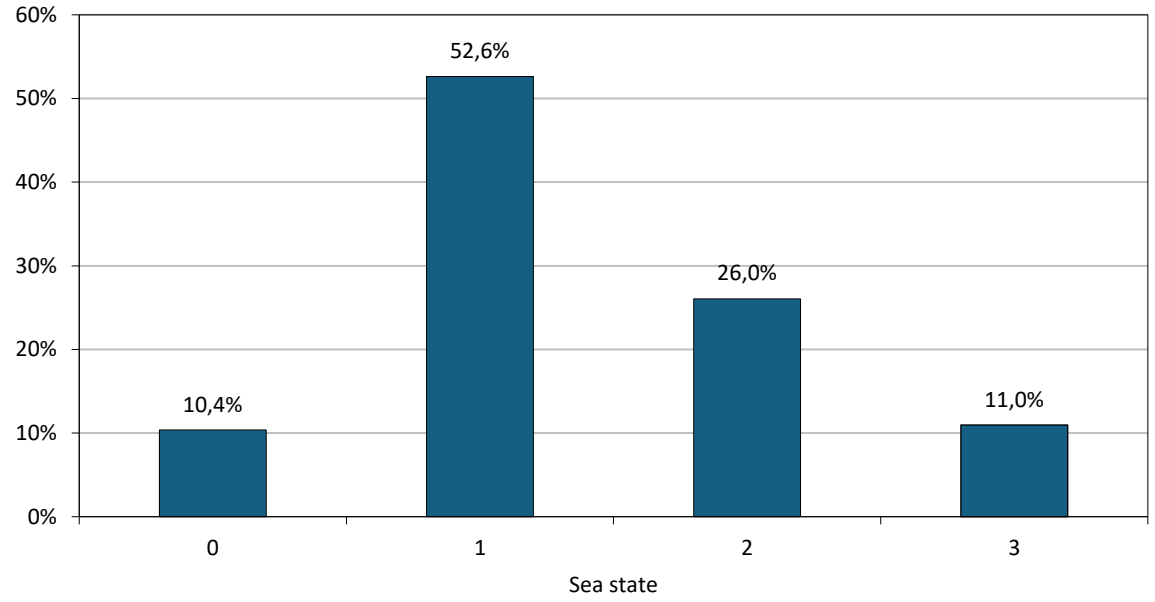


Figure 3.92. The proportion of the sea state categories recorded during all the campaigns in the survey area

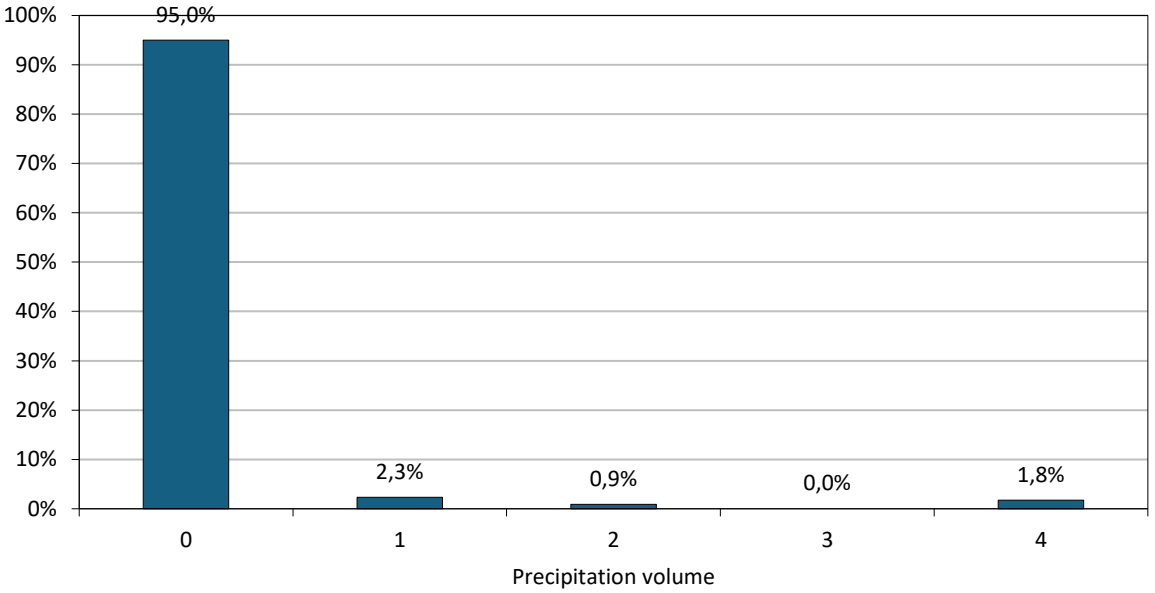


Figure 3.93. The proportion of the specific precipitation intensity categories recorded during all the campaigns in the survey area

0 – lack of precipitation, 1 – drizzle, 2 – precipitation not hindering the bird count, 3 – precipitation slightly hindering the bird count, 4 – precipitation hindering the bird count

3.5.1.4.1.2 The presence of other vessels within the transect strip

During the wintering period, 11 instances of other vessels passing through the transect strip in the survey area were recorded during observations lasting 41 hours and 6 minutes. One vessel was recorded during the survey campaign on 16 December 2022, the presence of which caused 40 herring gulls to aggregate in its vicinity. On 15 February 2023, a presence of a vessel within the transect strip

was recorded 10 times and in 8 cases the vessels were accompanied by flying European herring gulls ranging from 1 to 40 individuals and once by a great black-backed gull (1 individual).

In the spring migration period, during the observations lasting 43 hours and 2 minutes, only one fishing vessel was spotted within the transect strip – on 1 March 2023. Its presence attracted 26 European herring gulls.

During the observations lasting 42 hours and 54 minutes, carried out in summer, a fishing boat was spotted twice within the transect strip in the survey area. On 28 July 2023, its presence attracted 31 European herring gulls, and on 14 August 2023, 3 individuals of this species flew around the cutter.

In the autumn migration period, during the observations lasting 39 hours and 49 minutes, no other vessels were spotted within the transect strip.

During the wintering period, the spring migration and in the summer, the presence of other vessels within the transect strip in the survey area had a small influence on the increase in the number of European herring gulls recorded during five survey campaigns. Similarly to other gulls, the European herring gull accompanies fishing boats on fishing grounds, so aggregations of gulls accompanying fishing activities are typical of sea areas.

3.5.1.4.2 Reference area

A total of 23 survey campaigns consisting of one vessel passage and one campaign involving two vessel passage days were carried out in the reference area. In each case, birds were counted along all four transects [Table 3.47]. One bird count lasted from 3 hours 1 minute to 4 hours 44 minutes [Table 3.47]. During the 12-month survey period, the total time devoted to bird counting in the reference area was 94 hours and 43 minutes. Due to prolonged adverse weather conditions, it was impossible to carry out two survey campaigns planned for October 2023. In such a situation, the methodology of bird observation at sea (Meissner, 2011) as well as the methodology adopted in the surveys discussed herein both allow adopting the results of one vessel passage as representative for a given month. However, it was decided to conduct the missing vessel passage at a later date, on 30 November 2023 (Table 3.47: survey campaign 24), one day after the last survey campaign scheduled for the autumn migration period. Performing bird counts on two consecutive days and including them in the characterisation of the avifauna in a given period is not recommended because there is an extremely high chance of counting the same grouping of birds twice, so the data from one part of the month are over-represented in the sample analysed. This phenomenon is particularly significant when there are few days of observation. This is the reason why it was assumed in the survey methodology adopted that the minimum interval between consecutive survey vessel passages must be at least 7 days. Therefore, the results from the two survey vessel passages carried out on 29 and 30 November 2023 were not included in the report, whereas the average bird abundance from these two survey campaigns was taken into account. Similarly to the survey area, three survey campaigns were carried out in February, including one in lieu of a survey vessel passage that was not undertaken in January due to adverse weather conditions. However, in that month, the interval between survey campaigns was at least 7 days, which is in line with the methodology adopted.

Table 3.47. A list of dates of seabird observations in the reference area, including the names of people conducting the observations and the vessel used

Campaign no.	Vessel passage date	Vessel	Observers	Vessel passage beginning	Vessel passage end	Vessel passage duration
1	06.12.2022	Admirał II	Katarzyna Stępniewska, Dominik Marchowski, Zbigniew Kajzer	07:08	11:06	03:58
2	16.12.2022	Admirał II	Maciej Kozakiewicz, Adam Janczyszyn, Maciej Przybysz	08:07	12:02	03:55
3	19.01.2023	Admirał II	Mateusz Ściborski, Maciej Przybysz, Paweł Stańczak	07:47	11:34	03:47
4	06.02.2023	Admirał II	Krzysztof Stępniewski, Justyna Ciemińska, Michał Jasiński	08:26	12:21	03:55
5	15.02.2023	Admirał II	Krzysztof Stępniewski, Małgorzata Knitter, Maciej Przybysz	06:46	09:47	03:01
6	22.02.2023	Admirał II	Grzegorz Zaniewicz, Damiana Boroń, Piotr Zientek	09:47	13:43	03:56
7	01.02.2023 02.03.2023	Admirał III	Jakub Typiak, Krzysztof Stępniewski, Szymon Bzoma	14:08 05:02	14:59 08:43	00:51 03:01 03:52
8	21.03.2023	Admirał III	Grzegorz Zaniewicz, Łukasz Janocha, Samuel Sosnowski	05:44	09:07	03:23
9	06.04.2023	Admirał III	Adam Janczyszyn, Sabina Buczyńska, Andrzej Kośmicki	05:20	09:19	03:59
10	22.04.2023	Admirał III	Jakub Typiak, Katarzyna Stępniewska, Samuel Sosnowski	12:17	16:12	03:55
11	12.05.2023	Admirał III	Jakub Typiak, Adam Janczyszyn, Piotr Zientek	11:05	14:15	03:10
12	20.05.2023	Admirał III	Jakub Typiak, Cezary Wójcik, Samuel Sosnowski	10:36	14:36	04:00
13	08.06.2023	Admirał II	Adam Janczyszyn, Katarzyna Stępniewska, Szymon Bzoma	02:34	06:31	03:57
14	16.06.2023	Admirał II	Adam Janczyszyn, Grzegorz Zaniewicz, Marcin Sowa	02:53	07:01	04:08
15	10.07.2023	Admirał II	Adam Janczyszyn, Małgorzata Knitter, Piotr Zientek	02:52	07:01	04:09
16	28.07.2023	Admirał II	Krzysztof Stępniewski, Katarzyna Stępniewska, Jan Rapczyński	02:45	06:35	03:50

Campaign no.	Vessel passage date	Vessel	Observers	Vessel passage beginning	Vessel passage end	Vessel passage duration
17	05.08.2023	Admirał II	Jakub Typiak, Cezary Wójcik, Maciej Kozakiewicz	06:47	10:25	03:38
18	14.08.2023	Admirał III	Katarzyna Stępniewska, Justyna Ciemińska, Samuel Sosnowski	04:54	09:10	04:16
19	08.09.2023	Admirał II	Katarzyna Stępniewska, Marcin Dyduch, Marcin Sowa	04:02	08:07	04:05
20	26.09.2023	Admirał III	Jakub Typiak, Andrzej Kośmicki, Piotr Zientek	05:03	09:37	04:34
21	22.10.2023	Admirał II	Justyna Ciemińska, Mateusz Ściborski, Szymon Bzoma	05:42	08:58	03:16
22	11.11.2023	Admirał II	Cezary Wójcik, Samuel Sosnowski, Mateusz Ściborski	06:15	10:16	04:01
23	29.11.2023	Admirał II	Katarzyna Stępniewska, Samuel Sosnowski, Łukasz Janocha	07:45	12:29	04:44
24	30.11.2023	Admirał II	Katarzyna Stępniewska, Samuel Sosnowski, Łukasz Janocha	07:30	11:44	04:14

3.5.1.4.2.1 Weather conditions

All survey campaigns within the reference area were conducted at a sea state of 0–2 degrees according to the Douglas scale [

Figure 3.94]. Therefore, wave motion did not affect the quality of the data obtained.

No precipitation was observed during 95.9% of all weather conditions recorded. Drizzle and precipitation not hindering bird counts occurred in 1.1% and 1.4% of the cases, respectively. However, along 49 sections, which represent 34.3% of all the sections comprising transects in the reference area, precipitation which could hinder bird spotting at sea (precipitation intensity 4) was recorded [Figure 3.95]. This took place on 30 November 2023, when an additional vessel passage was performed instead of a survey campaign that had not been performed in October. The results of the vessel passage were averaged with those obtained on the previous day, hence the impact of the more intense precipitation recorded along 34.3% of the sections on 30 November 2023 could not have been substantial and it did not significantly affect the quality of the data obtained.

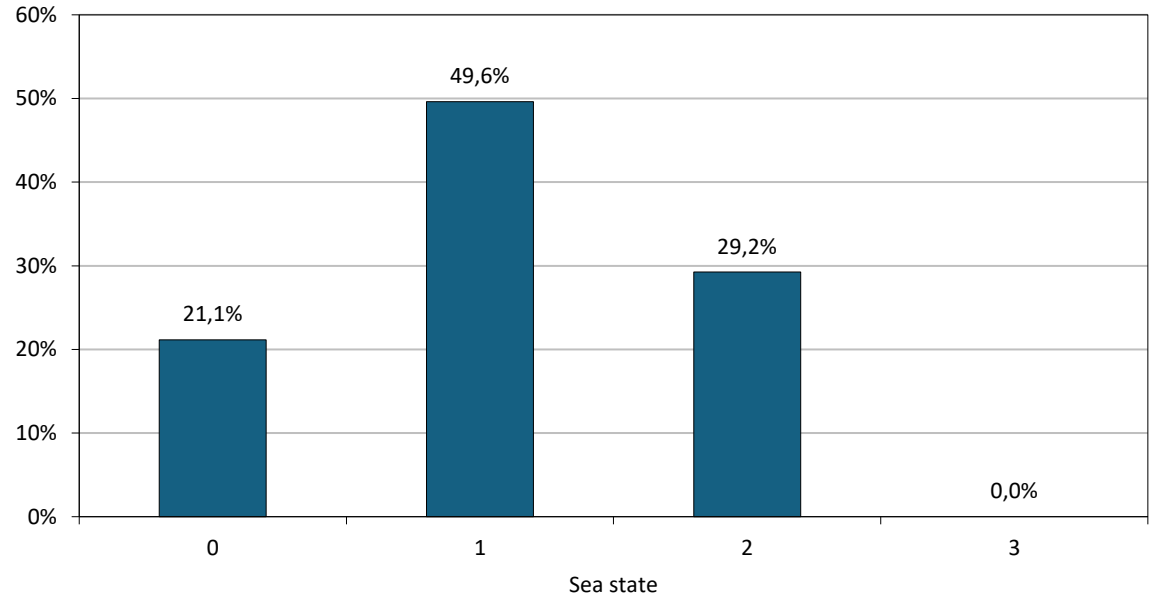


Figure 3.94. The proportion of the sea state categories recorded during all the campaigns in the reference area

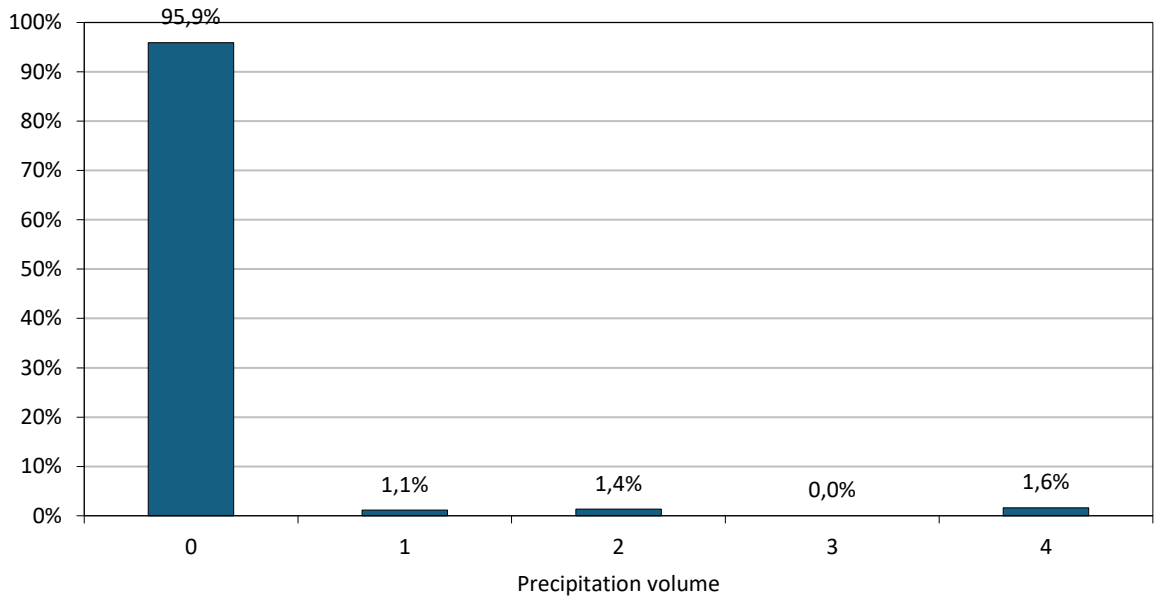


Figure 3.95. The proportion of the specific precipitation intensity categories recorded during all the campaigns in the reference area

0 – lack of precipitation, 1 – drizzle, 2 – precipitation not hindering the bird count, 3 – precipitation slightly hindering the bird count, 4 – precipitation hindering the bird count

3.5.1.4.2.2 The presence of other vessels within the transect strip

In the reference area, during the observations lasting 22 hours and 32 minutes, carried out during the wintering period, vessels navigating across the transect strip were recorded on two occasions. This took place on 15.02.2023 and resulted in two long-tailed ducks being scared off the transect strip the first

time, and a single long-tailed duck – the second time. Those birds were included in the database as individuals sitting on the water within the transect strip. Thus, that situation had no impact on the data obtained during the wintering period. In the periods of the spring migration, autumn migration, and summer, during observations lasting 82 hours and 3 minutes in total, no other vessels were recorded within the transect strip in the reference area.

3.5.1.5 Results

3.5.1.5.1 Avifauna species composition

Due to the significant differences in the abundance and grouping structure of waterbirds in the successive phenological periods and across the survey areas, this report presents the results for each phenological period separately, with a subsequent summary.

3.5.1.5.1.1 Survey area

3.5.1.5.1.1.1 Wintering period

In the wintering period, the average abundance index was 75.6 individuals per 10 km of the transect. The most abundant species found within the survey area were the long-tailed duck and the European herring gull, which together accounted for 82.8% of all the birds observed. The little gull and the razorbill exceeded the abundance of 100 individuals recorded during 6 survey campaigns. Other species were observed in small numbers within the sea area in question [Table 3.48]. The very abundant occurrence of the European herring gull during the survey campaign, on 6–7 February 2023, probably resulted from fishing boat operations in the area. The abundant presence of the European herring gull in offshore areas away from the coast is typical, as these birds accompany fishing vessels, aggregating in areas of fishing activity (Garthe et al., 2003). A detailed list of bird abundances for individual species recorded during 6 survey campaigns, broken down by the method of their recording, is included in Table 3.49.

Table 3.48. The abundance and proportion in the grouping of individual taxa of birds observed sitting on the water during successive survey campaigns within the survey area in the wintering period

Taxon	06.12.2022	16.12.2022	19.01.2023	06–07.02.2023	15.02.2023	22.02.2023	Total	Proportion [%]
Seabirds								
Long-tailed duck *Clangula hyemalis*	1227	103	181	125	40	53	1729	43.8
European herring gull *Larus argentatus*	39	68	15	1388	3	24	1537	39.0
Razorbill *Alca torda*	149	7	21	127	13	34	351	8.9
Little gull *Hydrocoloeus minutus*	3	5		100			108	2.7
Common guillemot *Uria aalge*	33	3	27	2	4	3	72	1.8
Black guillemot *Cepphus grylle*	4	4	5	3		2	18	0.5
Great black-backed gull *Larus marinus*	2				1	3	6	0.2
Velvet scoter *Melanitta fusca*	4						4	0.1
Red-throated diver *Gavia stellata*	3						3	0.1
Black-throated diver *Gavia arctica*	1						1	+
Yellow-billed diver *Gavia adamsii*						1	1	+

Taxon	06.12.2022	16.12.2022	19.01.2023	06–07.02.2023	15.02.2023	22.02.2023	Total	Proportion [%]
Waterbirds rarely encountered at sea far from the coast								
Common gull *Larus canus*	14	39		11	1	39	104	2.6
Red-breasted merganser *Mergus serrator*	2				5		7	0.2
Mallard *Anas platyrhynchos*	2						2	0.1
Black-headed gull *Chroicocephalus ridibundus*		1					1	+
Birds unidentified to species								
Unidentified diver *Gavia sp.*				1			1	+
Total	**1444**	**162**	**234**	**369**	**64**	**135**	**3945**	**100**

+ - percentage smaller than 0.1%

Table 3.49. The abundance of seabirds found within the survey area during the wintering period, broken down by the method of their recording

Taxon	Birds sitting on the water		Birds in flight		Total
	Within the transect strip	Outside the transect strip	Snap-shot technique	Besides the snap-shot technique	
European herring gull *Larus argentatus*	163	1374	153	2104	3794
Long-tailed duck *Clangula hyemalis*	1462	267	85	519	2333
Razorbill *Alca torda*	303	48	108	1509	1968
Common guillemot *Uria aalge*	50	22	8	130	210
Little gull *Hydrocoloeus minutus*	107	1	9	21	138
Black guillemot *Cepphus grylle*	17	1	2	21	41
Great black-backed gull *Larus marinus*	4	2	1	12	19
Common scoter *Melanitta nigra*				5	5
Velvet scoter *Melanitta fusca*	4		8	6	18
Red-throated diver *Gavia stellata*	3			3	6
Black-throated diver *Gavia arctica*		1		2	3
Yellow-billed diver *Gavia adamsii*	1				1
Birds unidentified to species					
Unidentified diver *Gavia sp.*	1		1	1	3
Total	**2115**	**1716**	**375**	**4333**	**8539**

The European herring gull and the razorbill were the most abundant species observed in flight over the reference area. Together they accounted for 75.3% of all the flying birds observed. The 10% proportion in the grouping was also exceeded by the long-tailed duck (11.7%). The other species were significantly less abundant and only in the case of the common gull and the common guillemot, over 100 individuals were observed in flight during all 6 survey campaigns [Table 3.50].

Table 3.50. The abundance and proportion in the grouping of individual taxa of birds observed in flight during successive survey campaigns within the survey area in the wintering period

Taxon	06.12.2022	16.12.2022	19.01.2023	06–07.02.2023	15.02.2023	22.02.2023	Total	Proportion [%]
Seabirds								
European herring gull *Larus argentatus*	50	90	40	1882	107	87	2256	43.8
Razorbill *Alca torda*	15	5	35	1464	44	54	1617	31.4
Long-tailed duck *Clangula hyemalis*	198	24	147	160	7	68	604	11.7
Common guillemot *Uria aalge*	40	13	37	7	35	6	138	2.7
Little gull *Hydrocoloeus minutus*	3	1	1		6	19	30	0.6
Black guillemot *Cepphus grylle*	1	5	6	5	3	3	23	0.4
Velvet scoter *Melanitta fusca*	13	1					14	0.3
Great black-backed gull *Larus marinus*	4	2	1	1	1	4	13	0.3
Common scoter *Melanitta nigra*					5		5	0.1
Red-throated diver *Gavia stellata*	1	2					3	0.1
Black-throated diver *Gavia arctica*				2			2	+
Waterbirds rarely encountered at sea far from the coast								
Common gull *Larus canus*	15	22	16	280	10	16	359	7.0
Mute swan *Cygnus olor*		9				12	21	0.4
Mallard *Anas platyrhynchos*	16						16	0.3
Goosander *Mergus merganser*	10				2		12	0.2
Whooper swan *Cygnus cygnus*		6					6	0.1
Red-breasted merganser *Mergus serrator*						5	5	0.1
Common goldeneye *Bucephala clangula*	1						1	+
Great crested grebe *Podiceps cristatus*	1						1	+
Birds of terrestrial environments								
Snow bunting *Plectrophenax nivalis*	1						1	+
Song thrush *Turdus philomelos*	1						1	+
Birds unidentified to species								
Unidentified swan *Cygnus* sp.		9			5		14	0.3
Unidentified ducks *Anatidae*					2		2	+
Unidentified diver *Gavia sp.*				1	1		2	+
Total	**370**	**189**	**283**	**3802**	**228**	**274**	**5146**	**100**

+ - percentage smaller than 0.1%

Individuals unidentified to species accounted for less than 0.1% of the birds observed on the water and 0.4% of the birds recorded in flight. Thus, their presence did not have an impact on the interpretation of the results obtained.

3.5.1.5.1.1.2 Spring migration period

During the spring migration period, 11 species of waterbirds closely associated with the marine environment were recorded in the survey area. The most numerous of the species was the long-tailed

duck constituting 96.3% of all the birds found. This result was most strongly influenced by the observation of 22 April 2023, when over 11 thousand individuals of this species were recorded along the vessel passage route. This very numerous appearance of long-tailed ducks meant that none of the other species exceeded 1% in the grouping. Relatively abundant (over 100 individuals) were the black-throated diver and the European herring gull, each species constituting 16.8% of the entire grouping. However, apart from the observation of 22 April 2023, the abundance of the entire group of birds staying in the survey area in spring was small and during the remaining 5 survey campaigns, from 25 to 440 individuals were found sitting on the water [Table 3.51]. During one survey campaign, the average number of birds sitting along the vessel passage route was high and amounted to 239.8 individuals detected per 10 km of the transect length. After excluding the results from two survey campaigns conducted in May, when the number of seabirds in the Polish zone of the Baltic Sea was already very low, its value was 355.8. This high value is due to the exceptionally numerous appearances of long-tailed ducks recorded during the second survey campaign in April. A detailed list of bird abundances for individual species recorded during 6 survey campaigns, broken down by the method of their recording, is included in Table 3.52.

Table 3.51. The abundance and proportion in the grouping of individual bird taxa sitting on water observed during subsequent campaigns in the survey area during the spring migration period

Taxon	**01.03.2023**	**21.03.2023**	**06.04.2023**	**22.04.2023**	**12.05.2023**	**20.05.2023**	**Total**	**Proportion [%]**
Seabirds								
Long-tailed duck *Clangula hyemalis*	315	372	145	11152	61	5	12050	96.3
European herring gull *Larus argentatus*	36	6	39	9		11	101	0.8
Black-throated diver *Gavia arctica*				66	29	6	101	0.8
Razorbill *Alca torda*	16	25	25	16	1	1	84	0.7
Common guillemot *Uria aalge*	4	4	3	21	11		43	0.3
Common scoter *Melanitta nigra*				28	2		30	0.2
Black guillemot *Cepphus grylle*	19	5	2	2			28	0.2
Little gull *Hydrocoloeus minutus*		4	2		4		10	0.1
Lesser black-backed gull *Larus fuscus*				4	2	1	7	0.1
Velvet scoter *Melanitta fusca*				6			6	+
Great black-backed gull *Larus marinus*	1						1	+
Waterbirds rarely encountered at sea far from the coast								
Common gull *Larus canus*	15	24		2			41	0.3
Red-breasted merganser *Mergus serrator*	2		4				6	0.0
Black-headed gull *Chroicocephalus ridibundus*				1			1	0.0
Birds unidentified to species								
Velvet scoter or common scoter *Melanitta* sp.				6			6	0.0
Unidentified diver *Gavia sp.*						1	1	0.0
Total	**408**	**440**	**220**	**11313**	**110**	**25**	**12516**	**100**

+ - proportion below 0.1%

Table 3.52. The abundance of seabirds found within the survey area during the spring migration period broken down by the method of their recording

Taxon	Birds sitting on the water		Birds in flight		Total
	Within the transect strip	Outside the transect strip	Snap-shot technique	Besides the snap-shot technique	
Long-tailed duck *Clangula hyemalis*	3477	8573	205	1373	13628
Common scoter *Melanitta nigra*	2	28	34	1358	1422
European herring gull *Larus argentatus*	66	35	36	179	316
Razorbill *Alca torda*	72	12	1	125	210
Black-throated diver *Gavia arctica*	100	1	2	34	137
Common guillemot *Uria aalge*	32	11	3	41	87
Velvet scoter *Melanitta fusca*	5	1	7	62	75
Black guillemot *Cepphus grylle*	27	1	1	28	57
Lesser black-backed gull *Larus fuscus*	6	1	6	20	33
Little gull *Hydrocoloeus minutus*	10			11	21
Red-throated diver *Gavia stellata*				13	13
Great black-backed gull *Larus marinus*	1			2	3
Common eider *Somateria mollissima*				1	1
Arctic skua *Stercorarius parasiticus*			1		1
Birds unidentified to species					
Unidentified diver *Gavia sp.*	1			9	10
Unidentified skua *Stercorarius* sp.				1	1
Total	**3799**	**8663**	**296**	**3257**	**16015**

During 6 survey campaigns conducted in spring, a total of 4 210 birds were recorded in flight over the survey area as the seabird counts were conducted. The two most abundant species of sea ducks were observed: the long-tailed duck and the common scoter, which together accounted for 70.5% of all the individuals spotted in flight. The great scaup and the common gull were also quite frequent (6.1% and 5.1% of the entire grouping, respectively). Other species were less common and, in total, birds typically found in terrestrial environments constituted only to 1.8% of all the individuals recorded in flight [Table 3.53].

Table 3.53. The abundance and proportion in the grouping of individual taxa of birds observed in flight during successive survey campaigns within the survey area in the spring migration period

Taxon	01.03.2023	21.03.2023	06.04.2023	22.04.2023	12.05.2023	20.05.2023	Total	Proportion [%]
Seabirds								
Long-tailed duck *Clangula hyemalis*	163	156	54	1175	26	4	1578	37.5
Common scoter *Melanitta nigra*		2	6	1361	21	2	1392	33.1
European herring gull *Larus argentatus*	53	44	50	24	30	14	215	5.1
Razorbill *Alca torda*	43	47	9	22	5		126	3.0

Taxon	01.03.2023	21.03.2023	06.04.2023	22.04.2023	12.05.2023	20.05.2023	Total	Proportion [%]
Velvet scoter *Melanitta fusca*			5	64			69	1.6
Common guillemot *Uria aalge*	11	9	7	7	10		44	1.0
Black-throated diver *Gavia arctica*		1		8	19	8	36	0.9
Black guillemot *Cepphus grylle*	11	2	8	7	1		29	0.7
Lesser black-backed gull *Larus fuscus*			2	17	3	4	26	0.6
Red-throated diver *Gavia stellata*		2		10	1		13	0.3
Little gull *Hydrocoloeus minutus*		4	7				11	0.3
Great black-backed gull *Larus marinus*				2			2	+
Arctic skua *Stercorarius parasiticus*					1		1	+
Common eider *Somateria mollissima*				1			1	+
Waterbirds rarely encountered at sea far from the coast								
Greater scaup *Aythya marila*				258			258	6.1
Greater white-fronted goose *Anser albifrons*		90	8				98	2.3
Common gull *Larus canus*	14	22	13	7	1	1	58	1.4
Great black cormorant *Phalacrocorax carbo*			1	15			16	0.4
Common teal *Anas crecca*			14				14	0.3
Greylag goose *Anser anser*					2	5	7	0.2
Whooper swan *Cygnus cygnus*	5	1					6	0.1
Tufted duck *Aythya fuligula*				6			6	0.1
Mallard *Anas platyrhynchos*					4		4	0.1
Birds of terrestrial environments								
Meadow pipit *Anthus pratensis*				17			17	0.4
Common chaffinch *Fringilla coelebs*			14				14	0.3
Eurasian skylark *Alauda arvensis*	1			10			11	0.3
Great tit *Parus major*		6					6	0.1
Common starling *Sturnus vulgaris*		2	1	1			4	0.1
White wagtail *Motacilla alba*				4			4	0.1
European robin *Erithacus rubecula*				3			3	0.1
Eurasian wren *Troglodytes troglodytes*				3			3	0.1
Goldcrest *Regulus regulus*				2			2	+
White wagtail *Motacilla flava*						2	2	+
Whimbrel *Numenius phaeopus*				2			2	+
Long-eared owl *Asio otus*			1				1	+
Northern goshawk *Accipiter gentilis*			1				1	+
Grey heron *Ardea cinerea*					1		1	+
Common chiffchaff *Phylloscopus collybita*				1			1	+
Eurasian siskin *Carduelis spinus*				1			1	+
Brambling *Fringilla montifringilla*				1			1	+
Hooded crow *Corvus corone*				1			1	+

Taxon	01.03.2023	21.03.2023	06.04.2023	22.04.2023	12.05.2023	20.05.2023	Total	Proportion [%]
White-tailed eagle *Haliaeetus albicilla*			1				1	+
Birds unidentified to species								
Unidentified passerines *Passeriformes*				61	2		63	1.5
Unidentified ducks *Anatidae*			5	32	3		40	1.0
Unidentified diver *Gavia sp.*					7	2	9	0.2
Unidentified seagulls *Laridae*		8		1			9	0.2
Unidentified tern *Sterna sp.*						2	2	+
Unidentified skua *Stercorarius* sp.						1	1	+
Total	**301**	**396**	**207**	**3124**	**137**	**45**	**4210**	**100**

+ - proportion below 0.1%

Individuals unidentified to species accounted for 0.1% of the birds observed on the water and 2.9% of the birds recorded in flight. Their presence did not have a significant impact on the interpretation of the results obtained.

3.5.1.5.1.1.3 Summer period

During the summer migration period, 6 species of waterbirds closely associated with the marine environment were recorded in the survey area. The most abundant of the species was the common guillemot, constituting 53% of all the birds found. In August, birds of this species begin to appear in sea areas situated away from the shore, because once the breeding period is over, they follow schools of fish together with their fledglings and young birds. A relatively high abundance (over 100 individuals) was recorded for the European herring gull, constituting 43.1% of the entire grouping. However, the abundance of the entire grouping of birds present in the survey area was low in summer and during 6 survey campaigns between 15 and 115 birds sitting on the water were recorded [Table 3.54]. The average number of birds sitting along the vessel passage route during one survey campaign was very low in the summer amounting to only 6.8 individuals detected per 10 km of the transect length. A detailed list of bird abundances for individual species recorded during 6 survey campaigns, broken down by the method of their recording, is included in Table 3.55.

Table 3.54 The abundance and proportion in the grouping of individual taxa of birds observed sitting on the water during successive survey campaigns within the survey area in the summer

Taxon	08.06.2023	16.06.2023	10.07.2023	28.07.2023	05.08.2023	14.08.2023	Total	Proportion [%]
Seabirds								
Common guillemot *Uria aalge*	3		4	59	52	69	187	53.0
European herring gull *Larus argentatus*	30	14	14	51	4	39	152	43.1
Lesser black-backed gull *Larus fuscus*	1		1	2		2	6	1.7
Razorbill *Alca torda*		1					1	0.3
Black-throated diver *Gavia arctica*				1			1	0.3
Common scoter *Melanitta nigra*	1						1	0.3

Taxon	08.06.2023	16.06.2023	10.07.2023	28.07.2023	05.08.2023	14.08.2023	Total	Proportion [%]
Waterbirds rarely encountered at sea far from the coast								
Brant goose *Branta bernicla*	1						1	0.3
Black-headed gull *Chroicocephalus ridibundus*				1			1	0.3
Common gull *Larus canus*						1	1	0.3
Great black cormorant *Phalacrocorax carbo*						1	1	0.3
Birds unidentified to species								
Unidentified seagull *Laridae*				1			1	0.3
Total	**36**	**15**	**19**	**115**	**56**	**112**	**353**	**100**

Table 3.55. The abundance of seabirds recorded within the survey area during summer, broken down by the method of their recording

Species	Birds sitting on the water		Birds in flight		Total
	Within the transect strip	Outside the transect strip	Snap-shot technique	Besides the snap-shot technique	
Common scoter *Melanitta nigra*	1		12	436	449
European herring gull *Larus argentatus*	96	56	11	81	244
Common guillemot *Uria aalge*	124	63		15	202
Lesser black-backed gull *Larus fuscus*	4	2	2	4	12
Razorbill *Alca torda*	1			2	3
Little gull *Hydrocoloeus minutus*				3	3
Black-throated diver *Gavia arctica*		1			1
Total	**226**	**122**	**25**	**541**	**914**

During 6 survey campaigns conducted in summer, a total of 639 birds were recorded in flight over the survey area as the seabird counts were conducted. The species observed in greatest abundance was the common scoter, which accounted for 71.0% of all the individuals observed in flight. The periods of the more numerous flights of the common scoter correspond to the periods of their migration across the Baltic Sea towards moulting areas in the western part of the Baltic Sea and in the Danish straits (Nehls and Zöllick, 1990). The European herring gull was also fairly abundant (13.2% of the grouping). Other species were less common and, in total, birds typically found in terrestrial environments constituted only 3.4% of all the individuals recorded in flight [Table 3.56].

Table 3.56. The abundance and proportion in the grouping of individual taxa of birds observed in flight during successive survey campaigns within the survey area in the summer

Taxon	08.06.2023	16.06.2023	10.07.2023	28.07.2023	05.08.2023	14.08.2023	Total	Proportion [%]
Seabirds								
Common scoter *Melanitta nigra*	25		160	245	6		436	71.0
European herring gull *Larus argentatus*	12	20	15	8	6	20	81	13.2

Taxon	08.06.2023	16.06.2023	10.07.2023	28.07.2023	05.08.2023	14.08.2023	Total	Proportion [%]
Velvet scoter *Melanitta fusca*			5		9	7	21	3.4
Common guillemot *Uria aalge*	3		11			1	15	2.4
Lesser black-backed gull *Larus fuscus*		1		1	1	1	4	0.7
Arctic tern *Sterna paradisaea*					4		4	0.7
Little gull *Hydrocoloeus minutus*					3		3	0.5
Razorbill *Alca torda*	2						2	0.3
Waterbirds rarely encountered at sea far from the coast								
Common gull *Larus canus*				3	1	3	7	1.1
Common tern *Sterna hirundo*				1	1	1	3	0.5
Great black cormorant *Phalacrocorax carbo*			1			2	3	0.5
Black-headed gull *Chroicocephalus ridibundus*			1	1			2	0.3
Mallard *Anas platyrhynchos*				2			2	0.3
Birds of terrestrial environments								
Eurasian curlew *Numenius arquata*		14		3			17	2.8
Common swift *Apus apus*			2				2	0.3
Grey plover *Pluvialis squatarola*					2		2	0.3
Birds unidentified to species								
Unidentified tern *Sterna sp.*						8	8	1.3
Unidentified seagulls *Laridae*				2			2	0.3
Total	**42**	**35**	**195**	**266**	**33**	**43**	**614**	**100**

Individuals unidentified to species accounted for 0.3% of the birds observed on the water and 1.6% of the birds recorded in flight. Their presence did not have a significant impact on the interpretation of the results obtained.

3.5.1.5.1.1.4 Autumn migration period

During the autumn migration period, 9 species of birds closely associated with the marine environment and 5 species of birds rarely encountered at sea away from the coast were recorded within the survey area. Three species were the most abundant during the observations: the long-tailed duck (60.7% of all the birds recorded), the European herring gull (17.5%) and the common guillemot (13.2%) [Table 3.57]. In total, they constituted 91.4% of the grouping residing in the sea area surveyed. Of all the birds observed, other species reaching the threshold of 1% in terms of abundance were the lesser black-backed gull (2.6%), the razorbill (2.2%), and the common scoter (1.2%). During the autumn migration period, the average abundance in the survey area amounted to only 23.8 individuals per 10 km of the transect length. A detailed list of bird abundances for individual species recorded during 6 survey campaigns, broken down by the method of their recording, is included in Table 3.58.

Table 3.57. The abundance and proportion in the grouping of individual taxa of birds observed sitting on the water during successive survey campaigns within the survey area in the autumn migration period

Taxon	08.09.2023	26.09.2023	22.10.2023	11.11.2023	29.11.2023	30.11.2023	Total	Proportion [%]
Seabirds								
Long-tailed duck *Clangula hyemalis*				121	29	605	755	60.7
European herring gull *Larus argentatus*	144	23	9	2	18	21	217	17.5
Common guillemot *Uria aalge*	112		16	19	14	3	164	13.2
Lesser black-backed gull *Larus fuscus*	27	5					32	2.6
Razorbill *Alca torda*			11	7	2	7	27	2.2
Common scoter *Melanitta nigra*	1			14			15	1.2
Little gull *Hydrocoloeus minutus*			5				5	0.4
Black guillemot *Cepphus grylle*						2	2	0.2
Black-throated diver *Gavia arctica*						1	1	0.1
Waterbirds rarely encountered at sea far from the coast								
Common gull *Larus canus*			1		3	7	11	0.9
Eurasian wigeon *Anas penelope*			3				3	0.2
Mallard *Anas platyrhynchos*			2				2	0.2
Goosander *Mergus merganser*						1	1	0.1
Eurasian coot *Fulica atra*	1						1	0.1
Birds unidentified to species								
Unidentified diver *Gavia sp.*					7		7	0.6
Total	**285**	**28**	**47**	**163**	**73**	**647**	**1243**	**100**

Table 3.58. The abundance of seabirds found within the survey area during the autumn migration period, broken down by the method of their recording

Taxon	Birds sitting on the water		Birds in flight		Total
	Within the transect strip	Outside the transect strip	Snap-shot technique	Besides the snap-shot technique	
Long-tailed duck *Clangula hyemalis*	720	35	33	605	1358
European herring gull *Larus argentatus*	98	119	39	296	552
Common guillemot *Uria aalge*	85	79	6	64	234
Razorbill *Alca torda*	23	4	3	30	60
Lesser black-backed gull *Larus fuscus*	23	9		3	35
Little gull *Hydrocoloeus minutus*	5		5	22	32
Common scoter *Melanitta nigra*	15			9	24
Great black-backed gull *Larus marinus*			2	7	9
Velvet scoter *Melanitta fusca*				8	8
Black guillemot *Cepphus grylle*	2			4	6
Red-throated diver *Gavia stellata*				5	5

Taxon	Birds sitting on the water		Birds in flight		Total
	Within the transect strip	Outside the transect strip	Snap-shot technique	Besides the snap-shot technique	
Arctic skua *Stercorarius parasiticus*				3	3
Pomarine skua *Stercorarius pomarinus*				1	1
Black-throated diver *Gavia arctica*	1				1
Black-legged kittiwake *Rissa tridactyla*				1	1
Red-necked grebe *Podiceps grisegena*				1	1
Birds unidentified to species					
Unidentified diver *Gavia sp.*	2	5		4	11
Total	**974**	**251**	**88**	**1032**	**2376**

During the survey campaigns carried out in the autumn migration period, a total of 1667 birds were recorded in flight over the survey area as the seabirds were counted. The species observed in greatest abundance was the long-tailed duck, which accounted for 38.0% of all the individuals observed in flight. Other abundant species were the European herring gull (20.0%) and the greater white-fronted goose (13.1%). The remaining species were less common and, in total, birds typically found in terrestrial environments constituted 8.6% of all the individuals recorded in flight [Table 3.59].

Table 3.59. The abundance and proportion in the grouping of individual taxa of birds observed in flight during successive survey campaigns within the survey area in the autumn migration period

Taxon	08.09.2023	26.09.2023	22.10.2023	11.11.2023	29.11.2023	30.11.2023	Total	Proportion [%]
Seabirds								
Long-tailed duck *Clangula hyemalis*			34	301	256	47	638	38.0
European herring gull *Larus argentatus*	37	44	44	29	47	134	335	20.0
Common guillemot *Uria aalge*	2	1	7	19	25	16	70	4.2
Razorbill *Alca torda*			2	4	9	18	33	2.0
Little gull *Hydrocoloeus minutus*	7	3	8	1	3	5	27	1.6
Common scoter *Melanitta nigra*	9						9	0.5
Red-throated diver *Gavia stellata*				1		8	9	0.5
Black guillemot *Cepphus grylle*			1	7			8	0.5
Great black-backed gull *Larus marinus*					3	2	5	0.3
Velvet scoter *Melanitta fusca*			1		1	2	4	0.2
Arctic skua *Stercorarius parasiticus*	1	2					3	0.2
Lesser black-backed gull *Larus fuscus*	2	1					3	0.2
Pomarine skua *Stercorarius pomarinus*		1					1	0.1
Red-necked grebe *Podiceps grisegena*				1			1	0.1
Black-legged kittiwake *Rissa tridactyla*						1	1	0.1
Waterbirds rarely encountered at sea far from the coast								
Greater white-fronted goose *Anser albifrons*			220				220	13.1

Taxon	08.09.2023	26.09.2023	22.10.2023	11.11.2023	29.11.2023	30.11.2023	Total	Proportion [%]
Common gull *Larus canus*	1	1	11	5	28	71	117	7.0
Great black cormorant *Phalacrocorax carbo*	1			12	1		14	0.8
Eurasian wigeon *Anas penelope*	8						8	0.5
Red-breasted merganser *Mergus serrator*					5	2	7	0.4
Goosander *Mergus merganser*	4		2				6	0.4
Mallard *Anas platyrhynchos*			3		2		5	0.3
Mute swan *Cygnus olor*					2		2	0.1
Black-headed gull *Chroicocephalus ridibundus*				2			2	0.1
Birds of terrestrial environments								
Eurasian siskin *Carduelis spinus*		46		2			48	2.9
White wagtail *Motacilla alba*	12	3					15	0.9
Goldfinch *Carduelis carduelis*				9			9	0.5
Whimbrel *Numenius phaeopus*	8						8	0.5
Eurasian skylark *Alauda arvensis*			2	1			3	0.2
Great white egret *Egretta alba*		2					2	0.1
Common starling *Sturnus vulgaris*						1	1	0.1
Twite *Carduelis flavirostris*				1			1	0.1
Eurasian wren *Troglodytes troglodytes*				1			1	0.1
Grey heron *Ardea cinerea*	1						1	0.1
Birds unidentified to species								
Unidentified passerines *Passeriformes*		2	52	2			56	3.3
Unidentified diver *Gavia sp.*	1				2	1	4	0.2
Total	**94**	**106**	**387**	**398**	**384**	**308**	**1677**	**100**

Individuals unidentified to species accounted for 0.6% of the birds observed on the water and 3.5% of the birds recorded in flight. Thus, their presence did not have an impact on the interpretation of the results obtained.

3.5.1.5.1.2 Reference area

3.5.1.5.1.2.1 Wintering period

In the wintering period, the average abundance index was 12.6 individuals per 10 km of the transect. Definitely, the long-tailed duck was the species occurring in greatest abundance, accounting for 80.6% of the entire grouping. The European herring gull and the razorbill (8.7% and 6.5% of the grouping, respectively) occurred in great numbers, whereas the other species were observed less frequently [Table 3.60]. A detailed list of bird abundances for individual species recorded during 6 survey campaigns, broken down by the method of their recording, is included in Table 3.61.

Table 3.60. The abundance and proportion in the grouping of individual taxa of birds observed sitting on the water during successive survey campaigns within the reference area in the wintering period

Taxon	06.12.2022	16.12.2022	19.01.2023	06.02.2023	15.02.2023	22.02.2023	Total	Proportion [%]
Seabirds								
Long-tailed duck *Clangula hyemalis*	288	431	932	78	822	607	3158	80.6
European herring gull *Larus argentatus*	32	42	5	257	5	1	342	8.7
Razorbill *Alca torda*	93	28	5	41	13	74	254	6.5
Common guillemot *Uria aalge*	61	3	8		3	3	78	2.0
Little gull *Hydrocoloeus minutus*	10						10	0.3
Black guillemot *Cepphus grylle*	1				2	1	4	0.1
Black-throated diver *Gavia arctica*	1			1	1		3	0.1
Red-throated diver *Gavia stellata*	3						3	0.1
Great black-backed gull *Larus marinus*					2		2	0.1
Yellow-billed diver *Gavia adamsii*	1						1	+
Waterbirds rarely encountered at sea far from the coast								
Common gull *Larus canus*	18	19	1	7	5	5	55	1.4
Red-breasted merganser *Mergus serrator*			2				2	0.1
Great crested grebe *Podiceps cristatus*	1						1	+
Birds unidentified to species								
Unidentified diver *Gavia sp.*	1	2	1				4	0.1
Total	**510**	**525**	**954**	**384**	**853**	**691**	**3917**	**100**

+ - percentage smaller than 0.1%

Table 3.61. The abundance of seabirds found within the reference area during the wintering period, broken down by the method of their recording

Taxon	Birds sitting on the water		Birds in flight		Total
	Within the transect strip	Outside the transect strip	Snap-shot technique	Besides the snap-shot technique	
Long-tailed duck *Clangula hyemalis*	2870	288	243	1436	4837
European herring gull *Larus argentatus*	91	251	29	207	578
Razorbill *Alca torda*	232	22	11	222	487
Common guillemot *Uria aalge*	43	35	3	67	148
Little gull *Hydrocoloeus minutus*	9	1		11	21
Black guillemot *Cepphus grylle*	4		2	4	10
Velvet scoter *Melanitta fusca*				10	10
Red-throated diver *Gavia stellata*	2	1		2	5
Black-throated diver *Gavia arctica*	3			1	4
Common scoter *Melanitta nigra*				4	4
Great black-backed gull *Larus marinus*	2			1	3
Yellow-billed diver *Gavia adamsii*		1			1
Birds unidentified to species					

Taxon	Birds sitting on the water		Birds in flight		Total
	Within the transect strip	Outside the transect strip	Snap-shot technique	Besides the snap-shot technique	
Unidentified diver *Gavia sp.*	4			6	10
Total	**3260**	**599**	**288**	**1971**	**6118**

The long-tailed duck was the most abundant species observed in flight over the reference area. It accounted for 69.1% of all the birds recorded in flight. During 6 survey campaigns, more than 100 individuals in flight were also observed in the case of the European herring gull, the razorbill and the common gull. The other species were less abundant [Table 3.62].

Table 3.62. The abundance and proportion in the grouping of individual taxa of birds observed in flight during successive survey campaigns within the reference area in the wintering period

Taxon	06.12.2022	16.12.2022	19.01.2023	06.02.2023	15.02.2023	22.02.2023	Total	Proportion [%]
Seabirds								
Long-tailed duck *Clangula hyemalis*	130	54	453	281	671	90	1679	69.1
European herring gull *Larus argentatus*	40	29	49	37	32	49	236	9.7
Razorbill *Alca torda*	2	29	21	56	59	66	233	9.6
Common guillemot *Uria aalge*	10	12	25	17	3	3	70	2.9
Little gull *Hydrocoloeus minutus*	4				2	5	11	0.5
Velvet scoter *Melanitta fusca*	3			4	1	2	10	0.4
Black guillemot *Cepphus grylle*	1		1	3	1		6	0.2
Common scoter *Melanitta nigra*						4	4	0.2
Red-throated diver *Gavia stellata*		1		1			2	0.1
Black-throated diver *Gavia arctica*						1	1	+
Great black-backed gull *Larus marinus*			1				1	+
Waterbirds rarely encountered at sea far from the coast								
Common gull *Larus canus*	15	23	28	23	20	13	122	5.0
Red-breasted merganser *Mergus serrator*			16				16	0.7
Mute swan *Cygnus olor*		9					9	0.4
Common goldeneye *Bucephala clangula*	1						1	+
Black-headed gull *Chroicocephalus ridibundus*	1						1	+
Birds unidentified to species								
Unidentified swan *Cygnus* sp.		20			2		22	0.9
Unidentified diver *Gavia sp.*		1	2			3	6	0.2
Total	**207**	**178**	**596**	**422**	**791**	**236**	**2430**	**100**

+ - percentage smaller than 0.1%

Individuals unidentified to species accounted for 0.1% of the birds observed on the water and 1.1% of the birds recorded in flight. Thus, their presence did not have an impact on the interpretation of the results obtained.

3.5.1.5.1.2.2 Spring migration period

During the spring migration period, 12 species of birds closely associated with the marine environment and 4 species of birds rarely encountered at sea away from the coast were recorded within the reference area. Long-tailed ducks were the most numerous species. In total, they constituted 91.6% of the grouping residing in the sea area surveyed. Of all the birds observed, other species exceeding 1% in terms of abundance were the razorbill (3.1%) and the common scoter (1.2%). The number of other species was very low and the total number of any of these species did not exceed 30 individuals [Table 3.63]. During the spring migration period, the average abundance in the reference area amounted to 95.1 individuals per 10 km of the transect length. After excluding the results from two survey campaigns conducted in May, when the number of seabirds in the Polish zone of the Baltic Sea is already very low, the value of this index is 140.4. A detailed list of bird abundances for individual species recorded during 6 survey campaigns, broken down by the method of their recording, is included in Table 3.64.

Table 3.63. The abundance and proportion in the grouping of individual taxa of birds observed sitting on the water during successive survey campaigns within the reference area in the spring migration period

Taxon	**01–02.03.2023**	**21.03.2023**	**06.04.2023**	**22.04.2023**	**12.05.2023**	**20.05.2023**	**Total**	**Proportion [%]**
Seabirds								
Long-tailed duck *Clangula hyemalis*	1245	176	237	1039	17	2	2716	91.6
Razorbill *Alca torda*	13	28	10	42			93	3.1
Common scoter *Melanitta nigra*				37			37	1.2
Black-throated diver *Gavia arctica*				10	14	2	26	0.9
European herring gull *Larus argentatus*	9	3	4		6	2	24	0.8
Common guillemot *Uria aalge*		2	6	14	1		23	0.8
Velvet scoter *Melanitta fusca*			2	5			7	0.2
Black guillemot *Cepphus grylle*				3		1	4	0.1
Lesser black-backed gull *Larus fuscus*						1	1	+
Yellow-billed diver *Gavia adamsii*				1			1	+
Red-throated diver *Gavia stellata*				1			1	+
Little gull *Hydrocoloeus minutus*				1			1	+
Waterbirds rarely encountered at sea far from the coast								
Common gull *Larus canus*	5	4	4	1			14	0.5
Red-breasted merganser *Mergus serrator*			4				4	0.1
Mallard *Anas platyrhynchos*			2				2	0.1
Common tern *Sterna hirundo*				1			1	+
Birds unidentified to species								
Unidentified diver *Gavia sp.*				10			10	0.3
Unidentified ducks *Anatidae*				1			1	+
Total	**1272**	**213**	**269**	**1166**	**38**	**8**	**2966**	**100**

+ - proportion below 0.1%

Table 3.64. The abundance of seabirds found within the reference area during the spring migration period broken down by the method of their recording

Taxon	Birds sitting on the water		Birds in flight		Total
	Within the transect strip	Outside the transect strip	Snap-shot technique	Besides the snap-shot technique	
Long-tailed duck *Clangula hyemalis*	2000	716	194	2735	5645
Common scoter *Melanitta nigra*	20	17	34	248	319
Razorbill *Alca torda*	56	37	2	99	194
European herring gull *Larus argentatus*	23	1	13	101	138
Common guillemot *Uria aalge*	11	12		44	67
Black-throated diver *Gavia arctica*	21	5	2	15	43
Little gull *Hydrocoloeus minutus*	1		1	12	14
Velvet scoter *Melanitta fusca*	7			7	14
Lesser black-backed gull *Larus fuscus*	1		1	9	11
Black guillemot *Cepphus grylle*	2	2		2	6
Red-throated diver *Gavia stellata*	1			3	4
Arctic tern *Sterna paradisaea*				2	2
Arctic skua *Stercorarius parasiticus*				1	1
Yellow-billed diver *Gavia adamsii*		1			1
Birds unidentified to species					
Unidentified diver *Gavia sp.*	2	8		10	20
Total	**2145**	**799**	**247**	**3288**	**6479**

During the spring migration period, 3843 birds flying over the reference area were spotted. The most numerous species, with over 100 individuals recorded, were the long-tailed duck, the common scoter, the common gull, the European herring gull and the razorbill. They constituted 92.5% of all the birds observed in flight. The remaining species were very scarce [Table 3.65].

Table 3.65. The abundance and proportion in the grouping of individual taxa of birds observed in flight during successive survey campaigns within the reference area in the spring migration period

Taxon	01–02.03.2023	21.03.2023	06.04.2023	22.04.2023	12.05.2023	20.05.2023	Total	Proportion [%]
Seabirds								
Long-tailed duck *Clangula hyemalis*	1794	837	98	188	10	2	2929	76.2
Common scoter *Melanitta nigra*		38	45	198	1		282	7.3
European herring gull *Larus argentatus*	29	23	30	16	5	11	114	3.0
Razorbill *Alca torda*	24	48	15	14			101	2.6
Common guillemot *Uria aalge*		5	27	3	9		44	1.1
Black-throated diver *Gavia arctica*				2	13	2	17	0.4
Little gull *Hydrocoloeus minutus*		2		3	8		13	0.3
Lesser black-backed gull *Larus fuscus*				8		2	10	0.3

Taxon	01–02.03.2023	21.03.2023	06.04.2023	22.04.2023	12.05.2023	20.05.2023	Total	Proportion [%]
Velvet scoter *Melanitta fusca*	2			5			7	0.2
Red-throated diver *Gavia stellata*			3				3	0.1
Arctic tern *Sterna paradisaea*						2	2	0.1
Black guillemot *Cepphus grylle*		1		1			2	0.1
Arctic skua *Stercorarius parasiticus*						1	1	+
Waterbirds rarely encountered at sea far from the coast								
Common gull *Larus canus*	88	31	4	1		5	129	3.4
Eurasian wigeon *Mareca penelope*			89				89	2.3
Red-breasted merganser *Mergus serrator*	2	3	16				21	0.5
Great black cormorant *Phalacrocorax carbo*			15				15	0.4
Greater white-fronted goose *Anser albifrons*			5				5	0.1
Pintail *Anas acuta*			3				3	0.1
Mallard *Anas platyrhynchos*			2				2	0.1
Common teal *Anas crecca*			2				2	0.1
Black-headed gull *Chroicocephalus ridibundus*		1			1		2	0.1
Birds of terrestrial environments								
Eurasian skylark *Alauda arvensis*	1	2					3	0.1
Grey heron *Ardea cinerea*		2	1				3	0.1
Great white egret *Egretta alba*				1			1	+
Eurasian wren *Troglodytes troglodytes*		1					1	+
Common starling *Sturnus vulgaris*			1				1	+
Song thrush *Turdus philomelos*		1					1	+
Goldcrest *Regulus regulus*			1				1	+
Birds unidentified to species								
Unidentified geese *Anserinae*		28					28	0.7
Unidentified diver *Gavia sp.*			1	6	3		10	0.3
Unidentified passerines *Passeriformes*				1			1	+
Total	**1940**	**1023**	**358**	**447**	**50**	**25**	**3843**	**100**

+ - proportion below 0.1%

Individuals unidentified to species accounted for less than 0.4% of the birds observed on the water and 1.0% of the birds recorded in flight. Thus, their presence did not have an impact on the interpretation of the results obtained.

3.5.1.5.1.2.3 Summer period

During summer, 4 bird species closely associated with the marine environment and 1 bird species rarely encountered at sea away from the coast were recorded within the reference area. As in the survey area, the most abundant species recorded was the common guillemot, which constituted 61% of the grouping present in the survey area. The European herring gull was also present in fairly high numbers (71 individuals, 32.6% of the grouping), but its high proportion is attributable to the low abundance of

the entire bird grouping. The abundance of other species was very low [Table 3.63]. During the spring migration period, the average abundance in the reference area amounted to only 7.0 individuals per 10 km of the transect length. A detailed list of bird abundances for individual species recorded during 6 survey campaigns, broken down by the method of their recording, is included in Table 3.67.

Table 3.66. The abundance and proportion in the grouping of individual taxa of birds observed sitting on the water during successive survey campaigns within the reference area in the summer

Species	08.06.2023	16.06.2023	10.07.2023	28.07.2023	05.08.2023	14.08.2023	Total	Proportion [%]
Seabirds								
Common guillemot *Uria aalge*	8		3	16	2	104	133	61.0
European herring gull *Larus argentatus*	43	5	3	8	5	7	71	32.6
Razorbill *Alca torda*	9						9	4.1
Lesser black-backed gull *Larus fuscus*			1	1		1	3	1.4
Waterbirds rarely encountered at sea far from the coast								
Common gull *Larus canus*				2			2	0.9
Total	**60**	**5**	**7**	**27**	**7**	**112**	**218**	**100**

Table 3.67. The abundance of seabirds recorded within the reference area during summer, broken down by the method of their recording

Species	Birds sitting on the water		Birds in flight		Total
	Within the transect strip	Outside the transect strip	Snap-shot technique	Besides the snap-shot technique	
Common scoter *Melanitta nigra*				345	345
Common guillemot *Uria aalge*	57	76		6	139
European herring gull *Larus argentatus*	12	59	13	43	127
Razorbill *Alca torda*	5	4	4	8	21
Velvet scoter *Melanitta fusca*				6	6
Lesser black-backed gull *Larus fuscus*	3			3	6
Arctic tern *Sterna paradisaea*				4	4
Sandwich tern *Thalasseus sandvicensis*				2	2
Little gull *Hydrocoloeus minutus*				1	1
Total	**77**	**139**	**17**	**418**	**651**

During summer, 505 birds passing over the reference area were recorded. Similarly to the survey area, the most abundant species was the common scoter. It accounted for 68.3% of all the birds recorded in flight. The remaining species were very scarce and only the European herring gull accounted for more than 10% of the grouping, but only 56 individuals of this species were recorded in the reference area during the 6 survey campaigns [Table 3.65].

Table 3.68. The abundance and proportion in the grouping of individual taxa of birds observed in flight during successive survey campaigns within the reference area in the summer

Taxon	08.06.2023	16.06.2023	10.07.2023	28.07.2023	05.08.2023	14.08.2023	Total	Proportion [%]
Seabirds								
Common scoter *Melanitta nigra*		1	36	306		2	345	68.3
European herring gull *Larus argentatus*	20	2	12	9	5	8	56	11.1
Razorbill *Alca torda*	12						12	2.4
Common guillemot *Uria aalge*	4		2				6	1.2
Velvet scoter *Melanitta fusca*					6		6	1.2
Lesser black-backed gull *Larus fuscus*	2		1				3	0.6
Sandwich tern *Sterna sandvicensis*	1				1		2	0.4
Arctic tern *Sterna paradisaea*				1		3	4	0.8
Little gull *Hydrocoloeus minutus*					1		1	0.2
Waterbirds rarely encountered at sea far from the coast								
Mallard *Anas platyrhynchos*	9		7				16	3.2
Common gull *Larus canus*			1	13	1		15	3.0
Common goldeneye *Bucephala clangula*	8						8	1.6
Common teal *Anas crecca*						7	7	1.4
Mute swan *Cygnus olor*				5			5	1.0
Common tern *Sterna hirundo*						3	3	0.6
Black-headed gull *Chroicocephalus ridibundus*		1					1	0.2
Great black cormorant *Phalacrocorax carbo*				1			1	0.2
Birds of terrestrial environments								
Common swift *Apus apus*			6				6	1.2
Barn swallow *Hirundo rustica*	1						1	0.2
Western yellow wagtail *Motacilla flava*						1	1	0.2
Birds unidentified to species								
Unidentified tern *Sterna sp.*				3		3	6	1.2
Total	**57**	**4**	**65**	**338**	**14**	**27**	**505**	**100**

Individuals unidentified to species accounted for only 0.9% of the birds sitting on the water and 1.2% of the birds recorded in flight. Thus, their presence could not have an impact on the interpretation of the results obtained.

3.5.1.5.1.2.4 Autumn migration period

During the autumn migration period, 8 species of birds closely associated with the marine environment and 3 species of birds rarely encountered at sea away from the coast were recorded within the reference area. The species observed in greatest abundance were the common guillemot (21.6%), the European herring gull (19.2%), the razorbill (17.4%) and the long-tailed duck (16.2%) [Table 3.69]. In total, they accounted for 74.3% of the grouping of waterbirds observed in this sea area. The abundance of birds in the reference area in the period discussed was very low and none of the species totalled more than 50 individuals [Table 3.69]. During the autumn migration period, the average abundance in

the reference area amounted to only 5.4 individuals per 10 km of the transect length. A detailed list of bird abundances for individual species recorded during the survey campaigns conducted, broken down by the method of their recording, is included in Table 3.70.

Table 3.69. The abundance and proportion in the grouping of individual taxa of birds observed sitting on the water during successive survey campaigns within the reference area in the autumn migration period

Taxon	08.09.2023	26.09.2023	22.10.2023	11.11.2023	29.11.2023	30.11.2023	Total	Proportion [%]
Seabirds								
Common guillemot *Uria aalge*	23	4	8		1		36	21.6
European herring gull *Larus argentatus*	8	1	12	3	7	1	32	19.2
Razorbill *Alca torda*			7	15	6	1	29	17.4
Long-tailed duck *Clangula hyemalis*					7	20	27	16.2
Common scoter *Melanitta nigra*	4	2					6	3.6
Little gull *Hydrocoloeus minutus*			2	2			4	2.4
Lesser black-backed gull *Larus fuscus*	2						2	1.2
Black-throated diver *Gavia arctica*					1		1	0.6
Waterbirds rarely encountered at sea far from the coast								
Common gull *Larus canus*			9		7	7	23	13.8
Goosander *Mergus merganser*						4	4	2.4
Eurasian coot *Fulica atra*			1				1	0.6
Birds unidentified to species								
Unidentified diver *Gavia sp.*					1		2	1.2
Total	**37**	**7**	**39**	**20**	**29**	**35**	**167**	**100**

Table 3.70. The abundance of seabirds found within the reference area during the autumn migration period, broken down by the method of their recording

Taxon	Birds sitting on the water		Birds in flight		Total
	Within the transect strip	Outside the transect strip	Snap-shot technique	Besides the snap-shot technique	
Long-tailed duck *Clangula hyemalis*	26	1	37	949	1013
European herring gull *Larus argentatus*	25	7	15	88	135
Common guillemot *Uria aalge*	31	5	1	33	70
Razorbill *Alca torda*	26	3	6	24	59
Common scoter *Melanitta nigra*	6		9	20	35
Little gull *Hydrocoloeus minutus*	4		2	14	20
Velvet scoter *Melanitta fusca*				11	11
Lesser black-backed gull *Larus fuscus*	1	1	2	4	8
Red-throated diver *Gavia stellata*				3	3
Black-throated diver *Gavia arctica*	1			1	2

Taxon	Birds sitting on the water		Birds in flight		Total
	Within the transect strip	Outside the transect strip	Snap-shot technique	Besides the snap-shot technique	
Black guillemot *Cepphus grylle*				2	2
Black-legged kittiwake *Rissa tridactyla*				1	1
Birds unidentified to species					
Unidentified diver *Gavia sp.*	2			7	9
Total	**122**	**17**	**72**	**1157**	**1368**

During the autumn migration period, 1508 birds were spotted in flight over the reference area. The most numerous species was the long-tailed duck, constituting 65.4% of all the birds observed in flight. The remaining species were very scarce and only the common gull and the European herring gull reached more than 5% of the proportion in the grouping [Table 3.71]. Birds associated with terrestrial environments accounted for only 1.0% of all the individuals recorded in flight.

Table 3.71. The abundance and proportion in the grouping of individual taxa of birds observed in flight during successive survey campaigns within the reference area in the autumn migration period

Taxon	08.09.2023	26.09.2023	22.10.2023	11.11.2023	29.11.2023	30.11.2023	Total	Proportion [%]
Seabirds								
Long-tailed duck *Clangula hyemalis*			24	553	322	87	986	65.4
European herring gull *Larus argentatus*	21	5	20	8	22	27	103	6.8
Common guillemot *Uria aalge*			5	6	9	14	34	2.3
Razorbill *Alca torda*		2	4	11	8	5	30	2.0
Common scoter *Melanitta nigra*	27		2				29	1.9
Little gull *Hydrocoloeus minutus*	8	2	5			1	16	1.1
Velvet scoter *Melanitta fusca*			1	7	2	1	11	0.7
Lesser black-backed gull *Larus fuscus*	4	2					6	0.4
Red-throated diver *Gavia stellata*	1					2	3	0.2
Black guillemot *Cepphus grylle*					2		2	0.1
Black-legged kittiwake *Rissa tridactyla*				1			1	0.1
Black-throated diver *Gavia arctica*				1			1	0.1
Waterbirds rarely encountered at sea far from the coast								
Common gull *Larus canus*	3	4	17	14	58	77	173	11.5
Eurasian wigeon *Anas penelope*		12	7				19	1.3
Mallard *Anas platyrhynchos*	3	7					10	0.7
Great black cormorant *Phalacrocorax carbo*	1			3			4	0.3
Goosander *Mergus merganser*						4	4	0.3
Red-breasted merganser *Mergus serrator*						2	2	0.1
Greater scaup *Aythya marila*			1				1	0.1

Taxon	08.09.2023	26.09.2023	22.10.2023	11.11.2023	29.11.2023	30.11.2023	Total	Proportion [%]
Birds of terrestrial environments								
Goldcrest *Regulus regulus*	1		1				2	0.1
White wagtail *Motacilla alba*	2						2	0.1
Common starling *Sturnus vulgaris*				1			1	0.1
Meadow pipit *Anthus pratensis*			1				1	0.1
European robin *Erithacus rubecula*			1				1	0.1
Birds unidentified to species								
Unidentified ducks *Anatidae*	5	1		15	15	4	40	2.7
Unidentified swan *Cygnus* sp.						11	11	0.7
Unidentified passerines *Passeriformes*		8					8	0.5
Unidentified diver *Gavia sp.*		1			5	1	7	0.5
Total	**76**	**44**	**89**	**620**	**443**	**236**	**1508**	**100**

Individuals unidentified to species accounted for 1.2% of the birds observed on the water and 4.4% of the birds recorded in flight. Thus, their presence did not have an impact on the interpretation of the results obtained.

3.5.1.5.2 Changes in avifauna abundance

Changes in the abundance of the entire avifauna grouping and the most numerous species were compared in the survey area and in the reference area. Such a comparison enabled a direct comparison of the dynamics of changes in abundance in both sea areas. It is also in line with the methodological assumptions, as the reference area was delineated in a sea area with similar habitat conditions as the area of the planned OWF and is intended as a reference to the results obtained in the survey area.

During the wintering period, the abundance of birds in the survey area was highly variable and during two of the six survey campaigns, it remained within the range of 7.7 to 28.6 individuals per 10 km. More birds were observed on 6 December 2022 and 6–7 February 2023, when 1483 and 1757 individuals, respectively, were recorded along the vessel passage route, which translated into the abundance rate of 170.5 and 202.0 respectively. During the survey campaign on 6–7 February 2023, birds in flight were also recorded in great abundance, i.e. 437 individuals per 10 km of the vessel passage route [Figure 3.96]. These were mainly the European herring gull and the razorbill, which accounted for as much as 88.0% of all the birds observed in flight during that survey campaign. In winter, the abundance of birds sitting on the water along the vessel passage route within the reference area was more uniform, with the maximum values recorded on 19 January 2023 and 15 February 2023, i.e. 183.5 and 164.0 individuals per 10 km of the vessel passage route, respectively [Figure 3.96].

In March, the number of birds in the survey area remained at the level of approximately 400 individuals. In early April, a decrease in the abundance of the grouping was recorded, but during the survey campaign on 22 April 2023, there was a sharp increase in the number of birds sitting on the water along the vessel passage route (11,313 individuals) and those in flight (3124 individuals). The corresponding values of the abundance index for this survey campaign were 1082.8 for sitting birds and 359.1 for flying birds per 10 km of the vessel passage route [Figure 3.96]. More than 98% of the birds present on

that day in the survey area were long-tailed ducks, and 81% of the birds passing through were two species of sea ducks, the long-tailed duck and the common scoter. In the reference area, the abundance of birds sitting along the vessel passage route fluctuated considerably during the same period. The highest abundances were recorded during the first survey campaign (1–2 March 2023) and on 22 April 2023, when the number of birds in the survey area also increased [Figure 3.96]. Moreover, during the vessel passage on 1–2 March 2023, an intensive passage was also observed, with 373.1 individuals per 10 km of the vessel passage route. In May, the abundance levels of birds observed on the water were already very low in both areas.

During the summer, the abundance of birds present in the two sea areas was low, not exceeding 120 individuals recorded along the vessel passage route. In July, an increase in the number of birds flying over both areas was observed [Figure 3.96]. A vast majority of the flights involved the common scoter migrating towards moulting areas in the western part of the Baltic Sea.

During the autumn migration period, an increase in the abundance of the grouping was noted in both areas, but it was not high. In the survey area, a maximum of 285 birds were recorded sitting on the water along the vessel passage route (on 8 September 2023), while in the reference area the highest abundance was only 39 individuals (on 22 October 2023). The abundance indices ranged from 9.2 to 32.8 individuals per 10 km of the vessel passage route [Figure 3.96]. In the autumn, birds recorded in flight were slightly more numerous. However, autumn migration over both areas was poorly represented during daytime. During the survey campaign, up to 45.7 birds were observed flying over the survey area and up to 122.1 over the reference area per 10 km of the vessel passage route. Both of these findings relate to the survey campaign conducted on 11 November 2023, with the most abundant bird observed in flight at that time being the long-tailed duck, representing 36.3% and 64.1% of the birds flying over the survey area and the reference area, respectively.

The numbers of birds sitting on the water and in flight were moderately correlated. The correlation coefficient for the survey area was 0.62, and for the reference area it was 0.65; in both cases, these were statistically significant values ($p = 0.01$ in both cases). This means that a large part of the flights over the surveyed areas observed may result from local movements of the birds staying there. However, it cannot be ruled out that during periods of intensive flights, some migrating birds stop here, adjourning their migration.

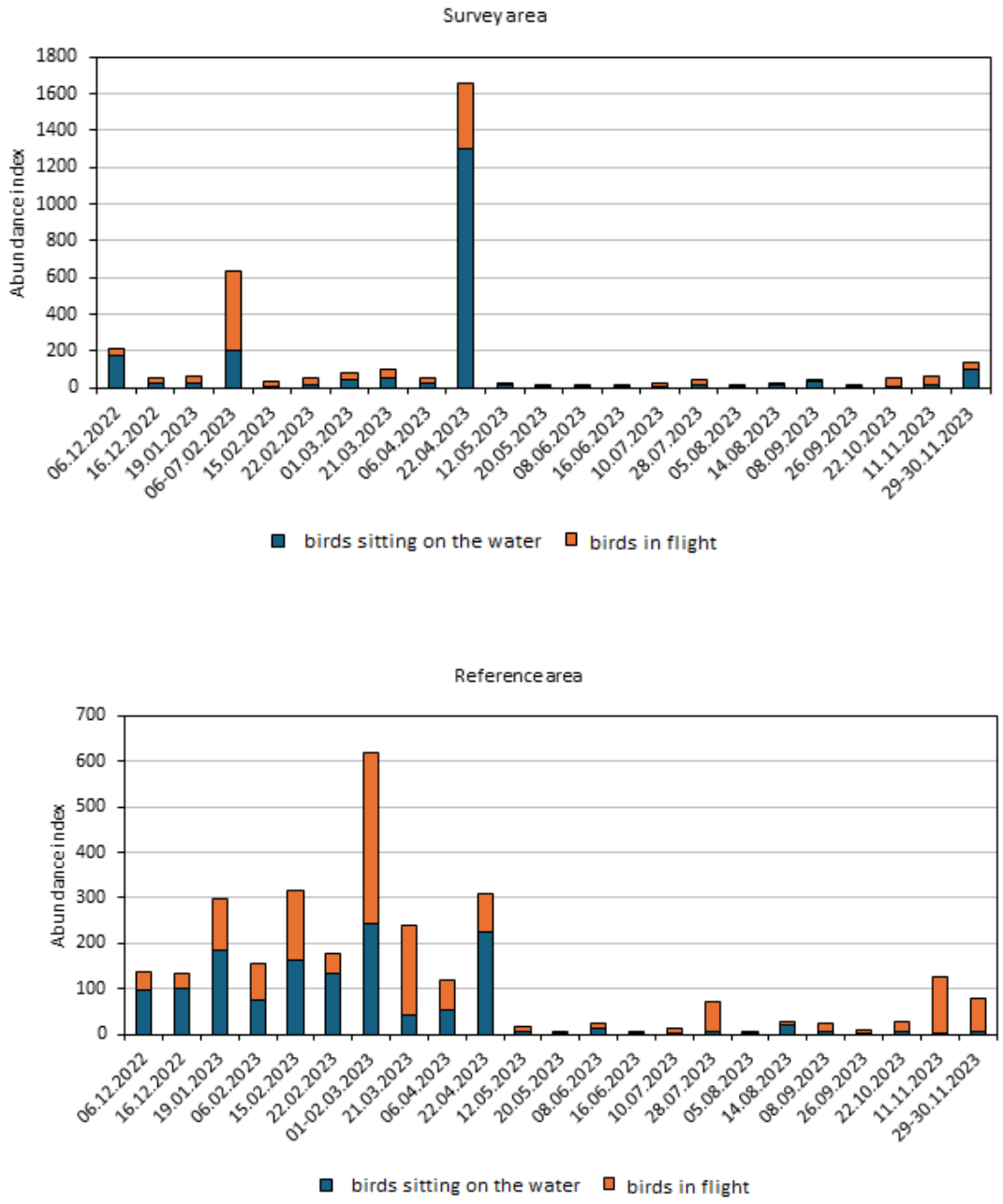


Figure 3.96. The changes in the abundance index of the entire bird grouping during successive survey campaigns within the survey area and the reference area

Between autumn and spring, the long-tailed duck was the most abundant species in both areas and its abundance largely determined changes in the abundance of the entire bird grouping. Within the survey area, the species was usually not very abundant. Apart from one observation on 22 April 2023, its abundance along the vessel passage route ranged from 4.3 (on 29–30 November 2023) to 141.0 individuals (on 6 December 2022) per 10 km of the vessel passage route. In the reference area, the maximum abundance of the long-tailed duck was 239.4 individuals per 10 km of the vessel passage route (on 1–2 March 2023), when an intense passage of this species was also observed [Figure 3.97]. On 22 April 2023, an exceptionally abundant presence of the long-tailed duck was observed in the survey area. 11,152 individuals sitting on the water and 1175 individuals in flight were recorded at that

time, and the abundance index was 1281.8 and 135.1 individuals per 10 km of the vessel passage route [Figure 3.97]. On the same day, there was also a marked increase in the abundance of the long-tailed duck in the reference area, following a decline in abundance observed since early March [Figure 3.97]. This coincidence indicates that the very abundant presence of the long-tailed duck on that day most likely concerned a much larger area than that covered by the observations.

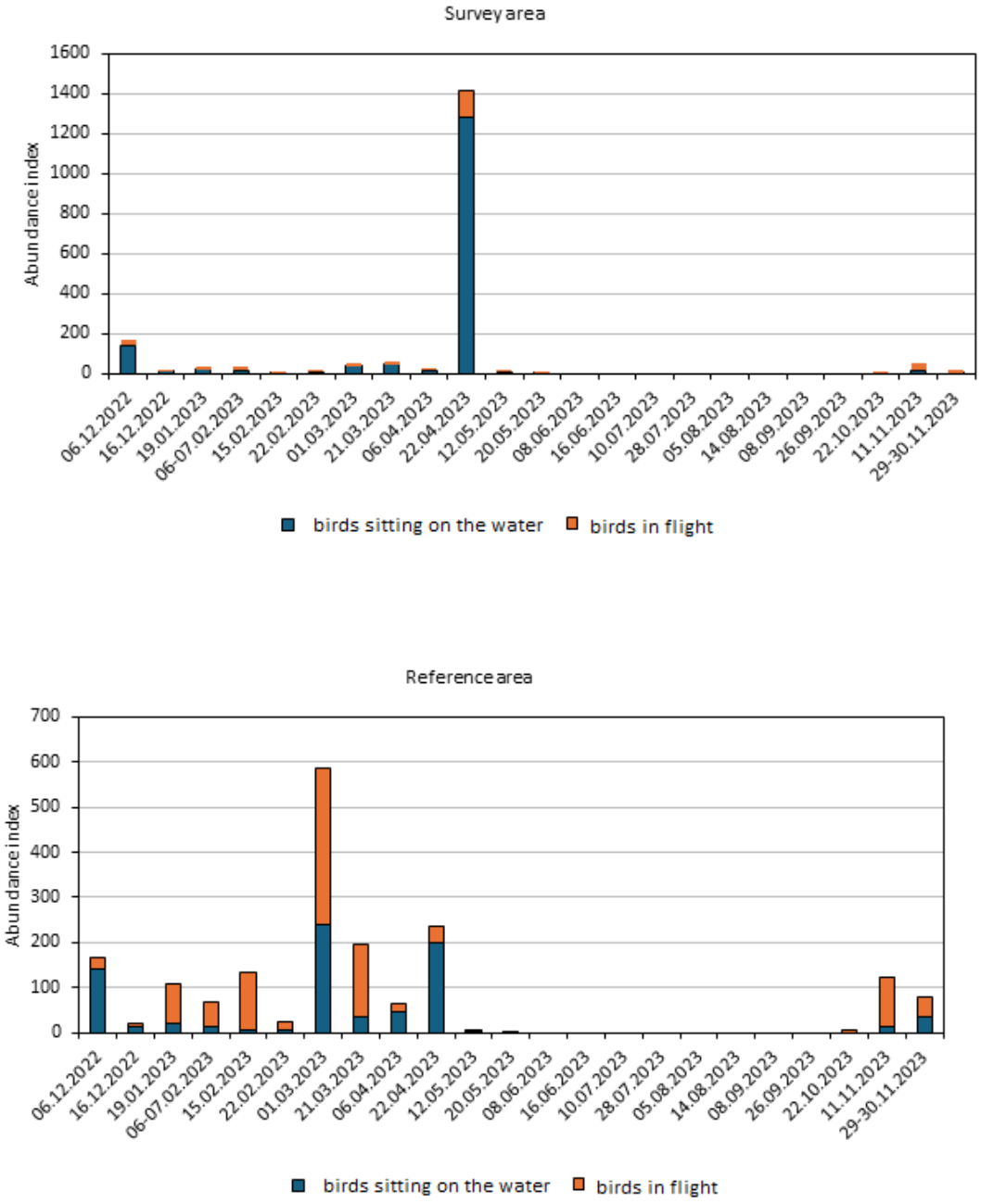


Figure 3.97. The changes in the abundance index of the long-tailed duck during successive survey campaigns within the survey area and in the reference area

The abundance of the European herring gull in both areas was typically not exceeding 70 individuals recorded on the water [Figure 3.98]. High and very high concentrations of this species were observed

in the survey area during the survey campaign conducted on 6–7 February 2023 (1388 individuals sitting on the water and 1882 in flight, i.e. the abundance index of 159.5 and 216.3 respectively) and on 8 September 2023 (144 individuals on the water, i.e. the abundance index of 16.6). In the reference area, the highest concentration of the European herring gull was recorded on 6 February 2023 (257 individuals on the water, i.e. the abundance index of 49.4) [Figure 3.98]. The European herring gull usually occurs in open sea areas in a scattered pattern while such high concentrations are usually associated with fishing activity (Garthe et al., 2003).

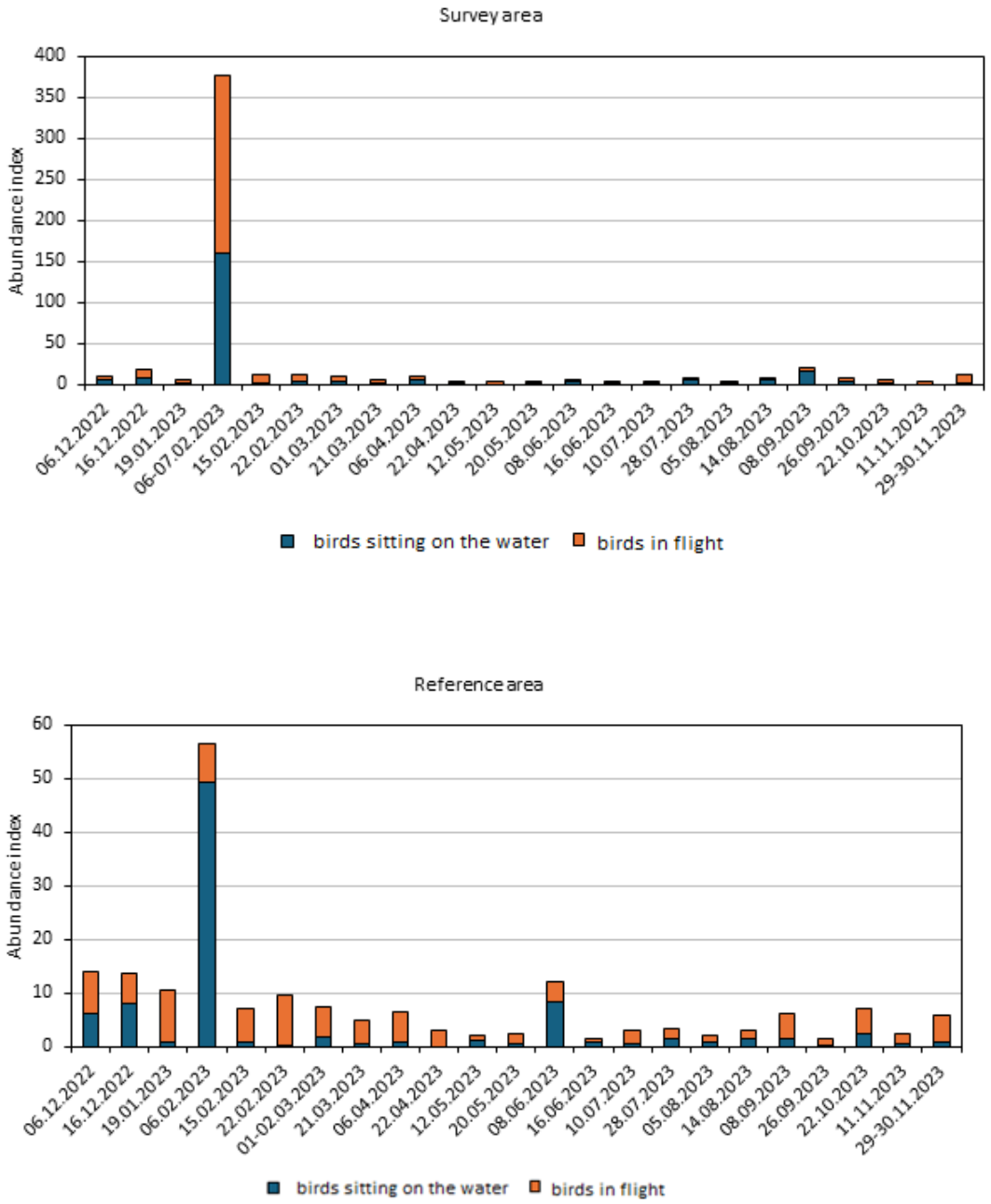


Figure 3.98. The changes in the abundance index of the European herring gull during successive survey campaigns within the survey area and in the reference area

Only in the winter, the abundance of the razorbill within the survey area twice exceeded 100 individuals sitting on the water along the vessel passage route, whereas, during the remaining survey campaigns, it was significantly lower, not exceeding 35 individuals. The maximum values of the abundance index for this species during this period were 17.1 (16.12.2022) and 14.6 (06–07.02.2023) individuals per 10 km of the vessel passage route. An exceptionally high number of razorbills flying over the sea area surveyed were observed during the survey campaign on 6–7 February 2023. In total, as many as 1464 individuals of this species were observed in flight at that time, which denoted the abundance index of 168.3 individuals in flight per 10 km of the vessel passage route [Figure 3.99]. In the reference area, the highest abundances of this species were also observed in the winter, when 93 and 74 birds were recorded sitting on the water on 6 December 2022 and 22 February 2023, respectively (the abundance index of 17.9 and 14.2 respectively [Figure 3.99]. In both sea areas, razorbills recorded in flight usually account for the majority of the observations of this species.

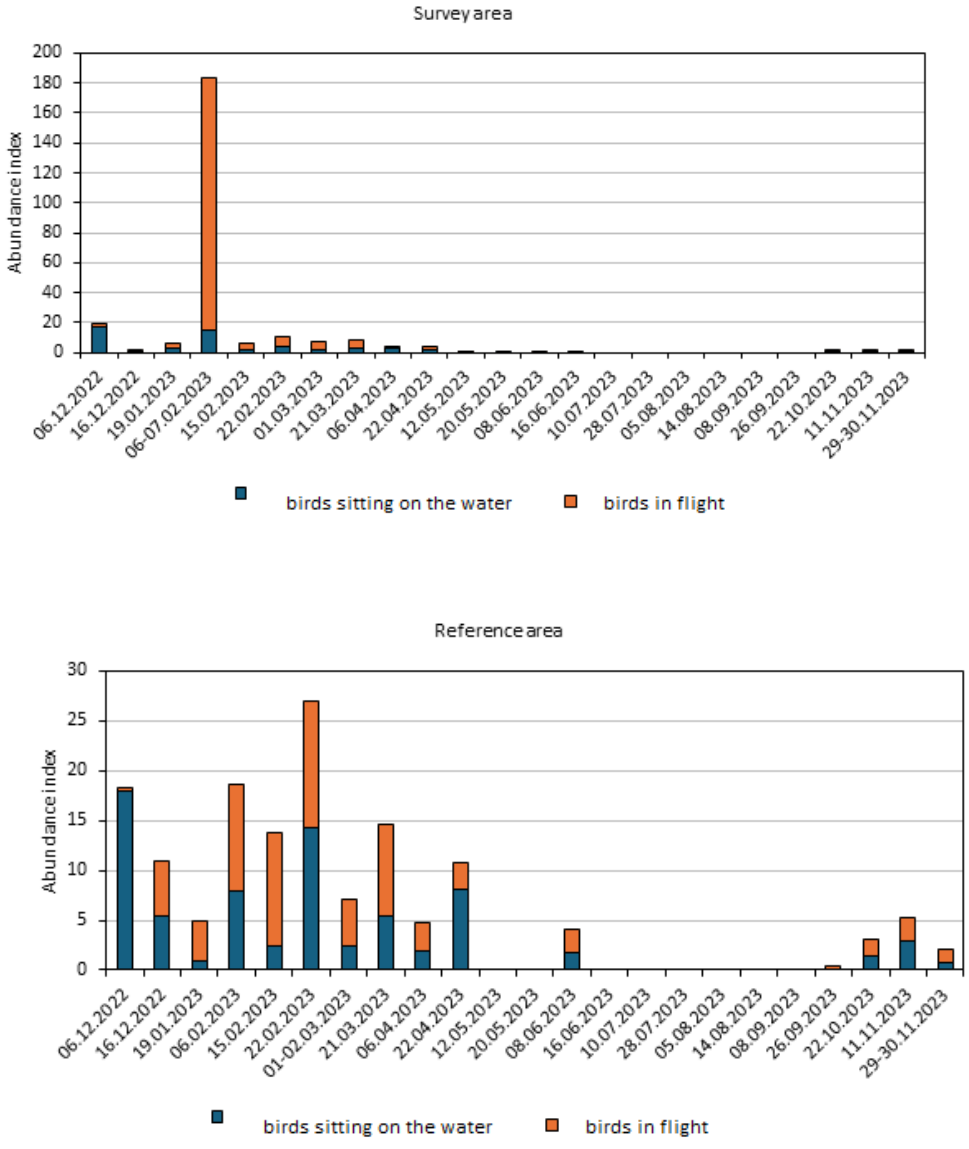


Figure 3.99. The changes in the abundance index of the razorbill during successive survey campaigns within the survey area and in the reference area

The phenology of the common guillemot occurrences differed considerably in the two areas discussed. In the survey area, by far the largest number of birds of this species was observed between late July and early September, when between 52 (on 5 August 2023) and 112 individuals (on 8 September 2023) were recorded along the vessel passage route, which translated into the abundance index ranging from 6.0 to 12.9 [Figure 3.100]. In the reference area, the common guillemot was most abundant on 6 December 2022, when 61 birds were recorded along the vessel passage route (with an abundance index of 11.7). Its abundance index during the remaining survey campaigns was low and, apart from three cases, did not exceed 2 individuals per 10 km of the vessel passage route [Figure 3.100]. During the period of the most abundant occurrence of the common guillemot in the survey area, in the reference area this species was extremely sparse and only on 8 September 2023, 23 birds of this species were recorded over there (the abundance index of 4.4 individuals per 10 km of the vessel passage route) [Figure 3.100].

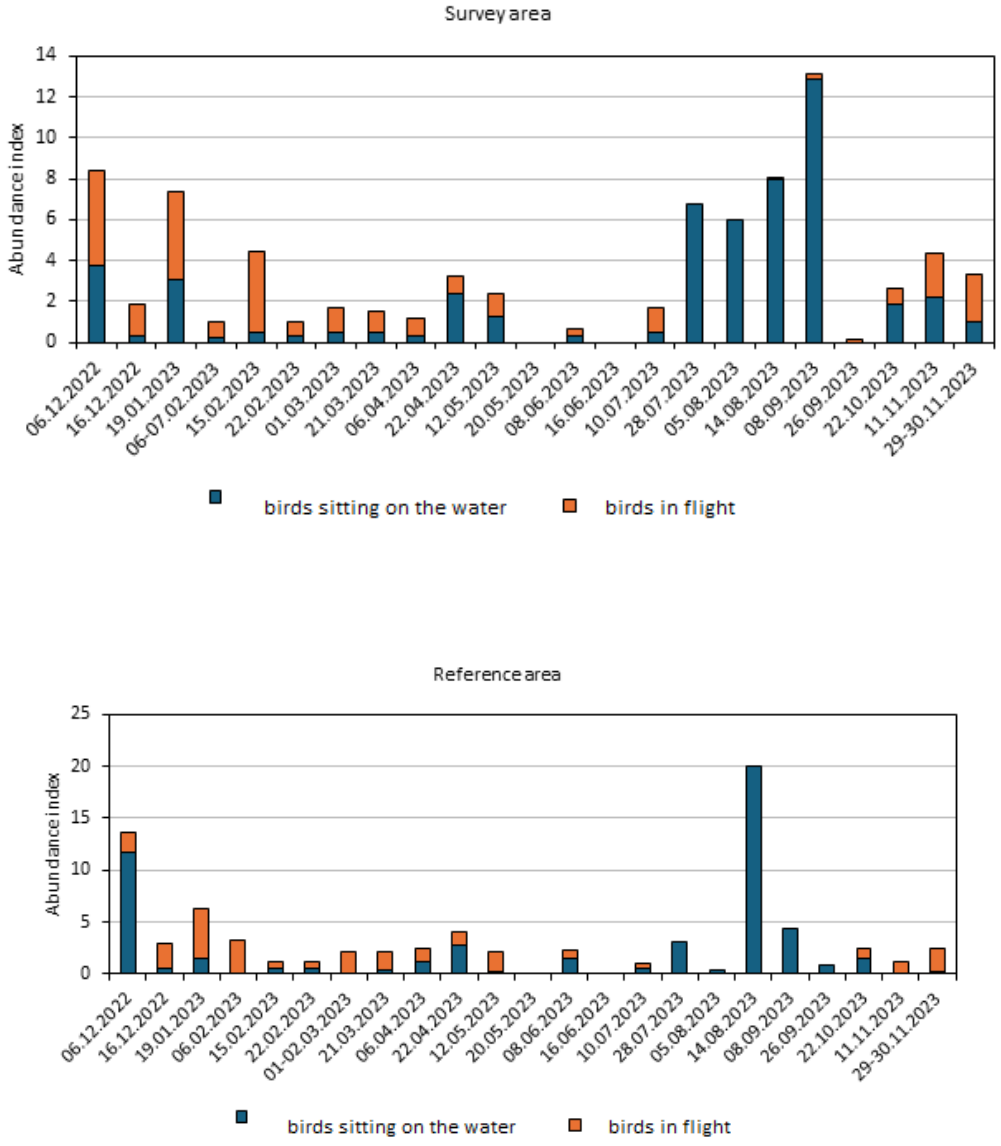


Figure 3.100. The changes in the abundance index of the common guillemot during successive survey campaigns within the survey area and in the reference area

3.5.1.5.3 Altitude of bird flights

3.5.1.5.3.1 Survey area

During all survey campaigns conducted in the survey area, a total of 11,673 birds flying over the water were recorded and their flight altitudes were determined. The average number of birds recorded in flight during one survey vessel passage was 486.4 individuals, including 857.8 during the wintering period, 701.7 during the spring migration period, 106.5 during the summer and 100.5 during the autumn migration period. The highest number of birds in flight was recorded during the survey campaign held on 6–7 February 2023 (3802 individuals) and on 22 April 2023 (3124 individuals) [Figure 3.101]. The observations conducted on 6–7 February 2023 concerned mostly the European herring gull and on 22 April 2023 – the long-tailed duck, which accounted for 79.0% and 85.4%, respectively, of all the birds observed in flight at that time. Outside these two survey campaigns, the number of birds flying over the survey area was low, not exceeding 400 individuals recorded during one survey campaign. During all survey campaigns, birds flying at collision heights (30–300 m) typically accounted for less than 10% of all birds recorded in flight. The threshold of 20% of flights at potential collision heights was recorded on five occasions, including as much as 49.4% of all passages recorded at these altitudes on 22 October 2023 [Figure 3.101]. However, these high values were observed on days characterised by very low flight intensity, when the abundance of birds passing over the survey area ranged from 36 to 387 individuals [Figure 3.101].

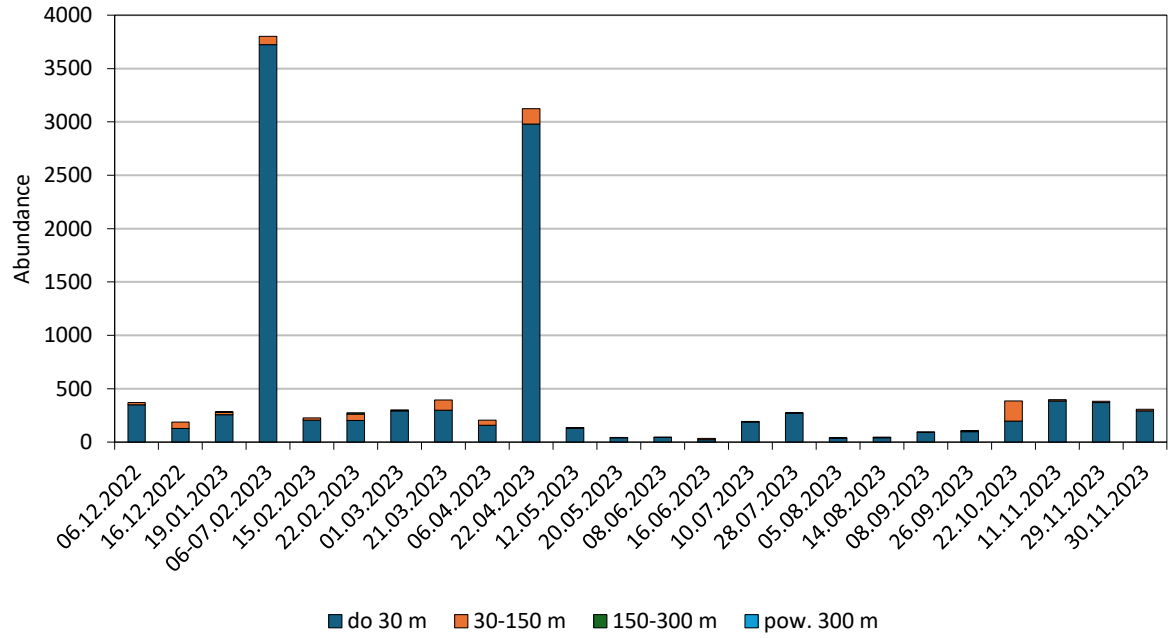


Figure 3.101. The changes in the abundance of birds flying over the survey area at various heights during successive inspections

As many as 92.5% of birds flying over the survey area were observed at the lowest altitudes, below 30 m ASL [Table 3.72]. Within the highest altitude zone, above 300 m, no birds were recorded. A total of 870 birds were recorded in flight at potential collision heights during the 24 survey campaigns, which accounted for 7.4% of all the flights observed. Such a result was mainly due to the observations of the greater white-fronted goose and the European herring gull [Table 3.72], which together constituted 70.5% of all the individuals spotted at this altitude.

Table 3.72. The abundance of individual bird species flying over the survey area at the heights specified and the proportion of flights in these zones

Taxon	≤30 m	30–150 m	150–300 m	>300 m	Total	Proportion [%]
Seabirds						
European herring gull *Larus argentatus*	2561	324	14		2899	24.8
Long-tailed duck *Clangula hyemalis*	2788	32			2820	24.2
Common scoter *Melanitta nigra*	1827	27			1854	15.9
Razorbill *Alca torda*	1778				1778	15.2
Common guillemot *Uria aalge*	265	2			267	2.3
Velvet scoter *Melanitta fusca*	100	12			112	1.0
Little gull *Hydrocoloeus minutus*	67	4			71	0.6
Black guillemot *Cepphus grylle*	56				56	0.5
Black-throated diver *Gavia arctica*	38				38	0.3
Lesser black-backed gull *Larus fuscus*	33	2			35	0.3
Great black-backed gull *Larus marinus*	20	4			24	0.2
Red-throated diver *Gavia stellata*	14	7			21	0.2
Arctic skua *Stercorarius parasiticus*	4				4	+
Arctic tern *Sterna paradisaea*	4				4	+
Red-necked grebe *Podiceps grisegena*	1				1	+
Black-legged kittiwake *Rissa tridactyla*	1				1	+
Common eider *Somateria mollissima*	1				1	+
Pomarine skua *Stercorarius pomarinus*	1				1	+
Waterbirds rarely encountered at sea far from the coast						
Common gull *Larus canus*	489	52			541	4.6
Greater white-fronted goose *Anser albifrons*	43	275			318	2.7
Greater scaup *Aythya marila*	194	64			258	2.2
Great black cormorant *Phalacrocorax carbo*	25	8			33	0.3
Mallard *Anas platyrhynchos*	27				27	0.2
Mute swan *Cygnus olor*	14	9			23	0.2
Goosander *Mergus merganser*	16	2			18	0.2
Common teal *Anas crecca*	14				14	0.1
Red-breasted merganser *Mergus serrator*	12				12	0.1
Eurasian wigeon *Anas penelope*	8				8	0.1
Greylag goose *Anser anser*	7				7	0.1
Tufted duck *Aythya fuligula*	6				6	0.1
Whooper swan *Cygnus cygnus*	11	1			12	0.1
Black-headed gull *Chroicocephalus ridibundus*	4				4	+
Common tern *Sterna hirundo*	3				3	+
Common goldeneye *Bucephala clangula*	1				1	+
Great crested grebe *Podiceps cristatus*	1				1	+
Birds of terrestrial environments						
Eurasian siskin *Carduelis spinus*	49				49	0.4

Taxon	≤30 m	30–150 m	150–300 m	>300 m	Total	Proportion [%]
White wagtail *Motacilla alba*	19				19	0.2
Meadow pipit *Anthus pratensis*	17				17	0.1
Eurasian curlew *Numenius arquata*	4	13			17	0.1
Eurasian skylark *Alauda arvensis*	14				14	0.1
Common chaffinch *Fringilla coelebs*	14				14	0.1
Whimbrel *Numenius phaeopus*	10				10	0.1
Goldfinch *Carduelis carduelis*	9				9	0.1
Great tit *Parus major*	6				6	0.1
Common starling *Sturnus vulgaris*	5				5	+
Eurasian wren *Troglodytes troglodytes*	4				4	+
European robin *Erithacus rubecula*	3				3	+
Common swift *Apus apus*	2				2	+
Grey heron *Ardea cinerea*	2				2	+
Great white egret *Egretta alba*	2				2	+
Western yellow wagtail *Motacilla flava*	2				2	+
Grey plover *Pluvialis squatarola*	2				2	+
Goldcrest *Regulus regulus*	2				2	+
Northern goshawk *Accipiter gentilis*	1				1	+
Long-eared owl *Asio otus*	1				1	+
Twite *Carduelis flavirostris*	1				1	+
Hooded crow *Corvus corone*		1			1	+
Brambling *Fringilla montifringilla*	1				1	+
White-tailed eagle *Haliaeetus albicilla*		1			1	+
Common chiffchaff *Phylloscopus collybita*	1				1	+
Snow bunting *Plectrophenax nivalis*	1				1	+
Song thrush *Turdus philomelos*		1			1	+
Birds unidentified to species						
Unidentified passerines *Passeriformes*	119				119	1.0
Unidentified ducks *Anatidae*	39	3			42	0.4
Unidentified diver *Gavia sp.*	11	4			15	0.1
Unidentified swan *Cygnus* sp.	7	7			14	0.1
Unidentified seagulls *Laridae*	11				11	0.1
Unidentified tern *Sterna sp.*	10				10	0.1
Unidentified skua *Stercorarius* sp.		1			1	+
Total	**10803**	**856**	**14**		**11673**	**100**
Proportion [%]	**92.5**	**7.3**	**0.1**	**0.0**	**100**	**-**

+ - proportion below 0.1%

3.5.1.5.3.2 Reference area

In the reference area, a total of 8256 birds migrating over water were recorded and their flight altitudes were determined. The average number of birds recorded in flight during one survey vessel passage was

344.0 individuals, including 405.0 during the wintering period, 640.5 during the spring migration period, 84.2 during the summer and 279.5 during the autumn migration period. The highest number of birds in flight was recorded during the first two survey campaigns, which were conducted in March. On 1–2 March 2023, 1940 individuals in flight were observed and on 21 March 2023 – 1023 individuals in flight [Figure 3.102]. These observations mostly concerned the long-tailed duck, which accounted for 92.5% and 81.8% of all birds observed in flight, respectively. Outside these two survey campaigns, the number of birds flying over the reference area was low, not exceeding 500 individuals recorded during one survey campaign. Only on 19 January 2023 and 15 February 2023, there were 596 and 791 individuals recorded, respectively, passing over the surveyed area [Figure 3.102]. Also in these cases, the long-tailed duck was the most abundant species, accounting for 76.0% and 84.8% of all the birds observed in flight. During all survey campaigns, birds flying at potential collision heights (30–300 m) typically accounted for less than 10%. The threshold of 20% at potential collision heights was recorded on four occasions, including as much as 50.0% of all passages recorded at these altitudes on 16 June 2023 [Figure 3.102]. However, these high values were observed on days characterised by very low flight intensity, when the abundance of birds passing over the survey area ranged from 4 to 236 individuals [Figure 3.102].

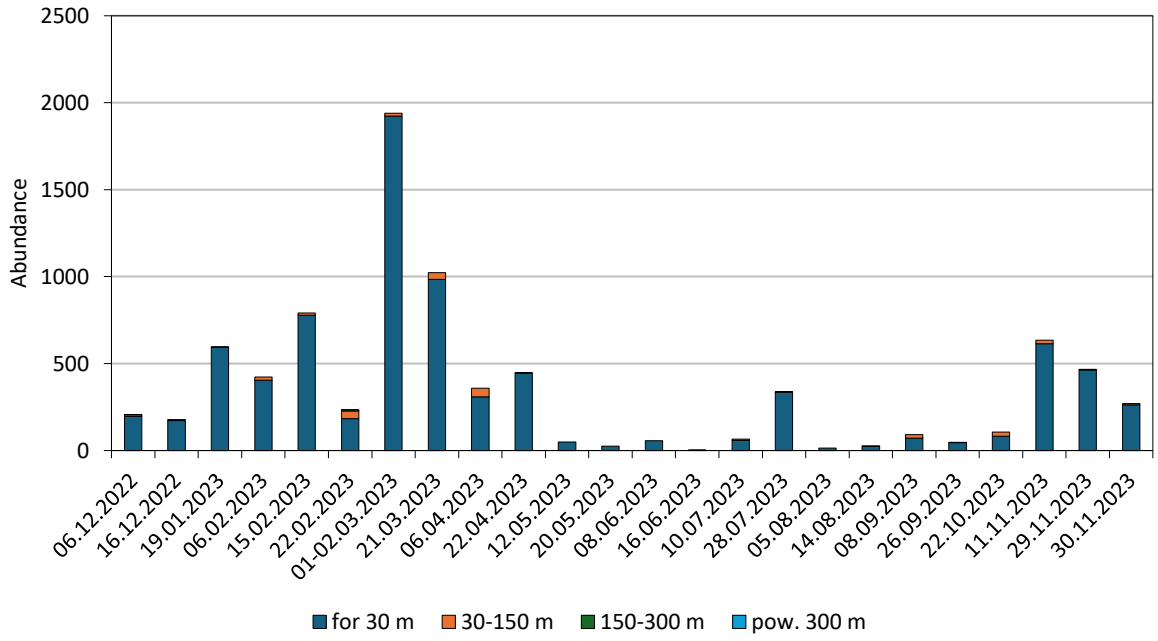


Figure 3.102. The changes in the abundance of birds flying over the reference area at various heights during successive inspections

As many as 96.8% of birds flying over the reference area were observed at the lowest altitude, below 30 m above the sea surface [Table 3.73]. In the highest zone, above 300 m, only two birds were recorded. A total of 297 birds were recorded in flight at potential collision heights during the 24 survey campaigns, which accounted for 3.2% of all the flights observed. This result was mainly due to the sightings of gulls, including the most abundant European herring gull [Table 3.73]. In total, gulls accounted for 74.3% of all the individuals recorded at that altitude.

Table 3.73. The abundance of individual bird species flying over the reference area at the heights specified and the proportion of flights in these zones

Taxon	≤30 m	30–150 m	150–300 m	>300 m	Total	Proportion [%]
Seabirds						
Long-tailed duck *Clangula hyemalis*	5616	15			5631	68.2
Common scoter *Melanitta nigra*	658	11			669	8.1
European herring gull *Larus argentatus*	385	130	7	2	524	6.3
Razorbill *Alca torda*	382				382	4.6
Common guillemot *Uria aalge*	154	1			155	1.9
Little gull *Hydrocoloeus minutus*	39	4			43	0.5
Velvet scoter *Melanitta fusca*	32	2			34	0.4
Lesser black-backed gull *Larus fuscus*	15	6			21	0.3
Black-throated diver *Gavia arctica*	19				19	0.2
Black guillemot *Cepphus grylle*	10				10	0.1
Red-throated diver *Gavia stellata*	5	3			8	0.1
Arctic tern *Sterna paradisaea*	6				6	0.1
Sandwich tern *Sterna sandvicensis*	2				2	+
Great black-backed gull *Larus marinus*	1				1	+
Arctic skua *Stercorarius parasiticus*	1				1	+
Black-legged kittiwake *Rissa tridactyla*	1				1	+
Waterbirds rarely encountered at sea far from the coast						
Common gull *Larus canus*	416	58	1		475	5.8
Eurasian wigeon *Anas penelope*	96	12			108	1.3
Red-breasted merganser *Mergus serrator*	37	2			39	0.5
Mallard *Anas platyrhynchos*	26	2			28	0.3
Great black cormorant *Phalacrocorax carbo*	16	5			21	0.3
Mute swan *Cygnus olor*	14				14	0.2
Common teal *Anas crecca*	9				9	0.1
Common goldeneye *Bucephala clangula*	9				9	0.1
Greater white-fronted goose *Anser albifrons*		5			5	0.1
Black-headed gull *Chroicocephalus ridibundus*	3	1			4	+
Goosander *Mergus merganser*	4				4	+
Pintail *Anas acuta*	3				3	+
Common tern *Sterna hirundo*	3				3	+
Greater scaup *Aythya marila*	1				1	+
Birds of terrestrial environments						
Common swift *Apus apus*	6				6	0.1
Eurasian skylark *Alauda arvensis*	3				3	0.0
Grey heron *Ardea cinerea*	3				3	+
Goldcrest *Regulus regulus*	3				3	+
White wagtail *Motacilla alba*	2				2	+
Common starling *Sturnus vulgaris*	2				2	+

Taxon	≤30 m	30–150 m	150–300 m	>300 m	Total	Proportion [%]
Meadow pipit *Anthus pratensis*	1				1	+
Great white egret *Egretta alba*	1				1	+
European robin *Erithacus rubecula*	1				1	+
Barn swallow *Hirundo rustica*	1				1	+
Western yellow wagtail *Motacilla flava*	1				1	+
Eurasian wren *Troglodytes troglodytes*	1				1	+
Song thrush *Turdus philomelos*	1				1	+
Eurasian siskin *Carduelis spinus*						
Birds unidentified to species						
Unidentified ducks *Anatidae*	40				40	0.5
Unidentified swan *Cygnus* sp.	33				33	0.4
Unidentified geese *Anserinae*		28			28	0.3
Unidentified diver *Gavia sp.*	19	4			23	0.3
Unidentified passerines *Passeriformes*	9				9	0.1
Unidentified tern *Sterna sp.*	6				6	0.1
Total	**7989**	**257**	**8**	**2**	**8256**	**100**
Proportion [%]	**96.8**	**3.1**	**0.1**	**+**	**100**	**-**

+ - proportion below 0.1%

3.5.1.5.4 Bird distribution

Averaging the densities of the entire grouping for the twelve-month survey period allows us to identify the fragments of the survey area in which seabirds aggregated in the highest numbers. There was a clear correlation between average density and depth – the highest average densities, exceeding 50 ind.·km^{-2}, were recorded in the shallowest part of the sea area surveyed. The area of high densities (10–50 ind.·km^{-2}) was mostly observed in the zone up to the 30-m isobath. On the other hand, in the deeper part of the sea area designated for the planned project, the average density of avifauna was below 5 ind.·km^{-2} [Figure 3.103]. Such a correlation was not observed in the reference area, in which the part of the sea area with the highest densities (10–50 ind.·km^{-2}) is situated in a wide depth range, between the 20 and 40-m isobaths [Figure 3.103].

The long-tailed duck was the most abundant species within both sea areas and its distribution largely determined the spatial distribution of average densities of the entire seabird grouping. In the shallowest part of the survey area, where the depth was less than 20 m, its densities were locally very high, exceeding 100 ind.·km^{-2} [Figure 3.104]. The example of this species, which feeds on benthic organisms, very clearly illustrates the dependence of its density on the depth of the sea area. In the depth zone exceeding 30 m, the long-tailed duck was recorded in small numbers and in a wide area it was not found at all [Figure 3.104]. In the reference area, on the other hand, the correlation between density and depth was not evident, while around the 20-m isobath the average density was very low [Figure 3.104]. The reason for this distribution of the long-tailed duck in the reference area may be due to a lower supply of food resources in the shallowest part of the sea area.

Summarising the data on the annual distribution of the European herring gull, it can be noted that the average densities in both areas were low (below 5 ind.·km^{-2}) and the correlation with depth was not

observed there [Figure 3.105]. Concentrations of the European herring gull in the open sea are related to the fishing activity of fishing vessels, hence the locations of the abundant presence of this species are not constant and the distribution of average densities is even over a large area.

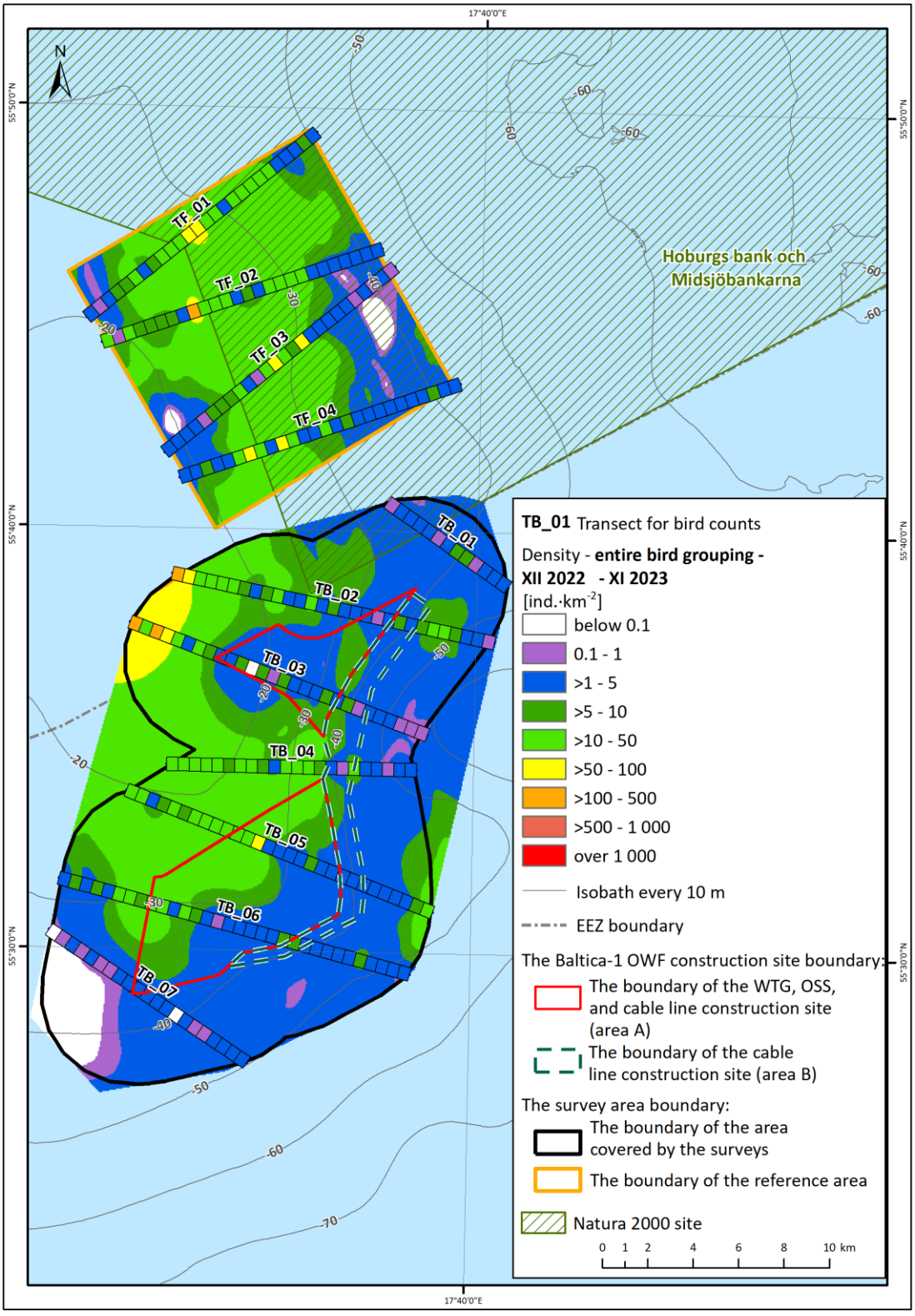


Figure 3.103. The spatial distribution of the average densities of all birds within the survey area and the reference area between December 2022 and November 2023

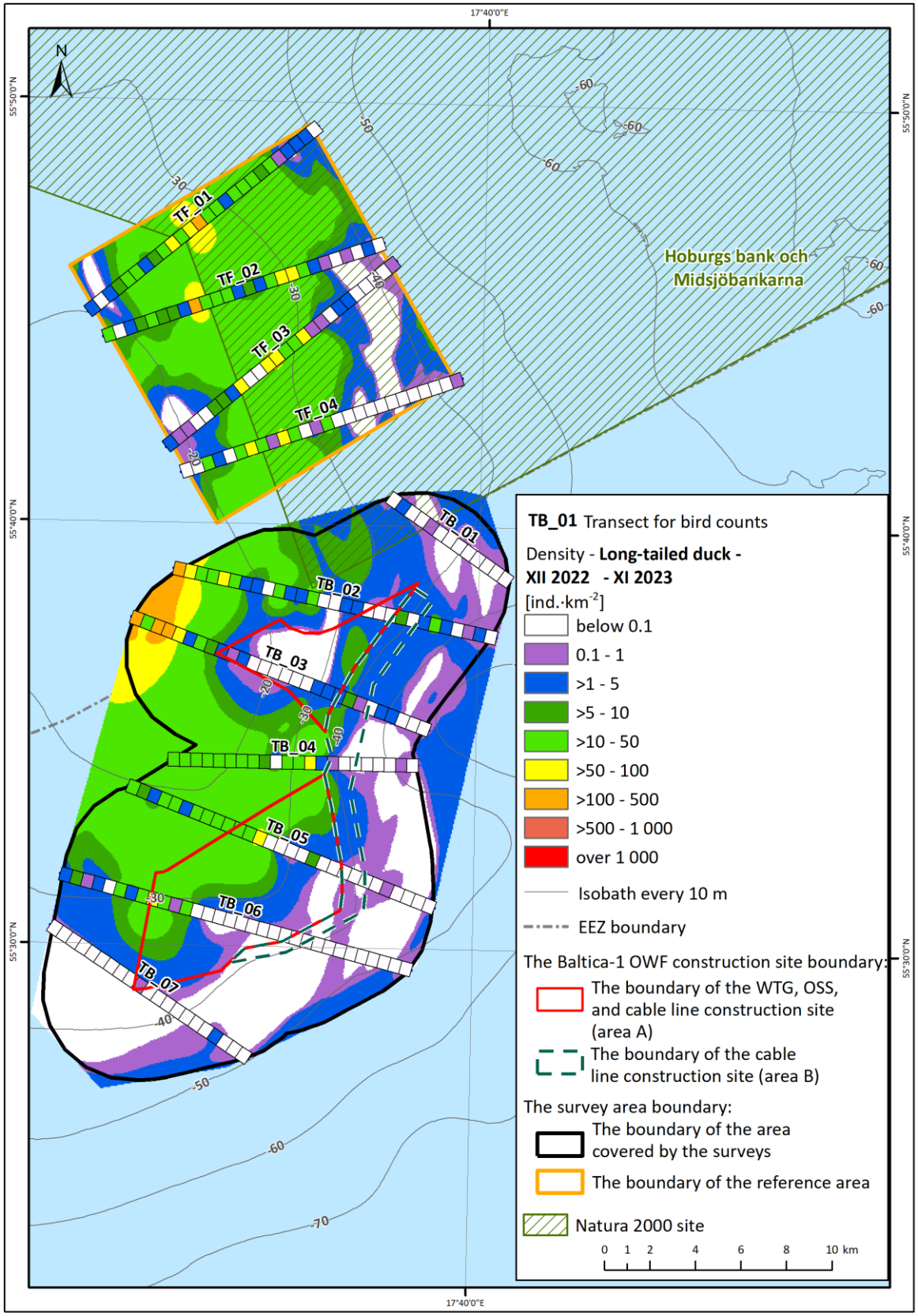


Figure 3.104. The spatial distribution of the average densities of the long-tailed duck within the survey area and the reference area between December 2022 and November 2023

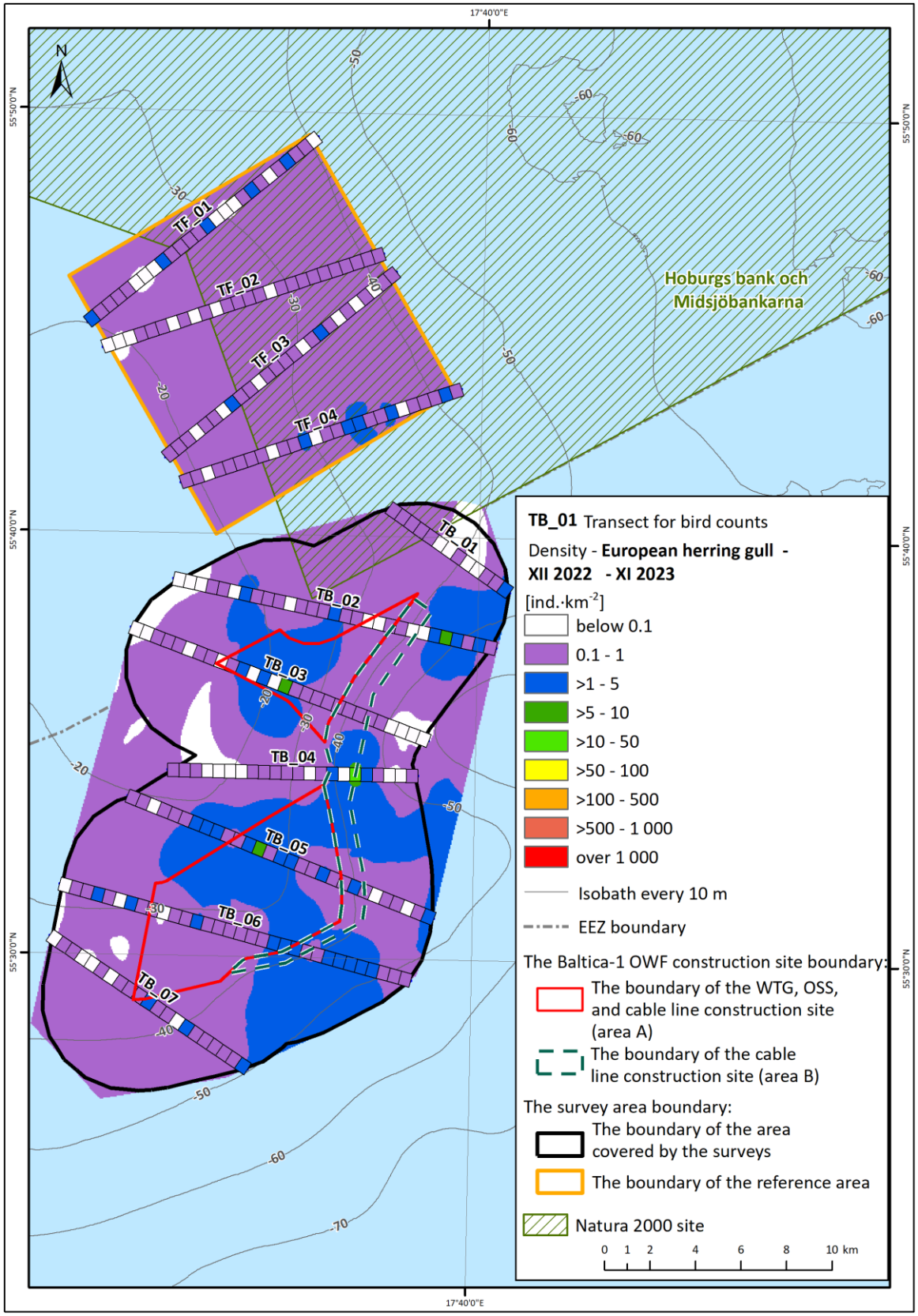


Figure 3.105. The spatial distribution of the average densities of the European herring gull within the survey area and the reference area between December 2022 and November 2023

3.5.1.5.4.1 Wintering period

During the winter period, the average densities of the entire grouping were slightly higher in the reference area than in the survey area. In the reference area, densities ranging from 10 to 50 ind.·km^{-2} prevailed; such values were recorded for approx. 70% of the surface of this sea area. On the other hand, in the survey area, densities ranging from 1 to 5 ind.·km^{-2} were recorded within more than 70% of its surface area, and the highest densities of avifauna in this area were found in its north-western part [Figure 3.106].

The long-tailed duck was the most abundant species within both sea areas, and its distribution largely determined the distribution of average densities. Within the survey area, the highest densities of the long-tailed duck were recorded in the north-western part of this sea area, where they exceeded 5 ind.·km^{-2}. Within the extensive south-eastern part of this area, which is also the deepest, no birds of this species were recorded [Figure 3.107]. Within the reference area, long-tailed ducks were found to be concentrated mainly in the central part of the area. The average densities for that area were higher than 10 ind.·km^{-2}. As in the case of the area intended for the construction of the wind farm, the lowest number of birds was observed within the deepest part of this sea area [Figure 3.107].

During the phenological period discussed, the European herring gull was distributed fairly evenly throughout the survey area. On 80% of the surface of this sea area, its average density reached 1 ind.·km^{-2} and was slightly higher only in the southern part of this sea area. A similar pattern of the European herring gull distribution was recorded in the reference area, with two locations of densities exceeding 1 ind.·km^{-2}. The spatial distribution of the average densities of the European herring gull was not conditioned by the sea area depth [Figure 3.108].

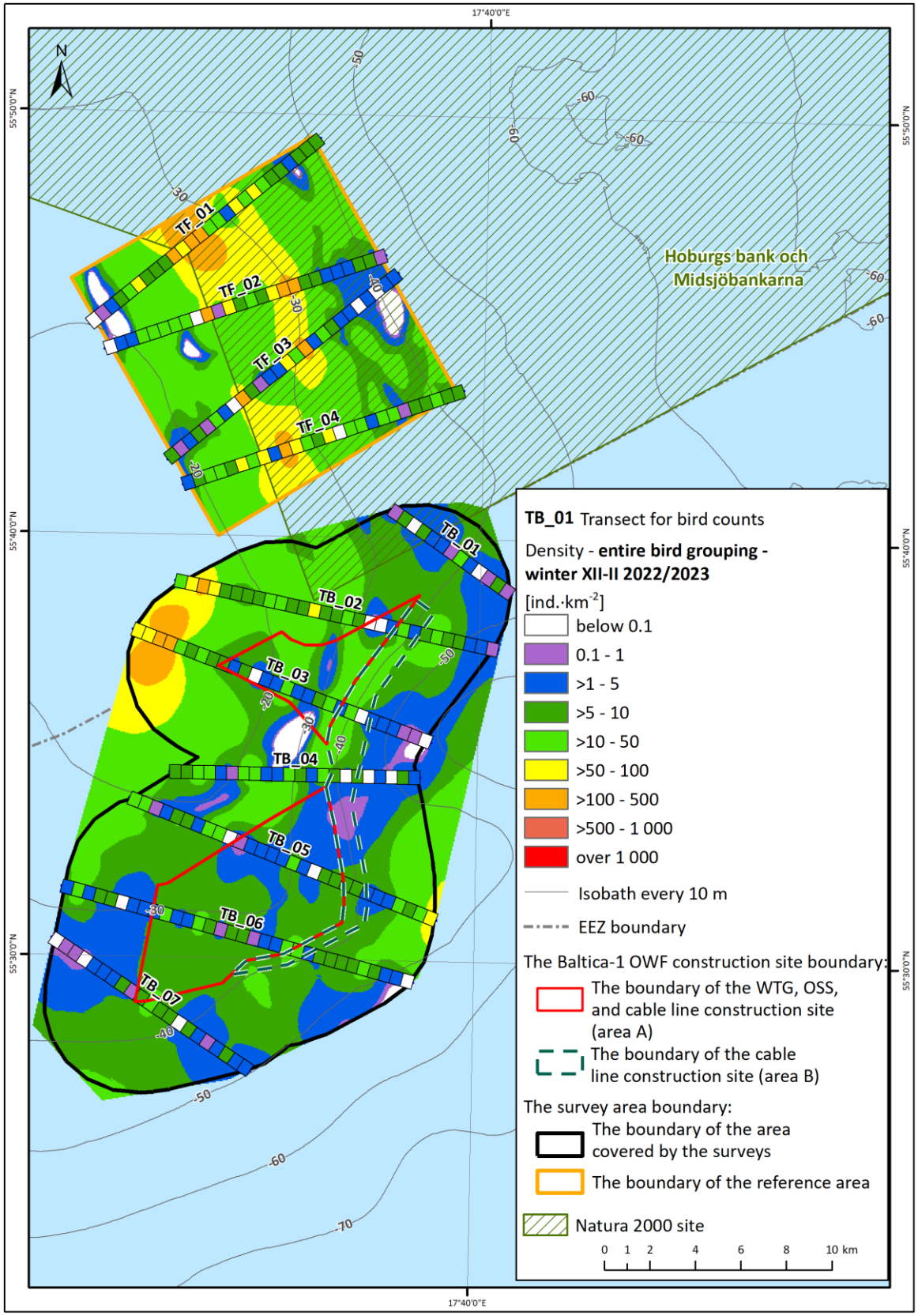


Figure 3.106. The spatial distribution of the average densities of all birds within the survey area and the reference area during the wintering period

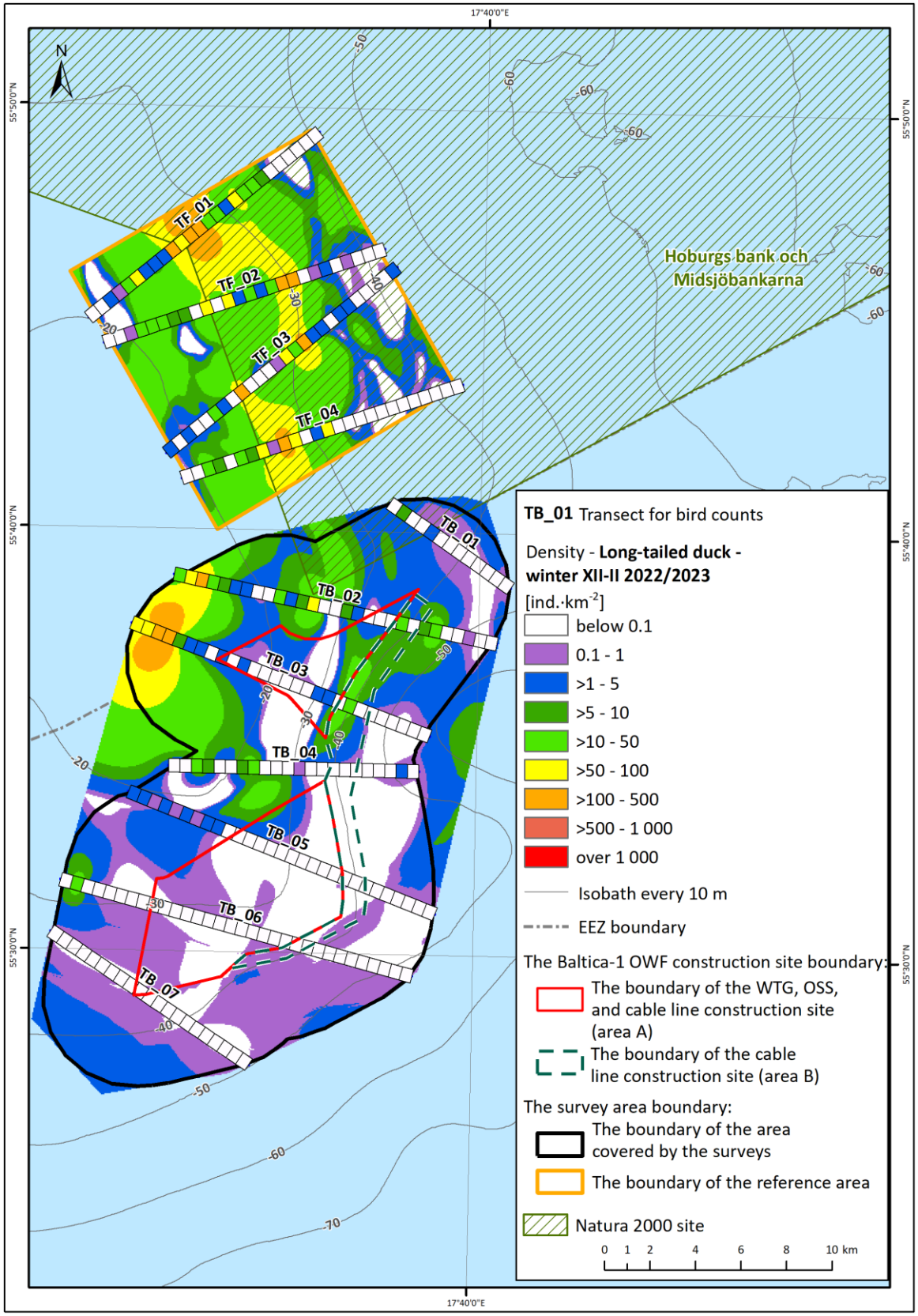


Figure 3.107. The spatial distribution of the average densities of the long-tailed duck within the survey area and the reference area during the wintering period



Figure 3.108. The spatial distribution of the average densities of the European herring gull within the survey area and the reference area during the wintering period

3.5.1.5.4.2 Spring migration period

During the spring migration, the average densities of the entire bird grouping were higher in the survey area, where in half of the area they remained within the range of 10–100 ind.·km^{-2}. The highest densities, above 50 ind.·km^{-2}, were recorded within approximately 20% of the entire survey area, in its western part [Figure 3.109]. In the reference area, the average bird densities above 50 ind.·km^{-2} occurred only locally, and densities within the range of 10–50 ind.·km^{-2} were found within approximately 75% of that sea area [Figure 3.109]. In the survey area, the tendency of densities decreasing with the increasing depth of the sea area was more pronounced than in the reference area.

The long-tailed duck was the most numerous species in both areas, and the largest number of birds of this species aggregated in the shallowest part of both sea areas. Densities recorded within the survey area were higher than in the reference area and, in approximately 15% of its area, they exceeded 50 ind.·km^{-2}, locally reaching up to 100 ind.·km^{-2} [Figure 3.110]. Although most of the sites with the highest densities are situated outside the boundaries of the future wind farm [Figure 3.110], it should be expected that after its construction, the majority of birds will be pushed out also from that part of the area (Petersen et al., 2006; Vanermen et al., 2014). In most of the reference area, the densities of long-tailed ducks ranged from 10 to 50 ind.·km^{-2}, and higher densities were recorded there only locally. In both areas, there is a strong tendency of the long-tailed duck density to decrease with the increasing depth of the sea area. In the deepest regions, these birds were not found, or the densities did not exceed 5 ind.·km^{-2} [Figure 3.110].

During the spring migration period, average densities of the European herring gull ranging from 0.1 to 1 ind.·km^{-2} prevailed in both sea areas [Figure 3.111]. Locally, in the survey area, they were slightly higher, reaching 5 ind.·km^{-2}. The results obtained indicate that this species occurs in both sea areas in a large dispersion and only locally forms slightly larger concentrations, most likely in places where fishing takes place.

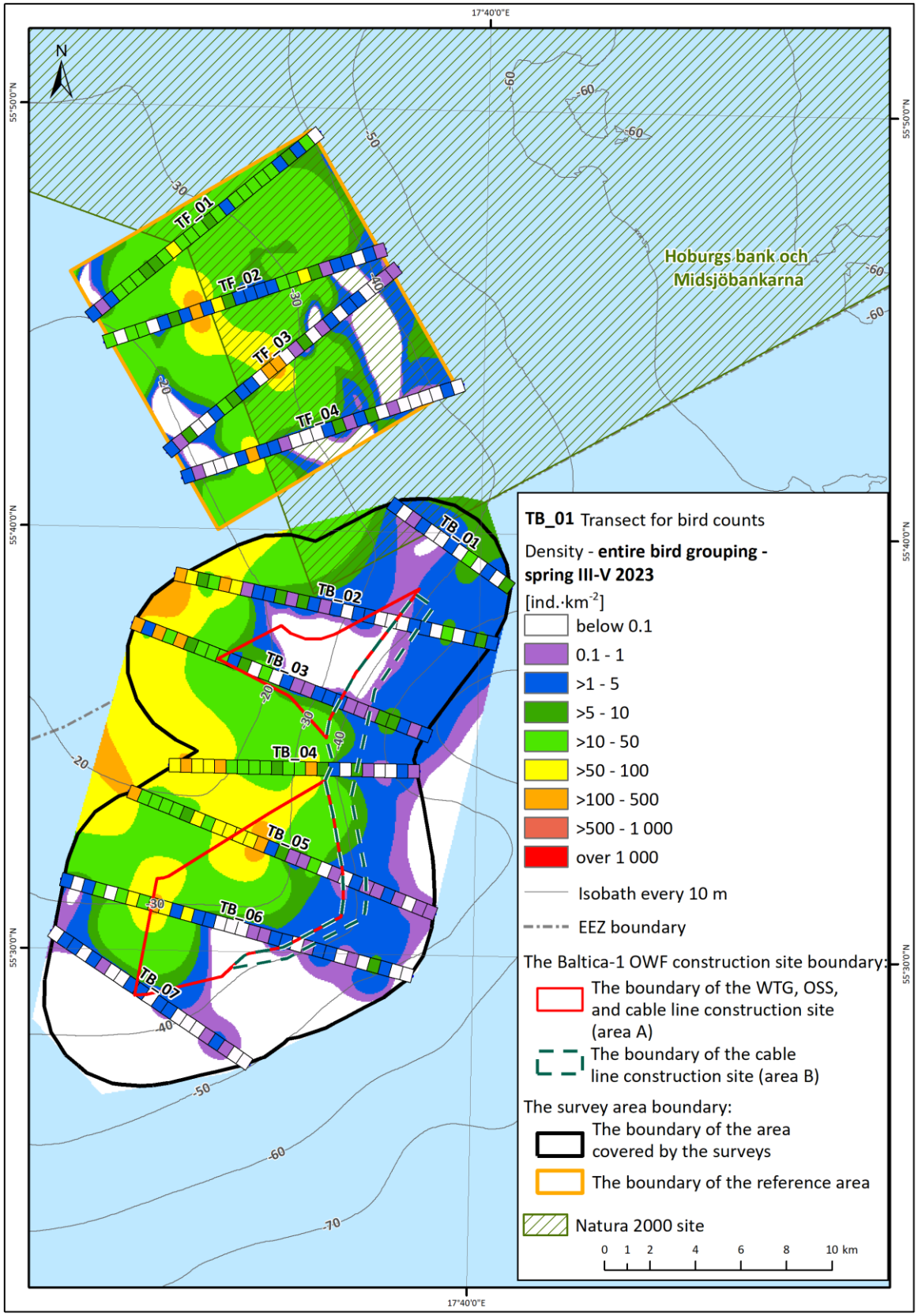


Figure 3.109. The spatial distribution of the average densities of all birds in the survey area and the reference area during the spring migration period

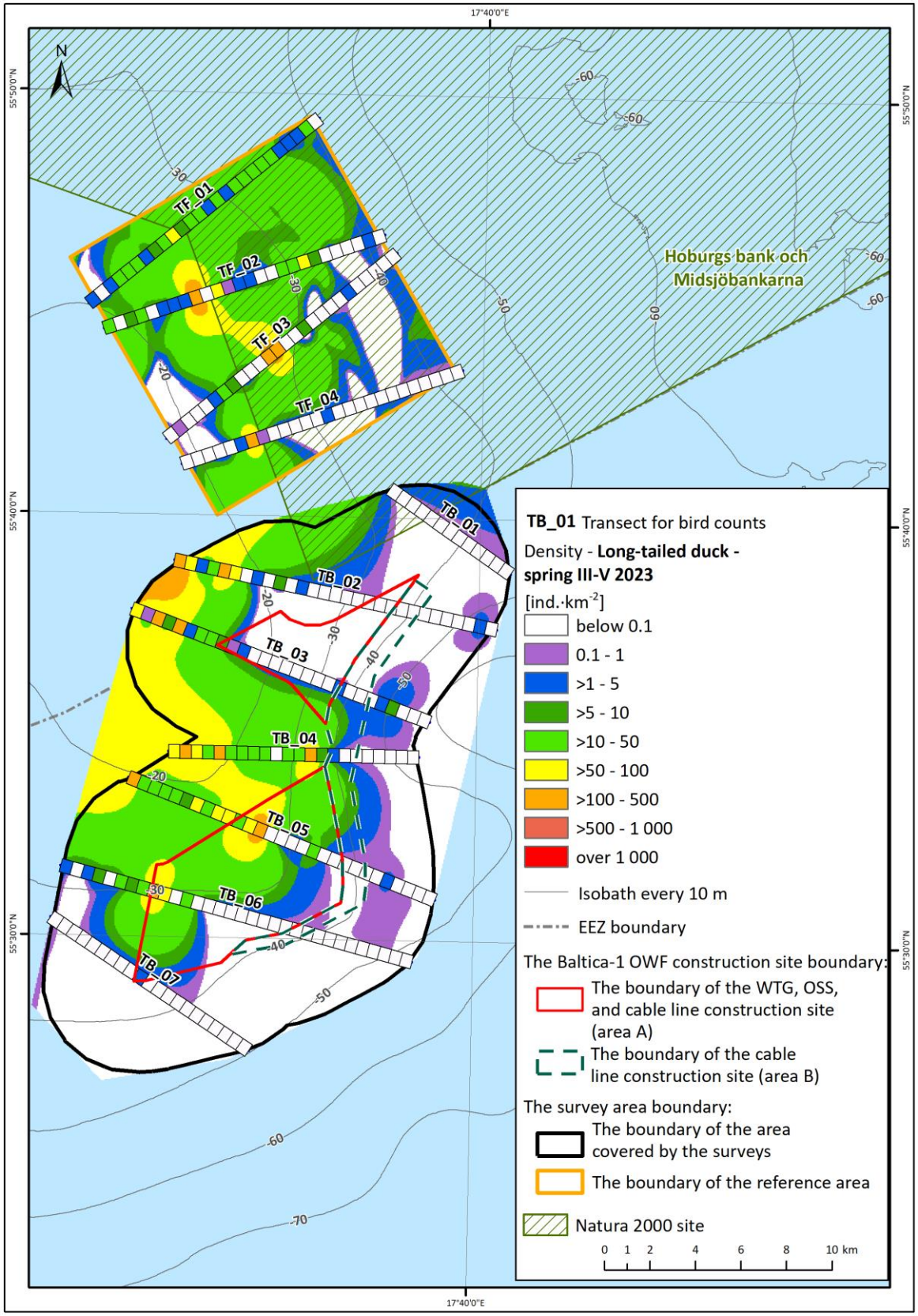


Figure 3.110. The spatial distribution of the average densities of the long-tailed duck within the survey area and the reference area during the spring migration period

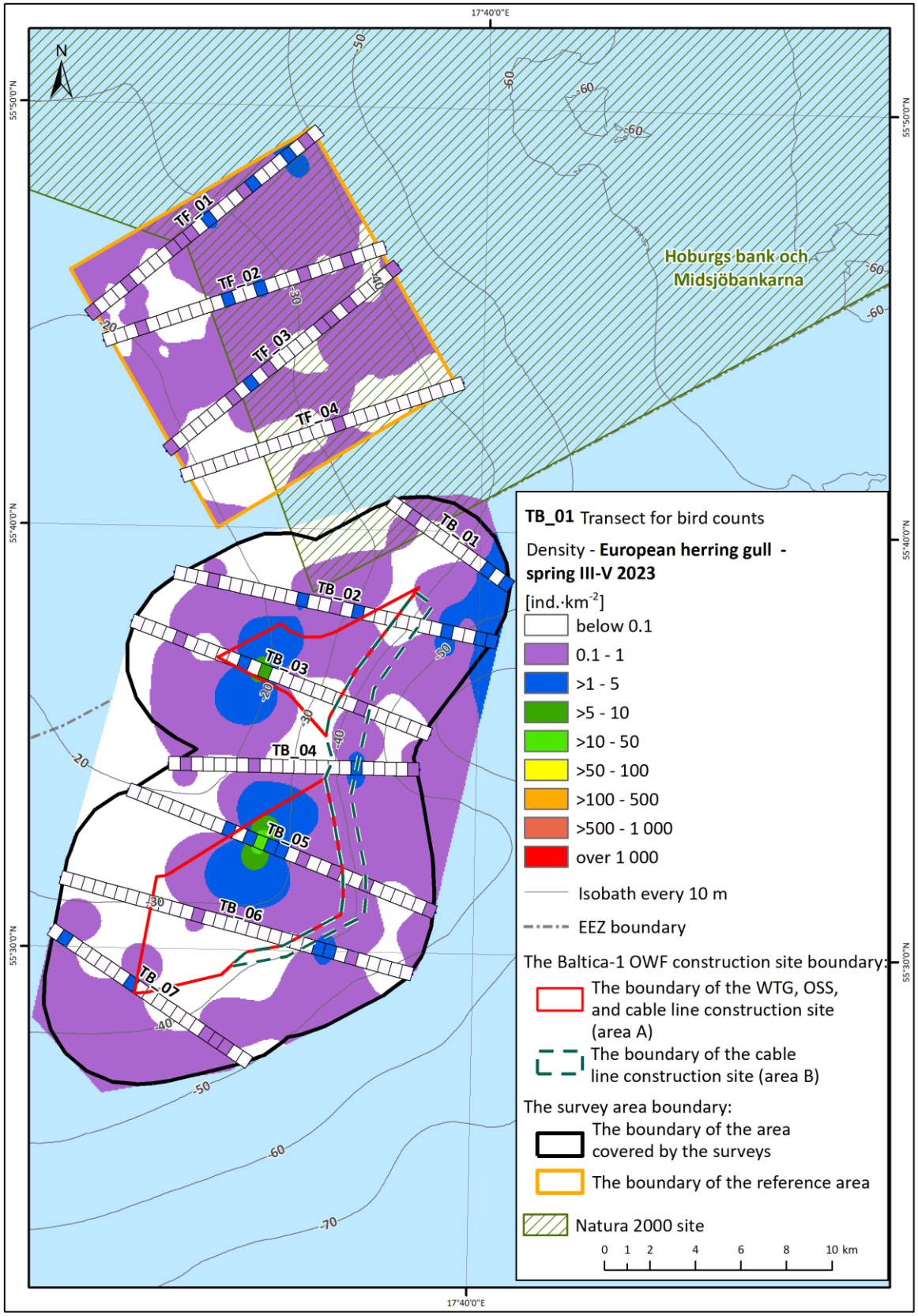


Figure 3.111. The spatial distribution of the average densities of the European herring gull within the survey area and the reference area during the spring migration period

3.5.1.5.4.3 Summer period

In summer, the average densities of the entire bird grouping in the survey area and in the reference area were very low, below 5 ind.·km^{-2}. The highest density, slightly exceeding the value of 5 and reaching up to 10 ind.·km^{-2} was recorded locally, in a small part of the central survey area, in its western part [Figure 3.112]. Contrary to the remaining phenological periods, during the summer there was no correlation between bird density and the depth of the sea area, which was due to the lack of benthophagous diving birds in the grouping – it is their presence that determines the occurrence of such a correlation.

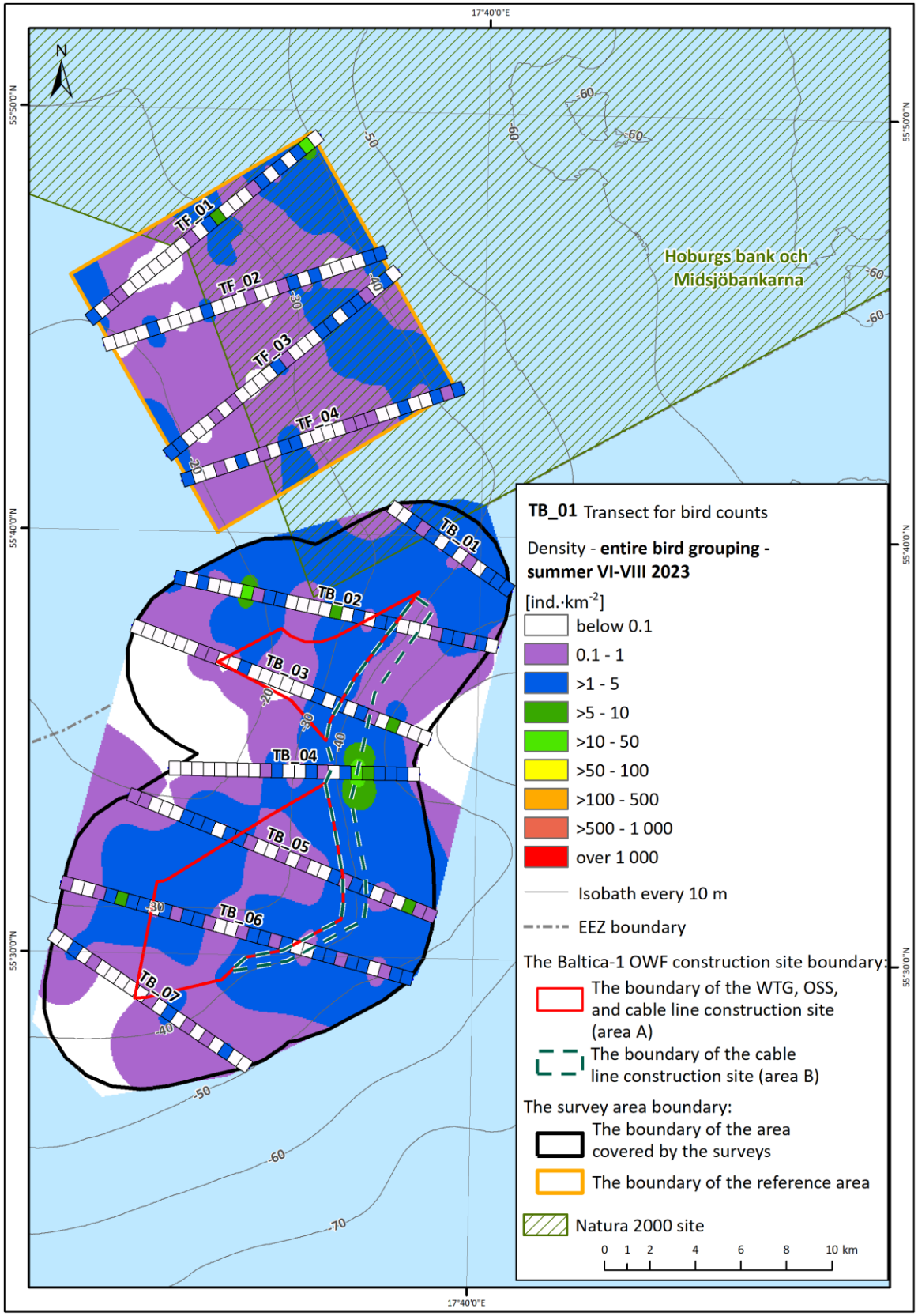


Figure 3.112. The spatial distribution of the average densities of all birds within the survey area and the reference area during summer

3.5.1.5.4.4 Autumn migration period

During the autumn migration period, the average densities of the entire avifauna grouping were higher in the survey area, exceeding 100 ind.·km^{-2} at the north-western end of the area, and remaining above 10 ind.·km^{-2} within a significant part of this sea area. In the rest of the survey area, however, the average bird densities were much lower, exceeding 5 ind.·km^{-2} only in small sections [Figure 3.113]. In the reference area, the average densities of avifauna were nowhere higher than 10 ind.·km^{-2}, remaining within the range of 1–5 ind.·km^{-2} within approximately 80% of the sea area [Figure 3.113].

The highest number of long-tailed ducks was observed in autumn in the north-western part of the survey area. Only there its average density was higher than 10 ind.·km^{-2}, locally exceeding even 100 ind.·km^{-2} [Figure 3.114]. The high concentration of birds of this species had a crucial influence on the pattern of the highest densities of the entire bird grouping in that sea area. In the remaining part of the survey area and in the reference area, long-tailed ducks were highly dispersed, with average densities reaching a maximum of 5 ind.·km^{-2} [Figure 3.114].

During the autumn migration period, the European herring gull was slightly more abundant in the survey area, with the average density locally exceeding 5 ind.·km^{-2}. However, the abundance of this species in the survey area and in the reference area its levels were low. The average densities below 1 ind.·km^{-2} prevailed in both sea areas, with that value being slightly exceeded in small parts of both of these areas [Figure 3.115].

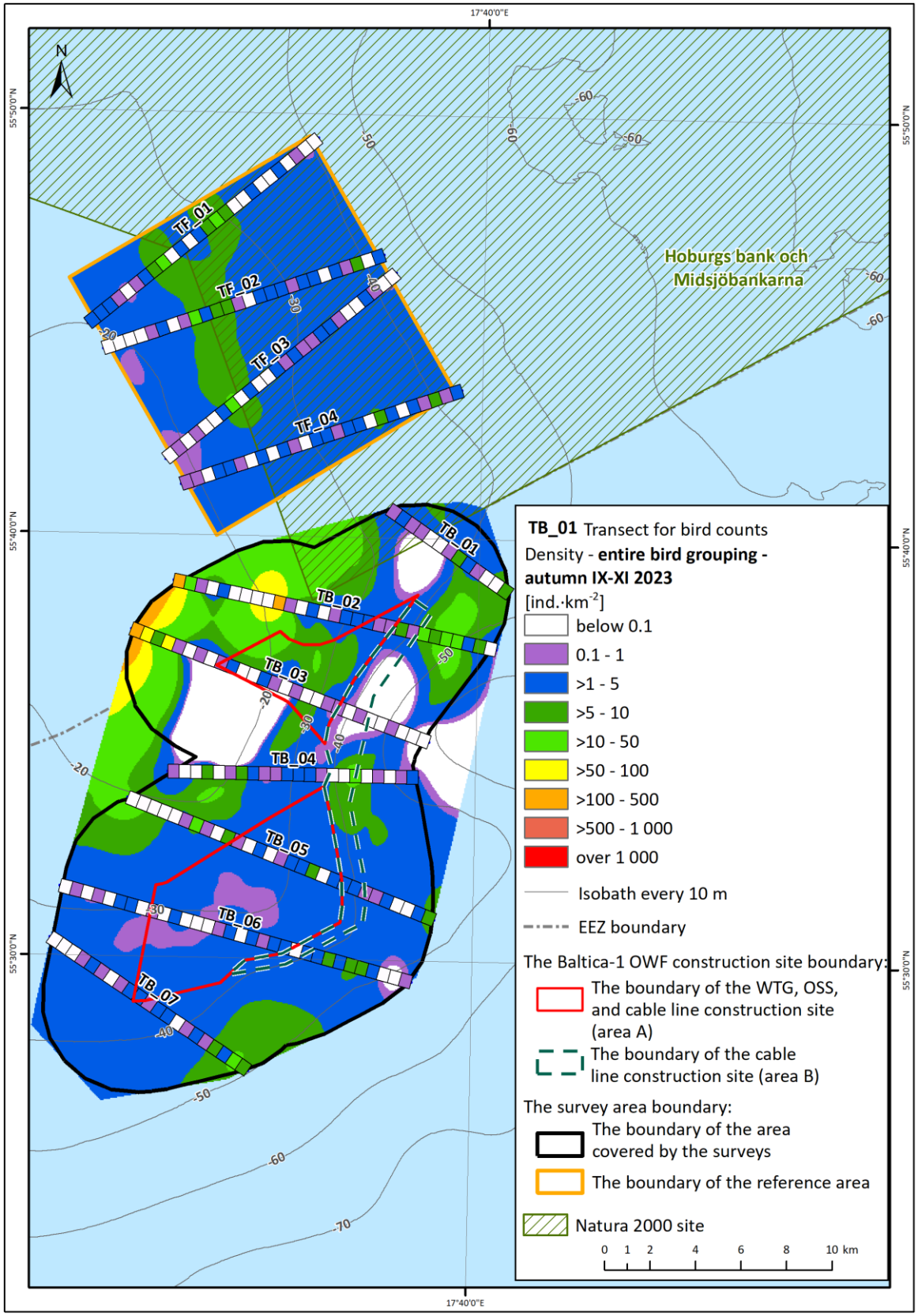


Figure 3.113. The spatial distribution of the average densities of all birds in the survey area and the reference area during the autumn migration period



Figure 3.114. The spatial distribution of the average densities of the long-tailed duck within the survey area and the reference area during the autumn migration period

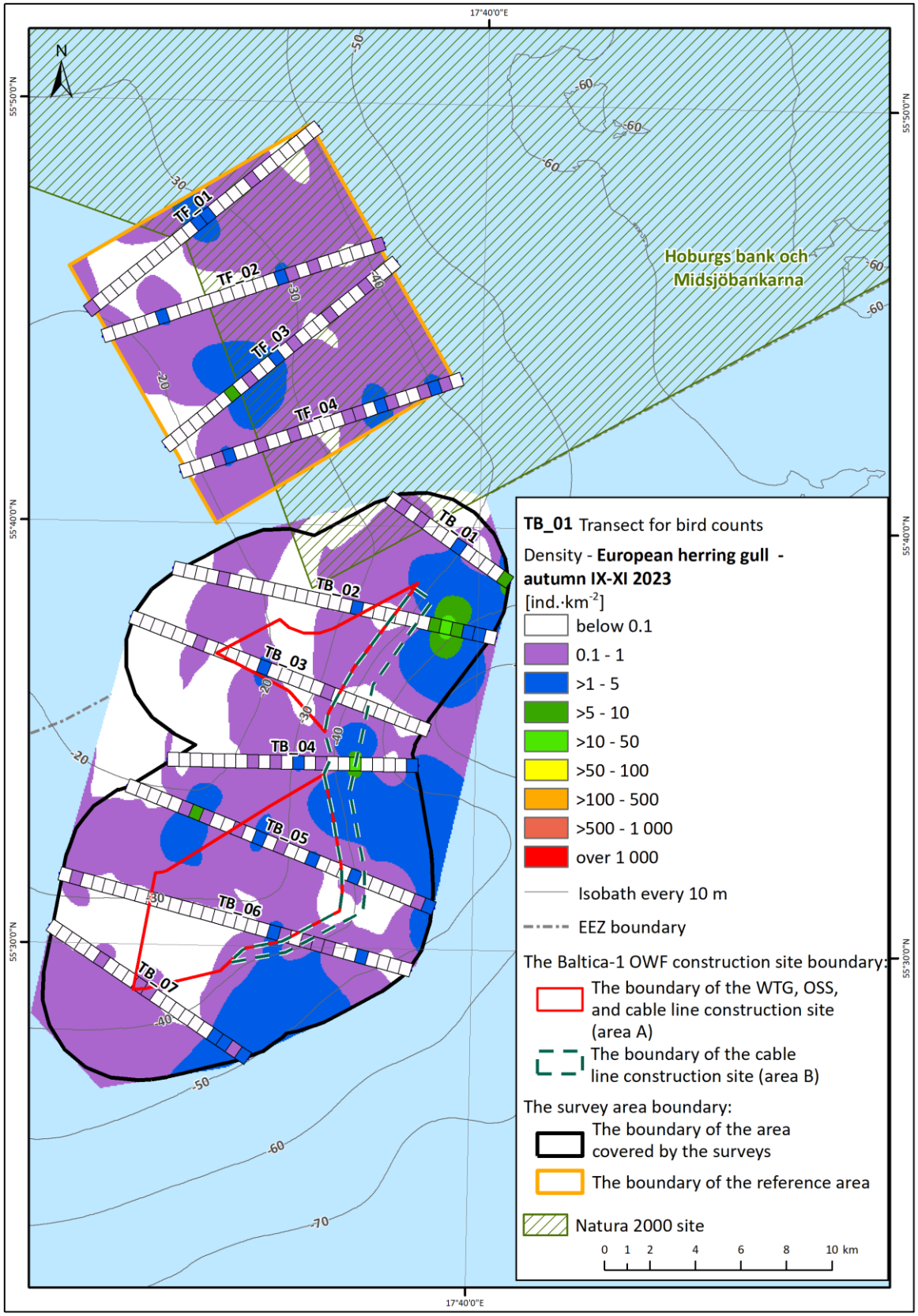


Figure 3.115. The spatial distribution of the average densities of the European herring gull within the survey area and the reference area during the autumn migration period

3.5.1.5.5 Conservation status of the seabird species identified

During the entire survey period, 13 seabird species were identified within the survey area, 4 of which were recorded in extremely low abundances. Those were the velvet scoter, the great black-backed gull, the yellow-billed diver and the red-throated diver. Therefore, it can be assumed that the survey area is not a significant location for them. Of the 9 remaining species, 8 are fully protected and one is under partial species protection in Poland [Table 3.74]. The black-throated diver and the little gull are listed in Annex I of the EU Birds Directive. Both these species have an elevated conservation status of SPEC 3 and a HELCOM threat category. The long-tailed duck has an elevated IUCN threat category, while the long-tailed duck and the velvet scoter have a HELCOM threat category [Table 3.74].

Among the species with an elevated conservation status, only the long-tailed duck was periodically very abundant in the survey area (during the spring migration period). The remaining species with an elevated conservation status were less numerous and their abundance indices did not exceed 10 individuals per 10 km of the transect length. However, it is also worth noting the exceptionally abundant occurrence of the black-throated diver during the spring migration period. This species appeared there in greater numbers on 22 April 2023 and that single observation influenced the higher abundance index during that phenological period. The razorbill was also clearly more abundant in the spring [Table 3.74].

Table 3.74. A list of seabird species present in the survey area, together with their conservation status and abundance indices [ind./10 km]. Species present in extremely low abundance were excluded

Species	**Abundance index in successive phenological periods: wintering/spring migration/summer/ autumn migration**	**Species protection in Poland[1]**	**Annex 1 of the EU Birds Directive**	**SPEC cate-gory[2]**	**IUCN threat category[3]**	**HELCOM threat category[3]**
Long-tailed duck *Clangula hyemalis*	33.1 / 230.8 / 0.0 / 5.0	SP	-	Non-SPEC	VU	EN
European herring gull *Larus argentatus*	29.4 / 1.9 / 2.9 / 4.5	PP	-	Non-SPEC	LC	LC
Razorbill *Alca torda*	6.7 / 1.6 / 0.0 / 05	SP	-	Non-SPEC	LC	LC
Common guillemot *Uria aalge*	1.4 / 0.8 / 3.6 / 3.6	SP	-	Non-SPEC	LC	LC
Little gull *Hydrocoloeus minutus*	2.1 / 0.2 / 0.0 / 0.1	SP	YES	SPEC 3	LC	NT
Black-throated diver *Gavia arctica*	0.0 / 1.9 / 0.0 / 0.2	SP	YES	SPEC 3	LC	CR
Black guillemot *Cepphus grylle*	0.3 / 0.5 / 0.0 / 0.0	SP	-	SPEC 2	LC	LC
Common scoter *Melanitta nigra*	0.0 / 0.6 / 0.0 / 0.3	SP	-	Non-SPEC	LC	EN

Species	Abundance index in successive phenological periods: wintering/spring migration/summer/ autumn migration	Species protection in Poland[1]	Annex 1 of the EU Birds Directive	SPEC cate-gory[2]	IUCN threat category[3]	HELCOM threat category[3]
Lesser black-backed gull *Larus fuscus*	0.0 / 0.1 / 0.1 / 0.6	SP	-	Non-SPEC	LC	LC

[1]pursuant to the Regulation of the Minister of Environment of 16 December 2016 on protection of animal species (Journal of Laws 2016, item 2183): Species protection in Poland: SP – strictly protected species; PP – partially protected species
[2]SPEC category: SPEC 2 – endangered species, the European population of which exceeds 50% of the global population and their conservation status was assessed as unfavourable; SPEC 3 – endangered species, the European population of which does not exceed 50% of the global population and their conservation status was assessed as unfavourable; non-SPEC – species not endangered
[3]IUCN threat category – classification according to the International Union for the Conservation of Nature also used by HELCOM: LC – least concern species, NT – near threatened species (species close to being classified as VU but not classified as such yet), VU – vulnerable species (species threatened with extinction in the near future but not as close to it as endangered species), EN – endangered species (species at high risk of extinction in the near future), CR – critically endangered species (species at the highest risk of extinction)

During the 12-month survey period, a total of 13 bird species strongly associated with the marine environment were identified in the reference area, of which 7 were present in extremely low numbers. These were the black guillemot, the white-billed diver, the red-throated diver, the velvet scoter, the little gull, the lesser black-backed gull and the great black-backed gull. Among the remaining species, the black-throated diver is listed in Annex I of the EU Birds Directive and has higher IUCN and HELCOM threat categories as well as a SPEC category [Table 3.75]. The long-tailed duck and the velvet scoter are HELCOM-listed as threatened species, and the long-tailed duck also has a higher IUCN threat category [Table 3.75]. The European herring gull is the only species in this group that is not strictly protected, but only partially protected.

The long-tailed duck was the only species that aggregated in large numbers in the reference area, although only during the wintering and autumn migration periods. Among the remaining species, only the European herring gull exceeded the abundance index value of 1. In the autumn, also the razorbill was observed in relatively high numbers in the reference area; the highest concentration of the razorbill was also observed in the wintering period with the abundance index of 8.1 [Table 3.75].

Table 3.75. A list of seabird species present in the reference area, together with their conservation status and abundance indices [ind./10 km]. Species present in extremely low abundance were excluded

Species	Abundance index in successive phenological periods: wintering/ autumn migration/ summer/spring migration	Species protection in Poland[1]	Annex 1 of the EU Birds Directive	SPEC categ ory[2]	IUCN threat category[3]	HELCOM threat category[3]
Long-tailed duck *Clangula hyemalis*	33.1 / 87.1 / 0.0 / 14.5	SP	-	Non-SPEC	VU	EN
European herring gull *Larus argentatus*	11.0 / 0.8 / 2.3 / 1.0	PP	-	Non-SPEC	LC	LC
Razorbill *Alca torda*	8.1 / 3.0 / 0.3 / 0.9	SP	-	Non-SPEC	LC	LC

Species	Abundance index in successive phenological periods: wintering/ autumn migration/ summer/spring migration	Species protection in Poland[1]	Annex 1 of the EU Birds Directive	SPEC category[2]	IUCN threat category[3]	HELCOM threat category[3]
Common guillemot *Uria aalge*	2.5 / 0.7 / 4.3 / 1.2	SP	-	Non-SPEC	LC	LC
Common scoter *Melanitta nigra*	0.0 /1.2 / 0.0 / 0.2	SP	-	Non-SPEC	LC	EN
Black-throated diver *Gavia arctica*	0.1 / 0.8 / 0.0 / 0.0	SP	YES	SPEC 3	LC	CR

[1]pursuant to the Regulation of the Minister of Environment of 16 December 2016 on protection of animal species (Journal of Laws 2016, item 2183): Species protection in Poland: SP – strictly protected species; PP – partially protected species
[2]SPEC category: SPEC 2 – endangered species, the European population of which exceeds 50% of the global population and their conservation status was assessed as unfavourable; SPEC 3 – endangered species, the European population of which does not exceed 50% of the global population and their conservation status was assessed as unfavourable; non-SPEC – species not endangered
[3]IUCN threat category – classification according to the International Union for the Conservation of Nature also used by HELCOM: LC – least concern species, NT – near threatened species (species close to being classified as VU but not classified as such yet), VU – vulnerable species (species threatened with extinction in the near future but not as close to it as endangered species), EN – endangered species (species at high risk of extinction in the near future), CR – critically endangered species (species at the highest risk of extinction)

In the survey areas, five species with a higher conservation status were observed regularly, but their abundance varied significantly. High and very high maximum values of the abundance index were found only for the long-tailed duck. In the survey area, this species reached very high values of that index (239.8); only in the reference area the abundance index was considerably lower, i.e. 125.5 ind./10 km [Table 3.76]. The maximum numbers of long-tailed ducks were recorded during the spring migration period in the survey area and in winter in the reference area. The numbers of other species were not as high. In the case of the black-throated diver, the maximum value of the abundance index was 1.9 during the spring migration period, while in the case of the little gull it was 2.1 during the wintering period. For both of these species, the maximum values apply to the survey area. However, in the case of the velvet scoter, the maximum value of the abundance index was 0.2, and in the case of the common scoter, it was 1.2. For both of these species, the maximum values apply to the reference area and the spring migration period [Table 3.76].

Table 3.76. A list of seabird species with an elevated conservation status present in the areas surveyed, together with their conservation status and maximum abundance indices [ind./10 km]. Species present in extremely low abundance were excluded

Species	Maximum abundance index value: survey area / RA[1]	Species protection in Poland[2]	Annex 1 of the EU Birds Directive	SPEC category[3]	IUCN threat category[4]	HELCOM threat category[4]
Long-tailed duck *Clangula hyemalis*	239.8 spr[5] / 125.5 win	SP	-	Non-SPEC	VU	EN
Velvet scoter *Melanitta fusca*	0.1 z spr / 0.2 spr	SP	-	Non-SPEC	VU	EN

Species	Maximum abundance index value: survey area / RA[1]	Species protection in Poland[2]	Annex 1 of the EU Birds Directive	SPEC category[3]	IUCN threat category[4]	HELCOM threat category[4]
Common scoter *Melanitta nigra*	0.6 spr / 1.2 spr	SP	-	Non-SPEC	LC	EN
Black-throated diver *Gavia arctica*	1.9 spr / 0.8 spr	SP	YES	SPEC 3	LC	CR
Little gull *Hydrocoloeus minutus*	2.1 win / 0.2 win aut	SP	YES	SPEC 3	LC	NT

[1]RA – reference area
[2]Pursuant to the Regulation of the Minister of Environment of 16 December 2016 on protection of animal species (Journal of Laws 2016, item 2183): Species protection in Poland: SP – strictly protected species; PP – partially protected species
[3]SPEC category: SPEC 2 – endangered species, the European population of which exceeds 50% of the global population and their conservation status was assessed as unfavourable; SPEC 3 – endangered species, the European population of which does not exceed 50% of the global population and their conservation status was assessed as unfavourable; non-SPEC – species not endangered
[4]IUCN threat category – classification according to the International Union for the Conservation of Nature also used by HELCOM: LC – least concern species, NT – near threatened species (species close to being classified as VU but not classified as such yet), VU – vulnerable species (species threatened with extinction in the near future but not as close to it as endangered species), EN – endangered species (species at high risk of extinction in the near future), CR – critically endangered species (species at the highest risk of extinction)
[5]Phenological period during which the highest value of the abundance index was recorded: win – wintering period, spr – spring migration period, sum – summer, aut – autumn migration period

3.5.1.5.6 Comparison of species composition of birds present in the survey area and in the reference area

A comparison of the species composition and dominance structure of the grouping of birds present in the survey area and in the reference area is provided separately for each phenological period. Account was taken of only those bird species present in the sea areas surveyed which outside the breeding season usually stay at sea, reaching the highest abundances in the offshore zone situated over 1 km away from the shore (seabirds). When comparing the species composition, the birds recorded in flight were excluded, because the observations of flying birds made during survey vessel passages in sea areas are only of ancillary nature and cannot constitute the basis for assessing the intensity of the flight.

3.5.1.5.6.1 Species composition and average abundance of seabirds in the wintering period

During the wintering period, similar numbers of species were identified in both sea areas, which is due to the great similarity of habitat conditions in these areas. Also, the average abundance of the entire seabird grouping, and the abundance index were similar [Table 3.77]. In the reference area, the long-tailed duck was recorded in significantly higher numbers throughout the survey period. During the same 12-month period, the average abundance and the abundance index of this species in the survey area were almost twice lower. Moreover, the European herring gull and the razorbill were more abundant in this area than in the reference area. Considerably more little gulls were observed in the survey area. The abundance of the common guillemot in both areas was fairly high and similar in both areas, with an abundance index above 1. The other species in the survey area and in the reference area showed similarly low values of average abundance and the abundance index [Table 3.77].

Table 3.77. Average abundance of seabirds per survey campaign and their abundance indices [ind./10 km] within the survey area and in the reference area during the wintering period

Species	Survey area	Reference area
Long-tailed duck *Clangula hyemalis*	**288.2 (33.1)**	**526.3 (60.5)**
European herring gull *Larus argentatus*	**256.2 (29.4)**	57.0 (6.6)
Razorbill *Alca torda*	58.5 (6.7)	42.3 (4.9)
Common guillemot *Uria aalge*	12.0 (1.4)	13.0 (1.5)
Little gull *Hydrocoloeus minutus*	18.0 (2.1)	1.7 (0.2)
Black guillemot *Cepphus grylle*	3.0 (0.3)	0.7 (0.1)
Great black-backed gull *Larus marinus*	1.0 (0.1)	0.3 (<0.05)
Red-throated diver *Gavia stellata*	0.5 (0.1)	0.5 (0.1)
Black-throated diver *Gavia arctica*	0.2 (<0.05)	0.5 (0.1)
Yellow-billed diver *Gavia adamsii*	0.2 (<0.05)	0.2 (<0.05)
Velvet scoter *Melanitta fusca*	0.7 (0.1)	
Total	638.5 (73.3)	642.5 (74.0)
Number of all species	11	10
Number of abundant species	2	1

**the average abundances and abundance indices exceeding respectively 100 and 10 individuals (numerous occurrences of the species) are in bold*

3.5.1.5.6.2 Species composition and average abundance of seabirds in the spring migration period

In the spring, the long-tailed duck was exceptionally abundant in the survey area. The average abundance of this species exceeded 2000 individuals, and the abundance index reached 230.8. Both of these values were more than four times higher and more than two times higher, respectively, than in the reference area, where the long-tailed duck was also classified as an abundant species [Table 3.78]. The long-tailed duck was the only species whose average abundance, as well as the abundance index value, exceeded the agreed level defining abundant occurrence and had a major impact on both of these values calculated for the entire seabird grouping. In the spring, the European herring gull and the black-throated diver were recorded in higher numbers in the survey area, compared to the reference area. The razorbill and the common scoter, on the other hand, were more numerous in the reference area [Table 3.78].

Table 3.78. The average abundance of seabirds per survey campaign and their abundance indices [ind./10 km] within the survey area and in the reference area during the spring migration period

Species	Survey area	Reference area
Long-tailed duck *Clangula hyemalis*	**2008.3 (230.8)**	**452.7 (87.1)**
Black-throated diver *Gavia arctica*	16.8 (1.9)	4.3 (0.8)
European herring gull *Larus argentatus*	16.8 (1.9)	4.0 (0.8)
Razorbill *Alca torda*	14.0 (1.6)	15.5 (3.0)
Common guillemot *Uria aalge*	7.2 (0.8)	3.8 (0.7)
Common scoter *Melanitta nigra*	5.0 (0.6)	6.2 (1.2)
Black guillemot *Cepphus grylle*	4.7 (0.5)	0.7 (0.1)
Little gull *Hydrocoloeus minutus*	1.7 (0.2)	0.2 (<0.05)
Lesser black-backed gull *Larus fuscus*	1.2 (0.1)	0.2 (<0.05)
Velvet scoter *Melanitta fusca*	1.0 (0.1)	1.2 (0.2)
Great black-backed gull *Larus marinus*	0.2 (<0.05)	

Species	Survey area	Reference area
Red-throated diver *Gavia stellata*		0.2 (<0.05)
Yellow-billed diver *Gavia adamsii*		0.2 (<0.05)
Total	2080.9 (238.5)	489.2 (93.9)
Number of all species	11	12
Number of abundant species	1	1

**the average abundances and abundance indices exceeding respectively 100 and 10 individuals (numerous occurrences of the species) are in bold*

3.5.1.5.6.3 Species composition and average abundance of seabirds in the summer period

In the summer, the number of birds present in both areas was very low. In the survey area, two more seabird species were identified than in the reference area. However, these were species recorded in very low numbers (abundance index below 0.05). None of the species were abundant; the most numerous species observed in both areas were the common guillemot and the European herring gull [Table 3.79]. All species identified in both areas showed similar abundance index values [Table 3.79].

Table 3.79. The average abundance of seabirds per survey campaign and their abundance indices [10 ind./10 km] within the survey area and in the reference area during the summer

Species	Survey area	Reference area
Common guillemot *Uria aalge*	31.2 (3.6)	22.2 (4.3)
European herring gull *Larus argentatus*	25.3 (2.9)	11.8 (2.3)
Razorbill *Alca torda*	0.2 (<0.05)	1.5 (0.3)
Lesser black-backed gull *Larus fuscus*	1.0 (0.1)	0.5 (0.1)
Black-throated diver *Gavia arctica*	0.2 (<0.05)	
Common scoter *Melanitta nigra*	0.2 (<0.05)	
Total	58.1 (6.6)	36.0 (7.0)
Number of all species	6	4
Number of abundant species	0	0

**the average abundances and abundance indices exceeding respectively 100 and 10 individuals (numerous occurrences of the species) are in bold*

3.5.1.5.6.4 Species composition and average abundance of seabirds in the autumn migration period

During the autumn migration period, the abundance of the seabird grouping within the two areas under discussion was low and none of the species appeared in high numbers. The number of seabird species identified in both sea areas was similar, but more species were observed within the area intended for the investment implementation [Table 3.80]. Compared to the reference area, the European herring gull and the long-tailed duck were more abundant in the survey area, while the razorbill was more abundant in the reference area [Table 3.80]. The abundance of the common guillemot in both areas was high, with abundance index values exceeding 3.5. The species was abundant during the summer and was still present in both sea areas during the autumn migration period.

Table 3.80. The average abundance of seabirds per survey campaign and their abundance indices [ind./10 km] within the survey area and in the reference area during the autumn migration period

Species	Survey area	Reference area
European herring gull *Larus argentatus*	39.5 (4.5)	5.6 (1.1)

Species	Survey area	Reference area
Common guillemot *Uria aalge*	31.1 (3.6)	7.2 (4.1)
Long-tailed duck *Clangula hyemalis*	31.6 (3.6)	2.8 (0.5)
Lesser black-backed gull *Larus fuscus*	6.4 (0.7)	0.4 (0.1)
Razorbill *Alca torda*	4.5 (0.5)	5.2 (1.0)
Common scoter *Melanitta nigra*	3.0 (0.3)	1.2 (0.2)
Little gull *Hydrocoloeus minutus*	1.0 (0.1)	0.8 (0.2)
Black-throated diver *Gavia arctica*	0.1 (<0.05)	0.2 (<0.05)
Black guillemot *Cepphus grylle*	0.2 (<0.05)	
Total	117.4 (13.3)	23.4 (7.2)
Number of all species	9	8
Number of abundant species	0	0

**the average abundances and abundance indices exceeding respectively 100 and 10 individuals (numerous occurrences of the species) are in bold*

3.5.1.5.6.5 Comparison of the abundance indices of the bird grouping

The highest abundance indices in the survey area were recorded during the spring migration period. At that time, the seabird grouping was significantly more abundant than in the reference area and the difference in the abundance index values exceeded 50% [Figure 3.116]. During the autumn migration period, more seabirds were observed in the survey area. During the remaining phenological periods, the abundance index values in both areas were very low [Figure 3.116].

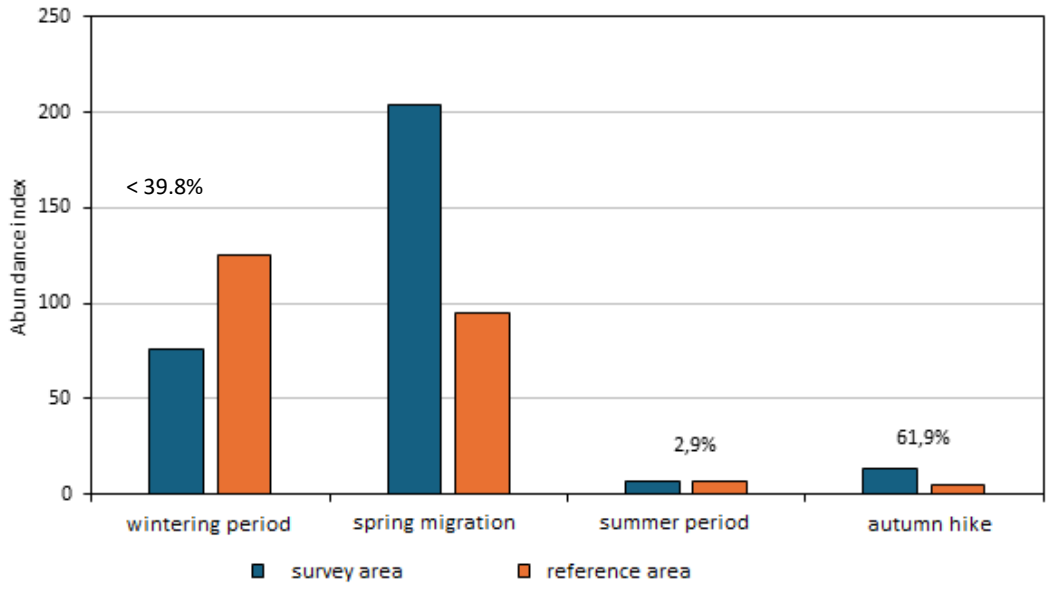


Figure 3.116. A comparison of abundance indices of the entire grouping of seabirds in the survey area and the reference area in successive phenological periods. The difference in percentage is provided in relation to the index value for the reference area

3.5.1.6 Summary of results and conclusions

Surveys in all areas were conducted in accordance with the assumptions and methodology adopted in advance. The data collected provided sufficient information to characterise the grouping of seabirds occurring in these sea areas in the four phenological periods distinguished.

During bird observations carried out from greater distances, it is often impossible to determine the species affiliation of all individuals. This is due to the difficult conditions under which observations are conducted (e.g. sea wave motion, long distance from the observer, unfavourable sunlight angle), as well as the high similarity of closely related species. During the 12-month survey period in the survey area and the reference area, a total of 13 individuals sitting on the water and 211 individuals in flight remained unidentified to species. They represented respectively 0.1% and 1.9% of all the birds observed during the surveys. On the one hand, this low proportion indicates the high qualifications of the ornithological team, and, on the other hand, it means that the presence of birds unidentified to species does not affect the quality and interpretation of the data obtained.

The reference area was selected so that the environmental conditions were similar to the survey area, which enables direct comparison of the avifauna groupings in both sea areas. The species composition in both areas was very similar but changed in successive phenological periods. The species structure of the seabird grouping was typical of most sea areas situated in the Polish zone of the Baltic Sea away from the coast (Durinck et al, 1994; Skov et al, 2011; Meissner, 2014a; Meissner, 2014b; Markones et al., 2015; Meissner, 2015), but out of the three most numerous wintering seabird species, only the long-tailed duck was abundant in both of these areas. This species has higher IUCN and HELCOM threat categories and therefore is likely to be the most important seabird species considered in formulating the environmental impact assessment for the proposed project. This assessment will also need to account for the black-throated diver, which also belongs to the species with an elevated threat category and appeared in large numbers in the survey area during the spring migration period, as well as the common guillemot, large post-breeding aggregations of which were observed. In the case of the common guillemot, as in other species of the auk family, juvenile birds leaving the breeding colonies are not yet prepared for independent life and require a long period under the care of adult birds (Cramp and Simmons, 1983). What is of key importance in this period for this species are sea areas with a sufficiently abundant food supply, where the young learn to feed themselves.

The high proportion of the common guillemot and the razorbill in the survey area and the reference area is a result that deviates from the existing knowledge on the species structure of seabird groupings within the Polish zone of the Baltic Sea. Knowledge of the occurrence of these species in the Baltic Sea outside of breeding colonies is still insufficient. During the non-breeding period, in the open sea, they usually are highly dispersed (Cramp and Simmons, 1983; Durinck et al., 1994), which is why they were omitted from the study by Skov et al. (2011). Larger concentrations of these species have been observed in winter, for example in the Danish Straits (Cramp and Simmons, 1983; Durinck et al., 1994), but their larger groupings have not been recorded in the available scientific literature concerning the Polish zone of the Baltic Sea (Tomiałojć and Stawarczyk, 2013). The high abundance of both species was also observed during the surveys conducted in the area of the planned Bałtyk II OWF (Meissner, 2015). This may indicate that, on the Polish coast, these species form aggregations in sea areas with greater depths than in places at which diving benthophagous birds gather and hence such sites have not been known so far, since the existing surveys were focused mainly on shallower areas in which high abundances of birds are expected, particularly of diving benthophagous birds (Chodkiewicz et al., 2018;

Wardecki et al., 2022). The presence of young birds indicates that after the breeding was over, they migrated there together with adult individuals. This is proved by the high abundance of the common guillemot in both areas during the summer, from late July onwards, which corresponds with the end of the breeding period in this species (Cramp and Simmons, 1983). In this species, as in other species of the auk family, juvenile birds leaving the breeding colonies are not yet prepared for independent life and require a long period under the care of adult birds. What is of key importance are sea areas with a sufficiently abundant food supply, where the young learn to feed themselves.

The results of seabird observations covering four phenological periods showed that the survey area is not a place of very high concentrations of seabirds during winter, summer and autumn migration. Only during the spring migration period, during one survey campaign conducted on 22 April 2023, a very high concentration of the long-tailed duck was recorded as the species was present in the shallowest, north-western part of the area [Figure 3.117]. This result had a major impact on the high values of the average densities and abundance index calculated for the entire spring migration period. During that survey campaign, extremely high densities of the long-tailed duck, exceeding 1000 ind.·km^{-2}, were recorded at 12 transects located in the depth zone up to approximately 30 m, some of which were situated in the buffer zone outside the project area [Figure 3.117]. During the same survey campaign, the black-throated diver, which usually does not form large concentrations, was also present in large numbers in the survey area; on 22 April 2023, as many as 66 individuals were recorded along a transect and, next to the long-tailed duck, this was the second most abundant species in the area. However, on the basis of one survey season, it is not possible to conclude whether the long-tailed duck and the black-throated diver regularly appear in large numbers in the survey area during the spring migration period, or whether this abundant appearance was incidental, for example, resulting from interrupted migration due to a sudden deterioration in weather conditions.

The abundance indices of the entire seabird grouping were higher within the survey area than in the reference area, with the greatest difference during the spring migration period, when the long-tailed duck appeared abundantly in the area of the planned project, on 22 April 2023. The long-tailed duck also aggregated in the area in greater numbers during the autumn migration period. In the winter, however, they were more abundant in the reference area. In the survey area, the black-throated diver was a species observed in larger abundance in the spring, while in the winter it was the razorbill, which was more abundant in the reference area during the autumn migration. The abundance of the European herring gull was higher within the area intended for the project during the wintering, as well as spring and autumn migration periods. The more frequent sightings of birds of this species in the survey area were most likely related to the higher activity of fishing boats in that sea area. Outside of the spring migration period, the abundance indices and average density of birds in both areas were not high and only locally reached very high values in the shallowest, north-western part of the survey area, during the spring and autumn migration periods. Although that part of the sea area is largely situated within a 4 km buffer strip, outside the area of the future OWF, once the OWF is constructed most birds are expected to be displaced from that part of the sea area as well (Petersen et al., 2006; Vanermen et al., 2014).

In terms of abundance in both areas during the wintering and spring migration periods, the long-tailed duck dominated, although its abundance and proportion was variable, but always above 43%. The common guillemot and the European herring gull were the most abundant species in the summer, when the total abundance of seabirds at sea areas away from the shore is very low. Together, they then

accounted for 96.1% and 93.6% of the birds observed in the survey area and the reference area, respectively.

Apart from one survey campaign on 22 April 2023, neither the total abundance nor the density of the long-tailed duck in the two areas were high, most likely due to the considerable depth of these sea areas. Depths of more than 30 m predominate there, which makes it more difficult for benthophagous birds to reach their food, because they incur high energy costs during diving. Although they can dive to considerable depths in search of benthic organisms (mainly bivalves), they prefer sites with shallower depths where the energy expenditure associated with diving is lower (Durinck et al., 1994). For sea ducks, the most energy efficient strategy is foraging in shallower (up to 20–25 m deep) nutrient-rich waters and only the decrease in the density of benthic organisms forces them to move to other places including the ones of greater depth (Kirk et al., 2008; Meissner, 2010). Both areas surveyed are located close to each other (less than 10 km between the extreme transect lines) and it cannot be ruled out that long-tailed ducks move between them. Similar changes in the diving benthophagous birds' distribution, including the long-tailed duck, between autumn and winter, were observed near Cape Rozewie (Meissner, 2010). The reasons for such movements can be attributed to the changes in the availability of food, since in the locations of large diving benthophagous bird concentrations, a gradual reduction in the density of bivalves, which are their main food component, takes place (Guillemette et al., 1996; Lewis et al., 2007), forcing the birds to seek new feeding grounds.

Thus, in the survey area, the dependence of the long-tailed duck densities recorded on the depth of the sea area was very evident. Its highest density was recorded in the shallowest, north-western part of the sea area surveyed, which also occurred during a very large occurrence of the long-tailed duck on 22 April 2023 [Figure 3.117]. On the other hand, in the case of the common guillemot and the razorbill, which feed on fish, a dependence between their density and the sea area depth should not be expected, since in the case of piscivorous birds, higher concentrations are most often connected to the presence of pelagic fish that constitute their food and are not as dependent on the depth of the sea area as is the case for benthophagous birds (Cramp and Simmons, 1983; Durinck et al., 1994).

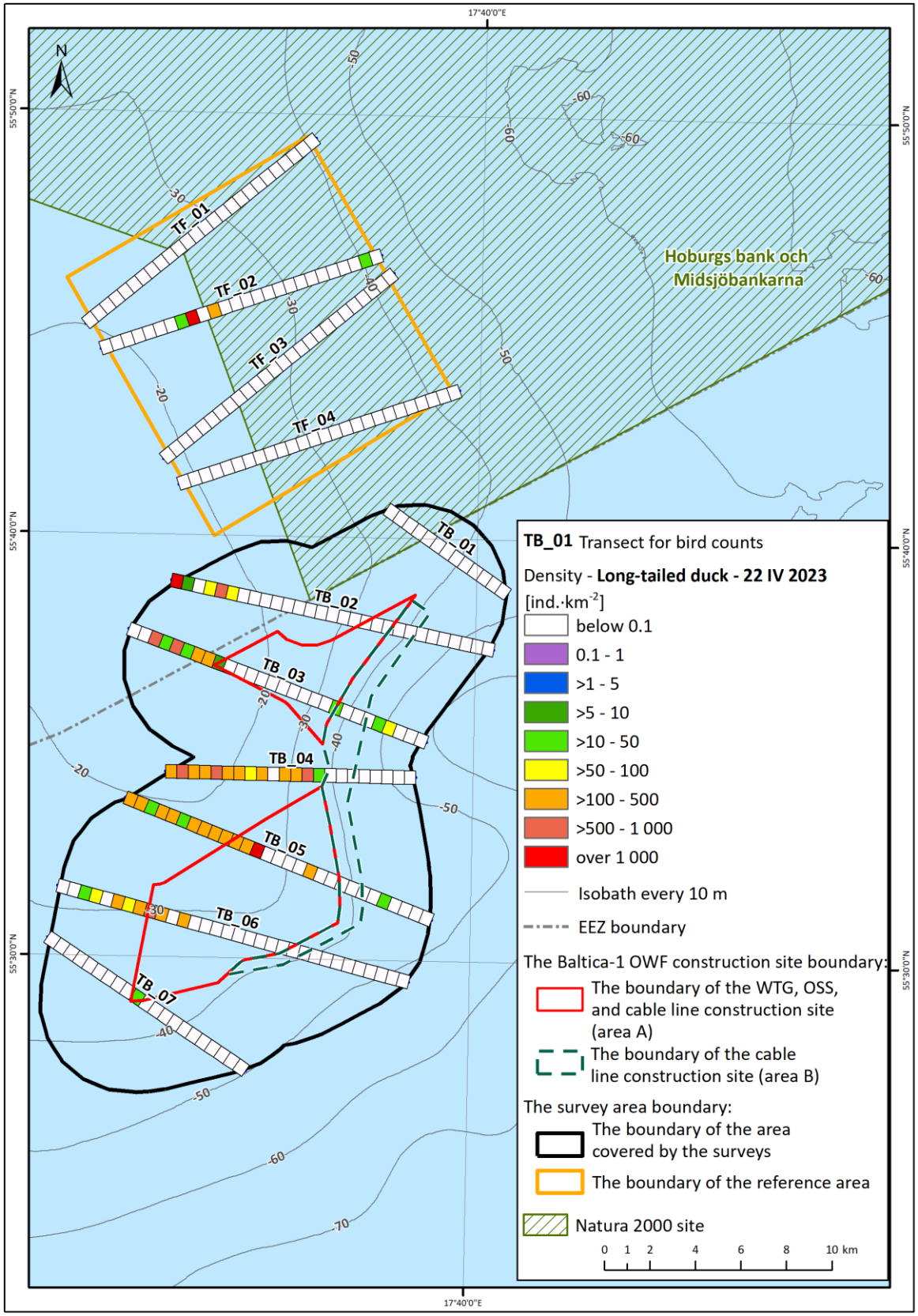


Figure 3.117. The spatial distribution of the long-tailed duck density in the transect strip within the survey area and in the reference area on 22 April 2023

During the 12-month period under analysis, also during the spring and autumn migration periods, no intensive bird migration was recorded over either the survey area or the reference area. The exception to this was the survey campaign conducted on 6–7 February 2023, when more than 1400 razorbills in flight were recorded over the area intended for the Baltica-1 OWF construction. Such intensive flights of that species had not been reported from the Polish zone of the Baltic Sea, except for a single observation in the vicinity of the port in Hel during the spring migration period (Meissner, 1989). No data on the intensity and scope of seabird migrations, including razorbills, is available for the wintering period. It can only be assumed that such migrations are probably due to the changes in the availability of food (pelagic fish) and are connected to searching for feeding grounds.

In July, a high abundance of the common scoter in flight was recorded in both areas. This corresponds to the periods of migration of this species towards moulting areas in the western part of the Baltic Sea (Nehls and Zöllick, 1990). More than 90% of the flights observed over the survey area and over the reference area took place within 30 m above the water, i.e. below the range assumed for wind turbine rotors. Nearly all flights of the sea ducks (the velvet scoter and the common scoter), as well as of the piscivorous birds (the razorbill and the common guillemot) were recorded low above the sea surface. The same results were obtained for other pre-investment surveys carried out for the purpose of offshore wind farms carried out in the Polish zone of the Baltic Sea (Meissner, 2014a, 2014b, 2015; Antczak and Meissner, 2018), as well as in the North Sea (Furness et al., 2013). However, it should be remembered that the results of visual observations of flying birds conducted during survey vessel passages cannot serve as the source of data that present a full picture of bird migrations over sea areas and cannot substitute the results acquired with the use of radars. In the case of passerines, the observations carried out during the day concern, to a large extent, individuals that did not fit into the typical pattern of crossing the barrier at night. The visual assessment of a flight altitude is certainly burdened with an error resulting from such factors as the position of an observer in relation to a flying bird, the movement of the ship deck resulting from the wave motion and the rapidly changing distance to the bird observed. Using specialist equipment to assess the distance in the case of counts focused on birds sitting on the water in a particular sea area surveyed is practically impossible when the vessel is in constant motion. The abundance of small body-size species can also be seriously underreported, because the effective range of observation of small species in flight is approx. 400 m. Thus, the methodology used does not provide a full picture of bird passages over the sea areas surveyed, and the data obtained can only have a supporting character.

The main conclusions resulting from the surveys conducted are summarised below:

1. The Baltica-1 OWF survey area is generally not a site of high concentrations of seabirds, as bird densities were not high over most of the area. However, during the spring migration period, a very high aggregation of long-tailed ducks and black-throated divers, i.e. species with an elevated conservation status, was recorded there. Without repeating the survey over one more season, it is impossible to state unambiguously whether the shallowest part of the survey area is a regularly used stopover site for the long-tailed duck and the black-throated diver during their migration towards breeding grounds, or whether their concentrations observed on one occasion were caused by weather conditions that forced the birds to temporarily stop their migration. Before formulating the environmental impact assessment, it would also be necessary to confirm whether the Baltica-1 OWF area is a permanent site of post-breeding concentrations of the common guillemot during the summer and autumn. In this species, as in other species of the auk family, juvenile birds

leaving the breeding colonies are not yet prepared for independent life and require a long period under the care of adult birds.

2. In both areas, concentrations of the common guillemot – significant for this species – were observed in July and August, i.e. after the breeding season in the nearby colonies on the Swedish coast. These birds lead their young to places with a plenitude of food. It can be assumed that the construction of the offshore wind farm will force them to leave that location. However, these birds will be able to move to other sea areas with a sufficiently high abundance of pelagic fish. In the case of piscivorous birds, the depth of the sea area does not affect their distribution as it does for diving benthophagous species.
3. Very few daytime passages of birds over the Baltica-1 OWF area and the reference area were recorded during the spring and autumn migration periods. More passages over the sea area were observed in the winter, most probably related to local flights in search of feeding grounds, and also in the summer, when the common scoter migrates across the Baltic Sea towards the moulting areas. A vast majority of the passages observed, i.e. 92.5% in the case of the survey area and 96.8% in the case of the reference area, took place low over the water surface, i.e. below the reach of turbine rotors. However, the results obtained on bird passages are only of ancillary nature. A comprehensive analysis of this phenomenon must be based on the results of radar surveys.

3.5.1.7 Shortcomings and gaps in the state of the art

The adopted division into phenological periods is arbitrary to a large extent, since various species migrate at slightly different times, and therefore the autumn migration of the common scoter is observed as early as in August, while the long-tailed ducks begin their autumn migration at the end of September (Meissner, 2014b; Meissner, 2015; Nehls and Zöllick, 1990). As shown by the results of the surveys in question as well as surveys related to other OWFs in the Polish zone of the Baltic Sea (Meissner, 2014a; 2015; 2014b; Antczak and Meissner, 2018), the spring migration period of sea ducks ends in April and for these species May should rather be considered a summer period. The division into four phenological phases adopted here enables grouping the observations into periods during which most of the waterbird species, the presence of which can influence project-related decisions, migrate, winter or aggregate mainly in the nearshore area, outside sea areas intended for offshore wind farms.

The results of visual observations of birds in flight conducted during survey vessel passages may constitute only a supplementary material in the analysis of data obtained in the course of surveys with the use of radars detecting birds flying over the OWF area. The vast majority of passerines cross the Baltic Sea at night. Observations conducted during daytime concern individuals that did not fit the typical pattern of behaviour, and therefore their migration over the sea does not have to take place at the same altitudes as at night. Moreover, the visual assessment of flight altitudes certainly involves a high risk of error resulting from, among others, the position of an observer in relation to a flying bird, the movement of the ship deck resulting from the wave motion and the quickly changing distance from the bird observed, as well as individual predispositions to assess the distance correctly without the use of special equipment. Additionally, birds, especially the ones of small species, are difficult to notice when they are flying at significant heights. Therefore, their abundance can be significantly underestimated during visual observations, since the effective range of observation of small species in flight is approximately 400 m. Thus, the methodology used does not provide a full picture of the flights over the sea areas surveyed and can only support the results acquired with the use of radars.

In this Report, the European herring gull is treated as a species *sensu lato*, i.e. a taxon including three differentiated nowadays but very similar species: the European herring gull *Larus argentatus – sensu stricto*, the Caspian gull *Larus cachinnans* and the yellow-legged gull *Larus michahelllis.* The surveys conducted in northern Poland indicate that a species that predominated decisively among the three is the European herring gull, and the two other species occur there rarely (Meissner and Betleja, 2007; Meissner et al., 2007).

3.5.2 Surveys of bird movements (migratory birds)

3.5.2.1 Non-specialist summary

This report summarizes surveys of migratory birds conducted in the area of the planned Baltica 1 OWF during winter 2022/2023, spring 2023 and autumn 2023.

The goal of the winter study was to find out how big the wintering population of seabirds staying within and in the vicinity of the Baltica-1 OWF area actually is and what their movements between known wintering grounds look like to assess the potential impact of the planned investment on the local bird migrations in the wintering period. The scope of the spring and autumn study was to describe the use of the survey area by migratory birds, i.e. timing, species composition, flight altitude, flight direction and the intensity of the passage of migratory birds termed “bird flux”.

The necessary data were collected from aboard two survey vessels, at survey points located within the boundaries of the Baltica-1 OWF construction area: at station LP_01 and at station LP_02 in the period from December 2023 to February 2023, at station MB_01 and at station MB_02 in the period from March to May 2023 and from July to December 2023. The used methods included visual observations aided with laser rangefinder (species composition and flight altitude), horizontal radar tracking aided with visual assessment of species, vertical radar (information about flight altitude and overall activity at the survey points) and acoustic recordings (identification species by their calls during spring and autumn migration).

The Baltica-1 OWF area is located close to the Swedish border and the Natura 2000 site *Hoburgs bank och Midsjöbankarna* (SE0330308, special area of habitat conservation and special bird protection area). The Southern Middle Bank excluded from the above Natura 2000 site is an IBA (Important Bird Area) as of 2016.

In total 24 bird species were observed during the surveys of local passages in the wintering period. Besides auks (common guillemot and razorbill) and long-tailed ducks, all the other species were observed rather in low numbers not exceeding 1% of the observations. Auks represent ichthyophagous birds – their diet consists mainly of fish, whereas the winter diet of sea ducks, which are diving benthophages, consists mainly of bivalves. Both groups prefer shallow waters (20–25 m) of the Baltic Sea, hence their most abundant aggregations were observed in the area of the Middle Bank. The flight altitude data obtained from the visual observations conducted shows that 98–99% (the variability among stations) of all the observed seabirds were flying at altitudes not exceeding 20 m ASL. No birds were observed at altitudes of more than 100 m ASL. Based on the data collected using vertical radar, it was found that the most intensive bird migration was recorded at altitudes of 30 to 60 m, in almost all months. In December 2022, at both survey stations, the radars detected relatively high bird activity at altitudes from 10 up to 280 m. This is due to capturing some of the late migrants migrating through the Baltic Sea (for example raptors, and pigeons). The lowest bird activity recorded by a vertical radar was observed in January. Low detections in January are reflected also by the visual observations and the

number of tracks registered by the horizontal radar. Elevated numbers of vertical radar recordings in February could suggest, that some of the long-tailed ducks started their spring migration (the migration peak should fall in April). The most frequently observed species was the razorbill. Razorbills were the most frequently encountered seabird with the highest numbers observed with a peak in February (at both stations over 1000 individuals) with numbers around ten times higher than in December and January. According to HELCOM, the razorbill population in the Baltic Sea experiences a moderate increase. General movement directions point at NE (towards shallower waters of the Middle Bank) and SW. The NE direction was especially pronounced at LP_01 station located slightly further away from the Middle Bank. This was true for most of the observations of benthophagous and pelagic species except for divers, which flew predominantly in the NW direction. At LP_02 located within the Baltica-1 OWF area, the movements in both, NE and SW directions are also visible when all the recorded tracks were analysed together. On the other hand, the recorded flights of the long-tailed duck, when analysed individually, indicate the species movement in all directions with the predominance of the N and W directions. The interpretation of such a pattern could be, that LP_02 station was capturing locally resting long-tailed ducks utilizing the area close to the survey station as foraging grounds.

In total 96 bird species were observed and recorded at both stations during spring surveys and 106 species in the course of the autumn migration studies. The number of species at both stations was similar, as well as the species composition. The long-tailed duck was the most frequently observed species throughout the spring survey period, followed by the common scoter and the razorbill. According to the flight flux analyses more than 26,000, slightly over 81,000 and close to 3800 long-tailed ducks flew through the survey area in March, April, and May, respectively. During the autumn migration studies, similarly as in spring, the most numerous species were common scoters and long-tailed ducks. The chaffinch and great cormorant were also observed in large numbers. Based on the flux estimates it is expected that more than 80,000 common scoters and over 13,000 long-tailed ducks can pass the study area in July and November, respectively. While the long-tailed duck was abundant during both, spring and autumn surveys, the common scoter was observed in large numbers mainly in spring months (except for observations performed in July). The relatively low abundance of the common scoter during autumn migration studies may be related to the different migration routes to the wintering grounds in the Kattegat, the Pomeranian Bay and the Gulf of Gdansk. During the spring migration studies, relatively high numbers of unidentified geese at MB_01 survey station and unidentified waders at MB_02 were also observed. Unidentified geese, ducks (long-tailed duck and common scoter included) and auks (razorbill included) were also noted during autumn migration studies, but the numbers were comparatively lower than in spring. Auks (mainly the razorbill) were observed throughout the spring and autumn surveys, although the spring numbers were relatively higher, especially in March and April. As the main wintering grounds for Baltic populations are located in the Gulf of Riga and Irbe Strait the numbers of auks observed in the study area are moderately low. The other species of auks (common and black guillemot) and other sea ducks (i.e. velvet scoter, common eider, common goldeneye, greater scaup) were observed in lower numbers. Passerines (mainly unidentified to species) were observed throughout the whole spring and autumn migration studies with the exception for July as most of the species were then still present at their breeding grounds and do not start the migration yet.

Flight altitude data obtained from the visual observations conducted in spring and autumn shows that 85–91% (the variability among stations) of all observed birds were flying at altitudes not exceeding 20 m ASL. The most numerous species observed were the long-tailed duck and the common scoter

with the majority of birds flying at the altitude up to 10 m ASL. Only about 0.1% of long-tailed ducks flew above 20 m ASL at both stations during spring surveys and about 2.6% in autumn months. 3.4% of common scoters did not exceed 20 m ASL in course of autumn migration studies. A few species were observed at altitudes ranging from 21 to 100 m ASL (in relatively low numbers) and only 2–7% of all birds were observed at altitudes more than 100 m ASL in spring and 0.05% in autumn. This is due to the fact that visual observations provide data on flight altitude that should be used as an aid to understand the movement of birds flying relatively low above the sea level. At altitudes higher than the very lowest, the vertical radar is considered more reliable in detecting birds.

In April, the radars detected relatively high bird activity at altitudes from 10 up to 100 m at both stations and from 1400–1500 m at survey station MB_02. Less numerous detections in March and May are reflected by the visual observations and number of tracks registered by the horizontal radar. Low numbers encountered in March were expected as for some of the species it is an onset of their spring migration. Elevated numbers in April indicate the spring migration peak occurring this month while the migration intensity recorded in May follows a more mixed pattern. In July and August, the vertical radars detected relatively low bird activity at all altitudes, with the highest reading around 1 track per hour in August from 10 up to 100 m at both stations. Lower detections in July (max 0.5 track per hour) are reflected by the visual observations and number of tracks registered by the horizontal radar. Low numbers encountered in July were expected as the autumn migration is just at its onset and not many species start their migration at that time. In September the number of tracks increased. Especially up to 75 m the number of echoes recorded by the radar tripled. In October and November number of recorded tracks drops back again below one track per hour at all altitudes. In October, the passage activity is more distinct at altitudes up to 100 m at MB_01 station and recorded in the whole operational range of the radar (up to 1500 m ASL) at MB_02 station, while in November very low number of tracks (less than 0.5 track per hour) are observed up to 350 m ASL at both stations. The track intensities recorded in September–November are below the expected ones. We can only assume that due to adverse weather conditions the migration peak might have occurred out of the sampling range, but we are not able to determine the exact reason for this at this point.

General spring movement direction points at NE-E at both stations. In sea ducks (long-tailed duck, common scoter, velvet scoter) clearly dominated NE-E direction as in the case of all tracks analysed together. In geese, two main flight directions were observed: NW-W and NE-E, all pointing into direction of the breeding sites located in north Russia, Finland and Sweden. The auks showed the NW-N flight direction, what is in line with the knowledge about their European breeding sites in Denmark and Sweden. The general pattern of autumn movement at both stations is as predicted – majority of birds flew S-SW-W, with a small portion of birds flying in opposite direction N-NE-E. In seaducks (long-tailed-duck, common scoter and velvet scoter) dominated SW-W direction what indicates the direction of their winter grounds in Danish Straits and Kattegat. Auks were tracked in all directions with the most dominant movement pattern showing opposite direction of W-SW and E-NE. This suggests that tracked auks were most likely local birds performing short trips and not necessarily documenting seasonal migration. Scattered movement patterns of gulls observed at both stations also suggest, that the recorded birds were only to some extent performing seasonal migration and a bigger portion of those gulls were local.

The main purpose of the acoustic analysis was to identify species migrating at night. This analysis also allows us to compare migration dynamics for individual species during daytime and at night. In total, in spring there were 9347 bird calls registered. Almost half of those calls belong to large gulls (e.g.

herring gull, great black-backed gull) – 4241 calls. In total, in autumn there were 11,456 bird calls registered of which 78% belonged to gull species. This activity does not necessarily explain migration movements, since the large gulls are most likely locally breeding (on the coast of Sweden, Gotland, and Poland) and remaining in the region the whole year. Gulls were most often recorded during the day. Passerine calls were registered most frequently in April thus expressing the migration movements toward breeding sites in Scandinavia and in September and October showing migration toward wintering grounds. In spring, the most abundantly recorded nocturnal migrant was the common blackbird, followed by other thrush species: the redwing, the European robin and the song thrush. The most frequently recorded diurnal migrants included the great tit, the white wagtail, and the goldcrest. The highest autumn vocal activity among nocturnally migrating birds was identified for song thrush, grey heron, European robin, redwing, common blackbird, common chaffinch and European herring gull. There were almost no nocturnal migrant calls in May, except for several calls of unidentified large gulls and unidentified passerines. There were also no nocturnal migrant calls in July at both stations, in November at MB_01 and in August at MB_02.

Among all the species recorded during the surveys, two are considered “endangered” on the European scale according to the international scale of the IUCN (BirdLife International, 2021): the common eider and Arctic skua. Seven species belong to the “near threatened” category: the Eurasian curlew, bar-tailed godwit, common swift, horned grebe, tufted duck, red-breasted merganser, and ruff. Ten species are recognised as “vulnerable”: black-legged kittiwake, common pochard, common snipe, curlew sandpiper, velvet scoter, rook, red-necked grebe, tundra swan, northern lapwing and northern pintail. Two species (wintering populations) are considered “critically endangered” according to HELCOM: the black-throated diver and the red-throated diver. Wintering populations of four species are recognised as “endangered”: bean goose, common scoter, red-necked grebe and long-tailed duck. The European population of the Mediterranean gull (both wintering and breeding), as well as dunlin (both wintering and breeding, however, the *C.a. schinzii* subspecies only) and the breeding population of black-legged kittiwake, are also considered “endangered”. Five species belong to the “near threatened” category: common ringed plover, little gull, northern lapwing, northern wheatear and tufted duck. As “vulnerable” were recognized eight species: the Caspian tern, common eider, greater scaup, horned grebe, lesser black-backed gull, red-breasted merganser, ruff and velvet scoter as well as the wintering population of the black-legged kittiwake.

Twenty-three of all observed and recorded species are listed in Annex I of the Birds Directive.

3.5.2.2 Spatial scope of the surveys

The spatial scope of the migratory bird surveys was the survey area covering the Baltica-1 OWF construction area, which is the construction area of the WTGs, OSSs, and cable lines (area A) and the construction area of cable lines (area B) together with a zone of no less than 4 km in width measured from the boundary of area A.

The surveys of bird flights during the wintering period (December2022 – February 2023) were carried out at 2 survey stations, LP_01 and LP_02 situated within area A and within the zone of no less than 4 km in width from the boundary of area A [Figure 3.118]

On the other hand, the surveys of bird flights in the spring migration period (March–May) and the autumn migration period (July–December) were conducted at two survey stations MB_01 and MB_02 situated within area A [Figure 3.119].

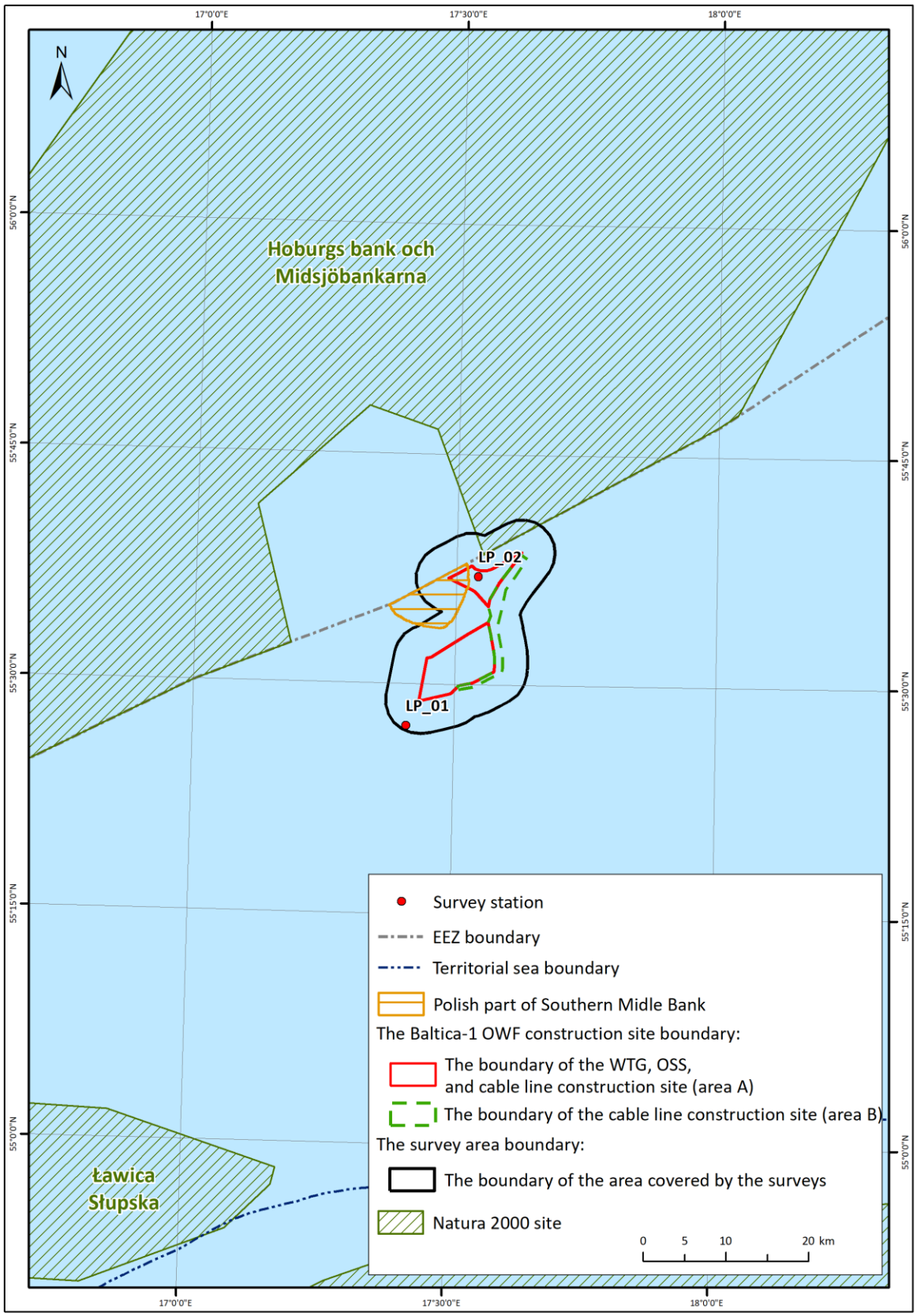


Figure 3.118. The location of survey stations as part of the surveys of bird movements during the wintering period against the background of the Natura 2000 sites and the Southern Middle Bank

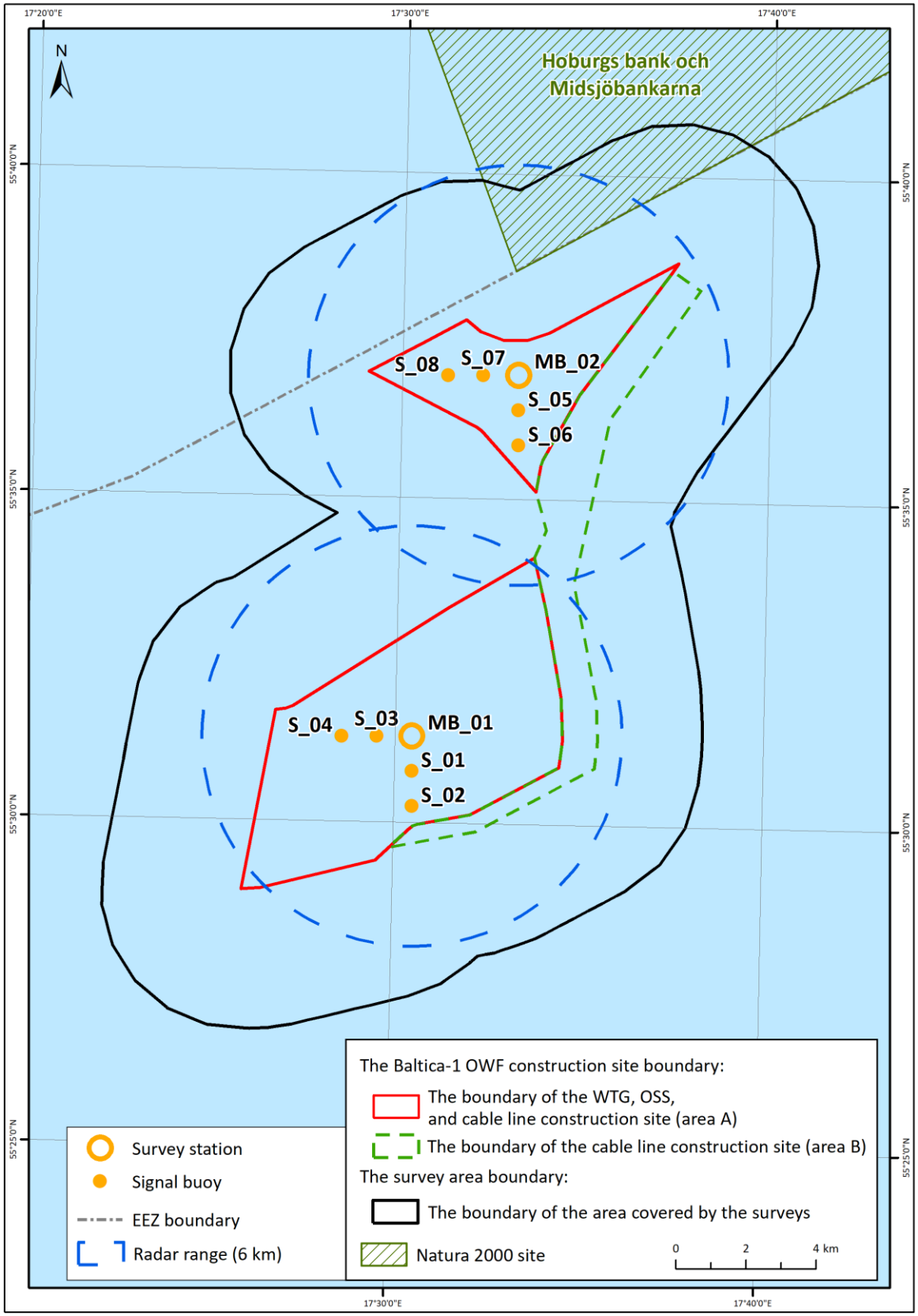


Figure 3.119. The location of survey stations as part of the surveys of bird movements during the spring and autumn migration periods

3.5.2.3 Methodology

During the wintering period, the surveys of local movements were conducted with the use of radar surveys and visual observations. The survey of bird movements during the spring and autumn migration period included surveys using simultaneous registration using vertical and horizontal radars as well as visual observations and acoustic monitoring.

3.5.2.3.1 Visual observations

Visual observations allow to identify species and determine the number of birds and flight directions of the most abundant migrants per day. Visual observations were conducted from aboard a survey vessel constituting a survey station. Two survey points located within the development area were determined so that the surveys could cover the largest possible part of the OWF area. The stations are located at a distance that ensures the coverage of two independent areas with observations (the scope of observations from two points does not overlap). The migration across the Baltic Sea takes place over a wide front and its intensity depends on, to a large extent, the regional and local weather conditions (for example, the wind strength and direction, precipitation, cloud cover, visibility), which means that there are Baltic Sea open sea waters with a constant, annually recurring intensity of bird movements. Therefore, the assumption that the observation area should cover the OWF area to the largest extent possible provides the possibility for conducting the most detailed survey of the migratory fauna.

Visual observations began 30 minutes before sunrise and were continued until 30 minutes after sunset. Observers recorded bird species, number of birds observed, flight altitude and direction, bird behaviour and time of observation at 15-minute intervals [15 minutes of observation and 15 minutes of assistance to the radar operator (flight altitude measurements, species identification)]. All bird observations were recorded in relation to two, 2 km long, north-south/east-west directed transects marked in the survey area with buoys as reference points [Figure 3.120]. The visual observations alternated between the two transects. Accordingly, numbers were only recorded in relation to one of the transects at a given time.

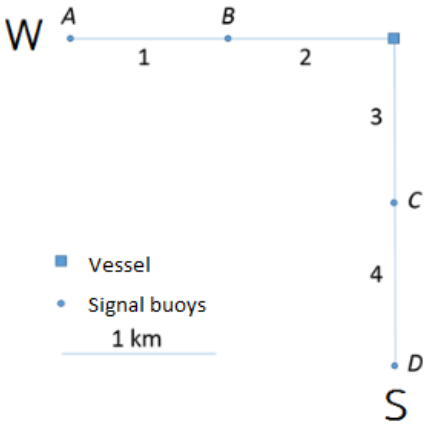


Figure 3.120. Transect segments (marked with numbers) and buoys (marked with dots and letters)

This is the so-called sampling technique: an observer monitors visually the area along the designated, north-south and east-west running transects. The observation of the designated transects enables the registration of birds flying in all directions. The sampling technique enables estimating the abundance of migratory birds over time and in units of area. If an observer tried to observe 360 degrees area, many birds would certainly be overlooked at both short and long distances and the standardisation would be very difficult. Due to the same reason, large gulls, especially European herring gulls, are

counted, however, with an indication that these are not migratory birds. The European herring gulls always accompany vessels, and it is impossible to determine which individuals are actually in the middle of their migration (real migration) and which belong to the locally living gulls that fly over the transect line multiple times. The horizontal radar registers targets omnidirectionally, therefore both methods complement each other thanks to mutual verification.

The flight altitude of birds was estimated visually by observers at approximate altitude ranges (1–10, 10–20, 20–30, 30–40, 40–50, 50–60, 60–70, 70–80, 80–90, 90–100, 100–120 m ASL) and whenever possible, altitude readings from the laser rangefinder were recorded. Four times per day, the observers had a 30-minute break that was not included in the observation time (i.e. that time is not included in the observation forms as a research effort), but the breaks were planned in such a way so as to ensure that the number of observations during the clock hour remains the same. The observations and radar tracking were carried out from the upper deck, behind the bridge (approx. 3.5 m ASL). Integrated surveys involving horizontal radar and visual observations to track the flight trajectory of flying birds were conducted during daytime (identification of flying species by observers is possible only during daytime). The horizontal radar operator shall closely cooperate with the observer on the vessel and remained in close communication with them, so that the identification of the birds tracked with a radar was correct.

The visual observations were continued until the sea state (provided according to the Douglas sea scale) reaches 5, while the horizontal radar surveys were continued up to the sea state 3 according to the Douglas sea scale; however, short periods of poor weather conditions do not preclude the use of radars (this depends on the observers' assessment of the situation).

The distances covered by visual observations depend on the bird species, flock size and environmental conditions determining visibility. Typically, large birds (waterbirds, raptors) can be reliably identified visually as to the species up to a distance of 2–3 km during good visibility conditions, while small passerines and waders can only be identified within a few hundred meters. Therefore, only the passerines observed within 1 km of the vessel should be recorded. For large birds, the main focus should be on migrants moving within a distance of 2 km from the observers. Similarly, the observation and identification of a bird to the species can be correctly determined with the visual method only up to the altitude of 100–300 m, depending on the weather conditions, species, and flock size (the angle of observation of a particular bird can also pose a problem, e.g. observation from the abdomen, when the bird flies over the observer on a sunny day can be very difficult, especially if the identifying features for the species are the plumage on the top of the body, wings, or tail). These limitations indicate that the vertical distribution of bird migration can be visually defined only in relative terms, as birds flying at high altitudes (usually more than 200 m, depending on the situation) will not be visible to the observer.

The data were recorded in special data sheets and included: the transect section, species, number, age, behaviour, distance, flight direction and altitude. The direction of flight was estimated with one digit accuracy using the wind rose. The distance was estimated with an accuracy of one digit. The flight altitude was estimated up to one meter. Additionally, the observer marked in the sheet if the altitude measurement was made with a laser rangefinder. Moreover, observers recorded the behaviour of the observed birds assigned to the following categories:

- M – migratory;
- L – local (including the foraging birds).

After each day or when no research effort is involved, visual observation data were entered into an Excel spreadsheet.

The observations were made using the following equipment:

- binoculars (personal for each observer);
- compass (one per vessel, used by an observer);
- laser range finder (one per vessel).

Before the first observation, each observer calculated the field of view of their personal binoculars by estimating the width of the field of view in meters at a distance of 1 km. The field of view is usually given as an angle. To calculate the field of view, the following formula should be used:

$$\text{Field of view (m)} = 1000 \tan(\alpha)$$

where α is the field of view in degrees indicated in the binocular's specification.

Requirements for the observer's binoculars: Magnification 7–12 ×, lens diameter 40–60 mm.

Main technical parameters of the Vector 21 Aero laser rangefinder:

- magnification: 7 ×;
- field of view: 120 miles/6.75° (or 120 m at a distance of 1 km);
- laser type: 1550 nm;
- range: 5–12 000 m;
- accuracy: ±5 m;
- azimuth accuracy (1σ) without tripod calibration: ±10 miles/±0.6°;
- inclination angle accuracy: ±3 miles/±0.2°.

In order to estimate the number of bird flights over the survey area, standardisation is carried out by determining the number of birds per one hour of observation, which is then averaged over a period of one month (the unit is the number of birds per hour). Such calculations are conducted only for the most abundant species whereas less abundant species are grouped into higher taxonomic units.

In the case of simultaneous observations at both survey points, the migratory flux will be counted separately for both points, and then averaged (added and divided by 2), to avoid doubling of the number of observations.

The passage of migratory birds across the survey area – referred to as the "migratory flux" – is calculated on the basis of the visual observation data using the step-by-step procedure illustrated in [Figure 3.122]:

- Stage 1: Bird visual observation data. This is a set of data collected by the visual observers at each survey station;
- Stage 2: Selection of bird observation at a designated distance from the survey station. Only bird sightings recorded up to a distance of 2 km are selected as this is the distance at which the majority of bird observations are made by observers, according to the migratory bird survey methodology. Observers often count migratory birds recorded at longer distances, but these observations will be excluded from the standard migratory flux calculations;
- Stage 3: Correction of the number of bird observations in order to detect distance deviations. It is quite likely that detection of smaller species of migratory birds declines with an increasing

distance from the observer. To determine this relationship, a distance analysis is carried out for groups of auks, waders and passerine species in order to calculate the function of observation distance for these groups during visual observations;

- Stage 4: Conversion of bird fluxes per kilometre per hour for headwind and tailwind. Bird observations are converted into the number of flights of a given species per one kilometre per hour. These calculations are made separately for each calendar month by dividing the total number of species observations (corrected using distance analysis) by the total number of observation time for that month. Additionally, these calculations will be conducted separately for headwind and tailwind. The division based on wind conditions is established due to the fact that the intensity of bird migration depends on wind conditions. Wind data modelled at a height of 10 m were obtained at 1-hour intervals from StormGeo website. Wind directions between degree 135 and degree 315 was defined as tailwind in spring and headwind in autumn [Figure 3.121].

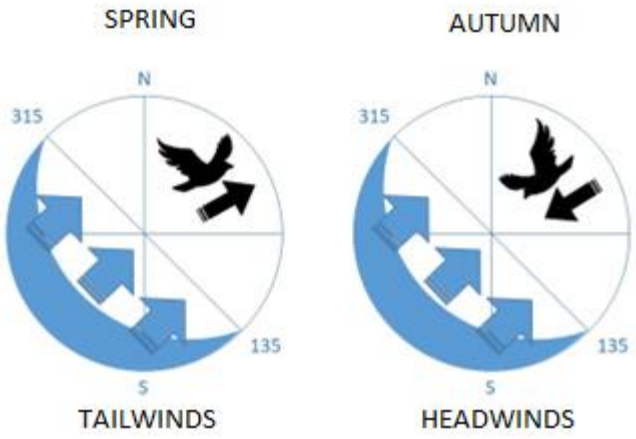


Figure 3.121. An illustration of headwinds and tailwinds during spring and autumn migration (marked in blue) for the dominant migratory bird flight directions (marked in black)

- Stage 5: Calculation of the number of bird flights per kilometre per month for headwind and tailwind. Calculations of bird flux rates observed were conducted for headwind and tailwind conditions, for each month of the bird winter migration period subject to monitoring.

$$Headwind\ bird\ flux = \left(\frac{\frac{Fpm}{2}}{NB}\right) * \%headwind$$

$$Tailwind\ bird\ flux = \left(\frac{\frac{Fpm}{2}}{NB}\right) * \%tailwind$$

where:

The headwind/tailwind bird flux is the number of birds flying per hour across a 1 km section of a transect [N/1 km/h] for the headwind and tailwind respectively; Fpm – the number of birds observed at a particular observation point flying during the surveys per month [N]; 2 – designated transect length (2 km) [km]; NB – research effort, i.e. the number of hours of

observation per month [h]; % of wind – percentage share of tailwind or headwind during observations.

Based on the proportion of birds flying either in headwind or tailwind, we extrapolated the number of birds passing each month while taking wind directions into account. Extrapolation of the migratory flux calculated per hour per kilometre (number of birds/km/hour) to bird flights per month (number of birds/km/month) was performed using the number of daylight hours per day in a given month. Daylight duration information was based on the United States Naval Observatory website for the location of the survey area. The extrapolation also accounted for wind directions during daylight hours in each month.

- Stage 6: Multiplying monthly bird flights by the width of the survey area to obtain daily migration flow throughout the survey area. The total flux of birds moving through the area was obtained by multiplying the monthly number of bird flights per linear kilometre by the width of the survey area.

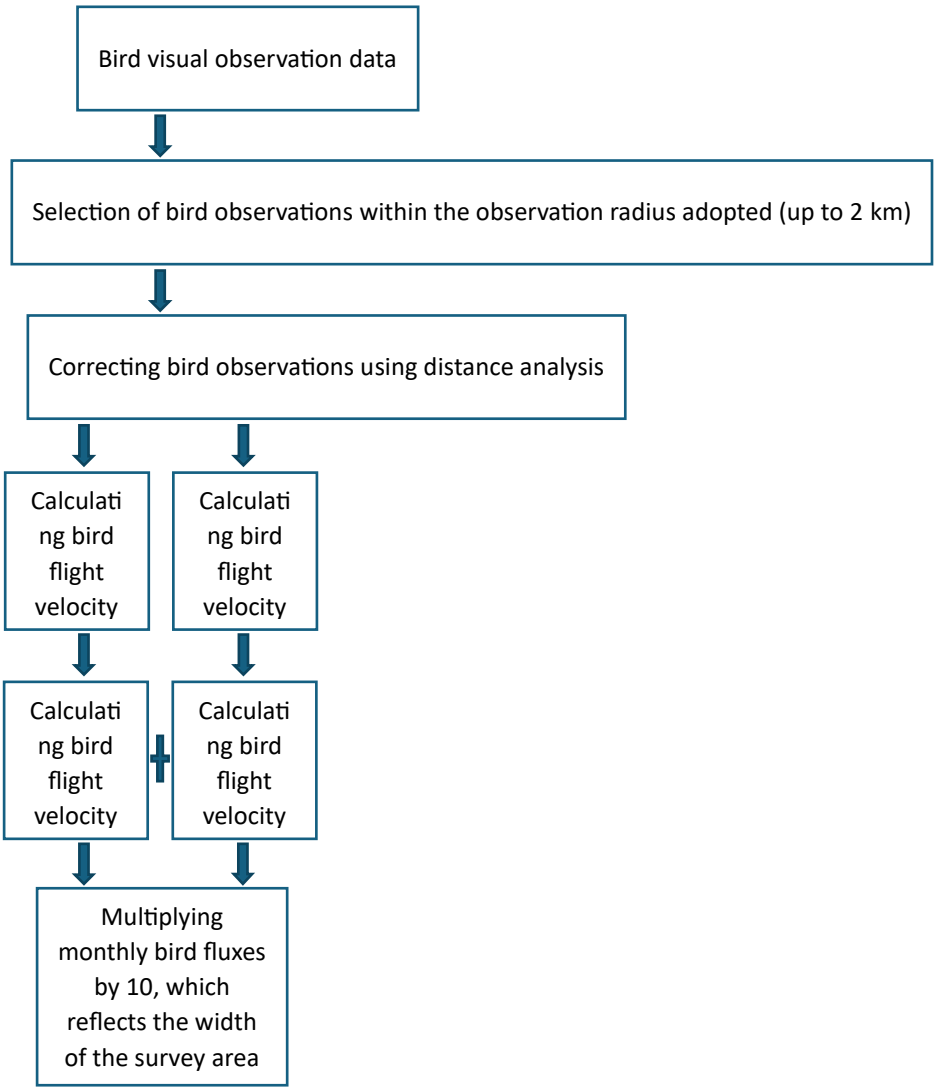


*Figure 3.122. A flow chart illustrating the main steps taken when estimating the total passage of migratory birds through the survey area based on visual daytime observations**

**the survey area width provided is not final and may differ from the exemplary value provided depending on the dominant bird flight directions*

The distance analysis was aimed at correcting the distance-related bias in bird observations carried out using the R distance package in R software. In other words, the purpose of this analysis was to determine which part of the observation should be included in the analysis of bird fluxes in order to avoid errors resulting from detection capabilities that decline as the distance from the observer increases. Distance analysis was carried out to calculate the distance function for the observation of smaller birds recorded during visual observations from anchored vessels. The distance analysis did not incorporate the vertical distance from an observer.

The detection of birds may decline with the distance from the observation position. The decline is typically non-linear, with high detection rates near the observer up to a point where bird detection capabilities gradually drop as the distance increases (function of observation distance).

All probability functions are included in R software package: uniform, half-normal hazard-rate, negative exponential and gamma. Each function is weighted using 0 to 5 expansion – simple polynomial, Hermite or cosine.

As a result, the best fitting function is selected on the basis of the smallest Akaike Information Criterion (AIC) values and control of the function fitting curve. The data are analysed by limiting the maximum survey distance between 1000 m and 2000 m, depending on the detection distance of a given species and control of detection function curves obtained using all data. This means that after establishing the measurement distance (1000 m or 2000 m), observations beyond the limit accepted have not been taken into account in further analyses.

Bird detection probabilities may vary depending on bird behaviour, weather conditions, observation platform and the observer's skills. However, sample size limits the degree of stratification that can be applied to survey data, therefore no stratification is applied for calculating species detection distance. Generalised detection functions were calculated for the entire dataset for each species with a sufficient number of sightings. If the number of observations was low at species level, distance detection functions were calculated for lower taxonomic groups.

The results of distance analysis are presented as a species-specific detection curve chart, detection curve function and its expansion as well as an estimated effective strip width (ESW).

The effective strip width (ESW) is a key parameter applied to correct bird numbers observed in order to specify distance detection bias, while the other parameters characterise the fit of the model. ESW represents the distance from the observation point, for which the probability of bird sighting beyond the ESW area is the same as the probability of no sighting within the ESW. Next, the ESW value was be used to estimate the number of birds that probably migrated within the observation strip. For example, if the observation distance (D) for a given species was 2000 m, and the estimated ESW was 800 m, the corrected number of birds (N_{cor}) is calculated by dividing the number of birds observed up to a distance of 2000 m (N_{obs}) by the ESW and multiplying by D:

$$N_{cor} = \frac{N_{obs}}{ESW} \times D$$

Flight direction of the birds observed was recorded by observers and presented in the form of radar charts cumulatively (for all data) and for the most abundant species. On the basis of the charts, it was possible to estimate the migration distribution in the survey area and to determine whether or not the individuals observed were resident or migratory birds.

The results of flight altitude estimations by the observers are presented in horizontal bar graphs for all data globally for both stations and individually for the most abundant species. Visually estimated data relating to the flight altitudes of migratory birds, although inclined towards smaller altitudes, provide crucial information relevant for the calculation of the collision risks of birds with offshore wind turbines.

3.5.2.3.2 Radar observations

The radar observations were carried out using 3Bird radar systems that are based on radar systems with a bird flight automatic detection algorithm, manufactured by the Dutch company RobinRadar and adjusted to operation aboard survey vessels by 3Bird. 3Bird radar systems consist of the following components:

1) horizontal radar: a pulsed radar, equipped with an antenna with a length of at least 3.6 m, rotating at a speed of at least 45 rpm, with 30 kW pulse power and at least 40 W average power, operating in S-Band frequency;
2) vertical radar: a pulsed radar, equipped with an antenna with a length of at least 2.4 m, rotating at a speed of at least 24 rpm, with 25 kW pulse power and at least 20 W average power, operating in X-Band frequency or a frequency-modulated continuous-wave radar equipped with an antenna with a length of at least 2.4 m, rotating at a speed of at least 20 rpm, with at least 0.4 W average power, operating in X-Band frequency;
3) 3BrosControl software used to optimise radar measurements in terms of the possibility of automatic bird flight detection in different sea wave motion conditions (significant wave height);
4) weather station monitoring air temperature, wind speed, wind direction, atmospheric pressure, and geographic coordinates;
5) satellite compass recording the position of the survey vessel from which surveys are conducted with a frequency of at least 1 Hz;
6) signalling processors with software used for automatic real-time detection of bird flights on the basis of radar images and recording of raw radar images (RAW format images) and bird flight routes in vector form (PostgreSQL database);
7) at least two external, rugged laptops with a wireless connection to the radar system, used for recording ornithological observations directly in the PostgreSQL data base;
8) a platform fixing the radar system to the deck of the survey vessel.

3.5.2.3.2.1 Horizontal radar surveys

Migratory bird tracking provides a detailed information on the flight direction of individual birds and bird flocks. Flight trajectories are determined automatically in real time on the basis of the analysis of radar images recorded by the 3BIRD radar operating in the S-Band. Flight trajectories were visualised in real time in the Robin Visualizer software and were saved in the PostgreSQL database as vector data in the form of lines and line breakpoints where pixels showing the place of detection of the presence of birds appear on the radar images. The radar range radius was no less than 6 km. The horizontal radar was installed on vessels and used S-band Furuno 30 kW or 60 kW technology and GPS stabilisation to ensure correct georeferencing of records. The geometry of bird tracks was recorded in real time in the vessel's local system (Head Up) and then converted in the post-processing mode to the geographic coordinate system (WGS 84, UTM Zone 33N, and PL-1992). The positioning of the radar was done by connecting the data recorded by a satellite compass, which ensured the calculation of the course with an accuracy of 1° in all directions. The radar system was optimised for the possibility of detecting birds

in changing sea states. For this purpose, the original 3BrosControl software was used, which performed automatic tuning of the radar system parameters depending on the current heights of significant waves. Significant wave heights were estimated by a radar analyst and ornithologists (observers). For estimation, auxiliary data on wind speed and direction were used, which will be displayed in real time in the window of 3BrosControl application.

The observation team, consisting of a radar analyst and observers, worked with the Robin Visualizer software [Figure 3.123] and added descriptive information on the species and the amount of data found to the tracked routes of the birds' flights. The observer team worked on at least two workstations running the Robin Visualizer software. Based on the estimation of the significant wave height by a radar analyst, the 3BROS software adjusted the parameters of the automatic process of detecting bird movements by the radar system.

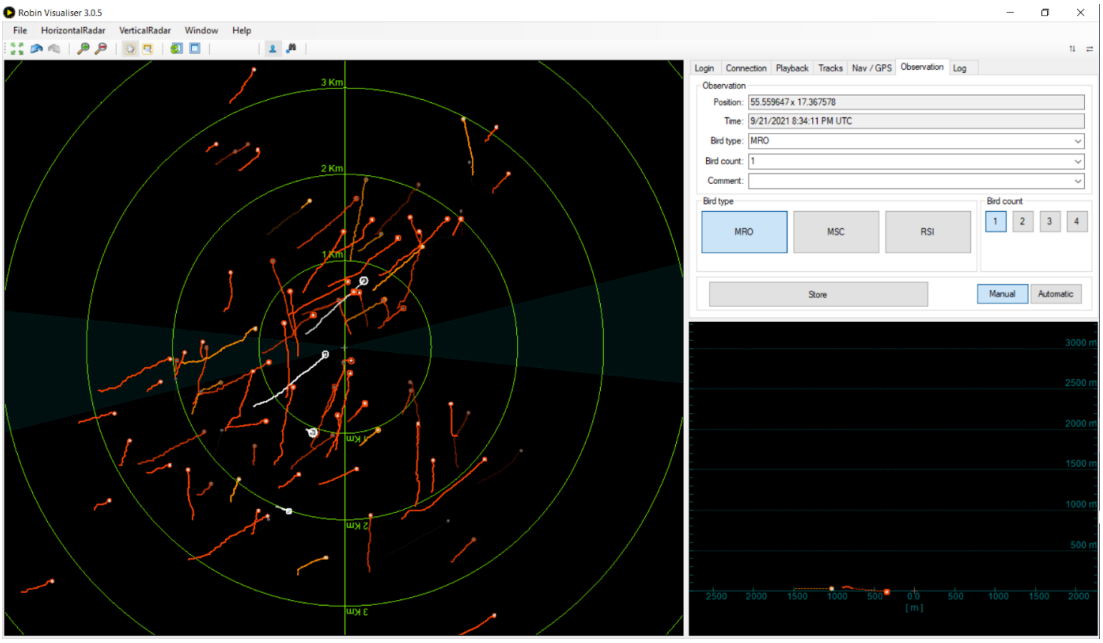


Figure 3.123. A screenshot of the Robin Visualiser display with radar screen as a background image on the left and editing console on the right. Continuous lines indicate flight trajectories automatically determined in real time by the horizontal radar

3.5.2.3.2.2 Vertical radar surveys

The flight altitude of migratory birds (the altitude at which flying birds are recorded) was recorded by a vertical radar, which operates continuously in a 24-hour mode. Flight altitude trajectories were determined automatically in real time on the basis of the analysis of radar images recorded by the 3BIRD radar operating in the X-Band. Flight altitude trajectories were visualised in real time in the Robin Visualizer software [Figure 3.124] and saved in the PostgreSQL database as vector data in the form of lines and line breakpoints where pixels showing the place of detection of the presence of birds appeared on the radar images. The radar range was not smaller than 1500 m. The radar installed on the vessels used X-band Furuno 25 kW technology and GPS stabilisation to ensure correct georeferencing of records. The radar positioning was performed using the data recorded by a satellite compass, which ensured the calculation of the course with an accuracy of 1° in all directions.

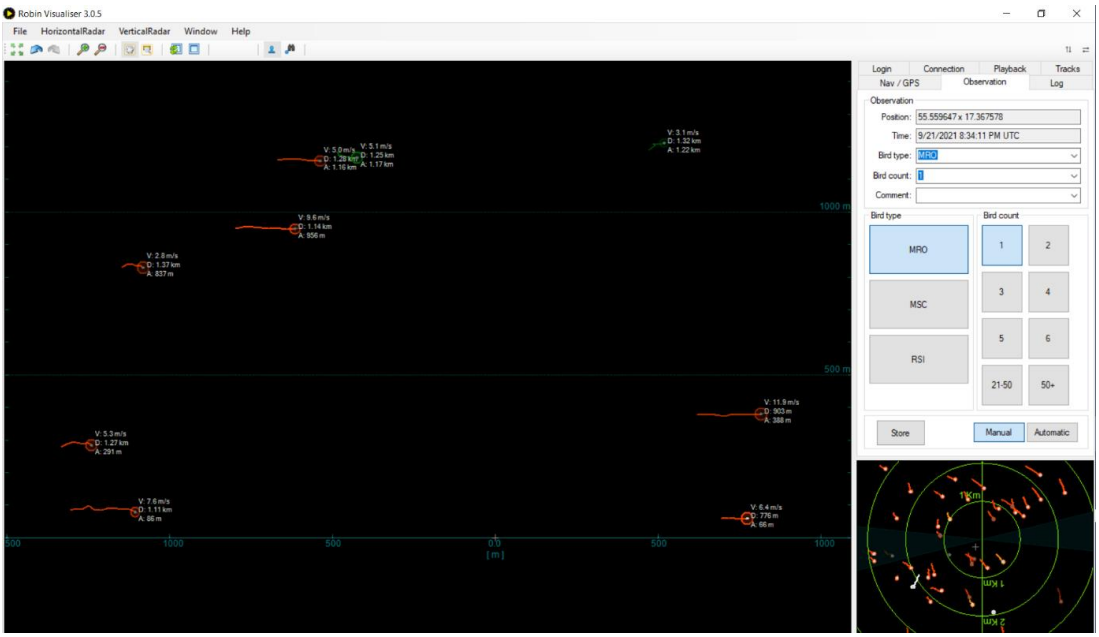


Figure 3.124. A screenshot of the Robin Visualiser display of a vertical radar presenting the passage routes of birds migrating at different altitudes

3.5.2.3.3 Acoustic monitoring

Acoustic recordings were made automatically with the use of a microphone and recording equipment. Acoustic recordings were made continuously by recording bird calls for 15 minutes every hour, both day and night. The recordings were analysed and processed by an experienced observer. Whenever possible, bird calls were identified down to the species level, counted and summed up for the 15-minute periods. No recordings should be made during heavy rain. In medium to strong winds, noise can also impair the quality of recordings. Observers and crew mustn't feed the seagulls at any time, since these birds, when attracted to the vessel, become a significant source of data disruption. Automatic acoustic recorders have been found to be able to detect more bird calls than a person listening to the birds on deck. Noise sources on the vessel should be limited.

The following equipment will be used for acoustic recordings:

- microphone;
- acoustic recorder SM2+ (Wildlife Acoustics).

Acoustic recordings enable the identification to the species level of those birds that fly close to the microphone of the recorder. They provide a qualitative assessment of the species composition, particularly important in the case of nocturnal migrations. Acoustic analysis is the only method enabling species identification, but it should be noted that it targets vocally active species. This means that, for example, flying ducks or auks, which are not highly vocally active during flight, are usually unrecorded. Acoustic data was analysed by an experienced ornithologist. The analyses were performed by viewing sonograms in Adobe Audition acoustic software. If the sound recordings on the sonogram were unrecognisable, the recordings were played back and identified by listening.

Key technical parameters of the SM2+ Wildlife Acoustics acoustic recorder:

- water-proof enclosure;

- autonomous internal power supply with 4 D-size batteries, which must be replaced every 5 days;
- data storage: 4 flash SD cards (SDHC class 10 to 32 GB);
- the number of channels: 1;
- programmable schedule;
- regulated sampling frequency: 4000–384 000 Hz (the sampling frequency 22 050 will be used which equals 11,025 Hz, and corresponds to bird calls within the range from 1200 to 9000 Hz);
- high-pass filter: 2-pole, 180–1800 Hz (1000 Hz filter will be used to remove the worst noise from the vessel. None of the relevant bird species produces sounds at frequencies below 1000 Hz);
- pre-amplifier: switch selectable for channels, at +0, +12, +24, +36, +48, or + 60 dB gain;
- output format: *.WAV files.

3.5.2.4 Activities performed

During the wintering period, at point LP_01 the surveys were performed using two survey vessels: Doktor Lubecki on the following dates: 9–10 December 2022, 9–10 January 2023, 19 January 2023, 6–8 February 2023 and 28 February 2023, and HEL-125 on 17 December 2022. At point LP_02, the surveys from aboard Doktor Lubecki were conducted on the following dates: 15–17 December 2022, and from the deck of HEL-125 on 9–10 January 2023, 12–20 January 2023, 6–8 February 2023, and 28 February 2023.

The total survey effort with a division into the methods of data collection is presented for points in Table 3.81 and Table 3.82.

Table 3.81. Total survey effort at LP_01 station in December 2022, January and February 2023

Date	Inspection start time	Inspection end time	Duration of inspection	Visual observations	Flight trajectory tracking using a horizontal radar [hh:min]	Laser rangefinder [hh:min]	Horizontal radar [hh:min]	Vertical radar [hh:min]
09.12.2022	06:05	14:50	08:45	08:14	08:14	08:14	08:30	08:30
10.12.2022	06:35	14:50	08:15	08:13	08:13	08:13	08:55	08:55
17.12.2022	04:30	15:50	11:20	08:08	10:30	08:08	10:30	10:30
09.01.2023	06:40	15:10	08:30	08:26	08:26	08:26	09:08	09:08
10.01.2023	06:40	15:15	08:35	08:29	08:29	08:29	09:29	09:29
19.01.2023	06:30	15:30	09:00	08:54	08:54	08:54	09:25	09:25
06.02.2023	06:00	16:05	10:05	10:00	10:00	10:00	18:40	18:40
07.02.2023	06:00	16:10	10:10	10:06	10:06	10:06	16:50	16:50
08.02.2023	06:00	16:10	10:10	10:10	10:10	05:00	11:11	11:11
28.02.2023	04:15	17:00	12:45	11:38	11:38	11:38	12:40	12:40
Total			97:35	92:18	94:40	87:08	115:18	115:18

Table 3.82. Total survey effort at LP_02 station in December 2022, January and February 2023

Date	Inspection start time	Inspection end time	Duration of inspection	Visual observations	Flight trajectory tracking using a horizontal radar [hh:min]	Laser rangefinder [hh:min]	Horizontal radar [hh:min]	Vertical radar [hh:min]
15.12.2022	06:40	14:50	08:10	08:05	08:05	08:05	08:59	08:59
16.12.2022	07:30	14:50	07:20	07:15	07:15	07:15	07:22	07:22
17.12.2022	06:40	14:50	08:10	08:03	08:03	08:03	08:45	08:45
09.01.2023	04:10	24:00	19:50	08:25	19:32	08:25	19:32	19:32
10.01.2023	00:00	15:10	15:10	08:27	15:11	08:27	15:11	15:11
19.01.2023	03:05	24:00	20:55	08:53	08:53	08:53	08:53	08:53
20.01.2023	00:00	15:35	15:35	08:56	08:56	08:56	08:56	08:56
06.02.2023	04:05	24:00	19:55	10:00	10:00	10:00	17:56	17:56

Date	Inspection start time	Inspection end time	Duration of inspection	Visual observations	Flight trajectory tracking using a horizontal radar [hh:min]	Laser rangefinder [hh:min]	Horizontal radar [hh:min]	Vertical radar [hh:min]
07.02.2023	00:00	23:55	23:55	10:04	10:04	10:02	00:00	00:00
08.02.2023	00:00	16:10	16:10	10:08	10:08	10:08	16:08	16:08
28.02.2023	05:15	17:00	11:45	11:38	11:38	11:38	12:10	12:10
Total			166:55	99:54	117:45	99:52	147:52	147:52

The collected data is sufficient for analysis of data on local bird movements during the wintering period between areas of significant importance for birds, i.e. the Southern Middle Bank and Natura 2000 sites: Hoburgs bank och Midsjöbankarna (SE0330308) and Słupsk Bank (PLC990001). Based on the interpretation of the data collected, it is possible to assess the potential impact of the Baltica-1 OWF on the local bird movements in the wintering period between areas of great significance for birds.

During the spring migration season, from March to the end of May 2023, 22 days of observations were carried out at survey station MB_01 and 22 days of observations at station MB_02. The surveys included visual observations, radar tracking using a vertical and horizontal radar, and acoustic monitoring.

At station MB_01, the surveys were conducted on the following dates: 1–3 March, 16–21 March, 25–26 March, 04–06 April, 12–18 April, 21–22 April, 2–4 May, 8–9 May and 19–22 May. At station MB_02, the surveys were conducted on the following dates: 1–2 March, 16–21 March, 25–26 March, 6–7 April, 12–17 April, 21–24 April, 8–11 May, 19–20 May, and 22–24 May.

The total survey effort with a division into the data collection methods is presented for both survey stations in Table 3.83 and Table 3.84.

Table 3.83. Total survey effort at MB_01 station in March, April and May 2023

Date	Start time of the observation day	End time of the observation day	Total duration of the observation day	Visual observations	Flight trajectory tracking using a horizontal radar [hh:min]	Laser rangefinder [hh:min]	Horizontal radar [hh:min]	Vertical radar [hh:min]	Acoustic monitoring [hh:min]
01.03.2023	00:05	00:00	23:55	11:43	11:43	11:43	23:55	23:55	23:55
02.03.2023	00:00	23:55	23:55	11:47	11:47	11:47	24:00	24:00	24:00
03.03.2023	00:00	00:05	00:05	00:00	00:00	00:00	00:05	00:05	00:05
16.03.2023	05:35	24:00	18:25	11:49	11:49	11:49	18:25	18:25	18:35
17.03.2023	00:00	05:35	05:35	01:00	01:04	01:00	05:31	05:31	05:31
18.03.2023	01:35	24:00	22:25	05:53	05:53	05:53	12:25	12:25	12:25
19.03.2023	00:00	24:00	24:00	00:50	00:50	00:50	24:00	24:00	24:00
20.03.2023	00:00	24:00	24:00	13:09	13:09	13:09	24:00	24:00	24:00
21.03.2023	00:00	18:30	18:30	13:09	13:09	13:09	17:30	17:30	17:30
25.03.2023	11:30	24:00	12:30	06:13	06:13	06:13	12:30	12:30	12:30
26.03.2023	00:00	14:15	14:15	02:39	02:39	02:39	14:15	14:15	14:15
				04:45	04:45	04:45	00:00	00:00	00:00
04.04.2023	08:00	24:00	16:00	10:02	10:02	10:02	16:00	16:00	16:00
05.04.2023	00:00	24:00	24:00	14:23	14:23	14:23	24:00	24:00	24:00
06.04.2023	00:00	08:00	08:00	04:21	04:21	04:21	08:00	08:00	08:00
12.04.2023	04:50	24:00	19:10	06:40	06:40	06:40	19:10	19:10	19:10
13.04.2023	00:00	24:00	24:00	15:00	15:00	15:00	24:00	24:00	24:00
14.04.2023	00:00	24:00	24:00	01:26	01:26	01:26	24:00	24:00	24:00
				13:27	13:27	13:27	00:00	00:00	00:00
15.04.2023	00:00	12:30	12:30	09:14	09:14	09:14	12:31	12:30	12:30
16.04.2023	01:40	24:00	22:20	02:46	02:46	02:46	04:16	04:16	04:16
				11:47	11:47	11:47	17:20	17:20	17:20
17.04.2023	00:00	24:00	24:00	15:17	15:17	15:15	24:00	24:00	24:00

Date	Start time of the observation day	End time of the observation day	Total duration of the observation day	Visual observations	Flight trajectory tracking using a horizontal radar [hh:min]	Laser rangefinder [hh:min]	Horizontal radar [hh:min]	Vertical radar [hh:min]	Acoustic monitoring [hh:min]
18.04.2023	00:00	04:30	04:30	01:20	01:20	01:20	04:30	04:30	04:30
21.04.2024	08:15	00:00	15:45	10:22	10:22	10:22	15:45	15:45	15:45
22.04.2024	00:00	08:15	08:15	05:16	05:16	05:16	08:15	08:15	08:15
02.05.2023	19:10	24:00	04:50	00:00	00:00	00:00	04:50	04:50	04:50
03.05.2023	00:00	24:00	24:00	16:26	16:26	16:26	24:00	24:00	24:00
04.05.2023	00:00	19:10	19:10	16:30	16:30	16:30	19:10	19:10	19:10
08.05.2023	05:40	24:00	18:20	13:30	13:30	13:30	18:20	18:20	18:20
09.05.2023	00:00	05:40	05:40	03:19	03:19	03:19	05:40	05:40	05:40
19.05.2023	00:00	24:00	24:00	17:27	17:27	17:27	24:00	24:00	24:00
20.05.2023	00:00	24:00	24:00	17:31	17:31	17:31	24:00	24:00	24:00
21.05.2023	00:00	24:00	24:00	17:34	17:34	17:34	24:00	24:00	24:00
22.05.2023	00:00	00:10	00:10	00:00	00:00	00:00	00:10	00:10	00:10
Total			534:15	306:35	306:39	306:33	522:33	522:32	522:42

Table 3.84. Total survey effort at MB_02 station in March, April and May 2023

Date	Start time of the observation day	End time of the observation day	Total duration of the observation day	Visual observations	Flight trajectory tracking using a horizontal radar [hh:min]	Laser rangefinder [hh:min]	Horizontal radar [hh:min]	Vertical radar [hh:min]	Acoustic monitoring [hh:min]
01.03.2023	00:00	24:00	24:00	11:42	11:42	11:42	24:00	24:00	24:00
02.03.2023	00:00	24:00	24:00	11:47	11:47	11:47	24:00	24:00	24:00
16.03.2023	03:15	24:00	20:45	12:52	12:52	12:52	21:00	21:00	21:00
17.03.2023	00:00	03:00	03:00	00:00	00:00	00:00	24:00	24:00	24:00
18.03.2023	04:00	24:00	20:00	13:00	13:00	13:00	24:00	24:00	24:00
19.03.2023	00:00	24:00	24:00	13:05	13:05	13:05	24:00	24:00	24:00

Date	Start time of the observation day	End time of the observation day	Total duration of the observation day	Visual observations	Flight trajectory tracking using a horizontal radar [hh:min]	Laser rangefinder [hh:min]	Horizontal radar [hh:min]	Vertical radar [hh:min]	Acoustic monitoring [hh:min]
20.03.2023	00:00	24:00	24:00	13:09	13:09	13:09	24:00	24:00	24:00
21.03.2023	00:00	06:00	06:00	01:10	01:10	01:10	06:08	06:08	06:15
25.03.2023	11:30	24:00	12:30	06:12	06:12	06:12	12:30	12:30	12:30
26.03.2024	00:00	14:15	14:15	02:33	02:33	02:33	10:08	10:08	10:08
				05:00	05:00	05:00	00:00	00:00	00:00
06.04.2023	10:45	24:00	13:15	07:21	07:21	07:21	13:15	13:15	13:15
07.04.2023	00:00	11:30	11:30	05:04	05:04	05:04	11:30	11:30	11:30
				02:25	02:25	02:25	00:00	00:00	00:00
12.04.2023	03:05	24:00	20:55	08:06	08:06	08:06	20:55	20:55	20:55
13.04.2023	00:00	24:00	24:00	15:00	15:00	15:00	24:00	24:00	24:00
14.04.2023	00:00	12:00	12:00	07:30	07:30	07:30	12:00	12:00	12:00
15.04.2023	15:15	24:00	08:45	03:04	03:04	03:04	08:45	08:45	08:45
16.04.2023	00:00	24:00	24:00	15:14	15:14	15:14	10:36	10:38	24:00
				00:00	00:00	00:00	12:29	12:29	00:00
17.04.2023	00:00	16:30	16:30	13:19	13:19	13:19	16:30	16:30	16:30
21.04.2023	01:35	24:00	22:25	15:35	15:35	15:35	22:29	22:22	22:22
22.04.2023	00:00	24:00	24:00	15:39	15:39	15:39	24:00	24:00	24:00
23.04.2023	00:00	24:00	24:00	15:45	15:45	15:42	24:00	24:00	24:00
24.04.2023	00:00	01:40	01:40	00:00	00:00	00:00	01:45	01:45	01:45
08.05.2023	02:05	24:00	21:55	16:47	16:47	16:47	21:55	21:55	21:55
09.05.2023	00:00	24:00	24:00	16:51	16:51	16:51	24:00	24:00	24:00
10.05.2023	00:00	24:00	24:00	16:55	16:55	16:55	24:00	24:00	24:00
11.05.2023	00:00	03:30	03:30	01:13	01:13	01:13	03:30	03:30	03:30
19.05.2023	06:10	24:00	17:50	13:21	13:21	13:21	17:50	17:50	17:50

Date	Start time of the observation day	End time of the observation day	Total duration of the observation day	Visual observations	Flight trajectory tracking using a horizontal radar [hh:min]	Laser rangefinder [hh:min]	Horizontal radar [hh:min]	Vertical radar [hh:min]	Acoustic monitoring [hh:min]
20.05.2023	00:00	24:00	24:00	04:09	04:09	04:09	06:10	06:10	06:10
22.05.2023	03:00	24:00	21:00	16:36	16:36	16:36	21:00	21:00	21:00
23.05.2023	00:00	24:00	24:00	17:41	17:41	17:41	24:00	24:00	24:00
24.05.2023	00:00	03:10	03:10	01:06	01:06	01:06	03:00	03:00	03:00
Total			538:55	319:11	319:11	319:08	541:25	541:20	542:20

The collected data is sufficient for analysis of data on the spring migration of birds through the Baltica-1 OWF area. Based on the interpretation of the data collected, it is possible to assess the potential impact of the Baltica-1 OWF on the spring migrations of birds in the area surveyed.

In the autumn migration period, between July and the beginning of December 2023, 22 days of observations were carried out at survey station MB_01 and 20 days of observations at survey station MB_02. The surveys included visual observations, radar tracking using horizontal and vertical radar, and acoustic monitoring.

At survey station MB_01, the surveys were conducted on the following dates: 28–29 July, 11–13 August, 17–21 August, 6–9 September, 24–27 September, 22–24 October, 27–29 October, 29–30 November and 1–4 December. At survey station MB_02, the surveys were conducted on the following dates: 27–28 July, 13–15 August, 21–23 August, 6–9 September, 25–28 September, 22–24 October, 27–29 October, 11–13 November, 29–30 November and 1–2 December.

The total survey effort with a division into the data collection methods is presented for both survey stations in Table 3.85 and Table 3.86.

Table 3.85. Total survey effort at MB_01 station in July, August, September, October, November and December 2023

Date	Start time of the observation day	End time of the observation day	Total duration of the observation day	Visual observations	Flight trajectory tracking using a horizontal radar [hh:min]	Laser rangefinder [hh:min]	Horizontal radar [hh:min]	Vertical radar [hh:min]	Acoustic monitoring [hh:min]
28.07.2023	05:30	24:00	18:30	13:54	13:54	13:54	18:20	18:20	18:20
29.07.2023	00:00	05:45	05:45	03:21	03:21	03:21	05:40	05:40	05:40
11.08.2023	11:50	24:00	12:10	07:14	07:14	07:14	12:09	12:09	12:09
12.08.2023	00:00	24:00	24:00	16:17	16:17	16:17	24:00	24:00	24:00
13.08.2023	00:00	13:35	13:35	02:42	02:42	02:42	13:31	13:31	13:31
13.08.2023				06:21	06:21	06:21	00:00	00:00	00:00
17.08.2023	18:50	24:00	05:10	00:00	00:00	00:00	05:02	05:02	05:02
18.08.2023	00:00	24:00	24:00	15:52	15:52	15:52	24:00	24:00	24:00
19.08.2023	00:00	24:00	24:00	08:46	08:46	08:46	24:00	24:00	24:00
20.08.2023	00:00	24:00	24:00	00:00	00:00	00:00	24:00	24:00	24:00
21.08.2023	00:00	18:45	18:45	15:38	15:38	15:38	18:42	18:42	18:42
06.09.2023	07:10	24:00	16:50	10:36	10:36	10:36	16:35	16:35	16:35
07.09.2023	00:00	24:00	24:00	14:24	14:24	14:24	24:00	24:00	24:00
08.09.2023	00:00	24:00	24:00	14:19	14:19	14:19	24:00	24:00	24:00
09.09.2023	00:00	07:25	07:25	03:46	03:46	03:46	07:25	07:25	07:25
24.09.2023	17:10	24:00	06:50	00:00	00:00	00:00	06:46	06:46	06:46
25.09.2023	00:00	24:00	24:00	13:02	13:02	13:02	24:00	24:00	24:00
26.09.2023	00:00	24:00	24:00	12:58	12:58	12:58	24:00	24:00	24:00
27.09.2023	00:00	18:55	18:55	12:53	12:53	12:53	18:20	18:20	18:45
22.10.2023	02:30	24:00	21:30	07:27	07:27	07:27	21:20	21:20	21:20
				01:49	01:49	01:49	00:00	00:00	00:00
23.10.2023	00:00	24:00	00:00	10:57	10:57	10:57	24:00	24:00	24:00
24.10.2023	00:00	07:05	07:05	07:00	01:53	01:53	07:00	07:00	07:00

Date	Start time of the observation day	End time of the observation day	Total duration of the observation day	Visual observations	Flight trajectory tracking using a horizontal radar [hh:min]	Laser rangefinder [hh:min]	Horizontal radar [hh:min]	Vertical radar [hh:min]	Acoustic monitoring [hh:min]
27.10.2023	07:40	24:00	16:20	07:19	07:19	07:19	15:25	15:25	15:25
28.10.2023	00:00	24:00	24:00	10:36	10:36	10:36	24:00	24:00	24:00
29.10.2023	00:00	10:05	10:05	00:00	00:00	00:00	05:30	05:30	10:05
				03:06	03:06	03:06	03:06	03:06	00:00
29.11.2023	11:00	24:00	13:00	03:50	03:50	03:50	12:55	12:55	12:55
30.11.2023	00:00	24:00	24:00	08:33	08:33	08:33	24:00	24:00	24:00
01.12.2023	00:00	24:00	24:00	08:31	08:31	08:31	24:00	24:00	24:00
02.12.2023	00:00	24:00	24:00	08:29	08:29	08:29	24:00	24:00	24:00
03.12.2023	00:00	24:00	24:00	08:26	08:26	08:26	24:00	24:00	24:00
04.12.2023	00:00	11:10	11:10	04:42	04:42	04:42	11:15	11:15	11:15
Total			539:05	262:48	257:41	257:41	535:01	535:01	536:55

Table 3.86. Total survey effort at MB_02 station in July, August, September, October, November and December 2023

Date	Start time of the observation day	End time of the observation day	Total duration of the observation day	Visual observations	Flight trajectory tracking using a horizontal radar [hh:min]	Laser rangefinder [hh:min]	Horizontal radar [hh:min]	Vertical radar [hh:min]	Acoustic monitoring [hh:min]
27.07.2023	01:55	24:00	22:05	03:44	03:44	03:44	03:45	03:45	03:45
				12:56	12:56	12:56	17:20	17:20	17:20
28.07.2023	00:00	03:00	03:00	00:38	00:38	00:38	02:56	02:56	02:56
13.08.2023	16:25	24:00	07:35	02:36	02:36	02:36	07:35	07:35	07:35
14.08.2023	00:00	24:00	24:00	16:10	16:10	16:10	24:00	24:00	24:00
15.08.2023	00:00	16:25	16:25	13:34	13:34	13:34	16:25	16:25	16:25
21.08.2023	21:35	24:00	02:25	00:00	00:00	00:00	02:18	02:18	02:18
22.08.2023	00:00	24:00	24:00	15:35	15:35	15:35	24:00	24:00	24:00

Date	Start time of the observation day	End time of the observation day	Total duration of the observation day	Visual observations	Flight trajectory tracking using a horizontal radar [hh:min]	Laser rangefinder [hh:min]	Horizontal radar [hh:min]	Vertical radar [hh:min]	Acoustic monitoring [hh:min]
23.08.2023	00:00	21:45	21:45	15:30	15:30	15:30	21:43	21:43	21:43
06.09.2023	04:45	24:00	19:15	13:01	13:01	13:01	19:00	19:00	19:00
07.09.2023	00:00	24:00	24:00	14:24	14:24	14:24	24:00	24:00	24:00
08.09.2023	00:00	24:00	24:00	14:19	14:19	14:19	24:00	24:00	24:00
09.09.2023	00:00	05:30	05:30	01:51	01:51	01:53	05:30	05:30	05:30
25.09.2023	01:05	24:00	22:55	13:00	13:00	13:00	22:40	22:40	22:40
26.09.2023	00:00	24:00	24:00	12:57	12:57	12:57	24:00	24:00	24:00
27.09.2023	00:00	24:00	24:00	12:52	12:52	12:52	24:00	24:00	24:00
28.09.2023	00:00	01:20	01:20	00:00	00:00	00:00	01:20	01:20	01:20
22.10.2023	11:00	24:00	13:00	04:04	04:04	04:04	12:00	12:00	12:00
23.10.2023	00:00	24:00	24:00	10:57	10:57	10:57	24:00	24:00	24:00
24.10.2023	00:00	13:05	13:05	06:53	06:53	06:53	12:00	12:00	12:00
27.10.2023	04:00	24:00	20:00	11:38	11:38	11:38	20:00	20:00	20:00
28.10.2023	00:00	24:00	24:00	11:32	11:32	11:35	24:00	24:00	24:00
29.10.2023	00:00	16:20	16:20	00:00	00:00	00:00	04:00	04:00	04:00
11.11.2023	10:25	24:00	13:35	04:55	04:55	04:55	13:33	13:33	13:35
12.11.2023	00:00	24:00	24:00	09:32	09:32	09:32	24:00	24:00	24:00
13.11.2023	00:00	10:35	10:35	04:36	04:36	04:36	10:27	10:27	10:25
29.11.2023	04:15	24:00	19:45	08:35	08:35	08:35	19:02	19:02	19:02
30.11.2023	00:00	24:00	24:00	08:32	08:32	08:32	24:00	24:00	24:00
01.12.2023	00:00	24:00	24:00	08:29	08:29	08:29	24:00	24:00	24:00
02.12.2023	00:00	05:10	05:10	00:00	00:00	00:00	05:00	05:00	05:00
Total			497:45	252:50	252:55	252:50	480:34	480:34	480:34

The collected data is sufficient for analysis of data on the autumn migrations of birds through the Baltica-1 OWF area. Based on the interpretation of the data collected, it is possible to assess the potential impact of the Baltica-1 OWF on the autumn migrations of birds in the area surveyed.

3.5.2.5 Results

3.5.2.5.1 Visual observations

3.5.2.5.1.1 Local bird movements in the wintering period

During the surveys of the local bird movements conducted at survey station LP_01, 20 species of birds were observed. Additionally, five categories were used in cases when a species could not be identified, for example, “unidentified diver”. Among all the birds observed, five species were recognised as long-distance migrants (migrating across the entire Baltic Sea area), i.e. the tundra swan, whooper swan, mute swan, greylag goose and Eurasian skylark (all observed in low numbers: 14, 9, 6, 2 and one individual respectively). Auks (razorbills, common guillemots) were observed in the highest numbers (in total N = 1428). Black guillemot observations were scarce – only two individuals were observed in February. Long-tailed ducks were the most numerous seaducks observed throughout the study (N = 143). The velvet scoter and the common scoter were observed in small numbers (17 and 4 individuals respectively). Among gulls, four species were recorded: great black-backed gull, European herring gull, little gull and common gull (in total N = 44).

The highest numbers of birds were observed in February making 78% of all the observations [Table 3.87].

Table 3.87. The local (L) and migratory (M) taxa observed at survey station LP_01 in December 2022, and January and February 2023

Taxon		**Local (L)/ migratory (M)**	**Number of observed individuals**			
English name	**Latin name**		**December**	**January**	**February**	**Total**
Razorbill	*Alca torda*	L	39	43	1033	1115
Unidentified auk	*Alca torda / Uria aalge*	L	77	20	178	275
Common guillemot	*Uria aalge*	L	20	4	12	36
Black guillemot	*Cepphus grylle*	L	0	0	2	2
Long-tailed duck	*Clangula hyemalis*	L	36	17	90	143
Common gull	*Larus canus*	L	14	8	6	28
Unidentified duck	*Melanitta indet.*	L	13	4	7	24
Velvet scoter	*Melanitta fusca*	L	2	3	12	17
Great black-backed gull	*Larus marinus*	L	11	1	2	14
Tundra swan	*Cygnus columbianus*	M	14	0	0	14
Red-breasted merganser	*Mergus serrator*	L	3	1	5	9
Whooper swan	*Cygnus cygnus*	M	0	0	9	9
Little gull	*Larus minutus*	L	6	1	0	7
Unidentified diver	*Gavia indet.*	L	7	0	0	7
European herring gull	*Larus argentatus*	L	6	0	0	6
Mute swan	*Cygnus olor*	M	4	0	2	6
Goosander	*Mergus merganser*	L	4	0	1	5
Great black cormorant	*Phalacrocorax carbo*	L	0	0	5	5
Red-throated diver	*Gavia stellata*	L	3	2	0	5
Common scoter	*Melanitta nigra*	L	4	0	0	4
Greater scaup	*Aythya marila*	L	3	0	0	3
Unidentified swan	*Cygnidae indet.*	M	3	0	0	3
Greylag goose	*Anser anser*	M	0	2	0	2
Red-breasted merganser/goosander	*Mergus serrator /Mergus merganser*	L	2	0	0	2
Eurasian skylark	*Alauda arvensis*	M	0	0	1	1
Total			**271**	**106**	**1365**	**1742**

During the surveys of the local movements of birds during the wintering period conducted at station LP_02, 18 species of birds were observed. Additionally, five categories were used in cases when a species could not be identified, for example, “unidentified diver”. Among all the birds observed, three species were migratory: the mute swan, common wood pigeon and Eurasian skylark (all observed in very low numbers, i.e. 5, 1, and 2 individuals respectively). Auks (mostly razorbills and common guillemots) were observed in the highest numbers (N = 1529). The black guillemot was the least abundant species in this category – 12 individuals throughout the study. Long-tailed ducks were the most numerous sea ducks observed (N = 583). The velvet scoter and common scoter were observed in small numbers (13 and 5 individuals respectively). Among gulls, four species were recorded: the black-headed gull, great black-backed gull, little gull and common gull (in total N = 26).

Similarly to survey station LP_01, the highest numbers of birds were observed in February making 75% of all the observations [Table 3.88].

Table 3.88. The local (L) and migratory (M) taxa observed at survey station LP_02 in December 2022, and January and February 2023

Taxon		Local (L) /Migratory (M)	Number of observed individuals			
English name	Latin name		December	January	February	Total
Razorbill	*Alca torda*	L	72	23	1153	1248
Unidentified auk	*Alca torda / Uria aalge*	L	34	82	104	220
Common guillemot	*Uria aalge*	L	35	11	3	49
Black guillemot	*Cepphus grylle*	L	3	1	8	12
Long-tailed duck	*Clangula hyemalis*	L	107	119	357	583
Common gull	*Larus canus*	L	0	10	8	18
Unidentified duck	*Melanitta indet.*	L	2	11	0	13
Velvet scoter	*Melanitta fusca*	L	0	0	12	12
Red-breasted merganser	*Mergus serrator*	L	4	3	2	9
Smew	*Mergellus albellus*	L	8	0	0	8
Common scoter	*Melanitta nigra*	L	5	0	0	5
Great black-backed gull	*Larus marinus*	L	0	1	4	5
Mute swan	*Cygnus olor*	M	5	0	0	5
Mallard	*Anas platyrhynchos*	L	4	0	0	4
Unidentified diver	*Gavia indet.*	L	1	2	0	3
Eurasian skylark	*Alauda arvensis*	M	0	0	2	2
Little gull	*Larus minutus*	L	2	0	0	2
Black-headed gull	*Larus ridibundus*	L	0	0	1	1
Common wood pigeon	*Columba palumbus*	M	0	1	0	1
Great black cormorant	*Phalacrocorax carbo*	L	0	0	1	1
Red-throated diver	*Gavia stellata*	L	1	0	0	1
Unidentified passerine	*Passeriformes indet.*	M	0	1	0	1
Unidentified swan	*Cygnidae indet.*	M	0	0	1	1
Total			**283**	**265**	**1656**	**2204**

3.5.2.5.1.2 Spring migration

During the spring migration surveys conducted at survey station MB_01, 61 species of birds were observed. Additionally, 12 categories were used in cases when an individual could not be identified to species, for example, “unidentified duck” or “common scoter/velvet scoter” [Table 3.89]. Long-tailed duck was the most numerous species observed throughout the survey period (2518 individuals) with the majority of observations (68%) made in April. Among other sea duck species, the common scoter was also observed in high numbers (in total of 1566 individuals). Velvet scoter observations were relatively less numerous with only 83 individuals observed throughout the whole study period. Numerous geese (unidentified to species) were observed mainly from the second half of March to the beginning of April (in total 833 individuals). Among auks, three species were observed (razorbill, common guillemot, black guillemot) with the most numerous razorbill (390 individuals in total).

Additionally, 276 unidentified auks (common guillemot/razorbill) were observed. Black guillemot observations were scarce, only 10 individuals were observed in March and 2 in April. Among gulls, six species were recorded with the most numerous little gull, lesser black-backed gull and common gull (133, 118, and 81 individuals, respectively). Black-headed gull, great black-backed gull and black-legged kittiwake observations were less numerous (22, 7, and 2 individuals respectively). The highest numbers of birds were recorded in April making 64% of all the observations [Table 3.89].

Table 3.89. The bird taxa observed at survey station MB_01 in the spring migration period

Taxon		**Number of observed individuals**			
English name	**Latin name**	**March**	**April**	**May**	**Total**
Long-tailed duck	*Clangula hyemalis*	663	1728	127	2518
Common scoter	*Melanitta nigra*	25	967	574	1566
Unidentified goose	*Anserini indet.*	436	390	7	833
Unidentified duck	*Melanitta indet.*	37	439	42	518
Razorbill	*Alca torda*	189	190	11	390
Unidentified auk	*Alca torda / Uria aalge*	87	163	26	276
Unidentified passerine	*Passeriformes indet.*	15	150	3	168
Eurasian curlew	*Numenius arquata*	0	152	0	152
Little gull	*Larus minutus*	35	97	1	133
Eurasian wigeon	*Anas penelope*	0	129	0	129
Lesser black-backed gull	*Larus fuscus*	5	86	27	118
Unidentified diver	*Gavia indet.*	3	17	65	85
Velvet scoter	*Melanitta fusca*	0	70	13	83
Common gull	*Larus canus*	33	44	4	81
Black-throated diver	*Gavia arctica*	1	8	57	66
Great black cormorant	*Phalacrocorax carbo*	4	47	14	65
Greylag goose	*Anser anser*	1	2	58	61
Greater white-fronted goose	*Anser albifrons*	50	0	3	53
Greater scaup	*Aythya marila*	0	48	0	48
Eurasian teal	*Anas crecca*	0	38	5	43
Common guillemot	*Uria aalge*	24	7	10	41
Eurasian siskin	*Spinus spinus*	40	0	0	40
Northern pintail	*Anas acuta*	0	37	2	39
Common starling	*Sturnus vulgaris*	6	33	0	39
White wagtail	*Motacilla alba*	1	29	1	31
Red-breasted merganser	*Mergus serrator*	10	20	0	30
Mute swan	*Cygnus olor*	21	1	8	30
Black-headed gull	*Chroicocephalus ridibundus*	6	11	5	22
Unidentified duck	*Melanitta indet.*	1	19	0	20
Eurasian skylark	*Alauda arvensis*	14	3	0	17
Unidentified swan	*Cygnidae indet.*	17	0	0	17
Barn swallow	*Hirundo rustica*	0	1	14	15
Black guillemot	*Cepphus grylle*	10	2	0	12

Taxon		Number of observed individuals			
English name	**Latin name**	**March**	**April**	**May**	**Total**
Common chaffinch	*Fringilla coelebs*	1	10	0	11
Red-throated diver	*Gavia stellata*	1	6	3	10
Great egret	*Ardea alba*	0	9	0	9
Common crane	*Grus grus*	0	7	1	8
Mallard	*Anas platyrhynchos*	0	8	0	8
Great black-backed gull	*Larus marinus*	7	0	0	7
Northern shoveler	*Anas clypeata*	0	7	0	7
Common/Arctic tern	*Sterna hirundo/paradisaea*	0	0	7	7
Meadow pipit	*Anthus pratensis*	0	6	0	6
Common wood pigeon	*Columba palumbus*	3	3	0	6
Hooded crow	*Corvus corone cornix*	0	3	2	5
Whooper swan	*Cygnus cygnus*	4	1	0	5
European robin	*Erithacus rubecula*	1	4	0	5
Grey heron	*Ardea cinerea*	0	4	1	5
Tufted duck	*Aythya fuligula*	0	2	2	4
Red-breasted merganser/goosander	*Mergus serrator/merganser*	1	3	0	4
Arctic skua	*Stercorarius parasiticus*	0	3	1	4
Arctic tern	*Sterna paradisaea*	0	0	4	4
Eurasian sparrowhawk	*Accipiter nisus*	1	2	0	3
Common tern	*Sterna hirundo*	0	1	2	3
Great tit	*Parus major*	2	1	0	3
Short-eared owl	*Asio flammeus*	0	2	1	3
Long-eared owl	*Asio otus*	0	2	0	2
Unidentified wader	*Limicolae indet.*	0	0	2	2
Black-legged kittiwake	*Rissa tridactyla*	2	0	0	2
Eurasian wren	*Troglodytes troglodytes*	0	2	0	2
Goldcrest	*Regulus regulus*	0	2	0	2
Unidentified owl	*Asio otus/flammeus*	0	1	1	2
Pomarine skua	*Stercorarius pomarinus*	0	0	2	2
Song thrush	*Turdus philomelos*	0	1	0	1
Goosander	*Mergus merganser*	1	0	0	1
Common eider	*Somateria mollissima*	0	1	0	1
Dunnock	*Prunella modularis*	0	1	0	1
Unidentified tern	*Sterna indet.*	0	0	1	1
Brambling	*Fringilla montifringilla*	0	1	0	1
Stock dove	*Columba oenas*	1	0	0	1
Barnacle goose	*Branta leucopsis*	1	0	0	1
Rook	*Corvus frugilegus*	0	0	1	1
Osprey	*Pandion haliaetus*	0	0	1	1

Taxon		Number of observed individuals			
English name	**Latin name**	**March**	**April**	**May**	**Total**
Common blackbird	*Turdus merula*	0	1	0	1
Total		**1760**	**5022**	**1109**	**7891**

During the spring migration surveys conducted at survey station MB_02, 60 species of birds were observed. Additionally, 11 categories were used in cases when an individual could not be identified to species, for example, "unidentified duck" or "common scoter/velvet scoter" [Table 3.90]. The long-tailed duck was the most numerous species observed throughout the study (5776 individuals) with the majority of observations (75%) made in April. Among other sea duck species, the common scoter was also observed in large numbers (in total 1449 individuals). Velvet scoter observations were relatively less numerous with only 92 individuals observed throughout the whole study period. Among auks, three species were observed (razorbill, common guillemot and black guillemot) with the most numerous razorbill (435 individuals in total). Additionally, 291 unidentified auks (common guillemot/razorbill) were observed. Black guillemot observations were scarce, with only 20 individuals observed throughout the study. Among gulls, six species were recorded with the most numerous European herring gull, lesser black-backed gull and common gull (100, 99, and 73 individuals respectively). Little gull, black-headed gull and great black-backed gull observations were less numerous (55, 13 and 5 individuals respectively). Similarly to survey station MB_01, the highest numbers of birds were recorded in April making 65% of all the observations [Table 3.90].

Table 3.90. The bird taxa observed at survey station MB_02 in the spring migration period

Taxon		Number of observed individuals			
English name	**Latin name**	**March**	**April**	**May**	**Total**
Long-tailed duck	*Clangula hyemalis*	1350	4311	115	5776
Common scoter	*Melanitta nigra*	187	1054	208	1449
Unidentified duck	*Melanitta indet.*	116	455	12	583
Razorbill	*Alca torda*	158	264	13	435
Unidentified wader	*Limicolae indet.*	0	0	382	382
Unidentified auk	*Alca torda / Uria aalge*	114	129	48	291
Eurasian curlew	*Numenius arquata*	139	1	0	140
Unidentified passerine	*Passeriformes indet.*	15	118	5	138
Unidentified diver	*Gavia indet.*	9	10	106	125
European herring gull	*Larus argentatus*	100	0	0	100
Lesser black-backed gull	*Larus fuscus*	0	80	19	99
Greater white-fronted goose	*Anser albifrons*	35	59	0	94
Velvet scoter	*Melanitta fusca*	10	79	3	92
Greater scaup	*Aythya marila*	40	38	13	91
Greylag goose	*Anser anser*	3	0	83	86
Common gull	*Larus canus*	33	39	1	73
Common starling	*Sturnus vulgaris*	11	55	1	67
Black-throated diver	*Gavia arctica*	3	10	50	63
Unidentified goose	*Anserini indet.*	30	0	28	58
Great black cormorant	*Phalacrocorax carbo*	16	26	16	58

Taxon		Number of observed individuals			
English name	**Latin name**	**March**	**April**	**May**	**Total**
Little gull	*Larus minutus*	13	36	6	55
Unidentified swan	*Cygnidae indet.*	45	1	6	52
Common guillemot	*Uria aalge*	16	23	4	43
Common crane	*Grus grus*	0	22	4	26
Red-breasted merganser	*Mergus serrator*	21	4	0	25
European golden plover	*Pluvialis apricaria*	0	23	0	23
White wagtail	*Motacilla alba*	3	19	0	22
Black guillemot	*Cepphus grylle*	15	3	2	20
Mallard	*Anas platyrhynchos*	2	17	0	19
Red-throated diver	*Gavia stellata*	4	5	9	18
Tufted duck	*Aythya fuligula*	0	16	0	16
Common chaffinch	*Fringilla coelebs*	7	9	0	16
Black-headed gull	*Chroicocephalus ridibundus*	5	7	1	13
Barn swallow	*Hirundo rustica*	0	0	12	12
Unidentified duck	*Melanitta indet.*	1	11	0	12
Eurasian teal	*Anas crecca*	3	8	0	11
Common/Arctic tern	*Sterna hirundo/paradisaea*	0	0	9	9
Mute swan	*Cygnus olor*	8	1	0	9
Great egret	*Ardea alba*	0	8	0	8
Whooper swan	*Cygnus cygnus*	8	0	0	8
Unidentified thrush	*Turdidae indet.*	7	0	0	7
Fieldfare	*Turdus pilaris*	0	7	0	7
Northern pintail	*Anas acuta*	7	0	0	7
Tundra swan	*Cygnus columbianus*	6	0	0	6
Common wood pigeon	*Columba palumbus*	3	3	0	6
Goosander	*Mergus merganser*	6	0	0	6
Great black-backed gull	*Larus marinus*	5	0	0	5
Rook	*Corvus frugilegus*	0	5	0	5
Eurasian wren	*Troglodytes troglodytes*	1	3	0	4
Arctic tern	*Sterna paradisaea*	0	0	4	4
Great tit	*Parus major*	4	0	0	4
Meadow pipit	*Anthus pratensis*	0	3	0	3
Eurasian skylark	*Alauda arvensis*	2	1	0	3
Eurasian siskin	*Spinus spinus*	1	2	0	3
Unidentified pipit	*Anthus indet.*	0	2	0	2
Song thrush	*Turdus philomelos*	1	0	1	2
Goldcrest	*Regulus regulus*	0	2	0	2
Long-eared owl	*Asio otus*	1	1	0	2
Eurasian sparrowhawk	*Accipiter nisus*	0	1	0	1
Stock dove	*Columba oenas*	0	1	0	1

Taxon		Number of observed individuals			
English name	**Latin name**	**March**	**April**	**May**	**Total**
Short-eared owl	*Asio flammeus*	0	1	0	1
Arctic skua	*Stercorarius parasiticus*	0	0	1	1
Red-necked grebe	*Podiceps grisegena*	0	1	0	1
Pomarine skua	*Stercorarius pomarinus*	0	0	1	1
Common goldeneye	*Bucephala clangula*	0	1	0	1
Eurasian blue tit	*Parus caeruleus*	1	0	0	1
Northern lapwing	*Vanellus vanellus*	1	0	0	1
Common kestrel	*Falco tinnunculus*	0	1	0	1
Horned grebe	*Podiceps auritus*	0	1	0	1
European robin	*Erithacus rubecula*	0	1	0	1
Black tern	*Chlidonias niger*	0	0	1	1
Total		**2566**	**6978**	**1164**	**10708**

3.5.2.5.1.3 Autumn migration

At the MB_01 station during the autumn migration studies, 50 species of birds were observed. Additionally, 11 categories were used in cases when a species could not be identified to species, for example, “unidentified duck” or “common scoter/velvet scoter” [Table 3.91]. The common scoter was the most numerous species observed with the observation peak recorded in July. The second most numerous species was the common chaffinch (including a single observation of 120 individuals) followed by the long-tailed duck. Unidentified ducks, geese and passerines were the most numerous categories of unidentified species. Except for the common scoter which was observed mainly in July or the long-tailed duck observed mainly in October, November, and December, other species were observed mainly in August and September (e.g. the great cormorant, little gull, lesser black-backed gull, common swift, unidentified ducks) [Table 3.91].

Table 3.91. The bird taxa observed at survey station MB_01 during the autumn migration surveys

Taxon		Number of observed individuals						
English name	**Latin name**	**July**	**August**	**September**	**October**	**November**	**December**	**Total**
Common scoter	*Melanitta nigra*	499	78	43	6	0	0	626
Unidentified duck	*Melanitta indet.*	6	42	111	33	2	2	196
Common chaffinch	*Fringilla coelebs*	0	0	186	0	0	0	186
Unidentified goose	*Anserini indet.*	0	0	8	162	0	0	170
Long-tailed duck	*Clangula hyemalis*	0	0	0	71	17	62	150
Unidentified passerine	*Passeriformes indet.*	0	8	83	53	0	0	144
Unidentified auk	*Alca torda / Uria aalge*	1	0	10	46	10	33	100
Great black cormorant	*Phalacrocorax carbo*	2	64	14	0	0	0	80
Common guillemot	*Uria aalge*	0	0	2	24	9	35	70
Common gull	*Larus canus*	3	2	8	10	24	18	65
Razorbill	*Alca torda*	1	0	0	14	6	42	63

Taxon		Number of observed individuals						
English name	Latin name	July	August	September	October	November	December	Total
Eurasian teal	*Anas crecca*	2	13	41	0	0	0	56
Little gull	*Larus minutus*	1	24	12	4	1	5	47
Lesser black-backed gull	*Larus fuscus*	4	16	22	2	0	0	44
Eurasian skylark	*Alauda arvensis*	0	0	42	0	0	0	42
Mallard	*Anas platyrhynchos*	0	0	0	4	26	2	32
Eurasian wigeon	*Anas penelope*	0	0	31	0	0	0	31
Common swift	*Apus apus*	0	30	0	0	0	0	30
Common/Arctic tern	*Sterna hirundo/paradisaea*	8	20	1	0	0	0	29
White wagtail	*Motacilla alba*	0	0	28	0	0	0	28
Common tern	*Sterna hirundo*	3	15	3	0	0	0	21
Grey heron	*Ardea cinerea*	3	0	17	0	0	0	20
Unidentified wader	*Limicolae indet.*	2	7	10	0	0	0	19
Unidentified swan	*Cygnidae indet.*	0	14	0	0	0	2	16
Black-headed gull	*Chroicocephalus ridibundus*	1	4	8	0	0	1	14
Velvet scoter	*Melanitta fusca*	0	0	5	9	0	0	14
Dunlin	*Calidris alpina*	0	0	13	0	0	0	13
Unidentified diver	*Gavia indet.*	0	0	6	4	0	1	11
Common crane	*Grus grus*	0	0	10	0	0	0	10
Northern shoveler	*Anas clypeata*	0	0	9	0	0	0	9
Black tern	*Chlidonias niger*	6	2	0	0	0	0	8
Unidentified sandpiper	*Calidris indet.*	0	8	0	0	0	0	8
Barn swallow	*Hirundo rustica*	0	2	5	0	0	0	7
Red-throated diver	*Gavia stellata*	0	0	2	2	0	3	7
Great black-backed gull	*Larus marinus*	0	0	0	0	1	4	5
Unidentified tern	*Sterna indet.*	5	0	0	0	0	0	5
Song thrush	*Turdus philomelos*	0	0	3	0	0	0	3
Western yellow wagtail	*Motacilla flava*	0	0	3	0	0	0	3
Arctic tern	*Sterna paradisaea*	2	0	0	0	0	0	2
Black guillemot	*Cepphus grylle*	0	0	0	0	2	0	2
Black-throated diver	*Gavia arctica*	0	0	0	1	0	1	2
Common redpoll	*Acanthis flammea*	0	0	0	1	0	1	2
Common shelduck	*Tadorna tadorna*	0	2	0	0	0	0	2
Greater scaup	*Aythya marila*	0	0	2	0	0	0	2
Grey plover	*Pluvialis squatarola*	0	2	0	0	0	0	2
Mute swan	*Cygnus olor*	0	0	2	0	0	0	2
Arctic skua	*Stercorarius parasiticus*	0	2	0	0	0	0	2
Barnacle goose	*Branta leucopsis*	0	0	0	1	0	0	1
Black-legged kittiwake	*Rissa tridactyla*	0	0	0	1	0	0	1

Taxon		Number of observed individuals						
English name	Latin name	July	August	September	October	November	December	Total
Common blackbird	*Turdus merula*	0	0	0	1	0	0	1
Eurasian blackcap	*Sylvia atricapilla*	0	0	1	0	0	0	1
Eurasian sparrowhawk	*Accipiter nisus*	0	0	1	0	0	0	1
Eurasian wren	*Troglodytes troglodytes*	0	0	0	1	0	0	1
European nightjar	*Caprimulgus europaeus*	0	0	1	0	0	0	1
Lesser whitethroat	*Sylvia curucca*	0	1	0	0	0	0	1
Osprey	*Pandion haliaetus*	0	0	1	0	0	0	1
Arctic/pomarine skua	*Stercorarius parasiticus/pomarinus*	0	0	1	0	0	0	1
Ruff	*Philomachus pugnax*	0	0	1	0	0	0	1
Sand martin	*Riparia riparia*	0	1	0	0	0	0	1
Snow bunting	*Plectrophenax nivalis*	0	0	0	1	0	0	1
Wood lark	*Lullula arborea*	0	0	0	1	0	0	1
Total		**549**	**357**	**746**	**452**	**98**	**212**	**2414**

At survey station MB_02, during the autumn migration studies, 49 species of birds were observed. Additionally, 12 categories were used in cases when a species could not be identified to species, for example, “unidentified duck” or “common scoter/velvet scoter” [Table 3.92]. The long-tailed duck was the most numerous species observed with the observation peak recorded in November. The second most numerous species was the great cormorant followed by the Eurasian wigeon and common scoter. Unidentified ducks and passerines were the two most numerous categories of unidentified species. Except for the long-tailed duck, auks (razorbill and common guillemot) and the common starling, which were observed mainly in October and November, other species were observed mainly in August and September (e.g. the great cormorant, lesser black-backed gull, common swift, Eurasian wigeon, unidentified waders) [Table 3.92]. Common scoters were observed in the highest numbers in September whilst velvet scoters mainly in October.

Table 3.92. The total observations of bird taxa recorded at survey station MB_02 during the autumn migration surveys

Taxon		Number of observed individuals						
English name	Latin name	July	August	September	October	November	December	Total
Long-tailed duck	*Clangula hyemalis*	0	0	1	386	672	36	1095
Unidentified duck	*Melanitta indet.*	0	0	89	107	74	4	274
Great black cormorant	*Phalacrocorax carbo*	0	150	26	3	23	0	202
Eurasian wigeon	*Anas penelope*	0	0	108	75	0	0	183
Common scoter	*Melanitta nigra*	20	18	88	11	26	0	163
Unidentified passerine	*Passeriformes indet.*	0	0	116	25	0	0	141
Unidentified auk	*Alca torda/Uria aalge*	1	0	9	48	63	4	125

Taxon		Number of observed individuals						
English name	Latin name	July	August	September	October	November	December	Total
Common starling	*Sturnus vulgaris*	0	0	0	3	80	0	83
Common guillemot	*Uria aalge*	0	0	5	41	25	6	77
Razorbill	*Alca torda*	0	0	2	37	32	5	76
Eurasian siskin	*Spinus spinus*	0	0	75	0	0	0	75
Little gull	*Larus minutus*	0	17	12	13	18	1	61
Common swift	*Apus apus*	0	58	0	0	0	0	58
Greylag goose	*Anser anser*	0	3	40	0	0	0	43
Unidentified wader	*Limicolae indet.*	2	24	15	0	0	0	41
Velvet scoter	*Melanitta fusca*	3	1	14	23	0	0	41
Unidentified goose	*Anserini indet.*	0	0	33	4	0	0	37
Lesser black-backed gull	*Larus fuscus*	1	8	26	0	0	0	35
Common/Arctic tern	*Sterna hirundo/ Sterna paradisaea*	6	26	0	0	0	0	32
Unidentified diver	*Gavia indet.*	0	3	4	9	8	7	31
European herring gull	*Larus argentatus*	0	0	25	0	0	0	25
Eurasian teal	*Anas crecca*	0	1	22	0	0	0	23
Common gull	*Larus canus*	3	0	7	12	1	0	23
White wagtail	*Motacilla alba*	0	0	17	0	1	0	18
Greater scaup	*Aythya marila*	0	0	2	15	0	0	17
Mute swan	*Cygnus olor*	14	0	0	0	0	3	17
Sanderling	*Calidris alba*	0	0	16	0	0	0	16
Unidentified duck	*Melanitta indet.*	14	0	0	0	0	0	14
Unidentified swan	*Cygnidae indet.*	0	0	0	0	9	0	9
Unidentified tern	*Sterna indet.*	4	1	2	0	0	0	7
European golden plover	*Pluvialis apricaria*	0	6	0	0	0	0	6
Grey heron	*Ardea cinerea*	0	1	4	0	0	0	5
Barn swallow	*Hirundo rustica*	0	4	0	0	0	0	4
Common linnet	*Linaria cannabina*	0	0	0	4	0	0	4
Common shelduck	*Tadorna tadorna*	0	0	4	0	0	0	4
Dunlin	*Calidris alpina*	2	2	0	0	0	0	4
Mallard	*Anas platyrhynchos*	0	0	1	3	0	0	4
Black-throated diver	*Gavia arctica*	0	0	1	2	0	0	3
Eurasian blue tit	*Parus caeruleus*	0	0	2	1	0	0	3
Common tern	*Sterna hirundo*	0	3	0	0	0	0	3
Goldcrest	*Regulus regulus*	0	0	3	0	0	0	3
Unidentified sandpiper	*Calidris indet.*	0	0	3	0	0	0	3
Arctic tern	*Sterna paradisaea*	1	1	0	0	0	0	2

Taxon		Number of observed individuals						
English name	Latin name	July	August	September	October	November	December	Total
Black-headed gull	*Chroicocephalus ridibundus*	0	0	0	2	0	0	2
Common chaffinch	*Fringilla coelebs*	0	0	2	0	0	0	2
Common redpoll	*Acanthis flammea*	0	0	0	1	0	1	2
Common snipe	*Gallinago gallinago*	0	0	2	0	0	0	2
European robin	*Erithacus rubecula*	0	0	2	0	0	0	2
Great black-backed gull	*Larus marinus*	0	0	0	1	0	1	2
Great tit	*Parus major*	0	0	2	0	0	0	2
Arctic skua	*Stercorarius parasiticus*	0	0	2	0	0	0	2
Western yellow wagtail	*Motacilla flava*	0	2	0	0	0	0	2
Black guillemot	*Cepphus grylle*	0	0	0	0	1	0	1
Black-legged kittiwake	*Rissa tridactyla*	0	0	0	0	1	0	1
Goosander	*Mergus merganser*	0	0	0	1	0	0	1
Grey plover	*Pluvialis squatarola*	0	1	0	0	0	0	1
Long-tailed/Arctic/Pomarine skua	*Stercorarius longicaudus/parasiticus /pomarinus*	0	0	1	0	0	0	1
Red-throated diver	*Gavia stellata*	0	0	0	1	0	0	1
Ruff	*Philomachus pugnax*	0	1	0	0	0	0	1
Sandwich tern	*Sterna sandvicensis*	0	1	0	0	0	0	1
Short-eared owl	*Asio flammeus*	0	0	1	0	0	0	1
Total		**71**	**332**	**784**	**828**	**1034**	**68**	**3117**

3.5.2.5.2 Migration fluxes (flight intensity)

The passage of migratory birds through the survey area, defined as a “bird flux”, was calculated using visual observation data. This was done by using the procedure described in Chapter 3.5.2.3. Migration flows illustrate the intensity of the flight of migrating birds during the seasonal migration from breeding grounds to wintering grounds and from wintering grounds to breeding grounds, which fly along the SW-NE and NE-SW axes.

Wintering seabirds move in different directions (so far, no unambiguous dominant flight directions have been determined for local migrations during any surveys conducted for the needs of the OWF in the region). The results of observations of local short migrations of wintering birds indicate that they do not follow specific routes and therefore, determining migration flows is not considered an adequate method for presenting this type of data.

Generalized detection functions were recalculated for the inventory report based on a complete data set from the entire survey period, for each species with a sufficient number of observations. Therefore, the migration flux values presented at the quarterly report stage may differ slightly from those presented in this report. Data from visual observations conducted in the first days of December were included in the analyses related to the calculation of migration flows during the autumn migration

period. Due to unfavourable weather conditions, the last November vessel passage was postponed by several days. This had not impact on the quality of the data obtained. Birds observed in the first days of December are most likely birds moving in the direction and staying in the course of their autumn migration. Based on empirical data, the figures below show the probability of detection depending on the distance from the observer taking account of the detection effect (detection error) for species with the highest flux values: long-tailed ducks [Figure 3.125], common scoters [Figure 3.126], common chaffinches [Figure 3.127], white wagtails [Figure 3.128] and razorbills [Figure 3.129]. The empirical distribution of the distance from the observer was presented as a scaled histogram, which means that a distance represented by bar with a value of 2, twice as many birds were counted at the distances the bar represents than at the distances a bar with a value of 1 represents. The line shown in the graph shows the estimated detection bias curve. The probability of detecting a bird at a certain distance is given by the y-axis value of the error line for that distance.

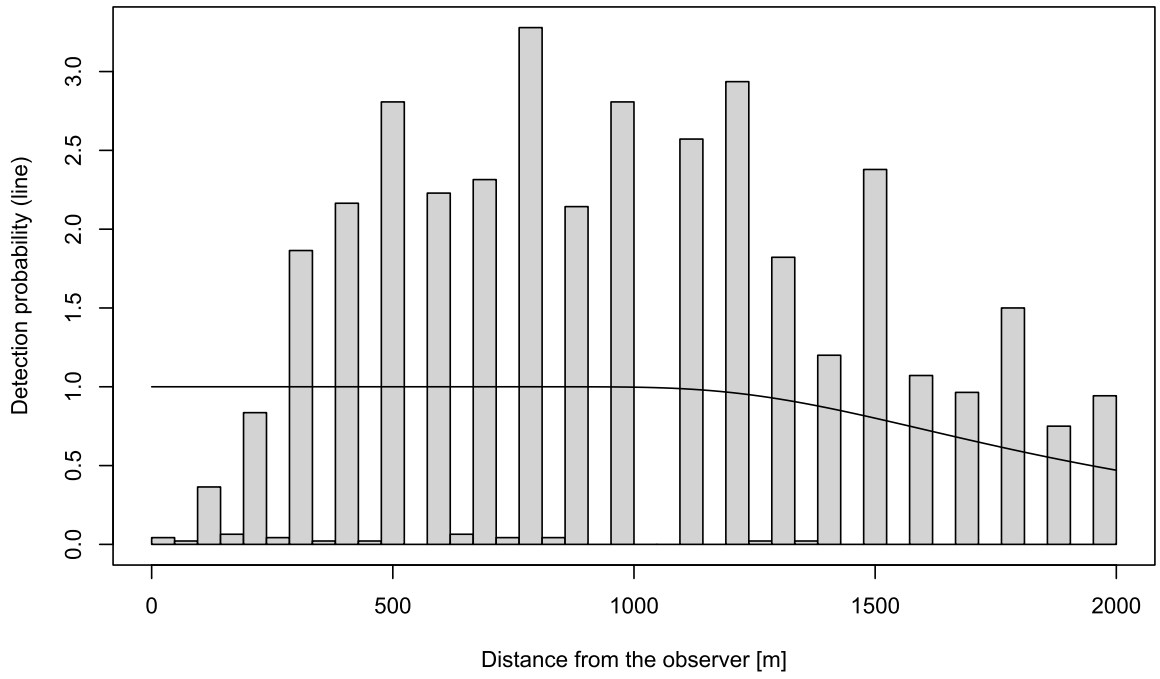


Figure 3.125. The probability of detection depending on the distance from the observer taking account of the observer effect (detection error) for the long-tailed duck

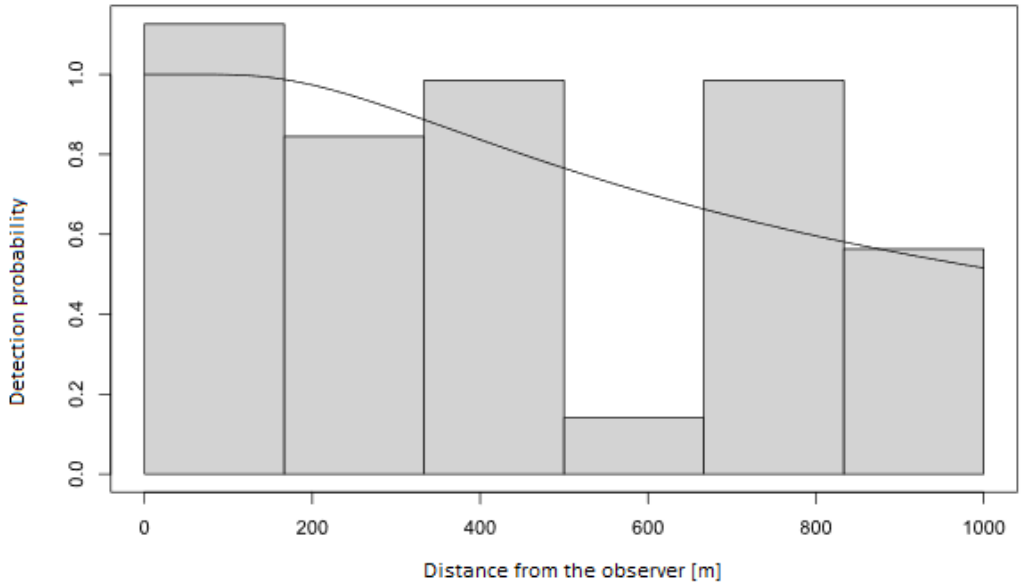


Figure 3.126. The probability of detection depending on the distance from the observer taking account of the observer effect (detection error) for the common scoter

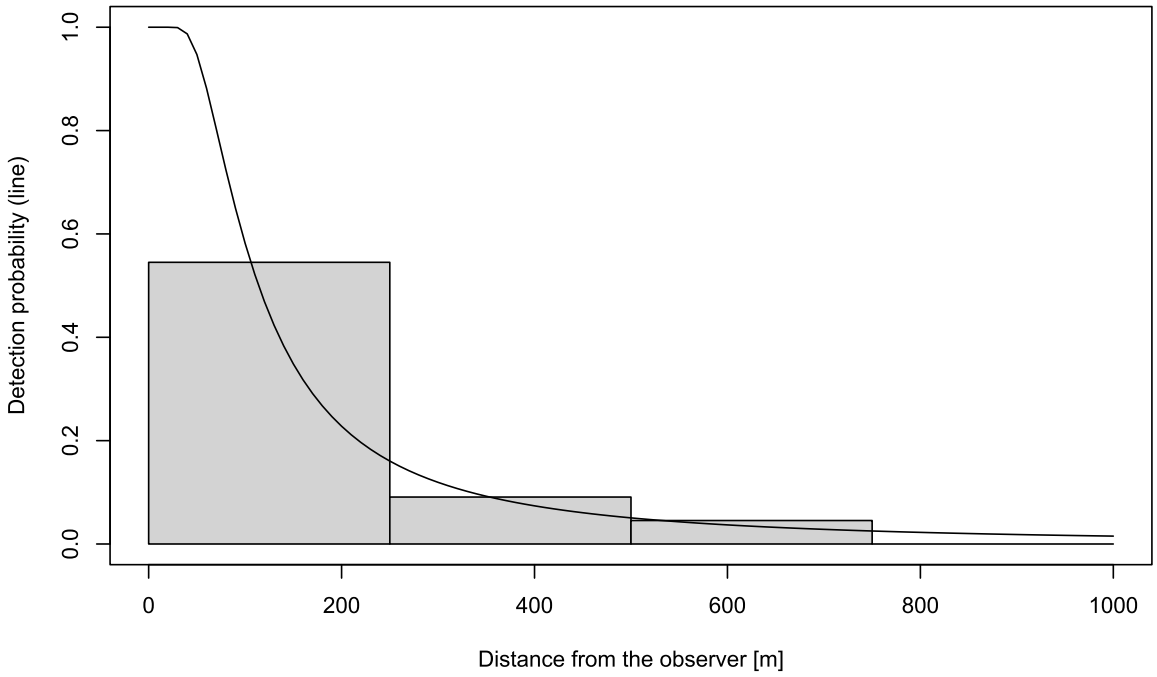


Figure 3.127. The probability of detection depending on the distance from the observer taking account of the observer effect (detection error) for the common chaffinch

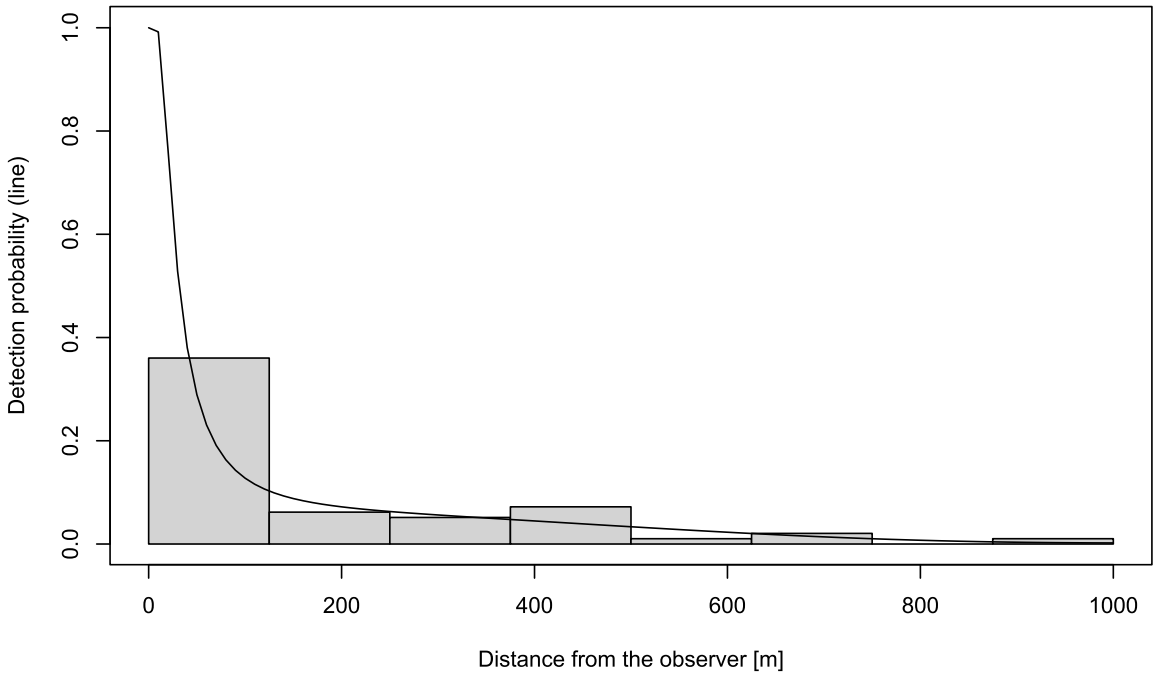


Figure 3.128. The probability of detection depending on the distance from the observer taking account of the observer effect (detection error) for the white wagtail

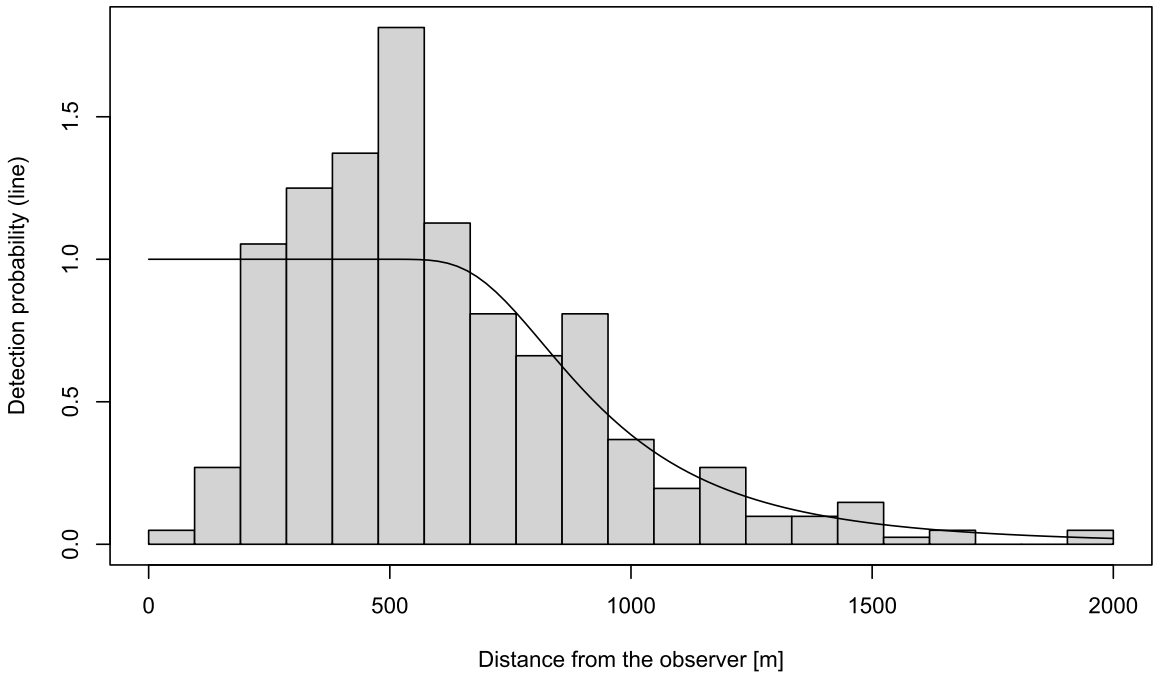


Figure 3.129. The probability of detection depending on the distance from the observer taking account of the observer effect (detection error) for the razorbill

Table 3.93. The effective sample width for long-tailed duck, common scoter, common chaffinch, white wagtail, and razorbill

Species	Effective sample width [m]
Long-tailed duck	1778.7
Common scoter	1823.1
Common chaffinch	170.3
White wagtail	73.3
Razorbill	1001.1

The fluxes calculated for the width of the planned Baltica-1 OWF (10 km) per each survey month (March–November) are the highest for the long-tailed duck in March, for the common scoter in April, May and July, for the common chaffinch in September, for the white wagtails in April and September, and for the razorbill in April – exceeding 10,000 individuals passing the planned OWF area [Table 3.94, Table 3.95]. The highest passage intensity for the long-tailed duck was identified in April while for the common scoter in July. According to the estimates, over 80,000 long-tailed ducks and 80,000 common scoters can pass the survey area in April and July, respectively [Table 3.94]. Quite big fluxes were also calculated for the common chaffinch, exceeding 30,000 individuals in September. High values were also obtained for white wagtails, exceeding 15,000 individuals. According to the estimates, slightly over 10,000 razorbills can pass the survey area in April. Comparable results were also obtained for unidentified ducks in April, exceeding 10,000 individuals. Quite big fluxes were also calculated for groups of species in almost all months: ducks (the long-tailed duck being included – almost 120,000 individuals in April), auks, geese, gulls, passerines, waders, divers in May only, swifts and cormorants in August and terns in July [Table 3.95]. Low flight intensity was observed for cranes, grebes, herons, nightjars, owls, pigeons, raptors, skuas and swans. For flux analysis, the total amount of time the transects were monitored was summed up.

Table 3.94. The migration fluxes of bird taxa in the survey area in subsequent months in the spring and autumn migration periods

Taxon	Month	Headwind per 1 km	Tailwind per 1 km	Total per 1 km	Total per 10 km
Arctic tern	March	-	-	-	-
Arctic tern	April	-	-	-	-
Arctic tern	May	9.37	1.63	10.99	109.95
Arctic tern	July	42.29	-	42.29	422.95
Arctic tern	August	1.78	0.38	2.16	21.63
Arctic tern	September	-	-	-	-
Arctic tern	October	-	-	-	-
Arctic tern	November	-	-	-	-
Barn swallow	March	-	-	-	-
Barn swallow	April	4.70	0.38	5.08	50.75
Barn swallow	May	131.64	22.87	154.51	1545.11
Barn swallow	July	-	-	-	-
Barn swallow	August	43.80	9.30	53.10	531.00
Barn swallow	September	23.19	5.56	28.75	287.52

Taxon	Month	Headwind per 1 km	Tailwind per 1 km	Total per 1 km	Total per 10 km
Barn swallow	October	-	-	-	-
Barn swallow	November	-	-	-	-
Barnacle goose	March	0.21	1.15	1.36	13.60
Barnacle goose	April	-	-	-	-
Barnacle goose	May	-	-	-	-
Barnacle goose	July	-	-	-	-
Barnacle goose	August	-	-	-	-
Barnacle goose	September	-	-	-	-
Barnacle goose	October	0.71	1.28	1.98	19.82
Barnacle goose	November	-	-	-	-
Black guillemot	March	7.71	41.11	48.82	488.24
Black guillemot	April	9.08	0.73	9.81	98.10
Black guillemot	May	3.86	0.67	4.54	45.36
Black guillemot	July	-	-	-	-
Black guillemot	August	-	-	-	-
Black guillemot	September	-	-	-	-
Black guillemot	October	-	-	-	-
Black guillemot	November	3.38	4.16	7.54	75.36
Black tern	March	-	-	-	-
Black tern	April	-	-	-	-
Black tern	May	1.19	0.21	1.40	14.02
Black tern	July	84.59	-	84.59	845.90
Black tern	August	3.16	0.67	3.82	38.25
Black tern	September	-	-	-	-
Black tern	October	-	-	-	-
Black tern	November	-	-	-	-
Black-headed gull	March	5.28	28.14	33.42	334.17
Black-headed gull	April	42.68	3.46	46.14	461.40
Black-headed gull	May	8.70	1.51	10.21	102.08
Black-headed gull	July	34.45	-	34.45	344.49
Black-headed gull	August	15.20	3.23	18.43	184.29
Black-headed gull	September	21.11	5.06	26.17	261.69
Black-headed gull	October	3.29	5.94	9.23	92.28
Black-headed gull	November	1.75	2.15	3.90	38.96
Black-legged kittiwake	March	-	-	-	-
Black-legged kittiwake	April	-	-	-	-
Black-legged kittiwake	May	-	-	-	-
Black-legged kittiwake	July	-	-	-	-
Black-legged kittiwake	August	-	-	-	-
Black-legged kittiwake	September	-	-	-	-
Black-legged kittiwake	October	0.71	1.28	1.98	19.82

Taxon	Month	Headwind per 1 km	Tailwind per 1 km	Total per 1 km	Total per 10 km
Black-legged kittiwake	November	0.66	0.82	1.48	14.81
Black-throated diver	March	1.03	5.47	6.50	64.97
Black-throated diver	April	27.83	2.25	30.08	300.84
Black-throated diver	May	174.46	30.31	204.76	2047.64
Black-throated diver	July	-	-	-	-
Black-throated diver	August	-	-	-	-
Black-throated diver	September	1.51	0.36	1.87	18.69
Black-throated diver	October	2.80	5.06	7.86	78.57
Black-throated diver	November	0.98	1.21	2.19	21.91
Unidentified duck	March	0.39	2.06	2.45	24.47
Unidentified duck	April	33.06	2.68	35.73	357.32
Unidentified duck	May	-	-	-	-
Unidentified duck	July	197.71	-	197.71	1977.09
Unidentified duck	August	-	-	-	-
Unidentified duck	September	-	-	-	-
Unidentified duck	October	-	-	-	-
Unidentified duck	November	-	-	-	-
Eurasian blue tit	March	0.34	1.79	2.12	21.22
Eurasian blue tit	April	-	-	-	-
Eurasian blue tit	May	-	-	-	-
Eurasian blue tit	July	-	-	-	-
Eurasian blue tit	August	-	-	-	-
Eurasian blue tit	September	4.28	1.03	5.30	53.03
Eurasian blue tit	October	1.38	2.49	3.87	38.66
Eurasian blue tit	November	-	-	-	-
Brambling	March	-	-	-	-
Brambling	April	2.19	0.18	2.36	23.65
Brambling	May	-	-	-	-
Brambling	July	-	-	-	-
Brambling	August	-	-	-	-
Brambling	September	-	-	-	-
Brambling	October	-	-	-	-
Brambling	November	-	-	-	-
Common blackbird	March	-	-	-	-
Common blackbird	April	2.13	0.17	2.30	23.04
Common blackbird	May	-	-	-	-
Common blackbird	July	-	-	-	-
Common blackbird	August	-	-	-	-
Common blackbird	September	-	-	-	-
Common blackbird	October	1.34	2.43	3.77	37.74
Common blackbird	November	-	-	-	-

Taxon	Month	Headwind per 1 km	Tailwind per 1 km	Total per 1 km	Total per 10 km
Common chaffinch	March	16.58	88.38	104.96	1049.64
Common chaffinch	April	245.74	19.89	265.63	2656.34
Common chaffinch	May	-	-	-	-
Common chaffinch	July	-	-	-	-
Common chaffinch	August	-	-	-	-
Common chaffinch	September	2420.66	580.75	3001.41	30014.10
Common chaffinch	October	-	-	-	-
Common chaffinch	November	-	-	-	-
Common crane	March	-	-	-	-
Common crane	April	24.25	1.96	26.22	262.18
Common crane	May	1.18	0.21	1.39	13.88
Common crane	July	-	-	-	-
Common crane	August	-	-	-	-
Common crane	September	10.69	2.57	13.26	132.58
Common crane	October	-	-	-	-
Common crane	November	-	-	-	-
Common goldeneye	March	-	-	-	-
Common goldeneye	April	1.11	0.09	1.20	12.03
Common goldeneye	May	-	-	-	-
Common goldeneye	July	-	-	-	-
Common goldeneye	August	-	-	-	-
Common goldeneye	September	-	-	-	-
Common goldeneye	October	-	-	-	-
Common goldeneye	November	-	-	-	-
Common kestrel	March	-	-	-	-
Common kestrel	April	1.11	0.09	1.20	12.03
Common kestrel	May	-	-	-	-
Common kestrel	July	-	-	-	-
Common kestrel	August	-	-	-	-
Common kestrel	September	-	-	-	-
Common kestrel	October	-	-	-	-
Common kestrel	November	-	-	-	-
Common linnet	March	-	-	-	-
Common linnet	April	-	-	-	-
Common linnet	May	-	-	-	-
Common linnet	July	-	-	-	-
Common linnet	August	-	-	-	-
Common linnet	September	-	-	-	-
Common linnet	October	5.25	9.49	14.75	147.46
Common linnet	November	-	-	-	-
Goosander	March	1.22	6.51	7.73	77.27

Taxon	Month	Headwind per 1 km	Tailwind per 1 km	Total per 1 km	Total per 10 km
Goosander	April	-	-	-	-
Goosander	May	-	-	-	-
Goosander	July	-	-	-	-
Goosander	August	-	-	-	-
Goosander	September	-	-	-	-
Goosander	October	0.66	1.19	1.84	18.43
Goosander	November	-	-	-	-
Common guillemot	March	16.56	88.30	104.86	1048.63
Common guillemot	April	69.26	5.61	74.86	748.62
Common guillemot	May	34.58	6.01	40.59	405.93
Common guillemot	July	-	-	-	-
Common guillemot	August	-	-	-	-
Common guillemot	September	15.68	3.76	19.44	194.45
Common guillemot	October	91.84	166.02	257.86	2578.58
Common guillemot	November	107.93	132.90	240.83	2408.27
Common redpoll	March	-	-	-	-
Common redpoll	April	-	-	-	-
Common redpoll	May	-	-	-	-
Common redpoll	July	-	-	-	-
Common redpoll	August	-	-	-	-
Common redpoll	September	-	-	-	-
Common redpoll	October	2.72	4.93	7.65	76.50
Common redpoll	November	2.72	3.35	6.07	60.70
Common scoter	March	40.41	215.41	255.82	2558.16
Common scoter	April	2385.82	193.15	2578.98	25789.75
Common scoter	May	1016.01	176.50	1192.51	11925.10
Common scoter	July	8027.14	-	8027.14	80271.40
Common scoter	August	166.59	35.37	201.96	2019.62
Common scoter	September	154.31	37.02	191.33	1913.34
Common scoter	October	12.70	22.96	35.66	356.62
Common scoter	November	18.93	23.30	42.23	422.30
Common shelduck	March	-	-	-	-
Common shelduck	April	-	-	-	-
Common shelduck	May	-	-	-	-
Common shelduck	July	-	-	-	-
Common shelduck	August	-	-	-	-
Common shelduck	September	4.28	1.03	5.30	53.03
Common shelduck	October	-	-	-	-
Common shelduck	November	-	-	-	-
Common snipe	March	-	-	-	-
Common snipe	April	-	-	-	-

Taxon	Month	Headwind per 1 km	Tailwind per 1 km	Total per 1 km	Total per 10 km
Common snipe	May	-	-	-	-
Common snipe	July	-	-	-	-
Common snipe	August	-	-	-	-
Common snipe	September	2.14	0.51	2.65	26.52
Common snipe	October	-	-	-	-
Common snipe	November	-	-	-	-
Common starling	March	8.15	43.45	51.60	515.95
Common starling	April	250.57	20.29	270.86	2708.59
Common starling	May	3.00	0.52	3.52	35.15
Common starling	July	-	-	-	-
Common starling	August	-	-	-	-
Common starling	September	-	-	-	-
Common starling	October	5.34	9.65	14.98	149.83
Common starling	November	137.14	168.86	306.00	3059.96
Common swift	March	-	-	-	-
Common swift	April	-	-	-	-
Common swift	May	-	-	-	-
Common swift	July	-	-	-	-
Common swift	August	202.63	43.02	245.65	2456.49
Common swift	September	-	-	-	-
Common swift	October	-	-	-	-
Common swift	November	-	-	-	-
Common tern	March	-	-	-	-
Common tern	April	4.43	0.36	4.79	47.90
Common tern	May	9.83	1.71	11.54	115.41
Common tern	July	175.84	-	175.84	1758.43
Common tern	August	113.15	24.02	137.18	1371.76
Common tern	September	13.68	3.28	16.97	169.66
Common tern	October	-	-	-	-
Common tern	November	-	-	-	-
Common wood pigeon	March	0.81	4.33	5.14	51.42
Common wood pigeon	April	6.62	0.54	7.16	71.57
Common wood pigeon	May	-	-	-	-
Common wood pigeon	July	-	-	-	-
Common wood pigeon	August	-	-	-	-
Common wood pigeon	September	-	-	-	-
Common wood pigeon	October	-	-	-	-
Common wood pigeon	November	-	-	-	-
Unidentified tern	March	-	-	-	-
Unidentified tern	April	-	-	-	-
Unidentified tern	May	19.12	3.32	22.44	224.41

Taxon	Month	Headwind per 1 km	Tailwind per 1 km	Total per 1 km	Total per 10 km
Unidentified tern	July	197.71	-	197.71	1977.09
Unidentified tern	August	77.63	16.48	94.11	941.13
Unidentified tern	September	1.07	0.26	1.33	13.28
Unidentified tern	October	-	-	-	-
Unidentified tern	November	-	-	-	-
Dunlin	March	-	-	-	-
Dunlin	April	-	-	-	-
Dunlin	May	-	-	-	-
Dunlin	July	28.20	-	28.20	281.97
Dunlin	August	3.57	0.76	4.33	43.27
Dunlin	September	14.26	3.42	17.68	176.84
Dunlin	October	-	-	-	-
Dunlin	November	-	-	-	-
Dunnock	March	-	-	-	-
Dunnock	April	2.13	0.17	2.30	23.04
Dunnock	May	-	-	-	-
Dunnock	July	-	-	-	-
Dunnock	August	-	-	-	-
Dunnock	September	-	-	-	-
Dunnock	October	-	-	-	-
Dunnock	November	-	-	-	-
Eurasian blackcap	March	-	-	-	-
Eurasian blackcap	April	-	-	-	-
Eurasian blackcap	May	-	-	-	-
Eurasian blackcap	July	-	-	-	-
Eurasian blackcap	August	-	-	-	-
Eurasian blackcap	September	2.19	0.53	2.72	27.21
Eurasian blackcap	October	-	-	-	-
Eurasian blackcap	November	-	-	-	-
Eurasian curlew	March	23.77	126.73	150.50	1505.03
Eurasian curlew	April	156.68	12.68	169.37	1693.66
Eurasian curlew	May	-	-	-	-
Eurasian curlew	July	-	-	-	-
Eurasian curlew	August	-	-	-	-
Eurasian curlew	September	-	-	-	-
Eurasian curlew	October	-	-	-	-
Eurasian curlew	November	-	-	-	-
Eurasian siskin	March	17.98	95.84	113.82	1138.17
Eurasian siskin	April	4.45	0.36	4.81	48.14
Eurasian siskin	May	-	-	-	-
Eurasian siskin	July	-	-	-	-

Taxon	Month	Headwind per 1 km	Tailwind per 1 km	Total per 1 km	Total per 10 km
Eurasian siskin	August	-	-	-	-
Eurasian siskin	September	160.39	38.48	198.88	1988.75
Eurasian siskin	October	-	-	-	-
Eurasian siskin	November	-	-	-	-
Eurasian skylark	March	12.90	68.79	81.70	816.96
Eurasian skylark	April	16.79	1.36	18.15	181.50
Eurasian skylark	May	-	-	-	-
Eurasian skylark	July	-	-	-	-
Eurasian skylark	August	-	-	-	-
Eurasian skylark	September	172.12	41.29	213.41	2134.13
Eurasian skylark	October	-	-	-	-
Eurasian skylark	November	-	-	-	-
Eurasian sparrowhawk	March	0.22	1.18	1.40	13.96
Eurasian sparrowhawk	April	3.24	0.26	3.51	35.07
Eurasian sparrowhawk	May	-	-	-	-
Eurasian sparrowhawk	July	-	-	-	-
Eurasian sparrowhawk	August	-	-	-	-
Eurasian sparrowhawk	September	1.07	0.26	1.33	13.26
Eurasian sparrowhawk	October	-	-	-	-
Eurasian sparrowhawk	November	-	-	-	-
Eurasian teal	March	0.63	3.38	4.02	40.18
Eurasian teal	April	58.12	4.70	62.82	628.22
Eurasian teal	May	7.46	1.30	8.76	87.60
Eurasian teal	July	35.59	-	35.59	355.94
Eurasian teal	August	27.86	5.91	33.77	337.75
Eurasian teal	September	85.74	20.57	106.31	1063.11
Eurasian teal	October	-	-	-	-
Eurasian teal	November	-	-	-	-
Eurasian wigeon	March	-	-	-	-
Eurasian wigeon	April	63.35	5.13	68.48	684.78
Eurasian wigeon	May	-	-	-	-
Eurasian wigeon	July	-	-	-	-
Eurasian wigeon	August	-	-	-	-
Eurasian wigeon	September	149.72	35.92	185.64	1856.37
Eurasian wigeon	October	50.93	92.06	142.98	1429.82
Eurasian wigeon	November	-	-	-	-
Eurasian wren	March	0.34	1.82	2.17	21.66
Eurasian wren	April	10.94	0.89	11.83	118.29
Eurasian wren	May	-	-	-	-
Eurasian wren	July	-	-	-	-
Eurasian wren	August	-	-	-	-

Taxon	Month	Headwind per 1 km	Tailwind per 1 km	Total per 1 km	Total per 10 km
Eurasian wren	September	-	-	-	-
Eurasian wren	October	1.41	2.55	3.96	39.63
Eurasian wren	November	-	-	-	-
European golden plover	March	-	-	-	-
European golden plover	April	25.61	2.07	27.68	276.79
European golden plover	May	-	-	-	-
European golden plover	July	-	-	-	-
European golden plover	August	10.71	2.27	12.98	129.80
European golden plover	September	-	-	-	-
European golden plover	October	-	-	-	-
European golden plover	November	-	-	-	-
European nightjar	March	-	-	-	-
European nightjar	April	-	-	-	-
European nightjar	May	-	-	-	-
European nightjar	July	-	-	-	-
European nightjar	August	-	-	-	-
European nightjar	September	1.10	0.26	1.36	13.60
European nightjar	October	-	-	-	-
European nightjar	November	-	-	-	-
European robin	March	0.43	2.29	2.72	27.21
European robin	April	10.81	0.88	11.68	116.84
European robin	May	-	-	-	-
European robin	July	-	-	-	-
European robin	August	-	-	-	-
European robin	September	4.28	1.03	5.30	53.03
European robin	October	-	-	-	-
European robin	November	-	-	-	-
Fieldfare	March	-	-	-	-
Fieldfare	April	15.59	1.26	16.85	168.48
Fieldfare	May	-	-	-	-
Fieldfare	July	-	-	-	-
Fieldfare	August	-	-	-	-
Fieldfare	September	-	-	-	-
Fieldfare	October	-	-	-	-
Fieldfare	November	-	-	-	-
Goldcrest	March	-	-	-	-
Goldcrest	April	8.72	0.71	9.42	94.22
Goldcrest	May	-	-	-	-
Goldcrest	July	-	-	-	-
Goldcrest	August	-	-	-	-
Goldcrest	September	6.42	1.54	7.96	79.55

Taxon	Month	Headwind per 1 km	Tailwind per 1 km	Total per 1 km	Total per 10 km
Goldcrest	October	-	-	-	-
Goldcrest	November	-	-	-	-
Great black-backed gull	March	5.94	31.67	37.61	376.10
Great black-backed gull	April	-	-	-	-
Great black-backed gull	May	-	-	-	-
Great black-backed gull	July	-	-	-	-
Great black-backed gull	August	-	-	-	-
Great black-backed gull	September	-	-	-	-
Great black-backed gull	October	1.72	3.11	4.83	48.33
Great black-backed gull	November	10.55	12.99	23.53	235.32
Great black cormorant	March	3.62	19.30	22.93	229.26
Great black cormorant	April	69.79	5.65	75.44	754.44
Great black cormorant	May	28.44	4.94	33.38	333.85
Great black cormorant	July	-	-	-	-
Great black cormorant	August	270.70	57.47	328.17	3281.75
Great black cormorant	September	33.23	7.97	41.20	412.05
Great black cormorant	October	1.97	3.57	5.54	55.39
Great black cormorant	November	15.29	18.82	34.11	341.10
Great egret	March	-	-	-	-
Great egret	April	1.07	0.09	1.15	11.52
Great egret	May	-	-	-	-
Great egret	July	-	-	-	-
Great egret	August	-	-	-	-
Great egret	September	-	-	-	-
Great egret	October	-	-	-	-
Great egret	November	-	-	-	-
Great tit	March	2.22	11.85	14.07	140.74
Great tit	April	2.19	0.18	2.36	23.65
Great tit	May	-	-	-	-
Great tit	July	-	-	-	-
Great tit	August	-	-	-	-
Great tit	September	4.28	1.03	5.30	53.03
Great tit	October	-	-	-	-
Great tit	November	-	-	-	-
Greater scaup	March	8.09	43.14	51.24	512.36
Greater scaup	April	144.42	11.69	156.12	1561.16
Greater scaup	May	-	-	-	-
Greater scaup	July	-	-	-	-
Greater scaup	August	-	-	-	-
Greater scaup	September	6.67	1.60	8.26	82.64
Greater scaup	October	15.89	28.72	44.61	446.09

Taxon	Month	Headwind per 1 km	Tailwind per 1 km	Total per 1 km	Total per 10 km
Greater scaup	November	-	-	-	-
Greater white-fronted goose	March	16.72	89.12	105.84	1058.38
Greater white-fronted goose	April	-	-	-	-
Greater white-fronted goose	May	3.58	0.62	4.21	42.06
Greater white-fronted goose	July	-	-	-	-
Greater white-fronted goose	August	-	-	-	-
Greater white-fronted goose	September	-	-	-	-
Greater white-fronted goose	October	-	-	-	-
Greater white-fronted goose	November	-	-	-	-
Grey heron	March	-	-	-	-
Grey heron	April	2.13	0.17	2.30	23.04
Grey heron	May	1.19	0.21	1.40	14.02
Grey heron	July	42.29	-	42.29	422.95
Grey heron	August	1.78	0.38	2.16	21.63
Grey heron	September	22.76	5.46	28.22	282.21
Grey heron	October	-	-	-	-
Grey heron	November	-	-	-	-
Grey plover	March	-	-	-	-
Grey plover	April	-	-	-	-
Grey plover	May	-	-	-	-
Grey plover	July	-	-	-	-
Grey plover	August	4.85	1.03	5.88	58.80
Grey plover	September	-	-	-	-
Grey plover	October	-	-	-	-
Grey plover	November	-	-	-	-
Greylag goose	March	1.24	6.63	7.87	78.73
Greylag goose	April	3.66	0.30	3.96	39.57
Greylag goose	May	216.58	37.62	254.20	2542.03
Greylag goose	July	-	-	-	-
Greylag goose	August	9.07	1.93	11.00	110.01
Greylag goose	September	34.44	8.26	42.70	427.02
Greylag goose	October	-	-	-	-
Greylag goose	November	-	-	-	-
European herring gull	March	17.10	91.17	108.28	1082.76
European herring gull	April	-	-	-	-
European herring gull	May	-	-	-	-
European herring gull	July	-	-	-	-
European herring gull	August	-	-	-	-
European herring gull	September	26.73	6.41	33.15	331.46
European herring gull	October	-	-	-	-
European herring gull	November	-	-	-	-

Taxon	Month	Headwind per 1 km	Tailwind per 1 km	Total per 1 km	Total per 10 km
Hooded crow	March	-	-	-	-
Hooded crow	April	6.45	0.52	6.97	69.73
Hooded crow	May	4.75	0.83	5.58	55.80
Hooded crow	July	-	-	-	-
Hooded crow	August	-	-	-	-
Hooded crow	September	-	-	-	-
Hooded crow	October	-	-	-	-
Hooded crow	November	-	-	-	-
Horned grebe	March	-	-	-	-
Horned grebe	April	1.11	0.09	1.20	12.03
Horned grebe	May	-	-	-	-
Horned grebe	July	-	-	-	-
Horned grebe	August	-	-	-	-
Horned grebe	September	-	-	-	-
Horned grebe	October	-	-	-	-
Horned grebe	November	-	-	-	-
Lesser black-backed gull	March	2.39	12.73	15.12	151.22
Lesser black-backed gull	April	360.49	29.18	389.68	3896.75
Lesser black-backed gull	May	110.70	19.23	129.92	1299.25
Lesser black-backed gull	July	156.72	-	156.72	1567.20
Lesser black-backed gull	August	72.71	15.44	88.14	881.43
Lesser black-backed gull	September	100.09	24.01	124.11	1241.08
Lesser black-backed gull	October	3.06	5.54	8.60	86.01
Lesser black-backed gull	November	-	-	-	-
Lesser whitethroat	March	-	-	-	-
Lesser whitethroat	April	-	-	-	-
Lesser whitethroat	May	-	-	-	-
Lesser whitethroat	July	-	-	-	-
Lesser whitethroat	August	3.16	0.67	3.82	38.25
Lesser whitethroat	September	-	-	-	-
Lesser whitethroat	October	-	-	-	-
Lesser whitethroat	November	-	-	-	-
Little gull	March	12.30	65.58	77.89	778.86
Little gull	April	186.05	15.06	201.12	2011.17
Little gull	May	10.67	1.85	12.53	125.29
Little gull	July	18.39	-	18.39	183.86
Little gull	August	88.24	18.73	106.97	1069.72
Little gull	September	33.87	8.12	41.99	419.90
Little gull	October	14.93	26.99	41.92	419.20
Little gull	November	22.01	27.10	49.11	491.08
Unidentified owl	March	-	-	-	-

Taxon	Month	Headwind per 1 km	Tailwind per 1 km	Total per 1 km	Total per 10 km
Unidentified owl	April	1.09	0.09	1.18	11.82
Unidentified owl	May	1.18	0.21	1.39	13.88
Unidentified owl	July	-	-	-	-
Unidentified owl	August	-	-	-	-
Unidentified owl	September	-	-	-	-
Unidentified owl	October	-	-	-	-
Unidentified owl	November	-	-	-	-
Long-eared owl	March	0.17	0.91	1.08	10.83
Long-eared owl	April	2.21	0.18	2.39	23.86
Long-eared owl	May	-	-	-	-
Long-eared owl	July	-	-	-	-
Long-eared owl	August	-	-	-	-
Long-eared owl	September	-	-	-	-
Long-eared owl	October	-	-	-	-
Long-eared owl	November	-	-	-	-
Long-tailed duck	March	414.58	2209.95	2624.52	26245.21
Long-tailed duck	April	7495.71	606.83	8102.55	81025.46
Long-tailed duck	May	320.79	55.73	376.51	3765.14
Long-tailed duck	July	-	-	-	-
Long-tailed duck	August	-	-	-	-
Long-tailed duck	September	1.20	0.29	1.49	14.91
Long-tailed duck	October	344.09	621.98	966.06	9660.64
Long-tailed duck	November	590.76	727.41	1318.18	13181.78
Unidentified skua	March	-	-	-	-
Unidentified skua	April	-	-	-	-
Unidentified skua	May	-	-	-	-
Unidentified skua	July	-	-	-	-
Unidentified skua	August	-	-	-	-
Unidentified skua	September	1.07	0.26	1.33	13.26
Unidentified skua	October	-	-	-	-
Unidentified skua	November	-	-	-	-
Mallard	March	0.45	2.38	2.83	28.28
Mallard	April	33.22	2.69	35.91	359.07
Mallard	May	-	-	-	-
Mallard	July	-	-	-	-
Mallard	August	-	-	-	-
Mallard	September	1.40	0.34	1.73	17.32
Mallard	October	6.26	11.32	17.57	175.75
Mallard	November	25.53	31.43	56.96	569.55
Meadow pipit	March	-	-	-	-
Meadow pipit	April	19.47	1.58	21.04	210.45

Taxon	Month	Headwind per 1 km	Tailwind per 1 km	Total per 1 km	Total per 10 km
Meadow pipit	May	-	-	-	-
Meadow pipit	July	-	-	-	-
Meadow pipit	August	-	-	-	-
Meadow pipit	September	-	-	-	-
Meadow pipit	October	-	-	-	-
Meadow pipit	November	-	-	-	-
Common gull	March	31.54	168.13	199.67	1996.71
Common gull	April	234.68	19.00	253.68	2536.76
Common gull	May	12.50	2.17	14.67	146.71
Common gull	July	222.97	-	222.97	2229.75
Common gull	August	8.20	1.74	9.94	99.40
Common gull	September	42.50	10.20	52.69	526.95
Common gull	October	39.34	71.11	110.46	1104.56
Common gull	November	79.35	97.71	177.06	1770.58
Unidentified auk	March	38.23	203.81	242.04	2420.40
Unidentified auk	April	319.66	25.88	345.54	3455.42
Unidentified auk	May	87.25	15.16	102.40	1024.01
Unidentified auk	July	28.24	-	28.24	282.44
Unidentified auk	August	-	-	-	-
Unidentified auk	September	20.52	4.92	25.44	254.40
Unidentified auk	October	63.69	115.12	178.81	1788.06
Unidentified auk	November	74.95	92.29	167.24	1672.40
Mute swan	March	1.67	8.91	10.58	105.78
Mute swan	April	2.18	0.18	2.36	23.55
Mute swan	May	-	-	-	-
Mute swan	July	-	-	-	-
Mute swan	August	-	-	-	-
Mute swan	September	-	-	-	-
Mute swan	October	-	-	-	-
Mute swan	November	1.99	2.45	4.44	44.42
Northern lapwing	March	0.17	0.91	1.08	10.83
Northern lapwing	April	-	-	-	-
Northern lapwing	May	-	-	-	-
Northern lapwing	July	-	-	-	-
Northern lapwing	August	-	-	-	-
Northern lapwing	September	-	-	-	-
Northern lapwing	October	-	-	-	-
Northern lapwing	November	-	-	-	-
Northern pintail	March	1.20	6.38	7.58	75.79
Northern pintail	April	17.44	1.41	18.86	188.57
Northern pintail	May	2.37	0.41	2.78	27.76

Taxon	Month	Headwind per 1 km	Tailwind per 1 km	Total per 1 km	Total per 10 km
Northern pintail	July	-	-	-	-
Northern pintail	August	-	-	-	-
Northern pintail	September	-	-	-	-
Northern pintail	October	-	-	-	-
Northern pintail	November	-	-	-	-
Northern shoveler	March	-	-	-	-
Northern shoveler	April	7.66	0.62	8.28	82.76
Northern shoveler	May	-	-	-	-
Northern shoveler	July	-	-	-	-
Northern shoveler	August	-	-	-	-
Northern shoveler	September	9.87	2.37	12.24	122.42
Northern shoveler	October	-	-	-	-
Northern shoveler	November	-	-	-	-
Osprey	March	-	-	-	-
Osprey	April	-	-	-	-
Osprey	May	1.18	0.21	1.39	13.88
Osprey	July	-	-	-	-
Osprey	August	-	-	-	-
Osprey	September	-	-	-	-
Osprey	October	-	-	-	-
Osprey	November	-	-	-	-
Arctic skua	March	-	-	-	-
Arctic skua	April	2.19	0.18	2.36	23.65
Arctic skua	May	2.35	0.41	2.76	27.63
Arctic skua	July	-	-	-	-
Arctic skua	August	3.11	0.66	3.77	37.71
Arctic skua	September	2.14	0.51	2.65	26.52
Arctic skua	October	-	-	-	-
Arctic skua	November	-	-	-	-
Unidentified skua	March	-	-	-	-
Unidentified skua	April	-	-	-	-
Unidentified skua	May	-	-	-	-
Unidentified skua	July	-	-	-	-
Unidentified skua	August	-	-	-	-
Unidentified skua	September	1.07	0.26	1.33	13.26
Unidentified skua	October	-	-	-	-
Unidentified skua	November	-	-	-	-
Pomarine skua	March	-	-	-	-
Pomarine skua	April	-	-	-	-
Pomarine skua	May	3.57	0.62	4.19	41.92
Pomarine skua	July	-	-	-	-

Taxon	Month	Headwind per 1 km	Tailwind per 1 km	Total per 1 km	Total per 10 km
Pomarine skua	August	-	-	-	-
Pomarine skua	September	-	-	-	-
Pomarine skua	October	-	-	-	-
Pomarine skua	November	-	-	-	-
Razorbill	March	135.30	721.24	856.54	8565.37
Razorbill	April	997.17	80.73	1077.89	10778.94
Razorbill	May	56.40	9.80	66.20	662.01
Razorbill	July	28.17	-	28.17	281.66
Razorbill	August	-	-	-	-
Razorbill	September	4.27	1.03	5.30	52.98
Razorbill	October	68.89	124.52	193.41	1934.13
Razorbill	November	116.93	143.98	260.91	2609.06
Red-breasted merganser	March	6.88	36.67	43.55	435.51
Red-breasted merganser	April	31.68	2.56	34.24	342.43
Red-breasted merganser	May	-	-	-	-
Red-breasted merganser	July	-	-	-	-
Red-breasted merganser	August	-	-	-	-
Red-breasted merganser	September	-	-	-	-
Red-breasted merganser	October	-	-	-	-
Red-breasted merganser	November	-	-	-	-
Red-breasted merganser/goosander	March	0.22	1.18	1.40	13.96
Red-breasted merganser/goosander	April	3.23	0.26	3.49	34.86
Red-breasted merganser/goosander	May	-	-	-	-
Red-breasted merganser/goosander	July	-	-	-	-
Red-breasted merganser/goosander	August	-	-	-	-
Red-breasted merganser/goosander	September	-	-	-	-
Red-breasted merganser/goosander	October	-	-	-	-
Red-breasted merganser/goosander	November	-	-	-	-
Red-necked grebe	March	-	-	-	-
Red-necked grebe	April	1.11	0.09	1.20	12.03
Red-necked grebe	May	-	-	-	-
Red-necked grebe	July	-	-	-	-
Red-necked grebe	August	-	-	-	-
Red-necked grebe	September	-	-	-	-
Red-necked grebe	October	-	-	-	-
Red-necked grebe	November	-	-	-	-
Red-throated diver	March	1.21	6.46	7.67	76.67

Taxon	Month	Headwind per 1 km	Tailwind per 1 km	Total per 1 km	Total per 10 km
Red-throated diver	April	14.90	1.21	16.11	161.10
Red-throated diver	May	17.60	3.06	20.65	206.53
Red-throated diver	July	-	-	-	-
Red-throated diver	August	-	-	-	-
Red-throated diver	September	2.94	0.71	3.65	36.46
Red-throated diver	October	2.76	4.99	7.75	77.47
Red-throated diver	November	2.89	3.55	6.44	64.39
Rook	March	-	-	-	-
Rook	April	11.13	0.90	12.03	120.34
Rook	May	2.37	0.41	2.78	27.76
Rook	July	-	-	-	-
Rook	August	-	-	-	-
Rook	September	-	-	-	-
Rook	October	-	-	-	-
Rook	November	-	-	-	-
Ruff	March	-	-	-	-
Ruff	April	-	-	-	-
Ruff	May	-	-	-	-
Ruff	July	-	-	-	-
Ruff	August	1.78	0.38	2.16	21.63
Ruff	September	1.07	0.26	1.33	13.26
Ruff	October	-	-	-	-
Ruff	November	-	-	-	-
Sand martin	March	-	-	-	-
Sand martin	April	-	-	-	-
Sand martin	May	-	-	-	-
Sand martin	July	-	-	-	-
Sand martin	August	3.16	0.67	3.82	38.25
Sand martin	September	-	-	-	-
Sand martin	October	-	-	-	-
Sand martin	November	-	-	-	-
Sanderling	March	-	-	-	-
Sanderling	April	-	-	-	-
Sanderling	May	-	-	-	-
Sanderling	July	-	-	-	-
Sanderling	August	-	-	-	-
Sanderling	September	17.11	4.10	21.21	212.13
Sanderling	October	-	-	-	-
Sanderling	November	-	-	-	-
Short-eared owl	March	-	-	-	-
Short-eared owl	April	2.21	0.18	2.39	23.86

Taxon	Month	Headwind per 1 km	Tailwind per 1 km	Total per 1 km	Total per 10 km
Short-eared owl	May	1.19	0.21	1.40	14.02
Short-eared owl	July	-	-	-	-
Short-eared owl	August	-	-	-	-
Short-eared owl	September	-	-	-	-
Short-eared owl	October	-	-	-	-
Short-eared owl	November	-	-	-	-
Snow bunting	March	-	-	-	-
Snow bunting	April	-	-	-	-
Snow bunting	May	-	-	-	-
Snow bunting	July	-	-	-	-
Snow bunting	August	-	-	-	-
Snow bunting	September	-	-	-	-
Snow bunting	October	1.34	2.43	3.77	37.74
Snow bunting	November	-	-	-	-
Song thrush	March	0.34	1.79	2.12	21.22
Song thrush	April	2.19	0.18	2.36	23.65
Song thrush	May	2.39	0.41	2.80	28.04
Song thrush	July	-	-	-	-
Song thrush	August	-	-	-	-
Song thrush	September	6.42	1.54	7.96	79.55
Song thrush	October	-	-	-	-
Song thrush	November	-	-	-	-
Stock dove	March	0.22	1.18	1.40	13.96
Stock dove	April	1.11	0.09	1.20	12.03
Stock dove	May	-	-	-	-
Stock dove	July	-	-	-	-
Stock dove	August	-	-	-	-
Stock dove	September	-	-	-	-
Stock dove	October	-	-	-	-
Stock dove	November	-	-	-	-
Tufted duck	March	-	-	-	-
Tufted duck	April	19.94	1.61	21.56	215.59
Tufted duck	May	2.37	0.41	2.78	27.76
Tufted duck	July	-	-	-	-
Tufted duck	August	-	-	-	-
Tufted duck	September	-	-	-	-
Tufted duck	October	-	-	-	-
Tufted duck	November	-	-	-	-
Tundra swan	March	1.01	5.36	6.37	63.67
Tundra swan	April	-	-	-	-
Tundra swan	May	-	-	-	-

Taxon	Month	Headwind per 1 km	Tailwind per 1 km	Total per 1 km	Total per 10 km
Tundra swan	July	-	-	-	-
Tundra swan	August	-	-	-	-
Tundra swan	September	-	-	-	-
Tundra swan	October	-	-	-	-
Tundra swan	November	-	-	-	-
Unidentified sandpiper	March	-	-	-	-
Unidentified sandpiper	April	-	-	-	-
Unidentified sandpiper	May	-	-	-	-
Unidentified sandpiper	July	-	-	-	-
Unidentified sandpiper	August	12.26	2.60	14.87	148.69
Unidentified sandpiper	September	3.21	0.77	3.98	39.78
Unidentified sandpiper	October	-	-	-	-
Unidentified sandpiper	November	-	-	-	-
Unidentified diver	March	2.19	11.65	13.83	138.33
Unidentified diver	April	29.56	2.39	31.95	319.52
Unidentified diver	May	202.11	35.11	237.22	2372.24
Unidentified diver	July	-	-	-	-
Unidentified diver	August	5.35	1.14	6.49	64.90
Unidentified diver	September	10.86	2.61	13.46	134.65
Unidentified diver	October	8.73	15.78	24.52	245.16
Unidentified diver	November	10.65	13.11	23.76	237.62
Unidentified duck	March	27.77	148.01	175.77	1757.71
Unidentified duck	April	984.73	79.72	1064.45	10644.49
Unidentified duck	May	64.11	11.14	75.24	752.44
Unidentified duck	July	84.59	-	84.59	845.90
Unidentified duck	August	65.14	13.83	78.98	789.76
Unidentified duck	September	216.30	51.89	268.20	2681.97
Unidentified duck	October	95.17	172.02	267.19	2671.90
Unidentified duck	November	54.58	67.20	121.78	1217.79
Unidentified goose	March	76.26	406.51	482.77	4827.71
Unidentified goose	April	424.33	34.35	458.68	4586.80
Unidentified goose	May	35.48	6.16	41.65	416.46
Unidentified goose	July	-	-	-	-
Unidentified goose	August	-	-	-	-
Unidentified goose	September	43.84	10.52	54.36	543.59
Unidentified goose	October	113.12	204.48	317.61	3176.05
Unidentified goose	November	-	-	-	-
Unidentified passerine	March	11.55	61.55	73.09	730.91
Unidentified passerine	April	586.89	47.51	634.40	6344.02
Unidentified passerine	May	18.76	3.26	22.02	220.17
Unidentified passerine	July	-	-	-	-

Taxon	Month	Headwind per 1 km	Tailwind per 1 km	Total per 1 km	Total per 10 km
Unidentified passerine	August	25.24	5.36	30.60	305.99
Unidentified passerine	September	426.69	102.37	529.06	5290.60
Unidentified passerine	October	105.35	190.43	295.77	2957.71
Unidentified passerine	November	-	-	-	-
Unidentified pipit	March	-	-	-	-
Unidentified pipit	April	4.45	0.36	4.81	48.14
Unidentified pipit	May	-	-	-	-
Unidentified pipit	July	-	-	-	-
Unidentified pipit	August	-	-	-	-
Unidentified pipit	September	-	-	-	-
Unidentified pipit	October	-	-	-	-
Unidentified pipit	November	-	-	-	-
Unidentified swan	March	11.37	60.62	71.99	719.94
Unidentified swan	April	1.11	0.09	1.20	12.03
Unidentified swan	May	6.96	1.21	8.16	81.64
Unidentified swan	July	-	-	-	-
Unidentified swan	August	21.46	4.56	26.02	260.20
Unidentified swan	September	-	-	-	-
Unidentified swan	October	-	-	-	-
Unidentified swan	November	7.40	9.11	16.51	165.14
Unidentified tern	March	-	-	-	-
Unidentified tern	April	-	-	-	-
Unidentified tern	May	1.19	0.21	1.40	14.02
Unidentified tern	July	126.88	-	126.88	1268.84
Unidentified tern	August	1.78	0.38	2.16	21.63
Unidentified tern	September	2.14	0.51	2.65	26.52
Unidentified tern	October	-	-	-	-
Unidentified tern	November	-	-	-	-
Unidentified thrush	March	2.39	12.76	15.16	151.59
Unidentified thrush	April	-	-	-	-
Unidentified thrush	May	-	-	-	-
Unidentified thrush	July	-	-	-	-
Unidentified thrush	August	-	-	-	-
Unidentified thrush	September	-	-	-	-
Unidentified thrush	October	-	-	-	-
Unidentified thrush	November	-	-	-	-
Unidentified wader	March	-	-	-	-
Unidentified wader	April	-	-	-	-
Unidentified wader	May	458.65	79.68	538.32	5383.22
Unidentified wader	July	56.39	-	56.39	563.93
Unidentified wader	August	53.56	11.37	64.93	649.28

Taxon	Month	Headwind per 1 km	Tailwind per 1 km	Total per 1 km	Total per 10 km
Unidentified wader	September	26.79	6.43	33.21	332.15
Unidentified wader	October	-	-	-	-
Unidentified wader	November	-	-	-	-
Velvet scoter	March	1.99	10.61	12.60	125.99
Velvet scoter	April	191.46	15.50	206.96	2069.64
Velvet scoter	May	22.11	3.84	25.95	259.53
Velvet scoter	July	49.61	-	49.61	496.12
Velvet scoter	August	2.09	0.44	2.54	25.37
Velvet scoter	September	23.96	5.75	29.71	297.11
Velvet scoter	October	25.76	46.56	72.32	723.16
Velvet scoter	November	-	-	-	-
White wagtail	March	19.82	105.66	125.48	1254.80
White wagtail	April	1424.31	115.31	1539.62	15396.21
White wagtail	May	32.57	5.66	38.23	382.33
White wagtail	July	-	-	-	-
White wagtail	August	-	-	-	-
White wagtail	September	1322.86	317.37	1640.24	16402.35
White wagtail	October	-	-	-	-
White wagtail	November	18.10	22.28	40.38	403.76
Whooper swan	March	0.86	4.58	5.44	54.42
Whooper swan	April	1.07	0.09	1.15	11.52
Whooper swan	May	-	-	-	-
Whooper swan	July	-	-	-	-
Whooper swan	August	-	-	-	-
Whooper swan	September	-	-	-	-
Whooper swan	October	-	-	-	-
Whooper swan	November	-	-	-	-
Wood lark	March	-	-	-	-
Wood lark	April	-	-	-	-
Wood lark	May	-	-	-	-
Wood lark	July	-	-	-	-
Wood lark	August	-	-	-	-
Wood lark	September	-	-	-	-
Wood lark	October	1.41	2.55	3.96	39.63
Wood lark	November	-	-	-	-
Western yellow wagtail	March	-	-	-	-
Western yellow wagtail	April	-	-	-	-
Western yellow wagtail	May	-	-	-	-
Western yellow wagtail	July	-	-	-	-
Western yellow wagtail	August	7.14	1.52	8.65	86.53
Western yellow wagtail	September	6.53	1.57	8.09	80.93

Taxon	Month	Headwind per 1 km	Tailwind per 1 km	Total per 1 km	Total per 10 km
Western yellow wagtail	October	-	-	-	-
Western yellow wagtail	November	-	-	-	-

Table 3.95. The migration fluxes of species groups in the survey area in subsequent months in the spring and autumn migration periods

Group of species	Month	Headwind per 1 km	Tailwind per 1 km	Total per 1 km	Total per 10 km
Auks	March	163.06	869.19	1032.24	10322.43
Auks	April	1178.92	95.44	1274.36	12743.57
Auks	May	184.69	32.08	216.78	2167.77
Auks	July	58.19	-	58.19	581.85
Auks	August	-	-	-	-
Auks	September	41.46	9.95	51.40	514.03
Auks	October	195.43	353.27	548.70	5486.98
Auks	November	257.42	316.96	574.38	5743.78
Cormorants	March	3.62	19.30	22.93	229.26
Cormorants	April	69.79	5.65	75.44	754.44
Cormorants	May	28.44	4.94	33.38	333.85
Cormorants	July	-	-	-	-
Cormorants	August	270.70	57.47	328.17	3281.75
Cormorants	September	33.23	7.97	41.20	412.05
Cormorants	October	1.97	3.57	5.54	55.39
Cormorants	November	15.29	18.82	34.11	341.10
Cranes	March	-	-	-	-
Cranes	April	24.25	1.96	26.22	262.18
Cranes	May	1.18	0.21	1.39	13.88
Cranes	July	-	-	-	-
Cranes	August	-	-	-	-
Cranes	September	10.69	2.57	13.26	132.58
Cranes	October	-	-	-	-
Cranes	November	-	-	-	-
Divers	March	3.81	20.32	24.13	241.30
Divers	April	60.38	4.89	65.27	652.71
Divers	May	339.40	58.96	398.37	3983.65
Divers	July	-	-	-	-
Divers	August	5.36	1.14	6.50	65.01
Divers	September	14.12	3.39	17.51	175.06
Divers	October	12.77	23.09	35.86	358.57
Divers	November	13.49	16.62	30.11	301.11
Ducks	March	472.90	2520.87	2993.77	29937.73
Ducks	April	10856.51	878.92	11735.43	117354.29
Ducks	May	1372.04	238.35	1610.39	16103.93

Group of species	Month	Headwind per 1 km	Tailwind per 1 km	Total per 1 km	Total per 10 km
Ducks	July	8063.33	-	8063.33	80633.27
Ducks	August	253.22	53.76	306.99	3069.85
Ducks	September	647.01	155.22	802.23	8022.30
Ducks	October	527.08	952.77	1479.85	14798.54
Ducks	November	648.45	798.45	1446.90	14468.95
Geese	March	110.11	586.96	697.08	6970.77
Geese	April	499.98	40.48	540.46	5404.55
Geese	May	195.58	33.98	229.55	2295.53
Geese	July	-	-	-	-
Geese	August	6.28	1.33	7.61	76.08
Geese	September	75.21	18.04	93.26	932.58
Geese	October	133.44	241.21	374.66	3746.57
Geese	November	-	-	-	-
Grebes	March	-	-	-	-
Grebes	April	2.23	0.18	2.41	24.07
Grebes	May	-	-	-	-
Grebes	July	-	-	-	-
Grebes	August	-	-	-	-
Grebes	September	-	-	-	-
Grebes	October	-	-	-	-
Grebes	November	-	-	-	-
Gulls	March	89.12	475.05	564.17	5641.67
Gulls	April	830.91	67.27	898.18	8981.81
Gulls	May	133.89	23.26	157.15	1571.48
Gulls	July	370.25	-	370.25	3702.47
Gulls	August	221.60	47.05	268.65	2686.52
Gulls	September	247.43	59.36	306.80	3067.96
Gulls	October	61.60	111.34	172.94	1729.42
Gulls	November	106.21	130.78	236.99	2369.93
Herons	March	-	-	-	-
Herons	April	3.20	0.26	3.46	34.62
Herons	May	1.20	0.21	1.40	14.04
Herons	July	42.37	-	42.37	423.66
Herons	August	1.79	0.38	2.17	21.67
Herons	September	22.80	5.47	28.27	282.69
Herons	October	-	-	-	-
Herons	November	-	-	-	-
Nightjars	March	-	-	-	-
Nightjars	April	-	-	-	-
Nightjars	May	-	-	-	-
Nightjars	July	-	-	-	-
Nightjars	August	-	-	-	-
Nightjars	September	1.10	0.26	1.36	13.60

Group of species	Month	Headwind per 1 km	Tailwind per 1 km	Total per 1 km	Total per 10 km
Nightjars	October	-	-	-	-
Nightjars	November	-	-	-	-
Owls	March	0.17	0.91	1.08	10.83
Owls	April	5.51	0.45	5.95	59.54
Owls	May	2.38	0.41	2.79	27.90
Owls	July	-	-	-	-
Owls	August	-	-	-	-
Owls	September	-	-	-	-
Owls	October	-	-	-	-
Owls	November	-	-	-	-
Passerines	March	157.91	841.76	999.67	9996.68
Passerines	April	3105.86	251.44	3357.31	33573.07
Passerines	May	281.37	48.88	330.25	3302.54
Passerines	July	-	-	-	-
Passerines	August	176.31	37.43	213.75	2137.48
Passerines	September	3674.90	881.65	4556.55	45565.48
Passerines	October	370.98	670.60	1041.58	10415.79
Passerines	November	328.82	404.88	733.70	7337.02
Pigeons	March	11.44	61.00	72.44	724.44
Pigeons	April	85.70	6.94	92.63	926.34
Pigeons	May	-	-	-	-
Pigeons	July	-	-	-	-
Pigeons	August	-	-	-	-
Pigeons	September	-	-	-	-
Pigeons	October	-	-	-	-
Pigeons	November	-	-	-	-
Raptors	March	0.22	1.18	1.40	13.96
Raptors	April	4.36	0.35	4.71	47.11
Raptors	May	1.18	0.21	1.39	13.88
Raptors	July	-	-	-	-
Raptors	August	-	-	-	-
Raptors	September	1.07	0.26	1.33	13.26
Raptors	October	-	-	-	-
Raptors	November	-	-	-	-
Skuas	March	-	-	-	-
Skuas	April	13.23	1.07	14.30	142.99
Skuas	May	35.83	6.22	42.05	420.55
Skuas	July	-	-	-	-
Skuas	August	18.81	3.99	22.80	228.04
Skuas	September	25.86	6.21	32.07	320.70
Skuas	October	-	-	-	-
Skuas	November	-	-	-	-
Swans	March	14.91	79.47	94.38	943.80

Group of species	Month	Headwind per 1 km	Tailwind per 1 km	Total per 1 km	Total per 10 km
Swans	April	4.36	0.35	4.71	47.11
Swans	May	6.96	1.21	8.16	81.64
Swans	July	-	-	-	-
Swans	August	21.46	4.56	26.02	260.20
Swans	September	-	-	-	-
Swans	October	-	-	-	-
Swans	November	9.39	11.56	20.96	209.55
Swifts	March	-	-	-	-
Swifts	April	-	-	-	-
Swifts	May	-	-	-	-
Swifts	July	-	-	-	-
Swifts	August	202.63	43.02	245.65	2456.49
Swifts	September	-	-	-	-
Swifts	October	-	-	-	-
Swifts	November	-	-	-	-
Terns	March	-	-	-	-
Terns	April	1.18	0.10	1.27	12.73
Terns	May	36.69	6.37	43.06	430.63
Terns	July	545.16	-	545.16	5451.57
Terns	August	123.12	26.14	149.26	1492.60
Terns	September	7.18	1.72	8.90	89.03
Terns	October	-	-	-	-
Terns	November	-	-	-	-
Waders	March	40.42	215.48	255.90	2558.99
Waders	April	307.73	24.91	332.64	3326.40
Waders	May	774.26	134.50	908.76	9087.64
Waders	July	142.80	-	142.80	1427.99
Waders	August	146.42	31.09	177.50	1775.02
Waders	September	109.01	26.15	135.16	1351.64
Waders	October	-	-	-	-
Waders	November	-	-	-	-

3.5.2.5.3 Flight altitude from visual observations

3.5.2.5.3.1 Local bird movements in the wintering period

98% of all visually observed birds (all auks and sea ducks) at LP_01 station flew at altitudes not exceeding 20 m ASL. Only several individuals were observed to fly at an altitude of more than 50 m ASL (whooper swan, unidentified mergansers, European herring gull and great black-backed gull) [Table 3.96, Figure 3.130].

Table 3.96. The flight altitude of birds observed at survey station LP_01 survey station in December 2022, and January and February 2023

Taxon		**Altitude [m]****						**Total**
English name	**Latin name**	**1–10**	**11–20**	**21–30**	**31–40**	**41–50**	**51–100**	
Black guillemot*	*Cepphus grylle*	2	0	0	0	0	0	2
Common merganser*	*Mergus merganser*	5	0	0	0	0	0	5
Common guillemot*	*Uria aalge*	36	0	0	0	0	0	36
Common scoter*	*Melanitta nigra*	4	0	0	0	0	0	4
Eurasian skylark*	*Alauda arvensis*	1	0	0	0	0	0	1
Great black-backed gull	*Larus marinus*	8	5	0	0	0	1	14
Great black cormorant	*Phalacrocorax carbo*	1	1	1	2	0	0	5
Greater scaup	*Aythya marila*	0	0	3	0	0	0	3
Greylag goose*	*Anser anser*	0	2	0	0	0	0	2
European herring gull	*Larus argentatus*	0	0	0	0	0	6	6
Little gull*	*Larus minutus*	3	4	0	0	0	0	7
Long-tailed duck	*Clangula hyemalis*	133	2	0	8	0	0	143
Common gull*	*Larus canus*	17	11	0	0	0	0	28
Unidentified auk*	*Alca torda / Uria aalge*	275	0	0	0	0	0	275
Mute swan	*Cygnus olor*	4	0	0	2	0	0	6
Razorbill*	*Alca torda*	1115	0	0	0	0	0	1115
Red-breasted merganser*	*Mergus serrator*	7	2	0	0	0	0	9
Red-breasted merganser/goosander	*Mergus serrator/Mergus merganser*	0	0	0	0	0	2	2
Red-throated diver*	*Gavia stellata*	1	4	0	0	0	0	5
Tundra swan*	*Cygnus columbianus*	14	0	0	0	0	0	14
Unidentified diver	*Gavia indet.*	5	1	1	0	0	0	7
Unidentified duck*	*Melanitta indet.*	12	12	0	0	0	0	24
Unidentified swan*	*Cygnidae indet.*	3	0	0	0	0	0	3
Velvet scoter*	*Melanitta fusca*	10	7	0	0	0	0	17
Whooper swan	*Cygnus cygnus*	0	0	0	0	0	9	9
Total		**1656**	**51**	**5**	**12**	**0**	**18**	**1742**

**taxa observed exclusively up to 20 m ASL*

***as the observations above 50 m ASL were scarce, observations in this altitude range are presented in cumulative form for the purposes of data presentation*

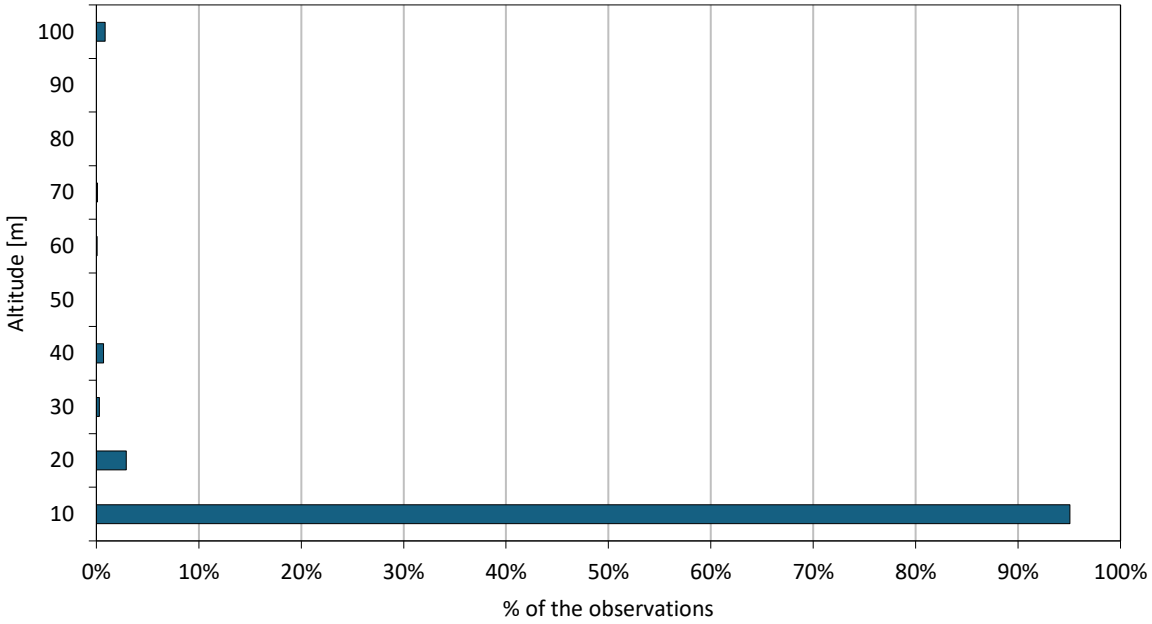


Figure 3.130. The proportion of all birds observed at individual altitudes at survey station LP_01 in December 2022, and January and February 2023

99.7% of all visually observed birds (all auks, gulls, divers, and sea ducks) at LP_02 station flew at altitudes not exceeding 20 m ASL. Only one individual (a cormorant) was observed flying at an altitude of between 51 and 60 m ASL [Table 3.97, Figure 3.131].

Table 3.97. The flight altitude of birds observed at survey station LP_02 survey station in December 2022, and January and February 2023

Taxon		**Altitude [m]****						**Total**
English name	**Latin name**	**1–10**	**11–20**	**21–30**	**31–40**	**41–50**	**51–100**	
Black guillemot*	*Cepphus grylle*	12	0	0	0	0	0	12
Black-headed gull*	*Larus ridibundus*	1	0	0	0	0	0	1
Common guillemot*	*Uria aalge*	49	0	0	0	0	0	49
Common scoter*	*Melanitta nigra*	5	0	0	0	0	0	5
Common wood pigeon*	*Columba palumbus*	1	0	0	0	0	0	1
Eurasian skylark*	*Alauda arvensis*	2	0	0	0	0	0	2
Great black-backed gull*	*Larus marinus*	5	0	0	0	0	0	5
Great black cormorant	*Phalacrocorax carbo*	0	0	0	0	0	1	1
Little gull*	*Larus minutus*	2	0	0	0	0	0	2
Long-tailed duck*	*Clangula hyemalis*	577	6	0	0	0	0	583
Mallard*	*Anas platyrhynchos*	0	4	0	0	0	0	4
Common gull*	*Larus canus*	13	5	0	0	0	0	18
Unidentified auk*	*Alca torda / Uria aalge*	220	0	0	0	0	0	220
Mute swan	*Cygnus olor*	0	0	5	0	0	0	5
Razorbill*	*Alca torda*	1248	0	0	0	0	0	1248
Red-breasted merganser*	*Mergus serrator*	9	0	0	0	0	0	9

Taxon		Altitude [m]**						Total
English name	Latin name	1–10	11–20	21–30	31–40	41–50	51–100	
Red-throated diver*	*Gavia stellata*	1	0	0	0	0	0	1
Smew*	*Mergellus albellus*	0	8	0	0	0	0	8
Unidentified diver*	*Gavia indet.*	1	2	0	0	0	0	3
Unidentified duck*	*Melanitta indet.*	13	0	0	0	0	0	13
Unidentified passerine*	*Passeriformes indet.*	1	0	0	0	0	0	1
Unidentified swan*	*Cygnidae indet.*	0	1	0	0	0	0	1
Velvet scoter*	*Melanitta fusca*	4	8	0	0	0	0	12
Total		**2164**	**34**	**5**	**0**	**0**	**1**	**2204**

**taxa observed exclusively up to 20 m ASL*

***as the observations above 50 m ASL were scarce, observations in this altitude range are presented in cumulative form for the purposes of data presentation*

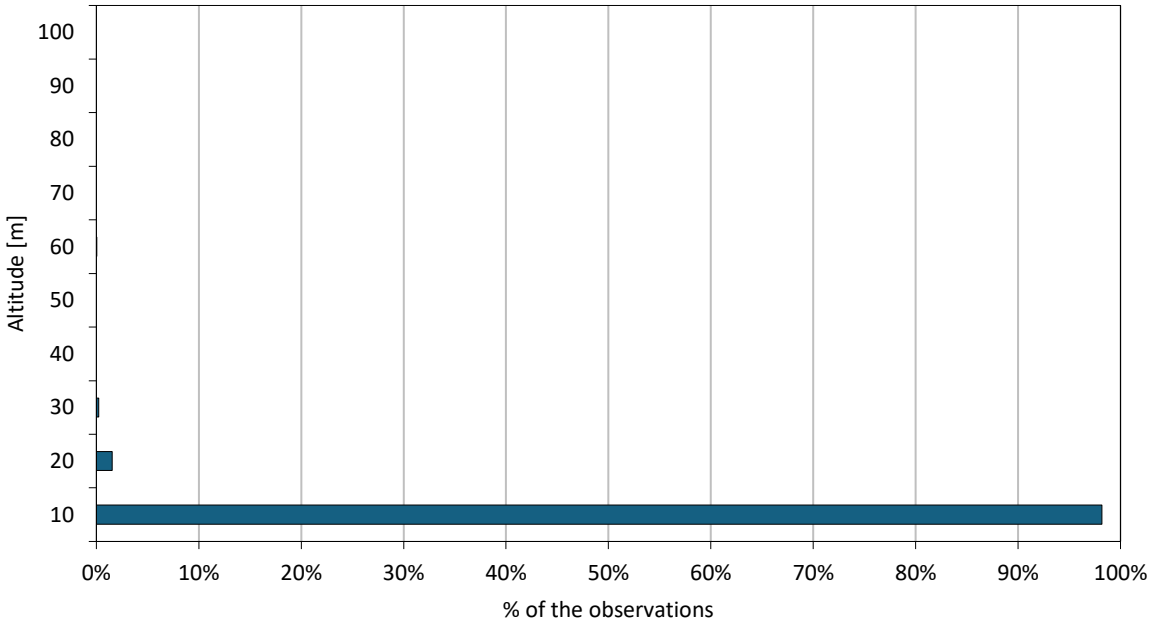


Figure 3.131. The proportion of all birds observed at individual altitudes at survey station LP_01 in December 2022, January and February 2023

3.5.2.5.3.2 Spring migration

85% of all visually observed birds at MB_01 station flew at altitudes not exceeding 20 m ASL. Long-tailed ducks were observed in the highest numbers with the vast majority at altitudes up to 10 m ASL. There were only 2 individuals of this species observed flying above 20 m ASL. 17 species were observed above 50 m ASL (common scoter, Eurasian wigeon, Eurasian curlew, lesser black-backed gull, common gull, black-headed gull, great cormorant, black-throated and red-throated diver, Eurasian teal, mute swan, barn swallow, common crane, common wood pigeon, tufted duck, short-eared owl and greater white-fronted goose) [Table 3.98, Figure 3.132]. The most numerous bird group observed above 50 m ASL (up to 200 m) were geese of unidentified species.

Table 3.98. The flight altitude of birds observed at survey station MB_01 in the spring migration period

Taxon		Altitude [m]**							Total
English name	Latin name	1–10	11–20	21–30	31–40	41–50	51–100	101–200	
Long-tailed duck	*Clangula hyemalis*	2503	13	0	2	0	0	0	2518
Common scoter	*Melanitta nigra*	1335	192	6	2	12	19	0	1566
Unidentified goose	*Anserini indet.*	120	0	4	262	32	237	178	833
Unidentified duck	*Melanitta indet.*	442	53	14	5	0	4	0	518
Razorbill*	*Alca torda*	390	0	0	0	0	0	0	390
Unidentified auk	*Alca torda / Uria aalge*	274	0	2	0	0	0	0	276
Unidentified passerine	*Passeriformes indet.*	150	11	3	3	0	1	0	168
Eurasian curlew	*Numenius arquata*	143	0	0	0	0	0	9	152
Little gull	*Larus minutus*	48	31	21	9	24	0	0	133
Eurasian wigeon	*Anas penelope*	37	18	47	13	0	13	1	129
Lesser black-backed gull	*Larus fuscus*	44	39	16	5	11	3	0	118
Unidentified diver	*Gavia indet.*	54	15	3	2	8	2	1	85
Velvet scoter	*Melanitta fusca*	35	41	6	0	1	0	0	83
Common gull	*Larus canus*	43	22	6	5	4	1	0	81
Black-throated diver	*Gavia arctica*	43	11	6	0	5	1	0	66
Great black cormorant	*Phalacrocorax carbo*	43	20	1	0	0	1	0	65
Greylag goose	*Anser anser*	50	1	0	10	0	0	0	61
Greater white-fronted goose	*Anser albifrons*	0	0	34	0	0	19	0	53
Greater scaup*	*Aythya marila*	31	17	0	0	0	0	0	48
Eurasian teal	*Anas crecca*	33	4	0	4	0	2	0	43
Common guillemot*	*Uria aalge*	41	0	0	0	0	0	0	41
Eurasian siskin*	*Spinus spinus*	40	0	0	0	0	0	0	40
Northern pintail	*Anas acuta*	14	4	21	0	0	0	0	39
Common starling	*Sturnus vulgaris*	20	18	1	0	0	0	0	39
White wagtail*	*Motacilla alba*	30	1	0	0	0	0	0	31
Red-breasted merganser*	*Mergus serrator*	19	11	0	0	0	0	0	30
Mute swan	*Cygnus olor*	12	0	0	2	0	16	0	30
Black-headed gull	*Chroicocephalus ridibundus*	12	7	1	0	0	2	0	22
Unidentified duck	*Melanitta indet.*	18	1	1	0	0	0	0	20
Eurasian skylark*	*Alauda arvensis*	17	0	0	0	0	0	0	17
Unidentified swan*	*Cygnidae indet.*	15	2	0	0	0	0	0	17
Barn swallow	*Hirundo rustica*	11	3	0	0	0	1	0	15
Black guillemot*	*Cepphus grylle*	12	0	0	0	0	0	0	12
Common chaffinch*	*Fringilla coelebs*	11	0	0	0	0	0	0	11
Red-throated diver	*Gavia stellata*	8	0	1	1	0	0	0	10

Taxon		Altitude [m]**							Total
English name	Latin name	1–10	11–20	21–30	31–40	41–50	51–100	101–200	
Great egret	*Ardea alba*	0	8	1	0	0	0	0	9
Common crane	*Grus grus*	0	0	1	0	0	7	0	8
Mallard	*Anas platyrhynchos*	4	0	0	0	0	4	0	8
Great black-backed gull	*Larus marinus*	4	1	0	2	0	0	0	7
Northern shoveler*	*Anas clypeata*	2	5	0	0	0	0	0	7
Common/Arctic tern*	*Sterna hirundo/paradisaea*	3	4	0	0	0	0	0	7
Meadow pipit*	*Anthus pratensis*	6	0	0	0	0	0	0	6
Common wood pigeon	*Columba palumbus*	3	1	0	1	0	0	1	6
Hooded crow	*Corvus corone cornix*	2	0	2	0	1	0	0	5
Whooper swan	*Cygnus cygnus*	1	0	0	4	0	0	0	5
European robin*	*Erithacus rubecula*	5	0	0	0	0	0	0	5
Grey heron	*Ardea cinerea*	2	1	0	0	2	0	0	5
Tufted duck	*Aythya fuligula*	0	0	2	0	0	2	0	4
Red-breasted merganser/goosander*	*Mergus serrator/merganser*	4	0	0	0	0	0	0	4
Arctic skua	*Stercorarius parasiticus*	3	0	0	0	1	0	0	4
Arctic tern*	*Sterna paradisaea*	4	0	0	0	0	0	0	4
Eurasian sparrowhawk*	*Accipiter nisus*	0	3	0	0	0	0	0	3
Common tern*	*Sterna hirundo*	2	1	0	0	0	0	0	3
Great tit*	*Parus major*	3	0	0	0	0	0	0	3
Short-eared owl	*Asio flammeus*	1	1	0	0	0	1	0	3
Long-eared owl*	*Asio otus*	2	0	0	0	0	0	0	2
Unidentified wader*	*Limicolae indet.*	2	0	0	0	0	0	0	2
Black-legged kittiwake*	*Rissa tridactyla*	2	0	0	0	0	0	0	2
Eurasian wren*	*Troglodytes troglodytes*	2	0	0	0	0	0	0	2
Goldcrest*	*Regulus regulus*	2	0	0	0	0	0	0	2
Unidentified owl*	*Asio otus/flammeus*	2	0	0	0	0	0	0	2
Pomarine skua	*Stercorarius pomarinus*	1	0	1	0	0	0	0	2
Song thrush*	*Turdus philomelos*	0	1	0	0	0	0	0	1
Common merganser*	*Mergus merganser*	1	0	0	0	0	0	0	1
Common eider*	*Somateria mollissima*	1	0	0	0	0	0	0	1
Dunnock*	*Prunella modularis*	1	0	0	0	0	0	0	1
Unidentified tern*	*Sterna indet.*	1	0	0	0	0	0	0	1
Brambling*	*Fringilla montifringilla*	1	0	0	0	0	0	0	1
Stock dove*	*Columba oenas*	1	0	0	0	0	0	0	1
Barnacle goose	*Branta leucopsis*	0	0	1	0	0	0	0	1
Rook*	*Corvus frugilegus*	1	0	0	0	0	0	0	1

Taxon		Altitude [m]**							Total
English name	Latin name	1–10	11–20	21–30	31–40	41–50	51–100	101–200	
Osprey*	*Pandion haliaetus*	1	0	0	0	0	0	0	1
Common blackbird*	*Turdus merula*	0	1	0	0	0	0	0	1
Total		**6168**	**562**	**202**	**332**	**101**	**336**	**190**	**7891**

**species and group of species observed exclusively up to 20 m ASL*

***as the observations above 50 m ASL were scarce, observations in this altitude range are presented in cumulative form for the purposes of data presentation*

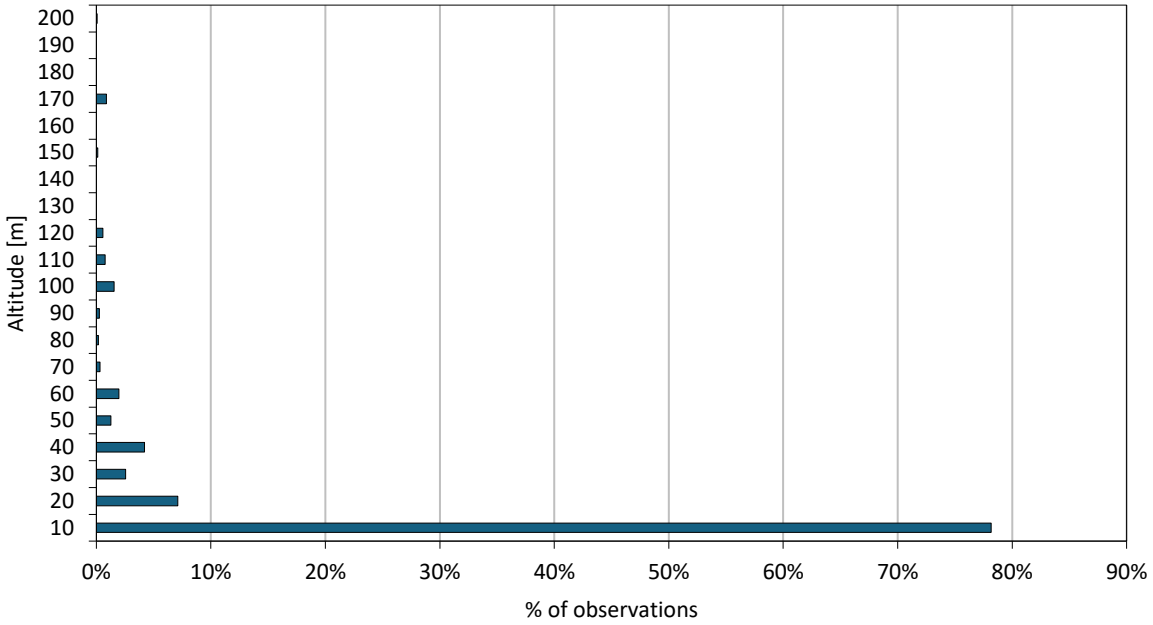


Figure 3.132. The proportion of all birds observed at individual altitudes at survey station MB_01 in the spring migration period

91% of all visually observed birds at MB_02 station flew at altitudes not exceeding 20 m ASL. Similarly to the results obtained at survey station MB_01, the most numerous species was the long-tailed duck, with a majority of observations at altitudes up to 10 m ASL (there were only 4 individuals of long-tailed duck observed flying above 20 m ASL). Nine species were observed at altitudes above 50 m ASL, i.e. the long-tailed duck (2 individuals), common scoter, lesser black-backed gull, greater white-fronted goose, common gull, black-throated diver, red-throated diver, great egret and common crane [Table 3.99, Figure 3.133]. From among those mentioned above, only two species (common crane and greater white-fronted goose) flew above 100 m ASL, along with a single flock of unidentified waders which were the most numerous birds observed at this altitude (150 m).

Table 3.99. The flight altitude of birds observed at survey station MB_02 in the spring migration period

Taxon		Altitude [m]**							Total
English name	Latin name	1–10	11–20	21–30	31–40	41–50	51–100	101–150	
Long-tailed duck	*Clangula hyemalis*	5682	90	2	0	0	2	0	5776
Common scoter	*Melanitta nigra*	1273	115	52	0	3	6	0	1449
Unidentified duck	*Melanitta indet.*	525	26	25	0	4	3	0	583
Razorbill*	*Alca torda*	435	0	0	0	0	0	0	435
Unidentified wader	*Limicolae indet.*	0	0	0	0	2	0	380	382
Unidentified auk*	*Alca torda / Uria aalge*	291	0	0	0	0	0	0	291
Eurasian curlew	*Numenius arquata*	90	0	0	0	50	0	0	140
Unidentified passerine*	*Passeriformes indet.*	122	16	0	0	0	0	0	138
Unidentified diver	*Gavia indet.*	71	40	7	6	1	0	0	125
European herring gull*	*Larus argentatus*	100	0	0	0	0	0	0	100
Lesser black-backed gull	*Larus fuscus*	46	28	14	1	2	8	0	99
Greater white-fronted goose	*Anser albifrons*	0	0	0	0	14	45	35	94
Velvet scoter	*Melanitta fusca*	85	6	1	0	0	0	0	92
Greater scaup	*Aythya marila*	32	17	37	0	5	0	0	91
Greylag goose	*Anser anser*	43	24	19	0	0	0	0	86
Common gull	*Larus canus*	45	19	5	0	2	2	0	73
Common starling	*Sturnus vulgaris*	12	5	0	0	50	0	0	67
Black-throated diver	*Gavia arctica*	37	14	9	0	0	3	0	63
Unidentified goose	*Anserini indet.*	0	0	8	0	10	40	0	58
Great black cormorant	*Phalacrocorax carbo*	13	27	1	17	0	0	0	58
Little gull	*Larus minutus*	33	15	6	0	1	0	0	55
Unidentified swan	*Cygnidae indet.*	7	0	0	0	0	45	0	52
Common guillemot*	*Uria aalge*	43	0	0	0	0	0	0	43
Common crane	*Grus grus*	0	0	17	4	1	0	4	26
Red-breasted merganser*	*Mergus serrator*	23	2	0	0	0	0	0	25
European golden plover	*Pluvialis apricaria*	0	0	0	23	0	0	0	23
White wagtail*	*Motacilla alba*	19	1	0	0	0	0	0	22
Black guillemot*	*Cepphus grylle*	20	0	0	0	0	0	0	20
Mallard	*Anas platyrhynchos*	14	0	5	0	0	0	0	19
Red-throated diver	*Gavia stellata*	6	8	3	0	0	1	0	18
Tufted duck*	*Aythya fuligula*	9	7	0	0	0	0	0	16
Common chaffinch*	*Fringilla coelebs*	16	0	0	0	0	0	0	16

Taxon		Altitude [m]**							Total
English name	Latin name	1–10	11–20	21–30	31–40	41–50	51–100	101–150	
Black-headed gull*	*Chroicocephalus ridibundus*	11	2	0	0	0	0	0	13
Barn swallow	*Hirundo rustica*	8	1	0	3	0	0	0	12
Unidentified duck	*Melanitta indet.*	9	2	1	0	0	0	0	12
Eurasian teal*	*Anas crecca*	11	0	0	0	0	0	0	11
Common/Arctic tern*	*Sterna hirundo/paradisaea*	9	0	0	0	0	0	0	9
Mute swan*	*Cygnus olor*	9	0	0	0	0	0	0	9
Great egret	*Ardea alba*	0	0	4	0	0	4	0	8
Whooper swan	*Cygnus cygnus*	0	0	8	0	0	0	0	8
Unidentified thrush*	*Turdidae indet.*	7	0	0	0	0	0	0	7
Fieldfare*	*Turdus pilaris*	7	0	0	0	0	0	0	7
Northern pintail	*Anas acuta*	0	0	0	0	7	0	0	7
Tundra swan*	*Cygnus columbianus*	6	0	0	0	0	0	0	6
Common wood pigeon	*Columba palumbus*	3	2	1	0	0	0	0	6
Common merganser*	*Mergus merganser*	6	0	0	0	0	0	0	6
Great black-backed gull*	*Larus marinus*	5	0	0	0	0	0	0	5
Rook*	*Corvus frugilegus*	5	0	0	0	0	0	0	5
Eurasian wren*	*Troglodytes troglodytes*	2	2	0	0	0	0	0	4
Arctic tern*	*Sterna paradisaea*	4	0	0	0	0	0	0	4
Great tit*	*Parus major*	4	0	0	0	0	0	0	4
Meadow pipit*	*Anthus pratensis*	3	0	0	0	0	0	0	3
Eurasian skylark*	*Alauda arvensis*	3	0	0	0	0	0	0	3
Eurasian siskin	*Spinus spinus*	1	0	2	0	0	0	0	3
Unidentified pipit	*Anthus indet.*	1	0	0	1	0	0	0	2
Song thrush*	*Turdus philomelos*	2	0	0	0	0	0	0	2
Goldcrest*	*Regulus regulus*	2	0	0	0	0	0	0	2
Long-eared owl*	*Asio otus*	1	1	0	0	0	0	0	2
Eurasian sparrowhawk*	*Accipiter nisus*	1	0	0	0	0	0	0	1
Stock dove*	*Columba oenas*	1	0	0	0	0	0	0	1
Short-eared owl	*Asio flammeus*	0	0	0	0	1	0	0	1
Arctic skua*	*Stercorarius parasiticus*	1	0	0	0	0	0	0	1
Red-necked grebe*	*Podiceps grisegena*	1	0	0	0	0	0	0	1
Pomarine skua*	*Stercorarius pomarinus*	1	0	0	0	0	0	0	1
Common goldeneye*	*Bucephala clangula*	1	0	0	0	0	0	0	1
Blue tit*	*Parus caeruleus*	1	0	0	0	0	0	0	1
Northern lapwing*	*Vanellus vanellus*	0	1	0	0	0	0	0	1

Taxon		Altitude [m]**							Total
English name	Latin name	1–10	11–20	21–30	31–40	41–50	51–100	101–150	
Common kestrel*	*Falco tinnunculus*	1	0	0	0	0	0	0	1
Horned grebe*	*Podiceps auritus*	1	0	0	0	0	0	0	1
European robin*	*Erithacus rubecula*	1	0	0	0	0	0	0	1
Black tern*	*Chlidonias niger*	1	0	0	0	0	0	0	1
Total		**9222**	**471**	**227**	**55**	**153**	**159**	**419**	**10708**

**species and group of species observed exclusively up to 20 m ASL*

***as the observations above 50 m ASL were scarce, observations in this altitude range are presented in cumulative form for the purposes of data presentation*

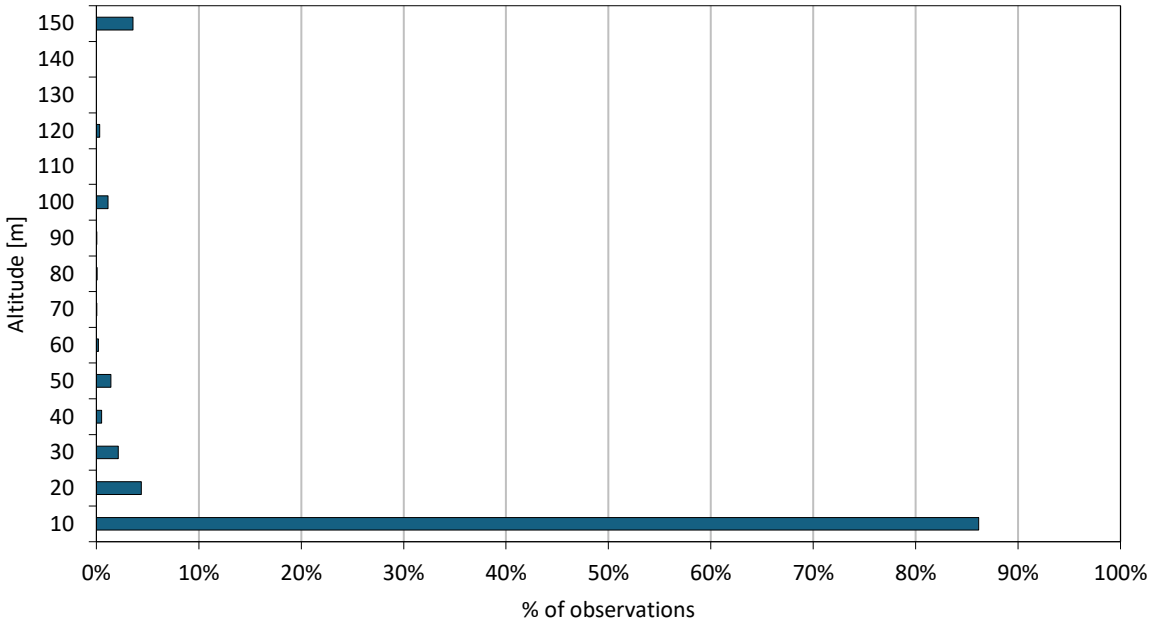


Figure 3.133. The proportion of all birds observed at individual altitudes at survey station MB_01 in the spring migration period

3.5.2.5.3.3 Autumn migration

88% of all visually observed birds at MB_01 station flew at altitudes not exceeding 20 m ASL. Twenty-three species or representatives of species groups were observed at an altitude of over 20 m ASL (e.g. great cormorant, unidentified ducks, unidentified geese, common swifts, little gull, lesser black-backed gull, Eurasian wigeon and common shelduck) [Table 3.100, Figure 3.134]. The most numerous bird category observed above 20 m ASL were unidentified ducks and unidentified geese. The only species observed above 100 m ASL was the osprey (one individual).

Table 3.100. The flight altitude of birds observed at survey station MB_01 in the autumn migration period

Taxon		Altitude [m]**								Total
English name	Latin name	1–10	11–20	21–30	31–40	41–50	51–80	81–100	101–200	
Arctic tern*	*Sterna paradisaea*	0	2	0	0	0	0	0	0	2
Barn swallow*	*Hirundo rustica*	7	0	0	0	0	0	0	0	7
Barnacle goose*	*Branta leucopsis*	1	0	0	0	0	0	0	0	1
Black guillemot*	*Cepphus grylle*	2	0	0	0	0	0	0	0	2
Black tern*	*Chlidonias niger*	8	0	0	0	0	0	0	0	8
Black-headed gull*	*Chroicocephalus ridibundus*	10	4	0	0	0	0	0	0	14
Black-legged kittiwake*	*Rissa tridactyla*	1	0	0	0	0	0	0	0	1
Black-throated diver	*Gavia arctica*	1	0	0	1	0	0	0	0	2
Common blackbird*	*Turdus merula*	1	0	0	0	0	0	0	0	1
Common chaffinch*	*Fringilla coelebs*	66	120	0	0	0	0	0	0	186
Common crane	*Grus grus*	0	0	0	10	0	0	0	0	10
Common guillemot*	*Uria aalge*	70	0	0	0	0	0	0	0	70
Common redpoll	*Acanthis flammea*	1	0	1	0	0	0	0	0	2
Common scoter*	*Melanitta nigra*	614	12	0	0	0	0	0	0	626
Common shelduck	*Tadorna tadorna*	0	0	0	0	2	0	0	0	2
Common swift	*Apus apus*	1	19	7	3	0	0	0	0	30
Common tern*	*Sterna hirundo*	16	5	0	0	0	0	0	0	21
Common/Arctic tern*	*Sterna hirundo/paradisaea*	16	13	0	0	0	0	0	0	29
Dunlin*	*Calidris alpina*	13	0	0	0	0	0	0	0	13
Eurasian blackcap*	*Sylvia atricapilla*	1	0	0	0	0	0	0	0	1
Eurasian skylark	*Alauda arvensis*	41	0	0	0	1	0	0	0	42
Eurasian sparrowhawk	*Accipiter nisus*	0	0	0	0	1	0	0	0	1
Eurasian teal	*Anas crecca*	38	0	0	0	18	0	0	0	56
Eurasian wigeon	*Anas penelope*	1	6	0	0	9	15	0	0	31
Eurasian wren*	*Troglodytes troglodytes*	1	0	0	0	0	0	0	0	1
European nightjar*	*Caprimulgus europaeus*	1	0	0	0	0	0	0	0	1
Great black-backed gull	*Larus marinus*	2	1	1	1	0	0	0	0	5
Great black cormorant	*Phalacrocorax carbo*	27	28	4	0	21	0	0	0	80
Greater scaup*	*Aythya marila*	2	0	0	0	0	0	0	0	2
Grey heron	*Ardea cinerea*	3	0	1	0	12	4	0	0	20
Grey plover*	*Pluvialis squatarola*	2	0	0	0	0	0	0	0	2
Lesser black-backed gull	*Larus fuscus*	27	8	6	2	0	1	0	0	44
Lesser whitethroat*	*Sylvia curucca*	1	0	0	0	0	0	0	0	1
Little gull	*Larus minutus*	40	4	1	0	2	0	0	0	47
Long-tailed duck	*Clangula hyemalis*	137	9	4	0	0	0	0	0	150
Mallard*	*Anas platyrhynchos*	29	3	0	0	0	0	0	0	32
Common gull	*Larus canus*	34	18	8	3	1	1	0	0	65

Taxon		Altitude [m]**								Total
English name	Latin name	1–10	11–20	21–30	31–40	41–50	51–80	81–100	101–200	
Unidentified auk*	*Alca torda / Uria aalge*	100	0	0	0	0	0	0	0	100
Mute swan	*Cygnus olor*	0	0	0	2	0	0	0	0	2
Northern shoveler*	*Anas clypeata*	0	9	0	0	0	0	0	0	9
Osprey	*Pandion haliaetus*	0	0	0	0	0	0	0	1	1
Arctic skua*	*Stercorarius parasiticus*	2	0	0	0	0	0	0	0	2
Arctic/Pomarine skua	*Stercorarius parasiticus/pomarinus*	0	0	1	0	0	0	0	0	1
Razorbill*	*Alca torda*	63	0	0	0	0	0	0	0	63
Red-throated diver	*Gavia stellata*	3	1	2	0	1	0	0	0	7
Ruff*	*Philomachus pugnax*	1	0	0	0	0	0	0	0	1
Sand martin*	*Riparia riparia*	0	1	0	0	0	0	0	0	1
Snow bunting*	*Plectrophenax nivalis*	1	0	0	0	0	0	0	0	1
Song thrush	*Turdus philomelos*	0	0	0	0	3	0	0	0	3
Unidentified sandpiper*	*Calidris indet.*	8	0	0	0	0	0	0	0	8
Unidentified diver*	*Gavia indet.*	3	8	0	0	0	0	0	0	11
Unidentified duck	*Melanitta indet.*	118	28	28	0	19	3	0	0	196
Unidentified goose	*Anserini indet.*	49	57	0	0	56	8	0	0	170
Unidentified passerine	*Passeriformes indet.*	84	54	0	0	0	6	0	0	144
Unidentified swan	*Cygnidae indet.*	14	0	0	0	2	0	0	0	16
Unidentified tern*	*Sterna indet.*	5	0	0	0	0	0	0	0	5
Unidentified wader	*Limicolae indet.*	17	0	0	0	0	0	2	0	19
Velvet scoter	*Melanitta fusca*	10	0	1	0	0	3	0	0	14
White wagtail*	*Motacilla alba*	27	1	0	0	0	0	0	0	28
Wood lark*	*Lullula arborea*	0	1	0	0	0	0	0	0	1
Western yellow wagtail	*Motacilla flava*	1	0	0	0	2	0	0	0	3
Total		**1721**	**412**	**65**	**22**	**150**	**41**	**2**	**1**	**2414**

**species and group of species observed exclusively up to 20 m ASL*

***as the observations above 50 m ASL were scarce, observations in this altitude range are presented in cumulative form for the purposes of data presentation*

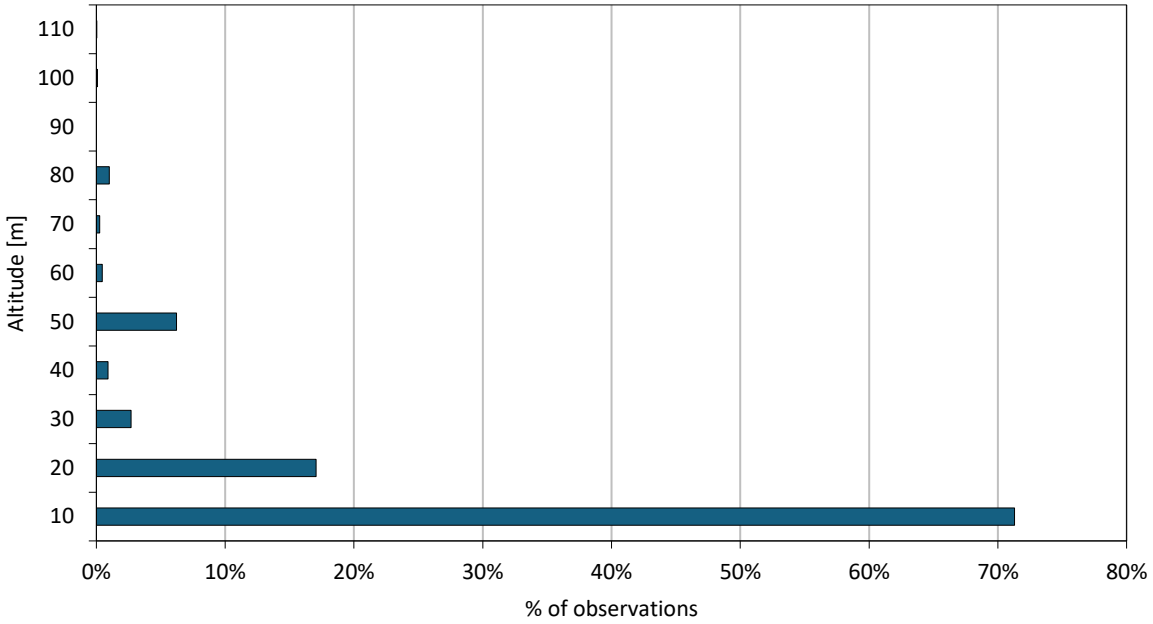


Figure 3.134. The proportion of all birds observed at individual altitudes at survey station MB_01 in the autumn migration period

89% of all visually observed birds at MB_02 station flew at altitudes not exceeding 20 m ASL. Eighteen species or representatives of species groups were observed at an altitude of over 20 m ASL (e.g. great cormorant, common swift, common/Arctic tern, little gull, lesser black-backed gull, velvet scoter, common gull, unidentified divers, unidentified terns, Eurasian wigeon) [Table 3.101, Figure 3.135]. It should be highlighted that the flight altitudes estimated based on visual observations are error-burdened, which is the consequence of this method's limitations, in particular, in the case of birds observed at high altitudes. For this reason, the data obtained using the above method should only be an auxiliary tool for drawing conclusions based on more precise data obtained from vertical radar.

Table 3.101. The flight altitude of birds observed at survey station MB_02 in the autumn migration period

Taxon		**Altitude [m]****										**Total**
English name	**Latin name**	**1–10**	**11–20**	**21–30**	**31–40**	**41–50**	**51–60**	**61–70**	**71–100**	**101–15**	**151–20**	
Arctic tern*	*Sterna paradisaea*	1	1	0	0	0	0	0	0	0	0	2
Barn swallow*	*Hirundo rustica*	4	0	0	0	0	0	0	0	0	0	4
Black guillemot*	*Cepphus grylle*	1	0	0	0	0	0	0	0	0	0	1
Black-headed gull*	*Chroicocephalus ridibundus*	2	0	0	0	0	0	0	0	0	0	2
Black-legged kittiwake*	*Rissa tridactyla*	1	0	0	0	0	0	0	0	0	0	1
Black-throated diver*	*Gavia arctica*	1	2	0	0	0	0	0	0	0	0	3
Unidentified duck*	*Melanitta indet.*	7	7	0	0	0	0	0	0	0	0	14
Blue tit*	*Parus caeruleus*	3	0	0	0	0	0	0	0	0	0	3
Common chaffinch*	*Fringilla coelebs*	2	0	0	0	0	0	0	0	0	0	2
Common linnet*	*Linaria cannabina*	4	0	0	0	0	0	0	0	0	0	4

Taxon		Altitude [m]**										Total
English name	Latin name	1–10	11–20	21–30	31–40	41–50	51–60	61–70	71–100	101–15	151–20	
Common merganser*	*Mergus merganser*	1	0	0	0	0	0	0	0	0	0	1
Common guillemot*	*Uria aalge*	77	0	0	0	0	0	0	0	0	0	77
Common redpoll*	*Acanthis flammea*	2	0	0	0	0	0	0	0	0	0	2
Common scoter	*Melanitta nigra*	116	20	27	0	0	0	0	0	0	0	163
Common shelduck*	*Tadorna tadorna*	4	0	0	0	0	0	0	0	0	0	4
Common snipe*	*Gallinago gallinago*	2	0	0	0	0	0	0	0	0	0	2
Common starling*	*Sturnus vulgaris*	83	0	0	0	0	0	0	0	0	0	83
Common swift	*Apus apus*	15	32	0	8	0	0	0	1	1	1	58
Common tern*	*Sterna hirundo*	3	0	0	0	0	0	0	0	0	0	3
Common/Arctic tern	*Sterna hirundo/paradisaea*	29	1	0	0	2	0	0	0	0	0	32
Dunlin*	*Calidris alpina*	4	0	0	0	0	0	0	0	0	0	4
Eurasian siskin*	*Spinus spinus*	75	0	0	0	0	0	0	0	0	0	75
Eurasian teal*	*Anas crecca*	22	1	0	0	0	0	0	0	0	0	23
Eurasian wigeon	*Anas penelope*	32	80	64	7	0	0	0	0	0	0	183
European golden plover*	*Pluvialis apricaria*	6	0	0	0	0	0	0	0	0	0	6
European robin*	*Erithacus rubecula*	2	0	0	0	0	0	0	0	0	0	2
Goldcrest*	*Regulus regulus*	3	0	0	0	0	0	0	0	0	0	3
Great black-backed gull*	*Larus marinus*	2	0	0	0	0	0	0	0	0	0	2
Great black cormorant	*Phalacrocorax carbo*	140	13	15	1	9	2	22	0	0	0	202
Great tit*	*Parus major*	2	0	0	0	0	0	0	0	0	0	2
Greater scaup*	*Aythya marila*	2	15	0	0	0	0	0	0	0	0	17
Grey heron	*Ardea cinerea*	1	0	4	0	0	0	0	0	0	0	5
Grey plover*	*Pluvialis squatarola*	0	1	0	0	0	0	0	0	0	0	1
Greylag goose	*Anser anser*	0	3	19	21	0	0	0	0	0	0	43
European herring gull*	*Larus argentatus*	25	0	0	0	0	0	0	0	0	0	25
Lesser black-backed gull	*Larus fuscus*	16	12	2	4	1	0	0	0	0	0	35
Little gull	*Larus minutus*	36	23	1	1	0	0	0	0	0	0	61
Long-tailed duck	*Clangula hyemalis*	1059	8	18	0	0	0	0	10	0	0	1095
Long-tailed/Arctic/ Pomarine skua*	*Stercorarius longicaudus/ parasiticus/pomarinus*	1	0	0	0	0	0	0	0	0	0	1
Mallard	*Anas platyrhynchos*	0	2	0	2	0	0	0	0	0	0	4
Common gull	*Larus canus*	10	4	7	2	0	0	0	0	0	0	23
Unidentified auk*	*Alca torda / Uria aalge*	125	0	0	0	0	0	0	0	0	0	125
Mute swan*	*Cygnus olor*	17	0	0	0	0	0	0	0	0	0	17
Arctic skua*	*Stercorarius parasiticus*	1	1	0	0	0	0	0	0	0	0	2
Razorbill*	*Alca torda*	76	0	0	0	0	0	0	0	0	0	76
Red-throated diver*	*Gavia stellata*	1	0	0	0	0	0	0	0	0	0	1

Taxon		Altitude [m]**										Total
English name	Latin name	1–10	11–20	21–30	31–40	41–50	51–60	61–70	71–100	101–15	151–20	
Ruff*	*Philomachus pugnax*	1	0	0	0	0	0	0	0	0	0	1
Sanderling*	*Calidris alba*	16	0	0	0	0	0	0	0	0	0	16
Sandwich tern*	*Sterna sandvicensis*	1	0	0	0	0	0	0	0	0	0	1
Short-eared owl*	*Asio flammeus*	1	0	0	0	0	0	0	0	0	0	1
Unidentified sandpiper*	*Calidris indet.*	3	0	0	0	0	0	0	0	0	0	3
Unidentified diver	*Gavia indet.*	12	11	1	0	5	2	0	0	0	0	31
Unidentified duck	*Melanitta indet.*	207	36	3	23	5	0	0	0	0	0	274
Unidentified goose	*Anserini indet.*	17	0	0	20	0	0	0	0	0	0	37
Unidentified passerine	*Passeriformes indet.*	113	3	25	0	0	0	0	0	0	0	141
Unidentified swan	*Cygnidae indet.*	7	0	0	0	2	0	0	0	0	0	9
Unidentified tern	*Sterna indet.*	6	0	1	0	0	0	0	0	0	0	7
Unidentified wader	*Limicolae indet.*	27	13	0	0	1	0	0	0	0	0	41
Velvet scoter	*Melanitta fusca*	24	7	10	0	0	0	0	0	0	0	41
White wagtail*	*Motacilla alba*	18	0	0	0	0	0	0	0	0	0	18
Western yellow wagtail*	*Motacilla flava*	2	0	0	0	0	0	0	0	0	0	2
Total		**2471**	**296**	**197**	**89**	**25**	**4**	**22**	**11**	**1**	**1**	**3117**

**species and group of species observed exclusively up to 20 m ASL*

***as the observations above 50 m ASL were scarce, observations in this altitude range are presented in cumulative form for the purposes of data presentation*

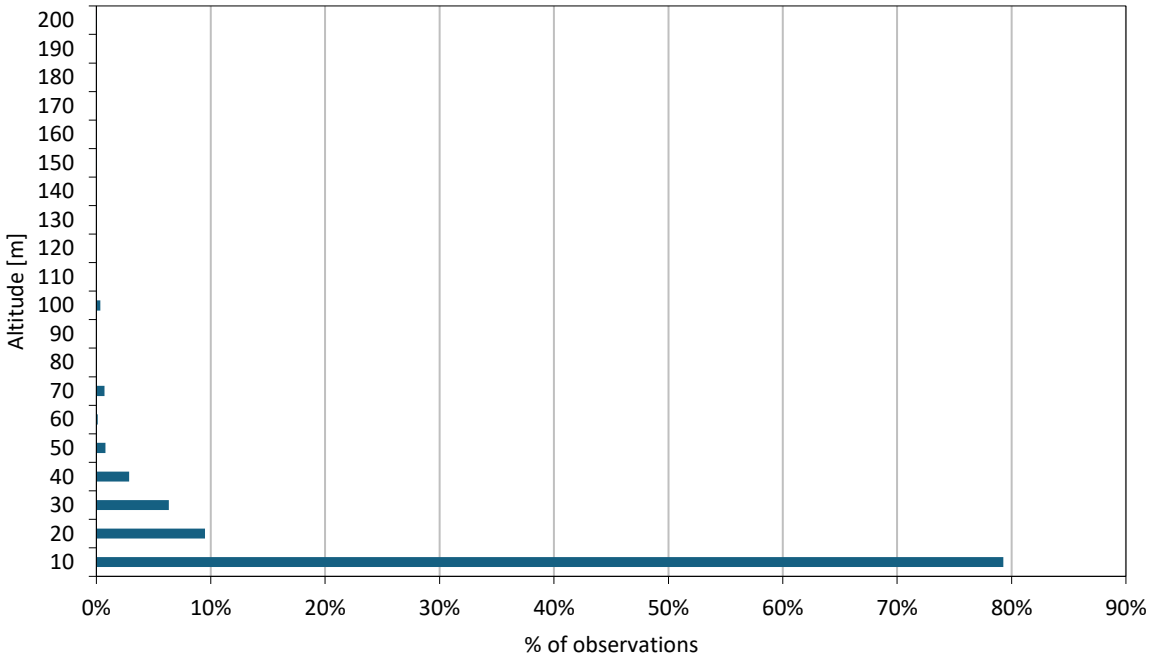


Figure 3.135. The percentage share distribution of all observations at different flight altitudes recorded at survey station MB_02 in the autumn migration period

3.5.2.5.4 Horizontal radar bird tracking

3.5.2.5.4.1 Local bird movements in the wintering period

In total, 1596 tracks were recorded at the two survey stations (LP_01: 660, LP_02: 936) [Table 3.102]. Among all tracked birds, 25 species were identified and 9 categories were used in the cases when a bird species could not be identified (for example, “unidentified duck”).

Table 3.102. The total number of birdtracks recorded at two survey stations during the wintering period (December 2022, January, and February 2023)

Survey station	December	January	February	Total
LP_01	337	69	254	660
LP_02	297	267	372	936
Total	**634**	**336**	**626**	**1596**

At the survey station LP_01, the highest number of tracks was recorded for auks (razorbills and common guillemots) and long-tailed ducks. Tracks of the auk species and of all divers were pooled together for data presentation purposes. The highest number of tracks was recorded in December 2022 [Table 3.103].

Table 3.103. The number of tracks of species and bird categories recorded at survey station LP_01 during the wintering period (December 2022, January and February 2023)

Taxon		December	January	February	Total
English name	**Latin name**				
Razorbill	*Alca torda*	53	14	168	235
Unidentified auk	*Alca torda / Uria aalge*	89	15	37	141
Long-tailed duck	*Clangula hyemalis*	46	27	21	94
Common guillemot	*Uria aalge*	37	4	2	43
Unidentified duck	*Melanitta indet.*	20	5	5	30
Unidentified diver	*Gavia indet.*	14	0	0	14
Velvet scoter	*Melanitta fusca*	9	0	4	13
Common gull	*Larus canus*	8	1	3	12
Great black-backed gull	*Larus marinus*	9	0	2	11
European herring gull	*Larus argentatus*	11	0	0	11
Little gull	*Larus minutus*	11	0	0	11
Goosander	*Mergus merganser*	3	1	2	6
Great black cormorant	*Phalacrocorax carbo*	5	0	1	6
Red-breasted merganser	*Mergus serrator*	3	0	3	6
Red-throated diver	*Gavia stellata*	4	2	0	6
Black-throated diver	*Gavia arctica*	2	0	2	4
Mute swan	*Cygnus olor*	2	0	2	4
Common scoter	*Melanitta nigra*	2	0	1	3
Whooper swan	*Cygnus cygnus*	1	0	1	2
Black-headed gull	*Larus ridibundus*	1	0	0	1
Unidentified duck	*Melanitta indet.*	1	0	0	1

Taxon		December	January	February	Total
English name	**Latin name**				
Greater scaup	*Aythya marila*	1	0	0	1
Grey heron	*Ardea cinerea*	1	0	0	1
Long-eared owl	*Asio otus*	1	0	0	1
Red-breasted merganser/goosander	*Mergus serrator/Mergus merganser*	1	0	0	1
Tundra swan	*Cygnus columbianus*	1	0	0	1
Unidentified swan	*Cygnidae indet.*	1	0	0	1
Total		**337**	**69**	**254**	**660**

At survey station LP_01, almost one fourth of all the tracks was registered for NE direction. The general pattern of bird movements observed at survey station LP_01 indicates the following directions: N, NE, and E [Figure 3.136].

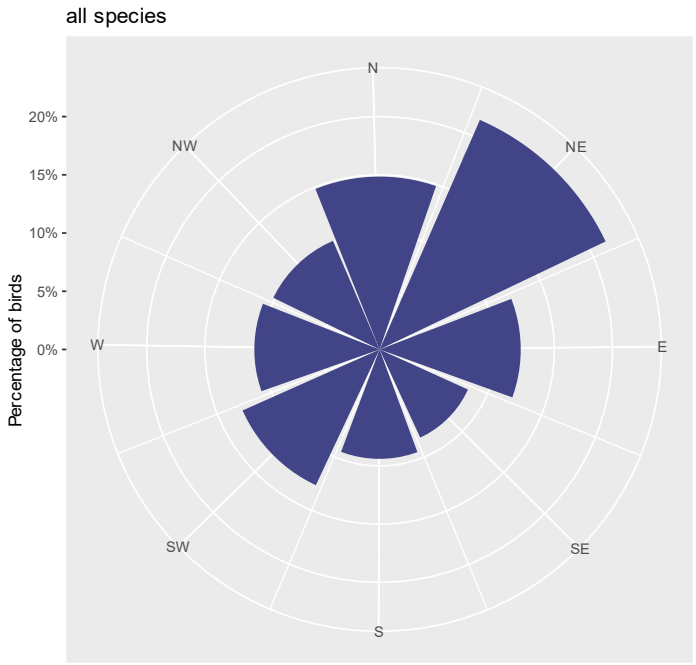


Figure 3.136. The flight directions of all tracked birds recorded at survey station LP_01 during the entire survey period (December 2022, January and February 2023)

The pattern of the directions of auk movement is consistent with the general pattern due to the fact that the flight registrations of this group of species were the most numerous. As in the case of all species analysed together, auks showed a tendency to move mainly in the NE and N and E directions [Figure 3.137].

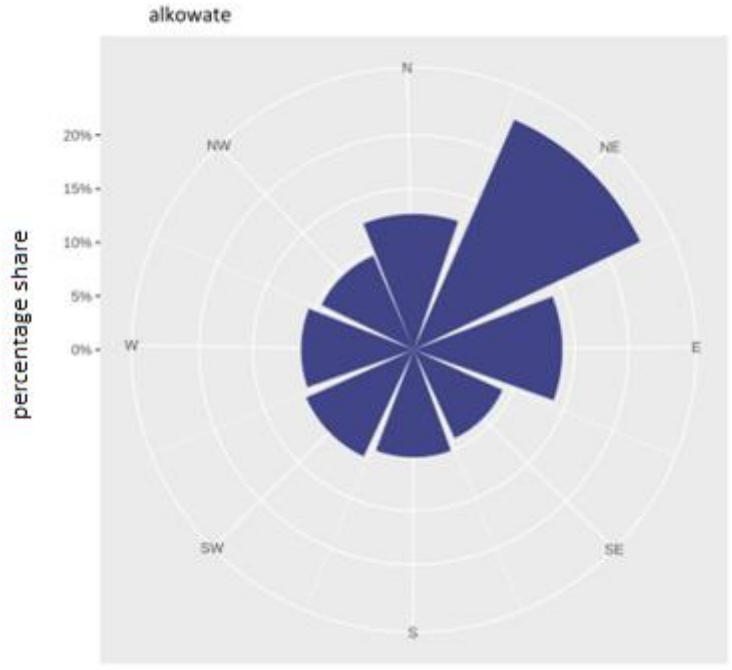


Figure 3.137. The flight directions of all tracked auks recorded at survey station LP_01 in the entire survey period (December 2022, January and February 2023)

In case of long-tailed duck tracks, over a half of the tracks indicate movements in N and NE direction [Figure 3.138].

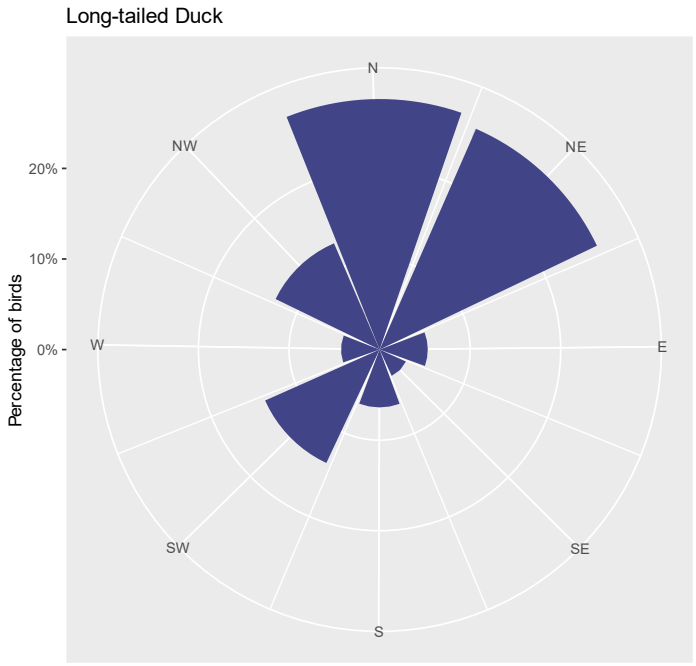


Figure 3.138. The flight directions of all tracked long-tailed ducks recorded at survey station LP_01 in the entire survey period (December 2022, January and February 2023)

One third of the divers flew in NW direction, with a smaller but equal proportion (17% of tracks each) heading N and W direction, showing a different movement pattern from the majority of the tracks recorded [Figure 3.139].

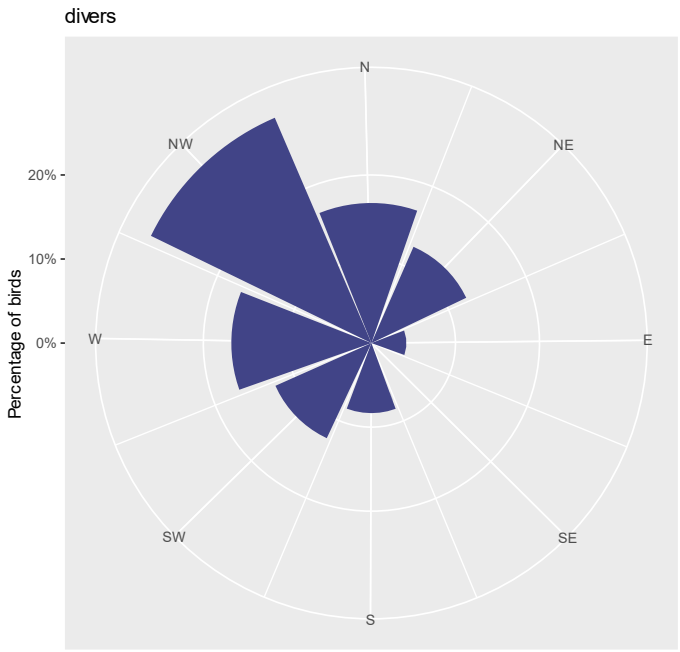


Figure 3.139. The flight directions of all tracked divers recorded at survey station LP_01 in the entire survey period (December 2022, January and February 2023)

Common scoter tracks showed three different directions. Given that tracks of common scoters were not very numerous (N = 3 tracks), it is difficult to draw any conclusion about their movement pattern within the area of the survey station [Figure 3.140].

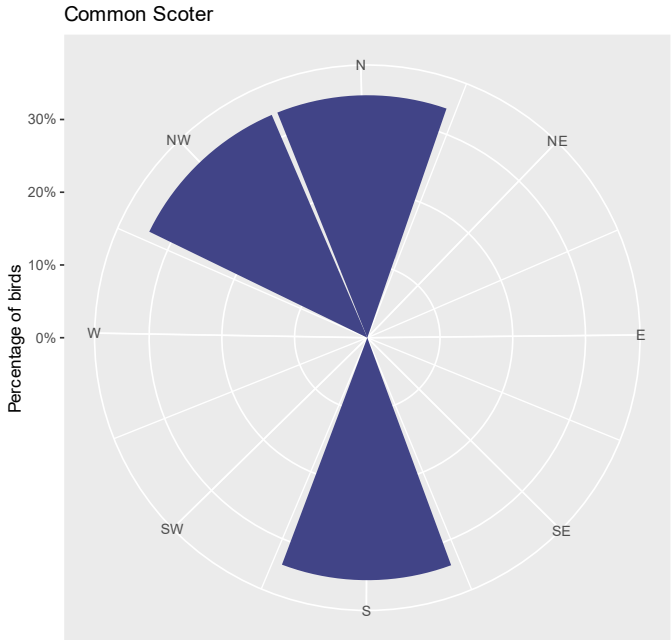


Figure 3.140. The flight directions of all tracked common scoters recorded at survey station LP_01 in the entire survey period (December 2022, January and February 2023)

No clear movement pattern was also a case for velvet scoters, however N-NE-E and W directions were dominating [Figure 3.141].

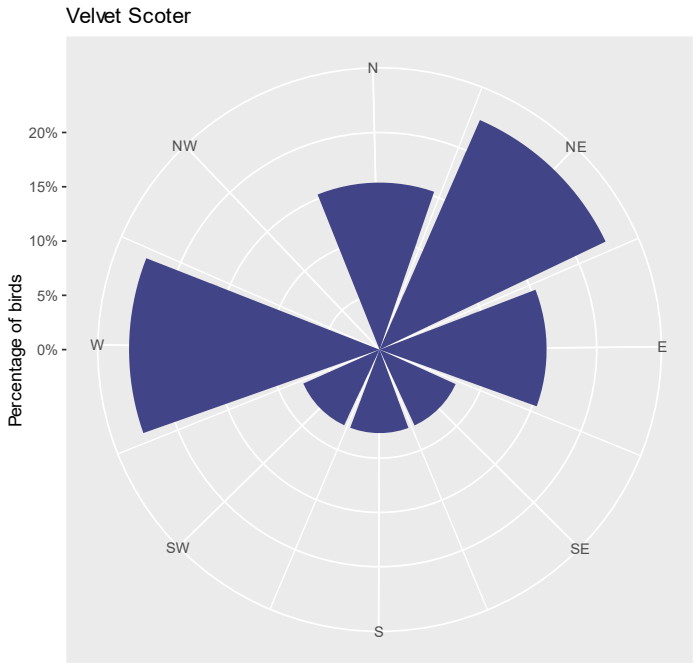


Figure 3.141. The flight directions of all tracked velvet scoters recorded at survey station LP_01 in the entire survey period (December 2022, January and February 2023)

At survey station LP_02, the highest number of tracks was recorded for long-tailed ducks and auks (razorbills and guillemots). In this Report, tracks of auks and divers were pooled together for data presentation purposes. The number of tracks recorded was the highest in February, while in December and January, the numbers of tracks recorded were similar [Table 3.104].

Table 3.104. The flight directions of individual bird taxa recorded at survey station LP_02 in the entire survey period (December 2022, January and February 2023)

Taxon		**December**	**January**	**February**	**Total**
English name	**Latin name**				
Long-tailed duck	*Clangula hyemalis*	94	106	112	312
Razorbill	*Alca torda*	46	21	184	251
Unidentified auk	*Alca torda / Uria aalge*	83	59	41	183
Unidentified duck	*Anatinae indet.*	10	33	6	49
Common guillemot	*Uria aalge*	34	9	3	46
Unidentified diver	*Gavia indet.*	5	11	0	16
Black guillemot	*Cepphus grylle*	2	2	7	11
Velvet scoter	*Melanitta fusca*	2	3	5	10
Red-breasted merganser	*Mergus serrator*	3	6	0	9
Common gull	*Larus canus*	0	6	2	8
Red-throated diver	*Gavia stellata*	5	2	0	7
Little gull	*Larus minutus*	3	2	0	5

Taxon		December	January	February	Total
English name	**Latin name**				
Mute swan	*Cygnus olor*	3	0	1	4
Great black-backed gull	*Larus marinus*	0	1	2	3
Great black cormorant	*Phalacrocorax carbo*	0	1	2	3
Common scoter	*Melanitta nigra*	2	1	0	3
Unidentified duck	*Melanitta indet.*	0	0	2	2
Unidentified gull	*Laridae indet.*	0	0	2	2
Black-headed gull	*Larus ridibundus*	0	1	1	2
Unidentified swan	*Cygnidae indet.*	1	0	1	2
Smew	*Mergellus albellus*	2	0	0	2
Unidentified thrush	*Turdidae indet.*	0	0	1	1
Black-throated diver	*Gavia arctica*	0	1	0	1
Red-breasted merganser/goosander	*Mergus serrator/Mergus merganser*	0	1	0	1
Unidentified gull	*Laridae indet.*	0	1	0	1
Common goldeneye	*Bucephala clangula*	1	0	0	1
Mallard	*Anas platyrhynchos*	1	0	0	1
Total		**297**	**267**	**372**	**936**

All tracks pooled together do not show a very clear pattern since the birds were tracked moving in all directions, but the main movement was registered along SW-W and N-NE axis [Figure 3.142].

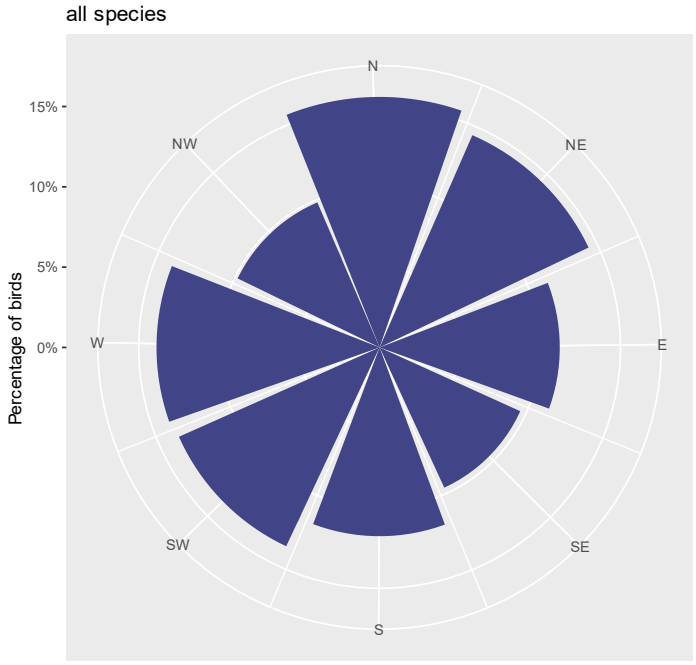


Figure 3.142. The flight directions of all tracked birds recorded at survey station LP_02 during the entire survey period (December 2022, January and February 2023)

Long-tailed ducks were observed flying mostly in W, N, and SW direction, however, the tracks were also recorded for all other directions, though with a smaller sample size [Figure 3.143].

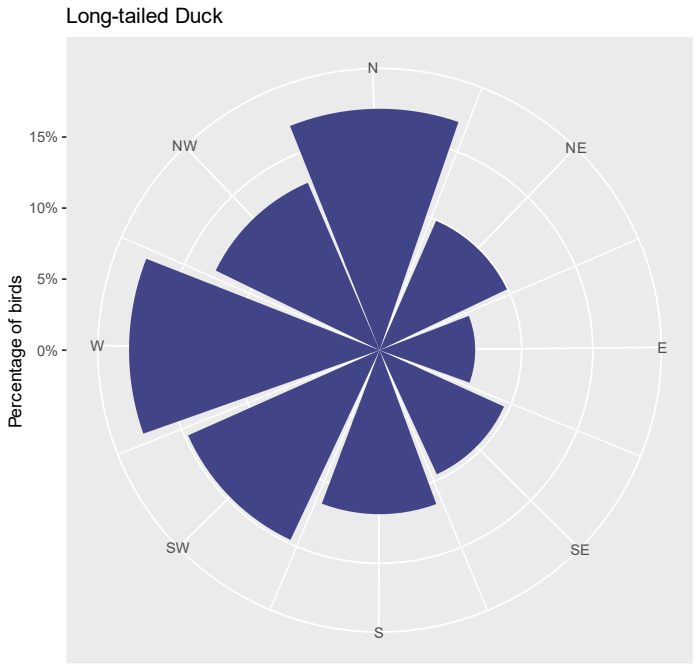


Figure 3.143. The flight directions of all tracked long-tailed ducks recorded at survey station LP_02 in the entire survey period (December 2022, January and February 2023)

Auks were flying mostly along the NE-SW direction, following the general pattern observed at survey station LP_02. Flights in the NE-SW axis dominated [Figure 3.144].

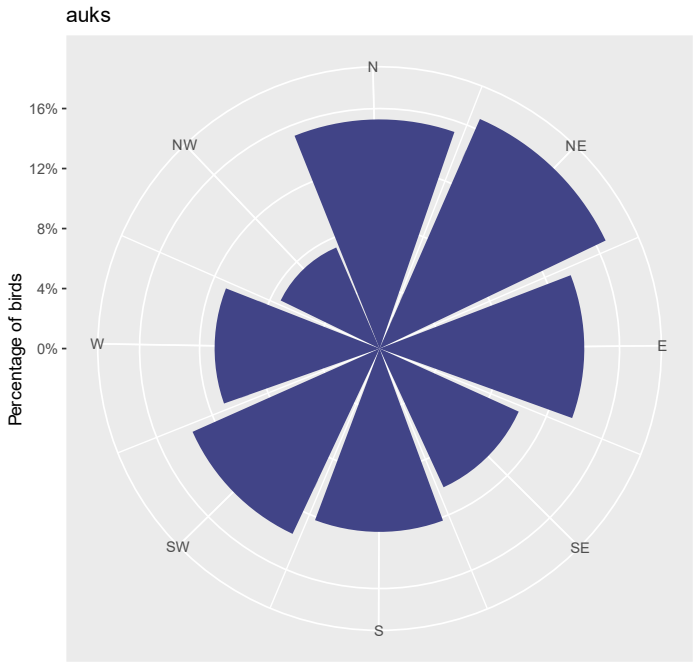


Figure 3.144. The flight directions of all tracked auks recorded at survey station LP_02 in the entire survey period (December 2022, January and February 2023)

The tracks of divers shown a pattern different from the auks. The majority of their tracks indicated the dominance of directions in the NW-N-NE-E axis [Figure 3.145].

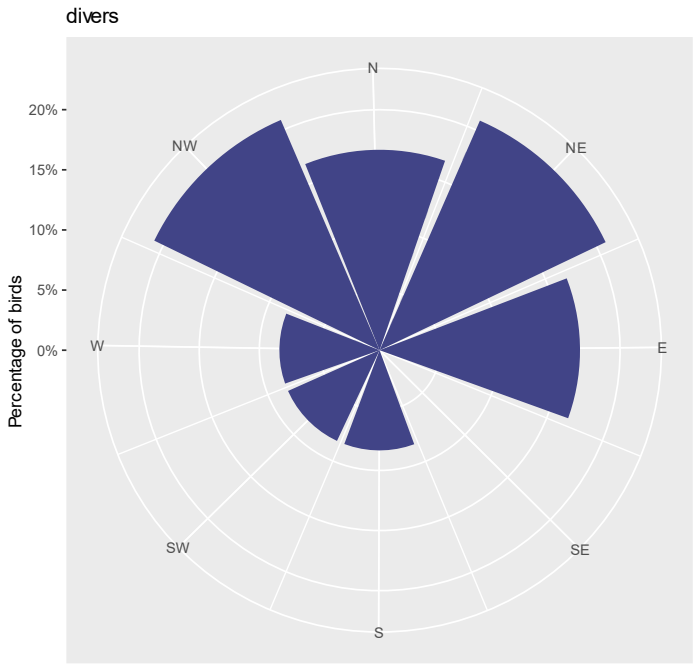


Figure 3.145. The flight directions of all tracked divers recorded at survey station LP_02 in the entire survey period (December 2022, January and February 2023)

Velvet scoters were following the overall pattern, similar to that of auks – along the NE-SW axis with a similar expression of NE, SW and E directions [Figure 3.146].

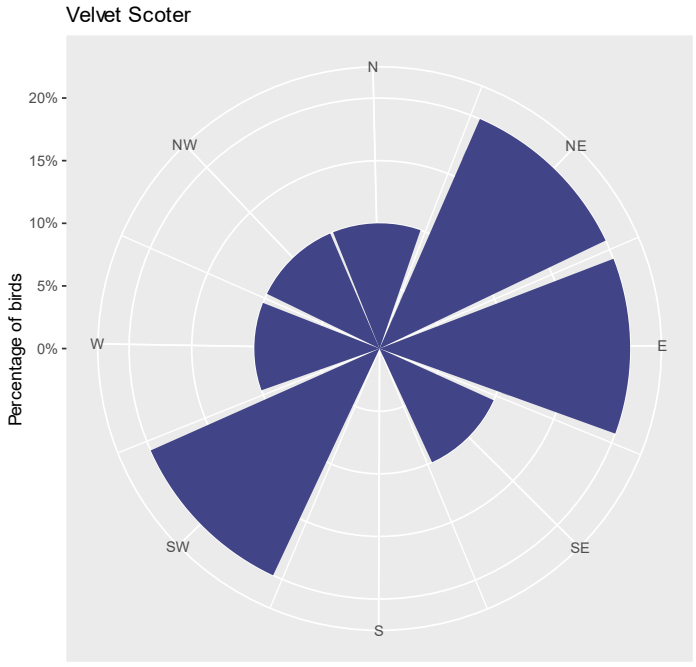


Figure 3.146. The flight directions of all tracked velvet scoters recorded at survey station LP_02 in the entire survey period (December 2022, January and February 2023)

3.5.2.5.4.2 Spring migration

In total, 9214 bird flight tracks were recorded at both survey stations (MB_01: 4567, MB_02: 4647) [Table 3.105]. Among all the tracked birds, 88 species were identified. 23 categories were used in cases when a bird species could not be identified to the level of species (for example, "unidentified duck", common/Arctic tern).

Table 3.105. The total number of all bird tracks recorded on the two survey stations during the spring migration period

Survey station	March	April	May	Total
MB_01	1094	2596	877	4567
MB_02	1118	2656	873	4647
Total	**2212**	**5252**	**1750**	**9214**

At survey station MB_01, the highest number of tracks was recorded for long-tailed ducks, common scoters, auks (razorbills and guillemots) and geese unidentified to the level of species. The highest number of tracks was recorded in April [Table 3.106].

Table 3.106. The number of tracks of individual bird taxa recorded at survey station MB_01 during the spring migration period

No.	Taxon		March	April	May	Total
	English name	Latin name				
1.	Long-tailed duck	*Clangula hyemalis*	348	666	47	1061
2.	Common scoter	*Melanitta nigra*	23	273	182	478
3.	Razorbill	*Alca torda*	179	251	13	443
4.	Unidentified duck	*Melanitta indet.*	66	274	74	414
5.	Guillemot/razorbill	*Uria aalge/Alca torda*	116	184	32	332
6.	Little gull	*Larus minutus*	70	157	2	229
7.	Unidentified diver	*Gavia indet.*	13	36	167	216
8.	Black-throated diver	*Gavia arctica*	1	24	155	180
9.	Unidentified passerine	*Passeriformes indet.*	11	131	10	152
10.	Lesser black-backed gull	*Larus fuscus*	0	93	32	125
11.	Common gull	*Larus canus*	24	59	3	86
12.	Velvet scoter	*Melanitta fusca*	11	59	4	74
13.	Common guillemot	*Uria aalge*	40	21	11	72
14.	Unidentified goose	*Anserini indet.*	35	14	3	52
15.	Great black cormorant	*Phalacrocorax carbo*	4	33	13	50
16.	Common starling	*Sturnus vulgaris*	17	31	0	48
17.	Black guillemot	*Cepphus grylle*	30	7	3	40
18.	Red-throated diver	*Gavia stellata*	5	22	12	39
19.	Red-breasted merganser	*Mergus serrator*	11	23	1	35
20.	Eurasian teal	*Anas crecca*	1	22	8	31

No.	Taxon		March	April	May	Total
	English name	Latin name				
21.	White wagtail	*Motacilla alba*	2	27	1	30
22.	Black-headed gull	*Chroicocephalus ridibundus*	9	14	3	26
23.	Eurasian wigeon	*Anas penelope*	0	24	0	24
24.	Greater scaup	*Aythya marila*	0	20	4	24
25.	Barn swallow	*Hirundo rustica*	0	2	21	23
26.	Common/Arctic tern	*Sterna hirundo/paradisaea*	0	0	21	21
27.	Eurasian curlew	*Numenius arquata*	0	16	1	17
28.	Eurasian skylark	*Alauda arvensis*	10	6	0	16
29.	Greylag goose	*Anser anser*	2	4	10	16
30.	Goosander	*Mergus merganser*	8	2	2	12
31.	Mallard	*Anas platyrhynchos*	2	9	0	11
32.	Great black-backed gull	*Larus marinus*	10	0	0	10
33.	Arctic skua	*Stercorarius parasiticus*	0	6	4	10
34.	Unidentified swan	*Cygnidae indet.*	8	1	1	10
35.	Mute swan	*Cygnus olor*	4	4	1	9
36.	Pintail	*Anas acuta*	0	8	1	9
37.	Common chaffinch	*Fringilla coelebs*	2	6	0	8
38.	Grey heron	*Ardea cinerea*	0	8	0	8
39.	Common crane	*Grus grus*	0	6	1	7
40.	Greater white-fronted goose	*Anser albifrons*	3	2	1	6
41.	Whooper swan	*Cygnus cygnus*	3	1	2	6
42.	Common tern	*Sterna hirundo*	0	1	4	5
43.	Common wood pigeon	*Columba palumbus*	3	2	0	5
44.	Meadow pipit	*Anthus pratensis*	2	3	0	5
45.	Short-eared owl	*Asio flammeus*	0	2	3	5
46.	Tufted duck	*Aythya fuligula*	0	4	1	5
47.	Eurasian siskin	*Spinus spinus*	3	1	0	4
48.	Eurasian sparrowhawk	*Accipiter nisus*	0	4	0	4
49.	Hooded crow	*Corvus corone cornix*	0	2	2	4
50.	Northern shoveler	*Anas clypeata*	0	4	0	4
51.	Common scoter/velvet scoter	*Melanitta nigra/fusca*	0	2	1	3
52.	Goldcrest	*Regulus regulus*	1	2	0	3
53.	Long-eared owl	*Asio otus*	0	3	0	3
54.	Red-breasted merganser/goosander	*Mergus serrator/merganser*	1	2	0	3
55.	Stock dove	*Columba oenas*	3	0	0	3

No.	Taxon		March	April	May	Total
	English name	Latin name				
56.	Rook	*Corvus frugilegus*	3	0	0	3
57.	Unidentified tern	*Sterna indet.*	0	0	3	3
58.	Barnacle goose	*Branta leucopsis*	1	0	1	2
59.	Black tern	*Chlidonias niger*	0	0	2	2
60.	Common blackbird	*Turdus merula*	0	2	0	2
61.	Eurasian wren	*Troglodytes troglodytes*	1	1	0	2
62.	Great egret	*Ardea alba*	0	2	0	2
63.	Great tit	*Parus major*	1	0	1	2
64.	Pomarine skua	*Stercorarius pomarinus*	0	0	2	2
65.	Unidentified c	*Falco indet.*	0	0	2	2
66.	Unidentified thrush	*Turdidae indet.*	1	1	0	2
67.	Unidentified wader	*Limicolae indet.*	0	0	2	2
68.	Yellowhammer	*Emberiza citrinella*	0	2	0	2
69.	Arctic tern	*Sterna paradisaea*	0	0	1	1
70.	Bean goose	*Anser fabalis*	1	0	0	1
71.	Brambling	*Fringilla montifringilla*	0	1	0	1
72.	Common eider	*Somateria mollissima*	0	1	0	1
73.	Common pigeon	*Columba livia*	0	0	1	1
74.	Common pochard	*Aythya ferina*	0	0	1	1
75.	Common reed bunting	*Emberiza schoeniclus*	1	0	0	1
76.	Common ringed plover	*Charadrius hiaticula*	0	1	0	1
77.	Dunnock	*Prunella modularis*	0	1	0	1
78.	Greenfinch	*Chloris chloris*	1	0	0	1
79.	European robin	*Erithacus rubecula*	1	0	0	1
80.	Gadwall	*Anas strepera*	0	0	1	1
81.	Northern lapwing	*Vanellus vanellus*	1	0	0	1
82.	Osprey	*Pandion haliaetus*	0	0	1	1
83.	Arctic/Pomarine skua	*Stercorarius parasiticus/pomarinus*	0	0	1	1
84.	Redwing	*Turdus iliacus*	0	1	0	1
85.	Sandwich tern	*Sterna sandvicensis*	0	1	0	1
86.	Song thrush	*Turdus philomelos*	0	1	0	1
87.	Unidentified owl	*Asio indet.*	0	1	0	1
88.	Unidentified curlew	*Numenius indet.*	0	1	0	1
89.	Unidentified pigeon	*Columba indet.*	1	0	0	1
90.	Unidentified pipit	*Anthus indet.*	0	1	0	1

No.	Taxon		March	April	May	Total
	English name	Latin name				
91.	Western marsh harrier	*Circus aeruginosus*	0	0	1	1
Total			**1094**	**2596**	**877**	**4567**

Based on the analysis of bird tracks recorded at survey station MB_01, it can be concluded that the general pattern of bird movement across the survey area in the spring migration period was towards the NE-E direction [Figure 3.147].

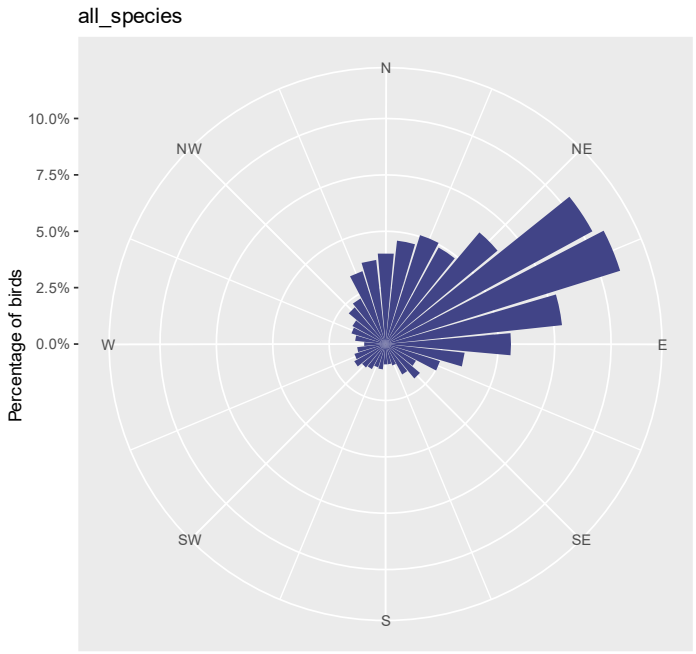


Figure 3.147. The flight directions of all tracked birds at survey station MB_01 during the spring migration period

The pattern of the long-tailed duck movement directions coincides with the general pattern since the registrations of flights of this species were the most numerous. As with all species analysed together, long-tailed ducks tended to show the same orientation mainly towards NE-E directions. Apart from the above pattern, long-tailed ducks indicate also a less intensive N-NE direction movement [Figure 3.148].

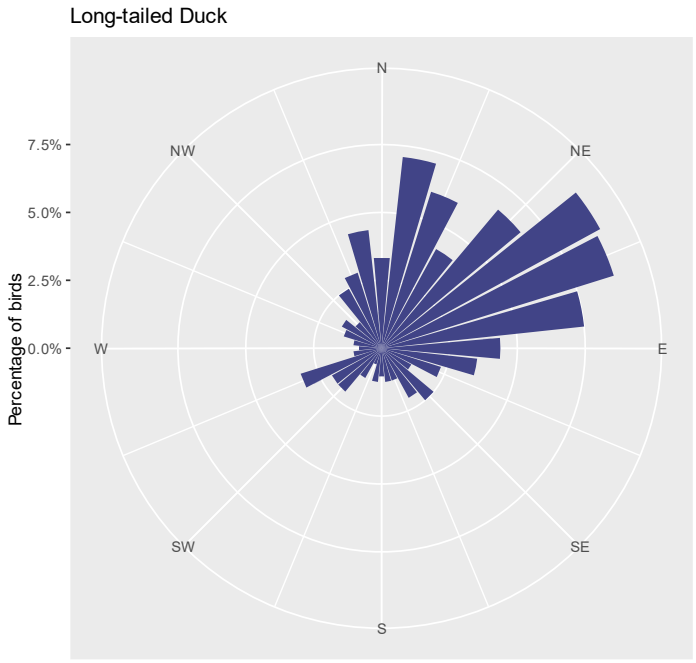


Figure 3.148. The flight directions of all tracked long-tailed ducks recorded at survey station MB_01 during the spring migration period

Common scoter and velvet scoter tracks indicates very similar pattern as for the general movement of all birds, showing orientation towards NE-E directions [Figure 3.149, Figure 3.150].

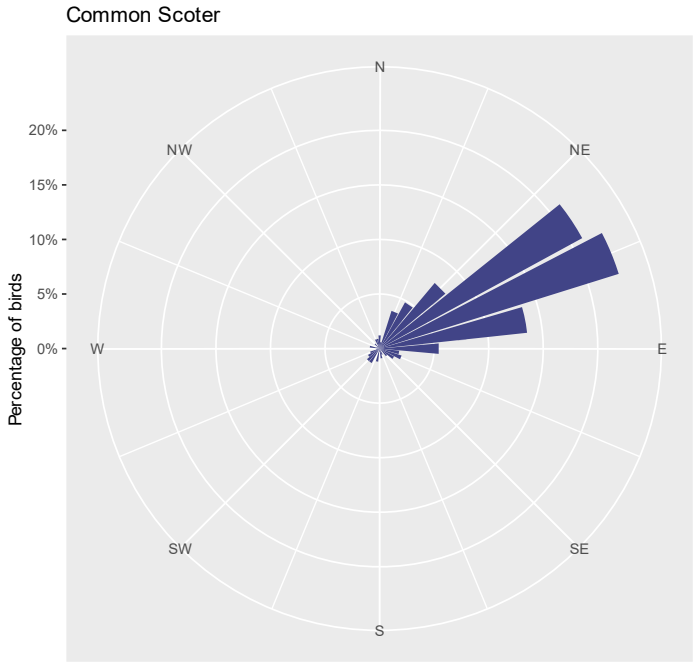


Figure 3.149. The flight directions of all tracked long-tailed ducks at survey station MB_01 during the spring migration period

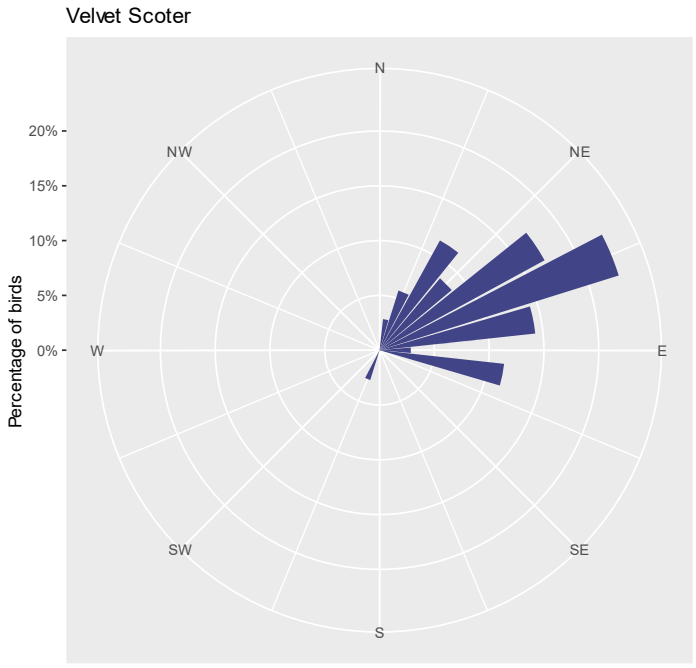


Figure 3.150. The flight directions of all tracked velvet scoters at survey station MB_01 during the spring migration period

Tracks recorded for all auks show a slightly different pattern with dominating movement directions of NW-N [Figure 3.151].

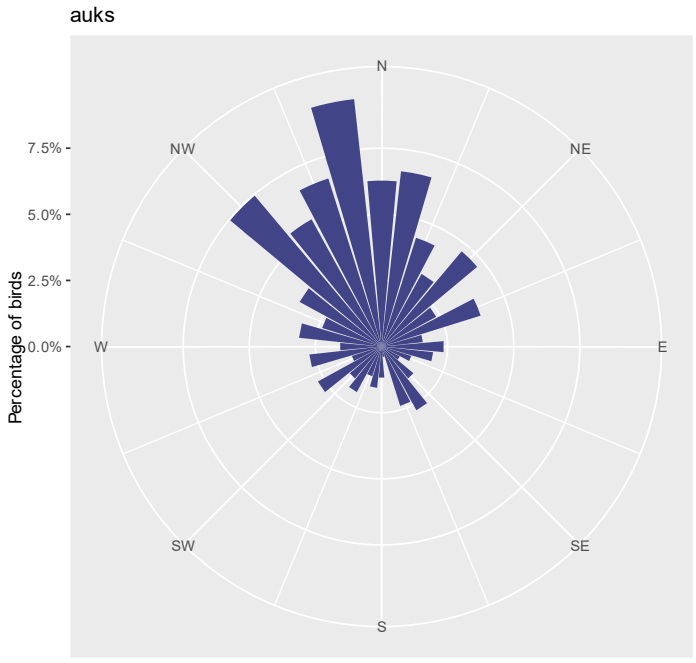


Figure 3.151. The flight directions of all tracked auks recorded at survey station MB_01 during the spring migration period

The tracks of all geese recorded indicate a clear split of movements into two main directions: NW-W and NE-E [Figure 3.152].

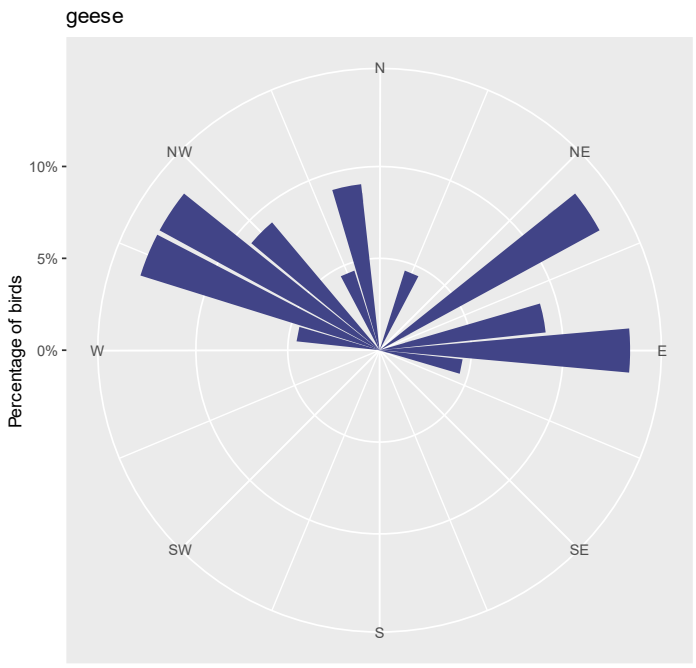


Figure 3.152. The flight directions of all tracked geese recorded at survey station MB_01 during the spring migration period

At survey station MB_02, the highest number of tracks was recorded for long-tailed ducks, common scoters, and razorbills. Numerous tracks were also recorded for ducks and divers unidentified to the level of species. The highest monthly number of tracks in the entire survey period was recorded in April [Table 3.107].

Table 3.107. The number of tracks of individual bird taxa recorded at survey station MB_02 during the spring migration period

No.	Taxon		March	April	May	Total
	English name	Latin name				
1.	Long-tailed duck	*Clangula hyemalis*	629	933	108	1670
2.	Common scoter	*Melanitta nigra*	11	464	63	538
3.	Razorbill	*Alca torda*	121	197	10	328
4.	Unidentified diver	*Gavia indet.*	10	37	266	313
5.	Unidentified duck	*Melanitta indet.*	36	208	54	298
6.	Guillemot/razorbill	*Uria aalge/Alca torda*	70	166	60	296
7.	Lesser black-backed gull	*Larus fuscus*	0	101	31	132
8.	Black-throated diver	*Gavia arctica*	2	29	86	117
9.	Unidentified passerine	*Passeriformes indet.*	11	73	9	93
10.	Common gull	*Larus canus*	36	44	2	82
11.	Common guillemot	*Uria aalge*	28	37	14	79
12.	Little gull	*Larus minutus*	14	45	18	77
13.	Velvet scoter	*Melanitta fusca*	3	50	3	56

No.	Taxon		March	April	May	Total
	English name	Latin name				
14.	Greater scaup	*Aythya marila*	0	52	1	53
15.	Great black cormorant	*Phalacrocorax carbo*	7	20	11	38
16.	Barn swallow	*Hirundo rustica*	0	0	32	32
17.	Red-throated diver	*Gavia stellata*	9	10	11	30
18.	Greylag goose	*Anser anser*	2	0	27	29
19.	Black guillemot	*Cepphus grylle*	16	5	4	25
20.	European herring gull	*Larus argentatus*	24	0	0	24
21.	Unidentified goose	*Anserini indet.*	7	6	10	23
22.	Common starling	*Sturnus vulgaris*	7	15	0	22
23.	Black-headed gull	*Chroicocephalus ridibundus*	7	7	7	21
24.	Common scoter/velvet scoter	*Melanitta nigra/fusca*	4	13	2	19
25.	Mallard	*Anas platyrhynchos*	1	16	2	19
26.	White wagtail	*Motacilla alba*	0	17	1	18
27.	Eurasian curlew	*Numenius arquata*	0	16	0	16
28.	Red-breasted merganser	*Mergus serrator*	7	6	3	16
29.	Common crane	*Grus grus*	1	7	6	14
30.	Eurasian teal	*Anas crecca*	1	10	0	11
31.	Great black-backed gull	*Larus marinus*	10	0	0	10
32.	Common wood pigeon	*Columba palumbus*	5	3	1	9
33.	Common chaffinch	*Fringilla coelebs*	2	6	0	8
34.	Common/Arctic tern	*Sterna hirundo/paradisaea*	0	0	8	8
35.	Unidentified tern	*Sterna indet.*	0	0	7	7
36.	Eurasian wigeon	*Anas penelope*	2	4	0	6
37.	Eurasian siskin	*Spinus spinus*	2	3	0	5
38.	Greater white-fronted goose	*Anser albifrons*	4	1	0	5
39.	Mute swan	*Cygnus olor*	3	2	0	5
40.	Pintail	*Anas acuta*	1	4	0	5
41.	Northern shoveler	*Anas clypeata*	0	5	0	5
42.	Goosander	*Mergus merganser*	2	1	1	4
43.	Northern lapwing	*Vanellus vanellus*	2	2	0	4
44.	Unidentified swan	*Cygnidae indet.*	4	0	0	4
45.	Eurasian skylark	*Alauda arvensis*	2	1	0	3
46.	Eurasian sparrowhawk	*Accipiter nisus*	0	2	1	3
47.	Horned grebe	*Podiceps auritus*	0	3	0	3
48.	Meadow pipit	*Anthus pratensis*	0	3	0	3

No.	Taxon		March	April	May	Total
	English name	Latin name				
49.	Short-eared owl	*Asio flammeus*	1	2	0	3
50.	Unidentified wader	*Limicolae indet.*	0	0	3	3
51.	Common goldeneye	*Bucephala clangula*	1	1	0	2
52.	European robin	*Erithacus rubecula*	1	1	0	2
53.	Goldcrest	*Regulus regulus*	0	2	0	2
54.	Great egret	*Ardea alba*	0	2	0	2
55.	Grey heron	*Ardea cinerea*	0	2	0	2
56.	Long-eared owl	*Asio otus*	1	1	0	2
57.	Red-necked grebe	*Podiceps grisegena*	0	2	0	2
58.	Rook	*Corvus frugilegus*	0	2	0	2
59.	Stock dove	*Columba oenas*	2	0	0	2
60.	Tufted duck	*Aythya fuligula*	0	2	0	2
61.	Tundra swan	*Cygnus columbianus*	2	0	0	2
62.	Unidentified pigeon	*Columba indet.*	0	2	0	2
63.	Unidentified pipit	*Anthus indet.*	0	2	0	2
64.	Unidentified thrush	*Turdidae indet.*	1	1	0	2
65.	Arctic tern	*Sterna paradisaea*	0	0	1	1
66.	Barnacle goose	*Branta leucopsis*	1	0	0	1
67.	Black tern	*Chlidonias niger*	0	0	1	1
68.	Caspian tern	*Hydroprogne caspia*	0	0	1	1
69.	Common blackbird	*Turdus merula*	1	0	0	1
70.	Common chiffchaff	*Phylloscopus collybita*	0	0	1	1
71.	Common kestrel	*Falco tinnunculus*	0	1	0	1
72.	Common swift	*Apus apus*	0	0	1	1
73.	Common tern	*Sterna hirundo*	0	0	1	1
74.	Eurasian wren	*Troglodytes troglodytes*	1	0	0	1
75.	European golden plover	*Pluvialis apricaria*	0	1	0	1
76.	European nightjar	*Caprimulgus europaeus*	0	0	1	1
77.	Fieldfare	*Turdus pilaris*	0	1	0	1
78.	Gadwall	*Anas strepera*	0	1	0	1
79.	Great crested grebe	*Podiceps cristatus*	0	1	0	1
80.	Long-tailed/Arctic/Pomarine skua	*Stercorarius longicaudus/parasiticus/ pomarinus*	0	1	0	1
81.	Arctic skua	*Stercorarius parasiticus*	0	0	1	1
82.	Pomarine skua	*Stercorarius pomarinus*	0	0	1	1

No.	Taxon		March	April	May	Total
	English name	Latin name				
83.	Red-breasted merganser/goosander	*Mergus serrator/merganser*	1	0	0	1
84.	Sandwich tern	*Sterna sandvicensis*	0	1	0	1
85.	Unidentified owl	*Asio indet.*	0	1	0	1
86.	Unidentified gull	*Laridae indet.*	1	0	0	1
87.	Unidentified skua	*Stercorarius indet.*	0	0	1	1
88.	Unidentified small gull	*Laridae indet.*	0	1	0	1
89.	Eurasian whimbler	*Numenius phaeopus*	0	1	0	1
90.	Whooper swan	*Cygnus cygnus*	1	0	0	1
91.	Western yellow wagtail	*Motacilla flava*	0	0	1	1
Total			**1118**	**2656**	**873**	**4647**

All tracks recorded at survey station MB_02 indicate a movement pattern towards NE and NE-E direction with a smaller but equal proportion of tracks in NW-N and SW-S [Figure 3.153].

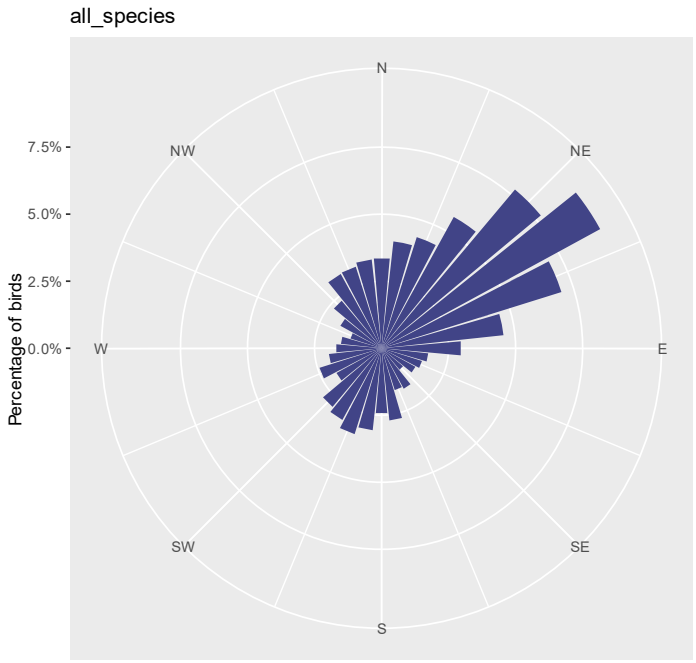


Figure 3.153. The flight directions of all tracked birds at survey station MB_02 during the spring migration period

In case of long-tailed ducks, about one fourth of recorded tracks indicated movements in SW-S directions, however, birds were observed flying also towards NE, which is in line with the general pattern observed at this station [Figure 3.154].

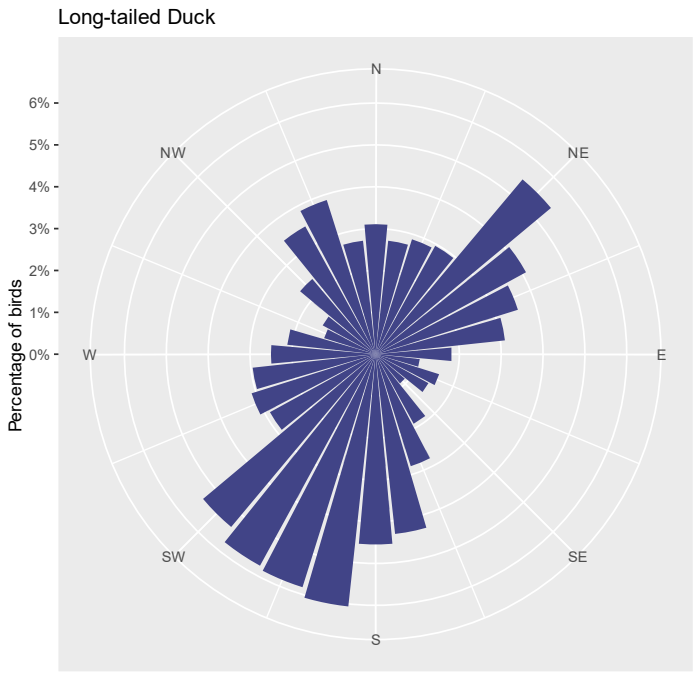


Figure 3.154. The flight directions of all tracked long-tailed ducks at survey station MB_02 during the spring migration period

Common and velvet scoters were flying almost exclusively following the general pattern observed at the survey station, i.e. NE-E [Figure 3.155, Figure 3.156].

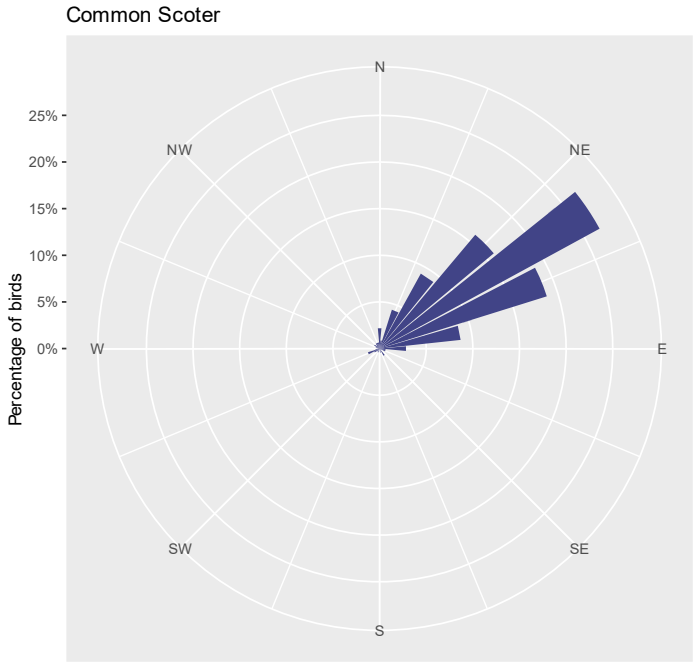


Figure 3.155. The flight directions of all tracked common scoters at survey station MB_02 during spring migration

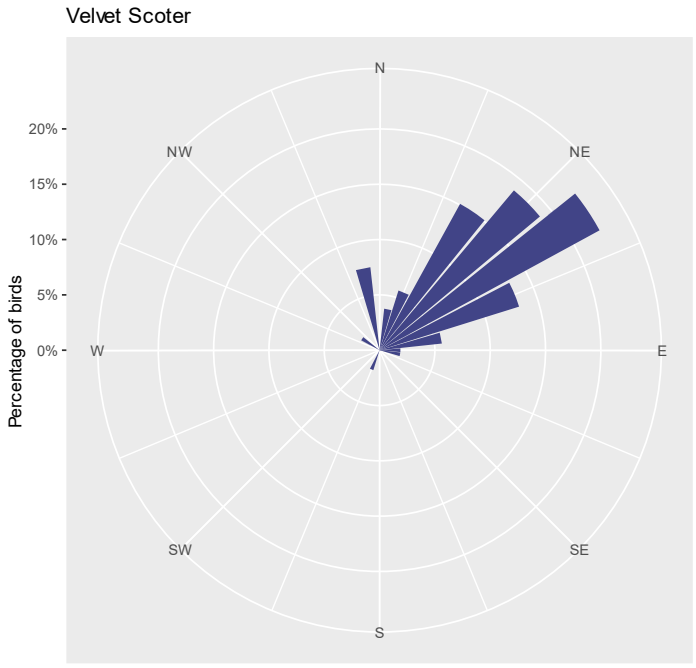


Figure 3.156. The flight directions of all tracked velvet scoters at survey station MB_02 during the spring migration period

Razorbills were observed flying mostly in N direction; however, the tracks were also recorded for all other directions though with a smaller sample size [Figure 3.157].

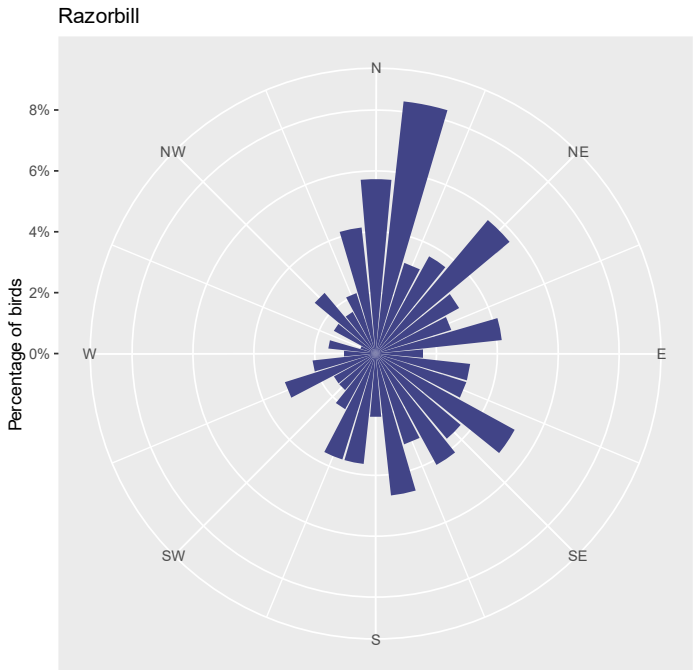


Figure 3.157. The flight directions of all tracked razorbills at survey station MB_02 during the spring migration period

3.5.2.5.4.3 Autumn migration

In total, 2968 bird flight tracks were recorded at both survey stations (MB_01: 1172, MB_02: 1796) [Table 3.108]. Among all the tracked birds, 81 species were identified. 15 categories were used in cases when a bird species could not be identified to the level of species (for example, "unidentified duck", common/Arctic tern).

Table 3.108. The total number of all bird tracks recorded at both survey stations during the autumn migration period

Survey station	July	August	September	October	November	December	Total
MB_01	63	252	457	188	85	127	1172
MB_02	32	282	389	568	508	17	1796
Total	**95**	**534**	**846**	**756**	**593**	**144**	**2968**

At survey station MB_01, the highest number of birdtracks was recorded for long-tailed ducks, common scoters, auks (razorbills and guillemots) and unidentified ducks. The highest number of tracks was recorded in October [Table 3.109]. At survey station MB_01, a total of 81 categories of birds was identified. Among those, there were distinguished 65 species, 12 categories of birds identified to an order or family, and 4 categories in which final identification was impossible and the category points at two most probable species.

Table 3.109. The number of tracks of species and bird categories recorded at survey station MB_01 during the autumn migration period

No.	Taxon		July	August	September	October	November	December	Total
	English name	Latin name							
1.	Unidentified duck	*Melanitta indet.*	1	23	54	27	8	8	121
2.	Long-tailed duck	*Clangula hyemalis*	0	0	0	37	17	34	88
3.	Common scoter	*Melanitta nigra*	14	34	30	6	0	1	85
4.	Unidentified auk	*Alca torda / Uria aalge*	4	0	6	36	15	17	78
5.	Lesser black-backed gull	*Larus fuscus*	4	10	60	0	0	0	74
6.	Little gull	*Larus minutus*	4	31	19	5	5	4	68
7.	Common guillemot	*Uria aalge*	0	0	3	16	20	22	61
8.	Great black cormorant	*Phalacrocorax carbo*	1	30	18	1	1	1	52
9.	Unidentified passerine	*Passeriformes indet.*	0	8	38	1	0	1	48
10.	Common/Arctic tern	*Sterna hirundo/paradisaea*	7	28	2	0	0	0	37
11.	Razorbill	*Alca torda*	0	0	4	13	6	13	36
12.	Velvet scoter	*Melanitta fusca*	0	3	21	8	0	2	34
13.	Common gull	*Larus canus*	3	5	7	4	6	7	32
14.	White wagtail	*Motacilla alba*	0	0	29	0	0	0	29
15.	Common swift	*Apus apus*	0	28	0	0	0	0	28
16.	Unidentified diver	*Gavia indet.*	0	0	16	7	2	1	26
17.	Eurasian teal	*Anas crecca*	2	5	18	0	0	0	25

No.	Taxon		July	August	September	October	November	December	Total
	English name	Latin name							
18.	Eurasian wigeon	*Anas penelope*	0	0	19	1	0	0	20
19.	Unidentified wader	*Limicolae indet.*	1	5	14	0	0	0	20
20.	Black-headed gull	*Chroicocephalus ridibundus*	3	6	5	1	0	0	15
21.	Unidentified goose	*Anserini indet.*	0	0	3	12	0	0	15
22.	Grey heron	*Ardea cinerea*	2	2	7	0	0	0	11
23.	Common tern	*Sterna hirundo*	3	6	1	0	0	0	10
24.	Red-throated diver	*Gavia stellata*	0	1	2	2	1	3	9
25.	Black tern	*Chlidonias niger*	4	4	0	0	0	0	8
26.	European herring gull	*Larus argentatus*	0	8	0	0	0	0	8
27.	Mallard	*Anas platyrhynchos*	1	0	3	2	0	2	8
28.	Great tit	*Parus major*	0	0	7	0	0	0	7
29.	Barn swallow	*Hirundo rustica*	0	1	5	0	0	0	6
30.	Northern shoveler	*Anas clypeata*	0	1	5	0	0	0	6
31.	Great black-backed gull	*Larus marinus*	1	2	0	0	1	1	5
32.	Greater scaup	*Aythya marila*	0	0	4	1	0	0	5
33.	European sand martin	*Pluvialis squatarola*	0	3	2	0	0	0	5
34.	Eurasian blue tit	*Parus caeruleus*	0	0	4	0	0	0	4
35.	Eurasian siskin	*Spinus spinus*	0	0	3	1	0	0	4
36.	Eurasian skylark	*Alauda arvensis*	0		4	0	0	0	4
37.	Mute swan	*Cygnus olor*	0	0	1	0	2	1	4
38.	Pintail	*Anas acuta*	0	0	4	0	0	0	4
39.	Osprey	*Pandion haliaetus*	0	1	3	0	0	0	4
40.	Red-breasted merganser	*Mergus serrator*	0	0	0	0	1	3	4
41.	Arctic tern	*Sterna paradisaea*	1	2	0	0	0	0	3
42.	Black guillemot	*Cepphus grylle*	0	0	0	0	0	3	3
43.	Black-throated diver	*Gavia arctica*	0	0	1	1	0	1	3
44.	Tufted duck	*Aythya fuligula*	0	0	3	0	0	0	3
45.	Unidentified tern	*Sterna indet.*	3	0	0	0	0	0	3
46.	Barnacle goose	*Branta leucopsis*	0	0	0	2	0	0	2
47.	Common blackbird	*Turdus merula*	0	0	0	2	0	0	2
48.	Common chaffinch	*Fringilla coelebs*	0	0	2	0	0	0	2
49.	Common kestrel	*Falco tinnunculus*	1	0	1	0	0	0	2
50.	Goosander	*Mergus merganser*	0	0	1	1	0	0	2
51.	Common shelduck	*Tadorna tadorna*	0	1	1	0	0	0	2
52.	Eurasian sparrowhawk	*Accipiter nisus*	0	1	1	0	0	0	2
53.	Arctic skua	*Stercorarius parasiticus*	0	0	2	0	0	0	2
54.	Song thrush	*Turdus philomelos*	0	0	2	0	0	0	2

No.	Taxon		July	August	September	October	November	December	Total
	English name	Latin name							
55.	Unidentified diving duck	*Aythyinae indet.*	2	0	0	0	0	0	2
56.	Unidentified gull	*Laridae indet.*	0	0	2	0	0	0	2
57.	Unidentified wagtail	*Motacilla indet.*	0	0	2	0	0	0	2
58.	Western yellow wagtail	*Motacilla flava*	0	0	2	0	0	0	2
59.	Bar-tailed godwit	*Limosa lapponica*	0	0	1	0	0	0	1
60.	Unidentified duck	*Melanitta indet.*	0	1	0	0	0	0	1
61.	Curlew sandpiper	*Calidris ferruginea*	0	0	1	0	0	0	1
62.	Dunlin	*Calidris alpina*	0	0	1	0	0	0	1
63.	Eurasian curlew	*Numenius arquata*	0	1	0	0	0	0	1
64.	Great egret	*Ardea alba*	0	0	1	0	0	0	1
65.	Greylag goose	*Anser anser*	0	0	1	0	0	0	1
66.	Horned grebe	*Podiceps auritus*	0	0	1	0	0	0	1
67.	Long-tailed skua	*Stercorarius longicaudus*	0	0	1	0	0	0	1
68.	Meadow pipit	*Anthus pratensis*	0	0	1	0	0	0	1
69.	Northern wheatear	*Oenanthe oenanthe*	0	0	1	0	0	0	1
70.	Arctic/Pomarine skua	*Stercorarius parasiticus/pomarinus*	0	0	1	0	0	0	1
71.	Red knot	*Calidris canutus*	0	0	1	0	0	0	1
72.	Red-necked grebe	*Podiceps grisegena*	0	0	1	0	0	0	1
73.	Ruff	*Philomachus pugnax*	0	0	1	0	0	0	1
74.	Sand martin	*Riparia riparia*	0	1	0	0	0	0	1
75.	Sanderling	*Calidris alba*	0	0	1	0	0	0	1
76.	Short-eared owl	*Asio flammeus*	0	0	0	1	0	0	1
77.	Tree pipit	*Anthus trivialis*	0	0	1	0	0	0	1
78.	Unidentified falconid	*Falco indet.*	0	0	1	0	0	0	1
79.	Unidentified bird-of-pray	*Accipitriformes indet.*	0	0	0	0	0	1	1
80.	Unidentified swan	*Cygnidae indet.*	0	0	0	0	0	1	1
81.	Wood sandpiper	*Tringa glareola*	1	0	0	0	0	0	1
Total			**63**	**252**	**457**	**188**	**85**	**127**	**1172**

General pattern of movement of all birds at survey station MB_01 is in line with the scheme predicted for autumn migration with the majority of birds flying to the S-SW-W, and with a small portion of birds flying in opposite direction – N-NE-E (primarily in October in November) [Figure 3.158]. Probably, this is a fraction of birds already wintering in the area and showing local, not migratory movements.

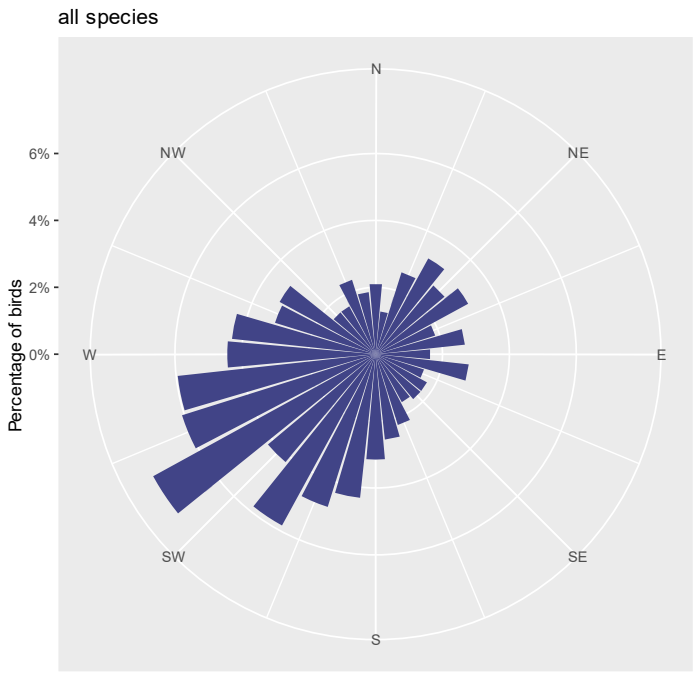


Figure 3.158. The flight directions of all tracked birds recorded at survey station MB_01 during the autumn migration period

The most numerous tracks were recorded for unidentified ducks, showing a unified direction of flight within W-SW-S direction [Figure 3.159].

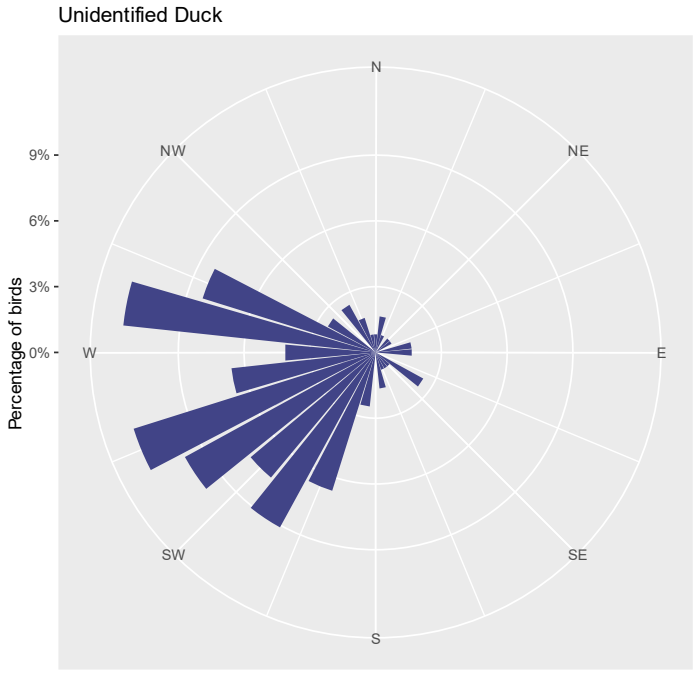


Figure 3.159. The flight directions of all tracked unidentified ducks recorded at survey station MB_01 during the autumn migration period

The majority of long-tailed duck movements were following the general autumn pattern recorded at survey station Mb_01, i.e. in S-W direction, however there was a portion of birds recorded in November and December flying in NW and NE direction (over 21% of all long-tailed ducks recorded in

both these months) [Figure 3.160]. In the case of common scoters, the pattern of movement is much more unified, with a vast majority of birds flying in SW-W direction [Figure 3.161].

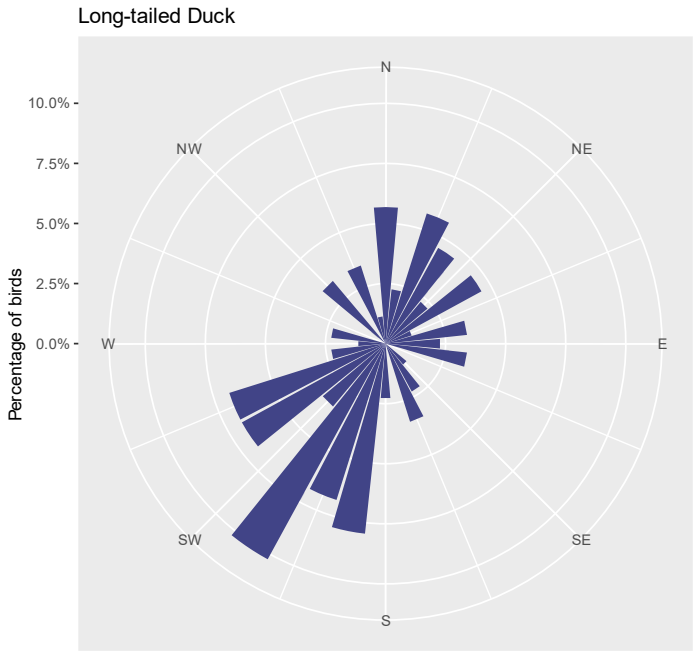


Figure 3.160. The flight directions of all tracked long-tailed ducks recorded at survey station MB_01 during the autumn migration period

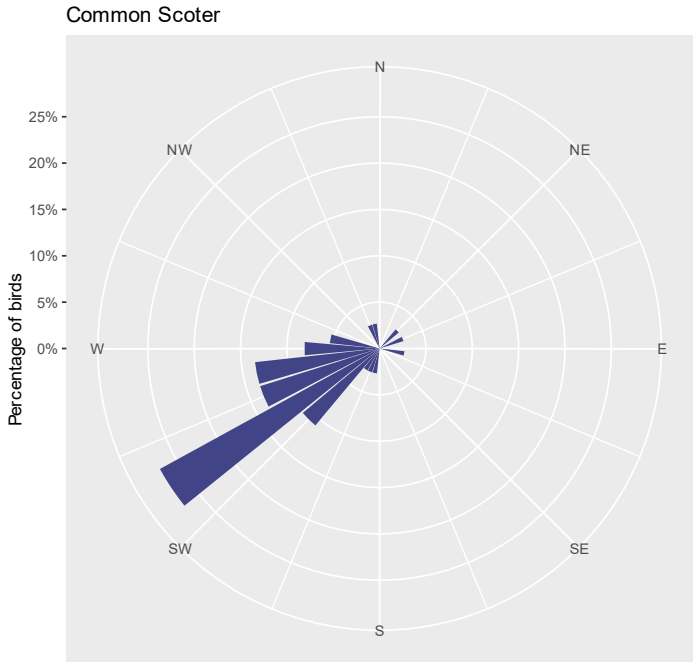


Figure 3.161. The flight directions of all tracked common scoters at survey station MB_01 during the autumn migration period

The tracks of all auks as well as categories of unidentified birds referring to auks (razorbill, common guillemot, black guillemot, auks unidentified to species) were combined together to obtain more robust and representative results. The flight paths of the auks indicate movement in almost all directions, with

two most dominant movement patterns showing opposite directions of E-NE and W-SW [Figure 3.162]. This suggests that the tracked auks were most likely local birds performing short trips and not necessarily taking part in seasonal migration.

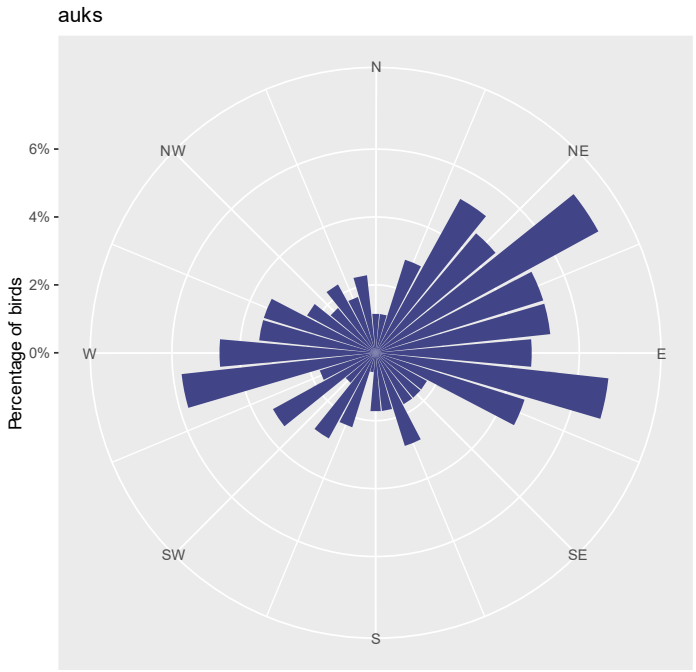


Figure 3.162. The flight directions of all tracked auks recorded at survey station MB_01 during the autumn migration period

Scattered movement patterns were recorded for the lesser black-backed gull and little gull also suggesting that the recorded birds were performing seasonal migration only to some extent and a bigger portion of those gulls were local [Figure 3.163, Figure 3.164]. This is especially supported by records from August and September showing that lesser black-backed gulls flew in NNE direction. Little gulls were tracked in the NNE-NE directions in August, September, and November.

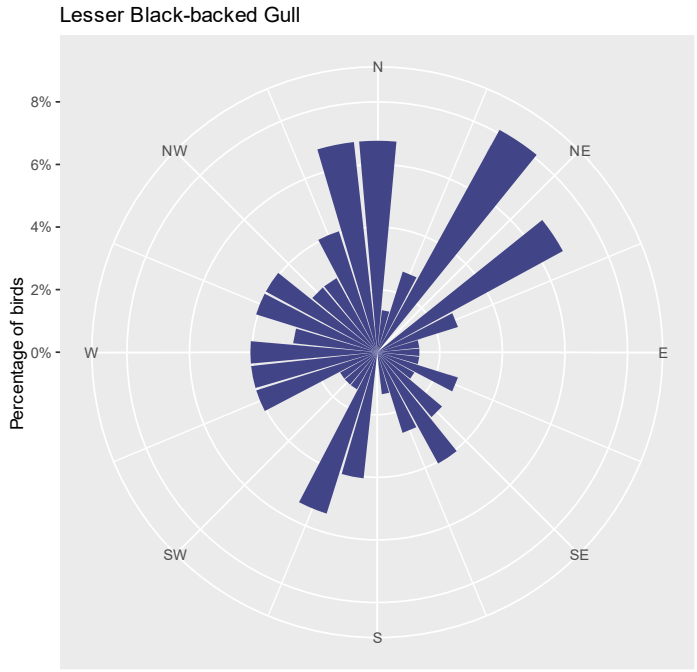


Figure 3.163. The flight directions of all tracked lesser black-backed gulls recorded at survey station MB_01 during the autumn migration period

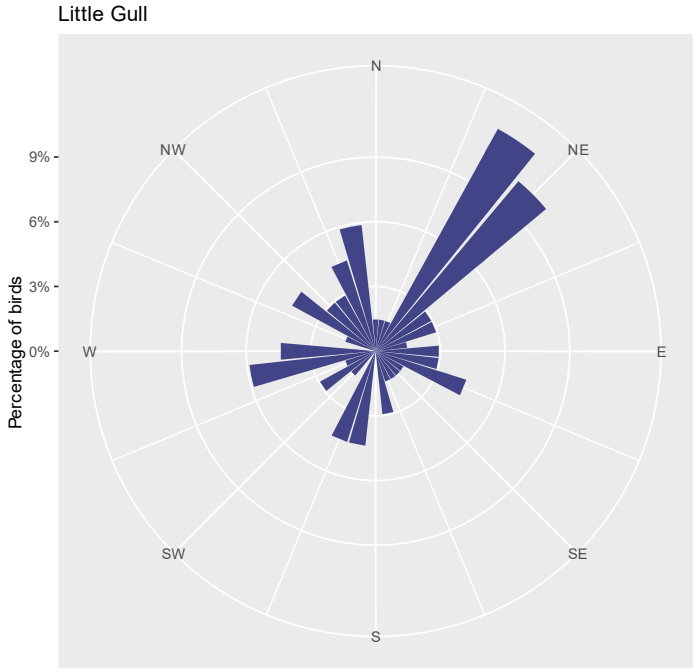


Figure 3.164. The flight directions of all tracked little gulls recorded at survey station MB_01 during the autumn migration period

Great cormorants flew mostly in W-SW and S directions with a small portion of birds (less than 5% in each direction) flying in the NW-N-NE-E and SE spectrum [Figure 3.165].

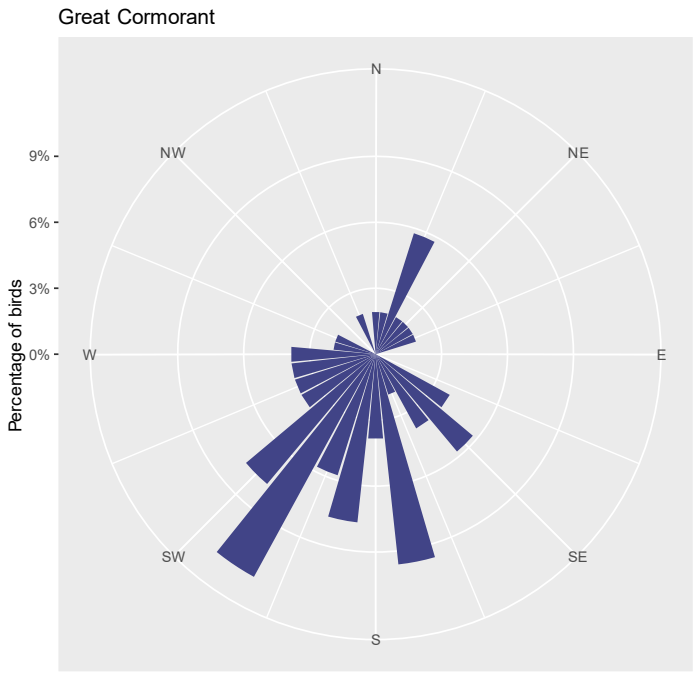


Figure 3.165. The flight directions of all tracked great cormorants recorded at survey station MB_01 during the autumn migration period

Passerine birds analysed together (both identified and unidentified species) showed a unified pattern of flight in SW-S direction with a small portion of birds flying NW, E and SE direction [Figure 3.166]. All species and categories of terns were pooled together for a better representation of flight patterns. Most of the terns flew in the range between NW and S direction. Very small numbers flew in opposite directions of N and NE [Figure 3.167].

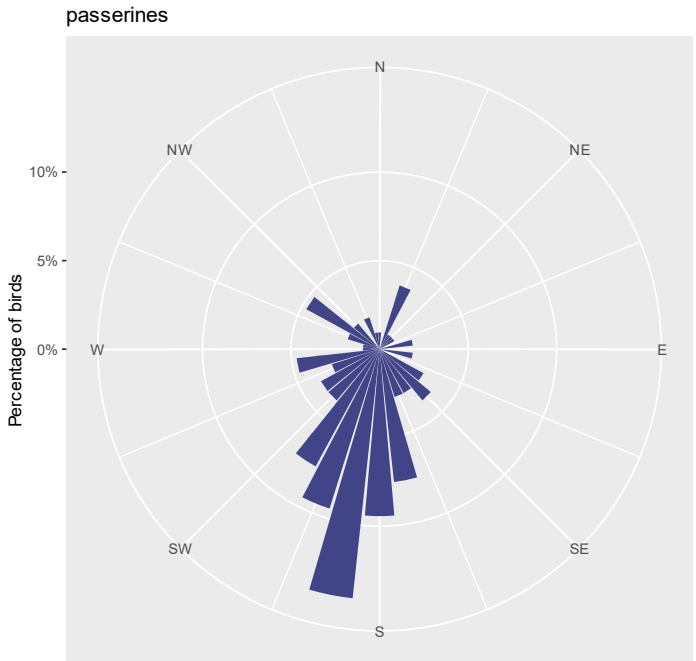


Figure 3.166. The flight directions of all tracked passerines recorded at survey station MB_01 during the autumn migration period

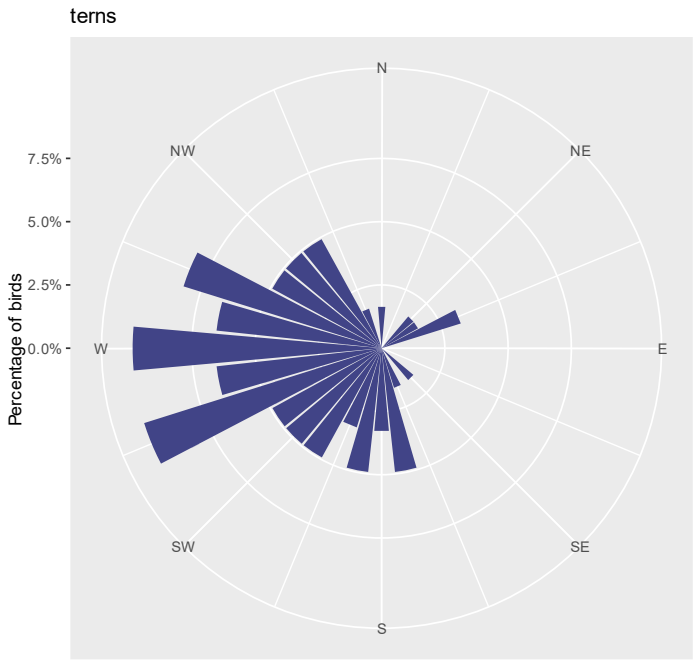


Figure 3.167. The flight directions of all tracked terns recorded at survey station MB_01 during the autumn migration period

At survey station MB_02, the highest number of bird tracks was recorded for long-tailed ducks, common scoters, auks (razorbills and guillemots) and unidentified ducks. The highest number of tracks was recorded in October [Table 3.110]. At survey station MB_02, a total of 80 categories of birds was identified. Among those, there were distinguished 64 species, 12 categories of birds identified to an order or family, and 4 categories in which final identification was impossible and the category points at two most probable species.

Table 3.110. The number of tracks of species and bird categories recorded at survey station MB_02 during the autumn migration period

No.	Taxon		July	August	September	October	November	December	Total
	English name	Latin name							
1.	Long-tailed duck	*Clangula hyemalis*	0	0	1	204	207	8	420
2.	Unidentified duck	*Melanitta indet.*	4	17	58	81	53	1	214
3.	Unidentified auk	*Alca torda / Uria aalge*	1	2	16	70	91	0	180
4.	Common guillemot	*Uria aalge*	0	0	11	51	38	1	101
5.	Razorbill	*Alca torda*	0	1	4	51	40	0	96
6.	Great black cormorant	*Phalacrocorax carbo*	1	50	17	1	4	0	73
7.	Common scoter	*Melanitta nigra*	4	16	29	11	8	0	68
8.	Little gull	*Larus minutus*	1	19	16	3	27	0	66
9.	Unidentified passerine	*Passeriformes indet.*	0	4	38	9	1	0	52
10.	Lesser black-backed gull	*Larus fuscus*	0	12	38	0	1	0	51
11.	Unidentified diver	*Gavia indet.*	0	3	8	19	15	3	48

No.	Taxon		July	August	September	October	November	December	Total
	English name	Latin name							
12.	Common swift	*Apus apus*	0	47	0	0	0	0	47
13.	Common/Arctic tern	*Sterna hirundo/paradisaea*	5	32	0	0	0	0	37
14.	Velvet scoter	*Melanitta fusca*	1	2	13	16	1	0	33
15.	Eurasian teal	*Anas crecca*	0	6	18	0	0	0	24
16.	Common gull	*Larus canus*	3	2	10	7	2	0	24
17.	Eurasian wigeon	*Anas penelope*	0	1	14	6	0	0	21
18.	European herring gull	*Larus argentatus*	0	19	0	0	0	0	19
19.	White wagtail	*Motacilla alba*	0	0	19	0	0	0	19
20.	Black-throated diver	*Gavia arctica*	0	1	4	7	1	0	13
21.	Unidentified wader	*Limicolae indet.*	0	5	7	0	0	0	12
22.	Unidentified goose	*Anserini indet.*	0	0	7	4	0	0	11
23.	Grey heron	*Ardea cinerea*	1	4	3	1	0	1	10
24.	Common tern	*Sterna hirundo*	1	7	0	0	0	0	8
25.	Mallard	*Anas platyrhynchos*	0	0	1	6	1	0	8
26.	Unidentified tern	*Sterna indet.*	3	4	1	0	0	0	8
27.	Black-headed gull	*Chroicocephalus ridibundus*	1	3	1	2	0	0	7
28.	Great tit	*Parus major*	0	0	7	0	0	0	7
29.	Red-throated diver	*Gavia stellata*	0	0	0	5	1	1	7
30.	Black guillemot	*Cepphus grylle*	0	0	0	0	6	0	6
31.	Eurasian siskin	*Spinus spinus*	0	0	6	0	0	0	6
32.	European golden plover	*Pluvialis apricaria*	0	5	1	0	0	0	6
33.	Great black-backed gull	*Larus marinus*	1	1	0	1	2	0	5
34.	Mute swan	*Cygnus olor*	2	0	0	0	2	1	5
35.	Barn swallow	*Hirundo rustica*	0	2	2	0	0	0	4
36.	Common chaffinch	*Fringilla coelebs*	0	0	4	0	0	0	4
37.	Goosander	*Mergus merganser*	0	0	0	3	1	0	4
38.	Greylag goose	*Anser anser*	0	1	3	0	0	0	4
39.	Unidentified diving duck	*Aythyinae indet.*	0	0	3	1	0	0	4
40.	Dunlin	*Calidris alpina*	0	3	0	0	0	0	3
41.	Greater scaup	*Aythya marila*	0	0	1	2	0	0	3
42.	European sand martin	*Pluvialis squatarola*	1	2	0	0	0	0	3
43.	Pintail	*Anas acuta*	0	2	1	0	0	0	3
44.	Northern shoveler	*Anas clypeata*	0	1	2	0	0	0	3
45.	Unidentified swan	*Cygnidae indet.*	0	0	1	1	1	0	3
46.	Common starling	*Sturnus vulgaris*	0	0	0	1	1	0	2
47.	Goldcrest	*Regulus regulus*	0	0	2	0	0	0	2
48.	Great crested grebe	*Podiceps cristatus*	0	1	1	0	0	0	2
49.	Great egret	*Ardea alba*	0	0	2	0	0	0	2

No.	Taxon		July	August	September	October	November	December	Total
	English name	Latin name							
50.	Long-tailed/Arctic/Pomarine skua	*Stercorarius longicaudus/parasiticus/ pomarinus*	0	0	2	0	0	0	2
51.	Arctic skua	*Stercorarius parasiticus*	0	1	1	0	0	0	2
52.	Red-breasted merganser	*Mergus serrator*	0	0	0	0	2	0	2
53.	Red-necked grebe	*Podiceps grisegena*	0	0	0	1	0	1	2
54.	Short-eared owl	*Asio flammeus*	0	0	1	1	0	0	2
55.	Tufted duck	*Aythya fuligula*	0	0	2	0	0	0	2
56.	Unidentified sandpiper	*Calidris indet.*	0	1	1	0	0	0	2
57.	Arctic tern	*Sterna paradisaea*	0	1	0	0	0	0	1
58.	Black-legged kittiwake	*Rissa tridactyla*	0	0	0	0	1	0	1
59.	Unidentified duck	*Melanitta indet.*	1	0	0	0	0	0	1
60.	Eurasian blue tit	*Parus caeruleus*	0	0	1	0	0	0	1
61.	Common kestrel	*Falco tinnunculus*	0	1	0	0	0	0	1
62.	Common pigeon	*Columba livia*	0	1	0	0	0	0	1
63.	Common redstart	*Phoenicurus phoenicurus*	0	0	1	0	0	0	1
64.	Common shelduck	*Tadorna tadorna*	0	0	1	0	0	0	1
65.	Common snipe	*Gallinago gallinago*	0	0	1	0	0	0	1
66.	Eurasian skylark	*Alauda arvensis*	0	0	1	0	0	0	1
67.	Eurasian tree sparrow	*Passer montanus*	0	1	0	0	0	0	1
68.	Northern wheatear	*Oenanthe oenanthe*	0	0	1	0	0	0	1
69.	Pomarine skua	*Stercorarius pomarinus*	0	0	1	0	0	0	1
70.	Sand martin	*Riparia riparia*	0	0	1	0	0	0	1
71.	Sanderling	*Calidris alba*	0	0	1	0	0	0	1
72.	Song thrush	*Turdus philomelos*	0	0	1	0	0	0	1
73.	Tundra swan	*Cygnus columbianus*	0	0	0	0	1	0	1
74.	Twite	*Linaria flavirostris*	0	0	0	1	0	0	1
75.	Unidentified curlew	*Numenius indet.*	0	1	0	0	0	0	1
76.	Unidentified bird-of-pray	*Accipitriformes indet.*	0	0	0	1	0	0	1
77.	Unidentified swallow	*Hirundo* indet.	0	0	1	0	0	0	1
78.	Eurasian whimbler	*Numenius phaeopus*	1	0	0	0	0	0	1
79.	Whooper swan	*Cygnus cygnus*	0	0	0	1	0	0	1
80.	Western yellow wagtail	*Motacilla flava*	0	0	1	0	0	0	1
Total			**32**	**282**	**389**	**568**	**508**	**17**	**1796**

The flight directions of all birds tracked at survey station MB_02 is unified and follows predictable pattern for autumn migration between W-S, with the biggest portion of birds flying in SW direction [Figure 3.168].

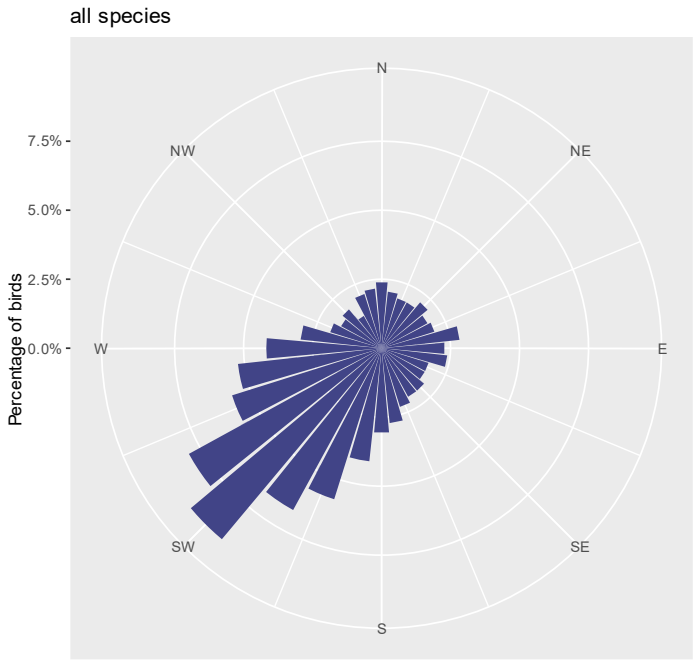


Figure 3.168. The flight directions of all tracked birds recorded at survey station MB_02 during the autumn migration period

The pattern of the long-tailed duck movements is unified and most of the birds were flying in SW direction, in a relatively narrow spectrum of the direction angle [Figure 3.169]. Unidentified ducks also fly in in a unified direction with a broader spectrum between W-S with two distinctive peaks in W and SW direction [Figure 3.170].

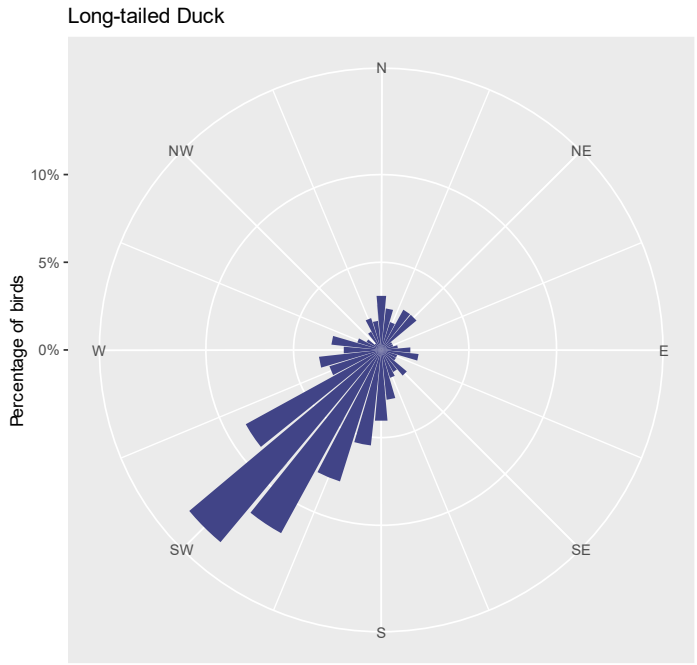


Figure 3.169. The flight directions of all tracked long-tailed ducks recorded at survey station MB_02 during the autumn migration period

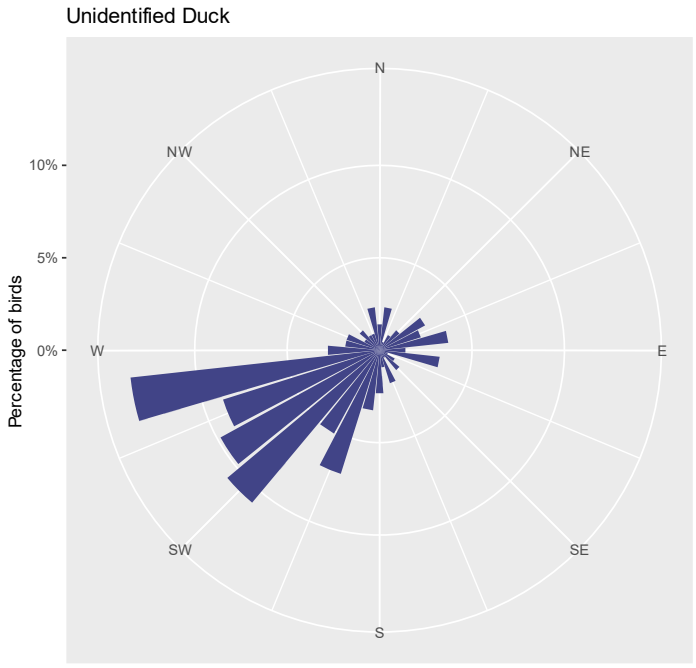


Figure 3.170. The flight directions of all tracked unidentified ducks recorded at survey station MB_02 during the autumn migration period

The tracks of all auks as well as categories of unidentified birds referring to auks (razorbill, common guillemot, black guillemot, auks unidentified to species) were combined together to obtain more robust and representative results. The flight paths of auks, similarly to those recorded at survey station MB_01, indicate movement in practically all directions. The only difference is that the dominant directions at station MB_01 were not opposite. Most of birds were tracked flying in the directions of NE-SE and W-S [Figure 3.171]. This suggests that auks tracked within the survey area were most likely local birds performing short trips and not necessarily taking part in the seasonal migration.

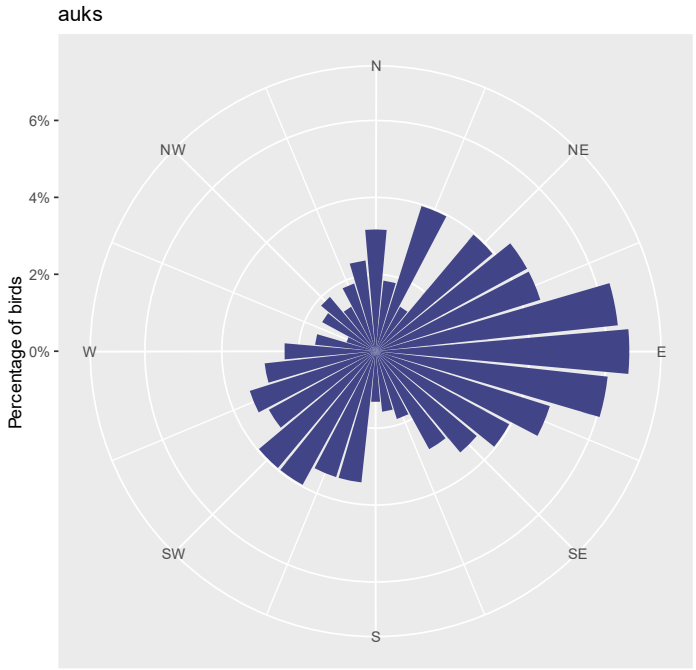


Figure 3.171. The flight directions of all tracked auks recorded at survey station MB_02 during the autumn migration period

Tracks of great cormorants show scattered flight directions, with a big portion of birds flying in W-S direction and substantial proportion in NE direction [Figure 3.172].

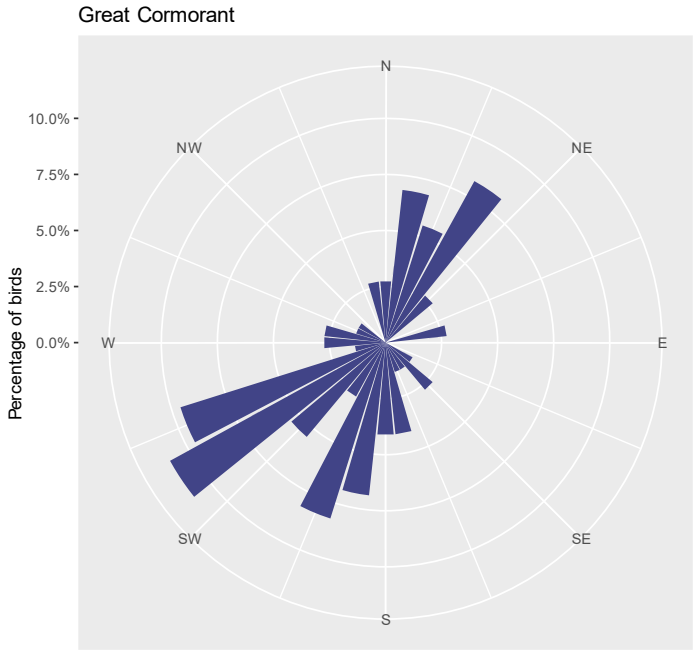


Figure 3.172. The flight directions of all tracked great cormorants recorded at survey station MB_02 during the autumn migration period

Almost all tracked common scoters flew in SW direction [Figure 3.173].

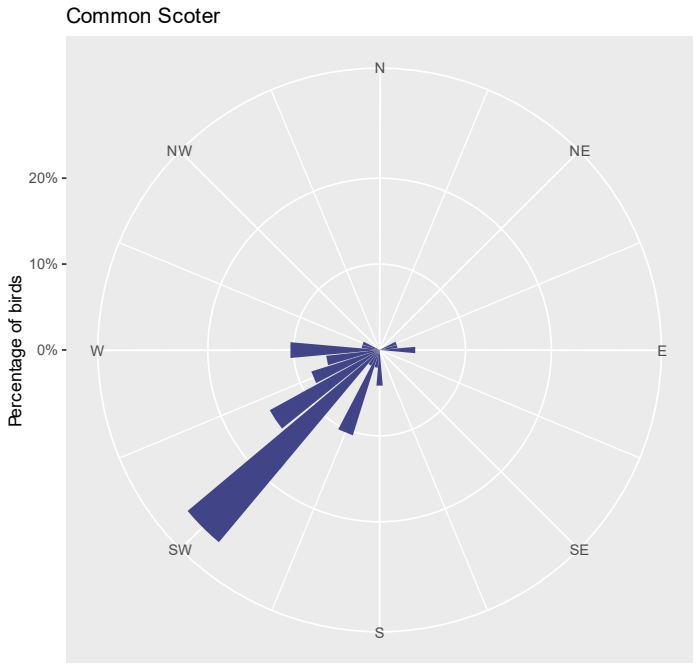


Figure 3.173. The flight directions of all tracked common scoters at survey station MB_02 during the autumn migration period

Little gulls showed a rather scattered pattern of movements, unlike lesser black-backed gull with almost all tracks falling within W-S direction [Figure 3.174, Figure 3.175].

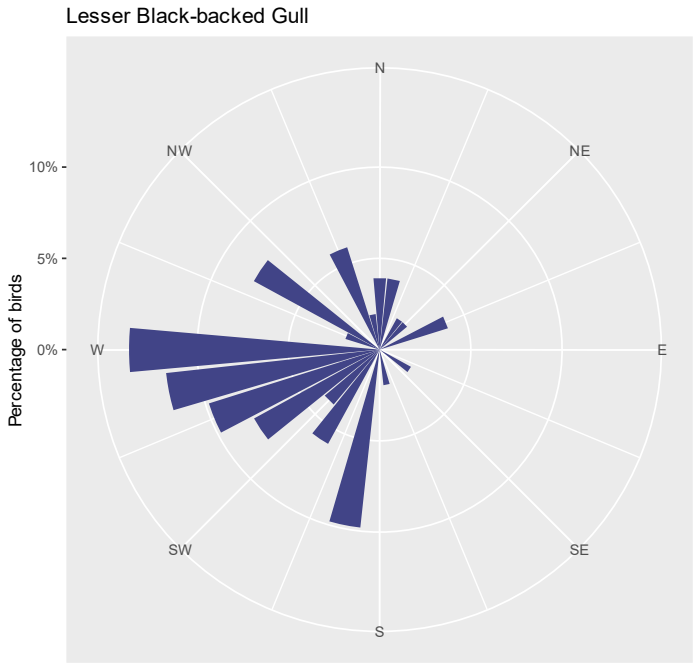


Figure 3.174. The flight directions of all tracked lesser black-backed gulls recorded at survey station MB_02 during the autumn migration period

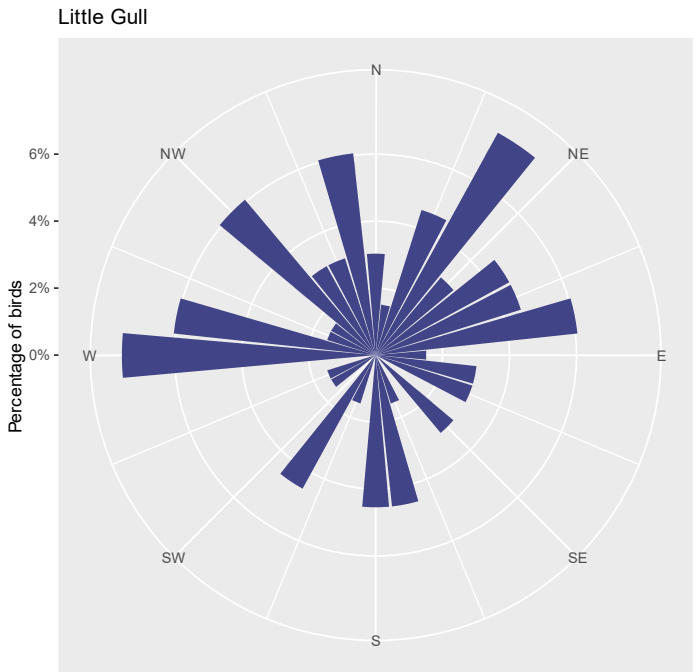


Figure 3.175. The flight directions of all tracked little gulls recorded at survey station MB_02 during the autumn migration period

Passerines tracked at survey station MB_02 flew in general SW-S direction with a small portion of birds following W trajectories as well as W, NW, N and E [Figure 3.176].

Unidentified divers flew without any particular pattern in all directions suggesting not a seasonal migration as a reason of movement [Figure 3.177].

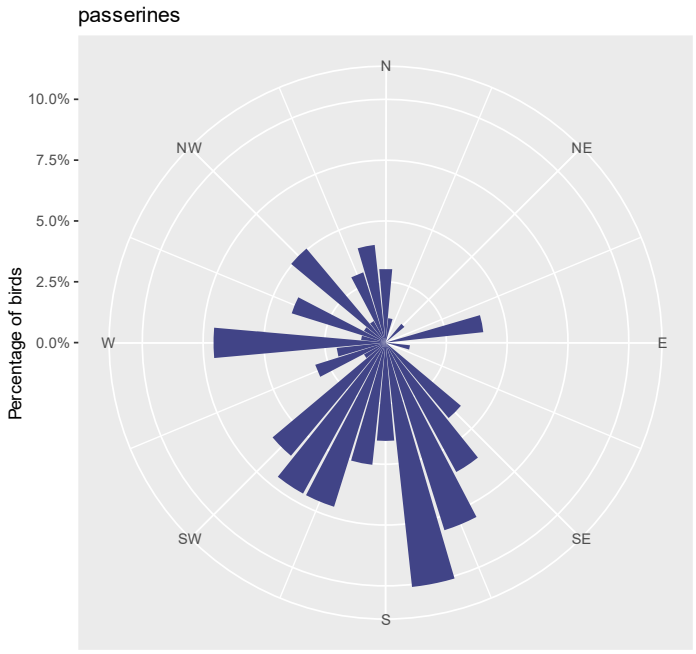


Figure 3.176. The flight directions of all tracked passerines recorded at survey station MB_02 during the autumn migration period

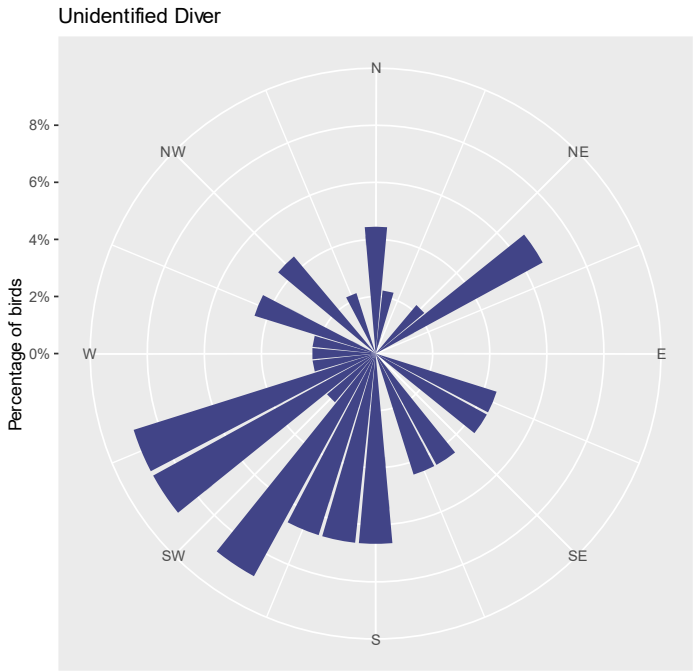


Figure 3.177. The flight directions of all tracked unidentified divers recorded at survey station MB_02 during the autumn migration period

3.5.2.5.5 Vertical radar results

3.5.2.5.5.1 Local bird movements in winter (wintering birds)

Vertical radar data are presented for 10-m altitude bins as a number of tracks per hour in a given month. The total number of tracks for every altitude bin for each month was divided by the total amount of effort hours for a given month (the total time of operating the vertical radar) in order to obtain the averaged number of tracks detected per hour. This procedure was performed separately for survey station LP_01 and LP_02. The resulting rates of tracks per hour were corrected for altitude-based detection biases (the observer effect). Due to most detections being at low altitude, the corrections accepted are very small.

In December, at survey station LP_02, significant bird movement was recorded up to the altitude of 240 m ASL. A relatively small number of birds were detected between 240 and 480 m ASL and only single tracks were recorded in December at altitudes higher than 480 m ASL [Figure 3.178].

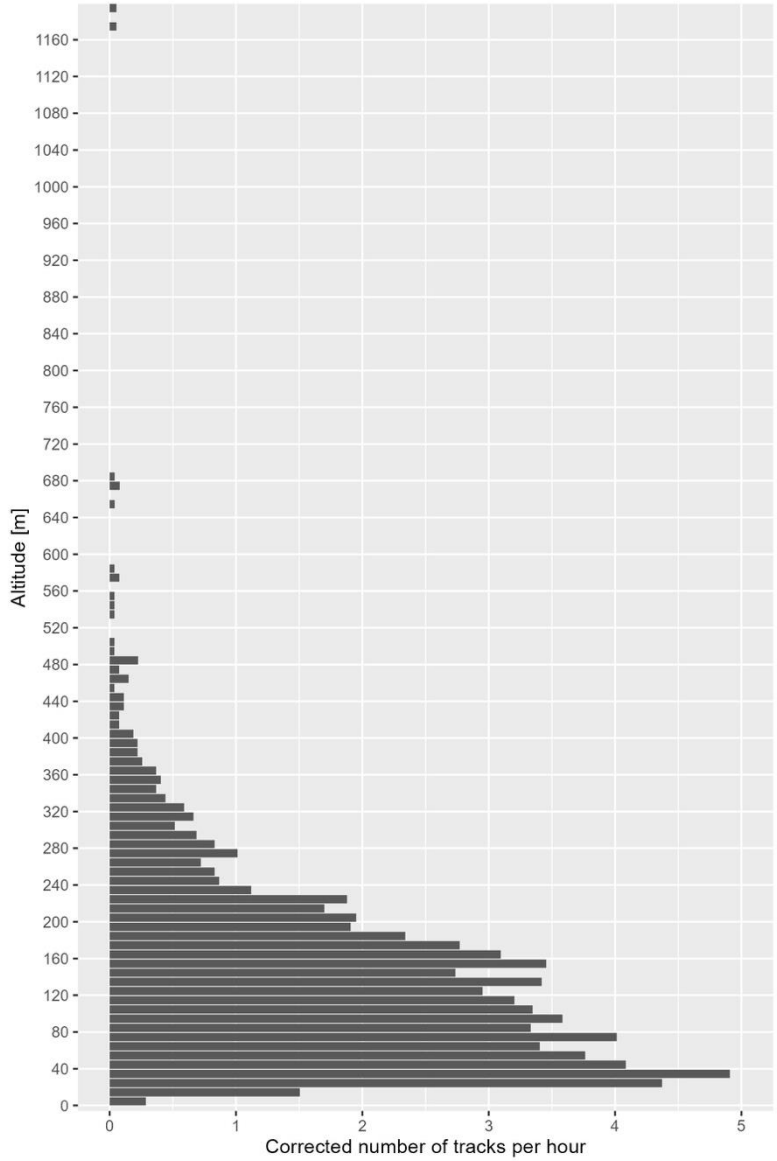


Figure 3.178. The distribution of bird flight altitudes recorded using vertical radar in December 2022 at survey station LP_01. The number of tracks was averaged with the total monthly effort of the vertical radar data collection

In January, the majority of bird tracks were recorded at altitude of up to 120 m ASL. Only single flights were recorded at an altitude of 500 m ASL [Figure 3.179]. No flights were recorded above this altitude. The peak of detections was recorded between 30–60 m ASL.

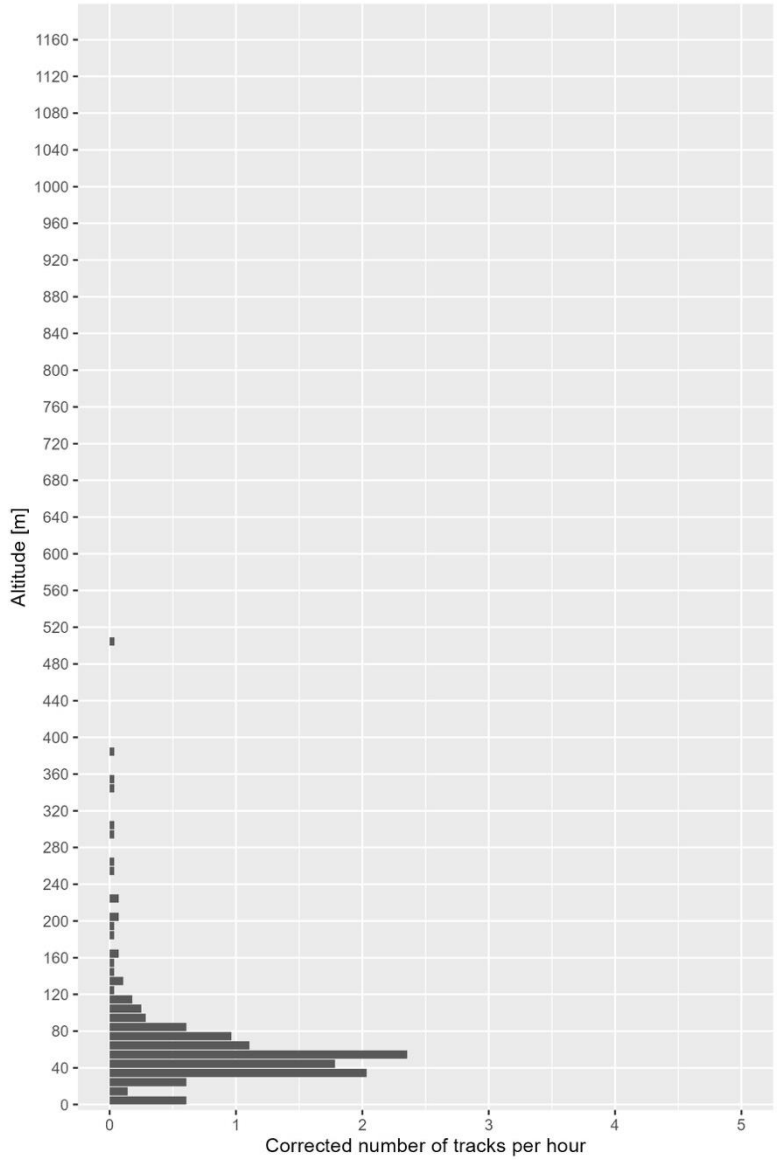


Figure 3.179. The distribution of bird flight altitudes recorded using vertical radar January 2023 at survey station LP_01. The number of tracks was averaged with the total time devoted to the vertical radar data collection in that month

In February, most flight paths were recorded at altitudes not exceeding 360 m ASL. More activity, however still rather scarce, was recorded at higher altitudes, up to 1080 m ASL [Figure 3.180]. Again, the peak of detections was recorded at the altitudes between 30–60 m ASL.

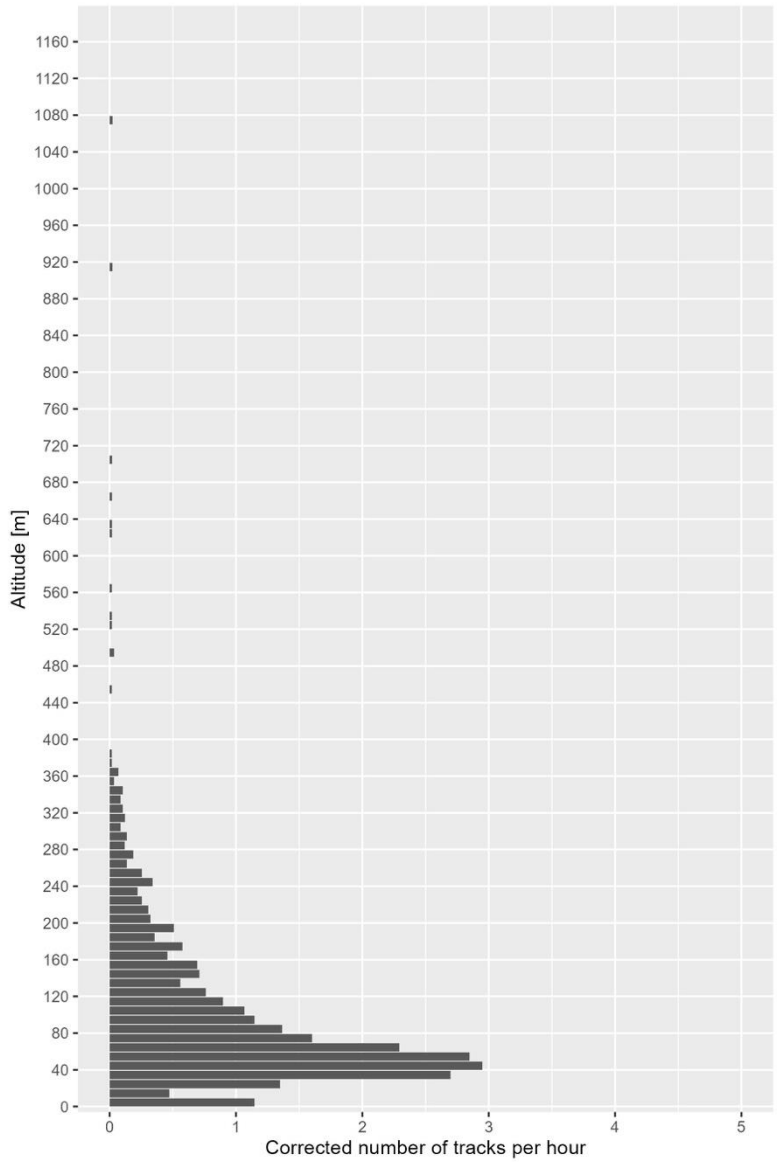


Figure 3.180. The distribution of bird flight altitudes recorded using vertical February 2023 at survey station LP_01. The number of tracks was averaged with the total time devoted to the vertical radar data collection in that month

At survey station LP_02, just as at survey station LP_01, more activity was recorded in December at higher altitudes, but it was not as pronounced as in the case of the results from the LP_01 point. The peak of detections was recorded between 20–50 m ASL. The second peak was recorded between 110 and 180 m ASL, which was not as pronounced as the first peak though. Most detections were recorded up to the level of 480 m ASL [Figure 3.181].

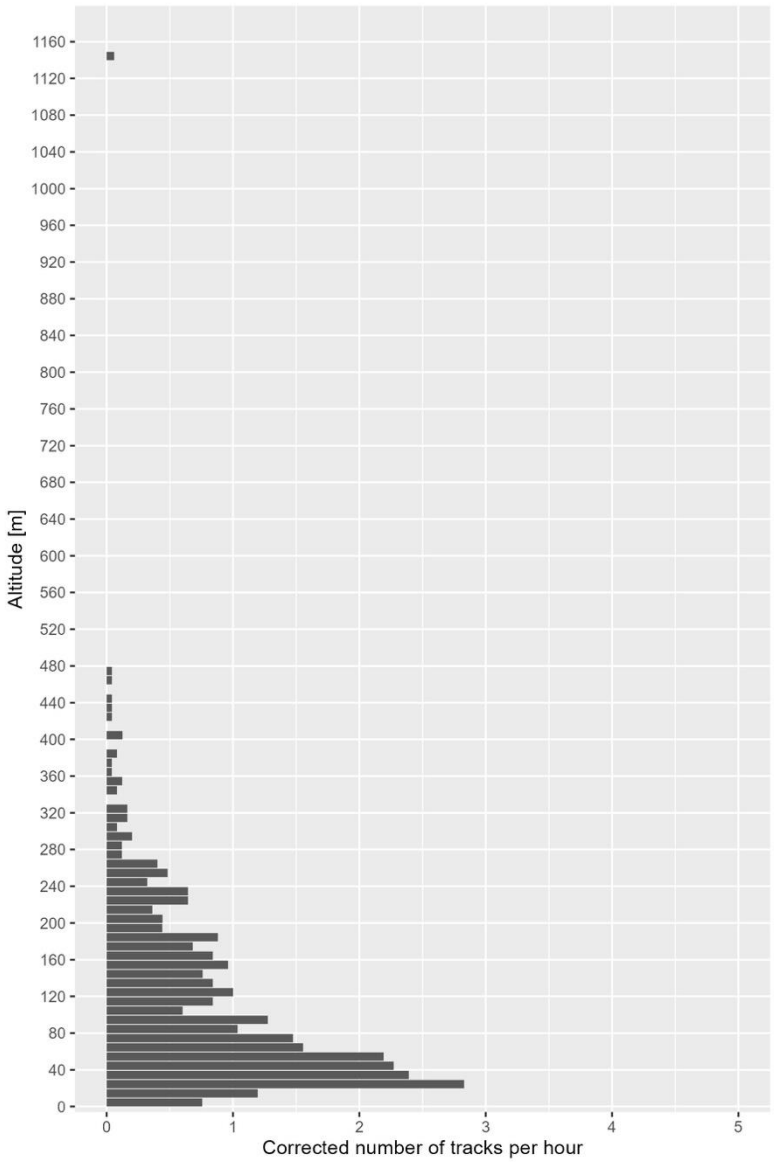


Figure 3.181. The distribution of bird flight altitudes recorded using vertical radar in December 2022 at survey station LP_02. The number of tracks was averaged with the total time devoted to the vertical radar data collection in that month

In January, at survey station LP_02, the smallest bird activity was recorded (among both stations in the whole local migration survey period). The average bird activity did not exceed 1 track per hour for the entire month. The peak of detected birds is placed similarly to the ones recorded in other months and at other stations – between 30 and 60 m ASL [Figure 3.182].

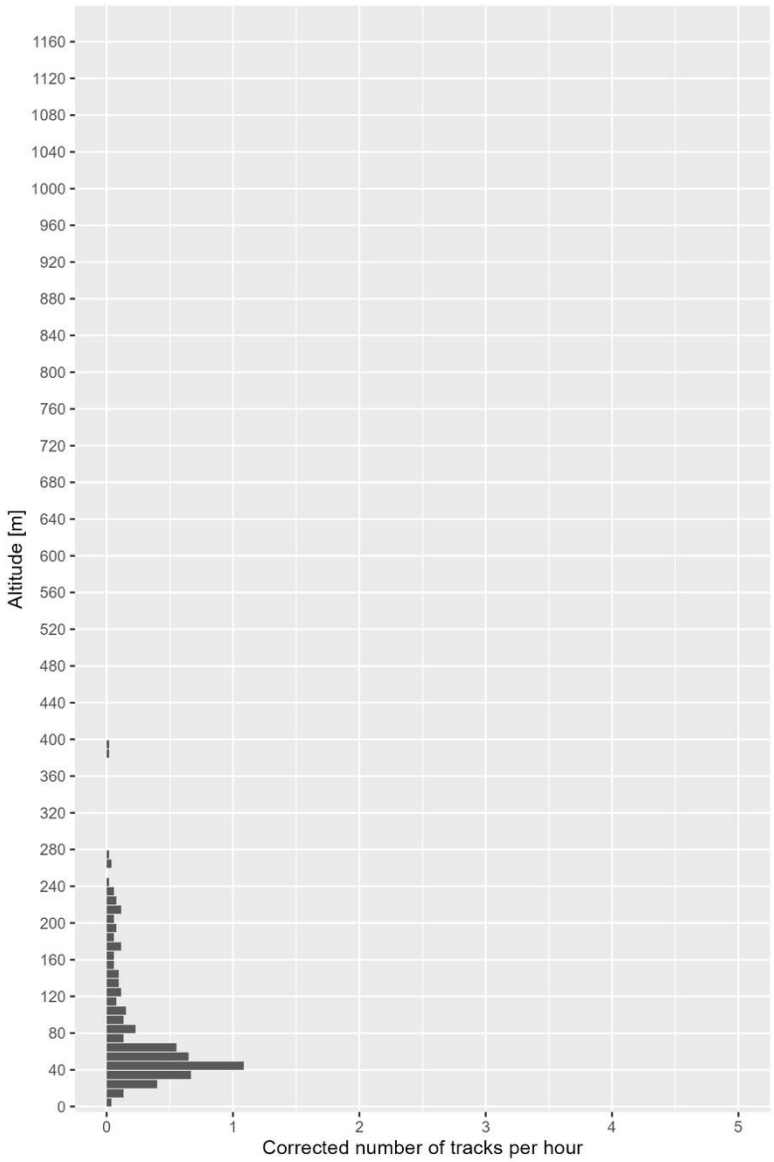


Figure 3.182. The distribution of bird flight altitudes recorded using vertical radar January 2023 at survey station LP_02. The number of tracks was averaged with the total time devoted to the vertical radar data collection in that month

In February, at survey station LP_02, the activity of birds was slightly higher than in January, with a similar peak of activity around 30–60 m ASL and scattered, not very numerous detections between 320 and 650 m ASL [Figure 3.183].

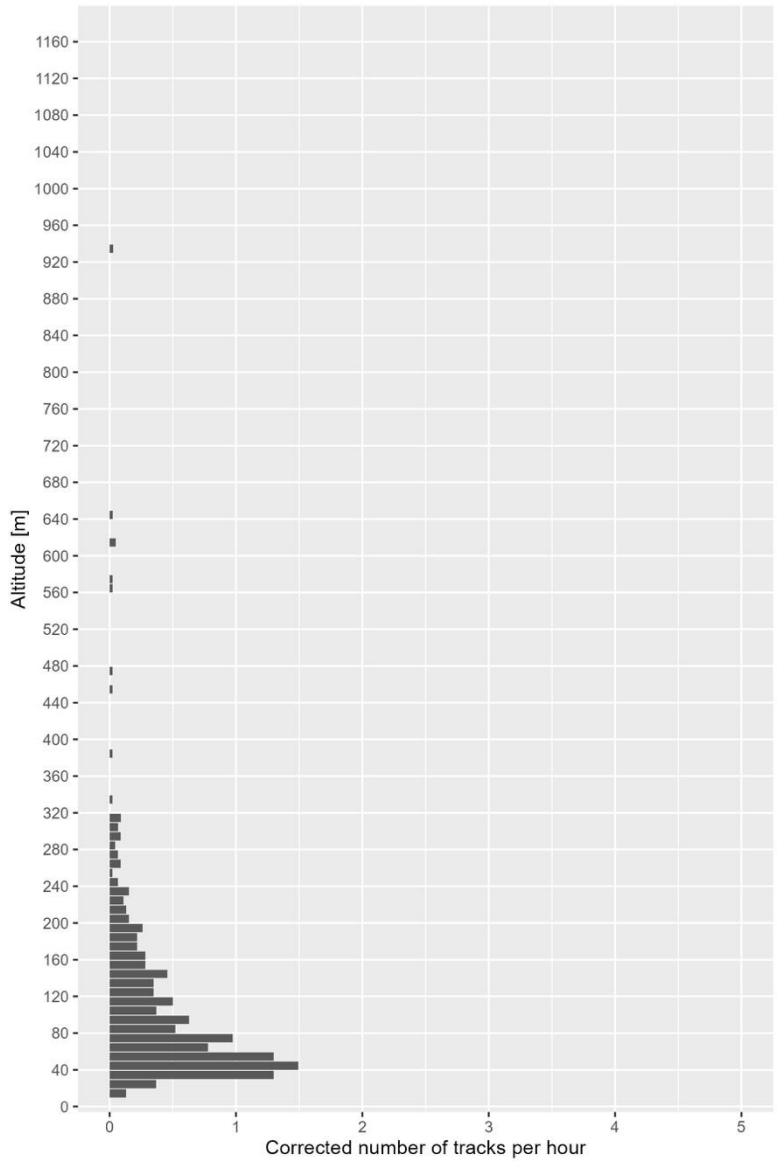


Figure 3.183. The distribution of bird flight altitudes recorded using vertical February 2023 at survey station LP_02. The number of tracks was averaged with the total time devoted to the vertical radar data collection in that month

3.5.2.5.5.2 Spring migration

Vertical radar data are presented for 10-m altitude bins as a number of tracks per hour in a given month. The total number of tracks for every altitude bin for each month was divided by the total amount of effort hours for a given month (the total time of operating the vertical radar) in order to obtain the averaged number of tracks detected per hour. This was performed separately for survey stations MB_01 and MB_02. The resulting rates of tracks per hour were corrected for altitude-based detection biases (the observer effect).

Due to low numbers of echoes recorded in March, the results for this month are presented on a scale up to 1 track per hour for better visual representation whereas the results for April and May are presented on a scale from 0 to 5 tracks per hour.

In March, at survey station MB_01, a small amount of bird movement was detected, mainly up to the altitude of 250 m ASL. Single tracks were recorded between 800 and 1050 m ASL [Figure 3.184]. The average bird activity did not exceed 1 track per hour for the whole month.

In April, the activity of birds was higher than in March, however, almost in all cases it did not exceed 1 track per hour. Birds were recorded at all altitudes up to 1500 m ASL with the clear peak of detections at altitudes up to 50 m ASL [Figure 3.185].

In May, similarly to April, the recorded mean number of bird flights at individual altitudes was lower than 1 track per hour in most cases. The peak of detected bird activity is placed around the altitude of 800–1000 m ASL [Figure 3.186].

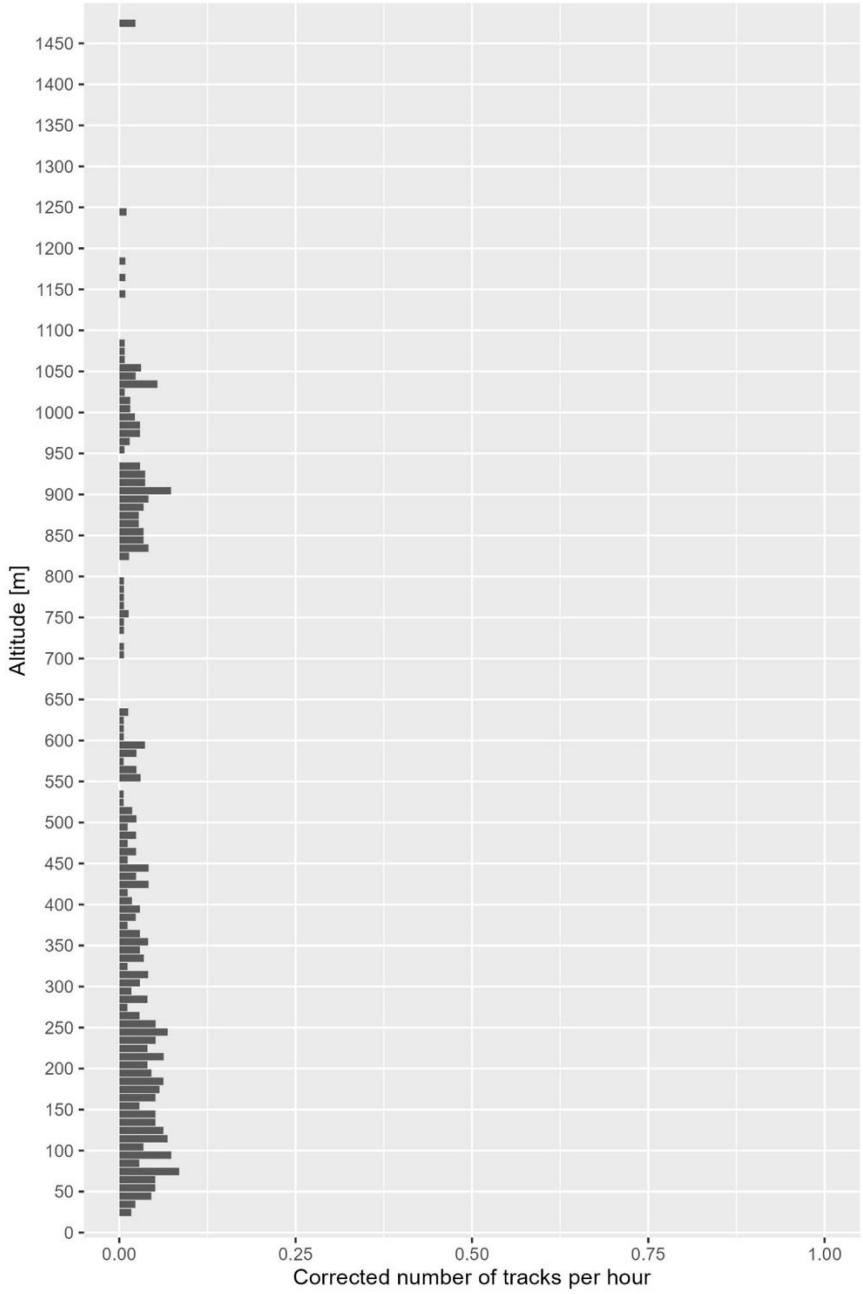


Figure 3.184. The distribution of bird flight altitudes recorded using vertical radar in March 2023 at survey station MB_01. The number of tracks was averaged with the total time devoted to the vertical radar data collection in that month

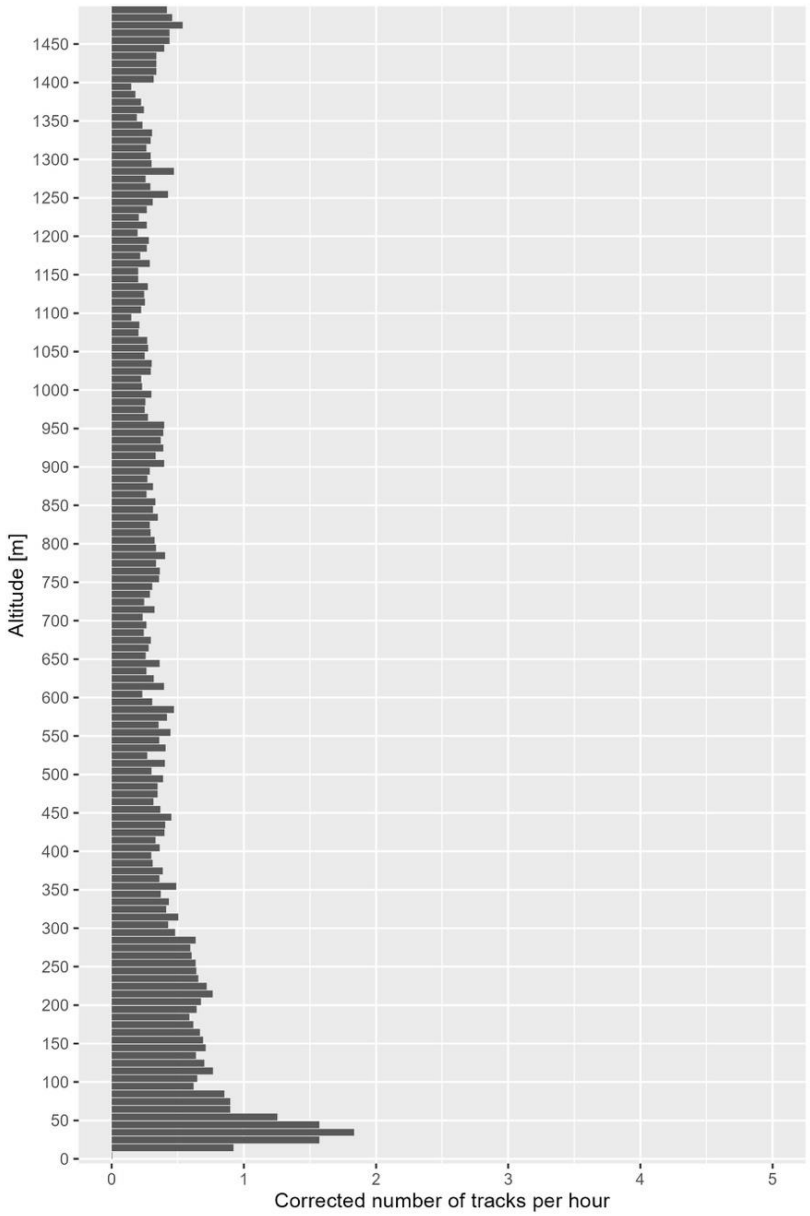


Figure 3.185. The distribution of bird flight altitudes recorded using vertical radar in April 2023 at survey station MB_01. The number of tracks was averaged with the total time devoted to the vertical radar data collection in that month

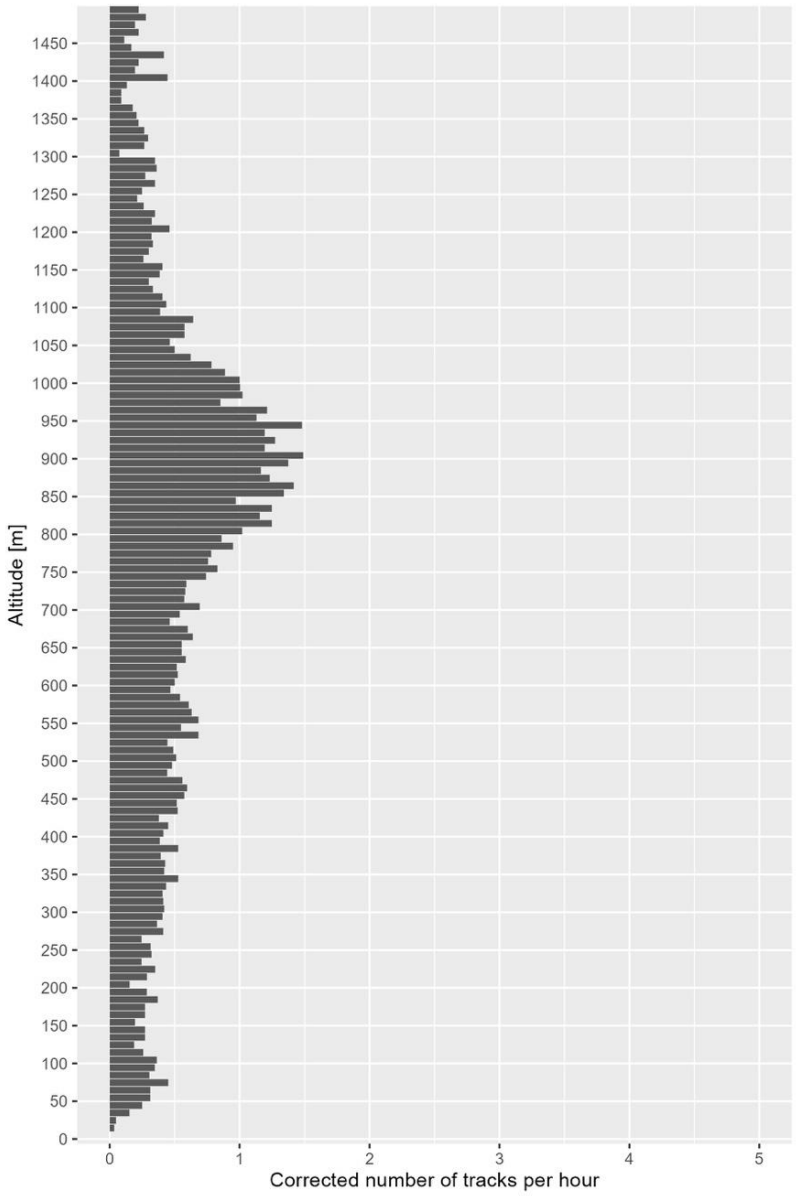


Figure 3.186. The distribution of bird flight altitudes recorded using vertical radar in May 2023 at survey station MB_01. The number of tracks was averaged with the total time devoted to the vertical radar data collection in that month

At survey station MB_02, just as in the case of survey station MB_01, the lowest bird activity was recorded in March. Scarce and scattered detections of bird flights were recorded at altitudes of up to 1225 m ASL. Most of birds were detected up to the level of 75 m ASL [Figure 3.187].

The bird activity recorded at survey station MB_02 in April was the highest among both survey stations in all survey months. A clear peak of bird track detections fell between the altitudes of 1400 and 1500 m ASL [Figure 3.188].

In May, regular but not very numerous detections were recorded at all altitudes with no clear peak of activity. Birds were detected from 10 up to 1500 m ASL [Figure 3.189].

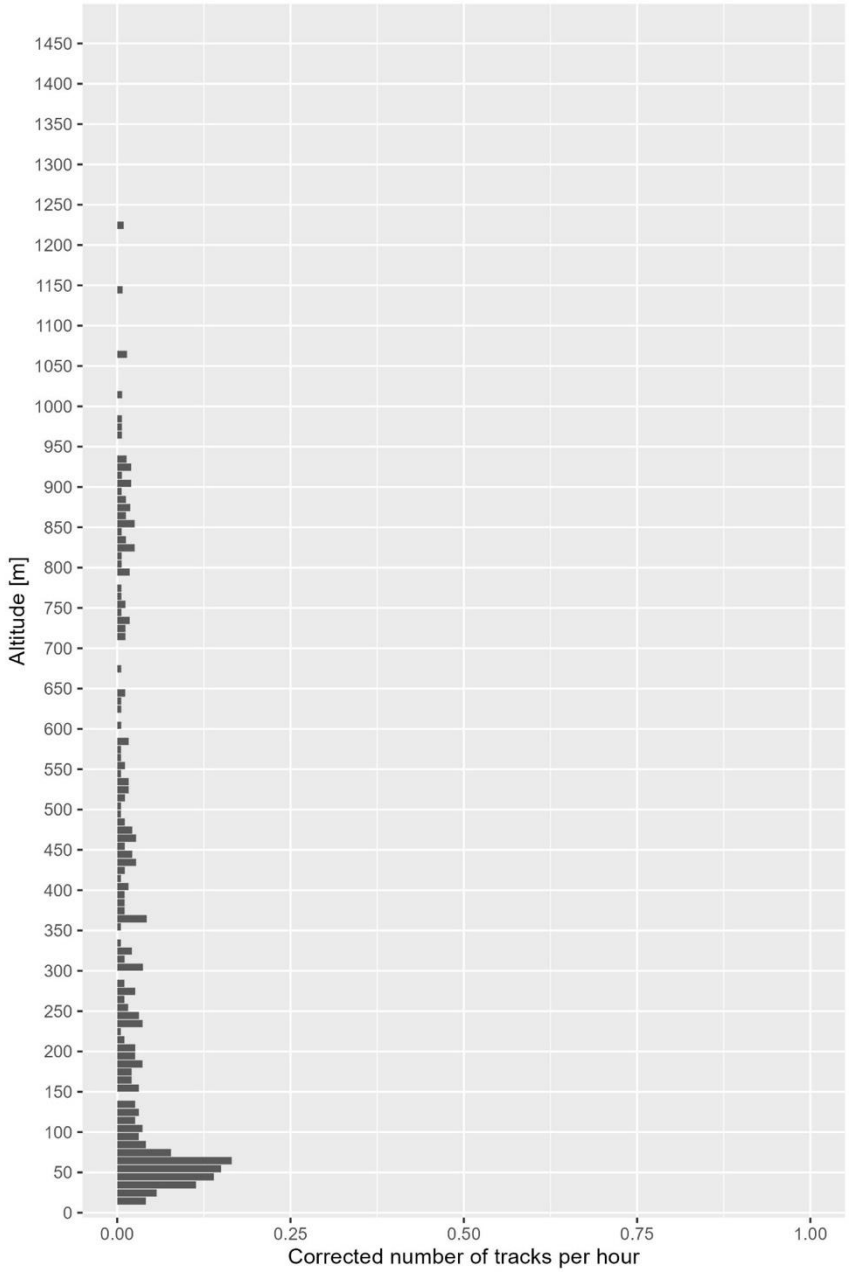


Figure 3.187. The distribution of bird flight altitudes recorded using vertical radar in March 2023 at survey station MB_02. The number of tracks was averaged with the total time devoted to the vertical radar data collection in that month

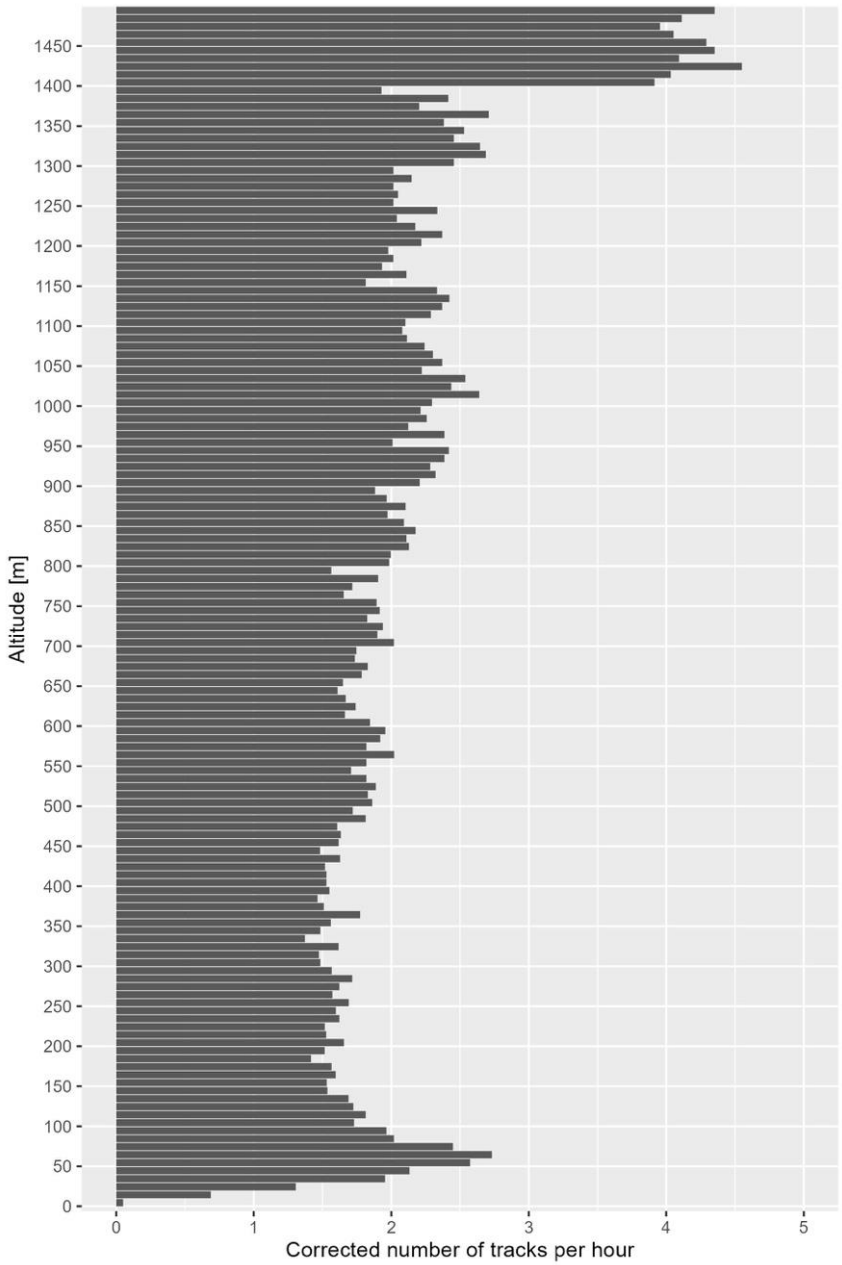


Figure 3.188. The distribution of bird flight altitudes recorded using vertical radar in April 2023 at survey station MB_02. The number of tracks was averaged with the total time devoted to the vertical radar data collection in that month

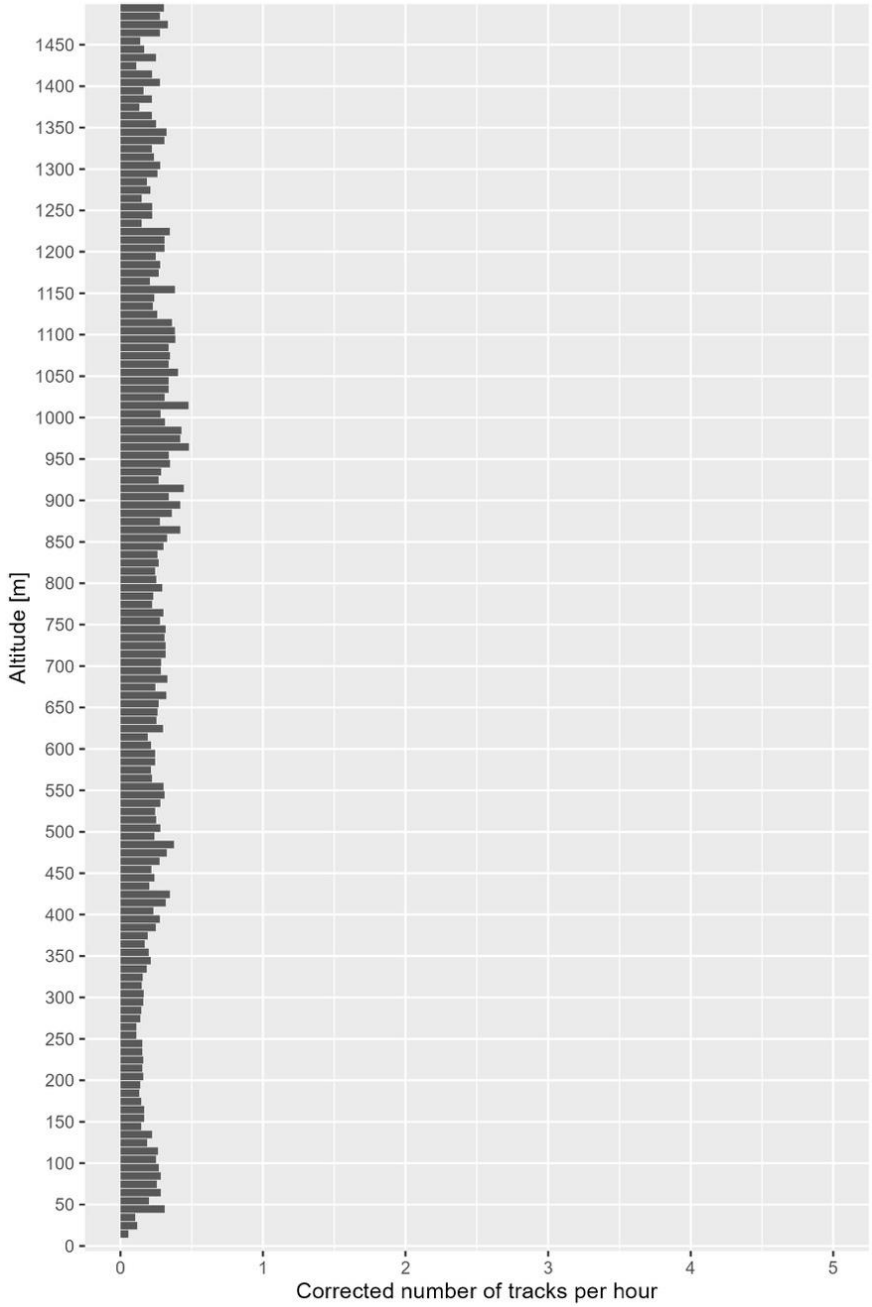


Figure 3.189. The distribution of bird flight altitudes recorded using vertical radar in May 2023 at survey station MB_02. The number of tracks was averaged with the total time devoted to the vertical radar data collection in that month

3.5.2.5.5.3 Autumn migration

Vertical radar data are presented for 10-m altitude bins as a number of tracks per hour in a given month. The total number of tracks for every altitude bin for each month was divided by the total amount of effort hours for a given month (the total time of operating the vertical radar) in order to obtain the averaged number of tracks detected per hour. This was performed separately for survey stations MB_01 and MB_02. The resulting rates of tracks per hour were corrected for altitude-based detection biases (the observer effect).

Due to low numbers of echoes recorded in July at survey station MB_02, the results for this month are presented on a scale up to 1 track per hour for better visual representation whereas for other autumn months, the results are presented on a scale from 0 to 5 tracks per hour.

In July, at survey station MB_01, there were recorded two peaks of activity at altitudes up to 100 m and between 300 and 450 m ASL. Yet, those peaks barely reached the level of 0.5 track per hour on average, hence, the activity can be considered low [Figure 3.190].

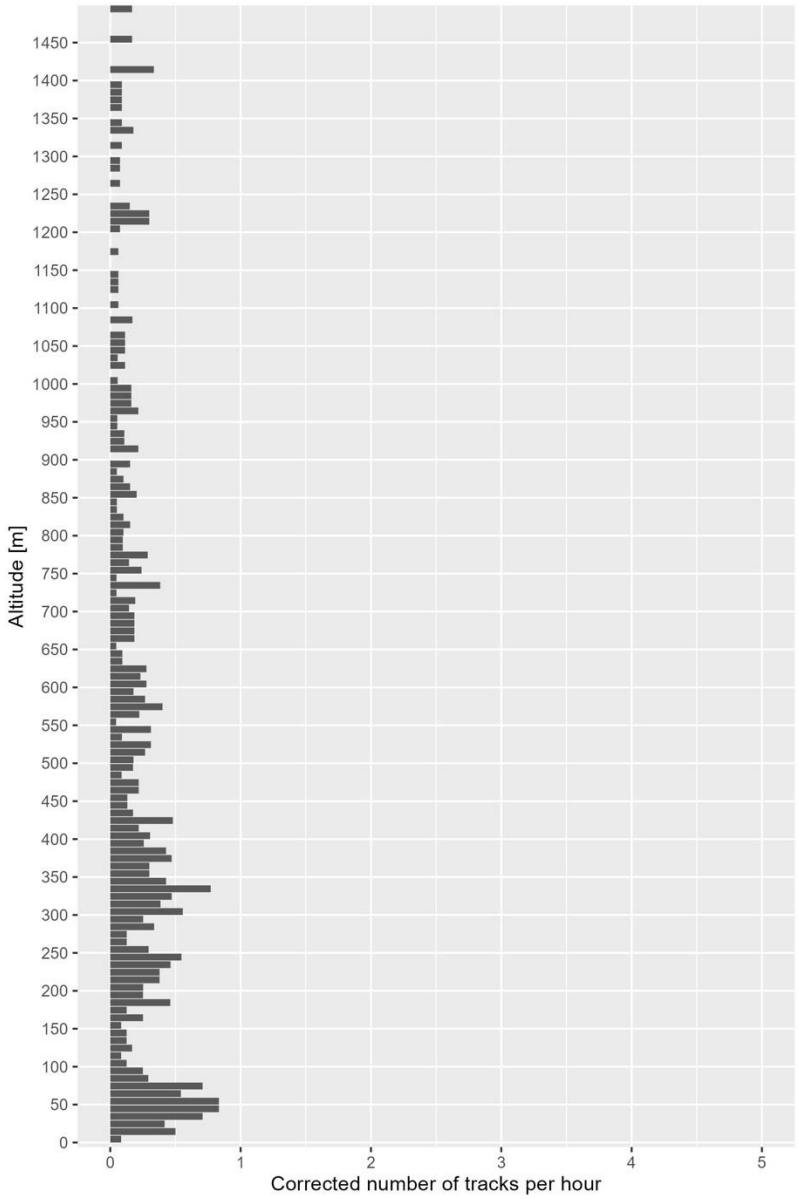


Figure 3.190. The distribution of bird flight altitudes recorded using vertical radar in July 2023 at survey station MB_01. The number of tracks was averaged with the total time devoted to the vertical radar data collection in that month

In August, the recordings from survey station MB_01 shown a uniform activity of around 0.5 track per hour at altitudes from the sea level of up to approximately 700 m ASL. Above 700 m, the activity decreases gradually down to a fraction of a track per hour, yet radar readings show bird movement up to the maximum range of the vertical radar, i.e. 1500 m ASL [Figure 3.191].

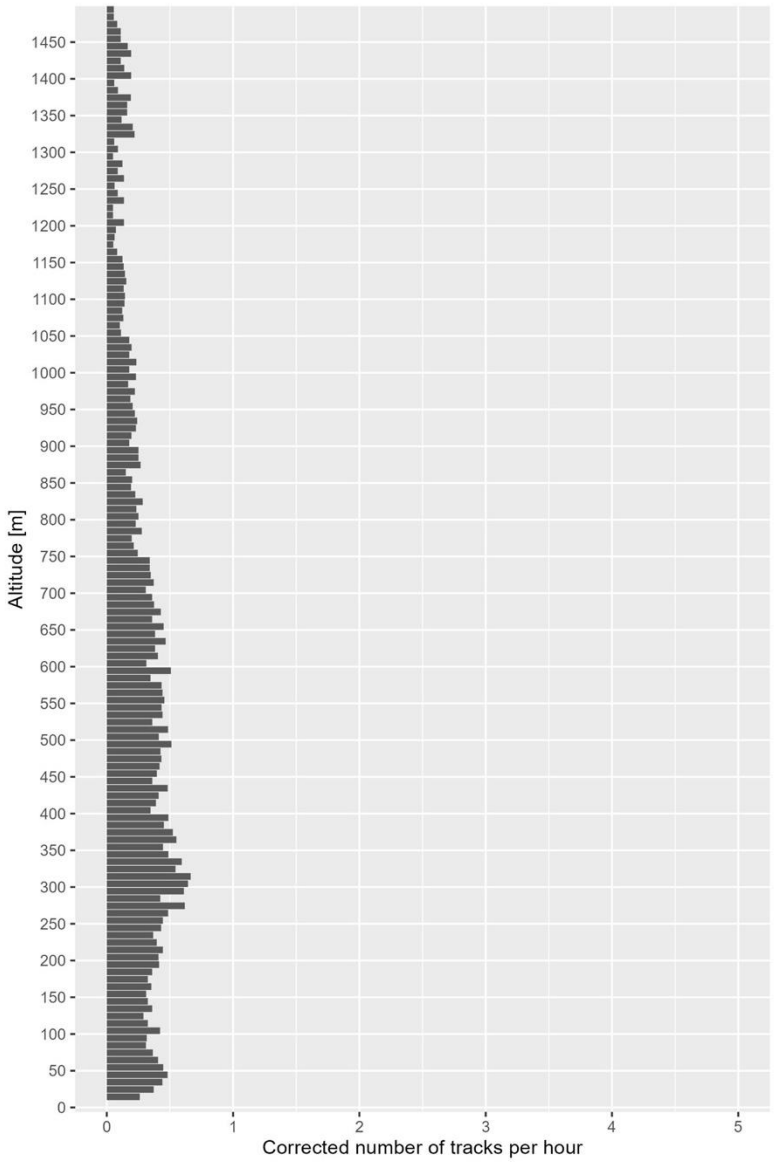


Figure 3.191. The distribution of bird flight altitudes recorded using vertical radar in August 2023 at survey station MB_01. The number of tracks was averaged with the total time devoted to the vertical radar data collection in that month

In September, the number of tracks was clearly higher. That increase was noticeable especially up to the level of 75 m ASL, the number of echoes recorded by the radar tripled in relation to previous months [Figure 3.192].

In October and November, we could observe again a drop in movement volume with less than one track per hour at all altitudes. In October, slightly higher activity was recorded up to an altitude of 100 m ASL. In November, very low bird activity was recorded mainly up to the altitude of 350 m ASL (less than 0.5 track per hour) [Figure 3.193, Figure 3.194].

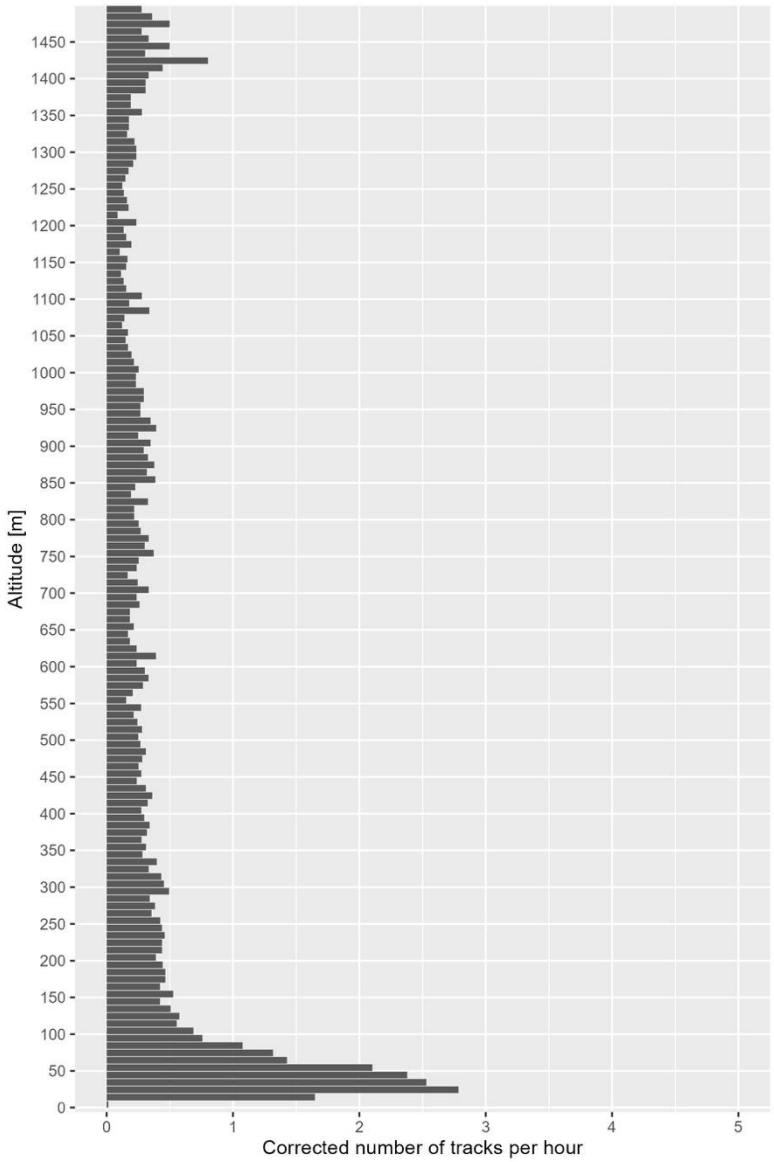


Figure 3.192. The distribution of bird flight altitudes recorded using vertical radar in September 2023 at survey station MB_01. The number of tracks was averaged with the total time devoted to the vertical radar data collection in that month

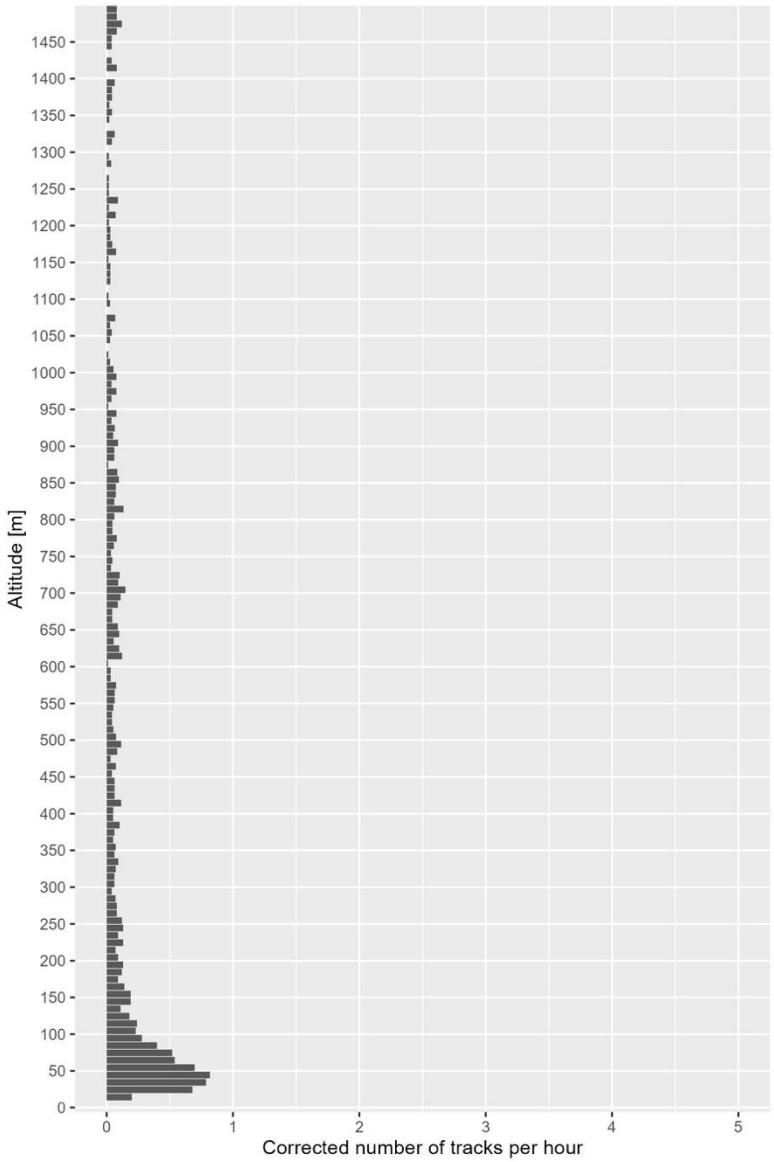


Figure 3.193. The distribution of bird flight altitudes recorded using vertical radar in October 2023 at survey station MB_01. The number of tracks was averaged with the total time devoted to the vertical radar data collection in that month

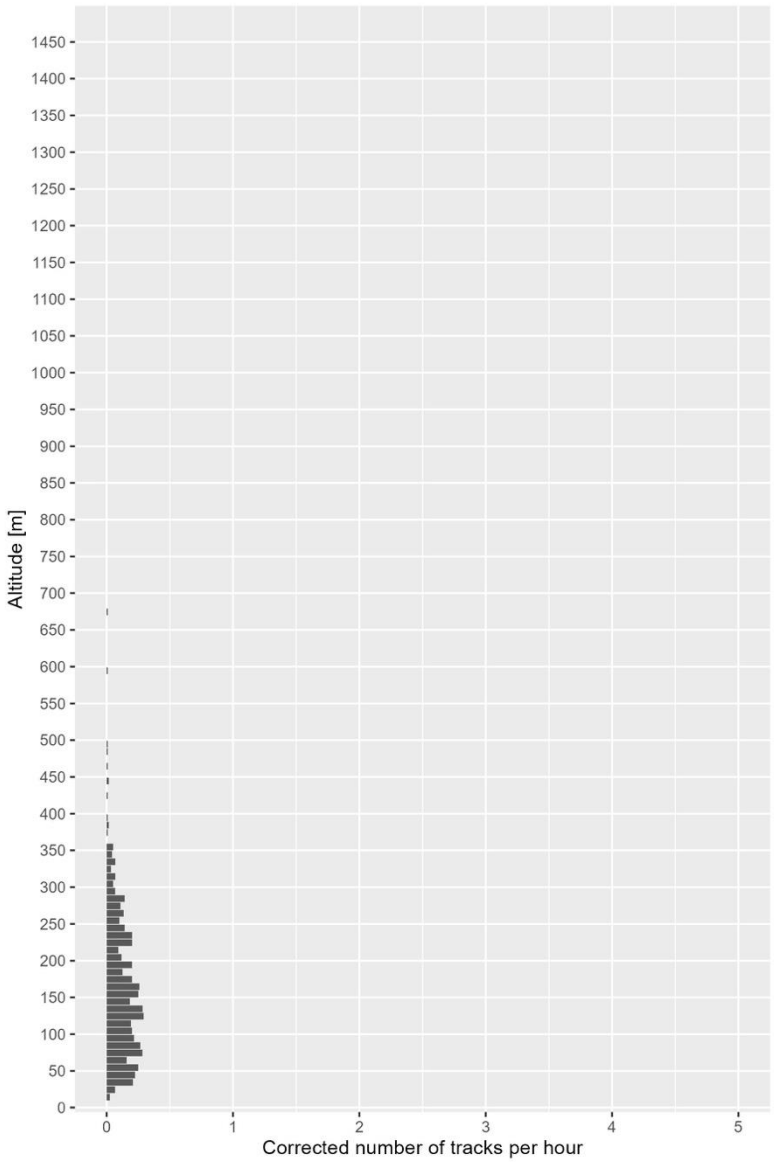


Figure 3.194. The distribution of bird flight altitudes recorded using vertical radar in November 2023 at survey station MB_01. The number of tracks was averaged with the total time devoted to the vertical radar data collection in that month

In July, at survey station MB_02, bird track recordings were scarcely distributed up to the level of 1350 m ASL with one peak from sea level up to 100 m ASL reaching only 0.25 track per hour [Figure 3.195]. In August, the recordings from survey station MB_02 were more numerous with reading of up to 1 track per hour on average between 0 and 100 m ASL. Rather uniform track recordings of approximately 0.5 track per hour were obtained at altitudes between 100 and 800 m ASL [Figure 3.196]. In both months, tracks were recorded along the whole operational spectrum of the vertical radar, i.e. to the level of 1500 m ASL.

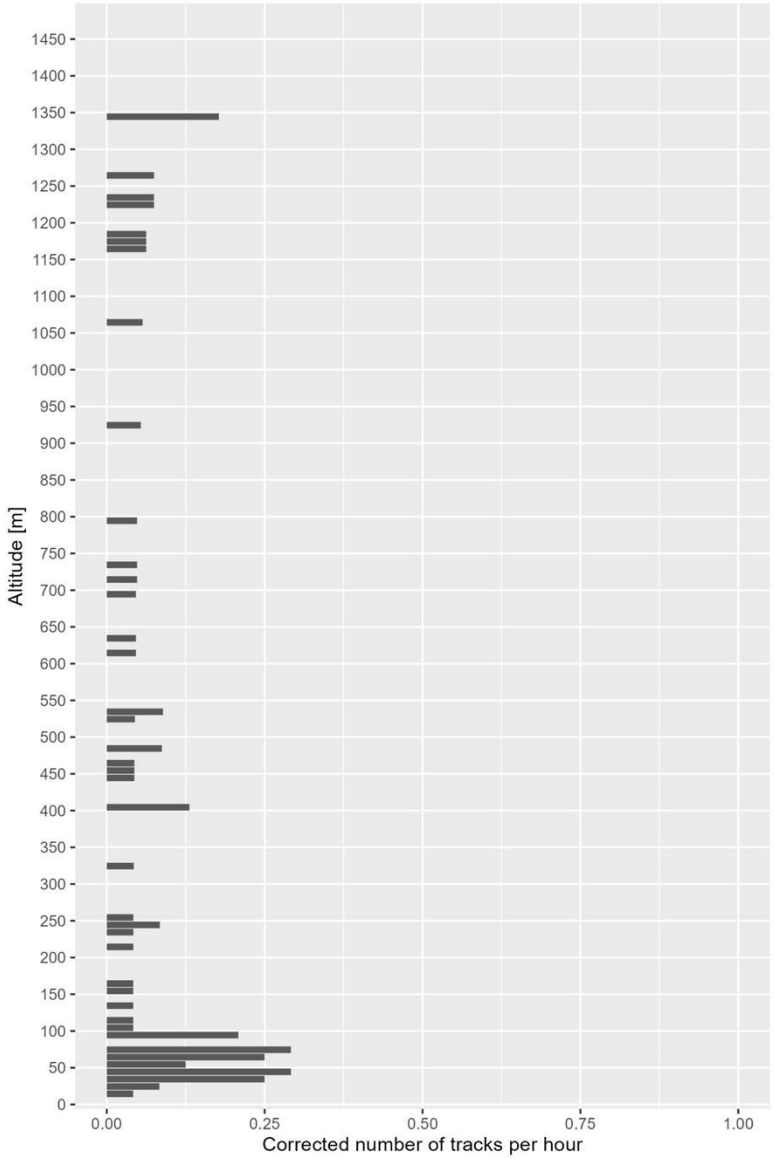


Figure 3.195. The distribution of bird flight altitudes recorded using vertical radar in July 2023 at survey station MB_02. The number of tracks was averaged with the total time devoted to the vertical radar data collection in that month

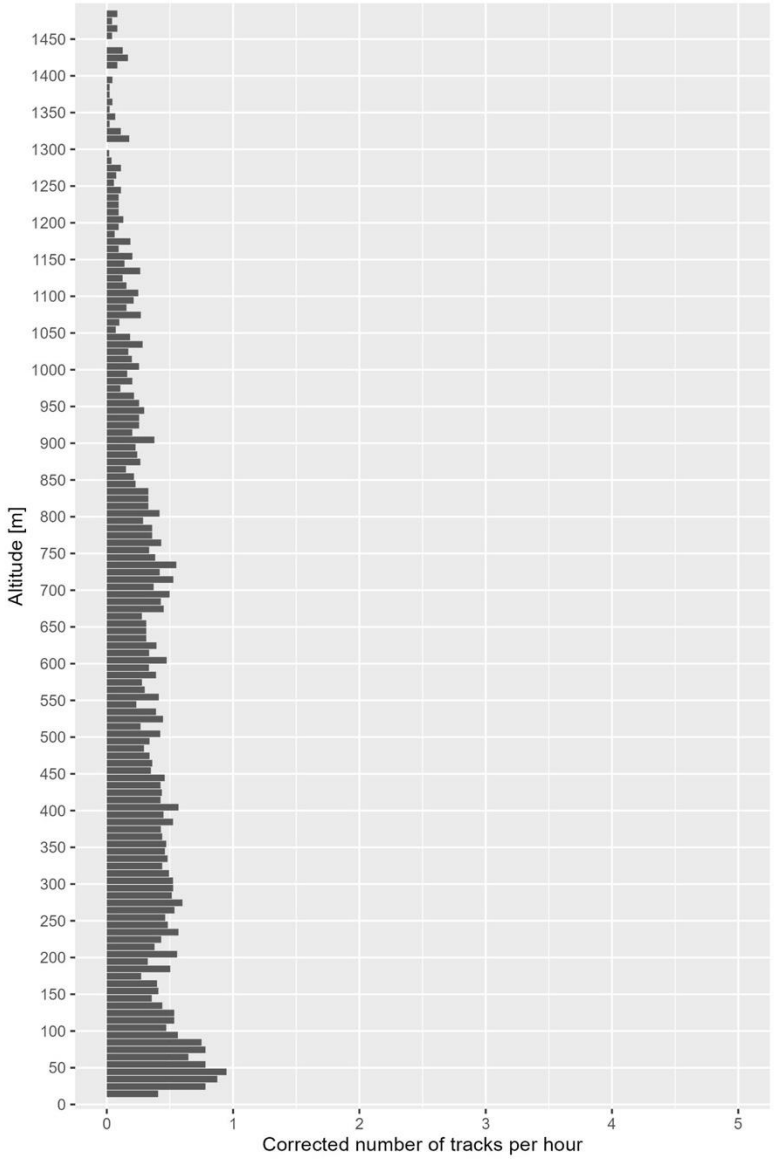


Figure 3.196. The distribution of bird flight altitudes recorded using vertical radar in August 2023 at survey station MB_02. The number of tracks was averaged with the total time devoted to the vertical radar data collection in that month

Results obtained at survey station MB_02 in September show (similarly to the ones from survey station MB_01) an increase in bird activity, especially up to the altitude of 75 m ASL. In October and November, the number of recorded tracks dropped back below 1 per hour, however, in October there were tracks recorded in the whole operational range of the vertical radar, whereas in November, the tracks were recorded only up to approximately 350 m ASL [Figure 3.197, Figure 3.198, Figure 3.199].

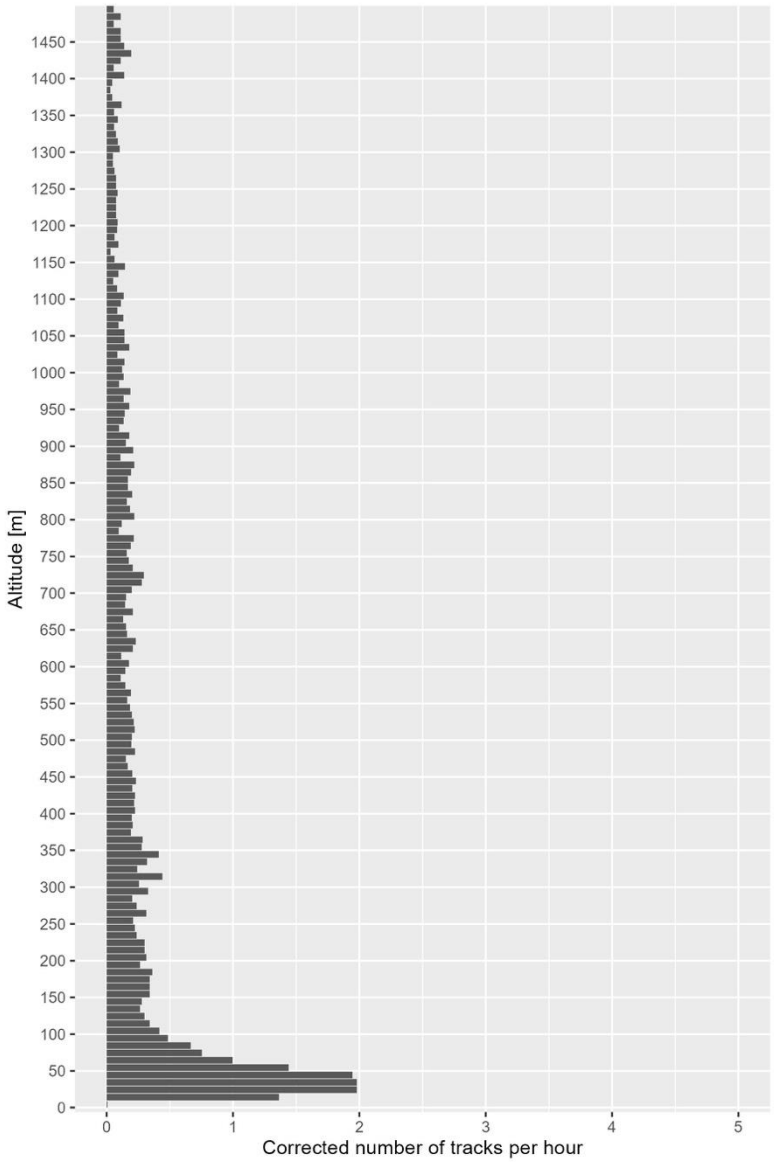


Figure 3.197. The distribution of bird flight altitudes recorded using vertical radar in September 2023 at survey station MB_02. The number of tracks was averaged with the total time devoted to the vertical radar data collection in that month

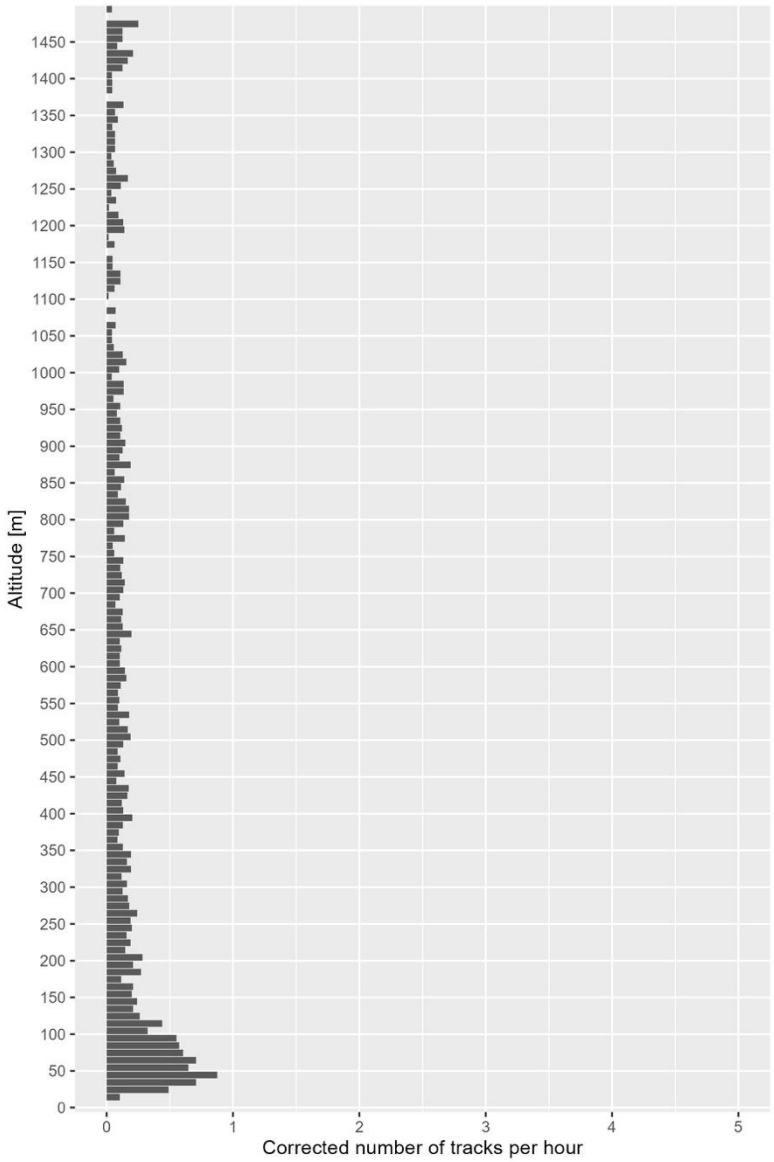


Figure 3.198. The distribution of bird flight altitudes recorded using vertical radar in October 2023 at survey station MB_02. The number of tracks was averaged with the total time devoted to the vertical radar data collection in that month

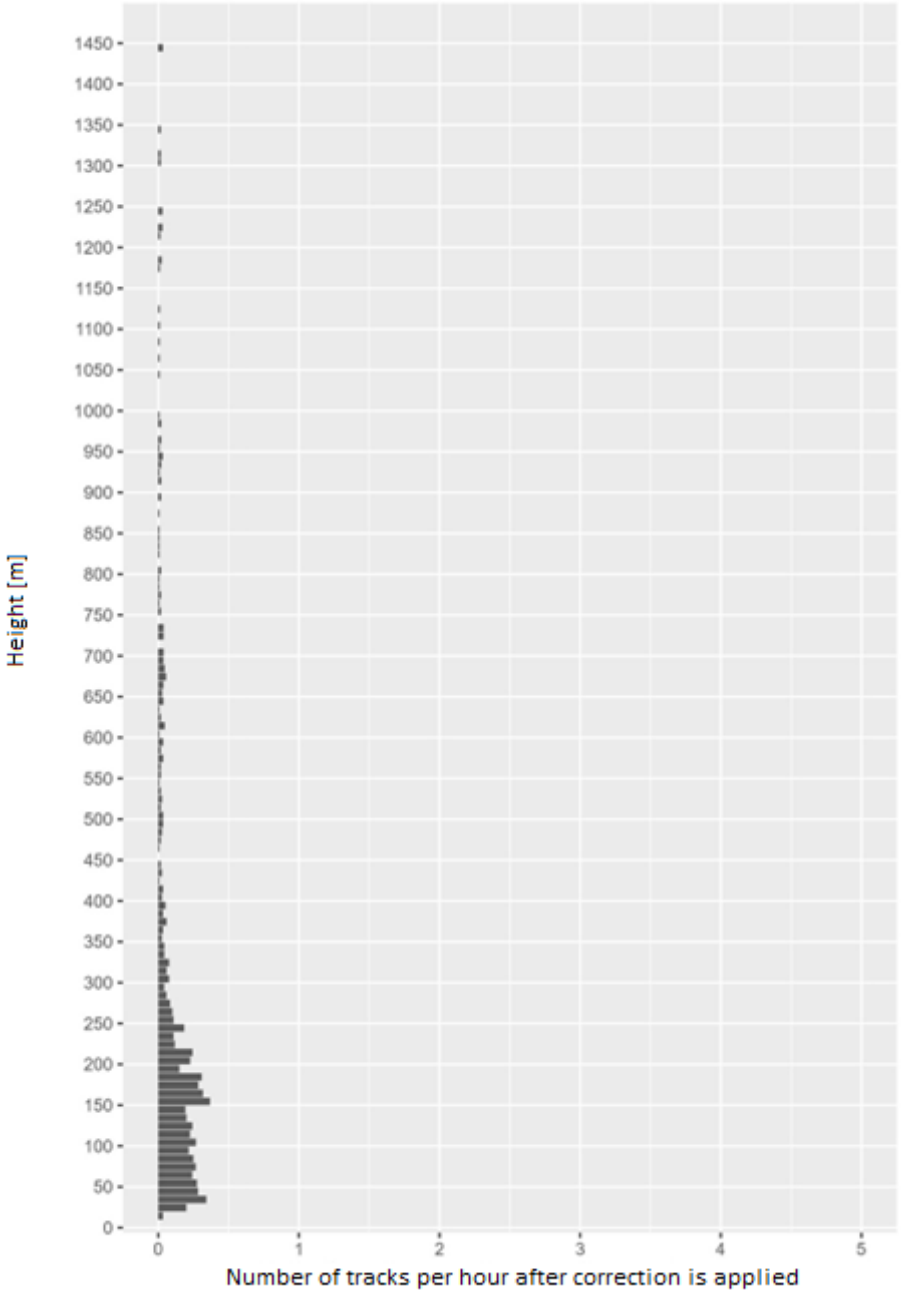


Figure 3.199. The distribution of bird flight altitudes recorded using vertical radar in November 2023 at survey station MB_02. The number of tracks was averaged with the total time devoted to the vertical radar data collection in that month

3.5.2.5.6 Acoustic monitoring

3.5.2.5.6.1 Spring migration

Based on the acoustic recordings conducted during the spring migration period, 23 bird species of diurnal migrants and 10 species of nocturnal migrants were tracked at survey station MB_01 [Table 3.111]. In cases when identification to species was impossible, birds were classified to 4 systematic groups with partial identification. A category of unidentified birds was used for unidentified calls

whenever determination of the taxonomic rank was impossible. In the entire period of spring migration studies, daytime vocal activity of birds was more pronounced [Figure 3.200].

The highest vocal diurnal activity was recorded for unidentified large gulls throughout the whole spring migration period (with the maximum vocal activity in March), and for goldcrests (only in April). Among gulls, 5 species were identified: black-headed gull, great black-backed gull, lesser black-backed gull, common gull, and herring gull being the most numerous. Vocal activity of small gulls (common gull or black-headed gull) was the highest in April, whilst the majority of large gulls' calls was recorded in March. Apart from the goldcrest, another frequently recorded passerine species was the white wagtail.

Despite the fact that gulls were most commonly recorded during daylight hours, unidentified large gulls were also the group most frequently recorded during the acoustic monitoring conducted at night [Table 3.111]. The highest vocal activity of passerines migrating at night was identified for thrushes (the common blackbird, redwing, song thrush).

Both diurnal and nocturnal migrants' vocal activity was the highest in April. There were almost no calls of nocturnal migrants in May, except for 1 call of a spotted flycatcher and 1 call of an unidentified passerine [Table 3.111,Figure 3.200].

Table 3.111. The summary of bird calls recorded at daylight and night hours at survey station MB_01 during the spring migration period

No.	Taxon		March	April	May	Total
	English name	Latin name				
Total of calls for daylight hours			**1653**	**1990**	**1106**	**4749**
1.	Unidentified large gull	*Larus indet.*	1459	868	1046	3373
2.	Goldcrest	*Regulus regulus*	0	638	0	638
3.	European herring gull	*Larus argentatus*	143	91	39	273
4.	White wagtail	*Motacilla alba*	2	104	8	114
5.	Common gull	*Larus canus*	15	75	0	90
6.	Yellowhammer	*Emberiza citrinella*	0	48	0	48
7.	Black-headed gull	*Chroicocephalus ridibundus*	0	44	0	44
8.	Great tit	*Parus major*	24	0	0	24
9.	Long-tailed duck	*Clangula hyemalis*	0	23	0	23
10.	Lesser black-backed gull	*Larus fuscus*	1	12	6	19
11.	Common chaffinch	*Fringilla coelebs*	1	11	0	12
12.	Unidentified bird	*Aves spec.*	0	12	0	12
13.	Common starling	*Sturnus vulgaris*	0	10	0	10
14.	Eurasian siskin	*Spinus spinus*	0	9	0	9
15.	Unidentified gull	*Laridae indet.*	0	9	0	9
16.	Unidentified passerine	*Passeriformes indet.*	1	8	0	9
17.	Eurasian blue tit	*Parus caeruleus*	0	8	0	8
18.	Meadow pipit	*Anthus pratensis*	0	6	1	7
19.	Great black-backed gull	*Larus marinus*	6	0	0	6
20.	Redwing	*Turdus iliacus*	1	0	4	5
21.	Song thrush	*Turdus philomelos*	0	5	0	5

No.	Taxon		March	April	May	Total
	English name	Latin name				
22.	European robin	*Erithacus rubecula*	0	3	0	3
23.	Common chiffchaff	*Phylloscopus collybita*	0	2	0	2
24.	Eurasian curlew	*Numenius arquata*	0	2	0	2
25.	Eurasian wigeon	*Anas penelope*	0	2	0	2
26.	Common linnet	*Linaria cannabina*	0	0	1	1
27.	Common whitethroat	*Sylvia communis*	0	0	1	1
Total calls for night hours			**278**	**450**	**2**	**730**
1.	Unidentified large gull	*Larus indet.*	25	172	0	197
2.	Common blackbird	*Turdus merula*	189	4	0	193
3.	Redwing	*Turdus iliacus*	7	110	0	117
4.	Song thrush	*Turdus philomelos*	2	75	0	77
5.	European herring gull	*Larus argentatus*	35	29	0	64
6.	Common gull	*Larus canus*	9	24	0	33
7.	European robin	*Erithacus rubecula*	7	13	0	20
8.	Eurasian curlew	*Numenius arquata*	0	15	0	15
9.	Lesser black-backed gull	*Larus fuscus*	0	7	0	7
10.	Unidentified duck	*Melanitta indet.*	3	0	0	3
11.	Unidentified passerine	*Passeriformes indet.*	0	1	1	2
12.	Black-headed gull	*Chroicocephalus ridibundus*	1	0	0	1
13.	Spotted flycatcher	*Muscicapa striata*	0	0	1	1
Total			**1931**	**2440**	**1108**	**5479**

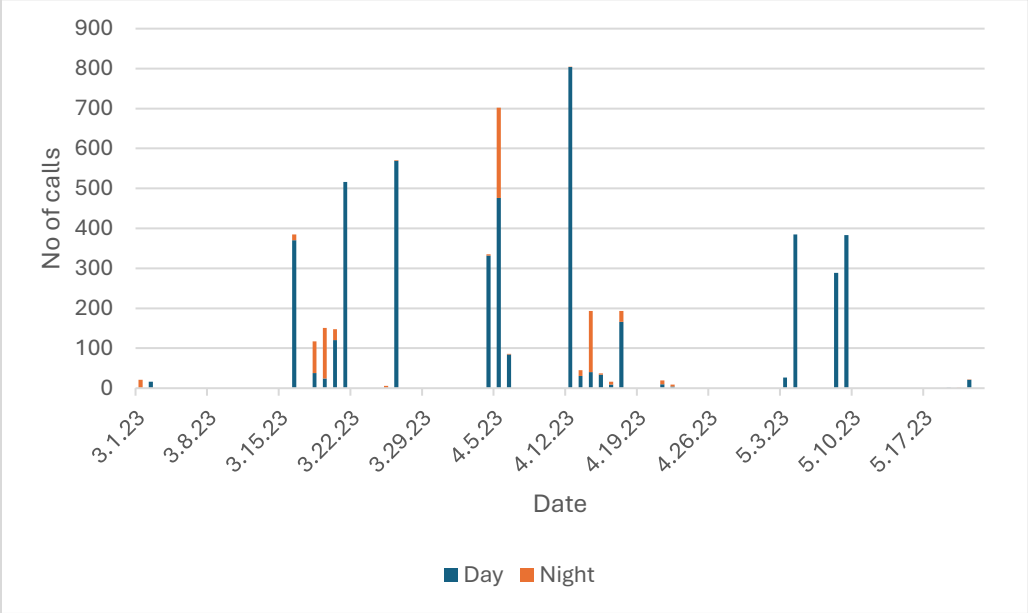


Figure 3.200. The number of bird calls in daylight and night hours recorded at survey station MB_01 in the spring migration period

Based on the acoustic recordings conducted at survey station MB_02, 19 bird species of diurnal migrants and 13 species of nocturnal migrants were recorded [Table 3.112]. The total number of calls

was lower than in the case of survey station MB_01. In the cases when identification to species was impossible, birds were classified to 3 systematic groups with partial identification. A category of unidentified birds was used for unidentified calls whenever determination of the taxonomic rank was impossible. During the spring migration study, daytime vocal activity of birds was more pronounced with an exception for the nocturnal migration in March [Figure 3.201]. In fact, this peak was due to numerous calls of common blackbirds recorded during a single recording session conducted on 16 March.

The highest diurnal activity was recorded for unidentified large gulls (with numerous calls recorded throughout the entire survey period and the peak of vocal activity in May) and for great tits (only in March). Among gulls, 5 species were identified (the black-headed gull, lesser black-backed gull, common gull, Mediterranean gull, and the herring gull being the most numerous species) were identified based on the calls recorded. In addition to the great tit, other passerines frequently recorded during daylight hours were the goldcrest and white wagtail.

Among nocturnal migrants, the most frequently recorded species was the common blackbird with the highest vocal activity in March [Table 3.112]. The song thrush, European robin, redwing, and Eurasian skylark were also recorded quite often.

Diurnal migrants' vocal activity was the highest (although not so strongly pronounced) in April whilst nocturnal migrants were recorded most numerously in March [Table 3.112]. Similarly to the records from survey station MB_01, there were almost no calls of nocturnal migrants in May, except for several calls of unidentified large gulls and unidentified passerines during one recording session on the 10 May [Figure 3.201].

Table 3.112. The summary of bird calls recorded at daylight and night hours at survey station MB_02 during the spring migration period

No.	Taxon		March	April	May	Total
	English name	Latin name				
Total of calls for daylight hours			**827**	**868**	**521**	**2216**
1.	Unidentified large gull	*Larus indet.*	378	265	401	1044
2.	Great tit	*Parus major*	290	0	0	290
3.	European herring gull	*Larus argentatus*	36	75	86	197
4.	Goldcrest	*Regulus regulus*	0	128	0	128
5.	White wagtail	*Motacilla alba*	0	112	3	115
6.	Unidentified gull	*Laridae indet.*	16	67	0	83
7.	Long-tailed duck	*Clangula hyemalis*	76	0	0	76
8.	European robin	*Erithacus rubecula*	0	48	0	48
9.	Common gull	*Larus canus*	2	41	0	43
10.	Common chaffinch	*Fringilla coelebs*	11	31	0	42
11.	Meadow pipit	*Anthus pratensis*	2	40	0	42
12.	Eurasian siskin	*Spinus spinus*	2	27	0	29
13.	Eurasian curlew	*Numenius arquata*	0	14	0	14
14.	Lesser black-backed gull	*Larus fuscus*	0	9	5	14
15.	Western yellow wagtail	*Motacilla flava*	0	0	13	13
16.	Eurasian skylark	*Alauda arvensis*	12	0	0	12
17.	Black-headed gull	*Chroicocephalus ridibundus*	0	0	8	8
18.	Unidentified bird	*Aves spec.*	0	4	0	4

No.	Taxon		March	April	May	Total
	English name	Latin name				
19.	Unidentified passerine	*Passeriformes indet.*	0	1	3	4
20.	Great tit/Eurasian blue tit	*Parus major/caeruleus*	0	3	0	3
21.	Mediterranean gull	*Ichthyaetus melanocephalus*	0	3	0	3
22.	Common blackbird	*Turdus merula*	2	0	0	2
23.	Tree pipit	*Anthus trivialis*	0	0	2	2
Total calls for night hours			**1054**	**575**	**23**	**1652**
1.	Common blackbird	*Turdus merula*	737	16	0	753
2.	Common gull	*Larus canus*	0	242	0	242
3.	European robin	*Erithacus rubecula*	49	96	0	145
4.	Redwing	*Turdus iliacus*	8	126	0	134
5.	Eurasian skylark	*Alauda arvensis*	126	0	0	126
6.	Unidentified large gull	*Larus sp.*	68	0	10	78
7.	Song thrush	*Turdus philomelos*	12	49	0	61
8.	European herring gull	*Larus argentatus*	53	0	0	53
9.	Eurasian wigeon	*Anas penelope*	0	29	0	29
10.	Unidentified passerine	*Passeriformes indet.*	0	3	13	16
11.	White wagtail	*Motacilla alba*	0	8	0	8
12.	Fieldfare	*Turdus pilaris*	0	3	0	3
13.	Eurasian curlew	*Numenius arquata*	0	2	0	2
14.	Mistle thrush	*Turdus viscivorus*	1	0	0	1
15.	Tree pipit	*Anthus trivialis*	0	1	0	1
Total			**1881**	**1443**	**544**	**3868**

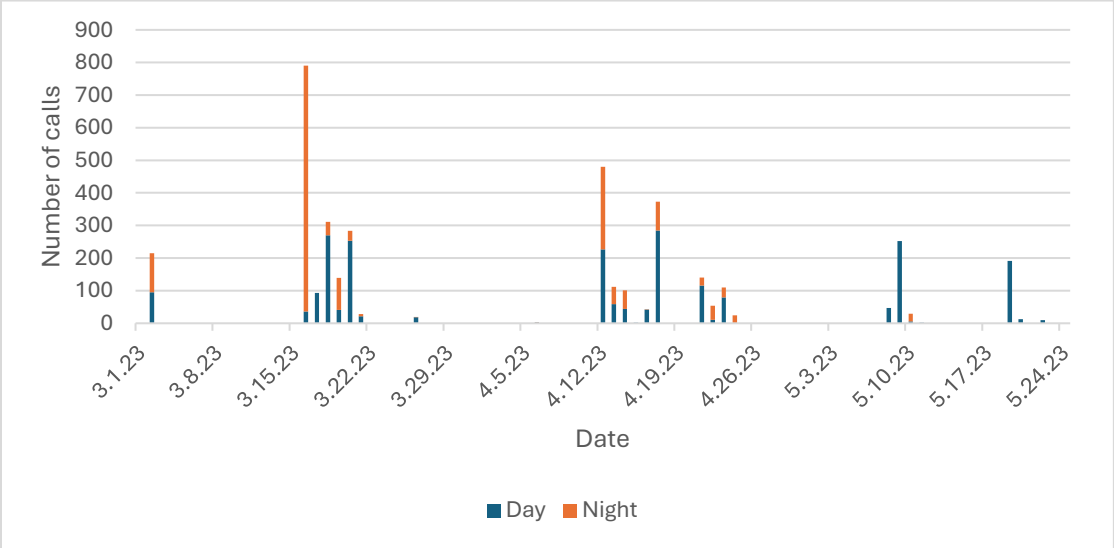


Figure 3.201. The number of bird calls in daylight and night hours recorded at survey station MB_02 in the spring migration period

3.5.2.5.6.2 Autumn migration

Based on the acoustic recordings conducted during the autumn migration at survey station MB_01, 5304 calls of 14 bird species were recorded during daylight hours (5 of these species were gulls) and 10 species were recorded during night time acoustic monitoring [Table 3.113]. In the cases when identification to species was impossible, birds were classified to 2 taxonomic groups with partial

identification (unidentified gulls and unidentified large gulls). During the entire period of autumn migration study, daytime vocal activity of birds was higher than night time activity. The highest numbers of calls, both in daylight and night hours, were recorded in September. There were almost no calls recorded in July (with the exception of a single call of a green sandpiper) and in December (11 calls of the herring gull and Caspian gull) [Table 3.113].

The highest vocal diurnal activity was recorded for the herring gull, Caspian gull, goldcrest, blue tit, and unidentified large gulls. Among gulls, 5 species were identified: the Caspian gull, common gull, herring gull, great black-backed gull and lesser black-backed gull.

The highest vocal activity among nocturnally migrating birds was identified for the song thrush, grey heron, European robin, redwing, and herring gull [Table 3.113]. There were no nocturnal migrant calls in July and November. Nocturnal migrants' vocal activity was the highest in September [

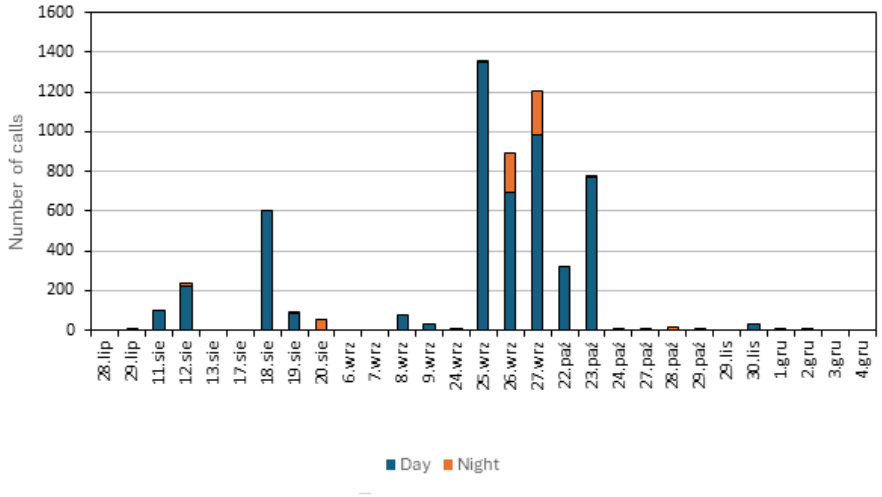


Figure 3.202].

Table 3.113. The summary of bird calls recorded at daylight and night hours at survey station MB_01 during the autumn migration period

No.	Taxon		July	August	September	October	November	December	Total
	English name	Latin name							
Total of calls in daylight hours			**1**	**1013**	**3150**	**1097**	**32**	**11**	**5304**
1.	Unidentified large gull	*Larus indet.*	0	268	1220	758	22	0	2268
2.	Caspian gull	*Larus cachinnans*	0	244	794	118	0	7	1163
3.	European herring gull	*Larus argentatus*	0	455	185	22	10	4	676
4.	Eurasian blue tit	*Parus caeruleus*	0	0	483	13	0	0	496
5.	Goldcrest	*Regulus regulus*	0	0	293	171	0	0	464
6.	Song thrush	*Turdus philomelos*	0	0	104	0	0	0	104
7.	White wagtail	*Motacilla alba*	0	0	36	0	0	0	36
8.	Common gull	*Larus canus*	0	22	0	12	0	0	34
9.	Unidentified gull	*Laridae indet.*	0	20	0	0	0	0	20

No.	Taxon		July	August	September	October	November	December	Total
	English name	Latin name							
10.	Lesser black-backed gull	*Larus fuscus*	0	2	17	0	0	0	19
11.	Common blackbird	*Turdus merula*	0	0	2	3	0	0	5
12.	European robin	*Erithacus rubecula*	0	0	5	0	0	0	5
13.	Great tit	*Parus major*	0	0	5	0	0	0	5
14.	Great black-backed gull	*Larus marinus*	0	2	2	0	0	0	4
15.	Meadow pipit	*Anthus pratensis*	0	0	4	0	0	0	4
16.	Green sandpiper	*Tringa ochropus*	1	0	0	0	0	0	1
Total of calls in night hours			**0**	**64**	**419**	**23**	**0**	**1**	**507**
1.	Song thrush	*Turdus philomelos*	0	0	362	0	0	0	362
2.	Grey heron	*Ardea cinerea*	0	51	0	0	0	0	51
3.	European robin	*Erithacus rubecula*	0	0	35	0	0	0	35
4.	Redwing	*Turdus iliacus*	0	0	3	21	0	0	24
5.	European herring gull	*Larus argentatus*	0	11	11	0	0	0	22
6.	Common snipe	*Gallinago gallinago*	0	0	4	0	0	0	4
7.	Caspian gull	*Larus cachinnans*	0	0	3	0	0	0	3
8.	Spotted flycatcher	*Muscicapa striata*	0	2	1	0	0	0	3
9.	Common blackbird	*Turdus merula*	0	0	0	1	0	0	1
10.	Common gull	*Larus canus*	0	0	0	0	0	1	1
11.	Unidentified large gull	*Larus indet.*	0	0	0	1	0	0	1

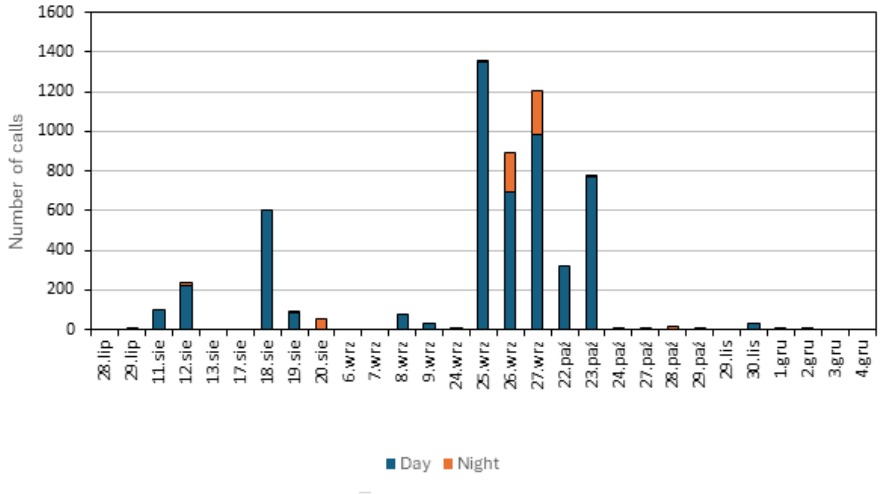


Figure 3.202. The number of bird calls in daylight and night hours recorded at survey station MB_01 in the autumn migration period

Based on the acoustic recordings conducted during the autumn migration period at survey station MB_02, 5441 calls of 14 bird species were recorded during daylight hours and 204 calls of 6 species were recorded during night-time acoustic monitoring [Table 3.114]. In the cases when identification to species was impossible, birds were classified to 2 taxonomic groups with partial identification

(unidentified gulls and unidentified large gulls). In the whole period of autumn migration studies, daytime vocal activity of birds was more pronounced than the night-time activity [Figure 3.203]. The diurnal vocal activity of birds was noticeably higher in August, September, and October [Table 3.114].

The highest vocal diurnal activity was recorded for the group of unidentified large gulls, the herring gull, Caspian gull, and goldcrest. Among gulls, 6 species were identified: the Caspian gull, black-headed gull, herring gull, great black-backed gull, common gull, and lesser black-backed gull.

The highest vocal activity of nocturnally migrating birds was identified for the redwing, song thrush, European robin, common blackbird, common chaffinch, and large gulls unidentified to species [Table 3.114]. There were no nocturnal migrant calls in July and August [Figure 3.203].

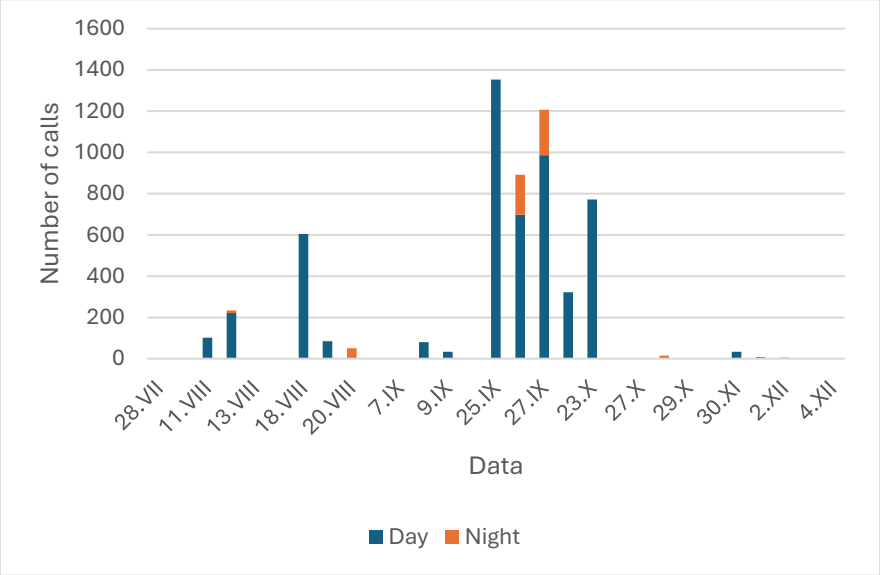


Table 3.114. The summary of bird calls recorded at daylight and night hours at survey station MB_02 during the autumn migration period

No.	Taxon		July	August	September	October	November	December	Total
	English name	**Latin name**							
Total of calls in daylight hours			**358**	**1452**	**1854**	**1205**	**105**	**467**	**5441**
1.	Unidentified large gull	*Larus indet.*	22	50	1039	1007	98	462	2678
2.	European herring gull	*Larus argentatus*	205	1099	0	0	3	5	1312
3.	White wagtail	*Motacilla alba*	0	0	477	0	0	0	477
4.	Caspian gull	*Larus cachinnans*	110	208	72	0	0	0	390
5.	Goldcrest	*Regulus regulus*	0	0	132	140	0	0	272
6.	Unidentified gull	*Laridae indet.*	7	80	0	0	0	0	87
7.	Common chaffinch	*Fringilla coelebs*	0	0	72	0	0	0	72
8.	Twite	*Linaria flavirostris*	0	0	0	50	0	0	50
9.	European robin	*Erithacus rubecula*	0	0	20	0	2	0	22
10.	Great black-backed gull	*Larus marinus*	14	5	0	0	0	0	19
11.	Western yellow wagtail	*Motacilla flava*	0	0	19	0	0	0	19
12.	Lesser black-backed gull	*Larus fuscus*	0	3	15	0	0	0	18
13.	Redwing	*Turdus iliacus*	0	0	2	8	0	0	10

No.	Taxon		July	August	September	October	November	December	Total
	English name	Latin name							
14.	Black-headed gull	*Chroicocephalus ridibundus*	0	7	0	0	0	0	7
15.	Song thrush	*Turdus philomelos*	0	0	6	0	0	0	6
16.	Common gull	*Larus canus*	0	0	0	0	2	0	2
Total of calls in night hours			**0**	**0**	**68**	**48**	**85**	**3**	**204**
1.	Unidentified large gull	*Larus indet.*	0	0	0	1	73	0	74
2.	Redwing	*Turdus iliacus*	0	0	1	32	3	0	36
3.	Song thrush	*Turdus philomelos*	0	0	32	0	0	0	32
4.	European robin	*Erithacus rubecula*	0	0	17	4	2	0	23
5.	Common blackbird	*Turdus merula*	0	0	1	11	4	1	17
6.	Common chaffinch	*Fringilla coelebs*	0	0	17	0	0	0	17
7.	European herring gull	*Larus argentatus*	0	0	0	0	3	2	5

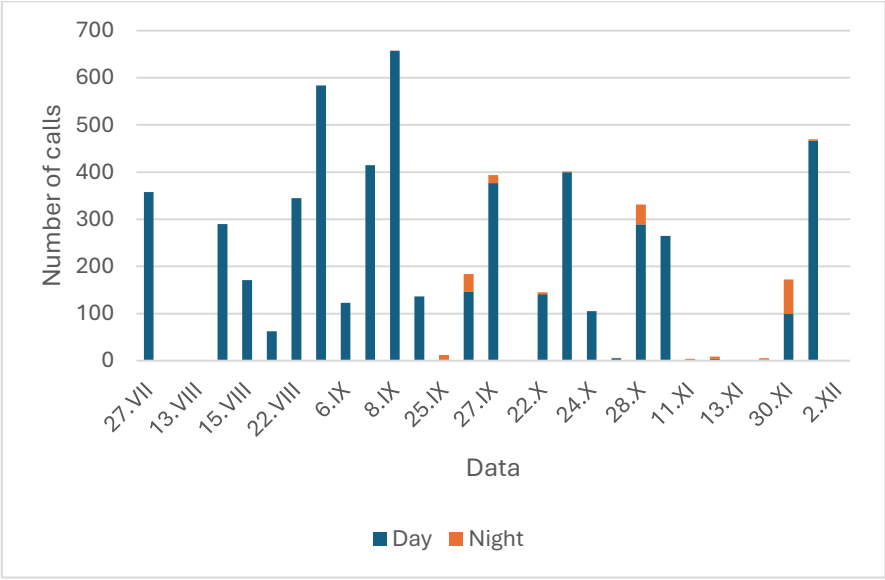


Figure 3.203. The number of bird calls in daylight and night hours recorded at survey station MB_02 in the autumn migration period

3.5.2.6 Summary of results and conclusions

Baltica-1 OWF is located in close proximity to the Swedish border and the Natura 2000 site *Hoburgs bank och Midsjöbankarna* (SE0330308, type: habitat and bird protection). The southern part of the Middle Bank is excluded from the above-mentioned Natura 2000 site, and it has been an IBA (Important Bird Area) since 2016 (Ramirez, 2010; Länsstyrelsen Kalmar län, 2021). The Natura 2000 site *Hoburgs bank och Midsjöbankarna* (SE0330308) is a protected habitat area where shoals and reefs are the subjects of protection. Bird species referred to in Article 4 of Directive 2009/147/EC and listed in Annex II of Directive 92/43/EEC are the long-tailed duck and common eider, which are diving benthophages, and the black guillemot (which is an ichthyophage).

A total of 120 species were recorded based on visual observations and acoustic monitoring during the winter surveys of local movements as well as the spring and autumn migration surveys [Table 3.115].

The local migration study was performed in December 2022 and January and February 2023 at two survey stations: LP_01 and LP_02. In total, 24 species were recorded at the two stations. The number of species at both stations was similar, as well as the species composition. Similar results regarding species composition were obtained during reference studies performed for Baltic Power OWF (Opioła et al., 2020). Beside auks (the common guillemot and razorbill) and long-tailed ducks, all the other species were observed in rather low numbers, not exceeding 1% of the observations. Although the Natura 2000 site *Hoburgs bank och Midsjöbankarna* refers to the black guillemot as a protected species, surveys conducted for Baltica-1 OWF and Baltic Power OWF in 2018/2019 shown that the most abundant species of the auk family are the razorbill and common guillemots, while the black guillemot is observed rather sparsely. Ichthyophages (auks) were the dominating foraging group in the area, followed by benthophages – seaducks. This is in contrast to winter surveys conducted on the Middle Bank for the Baltic Power OWF in 2019, which indicated that the prevailing species in the area is the long-tailed duck, however the general pattern with auks and long-tailed ducks being the most numerous in the area, is the same.

Flight altitude data obtained from the visual observations performed for the winter movement monitoring shows that 98–99% (the variability among stations) of all the observed seabirds were flying at altitudes not exceeding 20 m ASL and there were no observations at altitudes higher than 100 m ASL. This is due to the fact that visual observations provide data on flight altitudes that should be used only as an aid to understand the movement of birds flying relatively low above the sea level. At higher altitudes, the vertical radar is more reliable in detecting birds. A peak of bird activity was detected almost in all months between 30 and 60 m. These results are similar to the results obtained during surveys performed on the Middle Bank in 2019 for Baltic Power OWF (81.7% of all the observed birds flew at altitudes not exceeding 20 m and 2.4% of observations were higher than 100 m ASL) (Opioła et al., 2020).

In December, at both stations, a relatively high bird activity was detected at altitudes from 10 up to 230, and 280 m. This is due to capturing some of late migrants flying across the Baltic Sea (for example birds of prey, pigeons). Low detection levels in January are reflected also by a decreased abundance of birds in visual observations and lower number of tracks registered by the horizontal radar. Lower number of seabirds in January was also reported during the Baltic Power OWF surveys. Knowing, that the most important wintering ground for long-tailed ducks in the area is the Słupsk Bank, low numbers encountered at the survey stations in the southern end of the Middle Bank were expected, as it is not a primary wintering ground of that species. Elevated numbers in February could suggest that some of the long-tailed ducks had already started their spring migration; the migration peak should occur in April (Nilsson et al., 2016; Bellebaum et al., 2014).

Razorbills were the most frequently recorded seabirds with the highest numbers observed in February (over 1000 individuals at both stations) when the numbers were approximately ten times higher than in December and January. According to HELCOM, the razorbill population in the Baltic Sea is currently experiencing a moderate increase (HELCOM and Helsinki Commission, 2013). When comparing the numbers encountered in 2019 (Opioła et al., 2020) and during this survey in winter 2022/2023, it seems that there are more razorbills present in the survey area. However, the methods used in the two surveys are different (transect surveys in 2019 versus stationary surveys in the surveys discussed in this Report)

and the seasonal fluctuations might be substantial, so it is difficult to form general conclusions about population trends in the Middle Bank based on those two surveys only.

General movement directions point at NE (towards shallower waters of the Middle Bank) and SW. NE direction was especially pronounced at survey station LP_01, which is located slightly further away from the Middle Bank. This was true for the majority of observed benthic and pelagic feeders with the exception of divers, which flew predominantly in NW direction.

At survey station LP_02 located within the Baltica-1 OWF area, the movements in both, the above-mentioned NE and SW directions are also visible when all the recorded tracks are analysed together. Treated individually, the tracks of the long-tailed duck show different directions with dominating N and W direction. The interpretation of such pattern could be that survey station LP_02 was capturing locally resting long-tailed ducks tat were utilising the area in the close proximity to the survey station as foraging grounds.

Spring and autumn migration surveys were performed at two survey stations: MB_01 and MB_02, which are located in the area intended for the construction of Baltica-1 OWF, from March to May 2023 and from July to December 2023, respectively. In total, 96 bird species were observed and recorded at both stations during spring surveys and 106 species were reported in course of the autumn migration studies. The number of species at both stations was similar, as well as the species composition.

During the spring migration studies, the area was dominated by long-tailed ducks, common scoters, and razorbills at both stations with long-tailed ducks being the most frequently encountered. According to the estimates, it is expected that more than 26,000, slightly over 81,000 and close to 3800 of long-tailed ducks flew through the survey area in March, April and May, respectively. During the autumn migration studies, the most numerous species were the common scoter and long-tailed duck followed by the common chaffinch and great cormorant. Based on the flux estimates, it is expected that more than 80,000 of common scoters and over 13,000 of long-tailed ducks can cross the survey area in July and November, respectively. This relatively intense migration of the common scoter in early autumn months is related to their moulting period. Shortly after breeding, males head towards their staging grounds where during moult they become flightless. While the long-tailed duck was abundant during both spring and autumn surveys, the common scoter was observed more numerously only in spring months (except for observations performed in July). The low abundance of common scoter during autumn migration studies may be related to the different migration routes to the wintering grounds in the Kattegat, Pomeranian Bay, and the Gulf of Gdańsk. Common scoters nesting on the coasts of Sweden and Finland follow the coastline route in a westerly direction before crossing the Baltic Sea to reach Pomeranian Bay. Such movement pattern is similar to the results obtained for the Baltic Power OWF surveys (Opioła et al 2020). Long-tailed ducks are regularly and commonly observed in the Baltic Sea from October to May, where they winter in large numbers on sandy shallows of the Hoburgs Bank, northern and southern parts of the Middle Bank and Słupsk Bank (Zydelis et al., 2015a; Zydelis et al., 2015b; Bednarska et al., 2017; Gajko et al., 2018; Opioła et al., 2020; Gajewski et al., 2021). Baltica-1 OWF is located in close proximity to the Natura 2000 site *Hoburgs bank och Midsjöbankarna* and the southern parts of the Middle Bank, hence the almost constant presence of long-tailed ducks throughout the whole survey period. The Baltic winter population, which is centred on Pomeranian Bay, the Irbe Strait in the Gulf of Riga, the Hoburgs Bank and the Middle Bank, declined to approximately 1,500,000 birds by the end of the first decade of 21st century (Skov et al., 2011).

During spring migration studies relatively high numbers of unidentified geese were also observed at survey station MB_01 while a lot of unidentified waders were observed at survey station MB_02. The other species of auks (the common and black guillemot) and other seaducks (i.e. the velvet scoter, common eider, common goldeneye, and greater scaup) were observed in lower numbers. Unidentified geese, ducks (the long-tailed duck and common scoter included) and auks (the razorbill included) were also noted during autumn migration surveys, but the numbers were comparatively lower than in spring. Auks (mainly the razorbill and common guillemot) were observed throughout the spring and autumn surveys, although the spring numbers were relatively higher, especially in March and April. As the main wintering grounds for the Baltic populations are located in the Gulf of Riga and the Irbe Strait, the numbers of auks observed in the survey area are moderately low (HELCOM, 2009). The general species composition and dominant species abundance are in line with reference studies performed for the Baltic Power OWF (Opioła et al., 2020).

Passerines (mainly unidentified to species) were observed throughout the whole periods of spring and autumn migration surveys except July as most of the species were then still present at their breeding grounds. According to the estimates, more than 33,000 and 45,000 passerines may fly across the survey area in April and September, respectively. As the flux calculations are based on visual observation results (limited to light hours of a day), these estimates concern exclusively the species of diurnal migrants. Most likely, the values for nocturnal migrant species vastly exceed these numbers.

Flight altitude data obtained from the visual observations conducted in spring shows that 85–91% (mind the variability among stations) of all observed birds were flying at altitudes not exceeding 20 m ASL. The most numerous species observed at both survey stations was the long-tailed duck with the majority of birds flying at the altitude of up to 10 m ASL. Only about 0.05% of long-tailed ducks flew above 20 m ASL at both stations. These results are similar to the ones obtained during surveys performed on the Middle Bank in 2019 for Baltic Power OWF where only 1% (overall) of long-tailed ducks flew above 20 m ASL (Opioła et al., 2020). Several species were observed at altitudes in a range from 21 to 100 m ASL, but the numbers were relatively low (10 and 12% of all observed birds at survey stations MB_01 and MB_02, respectively). Only 2–7% of all birds were observed at altitudes exceeding 100 m ASL. This is because visual observations provide data on flight altitude that should be used as an aid to understand the movement of birds flying relatively low above sea level. At greater altitudes, the vertical radar is considered more reliable in detecting birds.

In April, the radars detected relatively high bird activity at altitudes from 10 up to 100 m at both stations and an altitude from 1400 to 1500 m at survey station MB_02. Lower detection rates in March and May are reflected by the visual observations and the number of tracks registered by the horizontal radar. Low numbers encountered in March were expected as for some of the species, this time is an onset of their spring migration. Elevated numbers recorded in April indicate the spring migration peak occurring this month while the migration intensity recorded in May follows a more mixed pattern.

The general movement direction points at NE-E at the two stations. For seaducks (the long-tailed duck, common scoter, velvet scoter), there clearly dominated the NE-E direction as in the case of all tracks analysed together; for geese, two main directions dominated: NW-W and NE-E, all pointing into direction of the breeding sites located in northern Russia, Finland, and Sweden (Skov et al., 2011; Bellebaum et al., 2014). The auks showed the NW-N flight direction, which is in line with the knowledge about their European breeding sites in Denmark and Sweden.

The main purpose of the acoustic analysis was to identify species migrating at night. This analysis also allows to compare migration dynamics for individual species during daytime and at night. In total, in spring there were 9347 bird calls registered. Almost half of those calls belonged to large gulls (e.g. the herring gull, great-black backed gull) – 4241 calls. There is no clear pattern in temporal voice activity of large gulls, however, high numbers of calls were recorded in March. This activity does not necessarily explain migration movements, since large gulls are most likely breeding locally (on the coast of Sweden, Gotland, and Poland) and remain in the region the whole year. Passerine calls were registered most frequently in April (with an exception for the common blackbird and Eurasian skylark, which migrated mainly in March) express the migration movements toward their breeding sites in Scandinavia. Gulls were recorded most often during light hours. Among the nocturnal migrants, the most numerous were the common blackbird followed by the redwing, European robin, and song thrush, while to the group of diurnal migrants there belonged the great tit, white wagtail, and goldcrest. There were almost no nocturnal migrant calls in May, except for several calls of unidentified large gulls and unidentified passerines.

Flight altitude data obtained from the visual observations conducted in autumn show that 88–89% of all observed birds were flying at altitudes not exceeding 20 m ASL. The most numerous species observed at survey station MB_01 was the common scoter while at survey station MB_02, it was the long-tailed duck. Most of these birds were flying at altitudes no higher than 10 m ASL. Only about 2.6% of long-tailed ducks and approximately 3.4% of common scoters flew above 20 m ASL at both stations. Several species were observed at altitudes from 21 up to 100 m ASL, but their numbers were relatively low as usually single individuals were recorded (12% and 11% of all observed birds at MB_01 and MB_02, respectively). The only species observed in the range between 101 and 200 m ASL were the osprey (1 individual) and the common swift (2 individuals).

In July and August, the vertical radars detected relatively low bird activity at all altitudes, with the highest reading of around 1 track per hour in August from 10 up to 100 m at both stations. Lower detection rates recorded in July (with a maximum of 0.5 track per hour) are reflected by the visual observations and the number of tracks registered by the horizontal radar. Low detection numbers encountered in July were expected as autumn migration is just at its onset at the time and not many species have started their migration already. In September, the number of tracks increased. Especially up to the level of 75 m ASL, the number of echoes recorded by the radar tripled. In October and November, the number of recorded tracks drops back again below one track per hour at all altitudes. In October, the flight activity was more distinct at altitudes up to 100 m ASL at survey station MB_01 and recorded in the whole operational range of the radar (up to 1500 m ASL) at survey station MB_02, while in November, a very low number of tracks (less than 0.5 track per hour) was observed up to 350 m ASL at both stations. The track intensities recorded in September–November are below the expected values. We can only assume that due to adverse weather conditions (strong storm front, strong wind), the migration peak might have occurred outside of the registration period but we are not able to determine the exact reason for this at this point.

The general pattern of movement on both stations was as predicted for autumn migration – the majority of birds flew S-SW-W, with a small portion of birds flying in opposite directions N-NE-E. With respect to seaducks (the long-tailed duck, common scoter, and velvet scoter), there dominated the SW-W direction, which indicates the direction of their winter grounds in the Danish Straits and Kattegat. However, there was a portion of long-tailed ducks observed in November and December at survey station MB_01 flying in NW and NE direction (21% for each month). Auks were tracked in all directions

with the most dominant movement pattern showing the opposite directions of W-SW and E-NE. This suggests that the tracked auks were most likely local birds performing short trips and not necessarily participating in seasonal migrations. Scattered movement patterns were recorded for the lesser black-backed gull at survey station MB_01 and the little gull observed at both stations, which also suggests that the recorded birds were performing seasonal migration only to some extent and a bigger portion of those gulls were local. Lesser black-backed gulls recorded at survey station MB_02 show a more specified movement pattern with almost all tracks falling within the W-S direction.

In total, in autumn, there were 11,456 bird calls registered, of which 78% belonged to gull species. This activity does not necessarily explain migration movements, since large gulls are most likely locally breeding (on the coasts of Sweden, Gotland, and Poland) and remaining in the region the whole year. The diurnal vocal activity of birds was noticeably higher in August. Apart from gulls, a relatively high number of calls was also recorded for the goldcrest and blue tit (at survey station MB_01 only). The highest diurnal vocal activity was recorded in September at both stations while any activity was hardly noted at survey station MB_01 in July (single calls only), November (32 calls), and December (11 calls). The highest vocal activity among nocturnally migrating birds was identified for the song thrush, grey heron, European robin, redwing, common blackbird, common chaffinch, and herring gull. Nocturnal migrants' vocal activity was the highest in September at survey station MB_01 and in November at survey station MB_02. There were no nocturnal migrants' calls recorded in July at any of the stations, in November at survey station MB_01, and in August at survey station MB_02.

Among all the species recorded during the surveys, two are considered "endangered" on the European scale (according to the international scale of the IUCN (BirdLife International, 2021): the common eider and Arctic skua (although they were recorded only in very small numbers). Seven species belong to the "near threatened" category: the Eurasian curlew, bar-tailed godwit, common swift, horned grebe, tufted duck, red-breasted merganser, and ruff. Ten species are recognised as "vulnerable": the black-legged kittiwake, common pochard, common snipe, curlew sandpiper, velvet scoter, rook, red-necked grebe, tundra swan, northern lapwing, and northern pintail [Table 3.115].

Two species (in the wintering populations) are considered "critically endangered" according to HELCOM: the black-throated diver and the red-throated diver. Wintering populations of four species are recognised as "endangered": bean goose, common scoter, red-necked grebe, and long-tailed duck. European population of the Mediterranean gull (both wintering and breeding) as well as the dunlin (both wintering and breeding, however, this concerns the *C.a. schinzii* subspecies only) and the breeding population of black-legged kittiwake are also considered "endangered". Five species belong to the "near threatened" category: the common ringed plover, little gull, northern lapwing, northern wheatear, and tufted duck. Eight species were recognised as "vulnerable": the Caspian tern, common eider, greater scaup, horned grebe, lesser black-backed gull, red-breasted merganser, ruff, and velvet scoter as well as the wintering population of the black-legged kittiwake [Table 3.115].

Twenty-three of all observed and recorded species are listed in Annex I of the Birds Directive.

Table 3.115. The conservation status of migrating bird species observed and recorded during the local winter movement studies, and the spring and autumn surveys conducted from December 2022 to December 2023

No.	Species		Species protection in Poland[1]	Annex 1 of the Birds Directive	IUCN[2]	HELCOM Red List category[3]
	English name	Latin name				
1.	Arctic tern	*Sterna paradisaea*	SP	Yes	LC	
2.	Bar-tailed godwit	*Limosa lapponica*	SP	Yes	NT	
3.	Barn swallow	*Hirundo rustica*	SP	No	LC	
4.	Barnacle goose	*Branta leucopsis*	SP	Yes	LC	
5.	Bean goose	*Anser fabalis*	GS	No	LC	EN (wp)
6.	Black guillemot	*Cepphus grylle*	SP	No	LC	
7.	Black tern	*Chlidonias niger*	SP	Yes	LC	
8.	Black-headed gull	*Chroicocephalus ridibundus*	SP	No	LC	
9.	Black-legged kittiwake	*Rissa tridactyla*	SP	No	VU	EN (bp) VU (wp)
10.	Black-throated diver	*Gavia arctica*	SP	Yes	LC	CR (wp)
11.	Eurasian blue tit	*Parus caeruleus*	SP	No	LC	
12.	Brambling	*Fringilla montifringilla*	SP	No	LC	
13.	Caspian gull	*Larus cachinnans*	SP	No	LC	
14.	Caspian tern	*Hydroprogne caspia*	SP	No	LC	VU
15.	Common blackbird	*Turdus merula*	SP	No	LC	
16.	Common chaffinch	*Fringilla coelebs*	SP	No	LC	
17.	Common chiffchaff	*Phylloscopus collybita*	SP	No	LC	
18.	Common crane	*Grus grus*	SP	Yes	LC	
19.	Common eider	*Somateria mollissima*	SP	No	EN/NT	VU (bp) EN (wp)
20.	Common goldeneye	*Bucephala clangula*	SP	No	LC	
21.	Common guillemot	*Uria aalge*	SP	No	LC	
22.	Common gull	*Larus canus*	SP	No	LC	
23.	Common kestrel	*Falco tinnunculus*	SP	No	LC	
24.	Common linnet	*Linaria cannabina*	SP	No	LC	
25.	Goosander	*Mergus merganser*	SP	No	LC	
26.	Common pigeon	*Columba livia*	PP	No	LC	
27.	Common pochard	*Aythya ferina*	GS	No	VU	
28.	Common redpoll	*Acanthis flammea*	SP	No	LC	
29.	Common redstart	*Phoenicurus phoenicurus*	SP	No	LC	
30.	Common reed bunting	*Emberiza schoeniclus*	SP	No	LC	
31.	Common ringed plover	*Charadrius hiaticula*	SP	No	LC	NT
32.	Common scoter	*Melanitta nigra*	SP	No	LC	EN (wp)
33.	Common shelduck	*Tadorna tadorna*	SP	No	LC	LC

No.	Species		Species protection in Poland[1]	Annex 1 of the Birds Directive	IUCN[2]	HELCOM Red List category[3]
	English name	Latin name				
34.	Common snipe	*Gallinago gallinago*	SP	No	VU/LC	
35.	Common starling	*Sturnus vulgaris*	SP	No	LC	
36.	Common swift	*Apus apus*	SP	No	NT/LC	
37.	Common tern	*Sterna hirundo*	SP	Yes	LC	
38.	Common whitethroat	*Sylvia communis*	SP	No	LC	
39.	Common wood pigeon	*Columba palumbus*	GS	No	LC	
40.	Curlew sandpiper	*Calidris ferruginea*	SP	No	VU/NT	
41.	Dunlin	*Calidris alpina*	SP	No	LC	EN (*schinzii*)
42.	Dunnock	*Prunella modularis*	SP	No	LC	
43.	Eurasian blackcap	*Sylvia atricapilla*	SP	No	LC	
44.	Eurasian curlew	*Numenius arquata*	SP	No	NT	
45.	Eurasian siskin	*Spinus spinus*	SP	No	LC	
46.	Eurasian skylark	*Alauda arvensis*	SP	No	LC	
47.	Eurasian sparrowhawk	*Accipiter nisus*	SP	No	LC	
48.	Eurasian teal	*Anas crecca*	GS	No	LC	
49.	Eurasian tree sparrow	*Passer montanus*	SP	No	LC	
50.	Eurasian wigeon	*Anas penelope*	SP	No	LC	
51.	Eurasian wren	*Troglodytes troglodytes*	SP	No	LC	
52.	European golden plover	*Pluvialis apricaria*	SP	Yes	LC	
53.	Greenfinch	*Chloris chloris*	SP	No	LC	
54.	European nightjar	*Caprimulgus europaeus*	SP	Yes	LC	
55.	European robin	*Erithacus rubecula*	SP	No	LC	
56.	Fieldfare	*Turdus pilaris*	SP	No	LC	
57.	Gadwall	*Anas strepera*	SP	No	LC	
58.	Goldcrest	*Regulus regulus*	SP	No	LC	
59.	Great black-backed gull	*Larus marinus*	SP	No	LC	
60.	Great black cormorant	*Phalacrocorax carbo*	PP	No	LC	
61.	Great crested grebe	*Podiceps cristatus*	SP	No	LC	
62.	Great egret	*Ardea alba*	SP	Yes	LC	
63.	Great tit	*Parus major*	SP	No	LC	
64.	Greater scaup	*Aythya marila*	SP	No	LC	VU
65.	Greater white-fronted goose	*Anser albifrons*	GS	No	LC	
66.	Green sandpiper	*Tringa ochropus*	SP	No	LC	
67.	Grey heron	*Ardea cinerea*	PP	No	LC	
68.	European sand martin	*Pluvialis squatarola*	SP	No	LC	
69.	Greylag goose	*Anser anser*	GS	No	LC	
70.	European herring gull	*Larus argentatus*	PP	No	LC	

No.	Species		Species protection in Poland[1]	Annex 1 of the Birds Directive	IUCN[2]	HELCOM Red List category[3]
	English name	Latin name				
71.	Hooded crow	*Corvus corone cornix*	PP	No	LC	
72.	Horned grebe	*Podiceps auritus*	SP	Yes	NT/VU	VU (bp) NT (wp)
73.	Lesser black-backed gull	*Larus fuscus*	SP	No	LC	VU
74.	Lesser whitethroat	*Sylvia curucca*	SP	No	LC	
75.	Little gull	*Larus minutus*	SP	Yes	LC	NT
76.	Long-eared owl	*Asio otus*	SP	No	LC	
77.	Long-tailed duck	*Clangula hyemalis*	SP	No	LC/VU	EN (wp)
78.	Long-tailed skua	*Stercorarius longicaudus*	SP	No	LC	
79.	Mallard	*Anas platyrhynchos*	GS	No	LC	
80.	Meadow pipit	*Anthus pratensis*	SP	No	LC	
81.	Mediterranean gull	*Ichthyaetus melanocephalus*	SP	Yes	LC	EN
82.	Mistle thrush	*Turdus viscivorus*	SP	No	LC	
83.	Mute swan	*Cygnus olor*	SP	No	LC	
84.	Northern lapwing	*Vanellus vanellus*	SP	No	VU/NT	NT
85.	Pintail	*Anas acuta*	SP	No	VU/LC	
86.	Northern shoveler	*Anas clypeata*	SP	No	LC	
87.	Northern wheatear	*Oenanthe oenanthe*	SP	No	LC	NT
88.	Osprey	*Pandion haliaetus*	SP	Yes	LC	
89.	Arctic skua	*Stercorarius parasiticus*	SP	No	EN/LC	
90.	Pomarine skua	*Stercorarius pomarinus*	SP	No	LC	
91.	Razorbill	*Alca torda*	SP	No	LC	
92.	Red knot	*Calidris canutus*	SP	No	LC/NT	
93.	Red-breasted merganser	*Mergus serrator*	SP	No	NT/LC	VU
94.	Red-necked grebe	*Podiceps grisegena*	SP	No	VU/LC	EN (wp)
95.	Red-throated diver	*Gavia stellata*	SP	Yes	LC	CR (wp)
96.	Redwing	*Turdus iliacus*	SP	No	LC/NT	
97.	Rook	*Corvus frugilegus*	PP	No	VU/LC	
98.	Ruff	*Philomachus pugnax*	SP	Yes	NT/LC	VU
99.	Sand martin	*Riparia riparia*	SP	No	LC	
100.	Sanderling	*Calidris alba*	SP	No	LC	
101.	Sandwich tern	*Sterna sandvicensis*	SP	Yes	LC	LC
102.	Short-eared owl	*Asio flammeus*	SP	Yes	LC	
103.	Smew	*Mergellus albellus*	SP	Yes	LC	
104.	Snow bunting	*Plectrophenax nivalis*	SP	No	LC	
105.	Song thrush	*Turdus philomelos*	SP	No	LC	
106.	Spotted flycatcher	*Muscicapa striata*	SP	No	LC	

No.	Species		Species protection in Poland[1]	Annex 1 of the Birds Directive	IUCN[2]	HELCOM Red List category[3]
	English name	Latin name				
107.	Stock dove	*Columba oenas*	SP	No	LC	
108.	Tree pipit	*Anthus trivialis*	SP	No	LC	
109.	Tufted duck	*Aythya fuligula*	GS	No	NT/LC	NT
110.	Tundra swan	*Cygnus columbianus*	SP	No	VU/LC	
111.	Twite	*Linaria flavirostris*	SP	No	LC	
112.	Velvet scoter	*Melanitta fusca*	SP	No	VU	VU (bp) EN (wp)
113.	Western marsh harrier	*Circus aeruginosus*	SP	Yes	LC	
114.	Eurasian whimbler	*Numenius phaeopus*	SP	No	LC	
115.	White wagtail	*Motacilla alba*	SP	No	LC	
116.	Whooper swan	*Cygnus cygnus*	SP	Yes	LC	
117.	Woodlark	*Lullula arborea*	SP	Yes	LC	
118.	Wood sandpiper	*Tringa glareola*	SP	Yes	LC	
119.	Western yellow wagtail	*Motacilla flava*	SP	No	LC	
120.	Yellowhammer	*Emberiza citrinella*	SP	No	LC	

[1]Regulation of the Minister of the Environment of 16 December 2016 on the protection of animal species; Regulation of the Minister of the Environment of 11 March 2015 on the establishing a list of game species: SP – strict protection, PP – partial protection, GS – game species
[2]IUCN: EN – endangered, VU – vulnerable, NT – near threatened, LC – least concern (European/Global population)
[3]HELCOM: CR – critically endangered; EN – endangered; VU – vulnerable, NT – near threatened, LC – least concern; wp – wintering population, bp – breeding population

3.5.2.7 Shortcomings and gaps in the state-of-the-art

The technology and methods used for collecting bird migration data provide the most accurate and detailed information about seasonal movements of birds at sea and up to this date, there is no other technology that could offer more accurate data collection methods. It is still not possible to study in detail the nocturnal bird migration, given the fact, that acoustic recorders do not capture species flying at higher altitudes as well as a certain portion of nocturnal migrants are not vocally active, therefore, there are no records of those species. The range of the acoustic recorder is limited (depending on background acoustic noise, e.g. form waves, wind, precipitation). Registration will depend on the species, birds such as seagulls can be recorded in ideal conditions (without background sea noise) up to about 100 m, passerines are many times quieter and can be recorded from 30–50 m at most. The microphone sensitivity range in dB given by the manufacturer is -36 ± 4 dB, however, the exact operating range in meters cannot be determines for the above-stated reasons. Next, it should be taken into account that not all birds flying over the recorder call out and get recorded. However, by means of combining acoustic data with vertical radar data, it was possible to obtain reliable results describing nocturnal migration across the Baltic Sea in the region of planned OWF. The study effort during the spring and autumn migrations, as well as the study effort concerning the surveys of local movements in winter provides enough information to finalise conclusions for this Report. The data is also sufficient to conduct collision risk modelling for the EIA Report.

3.6 CHIROPTEROFAUNA (BATS)

3.6.1 Non-specialist summary

The monitoring completed in 2023 aimed to conduct surveys aimed to determine the bat activity within the Baltica-1 OWF survey area as well as to identify the impact of the proposed offshore wind farm on the bat population within this area. The monitoring methodology complied with the survey methodology proposed in the "Guidelines for Assessing the Impact of Wind Farms on Bats" (Kepel et al., 2011). Bat activity recordings were made as part of 35 all-night surveys during two bat migration seasons (April–May and August–October). The surveys covered a transect comprising four linear sections and four static acoustic monitoring points. Bats were detected based on the recordings made using specialist recording equipment under favourable weather conditions.

Four bat species not threatened by extinction and characteristic of northern Poland were found within the monitoring area. No species listed in Annex II of the Habitats Directive were found. The most abundant group was the common noctule, which is a long-distance migrant. The northern bat was found to be quite abundant, whereas the other species, the Nathusius' pipistrelle and the parti-coloured bat, were scarcely recorded. The bat activity was recorded at low to high levels in terms of all-night surveys and at a low level in terms of the phenological season.

3.6.2 Spatial scope of the surveys

The acoustic monitoring of bats was conducted in the Baltica-1 OWF survey area [Figure 3.204].

The recording of acoustic signals was conducted during vessel passages along the established transect divided into 4 sections: NT_01, NT_02, NT_03 and NT_04, with a total length of approx. 47.5 km [Table 3.116] and at four survey stations constituting the acoustic monitoring points [Table 3.117]. Two of the four planned survey stations were the same as the stations established as part of the surveys of bird movements.

The route of the transect (divided into sections) and the location of the survey stations were designed so as to ensure an even coverage of the survey area and to provide data distributed approximately evenly across the potential flux of bat flights [Figure 3.204].

Table 3.116. The coordinates of particular survey transect sections within the survey area

Survey transect section	Two-dimensional Cartesian coordinate system PL-1992 [m]				Length [km]
	Transect section beginning		Transect section end		
	y	x	y	x	
NT_01	847284.85	399723.63	854041.08	411140.46	13.3
NT_02	860221.34	411211.74	847284.85	399723.63	17.3
NT_03	863525.04	404177.29	860221.34	411211.74	7.8
NT_04	863576.34	413332.80	863525.04	404177.29	9.2

Table 3.117. The coordinates of the acoustic monitoring points in the survey area

Acoustic monitoring point	Two-dimensional Cartesian coordinate system PL-1992 [m]		Comments
	y	x	
NS_01	848418.95	402892.39	-

NS_02	852077.75	405812.03	Station identical to survey station MB_01
NS_03	856163.31	408958.82	-
NS_04	862368.09	408860.67	Station identical to survey station MB_02

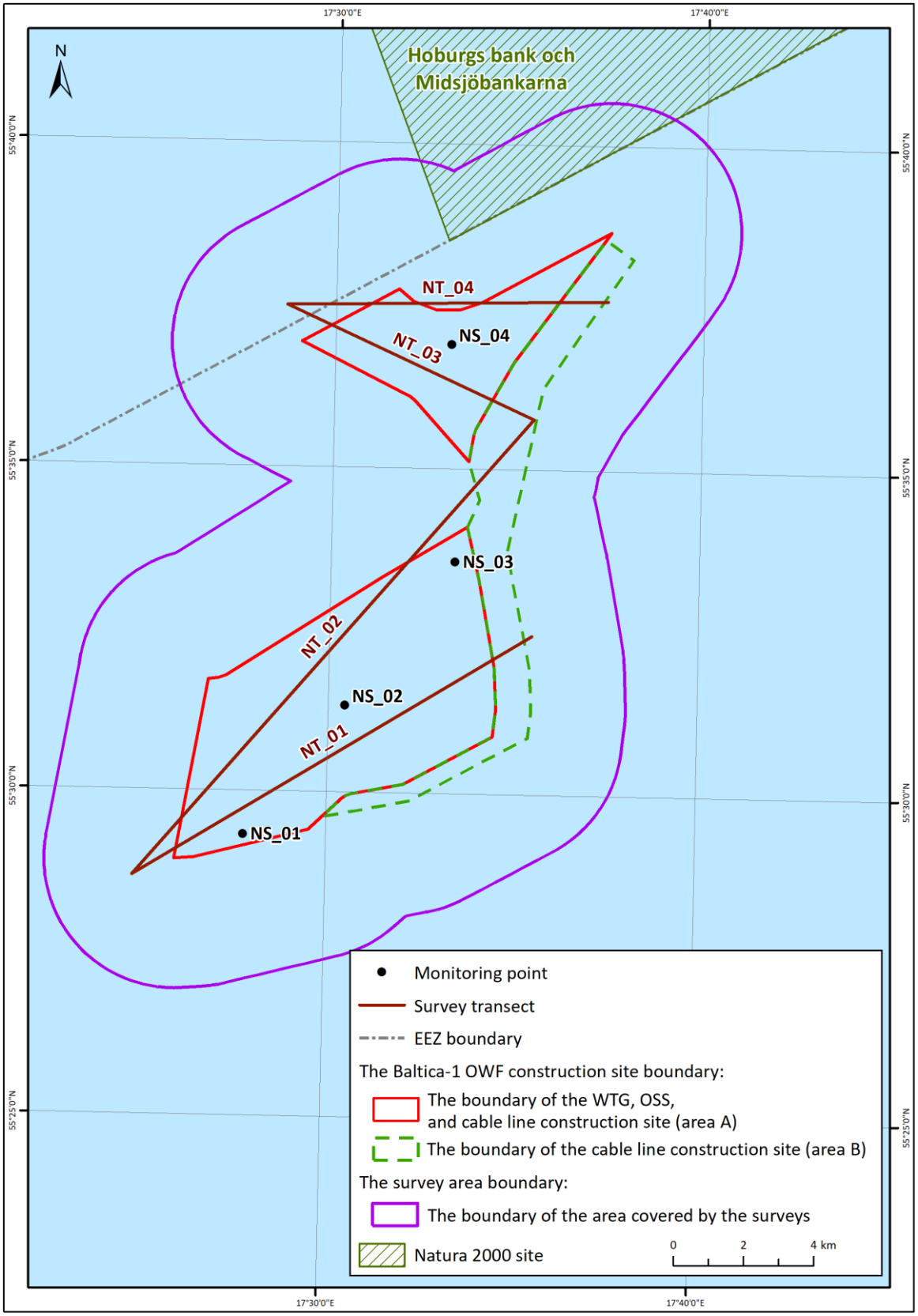


Figure 3.204. The bat acoustic monitoring sites; NT_01–NT_04 – transects, NS_01–NS_04 – static monitoring points

3.6.3 Methodology

The survey methodology was based on the draft "Guidelines for assessing the impact of wind farms on bats" prepared by Polish specialists and practitioners on behalf of the General Directorate for Environmental Protection in 2013 (Kepel et al., 2013) and on the Annex to the Resolution 7.5 The Agreement on the Conservation of Populations of European Bats EUROBATS (Rodrigues et al., 2015).

According to the guidelines, the surveys of bat activity within the B1 OWF survey area were conducted following the same principles as in the case of onshore bat monitoring. However, all the surveys were conducted throughout the night and, during the spring migration, included at least 7 surveys along the transects and two surveys at each survey station (of which one was conducted in April and one in May) as well as, during the autumn migration, at least 7 surveys along the transects and two surveys at each survey station (of which one was conducted in August and one in September).

The minimum interval between the surveys along the survey transect (divided into sections) was 7 days. The minimum interval between the surveys at the same survey station was 7 days. It was allowed to conduct surveys along the survey transect and at different survey stations on the same day or on consecutive days. All surveys took place in favourable weather conditions, in the absence of continuous precipitation and fog, at wind speed up to 6 $m \cdot s^{-1}$ and temperature above 0°C. The wind speed was measured at the mounting height of the microphone, i.e. approx. 2.5–5 m ASL, which varies by survey vessel and depends on the possibility of safe and efficient mounting of the measuring devices. The weather parameters were checked every 6 hours using an on-board weather station. In the absence of a weather station, weather parameters were checked using on-line weather forecasts. In the event of long-term adverse weather conditions, it was allowed to reduce the survey interval in order to achieve the planned number of surveys during a given migration season.

The surveys at the survey stations were conducted from aboard an anchored vessel. In the case of vessel traffic near the survey station, for safety reasons, maintaining position by drifting and manoeuvring using the vessel propulsion was allowed. In the case of the surveys along the survey transect (divided into sections), recording was made from a vessel moving at a speed not exceeding 8 knots (vessel speed below 15 $km \cdot h^{-1}$) in order to minimise the impact of background noise on the acoustic signals being recorded. To minimise the risk related to the recording of the activity of bats that arrived at the survey area together with the survey vessel, bats recorded within the first 15 minutes from sunset were excluded from further analyses. The occurrence of the same species later in the night were considered individually, and the inclusion or exclusion of the bats recorded at that time in further analyses was decided on the basis of expert knowledge. Additionally, before the beginning of the surveys, the survey vessel was inspected for the presence of bats.

The bat activity monitoring along transects was carried out using one survey vessel. During short nights (May), it was permitted to conduct bat activity monitoring using two survey vessels. The bat activity monitoring at a single survey station was conducted using one survey vessel.

To monitor bat activity along the survey transect (divided into sections) and at the survey stations, a system for detecting and recording bats was used which saved acoustic data in a lossless or low loss *.WAV format on a storage medium for subsequent analysis. This system is intended for long-term surveys, which enable continuous assessment of bat activity in the same place throughout the night as well as along the established survey transect. The bat detection and recording system consisted of Song Meter „SM4BAT FS” recorders by Wildlife Acoustic (https://www.wildlifeacoustics.com) used for

recording ultrasounds and SMM-U2 low-noise ultrasound microphones. To ensure the high quality of survey data, the survey systems were located in a place with an unlimited field of detection, away from water and its splashes and from noise emitters such as exhausts, chimneys, engines, loose objects that could generate metallic sounds or sources of strong electromagnetic interference such as antennas or radars, and their location allowed their safe operation by the Party Chief.

Due to the high sensitivity of the microphone required for the bat activity monitoring, there was a possibility that the ambient noise could be recorded. Nevertheless, the spectral analysis of the recorded sound, taking into account the knowledge of bat sonographs, allowed separating the recorded bat sounds from potential other sounds that could also be recorded; thus no masking of bat calls took place. To minimise the risk of data loss, the bat detection and recording system used for bat activity monitoring along the survey transect and at individual survey stations consisted of two Song Meter "SM4BAT FS" recorders of the same type, equipped with ultrasonic SMM-U2 microphone. A Party Chief marked the recorders as the main recorder and the backup recorder and the information about the functions assigned was included in the vessel passage documentation. Both systems operated simultaneously, however, only the data from the main recorder were analysed further. The data from the second recorder were used for further analysis and interpretation only if no signals were recorded by the main recorder or the number of files recorded was much smaller than the one recorded by the backup recorder.

The parameters of the recorder settings that were used during the surveys along the survey transect and at the survey stations are presented below:

- time and date: UTC;
- sampling frequency: 384 kHz;
- 16 k filter: OFF;
- minimum duration of a signal: 1.5 ms;
- maximum duration of a signal: none;
- minimum trigger frequency: 16 kHz;
- trigger level: 12 dB;
- trigger window: 1 s;
- maximum length: 15 s.

After each completed survey, the data in *WAV format was downloaded from the recorder to external storage media and, together with a vessel passage data package, was submitted to the team responsible for the analysis and interpretation of acoustic data. The acoustic data analysis and interpretation team processed the data collected for the potential occurrence of bat signals. The data were analysed manually in order to identify bat signals using the bioacoustics software BatSound.

As a result of the preliminary analysis, the number of files containing sequences of bat calls identified to the species was indicated. If it was impossible to identify a given sequence to the specific species, the sequence was classified to a group of species or genera (e.g. *Nyctalus* spp. or *Nyctalus* + *Eptesicus* + *Vespertilio* spp.).

At the final stage of data analysis, bat activity was examined in relation to the total recording time at a given survey station or along the survey transect and its particular section (the monitored recording time of individual signals enabled the assignment of a given recording to a specific fragment of a transect and/or its section). A bat activity unit was defined as an uninterrupted sequence of

echolocation signals produced by a single individual with a length ranging from one pulse to 5 seconds. If an uninterrupted sequence of calls longer than 5 seconds was recorded, it was treated as a number of activity units corresponding to the result of dividing the recording time expressed in seconds by 5, rounded up to the nearest integer. Bat activity units were, whenever possible, counted separately for individual species or groups of species. Based on activity units, an evaluation of the acoustic data analysed was carried out according to Kepel et al. (2013). To this end, bat activity indices were calculated in activity units/hour [$n \cdot h^{-1}$] according to the following formula:

$Ix = Lx * 60 / T$

where:

Ix – bat activity index for species or group of species "x"
Lx – number of bat activity units
T – time of a given recording (or all recordings taken into account) expressed in minutes

The bat activity indices were calculated for individual surveys, broken down by particular species or groups of species, or genera. The activity indices calculated in that way were used to calculate the average activity index for a selected survey period. The value of the average activity index was calculated on the basis of an arithmetic mean of the activity indices from individual surveys during a particular migration period.

Based on the values of the activity indices and the average activity index for a given migration period, the level of bat activity within the survey area was determined according to the reference scale after Kepel et al. (2013) [Table 3.118].

Table 3.118. The boundaries of bat activity categories for individual taxa according to Kepel et al. (2013)

Taxon	**Boundary of activity range***		
	A	**B**	**P**
Nyctalus spp.	2.5	4.3	8.6
Eptesicus spp.	2.5	4.0	8.0
Nyctalus + *Eptesicus* + *Vespertilio* spp.	2.7	5.0	9.0
Pipistrellus spp.	2.5	4.1	8.0
all bats	3.0	6.0	12.0

** the given values determine the top limits of activity: A – low, B – moderate, C – high (activities > C are described as "very high")*

Due to the scope of the bat activity surveys and the standards indicated, the value of the measurement or calculation error is not determined.

3.6.4 Activities performed

Within the survey period, a total of 14 survey vessel passages along the survey transect were made [Table 3.119]. During the transect vessel passages, the wind speed recorded was between 1 m s^{-1} and 5 m s^{-1}, the air temperature was above zero and no heavy or prolonged precipitation was recorded.

Table 3.119. A list of dates of bat survey vessel passages along the transects within the survey area including the names of people carrying out the observations and the vessel used

Survey no.	Vessel passage date	Observer	Start of recording	End of recording	Recording duration [min.]	Wind velocity [m·s^{-1}]
1	05–06.04.2023	Sebastian Blaszke	17:30	04:09	639	2–3
2	13–14.04.2023	Sebastian Blaszke	17:50	03:50	600	3
3	21–22.04.2023	Krzysztof Plewka	18:06	03:29	563	1
4	28–29.04.2023	Krzysztof Plewka	18:18	03:15	537	4–5
5	07–08.05.2023	Krzysztof Plewka	18:36	02:55	499	2–4
6	18–19.05.2023	Sebastian Blaszke	18:55	02:35	460	2
7	26–27.05.2023	Sebastian Blaszke Krzysztof Plewka	19:10 00:00	02:22 02:22	432 142	3–2
8	11–12.08.2023	Katarzyna Borzym	18:35	03:15	520	5–2
9	19–20.08.2023	Artur Wojtasik	18:19	03:29	550	5–4
10	24–25.08.2023	Sebastian Blaszke	18:07	03:40	573	3–4
11	08–09.09.2023	Krzysztof Plewka	16:30	04:10	760	1–3
12	25–26.09.2023	Sebastian Blaszke	15:41	04:40	779	2–4
13	09–10.10.2023	Sebastian Blaszke	16:07	05:07	780	3–2
14	23–24.10.2023	Krzysztof Plewka	15:35	05:35	840	5–3

During the survey period, a total of 17 survey vessel passages were made at the acoustic monitoring points, one vessel passage per month per each survey station [Table 3.120]. During the surveys, the wind speed recorded was between 2 and 7 m s^{-1}, the air temperature was above zero and no prolonged or heavy precipitation was recorded.

Table 3.120. A list of dates of bat survey vessel passages to the survey stations within the survey area including the names of people carrying out the observations and the vessel used

Survey no.	Acoustic monitoring point	Vessel passage date	Observer	Start of recording	End of recording	Recording duration [min.]	Wind velocity [m·s^{-1}]
1	NS_01	11–12.04.2023	Krzysztof Plewka	17:45	03:57	612	2
1	NS_03	11–12.04.2023	Sebastian Blaszke	17:46	03:54	608	2–3
1	NS_04	12–13.04.2023	Katarzyna Borzym	17:43	03:50	607	2–5
1	NS_02	16–17.04.2023	Maciej Kozakiewicz	17:56	03:40	580	4
2	NS_04	08–09.05.2023	Marcin Sołowiej	18:40	02:51	491	2–3
2	NS_01	12–13.05.2023	Krzysztof Plewka	18:46	02:43	477	3–5
2	NS_03	13–14.05.2023	Sebastian Blaszke	18:49	02:50	481	3
2	NS_02	19–20.05.2023	Małgorzata Knitter	19:00	02:31	451	4–5
3	NS_01	11–12.08.2023	Krzysztof Plewka	18:35	03:15	520	5–2
3	NS_04	11–12.08.2023	Grzegorz Zaniewicz	18:35	03:15	520	5–3
3	NS_03	16–17.08.2023	Sebastian Blaszke	18:26	03:23	537	6–4
3	NS_02	18–19.08.2023	Grzegorz Zaniewicz	18:19	03:29	550	4–5
4	NS_04	22–23.08.2023	Grzegorz Zaniewicz	18:10	03:35	573	7–3
5	NS_04	07–08.09.2023	Adam Janczyszyn	17:31	04:05	634	3–2

Survey no.	Acoustic monitoring point	Vessel passage date	Observer	Start of recording	End of recording	Recording duration [min.]	Wind velocity [m·s^{-1}]
4	NS_01	07–08.09.2023	Krzysztof Plewka	17:29	04:08	639	4–3
4	NS_03	08–09.09.2023	Sebastian Blaszke	17:29	04:07	638	2
4	NS_02	26–27.09.2023	Grzegorz Zaniewicz	15:10	04:45	805	5–3

3.6.5 Results

The results covered two periods: the spring migration period, i.e. the period from 1 April to 31 May 2023, and the autumn migration period, i.e. the period from 1 August to 31 October 2023.

3.6.5.1 Bat species composition

During the acoustic monitoring within the area surveyed, a total of 111 activity units [a.u.] were recorded, which were attributed to 4 species [Figure 3.205 and Figurep 3.206]: the common noctule *Nyctalus noctula* – 72 activity units (64.9% of all the calls recorded), the northern bat *Eptesicus nilsonii* – 30 (27%), the parti-coloured bat *Vespertilio murinus* – 4 (3.6%) and the Nathusius' pipistrelle *Pipistellus nathusii* – 5 (4.5%). Of the species recorded, the genera Nyctalus, Vespertilio and Pipistrellus are the species considered to be very highly vulnerable to collisions with wind turbines, whereas the northern bat is classified as a species with a moderate level of collision mortality risk (Kepel et al., 2011). Only 1 activity unit for the Nathusius' pipistrelle was recorded along the transects during the surveys on 19/20 August 2023. The other activity was recorded during the surveys at the acoustic monitoring stations.

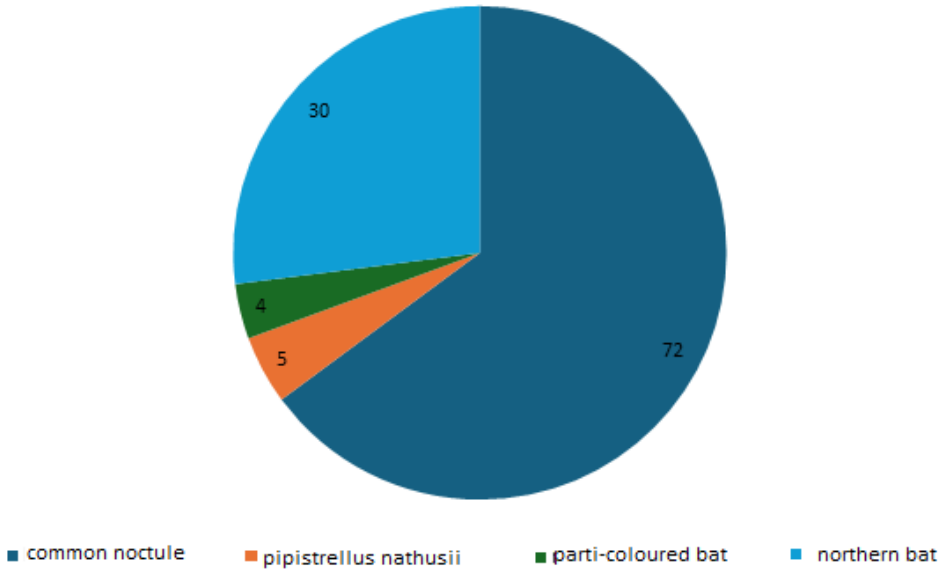
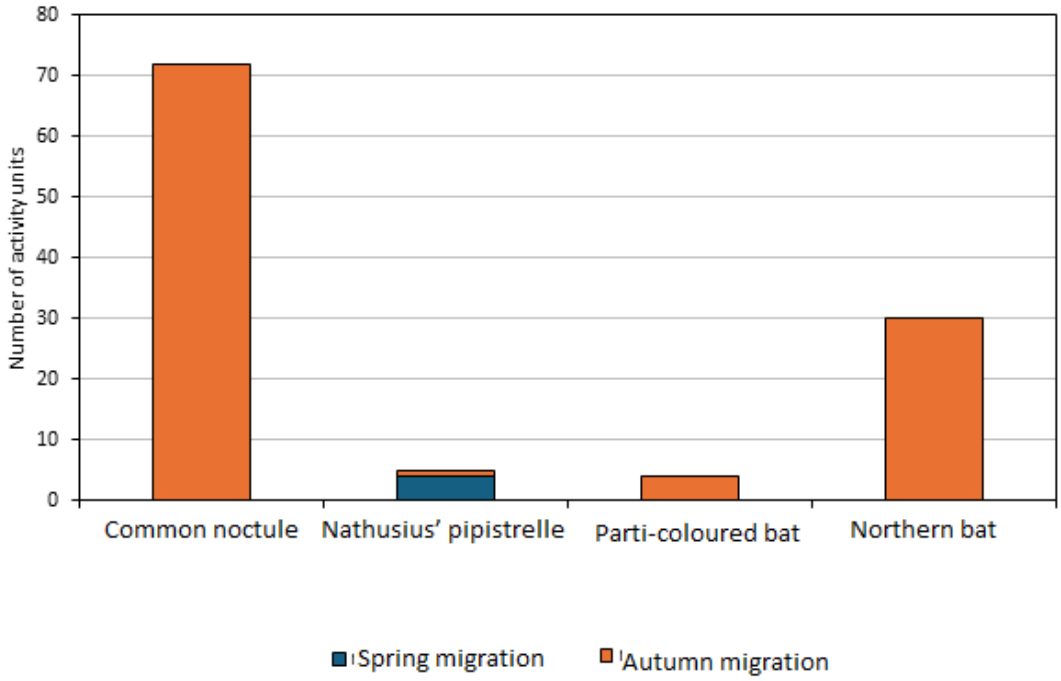


Figure 3.205. The bat species composition and the total number of activity units recorded using ultrasound detection within the survey area between 1 April and 31 October 2023



Figurep 3.206. The bat species composition – the number of activity units recorded using ultrasound detection between 1 April and 31 October 2023 broken down by phenological seasons – spring migration and autumn migration

All the bat species found are strictly protected (Regulation of the Minister of the Environment of 16 December 2016 *on the protection of animal species*, Journal of Laws of 2016, item 2134) and protected under the Bern Convention (Appendix III – the common pipistrelle and the soprano pipistrelle, Appendix II – the other species), the Bonn Convention, Annex IV of the European Union Habitats Directive and the Agreement on the Conservation of Populations of European Bats (EUROBATS) ratified by Poland. No species with the highest conservation status, i.e. listed in Annex II of the EU Habitats Directive, were recorded. The species found within the area surveyed are common and widespread across Poland and are assigned the LC (Least Concern) category according to the IUCN (International Union for Conservation of Nature and Natural Resources). In the northern lake district, it is worth mentioning the northern bat, which has been observed only in winter (Sachanowicz et al., 2006; Zapart et al., 2022).

3.6.5.2 Seasonal activity dynamics

In spring, 4 activity units for the Nathusius' pipistrelle were recorded at station NS_01 during the surveys on 12/13 May 2023. The activity index calculated for this survey was 0.5 units per hour [n h^{-1}]. For the entire spring period, the index was 0.2 n h^{-1}, remaining within the low-value range [Table 3.121 and Table 3.122].

Table 3.121. A list of results of bat survey vessel passages at the acoustic monitoring point within the survey area including the bat species recorded and the level of the activity index for the survey night

Survey no.	Acoustic monitoring point	Season	Survey date	Recording duration for analysis [min.]	Species	Activity units	Activity index*
1	NS_01	Spring migration	11–12.04.2023	597	-	0	0.0
1	NS_03		11–12.04.2023	593	-	0	0.0
1	NS_04		12–13.04.2023	592	-	0	0.0
1	NS_02		16–17.04.2023	565	-	0	0.0
2	NS_04		08–09.05.2023	476	-	0	0.0
2	NS_01		12–13.05.2023	462	Nathusius' pipistrelle	4	0.5
2	NS_03		13–14.05.2023	466	-	0	0.0
2	NS_02		19–20.05.2023	436	-	0	0.0
3	NS_01	Autumn migration	11–12.08.2023	505	-	0	0.0
3	NS_04		11–12.08.2023	505	-	0	0.0
3	NS_03		16–17.08.2023	522	-	0	0.0
3	NS_02		18–19.08.2023	535	Common noctule	72	8.1
4	NS_04		22–23.08.2023	558	Northern bat	30	3.2
4	NS_01		07–08.09.2023	624	-	0	0.0
5	NS_04		07–08.09.2023	619	Parti-coloured bat	4	0.4
4	NS_03		08–09.09.2023	623	-	0	0.0
4	NS_02		26–27.09.2023	980	-	0	0.0

**The low level of activity is shown in green, moderate – in yellow, and high – in red.*

In autumn, all the bat passes were recorded during the surveys between 17 August and 8 September 2023. The highest number of activity units were recorded at station NS_02 during survey night from 18 to 19 August 2023. 72 activity units for the common noctule were recorded then, and the activity index obtained was 8.1 n h^{-1}, respectively. The activity level observed during this survey was classified as high. However, throughout autumn, the activity index obtained for station NS_02 remained at a low level – 1.2 n h^{-1}.

During the survey conducted between 22 and 23 August 2023 at station NS_04, 30 activity units were recorded for the northern bat. The activity index calculated for this survey was 3.2 n h^{-1} (moderate level). On 7 September 2023, 4 activity units for the parti-coloured bat were recorded (activity index of 0.4 n h^{-1} – low level). Throughout autumn, the activity index obtained for station NS_04 remained at a low level – 1.2 n h^{-1}.

At station NS_03, no bat passes were recorded throughout the survey period.

On 20 August 2023, along transect NT_02, the Nathusius' pipistrelle was recorded once. The activity index obtained for this section during this survey was 0.9 n h^{-1}, remaining within the low-value range. Throughout the phenological season, the activity index for this section was 0.1 n h^{-1}, which means that the activity remained at a low level.

According to the methodology included in the guidelines for assessing the impact of WTGs on bats (Kepel et al., 2013), the autumn migration period is divided into two phenological periods: late summer – from early August to mid-September, where increased bat activity is usually recorded, associated

with the dispersal of breeding colonies, the beginning of migration and the mating period, and early autumn – from mid-September to the end of October, when autumn migration and the mating period of bats are recorded.

Table 3.122. A list of activity indices obtained for the survey periods (01.04–31.05 – spring migration, 01.08–15.09 and 15.09–31.10 – autumn migration) during the bat survey vessel passages at the monitoring stations and along the survey transect,***

Transect section / acoustic monitoring station	Period covered	Pipistrellus		Nyctalus		Vespertilio		All	
		AU	IA	AU	IA	AU	IA	AU	IA
NT_01	01.04–31.05	0	0.0	0	0.0	0	0.0	0	0.0
NT_02		0	0.0	0	0.0	0	0.0	0	0.0
NT_03		0	0.0	0	0.0	0	0.0	0	0.0
NT_04		0	0.0	0	0.0	0	0.0	0	0.0
NS_01		4	0.2	0	0.0	0	0.0	4	0.2
NS_02		0	0.0	0	0.0	0	0.0	0	0.0
NS_03		0	0.0	0	0.0	0	0.0	0	0.0
NS_04		0	0.0	0	0.0	0	0.0	0	0.0
NT_01	01.08–15.09	0	0.0	0	0.0	0	0.0	0	0.0
NT_02		1	0.1	0	0.0	0	0.0	1	0.1
NT_03		0	0.0	0	0.0	0	0.0	0	0.0
NT_04		0	0.0	0	0.0	0	0.0	0	0.0
NS_01		0	0.0	0	0.0	0	0.0	0	0.0
NS_02		0	0.0	113	4.1	0	0.0	113	1.9
NS_03		0	0.0	0	0.0	0	0.0	0	0.0
NS_04		0	0.0	0	0.0	34	1.2	34	1.2
NT_01	15.09–31.10	0	0.0	0	0.0	0	0.0	0	0.0
NT_02		0	0.0	0	0.0	0	0.0	0	0.0
NT_03		0	0.0	0	0.0	0	0.0	0	0.0
NT_04		0	0.0	0	0.0	0	0.0	0	0.0

**AU – activity unit, AI – activity index*

*** low level of activity is shown in green*

3.6.6 Summary of results and conclusions

During the surveys, four bat species were recorded: the common noctule *Nyctalus noctula*, the Nathusius' pipistrelle *Pipistrellus nathusii*, the northern bat *Eptesicus nilssonii* and the parti-coloured bat *Vespertilio murinus*. Of the species recorded, the genera Nyctalus, Vespertilio and Pipistrellus are species considered to be very highly vulnerable to collisions with wind turbines, whereas the northern bat is classified as a species with a moderate level of collision mortality risk. A total of 111 activity units were recorded, 64.9% of which were attributed to the common noctule.

During the spring migration, 4 activity units for the Nathusius' pipistrelle were recorded at station NS_01. During the autumn migration season, all the bat passes recorded were observed at stations NS_02 and NS_04 and the activity indices obtained during these surveys are classified as moderate and high levels. The activity level throughout this period remained within the low-activity range.

Along the acoustic monitoring transects, only one Nathusius' pipistrelle call was recorded during the autumn migration. The bat activity during the phenological period is classified as low.

All the species are protected by Polish law. The Nathusius' pipistrelle is a species not threatened by extinction, abundant or moderately abundant in Poland and in Gdańsk Pomerania, however, it was very rarely encountered within the project area during the surveys. Its resources can be considered insignificant. The common noctule, which was the species most frequently recorded, is also not threatened by extinction and abundant in Pomerania, and its resources should be considered as insignificant. The northern bat and the parti-coloured bat, however, are rare or quite rare in Poland and in Gdańsk Pomerania, therefore their resources should be considered as of a low value.

3.6.7 Shortcomings and gaps in the state-of-the-art

Due to a lack of binding legal regulations concerning the methodology of bat monitoring and the analysis of the impact of wind farms on their population, in order to monitor and analyse the population of bats within the proposed project area, a methodology based on the draft "Guidelines for assessing the impact of wind farms on bats" prepared by Polish specialists and practitioners on behalf of the General Directorate for Environmental Protection in 2011 (Kepel et al., 2011) was adopted. It involves all-night acoustic monitoring along transects covering the entire survey area as well as at static acoustic monitoring points. The survey methods used, the analyses and the results mainly apply to onshore wind farms and were adjusted to specific features of bat activity at sea. The presence of intensely lit vessels may make it difficult to estimate the actual activity of bats in the survey area, as bats may be attracted to a vessel in this way. A vessel may also be home to bats called "stowaways" that may become active around the vessel at night, thus distorting the survey results.

Moreover, there are no models enabling reliable prediction of bat mortality within the planned wind farm based on pre-investment results. It is only known that this mortality is positively correlated with the level of bat activity in a given location, including the activity recorded at ground level (Kunz et al., 2007a; Heist and Johnson, 2013). Currently, the only possible method for assessing the pre-investment results is comparing the recorded activity levels (activity indices) with available reference scales. These scales allow to determine if the obtained results exceed the average values and, thus, whether the planned wind farm is located in a place of a higher-than-average importance for bats. The scale presented in the draft "Guidelines for assessing the impact of wind farms on bats" published by GDEP, which the monitoring methodology was based on, was developed on the basis of the data obtained from onshore wind farms. For this purpose, the data from the pre-investment surveys (Kepel et al., 2011) were used as no database containing information on sea areas was available. It should also be noted that only few surveys on bat migration routes within the area surveyed have been described, both in Polish and in international literature.

The most up-to-date survey tools and methodologies were used to carry out the work, during the work, no exceptional phenomena related to the bat activity occurred and the survey material collected is complete and does not contain gaps. Therefore, no reasons which could negatively affect the reliability of results, analyses and conclusions aimed at a comprehensive assessment of the project impact on bats have been indicated in the case of the project discussed.

4 REFERENCES

Aguilar de Soto N., Delorme N., Atkins J. et al., 2013. Anthropogenic noise causes body malformations and delays development in marine larvae. Sci. Rep., 3: 2831.

Ahlen I., 1997. Migratory behavior of bats at South Swedish coasts. Z. Saugetierkunde, 62: 375–380.

Ahlen I., Bach L., Baagoe H.J., Pettersson J., 2007. Bats and offshore wind turbines studied in southern Scandinavia. Report 5571. The Swedish Environmental Protection Agency.

Ahlen I., Baggoe H.J., Bach L., 2009. Behavior of Scandinavian bats during migration and foraging at sea. Journal of Mammalogy, 90(6): 1318–1323.

Ainslie M., Dekeling R.P.A., 2018. Proposals for TG Noise 2019 update. TG-Noise meeting. 6th November 2018, Conference Centre Albert Borschette, Brussels, Belgium.

Alerstam T., 1978. Analysis and a theory of visible bird migration. Oikos, 30(2): 273–349.

Alloway B.J., Ayers D.C., 1999. Chemiczne podstawy zanieczyszczenia środowiska. Wydawnictwo Naukowe PWN, Warszawa.

Aminot A., 1995. Quality assurance of pre-determination steps for dissolved nutrients in marine samples, [in:] P. Quevauviller (Ed.), Quality assurance in environmental monitoring. Sampling and sample pretreatment. VCH Verlagsgcsellschaft mbH, Weinheim, pp. 92–112.

Anderson P.A., Berzins I.K., Fogarty F. et al., 2011. Sound, stress, and seahorses: the consequences of a noisy environment to animal health. Aquaculture, 311(1–4): 129–138.

Andersson M.H., 2011. Offshore wind farms – ecological effects of noise and habitat alteration on fish. Doctoral dissertation. Department of Zoology, Stockholm University.

André M., Sole M., Lenoir M. et al., 2011. Low-frequency sounds induce acoustic trauma in cephalopods. Front. Ecol. Environ., 9(9): 489–493.

Andrulewicz E., Szymelfenig M., Urbański J., Węsławski J.M., Węsławski S., 2008. Morze Bałtyckie – o tym warto wiedzieć. Polski Klub Ekologiczny, Okręg Wschodnio Pomorski, Gdynia, pp. 84–93.

ANSI, ANSI/ASA S1.11-2004 (R2009), 2009. Specification For Octave-band And Fractional-octave-band Analog And Digital Filters. American National Standards Institute.

Antczak J., Meissner W., 2018. Wyniki monitoringu ptaków morskich, [in:] Raport o oddziaływaniu na środowisko morskiej farmy wiatrowej FEW Baltic II. Tom II, Załącznik 4. Baltic Trade and Invest Sp. z o.o., Słupsk.

Antizar-Ladislao B., 2008. Environmental levels, toxicity and human exposure to tributyltin (TBT)-contaminated marine environment. A review. Environment International, 34(2): 292–308.

Aps R., Ustinova L., Gentzen B. et al., 1992. Guide for the use of Baltic sprat otoliths in fisheries studies. Part I. [in:] Guide for the use of Baltic sprat and herring otoliths in fisheries studies. Fischerei-Forsch., Sonderheft, Wissen. Zeit. des IfH Rostock-Marienehe, pp. 3–17.

Arnett E.B, Huso M.M.P., Schirmacher M.R., Hayes J.P., 2011. Altering turbine speed reduces bat mortality at wind – energy facilities. Frontiers in Ecology and Environment, 9(4): 209–214.

Arnett E.B., Brown W.K., Erickson W.P. et al., 2008. Patterns of Bat Fatalities at Wind Energy Facilities in North America. Journal of Wildlife Management, 72: 61–78.

Aro E., 1989. A review of fish migration patterns in the Baltic. Rapp. P.-v. Réun. Cons. Int. Explor. Mer, 190: 72–96.

Aro E., 2002. Fish migration studies in the Baltic Sea – a historical review. ICES Mar. Sci. Symp. 215: 361–370.

ASTM D5334-14. Standard Test Method for Determination of Thermal Conductivity of Soil and Soft Rock by Thermal Needle Probe Procedure.

Bach L., 2001. Fledermäuse und Windenergienutzung – reale Probleme oder Einbildung? Vogelk. Ber. Niedersachs., 33: 119–124.

Bach L., Rahmel U., 2006. Fledermäuse und Windenergie – ein realer Konflikt? Inform.d. Naturschutz Niedersachs., 26(1): 47–52.

Bach P., Voigt C.C., Göttsche M. et al., 2022. Offshore and coastline migration of radio-tagged Nathusius' pipistrelles. Conservation Science and Practice, 4(10): e12783.

Baerwald E.F., Barclay R.M.R., 2009. Geographic variation in activity and fatality of migratory bats at wind energy facilities. Journal of Mammalogy, 90(6): 1341–1349.

Baerwald E.F., D'Amours G.H., Klug B.J., Barclay R.M.R., 2008. Barotrauma is a significant cause of bat fatalities at wind turbines. Current Biology, 18(16): R695–R696.

Baerwald E.F., Edworthy J., Holder M., Barclay R.M.R., 2009. A Large – Scale Mitigation Experiment to Reduce Bat Fatalities at Wind Energy Facilities. Journal of Wildlife Management, 73(7): 1077–1081.

Bagge O., 1981. Demersal fishes, [in:] A. Voipio (Ed.), The Baltic Sea Elsevier Oceanographic Series No. 30. Elsevier Scientific Publishing Company, Amsterdam–Oxford–New York, pp. 311–333.

Bagge O., Bay J., Steffensen E., 1993. Fluctuations in Abundance of the Baltic Cod (Gadus morhua) Stock in Relation to Changes in the Environment and the Fishery. NAFO Sci. Coun. Studies. 18: 35–42.

Barańska A., Dziaduch D., Osowiecki A., Tarała A., Galer-Tatarowicz K., Dembska G., Pazikowska-Sapota G., Flasińska A., Littwin M., Szczepańska K., Ostrowska D., Bojke A., Wróblewski R., Kubacka M., Dworniczak J., Rogowska K., Kołakowski M., Ginał K., Bogucki M., Gajewski Ł., Załęski K., Nawrotek I., Brzezińska A., Edut J., Pylhun A., Warchhold K., Zelewska I., Nowak J., Gajewski L., Kusio T., Greszczuk M., Gajewski P., Druzd N., Kapiński J., Kałas M., Misiewicz E., Meissner W., Schönberger L., Pick D., Jasper B., Nermer T., Fey D., Radtke K., Grygiel W., Wyszyński M., Mirny Z., Schmidt B., Szymanek L., Lisimenka A., Brocławik O., Kołakowska E., Nocoń M., Sarnocińska J., 2020. Załącznik 1 – Raport z inwentaryzacji zasobów abiotycznych i biotycznych obszaru badań MFW Baltic Power.

Barclay R.M.R., Baerwald E.F., Gruver J.C., 2007. Variation in bat and bird fatalities at wind energy facilities: assessing the effects of rotor size and tower height. Can. J. Zool., 85: 381–387.

Bednarska M., Brzeska-Roszczyk P., Dawidowicz D., Dembska G., Drgas A., Dworniczak J., Fey D., Gajewski J., Gajewski L., Gajewski Ł., Galer-Tatarowicz K., Hac B., Kaczmarek N., Kałas M., Kapiński J., Keslinka L., Koszałka J., Kruk-Dowgiałło L., Kubacka M., Kuzebski E., Meissner W.,

Nermer T., Opioła R., Osipowicz I., Osowiecki A., Pazikowska-Sapota G., Rudowski S., Skov H., Spich K., Szefler K., Świstun K., Thomsen F., Typiak M., Tyszecki A., Wąś M., Wróblewski R., Yalçın G., Zydelis R., 2017. Report on the Environmental Impact Assessment of the Baltica OWF, Gdańsk.

Belkina N.A., 2006. Pollution of bottom sediments in Petrozavodsk Bay of Lake Onega with oil products. Water Resources, 33(2): 163–169.

Bellebaum J., Kube J., Schulz A., Skov H., Wendeln H., 2014. Decline of Long-tailed Duck Clangula hyemalis numbers in the Pomeranian Bay revealed by two different survey methods. Ornis Fenn., 91(3): 129–137.

Bellefontaine S.C., Hamilton D.J., 2023. Shorebirds exhibit niche partitioning on multiple dimensions at a small staging site on the Northumberland Strait, New Brunswick, Canada. FACETS, 8: 1–12.

Bellmann M.A., Brinkmann J., May A., Wendt T., Gerlach S., Remmers P., 2020. Underwater noise during the impulse pile-driving procedure: Influencing factors on pile-driving noise and technical possibilities to comply with noise mitigation values. Supported by the Federal Ministry for the Environment, Nature Conservation and Nuclear Safety [Bundesministerium für Umwelt, Naturschutz und nukleare Sicherheit (BMU)], FKZ UM16 881500. Commissioned and managed by the Federal Maritime and Hydrographic Agency [Bundesamt für Seeschifffahrt und Hydrographie (BSH)]. Order No. 10036866. Edited by the itap GmbH.

Bernard P.C., Van Grieken R.E., Brügmann L., 1989. Geochemistry of suspended matter from the Baltic Sea. 1. Results of individual particle characterization by automated electron microprobe. Marine Chemistry, 26(2): 155–177.

Betke K., Folegot T., Matuschek R. et al., 2015. BIAS Standards for Signal Processing. Aims, Processes and Recommendations. Amended version. U.K. Verfuss, P. Sigray (Ed.).

Bidleman T., Agosta K., Andersson A., Brorström-Lundén E., Haglund P., Hansson K., Laudon H., Newton S., Nygren O., Ripszam M., Tysklind M., Wiberg K., 2015. Atmospheric pathways of chlorinated pesticides and natural bromoanisoles in the northern Baltic Sea and its catchment. Ambio, 44(Suppl 3): 472–483.

BirdLife International, 2017. European birds of conservation concern: populations, trends and national responsibilities. BirdLife International, Cambridge, UK.

BirdLife International, 2021. European Red List of Birds. Publications Office of the European Union, Luxembourg.

Birjukov N.P., 1980. Baltijskij shprot (Biologikheskije sostojanie i khozaijstviennoie ispolzovanie). Pushkin Leningrad State University, Leningrad.

Błeńska M., Bogdaniuk M., Brzeska P., Bubak I., Dembska G., Dubiński M., Kruk-Dowgiałło L., Michałek M., Nowacki J., Olenycz M., Opioła R., Sapota G., Tarała A., 2010. Wykonanie kompleksowych poinwestycyjnych badań i pomiarów w rejonie Mechelinek w celu monitorowania wód Zatoki Puckiej w związku ze zrzutem solanki pochodzącej z budowy PMG Kosakowo. Internal Publication of the Maritime Institute in Gdańsk no. 6732. L. Kruk-Dowgiałło, J. Nowacki, M. Błeńska (Eds).

Błeńska M., Osowiecki A., Brzeska P., Kruk-Dowgiałło L., Barańska A., Dziaduch D., 2015a. Badania bentosu na obszarze Morskiej Infrastruktury Przyłączeniowej (MIP). Raport końcowy z wynikami badań, [in:] Morska infrastruktura przesyłowa energii elektrycznej. Raport o oddziaływaniu na środowisko. Volume III, Chapter 2, Subchapter 2.13. Biuro Doradztwa Ekologicznegi i Inwestycyjnego Sp. z o.o.

Błeńska M., Osowiecki A., Brzeska P., Dziaduch D., Barańska A., 2014. Badania bentosu na obszarze morskiej farmy wiatrowej Bałtyk Środkowy III. Raport końcowy z wynikami badań, [in:] Morska farma wiatrowa Bałtyk Środkowy III. Raport o oddziaływaniu na środowisko. Volume III, Chapter 6. Grupa Doradcza SMDI, Warszawa.

Błeńska M., Osowiecki A., Brzeska P., Kruk-Dowgiałło L., Dziaduch D., Barańska A., 2015b. Badania bentosu na obszarze morskiej farmy wiatrowej Bałtyk Środkowy II. Raport końcowy z wynikami badań, [in:] Morska farma wiatrowa Bałtyk Środkowy II. Raport o oddziaływaniu na środowisko. Volume III, Section 6. Grupa Doradcza SMDI, Warszawa.

Bogdaniuk M., Sapota G., Dembska G., Aftanas B., 2012. Determination of PAHs and PCBs in the Polish area of shipwreck exploration. Polish Journal Environmental Studies, 21(2): 297–306.

Bolałek J. (Ed.), 2010. Fizyczne, biologiczne i chemiczne badania morskich osadów dennych. The University of Gdańsk Publishing House, Gdańsk.

Bolałek J., Falkowska L., 1999. Analiza chemiczna wody morskiej. Tom 1. Makroskładniki i gazy rozpuszczone w wodzie morskiej. Wydawnictwo Uniwersytetu Gdańskiego, Gdańsk.

Boonman M., 2018. Mitigation measures for bats in offshore wind farms. Evaluation and improvement of curtailment strategies. Bureau Waardenburg Report no. 18-278. Bureau Waardenburg, Culemborg.

Böhner J., Antonić O., 2009. Chapter 8 Land-Surface Parameters Specific to Topo-Climatology, [in:] Geomorphometry – Concepts, Software, Applications. Vol. 33. Elsevier, pp. 195–226.

Brabant R., Laurent Y., Jonge Poerink B., Degraer S., 2021. The Relation between Migratory Activity of Pipistrellus Bats at Sea and Weather Conditions Offers Possibilities to Reduce Offshore Wind Farm Effects. Animals, 11(12): 3457.

Breiman L., 2021. Random Forests. Machine Learning, 45(1): 5–32.

Brinkmann R., 2006. Survey of possible operational impacts on bats by wind facilities in southern Germany. Administrative district of Freiburg – Department 56 Conservation and Landscape Management. Gundelfingen.

Brocławik O., Nocoń M., Sarnocińska J., Thomsen F., Sadowska U., 2022. Morska farma wiatrowa MFW Bałtyk I. Ssaki morskie. Raport końcowy z wynikami badań, [in:] Morska farma wiatrowa Bałtyk I. Raport o oddziaływaniu Przedsięwzięcia na środowisko. Appendix 3, Mammals. ERM Polska Sp. z o.o., Warszawa.

Brutemark A., Engström-Öst J., Vehmaa A., 2011. Long-term monitoring data reveal pH dynamics, trends and variability in the western Gulf of Finland. Oceanological and Hydrobiological Studies, 40(3): 91–94.

Brzeska-Roszczyk P., Brzezińska A., Bujnik B., Dembska G., Drgas A., Duljas E., Dworniczak J., Dyndo M., Dziaduch D., Edut J., Fey D., Flasińska A., Gajewski J., Gajewski L., Gajewski Ł., Gajewski P., Galer-

Tatarowicz K., Gałka K., Górnowicz D., Grygiel W., Horbowa K., Jażdżewska O., Jóźwik A., Kaczmarek N., Kałas M., Kamieńska K., Kapiński J., Kargol J., Knitter R., Kołakowski M., Kowalczyk J., Kowalewska A., Kozłowska H., Kunicki M., Kuzebski E., Kwiatkowski M., Lednicka B., Markowska M., Mirny Z., Misiewicz E., Mokwa T., Moroz-Kunicka T., Mróz M., Mytnik J., Nerkowski P., Nermer T., Olenycz M., Opioła R., Pazikowska-Sapota G., Pylhun A., Radtke K., Rogowska K., Rutkowska A., Rutkowski P., Rydzkowski P., Schmidt B., Strzelecki D., Sularz W., Szeniawska K., Szuba M., Szymanek L., Warchhold K., Wróblewski R., Wyszyński M., Zelewska I., Zieliński S. 2021, Raport o oddziaływaniu Infrastruktury Przyłączeniowej Morskiej Farmy Wiatrowej Baltic Power na środowisko. MEWO S.A., MI UMG, Gdańsk–Gdynia.

Brzeska-Roszczyk P., Kruk-Dowgiałło L. 2017, Preliminary results of monitoring studies on macrophytes in the area of brine discharge from the creation of gas storage caverns (Puck Bay, Baltic). Bulletin of the Maritime Institute in Gdańsk, 32(1): 50−57.

Bundesamt für Seeschifffahrt und Hydrographie (BSH), 2011. Offshore-windparks. Messvorschrift für unterwasserschallmessungen. Aktuelle vorgehensweise mit anmerkungen. Anwendungshinweise. Hamburg.

Burnham K.P., Anderson D.R., 2002. Model selection and multimodel inference. A practical information − theoretic approach. Springer, New York.

Burska D., Pryputniewicz D., Falkowska L., 2005. Stratification of particulate organic carbon and nitrogen in the Gdańsk Deep (southern Baltic Sea). Oceanologia, 47(2): 201–217.

Carlén I., Thomas L., Carlström J., Amundin M., Teilmann J., Tregenza N., Tougaard J., Koblitz J.C., Sveegaard S., Wennerberg D., Loisa O., Dähne M., Brundiers K., Kosecka M., Kyhn L.A., Ljungqvist C.T., Pawliczka I., Koza R., Arciszewski B., Galatius A., Jabbusch M., Laaksonlaita J., Niemi J., Lyytinen S., Gallus A., Benke H., Blankett P., Skóra K.E., Acevedo-Gutiérrez A., 2018. Basin-scale distribution of harbour porpoises in the Baltic Sea provides basis for effective conservation actions. Biological Conservation, 226: 42–53.

Carman R., 2003. Carbon and nutrients, [in:] M. Perttilä (Ed.), Contaminants in the Baltic Sea Sediments. Results of the 1993 HELCOM/ICES Baltic Sea Sediment Baseline Study. MERI, Report Series of the Finnish Institute of Marine Research No. 50. Helsinki.

Carman R., Cederwall H., 2001. Sediments and macrofauna in the Baltic Sea – characteristics, nutrient contents and distribution, [in:] F.V. Wulff, L.A. Rahm, P. Larsson (Ed.), A systems analysis of the Baltic Sea. Ecological Studies, Vol. 148. Analysis and synthesis. Springer-Verlag, Berlin Heidelberg, pp. 289–327.

Carman R., Jonsson P., 1991. Distribution patterns of different forms of phosphorus in some surficial sediments of the Baltic Sea. Chemical Geology, 90(1–2): 91–106.

Casini M., Cardinale M., Arrhenius F., 2004. Feeding preferences of herring (Clupea harengus) and sprat (Sprattus sprattus) in the southern Baltic Sea. ICES J. Mar. Sci., 61(8): 1267–1277.

Chałacińska I., Kałas M., Kapiński J., Zasońska A., Dembska G., Sapota G., Galer-Tatarowicz K., Littwin M., Zegarowski Ł., Aftanas B., 2015. Badania warunków hydrologicznych i hydrochemicznych na obszarze MFW Bałtyk Środkowy II. Raport końcowy z wynikami badań, [in:] Morska farma wiatrowa Bałtyk Środkowy II. Raport o oddziaływaniu na środowisko. Volume III, Section 2. Grupa Doradcza SMDI, Warszawa.

Chałacińska I., Kałas M., Kapiński J., Zasońska A., Dembska G., Sapota G., Galer-Tatarowicz K., Littwin M., Zegarowski Ł., Aftanas B., 2014. Badania warunków hydrologicznych i hydrochemicznych na obszarze MFW Bałtyk Środkowy III. Raport końcowy z wynikami badań, [in:] Morska farma wiatrowa Bałtyk Środkowy III. Raport o oddziaływaniu na środowisko. Volume III, Chapter 2. Grupa Doradcza SMDI, Warszawa.

Chapman C.J., Hawkins A.D., 1973. A field study of hearing in the cod, Gadus morhua L. J. Comp. Physiol., 85(2): 147–167.

Chen C.T., Millero F.J., 1977. Speed of Sound in Seawater at High Pressures. J. Acoust. Soc. Am., 62(5): 1129–1135.

Chodkiewicz T., Neubauer G., Sikora A., Ławicki Ł., Meissner W., Bobrek R., Cenian Z., Bzoma S., Betleja J., Kuczyński L., Moczarska J., Rohde Z., Rubacha S., Wieloch M., Wylegała P., Zielińska M., Zieliński P., Chylarecki P., 2018. Monitoring Ptaków Polski w latach 2016–2018. Biuletyn Monitoringu Przyrody, 17: 1–90.

Christensen M., Kristian P., Petersen K., 2022. Energy Island Bornholm. Environmental baseline note for WP-H Bats. WSP Denmark A/S.

Cichocki W., Ważna A., Cichocki J., Rajska-Jurgiel E., Jasiński A, Bogdanowicz W., 2015. Polskie nazewnictwo ssaków świata. Muzeum i Instytut Zoologii PAN, Warszawa.

Ciechanowski M., Jakusz-Gostomska A., Żmihorski M., 2016. Empty in summer, crowded during migration? Structure of assemblage, distribution pattern and habitat use by bats (Chiroptera: Vespertilionidae) in a narrow, marine peninsula. Mammal Research, 61: 45–55.

Codarin A., Wysocki L.E., Ladich F, Picciulin M., 2009. Effects of ambient and boat noise on hearing and communication in three fish species living in a marine protected area (Miramare, Italy). Mar. Pollut. Bull., 58(12): 1880–1887.

Collins J., Jones G., 2009. Differences in bat activity in relation to bat detector height: implications for bat surveys at proposed windfarm. Acta Chiropterologica, 11(2): 343–350.

Cramp S., Simmons K.E.L., 1983. The Birds of the Western Palearctic. Vol. III. Oxford University Press, Oxford.

Cryan P.M., Brown A.C., 2007. Migration of bats past a remote island offers clues towards the problem of bat fatalities at wind turbines. Biological Conservation, 139(1–2): 1–11.

Dadlez R., 1995, Mezozoik, [in:] J.E. Mojski (Ed.), Atlas geologiczny południowego Bałtyku. Tabl. VIII. Państwowy Instytut Geologiczny, Sopot–Warszawa.

Degraer S., Brabant R., Rumes B., Vigin L. (Eds), 2018. Environmental Impacts of Offshore Wind Farms in the Belgian Part of the North Sea: Assessing and Managing Effect Spheres of Influence. Royal Belgian Institute of Natural Sciences, OD Natural Environment, Marine Ecology and Management, Brussels.

Dekeling R.P.A., Tasker M.L., Van der Graaf A.J. et al., 2014. Monitoring Guidance for Underwater Noise in European Seas. Part I: Executive Summary. JRC Scientific and Policy Report EUR 26557 EN. Publications Office of the European Union, Luxemburg.

Dekeling R.P.A., Tasker M.L., Van der Graaf A.J. et al., 2014. Monitoring Guidance for Underwater Noise in European Seas. Part II: Monitoring Guidance Specifications. JRC Scientific and Policy Report EUR 26555 EN. Publications Office of the European Union, Luxemburg.

Dekeling R.P.A., Tasker M.L., Van der Graaf A.J. et al., 2014. Monitoring Guidance for Underwater Noise in European Seas. Part III: Background Information and Annexes. JRC Scientific and Policy Report EUR 26556 EN. Publications Office of the European Union, Luxemburg.

Dembska G., 2003. Metale śladowe w osadach Portu Gdańskiego. PhD Thesis. University of Gdansk – *Faculty of* Biology*,* Geography and Oceanology.

Dietz C., Helversen O. v., Nill D., 2009. Bats of Britain, Europe and Northeastern Africa. A & C Black.

Dojlido J.R., 1995. Chemia wód powierzchniowych. Wydawnictwo Ekonomia i Środowisko, Białystok.

Downs N.C., Racey P.A., 2006. The use of habitat features in mixed farmland in Scotland. Acta Chiropterologica, 8: 169–186.

Drgas A., Janusz J., Andrulewicz E., Łączkowski T., Szymanek L., Fey D., Margoński P., Trella K., Gromisz S., Mirny Z., Warzocha J., Grygiel W., Nadolna K., Witalis B., Grzyb A., Ochman A., Wodzinowski T., Horbowa K., Pawlikowski K., Wójcik I., Horbowy J., Psuty I., Wróblewska H., Kownacka J., Radtke K., Wyszyński M., Krajewska A., Spich K., Zaporowski R., 2014. Monitoring ichtiofauny obszaru morskiej farmy wiatrowej Bałtyk Środkowy III. Raport końcowy z wynikami badań, [in:] Morska farma wiatrowa Bałtyk Środkowy III. Raport o oddziaływaniu na środowisko. Volume III, Chapter 7. Grupa Doradcza SMDI, Warszawa.

Drgas A., Janusz J., Andrulewicz E., Łączkowski T., Szymanek L., Fey D., Margoński P., Trella K., Gromisz S., Mirny Z., Warzocha J., Grygiel W., Nadolna K., Witalis B., Grzyb A., Ochman A., Wodzinowski T., Horbowa K., Pawlikowski K., Wójcik I., Horbowy J., Psuty I., Wróblewska H., Kownacka J., Radtke K., Wyszyński M., Krajewska A., Spich K., Zaporowski R., 2015. Monitoring ichtiofauny obszaru morskiej farmy wiatrowej Bałtyk Środkowy II. Raport końcowy z wynikami badań, [in:] Morska farma wiatrowa Bałtyk Środkowy II. Raport o oddziaływaniu na środowisko. Volume III, Section 7. Grupa Doradcza SMDI, Warszawa.

Durinck J., Skov H., Jensen F.P., Pihl S., 1994. Important marine areas for wintering birds in the Baltic Sea. EU DG XI research contract no. 2242/90-09-01. Ornis Consult Report. Copenhagen.

Dürr T., 2007. Möglichkeiten zur Reduzierung von Fledermausverlusten an Windenergieanlagen in Brandenburg. Nyctalus (N.F.), 12(2–3): 238–252.

Dürr T., Bach L., 2004. Fledermäuse als Schlagopfer von Windenergieanlagen – Stand der Erfahrungen mit Einblick in die bundesweite Fundkartei. Bremer Beiträge für Naturkunde und Naturschutz, 7: 253–263.

Edlund G., Carman R., 2001. Distribution and diagenesis of organic and inorganic phosphorus in sediments of the Baltic proper. Chemosphere, 45 (6–7): 1053–1061.

Eero M., 2008. Dynamics of the eastern Baltic cod (Gadus morhua) stock in the 20th century under variable climate and anthropogenic forcing. Ph.D. thesis. University of Southern Denmark, Faculty of Humanities and Technical University of Denmark, National Institute of Aquatic Resources.

Enger P.S., 1967. Hearing in herring. Comp. Biochem. Physiol., 22(2): 527–538.

Falkowska L., Bolałek J., Łysiak-Pastuszak E., 1999. Analiza chemiczna wody morskiej. Tom 2. Pierwiastki biogeniczne N, P, Si, Fe. The University of Gdańsk Publishing House, Gdańsk.

Fewtrell J.L., McCauley R., 2012. Impact of air gun noise on the behaviour of marine fish and squid. Mar. Pollut. Bull., 64(5): 984–993.

Fey D.P., Lejk A., Margonski P. et al., 2014. HERRING: An analysis of spawning ground management, ecological conditions and human impacts in Greifswald Bay, Vistula Lagoon and Hanö Bight.

Filipkowska A., Kowalewska G., Pavoni B., 2014. Organotin compounds in surface sediments of the Southern Baltic coastal zone: a study on the main factors for their accumulation and degradation. Environmental Science and Pollution Research, 21(3): 2077–2087.

Flaquer C., Puig-Montserrat X., Goiti U., Vidal F., Curco A., Russo D., 2009. Habitat selection in Nathusius' pipistrelle (Pipistrellus nathusii): the importance of wetlands. Acta Chiropterologica, 11(1): 149–155.

Foody G.M., 2022. Status of land cover classification accuracy assessment. Remote Sensing of Environment, 80(1): 185–201.

Furness R.W., Wade H.M., Masden E.A., 2013. Assessing vulnerability of marine bird populations to offshore wind farms. Journal of Environmental Management, 119: 56–66.

Gajewski J., Opioła R., Brzezińska A., Barańska A., Brocławik O., Dembska G., Drgas A., Dworniczak J., Dziaduch D., Edut J., Flasińska A., Gajewski Ł., Galer-Tatarowicz K., Jasiński P., Jasper B., Kaczmarek N., Kałas M., Kapiński J., Kargol J., Kołakowska E., Kunicki M., Kuzebski E., Lisimenka A., Littwin M., Marcinkowski T., Matczak M., Misiewicz E., Meissner W., Moroz-Kunicka T., Nermer T., Nocoń M., Olenycz M., Olszewski T., Pazikowska-Sapota G., Pick D., Pylhun A., Rydzkowski P., Sadowska U., Sarnocińska-Kot J., Schönberger L., Skov H., Stöber U., Strzelecki D., Szczepańska K., Szymańska M., Thomsen F., Wróblewski R., Zelewska I., 2021. Raport o oddziaływaniu Morskiej Farmy Wiatrowej BC-Wind na środowisko. Gdańsk.

Gajko K., Ksepko J., Lewsza S., Siuchno R., Zbyryt A., 2018. Wyniki monitoringu ptaków migrujących, [in:] Raport o oddziaływaniu na środowisko morskiej farmy wiatrowej FEW Baltic II. Tom II, Załącznik 5. Baltic Trade and Invest Sp. z o.o., Słupsk.

Galer K., Makuch B., Wolska L., Namieśnik J., 1997. Toksyczne związki organiczne w osadach dennych: problemy związane z przygotowaniem próbek i analizą. Chemia i Inżynieria Ekologiczna (Ecological Chemistry and Engineering), 4: 285.

Galer K., Wolska L., Namieśnik J., 2001. Evaluation of effect of SPM filtration on determination of PCB and PAH in surface waters. Chemia i Inżynieria Ekologiczna (Ecological Chemistry and Engineering), 8(8–9): 817–824.

Garthe S., Scherp B., 2003. Utilization of discards and offal from commercial fisheries by seabirds in the Baltic Sea. ICES Journal of Marine Science, 60: 980–989.

Gauger M., Jansen C., Hagedorn B., Culik B., 2012. Testing POD detection range under optimal field conditions, [in:] B. McGovern, S. Berrow, E. McKeogh, I. O'Connor (Eds), Information and Ideas Worth Sharing. 26th European Cetacean Society Meeting, 26th–28th, March 2012, Galway, Ireland, p. 52.

Gaultier S., Blomberg A., Ijäs A., Vasko V., Vesterinen E., Brommer J., Lilley T.M., 2020. Bats and Wind Farms: The Role and Importance of the Baltic Sea Countries in the European Context of Power Transition and Biodiversity Conservation. Environmental Science and Technology, 54(17): 10385−10398.

Chief Inspectorate of Environmental Protection (*GIOŚ*), 2018. Metodyka monitoringu i oceny stanu ochrony − 1170 Skaliste i kamieniste dno morskie, rafy.

Chief Inspectorate of Environmental Protection (*GIOŚ*), 2018. Pilotażowe wdrożenie monitoringu gatunków i siedlisk morskich w latach 2015–2018. Raport końcowy.

Chief Inspectorate of Environmental Protection (*GIOŚ*), 2022. Monitoring gatunków i siedlisk morskich w latach 2020–2022: część III – gatunki ssaków, morświn.

Girjatowicz J.P., 1985. Atlas zlodzenia wód polskiego wybrzeża Bałtyku. Wydawnictwo Zakładu Upowszechniania Postępu, Szczecin.

Głód D., 1995. N-alkany (n-C16-33), fenantren, fluoranten i piren w stratyfikowanych osadach Zatoki Gdańskiej. The Uniwersity of Gdańsk, Gdańsk.

Goudie R.I., Ankney C.D., 1988. Patterns of habitat use by sea ducks wintering in southeastern Newfoundland Ornis Scandinavica Ornis Scandinavica (Scandinavian Journal of Ornithology), 19(4): 249–256.

Grauman G.B., 1980. Long-term changes of sprat eggs and larvae abundance in the Baltic Sea. [Mnogoletnie izmenienia chislennosti ikryi lichinok szprota w Baltijskom More]. Rybokhozyaistvennye Issledovania (BaltNIIRKh), Riga, Avots, 15: 138–154.

Grauman G.B., 1981. Spatial distribution of flounder eggs and larvae in the Baltic Sea. [Prostranswennoje rozpredelenie ikry i lichinok rechnoj kambaly w Baltijskom More]. Rybokhozyaistvennye Issledovania (BaltNIIRKh), Riga, Avots, 16: 28–38.

Grygiel W., 1987. Młodzież śledzi i szprotów, [in:] Raporty Mor. Inst. Ryb. 1984–1985, Gdynia, pp. 70–74.

Grygiel W., 1997. Charakterystyka biologiczno-technologiczna szprotów południowego Bałtyku, [in:] Prognoza możliwości połowów śledzi i szprotów bałtyckich z uwzględnieniem sezonowości, relacji międzygatunkowych i jakości ryb jako surowca na tle danych wieloletnich. Stud. Mater. Mor. Inst. Ryb., Gdynia, ser. B/69: 124–159.

Grygiel W., 1999. Rozmieszczenie i liczebność młodych śledzi i szprotów w południowym Bałtyku (lata 1976–1991). Monografia. Wydaw. Mor. Inst. Ryb., Gdynia.

Grygiel W., 2006a. Baltic sprat sampling and age determination in Poland. Working paper on the BSRP Sprat Age Reading Workshop, 24–27.01.2006 – Charlottenlund, Denmark [mimeo].

Grygiel W., 2006b. The techniques and criteria of the Baltic sprat age determination. Working document on the BSRP Sprat Age Reading Workshop, 24–27.01.2006 – Charlottenlund, Denmark [mimeo].

Grygiel W., 2015. Zasoby i liczebność rekrutujących pokoleń bałtyckich śledzi, szprotów i dorszy, na podstawie rejsów badawczych. Wiadomości Rybackie, Pismo Mor. Inst. Ryb. – Pań. Inst. Badaw., 9–10(207): 19–23.

Grygiel W., 2016. Biologiczna charakterystyka zasobów szprotów bałtyckich, [in:] Zadanie 1 – Opracowanie roczne statutowego tematu badaw. DOT16/NB/Zasoby „Dynamika populacji ważniejszych ryb użytkowych w świetle czynników środowiskowych wraz z implikacjami dotyczącymi racjonalnego gospodarowania zasobami", prac. zbior. pod kierow. J. Horbowego, The National Marine Fisheries Institute, Gdynia [mimeo].

Grygiel W., Radtke K., 2017. Występowanie szprotów i dorszy w polskiej części Bałtyku (2016 r.). Wiadomości Rybackie, Pismo Mor. Inst. Ryb. – Pań. Inst (The National Marine Fisheries Institute), 9–10(219): 22–26.

Grygiel W., Radtke K., Mirny Z., Wyszyński M., 2016. Bałtyckie rejsy badawcze jako podstawa oceny rozmieszczenia i liczebności rekrutujących pokoleń dorszy, śledzi, szprotów i storni, [in:] 95-lecie Morskiego Instytutu Rybackiego: aktualne tematy badań naukowych. Monografia. Tom 1. Zasoby ryb i rybołówstwo. The National Marine Fisheries Institute, Gdynia, pp. 17–32.

Guillemette M., Reed A., Himmelman J.H., 1996. Availability and consumption of food by common eiders wintering in the Gulf of St. Lawrence. Evidence of prey depletion. Canadian Journal of Zoology, 74(1): 32–38.

Guz W., Bolałek J., Aftanas B., Dembska G., Wiśniewski S., 2000. Zawartość wielopierścieniowych węglowodorów aromatycznych w osadach dennych kanałów portu Gdańskiego. Konferencja naukowo-techniczna z okazji 50-lecia Instytutu Morskiego, Gdańsk, 19–20 October 2000. Internal Materials of the Maritime Institiute in Gdańsk no 897.

Haslob H., Rabade-Uberos S., Saborido-Rey F., 2013. Seasonal variability of fecundity and spawning dynamics of Baltic sprat. Fisheries Research, 138: 99–109.

Hastings M.C., Popper A.N., Finneran J.J. et al., 1996. Effects of low-frequency underwater sound on hair cells of the inner ear and lateral line of the teleost fish Astronotus ocellatus. J. Acoust. Soc. Am., 99(3): 1759–1766.

Hawkins A.D., Johnstone A.D.F., 1978. The hearing of the Atlantic salmon, *Salmo salar*. J. Fish. Biol., 13(6): 655–673.

Heinemann D., 1981. A range finder for pelagic bird censusing. Journal of Wildlife Management, 45(2): 489–493.

Heist K., Johnson D., 2013. Predicting Bat Fatality Risk at Prospective Wind Farm Sites Using Acoustic Detectors. 16th International Bat Research Conference & 43rd North American Symposium on Bat Research. August 11–15, 2013. San Jose, Costa Rica. Abstracts.

HELCOM, 2013a. HELCOM core indicators. Final report of the HELCOM CORESET project. Baltic Sea Environment Proceedings No. 136.

HELCOM, 2002. Environment of the Baltic Sea area 1994–1998. Baltic Sea Environment Proceedings No. 82B.

HELCOM, 2009. Biodiversity in the Baltic Sea. An integrated thematic assessment on biodiversity and nature conservation in the Baltic Sea. Baltic Sea Environment Proceedings No. 116B.

HELCOM, 2009. Ensuring safe shipping in the Baltic.

HELCOM, 2013b. HELCOM Red List of Baltic Sea species in danger of becoming extinct. Baltic Sea Environment Proceedings No. 140.

HELCOM, 2018. Population trends and abundance of seals. HELCOM core indicator report. Online: http://www.helcom.fi/baltic-sea-trends/indicators/population-trends-and-abundance-of-seals/.

HELCOM, 2018. Tributyltin (TBT) and imposex. HELCOM core indicator report.

HELCOM, 2021, Manual for Marine Monitoring in the COMBINE Programme of HELCOM. Part C. Programme for monitoring of eutrophication and its effects. Anne C-8. Soft bottom macrozoobenthos.

HELCOM, 2021. Essential fish habitats in the Baltic Sea – Identification of potential spawning, recruitment and nursery areas.

HELCOM, 2021. HELCOM Guidelines for monitoring continuous noise. Updated HELCOM Guidelines as noted by State & Conservation 14-2021.

HELCOM, 2023. Lead. HELCOM Core Indicator Report. Online (Access: 20.01.2024); https://indicators.helcom.fi/wp-content/uploads/2023/04/Lead_Final_For_April_2023-1.pdf.

HELCOM, 2023. Metals (cadmium). HELCOM Core Indicator Report. Online (Access: 20.01.2024); https://indicators.helcom.fi/wp-content/uploads/2023/04/Cadmium_Final_July_2023.pdf.

HELCOM, 2023. Radioactive substances: Caesium-137 in fish and surface seawater. HELCOM core indicator report. Online (Access: 20.01.2024); https://indicators.helcom.fi/wp-content/uploads/2023/04/Radioactive-substances_Final_April_2023-2.pdf.

HELCOM, Activities 2005. Overview, Baltic Sea Environment Proceedings No. 107.

HELCOM, Activities 2011. Overview, Baltic Sea Environment Proceedings No. 132.

Herra T., 1988. Sezonowa i wieloletnia zmienność ichtioplanktonu Bałtyku Południowego i czynniki ją warunkujące. 107/C [mimeo].

Hjalmarsson S., Wesslander K., Anderson L.G., Omstedt A., Perttilä M., Mintrop L., 2008. Distribution, long-term development and mass balance calculation of total alkalinity in the Baltic Sea. Continental Shelf Research, 28(4–5): 593–601.

Hoekman S.T., Moynahan B.J., Lindberg M.S., Sharman L.C., Johnson W.F., 2011. Line transect surveys for murrelets: accounting for incomplete detection and identification. Marine Ornithology, 39: 35–44.

Horackiewicz J., Skóra K., 1996. Występowanie babkowatych (Gobiidae, Pisces) w polskiej strefie przybrzeżnej Morza Bałtyckiego. Zoologica Poloniae, 41(Suppl.): 179–188.

Horackiewicz J., Skóra K., 1998. A seasonal pattern of occurrence of gobiid fish (Gobiidae) in the shallow littoral zone (0–1 m depth) of Puck Bay. Oceanological Studies, 27: 3–17.

Horbowa K., Fey D., 2013. Atlas wczesnych stadiów rozwojowych ryb. 34 gatunki ryb Bałtyku Południowego i jego zalewów. The National Marine Fisheries Institute., Gdynia.

Horn J.W., Arnett E.B., Kunz T.H., 2008. Behavioral Responses of Bats to Operating Wind Turbines. Journal of Wildlife Management, 72: 123–132.

Hüppop O., Hüppop K., Dierschke J., Hill R., 2016. Bird collisions at an offshore platform in the North Sea. Bird Study, 63(1): 73–82.

Hutterer R., Ivanova T., Meyer-Cords C., Rodrigues L., 2005. Bat migrations in Europe. A review of banding data and literature. Federal Agency for Nature Conservation in Germany, Bonn.

ICES, 2010. Report of the Study Group on Standards in Ichthyoplankton Surveys (SGSIPS). 11–15 October 2010, Ijmuiden, The Netherlands. ICES CM 2010/SSGESST:21.

ICES, 2012. Report of the Study Group on Standards in Ichthyoplankton Surveys (SGSIPS). 8–10 May 2012, Hamburg, Germany. ICES CM 2012/SSGESST:10.

ICES, 2022. Report of the Baltic Fisheries Assessment Working Group (WGBFAS). ICES Scientific Reports, 4:44.

ICES, 2023. Baltic Fisheries Assessment Working Group (WGBFAS). ICES Scientific Reports, 5:58.

IEC 61260-1:2014. Electroacoustics – Octave-band and fractional-octave-band filters. Part 1: Specifications, 2014. International Electrotechnical Commission, Geneva.

Inspekcja Ochrony Środowiska, 2020. A. Kolada (Ed.) Podręcznik do monitoringu elementów biologicznych i klasyfikacji stanu ekologicznego wód powierzchniowych. Aktualizacja metod. Biblioteka Monitoringu Środowiska, Warszawa.

International Atomic Energy Agency (IAEA), 2005. Worldwide marine radioactivity studies (WOMARS). Radionuclide levels in oceans and seas. Final report of a coordinated research project. IAEA-TECDOC-1429.

IUCN, 2023. The IUCN Red List of Threatened Species. Version 2023-1. https://www.iucnredlist.org.

Jönsson A., Danielsson Å., Rahm L., 2005. Bottom-type distribution based on wave friction velocity in the Baltic Sea. Continental Shelf Research, 25(3): 419–435.

Kajzer Z., Barcz M., Guentzel S., Jasiński M., 2010, Liczebność ptaków wodno-błotnych na zachodnim wybrzeżu Bałtyku w sezonach 2008/2009–2010/2011. Ptaki Pomorza, 3: 87–99.

Kastak D., Schusterman R.J., 1998. Low-frequency amphibious hearing in pinnipeds: methods, measurements, noise and ecology. J. Acoust. Soc. Am., 103(4): 2216–2228.

Kastelein R.A., Bunskoek P., Hagedoorn M., Au W.W., de Haan D., 2002. Audiogram of a harbor porpoise (Phocoena phocoena) measured with narrow-band frequency-modulated signals. J. Acoust. Soc. Am., 112(1), 1: 334–344.

Kastelein R.A., van der Heul S., Verboom W.C. et al., 2008. Startle response of captive North Sea fish species to underwater tones between 0.1 and 64 kHz. Mar. Env. Res., 65(5): 369–377.

Kepel A. (Ed.), Ciechanowski M., Furmankiewicz J., Górawska M., Hejduk J., Jaros R., Jaśkiewicz M., Kasprzyk K., Kowalski M., Przesmycka A., Stopczyński M., Urban R., 2009a. Tymczasowe wytyczne dotyczące oceny oddziaływania elektrowni wiatrowych na nietoperze (na rok 2009).

Kepel A. (Ed.), Ciechanowski M., Furmankiewicz J., Gottfried T., Górawska M., Ignaczak M., Jaros R., Jaśkiewicz M., Kasprzyk K., Kmiecik P., Kowalski M., Popczyk B., Szkudlarek R., Urban R., Wojtaszyn G., Wojtowicz B., 2009b. Tymczasowe wytyczne dotyczące oceny oddziaływania elektrowni wiatrowych na nietoperze (wersja II, grudzień 2009).

Kepel A., Ciechanowski M., Jaros R., 2011. Wytyczne dotyczące oceny oddziaływania elektrowni wiatrowych na nietoperze. Chief Inspectorate of Environmental Protection (*GIOŚ*), Warszawa.

Kepel. A., Ciechanowski M., Jaros R., 2013. Wytyczne dotyczące oceny oddziaływania elektrowni wiatrowych na nietoperze. Projekt – wersja z XI 2013. Chief Inspectorate of Environmental Protection, Poznań.

Khanh N.V., Drzycimski I., Chojnacki J., 1972. Feeding and food composition of sprat from the Bornholm Depth. Acta Ichthyologica et Piscatoria, II(2): 55–66.

Kirk M., Esler D., Iverson S.A., Boyd W.S., 2008. Movements of wintering surf scoters: predator responses to different prey landscapes. Oecologia, 155(4): 859–867.

Klug B.J., Baerwald E.F., 2010. Incidence and management of live and injured bats at wind energy facilities. J. Wildlife Rehab., 30: 11–16.

Klusek Z., 1977a. Charakterystyczne elementy szumów akustycznych w toni wodnej Południowego Bałtyku. PhD Thesis. The Oceanology Department of the Polish Academy of Sciences, Sopot.

Klusek Z., 1977b. Charakterystyki kierunkowe pola szumów w Południowym Bałtyku. Studia i Materiały Oceanologiczne KBM PAN, 17: 83–106.

Klusek Z., 1990. Warunki propagacji dźwięku w Południowym Bałtyku. The Oceanology Department of the Polish Academy of Sciences, Sopot.

Klusek Z., 2000. Monte-Carlo Modelling of Seasonal Changes of the Ambient Sea Noise Field Characteristics in the Baltic Sea, [in:] M.E. Zakharia (Ed.), Proc. 5th European Conference on Underwater Acoustics, ECUA, Lyon, France, pp. 705–710.

Klusek Z., Lisimenka A., 2016. Seasonal and diel variability of the underwater noise in the Baltic Sea. J. Acoust. Soc. Am., 139(4): 1537–1547.

Komdeur J., Bertelsen J., Cracnell G. (Eds), 1992. Manual for Aeroplane and Ship Surveys of waterfowl and Seabirds. IWRB Special Publication No. 19, Slimbridge.

Konat J., Kowalewska G., 2001. Polychlorinated biphenyls (PCBs) in sediments of the southern Baltic Sea – trends and fate. Science of the Total Environment, 280(1–3): 1–15.

Kostrichkina E.M., Starodub M.L., Davidyuk A.P., 1980. Pitanje sieldi i shprota v vostochnom i jugo-vostovhnom Baltijskom morie. Rybohoz. issl. v bass. Baltijskogo moria, 15: 130–137.

Kot-Wasik A., Dębska J., Namieśnik J., 2004. Monitoring of organic pollutants in coastal waters of the Gulf of Gdańsk, Southern Baltic. Marine Pollution Bulletin, 49(3): 264–276.

Kowalewska G., Konat J., 1999. Determination of polychlorinated biphenyls in the marine sediments using gas chromatography. Chemical Analysis, 44(2): 223–233.

Kramarska R., 1995a. Osady na głębokości 1 m poniżej powierzchni dna, [in:] J.E. Mojski (Ed.), Atlas geologiczny Południowego Bałtyku. Tab. XXI. Polish Geological Institute, Sopot–Warszawa.

Kramarska R., 1995b. Osady powierzchni dna, [in:] J.E. Mojski (Ed.), Atlas geologiczny Południowego Bałtyku. Tab. XXIV. Polish Geological Institute, Sopot–Warszawa.

Kramarska R., Jegliński W., Jurys L., Przezdziecki P., Uścinowicz S., Zachowicz J., 2005. Atlas parametrów litologicznych osadów powierzchniowych południowego Bałtyku ze szczególnym

uwzględnieniem geologiczno-górniczych warunków występowania surowców okruchowych. Tab. nr 17, Złoża i obszary perspektywiczne surowców okruchowych. Polish Geological Institute – Marine Geology Department, Gdańsk.

Kramarska R., Krzywiec P., Dadlez R., 1999. Mapa geologiczna dna Bałtyku bez utworów czwartorzędowych. Polish Geological Institute, Warszawa.

Kramarska R., Krzywiec P., Dadlez R., Jegliński W., Papiernik B., Przeździecki P., Zientara P., 1999. Mapa geologiczna dna Bałtyku bez utworów czwartorzędowych w skali 1:500 000 wraz z tekstem objaśniającym. Polish Geological Institute, Gdańsk–Warszawa.

Kramarska R., Przezdziecki P., Uścinowicz S., Zachowicz J., 1995. Przekroje geologiczne (I), [in:] J.E. Mojski (Ed.), Atlas geologiczny Południowego Bałtyku. Tab. XIX. Polish Geological Institute, Sopot–Warszawa.

Kramarska R., Szarafin T., Pączek U., Frydel J., Koszka-Maroń D., Kaulbarsz D., Piotrowski A., Relisko-Rybak J., Mil L., 2019. Mapa geośrodowiskowa polskich obszarów morskich w skali 1:250 000 wraz z objaśnieniami. Polish Geological Institute-National Research Institute, Gdańsk–Warszawa.

Krasovskaya N., 2002. Spawning of the Baltic herring in the Vistula Lagoon: effects of environmental conditions and stock parameters. Bull. Sea Fish. Inst. 1(155): 3–25.

Kruk-Dowgiałło L., Kramarska R., Gajewski J. (Ed.), 2011. Siedliska przyrodnicze polskiej strefy Bałtyku. T. 1. Głazowisko Ławicy Słupskiej. Maritime Institute in Gdańsk, Polish Geological Institute-National Research Institute, Gdańsk.

Krzymiński W. (Ed.), 2018. Ocena stanu środowiska polskich obszarów morskich Bałtyku na podstawie danych monitoringowych z roku 2017 na tle dziesięciolecia 2007–2016. Inspectorate of Environmental Protection.

Krzymiński W. (Ed.), 2013. Wstępna ocena stanu środowiska wód morskich polskiej strefy Morza Bałtyckiego. Raport do Komisji Europejskiej. Chief Inspectorate of Environmental Protection, Warszawa.

Kunz T.H., Arnett E.B., Cooper B.M., Erickson W.P., Larkin R.P., Mabee T., Morrison M.L., Strickland M.D., Szewczak J.M., 2007. Assessing Impacts of Wind-Energy Development on Nocturnally Active Birds and Bats: A Guidance Document. J. Wildlife Manage., 71(8): 2449–2486.

Kursa M.B., Rudnicki W.R., 2010. Feature selection with the Boruta Package. Journal of Statistical Software, 36(11): 1–13.

La Manna G., Manghi M., Perretti F. et al., 2016. Behavioral response of brown meagre (Sciaena umbra) to boat noise. Mar. Pollut. Bull., 110 (1): 324–334.

Lagerveld S., Mostert K., 2023. Are offshore wind farms in the Netherlands a potential threat for coastal populations of noctule? Lutra, 66(1): 39–53.

Lagerveld S., Noort C.A., Meesters L., Bach L., Bach P., Geelhoed S., 2020. Assessing fatality risk of bats at offshore wind Turbines. Wageningen Marine Research report C025/20.

Lagerveld S., Poerink B.J., Haselager R., Verdaat H., 2014. Bats in Dutch offshore wind farms in autumn 2012. Lutra, 57(2): 61–69.

Lagerveld S., Wilkes T., van Puijenbroek M,·Noort B., Geelhoed S., 2023. Acoustic monitoring reveals spatiotemporal occurrence of Nathusius' pipistrelle at the southern North Sea during autumn migration. Environ Monit Assess 195: 1016.

Länsstyrelsen Kalmar län, 2021. Bevarandeplan för Natura 2000-området SE0330308 Hoburgs bank och Midsjöbankarna.

Lewis T.L., Esler D., Boyd W.S., 2007. Effects of predation by sea ducks on calm abundance in soft-bottom intertidal habitats. Marine Ecology Progress Series, 329: 131–144.

Lisimenka A., 2007. Identification of sound scattering layers and some hydrometeorological characteristics using ambient sea noise in the Baltic Sea. PhD Thesis. The Oceanology Department of the Polish Academy of Sciences, Sopot.

Lundgren R.B.C., Nielsen A., Krüger-Johnsen M., Righton D., Mion M., Radtke K., Plikshs M., Leskelä A.I., Raitaniemi J., Griffiths C.A., Casini M., Krumme U., Hüssy K., 2022. Examining fish movement in terms of advection or diffusion: a case study of northeastern Atlantic cod. Mar. Ecol. Prog. Ser., 691: 115–129.

Luoma S.N., Bryan G.W.W., 1981. A statistical assessment of the form of trace metals in oxidized estuarine sediments employing chemical extractants. Science of the Total Environment, 17(2): 165–196.

Maciejowski M., Lenart W. (Eds), 1995. Leksykon ochrony środowiska ze słownikami polsko-angielskim, angielsko-polskim, polsko-niemieckim, niemiecko-polskim. Fundacja Ecobaltic, Gdańsk.

Mackie I., Racey P., 2007. Habitat use varies with reproductive state in noctule bats (Nyctalus noctula): implications for conservation. Biological Conservation, 140(1–2): 70–77.

Maier H.N., 1908. Beiträge zur Altersbestimmung der Fische. Wissenschaftliche Meeresuntersuchungen (Abt. Helgoland, N. F.), 8(1): 60–115.

Mańkowski W., 1947. Odżywianie się i pokarm szprota (Clupea sprattus L.) Bałtyku Środkowego. Arch. Hydrobiol. i Ryb., 13: 37–90.

Mańkowski W., 1951. Ichtiologia dla rybaków morskich. Wydaw. Morskie, Gdańsk.

Margoński P. et al., 2014. Troficzne interakcje pomiędzy ichtioplanktonem i zooplanktonem południowego Bałtyku – badania mechanizmów rekrutacji. Kierownik projektu: dr Piotr Margoński. Kierownik zadania: dr Aleksander Drgas. Sprawozdanie z realizacji tematu statutowego, Gdynia. Temat realizowany przez Zakład Oceanografii Rybackiej i Ekologii Morza, Gdynia.

Margoński P., Ameryk A., Andrulewicz G., Fey D., Grelowski A., Gromisz S., Horbowa K., Kownacka J., Krajewska A., Maciejewska K., Pastuszak M., Pawlikowski K., Szymanek L., Tomczak M., Wodzinowski T., Wróblewska H., Zalewski M., 2007. Troficzne interakcje pomiędzy ichtioplanktonem zooplanktonem południowego Bałtyku – badania mechanizmów rekrutacji – sprawozdanie z realizacji tematu statutowego, Gdynia.

Margoński P., Ameryk A., Andrulewicz, E., Drgas A., Fey D., Gromisz S., Horbowa K., Krajewska A., Jakubowska A., Kownacka J., Krajewska A., Linkowski T., Pastuszak M., Pawełczyk A., Pawlikowski K., Schmidt B., Słembarski J., Szymanek L., Warzocha J., Witalis B., Wodzinowski T., Woźniczka A. Wróblewska H., Zalewski M., 2012. Podstawy do ekosystemowego podejścia do zarządzania:

Troficzne interakcje pomiędzy ichtioplanktonem i zooplanktonem południowego Bałtyku: badania mechanizmów rekrutacji – sprawozdanie z realizacji problemu badawczego P2, Gdynia.

Margoński P., Ameryk A., Białowąs M., Bielak M., Choma-Stolarek K., Dembek M., Horbowa K., Nadolna-Ałtyn K., Nowak A., Nurek B., Pawlak J., Rosa P., Witalis B., Wodzinowski T., Woźniczka A., Wróblewska H., Zalewski M., 2020. Rekrutacja wybranych gatunków ryb a warunki hydrologiczne oraz skład i dostępność bazy pokarmowej. Gdynia.

Margoński P., Ameryk A., Białowąs M., Czugała A., Dembek M., Horbowa K., Jakubowska A., Nurek B., Pawlikowski K., Rosa P., Spich K., Warzocha J., Witalis B., Wodzinowski T., Woźniczka A., Wróblewska H., Zalewski M., 2018. Rekrutacja wybranych gatunków ryb a warunki hydrologiczne oraz skład i dostępność bazy pokarmowej. Gdynia.

Margoński P., Ameryk A., Białowąs M., Dembek M., Horbowa K., Nadolna-Ałtyn K., Nurek B., Pawlak J., Pawlikowski K., Witalis, B., Wodzinowski T., Woźniczka A., Wróblewska H., Wybierała I., Zalewski M., 2019. Rekrutacja wybranych gatunków ryb a warunki hydrologiczne oraz skład i dostępność bazy pokarmowej. Gdynia.

Margoński P., Ameryk A., Celmer Z., Czugała A., Fey D., Horbowa K., Pawlikowski K., Rosa P., Słembarski J., Szymanek L., Vaniala A., Warzocha J., Wodzinowski T., Woźniczka A., Zalewski M., 2017. Relacje pomiędzy rekrutacją wybranych gatunków ryb a czynnikami je warunkującymi, takimi jak warunki hydro-meteorologiczne oraz skład i dostępność bazy pokarmowej – sprawozdanie z realizacji statutowego problemu badawczego P7-1, temat DOT 16/rekrut. Gdynia.

Margoński P., Ameryk A., Drgas A., Fey D., Gromisz S., Grzyb A., Horbowa K., Jakubowska A., Jankowska-Tessmer A., Kownacka J., Krajewska A., Pastuszak M., Pawełczyk A., Pawlikowski K., Schmidt B., Słembarski J., Spich K., Szymanek L., Warzocha J., Witalis B., Wodzinowski T., Woźniczka A. Wróblewska H., Zalewski M., 2013. Podstawy do ekosystemowego podejścia do zarządzania: Troficzne interakcje pomiędzy ichtioplanktonem i zooplanktonem południowego Bałtyku: badania mechanizmów rekrutacji – sprawozdanie z realizacji problemu badawczego P2, Gdynia.

Margoński P., Ameryk A., Drgas A., Fey D., Gromisz S., Horbowa K., Jakubowska A., Kownacka J., Krajewska A., Pawełczyk A., Pawlikowski K., Schmidt B., Szymanek L., Warzocha J., Witalis B., Wodzinowski T., Woźniczka A., Wróblewska H., Zalewski M., 2011. Troficzne interakcje pomiędzy ichtioplanktonem i zooplanktonem południowego Bałtyku – badania mechanizmów rekrutacji – sprawozdanie z realizacji tematu statutowego, Gdynia.

Margoński P., Ameryk A., Dziaduch D., Fey D., Grelowski A., Gromisz S., Horbowa K., Kownacka J., Krajewska A., Maciejewska K., Pawlikowski K., Sitek S., Szymanek L., Warzocha J., Wodzinowski T., Woźniczka A., Wróblewska H., Zalewski M., 2008. Troficzne interakcje pomiędzy ichtioplanktonem i zooplanktonem południowego Bałtyku – badania mechanizmów rekrutacji – sprawozdanie z realizacji tematu statutowego, Gdynia 2008.

Margoński P., Ameryk A., Dziaduch D., Fey D., Gromisz S., Horbowa K., Kownacka J., Krajewska A., Maciejewska K., Pawlikowski K., Schmidt B., Szymanek L., Wodzinowski T., Wróblewska H., Zalewski M., 2009. Troficzne interakcje pomiędzy ichtioplanktonem i zooplanktonem południowego Bałtyku – badania mechanizmów rekrutacji – sprawozdanie z realizacji tematu statutowego, Gdynia.

Margoński P., Ameryk A., Fey D., Grelowski A., Gromisz S., Horbowa K., Kownacka J., Krajewska A., Linkowski T., Maciejewska K., Pastuszak M., Pawlikowski K., Szymanek L., Świtek K., Tomczak M., Witek Z., Wodzinowski T., Wróblewska H., Zalewski M., 2006. Troficzne interakcje pomiędzy ichtioplanktonem i zooplanktonem południowego Bałtyku – badania mechanizmów rekrutacji – sprawozdanie z realizacji tematu statutowego, Gdynia.

Margoński P., Ameryk A., Fey D., Grelowski A., Gromisz S., Horbowa K., Kownacka J., Krajewska A., Pawlikowski K., Piwosz K., Schmidt B., Szymanek L., Warzocha J., Witalis B., Wodzinowski T., Wróblewska H., Zalewski M., Jakubowska A., Pawełczyk A., Woźniczka A., 2010. Troficzne interakcje pomiędzy ichtioplanktonem i zooplanktonem południowego Bałtyku – badania mechanizmów rekrutacji – sprawozdanie z realizacji tematu statutowego, Gdynia.

Margoński P., Czugała A., Drgas A., Fey D., Horbowa K., Jankowska-Tessmer A., Pawlikowski K., Rosa P., Schmidt B., Słembarski J., Szymanek A., Vaniala A., Wodzinowski T., Wróblewska H., Zalewski M., 2016. Relacje pomiędzy rekrutacją wybranych gatunków ryb a czynnikami je warunkującymi, takimi jak warunki hydro-meteorologiczne oraz skład i dostępność bazy pokarmowej. Kierownik zadania: dr Piotr Margoński. Gdynia.

Markones N., Guse N., Borkenhagen K., Schwemmer H., Garthe S., 2015. Seevogel-Monitoring 2014 in der deutschen AWZ von Nord- und Ostse. Bundesamt für Naturschutz (BfN), Bonn.

Matzner S., Cullinan V., Duberstein C., 2015. Two-dimensional thermal video analysis of offshore bird and bat flight. Ecological Informatics, 30(2015): 20–28.

McCauley R., Day R.D., Swadling K.M. et al., 2017. Widely used marine seismic survey air gun operations negatively impact zooplankton. Nat. Ecol. Evol., 1(7): 1–8.

McCauley R.D., Fewtrell J., Popper A.N., 2003. High intensity anthropogenic sound damages fish ears. J. Acoust. Soc. Am., 113(1): 638–642.

Medwin H., Clay C.S., 1998. Fundamentals of Acoustical Oceanography, Academic Press.

Meissner W., 2010. Sezonowe zmiany liczebności i rozmieszczenia lodówki Clangula hyemalis, markaczki Melanitta nigra i uhli M. fusca w rejonie Przylądka Rozewie. Ornis Polonica, 51: 275–284.

Meissner W., 2011. Ptaki morskie, [in:] Sikora A., Chylarecki P., Meissner W., Neubauer G. (Eds), Monitoring ptaków wodno-błotnych w okresie wędrówek. Poradnik metodyczny. GDOŚ, Warszawa, pp. 93–102.

Meissner W., 2014a. Monitoring ornitologiczny obszaru Natura 2000 Ławica Słupska (PLC 990001). Raport końcowy z wynikami badań, [in:] Morska farma wiatrowa Bałtyk Środkowy II. Raport o oddziaływaniu na środowisko. Volume III, Section 8. Grupa Doradcza SMDI, Warszawa.

Meissner W., 2014b. Monitoring ptaków morskich obszaru przeznaczonego pod budowę MFW Bałtyk Środkowy III. Raport końcowy z wynikami badań, [in:] Morska farma wiatrowa Bałtyk Środkowy II. Raport o oddziaływaniu na środowisko. Volume III, Section 8. Grupa Doradcza SMDI, Warszawa.

Meissner W., 2015. Monitoring ptaków morskich obszaru przeznaczonego pod budowę MFW Bałtyk Środkowy II. Raport końcowy z wynikami badań, [in:] Morska farma wiatrowa Bałtyk Środkowy

II. Raport o oddziaływaniu na środowisko. Volume III, Section 8. Grupa Doradcza SMDI, Warszawa.

Meissner W., Betleja J., 2007. Skład gatunkowy, liczebność i struktura wiekowa mew Laridae zimujących na składowiskach odpadów komunalnych w Polsce. Notatki Ornitologiczne, 48: 11–27.

Meissner W., Staniszewska J., Bzoma S., 2007. Liczebność oraz struktura gatunkowa i wiekowa mew Laridae w regionie Zatoki Gdańskiej w okresie pozalęgowym. Notatki Ornitologiczne, 48: 67–81.

Michałek M., Osowiecki A., Barańska A., Wróblewski R., Rydzkowski P., Kośmicki A., Strzelecki D., Meissner W., Pieckiel P., Kuczyński T., Gajewski L. 2020, Dokumentacja przyrodnicza, tj. opis tekstowy, zestawienia tabelaryczne, przedstawienia graficzne, kartograficzne oraz dane stanowiące podstawę sformułowania projektu planu ochrony morskiego obszaru Natura 2000 Ławica Słupska PLC990001. MI GMU publications 7374. Maritime Institute of the Gdynia Maritime University, MEWO S.A., Gdańsk.

Miętus M., Sztobryn M., (Eds), 2011. Stan środowiska polskiej strefy przybrzeżnej Bałtyku w latach 1986–2005. Wybrane zagadnienia. Institute of Meteorology and Water Management – National Research Institute, Warszawa.

Ministerstwo Przemysłu, 1988. Kryteria bilansowości dla złóż kruszywa naturalnego w polskim obszarze Bałtyku, Warszawa.

Møhl B., 1968. Auditory sensitivity of the common seal in air and water. Journal of Auditory Research, 8(1): 27–38.

Momigliano P., Denys G.P.J., Jokinen H., Merilä J., 2018. Platichthys solemdali sp. nov. (Actinopterygii, Pleuronectiformes): A New Flounder Species From the Baltic Sea. Frontiers in Marine Science, 5: 1–21.

Mustonen M., Klauson A., Andersson M. et al., 2019. Spatial and Temporal Variability of Ambient Underwater Sound in the Baltic Sea. Sci. Rep., 9(1): 13237.

Namieśnik J., 2001. Modern trends in monitoring and analysis of environmental pollutants. Polish Journal of Environmental Studies, 10(3): 127–140.

Nedelec S.L., Radford A.N., Pearl L. et al., 2017. Motorboat noise impacts parental behaviour and offspring survival in a reef fish. Proc. R. Soc. B, 284(1856): 20170143.

Nedelec S.L., Radford A.N., Simpson S.D. et al., 2014. Anthropogenic noise playback impairs embryonic development and increases mortality in a marine invertebrate. Sci. Rep., 4: 5891.

Nedelec S.L., Simpson S.D., Morley E.L. et al., 2015. Impacts of regular and random noise on the behaviour, growth and development of larval Atlantic cod (Gadus morhua). Proc. R. Soc. B, 282(1817): 20151943.

Nehls H.W., Zöllick H., 1990. The moult migration of Common Scoter (Melanitta nigra) off the coast of the GDR. Proc. Conf. Baltic Birds 5, Riga, pp. 36–46.

Nichols T.A., Anderson T.W., Širović A., 2015. Intermittent noise induces physiological stress in a coastal marine fish. PLoS ONE, 10(9): e0139157.

Niemirycz E., Sapota G., 2010. Pestycydy i polichlorowane bifenyle, [in:] J. Bolałek (Ed.), Fizyczne, biologiczne i chemiczne badania morskich osadów dennych. The University of Gdańsk Publishing House, Gdańsk.

Nikanorov A.M., Stradomskaya A.G., 2003. Oil Products in Bottom Sediments of Freshwater Bodies. Water Resources, 30(1): 98–102.

Nilsson L., Ogonowski M., Staveley T.A.B., 2016. Factors affecting the local distribution of the Long-tailed Duck Clangula hyemalis in Baltic offshore waters. Wildfowl, 66: 142–158.

Nissling A., Westin L., Hjerne O., 2002. Reproductive success in relation to salinity for three flatfish species, dab (Limanda limanda), plaice (Pleuronectes platessa), and flounder (Pleuronectes flesus), in the brackish water Baltic Sea. ICES J. Mar. Sci. 59(1): 93–108.

NMFS, 2018. Revisions to: Technical Guidance for Assessing the Effects of Anthropogenic Sound on Marine Mammal Hearing (Version 2.0): Underwater Thresholds for Onset of Permanent and Temporary Threshold Shifts. U.S. Dept. of Commer., NOAA. NOAA Technical Memorandum NMFS-OPR-59.

NMFS, 2023. National Marine Fisheries Service: Summary of Endangered Species Act acoustic thresholds (marine mammals, fishes and sea turtles).

Nowak J., Hac B., Malottki A., Niemkiewicz M., Jacob K., Jażdżewski M., Sitarz M., Spacjer R., Cichowska D., Szyłejko W., Wysocki P. 2017, Wykonanie projektu i budowa działającego modelu urządzenia do poboru prób biologicznych z obiektów stałych zalegających na dnie morza. Internal Publications of the Maritime Institute in Gdańsk no. 7140A.

Nriagu J.O., 1988. A silent epidemic of environmental metal poisoning? Environmental Pollution, 50(1–2): 139–161.

Odum E. 1982, Podstawy ekologii. Wydanie III. Państwowe Wydawnictwo Rolnicze i Leśne, Warszawa.

Ojaveer E., Jevtjukhova B., Rechlin O., Strzyzewska K., 1981. Results of investigation of population structure and otoliths of Baltic spring spawning herring. CM 1981/J19 Balt Fish Com.

Ojaveer E., Kalejs M., 2010. Ecology and long-term forecasting of sprat (Sprattus sprattus balticus) stock in the Baltic Sea: a review. Rev. Fish Biol. Fish. 20(2): 203–217.

Ojaveer H., Lankov A., Raid T. et al., 2018. Selecting for three copepods—feeding of sprat and herring in the Baltic Sea. ICES J Mar Sci., 75(7): 2439–2449.

Olsen M., Petersen K., Lehoux A.P., Leppänen M., Schaanning M., Snowball I., Øxnevad S., Lund E., 2019. Contaminated Sediments : Review of solutions for protecting aquatic environment TemaNord 2019:514.

Opioła R., Barańska A, Kruk-Dowgiałło L., Dziaduch D., Brzeska-Roszczyk P., Pieckiel P., Łysiak-Pastuszak E., Osowiecki A., Olenycz M., Zaboroś I., Mioskowska M., Kuczyński T., Błeńska M., Dembska G., Pazikowska-Sapota G., Galer-Tatarowicz K., Flasińska A., Nowogrodzka K., Boniecki W., Cichowska A., Boniecka H., Gawlik W., Gajda A., Kaźmierczak A., Bajkiewicz-Grabowska E., Markowski M., Kozłowski K., Malinga M., Świstun K., Yalçin G., Błaszczyk Ł., Mroczek K., Pyra A., 2017. Pilotażowe wdrożenie monitoringu gatunków i siedlisk morskich w latach 2015–2018. Raport z prac wykonanych w III etapie. Internal Publications of the Maritime Institute in Gdańsk

no. 7124, Study carried out as part of the state Environmental Monitoring commissioned by the Chief Inspectorate for Environmental Protection.

Opioła R., Gajewski J., Kaczmarek N., Barańska A., Bojke A., Brocławik O., Brzezińska A., Celmer Z., Cuttat F., Dembska G., Drgas A., Druzd N., Dworniczak J., Dziaduch D., Edut J., Eisen M., Fey D., Flasińska A., Gajewski Ł., Galer-Tatarowicz K., Grygiel W., Horbowa K., Jasper B., Kałas M., Kapiński J., Kołakowska E., Kubacka M., Kunicki M., Kuzebski E., Lisimenka A., Littwin M., Marcinkowski T., Meissner W., Mirny Z., Misiewicz E., Mortensen L., Nermer T., Nocoń M., Olenycz M., Olszewski T., Ostrowska D., Pazikowska-Sapota G., Pick D., Radtke K., Rydzkowski P., Sadowska U., Sarnocińska J., Schack H., Schmidt B., Schönberger L., Skov H., Strzelecki D., Stöber U., Suska M., Szczepańska K., Szymanek L., Thomsen F., Tuhuteru N., Wróblewski R., Wyszyński M., Załęski K., 2020. Raport o oddziaływaniu Morskiej Farmy Wiatrowej Baltic Power na środowisko, Gdańsk.

Orio A., Bergström U., Florin A.B., Lehmann A., Šics I., Casini M., 2019. Spatial contraction of demersal fish populations in a large marine ecosystem. Journal of Biogeography, 46(3): 633–645.

Osowiecki A., Błeńska M. 2020, Makrozoobentos w wodach przejściowych i przybrzeżnych, [in:] A. Kolada (Ed.), Przewodnik do monitoringu elementów biologicznych i klasyfikacji stanu ekologicznego wód powierzchniowych. Aktualizacja metod. Biblioteka Monitoringu Środowiska, Warszawa, pp. 345–367.

Osowiecki A., Błeńska M., Michałek-Pogorzelska M., 2009. Ocena jakości ekologicznej wyrobisk i rejonu ich lokalizacji w Zatoce Puckiej na podstawie zoobentosu, [in:] L. Kruk-Dowgiałło (Ed.), Program rekultywacji wyrobisk w Zatoce Puckiej. Maritime Institute in Gdańsk, Gdańsk.

Osowiecki A., Łysiak-Pastuszak E., Kruk-Dowgiałło L., Błeńska M., Brzeska P., Kraśniewski W., Lewandowski Ł., Krzymiński W. 2012, Development of tools for ecological quality assessment in the Polish marine areas according to the water Framework Directive. Part IV – Preliminary assessment. Oceanological and Hydrobiological Studies, 41(3), 1–10.

Owen K., Sköld M., Carlström J., 2021. An increase in detection rates of the critically endangered Baltic Proper harbor porpoise in Swedish waters in recent years. Conservation Science and Practice, 3(8): e468.

Pachur M., Horbowy J., 2013. Food composition and prey selection of cod, Gadus morhua (Actinopterygii: Gadiformes: Gadidae), in the southern Baltic Sea. Acta Ichthyologica et Piscatoria, 43(2): 109–118.

Pachur M.E., Pawlak J., 2016. Zmiany w składzie pokarmu i odżywianie się dorsza (Gadus morhua) w południowym Bałtyku na przestrzeni ostatnich lat, [in:] 95-lecie Morskiego Instytutu Rybackiego: aktualne tematy badań naukowych. Tom II – Stan środowiska południowego Bałtyku. The National Marine Fisheries Institute, Gdynia, pp. 87–96,

Pęcherzewski K., 1972. Zawartość i rozmieszczenie substancji organicznych oraz azotu i fosforu w osadach dennych południowego Bałtyku, [in:] K. Siudziński (Ed.), Ekosystemy Morskie. Polska Akademia Nauk, Instytut Biologii, Morski Instytut Rybacki, Zakład Oceanografii, Gdynia, pp. 51–76.

Pęcherzewski K., Ławacz W., 1975. Wstępne wyniki badań nad ilością C org. (DOC i POC) w wodach Południowego Bałtyku. Zeszyty Naukowe Wydziału Biologii i Nauk o Ziemi. Oceanografia, 4: 25–45.

Pelletier S.K., Omland K., Watrous K.S., Peterson T.S., 2013. Information Synthesis on the Potential for Bat Interactions with Offshore Wind Facilities – Final Report. U.S. Dept of the Interior, Bureau of Ocean Energy Management, Headquarters, Herndon, VA. OCS Study BOEM 2013-01163.

Pempkowiak J., Chiffoleau J.F., Staniszewski A., 2000. The vertical and horizontal distribution of selected trace metals in the Baltic Sea off Poland. Estuarine, Coastal and Shelf Science, 51(1): 115–125.

Petalas C., Lazarus T., Lavoie R.A., Eliott K.H., Guigueno M.F., 2021. Foraging niche partitioning in sympatric seabird populations. Scientific Reports, 11: 2493.

Petersen I.K., Christensen T.K., Kahlert J., Desholm M., Fox A.D., 2006. Final results of bird studies at the offshore wind farms at Nysted and Horns Rev, Denmark. National Environmental Research Institute, Denmark.

Pētersons G., 2004. Seasonal migrations of north-eastern populations of Nathusius' bat Pipistrellus nathusii (Chiroptera). Myotis, 41–42: 29–56.

Pikies R., 1990. Mapa geologiczna dna Bałtyku w skali 1:200 000. Arkusz Południowa Ławica Środkowa. Polish Geological Institute, Warszawa.

Pikies R., 1992, Mapa geologiczna dna Bałtyku 1:200 000. Ark. 15 – Południowa Ławica Środkowa. Polish Geological Institute, Warszawa.

Pikies R., 1995, Objaśnienia do Mapy geologicznej dna Bałtyku 1:200 000. Arkusze Południowa Ławica Środkowa, Basen Gotlandzki, Próg Gotlandzko-Gdański. Polish Geological Institute, Warszawa.

Pikies R., 2005. Procesy erozji i akumulacji glacjalnej w południowej części Basenu Gotlandzkiego w zapisie rzeźby podłoża czwartorzędu oraz rozprzestrzenienia osadów plejstoceńskich. Bulletin of the Polish Geological Institute, 416: 81–114.

Plichta I., Kosecka M., Thomsen F., Świątek D., 2015. Monitoring ssaków morskich na obszarze morskiej farmy wiatrowej Bałtyk Środkowy II. Raport końcowy z wynikami badań, [in:] Morska farma wiatrowa Bałtyk Środkowy II. Raport o oddziaływaniu na środowisko. Volume III, Section 10. Grupa Doradcza SMDI, Warszawa.

Plichta I., Kosecka M., Thomsen F., Świątek D., 2014. Monitoring ssaków morskich na obszarze morskiej farmy wiatrowej Bałtyk Środkowy III. Raport końcowy z wynikami badań, [in:] Morska farma wiatrowa Bałtyk Środkowy III. Raport o oddziaływaniu na środowisko. Volume III, Section 10. Grupa Doradcza SMDI, Warszawa.

SEM (*PMŚ*) 2002−2022. Dane Państwowego Monitoringu Środowiska dotyczące fitobentosu w polskich obszarach morskich – Data from the State Environmental Monitoring programme on phytobenthos in Polish sea areas.

Poerink B.J., Lagerveld S., Verdaat H., 2013. Bat activity in the dutch offshore wind farm OWEZ and PAWP. Pilot study. IMARES report No. C026/13 – tFC 20120402.

Poleszczuk G., 1996. General chemical indicators of water quality in Roztoka Odrzanska (Odra River mouth, NW Poland). Oceanological Studies, 25(3): 55–65.

Polivajko A.G., 1982. O sozrievanii i nieriestje baltijskogo shprota, [in:] Rybokhozjaistviennyje issliedovanija v basseinie Baltijskogo morja. Riga, BaltNIIRH; 29–45 (in Russian).

Porębski J., 1995. Ichtioplankton Zatoki Pomorskiej w sezonie 1994 r. ze szczególnym uwzględnieniem śledzia wiosennego. National Marine Fisheries Research Institute (MIR) Reports 1993–1994: 325–341.

Radtke K., Wodzinowski T., Wójcik I., Šics I., 2023. Podsumowanie wyników oceanograficzno-rybackich badań rejsu r.v. Baltica na przełomie lutego i marca 2023 roku z obiecująco liczniejszym występowaniem małych dorszy. Wiadomości Rybackie, Pismo Mor. Inst. Ryb. – Pań. Inst. Badaw., 3–4 (252): 3–7.

Ramirez I. (Ed.), 2010. Marine IBAs in the European Union. BirdLife International, Belgium.

Opioła R., Gajewski J., Kaczmarek N., Barańska A., Bojke A., Brocławik O., Brzezińska A., Celmer Z., Cuttat F., Dembska G., Drgas A., Druzd N., Dworniczak J., Dziaduch D., Edut J., Eisen M., Fey D., Flasińska A., Gajewski Ł., Galer-Tatarowicz K., Grygiel W., Horbowa K., Jasper B., Kałas M., Kapiński J., Kołakowska E., Kubacka M., Kunicki M., Kuzebski E., Lisimenka A., Littwin M., Marcinkowski T., Meissner W., Mirny Z., Misiewicz E., Mortensen L., Nermer T., Nocoń M., Olenycz M., Olszewski T., Ostrowska D., Pazikowska-Sapota G., Pick D., Radtke K., Rydzkowski P., Sadowska U., Sarnocińska J., Schack H., Schmidt B., Schönberger L., Skov H., Strzelecki D., Stöber U., Suska M., Szczepańska K., Szymanek L., Thomsen F., Tuhuteru N., Wróblewski R., Wyszyński M. i Załęski K. Raport o oddziaływaniu morskiej farmy wiatrowej Baltic Power na środowisko, 2020.

Ridgway S.H., Joyce P.L., 1975. Studies on seal brain by radiotelemetry. Rapp. P.-v. Reun. Cons. Int. Explor. Mer, 169: 81–91.

Rodrigues L., Bach L., Biraschi L., Dubourg-Savage M.J., Goodwin J., Harbusch C., Hutson T., Ivanova T., Lutsar L., Parsons K., 2006. Wind Turbines and Bats. Guidelines for the planning process and impact assessment. Annex 1 to Resolution 5.6. EUROBATS Publication Series. UNEP/EUROBATS Secretariat, Bonn.

Rodrigues L., Bach L., Dubourg-Savage M.J., Goodwin J., Harbusch C., 2008. Guidelines for consideration of bats in wind farm projects. EUROBATS Publication Series No. 3 (English version). UNEP/EUROBATS Secretariat, Bonn.

Ronconi R.A., Burger A.E., 2009. Estimating seabird densities from vessel transects. Distance sampling and implications for strip transects. Aquatic Biology, 4(3): 297–309.

Regulation of the Minister of the Environment of 1 July 2015 on the geological documentation of mineral deposits, excluding hydrocarbon deposits (Journal of Laws 2015, item 987);

Regulation of the Minister of the Environment of 11 May 2015 on the recovery of waste outside the installations and facilities (Journal of Laws 2015, item 796).

Regulation of the Minister of Environment of 11 March 2005 on establishment of a list of game species (Journal of Laws 2005, No. 45, item 433).

Regulation of the Minister of Environment of 16 December 2016 on protection of animal species (Journal of Laws 2016, item 2183).

Regulation of the Minister of the Environment of 9 October 2014 on protection of plant species (Journal of Laws 2014, item 1409).

Regulation of the Council of Ministers of 14 April 2021 on the adoption of the spatial development plan for the internal sea waters, the territorial sea and the exclusive economic zone at the scale of 1:200 000 (Journal of Laws 2021, item 935). Russell D., Hastie G.D., Thompson D., Janik V.M., Hammond P.S., Scott-Hayward L.A., McConnell B.J., 2016. Avoidance of wind farms by harbour seals is limited to pile driving activities. Journal of Applied Ecology, 53(6): 1642–1652.

Rydell J., Bach L., Bach P. et al., 2014. Phenology of migratory bat activity across the Baltic Sea and the south-eastern North Sea. Acta Chiropterologica, 16(1): 139–147.

Rydell J., Bach L., Dubourg-Savage M.J., Green M., Rodrigues L., Hendenström A., 2010. Bat mortality at wind farms in northwestern Europe. Acta Chiropterologica, 12: 261–274.

Rydell J., Bach L., Dubourg-Savage M.J., Green M., Rodrigues L., Hendenström A., 2010. Mortality of bats at wind turbines links to nocturnal insect migration? European Journal of Wildlife Research, 56(6): 823–827.

Sachanowicz K., Ciechanowski M., Piksa K., 2006. Distribution patterns, species richness and status of bats in Poland. Vespertilio, 9–10: 151–173.

Salbu B., Oughton D.H., 1994. Strategies of sampling, fractionation and analysis, [in:] B. Salbu, E. Steinnes (Eds), Trace elements in natural waters. CRC Press, Boca Raton pp. 41–69.

SAMBAH, 2016. Final report for LIFE+ project SAMBAH LIFE08 NAT/S/000261 covering the project activities from 01/01/2010 to 30/09/2015.

Saniewski M., Zalewska T., 2016. Atmospheric deposition and riverine load of 90Sr and 137Cs to the Gulf of Gdańsk (southern Baltic Sea) in the period 2005–2011. J. Environ. Radioactiv., 151: 1–11.

Saniewski M., Zalewska T., Kraśniewski W., 2022. Benthic macroinvertebrates as reference indicators for monitoring of anthropogenic isotope 137 Cs contamination in the marine environment. Environmental Science and Pollution Research, 29: 13822–13834.

Sapota G., 2004. Polychlorinated biphenyls (PCBs) and organochlorine pesticides (OCPs) in seawater of the southern Baltic Sea. Desalination, 162(1–3): 153–157.

Sapota G., 2006. Persistent organic pollutants (POPs) in bottom sediments from the Baltic Sea. Oceanological and Hydrobiological Studies, 35(4): 295–306.

Sapota G., 2011. Environmental Policy and Legislation on Dredged Material in the Baltic Sea Region. Raport SMOCS. Baltic Sea Region Programme Project No 39.

Sapota G., Dembska G., Bogdaniuk M., Holm G., 2012. Contamination in sediments from the Baltic Sea region – analysis, [in:], IEEE/OES Baltic International Symposium (BALTIC), Klaipeda, Lithuania.

Savvides C., Papadopoulos A., Haralambous K.J.J., Loizidou M., 1995. Sea sediments contaminated with heavy metals. Metal speciation and removal. Water Science and Technology, 32(9–10): 65–73.

Seitz R.D., Wennhage H., Bergström U. et al., 2014. Ecological value of coastal habitats for commercially and ecologically important species. ICES J. Mar. Sci., 71: 648–665.

Shannon G., McKenna M.F., Angeloni L.M. et al., 2016. A synthesis of two decades of research documenting the effects of noise on wildlife. Biol. Rev., 91(4): 982–1005.

Shvetsov F., Rudneva A., 1994. The growth and feeding of sprat in Eastern Baltic. ICES C.M., J:10: 1–8.

Siepak J. (Ed.), 1998. Analiza specjacyjna metali w próbkach wód i osadów dennych. Adam Mickiewicz University, Poznań.

Sjöberg M., Ball J.P., 2000. Grey seal, *Halichoerus grypus*, habitat selection around haulout sites in the Baltic Sea: bathymetry or central-place foraging? Canadian Journal of Zoology, 78(9): 1661–1667.

Skjellerup P., Maxon C.M., Tarpgaard E., Thomsen F., Schack H.B., Tougaard J. et al., 2015. Marine mammals and underwater noise in relation to pile driving. Working Group 2014. Energinet.dk.

Skov H., Heinänen S., Žydelis R., Bellebaum J., Bzoma S., Dagys M., Durinck J., Garthe S., Grishanov G., Hario M., Kieckbusch J.J., Kube J., Kuresoo A., Larsson K., Luigujoe L., Meissner W., Nehls H.W., Nilsson L., Petersen I.K., Roos M.M., Pihl S., Sonntag N., Stock A., Stipniece A., Wahl J., 2011. Waterbird populations and pressures in the Baltic Sea. Nordic Council of Ministers, Copenhagen.

Smith P.E., Richardson S.L., 1977. Standard techniques for pelagic fish egg and larva surveys. FAO Fisheries Technical Paper No. 175. Food and Agriculture Organization of the United Nations, Rome.

Solé M., Sigray P., Lenoir M. et al., 2017. Offshore exposure experiments on cuttlefish indicate received sound pressure and particle motion levels associated with acoustic trauma. Sci. Rep., 7: 45899.

Spiga I., Caldwell G.S., Bruintjes R., 2016. Influence of pile driving on the clearance rate of the blue mussel, Mytilus edulis (L.). Proc. Mtgs. Acoust., 27(1): 040005.

Spurr E.B., Borkin K.M., Drew K.W., 2012. Line-transect distance sampling compared with fixed-width strip-transect counts for assessing tomtit (Petroica macrocephala) population trends. New Zealand Journal of Ecology, 36(3): 365–370.

Stroomberg G.J., Freiriks I.L., Smedes F., Cofino W.P., 1995. Quality assurance and quality control of surface water sampling, [in:] P. Quevauviller (Ed.), Quality assurance in environmental monitoring. Sampling and sample pretreatment. VCH Verlagsgcsellschaft mbH. Weinheim–New York–Basel–Cambridge–Tokyo, pp. 51–90.

Šuba J., Petersons G., Rydell J., 2012. Fly-and-forage strategy in the bat *Pipistrellus nathusii* during autumn migration. Acta Chiropterologica, 14(2): 379–385.

Svedäng H., Hornborg S., 2017. Historic changes in length distributions of three Baltic cod (Gadus morhua) stocks: Evidence of growth retardation. Ecology and Evolution, 7: 6089–6102.

Szczepańska T., Uścinowicz S., 1994. Atlas geochemiczny Południowego Bałtyku. Polish Geological Institute – National Research Institute, Warszawa.

Szefer P., 2002. Metals, Metalloids and Radionuclides in the Baltic Sea Ecosystem. Elsevier Science B.V., Amsterdam.

Terhune J.M., 1988. Detection thresholds of a harbour seal to repeated underwater high-frequency, short-duration sinusoidal pulses. Can. J. Zool., 66(7): 1578–1582.

Terhune J.M., Ronald K., 1975. Underwater hearing sensitivity of two ringed seals (Pusa hispida). Can. J. Zool., 53: 227–231.

Thomas L., Buckland S.T., Rexstad E.A., Laake J.L., Strindberg S., Hedley S.L., Bishop J.R.B., Marques T.A., Burnham K.P., 2010. Distance software. Design and analysis of distance sampling surveys for estimating population size. Journal of Applied Ecology, 47: 5–14.

Thomsen F., Laczny M., Piper W., 2004. Methodik zur Erfassung von Schweinswalen (Phocoena phocoena) und anderen marinen Säugern mittels Flugtransekt-Zählungen. Seevögel, 25(1): 3–12.

Thomsen F., Lüdemann K., Kafemann R. et al., 2006. Effects of offshore wind farm noise on marine mammals and fish. biola, Hamburg, Germany on behalf of COWRIE Ltd.

Tomiałojć L., Stawarczyk T., 2003. Awifauna Polski. Rozmieszczenie, liczebność i zmiany. Polskie Towarzystwo Przyjaciół Przyrody „proNatura", Wrocław.

Trojan P., 1980. Ekologia ogólna. PWN, Warszawa.

Ulfsbo A., Hulth S., Anderson L.G., 2011. pH and biogeochemical processes in the Gotland Basin of the Baltic Sea. Marine Chemistry, 127(1–4): 20–30.

Urick R.J., 1984. Ambient Noise in the Sea. Undersea Warfare Technology Office, Naval Sea System Command, Department of the NAVY, Washington D.C.

Uścinowicz S. (Ed.), 2011. Geochemia osadów powierzchniowych Morza Bałtyckiego. Polish Geological Institute – National Research Institute, Warszawa.

Uścinowicz S., 1995, Miąższość czwartorzędu, [in:] Mojski J.E. (Ed.), Atlas geologiczny południowego Bałtyku. Tabl. XIII. Polish Geological Institute – National Research Institute, Sopot–Warszawa.

Uścinowicz S., Zachowicz J., 1988. Mapa geologiczna dna Bałtyku w skali 1: 200 000. Arkusz Łeba, Słupsk. Polish Geological Institute – National Research Institute, Warszawa.

Uścinowicz S., Zachowicz J., 1991. Objaśnienia do Mapy geologicznej dna Bałtyku w skali 1:200 000, arkusz Łeba, Słupsk. Polish Geological Institute – National Research Institute, Warszawa.

Abraham M., Westphal L., Hand I., Lerz A., Jeschek J., Bunke D., Leipe T., Schulz-Bull D., 2017. TBT and its metabolites in sediments: Survey at a German coastal site and the central Baltic Sea. Marine Pollution Bulletin, 121(1–2): 404–410.

Geological and Mining Law Act of 9 June 2011 (Journal of Laws 2022, item 1072, as amended)

Van der Graaf A.J., Ainslie M.A., André M. et al., 2012. European Marine Strategy Framework Directive – Good Environmental Status (MSFD GES). Report of the Technical Subgroup on Underwater noise and other forms of energy.

Vanermen N., Onkelinx T., Courtens W., Van de walle M., Verstraete H., Stienen E.W.M., 2014, Seabird avoidance and attraction at an offshore wind farm in the Belgian part of the North Sea. Hydrobiologia, 756: 51–61.

Voigt C.C., Kionka J., Koblitz J.C., Stilz P.C., Pētersons G., Lindecke O., 2023. Bidirectional movements of Nathusius' pipistrelle bats (Pipistrellus nathusii) during autumn at a major migration corridor. Global Ecology and Conservation, 48: e02695.

Voigt C.C., Popa-Lisseanu A.G., Niermann I., Kramer-Schadt S., 2012. The catchment area of wind farms for European bats. A plea for international regulations. Biol Conserv., 153: 80–86.

Wagstaff R.A., Newcomb J., 1987. Omnidirectional Ambient Noise Measurements in the Southern Baltic Sea During Summer and Winter, [in:] H. Mercklinger (Ed.), Progress in Underwater Acoustics. Springer, Boston, pp. 445–452.

Wardecki Ł., Chodkiewicz T., Beuch S., Smyk B., Sikora A., Neubauer G., Meissner W., Marchowski D., Wylegała P., Chylarecki P., 2022. Monitoring Ptaków Polski w latach 2018–2021. Biuletyn Monitoringu Przyrody, 22(2): 1–80.

Wenz G.M., 1962. Acoustic Ambient Noise in the Ocean. Spectra and Sources. J. Acoust. Soc. Am., 34(12): 1936–1956.

Więcaszek B., 2010. Analiza statusu taksonomicznego dorsza Gadus morhua Linnaeus, 1758 z Morza Bałtyckiego na podstawie cech morfologicznych, biologicznych i genetycznych populacji z różnych rejonów rozsiedlenia. Zachodniopomorski Uniwersytet Technologiczny w Szczecinie, Szczecin.

Wille P.C., Geyer D., 1984. Measurements on the origin of the wind-dependent ambient noise variability in shallow water. J. Acoust. Soc. Am., 75(1): 173–185.

Winstral A., Elder K., Davis, R.E., 2002. Spatial Snow Modeling of Wind-Redistributed Snow Using Terrain-Based Parameters. Journal of Hydrometeorology, 3(5), 524-538.

Witt G., 1995. Polycyclic aromatic hydrocarbons in water and sediment of the Baltic Sea. Marine Pollution Bulletin, 31(4–12): 237–248.

Witt G., 2002. Occurrence and transport of polycyclic aromatic hydrocarbons in the water bodies of the Baltic Sea. Marine Chemistry, 79(2): 49–66.

World Meteorological Organization, 2012. Guide to Meteorological Instruments and Methods of Observation. 2008 edition updated 2010. WMO No. 8. Geneva.

World Register of Marine Species (WoRMS); http://www.marinespecies.org/index.php.

WWF, 2019. Projekt: „Restytucji i ochrony fok szarych w Polsce". Raport z realizacji zadania w roku 2019, „Wprowadzenie osobników fok do środowiska w ramach restytucji".

WWF, 2020. Raport z projektu „Ochrona ssaków i ptaków morskich i ich siedlisk" 2016–2020. Fundacja WWF Polska, Warszawa.

WWF, 2023a. Raport z projektu Ochrona ssaków i ptaków morskich – kontynuacja 2020–2023. Fundacja WWF Polska, Warszawa.

WWF, 2023b. Data collected in the WWF marine mammal and bird observation database. Available on the website: https://link.wwf.pl/baza_ssaki/public/mapa.

Wysocki L.E., Dittami J.P., Ladich F., 2006. Ship noise and cortisol secretion in European freshwater fishes. Bio. Conserv., 128(4): 501–508.

Zabiegała B., 2002. Oznaczanie zawartości węgla całkowitego, całkowitego węgla organicznego oraz węgla nieorganicznego w próbkach środowiskowych z kulometrycznym oznaczeniem końcowym. Katedra Chemii Analitycznej, Wydział Chemiczny, Politechnika Gdańska, Gdańsk.

Zalewska T., Kraśniewski W., 2019. Ocena stanu środowiska polskich obszarów morskich Bałtyku na podstawie danych monitoringowych z roku 2018 na tle dziesięciolecia 2008–2017. Biblioteka Monitoringu Środowiska.

Zalewska T., Kraśniewski W., 2022. Ocena stanu środowiska polskich obszarów morskich Bałtyku na podstawie danych monitoringowych z roku 2021 na tle dziesięciolecia 2011–2020. Biblioteka Monitoringu Środowiska.

Zalewska T., Suplińska M., 2013. Anthropogenic radionuclides ^{137}Cs and ^{90}Sr in the southern Baltic Sea ecosystem. Oceanologia, 55(3): 485–517.

Zapart A., Kończak J., Ciechanowski M., Wikar Z., Bidziński K., Jankowska-Jarek M., 2022. Nordowe Nocki – skład gatunkowy, rozmieszczenie i liczebność nietoperzy w najdalej na północ wysuniętym zimowisku w Polsce, [in:] XXIX Ogólnopolska Konferencja Chiropterologiczna. Poznań 16–18 września 2022 r. Streszczenia. Polskie Towarzystwo Ochrony Przyrody „Salamandra", Poznań, pp. 37.

Zevenbergen L.W., Thorne C.R., 1987. Quantitative analysis of land surface topography. Earth Surface Processes and Landforms, 12(1): 47–56.

Zydelis R., Skov H., Heinanen S., Hoigaard Holst M., Jankowiak A., Łuczak A., Tryjanowski P., 2015a. Morska farma wiatrowa Bałtyk Środkowy II. Raport o oddziaływaniu na środowisko. Volume IV, Section 5, Part 2. Grupa Doradcza SMDI, Warszawa.

Zydelis R., Skov H., Heinanen S., Hoigaard Holst M., Jankowiak A., Łuczak A., Tryjanowski P., 2015b. Morska farma wiatrowa Bałtyk Środkowy III. Raport o oddziaływaniu na środowisko. Ocena oddziaływania na ptaki. Cz. 2. Ptaki migrujące. [in:] Morska farma wiatrowa Bałtyk Środkowy III. Raport o oddziaływaniu na środowisko. Volume IV, Section 5, Part 2. Grupa Doradcza SMDI, Warszawa.